
Society of Petroleum Engineers

Chemistry for Enhancing the Production of Oil and Gas

Wayne W. Frenier

Murtaza Ziauddin

Chemistry for Enhancing the Production of Oil and Gas

Chemistry for Enhancing the Production of Oil and Gas

Wayne W. Frenier

Frenier Chemistry Consultants

Murtaza Ziauddin

Schlumberger

Society of Petroleum Engineers

© Copyright 2013 Society of Petroleum Engineers

All rights reserved. No portion of this book may be reproduced in any form or by any means, including electronic storage and retrieval systems, except by explicit, prior written permission of the publisher except for brief passages excerpted for review and critical purposes.

Manufactured in the United States of America.

ISBN 978-1-61399-317-0
ISBN 978-1-61399-393-4 (Digital)

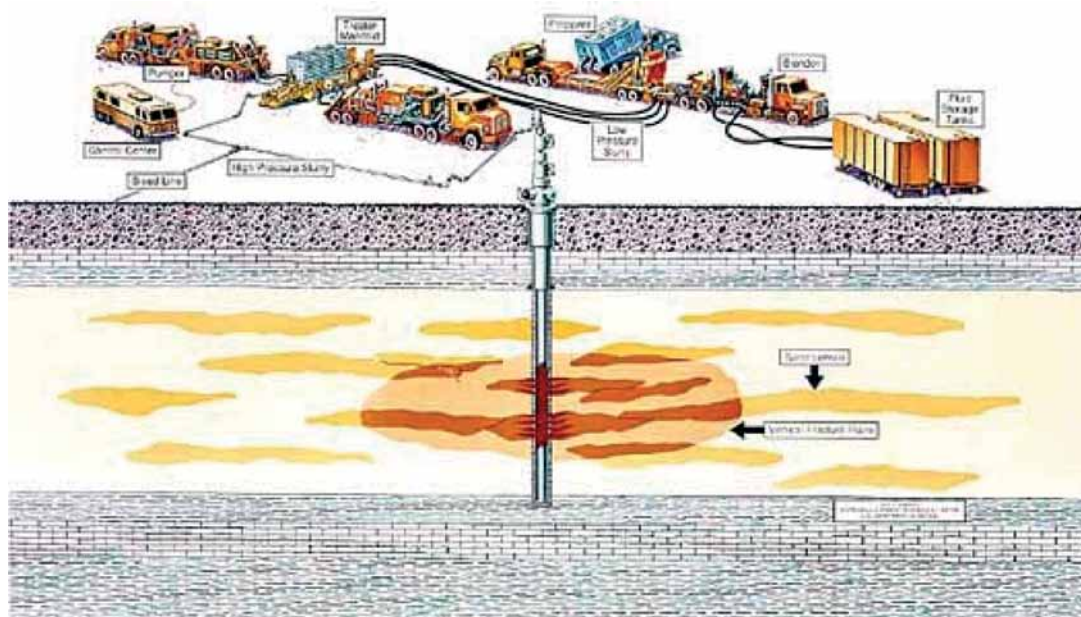
Society of Petroleum Engineers
222 Palisades Creek Drive
Richardson, TX 75080-2040 USA

<http://www.spe.org/store>
service@spe.org
1.972.952.9393

Preface

In approximately 1983, Al Look* (at that time the President of the Dowell Division of the Dow Chemical Company) noted that each day, hundreds (possibly thousands) of small chemical plants are set up in the world's oil/gas fields, and hundreds of thousands of pounds of chemicals are pumped into the Earth to enhance and maintain the flow of oil and gas. Frequently at the end of the treatment, these “mini-plants” [see Fig. P.1 in API (2008) for drawing of a hydraulic fracturing set up] are broken down and transported to a new site. The chemistry applied is the same as might happen in a refinery or a chemical plant, but here, most of the reactions take place out of sight and control of the process engineers. Thus, the design of the *chemistry* is of particular importance because usually it cannot be changed once it is pumped. This book will describe how these underground reactions work to keep the world's hydrocarbon life lines flowing.

This document has been written to provide an improved understanding of the role of chemical reactions for enhancing and maintaining the production of oil and gas. There are several books that describe the thousands of production chemicals in use and include those by Fink (2003), Fink (2011), and Kelland (2009). These documents are useful references and have been cited frequently by the authors of this book. In addition, the reviews in Economides and Nolte (2000) have several excellent chapters (Constein et al. 2000; Hill and Schechter 2001) on some aspects of production chemistry and their applications in acid and hydraulic prop stimulation. This current book will also review many new aspects of the application of chemistry for enhancement oil and gas production that have reached the market since 2000 and will provide new mechanistic information.



*Al Look. 1983. Private communication.

This publication will provide an overview of the science and technology of the use of many production chemicals to a general technically trained audience, with emphasis placed on the basic chemical and physical principles by which the chemicals can enhance or maintain oil and gas production.

The introductory chapter describes the production environment, problems that require chemical intervention, and thus, the need for the thousands of different chemicals that are in use. This chapter also reviews the important chemical and physical principles that are common to most if not all of the enhancement treatments. This also places the technical aspects of production management in the perspective of the upstream oil and gas business. Subsequent chapters discuss aspects of the use and mechanisms of the complex chemistries that take place with the application of flow assurance chemicals, during stimulation (reactive chemistry and prop fracturing) and chemically improved oil recovery, including the use of chemical tracers. A separate chapter (Chapter 6) emphasizes the importance of health, safety, and environmental compliance in all aspects of oilfield treatments. Most of the chapters of the book end with a section where successful chemical enhancement or control methods have been used to solve specific production problems.

An outline for analysis is

- Is there a problem that requires an intervention?
- If there is a problem, how bad will it be?
- Can the problem be managed through engineering, and/or chemical means?
- Evaluate the results of an intervention or control strategy.

Each major section and most subsections will include reviews of current literature as well as summaries of the consensus understandings from the literature cited.

Chapter 1—Introduction

This section describes the reasons producing formations require intervention to enhance or maintain production, and the various types of chemical intervention in use. This chapter also reviews basic chemical and engineering processes that occur in production operations. It emphasizes the commonality of many of the chemical and engineering processes across the various production enhancement processes.

Chapter 2—Chemistry of Production Impairment

This chapter describes processes that impair the production of oil and gas such as formation damage and formation (and then mitigation) of emulsions in the production stream. It also updates techniques for mitigating and inhibiting deposition of inorganic and organic materials using references from earlier sources (Frenier and Ziauddin 2008; Frenier et al. 2010).

Chapter 3—Formation Stimulation With Reactive Chemicals

This chapter reviews the chemicals and mechanisms of reactive fluids (including acids) stimulation of oil and gas formations.

Chapter 4—Propped Fracturing Chemistry and Applications

This chapter discusses techniques and chemicals for formation stimulation using hydraulic fracturing using essentially nonreactive fluids.

Chapter 5—Improved Oil Recovery Chemical Applications

This chapter provides details of the chemicals and formation interactions that allow chemical sweep methods and conformance control processes to enhance hydrocarbon recovery. This chapter also gives a short review of the use of chemical tracers.

Chapter 6—Health, Ecology, and Safe Handling of Treating Chemicals and Produced Fluids

This chapter reviews general guidelines for planning and use of potentially toxic or hazardous chemicals that are frequently part of a treatment. Included is a discussion of the hazards associated with flowing back fluids. This chapter also reviews the use of chemicals to remediate spills of crude oil or production chemicals.

Chapters 1 through 5 each conclude with a “Things to Think About” section that summarizes the major findings revealed by the review of the technologies that were discussed and how this knowledge can be applied to chemical production management projects. Chapters 2 through 5 also have a section titled Histories and Best Practices (based on the technologies in that chapter). Here, the science and engineering principles described in the earlier sections are illustrated through practical demonstrations of chemical intervention and remediation.

Definition of the Upstream Oilfield Environment

The scope of this document is limited to chemical intervention and enhancement in the production (“upstream”) oilfield environment. This includes the entire production field including injection wells, the producing formation, and especially the near wellbore area as well as flowlines and gathering lines. This includes the natural or artificial tubulars, subsurface devices, gathering lines, and wellsite surface equipment. The book *will not* describe chemicals in use to drill, complete, or cement the well field. See the books by Growcock (2005) and Nelson and Guillot (2005). The discussion will also *not* include problems in transmission pipelines or refineries. However, many of the techniques and technologies needed are very similar to those described in this book and could be applied with appropriate modifications. See Frenier (2001b) for a review of cleaning of industrial equipment, including the downstream oil and gas equipment.

Acknowledgment

The authors acknowledge the help and encouragement of Schlumberger Technology Company. In particular, we thank Schlumberger for releasing significant portions of text and illustrations from company files for use in the document. Olga Kresse, Bruno Lecerf, Philippe Enkababian, Eric Clum, and Greg Kubala, (all of Schlumberger) reviewed some of the portions of the text and provided very useful suggestions for improvements. We also acknowledge the help and encouragement of Prof. Mojdeh Delshad, University of Texas at Austin.

SPE would like to thank Mojdeh Delshad for his generous contributions to the oversight of this book project on behalf of the Books Development Committee. We appreciate his contributions in working with the author and ensuring that timelines and quality standards were upheld throughout the process.

This book is dedicated to my wife, Dolores, and our children, Andrew Frenier and Kathleen Turner, as well as our grandchildren. They inspire me to continue to work, learn, and become a better person.

–Wayne W. Frenier

I humbly dedicate this modest endeavor to the 52nd *Dai al Mutlaq*, His Holiness, Dr. Syedna Mohammed Burhanuddin (TUS), on the occasion of his 102nd birthday and 50 years as *Dai al Mutlaq*. I pray that Allah may grant him a long and healthy life.

–Murtaza Ziauddin

Contents

Preface

| | |
|---|------------|
| 1. Introduction..... | 1 |
| 1.1 Chemical Applications in the Reservoir Life Cycle | 1 |
| 1.2 Need for Chemical or Engineering Practices to Enhance Production | 4 |
| 1.3 Production Chemistry Economics | 11 |
| 1.4 Basics of Fluid Chemistries | 12 |
| 1.5 Key Production Chemistry Concepts | 23 |
| 1.6 Injecting Fluids Into the Earth..... | 39 |
| 1.7 Treating Equipment on the Wellsite | 49 |
| 1.8 Electronic Sources of Oilfield Chemistry Information | 53 |
| 2. Chemistry of Production Impairment | 55 |
| 2.1 Introduction to Production Impairment Processes | 55 |
| 2.2 Organic and Inorganic Deposits | 57 |
| 2.3 Formation Damage | 87 |
| 2.4 Formation and Control of Emulsions in Production Operations | 99 |
| 2.5 Flow Enhancers | 116 |
| 2.6 Case Histories and Best Practices for Use of Production Chemicals | 118 |
| 2.7 Things to Think About..... | 120 |
| 3. Formation Stimulation With Reactive Chemicals | 121 |
| 3.1 Introduction to Stimulation Using Reactive Chemicals..... | 121 |
| 3.2 Laboratory Test Methods for Matrix Reactive Fluid Treatments | 126 |
| 3.3 Matrix Stimulation of Carbonate Formations | 132 |
| 3.4 Chemical Formulations for Stimulation of Carbonate Reservoirs..... | 142 |
| 3.5 Sandstone Matrix Stimulation | 163 |
| 3.6 Additives—What Is in the Reactive Fluid? | 184 |
| 3.7 Placement of Matrix Fluids | 206 |
| 3.8 Fracture Stimulation of Carbonates and Sandstone Using Reactive Fluids | 231 |
| 3.9 Best Practices and Case Histories of Use of Reactive Chemicals for Stimulation | 253 |
| 3.10 Things to Think About | 257 |
| 4. Propped Fracturing Chemistry and Applications | 259 |
| 4.1 Introduction to Propped Fracturing Processes | 259 |
| 4.2 Characteristics of Fracturing Fluids, Additives, and Proppants | 271 |
| 4.3 Introduction to Fracture Fluid/Proppant Chemistry Using HPG as an Example | 284 |
| 4.4 Water-Based Fluids..... | 291 |
| 4.5 Nonwater-Based Fluids..... | 312 |
| 4.6 Fluid Loss Agents and Breakers | 313 |
| 4.7 Additional Frac Additives | 322 |
| 4.8 Reactions of Fracturing Fluids With Formations and Well Fluids..... | 331 |
| 4.9 Proppants and Proppant Aids | 333 |

| | |
|--|------------|
| 4.10 Fluid Selection/Proppant Selection | 345 |
| 4.11 Fracture Planning and Models: Combining Chemistry and Engineering | 353 |
| 4.12 Case Histories and Best Practices for Proppant Fracturing | 366 |
| 4.13 Things to Think About | 369 |
| 5. Improved Oil Recovery Chemical Applications | 371 |
| 5.1 Basic Principles of IOR | 373 |
| 5.2 Selection Criteria for IOR Treatments | 384 |
| 5.3 Testing Methods for IOR Processes | 389 |
| 5.4 Immiscible Displacement Processes | 395 |
| 5.5 Miscible Displacement Processes | 414 |
| 5.6 Chemical Methods for Improving Sweep Efficiency (Mobility Control) | 445 |
| 5.7 Use of Chemical Tracers | 456 |
| 5.8 Case Histories and Best Practices for Chemical EOR | 460 |
| 5.9 Things to Think About | 462 |
| 6. Health, Ecology, and Safe Handling of Treating Chemicals and Produced Fluids | 463 |
| 6.1 Safety Considerations During Production Enhancement Operations | 463 |
| 6.2 Health, Safety, and Environmental (HSE) Management | 467 |
| 6.3 Handling, Reuse, and Disposal of Flowback Fluids | 476 |
| 6.4 Control and Remediation of Spills in Water Bodies and on Land | 489 |
| 6.5 Continual Quality Improvements With Oilfield Chemistry | 505 |
| Nomenclature | 509 |
| References | 513 |
| Author Index | 577 |
| Subject Index | 593 |

Chapter 1

Introduction

This chapter provides an introduction to the use of chemicals for production stimulation and maintenance of production after it has commenced. The life cycle of a well affects the need for chemical intervention. Many different types of chemicals may be used and the thermodynamic and kinetic parameters that characterize the reactions come into play as the chemicals are injected and react in the Earth or in the production flow paths. The treatments are conducted using “minichemical plants” that are custom assembled on site using a wide variety of portable equipment. For some applications, such as improved-oil-recovery (IOR) processes, the various chemical plants and storage vessels may be in place for several years.

Basic chemical and engineering principles that are required to understand the applications of production-enhancement chemicals also are reviewed in this chapter. The dominant theme that is described in this chapter (and emphasized throughout the book) is that *similar* chemical and engineering practices are used in many and possibly all aspects of the oil and gas production environment. So, it is possible to understand many different procedures by understanding some basic principles. An additional dominant theme is that surface-active chemicals are used throughout the processes in the producing formation and in the production tubing. These chemicals react with each other, with the fluids in the earth and frequently with the formation or with the solids in the tubing to *change* the flow paths of the hydrocarbons. If these chemical/engineering processes are preformed properly, improved production will be achieved.

1.1 Chemical Applications in the Reservoir Life Cycle

The phases of the life cycle of a hydrocarbon producing reservoir have been identified in the industry (POSC 2006) as exploration (discover), appraisal (define), development (develop), production (deplete), and abandonment (dispose). Except for the earliest phases of exploration where geologic and seismic methods are used to find promising areas where hydrocarbons may be located, large volumes of chemicals are employed. They are applied during the drilling, completion, production, and abandonment phases. However, *chemistry* is important in all of the phases (see [Fig. 1.1](#)) even when additional chemicals are not used. Examples are given.

- Exploration/appraisal: The geochemistry of the formation and chemistry of the fluids are elucidated.
- Development: Drilling and cementing chemicals are applied to help form and complete the well.
- Production: Chemicals are applied for:
 - Stimulation
 - Flow Assurance
 - Mature Field: IOR
 - Characterization: Tracers
- Abandonment: Cementing chemicals are used to seal the well and to monitor the seal.

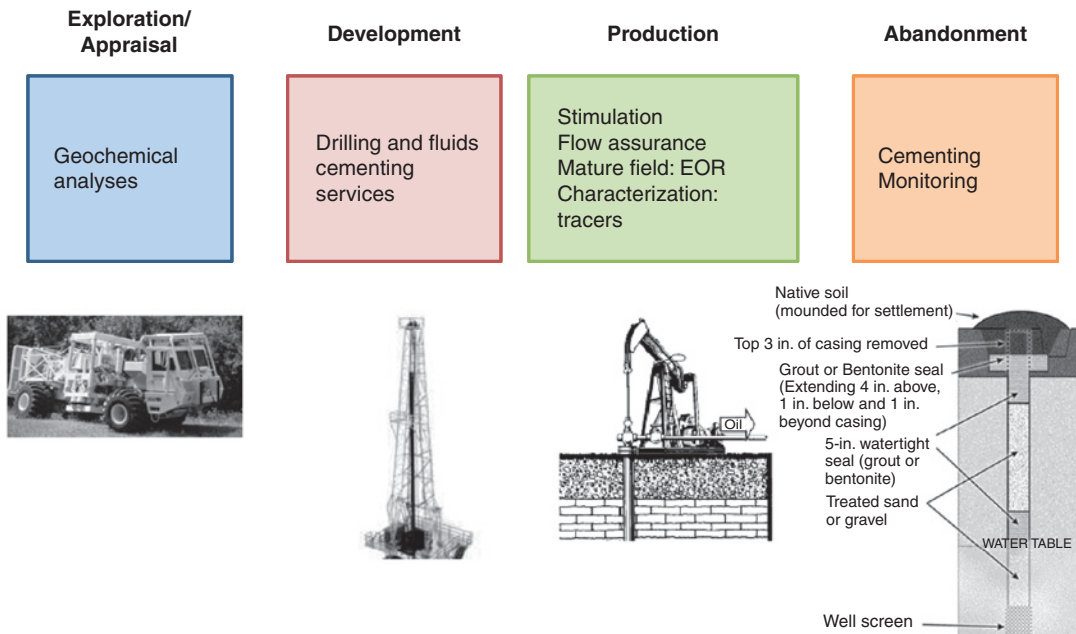


Fig. 1.1—Chemistry in the production phases of a well's life.

In “Exploration and Appraisal,” geochemical analyses are performed based on seismic and well-probe data and analyses of outcrops or cores. McCarthy et al. (2011) has described the tests that geochemists have used to determine the hydrocarbon producing potential of a formation from the rock samples collected. These include total organic carbon analysis to find the maximum amount of carbon in the rock, as well as a pyrolysis process where the rock is heated to increasing temperatures and the effluents are analyzed by several methods described in the papers. Fluids may be captured in test wells for evaluation and chemical probes also may be placed using wireline or coiled tubing. Short summaries of methods used to analyze the liquid samples are described in Chapter 3 of Frenier et al. (2010).

Various water-based and oil-based fluids are used in drilling (development) most wells. Complex oilfield cements are then employed to stabilize the production tubing and to isolate various zones from communication with the surface and from nonproducing formations. Completion fluids also may be used to maintain and control the well's pressure balance.

Various chemicals are applied during all of the phases of Production to maintain, control, and frequently enhance the flow of the oil, gas, and aqueous phases. This is the major theme of this book. The production phase has sub phases based on the nature of production enhancements needed and are designated as Primary, Secondary, and Tertiary.

- *Primary*: In this phase, the reservoir fluids flow mostly because of the initial and internal pressure of the reservoir. Note that the production is controlled by the pressure differential between the formation and the bottomhole well pressure. While the pressures may be sufficient for initial production, stimulation using fracturing (Chapter 4) and/or reactive chemical treatments (Chapter 3) may be applied to some wells to remove formation damage or to improve returns from tight formations (such as shale plays). Other production chemicals can also be used to maintain flow (including inhibitors and surfactants described in Chapter 2 and in Frenier and Ziauddin (2008) and Frenier et al. (2010). For the most part, during the primary phase, chemicals (including any injected water or gas) are not added to the reservoir (except near the wellbore), so it is not changed significantly from a chemical standpoint. However, just by flowing the wells, important equilibrium conditions may be changed. At some point (either early or very late in the production phase) pressure maintenance may be required.
- *Secondary*: The pressure to move the fluids through the formations (see Section 1.2) can be maintained or enhanced by adding a downhole pump (to reduce the flowing pressure) or by

injecting fluids into the formation (Chapter 5). This presents a radical change to the reservoir since a large number of injection wells may be required. Many chemical treatments can be employed in this phase to maintain production including inhibitor injections as well as reactive chemical and prop fracture treatments. These are described in more details in Chapters 2, 3, and 4 of this book. At some point in the life of many reservoirs, the removal of additional hydrocarbons is not possible (or economically productive) because the oil is trapped in the pore spaces and so strongly adsorbed onto the rock surfaces that injection of water, natural gas, or steam cannot remove economic amounts. Because of uneven coverage of the reservoir because of permeability differences, oil also may have been bypassed by the sweep fluids. At this point, the massive injection of external chemicals may be planned, and the well may be considered to be in the tertiary production phase.

- *Tertiary*: As much as 2×10^{12} bbl of conventional oil and as much as 5×10^{12} bbl of heavy oil will remain in the world's reservoirs after the primary and secondary production has reached their economic limit (note that steam injection may be used at earlier phases in some heavy oil fields) (Thomas 2008). This incremental production is difficult and expensive but will remain as one of the methods for prolonging production from mature fields. Thus, the injection of large amounts of chemicals to remove some of this oil usually defines the tertiary phase. Much of the current interest is driven by the high price of oil.

Lastly, when the well is abandoned, cements and other chemicals are employed to make sure that the hydrocarbons or other fluids will not reach the surface or pollute aquifers or damage property.

The hydrocarbon chemical makeup, reservoir saturation, and morphology control the recovery of these valuable chemicals. The petroleum industry classifies “crude oil” using a number of different systems. These include classification by the location of its origin (e.g., “West Texas Intermediate, WTI (aka Texas Light Sweet)” or “Brent”) and often by its relative weight (API gravity—defined below) and viscosity. Note that these are also pricing bench mark crude oils based on other characteristics but are typical from the region of origin. See the definitions in Wikipedia (2009a).

Refiners may also refer to the fluid as “sweet,” which means it contains relatively little sulfur, or as “sour,” which means it contains substantial amounts of hydrogen sulfide or mercaptans and requires more refining to meet product specifications. Low sulfur crude oil contains less than 0.5% sulfur and high sulfur oil may contain more than 2% sulfur (Simanzhenkov and Idem 2003). Each crude oil has unique molecular characteristics that can be determined by various analyses in petroleum laboratories and that are described in detail in Chapter 3 of Frenier et al. (2010). The petroleum production industry developed in stages and different terms have been, and continue to be, used to describe and characterize petroleum crude oil.

The API gravity of petroleum liquids is frequently used as a descriptor and is defined as

$$\text{API gravity} = (141.4/\text{Sp. Gr (SG) at } 60^\circ\text{F}) - 135.5. \dots\dots\dots (1.1)$$

The temperature (60°F) and pressure (1 atm) will be specified for specific gravity. Usually, oils with higher API gravity values have a greater commercial value and lower API gravity value crude oils have lower commercial value. This general rule only holds up to 45°API gravity since beyond this value, the fraction of useable motor fuel that can be distilled from the liquid diminishes or is too volatile. Crude is also classified as light, medium, or heavy, according to its measured API gravity. Light crude oil is defined as having API gravity higher than about 30°API. Medium oil is defined as having API gravity between 20°API and 30°API. Heavy oil is defined as having API gravity below 20°API. Extra heavy oils are defined as API gravity below 10°API. In 1982, UNITAR (Kayhan 1982), an international working group, defined heavy oil to be gas-free oil between 100 cp and 10,000 cp at original reservoir temperature, with a density between 10° and 20°API gravity.

At a given pressure, the flow rate of a fluid is inversely proportional to the viscosity, so viscosity of the crude oil is an important value. The viscosity of the live oil is typically correlated with the gas content, API gravity, and temperature. Oil with high API gravity usually has low viscosity values. Oil that will not flow at normal temperatures or without dilution is usually called “bitumen” may have

viscosities of $>10,000$ cp and the API gravity is generally less than 10° API. Bitumen derived from the oil sands deposits in the Alberta, Canada area has an API gravity of around 8° API. It is upgraded to an API gravity of 31° API to 33° API and the upgraded oil is known as synthetic oil. These upgraded fluids will have viscosity values less than 100 cp. See Beal (1946a, 1946b). The various chemical enhancement methods described in this book aid in the recovery of the hydrocarbon products and possibly at an increased rate.

A report (Freedoniagroup 2008) estimates the global oilfield chemical market at \$15.2 billion and growing at 5.7%/year through 2012. There are thousands of individual chemicals employed in the various parts of the industry and many thousands of complex formulations that are custom-mixed each day to drill, complete, and treat the wells and auxiliary equipment associated with the upstream portion of the hydrocarbon supply chain. The books by Fink (2003), Fink (2011), and Kelland (2009) describe virtually all of the types of different chemicals employed in all of the phases of the life cycle of a producing reservoir and provide the identification of the structures of hundreds of these chemicals. These books cover different areas of oilfield chemicals (with some overlap) with thousands of references.

This current book concentrates on the chemical reactions and the application of chemical substances during the production phase to enhance and maintain the flow of oil and gas. Books by Growcock (2005) and Darley and Gray (1988) describe various aspects of drilling and completion fluid chemistries. Brooks (1992) and Nelson and Guillot (2005) review cementing chemistry and practice. There are many introductory books in chemistry that may be useful for further reading. The authors have consulted Solomons (1992a) in the Chapter 4 on frac fluids and Cotton et al. (1999) for references about inorganic compounds. The compilation by Clegg (2007) has been consulted for many engineering topics.

1.2 Need for Chemical or Engineering Practices to Enhance Production

Enhancing the performance of an oil and gas production system involves analyzing the system as a whole, identifying bottlenecks, and eliminating excessive energy dissipations or pressure losses in all system components. For optimal performance of the production system efficient use of energy is a must. The main components of the production system are

- The reservoir
- The completion, such as stimulation, perforation and gravel pack
- The tubing string
- The artificial lift system, such as pumps and gas lift valves
- The flow control devices, such as chokes and safety valves
- The surface flowline with chokes, valves, and elbows
- The separator and surface treaters

1.2.1 Analyzing Production Problems. Mach et al. (1982) introduced a systematic approach for analyzing performance of production systems. Their method involves defining computational nodes at various points in the system and calculating pressure as a function of flow rate for fluids flowing in and out of the node. Fig. 1.2 shows a typical location of the computational node [large black dot (•) in the wellbore diagram]. Pressures at key points in the system are marked on the figure and are denoted as p_e , the pressure at the external reservoir boundary, p_{wf} for downhole flowing pressure, p_{wh} for pressure at the wellhead, and p_{sep} for pressure at the separator. For producing fluids from the reservoir to the surface, $p_e > p_{wf} > p_{wh} > p_{sep}$. Both inflow and outflow performance of the well must be considered.

Fig. 1.3a shows a plot of p_{wf} as function of flow rate for flow into the node, commonly known as the inflow performance relationship (IPR) curve. The equations in the figures are described later in the text.

The linear relationship between flow rate, q , and the downhole flowing pressure, p_{wf} , shown in the figure is for a single phase fluid flowing into the well from the porous reservoir rock. This relationship can be easily derived from the well known Darcy's law, which for horizontal, linear single phase flow of an incompressible fluid is expressed by Darcy (1857) and Dake (1995) as

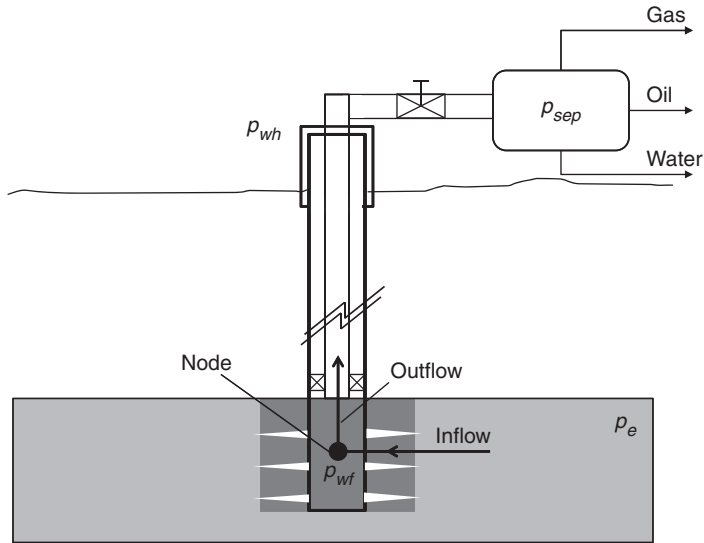


Fig. 1.2—An oil and gas production system showing the location of a computational node used in analyzing the performance of the system.

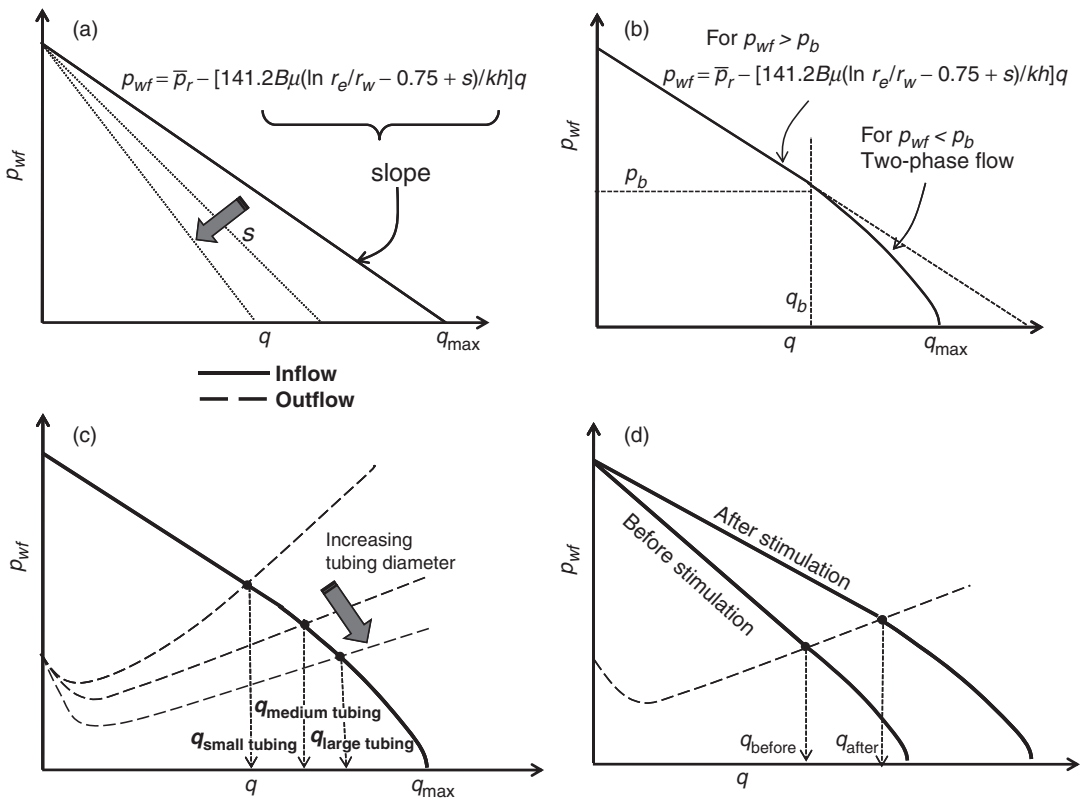


Fig. 1.3—(a) Inflow and outflow relationships for a node near the sandface, (b) inflow performance relationship (IPR) for flow of single-phase fluid, (c) inflow performance for two-phase fluid flow, and (d) outflow from the node for various tubing diameters.

$$q = \frac{Ak}{\mu} \frac{dp}{dl}, \dots \dots \dots (1.2)$$

where q is the flow rate, A is the cross-sectional area, k is the permeability, μ is the fluid viscosity, p is the pressure, and l denotes distance, which is taken as positive in the *opposite* direction to the fluid flow. The permeability is the property of the porous medium and is a constant. Hence for a fluid with constant viscosity the flow rate is proportional to the pressure gradient (dp/dl). For flow of oil and gas into a vertical well, the radial form of Darcy’s law is generally used. If flow from the reservoir into the well is taken as positive and the radial distance is taken as positive in the opposite direction, then the flow rate can be expressed as

$$q = \frac{Ak}{\mu} \frac{dp}{dr} = 2\pi rh \frac{k}{\mu} \frac{dp}{dr}, \dots \dots \dots (1.3)$$

where, r denotes radial distance from the center of the wellbore and h is the height of the pay zone. Separating and integrating the previous equation and specifying the wellbore flowing pressure and the pressure at the external boundary, the expression for the flow rate in the well becomes

$$q = \frac{2\pi kh}{\mu} \frac{(p_e - p_{wf})}{\ln(r_e / r_w)}, \dots \dots \dots (1.4)$$

where, p_e and r_e are the pressure and radial distance respectively to the external boundary, and p_{wf} and r_w , respectively, are the flowing wellbore pressure and wellbore radius. The previous equation can be rearranged and expressed as in terms of p_{wf} as

$$p_{wf} = p_e - q \left[\frac{\mu}{2\pi kh} \ln \frac{r_e}{r_w} \right], \dots \dots \dots (1.5)$$

Because the pressure at the external reservoir boundary is generally difficult to measure; a more useful form of the expression is in terms of *average* reservoir pressure, \bar{p}_r ,

$$p_{wf} = \bar{p}_r - q \left[\frac{\mu}{2\pi kh} \left(\ln \frac{r_e}{r_w} - \frac{3}{4} \right) \right], \dots \dots \dots (1.6)$$

This equation (Eq. 1.6) is for an undamaged well. Formation damage (**Fig. 1.4** and Section 2.3) may result in a region of reduced permeability near the wellbore, which may cause an additional pressure drop. A stimulation treatment, on the other hand, may reduce the pressure drop. The pressure drop, $p_{\Delta skin}$, because of a region of altered permeability near the wellbore was shown by van Everdingen and Hurst (1949) as

$$p_{\Delta skin} = \frac{q\mu}{2\pi kh} s, \dots \dots \dots (1.7)$$

where s (frequently called skin) is dimensionless and accounts for the altered permeability near the wellbore.

Hawkin’s formula is often used to estimate the skin effect, s (Hawkins 1956).

$$s = \left[\frac{k}{k_s} - 1 \right] \ln \frac{r_s}{r_w}, \dots \dots \dots (1.8)$$

where, r_s and k_s are the radial depth and permeability of the damaged or stimulated region. For an undamaged well $s = 0$, while for a damaged well, $s > 0$ and for a stimulated well $s < 0$. Adding $p_{\Delta skin}$ and converting to oilfield units the equation radial inflow of a single phase incompressible fluid into a vertical well becomes (see Fig. 1.3a)

$$p_{wf} = \bar{p}_r - q \left[\frac{141.2B\mu}{kh} \left(\ln \frac{r_e}{r_w} - \frac{3}{4} + s \right) \right], \dots \dots \dots (1.9)$$

Here, B is the formation volume factor, defined as the ratio of the volume of oil a reservoir condition to that at stock tank (surface conditions). If the reservoir pressure is above the bubblepoint (p_b) and the flowing bottomhole pressure is below p_b , then there will be two-phase flow near the wellbore.

Note from Fig. 1.3b that the inflow performance relationship is no longer a straightline as in Fig. 1.3a. Vogel (1968) and Fetkovich (1973) have both developed empirical correlations to account for effects of two-phase flow. The Vogel relationship for pseudosteady state is (from Economides et al. 1994)

$$q = q_{0,max} \left[1 - 0.2 \frac{p_{wf}}{p_b} - 0.8 \left(\frac{p_{wf}}{p_b} \right)^2 \right]$$

$$q_{0,max} = \left(\frac{1}{1.8} \right) \frac{k_o h \bar{p}_r}{141.2B_o \mu_o [\ln r_e / r_w - 3 / 4 + s]} \dots \dots \dots (1.10)$$

Here, the permeability to oil is k_o , the viscosity of oil is μ_o and B_o are all evaluated at \bar{p}_r . The convenience of the Vogel (1968) relationship is that only the prosperities for the oil are required to predict the two-phase behavior. Although convenient, Vogel’s relationship does not provide a good fit to data in many cases. Fetkovich (1973) proposed as simple relationship with the adjustable parameters.

$$q = C \left[\bar{p}_r^2 - p_{wf}^2 \right]^n \dots \dots \dots (1.11)$$

The parameters C and n are specific to a well and must be determined from stabilized flow data for the well.

Fig. 1.3c depicts the outflow performance relationship of the well for three tubing sizes. The intersection of the *inflow* and *outflow* performance curves indicates the flow deliverability of the system under stabilized conditions for each tubing size. For the case illustrated in the figure, increasing tubing size results in an increased flow rate from the well as excessive pressure drop in the production tubing is reduced.

The pressure drop over a distance, L , of a single phase incompressible fluid can be obtained from the mechanical energy balance equation as (Economides et al. 1994)

$$\Delta p_L = \Delta p_{PE} + \Delta p_F + \Delta p_{KE}, \dots \dots \dots (1.12a)$$

and in an expanded form becomes

$$\Delta p_L = \left(\frac{g}{g_c} \right) \rho L \sin \theta + \frac{2f_f \rho v^2 L}{g_c D} + \frac{\rho}{2g_c} \Delta v^2 \dots \dots \dots (1.12b)$$

Δp_L is the difference between the upstream and the downstream pressure. Δp_{PE} is the pressure drop caused by potential energy change. It is the hydrostatic head of the fluid and accounts for the pressure change because of the weight of the column of fluid. ρ is the fluid density and θ , is the well deviation. The hydrostatic head for a horizontal well ($\theta = 0^\circ$) is zero. For a vertical well, $\theta = 90^\circ$ for upward flow and $\theta = -90^\circ$ for downward flow. For fresh water, the potential energy pressure drop per foot of vertical distance is 0.433 psi/ft. Δp_F is the pressure drop caused by wellbore friction, and it is obtained from the Fanning (John Thomas Fanning 1837–1911) equation:

$$\Delta p_F = \frac{2f_f \rho v^2 L}{g_c D}, \dots \dots \dots (1.13)$$

where v is the fluid velocity and D is the pipe diameter. For a pipe with a constant cross section the fluid velocity can be expressed in terms of flow rate, q as

$$v = \frac{4q}{\pi D^2} \dots \dots \dots (1.14)$$

The Fanning friction factor, f_f for laminar flow is

$$f_f = \frac{16}{N_{Re}} = \frac{4\pi D\mu}{q\rho} \dots \dots \dots (1.15)$$

where $N_{Re} = 4q\rho / (\pi D\mu)$ is the Reynolds number for the flow. Substituting v and f_f in the expression for Δp_F , yields the Hagen-Poiseuille law for pressure drop in a pipe (Hagen 1839; Poiseuille 1840):

$$\Delta p_F = \frac{128 \mu q L}{\pi g_c D^4} \dots \dots \dots (1.16)$$

From Eq. 1.12, note that Δp_{KE} is the pressure drop because of change in kinetic energy between various positions in the pipe. Generally, it is much smaller compared to Δp_{PE} and Δp_F . It is equal to zero if there is no change in fluid velocity between the two points of measurement. For example, an incompressible fluid flowing through a pipe of uniform cross-sectional area the velocity does not change and Δp_{KE} is equal zero. In cases of high gas volumes or high-gas oil ratios, a rapid change in velocity may occur, but even then, Δp_{KE} generally accounts for less than 10% of the pressure loss.

For two-phase fluid flow the flowrate is not a monotonic function of flowing bottomhole pressure. At low flow rates the pressure drop may decrease as the flow rate increases (Fig. 1.3c and 1.3d). However, operation in this region is unstable.

1.2.2 Production Enhancement Processes. To enhance production of the oil and gas production system, one must first identify the condition limiting the performance. If the outflow from the well is limiting the performance, such as because of subsized tubulars (Fig. 1.3c), improving the inflow performance will obviously not result in a significant production increase, and vice versa.

A useful measure for evaluating the performance of a well is its productivity index, J^* . It is defined as the ratio of flow rate of the fluids (q) to the pressure difference (Δp):

$$J^* = \frac{q}{p - p_{wf}} \dots \dots \dots (1.17)$$

The inflow and outflow performance for a single phase incompressible fluid can be rearranged and expressed in terms of flow rate in SI units as:

$$q_{in} = \frac{2\pi kh(\bar{p}_r - p_{wf})}{\left[\mu \left(\ln(r_e / r_w) - 0.75 + s \right) \right]} \dots \dots \dots (1.18)$$

and

$$q_{out} = \frac{\pi g_c D^4}{128 \mu L} \left[p_{wf} - p_{wh} - \left(\frac{g}{g_c} \right) \rho L \sin \theta \right] \dots \dots \dots (1.19)$$

For steady-state operation, $q_{in} = q_{out}$. This is the intersection point of the inflow and outflow curves on Fig. 1.3c and 1.3d. Although the equations have been derived for simplistic conditions of flow of a single phase incompressible fluid, some valuable observations can be made. It is evident from the inflow equation that the flow rate can be improved by increasing the average reservoir pressure, \bar{p}_r or reducing downhole flowing pressure, p_{wf} , or fluid viscosity, μ , or skin, s . Similarly, from the outflow

performance equation it is evident that the flow rate can be increased by increasing the tubing diameter $q_{\text{out}} \propto D^4$ or by reducing the hydrostatic head (i.e., the fluid density).

Production enhancement can be achieved by both chemical and mechanical methods; however, only the chemical methods are presented in this book. Mechanical means of production enhancement such as, lifting of the wellbore fluids by gas lift or pumps or drilling additional wells are not discussed.

Chapter 2 in the book discusses inorganic and organic scales, which may restrict flow in the tubing and severely impact outflow performance. Many well construction and production operations can cause of near-wellbore (NWB) damage. Fig. 1.4 shows some of the damage types and the areas where these forms of damage may be located. The graphic predicts the possible severity of the damage (based on the experience of the authors) by the darkness of the shading with black as most severe. Additional details of possible formation damage and mechanism are described in Section 2.3. The causes of organic solids and inorganic scale formation and NWB damage have been described in books by Frenier and Ziauddin (2008) and Frenier et al. (2010). Silicate damage usually is the result of fines migration and damage by drilling fluids and is one of the most common reasons for performing stimulation processes. Section 2.3 of this book gives additional details on formation damage. Also refer to the publications by Civan (2000) and Sharma (2007) for more information on additional causes of formation damage. Matrix treatments and hydraulic fracturing (HF) may be used to remove/bypass the damage.

Chapters 3 and 4 present matrix and hydraulic fracture stimulation methods. These methods improve production by reducing the wellbore skin. Chapter 3 focuses mainly on matrix stimulation treatments for sandstone and carbonate reservoirs. Matrix stimulation treatments improve the NWB permeability by reactive dissolution may reduce the skin value of a damaged well from several tens to close to zero. Chapter 4 focuses on hydraulic fracture treatments. These are much longer range than matrix treatments and can be applied to reservoirs where the production is limited by the reservoir permeability, such as shale reservoirs. Fracturing also may be used as an initial production enhancement for very tight formations, as without it, the wells do not produce at an economical rate.

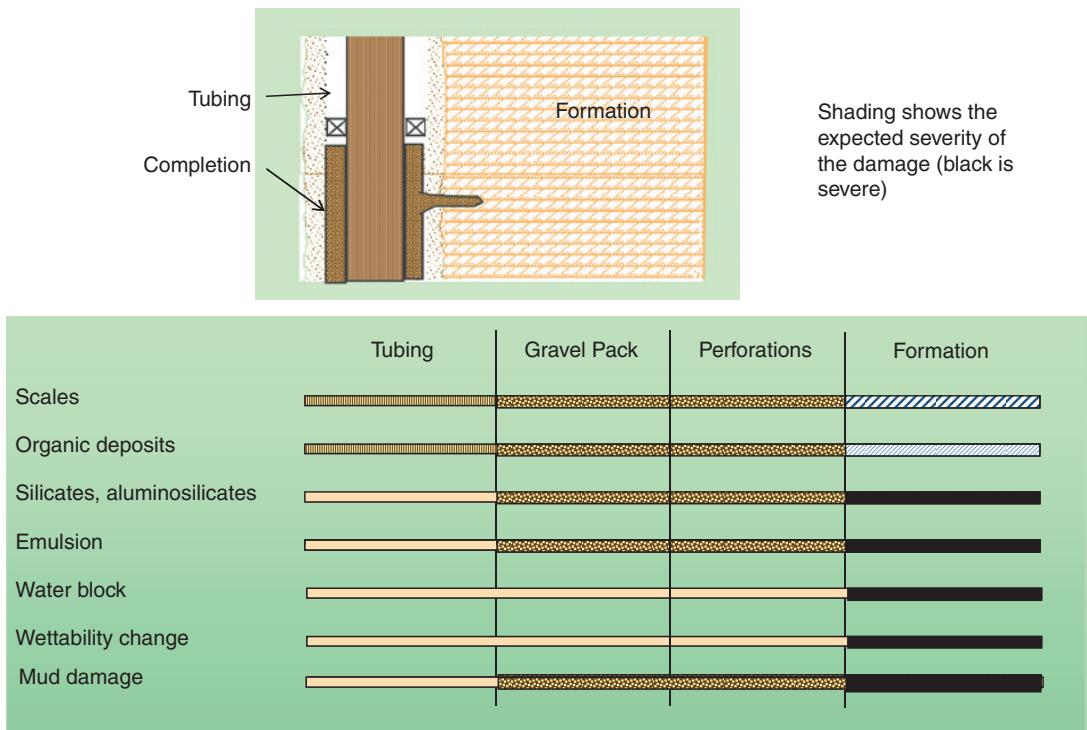


Fig. 1.4—Areas for formation damage in tubing, completion, and formation.

As the fluids are produced, the formation pressure will be reduced. Maintenance of pressure by reinjection of produced natural gas, or produced brine can be used to maintain flow. Additional injection of N_2 or CO_2 may also act to maintain pressure as well as to reduce the viscosities of the fluids. Injection of chemicals including pH modifiers, surfactants, and polymers are in use as part of chemical enhanced-oil-recovery (EOR) processes (Chapter 5) that also may change the wetting characteristics in the formation pores and increase ultimate hydrocarbon yields. Chapter 5 presents IOR methods, which aim to increase production by increasing the average reservoir pressure and areal contact, reducing fluid viscosity or affecting reservoir wettability.

Additional problems also occur as the production process life cycle proceeds. Usually the oil/water ratio becomes smaller and emulsions start to occur. Various chemicals are in use to help reduce water cuts and to resolve emulsions. The changes in the oil or gas/water ratios also exacerbate scaling and corrosion problems, requiring more or different scale and corrosion control chemicals. Changes in water cut, pressures, temperatures, and production practices also may cause the formation of wax, asphaltenes, hydrates, and naphthenates (Frenier et al. 2010).

Completely mechanical methods (such as drilling additional wells) are beyond the scope of this book. The chemical solutions (applied with pumping) to all of these problems will be described in subsequent chapters. Chapters 2 through 5 are arranged in that order because this also describes an increasing degree of intervention (and cost and equipment). The use of flow assurance chemistries and stimulation with reactive materials may require a minimal amount of equipment but possibly a lot of chemicals to return (or maintain) productivity at an original value. Prop fracturing may greatly improve productivity, especially in tight formations, but requires much larger investments in equipment and chemicals. Finally, some IOR campaigns may last for years and will require many tons of chemicals.

Fig 1.5 provides a visualization of the *distance* (in the formation) treated by each type of service. From the *volume* of formation treated, an estimate of the amount of fluids needed also can then be determined. The various inhibitors needed for control of deposits usually treat only the tubing unless they are placed as part of a matrix service. Matrix treatments contact the NWB area of about 10 ft from

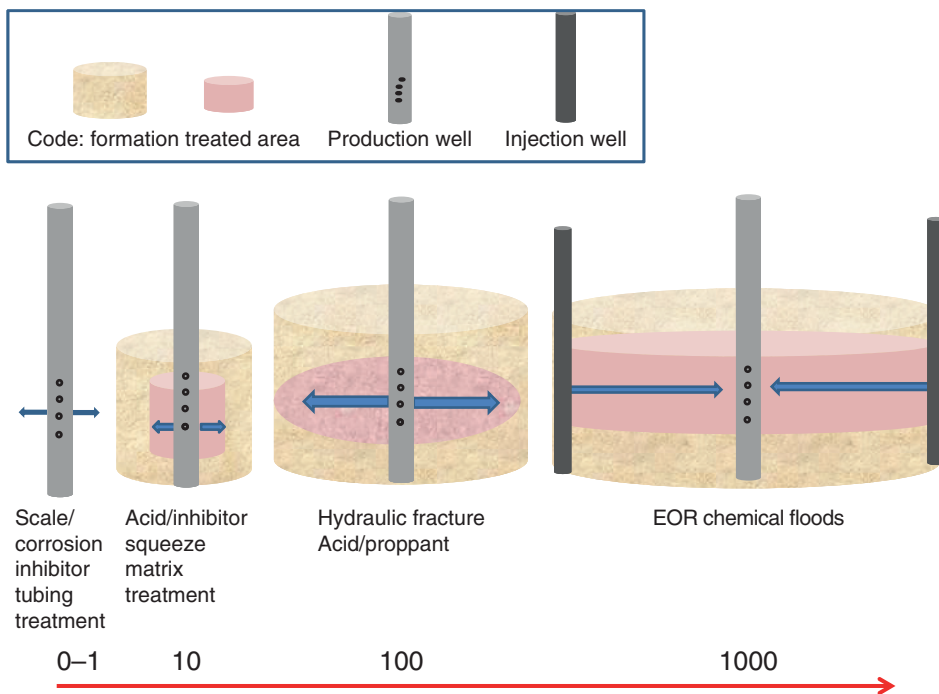


Fig. 1.5—Relative formation areas treated by various production enhancement services.

the tubing. Fracture jobs may penetrate 100 ft into the rock and for multiple stages, possibly hundreds of feet. IOR floods are designed to treat the entire distance from the injection wells to the production wells. The actual volume of fluid pumped also varies greatly. Scale/corrosion inhibitor treatments usually are based on the amount of water produced and 10–1,000 ppm of an inhibitor may be needed for years (possibly the life of the well). A small acid matrix job could need only 500 gallons, but acid or prop fracturing projects can range from thousands to millions of gallons of fluid. IOR treatments also can require millions of gallons of fluid spread over a decade.

Each level of intervention also may increase the environmental impact of the treatments. Chapter 6 describes health, safety, and environment issues, including flowback, disposal, and (sometimes) spill control of well fluids. This book will also emphasize the many connections between the various enhancement processes and common themes such as flow and reactions in the subsurface matrices and chemical reactions that must happen in a planned sequence.

1.3 Production Chemistry Economics

Chemical treatments are performed for many different reasons, and the oilfield chemicals market may exceed 15 billion USD (Freedoniagroup 2008). Flow assurance (FA) activities such as the use of corrosion, scale, and organic deposit inhibitors, as well as the application of demulsifiers are employed to prevent problems from occurring. Matrix chemical fluids and deposit removal techniques are used to remove damage that is impeding the production of the hydrocarbons. Some HF activities also are used to bypass NWB damage to restore flow to an original value. EOR chemicals and tracers are frequently pumped to enable trapped hydrocarbons to be accessed and prolong the life of depleted reservoirs.

In the case of tight formations, HF methods are employed initially to cause enough conductivity to allow the well to produce economical amounts of hydrocarbons. Fracturing activities, along with directional drilling in shale oil/gas formations may produce enough hydrocarbons to change the entire energy calculus of countries and regions of the world. Jaffe (2010) has written an article that says that there may be enough gas potentially available because of these methods to change some geopolitical balances of power. Discoveries of retrievable liquid hydrocarbons associated with various shale plays (RRC 2011) also may greatly affect hydrocarbon supplies and economics.

For all of these methods, there is an economic element (note the extent of the treatments in Section 1.2 and Fig. 1.5) that also includes environmental and political (Hess 2010) questions that require consideration in the business calculations before a decision is made to pump chemicals. Initially, a calculation must be made on whether or not any stimulation/enhancement should be considered. Then, there may be a decision on which method should be employed. The decision on the type of treatment may involve more than economic issues. Examples are the formation type, location, equipment availability, time constraints, local chemical availability, and the urgency of trying to treat a problem. If enough information is available to add up all of the potential costs as well as the loss/gain of products, then the economic equations described below can be used.

Economides and Boney (2001) discuss some calculation methods and decisions that should be made to decide on a project.

Several indicators discussed by these authors are:

- Payout time—This includes the total costs associated with the project but not the value of the money or the profit. This is a measure of liquidity for the project.
- Net present value (NPV)—This equation (Eq. 1.20) is the definition for cumulative discounted cash flow. The NPV is the maximum of this cumulative discounted cash flow. NPV gives a dollar value added to the property at present time. If it is positive, the investment is attractive; if it is negative, it means an undesirable investment. According to these authors, NPV is the most widely used indicator showing a dollar amount of net return. Here ΔS_n is the incremental revenue (minus the incremental expenses and taxes that are because of operations), n is the time period increments (e.g., years) and i is the interest rate.

$$NPV = \sum_{n=1}^n \frac{\Delta\$}{(1+i)^n} - \text{cost} \dots \dots \dots (1.20)$$

- Rate of return—This is a comparison with other investments and is determined by setting $i = 0$.
- Return on investment (ROI)—The payback is the total amount of money earned from the investment in the project. Investment relates to the amount of resources put into generating the given payback.

$$ROI = \frac{(\text{Payback} - \text{Investment})}{\text{Investment}} \cdot 100 \dots \dots \dots (1.21)$$

- Corporate goals and risk—These are less tangible but important considerations for judging projects. These also include matching or exceeding the capabilities of the competition in some markets. Risks may include environmental or ecotox issues.

Economides and Boney (2001) also have described some of the methods for determining which type of stimulation/intervention method is possible. Some of the considerations are

- Maximum allowable treating pressure limits injection rates and the type of treating fluids.
- Tubular size limits rates and pipe erosion.
- Well location size limits the equipment and materials that can be used.
- Tubular integrity prevents or limits the type of treatments that can be employed without compromise.
- Completion tools and their location limit where the treatment is placed and the magnitude of the rates and volumes.
- Zonal isolation is whether the zone can be isolated from other intervals through perforating and/or pipe integrity limitations.
- Typical reservoir constraints include
 - Production failures: water or gas coning or influx, formation sanding.
 - Physical location of the zones and their thicknesses: pay zone qualities limit or dictate treatments.

1.4 Basics of Fluid Chemistries

This section will provide a brief review of the primary fluid types and chemistry classifications of formulations that are used in production treatments. These four classifications of fluids as well as the individual chemicals in them are used in many different types of production enhancement fluids. The classifications and definitions to be used in this book are

- Solutions of monomers and salts—A homogeneous (thermodynamically stable) mixture of two or more substances, which may be solids, liquids, gases, or a combination of these.
- Surfactant fluids—Solutions containing surface-active monomers in aqueous or organic liquids.
- Polymer fluids—Solutions of molecules that contain multiple repeat units (of monomers) in aqueous or organic liquids.
- Dispersions including foams, emulsions and solid particle slurries—Materials comprising more than one phase where at least one of the phases consists of finely divided domains, often in the colloidal size range, distributed throughout a continuous phase domain.

Short descriptive sections of each type follows.

1.4.1 Monomer and Salt Solutions. Various salts as well as organic molecules form stable (permanent) solutions in water, organic liquids, and mixed solvents. A thermodynamic solubility product equation (described in Section 1.5.1) can be used to calculate the solubility limits of many of these

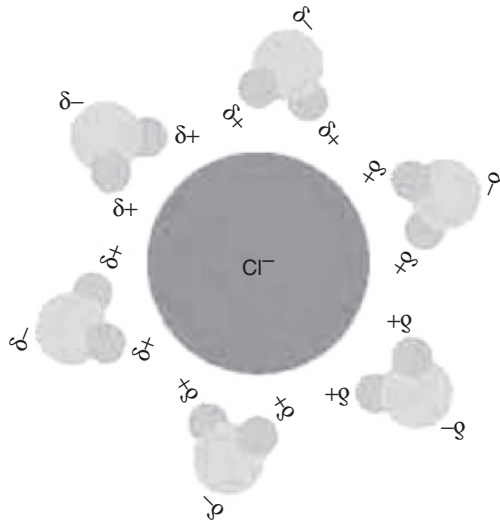


Fig. 1.6—Hydrated chloride anion (Berg 2004).

solutions. In these fluids, the solute is surrounded by the solvent molecules and maintained in solution, usually by electro static or hydrogen bonding forces; see Fig. 1.6 for a depiction of a chloride anion solvated by water dipoles. In most aqueous salt solutions, the cations and anions will be separated by the water molecules, but the entire solution will have electrical neutrality. Also see the discussions of solubility in Frenier and Ziauddin (2008).

A large number of fluids used in treatment of various formations are true single-phase solutions and include acids (such as HCl), salts (such as KCl), and hydrocarbon mixtures (such as diesel oil). Aqueous/organic solutions such as various alcohols in water are also true solutions that may be termed *miscible*. This means they are mutually soluble in all proportions. Some water/organic molecule solutions (as well as other organic/organic solutions) would have solubility limits that can be described by mixing rules (Kwak et al. 1985). Crude oil fluids at reservoir conditions are considered to be a single solution phase and the thermodynamic properties (pressure, volume, and temperature) are calculated based on that assumption [see Frenier et al. (2010)]. However, water in contact with the crude oil may also exist as an emulsion.

Surfactants and/or polymers may be added to (or exist as a part of) these solutions and make up the more complex fluids described in subsequent paragraphs.

1.4.2 Surfactant Fluids. Surface active agents (surfactants) are predominantly organic molecules that have a *separation* of charges (they are dipoles—a schematic drawing of separation of charges in a dipole is in Fig. 1.7) and have a hydrophobic (usually a hydrocarbon) end and a hydrophilic end (the more highly charged part). The surfactant may have a formal positive (cationic) or negative (anionic) charge or contain groups of hydrophilic atoms (frequently oxygen) that have a net negative charge. Fig. 1.8 shows examples of the three most common types of surfactants (cationic, anionic, and non-ionic). Amphoteric surfactants that can change charge as a function of pH also are in wide use and will be described in Sections 3.7.2 and 4.4.4.

When present in a liquid, the surfactant molecules will migrate to any surface and orient themselves with respect to the surface and its force vector (see Section 1.6.1). The presence of the surfactant at these surfaces can dramatically change the interfacial surface tension (IST) (γ) and thus the balance of



Fig. 1.7—Surfactant dipole.

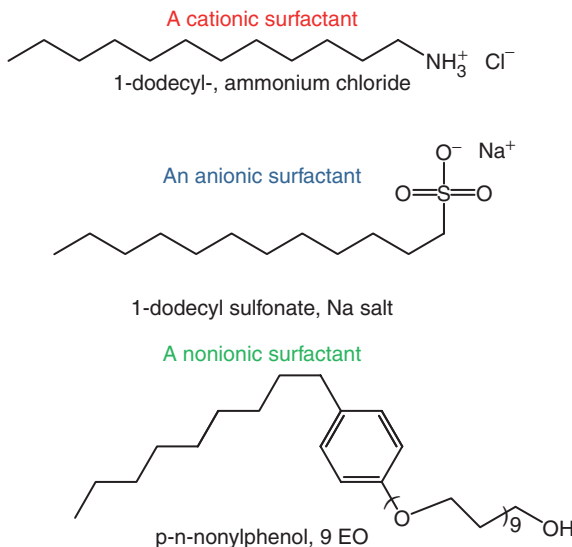


Fig. 1.8—Surfactant types: cationic, anionic, and nonionic (from top).

the forces at the two surfaces. For example, pure water (See Section 1.6.1) has an IST value (vs. air) of about 72 dyne/cm and small amounts of many surfactants lower this value to 20–30 dyne/cm. The surfactants also may change the contact angle, θ , between phases. This ability to orient at various surfaces and affect the balance of the forces is at the heart of the widespread use of these types of molecules in various oilfield fluids including emulsions and foams described in later paragraphs. Surfactants are also used extensively in many stimulation and EOR fluids.

The ability of a surfactant or other surface-active molecule to cover a surface has been described by the Langmuir equation (aka Langmuir isotherm) that relates the coverage or adsorption of molecules on a solid surface to gas pressure or concentration of a medium above the solid surface at a fixed temperature (thus an isotherm). The equation was developed by Irving Langmuir in 1916. The equation is stated as

$$\theta = \frac{\alpha C}{1 + \alpha C} \dots \dots \dots (1.22)$$

In this equation, θ is the fractional coverage of the surface, C is the concentration, α is a constant dependent on the individual molecule and fluid. The constant α is called the Langmuir adsorption constant and increases with an increase in the binding energy of adsorption and with a decrease in temperature. A generalized plot of the Langmuir isotherm with different values of α (different colored curves denoting different surfactants) is shown in **Fig. 1.9**.

The Langmuir adsorption model may deviate significantly from the measured behavior in many cases, primarily because it fails to account for the surface roughness of the adsorbate. Rough inhomogeneous surfaces have multiple sites available for adsorption (also it is hard to get a true value for the surface area and thus, to calculate total coverage); the heat of adsorption varies from site to site. Thus, the adsorption behavior may fit different isotherm equations (Masel 1996), and these different models may reveal information about the binding and orientation of the molecules at a surface.

The presence of the hydrophobic and hydrophilic parts of the surfactant also may cause the surfactant molecules to aggregate into structures (variously called micelles or vesicles depending on the structure) as the concentration increases. The concentration at which the micelles start to form is called the critical micelle concentration (CMC). An example of one depiction of a micelle is in **Fig. 1.10** that shows the hydrocarbon ends in the center and the more polar heads at the water surface.

The CMC is frequently determined by measuring (see Section 1.6.1) the IST and plotting this value vs. concentration and noting an abrupt change in the slope of this plot (**Fig. 1.11**). Some properties of surfactant containing solutions depend on the concentration in solution being above the CMC, and

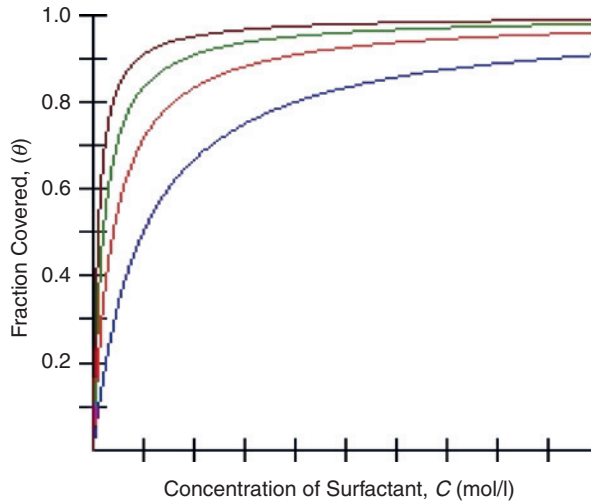


Fig. 1.9—Plots of Langmuir adsorption isotherms for different surfactants and thus values of α .

others do not. One widely used type of surfactant class are called viscoelastic surfactants because the micelles formed by solutions of these materials can themselves interact and form pseudopolymer structures that can greatly increase the fluid's viscosity.

Yang (2002) describes various types of associations of surfactant molecules that include the spherical micelle, wormlike micelle, vesicle, hexagonal liquid crystal, and lamellar liquid crystal. This author states that the association can be correlated with molecular geometry, a packing parameter that is defined as ratio of the volume (v) of hydrophobic group to the product of the length (l) of this group and the cross-sectional area (A) of the hydrophilic group. These different aggregation structures have characteristic rheological properties. For example, this author contends that the microstructure of a wormlike micelle is correlated to a packing parameter of approximately $\frac{1}{2}$. Thus, the effective head group area (A) is affected by additives in the solution and transition to wormlike micelle can be induced. In addition, the transition from spherical micelle to wormlike micelle corresponds to a drastic increase of elasticity and viscosity of the fluid. See Fig. 1.12 for a theoretical example of the interaction of wormlike micelles.

More examples of viscoelastic surfactants and the uses of these chemicals will be given in Chapters 3 and 4. Surfactants are also used to facilitate formation of foams and emulsions as well as to change the wetting properties of the fluid. Reactive fluids such as HCl or chelating agents will react at surfaces

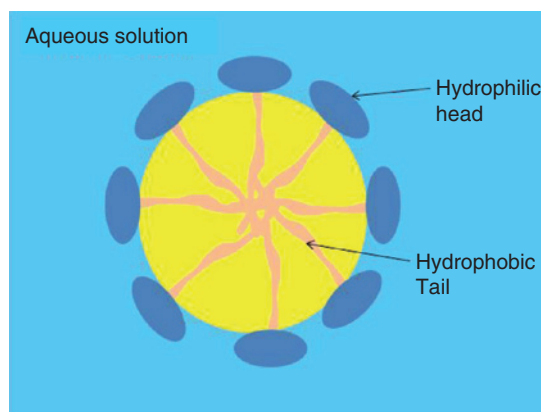


Fig. 1.10—Micelle in water.

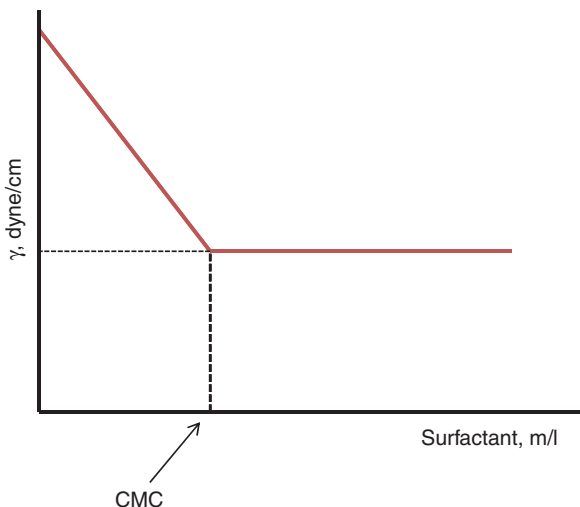


Fig. 1.11—Measurement of the critical micelle concentration (CMC).

and surfactants may help them wet the surface and possibly remove hydrocarbon films. Surfactants are also very important for changing the wetting properties of formation minerals during EOR floods (Chapter 5).

1.4.3 Polymer Fluids. Many varieties of polymer-containing fluids (possibly also containing surfactants and many other additives) are used or encountered in oilfield services and production operations. Polymers contain repeating units of groups of molecular fragments (monomers) that then react to produce large molecules. The definition of a polymer is somewhat arbitrary. A dimer of two ethylene imine molecules is called ethylenediamine but would not be called a polymer. However, at some point a material with many ethylene imine units would be called a polyethyleneimine. The size of a final polymer’s molecular weight can range from about 10^3 daltons to more than 5×10^6 daltons.

Water soluble as well as oil soluble polymer additives are used in many oilfield fluids. A very common use for polymers is to increase the viscosity of the fluid. This happens when the polymer is solvated (hydrated in water is one example) by the fluid and takes on an extended form or shape in the fluid. A common form is a random coil. Note that a random coil is a polymer conformation where the monomer subunits are oriented randomly while still being bonded to adjacent units. It is not one specific shape, but a statistical distribution of shapes for all the chains in a population



Fig. 1.12—Wormlike micelle aggregation (Yang 2002).

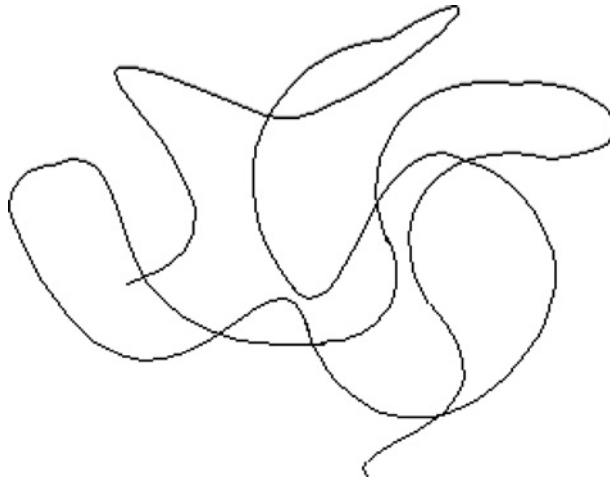


Fig. 1.13—Random coil polymer conformation in solution.

of macromolecules. The conformation's name is derived from the idea that, in the absence of specific, stabilizing interactions, a polymer backbone will “sample” all possible conformations randomly. Many linear, unbranched homopolymers—in solution, or above their melting temperatures—assume (approximate) random coils. Even copolymers with monomers of unequal length will distribute in random coils if the subunits lack any specific interactions. The parts of branched polymers may also assume random coils. The authors of this book's depiction of a random coil is in [Fig. 1.13](#); however, there could be a very large number of possible structures and permutations as well as more ordered polymer structures in a fluid.

In an analogy with the surfactants, at a critical concentration of polymer molecules in solution (called C^*), the solvated polymer molecules may start to overlap and interact, thus forming a larger structure that causes an additional increase in the fluid's viscosity. In addition to uses as thickening agents (used in fracturing and acidizing), polymers are used as scale/deposit inhibitors and as additives in IOR sweeps.

1.4.4 Dispersions Including Emulsions, Foams, and Solid Particle Slurries. Dispersions are thermodynamically *unstable* mixtures of one (or more) phase in another phase. Included are liquid/liquid *emulsions*, gas/liquid *foams* and liquid/solid *slurries* and gas/solid *dispersions*. Dispersions containing four phases also are known. Common examples are homogenized milk (an emulsion), the “head” on a glass of beer (a foam), a slurry of water and sand at the beach, and a dust cloud. While all of these fluids will separate into the individual phases if given a sufficient time at rest for the denser phase to settle, the induction time (t_{ind}) can be very long. Formation of semistable dispersions requires forces (usually shear forces) to reduce the particle size of the internal phase and mix the phases as well as some type of surface active agent to form at the interface and to resist the coalescence and settling forces that will cause the phase to separate.

Emulsions. These fluids are defined by Kokal (2006) as a dispersion (droplets) of one liquid in another immiscible liquid. The phase that is present in the form of droplets is the dispersed or *internal phase*, and the phase in which the droplets are suspended is called the continuous or *external phase*. For naturally occurring oilfield emulsions, one of the liquids is water (usually with dissolved salts) and the other is crude oil. The amount of water that emulsifies with crude oil varies widely from condition to condition. It can be less than 1% and sometimes greater than 80%. Other types of emulsions are made to perform as oilfield treatment fluids. These include acid emulsions, fracturing fluid emulsions, and formulations to disperse oil spills. Oil in water (O/W) and water in oil (W/O) emulsions can form depending on the phase ratios and the conditions of formation.

No emulsions are stable from a thermodynamic view point because most of the “solute” is not actually dissolved at a molecular level. However, each O/W couple will have a true solubility equation:

$$O + W = O_{sw} \dots\dots\dots (1.23)$$

and

$$O + W = W_{sw} \dots\dots\dots (1.24)$$

Solubility values can be determined for these equations (see the discussion in Section 1.5.1). The thermodynamic solubility depends on the polarity differences between the oil and water phases. Generally, the larger the differences in polarity, the lower the solubility. Paraffin mineral oils (very low polarity) have low O/W solubilities (50–200 ppm), and the value depends on temperature. Octyl alcohol (more polar) has a solubility of more than 500 ppm. Page et al. (2000) has determined that the solubility of naphthalene in water is approximately 0.2 ppm. Each component in crude oil will have solubility values in water, but generally, they are very low.

However, in an emulsion, discrete droplets of water or oil or mixtures can be seen suspended in the other phase. Kokal (2006) has provided micrographs of W/O emulsions (the yellow spheres in Fig. 1.14) and O/W emulsions (the brown spheres in Fig. 1.15). Note also in each figure that the dispersed phase droplets are surrounded by an interface layer that resists coalition.

Emulsions are used in production chemistry as a method of providing both an aqueous phase and an oil phase in one fluid. Oilfield emulsions also pose problems in that they may affect production and flow assurance. Because emulsions are not thermodynamically stable, chemical agents must

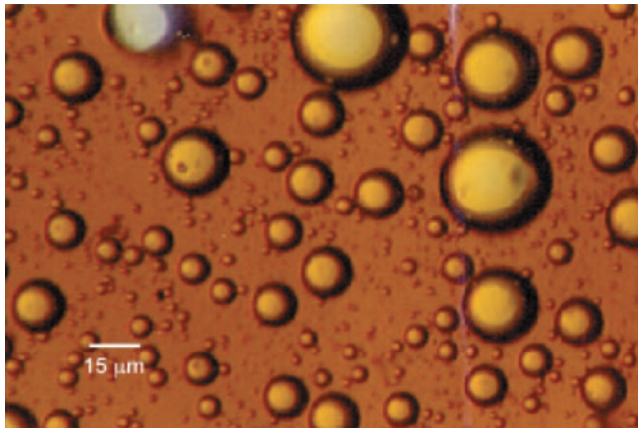


Fig. 1.14—Photomicrograph of W/O emulsion (Kokal 2006).

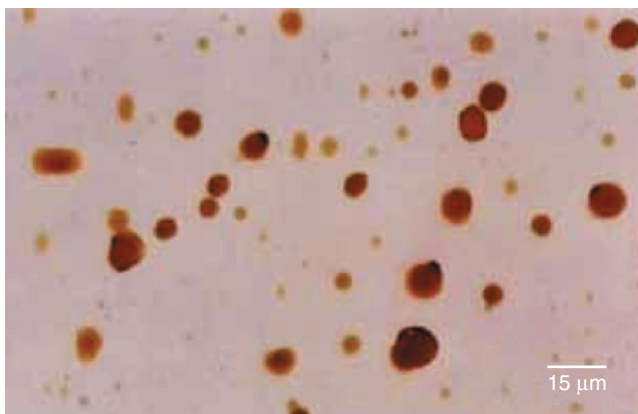


Fig. 1.15—Photomicrograph of O/W emulsion (Kokal 2006).

be present to prevent the internal phase from separating and coalescing. Because these are essentially super saturated systems, the driving force will cause the droplets to coalesce and the emulsion will eventually break. The *rate* of breaking, and thus the stability of oilfield emulsions vary greatly depending on

- The water phase composition
- The oil composition
- The presence of numerous surface active agents (solids, liquids, gasses, and individual molecules)
- The temperature
- The shear conditions and the shear history

Weiss (2008) shows a diagram (Fig. 1.16) of the processes of formation of emulsions and notes that the *order* of addition of the phases and the emulsifier chemical (different surfactants as well as possibly solids) can affect the stability of the emulsion as well as the inner and outer phases. The three stages described in this figure shows initial mixing, formation of an initial dispersion, and then the formation of small semistable droplets.

In the nomenclature of the field a “normal” emulsion is O/W while an “invert” emulsion is W/O. Many additional details of emulsion formation and breaking are in Section 2.4.

Microemulsions (MEs) are a special class of liquid/liquid dispersions that are treated as if they are thermodynamically stable. These are defined as having an internal phase droplets size that is less than 100 nm (usually 5–50 nm) in radius. At this level, the fluids appear to be one phase. Note that this radius is still much larger than true solutions where the solute/solvent clusters are less than 1 nm in radius. There can be W/O or O/W MEs depending on the surfactants and liquid phases.

They are very important in the oil industry and are used in EOR and as part of chemical delivery systems. Collins and Hewartson (2002) give an excellent description of MEs, the components in them and how and why they are formed. The four components needed are an aqueous brine phase, an oil phase, a primary surfactant and a cosurfactant. The primary surfactant can be any of the three types noted in Fig. 1.8. The cosurfactant is very important and frequently is a partially water soluble (35 g/100 ml) alcohol such as 2-butanol. According to Collins et al. (2001) MEs can only be formed if the interfacial tension between the oil and water is so low that the remaining free energy of the interface can be overcompensated by the entropy of the dispersion forces. The surfactants do lower the interfacial tension but generally not enough to permit ME formation. The addition of a co surfactant is often necessary to lower the interfacial tension further. The cosurfactant also serves another vital purpose in these systems. It acts to decrease the viscosity of ME systems.

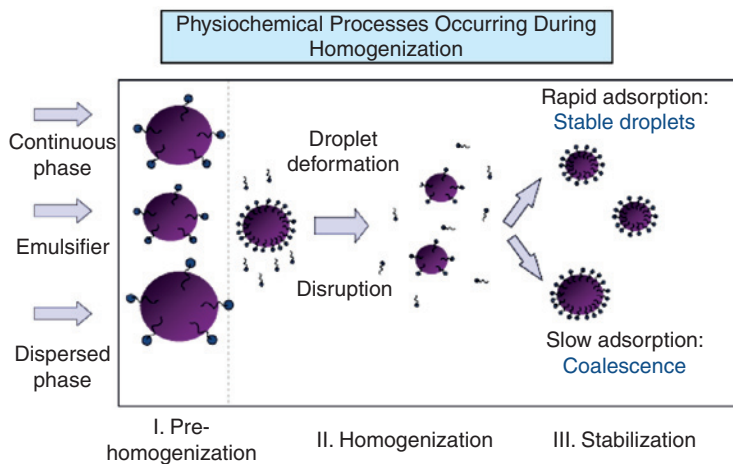
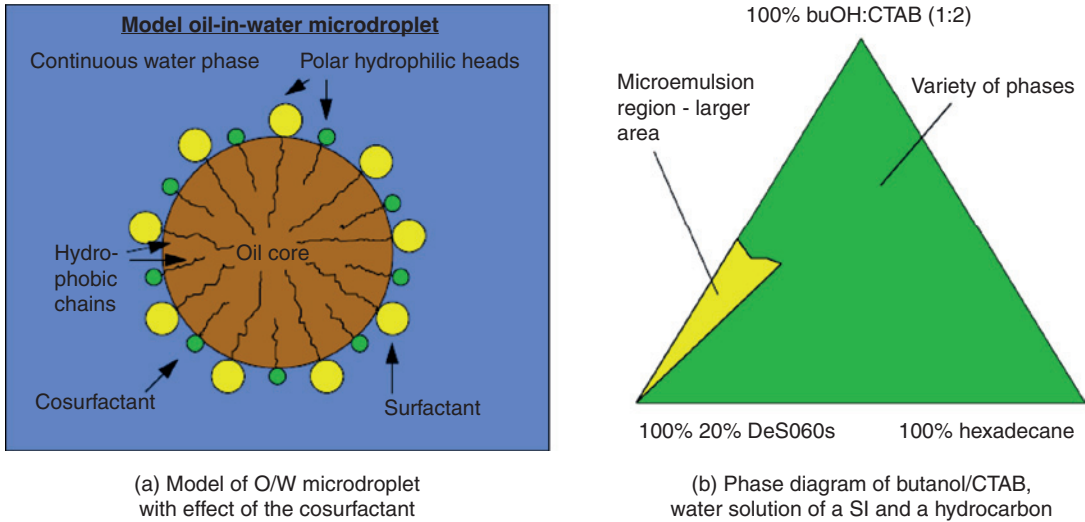


Fig. 1.16—Physiochemical processes in emulsion formation (Weiss 2008).



(a) Model of O/W microdroplet with effect of the cosurfactant

(b) Phase diagram of butanol/CTAB, water solution of a SI and a hydrocarbon

Fig. 1.17—Microemulsion formation mechanism (Collins and Vervoort 2003).

In **Fig. 1.17a**, a cosurfactant is shown to mingle in with the surfactant at the monomolecular film dividing the two immiscible counterparts. However, unlike the surfactant that resides only at this interface, the smaller cosurfactant molecule is not static. The cosurfactant constantly migrates in and out of the dispersed and continuous phases increasing the mobility of the monomolecular interface, hence decreasing the viscosity of such systems. Collins and Vervoort (2003) claim that the cosurfactant also serves to increase the entropy of the dispersion and hence discourage the formation of liquid crystals within the ME. It does this by increasing the disorder at the mixed film where the surfactant is located. In **Fig. 1.17b**, the phase diagram of an aqueous solution of a scale inhibitor (DeS060s) is seen with a hydrocarbon and the mixture of a cationic surfactant/butanol. A small region of the ME is seen in yellow. This illustrates that the ME can only form when the concentrations of the four components are carefully adjusted. Many other MEs with other types of surfactants and cosurfactants are described in other sections (3.6.2 and 5.5). The order of addition also may affect the formation [see Miles et al. (2003)].

MEs employed in EOR treatments are frequently described in the Winsor nomenclature (Winsor 1954). A phase diagram using this system is seen as **Fig. 1.18**. Paul and Moulik (2001) explains the

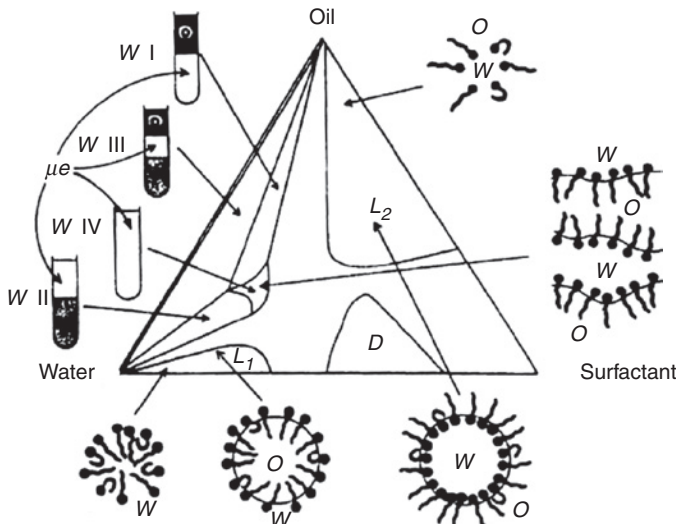


Fig. 1.18—Winsor microemulsion phase diagram.

schematic ternary phase diagram of water/oil-surfactant mixtures representing Winsor classification and probable internal structures. These include L1, a single phase region of normal micelles or O/W MEs; L2, reverse micelles or W/O MEs; and *D*, anisotropic lamellar liquid crystalline phase. The ME is marked by μe , oil by *O*, and water by *W*. This author also notes that the MEs are formed at low surfactant concentrations, and there is a sequence of equilibrium between phases, commonly the Winsor I: with two phases, the lower (O/W) ME phase in equilibrium with the upper excess oil; Winsor II: with two phases, the upper ME phase (W/O) in equilibrium with excess water; Winsor III: with three phases, middle ME phase (O/W plus W/O, called bicontinuous) in equilibrium with upper excess oil and lower excess water; Winsor IV: in single phase, with oil, water, and surfactant homogeneously mixed.

This diagram does not show a cosurfactant (as does Fig. 1.17), but the cosurfactant helps to stabilize the ME phases and makes them much more useful because it is clear that these are very small portions of the phase diagrams. ME uses as well as the Winsor nomenclatures are used in the discussions of emulsion issues in Section 2.2.3 and for EOR in Section 5.9.4.

Nanoparticles in Oil and Gas Production. Nanoscale particles are not new in either nature or science (Ritter 2011). Nanotechnology is considered to involve particles in the scale range of 1 to 100 nm, following the definition used by the National Nanotechnology Initiative (NNI 2011). The lower limit is set by the size of atoms (hydrogen has the smallest atoms, which are approximately a quarter of a nm in diameter) because nanotechnology must build its devices from atoms and molecules, the upper limit is more or less arbitrary but is approximately the size where a phenomena not observed in larger structures start to become apparent and can be made use of in the nano device or particles (Prasad 2008).

Many MEs involve nanosize particles. Frequently at this scale, particles have unusual properties and may be affected by quantum as well as higher scale physical effects. New oilfield products are being claimed to contain nanoparticles; however, special capabilities based on the small size may not be claimed or proven. Products for placement of fracturing additives (Section 4.7), EOR chemicals (Section 5.5) and other additives that have nanoscale components are described in the appropriate sections of this book. In most cases, the nanoparticles are also part of an emulsion, foam, or slurry.

Foams. Dispersions of gases in a liquid are called foams. Most of the common foams constitute a two-phase medium of gas and liquid with a particular structure consisting of gas pockets trapped in a network of thin liquid films and plateau borders. Kam and Rossen (2003) notes that foams used in drilling, fracturing, cementing, and wellbore cleanup are called *bulk foams* because in each case the foam bubbles are much smaller than the geometry of the flow channel in which foam acts. In the other applications (such as diversion and EOR applications), foam enters and acts in the pores of the formation. In the oilfield, foams usually are made using CO₂ or N₂ and the external phase can be a number of salt solutions, acids, alcohols, hydrocarbons or sometime mixtures of these.

There are several important differences between bulk foams and foams in porous media. Kam and Rossen (2003) claim that because the bubbles in bulk foam are small compared to the flow channel, bulk foam can be treated as a locally homogeneous, if rheologically complex, fluid. In porous media, they also claim that one must account for the separate mobilities of gas and liquid and, in particular, for the huge effect of foam on the mobility of gas. Second, the stability of bulk foam is governed by diffusion and the rate at which liquid drains through the foam over relatively large distances (much greater than the bubble size) under gravity. In such a case, for instance, viscosifying the liquid can slow down the rate of liquid drainage and stabilize the foam. In porous media, bubbles are thought to be as large as, or larger than, individual pores (Ettinger and Radke 1992).

The authors (Kam and Rossen 2003) note that diffusion is relatively unimportant to foam in porous media once bubbles are as large as pores (Rossen 1995). Liquid drains from the liquid films, or lamella between bubbles in response to capillary pressure to nearby pores, over a distance of order of pore size. Thus, the lamellae in foam rapidly come to equilibrium with the capillary pressure of the surrounding medium. Therefore, foam in porous media is more directly sensitive to the ability of the surfactant to stabilize lamellae between bubbles than in bulk foam, which can be stabilized simply by viscosifying the liquid. Also, creation of bulk foam often involves turbulent flow or bubbling gas through narrow

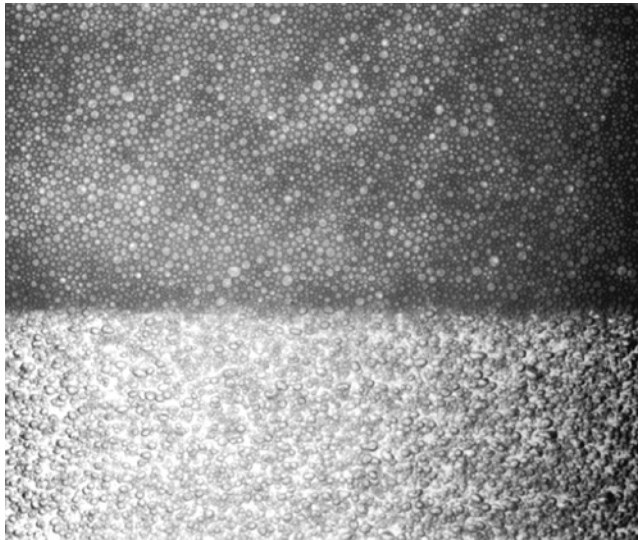


Fig. 1.19—Foam settling (butanol/water/SDS) (Joseph 1997).

tubes into the liquid. In porous media, processes of both creation and destruction of foam are dominated by capillary forces (Kam and Rossen 2003).

Joseph (1997) notes that static foams are inherently unstable. Fig. 1.19 shows foam made in air from water/butanol with sodium dodecyl sulfate as the surface active agent. Foams collapse by draining and film rupture. To keep foam from collapsing, it is necessary to oppose the draining by surface tension gradients induced by the surfactants or to provide continuous shear forces (or both). In Fig. 1.19, the highly dispersed foam is in the top section and the coalescing foam in the bottom of the figure. It is relatively easy to assess the stability of bulk foam. The foamed fluid is placed in a graduated cylinder and the rate of formation of liquid is determined. The time to breakout of ½ of the liquid is called the foam half-life and is used to compare surfactants and fluids. Methods to test oilfield foams are also described by Chambers (1994).

Assessment of the effectiveness of foam in porous media is more complex and requires the use of sand packs or cores (see the discussion by Kam and Rossen 2003). More details of foams used as diverting agents are in Section 3.7.2, and Section 4.7.2 describes foamed fracturing fluids.

The petroleum industry uses the nomenclature of “foam quality” to describe the volume percentage of gas phase to liquid phase. The definition is:

$$\text{Foam quality} = \frac{V_g}{V_g + V_l} \cdot 100 \dots\dots\dots (1.25)$$

Here V_g is the volume of the gas and V_l is the volume of the liquid. The sum is the volume of the foam. Foam quality is considered to range from 52 to 95%. Above 95%, the foam usually changes to a mist, with gas as the continuous phase. Below 52%, stable foam does not exist because there are no bubble/bubble interactions to provide resistance to flow or to gravity separation. Above 52% gas, the gas concentration is high enough that the bubble surfaces touch. Fluids with less than 90% quality are frequently called energized fluids and foams are fluids in the 90-95% range. Note that this same equation (Eq. 1.25) also can be used to calculate a foam quality with a liquid/gas flow rate, as long as the volumes/time is known.

Slurries. These materials consist of multiphase fluids that may contain liquids, solids, and possible gasses (foams) and surfactants as well as polymers. The fracturing proppant slurries are described in Section 4.3.1 and are the major example in oilfield operations. These are very complex fluids, and the rheological properties are described in Chapter 4.

1.5 Key Production Chemistry Concepts

The concepts of chemical thermodynamics, reaction rates (especially at surfaces), and the complex properties of fluids are critical to understanding the use of chemicals for production enhancement. Some of these concepts are previewed in this section and will be explained in more details and applied in the other Chapters (2 through 5) of the book.

1.5.1 Thermodynamic Equilibrium Processes. The concepts of aqueous solution thermodynamics are crucial for understanding many processes in oilfield chemistry. The topic is covered in great depth in text books on aqueous chemistry. For example see Zemaitis et al. (1986) and Langmuir (1997). Therefore, only a simplified description of important principles is presented here. The reader should consult the previously mentioned texts for a more in-depth discussion.

A system at chemical equilibrium represents a dynamic state in which two or more opposing reactions are taking place at the same time and at the same rate. Fig. 1.20 shows the approach of a chemical system to equilibrium. At early time the rate of forward reaction (r_1) (i.e., the formation of products from reactants) is large. As the system progresses in time, the rate of forward reaction decreases and the rate of reverse reaction (r_2) increase. When the rates are equal, the system is in equilibrium and the net rate (i.e., rate of formation of products—rate of formation of reactants) is equal to zero. Once a closed system reaches chemical equilibrium it implies that from that point on, the chemical composition of the system is independent of time and previous history.

Equilibrium constants are used to relate the amounts of reactants and products at equilibrium. Consider, for example, a simple ideal chemical system consisting of reactants A and B , and products C and D , for which the reaction stoichiometry is given by:



These would imply that the forward and reverse reactions are



If the system is ideal then the equilibrium constant for the system can be expressed in terms of concentrations as:

$$K_{eq} = \frac{[C]^c [D]^d}{[A]^a [B]^b}, \dots\dots\dots (1.29)$$

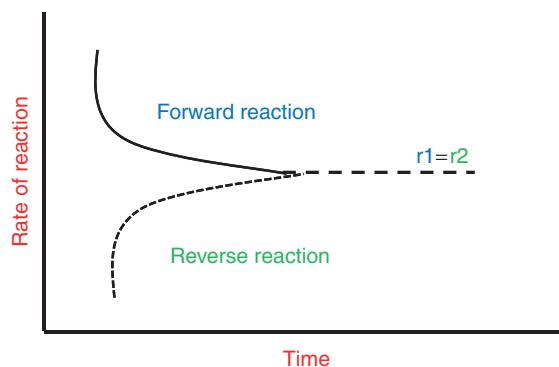


Fig. 1.20—Approach of a chemical system to equilibrium.

where K_{eq} is the equilibrium constant and [] denotes concentration of the species. The equilibrium constant can also be expressed in terms of the free energy change for the reaction (ΔG°) as:

$$K_{eq} = \exp\left(\frac{-\Delta G^\circ}{RT}\right), \dots \dots \dots (1.30)$$

where, R is the gas constant, and T is the temperature. The K_{eq} is a function of temperature and pressure only and does not depend on composition of the system. Therefore, if the composition of the system changes by subsequent reactions or addition of new reactants or products to the system, the same value of the equilibrium constant(s) can be used to calculate the equilibrium distribution in the new system provided the temperature and pressure remain constant and the equilibrium assumption is valid.

Equilibrium constants are not “constants” in the true sense because they do depend on temperature and pressure. An increase in temperature may affect the forward and reverse reactions differently. The reaction that absorbs the most heat will increase that rate to a larger extent than the other reaction. A new equilibrium constant will now represent the new situation. The simple equation by van’t Hoff (proposed by Dutch chemist J.H. van’t Hoff in 1884) can be used to compute the change in equilibrium constant caused by change in temperature. The equation can be expressed as

$$\frac{d \ln K_{eq}}{dT} = \frac{\Delta H^\circ}{RT^2}, \dots \dots \dots (1.31)$$

where ΔH° is the standard enthalpy change of reaction, T is the temperature, and R is the gas constant. If the reaction is exothermic (i.e., if ΔH° for the reaction is negative), then the equilibrium constant decreases as temperature increases. Conversely, K_{eq} increases with temperature for an endothermic reaction.

If the standard enthalpy change of reaction is assumed independent of temperature, then integrating of Eq. 1.31 gives an even simpler result:

$$\ln \frac{K_{eq}}{K_{eq,ref}} = -\frac{\Delta H^\circ}{R} \left[\frac{1}{T} - \frac{1}{T_{ref}} \right], \dots \dots \dots (1.32)$$

Here $K_{eq,ref}$ is the value of the equilibrium constant at the reference temperature $T_{eq,ref}$. This approximate equation implies that a plot of $\ln K_{eq}$ vs. the reciprocal temperature gives a straight line. This equation is helpful in interpolating and extrapolating equilibrium constant data with reasonable accuracy.

The effect of pressure on equilibrium constants is typically smaller than the effect of temperature. However, for deep wells it can be significant and needs to be considered along with the change in temperature. The pressure dependence of the equilibrium constant can be calculated from

$$\left(\frac{\partial \ln K_{eq}}{\partial P} \right)_T = \frac{\Delta V^\circ}{RT}, \dots \dots \dots (1.33)$$

where ΔV° is the molar volume of change of the reaction with all reactants and products in their standard states (Langmuir 1997). If the molar volume change of the reaction is independent of pressure then the integration of the above equation yields

$$\ln \frac{K_{eq}}{K_{eq,ref}} = -\frac{\Delta V^\circ(P - P_{ref})}{RT}, \dots \dots \dots (1.34)$$

where K_{eq} is the equilibrium constant at the desired pressure P . $K_{eq,ref}$ is the equilibrium constant at P_{ref} , which is typically 1 bar.

In very dilute aqueous solutions, the anions and cations behave in an “ideal” manner where each ion will act as if it is independent of all other ions in the solution. In real solutions, especially where there

are high concentrations of other ions (such as in a produced brine), the ions are affected by the other ions in solution and the fluid may not behave as if it has exactly the same number of ions as described by the concentration. The equilibrium constants in such nonideal systems are then expressed in terms of species activity. For example, if the chemical system considered previously of components A , B , C , and D is nonideal then the equilibrium constant is given by

$$K_{eq} = \frac{\{C\}^c \{D\}^d}{\{A\}^a \{B\}^b} = \exp\left(\frac{-\Delta G^\circ}{RT}\right), \dots\dots\dots (1.35)$$

where $\{ \}$ denotes the *activity* of the species. The activity of the species can be thought of as an effective concentration of the species in solution. Programs to calculate or estimate the activity coefficients have been developed but are beyond the scope of this discussion. Refer to several general purpose geochemical models available in the public domain that can be used to predict formation of oilfield scale. Most of them are available at no or minimal charge from the Internet. They have been extensively reviewed in texts on aqueous chemistry and include Mangold and Tsang (1991), Glynn et al. (1992), Wolery (1992), van der Heijde and Elnawawy (1993), Langmuir (1997), and Butler and Cogley (1998).

The solubilities of inorganic salts and organic solids can be predicted using equilibrium models that have been described in Frenier and Ziauddin (2008) and Frenier et al. (2010).

1.5.2 Solubility and Solubility Parameters of Organic-Based Fluids. Solvents and solutions make up a large part of many of the formulations used in production chemistry. This includes corrosion and scale inhibitors as well as dispersant and antidisperants and solvents for removing organic residues from surfaces. The choice of the solvent in a particular situation involves many factors, including the flash point, solution viscosity, or environmental and health concerns, and often the effectiveness of a solvent depends on its ability to adequately dissolve one material while leaving other materials unaffected. Burke (1984) notes that the selection of solvents or solvent blends to satisfy such criterion is a fine art, based on experience, trial and error, and intuition guided by such rules of thumb as “like dissolves like” and various definitions of solvent “strength.” While rule-of-thumb methods may be suitable in many situations, any dependence on experiential reasoning at the expense of scientific method has practical limitations. This author has provided a useful review of the technical basis of solubility theories and quantitative solubility parameters. Solubility and solubility parameters also can be used to describe the behavior of crude oil fluids and the precipitation of asphaltenes [see Frenier et al. (2010)]. The theories and models of Hildebrand and Scott (1950), Hansen (1967), and Teas (1968) are described in the review by Burke (1984). A short abstract is included in this section because formulators in the production chemistry industry (including the authors of this book) have used these principles for developing stable, effective treating formulations.

The Hildebrand solubility parameter of a liquid is a numerical value that indicates the relative solvency behavior of a specific solvent. It is derived from the cohesive energy density of the solvent, which in turn is derived from the heat of vaporization and may be estimated from the molar vaporization energy of a liquid. Eq. 1.36 (Barton 1983) allows the calculation of the Hildebrand parameter (δ) from the molar volume and enthalpy of vaporization (ΔU) at normal pressures and here v_m is the molar volume.

$$\delta = \left(\frac{\Delta U}{v_m} \right)^{1/2} \dots\dots\dots (1.36)$$

This single parameter [listed in Burke (1984)] article ranks solvents from the very hydrophobic (pentane) to most hydrophilic (water). It is also understood that the same value can be obtained by mixtures of solvents and that there are several components of solubilization that included a dispersion component, a hydrogen bonding component, and a polar component.

A three-component (Hansen 1967; Hansen 2000) solubility parameter model, accounting for the different contributions of interaction energy, was developed (Mannistu et al. 1997; Frost et al. 2008). Eq. 1.37 shows the components of δ .

$$\delta^2 = \delta_d^2 + \delta_p^2 + \delta_h^2 \dots \dots \dots (1.37)$$

These represent the three basic interactions that are

1. Dispersion interactions (nonpolar interactions) that give rise to the dispersion cohesive energy, E_d . This is most important for hydrocarbons that have low polarity values.
2. The permanent dipole-permanent dipole interactions (polar interactions) that provide the polar cohesive energy, E_p . Polar molecules tend to arrange themselves head to tail, positive to negative, and these orientations lead to further increases in intermolecular attraction.
3. The hydrogen bonding interactions that result in the hydrogen bonding cohesive energy, E_h . This is important in many molecules including water, alcohols, and amines.

In this model, each of the Hansen solubility parameters defines one axis in 3D space. The center of the sphere corresponds to the Hansen solubility parameters for the solute. The radius (r), defines the sphere of solubility of the solute in a particular solvent or solvent mixture. That is, if the Hansen solubility parameters for a solvent or solvent mixture lie within the Hansen solubility parameter sphere for a solute, then that particular solvent or solvent mixture is considered to be a good solvent for the solute with Hansen solubility parameters corresponding to the center of the sphere. See Fig. 1.21 for a depiction from Burke (1984) that plots the 3 components (Eq. 1.37) on the x , y , and z axes of a 3D figure.

Burke (1984) describes a method to determine the numerical values for the component. First, the dispersion force for a particular liquid is calculated using what is called the homomorph method. The homomorph of a polar molecule is the nonpolar molecule most closely resembling it in size and structure (*n*-butane is the homomorph of *n*-butyl alcohol). The Hildebrand value for the nonpolar homomorph (being entirely because of dispersion forces) is assigned to the polar molecule as its dispersion component value. This dispersion value (squared) is then subtracted from the Hildebrand value (squared) of the liquid, the remainder designated as a value representing the total polar interaction of the molecule. Through trial and error experimentation on numerous solvents and polymers, Hansen (1967) separated the polar value into polar and hydrogen bonding component parameters best reflecting empirical evidence. Burke (1984) lists Hansen parameters for several solvents. Using (usually 2)

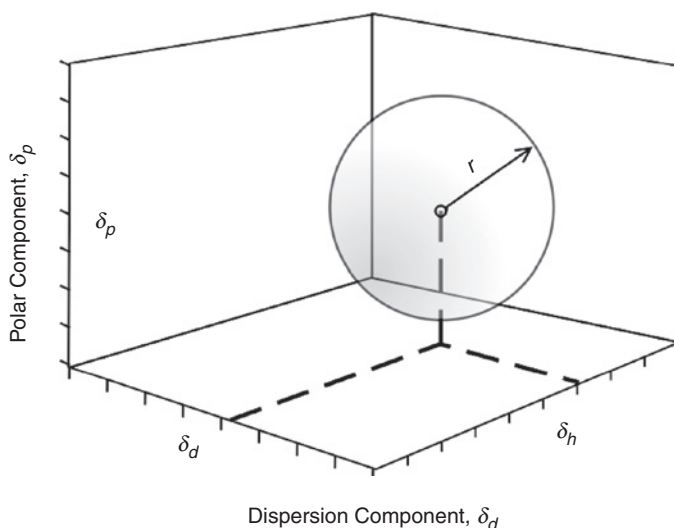


Fig. 1.21 — Hansen plot.

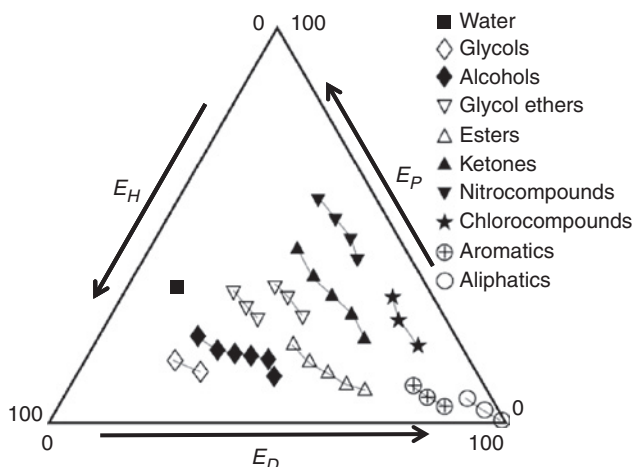


Fig. 1.22—Teas classes (Burke 1984).

Hansen parameters, solubility of some solutes can be predicted (Samuelson 1991; Frost et al. 2008) for some solvent mixtures.

A possibly more practical graphic is the Teas (1968) graph, which is an overlay of three solubility scales where fractions of solubility functions (such as the Hansen parameters) are determined. The overlay is a ternary plot such as Fig. 1.22 (modified from Burke 1984) where *classes of solvents* are plotted, and the trends in the effect of the three parameters are shown. According to this author, it illustrates that for solvents of increasing molecular weight within each class shifts the relative position of a solvent on the graph closer to the bottom right apex. This is because, as molecular weight increases, the polar part of the molecule that causes the specific character identifying it with its class, called the functional group, is increasingly “diluted” by progressively larger, nonpolar “aliphatic” molecular segments. This gives the molecule as a whole relatively more dispersion force and less of the polar character specific to its class.

Several other solubility models and methods are also described by Burke (1984) of which the Kauri-Butanol number (KB) is a method that is used in production chemistry formulation technologies. The KB of a solvent represents the maximum amount of that solvent that can be added to a stock solution of kauri resin (a fossil copal) in butyl alcohol without causing cloudiness. Because kauri resin is readily soluble in butyl alcohol but not in hydrocarbon solvents, the resin solution will tolerate only a certain amount of dilution. Stronger solvents such as toluene can be added in a greater amount (and thus have a higher KB value) than weaker solvents like hexane. *ASTM D1133-10* (2010) is the ASTM method for determining KB. The Burke (1984) publication is very useful because there are multiple tables with the various solubility “parameter” values for many of the systems described.

Various types of solubility parameter studies as well as the values appear in theoretical and practical studies of the interactions of organic molecules and solvents in various oilfield production systems that are described in Chapters 2 and 3 of this book.

1.5.3 Mechanical Properties of Solids and Liquids. This section provides a brief review of the mechanical properties of solids and liquids. These properties are critical for understanding and designing for HF treatments and any treatment that pumps fluids into the formation. Applications will be described in Section 1.6.3.

Any stress (σ) placed on a solid or fluid is measured in the units of force/area and has the same units as pressure (SI units are Pascals, $1 \text{ Pa} = 1 \text{ N/m}^2$). As seen in Fig. 1.23, a stress at the center of mass causes a deformation in either the axial or lateral direction. If the solid is confined, stresses in 3 directions (triaxial) could be imposed. The amount of the deformation of the solid is called the strain (ϵ). Note that liquid formulations also have properties described by stress/strain curves (this is described as viscosity).

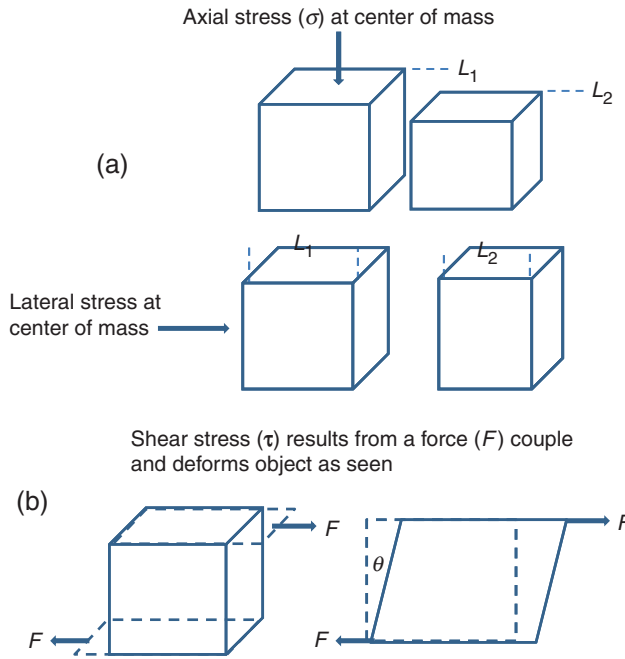


Fig. 1.23—Stress and deformation of solids.

The stress and strain on solids could be compressional, as in Fig. 1.23, or could be a *tension* that would cause an elongation of the solid. Compression loads on the solids in the earth usually would be found during pumping activities, but the various well-piping components may also be in tension. Eq. 1.38 shows the *strain* caused by the load. Here, L is the lengths and ΔL is the change in the length caused by the load.

$$\epsilon = \frac{\Delta L}{L_1} \dots \dots \dots (1.38)$$

The relationship between the stress and the strain of a solid is known as Young’s modulus (E) and is an important characteristic of the solid.

$$E = \frac{\sigma}{\epsilon} \dots \dots \dots (1.39)$$

The ratio of the lateral and axial strain is called Poisson’s ratio (ν). When a material is compressed in one direction, it usually tends to expand in the other two directions perpendicular to the direction of compression. This phenomenon is called the *Poisson effect*. Poisson’s ratio, ν (Eq. 1.40) is a measure of the Poisson effect. The Poisson ratio is the ratio of the fraction (or percent) of expansion divided by the fraction (or percent) of compression, for small values of these changes and is also an important descriptor for the solid.

$$\nu = \frac{\epsilon_y}{\epsilon_z} \dots \dots \dots (1.40)$$

If the stress is not at the center of mass, but consists of a force couple that causes a shear stress (τ), then a deformation is seen as in Fig. 1.23b. The shear strain (γ) defines the extent that the plane is displaced.

$$\gamma = \tan \theta = \frac{\Delta L}{L} \dots \dots \dots (1.41)$$

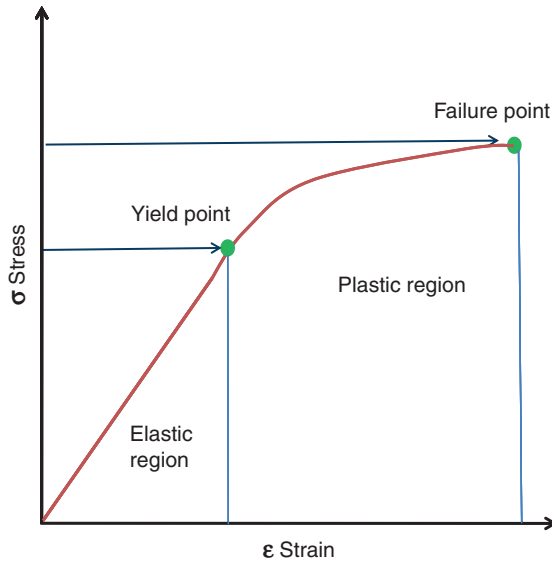


Fig. 1.24—Stress/strain curve for a solid.

The relationship between shear stress and shear strain is called the shear modulus (G).

$$G = \frac{\tau}{\gamma} \dots \dots \dots (1.42)$$

For linear, isotropic materials, E and G are related as:

$$G = \frac{E}{2(1 + \nu)} \dots \dots \dots (1.43)$$

The value of the stress/strain provides a lot of information about the solid. All of the equations previously (Eq. 1.41 through 1.43) are for the elastic region of Fig. 1.24.

Very malleable solids such as metals may have a large plastic region, while very brittle solids such as a glass may have no plastic region.

1.5.4 Transport Properties. The transport properties of fluids include viscosity (momentum transport), diffusion (mass transport), and thermal conductivity (heat transport) and have similar descriptor equations. These properties are critical for using the fluids in the various production-enhancement processes.

Viscosity. The viscosity of a fluid is an essential property for characterization of the flow behavior. This property is a measure of the resistance of a fluid to being deformed by either shear stress or tensile stress. Viscosity describes a fluid’s internal resistance to flow and may be thought of as a measure of fluid friction. Note the similarity to the stress/strain on a solid (Eq. 1.39). Wikipedia (2009b) claims that James Clerk Maxwell (13 June 1831–5 November 1879) called viscosity *fugitive elasticity* because of the analogy that elastic deformation opposes shear stress in solids, while in viscous fluids, shear stress is opposed by rate of deformation.

It is a function of the chemical composition and the physical state (usually temperature) of the fluid. Two different definitions of viscosity are in common use. Absolute (intrinsic) viscosity (η) is a measure of the resistance to flow that a fluid offers when it is subjected to shear stress (Eq. 1.44). This equation relates the shear stress (σ) exerted on a fluid to the resultant strain rate ($\dot{\gamma}$). Kinematic viscosity (ν) is defined as the ratio of absolute viscosity to the density of the fluid at the same temperature. The apparent (measured) viscosity (μ_a) is the value usually reported in oilfield application and may depend on the shear rate.

$$\sigma = \eta \dot{\gamma} \dots \dots \dots (1.44)$$

The viscosity of the crude oil as well as the viscosities of various treating fluids described in this book is critical values. In general, the viscosity of crude oil increases with its density (i.e., the lower the API gravity of a crude oil (denser oil), higher the viscosity). Typically, the viscosity of dead oil is experimentally determined as a function of temperature, and the viscosity of live oil is determined as a function of pressure at reservoir temperature (for reservoir-engineering purposes) and at a lower temperature (for facility design purposes). In addition, the viscosity of various petroleum fractions is important in midstream and downstream applications.

The viscosity of petroleum fractions also increases with a decrease in the API gravity; for residues and heavy oils with API gravity of less than 10 (specific gravity of above 1), the viscosity varies from several thousands to several million poises. Viscosity is a bulk property that can be measured for all types of petroleum fractions in liquid form. Kinematic viscosity is a useful characterization parameter for heavy fractions in which boiling point data are not available because of thermal decomposition during distillation. Not only is viscosity an important physical property, but it is a parameter that can be used to estimate other physical properties as well as composition and quality of undefined petroleum fractions (Riazi 2005). Generally the kinematic viscosities of petroleum fractions are measured at standard temperatures 37.8°C (100°F) and 98.9°C (210°F).

The viscosity of various treating fluids is of great importance because it affects the physical and chemical properties. The measurement of viscosity is accomplished by several techniques. In general, either the fluid remains stationary and an object moves through it, or the object is stationary and the fluid moves past it. The *drag* caused by relative motion of the fluid and a surface is a measure of the viscosity. The flow conditions must also have a sufficiently small value of the Reynolds (R_e) number for there to be laminar flow.

For Newtonian liquids (viscosity that is independent of shear rate), viscosity can be measured by capillary U-tube viscometers (Fig. 1.25). The time it takes for the test liquid to flow through a capillary of a known diameter of a certain factor between two marked points is measured. By multiplying the time taken for the fluid to flow, by the factor of the viscometer, the kinematic viscosity is obtained. The viscometers are usually placed in a constant temperature water bath for this measurement. A test method is described in more detail in *ASTM D445-04el* (2004), which is equivalent to *ISO 3104:1994* (1994) method, and kinematic viscosity is measured at temperatures from 15 to 100°C (approximately 60–210°F). In this method, repeatability and reproducibility are 0.35 and 0.7% respectively (Denis and Briant 1997). Additional methods are described in Chapter 4.

Another type of viscometer is a rotary viscometer, which is used for a wide range of shear rates, especially for low shear rate and viscous fluids such as lubricants and heavy petroleum fractions and fracturing fluids. In these viscometers, fluid is placed between two surfaces, one is fixed and the other is rotating. Rotational viscometers use the idea that the torque required to turn an object in a fluid is a

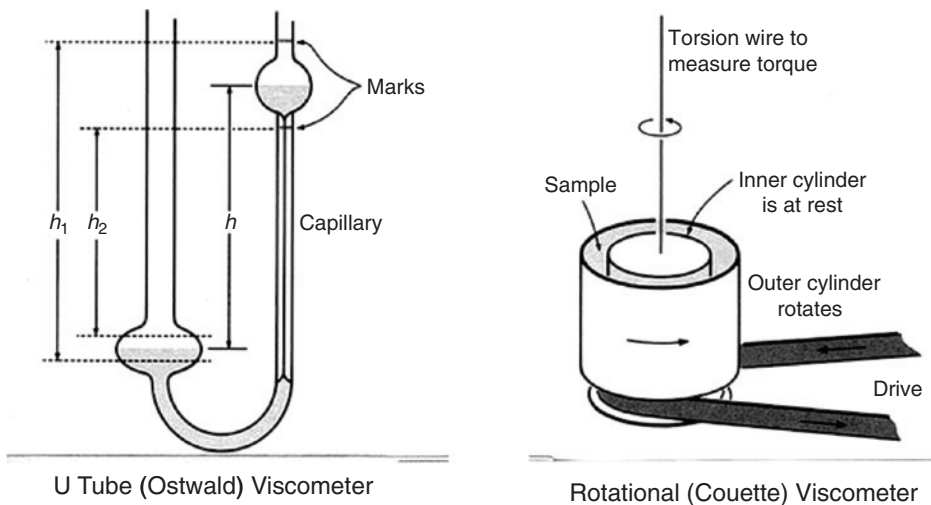


Fig. 1.25—Viscometer types.

function of the viscosity of that fluid. They measure the torque required to rotate a disk or bob in a fluid at a known speed. “Cup and bob” viscometers work by defining the exact volume of a sample that is to be sheared within a test cell; the torque required to achieve a certain rotational speed is measured and plotted. There are two classical geometries in cup and bob viscometers, known as either the Couette or Searle systems—distinguished by whether the cup or bob rotates. The rotating cup is preferred in some cases because it reduces the onset of Taylor vortices (axisymmetric toroidal vortices), but is more difficult to measure accurately. See Fig. 1.25 for diagrams of the two types of viscometers. Also see Wikipedia (2009b) for examples of other types of viscometers. Viscometry measurement devices for specific fluids such as fracturing fluids are described in Section 4.2.2.

The above methods are used to measure viscosity of liquids at atmospheric pressure. To measure the viscosity of the live fluid, the viscometers must operate under pressure. Typically, three types of viscometers are used for these measurements: a rolling ball viscometer, capillary flow viscometer, and an electromagnetic viscometer. The reservoir fluid sample is transferred to the viscometer at an elevated pressure to ensure monophasic transfer.

In the rolling ball viscometer, a ball is allowed to fall through the fluid and the time required for the ball to travel through the fluid is correlated to the fluid viscosity. In the capillary flow viscometer, the live fluid is allowed to flow under pressure through a long capillary tube. The pressure drop across the tube is measured, and the viscosity of the fluid is calculated based on the Hagen-Poiseuille equation for laminar flow. An electromagnetic viscometer is available from Cambridge Viscosity (CVI 2010). In this method, a piston moves back and forth through the pressurized fluid, and the drag on the piston is measured, thus, inferring the viscosity. Examples are in Section 4.2.2.

Diffusivity. The diffusivity or the diffusion coefficient is the proportionality constant between the molar flux caused by molecular diffusion and the gradient in the concentration of the species (or the driving force for diffusion). Diffusivity is described in Fick’s law:

$$J_i = -D_i \frac{\partial \phi}{\partial x}, \dots \dots \dots (1.45)$$

where J is the diffusion flux [(amount of substance) per unit area per unit time], example mol/m²/s. J measures the amount of substance that will flow through a small area during a small time interval. D_i is the diffusion coefficient or diffusivity of species i in dimensions of [length² time⁻¹], example m²/s. ϕ (for ideal mixtures) is the concentration in dimensions of [(amount of substance) length⁻³], example mol/m³. x is the position [length].

Diffusion is a very important factor in reactions at surfaces (solid as well as insoluble liquid) where the reactants and products may diffuse to or away from the surfaces, and this process may control the surface reaction rate (see Section 1.5.7).

The diffusivity of chemical species frequently can be measured using a chemical reaction where the rate can be proven to be under mass transfer (diffusion) control. In these cases, a rotating disk electrode (or a rotating reactive surface such as a mineral such as calcite in HCl) is used to measure the change in the reaction rate vs. angular velocity, and the diffusion coefficient can be calculated. See Sections 3.2 and 3.8.1 of this book and Frenier and Kennedy (1986). Diffusion cells (de Rozières et al. 1994) also can be employed to measure the movement of protons (H⁺) in acid emulsions.

Thermal Conductivity. The thermal conductivity of a material is defined by the Fourier’s Law of heat conduction, which states that the heat flux by conduction is proportional to the temperature gradient. The 1D form of the law can be expressed as:

$$q_y = -k \frac{dT}{dy}, \dots \dots \dots (1.46)$$

where q_y is the heat flow per unit area or heat flux in the positive y direction, and T is the temperature. The proportionality constant, k is the thermal conductivity of the material. The thermal conductivity is not truly as constant because it varies with temperature. Units of measurement of thermal conductivity

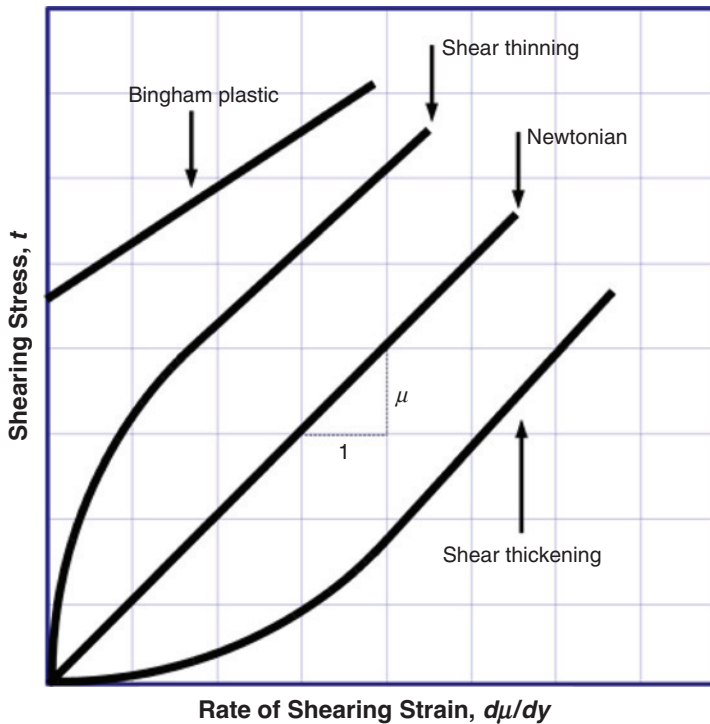


Fig. 1.26—Types of viscous responses.

are BTU/(hr-ft-°F) in oilfield units and Wm-1K-1 in metric units. *ASTM D5334-08* (2008) describes one method for determining thermal conductivity in geological specimens.

1.5.5 Rheology. A large variety of complex fluids are encountered in oilfield treatments; especially in reactive stimulation, HF, and EOR. These are fluids that behave neither like a liquid nor like a solid under flow, but show a mixed behavior. The study of these types of fluids is called *rheology*. The simplest definition of rheology is the study of the flow of matter. For simple fluids such as water or many organic liquids (including some very viscous fluids), the relationship of the shear stress (σ) applied to the resultant shear strain rate (γ) is linear and the ratio of these quantities is the liquid viscosity (ν or η) as defined in Eq. 1.44. These fluids are called Newtonian fluids. **Fig. 1.26** shows types of stress/strain responses for several different types of fluids that include Newtonian and non-Newtonian materials.

Note that a Bingham plastic has a yield value and does not respond until that point; however, then, it acts like a Newtonian fluid. For many types of complex fluids such as emulsions, suspensions, slurries, gels, foams, polymer solutions, and other complex mixtures of substances, the shear stress/shear rate relationship cannot be characterized by a single value of viscosity (ν) (at a fixed temperature). Instead, the viscosity is a function of the operating conditions such as the shear rate. One of the tasks of rheology is to establish the relationships between deformations and stresses by adequate measurements and modeling. Two examples of the non-Newtonian behavior are *shear thinning* and *shear thickening* fluids. *Thixotropic fluids* are even more complex because a scan of stress vs. strain does not have the same values when the strain is reversed. Latex paints provide an example of a thixotropic fluid.

For polymer melts (and wax/oil mixtures) and suspensions, generally, the viscosity decreases as the shear rate increases. This type of behavior, called *shear thinning*, is of considerable industrial significance. For example, frac fluids are shear thinning. Some fluids exhibit different types of behavior depending on the shear field. Carbohydrate-based frac fluids (such as hydroxypropyl guar) in water exhibit such complex behavior. **Fig. 1.27** shows plots of 0.48% hydroxypropyl guar in water as a function of shear rate and temperature (Guillot and Dunand 1985). Two models will be required to fit this

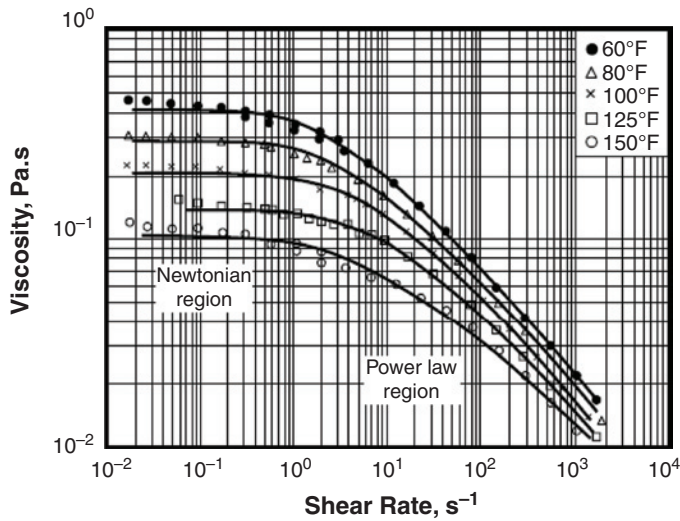


Fig. 1.27—HPG rheology as a function of temperature.

type of data. Eq. 1.44 is useful in the linear (Newtonian) low-shear region, but a power-law model, gives an *apparent viscosity* (μ_a):

$$\mu_a = K / \dot{\gamma}^{(1-n)} \dots \dots \dots (1.47)$$

This is required for the high-shear region. Here K is the consistency index in lbf-sⁿ/ft² or kPa-sⁿ and n is the flow behavior index (dimensionless). These relations hold for most fracturing fluids over the range of shear rates in which the fluid displays non-Newtonian behavior. A log-log plot of σ vs. γ usually yields a straight line over a portion of the shear range. The slope of the straight-line portion is equal to the behavior index n , and the value of the viscosity at $\gamma = 1.0 \text{ s}^{-1}$ is equal to the consistency index K . A log-log plot of μ_a vs. γ has a straight-line slope of $n - 1$ when the power-law model is applicable. The slope is zero for Newtonian behavior (Constein et al. 2000). To better predict the full range of fracturing fluid viscosity, a rheology model must use not only n and K but also a zero-shear viscosity term. The Ellis model (Matsuhisa and Bird 1965) adds zero-shear viscosity at γ_o to the power-law model to improve viscosity prediction:

$$\frac{1}{\mu_a} = \frac{1}{\mu_o} + \frac{1}{K\gamma^{n-1}}, \dots \dots \dots (1.48)$$

where n and K are defined from the high-shear data.

Shear thickening is a less frequently observed phenomenon whereby the material exhibits an increasing viscosity with increasing shear rate. *Thixotropy* is a property of some complex fluids (for example, some types of clay in water and latex paint noted in the previous paragraph), which refers to time-dependent viscosity. A thixotropic fluid displays a decreasing viscosity with time at a constant shear rate. Materials that exhibit the opposite behavior (i.e., increasing viscosity with time at a constant shear rate) are called *rheopectic*. A complex fluid may also exhibit a yield stress. Below a certain value of applied stress, called the yield stress, the fluid does not flow, but above this stress, the fluid flows. It may be noted that waxy crude oils, for example, are usually both shear thinning and thixotropic and may exhibit a yield stress at lower temperatures as well.

A rheometer is an instrument that is used to measure the rheology of fluids. In addition to applying a constant shear stress or a constant shear rate, rheometers can also apply oscillatory motion. This is called dynamic oscillatory rheometry (DOR).The response to the oscillatory motion can be used to determine the solid-like behavior and the liquid-like behavior of the fluid. Further, the stress

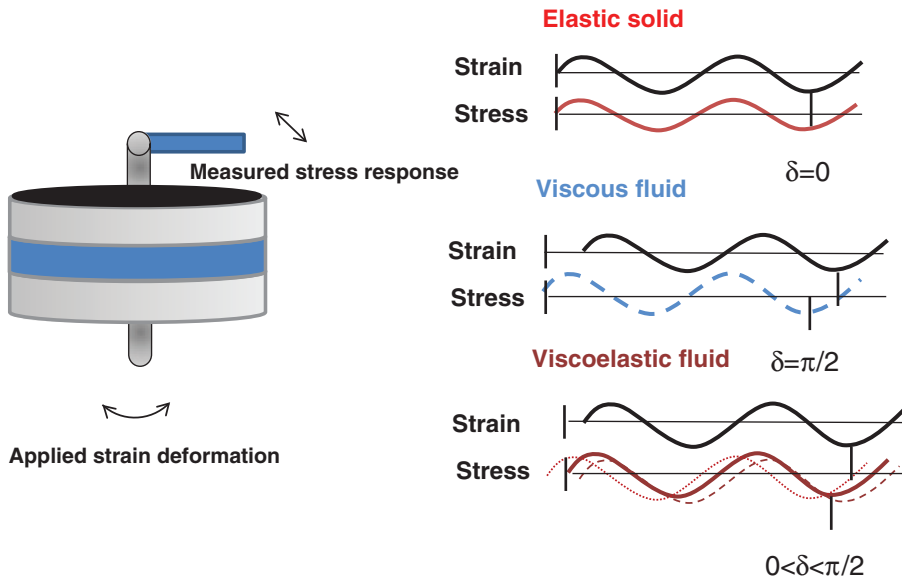


Fig. 1.28—Dynamic oscillation rheometry.

in the direction normal to the flow can also be measured. Thus, the stress tensor can be related to the strain. The measured response can be factored into two components: the in-phase response defines the storage modulus, G' that gives information on the elasticity and the 90° out of phase (G'') is the loss modulus that gives information about the viscous properties of the fluid. To do the experiment, a sinusoidal stress is applied at a frequency, ω , and the strain (in phase and out of phase) are plotted vs. the frequency. See Fig. 1.28.

Rheometers can be programmed to run temperature sweeps, shear sweeps, creep etc. to determine various rheological properties of fluids. Several specific types are described in Chapter 4. A study of the behavior can provide mechanistic information about the arrangement and rate of change of the polymer molecules that cause the viscosity properties.

1.5.6 Chemistry of Minerals in Producing Formations. This section reviews characteristics of some of the solids that are encountered in the oilfield. These include those that are *crystalline* (having a specific orientation of the atoms in the solids) as well as those that have an *amorphous* structure, such as glasses (including some polymers at certain temperatures). These materials do not have a specific orientation of the atoms and molecules and could be considered to be very viscous liquids. These solids constitute the physical structure of the oil and gas producing formations.

Naturally occurring crystalline solids usually are called minerals, and the producing formations are made up of an almost infinite variation of these minerals. The metallic components that make up the producing hardware usually are man-made crystalline materials, and the cement that isolates the well from the environment is mostly composed of man-made crystalline solids. See Sections 2.2.2 and Chapter 3. The mineralogy database assembled by Barthelmy (2009) is an important source of information for thousands of natural and man-made minerals. This database also is a good source for information on the crystal structure of important minerals as these structures may affect reactivity. A few definitions show the wide variety of ideas about what constitutes a mineral. Most of the definitions include the designation of an inorganic compound, but many organic compounds (including some of interest to the oilfield production such as waxes and gas hydrates) form crystals and some are also naturally occurring minerals.

- A mineral is an element or chemical compound that is normally crystalline and that has been formed as a result of geological processes (Nickel 1995).

- Minerals are naturally occurring inorganic substances with a definite and predictable chemical composition and physical properties. (O'Donoghue 1990).
- These ... minerals ... can be distinguished from one another by individual characteristics that arise directly from the kinds of atoms they contain and the arrangements these atoms make inside them (Sinkankas 1966).

The authors of this book will use the more general definition of a crystalline solid, where each mineral precipitates from solution to form a specific geometric configuration of the atoms (and/or ions) called a unit cell. For example, NaCl (halite) forms a square crystal unit cell with 12 Na⁺ and 12 Cl⁻ ions. Using x-ray diffraction methods, the dimensions of the unit cell can be calculated, and these dimensions may be used to draw some conclusions about the properties of the solid. As more halite precipitates onto the incipient crystal, the square shape may be maintained if the fluid is very pure. Barium sulfate (BaSO₄—barite) forms a somewhat more complex dipyramidal cell with 14 Ba²⁺ and 14 SO₄²⁻ ions. In more complex crystalline minerals such as the clay kaolinite, even larger structures of Al³⁺, Si⁴⁺, O²⁻, and OH⁻ may be arranged in layers. Because particular atoms/ions may be exposed on the surface (and to a treating fluid), the structure of the mineral may affect reactivity and must be considered by the engineer when designing treatments.

While carbonate formations consist of mostly calcite (CaCO₃) or dolomite [CaMg(CO₃)₂], sandstone formations are much more complex and contain carbonate minerals, silica (SiO₂), iron and manganese compounds, and most importantly, various types of aluminosilicates. These complex minerals are classified structurally as phyllosilicates (clays) and tectosilicates (feldspars, zeolites, and other minerals).

The clays are aluminosilicates that have a unit cell but also are layered in microstructure and in the macrostructure. **Fig. 1.29** shows the structure of kaolinite and chlorite, two layered clays that are important in many sandstone formations. Some of the important chemistry is illustrated. All of the silicon ions (Si⁴⁺) exist in 4-coordinate tetrahedral (“T”) structures with O²⁻ ions at the corners of the tetrahedrons. In kaolinite, Al³⁺ ions are in an octahedral (“O”—6-coordinate) structure with O²⁻ and OH⁻ ions balancing the charges. While the kaolinite macrostructure is layered like a deck of cards (see **Fig. 1.30**, which is a scanning electron microscope photo). Note that chlorite is “layered” even at the unit cell level and has additional metal ions in the “sandwich.”

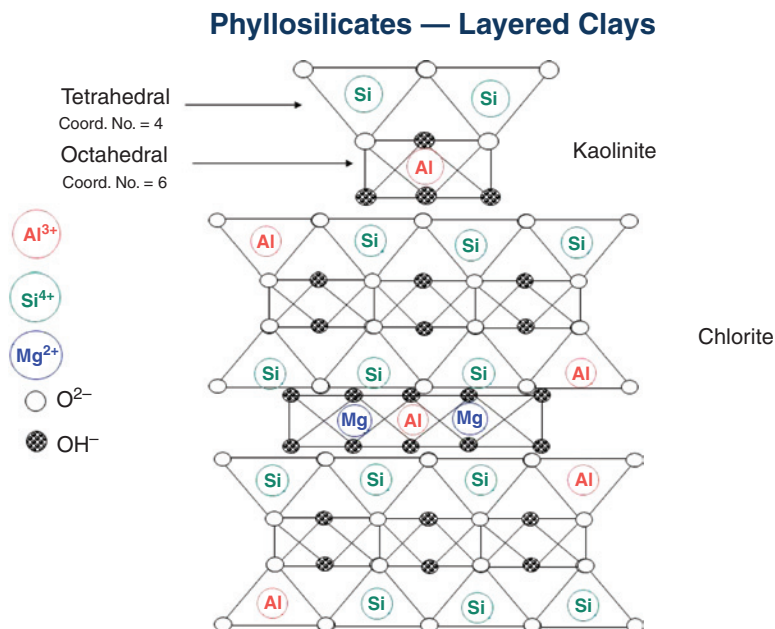


Fig. 1.29—Phyllosilicates structures.



Fig. 1.30—SEM photo of kaolinite.

Kaolinite is the only clay with a single balanced Al/Si structure in the unit cell. It is, thus, easy to test in dissolution experiments that follow Al and Si ions in solution. All of the other petroleum-formation significant clays have more complex structures such as that seen for chlorite and montmorillonite in Fig. 1.31 with a T-O-T microstructure.

A consequence of the clay microstructure and macrostructure is that surface charges frequently are not perfectly balanced and cations (Na^+ , K^+ , Ca^{2+} , etc.) migrate from the water phase to balance the charges. Clays, thus, have an ion-exchange capacity that helps (or hinders) the physical stability of the clays in the formation. That is, changes in salinity or water composition may cause the clays to clump or to be dispersed.

Characteristics that cause the clays to stay in place or to disperse in a fluid (such as water or brine) are related to the electrical double layer (Fig. 1.32a) that exists around each particle. The liquid layer

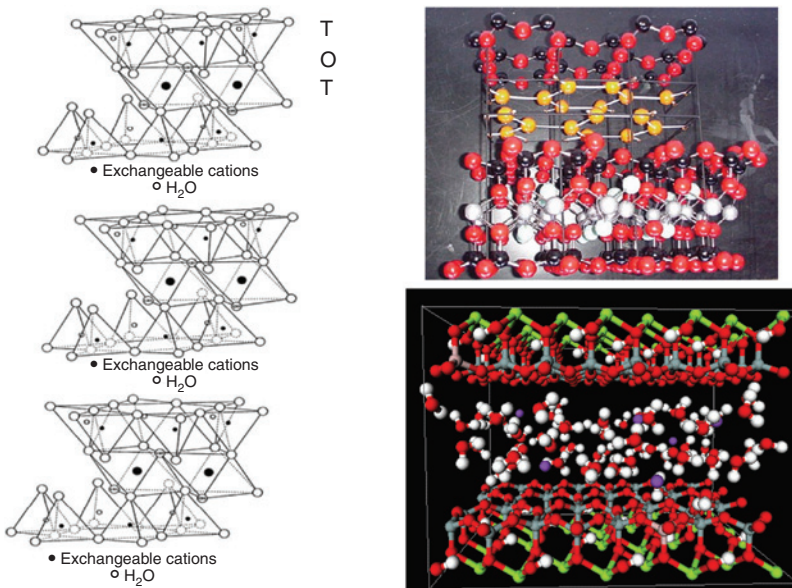


Fig. 1.31—Montmorillonite structure.

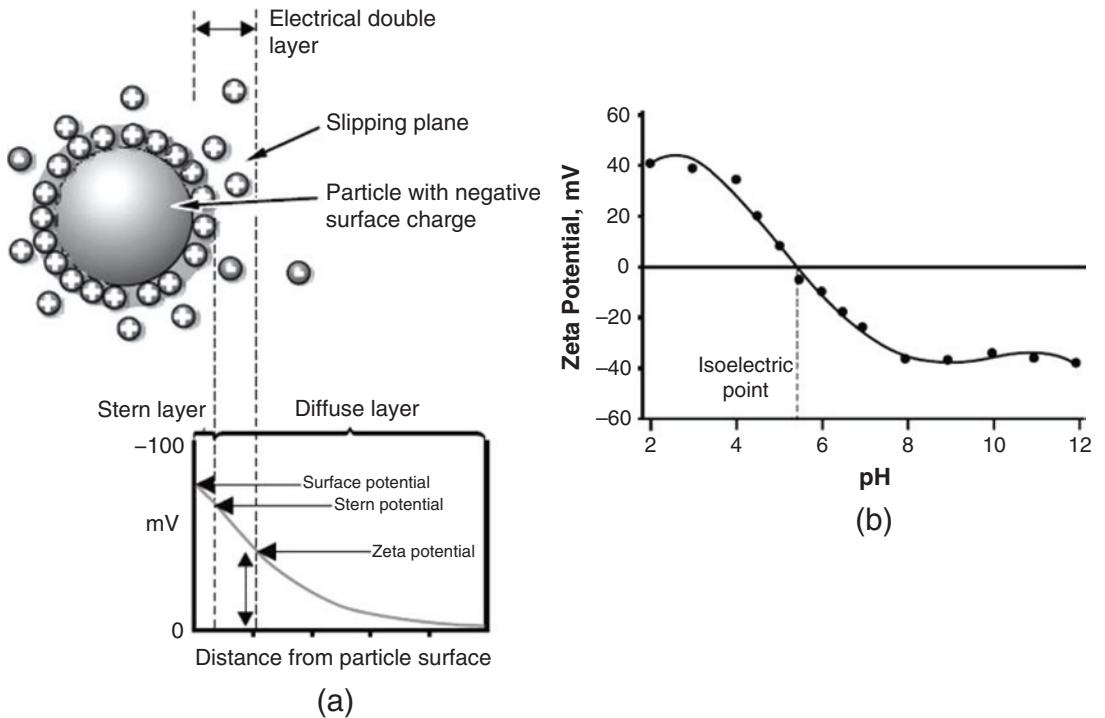


Fig. 1.32— Charge on a particle.

surrounding the particle exists as two parts; an inner region, called the stern layer, where the ions are strongly bound, and an outer, diffuse, region where they are less firmly attached. Within the diffuse layer there is a notional boundary inside which the ions and particles form a stable entity. When a particle moves (e.g., because of gravity), ions within the boundary move with it, but any ions beyond the boundary do not travel with the particle. This boundary is called the surface of hydrodynamic shear or the slipping plane. The electrical potential that exists at this boundary is known as the zeta potential, ζ . If cations such as protons or anions including hydroxyl ions are added to the solution, a titration curve will give the isoelectric point (Fig. 1.32b) of the particle (this is also called the potential of zero charge, pzc). The clays usually are least stable at the isoelectric point. The isoelectric point also could be determined by adding other cations or anions.

Note that the zeta potential is *not* the same as the surface charge but will usually be the same sign and does reflect that charge. Significantly, it is measurable using simple electrophoretic devices (Malvern 2003), while the actual surface charge is not easily determined. The velocity of a particle in an electric field is commonly referred to as its electrophoretic mobility. With this measurement, the zeta potential of the particle can be determined by application, which can be determined by Henry’s equation (William Henry, born in 1803):

$$U_E = \frac{2e\zeta f(K_a)}{3\eta}, \dots \dots \dots (1.49)$$

where ζ is zeta potential; U_E is electrophoretic mobility; ϵ is a Dielectric constant; η is viscosity; and $f(K_a)$ is Henry’s function. Two values are generally used as approximations for the $f(Ka)$ determination, either 1.5 or 1.0.

The various microstructures and macrostructures greatly affect the reactivity of clays in the various possible stimulation solutions. These characteristics may cause formation damage because of clay migration that is described in more detail in Section 2.3.3.

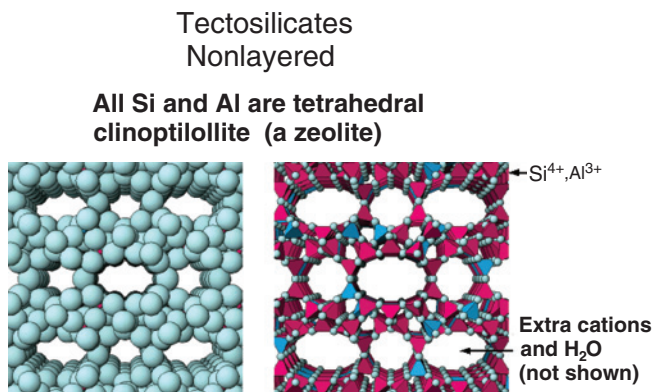


Fig. 1.33—Tectosilicate structure.

Some clay minerals also may contain iron, nickel, or manganese ions. An example is the chlorite family (see Fig. 1.29). Specific examples are:

- Clinocllore: $(\text{Mg}_5\text{Al})(\text{AlSi}_3)\text{O}_{10}(\text{OH})_8$
- Chamosite: $(\text{Fe}_5\text{Al})(\text{AlSi}_3)\text{O}_{10}(\text{OH})_8$
- Nimite: $(\text{Ni}_5\text{Al})(\text{AlSi}_3)\text{O}_{10}(\text{OH})_8$
- Pennantite: $(\text{Mn},\text{Al})_6(\text{Si},\text{Al})_4\text{O}_{10}(\text{OH})_8$

The other category of aluminosilicates in sandstone formations are the tectosilicates, that include feldspars, micas, and zeolites (see Fig. 1.33). These materials are not layered, and all Si and Al ions are in a tetrahedral (4-coordination structure) with O^{2-} ions. This usually confers a significant resistance to dissolution by acids. An exception is some of the zeolites where the large cavities allow some acids (such as HCl) to enter into the structure and remove Al^{3+} ions and thus, destabilize the aluminosilicate (Hartman et al. 2003). The zeolites and several other minerals are considered to be “acid-sensitive” and susceptible to damage in the presence of HCl at high temperatures. See discussions in Section 3.5.2.

Shales are compressed mud stones that are made up of fine-grained clays and carbonates and have very low permeability values. Shales frequently form the barriers in the earth that trap various hydrocarbons in producing formations. However, shales also may contain hydrocarbons in their matricides and now can be produced using directional drilling and HF. A short discussion on physical structure and the hydrocarbon potential of these formations is in Section 4.1.

The hydrocarbons in the producing formations also may greatly affect the various enhancement and stimulation processes, though most of the tests described in the book are done on model rocks (such as Berea sandstone and Indiana limestone) because these are readily available from construction quarries. Occasionally, samples from outcrops of producing formations are also used. Because the presence of the hydrocarbons would affect surface reactions in unpredictable ways, tests with hydrocarbons present in cores are only performed when very necessary for a particular test (see Section 5.3.4). A short review of the chemistries of the various petroleum hydrocarbons is in Section 2.2.4. Because the various hydrocarbon chemicals may improve or interfere with a particular enhancement treatment, some of these interactions are described explicitly in Sections 2.3.3, 2.4, 3.6, 4.7, 4.8, and 5.3.4.

This section (1.5.6) has described the minerals that make up sedimentary petroleum-bearing rock but not the complex formations themselves. Some aspects of sandstone and carbonate formation rock are in Chapter 3. More details of petroleum geology and geochemistry are in Holstein (2007), McCarthy et al. (2011), and Alexander et al. (2011). A short description of some shale formations is in Section 4.1.

1.5.7 Preview of Reaction Chemistry of Minerals. The processes described in this book involve both homogeneous and heterogeneous chemical reactions. Review Section 1.5.1 as the equations (such as Eq. 1.29) will apply to this section.

For homogeneous reactions (in a single phase), the rate of the reaction to form a product C (in Eq. 1.50) is:

$$\frac{d[C]}{dt} = k_r [A]^m [B]^n \dots \dots \dots (1.50)$$

Here, k_r is the reaction rate coefficient and the exponents denote the order of the reaction, which can be fractions or whole numbers. The temperature dependence of k_r is given by

$$k_r = A \exp\left(\frac{-E_a}{RT}\right) \dots \dots \dots (1.51)$$

Here, A is called the pre-exponential term and E_a is the activation energy term, and both depend on the individual reactions.

Heterogeneous reactions such as the dissolution of solids or other reactions at various surfaces can be more complex. The dissolution of solids is important in acidizing and solids removal as well as for other reactions at a surface. The dissolution rates and the amount of solid that can be dissolved (capacity) of solids vary greatly depending on the composition of the solid, morphology, the composition of the solvent, as well as the temperature of the fluid at the point of contact.

The overall rate of dissolution (and thus the time needed to remove a given amount of the solid) depends on

- The surface reaction rate (SRR) between minerals being dissolved in the solvent chosen.
- The surface area of contact.
- Mass transport (including diffusion) of solvent or reaction products.
- Solvent concentration and amount.
- Composition and structure of the solid itself (morphology).

Further, the overall rate of reaction is influenced by the limiting reactant, which could be the solvent or the solid. If the solvent is in far excess, then the overall rate will be favored in the forward direction and is far from equilibrium.

The SRR varies by many orders of magnitude from very reactive couples such as HCl reacting with calcite (Hill and Schechter 2001; Lund et al. 1975) to barium sulfate reacting with ethylenediaminetetraacetic acid (Eylander et al. 1998). The SRR also depends on the temperature and frequently on the concentration of the solvent; however, some solvents, such as chelating agents may display an essentially zero order dependence on concentration. The SRR may be the slowest part of the overall process or transport may be the slowest step. Complete dissolution of a solid frequently follows an S-shaped curve (also called sigmoid) where the rate is low initially and increases dramatically as the solid opens up and the surface area, on which the solvent acts, increases dramatically, then slows as the solid is depleted. Additional information on solids dissolution is in Section 3.3 and typical rate curves will be shown in Section 3.5.3.

1.6 Injecting Fluids Into the Earth

Most of the processes and treatments described in this book have one characteristic in common: fluids are injected into the ground through various types of tubing. Then, usually, the fluids flow into underground geologic formations. Chemical reactions produce various products that change portions of the formation either physically and/or chemically. Subsequently, the reaction products and the hydrocarbons and brines flow to the surface through the production tubing. On emerging from the wellhead, the fluids go through gathering lines and surface/subsurface treating facilities before going to additional locations. The reactions that are taking place will be affected by the tubing, the fluid dynamics, and by the rock matrix. Thus, the processes involve flow and reactions in porous media as well as flow and reactions in various devices with higher diameters than the capillaries in the rocks.

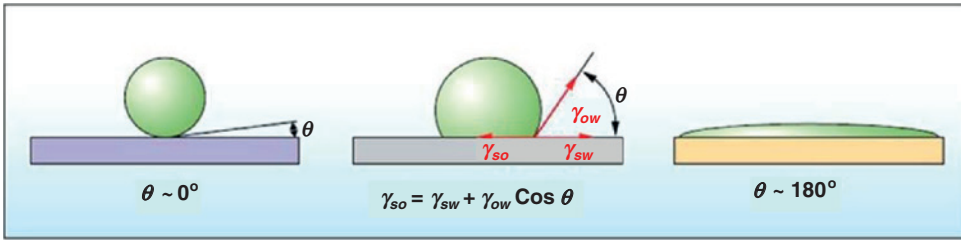


Fig. 1.34—Wetting angles of water/oil/mineral surface (Abdallah et al. 2007).

In this section, we will discuss several general principles with specifics delayed until later chapters. In Section 1.6.1, the authors of this book will describe how the chemistry and physics of surfaces affects a great number of processes and services performed in oil and gas production that apply both to solids and liquids. Section 1.6.2 describes equations and conditions for pumping fluids in the tubing and in the porous media. Section 1.6.3 describes the applications of solid-state mechanics to the geological formations and Section 1.6.4 provides a qualitative overview to mobility control during production enhancement operations.

1.6.1 Surface Chemistry, Wetting, and Nonwetting Surfaces. The chemistry and physics of surfaces affects a great number of processes and services performed in oil and gas production and apply both to solids and liquids. In Section 1.5.6, we noted that the chemistry of a mineral may affect reactivity. The surface of any solid or liquid is an interface between that medium and some other that could be a solid, liquid, or a gas. The chemistry of the interface is affected by both surfaces. In one example (Fig. 1.34), a drop of oil is placed on a solid surface in a jar of water. The forces at that surface (IST, γ) is caused by the cohesion of the molecules in that surface and depends on the molecules in both surfaces.

Therefore, it is not a property of the liquid alone but of the liquid’s interface with another material. In Fig. 1.34, the surface (on the left) is covered with a water film (it is hydrophilic) and the oil drop is repelled and the contact angle (θ) is close to 0° . In the middle case, the surface is partially oil wetting, and in the right figure, the surface is completely oil wet and the oil droplet spreads out on the surface.

If a liquid is in a container (such as a pipe or tank), then there will be a liquid/air interface at its top surface and there is also an interface between the liquid and the walls of the container. The IST between the liquid and air is usually different than its IST with the walls of a container. Where two surfaces meet, the consequence must also be such that all forces are in balance. As noted above, where the two surfaces meet (and 3 phases), they form a contact angle, θ , which is the angle that is tangent to the surface that meets with the solid surface. Fig. 1.35 shows an example of solid, liquid, and gas interfaces. Here, tension forces (f) are shown for the liquid-air interface, the liquid-solid interface, and the solid-air interface. Both the vertical and horizontal forces must cancel exactly at the contact point. The horizontal component of f_{la} is canceled by the adhesive force, f_A .

$$f_A = f_{la} \sin \theta. \dots\dots\dots (1.52)$$

The other balance of forces is in the vertical direction. The vertical component of f_{la} must exactly cancel the force, f_{ls} .

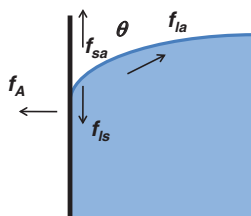


Fig. 1.35—Forces at surfaces.

TABLE 1.1—CONTACT ANGLE VALUES SOLID LIQUID (SEARS AND ZEMANSKI 1955) CONVERTED TO OILFIELD CONVENTION

| Liquid | Solid | Contact Angle |
|----------------------|-----------------|---------------|
| Water | | |
| Ethanol | | |
| Diethyl ether | Soda-lime glass | |
| Carbon tetrachloride | Lead glass | 180° |
| Glycerol | Fused quartz | |
| Acetic acid | | |
| Water | Paraffin wax | 73° |
| | Silver | 90° |

TABLE 1.2—IST OF VARIOUS LIQUIDS IN AGAINST AIR (DEAN 1961)

| Liquid | Temperature (°C) | IST, γ (dyne/cm) |
|--|------------------|-------------------------|
| Acetic acid | 20 | 27.6 |
| Acetic acid (40.1%) + water | 30 | 40.68 |
| Acetic acid (10.0%) + water | 30 | 54.56 |
| Acetone | 20 | 23.7 |
| Diethyl ether | 20 | 17.0 |
| Ethanol | 20 | 22.27 |
| Ethanol (40%) + water | 25 | 29.63 |
| Ethanol (11.1%) + water | 25 | 46.03 |
| Glycerol | 20 | 63 |
| <i>n</i> -Hexane | 20 | 18.4 |
| Hydrochloric acid 17.7M aqueous solution | 20 | 65.95 |
| 2-proponal | 20 | 21.7 |
| Methanol | 20 | 22.6 |
| <i>n</i> -Octane | 20 | 21.8 |
| Sodium chloride 6.0M aqueous solution | 20 | 82.55 |
| Sucrose (55%) + water | 20 | 76.45 |
| Water | 0 | 75.64 |
| Water | 25 | 71.97 |
| Water | 50 | 67.91 |

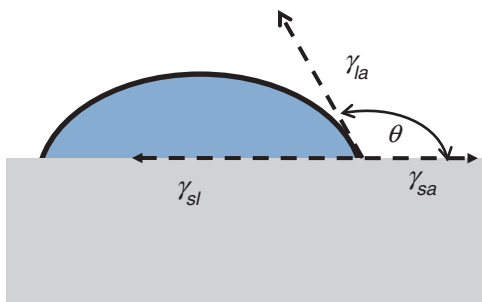
$$f_{ls} = f_{sa} + f_{la} \cos \theta \dots \dots \dots (1.53)$$

Because the forces are in direct proportion to their respective surface tensions, we also have

$$\gamma_{ls} = \gamma_{sa} + \gamma_{la} \cos \theta, \dots \dots \dots (1.54)$$

where γ_{ls} are the liquid-solid IST, γ_{sa} is the solid-air IST, and γ_{la} is the liquid-air IST. This is known as Young’s equation.

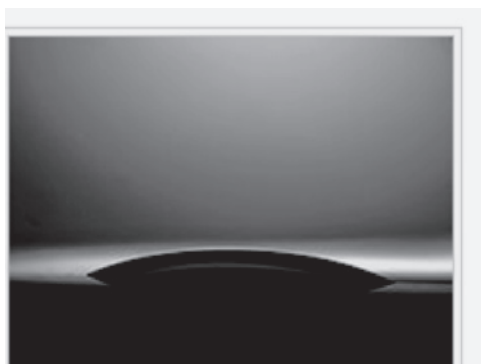
Table 1.1 lists some contact angle data for common fluids. **Table 1.2** shows some IST values for a number of liquids with air. The values of the contact angles and the IST control many of the properties of processes that will be described in subsequent chapters. Note in Table 1.2 that the IST of pure water is much higher than solutions of ethanol and water. Many surface active agents (surfactants) also lower the IST of water and thus affect the contact of water with surfaces. The convention used in the oil and



(a) Illustration of sessile drop method with liquid droplet partially wetting a solid substrate



(b) Water droplet immersed in oil resting on a brass surface



(c) Water droplet immersed in oil resting on a glass surface

Fig. 1.36—Sessile drop method showing examples of wetting and nonwetting conditions.

gas industry is that a near 180° contact angle indicates that the liquid will spread (wet) on that surface. The reader should note which convention is being used when comparing data, as some conventions call wetting with a 0° contact angle.

The contact angle and IST can be measured in several ways. The sessile drop method is illustrated in **Fig. 1.36a**. Here a drop of liquid is seen after it has been placed on a surface in air, and the three IST vectors are seen. The contact angle (θ), can be measured visually by taking a photograph of the surface, usually using a microscopic device. See Howard et al. (2010) for a specific example. Figs. 1.36b and 1.36c illustrate the importance of the solid surface itself. In these examples, a water drop has been placed on two surfaces in an oil medium. When brass (**Fig. 1.36b**) is the solid, the water does not displace the oil; while in (**Fig. 1.36c**) on glass, the water does displace the oil and wets the surface.

This (**Fig. 1.36**) also illustrates a possible caution when interpreting literature information because either the acute or the obtuse angle could be reported. If water is used to test the wetting of a surface, low numbers refer to a hydrophilic surface and high values refer to a hydrophobic surface. Also see Tadmor (2004).

The IST of a liquid vs. air can be measured using a Du Nouy ring manual method (**Fig. 1.37**). This is the traditional method used to measure surface or interfacial tension. Wetting properties of the surface or interface have little influence on this measuring technique. Maximum pull force exerted on the platinum (Pt) ring by the surface is measured (PHYWE 2004). The most important experimental issues are using very clean equipment and fire cleaning the Pt ring used in the test.

Another method especially suited to check surface tension over long time intervals is the Wilhelmy plate method that is described in **Fig. 1.38**. A vertical plate of known perimeter is attached to a balance, and the force caused by wetting is measured. This method uses the interaction of a test plate with the liquid being tested. BiolinScientific (2009) describes one instrument that uses this method. The calculations for this technique are based on the geometry of a fully wetted plate in contact with but

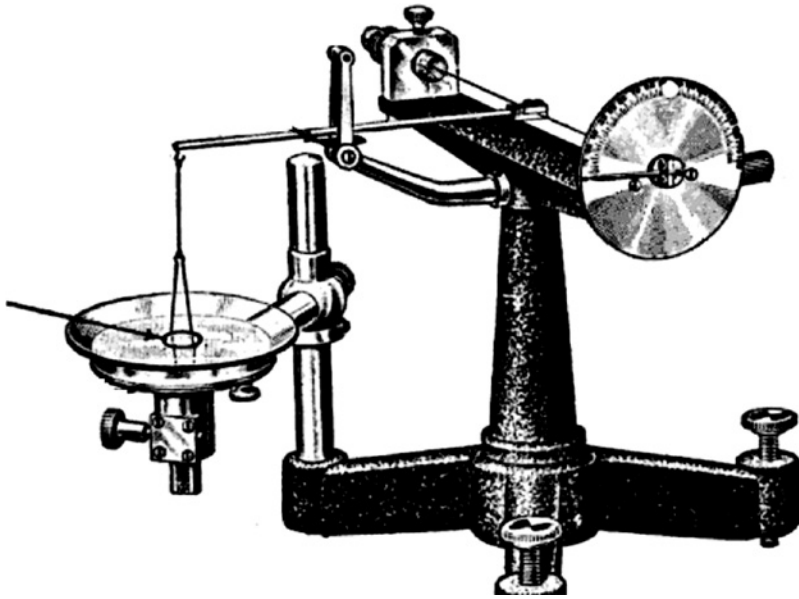


Fig. 1.37—Du Noüy ring (Wikipedia 2010g).

not submerged in the liquid phase. In this method, the position of the probe relative to the surface is significant. As the surface is brought into contact with the probe the instrument will notice this event by the change in forces it experiences. It will register the height at which this occurs as the ‘zero depth of immersion.’ The plate will then be wetted to a set depth to ensure that there is indeed complete wetting of the plate (zero contact angle). When the plate is later returned to the zero depth of immersion, the force it registers can be used to calculate surface tension. See Eq. 1.55.

$$\gamma_{la} = \frac{F}{2l \cos\theta}; l = 2w + 2d \dots \dots \dots (1.55)$$

A number of important properties and uses of production chemicals are related to wetting and capillary forces during pumping in the formation. Howard et al. (2010) explains that both the Laplace and Washburn equations can be of importance (Grattoni et al. 1995). The Laplace (Pierre-Simon,

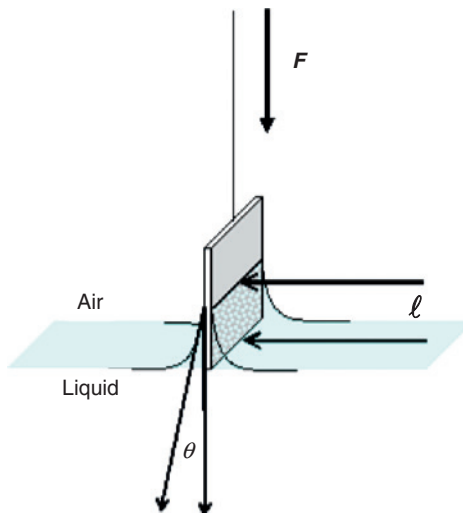


Fig. 1.38—Wilhelmy plate method.

marquis de Laplace, 23 March 1749–5 March 1827) equation (Eq. 1.56) relates capillary pressure (the difference between the phase pressures of a nonwetting (P_2) and a wetting phase (P_1) such as water and oil, P_c) to surface tension, γ , and contact angle, θ . Here r is the radius of a capillary tube, L is the height of the fluid rise in the tube, ρ is the density of the fluid, and g is the gravitational acceleration (980 cm/sec²).

$$(P_2 - P_1) = P_c = L\rho g = 2\gamma \cos\theta/r. \dots\dots\dots (1.56)$$

To evaluate wetting of two fluids in the same geometry, the ratio of two Laplace equations can be used. For example, using water (w) and a solution with unknown (u) properties:

$$L_w \rho_w g = 2\gamma_w \cos\theta_w / r, \dots\dots\dots (1.57)$$

and

$$L_u \rho_u g = 2\gamma_u \cos\theta_u / r. \dots\dots\dots (1.58)$$

Dividing one by the other and removing constants gives

$$\frac{L_u}{L_w} = \frac{\gamma_u \cos\theta_u}{\gamma_w \cos\theta_w} \dots\dots\dots (1.59)$$

The Washburn equation (Washburn 1921) relates that the rate of capillary rise is also an important relationship, such as in an imbibition test (wetting fluid displacing nonwetting fluid). The method of Grattoni et al. (1995) gives:

$$M^2 = (A^2 \rho^2 \alpha \gamma t \cos\theta) / 2\eta. \dots\dots\dots (1.60)$$

In Eq. 1.60, the area A and the term α relating to the structure of the core (α) have replaced the r term in the Laplace equation (Eq. 1.56). M is the mass of fluid imbibed into the core and η is the fluid viscosity. Time is t . Plotting M^2 vs. time should give a straight line as the limit of the Laplace equilibrium is approached. The slope of the line is related to core terms (A and α) and fluid-property terms ($\gamma \cos\theta$). Capillary forces increase linearly with the inverse of pore size; so, they are much more important in lower-permeability reservoirs. These equations are important for understanding EOR (Section 5.1.1) as well as the use of flowback aids in tight gas fracturing (Section 4.7.2) (Howard et al. 2010).

1.6.2 Pumping and Flow of Fluids in the Tubing and in Porous Media. During the well treatments that will be reviewed in this book, various (and complex fluids) will be transported through the surface equipment, then through the well tubing and finally into the earth. After the treatments are complete, the well fluids and treatment reaction products will be returned through part of the subterranean formations, through the well equipment and then to the surface. These present very different flow regimes. In the man-made part of the production environment, the diameter of the tubing and production equipment may range from about 3 cm to about 20 cm.

In the formation, the fluid will be subjected to flow in a porous media. The pore-throat sizes in siliciclastic rocks form a continuum (Nelson 2009) from the sub millimeter to the nanometer scale. The author notes that the pore-throat sizes (diameters) are generally greater than 2 μm in conventional reservoir rocks but range from about 2 to 0.03 μm in tight-gas sandstones, and range from 0.1 to 0.005 μm in shales.

Two different transport regimes can be described by different models of the inflow (in the formation) and the outflow (in the piping) are covered in detail (with the equations) in Section 1.2. From the previous definitions and equations in that section, we can see that, for a given flow rate (Eq. 1.16), the pressure drop is proportional to $1/D^4$ for laminar flow, and for turbulent flow in a smooth pipe, the pressure drop is proportional to $1/D^{4.75}$. Hence, any reduction in effective pipe diameter caused by deposit

buildup can lead to a drastic increase in pressure drop and hence a similar decrease in the production from the reservoir.

We also note that the viscosity is a transport properties (see Section 1.5.4). For comparisons, it is useful to note that Eqs. 1.44–1.46 have elements that are similar to Ohm’s law:

$$\Delta V = IR, \dots \dots \dots (1.61)$$

where V is voltage, I is current, and R is resistance.

Once the fluid enters the formation with many small flow paths, it would be very difficult to describe the flow using the Hagen–Poiseuille law (Eq. 1.16). See illustrations of a porous media and the possible flow paths in **Figs. 1.39 and 1.40**. Flow in porous media at laminar velocities can be described by the Darcy relationships (Eqs. 1.2 through 1.5). This is a simple proportional relationship between the instantaneous discharge rate through a porous medium, the viscosity of the fluid, and the pressure drop over a given distance. It was developed using empirical experiments (Darcy 1857) but can be developed also from first principles (Whitaker 1986). The major determinants of flow at a given pressure drop are thus, viscosity of the fluids and the permeability (κ), which is a very complex characteristic of the formation. Formation enhancement engineers, viscosity, and Δp are the only controllable

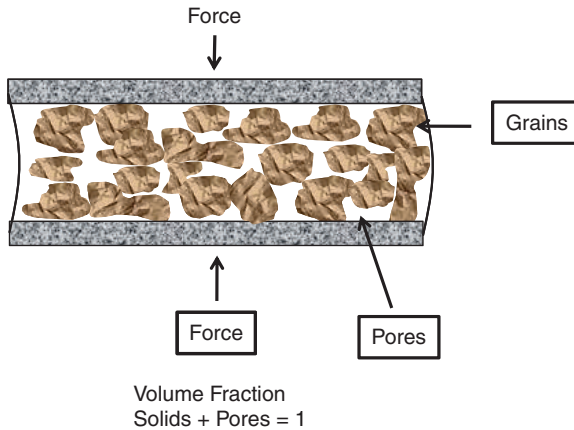


Fig. 1.39—Porous media.

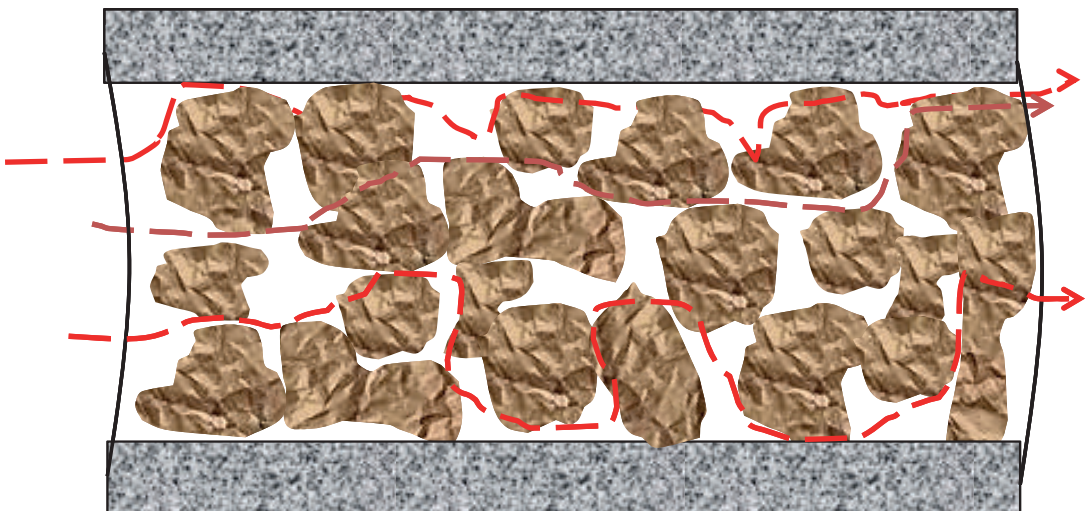


Fig. 1.40—Flow in porous media.

parameters for affecting penetration of the formation. When fluids are returned to the surface, Darcy's equations also will apply as long as laminar flow is present.

In some high flow situations including HF and production from high flow wells, non-Darcy conditions results in turbulent flow. Because most of the turbulent flow takes place near the wellbore in producing formations, the effect of non-Darcy flow is seen as a rate-dependent skin effect in Eq. 1.8.

The flow and reactions in oil and gas formations have many similarities with microreaction technologies (MRT) that are in wide use to scale up bench-type processes to production plant systems. Wiles and Watts (2010) claim that because of the excellent heat and mass transfer, and predictable flow properties exhibited by MRT systems a high degree of reaction control is attainable. These systems frequently are produced using a plate (materials compatible for the reactions) 40 μm deep and up to 100 μm wide and are thus, similar to some rock dimensions. Surface wetting is a similar issue as in formation improvement reactions. The large difference is that the "reactor" in the earth may become part of the chemistry, while the MRT systems usually are inert. See also the book by Wiles and Watts (2011).

1.6.3 Reservoir Geomechanics. Geomechanical analyses of the stress state in the reservoir and surrounding formations are necessary to enable operators to predict how drilling, stimulation, production, and injection of fluids will affect the field. Injection of fluid into the formation causes mechanical changes as well as chemical changes. A few geomechanical concepts are presented that are necessary to understand aspects of HF that are conducted above the fracture pressure. The other treatments such as matrix treatments and IOR are performed at pressures below the fracture pressure, but the flow in the matrix will still be determined by the pressures acting on the fluids and it is still necessary to know the fracture pressure to avoid unwanted cracking of the formation.

Some of these concepts below are abstracted from Thiercelin and Roegiers (2001). They note that important aspects of rock mechanics can be used to characterize the mechanical behavior of reservoirs and adjacent layers (Fig. 1.41), as applied to the stimulation process. The mechanical properties of solids and liquids described in Section 1.5.3 are applied to the subterranean solid structures. They (Thiercelin and Roegiers 2001) claim that the general state of *stress* underground expressed by the



Fig. 1.41—Depiction of geologic layers (Schlumberger 2009a).

three principal stresses axes (σ_x , σ_y , and σ_z) are unequal. For tectonically relaxed areas characterized by normal faulting, the minimum stress should be horizontal. More details are in Section 4.1. Other formations will be more complex (also see Section 4.1.1).

To know how much pressure to apply to produce a fracture, knowledge of the stress/strain response of a solid is required. From the simple diagrams of a porous medium such as seen in Figs. 1.39 and 1.40, it is assumed that the pore spaces are filled with a fluid (gas or liquid) and the medium is being confined by the overburden of the pressure of the earth.

When a rock specimen or an element of the earth is subjected to a load, it deforms; the higher the stress level, the more strain the rock experiences. It is an important aspect of rock mechanics, and solid mechanics in general, to determine the relationship between stress and strain. Note that these same concepts apply to fluid flow (Section 1.5.5).

The slope of the stress-strain curve at any point is called the tangent modulus. The tangent modulus of the initial, linear portion of a stress-strain curve is Young’s modulus (E) (see Eq. 1.39), this is also known as the tensile modulus. It is defined as the ratio of the uniaxial stress over the uniaxial strain in the range of stress in which Hooke’s Law holds. It is also a measure of the stiffness of an elastic material and is a quantity used to characterize materials. It can be experimentally determined from the slope of a stress-strain curve (B) created during tensile tests conducted on a sample of the material.

Also when a rock specimen is compressed in one direction, not only does it shorten along the loading direction, but it also expands in the lateral directions. This effect is (Poisson’s ratio, ν), which is defined as the ratio of lateral expansion to longitudinal contraction. See Eq. 1.40. Eq. 1.41 also applies to formation rocks. Thiercelin and Roegiers (2001) point out that another coefficient that is commonly used is the bulk modulus K , which is the coefficient of proportionality between the mean stress σ_m and volumetric strain ϵ_v during a hydrostatic test. In such a test, all three normal stresses are equal, and, consequently, all directions are principal. For this case:

$$K = \frac{E}{3(1-2\nu)} \dots \dots \dots (1.62)$$

Pore fluids (and thus the pore pressure) in the reservoir rock play an important role because they support a portion of the total applied stress. Hence, only a portion of the total stress, namely, the effective stress component (σ), is carried by the rock matrix (Fig. 1.39 and Fig. 1.42). Also, we note that the effective stress changes over the life of the reservoir. In addition, the mechanical behavior of the porous rock modifies the fluid response.

Fracture Mechanics. Thiercelin and Roegiers (2001) state that fracture mechanics studies the stability of preexisting defects that are assumed to pervade a continuum of the formation. These inclusions induce high stress concentrations in their vicinity and become the nucleus for crack initiation and/or propagation. The approach presented by them states that the energy that is consumed by the creation of new surfaces should be balanced by the change in the potential energy of the system:

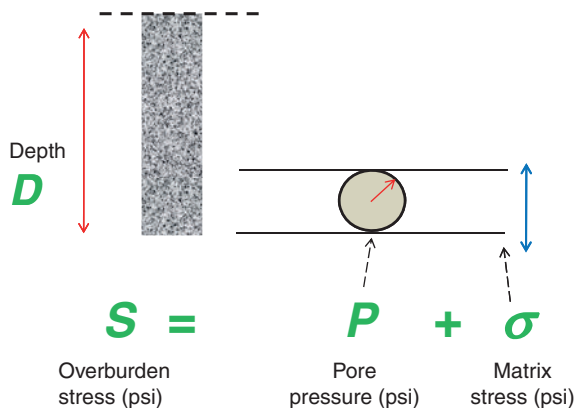


Fig. 1.42—Formation pressure and matrix stress.

$$0 = dW_{elas} + dW_{ext} + dW_s + dW_{kin}, \dots \dots \dots (1.63)$$

where dW_{elas} represents the change in elastic energy stored in the solid, dW_{ext} is the change in potential energy of exterior forces, dW_s is the energy dissipated during the propagation of a crack, and dW_{kin} is the change in kinetic energy. Energy dissipated as heat is neglected. They (Thiercelin and Roegiers 2001) also assume that the energy dW_s required to create the new elementary fracture surfaces, $2dA$, is proportional to the area created:

$$dW_s = 2\gamma_f dA. \dots \dots \dots (1.64)$$

Here, γ^F is the fracture surface energy of the solid, which is the energy per unit area required to create new fracture surfaces (similar to the surface tension of a fluid). The factor 2 comes from a consideration that two new surfaces are created during the separation process. They (Thiercelin and Roegiers 2001) claim that the propagation of the fracture is unstable if the kinetic energy increases; thus, $dW_{kin} > 0$ gives:

$$G_e > 2\gamma_f, \dots \dots \dots (1.65)$$

where the strain energy release rate G_e is defined as:

$$G_e = -\frac{d(W_{elas} + W_{ext})}{dA}. \dots \dots \dots (1.66)$$

The onset of crack propagation, which is referred to as the Griffith criterion (1921), is

$$G_e = 2\gamma_f. \dots \dots \dots (1.67)$$

The fracture gradient is defined as the pressure required for inducing a fracture in rock at a given depth and is an important value for drilling, injection of fluids, and for HF. Fig. 1.42 shows a diagram of formation pressure and matrix stresses. Important values are the depth, the overburden stress, the matrix stress, and the pore pressure. The overburden stress depends on the rock type and usually varies from about 0.8–1.1 psi/ft (Eaton 1969).

Eaton (1969) developed a method of predicting formation fracture gradients (F , in psi/ft), where it was found that overburden load, Poisson’s ratio (γ) for rocks, and pressure gradients vary with depth. Although the method was developed specifically for the Gulf Coast, the author claims it is reliable for all areas, provided that the variables reflect the conditions in the specific area being considered. The equation developed (using the terms in Fig. 1.42) is

$$F = \left(\frac{S - P}{D} \right) x \left(\frac{\gamma}{1 - \gamma} \right) + \frac{P}{D}. \dots \dots \dots (1.68)$$

An alternative equation is

$$F = \left(\frac{K_i \sigma}{D} \right) + \frac{P}{D}. \dots \dots \dots (1.69)$$

This is from Matthews and Kelly (1967), and K_i is the matrix stress coefficient and σ is the vertical matrix stress in psi (see Fig. 1.42). Note that this uses the concept of a variable horizontal-to-vertical stress ratio (K_i). This is determined graphically.

Fracture Pressure. Thiercelin and Roegiers (2001) note that the in-situ stress, and in particular the minimum in-situ stress, σ_c (the term used for the fracture closure pressure for nonhomogeneous zones,) is the *dominant parameter* controlling fracture geometry. Thus, for many relaxed geologic environments, the minimum in-situ stress is generally horizontal, and thus, vertical fractures formed when a vertical wellbore broke remains vertical and is perpendicular to this minimum stress.

The result is that hydraulic fractures are always perpendicular to the minimum stress, except in some complex cases (more details of fracture geometries are in Section 4.1.2). This occurs because that is the least resistant path for the fluids. The result is that opening a fracture in any other direction requires higher pressure and more energy. The minimum stress controls many aspects of the value of the minimum stress. At typical reservoir depths, the fracturing pressure is a strong function of the minimum stress (or closure pressure). An engineer must know the magnitude of the minimum in-situ stress for the pay zone and over- and underlying zones and in some cases must know the direction for the three principal stresses. For a simple, relaxed geology with normal pore pressure, the closure stress is typically between 0.6 and 0.7 psi/ft of depth (true vertical depth). More generally, the minimum stress is related to depth and reservoir pressure by (Smith and Shlyapobersky 2001):

$$\sigma_c \cong K_o (\sigma_v - p_r) + p_r + T, \dots \dots \dots (1.70).$$

where K_o is a proportionality constant related to the rock properties of the formations (possibly to both the elastic properties and the faulting or failure properties), σ_v (equivalent to S in Fig. 1.42) is the vertical stress from the weight of the overburden, p_r is the reservoir pore pressure, and T accounts for any tectonic effects on the stress (for a relaxed, normal fault geology, T is typically small). K_o is typically about 1/3. Note an example a fracture gradient of 0.7 psi/ft [0.15 kPa/m] in a well with a true vertical depth of 8,000 ft [2440 m] would predict a *fracturing pressure* of 5,600 psi [38.6 MPa].

1.6.4 Mobility Control. Control of the direction and volume of the fluids injected into the 3D matrix is of great concern in almost all of the production enhancement services. In acidizing, this control is frequently called diversion or placement. In the other services, such as fracturing and EOR the term, mobility control is used for processes that direct or frequently impede the flow of fluids into specific zones of the formation. If fluids are pumped without control (termed bullhead) the volume that enters a particular zone will be determined only by the Darcy equations (Eqs. 1.2 and 1.3). The determining control values that are available to the engineer are usually only pressure (p), volume of fluid and viscosity (μ) since the permeability (κ) and well radius (r) depend on the formation zone and the well configuration. Less frequently, temperature may also be a control variable.

Preplanning of the construction of the well can have a very great influence on distribution of the fluids by controlling the direction, number, and size of perforations. Selection of screens and other “smart” downhole devices also can be very useful. However for older wells, the engineer can usually only use devices such as balls, packers and coil tubing for mechanical control (described in Section 3.7). Many chemical techniques that selectively (in time and space) control the viscosities (and chemical reactivates) of various fluids become the very hearts of the treatment processes that will be described in Chapters 2 through 5. The fluid developers are always trying to produce smart fluids that will react in a predictable manner to produce a desired change in a controllable property. As noted this usually is viscosity, but also, a change in temperature or the production/dissolution of solids or gasses may be used to affect a useful change. While many chemical changes can be affected using catalysts, encapsulating agents (or other effects not now known), the knowledge of the chemistry and physics of the formation/fluids at a particular location in the earth frequently is not known with the precision needed to have adequate control. As geochemical monitoring processes improves so will the control of the injected fluids.

1.7 Treating Equipment on the Wellsite

The idea that small chemical plants are created, processes are performed in the earth, and then the equipment is moved to a new site requires an examination of the equipment and how it is used to perform these operations. Chemist and chemical engineers routinely mix chemicals in precise proportions and in set sequences, and then apply specific temperatures, flow rates, and contact with surfaces (frequently catalysts) to produce new chemical compounds. Similar unit operations take place in the various processes that will be described in this book, but the engineers have much less control of the

variables. Never the less, chemical are mixed, pumped, and heated (usually by the earth) and new chemical species are produced. The mixing and pumping is done at the wellsite (and as the fluids descend or return through production tubing) using a remarkable assortment of portable equipment. Most of the examples below are from land-based operations, but the same sort of operations are performed offshore using special work boats as well as using rig-based equipment. The chemicals used and the chemistry performed must be able to be effective under *continually* changing conditions of temperature, pressure, shear and surface contact as the fluids go from the surface into the reservoir (and then back to the surface). It is very important to note that treatments are performed from the arctic to the equator, on land and at sea and from urban to impenetrable forest environments. The equipment and chemicals must be adjusted to them. Important requirements include the following mechanical requirements.

1.7.1 Transportation and Storage. Depending on the size and type of the treatment, equipment ranging from single trucks, through multiple transports and large tanks that are called frac tanks, may be required at the wellsite. For examples see Schlumberger (2004a), Fig. P.1 as well as the illustrations in Sections 4.1 and 4.3. Usually onshore, all chemicals, including water, many pounds of chemicals, and tons of sand (for frac jobs) must be transported and stored. Water is of particular concern because a domestic (or otherwise purified) water source is rarely available; the water must be transported to the site and stored. Water quality also may greatly affect some of the necessary reactions, so testing is required and the chemistry may be adjusted. While insulated or heated, tanks may sometimes be available, the water temperature usually will reflect the local ambient temperature at the time of the treatment. All of this equipment has to be transported to the job site (frequently over unimproved roads) and then assembled. Several of the important engineering steps are noted. For some types of treatments, onsite storage of concentrated or mixed chemicals must be provided.

1.7.2 Mixing. With the exception of small reactive chemical (acid) treatments, chemicals are frequently mixed on site. Small amounts of dry or liquid additives may be mixed in line or with the use of skid-mounted mixers. For larger jobs, mobile units with very large mixing and hydrating (for polymers) capabilities may be required. For examples see Schlumberger (2004a), Fig. P.1 as well as the illustrations in Sections 4.1 and 4.3. Depending on the treatment, the mixed chemicals may be stored temporally or directly injected into a stream for transport into the well.

1.7.3 Pumping. The mixing stage requires pumps and tanks, but the most important pumping equipment is that which is designed for injecting the fluids into the well. For matrix treatments (with fluid injected at rates below the frac pressure and into the NWB region), pumpers such as seen in [Fig. 1.43](#), may be adequate. These types of units use diesel motor-driven centrifugal pumping units.



Fig. 1.43—Pumper for matrix acid and cement placement (Halliburton 2006).



Fig. 1.44—Portable high pressure frac pump (Schlumberger).

This type of equipment is capable of providing flow volumes up to about 400 gal/min at pressures up to approximately 10,000 psi. Some mixing and storage capabilities frequently are present, but additional fluid storage also could be used.

For fracture stimulation applications, many different types of high pressure pumping units are in use. **Fig. 1.44** shows one type of high pressure (20,000 psi) triplex pumper. These pumps are positive displacement, piston units that can also handle large volumes of slurries of chemicals and proppants. For especially large jobs, groups of pumps may be needed (described later).

For IOR or other types of chemical treatments, the polymers, surfactant, or additional chemical must be dissolved in the treatment brine (or hydrocarbon fluids) and then injected. This can be accomplished using a mixing tank or the equipment described in Schlumberger (2004a), Fig. P.1 as well as the illustrations in Sections 4.1 and 4.3. For the actual injection, SNF (2010) recommends the use of small progressive cavity pumps for their easy maintenance and low shear. These pumps are optimized for the needed injection pressure and flow rate. Because of the very large number of different chemical treatments, specialized storage, mixing, and pumping equipment will be provided depending on the pressures, volumes, and flow rates required. All of the equipment must be compatible with the corrosivity, viscosity, and other physical and chemical properties of the fluids.

1.7.4 Material Requirements—Metallurgy of Treating Iron and Pressure Hoses. To assemble our minichemical plants, we may need hundreds of feet of piping and hoses to connect the equipment together and then to the wellhead.

- The treating iron metallurgy usually consists of carbon steel and alloy steel and needs to be lightweight. This integral treating iron described below is capable of handling a variety of fluids at cold working pressure of 15,000 psi. They are also available for sour service up to a critical working pressure of 10,000 psi and in other lengths if required. See **Fig. 1.45**. Treating iron (not hoses) with hammer unions for connections are much safer and are preferred on the high pressure side of all treatments. They must be able to withstand the pressure, abrasiveness, and possible corrosivity of the fluids.
- Appropriate hoses that are needed to connect equipment are frequently also in use. Multilayer, braided chemical resistant hoses should be used, especially for acid service (the manufactures require rinsing to neutral pH after acid service).

1.7.5 Wellsite Placement and Control. Our chemical plant is finally assembled at the wellsite and the job is being executed. For examples see Schlumberger (2004a), Fig. P.1 as well as the illustrations in

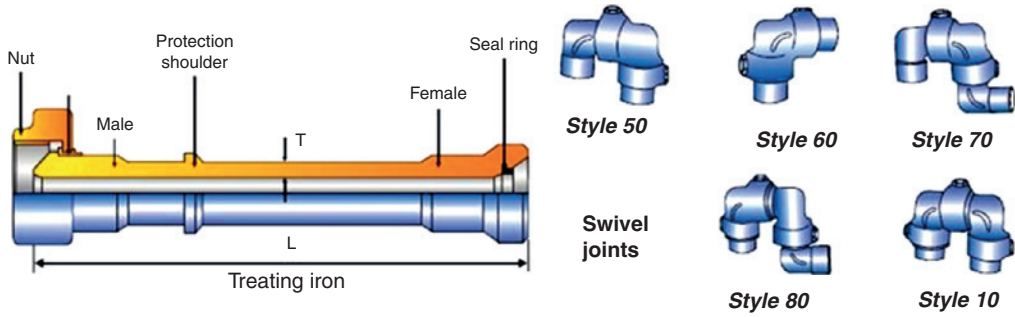


Fig. 1.45—Treating iron ACT (American Completion Tools 2010).

Sections 4.1 and 4.3. In these many pumps and massive amounts of water and chemicals will be on the site. In some jobs as much as 5,000,000 lbs of proppant could be pumped. Note that several control vans may be used to monitor and coordinate the equipment and the people. In some cases, a coil tubing rig (Fig. 1.46) is used to convey the treating fluids to a specific zone in the formation.

The wellsite during any treatment, but especially a massive hydraulic fracture can be a very hazardous place. Large numbers of people from different companies and trades are involved in high pressure operations involving potentially hazardous chemicals. So, planning, command, and control is essential. A number of health, safety, and environmental concerns that apply to work during chemical treatments are considered in Chapter 6.

Offshore, chemicals, and some pumping capacity may be provided by a specially designed work boat. See an example of a service boat at an offshore wellsite in Bigorange (2010).

1.7.6 Heat/Cooling. As Eqs. 1.50 and 1.51 demonstrate, the rates of chemical reactions are partially controlled by the temperatures at which they are conducted. Each reaction has a characteristic

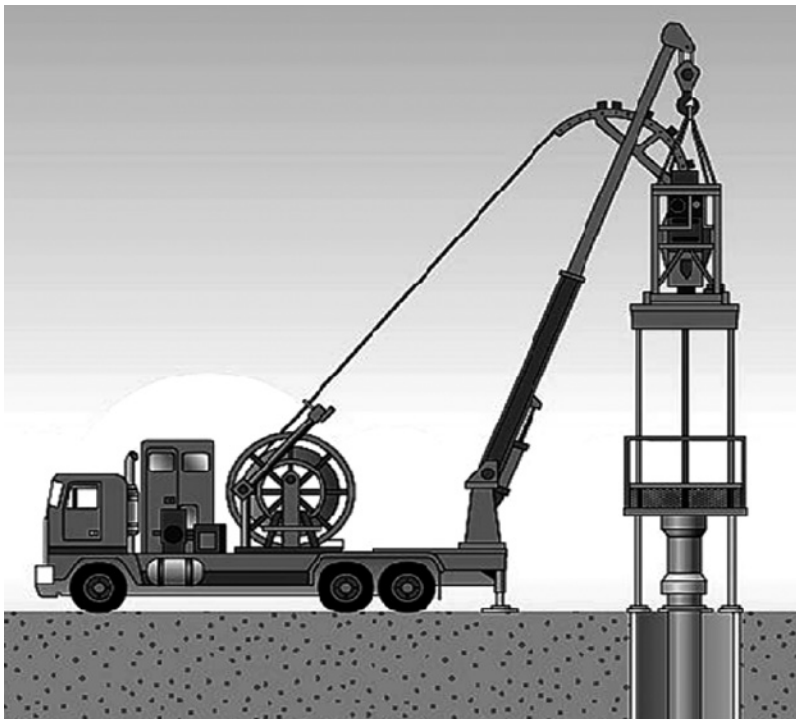


Fig. 1.46—Coil tubing rig.

activation energy (E_a) associated with it, and the rate may be increased or decreased in accordance with this value. In a controlled environment, engineers and chemists use this knowledge to control the reaction to give a desired product. In well treatments, the great heat capacity of the earth will dictate the reaction temperature environment. Therefore, the developers of the treatment must design the chemicals to be appropriate for the expected temperatures and to take advantages of the changes that will take place. Usually, the fluids will be initially colder than the formation, and the temperature will increase during the treatment until all of the fluid is at the temperature of the formation.

Some manipulation of temperature is possible by pumping fluid slugs to cool the formation and the treating pipe. Occasionally, “hot oilers” may be employed to heat the treatment zone and exothermic chemical reactions may also be employed. However, the engineers usually employ heat transfer equations to estimate the temperature based on the fluid mass pumped and the heat flux from the rock.

1.7.7 Rig Down and Disposal of the Flowback Fluids. After a treatment has been pumped and any shut-in time has expired, the well will be “turned around” and flowback of the fluids will commence. These fluids will be quite different than the injected fluids. Acids may be reacted, polymer fluids will be broken and the viscosities will have changed. In addition, the fluids may be contaminated by flammable and toxic well fluids (and gasses such as H_2S). Adequate tankage must be available to store the fluids until they can be transported for disposal or recycle. See Section 6.3.2. Some jobs will have many stages and the character of the fluids may change and there may be a need to segregate them.

Ultimately, the well will clean up, the equipment will be disassembled and transported to a new site. Hopefully good planning and execution will result in an improvement in the well’s productivity.

1.7.8 Evaluation of the Treatment. The logs from a treatment, production logs, and frequently, samples of the returned fluids can be used to evaluate the treatment and to propose needed improvements.

The following chapters describe how various stimulation, enhancement, and maintenance treatments use complex chemistry that is applied using mostly temporary equipment in the oil and gas production environment. Chapters 3 and 4 cover subjects that are usually called stimulation while Chapter 5 describes chemical IOR methods.

1.8 Electronic Sources of Oilfield Chemistry Information

Electronic/digital sources of information are available from many locations. To locate, review, and ultimately source the many books and published information that are cited (in the text) a number of information databases were used by the authors of this book. The most used sources of information are listed. Note that there are many others and organizations such as NIST (2012) that provide databases of scientific databases. Also, there are a variety of access controls (some at no cost to members, others at various prices) to obtain the electronic documents, but usually, the abstracts and detailed citations can be downloaded without charge.

- Society of Petroleum Engineers: Connects to a number of petroleum-related sites. <http://www.onepetro.org>
- NACE International: Corrosion/scale-related publications and standards. <http://www.NACE.org/>
- Elsevier: A variety of scientific journals: <http://www.elsevier.com/>
- American Chemistry Society: A variety of chemical-related journals. <http://portal.acs.org/portal/acs/corg/content>
- American Institute of Chemical Engineers: Several engineering/chemical journals. <http://www.aiche.org/>
- Wiley online library: <http://onlinelibrary.wiley.com/>
- Chemical Abstracts: One of the world’s largest search services. <http://www.cas.org>
- Petroleum Abstracts: Petroleum-related search service. <http://www.pa.utulsa.edu/>

- Google Scholar: Searches technical and patent documents. <http://scholar.google.com>
- US Patent Office: No-cost search/access of USPO issued and applied patents. <http://patft.uspto.gov>
- European Patent Office: No cost search/access of European/World issued and applied patents. www.epo.org
- *Schlumberger Oilfield Review*: Reviews of selected oilfield technologies. (http://www.slb.com/resources/publications/oilfield_review.aspx)
- Mineralogy database: Lists information on thousands of minerals. (<http://www.webmineral.com/>)

Chapter 2

Chemistry of Production Impairment

This chapter describes many of the causes of impairment of the production of hydrocarbons as well as some of the methods for eliminating or inhibiting these processes. Short segments (in Section 2.2) also reprise and update discussion in previous books by the current authors on the formation and treatment of inorganic and organic deposits (Frenier and Ziauddin 2008; Frenier et al. 2010). These short discussions are included in this book because these types of fouling deposits affect many processes described in later sections of the current publication. These include the formation of emulsions as well as problems during EOR operations. This chapter will also describe the types and mechanisms of formation damage. The various types of damage (Section 2.3), especially in the near wellbore (NWB), are frequently treated and relieved by the use of chemicals as well as through the various stimulation treatments described in Chapters 3 and 4. The current chapter also will describe (in Section 2.4) the formation and treatments for emulsions that form in the flow paths and that especially impact the functioning of surface equipment. These materials are greatly affected by the solids described in Section 2.2.

2.1 Introduction to Production Impairment Processes

A large number of individual chemicals as well as a very large quantity of chemicals are used in various processes to help maintain the flow of petroleum products after they leave the formation. These include corrosion and scale inhibitors, inhibitors for wax, asphaltenes, naphthenates, and hydrates. A major category of production chemicals are those designed to prevent/resolve emulsions, as well as surfactants and solvents for spill cleanup. A significant number of chemicals (some of which will be described in Chapter 3 as part of stimulation treatments) are also in use to dissolve/disperse inorganic and organic solids. These dissolution processes are described in much more detail in Frenier and Ziauddin (2008) and Frenier et al. (2010).

The production from an oil/gas field can be severely impaired if scale or organic deposits from anywhere from the NWB matrix and in the tubulars leading from the reservoir to the sales point. Scale in the NWB area leads to a skin described in Eq. 1.8. The deposition in tubulars reduces the diameter of the tubular available for flow and can, therefore, choke the production from the reservoir. The additional pressure drop caused by deposit buildup in the tubulars can be quite large. The pressure drop relationship to the flow rate for single-phase pipe flow is given Eqs. 1.13 and 1.16. The reader can also review Sections 1.2 and 1.6.2.

In Eq. 1.16, L is the length of the pipe, D is the pipe diameter, ρ is the fluid density, f is the friction factor and u is the average fluid velocity defined as $u = 4q/(\pi D^2)$, where q is the volumetric flow rate. For laminar flow, the friction factor is defined as $f = 16/\text{Re}$, where Re is the Reynolds number. For turbulent flow in a smooth pipe, $f = 0.079/\text{Re}^{0.25}$. Note that the definition of the Reynolds number, $N_{\text{Re}} = 4q\rho / (\pi D\mu)$.

In this relationship, μ is the fluid viscosity. From the previously mentioned definitions and equations, we can see that, for a given flow rate, the pressure drop is proportional to $1/D^4$ for laminar flow,

and for turbulent flow in a smooth pipe, the pressure drop is proportional to $1/D^{4.75}$. Hence, any reduction in effective pipe diameter because of deposit buildup can lead to a drastic increase in pressure drop and hence a similar decrease in the production from the reservoir.

Excessive pressure drops in the NWB and tubulars can hinder the ability to flow reservoir fluids to the point of sale. The term flow assurance (FA) is often used in the oil industry to describe such issues. Brown (2002) describes FA as the “production operation that generates a reliable, manageable, and profitable flow of fluids from the reservoir to the sales point.” FA is especially critical for deepwater assets. Because of limited access to the seafloor infrastructure in deepwater assets, blockages in tubulars caused by deposit formation may lead to expensive workovers and sometimes prohibitively so (Brown 2002). Comprehensive reservoir fluid characterization is essential to every aspect of FA. The pressure/volume/temperature characteristics; analysis of saturates, aromatics, resins, asphaltenes, paraffins, and naphthalene; water chemistry; and drilling-mud characteristics are required for development of an asset. An adequate number of high-quality reservoir fluids samples are required to determine the economic risk boundaries within which the reservoir, wells, risers, and flowlines, and the process must operate to avoid FA problems.

Some of the consequences of skin and tubing blockages were described in Section 1.2.1. In addition, Fig. 2.1 presents a general depiction of formation of deposits in a producing well. Here various types of scale and organic solids are shown, including iron, calcium, and possibly barium scale deposits as well as asphaltenes and wax deposits. The blowup shows a proposed sequence of deposition. Because most production tubing and lines are constructed from ferrous alloys, the first layer usually will be an iron oxide. Inorganic scales (usually calcite or barium sulfate) readily can be deposited onto the iron oxide.

Organic solids such as asphaltenes and or waxes will deposit on or mix with the inorganic scale. The authors of this book contend that mixed deposits, especially in the tubulars, are the rule rather than the exception, and all types of deposits must be addressed in a successful FA program. More details of the formation of organic as well as mix deposits are described in Frenier et al. (2010) and the subjects are also reviewed briefly in Sections 2.2.4 and 2.3.3 of the current book.

Typical activities involved in FA studies are shown in Fig. 2.2. The rectangles are process steps and the ovals represent additional activities or outcomes. As seen from Fig. 2.2, FA involves the combination of production chemistry and multiphase flow. A key first step in any FA study is the collection

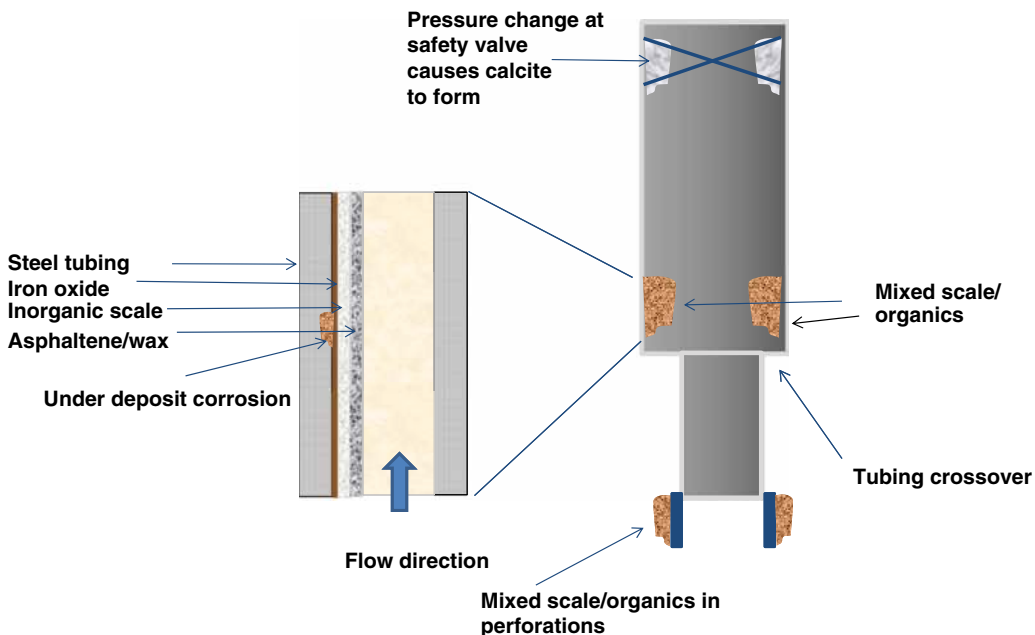


Fig. 2.1—Scale and organic solids formation in a well.

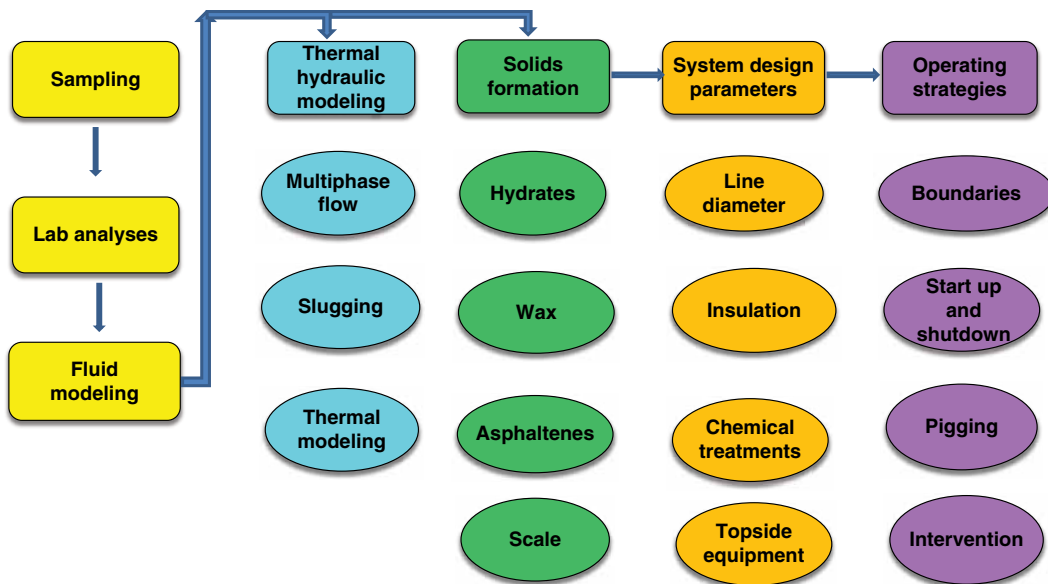


Fig. 2.2—Best practice for FA in mixed deposit environment (courtesy of Chevron).

of a representative fluid sample. The ideal sample would be collected contamination-free from the reservoir at constant temperature and pressure and transported intact to the laboratory, maintaining both temperature and pressure. In practice, this is probably not possible today. A more realistic goal is to reduce the potential for phase changes through pressure and potentially temperature compensation. FA studies based on unrepresentative samples may lead to overdesign or underdesign of production facilities, both of which can be costly to remediate later. The authors of this book contend that this *cannot* be overemphasized.

After collection, care must be exercised to preserve the integrity of samples during transportation to the laboratory and while at the laboratory. Once the samples arrive in the laboratory, preliminary phase behavior and solids screening is done after reconditioning of the samples to an appropriate pressure and temperature environment. Depending on the type of inorganic scale, organic deposits expected, wax content, pour point, wax appearance temperature (WAT); saturate, aromatic, resin, and asphaltene analysis; asphaltenes onset determination; and hydrate formation analyses may be performed. Inorganic scaling and emulsion studies also may be performed. Measured data from appropriate sources are then used in numerical simulations of the phenomena and entire process to predict the severity of probable FA issues in the field. This will be done considering the forecast production profile for a given asset to be developed and for various operating conditions. The results help optimize the design of production system, export lines, pigging frequency, pigging type, effective insulation, injection facilities, slugging, shut-in and startup, inhibition and so on. A final validation of numerical simulation results may be made with further experimental studies on an as-needed basis. Details of these experiments, simulations, and strategies are described in various sections of Frenier and Ziauddin (2008) and Frenier et al. (2010).

Very brief discussions of the formation of inorganic scale are in Section 2.2.2 of the current book and organic deposits are described in Section 2.2.4. These descriptions are included in this book because these types of deposits also impact formation damage (Section 2.3) and the formation of emulsions that are considered in Section 2.4. That section will also discuss methods (mechanical and chemical) to resolve the emulsions.

2.2 Organic and Inorganic Deposits

This section gives a brief review of the formation of inorganic and organic deposits. These types of solids have a significant effect on many of the chemistries described in the subsequent chapters as well as on the emulsions described in Section 2.4 of this chapter and are the cause of much of the formation damage

discussed in Section 2.3. More details of the mechanism and control of the various deposit types are available in Frenier and Ziauddin (2008) and Frenier et al. (2010). Sections 2.2.3 and 2.2.5 of this current book also describe new developments in inorganic scale and organic deposit control technologies.

2.2.1 Why and Where Inorganic Scale and Organic Deposits Form. Before a well is drilled and completed, the fluids in the formation are in equilibrium with their surroundings. However, when the well starts to flow, the equilibrium is disturbed and solids may start to precipitate. Inorganic deposits are called scales [see Fig. 2.3 for a photo of gypsum scale (a) and calcite scale (b) in tubing] and organic deposits are further referred to as waxes (saturated hydrocarbons) or asphaltenes (unsaturated and cyclic hydrocarbons).

Additional types of organic fouling solids include naphthenates, diamondoids, and clathrate gas hydrates. Any of these materials can precipitate in the formation, in the NWB region, perforations, tubulars, on downhole completion equipment, and in surface equipment such as gathering lines, separation equipment, and pipelines. An important but overlooked source of scale is corrosion. The iron produced because of corrosion of the tubular materials and surface equipment provides the cations for formation of iron carbonate, iron oxide, and iron sulfide scales. The corrosion process also can damage the equipment and cause a failure and loss of product to the environment.

Organic deposits such as those formed from organic solids (primarily waxes, asphaltenes, clathrate hydrates, and naphthenates) can cause interruption in flow in piping as well as formation damage. A photograph of wax blocking tubing is in Fig. 2.4. In the subsea production environment (which is most important for new large scale developments), tube blockages caused by formation of clathrate

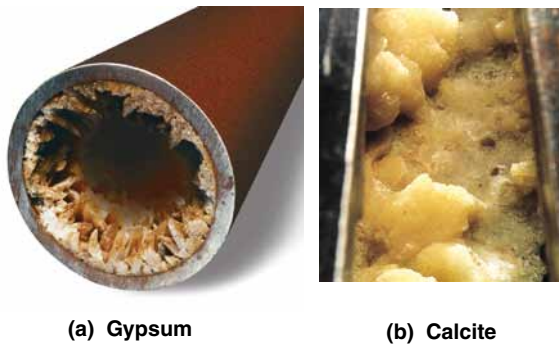


Fig. 2.3—Tubing fouled with gypsum scale and calcite scale (Crabtree 1999). Courtesy of Schlumberger.



Fig. 2.4—Wax in a tubing.

gas hydrates is thought (opinion of the authors of this book) to be the major cause of FA problems. Paraffin deposition also is a critical issue in this area because the seafloor temperature of about 4°C is below the WAT of most crude oil streams.

Wherever the precipitates form, flow can be reduced to varying degrees and may even cause abandonment of the well. Fig. 2.5 shows a depiction of formation scale that is blocking the spaces in the formation matrix. The formation of the fouling deposits can be minimized by mechanical means or by addition of “inhibitors.” The conditions that allow scale or organic solids to form can be predicted, but the exact location where deposition does form is more difficult to determine. After the deposits have formed, various chemical and mechanical methods can be employed to remove them. Because both acidizing and fracturing may be applied to bypass formation damage a short review of formation damage mechanisms (including inorganic solids scaling) is in Section 2.3.

2.2.2 Formation of Inorganic Deposits. Inorganic scales are minerals that form on a surface because of the saturation of the local environment with an inorganic salt. The major categories of scales are as follows: carbonates [Ca(II), Mg(II), Fe(II)]; sulfates [Ca(II), Ba(II), Sr(II), Ra(II)]; oxides and hydroxides [Fe(II), Fe(III), Mg, Cu(II)]; sulfides [Fe(II), Cu(II) and Zn(II)]; and silicates [Ca(II), Mg(II), Al(III) and Na(I)]. Table 2.1 gives a summary of common inorganic scale forming compounds. A previous book, Frenier and Ziauddin (2008), describes more details of the scale forming process. A more comprehensive list of scaling deposits found in industrial water is described in Table 1.1a of Cowan and Weintritt’s 1975 (revised in 2004) review of scale and deposit literature. This book (Cowan and Weintritt 2004) covers many aspects of scaling and scale prevention.

Debris is defined as any collection of material that forms elsewhere and is transported to a surface where it may cause a disruption in flow and/or heat transfer. Thus, debris is a “mobile” scale. The problem of migration and pore plugging caused by formation “fines” is an example of debris damage. Some of the basic information on scale formation comes from the cooling water literature, where it is difficult to separate corrosion inhibition from scale inhibition. This is also true of the oilfield environment where corrosion of tubulars and surface equipment contributes to the production of iron-containing scale.

Prediction of scaling tendencies can be accomplished if the composition of the water downhole is known with a high degree of accuracy. One of the first methods for estimating scaling tendencies was developed by Langelier (1988) and used thermodynamic and empirical values to calculate the saturation index or scaling index (SI) of the water and, thus, predict the scaling tendency of the water source.

A calculation useful for prediction of possible problems for saturated solutions is the saturation ratio (SR): A generalized equation for any salt solution is

$$SR = \{M^{z+}\}^m \{X^{z-}\}^x / K_{sp} \dots \dots \dots (2.1)$$

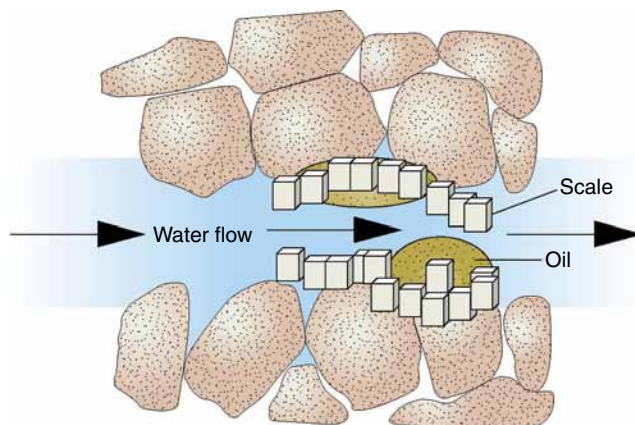


Fig. 2.5—Depiction of scale blocking formation pores (Crabtree et al. 1999).

TABLE 2.1—SUMMARY OF COMMON INORGANIC SCALE FORMING COMPOUNDS

| Mineral Name | Common Name | Chemical Formula |
|-------------------|-----------------------------------|--|
| Acmite | Sodium iron silicate | NaFe(SiO ₃) ₂ |
| Analcite | Sodium aluminum silicate | NaAlSi ₂ O ₆ ·H ₂ O |
| Anhydrite | Calcium sulfate | CaSO ₄ |
| Aragonite | Calcium carbonate-rhombic | CaCO ₃ |
| Barite | Barium sulfate | BaSO ₄ |
| Brucite | Magnesium hydroxide | Mg(OH) ₂ |
| Calcite | Calcium carbonate-hexagonal | CaCO ₃ |
| Chalcocite | Copper sulfide | Cu ₂ S |
| Chalcopyrite | Copper iron sulfide | CuFeS ₂ |
| Chromite | Iron chromium spinels | CrFe ₂ O ₄ |
| Copper | Copper | Cu |
| Covellite | Copper sulfide | CuS |
| Cuprite | Copper oxide | Cu ₂ O |
| Gibbsite | Aluminum hydroxide | Al(OH) ₃ |
| Goethite | Hydrous ferric oxide | FeOOH |
| Gypsum | Calcium sulfate dehydrate | CaSO ₄ ·2H ₂ O |
| Halite | Salt | NaCl |
| Hematite | Ferric oxide | Fe ₂ O ₃ |
| Hydromagnesite | Magnesium carbonate and hydroxide | 3MgCO ₃ ·Mg(OH) ₂ ·3H ₂ O |
| Hydroxyapatite | Calcium phosphate | Ca ₁₀ (OH) ₂ (PO ₄) ₆ |
| Mackinawite | Iron sulfide | Fe _x S _y |
| Magnesia | Magnesium oxide | MgO |
| Magnetite | Ferric-ferrous oxide | Fe ₃ O ₄ |
| Magnesite | Magnesium carbonate | MgCO ₃ |
| Montmorillonite | Aluminum silicate | Al ₂ O ₃ ·4SiO ₂ ·4H ₂ O |
| Noselite | Sodium aluminum silicate | Na ₆ Si ₂ O ₇ O ₂₄ ·H ₂ O |
| Pyrite | Iron sulfide | FeS ₂ |
| Pyrolusite | Manganese dioxide | MnO ₂ |
| Pyrrhotite | Iron sulfide | FeS ₂ |
| Serpentine | Magnesium silicate | Mg ₃ Si ₂ O ₇ ·2H ₂ O |
| Siderite | Iron carbonate | FeCO ₃ |
| Silica | Quartz | SiO ₂ |
| Silica, amorphous | Hydrated silica | SiO ₂ ·2H ₂ O |
| Sodalite | Sodium aluminum silicate | Na ₈ Al ₆ Si ₆ O ₂₄ ·2Cl |
| Wüstite | Ferrous oxide | FeO |

Here, M represents the activity (noted by the braces) of any cation, while X represents the activity of an anion. Also m is the number of the cations with a charge z^+ and x is the number of the anions with a charge of z^- . K_{sp} is the solubility product of the solid salt (see Frenier and Ziauddin 2008). The saturation ratio for a salt measures the degree of its supersaturation. Precipitation can only occur when $SR > 1.0$.

Much of the art and science of prediction of scaling involves calculation of the real SR in complex brines. The log (SR) is called the saturation index (SI). This is a convenient designation with small numbers. Various correlations are available in the literature for estimating SI in terms of easily measurable quantities such as pH, alkalinity (Alk), and concentration of dissolved ions and ionic strength of the fluid. For example, the saturation index from Stiff and Davis (1952) is calculated

$$SI = pH - k - pCa^{2+} - pAlk \dots \dots \dots (2.2)$$

In this equation, that only applies to the supersaturation of calcium carbonate, Ca^{2+} is the concentration of the dissolved calcium and Alk is the measured alkalinity (a titration) that is a general measure of the bicarbonate (HCO_3^-) concentration. Many other empirical saturation indices have been used in various industries to predict scaling conditions. See Davies and Scott (2006) and Frenier and Ziauddin (2008).

Under the best of conditions, scaling and corrosion can be controlled with minimal use of chemicals if pH, $[\text{Ca}^{2+}]$ and $p[\text{CO}_2]$ are tightly controlled. This approach is very difficult to achieve in practice, so various scale and corrosion inhibitors (CIs) are also employed. Carbonate scales form in the NWB region, in fractures, sand packs, screens, downhole equipment, and tubulars, and on surface equipment. The mixing of incompatible waters (such as seawater and formation water) when the solubility product of a salt is exceeded in a local environment usually causes sulfate scales. These are found in most of the same environments as carbonates (though usually not at the same time) but are not seen frequently in surface equipment. This type of scale can form in the matrix, in the perforations, screens, tubing, and connections lines. Of particular concern is scale formation in electrical submersible pumps (ESP), where these deposits can cause a pump failure (MacDonald and Engwall 1983). Another example is fouling of injection wells because of placement of seawater into an incompatible formation. Barium sulfate scale is a particularly important scale formed from mixing incompatible water because it is very difficult to redissolve (Frenier and Ziauddin 2008).

Iron-based scale forms caused by the reaction of a corrosive fluid with any iron-containing metal (tubulars, surface equipment) and is followed by precipitation of an insoluble salt. Examples are hydrous iron oxides (rust), found in tubulars and surface equipment, magnetite (Fe_3O_4) in boilers, iron sulfide in NWB regions and tubulars of sour wells and iron carbonate found in sweet wells. A book by Becker (1998) reviews some additional details of the chemistry of scale and corrosion. The book by Byars (1999) also covers many details of corrosion of iron alloys in oil and gas production equipment that are beyond the scope of the current discussion.

Crabtree et al. (1999) proposed a mechanism of formation of the most common types of inorganic scale including calcium carbonate and alkaline earth sulfate deposits. These are categorized as salt formers. Although the driving force for scale formation may be a temperature or pressure change, outgassing, a pH shift, or contact with incompatible water, many produced waters that have become oversaturated and scale-prone do not always produce a fouling scale.

For a scale to form, it must grow from solution. The first development within a saturated fluid (see discussion of Eq. 2.1 in the previous paragraphs) is a formation of unstable clusters of atoms, a process called homogeneous nucleation. Fig. 2.6 depicts this process from supersaturation to formation of ion pairs to the final deposition of a crystal. The final part of the process is deposition of scale crystals on a surface. This part of the process can occur coincidental to nucleation and crystal growth or subsequent to the first two steps. Fig. 2.7 shows microscopic views of some incipient BaSO_4 scale crystals. Deposition onto a surface is frequently the most damaging process (for FA), but mobile solids also can plug the formation as well as filters and may affect other processes such as the stability of emulsions (see Section 2.4.1).

Processes to control inorganic scale include dissolution chemistries that are in Sections 3.1.3 and 3.4 of this book. As noted in those sections, matrix stimulation of producing formations, as well as the cleanout of the tubulars is the major reason for doing a reactive fluid stimulation. A wide range of CIs and inhibitors for preventing mineral scales are in use and many are placed in the formation using acidizing and fracturing methods. Details are in Frenier and Ziauddin (2008) and a short update is in Section 2.2.3 of this book.

2.2.3 New Developments in Inorganic Scale/Corrosion Control Technology. This section supplements and updates discussions of the literature on inorganic scale and corrosion control methods that were described in Frenier and Ziauddin (2008). The emphasis of this section (2.2.3) is on the use and new developments of production stage CIs and scale inhibitors. This is a large and growing industry and is of very great importance to the efficient production of hydrocarbons, FA, and environmental protection. A short section also will review the use of downhole water quality sensors that may aid in prediction scale formation or corrosion.

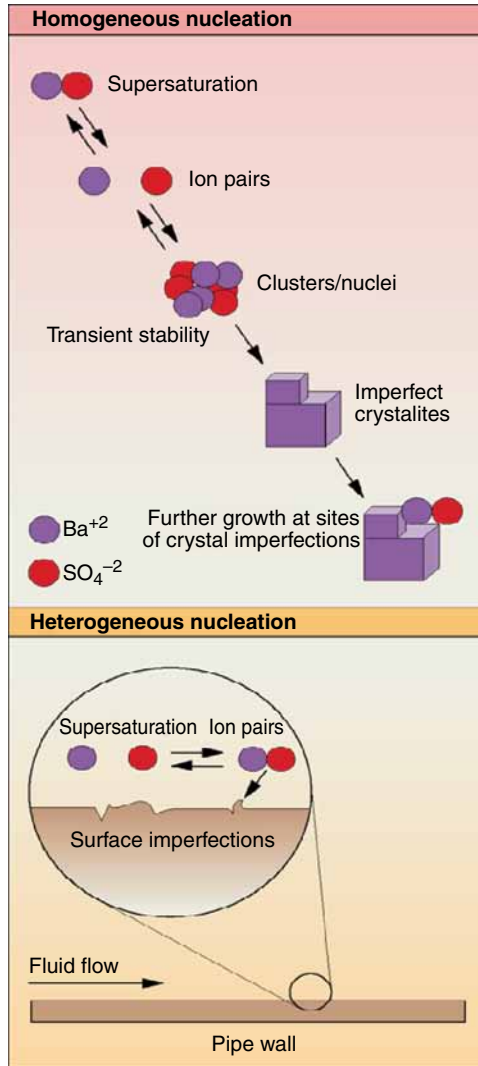


Fig. 2.6—Formation mechanisms of inorganic scale (Crabtree et al. 1999).

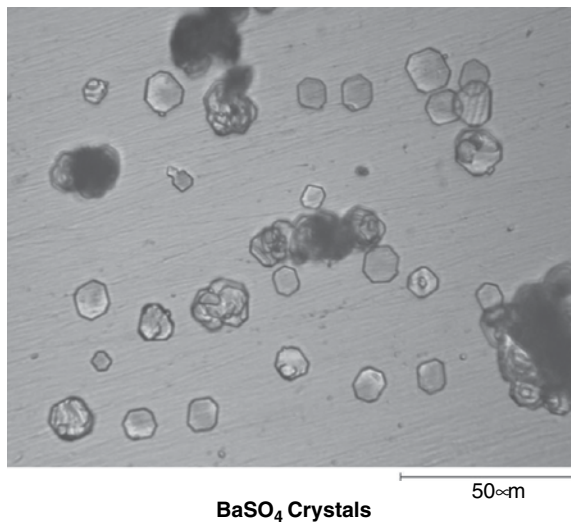
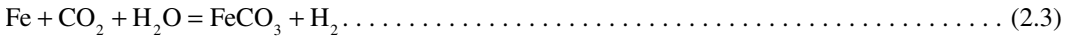


Fig. 2.7—Barium sulfate crystals (Graham et al. 2004).

As noted in the previous section (2.2.2), scale control and corrosion control can be intertwined. The formation of iron-based scale itself can cause flow problems, but the corrosion process may also cause the well tubing or transfer lines to perforate and leak large quantities of hydrocarbons (Isidore 2006). This is frequently initiated by a scale deposit (the process called underdeposit corrosion) and the formation of a pit. As the diagram of a corrosion pit (Fig. 2.8) shows, the corrosion product causes the pit bottom to be anodic to the surface and, thus, accelerates the loss of metal. The right side of this figure shows a large pit with scale and thinning of the tube wall.

Acid gases that include CO₂ and H₂S, as well as natural short-chain organic acids (such as acetic acid) provide the oxidizing agents (H⁺ ions, see Eqs. 2.3 and 2.4). Much more information on corrosion in oil and gas production is described in Byars (1999), Becker (1998), Fontana (1986), and Uhlig (1971). Heidersbach (2011) has a very useful chapter (8) on Oilfield Equipment that reviews specific corrosion risks in various types of oilfield units such as drilpipe, wellheads, and well tubulars. The other chapters in his book are concerned with general aspects of corrosion and control including inhibitors, cathodic protection, and coatings. Several specific scale/corrosion processes are noted in the subsequent paragraphs as part of the current review.

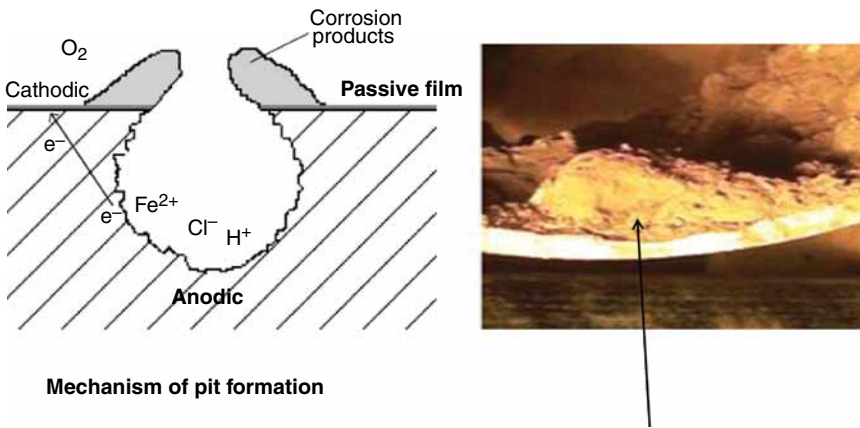
Siderite is a scale produced primarily by a corrosion product reaction in the presence of CO₂. The formation reaction is



Note that this is an acidic corrosion reaction because iron is dissolved and hydrogen gas (H₂) is evolved. This scale can be protective when it forms initially on the surface. Natural CIs in the crude oil as well as added materials influence the thickness of the scale and the protection provided by it (see discussions in Section 2.2.3). Siderite placed in carbonate-free water is extremely insoluble but pH and other gases greatly change the overall solubility.

The corrosion produced by the reaction in Eq. 2.3 can cause very severe damage to unprotected steel exposed to CO₂ and aqueous oilfield brines. A significant leak, such as that which occurred in a flowline to a structure such as the Alaskan pipeline (Isidore 2006) can cause a major shutdown and loss of product to the market.

Zhang et al. (2011) has studied the corrosion and inhibition of steel in supercritical CO₂ [used for CO₂ enhanced oil recovery (EOR), see Section 2.2.3] and found very high corrosion rates for carbon steel even at 80°C. While some of the inhibitors shown in “Production Phase Corrosion Inhibitor Chemistry” were somewhat effective in reducing the corrosion rates, the authors of the paper recommend using 13-Cr steel in contact with aqueous-supercritical fluids. Because these fluids are commonly used in EOR projects, corrosion and siderite scale prevention must be a consideration of the production engineers.

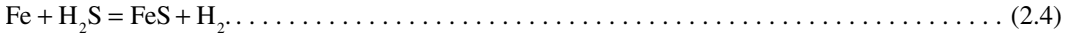


Iron scale in a pit and thinning tube wall

Fig. 2.8—Corrosion pit and scale.

If any H₂S is present, corrosion by this acid gas and formation of iron sulfides can occur. As noted in Section 2.2.4 of Frenier and Ziauddin (2008), iron sulfides can be formed in a number of different ways. If a well has sour fluid, a corrosion reaction is the most likely method for forming iron sulfide scale.

The net corrosion reaction is



It is also noted in that reference (Frenier and Ziauddin 2008) that a number of different iron sulfide species can form that include mackinawite, pyrrhotite, and pyrite. These minerals have different crystal structures as well as different ratios of Fe/S. The first two solids are soluble in HCl, but pyrite is very insoluble. The type of solid formed is controlled by the ratios of the partial pressures of CO₂/H₂S as well as the time of exposure. See the discussions in the cited book (Frenier and Ziauddin 2008) as well as in Smith and Pacheco (2002) and Dunlop et al. (1985).

Wells that are on CO₂ EOR treatments (see Section 5.5) may have both corrosion and precipitations from FeS, FeCO₃, CaCO₃, and alkaline earth sulfates. The species formed will depend on the various equilibrium present. Note that EOR treatments can cause major changes in the chemistries of the formation, so the operators should be prepared for different scales and blockages in the production and the injector wells. Singer et al. (2007) have looked at the combined effects of H₂S, CO₂, and acetic acid on corrosion of steel and precipitation of FeS and FeCO₃. Fig 2.9 shows the phases that exist under different conditions and note that that if any H₂S is present, it takes a lot of CO₂ to suppress the sulfide formation (the “sweet regime” in the graph).

Sun (2006) has shown that as the pH becomes less than about 4.0, the formation of FeS may be suppressed, depending on the amount of CO₂ present in the fluid, the amount of H₂S, and the [Fe]. Because of the changes in the ratios of the partial pressures during production, the precipitation of FeS as well as calcite may still be present at different places in the fluid paths.

The carbonate/sulfide scales may be partially protective, and the corrosion rates depend on the composition of the crude oil [note that there are natural surfactants that have nitrogen and sulfur moieties that are similar to some synthetic CIs. See structures in Section 2.2.4 of this book as well as in Frenier et al. (2010)]. The composition of the corrosive gases are also critical as well as the composition of the brine. Therefore, the need for and the selection of a production inhibitor as well as the placement of the material requires a significant amount of testing, chemistry, and engineering. Details are beyond the scope of this book, but the authors will review several recent trends. Additional information is in Palmer et al. (2004) as well as in specific references cited in this section.

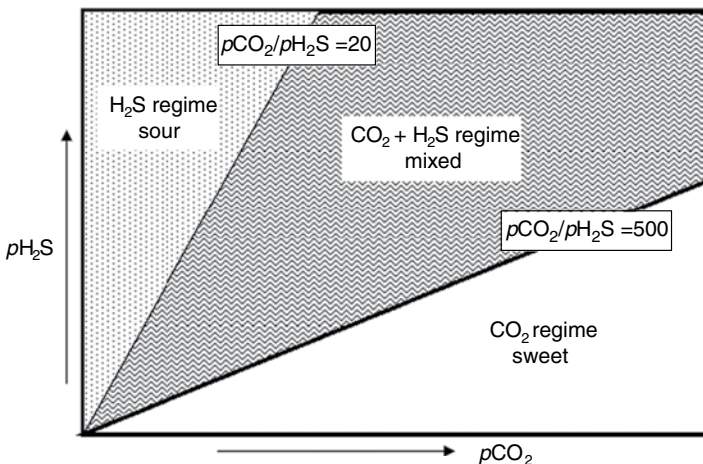


Fig. 2.9—Corrosion/precipitation regimes for FeS and FeCO₃ (Singer et al. 2007).

Alkaline earth mineral scales (calcite, barite, and anhydrite) can be inhibited using scale inhibitor molecules described in Frenier and Ziauddin (2008). Several new developments on the use of these materials are in Sections 2.2.4 and 2.2.3.

Production Phase CI Chemistry. A large number of inhibitors (Kelland 2009; Fink 2011) are claimed to be effective in protecting steel from corrosive, acidic well fluids (salt brines containing CO_2 , H_2S , and natural organic acids). The list of chemical types have included imidazolines, amines, and quaternary ammonium compounds (Schmitt and Labus 1994; Jayarman and Saxena 1996) and organic esters of phosphoric acid. Typical inhibitor structures are shown in Fig. 2.10.

Additional inhibitors include coco dimethyl benzyl ammonium chloride, salted aminoethyl fatty imidazolines, and alkyl pyridinium ammonium chloride. Some of these materials may be used in acid inhibitor formulations described in Section 3.6.1. A larger list of the various types of production CIs are in Fink (2003), Fink (2011), and Kelland (2009). Useful references also are in Raman and Labine (1993) and Kuron (1995).

While these chemicals are effective as CIs, many of these compounds are toxic to marine (and other) organisms. Because a lot of oil and gas come from offshore sources and the inhibitors become part of the produced fluid as it emerges from the well, the effect of the inhibitors on marine life has become a major concern of governments worldwide and this is a major theme of the inhibitor literature. Many additional molecules have been proposed in recent years to produce more environmentally friendly

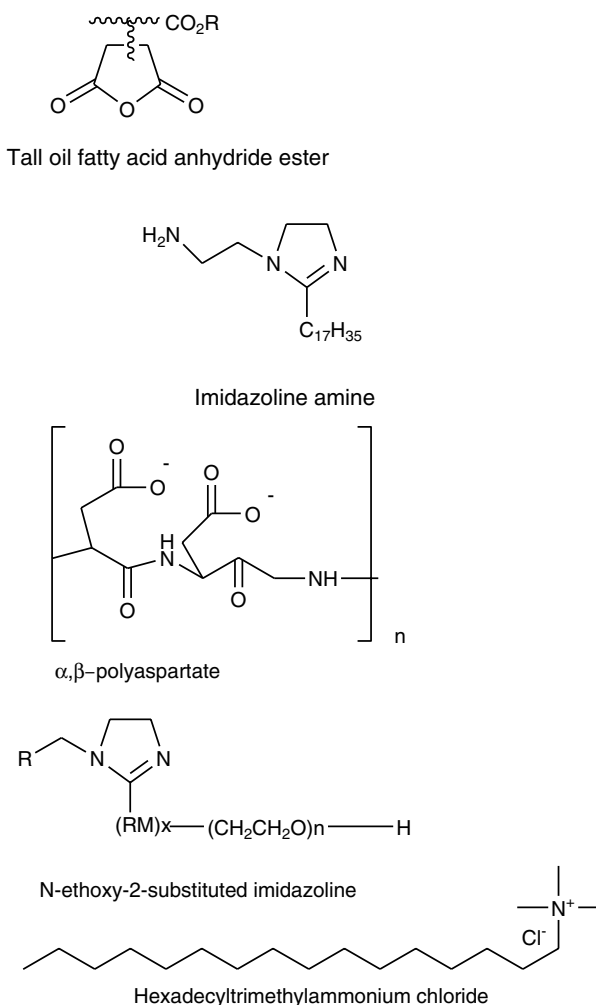


Fig. 2.10—Typical production corrosion inhibitor structures.

formulations. To address these concerns, Clewlow et al. (1994) patented molecules that are the product of a condensation reaction between a di or polyamine and a fatty acid. Subsequently, the mixture is reacted with an unsaturated carboxylic acid or halocarboxylic acid. The resulting material is an unsaturated heterocyclic compound. The author claims toxicity values (LC_{50}) for *Tisbe Battagliai* (a marine organism) of 10–1000 ppm. This is a low toxicity value compared with previous formulations.

Formulations to be used in the North Sea area must meet several stringent requirements (see Section 6.2). These included being biodegradable to at least 70% in 28 days. In addition, there should be reduced toxicity toward several marine organisms including *Skeletonemia costatum*. Also, it is desirable that the material is water soluble so it will not bioaccumulate. Martin et al. (1995) have claimed an inhibitor that comprises an N-ethoxy-2-substituted imidazolines material.

The ethoxy moiety gives the compound increased water solubility. If sulfide is not present, the formulation also may include a phosphate ester. Increasing water solubility of the inhibitor can be a major achievement because marine toxicity frequently is related to solubility of the material in the cell's lipid bilayer (Clewlow 1995). Water-soluble inhibitors also will not need toxic hydrocarbon solvents. Fischer and Parker (1997) have increased water solubility of the classic tall oil fatty acid condensate by making the anhydride of the fatty acid, then partially neutralizing it to an ammonium or potassium salt. The authors claim good film persistency and corrosion inhibition properties. Additional information on health, safety, and environmental issues is in Section 6.2.

A major advancement in the production of “greener” petroleum production inhibitors has come from the work of Bockris et al. (1995), Singh and Bockris (1996), and Singh et al. (1998). This work was the result of a consortium formed at Texas A&M University to develop less toxic petroleum production inhibitors in a systematic manner by applying the types of chemical computational methods that have been successful in the pharmaceutical industry. Toxicity prediction parameters as well as corrosion inhibition prediction parameters would have to be developed. The first model of toxicity was based on the assumption that the inhibitor must pass through the lipid bilayer of an organism's cell. Thus, a standard measure of the partition of a molecule between water and octanol ($\text{Log}P$) was the first toxicity predictor (LC_{50} = lethal concentration of inhibitor for 50% of the fish). A large number of potential inhibitor compounds fit the model:

$$\text{Log}(1 / LC_{50} - \text{fathead minnow}) = a\text{Log}P + b. \dots\dots\dots (2.5)$$

Three themes that are reviewed in this section and include mechanisms of action, mixed inhibitors, and new application methods.

Jenkins (2011b) claims to have synthesized and tested a series of new CO_2 brine-targeted chemicals and that the three most effective CIs that met UK (see Section 6.2.1) environmental regulations, also gave excellent performance in corrosion tests. All of the three molecules developed were modified quaternary amine compounds. The authors describe the kettle method, rotating cylinder electrode and autoclave tests in this paper. Also see Kelland (2009) for additional test protocols.

Mechanisms of Action of Production CIs. Production CIs are frequently added to the well fluids at the bottom of the well or injected into a flowline on the surface. They must contact relatively scale-free surfaces to have maximum effectiveness. They cannot penetrate a heavy deposit.

The classic film formation mechanism of inhibition is explained by Kelland (2009). In this mechanism (Fig. 2.11), a polar inhibitor molecule that has a reactive head group is attracted to and possibly

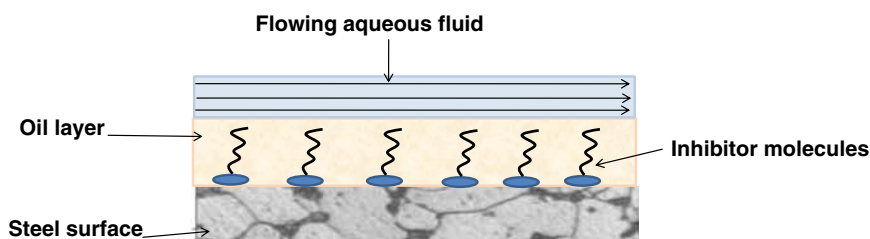


Fig. 2.11—Film forming inhibitor mechanism.

forms a weak bond with the iron ions in the steel surface (or possibly in the scale film). The hydrophobic tail attracts a film of hydrocarbon, and this combined film protects the surface from the corrosive aqueous fluid. Also, note the structures in Fig. 2.10. For film-forming inhibitors, the tenacity of the film may be very important because the flow-shear conditions vary greatly. Various complex corrosion tests are in use to evaluate various scenarios. Kelland (2009) lists the following tests types for evaluating production inhibitors:

- Bubble/kettle tests
- Rotating cylinder and disk electrochemical electrode tests that give a defined shear field
- Impinging jet tests (electrochemical or weight loss/microscopic)
- High-shear autoclave and rotating cage tests
- Flow loops
- Wheel tests
- Static tests (weight-loss or electrochemical)

Details of the various tests are in the Kelland (2009) book as well as in the reference lists of the papers cited in Chapter 8 of his book. Other test protocols are available from *NACE PR0497* (2004), *NACE TM0169-2000* (2000), and Nyborg and Gulbrandsen (2007).

Many years of observation of the corrosivity of hydrocarbon/brines by Byars (1999), Efirid and Smith et al. (2004), and Crolet and Bonis (1985) have lead investigators to conclude that the native corrosion rates of an oil/brine system depend partially on the chemistry of the crude oil as well as the aqueous phase. The crude oil effect is because of the presence of natural surfactants and various N, O, and S containing chemicals in different crude oil streams. See the discussions in Section 2.2.4 as well as Chapter 3 of Frenier et al. (2010). However, Ayello et al. (2011) claim that the effect of crude oil chemistry on corrosion processes is still poorly understood. These authors have examined a wide range of natural surfactant model chemicals (aromatics—tetrahydronaphthalene; organic acids—a commercially available naphthenic acid mixture; S compounds—1-tetradecanethiol; and N compounds—carbazole). These materials were tested in corrosive (CO₂) hydrocarbon-brine mixtures and the results were determined using corrosion tests as well as IST/steel wettability and adsorption tests (see Section 1.6.1). The conclusions are noted:

- The corrosion inhibition by the crude oil chemicals is induced by the accumulation of surface active compounds at the metal surface (see Fig. 2.11).
- The wettability of steel is altered by accumulation of surface active compounds at the metal surface.
- The flow pattern is modified by accumulation of surface active compounds at the oil/water interface.
- The sulfur, nitrogen and the oxygen-containing compounds were more effective as CIs compared to aromatic-only compounds; however, the surface wettability may be affected, as well, without changing the corrosion rates.
- The corrosion protection depended on the weight of the compound that was adsorbed.

While, the chemicals in the crude oil may influence the native corrosivity of the crude/brine mixtures, the interactions with artificial CIs must be examined on a case-by-case basis because there may be positive or negative interactions. For initial screening of inhibitors, an artificial oil (or no oil) may be used, but for field-level tests, the effects of the oil/brine being treated should be determined.

A paper by Ramachandran and Jovancievcic (1998) describe systematic studies of various imidazolines derivatives with the use of surface molecular modeling to understand the inhibition mechanism. The corrosion inhibition increased with increasing aliphatic chain length, and for a given chain length, imidazolines were more effective than amides or amines. The imidazolines were arranged on a magnetite surface as a bilayer. The effects and the consequence of the corrosion product layer also may affect the ultimate corrosion protection.

Ramachandran et al. (2000) determined that CIs are known to adsorb to a variety of corrosion product layers. Under conditions of high shear, the fracture of corrosion product scale is one important aspect affecting corrosion. In this paper, molecular mechanics was used to calculate the Young's modulus of a ferrous carbonate scale. They found that the tangential tensile stresses are larger than axial tensile stresses introduced by wall shear stress. The Young's modulus decreases with increases in microporosity was found to better represent simulation. The high-strain model of metal loss presented in their paper agrees both with simulation and other experimental observations on the corrosion product layer thickness. The results indicate that defects are introduced into surface grain during the process of corrosion placing it under a condition of high strain. Some CIs like trimethyl n-octadecyl ammonium bromide increase the Young's modulus of the corrosion product scale. Based upon the previously mentioned developed theory, this suggests that the inhibitor strengthens the corrosion product film, enhancing the protectiveness of this film under shear. Depending on the acid gas, different type of inhibitors may be required.

“Sweet (CO₂)” Fluid CIs. These inhibitors are the most used category of production inhibitors, so there have been a significant number of reports about the mechanisms of these materials that are used in the presence of CO₂ and with siderite on the metal surfaces. The next paragraphs summarize some of the investigations.

Henry et al. (2005) studied bis amine (quat) inhibitors and found them to be better inhibitors than mono-quats. These authors invoked a chelate effect argument to explain the increased surface bonding and improved inhibitor efficiencies. A number of papers have looked at the effects of inhibitors on the siderite scale layers.

Sun et al. (2005) have shown that the generic imidazolium CIs used in their study worked by slowing down the anodic as well as cathodic reactions. In addition above a certain threshold concentration [called the minimum inhibitor concentration (MIC)], both inhibitors tested hampered the growth of the iron carbonate scale. See Fig. 2.12 that shows different surface morphologies of the siderite scale with and without an inhibitor. According to the authors (Sun et al. 2005), the effect could be a result of a decreased concentration of Fe²⁺ ions at the surface of the steel and/or scale inhibition properties of the CI. However, they did not find conditions under which inhibitor and scale interacts in an antagonistic manner. In all of the conditions investigated, the combination of inhibitor and iron carbonate scale *never* failed to reduce the corrosion rate.

Wong and Park (2008) explored the adsorption of quaternized amine inhibitors during iron carbonate scale formation through electrochemical and post-test microscopic analysis. They found that there is evidence that quaternized amines increase the precipitation rate of iron carbonate to enhance the already protective passivation layer, which is the opposite that was observed in previous work where the inhibitor prevented further iron carbonate from forming. They used rotating cylinder electrode methods (referenced in the paper) to study the corrosion rates. Conclusions were as follows:

- Iron carbonate scale is affected as observed through electrochemical spectra and scanning electron microscope (SEM) images when quaternized amine is present during scale formation.

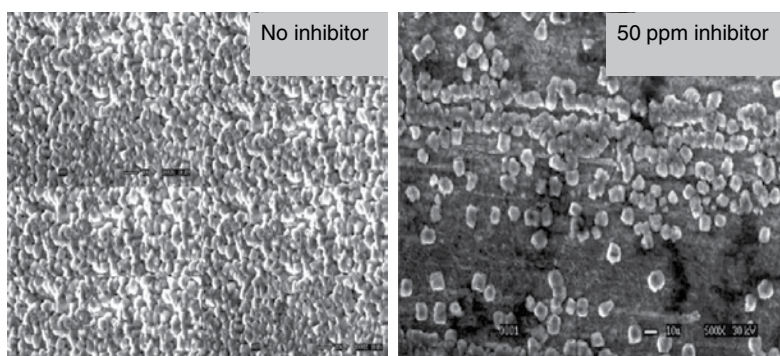


Fig. 2.12—Effect of imidazolium inhibitors on siderite formation (Sun et al. 2005).

- The rate of growth of the iron carbonate scale is increased when quat amine is present because the impedance of the resulting scale is higher vs. nontreated iron carbonate scales. Also, the scale is thinner and is comprised of iron carbonate crystals that are smaller vs. nontreated conditions.
- This quaternized amine inhibitor does not completely prevent iron carbonate growth when the concentration is 50 ppm.
- The corrosion rate is decreased the most when the concentration of Fe^{2+} is 100 ppm or greater and the concentration of quat is 50 ppm.

Wong and Park (2009) also investigated the interaction of iron carbonate and three inhibitor types—quaternary amine, imidazoline, and a phosphate ester (see Fig. 2.10). This study is claimed to have examined two more additional generic compounds [see previous work by Wong and Park (2008)]: quaternary amine dimer and alkyl pyridine quaternary amine. Linear polarization resistance and electrochemical impedance spectroscopy were used to measure corrosion rates and to monitor the active-scale interaction. SEM was used to observe the morphology of the iron scale layer. See details of the methods in the following papers: Wong and Park (2009) and Heidersbach (2011).

The study showed that the growth of iron carbonate scale is affected by the addition of quaternized amine and the resulting scale is comprised of smaller crystalline formations that are tightly packed together. They found that the impedance of this scale can be doubled in value compared to an iron carbonate scale. The inhibitors tested were an imidazolium and a phosphate ester. Their data showed that the combination of 50 ppm an imidazoline and 100 ppm Fe^{2+} yields an adsorbed film with impedance ranging from 4000 to 5000 ohms. This shows that neither species dominates the adsorbed film; however, a synergistic relationship has occurred.

Conclusions of the study are

- There is evidence that the imidazoline inhibitor and Fe^{2+} interact with each other, creating an adsorbing film that decreases the corrosion rate and increases film impedance more so than when either species is alone.
- The resulting impedance of the film is higher than of the FeCO_3 scale formed when no inhibitor was present. They speculate that it is possible that the added Fe^{2+} formed a complex with the imidazoline inhibitor, which was reduced and then subsequently oxidized in the potentiodynamic studies.

The paper also says that the phosphate ester inhibitor has a tendency to adsorb to the surface of carbon steel.

Additional work from Tsui et al. (2010) also shows that there is a *synergism* between the iron carbonate scale and different quaternary CIs; however, the inhibition effects are not improved after the CMC (see discussion in Section 1.4.2) is exceeded.

Mechanistic details suggested by the study were

- When alkyl pyridine quaternary amine was added to a scaled surface, the final corrosion rate was lower compared to when either species was used alone. Therefore, a complementary effect was also observed when the inhibitor was introduced after the complete formation of the iron carbonate scale.
- Corrosion inhibition performance by a certain inhibitor active can be predicted using its CMC value.

Because inhibitors must be effective under some high-shear conditions, Akbar et al. (2011) conducted tests at a temperature of 70°C, pH of 5.9 and 4.5 $\text{g/cm}\cdot\text{s}^2$ wall shear stress (τ_w) using both uninhibited and inhibited Forties brine with 25 ppm of inhibitor saturated with carbon dioxide (CO_2) and silica sand. Weight gain/loss was measured for as well as a number of surface analytical methods. The authors found that the weight loss of as-received surfaces was reduced by more than 43% when 25 ppm of inhibitor was introduced.

However, the inhibitor was found *not* to be effective in reducing weight loss of prescaled surfaces. Note that these tests used a very low dose (25 ppm of an unidentified) inhibitor and higher doses may be more effective in protecting prescaled surfaces. The conclusion is that the inhibitors work best on cleaned surfaces and act to make the siderite scale thinner but more compact.

The authors of this book note that the papers abstracted previously are not completely in agreement on the interaction between the forming siderite and the various inhibitors, but all do seem to indicate there is an interaction that increases the impedance of the film (this is equivalent to the electrical resistance in an alternating current circuit) and that it depends on the concentration of the inhibitor.

Sour Brine CIs. Most of the studies described previously have been directed at inhibitors for *sweet* systems where the corrosion reactions involve CO_2 . Sour (H_2S) wells and pipeline fluids also must be inhibited. The types of inhibitors used for fluids in contact with CO_2 as well as elemental sulfur and H_2S include coco dimethyl benzyl ammonium chloride as well as aminoethyl fatty imidazolines and alkyl pyridinium ammonium chloride. These are similar in structure to some CO_2 inhibitors. See Fig. 2.13 for typical sour fluid inhibitors, but they usually must be specially formulated to be dispersible in the more acidic H_2S environments and in the presence of an FeS-containing scale.

Moore and Liu (2009) have addressed some of the principal properties of CIs and how these properties impact the ultimate fate of an inhibitor in a production system. Specifically, affinities of various CIs for sand, iron sulfide, barium sulfate, iron carbonate, and emulsion drop surfaces were presented. This paper reports the behaviors and performance of selected CIs in the presence of elemental sulfur. This study looked at systems where corrosion was taking place under a deposit of sulfur and a cell for such studies is described in the report. They found that the quaternary inhibitors will adsorb on sand and sulfur and, thus, the effectiveness may be reduced.

Ramachandran et al. (2002) used a force field program that was developed to understand mackinawite, an important iron sulfide scale formed during H_2S corrosion. They claim the inhibitors retard the dissolution of scale by binding to it and preventing acidic attack of the scale. This work is claimed to form an important step in using molecular modeling techniques to study the corrosion of iron in H_2S environments and its inhibition. The CI used in the study was 1-benzyl-2, 6 dimethylpyridinium chloride. The calculations showed that the lowest energy structure arrived through annealed dynamics is that the pyridine ring of 1-benzyl-2, 6 dimethylpyridinium chloride does not follow a flat orientation with the surface but adopts a 70° angle with the surface. The most favorable interactions are those in which the hydrogen atoms of the pyridine ring bind with the surface sulfur atoms of mackinawite.

Park et al. (2009) proposed to test the idea that the performance of the inhibitor is determined not only by adsorption to the steel surface but by its ability to bind into the product layer providing protection and by changing the morphology of future scale growth. Comparison of film persistency on bare steel

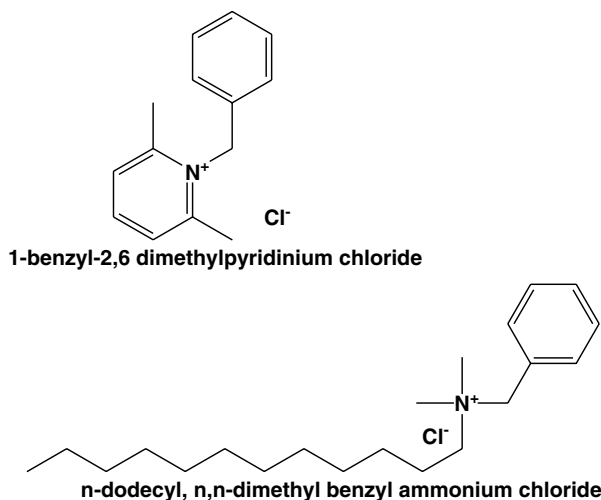


Fig. 2.13—Sour (H_2S) corrosion inhibitors.

surfaces and precorroded surfaces under differing corrosion environments was tested in high-pressure autoclaves. Corrosion rate analysis was conducted by weight loss, electrical impedance spectroscopy. Scale analysis was conducted by SEM/electron dispersive X-ray and X-ray diffraction analysis.

The proposed theory developed from this study is the affinity of the CI to bind into the iron sulfide layer providing a stronger persistency, slowing the rate of iron sulfide growth, and reducing the dissolution of the layer. They found that the addition of CI appears to change the crystal morphology and indicate that the inhibitor does bind into the corrosion product layer and change the morphology, but may not determine the overall inhibitor’s effectiveness.

Jenkins (2010) describes the laboratory selection procedure performed to develop a CI that was effective in preventing both localized and general corrosion. The results illustrate that to mitigate localized corrosion a substantially *higher* inhibitor dose rate is required compared to the concentration needed to prevent general corrosion. They claim that in sour systems iron sulfide will form, and it will precipitate on the metal surface reducing the general corrosion rate. However, if the metal surface is not fully covered with iron sulfide or if the film breaks down in certain locations, there will be exposed anodic sites on the metal surface. The areas covered by iron sulfide are cathodic, and consequently, there will be a small anode and large cathode set up on the metal that will result in accelerated corrosion at the anodic sites. This will cause pits to form at the anodic sites followed by subsequent failures.

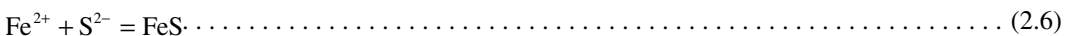
A major conclusion of the various studies is that in oilfield systems where pitting or localized corrosion is likely, the use of electrical resistance (standard or high-sensitivity) corrosion monitoring probes in combination with corrosion side stream should not be solely relied upon when optimizing CI treatments. Corrosion monitoring techniques that assess pitting corrosion rates should also be used (e.g., corrosion weight loss coupons).

Several other general conclusion on the use of production stage CIs are

- The native corrosivity of a oil/brine system depends on the acid gases as well as the chemistry of the crude oil, and these chemicals must interact effectively with any added inhibitors.
- There is a complex interaction of the inhibitor and the forming corrosion product layer (siderite or an iron sulfide) that may enhance the inhibition process.
- Most lab tests are done on cleaned steel, and the extrapolation to a heavily scale-covered surface is not predictable but may require additional inhibitor for good protection or precleaning.
- Many markets require more environmentally friendly inhibitor chemistries.

Control of H₂S and FeS Precipitation. Iron sulfides can be formed in several different ways. If a well has sour fluids (H₂S present), a corrosion reaction is the most likely method for forming iron sulfide scale. Control of direct deposition (usually on the steel tubing) of FeS, by inhibition of the corrosion reactions was described in Section 2.2.3.

Iron sulfides also can form because of mixing of iron-containing fluids with sulfide-containing liquids. Even if these scales do not directly cause corrosion, their mere presence can induce under deposit corrosion and may also affect the use of the various CI that are applied. This type of precipitation also may result in formation damage in the matrix or perforations as well as on the tubulars and the migration of the solids may foul screens and filters for injection wells. A major cause of this type of FeS solid is the use of acidizing fluids (see Chapter 3). This is possible because these types of treatments may produce large amounts of iron from the acid itself as well as from corrosion of the well tubulars. This represents formation of FeS because of more conventional precipitation of a salt when the solubility of FeS is exceeded because of changes in water quality and is analogous to the formation of calcite and sulfate scales. If the formation has naturally occurring dissolved iron from the minerals in the matrix, this may combine with dissolved sulfide in different water streams. In either case an iron sulfide solid is formed:



As noted in Section 2.2.3, several different crystalline iron sulfide minerals may form (as well as an amorphous solid) depending on the concentrations and pH values of the fluids. In the oilfield environment, both modes of formation (corrosion and salt formation) can be important. The authors of this

book contend that FeS is a particularly significant scale because it can cause flow reduction problems and severe health/environmental concerns because removal can regenerate toxic H₂S. The solubility product of FeS is very low (8×10^{-19} for Mackinawite), so precipitation may occur at low concentrations of iron and sulfide ions. Because corrosion-induced FeS scale usually will form on the tubulars, this will affect flow but is not likely to cause formation damage. The formation of FeS from mixing incompatible fluids *could* cause formation damage (see Section 2.3).

Control of precipitated FeS can be affected by controlling the iron and/or the sulfides as well as by FeS-specific scale inhibitors.

Iron control of reaction Eq. 2.6 includes

1. Sour fluid CIs described in Section 2.2.3.
2. Reducing total iron concentration in the injected acid to the lowest practical level.
3. Pickle tubing, mixing tanks, and lines before the acid treatment is necessary to limit the iron concentration.
4. Effective use of CIs in the stimulation fluids [see Frenier and Ziauddin (2008) and Section 3.6.1].
5. Adding chelating agents to the acid. Included are ethylenediaminetetraacetic acid, hydroxyethylethylenediaminetriacetic acid (HEDTA), and nitrilotriacetic acid. See Frenier et al. (2000). These materials will complex the iron, and thus, reduce precipitation, and they are described in detail in Section 3.6.1.

Sulfide Scavengers. Control of the sulfide part of the solid formation reaction (Eq. 2.6) may be accomplished using sulfide/H₂S scavengers. Nasr-el-Din et al. (2000c) have described the formation of various types of iron sulfide as well as the use of scavengers to prevent the formation of this scale. Kelland (2009) also has described several categories of H₂S scavengers.

Aldehydes and triazines are in commercial use as sulfide control agents. Fig. 2.14 shows the base reactions of aldehydes with H₂S. Note that the first step is the formation of a thioaldehyde that then reacts to form a more complex sulfide. The reaction with formaldehyde is a low solubility material (trithiane if the aldehyde is formaldehyde), while other aldehydes (Fig. 2.15) also form complex [that are frequently more soluble (see Kelland 2009)] compounds. Acrolein is in commercial use as a sulfide scavenger, as is glutaraldehyde, but they are also quite toxic. Possible advantages of these materials are that they are also biocides and, thus, may control sulfate-reducing bacteria and other microbiological problems such as MIC.

Frenier and Hill (2002) and Nasr-El-Din et al. (2000b) have described the use of glyoxal, glyoxylic acid, and cinnamaldehyde as H₂S scavenger agents in acids.

The authors of these reports claim that these materials are effective as sulfide scavengers, yet allow any precipitated FeS to be dissolved by the HCl. More details of the use of sulfide suppressors during acidizing are in Section 3.6.3.

Triazines are the reaction product of an amine with an aldehyde. They frequently are produced from condensation of an ethanolamine and formaldehyde [see the detailed discussion in Kelland (2009) that has 75 references]. These materials are called triazines, but as the structure in Fig. 2.16 shows these materials are actually know as 1,3,5 hexahydrotriazines. The reaction products with H₂S are claimed

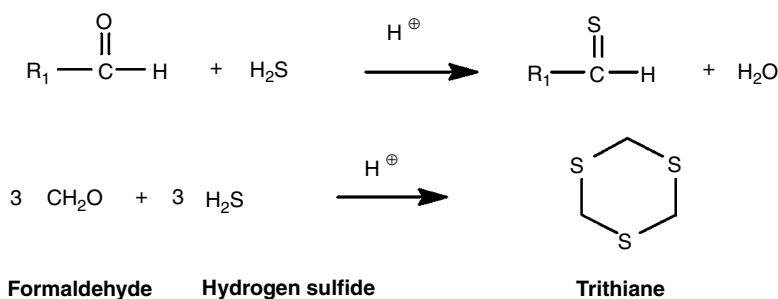


Fig. 2.14—Reaction of H₂S with aldehydes.

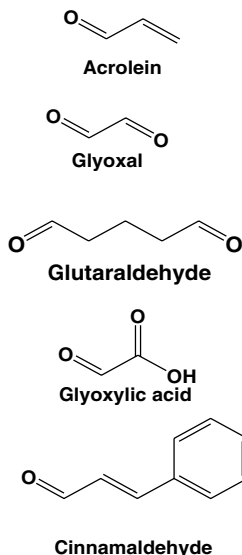
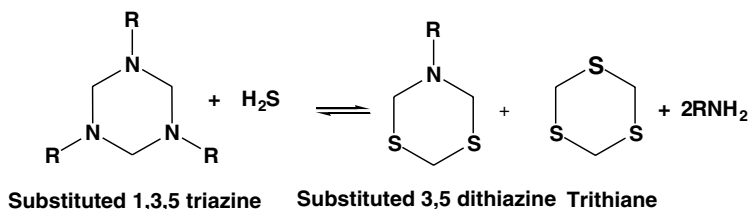


Fig. 2.15—Aldehydes used in oilfield fluids.

Fig. 2.16—Reactions of triazines with H_2S .

be to mix of a dithiazine and trithiane (Bakke et al. 2001; Dillon 1990). They are analogous to hexamethylenetetraamine (HMTA) (Fig. 2.17). This is essentially a solid form of formaldehyde (formed from the condensation of formaldehyde and ammonia). As such the reactions with H_2S are similar to the reactions with aldehydes. Compare Fig. 2.14 with Fig. 2.16.

Some of the triazines also may act as biocides by releasing an aldehyde into the fluid; however, as an amine they also may raise the pH of the fluid, thus increasing the possibility of precipitation of calcite scale. Taylor and Matherly (2011) have tested several commercial scavengers including formaldehyde, glyoxal, and Tris (2-hydroxyethyl)hexahydro-s-triazine (THHT) (Fig. 2.18). The experiments used a column that contained control chemicals and where H_2S was flowed over it. The test fluids were tested using a sulfur specific flame photometric detector. They provided data that indicate that THHT is more efficient than trimethyl-hexahydro-s-triazine and is more efficient on an equivalent basis (and on a weight basis) than formaldehyde and glyoxal based on the H_2S detected by the test.

Taylor and Matherly (2011) also claim that the reaction with THHT produces monoethanol amine as a byproduct that itself can react with H_2S , this increasing the efficiency (Bakke et al. 2001) of the suppression. See Fig. 2.19. These authors also tested the effects of CO_2 on the removal efficiency of the scavengers. They found that high concentrations (>15,000 ppm) reduced the breakthrough time significantly. A likely mechanism is the reduction in pH of the fluid that would shift the equilibrium seen in Fig. 2.19 to the left.

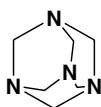


Fig. 2.17—Hexamethylene tetraamine diagram.

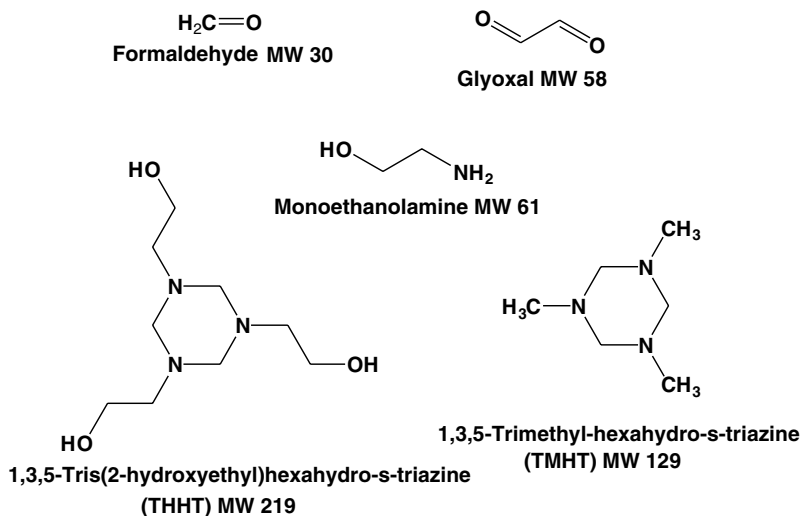


Fig. 2.18—H₂S scavengers.

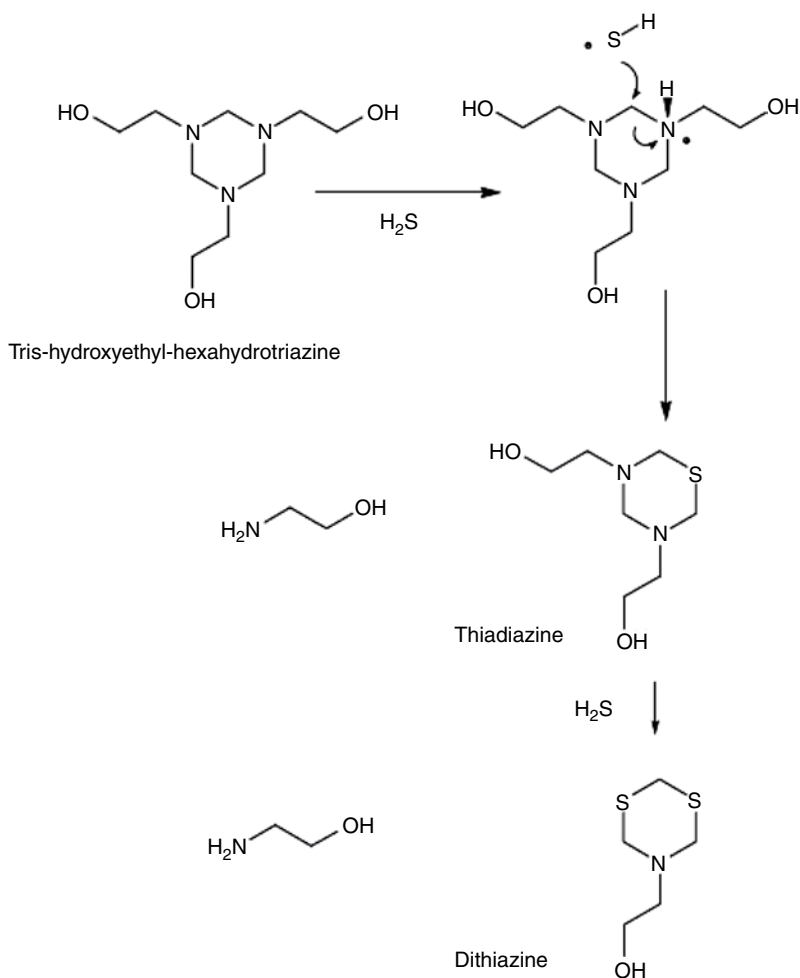


Fig. 2.19—H₂S removal by THHT (Taylor and Matherly 2011).

FeS Scale Inhibitors. These also have been proposed. All scale inhibitors affect the *rate* of formation/precipitation of scale when the scaling index is >1 , and the field of inhibition is mature (Frenier and Ziauddin 2008) for calcite, barite, and other sulfate scale treatments but not for FeS. However, Chen et al. (2009) claim to have developed a novel iron sulfide test method to test the performance of iron sulfide inhibition. Compared with the traditional static jar test and dynamic loop test, this novel developed test method is claimed to show good reproducibility and provides a quick and effective way to evaluate the performance of iron sulfide scale inhibition. While the structures are not disclosed, the references to “environmentally friendly” inhibitors may indicate that polyaspartate-based materials [see Kohler et al. (2002) and Frenier and Ziauddin (2008), Chapter 4] are in use instead of the phosphate-types of inhibitors. They also claim an environmentally friendly iron sulfide scale inhibitor has been developed based on this novel test method. They claim that it provided good performance on iron sulfide inhibition in synthetic field water (no carbonate present). They claim that the tested inhibitor reduces the agglomeration of FeS particles. The authors of this book are not personally familiar with FeS (kinetic) inhibitors, but they are worth investigating because other types of scale inhibitors are being proposed for use in CO₂-flooded wells.

A chapter in Kelland (2009) also mentions the use of Zn complexes that can remove sulfide as a Zn solid. These types of materials as well as the use of alkanolamines are appropriate only when the solids can be easily removed, such as for treatment of natural gas after production. See Abdel-Aal et al. (2003) for more information on gas-processing methods.

2.2.4 New Formulations for Application of Production Corrosion and Scale Inhibitors. The use of microemulsions (see Section 1.4.4) to place and disperse an inhibitor is reviewed. Collins and Hewartson (2002) claim that as the industry moves towards increasing deepwater production, the very high cost of well intervention places large constraints upon the performance of scale-control options. The paper discusses using EOR-type surfactant systems (see Section 5.5.3) in conjunction with scale inhibitors to extend the squeeze inhibitor treatment lifetime.

The authors (Collins and Hewartson 2002) contend that the treatment lifetime is extended by the miscible displacement of organic material from formation surfaces thereby increasing the surface area available for the scale inhibitor to adsorb onto the surface that are placed in microemulsions (Section 1.4.4). This is a very extensive paper with a lot of details on the preparation of the microemulsions and incorporating various oilfield chemicals in them.

Several patents provide useful details of using microemulsions for placing scale and CIs. A patent by Collins and Vervoort (2003) describes a microemulsion comprising (i) an oil phase, (ii) an aqueous phase comprising an aqueous solution of a water soluble oilfield or gasfield production chemical or an aqueous dispersion of a water dispersible oilfield or gasfield production chemical, and (iii) at least one surfactant, wherein the aqueous phase is distributed in the oil phase in the form of droplets having a diameter in the range 1 to 1000 nm or in the form of microdominans having at least one dimension of length, breadth, or thickness in the range 1 to 1000 nm.

Yang and Jovancicevic (2009b) and Yang and Jovancicevic (2010) also claim patents for microemulsions that have CIs in the internal phase and an external phase and at least one surfactant that helps define the emulsion. The CI itself is claimed to have its pH adjusted so that it also serves the role of surfactant. The CIs form microemulsions with particle or droplet diameters of about 10 to about 300 μm . The microemulsions may be oil-in-water, water-in-oil or bicontinuous. The microemulsions are claimed to increase the dispensability of the oilfield chemical (e.g., a CI) into fluids, such as dispersed fluids, and thus increase the performance of the oilfield chemical (e.g., inhibitor). Microemulsions may also incorporate other incompatible oil-soluble oilfield chemicals and water-soluble oilfield chemicals as alternatives to or additions to the one initially used. For instance, the oil-soluble oilfield chemical such as a CI may be in the internal phase, whereas the water-soluble scale inhibitor may be in the aqueous external phase.

A list of CIs that can be used in the microemulsions are described by Yang and Jovancicevic (2010) and include alkanolamides, alkyl phosphate esters, thiophosphate esters, fatty acids such as alkyl dimeric acids, maleated fatty acids, imidazolines, sulfur-containing inhibitors, and the like. The alkyl chain lengths may range from 8 to 24 carbon atoms. In one nonlimiting embodiment, an unsaturated

chain such as oleyl may be used. Other examples of CIs are compounds for inhibiting corrosion on steel, especially under anaerobic conditions, and may especially be film formers capable of being deposited as a film on a metal surface (e.g., a steel surface such as a pipeline wall). Such compounds may be nonquaternized long aliphatic chain hydrocarbyl N-heterocyclic compounds, where the aliphatic hydrocarbyl group may have from 5 to 12 or more carbon atoms; mono- or di-ethylenically unsaturated aliphatic groups (e.g., of 8–24 carbons such as oleyl, etc.). The N-heterocyclic group can have 1–3-ring nitrogen atoms with 5–7-ring atoms in each ring; imidazole and imidazoline rings are suitable in one nonlimiting embodiment.

Yang and Jovancicevic (2009a) described imidazoline dimer-type compounds, which are prepared by the reaction of dimer fatty acid and a dialkylene triamine, such as diethylenetriamine, are useful for corrosion inhibition in water-containing fluids contacting metal, particularly fluids containing CO₂ and/or H₂S. When the reaction is conducted with molar excess of the polyamine, the resulting imidazoline dimer or oligomer is surprisingly more effective at corrosion inhibition than conventional monomeric imidazoline. Also unexpected is the better water solubility of the reaction product as compared with the conventional monomeric imidazoline.

Improvements in Scale Inhibitor Delivery. The major types of scale inhibitors used to delay the deposition of mineral scales are phosphonates, phosphonocarboxylic acids, and polyvinyl sulfonates. See Fig. 2.20 for typical structures. “Green” scale inhibitors also are in use and include various polymers from natural products. See the discussion in Frier and Ziauddin (2008). Scale inhibitors can be applied in a continuous manner using a pump from the surface (or a subsea pump), “squeezed” into the formation in the same manner as a matrix acidizing treatment [Sections 3.3, 3.5, and Frier and Ziauddin (2008)]. The scale inhibitors also can be applied as a component in a hydrofluoric acid (HF) treatment (Bourne 1995; Bourne et al. 2000; Norris et al. 2001; Szymczak et al. 2012). A short review is given later in the current section. Short discussions of various alternative methods that have been developed since 2007 are also reviewed in this section.

Improved Squeeze Treatments. The retention of a scale inhibitor in the formation is the determining factor on the squeeze life (time to MIC). As noted in Frier and Ziauddin (2008), a precipitation squeeze, where the anionic inhibitor (usually a phosphonate or a polyacrylate with phosphorous as an

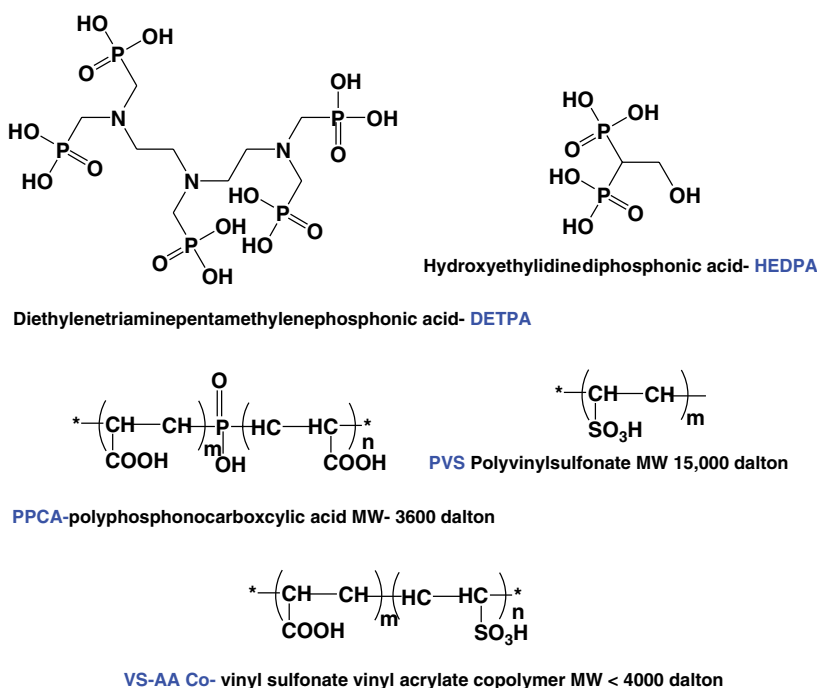


Fig. 2.20—Chemical structure of generic SIs.

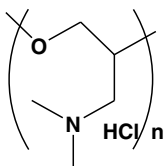
analytical tag) is precipitated as a Ca^{2+} salt, usually lasts longer than an adsorption squeeze where the inhibitor molecules adhere directly to the limestone, sandstone, and clays. A number of other ways to enhance the lifetime of a squeeze also have been proposed.

Kelland (2009) has a short discussion of a number of “squeeze enhancement” methods that include Ca^{2+} , Zn^{2+} , the quats to be mentioned later as well as kaolin clays. As noted in the previous paragraph, the use of Ca^{2+} has been extensively researched (Frenier and Ziauddin 2008).

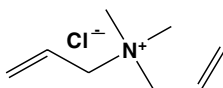
Patents by Shuler (1991, 1993) have some good teachings on squeeze technologies and inhibitors that can be reviewed by the reader. They claim a method that involves injecting an aqueous solution of polyquaternary amines into the formation. This solution of polyquaternary amines can be injected before, simultaneously with, or after the injection of the scale inhibitors. The scale inhibitors are preferably a blend of nonpolymeric and polymeric scale inhibitors. Preferably, the polyquaternary amine is a poly-dimethylamine/co-epichlorohydrin or a poly-diallyldimethylammonium chloride. Shuler says that materials such as the clay stabilizer polyepichlorohydrin are effective. In a typical process, an amine polymer solution is injected into a well, followed by injection of a scale inhibitor and an overflush. The well is then shut in for 20–24 hours before production recommences. To ensure facile injection of the polyquaternary amines into the formation during the process the Shuler patents teaches that their molecular weight should be below 50,000.

Selle et al. (2003), Chen et al. (2006), and Montgomerie et al. (2010) claim (in several publications and patent applications) that the life of the squeeze can be extended if a cationic monomer or polymer is placed into the formation before the inhibitor is squeezed. These chemicals are the same (or similar) to quaternary clay control chemicals described in Sections 3.6.4 and 4.7.5 of this book. Montgomerie et al. (2010) use of a homopolymer formed from diallyl dimethyl ammonium chloride. Possible structures of bridging agents are in shown in Fig. 2.21.

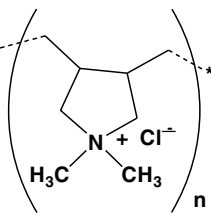
These compounds are then followed by the scale inhibitors of the types mentioned by Frenier and Ziauddin (2008) and Kelland (2009). They propose (Montgomerie et al. 2010) a mechanism by which the use of charged polymers such as those described in the previously mentioned applications enhances retention of scale inhibitors in subterranean formations by a mechanism wherein the adsorption of the



Poly(dimethylamine-co-epichlorohydrin)



**Diallyldimethylammonium chloride
DADMAC**



PolyDADMAC

Fig. 2.21—Possible polymer repeat unit structures for squeeze enhancements.

positively charged compounds to the formation reduces its negative charge. As a result, scale inhibitors, which are often negatively charged, are more readily retained on the formation.

This mechanism may also involve a combination of effects, including modification of the formation surface to enhance adsorption and precipitation. It is believed by Montgomerie et al. (2010) that when polymers formed from a diallyl ammonium salt as they are combined with scale inhibitors, and in particular scale inhibitors comprising a carboxylate group, a solid (e.g., gel) forms. This gel acts like a precipitate in that it is easily retained in a hydrocarbon well. However, the reaction to form the solid (e.g., gel) is believed to be reversible.

The method of the invention (Montgomerie et al. 2010) is claimed to be *different* from those previous art techniques employing relatively low molecular weight polyquaternary amines (Shuler 1991) salts as these earlier methods rely solely on adsorption of the amine to the rock to improve retention of scale inhibitor. It is also claimed to be different from the previous art technique of employing Ca^{2+} because the polymer formed from a diallyl ammonium salt can itself be adsorbed onto a rock surface, preferably in a preconditioning step. Thus, a further advantage of the method of the invention is that the polymer formed from a diallyl ammonium salt can be preinjected followed by an injection of a scale inhibitor. This is claimed to reduce or prevent formation damage (e.g., loss in permeability).

Chen et al. (2006) describe a detailed method and field results based on the treatments using the polymer-like inhibitor and additive package in the oil field. The application of polymer interaction packages are claimed to significantly improve the inhibitor squeeze life. Satisfactory results have been achieved from the field trials. This paper provides quite a large amount of detail. Selle et al. (2003) provide more details on the chemistry.

Kan et al. (2009) have tested a number of cations to enhance a precipitation squeeze and claim that the stronger solution complex formation with Zn^{2+} may be attributed to the observed enhanced inhibition efficiency. Because of the lower solubility of Zn^{2+} -scale inhibitor salts, Zn^{2+} added to the inhibitor pill significantly improves the retention of some scale inhibitors during squeeze treatment. In this paper, the projected squeeze life is defined. When Zn^{2+} is used in the inhibitor pill, the projected squeeze life for Bis-hexamethylene triamine-penta(methylene phosphonic) acid is claimed to be increased by a factor of 60 without significantly affecting the cost. There is a significant amount of mechanistic work in this paper to give some confidence in the use of Zn^{2+} . No field uses have been described.

The question from the authors of this book involves formation damage and if this can be tested adequately. The planning using the squeeze software must account for the perm/porosity of the formation and whether it can accommodate the precipitated/bridged solids without reducing fluid flow. The authors of this book also note that some possible enhancement agents (some polymers as well as metals such as Zn) appear on international lists [such as the priority pollutants list from the US Environment Protection Agency (USEPA 2011b)] and may not be acceptable in some markets. More details of toxicity and environmental protection in the oil/gas production industries are described in Chapter 5.

Patterson et al. (2012) and Jordan (2012) report on field applications of combining (or following) acidizing treatments with a scale inhibitor treatment for both carbonate and sandstone wells. Also see Chapter 3 of this book as well as the discussions in Section 5.2.6 of Frenier and Ziauddin (2008) of acidizing and mixing scale inhibitors with acids.

The authors (Patterson et al. 2012; Jordan 2012) claim that

- The approach of deploying the stimulation step and the squeeze step (the authors call this “squimulation”) into one pumping operation not only benefits the stimulation by displacing the spent acid and reagents away from the immediate wellbore area, but pumping of the treatments stages provides a cost saving with only a single mobilization now being required for the combined treatment.
- The development for sandstone reservoirs of a “nonconventional” batch chemical applications where bullhead stimulation treatments (HCl and HCl/HF) have been displaced deep into the formation (>20 ft) using a scale inhibitor overflush has been proved to be effective in the four wells treated to date.

- Scale inhibitor return profile look excellent for phosphonate in carbonate reservoir applied as conventional squeeze or as part of squimulation-type treatment. These authors claim that mixing phosphonates directly with acid in carbonate stimulation is not acceptable because of precipitation. Frenier and Ziauddin (2008) and Frenier and Garcia (2004) reached the same conclusion but found that phosphono-poly acrylate inhibitors SIs could be used in this type of treatment.

Squeeze treatments and other scale inhibitor treatments may be required in very hot wells. Wang et al. (2013) have tested several phosphonate and polymeric SIs at temperatures up to 200°C to determine the thermal stability and, thus, the effectiveness of the materials for delaying precipitation of BaSO₄. Using scale delay tests and chemical analyses, the authors found that all of the inhibitors tested (3 phosphonates and 3 polymers) were quite stable up to about 150°C, but the polymers were more stable at 200°C. However, adsorption on sandstone core materials materially improved the stability of diethylenetriaminepentamethylenephosphonic acid (DTPMP), even at 200°C. The implication is that squeezing the inhibitor applications will stabilize the inhibitor in very hot wells.

Use of Scale Inhibitors Added to Hydraulic Fracturing Treatments. As noted at the beginning of this section, inhibitors of various scaling solids can be added to HF fluids (see Section 4.7.5). Bourne (1995), Bourne et al. (2000), and Norris et al. (2001) have used very porous ceramic particles that have been soaked in an SI solution then the water is evaporated and the SI-ceramic is added to the frac sand. These authors report that the time to MIC can be greatly increased with this type of SI treatment. See Figs. 5.22–5.24 in Frenier and Ziauddin (2008) for one proposed mechanism of action.

Gupta et al. (2009), Gupta et al. (2010), and Szymczak et al. (2012) have reported on the use of SIs that are adsorbed onto to various solids (including activated carbon, silica particulate, precipitated silica, zeolite, diatomaceous earth, ground walnut shells, fuller’s earth, and organic synthetic high molecular weight water-insoluble adsorbents). The authors claim that scores of wells have been treated successfully with these types of adsorbed SIs. Szymczak et al. (2012) also reports that low-toxicity, high-biodegradable (chemistry not described) SIs have been developed for the systems described in the previous paragraph. They also claim that these materials have been used to maintain the conductivity of the HF pack from scaling in Bakken play shale wells. The authors also note that these types of wells (including in the Marcellus plays) do not have flowable connate water and much of the water returned is frac water that has come into contact with the formation rocks. See discussions of water reuse in Section 6.3 of this book.

“Live Formation Water” In-Situ Analyses. The SI of formation water [see Eqs. 2.1 and 2.2 and Frenier and Ziauddin (2008)] and the corrosion potential of fluids usually are determined using stock-tank surface-sampled water. Because the pH and the amount of scaling ions present will change as the temperature and pressure changes between the formation and the surface, a much more accurate evaluation would be available using the live bottomhole water.

Børreng et al. (2003) describe development of a pH sensor system for downhole use. It is claimed that a field test of this system by running it in a well with a “single phase” fluid sampling chamber. The water sample captured downhole was used to get a laboratory measurement of the pH in the formation water at reservoir temperature and pressure. This sample was then flashed to standard conditions and a full water and gas analysis was performed. The authors claim that results were used in the MultiScale software program (Multiscalelab 2011) to calculate a pH value. The results indicated good correspondence between the pH values obtained from the downhole sensor, the water sample, and the pH value calculated with the scale prediction program. Expro (2007) describe a measurement probe system contains instruments for the measurement of pH. A platinum temperature element is integrated in the sensor system for measurement of well temperature. The pH is temperature dependent and accurate temperature measurement is, therefore, very important.

Abdou et al. (2011) have reviewed the use of formation water analyses as a technique for better prediction of scaling, corrosion, and the chemistry of the formation during the various stages of the reservoir life cycle (see Section 1.10). The authors claim that live water samples can be obtained using a pressurized wireline vessel once the well has cleaned up (Creek et al. 2009). The wireline vessel described also allows some measure of pH and pCO₂ that can be used for scale prediction. The water samples obtained by this probe could be analyzed on the surface, but they have had changes

in temperature and pressure. The pH is measured by injecting a pH dye indicator and then noting the absorbance of the signal using a filter colorimeter.

The live formation water analyses described by Abdou et al. (2011) are, thus, claimed to show that this type of data (base on in-situ pH and $p\text{CO}_2$) can be used directly to show that the formation water was stable and would not form scale at that time and location.

2.2.5 Formation and Control of Organic Deposits. This section provides a short review of organic deposits that may affect the formation of emulsions or cause formation damage. Crude oil is a complex mixture of different types of molecules comprised primarily of hydrogen and carbon (hydrocarbons). These molecules range in size from the very small (H_2 and CH_4) to chemicals with molecular weights in the thousands. Paraffins and aromatic hydrocarbon molecules are composed only of hydrogen and carbon, with each type of molecule having distinctive chemical structure and properties. Other species present in some crude oil molecules include sulfur, nitrogen, and oxygen. These frequently are called the *hetero atoms* because they are not carbon and hydrogen. In addition, metal atoms including iron, nickel, and vanadium may form complex associations with the aromatic and heteroatomic species. Fig. 2.22 shows some of the chemical types that are in crude oil.

Oil and gas production is usually accompanied by water production. Hence, the interaction of oil, gas, and water form emulsions and foams, but foremost the clathrate gas hydrate compounds. These ice-like solids form at low temperatures when molecules form from a cage of water molecules and a

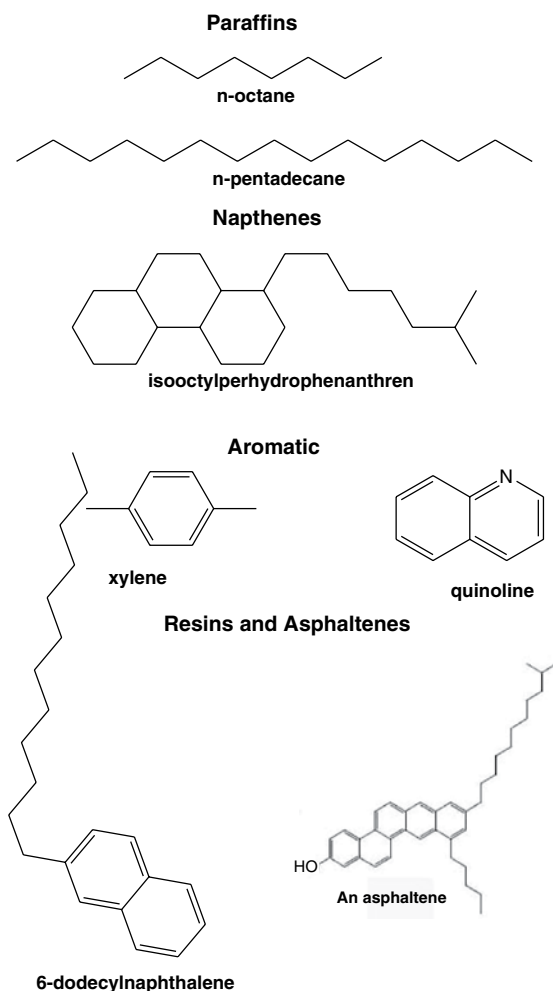


Fig. 2.22—Chemical types in crude oil.

smaller guest molecule (like methane). The formation of solids such as hydrates, waxes, asphaltenes, and naphthenates cause problems in production operations (in addition to the inorganic scales discussed Section 2.2.1). In this section, the basic principles associated with the formation of organic solids are discussed. The formation of organic deposits, in the formation and tubulars requires the use of various reactive chemicals described in Section 3.6.2 to remove them.

There are four broad types of organic deposits that may contribute to foulant production in the NWB formation, in the production lines and in surface equipment. These are

- Wax (paraffin)
- Asphaltenes
- Gas hydrates
- Naphthenic acid salts

Waxes (a.k.a. Paraffins). Waxes are organic solids that precipitate from the crude oil primarily as a function of temperature. The waxes are usually considered to be composed of predominantly normal paraffins (straight chains) and occasionally some iso (branched) and cyclo-paraffins. Cyclo-paraffins are termed naphthenes in the petroleum industry. See Fig. 2.22. Normal paraffins, nC_{16} and lighter are liquids at ambient conditions. Therefore only those paraffins C_{17} and above and can usually crystallize from wax and deposit in a meaningful way. The carbon number range of interest is from $n-C_{20}$ to $n-C_{80}$ or more. Waxes may precipitate in flowlines and production tubing when the temperature of the oil cools below the cloudpoint (CP) of the oil. The CP is the highest temperature where cloudiness starts to appear as a crude oil sample is cooled. The terms wax WAT and wax precipitation temperature also are used interchangeably with the CP.

Asphaltenes. Asphaltene are a solubility class of compounds that are precipitated by alkanes and are soluble in aromatic chemicals such as toluene or benzene. This class of materials contains varying degrees of condensed rings, alkyl substitutions, and functionalities. They constitute a compositional continuum with respect to molar mass and polarity. Resins (described previously) also may be considered in the asphaltene classification. Divisions into various asphaltenes are arbitrary, depending on the analysis methods or solvents employed. Figs. 2.22 and 2.23 show structures of polyaromatic hydrocarbons with alkyl appendages that would fit into the asphaltene class. Hetero atoms of N, S, and O also are in some of the rings. The solid asphaltene, when separated or precipitated, is brown to black in color and has no definite melting point. In general, many asphaltenes decompose at temperature conditions of above $150^{\circ}C$. Fig. 2.23 also shows an aggregation of asphaltene molecules that occur when the concentration of asphaltenes exceeds a value called the critical aggregation concentration. Asphaltenes are a major cause formation damage and of the emulsions and details described in Sections 2.4.1.

New Developments in Organic Deposit Control Technology. Soulgani et al. (2009) claim that accurate modeling of the asphaltenes precipitation from asphaltenic crude oil is essential to possible preventive and curative measures for the potential problem of asphaltene deposition occurring during oil production, transport, and refining operations.

They claim a simple method based on a scale equation has been developed for prediction of asphaltene precipitation modeling from live oil. The authors claim that extensive experimental results were applied over a wide range of temperature and pressure on the different Iranian oil fields. The models are claimed to be adequate to represent a wide range of the experimental results. The predictions of

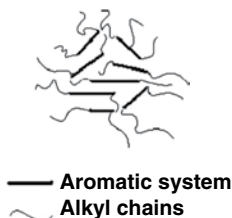


Fig. 2.23—Aggregation of asphaltene molecules (Mullins 2005).

the suggested modified scaling equations for asphaltene deposition from live oil are compared with present results and the data that are reported by other investigators for live oil from other reservoirs. Good agreements are observed that confirm the suitability of the models are claimed.

Wylde and Slayer (2009) describes details of the development of a cleaning chemical for heavy oil and gas pipelines. Information is offered regarding the reason for development, the research involved in formulation of the new product, and the laboratory testing.

A literature review of the current theory in the chemistry of pipeline-cleaning chemicals is presented (Frenier et al. 2010), together with a critical account of the key properties required of these chemistries that include

- Wettability alteration
- Solubilization efficacy of organic materials
- Emulsification of phases
- Dispersion, detergency
- Defoaming

One case history details how a pipeline operator unsuccessfully tried to clean a 12-in., 9-mile section of pipeline with a pig. The pig was launched and became stuck along the length of the pipeline. Application of the newly developed product was able to free the stuck pig and removed significant debris. By way of conclusion, the paper offers suggestions on how chemicals can be most efficiently used in conjunction with these programs.

A patent by Smith et al. (2011a) has claimed production of a single acidizing fluid for dissolving organic and inorganic components fouling wells. It contains a miscibility solvent that substantially prevents any phase separation between the constituents and lack of dispersion of the additives in the fluid. One aspect of the invention is the production of a single fluid acidizing formulation that comprises a relatively high concentration of mineral or organic acid, a miscibility solvent, a surfactant, and at least an anticorrosion additive, which, when premixed, is stable for extended periods and substantially for periods such as exceeding 1 year and possibly longer at both ambient and wellbore temperatures (when under wellbore pressure). The major claim is that an aqueous 15% hydrochloric acid solution being about 13.8% by weight of the formulation, a miscibility solvent being about 59% by volume of the formulation for forming a substantially stable single fluid, the miscibility solvent further comprising: about 15 wt% of an aromatic solvent; about 63 wt% of a blend of alcohols, the blend of alcohols being about 5 wt% to about 15 wt% long chain alcohols and about 40 wt% to about 60 wt% short chain alcohols; and about 19 wt% to about 24 wt% of a surfactant; a CI being about 1.5 wt% of the formulation; a demulsifier being about 0.04 wt% of the formulation; an antisludge additive being about 0.4 wt% of the formulation; an iron control additive being about 1.5 wt% of the formulation; and the balance being water.

Additional multifunctional solvents are described in Section 3.6.2 of this book.

2.2.6 Additional Fouling Precipitates and Mixed Deposits. In addition to the waxes, asphaltenes, and hydrates, the industry also recognizes calcium or magnesium salts of organic acids that include the complex class called naphthenates as capable of causing fouling. These chemicals also make up the major class of natural surfactants that cause oilfield emulsions to be stabilized and are also used in alkaline EOR floods (Section 5.5.4). If high temperatures are encountered during the production process (such as in separators), polymeric reaction products may form.

Mixed Deposit Chemistries. Mixed deposits are the rule rather than the exception in nature and during oil and gas production. Fig. 2.24 shows a photo of the naturally occurring minerals rose barite (Oklahoma Rose Stone) and Selenite (a mixture of gypsum, sand clay, and probably iron). These minerals have formed in salty seas and may include sand, clay, and iron. These are conditions that are similar to those present in oilfield brines.

Frenier and Ziauddin (2010) have investigated the formation of real world deposits in the oil and gas production that are mixtures of different inorganic salts as well as several organic solids. A photo of a

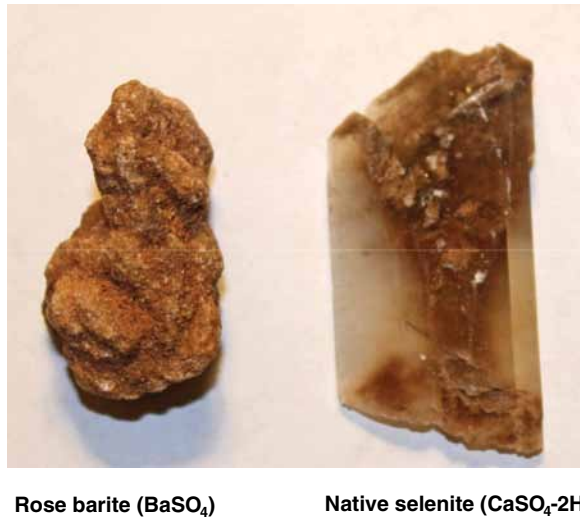


Fig. 2.24—Mixed natural minerals.

mixed deposit from an undersea pipeline in a [Fig. 2.25](#). This deposit contains black powder (Sherik et al. 2008) and organics such as wax and possibly gas hydrates.

The pressure and temperature changes taking place during production produce the conditions for formation of asphaltenes and scale. Because many oil wells are using CO₂ EOR methods to increase recovery (see Section 5.5.2). Both asphaltene deposition and inorganic scales may be exacerbated. This factor absolutely complicates the solubility calculations and estimates (Frenier et al. 2010; Graham and McMahon 2002; Kalantari-Dahaghi et al. 2006; Gonzalez et al. 2007).

However, as noted above, the situation where asphaltenes deposit is complex. Corraera et al. (2010) claim that CO₂ injection allows producers to reach a twofold objectives of increasing the amount of crude oil extracted from an oil field as well as mitigating the contribution of emissions to global. The authors also propose that an intervention is planned in an oil production field in Sicily, Italy, by employing a CO₂ stream already available from an oil refinery located near to the field. However, the producers are concerned that the injected CO₂ could destabilize the asphaltene fraction, leading to the formation of a sludge or a solid phase that would plug the formation pores and, ultimately, decrease



Fig. 2.25—Mixed deposit in pipeline (Bell et al. 2008). Photograph courtesy of Rick Armstrong.

injectivity and productivity. To assess this risk, the authors employed an in-house-developed asphaltene deposition model to investigate various conditions close to the expected operating conditions.

Problems with fouling around an ESP also has been noted (Gagmer and Wolfe 2010), who report that wells on high concentrations of CO₂ flooding have higher amounts of asphaltene and calcite scale on the pump. See Fig. 2.26 for an example of a well in a different field (in West Texas) where asphaltenes have formed onto a mixture of calcite and sulfate scales. These types of deposits will completely stop the ESP.

Shimokata and Yamada (2010) also report that the buildup of asphaltene and CaCO₃ scale is a large problem that will be faced with ESP wells. Once scale is deposited at the downhole, it is difficult to remove and, as a result, oil production will decrease. The authors of the report claim that to avoid asphaltene deposit, xylene is injected into the annulus periodically. To avoid CaCO₃ scale deposition, the brine pH is controlled during stimulation and, if necessary, a scale inhibitor is squeezed after stimulation. Conditions for the deposition of asphaltenes as well as calcite because of pressure changes will be described in Section 2.3.3.

Mixed Inhibitor Treatments for Complex Deposits. There are a number of recent examples of treatments using mixtures of CIs, scale inhibitors, and wax and/or asphaltene inhibitors to treat multiple problems (Frenier and Ziauddin 2010). Note that some details of organic deposits and control method are described in Section 2.2.5. There are benefits from multiple treatments that are included in a single fluid, as well as possible problems. Haynes and Lenderman (1986) described a squeeze treatment method where the aim was to put a slowly dissolving solid paraffin inhibitor into the formation. The paraffin inhibitor was squeezed into the formation in liquid form and then caused to precipitate by an activator. Before the squeeze treatment, these two wells were being treated by hot oiling 3–4 times every year. A step-by-step procedure was followed to perform squeeze treatment in one of the wells in West Texas and is as follows:

- Injection and circulation of hot oil with one drum of paraffin dispersant down the annulus and up the tubing to preflush the wellbore before the squeeze treatment.
- Injection of 10 bbl of crude oil down the annulus, mixed with six drums of activator.
- Injection of 10 bbl of water into the annulus to separate the activator from the inhibitor.
- Injection of a mixture containing six drums of paraffin inhibitor with 60 bbl of crude oil down the annulus.
- Over flush of 270 bbl of water into the annulus to push the previous injected fluids into the formation.
- Shut in the well for 24 hours.

Swanson et al. (2005) discusses the use of a kinetic hydrate inhibitor (KHI) [see Frenier et al. (2010) and Kelland (2009) for details of KHIs and other hydrate inhibitors] used with wax inhibitors. This field application was conducted on a pipeline for a newly recompleted well, which was predicted to have water cuts in the 20% range. Actual water cuts have typically been about 35% but have also increased to above 60% at times. They note that the continuing evaluation of different chemistries, and consequently, different mechanisms for preventing hydrate and wax problems in a subsea pipeline



Fig. 2.26—Asphaltene and calcite scale on ESP screen (anonymous producer).

is reviewed. A KHI was injected after the production rates had stabilized. A wax inhibitor [see Frenier et al. (2010) for discussions of wax inhibitors] was also used because of previous concerns about possible wax blockage.

They found that KHI hydrate inhibitors as well as antiagglomeration-type inhibitors could be used with wax inhibitors using continuous injection application in the deepwater Gulf of Mexico. They claim that the KHIs work well with the paraffin control additives, and there were no incompatibilities. However, a wax crystal modifier was more effective than the wax dispersant at reducing the deposition (plating out) of the wax in the condensate. In addition, there were no major water quality issues caused by using the low dose hydrate inhibitors (LDHIs) continuously. They also concluded that because most previous KHI case histories have typically been from the North Sea, this continuous injection application in the deepwater Gulf of Mexico is somewhat unique and increasingly complex with the addition of paraffin control additives. This paper contained a very comprehensive list of LDHI patents that demonstrates the variety of work in this area as well as a long list of wax inhibitors. See Frenier et al. (2010) for more details of various organic deposit inhibitors.

Potential problems with the use of KHI materials to inhibit hydrate formation in sour gas wells or pipelines have been noted by Graham et al. (2001) and Fu (2007), especially if it is also necessary to inject CIs to protect the metal surfaces from acid gas attack. Because the KHI chemicals and the CI chemicals are all surface active materials [see discussions in Frenier and Ziauddin (2008)], the KHI materials could affect corrosion inhibition and the CI materials could affect hydrate inhibition. A study by Fu (2007) did find that the presence of CI can significantly decrease the performance of KHI. The adverse effect is attributed to the interference between these two types of molecules.

In this case, the KHI materials were described as a homopolymer based on polyvinylcaprolactam chemistry (Bakeev et al. 2000; Fu et al. 2001). The CI chemistries were not described. Only by testing a wide range of KHI and CI chemistries were the authors able to develop KHI/CI formulations that were able to inhibit hydrates as well as corrosion using a single injection package. Data in a paper by Mcfarland et al. (2008) describes the selection process for CI and kinetic hydrate inhibitors in a highly corrosive gas field. Also, Moloney et al. (2008) discusses the work to develop two CI/KHI combinations exhibiting excellent compatibility in terms of corrosion inhibition performance (both general corrosion inhibition as well as, more importantly, pitting corrosion inhibition), hydrate inhibition performance, and high-temperature injection conditions in corrosive wells.

Peytavy et al. (2007) also found that the effectiveness of KHI chemicals was sensitive both to the presence of CI chemicals as well as to the pressure of the well. In a high pressure well (130 bar), the authors found that both the presence of a CI and the pressure required the use of both a high concentration of a KHI plus addition of large amounts of monoethylene glycol to allow an acceptable shut-in time (120 hours) to be possible. Tests at lower pressures and without the CI indicated that the goal could be accomplished with only the KHI material present.

Moore et al. (2009) have performed mechanistic studies on the interactions of CI and KHI materials. Two distinct ideas were explored. See Fig. 2.27 for a diagram of the two theories using chemical models. The first proposed theory (left on the figure) is that KHI and CI are in competition for the surface interface. Both KHI and CI molecules can reside on the interface; if incompatibilities exist between KHI and CI molecules, then the exclusion of the KHI and/or CI could impact performance. Additionally, the interaction could impact packing efficiency also leading to changes in performance if the KHI relies on being in certain position on the interface for maximum performance. The second theory (right side) involves chemical interaction between the KHI and CI at a molecular level. The KHI polymer, in theory (Moore et al. 2009), has anchor points that work by distorting the hydrate structure thereby increasing the amount of energy needed to form hydrates and, thus, slowing down the reaction kinetics.

A publication (Makogon and Sloan 2002) proposed that by being absorbed onto the hydrate crystal, the polymer forces the crystals to grow around and between polymer strands and consequently block the diffusion of gas to the hydrate surface. Therefore, if CI molecules have an affinity to chemically adsorb onto the polymer at these anchor points, this could interfere with the polymer's ability to prevent hydrates. The two mechanisms described above were explored through surface tension measurements and liquid chromatography/mass spectroscopy (Moore et al. 2009). Theory one was explored

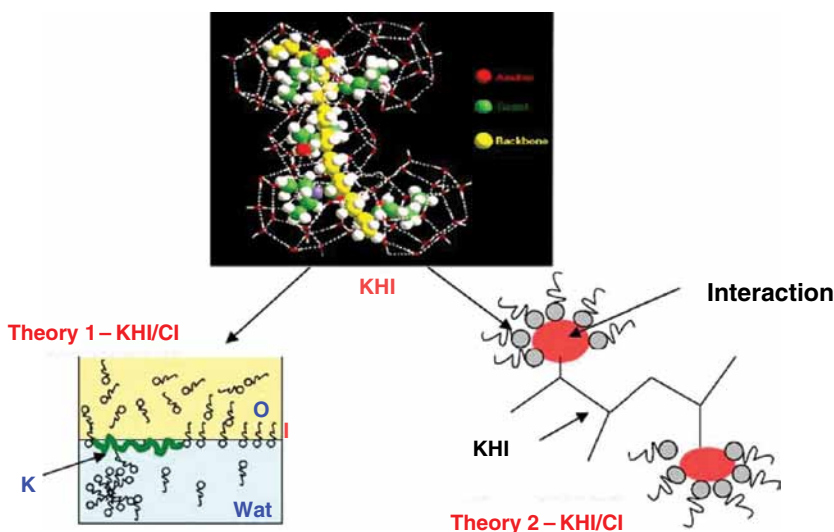


Fig. 2.27—Illustration of two theories of CI/KHI interactions (Moore et al. 2009).

by observing the behavior of the KHI and CI at the surface by means of surface tension measurement. The surface tension measurements were carried out on the CI in the absence or presence of KHI. The KHI concentrations were held constant and various amount of CI were added. Comparison between the surface behavior of CI and/or CI + KHI was investigated. The second theory of interaction was studied by means of absorption techniques. The chemicals chosen in the paper are commercially available and described in [Table 2.2](#).

The results from the corrosion testing (Moore et al. 2009) indicate that minimal performance interference was observed. All three CIs performed the same or better in the presence of the KHI. With the knowledge obtained from performance date the two ideas regarding the interaction were explored. The first theory involves the competition of KHIs and CIs at the surface interface and this was explored though surface tension measurement. Results of the tests indicate that all CIs tested had an impact on the structure of the polymer. In the case of C1, the CI interference was overcome by the incorporation of C1 into the polymer end-groups. C2 observes similar phenomenon; however, association into the polymer was not as complete as C1. Finally, they found that the C3 results indicate the same interference, but in this case, C3 was not able to associate with the polymer end-groups, and consequently, the KHI polymer is altered and the resulting polymer is not able to perform in the presence of C3.

Masoudi and Tohidi (2005) also have looked for interferences between KHI materials and other oil-field chemicals such as mineral scale inhibitors. In this work, an experimental investigation has been carried out, using a hydrate kinetic rig with mixing capability, on the effect of three commercial scale inhibitors called LUVICAP, a known LDHI in the industry. This material contains 40 mass% polyvinyl caprolactam and 60 mass% monoethylene glycol. The scale inhibitors were aqueous solutions of phosphine carboxylic acid polymer, polyvinyl sulfonate, and DTPMP. These materials are some of the most used as well as the most studied inorganic scale inhibitors (Frenier and Ziauddin 2008). The investigators (Masoudi and Tohidi 2005) found that phosphine carboxylic acid polymer was more

TABLE 2.2—CHEMICALS USED IN INTERFERENCE EXPERIMENTS

| Code | Chemistry |
|-----------|--|
| CI A (C1) | Coco dimethyl benzyl ammonium chloride |
| CI B (C2) | Aminoethyl fatty imidazoline |
| CI C (C3) | Ethylene oxide-phosphate ester |
| KHI-1 | PV-CAP polymer |

effective and has more synergist effect than polyvinyl sulfonate or DTPMP. The investigators did not study the effect of the LDHI on the effectiveness of the scale inhibitors.

2.3 Formation Damage

As noted in Section 1.2, a number of factors and operations can cause damage to the NWB formation, and this can seriously affect the flow of hydrocarbons from production wells and may impact the operation of injection wells. Fig. 1.4 describes some of the major types of formation damage and the locations in the flow paths where it may occur. Damage can be caused by organic deposits, inorganic scale, formation fines, mud infiltration, and water/emulsion blocks as well as by mechanical problems. This damage can be described as a skin factor that is equivalent to a resistance (or pressure drop) placed in the flow paths at a critical area. Much of this damage is caused by the solids described in Section 2.2. Additional types and details of the causes of damage are described in this Sections 2.3.1, 2.3.2, and 2.3.3.

2.3.1 Introduction to Formation Damage and Analyses. Sharma (2007) shows a diagram of the pressure profile in a damaged (light yellow) wellbore (Fig. 2.28) and the pressure drop across this damage as fluid flows through it. The skin factor(s) is calculated using Eq. 2.7 (also see Eqs. 1.8 and 1.9 for calculation equations in linear and radial flow). Here (in field units) k is the permeability, h is the thickness of the formation, q is the flow rate, μ is the viscosity, and B is a conversion factor for non-Darcy flow (high rates).

$$S = \left(\frac{kh}{1.41.2q\mu B} \right) \Delta P_{skin} \dots \dots \dots (2.7)$$

The effect of the formation skin (and thus the formation damage) is given by a flow efficiency factor, F :

$$F = \frac{P_R - P_{wf} - \Delta P_{skin}}{P_R - P_{wf}} \frac{\text{Ideal drawdown}}{\text{Actual drawdown}} \dots \dots \dots (2.8)$$

Various factors can contribute to this damage. Bennion (1999) and Thomas and Bennion (1999) gave a general review of various types of *organic solids* damage that can affect production of hydrocarbons (see information and references in Section 2.2.4). They conclude that many oils exhibit high WAT values, which could result in the crystallization of waxes from solution in the oil. These solids can result in the formation of bridging plugs of paraffin at or near the perforations (common in high drawdown wells because of localized cooling near the perforations), as well as in tubing and surface equipment. Fan and Llave (1996) report that paraffin deposition in the NWB formation frequently is caused by improper production techniques such as hot oiling or introduction of cold fluids.

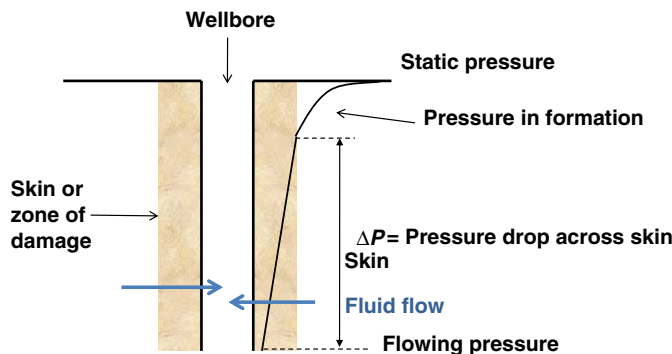


Fig. 2.28—Pressures in NWB areas due to formation damage (from Sharma 2007).

Damage by asphaltenes are more common when production is near the bubblepoint (Bp) pressure [also see Section 4.2 of Frenier et al. (2010)]. Another group of foulants includes diamondoids, which are the gas reservoir equivalent of asphaltenes and hydrates. These problems are frequently treated with solvents, diluents, heat or crystal inhibitors, and wax deposition, but can be extremely damaging in many situations.

Deposition, especially from organic solids, can change the wettability of a hydrocarbon producing formation (Abdallah et al. 2007). Most formations are water-wet before production and hydrocarbons are able to flow between the pore spaces because the water is absorbed onto the rock surfaces. Deposition of organic scale such as asphaltenes may cause the formation to become partially or fully oil-wet, and then the hydrocarbons will cling to the rock surfaces and will not flow to the well during production operations.

The various types of inorganic scales described in Table 2.1 also can precipitate in the formation and in the tubulars because of chemical and mechanical changes that occur during production. Their removal is a major reason for conducting the various “acid” matrix stimulation procedures described in Chapter 3. A simple diagram of scale damage is in Fig. 2.5.

The movement of the fluids during production including the aqueous and the hydrocarbons phases may cause formation fines to migrate and possibly change the permeability of the NWB area. This is termed fines migration. Photomicrographs of several different types of formation damage are described in Fig. 2.29 by Corex (2010). These types of damage include drilling mud, filtrate damage (very fine solids), emulsion and water blocks, and damage from the migration of various types of formation fines. The particles could include broken sand grains as well as various clays that have been destabilized by a change in salinity.

Formation damage can also be caused by well servicing that is not appropriate for the formation or the well fluid. For example, acidizing a well that has an asphaltic crude oil may cause asphaltenes to precipitate. Use of HCl to acidize some sandstone formations may destroy some clay minerals (such as zeolites) and cause additional damage. Some of these factors are described in Chapter 3 of this book.

McLeod (2007) notes that damage near to the wellbore has a great effect on the flow from the well. Fig. 2.30 shows hypothetical cases that cause various amounts of damage and the effects on flow.

These graphs note that most of the reduction in flow happens within 1–2 ft of the wellbore. Sharma (2007) describes several methods for determining the extent of skin (formation) damage. These include multirate tests at stabilized flow rates and more commonly pressure buildup tests. In this test, a well

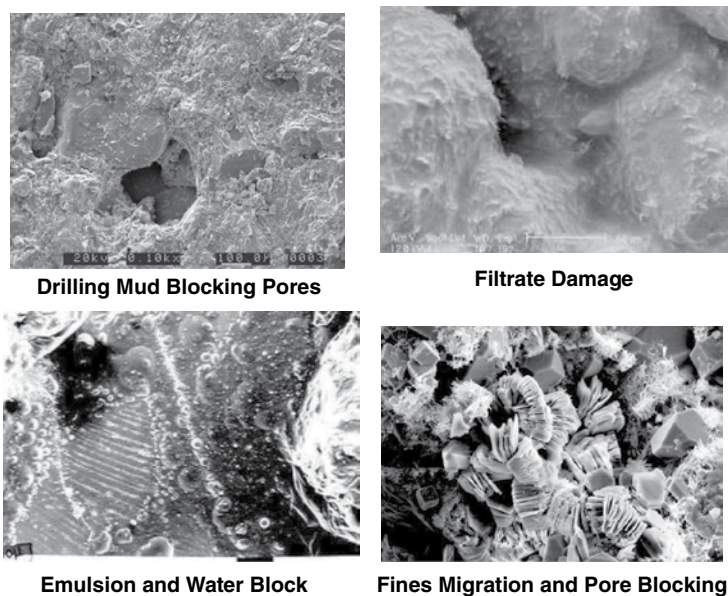


Fig. 2.29—Formation damage photos (Corex 2010).

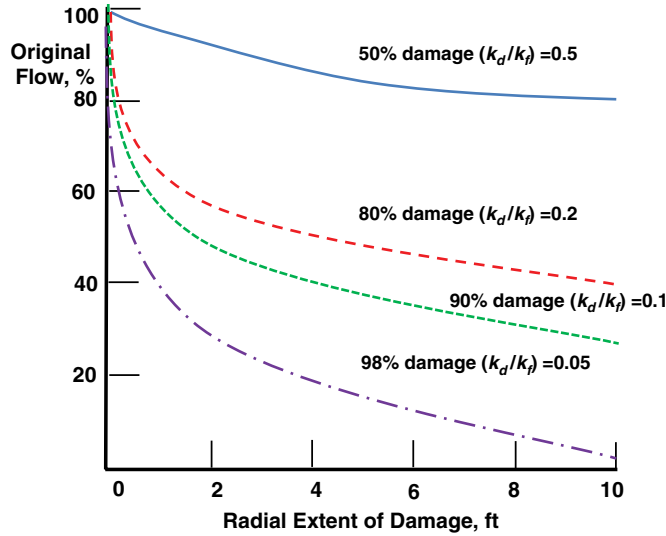


Fig. 2.30—Flow reduction effect of damage on flow McLeod (2007).

that is producing for a time (t) is shut in for a time (Δt). The pressure is then allowed to build up. One type of analytical test based on pressure build up processes uses the Horner (1951) plot (Fig. 2.31), and then Eq. 2.9 to calculate the skin (S):

$$S = 1.15 \left[\frac{P_{wf} - P_{ws,1hr}}{m} - \log \left(\frac{k}{\mu c r_w^2} \right) + 3.23 \right] \dots \dots \dots (2.9)$$

In this equation, m is the slope of the straightline portion of the Horner plot, $p_{ws,1hr}$ is the extrapolated shut-in pressure at 1 hour, and c is the compressibility of the oil. In Fig. 2.31, the x axis is known as the Horner time where t is the time of constant flow and the shut-in for a time (Δt).

These following sections (Sections 2.3.2 and 2.3.3) provide brief reviews of the various types of formation damage that may necessitate the use of the stimulation methods described in Chapters 3 and 4. Also see the texts by Civan (2000) and Sharma (2007) for a more comprehensive description of formation damage and various causes. Several additional assessment methods including core flood tests as well as the use of SEM are referenced in the various sections below.

2.3.2 Drilling- and Completion-Induced Damage. The drilling and completion process uses many chemicals and fluids that are necessary for lubricating the drill bit, for moving the cuttings to the

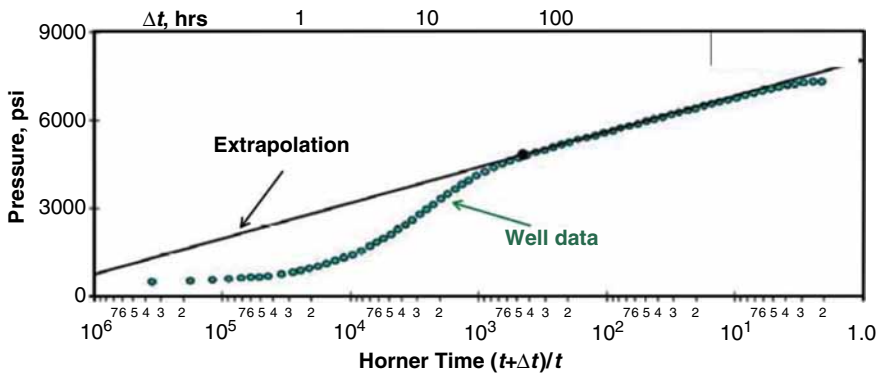


Fig. 2.31—Horner plot.

surface, and for controlling the well pressure. These fluids can be water-based as well as oil-based, but they usually contain suspended solids and surface active agents that may damage the formation if they cannot be removed completely.

Drilling mud is a complex dispersion of various clays and thickeners and weighting (Growcock 2005). A filter cake will build up on the formation face, and both small particles as well as fluids can then invade the formation. Thus, drilling mud infiltration can be a major impairment of the flow paths in the NWB area. Fig. 2.29 shows photomicrographs of mud-blocking pores, filtrate damage, as well as fines migration and water block damage.

To describe mud damage, Lohne et al. (2010) have produced a simulation model for computing the damage imposed on the formation during overbalanced drilling (a higher pressure than the formation). The main parts of the model are filter-cake buildup under both static and dynamic conditions; fluid loss to the formation; transport of solids and polymers inside the formation, including effects of pore-lining retention and pore-throat plugging; and salinity effects on fines stability and clay swelling. The developed model is claimed to handle multicomponent water-based-mud systems at both the core scale (linear model) and the field scale (2D radial model). Among the computed results are fluid loss vs. time, internal damage distribution, and productivity calculations for both the entire well and individual sections.

According to Sharma (2007), damage by water-based drilling fluids (that contain salts, surfactants, polymers, and most significantly, bentonite clay) usually is restricted to the first 8 in. from the wellbore. Fig. 2.29 shows micrographs of drilling mud and filtrate damage and Fig. 2.30 shows the effect of the damage on flow.

In some formations, just the water as well as the clays may cause damage. Lakatos et al. (2010) have described a detailed laboratory study that has been carried out with the aim at restricting the spontaneous imbibition (see Section 1.6 for definitions and equations) and penetration of drilling fluids into tight gas sand and basin-concentrated gas accumulation reservoirs. Based on the experimental results, it was clearly indicated that the water can be a natural blocking phase, causing serious formation damaging that is hard to cure. Thus, if the formation was ever contacted by water, production of the gas would be very difficult.

Consequently, the authors claim that the fluid penetration from drilling fluids can be modified only by surface (interfacial) tension lowering and wettability alteration (from strongly water-wet to intermediate or oil-wet state). In addition, proper selection of the cake forming components may significantly decrease the liquid uptake in tight, low permeable sandstones. The laboratory studies indicated that when using special (oil-wetting) surfactants, organic water miscible solvents, and special high-molecular weight additives, the spontaneous imbibition and penetration of liquid phase of the water-based drilling mud can be significantly influenced in unconventional gas reservoirs, thus mitigating the formation damage often encountered in tight sands and basin-concentrated gas accumulation. These authors mention the use of ethoxylated alkylphenols with reduced ethoxy numbers as a way to control the wetting properties of the fluids.

Oil-based drilling mud contains water dispersed in an oil and the thickening/weighting agent will include an organophilic clay may be employed to reduce damage by water. These materials can be produced by adsorbing a hydrophobic surfactant (such as dimethyl benzyl lauryl ammonium chloride—Fig. 2.32) onto bentonite clay. The clay particles and the oil can also invade the formation if the filter cake does not develop properly and can cause filtrate/solids plugging as well as affect the

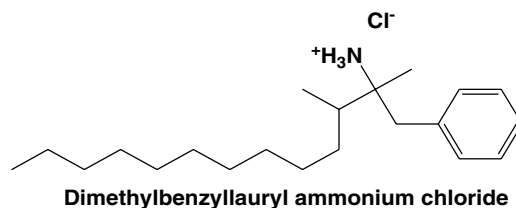


Fig. 2.32—Dimethylbenzyl lauryl ammonium chloride.

wetting characteristics of the NWB formation. Both water-based and oil-based mud damage types are frequently treated using the matrix acidizing methods described in Chapter 3. The conclusions from the previous paragraphs are that water-based and oil-based drilling fluids can cause damage by invading the NWB formation with solids (clays), precipitated salts, surfactants, oils, and possibly just water. Physical blocking as well as wettability changes may, thus, affect the NWB permeability. The authors of this book note that similar chemistry is associated with several chemical EOR processes (See Section 3.7).

Completion and workover fluids are used to contain the well pressure after the well is drilled as well as to apply sand control gravel. Clear brine includes heavy Ca and Zn salt solution (CaCl_2 , CaBr_2 , and ZnBr_2). These can cause precipitations to form if they come in contact with incompatible well fluids that contain sulfate ions or if the pH is raised. These materials, especially the Zn-containing brines (these are Lewis acids) can also cause corrosion damage and corrosion solids if not properly inhibited (Coffey 1980).

2.3.3 Production Processes That Induce Damage. The production process themselves are a major cause of damage because fluids are flowing through new and unnatural pathways and new chemicals are being introduced into the formation. Several types of production-induced damage are reviewed in this section.

Fines Migration. Migration of formation fines can take place in any formation, but it is particularly important in predominantly sandstone matrices because the components are soluble mostly in HF containing solvents and, thus, very difficult to remove. Some details of sandstone formations are described in Section 3.5.2. Because the mobile particles are usually clay fines (aluminosilicates—details of some clay structures are in Section 1.5.6) these particles can be detached, especially if there is a change in the water salinity. Many types of clay and other aluminosilicates have large ion exchange capacities because of surface charges (see Section 1.5.6). Fig. 2.33 shows the microstructure of two types of clays and the layered structure that can attract anions and cations to satisfy any charge difference. This figure also shows an example of the layered structure of kaolinite (right) that is held together by chemical forces between the various layers.

Sharma (2007) notes that the different types of fine particles in the matrix are held together by van der Waal forces, and as the salinity is reduced, repulsive forces will cause some of these to disperse. This can cause plugging of the pore throats and loss of flow. A classic example of this type of damage uses the water shock test. In this experiment, the investigator uses a pump to flow a salt brine through a core, and then follows with by a fresh water flow. Fig. 2.34 plots the change in permeability vs. pore volume of injected fluids and shows typical results of the change in salinity, the temporary return in

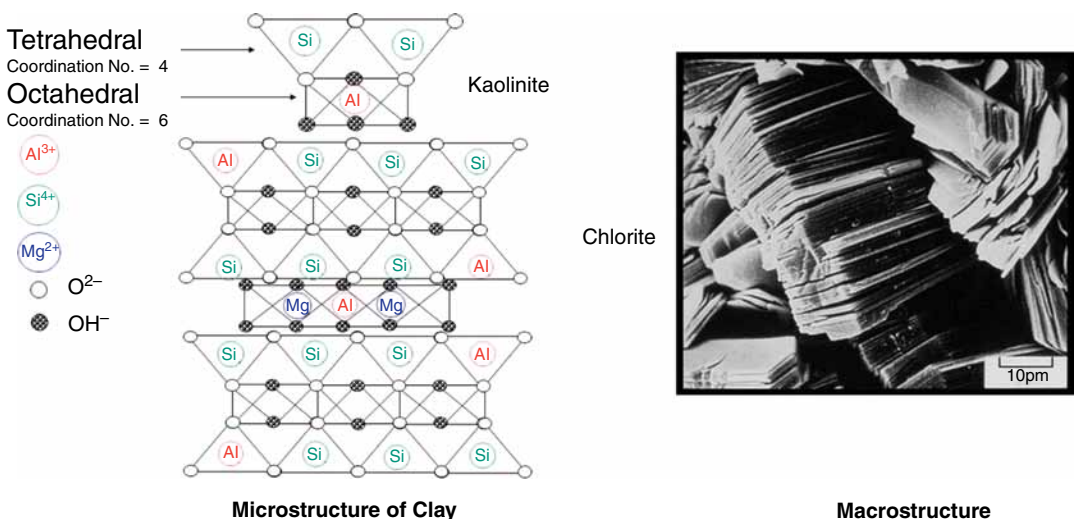


Fig. 2.33—Clay micro and macrostructure.

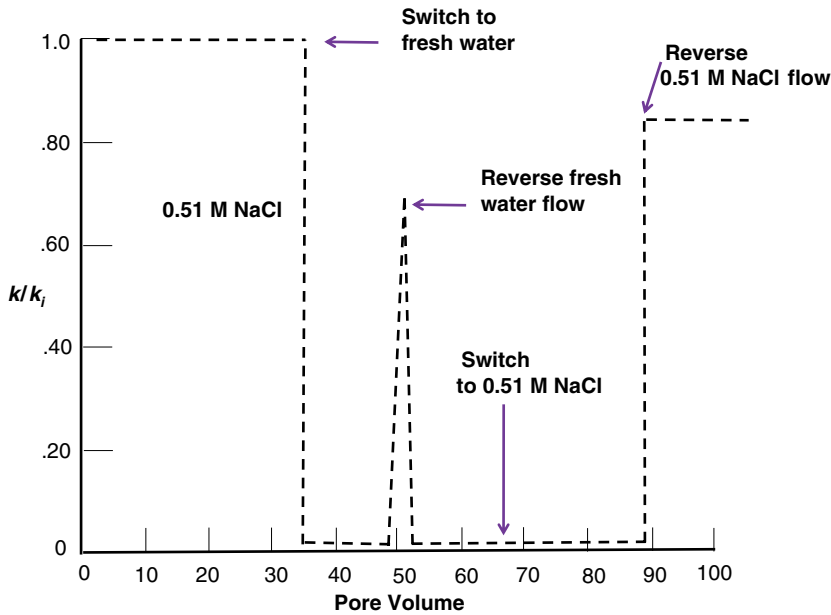


Fig. 2.34—Water shock test on a Berea sandstone core (from Sharma 2007).

permeability, and the reattachment of the particles as the flow of salt solution is reversed. A change in the type of cation also may affect the dispersal of some clay types. For example, calcium ions compact bentonite clays and sodium ions may allow the dispersal of them.

Montmorillonite, smectite, and some illite clay may cause a type of formation damage called clay swelling that is different from fines migrations. A change in salinity or the type of the ions in the water may greatly increase the volume as water that invades the layers of the macrostructure. Sharma (2007) describe a three step process:

- Crystalline swelling takes place as water invades the space between the layers (seen in the left part of Fig. 2.33).
- Hydration swelling takes place as more water hydrates the ions between the macroclay layers.
- When the clays have adsorbed enough water and the layers are approximately 50 Å apart, free swelling causes complete dispersal and more plugging.

A number of clay control chemicals are available to reduce the effects of fines migration. These include NH_4Cl , KCl, metal salts, and various nitrogen quats. Section 3.6.4 provides more information on clay control chemicals used in acidizing fluids. Clay control chemicals are also used during fracturing treatments (Section 4.7.5). They are thought to adsorb on the clay surfaces and stabilize the charges. Also see the descriptions of clay control chemicals in Chapter 3 of Fink (2011).

Formation Damage Caused by Organic Solids and Inorganic Scales. Sharma (2007) states that one of the most common causes of formation damage in mature wells is organic solids including paraffin wax and asphaltenes that form in the wellbore and in the NWB formation. Fig. 2.4 shows wax blocking a production tubing. Also see the discussion by Bennion (1999).

Leontaritis (1998) developed a model for formation damage caused by asphaltenes. Three possible mechanisms of asphaltene-induced formation damage have been discussed by this author. Asphaltenes can reduce the hydrocarbon effective mobility by

1. Blocking pore throats, thus reducing the rock permeability, k .
2. Adsorbing onto the rock and altering the formation wettability from water-wet to oil-wet, thus diminishing the effective permeability to oil, k .
3. Increasing the reservoir fluid viscosity, pressure, by nucleating water-in-oil emulsions.

Boek et al. (2008) studied the aggregation and deposition of colloidal asphaltene in reservoir rock. To obtain a fundamental understanding of this phenomenon, they have studied the deposition and aggregation of colloidal asphaltene in capillary flow by experiment and simulation using the stochastic rotation dynamics method, in which the solvent hydrodynamic emerges from the collisions between the solvent particles, while they claim that Brownian motion emerges naturally from the interactions between the colloidal asphaltene particles and the solvent. In this model, the asphaltene colloids interact through a screened Coulomb potential. They observed that the solvent flow rate decreases when the asphaltene particles become more sticky. Descriptions of asphaltene coagulation is also described in Section 2.4 where it is associated with stabilization of emulsions.

Yi et al. (2009) have described a study of the effect of asphaltene on the development of the Marrat field using a compositional simulation with asphaltene modeling facility for this field. They claim that the model enables the simulation of asphaltene precipitation, flocculation, and deposition including adsorption, plugging, and entrainment, and the resulting reduction in porosity and permeability and changes in oil viscosity and rock wettability.

In this work, asphaltenes were characterised by a set of hydrocarbon component(s) that are dissolved into oil and can precipitate from the oil and deposit on the rock surface changing the properties of the fluids and the formation, as illustrated in Fig. 2.35 that has three stages of precipitation, flocculation, and finally deposition. This process is considered to be reversible if the triggering variable(s) changes are reversed. The process is then modeled by a dissolution-like procedure, in which the amount of precipitate coming out of the oil solution at a given value of the variable(s) represents the ability of the oil solution to dissolve the asphaltene component(s). The amount of precipitate corresponds to the excess of a specified component in the oil phase with respect to the solubility limit defined in the model as a function of P , T , or Z (or two of those variables) and based on laboratory data. They (Yi et al. 2009) claim that this provides a simple and flexible way to use laboratory data directly in the simulator. In Fig. 2.35, the change in wettability is shown in the insert.

Formation damage by inorganic salts includes blockages by carbonates as well as sulfates. Fig. 2.1 shows examples of damage to tubing caused by inorganic scales. A short review of the formation or inorganic scale and organic foulants are in Section 2.2. Much more details of formation damage by these solids are described in Frenier et al. (2010) and Frenier and Ziauddin (2008).

One of the most common mechanisms for the formation of calcite in sandstone formations and production tubulars is flash scaling, which is initiated by a pressure drop. Fig. 2.36 shows a depiction of flash scaling. The mechanism is keyed to the 5 equilibrium shown on the drawing. Simple precipitation of solid CaCO_3 is controlled by the bicarbonate ions in the solution formed from dissolution of CO_2 in water. At the low pH values expected from high CO_2 partial pressures, calcite will not form. As CO_2 leaves solution because of a pressure drop, the pH raises enabling bicarbonate to be converted

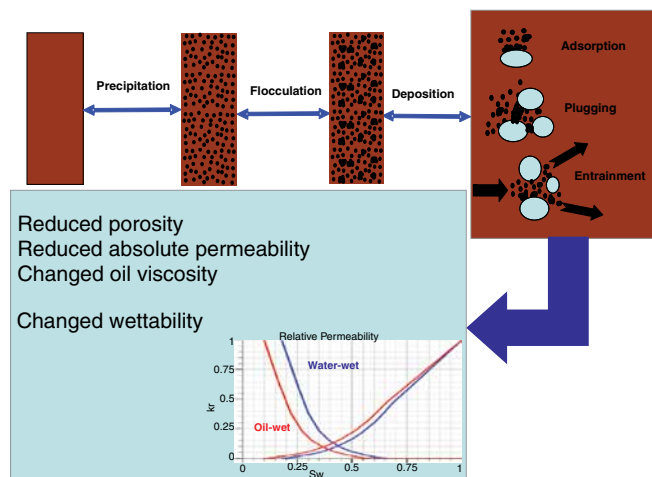
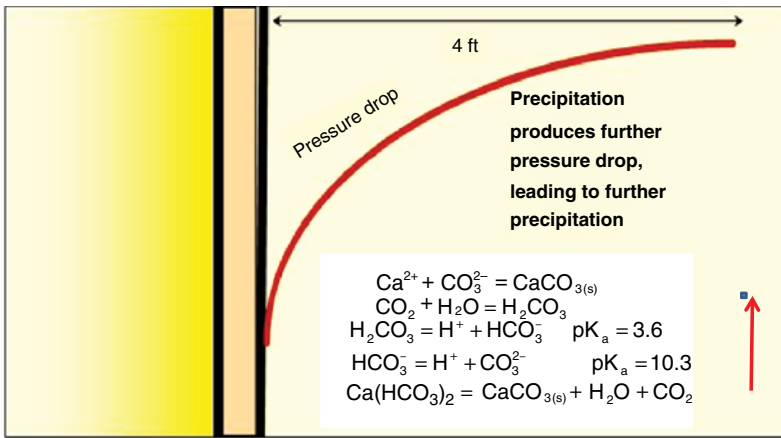


Fig. 2.35—Asphaltene modeling (Yi et al. 2009).



Pressure drop causes CO_2 to break out of solution, causing precipitation of calcium carbonate scale

Fig. 2.36—Flash scaling as pressure changes.

to carbonate ions, then calcite scale forms very rapidly. The authors of this book have observed flash scaling in the lab in a few seconds after releasing pressure from a test flask.

A pressure drop also may induce precipitation of asphaltenes (Hammami and Ratulowski 2007), resulting in a mixed deposit of asphaltenes and calcite. Section 2.2.3 describes problems with precipitation and migration of FeS particles that may affect injection wells used in EOR enhancement treatments. Fig. 2.26 shows a photo of an ESP that is badly fouled by a mixture of scale and asphaltenes and the proposed mechanisms involve the various pressure changes during production.

Injection of Produced Water. Produced water is often used as an injection fluid (see the discussions of water flooding in Section 5.4.1) for pressure maintenance and various EOR processes. The use of the produced water may reduce the potential of causing formation damage because of incompatible fluids, although the risk of scaling or corrosion in injection wells' flowlines or tubing remains. Also, the produced water can be contaminated with hydrocarbons, bacteria (including sulfate-reducing bacteria), and solid, and at some point must be disposed of in some manner. Disposal at sea or in a river will require a certain level of cleanup of the water stream first. However, the processing required to render produced water fit for reinjection may be equally costly. See additional discussions of the use and disposal of produced water in Section 6.3.

Zhang et al. (1993) claim that produced oily water injection is under consideration in offshore waterflooding fields because of the possible environmental impact of the alternative of sea disposal. The amount of produced water containing heavy metals, chemicals, and other organics is estimated to be the range of 50 million tons each year.

Among the advantages of produced water injection (according to these authors) are that the water quality treatment for produced oily water injection may be less than that for raw seawater and other sources of water and produced water is normally compatible with the reservoir fluids and seldom causes scale problems. However, because the produced water has had lengthy contact with crude oil and other mineral material at reservoir temperatures, as well as experiencing mixing during flow from the reservoir to the surface, oil droplets and solid particles may be dispersed in it. These oil droplets and solids may cause severe formation damage if the produced water is injected into the reservoir. The results of the authors' (Zhang et al. 1993) study claim that produced oily water containing oil droplets and solid particles can contribute to the permeability decline observed in the cores. The permeability alteration resulting from a combination of both oil droplets and solid particles is more severe than obtained from the systems individually. Note the information in Section 2.3.3 on emulsion damage and on wettability issues.

Al-Abduwani et al. (2005) claim that the importance of produced water reinjection is unquestionable. It is in many cases the cheapest and most environmentally friendly solution for wastewater disposal. It is also a feasible method for EOR as a waterflooding mechanism.

The authors claim that produced water reinjection suffers from a major limitation, which include the current inability of accurately predicting the lifespan and performance of its injection wells. This is because of the multitude of parameters that affect it. Some of the issues include containing changes in composition and pH values. These changes can cause changes in scaling patterns as well as changes in corrosion control strategies. See discussions in Sections 2.2.3, 2.2.4, 6.3, and Frier and Ziauddin (2008).

Injection of Seawater. The previous section described scaling and problems from oil during injection of produced water. This section describes scaling from injecting seawater. This is very common for pressure maintenance and EOR activities offshore.

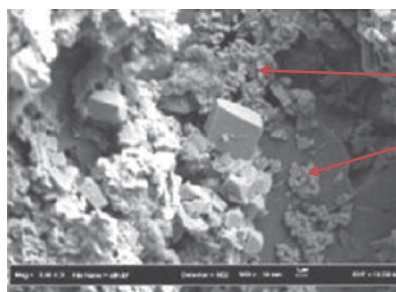
Two waters are incompatible if they interact chemically and precipitate minerals when mixed (see the Eqs. 2.1 and 2.2). A few more details are in Section 2.2.2 and much more information is in Frier and Ziauddin (2008). Typical examples of problems are seawater, with high concentration of sulfate ion and formation waters, with high concentrations of calcium, barium, and strontium ions. Mixing of these waters, therefore, could cause precipitation of calcium sulfate, barium sulfate, and/or strontium sulfate. However, seawater injection will continue to be necessary for pressure maintenance, so several examples of use problems are abstracted.

Merdhah and Yassin (2009) conducted an investigation of the permeability reduction caused by deposition of calcium, strontium, and barium sulfates in sandstone cores from mixing of injected Malaysian sea waters (from the Angsi and Barton fields) and formation water that contained high concentration of calcium, barium, and strontium ions at various temperatures (60–90°C) and differential pressures (125–175 psig).

Results (Merdhah and Yassin 2009) have shown that a large extent of permeability damage caused by calcium, strontium, and barium sulfates that deposited on the rock pore surface. The rock permeability decline indicates the influence of the concentration of calcium, barium, and strontium ions. At higher temperatures, the deposition of CaSO_4 and SrSO_4 scales increases and the deposition of BaSO_4 scale decreases because the solubilities of CaSO_4 and SrSO_4 scales decreases and the solubility of BaSO_4 increases with increasing temperature. The deposition of CaSO_4 , SrSO_4 , and BaSO_4 scales during flow of injection waters porous media was shown by SEM micrographs. See Fig. 2.37 for images of sandstone cores before and after injection of the seawater. Scale is noted in the after examination.



SEM Image of Unscaled Sandstone Core



SEM Image of CaSO_4 and SrSO_4 Scale in Sandstone Core

Fig. 2.37—Effects of injection of mixed waters on sandstone cores using SEM (Merdhah and Yassin 2009).

Coreflood (Malaysian Sandstone) Tests with Seawater and Barium

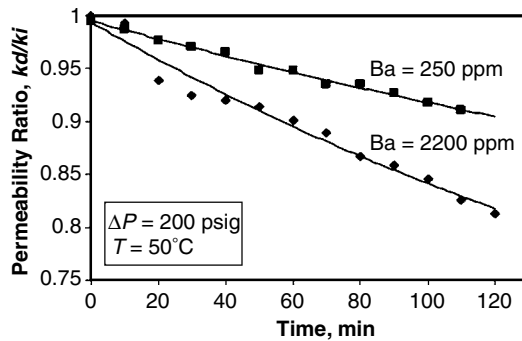


Fig. 2.38—Permeability loss using coreflood tests with sandstone and barium sulfate precipitation (Merdhah and Yassin 2009).

Fig. 2.38 shows permeability loss because of formation damage from seawater containing barium based on coreflood tests. Fig. 2.39 presents a schematic of the production system and the projected areas for expecting scale damage in the well system. The list of possible damage areas is extensive, possibly requiring addition of scale inhibitors or changing operating conditions.

In-Situ Emulsification. A consequence of mixing various aqueous and organic well fluids may be the formation of emulsions in the reservoir that can cause damage. Section 2.4 provides very extensive information on formation and control of emulsions in the topside production equipment. The shear forces that cause emulsions to form also take place in the production matrix. Section 2.2.5 described damage because of wax and asphaltenes and inorganic scale. These three solid types also can stabilize emulsions if a surface active chemical is present in the crude oil or in the production water. Natural as well as introduced surfactants may present to stabilize the emulsion. Naturally occurring surfactants include the various many naphthenates present in many acidic crude oils and quantities of surfactants and are employed in EOR operations (Chapter 5).

One EOR process uses alkaline fluids to generate these surfactants in-situ. Sharma (2007) notes that there are ways to reduce the effect of in-situ emulsions including using demulsifiers (DMs) and solvents (also described in Section 2.4); however, the best remedy is testing the fluids before production to try to eliminate formation of them.

Water Block and Wettability Alterations. Water blocks and other wettability alterations are associated with the surface energy and wetting technologies described in Section 1.5.6 and Figs. 1.34 and 1.35.

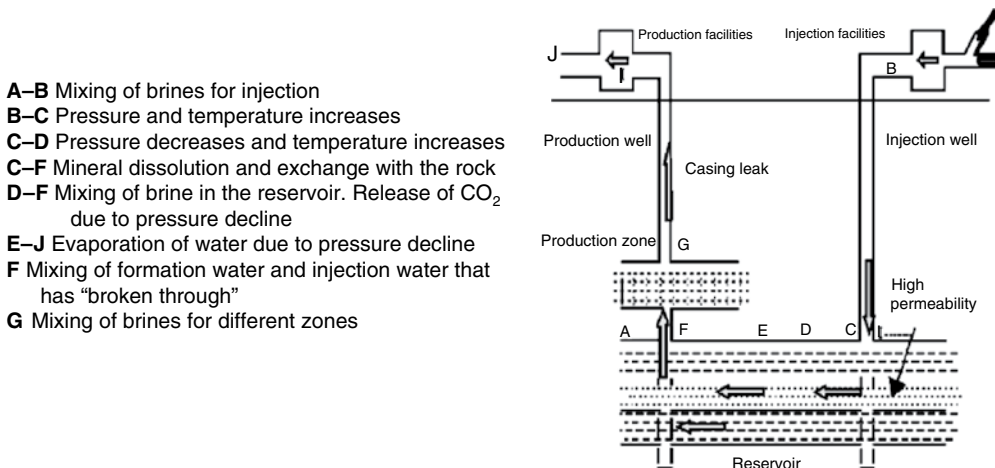


Fig. 2.39—Location of fouling due to injected water (Merdhah and Yassin 2008).

Sharma (2007) says that if a large amount of water is lost during drilling, a water block may exist around the wellbore. This may cause water to block the flow of hydrocarbons. Fig. 2.29 shows a micrograph of a water block. This author (Sharma 2007) claims that the duration of the block may depend on the balance of capillary forces in the NWB formation. Surfactant or mutual solvent washes of this area may resolve the blockage.

Deposition, especially from organic solids, can change the wettability of a hydrocarbon producing formation (Abdallah et al. 2007). Most formations are water-wet before production and hydrocarbons are able to flow between the pore spaces because the water is absorbed onto the rock surfaces. Deposition of organic scale such as asphaltenes may cause the formation to become partially or fully oil-wet, and then the hydrocarbons will cling to the rock surfaces and will not flow to the well during production operations. Fig. 2.40 is a depiction of a water-wet and oil-wet formation and the location of the oil and water phases. Changes from water-wet to oil-wet will block the flow of hydrocarbons because the connate water cannot be displaced by the formation pressure of the flowing fluids. This may be caused by a loss of surfactants or as a natural process as the reservoir is depleted of oil and connate water. Application of solvents or water-wetting surfactants may resolve these problems. Also see the discussion of the need for oil/organic drilling fluids for use in tight gas formations (Lakatos et al. 2010) to reduced the imbibition of water and, thus, prevent water blocks.

Bazin et al. (2010) claim that invasion of aqueous drilling, completion, or fracturing fluids can reduce the relative permeability to gas and thereby causes a water block. In the case of low-permeability formations, the capillary pressure tends to be high because of the small pore size. Cleanup of water blocks requires high drawdown unless water vaporization by the flowing gas is improved by using specific additives such as alcohols. Bazin et al. (2010) investigated fracture-face damage by measuring petrophysical parameters including: absolute-permeability damage and gas return permeabilities. They tested shaley sandstone (Moliere) that contains approximately 13 vol% of illite clay. The absolute gas permeability was 1–10 μD . The test fluids included a borate crosslinked carboxymethyl hydroxypropyl guar (CMHPG) as well as 25 vol% methanol. They found that adding alcohol in the fracturing fluid has a striking effect on resolving water blocks. See Fig. 2.41, which shows the return permeability values from coreflood tests using fluids that contained CMHPG and CMHPG + 25% methanol.

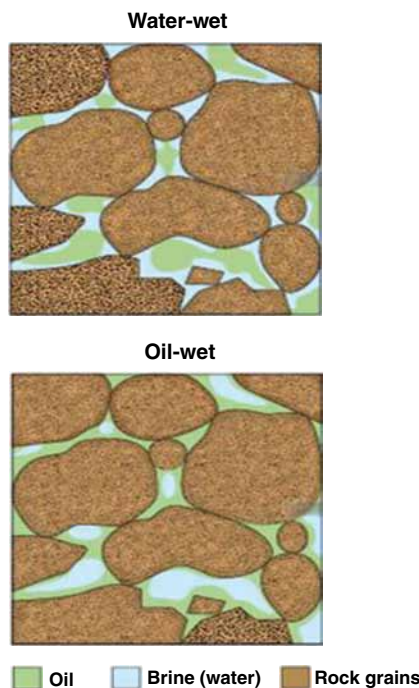


Fig. 2.40—Water-wet and oil-wet formation (Abdallah et al. 2007).

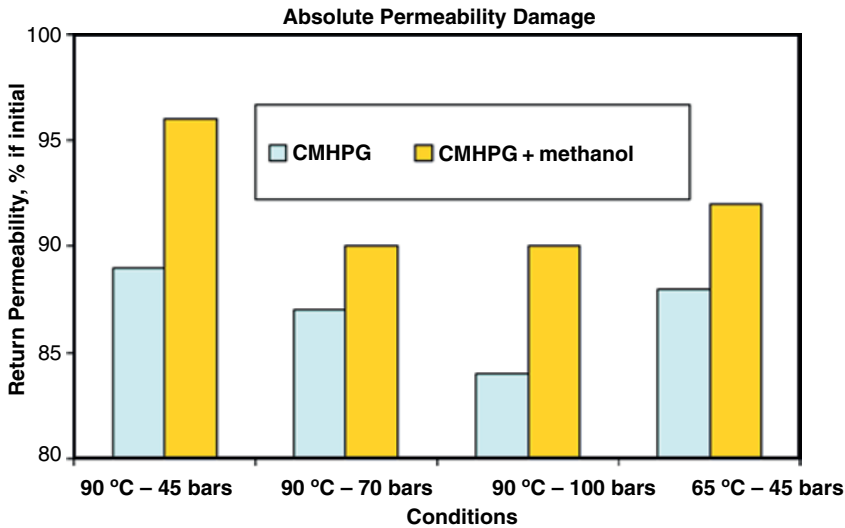


Fig. 2.41—Return permeability values after filtration of Moliere sandstone with fracturing fluids (Bazin et al. 2010).

Ahmadi et al. (2011) claim to have tested chemicals that contain fluorinated nonionic surfactants deployed in alcohol-type solvents (Bang et al. 2010) to relieve liquid blocking in gas wells. These authors claim that the use of these chemicals can increase the gas permeability by 80%, compared with controls.

Damage Because of Stimulation Treatments. Stimulation treatments (especially HCl treatments) are known to cause formation damage unless they are properly executed. Refer to Chapter 3 and Section 1.6.1 for details on reactive chemicals treatments that are actually designed to remove damage. Several types of damage are reviewed.

Bryant and Buller (1990) note that well treatments with only HCl are potentially damaging in formations that contain aluminosilicates minerals (clays, feldspars, and micas) because HCl reacts significantly with aluminosilicates, leaching aluminum and forming hydrated silica. Fluid flow past leached mineral particles liberates mineral fragments and amorphous silica within the pore network. These fines can block pore throats, reducing the rock permeability. Both field data and reservoir-condition coreflood test results were found to be consistent with this chemical reaction and permeability impairment mechanism. The average permeability reduction in the coreflood test described by these authors was 35%.

El-Monier and Nasr-El-Din (2011c) and Khilar and Fogler (1998) propose that clays released from water-sensitive Berea sandstone cores because of contact with either acidic or highly alkaline fluids remain dispersed until captured in the pore throats, thus initiating formation damage. Therefore, acidizing as well as prop fracture treatments (usually high pH) also may cause fines release and cause damage.

Aluminum and metal ions are extracted from the mineral, leaving behind a siliceous residue. Because aluminum is an essential constituent of aluminosilicate mineral lattices, its removal by HCl must weaken the structure of the mineral particles. HCl and mud (HCl/HF) acids used in many sandstone treatments can, thus, produce damage to clay release and precipitation of silica (Ali and Hinkel 2001). These reactions are described in more detail in Section 3.5.5. El-Monier and Nasr-El-Din (2011c) also claim that the fraying and fragmentation of aluminosilicates exposed to strong acid are well documented. More details of these reactions as well as solutions to these problems are in Section 3.5 of the current book.

Jacobs and Thorne (1986) studied asphaltene precipitation during acid stimulation treatments. They found that iron contamination promoted the precipitation of asphaltenes when acidizing certain oil-bearing zones. This can cause severe formation damage. Standard antisludging agents (see

Section 2.4.4), normally used to prevent this, may not be effective in the presence of iron. Commonly used iron sequestrants were found not to prevent the asphaltic sludging. Proposed mechanisms to explain these observations are presented along with a new iron control additive that does prevent the precipitation when used with conventional antisludging agents (chemistry not listed).

Section 2.2.3 describes methods for controlling of FeS precipitation damage. Alternative treatments are described in Section 3.6.3 of this book. Also fracturing treatments may cause water blocks (Bazin et al. 2010). As will be discussed in Sections 4.2 and 4.8.1, fracturing fluids must be designed to be compatible with the formation and damage including fines release and loss of native permeability from the frac gels must be understood and evaluated. Clay stabilizers are described in both Sections 3.6.4 and 4.7.5.

It is clear from the text in this section that there is considerable overlap with the various causes of formation damage and the fundamental chemical/physical forces must be analyzed to prevent or alleviate the damage.

2.4 Formation and Control of Emulsions in Production Operations

During oil production and transportation, water and oil phases are coproduced, and if the fluids are exposed to sufficient mixing energy, they will form dispersions of water droplets in oil (W/O) and, conversely, oil droplets in water (O/W). See Section 1.4.4 that briefly introduces concepts of the formation of emulsions. Unfortunately, the crude oil may contain a number of components, which may act to form emulsions. These natural surfactants include asphaltenes, resins, and naphthenic acids and other carboxylic acids as well as amines and sulfur-containing organic molecules. These compounds may accumulate at the water-oil interface and hinder the droplets from reforming a separate phase (Auflem 2002).

Water-in-crude oil emulsions can form during the processing of fluids from hydrocarbon reservoirs to the refinery or in production facilities during extraction and cleaning. The emulsified water adds significant volume to the crude oil; it also may cause corrosion (Section 2.2.2) in the pipelines and increase the cost of transportation and refining. Kalra et al. (2012) claim that the viscosity (and thus the more complex rheology) of an oilfield emulsion can have a significant effect on a topside facility and must be considered in sizing piping and pumps. This may especially influence work in EOR-surfactant floods (see Section 5.5.3).

Al-Asmi et al. (1999) note that it is difficult to describe and predict the effects of emulsified water in pipelines without extensive tests because both Newtonian and non-Newtonian flow behavior may occur. During production operations, both W/O and O/W emulsions may form.

Because the amount of water in the oil affects pipeline operations (and will have to be separated at some point) and the amount of oil that is allowable in produced water before discharge or reuse is small [usually < 42 mg/l (USDOE 2007)], resolution of these emulsions is an absolute requirement. Chemicals (demulsifiers) and mechanical equipment are in use to separate the aqueous and hydrocarbon phases during the final stages of production.

If a spill of crude or other hydrocarbon products should occur in a stream, lake, or in the ocean, emulsifiers (dispersants) may be used as part of the cleanup plan to reduce the effects of the oil on shore facilities or to clean up wildlife or other affected items. These types of purpose-caused emulsions usually are of the O/W type. W/O emulsions also can form during oceanic spills. These emulsions are very stable and the oil phase is difficult to recover, leading to great environmental damage. Because of their color and semisolid consistency, they are often named chocolate mousse (Auflem 2002). See [Fig. 2.42](#) to see this phenomenon. In this photo, the oil emulsion is the orange/brown mass on the surface of the blue water.

This section will review the literature on the formation and resolution of crude oil-water emulsions by describing the mechanism of formation and the chemicals and mechanical methods of demulsification. Compilations of additional information on emulsions and antiemulsion chemicals are included in the books by Becker (1997), Fink (2003), Fink (2011), Kelland (2009), and Kokal (2006).

The authors of this book note that emulsions are used in both reactive stimulation of formations, in hydraulic fracturing, and in EOR. Those useful aspects of emulsions are described in Sections 3.8.1 and 5.5.3. Specific information on spill cleanup (where O/W emulsions are also formed deliberately) will be addressed in Section 6.4.



Fig. 2.42—Chocolate mousse emulsion (NGS 2010).

2.4.1 Introduction to Production Phase Emulsion Formation Mechanisms. Micrographs of simple emulsions are seen as Figs. 1.14 through 1.15. A photomicrograph of a more complex W/O in water emulsion is seen as Fig. 2.43. In the figure, the water is the white phase, the oil is brown, and the W/O phase is yellow.

These more complex emulsions as well as the simpler production-produced emulsions are described by Kokal (2006), who claims that W/O emulsions are more common in the production environment; however, the more complex cases are also encountered. In these cases just described, the droplet diameters are 5–15 μm in range. These are called macroemulsions (droplet size $> 1 \mu\text{m}$). Because these are essentially supersaturated systems, physical (gravity) and chemical driving forces will cause the droplets to coalesce and the emulsion will eventually break. The rate of breaking and, thus, the problems caused by oilfield emulsions, vary greatly depending on

- The water composition
- The oil composition
- The presence of numerous surface active agents (solids, liquids, gasses, and individual molecules)
- The temperature
- The shear conditions and the shear history

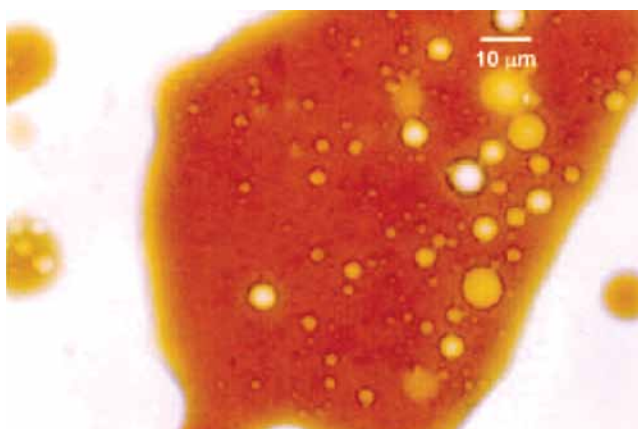


Fig. 2.43—Photomicrograph of W/O in water emulsion (Kokal 2006).

The unstable macroemulsions are usually the system encountered in the oil production areas. Microemulsions exist where the droplets may be in the 10 nm size range. These are very stable, usually are formed using solvents and cosurfactants (Collins et al. 2001), and are not usually encountered unless they are created for a purpose. There is a discussion of the use of microemulsions in Section 2.2.4 and microemulsions are used in EOR formulations. See Section 5.5.3.

Kalra et al. (2012) also claim that the rheological properties of the emulsion formed is an important property that must be measured and considered in facilities planning. Their work has shown that the viscosity of native W/O depends on several factors:

- Shear rate—high shear usually results in lower viscosities, but some fluids may be non-Newtonian.
- API gravity (and composition of the oil)—it usually is higher for heavier oils.
- Water cut—this is critical as the viscosity increases with water cut until an inversion point where an W/O emulsion forms and the viscosity falls.
- Temperature—their data shows that (with other variables constant) viscosity increases with increasing temperatures. The authors do not have a satisfactory explanation for this observation.
- Additional surfactant—this addition caused by EOR activities may increase the viscosity because of the formation of smaller droplets and, thus, a more stable emulsion.

2.4.2 Details of the Formation of Oilfield Emulsions. These emulsions are considered to be liquid-in-liquid colloidal dispersions. Two critical factors for forming them are shear forces and emulsifying agents that can be located at the surface of the discontinuous phase. During production, aqueous brines and hydrocarbons are in contact. Kokal (2006) claims that the internal phase usually is the one with the lower relative concentration. During the production operations, there are a lot of opportunities for shear. Included are

- Flow through reservoir rock
- Bottomhole perforations
- Pumping operations
- Flow through tubing, flowlines, and production headers; valves, fittings, and chokes
- Surface equipment
- Gas bubbles released because of phase change

The amount of mixing/shear depends on many different factors and is difficult to avoid. In general, though, the greater the shearing forces, the smaller the droplets of water dispersed in the oil and the tighter the emulsion. Because shear is also difficult to measure in individual cases, and probably more difficult to eliminate or control, much of the research in the field has concentrated on understanding the role of different emulsifying chemicals and more complex systems such as solids.

The kinetic stability (the time to be resolved) of emulsions is a consequence of small droplet size and the presence of an interfacial film around water droplets and is caused by *stabilizing agents* (or emulsifiers). These stabilizers suppress the mechanisms involved (sedimentation, aggregation or flocculation, coalescence, and phase inversion) that would otherwise break down an emulsion. Definitions applicable to the production environment are given.

- Sedimentation is the falling of water droplets from an emulsion because of the density difference between the oil and water.
- Aggregation or flocculation is the grouping together of water droplets in an emulsion without a change in surface area.
- Coalescence is the fusion of droplets to form larger drops with reduced total surface area (Kokal 2006). As compared with the use of emulsifiers to deliberately disperse an oil spill, the surface active agents are already present during the production process.

Crude oil contains a number of natural surfactant-like molecules that may be able to stabilize some W/O or O/W emulsions. See Fig. 2.22 for drawings of some of the types of materials in crude oil.

Natural surfactants include simple carboxylic acids, naphthenic acids (a more complex carboxylic acid), resins, asphaltenes, and organic nitrogen bases. The fatty acids include low in molecular weight formic and acetic acid as well as saturated and unsaturated acids based on single and multiple five- and six-member rings.

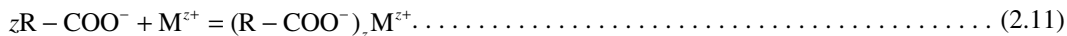
The name for the naphthenic acid category of chemicals comes from the naphthene fraction (see Fig. 2.22 for a model structure) of the crude oil that when it is cracked or oxidized (Petrov and Ivanov 1932), yields a naphthenic acid. When reacted with alkaline or alkaline earth cations (Na⁺, Ca²⁺, and Mg²⁺) the salts may cause fouling deposits or emulsions to form in the production areas, especially in the separators. This class of chemicals includes a nonspecific mixture of a large number of cyclopentyl and cyclohexyl carboxylic acids with molecular weight (MW) of 120 to well over 700 g/mol. The main fractions are carboxylic acids with a carbon backbone of 9 to 20 carbons. However some large molecules with 80 carbons have been identified. Experimental work by Shepherd et al. (2005) have added new details to the mechanistic picture of naphthenate scale and emulsion formation.

One of the most important classes of naphthenate surfactants are the “ARN Acids” (Vindstad et al. 2007). One possible structure is seen in Fig. 2.44.

The naphthenic acids, R-CO₂H, that are present in many crude oils and the hydrophilic nature of the carboxylic acid group means that they congregate at the oil-water interface. As the pressure drops during production, carbon dioxide (Rousseau et al. 2001) is lost from solution, the pH of the brine increases, which in turn leads to dissociation of the naphthenic acid (RCO₂H ----> RCO₂⁻). The dissociation of acid is expressed by

$$K_{diss} = \frac{[R - COO^-][H^+]}{[R - COOH]} \dots \dots \dots (2.10)$$

The equilibrium expression depends on the *pK_a* of each carboxylate group and the total structure of the molecule, while the total amount of dissociation is controlled by the fluid pH value and the buffer capacity of that fluid. In the presence of the salts present in oilfield brines, the carboxylic acids will associate with the metals ions:



For sodium salts, the result is R-COONa and for calcium salts, (R-COO⁻)₂Ca²⁺. For the formation of solids to take place, the solubility product,

$$K_{sp} = [M^{z+}][R - COO^-]^z, \dots \dots \dots (2.12)$$

of the salt must be exceeded and this will depend on the structure of the organic acid as well as the cation and the pH. So the discussions mentioned previously concerning the chemical structure and compositions of the naphthenic acids found in various crude oils are very significant. The formation of the calcium naphthenates is thus similar to flash scaling of calcium carbonate, which also is caused by a change of pressure and a rise in fluid pH.

Sjoblom et al. (2003) claim that because of the introduction of fatty acids (naphthenic acids) in the crude oil, the interaction pattern will undergo changes. One of the most fundamental properties in systems of fatty acid/salt water is the formation of a lamellar lyotropic liquid crystalline D-phase.

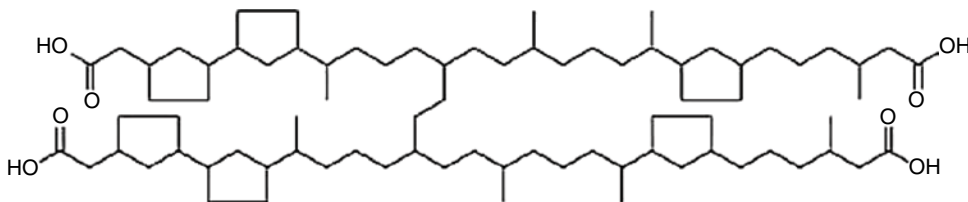


Fig. 2.44—ARN acid structure (after Lutnais et al. 2006).

This phase has a microstructure involving bilayers of the surfactant and intervening water layers. They (Sjöblom et al. 2003) claim that it has been unambiguously shown that such structures will enhance the stability of W/O emulsions. They also have shown from critical micelle concentration (CMC) measurements that the naphthenic acid salts behave as micelle forming surfactants at appropriate pH values. Friberg (2007) also has documented the importance of the existence of a lamellar liquid crystal (the D-phase) and a corresponding increase in emulsion stability. For more information on the thermodynamics of salt scale formation including naphthenates, refer to Frenier and Ziauddin (2008). The documents described later in this book also implicate formations fines and scales with the formation of W/O emulsions.

Asphaltenes and resins constitute a very important solubility class of aromatic compounds that exist in many crude streams. As seen in the structures depicted in Figs. 2.22 and 2.23, these materials are oil-soluble surfactants. They are described very briefly in Section 2.2.4 as well as in the books by Frenier et al. (2010), Mullins et al. (2007), and Buckley et al. (2007).

Several references (Kokal 2006; Sjöblom et al. 2007) consider these chemicals as well as the naphthenates to be the primary stabilizing chemicals for crude oil emulsions. The mechanisms proposed by these investigators is that the asphaltenes and other surface active materials become associated at the water/oil interface and produce a macro film that then resists the agglomeration of the water droplets.

Fig. 2.45 by Kokal (2006) shows a photomicrograph of a W/O emulsion where interfacial films are seen as the yellow rings around the water droplets. According to the work by Mullins et al. (2007) and Akbarzadeh et al. (2007), asphaltene molecules become associated in the crude oil solution into nanoaggregates (Fig. 2.23) when the concentration is higher than the critical nanoaggregate concentration. This is analogous to the CMC for surfactants in aqueous solutions. As the solubility of the asphaltenes in decreases during production, larger aggregates may form, and precipitation may actually occur.

Fig. 2.46 depicts the growth of the asphaltene nanoaggregates as a function of concentration into a mass that can precipitate and foul the well surfaces. The decrease in solubility of the asphaltenes frequently occurs during production as the pressure is decreased to the bubblepoint of the fluid (B_p) and dissolved gas leaves the solution. See the discussions and numerous references in Frenier et al. (2010).

Asphaltene precipitation in the surface separation facilities and pipelines can cause tremendous problems as the flocculated material deposits on just about everything with which the crude oils contacts. The biggest impact of this problem is on safety and process control equipment.

To predict precipitation in surface equipment such as separators, Gharfeh et al. (2007) have used the modified solubility parameter model (Buckley et al. 2007). This model was used to correctly predict and explain precipitation of asphaltenes during the blending of a North Sea crude oil and a condensate. The modification uses the Gibbs free energy mixing rule:

$$\delta_{\text{LiveOil}} = \phi_{\text{STO}}\delta_{\text{STO}} + \phi_{\text{DG}}\delta_{\text{DG}} \dots \dots \dots (2.13)$$

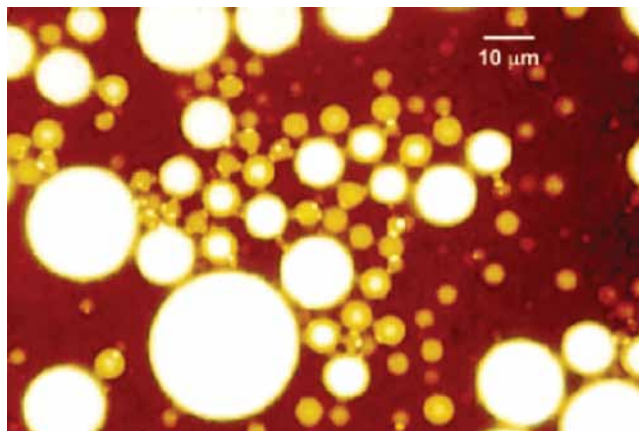


Fig. 2.45—Photomicrograph of a W/O emulsion showing interfacial films (Kokal 2006).

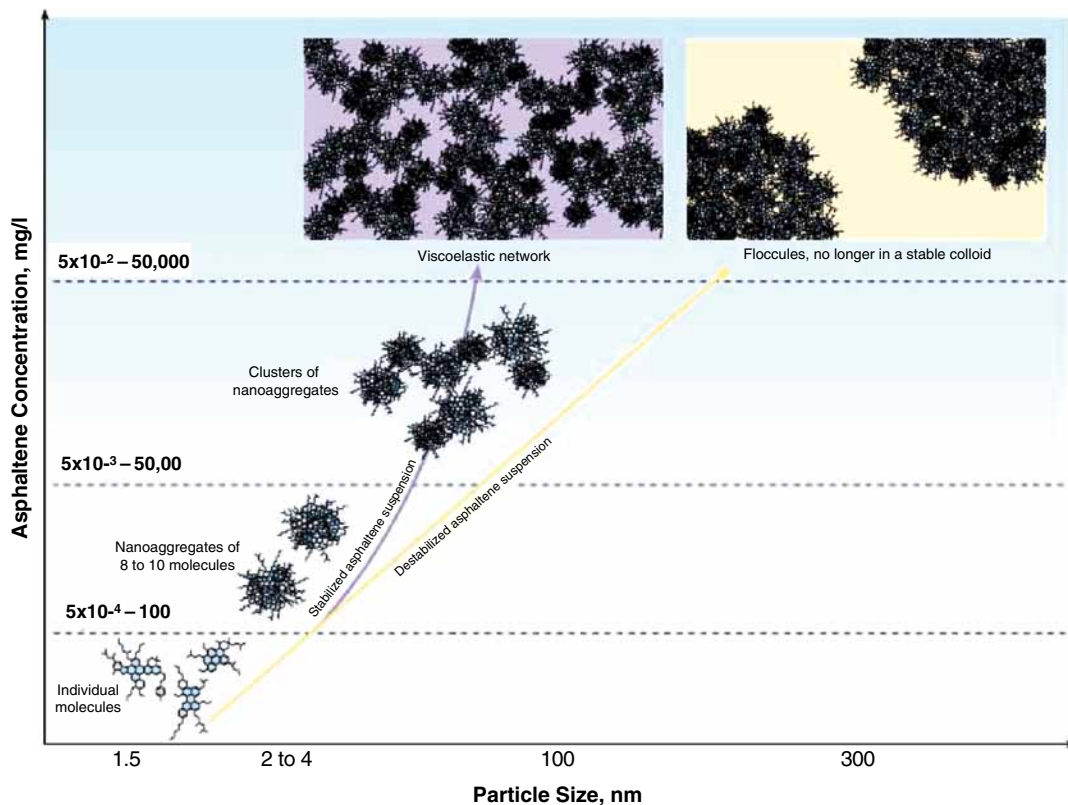


Fig. 2.46—Growth of asphaltene aggregates (Akbarzadeh et al. 2007).

Here the terms are the volume fraction (ϕ) and solubility parameters (δ) for the crude oil that has been vented at atmospheric pressure (frequently called stock-tank oil) and dissolved light ends for the condensate, respectively. This method was able to predict and explain asphaltene precipitation in the medium separator in an offshore North Sea field. In this case, condensate was being mixed with a crude oil stream.

In addition to damage caused by asphaltene precipitates, Sjöblom et al. (2007) claim that the aggregation state of the asphaltenes plays a decisive role on the stability of an emulsion. They cite literature (Førde dal et al. 1995) that claims that aggregated (precipitated) asphaltenes (top of Fig. 2.47) are much more likely to stabilize an emulsion compared with very small clusters. These researchers also have studied the effects of separator operational characteristics on the stability of emulsions. They found that three things affected the stability of emulsions where asphaltenes are a factor:

1. An increased separation with increasing pressure drop (ΔP) below the bubble pressure.
2. An increased ΔP above the bubble pressure increased emulsion stability.
3. Addition of toluene resulted in less stable emulsions.

Note that all of these items are also associated with asphaltene stability in crude oils; however, they also propose that the loss of gas below B_p will cause the surface films to tear and this destabilizes the emulsion.

The mechanism proposed by Kokal (2006) (see Fig. 2.47) for the affect of asphaltenes is that the nanoaggregates of asphaltenes associate and strengthen the film around the water droplets. Auflem (2002) claim that the interactions are through polar and hydrogen bonding forces. More details are probably not possible because the exact composition of an asphaltene deposition changes with the crude oil as well as depends on the exact production conditions. Auflem (2002) and Sjöblom and

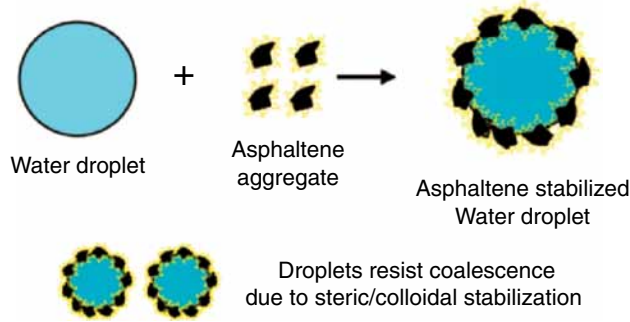


Fig. 2.47—Mechanism of emulsion stabilization by asphaltene aggregates (Kokal 2006).

Aske et al. (2003) have conducted very extensive investigations on the formation/destabilization of the W/O films, and the reader is directed to these works for more details.

The mechanisms described previously are associated with the stabilizations by molecules or aggregations of molecules. Gross solids such as precipitated asphaltenes, inorganic scales, formation fines, and calcium naphthenate solids also may act to stabilize the film that forms around the water droplets suspended in the oil. The effectiveness of these solids in stabilizing emulsions depends on factors such as the solid particle size, interparticle interactions, and the wettability of the solids. Solid particles stabilize emulsions by diffusing to the oil/water interface, in which they can form rigid films that can sterically inhibit the coalescence of emulsion droplets. Furthermore, solid particles at the interface may be electrically charged, which may also enhance the stability of the emulsion. Particles must be much smaller than the size of the emulsion droplets to act as emulsion stabilizers. Typically, these solid particles are submicron to a few microns in diameter. [Fig. 2.48](#) shows a photomicrograph with solids (rings around bright spots of water) visible in the oil fluid.

Kokal (2006) claims that the wettability of the particles also plays an important role in emulsion stabilization. Wettability (Buckley and Wang 2002; Abdallah et al. 2007) is the degree to which a solid is wetted by oil or water when both are present. This is described by the solid/fluid contact angle (θ). When the contact angle, θ , is less than 90° , the solid is preferentially oil-wet (also see the discussion in Section 1.5.3). Similarly, when the contact angle is greater than 90° , the solid is preferentially water-wet. Contact angles close to 90° result in an intermediately wetted solid that generally leads to the tightest emulsions. If the solid remains entirely in the oil or water phase, it will not be an emulsion stabilizer. For the solid to act as an emulsion stabilizer (Kokal 2006), it must be present at the interface and must be wetted by both the oil and water phases. In general, oil-wet solids stabilize a W/O emulsion. Oil-wet particles preferentially partition into the oil phase and prevent the coalescence of water

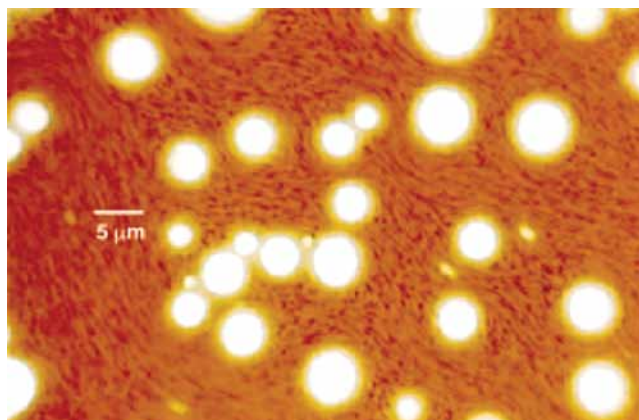


Fig. 2.48—Photomicrograph showing the presence of solids (yellow rings around the white oil droplets) (Kokal 2006).

droplets by steric hindrance. Similarly, water-wet solids stabilize a water-continuous or an O/W emulsion. Examples of oil-wet solids are asphaltenes and waxes. Inorganic solids will normally be water-wet; however, these particles may be coated with a hydrocarbon film that would render them oil-wet. Sullivan and Kilpatrick (2002) did work that indicates that the change in particle wettability, because of adsorption of resins and asphaltenes from the crude oil, is the primary reason for the accumulation of particles at the interface. See Fig. 2.49 that diagrams the asphaltenes accumulating on the surface of a solid particle rendering it oil-wet.

These investigators performed quantitative studies [water resolution tests described in the report (Sullivan and Kilpatrick 2002)] on the addition of solid particles such as calcite and iron oxide to asphaltene-stabilized W/O emulsions. They found that both Fe₂O₃ and Ca(OH)₂ significantly increased emulsion stability over a large range in particle concentration. In some cases, the presence of particles caused the emulsion to invert to an O/W emulsion. They found that the details are very complex. Some qualitative conclusions that are possible indicate parameters include the size and surface energy of the stabilizing particles and the state of asphaltene aggregation.

Sjoblom et al. (2003) claim that the presence of gas in the oil phase may weaken the emulsion film when the pressure is reduced and the CO₂ or light hydrocarbons leave solution. See Fig. 2.50. However, a loss of carbon dioxide also will raise the pH and this may cause naphthenate salts to form that could then strengthen the film.

A summary from the previous paragraphs of the chemical factors that affect an emulsions stability are noted:

- The type and amount of naphthenic acids in the crude oil
- Type and amount of asphaltenes and oil wetting by them
- Presence of gross solids
- Presence of gas bubbles
- Temperature

There are other significant sources of production activities that may affect the formation/resolution of emulsions. These may include essentially all of the other production enhancement methods performed before the fluids reach the surface. Acidizing, fracturing, EOR, and any use of scale, corrosion, and organic solids inhibition activities may introduce surface active chemicals or solids into the fluid streams. For example, acidizing and fracturing procedures described in Chapters 3 and 4 likely will produce solids or fines, at least during the flowback/cleanup phases. Inhibitors for various individual and mixed deposits (Frenier and Ziauddin 2008; Frenier et al. 2010) are very surface active by design and may cause/enhance emulsions. Produced and broken frac gels may include emulsion enhancing solids. The key to control is awareness that these effects are possible and are made a part of the FA plan (Fig. 2.2).

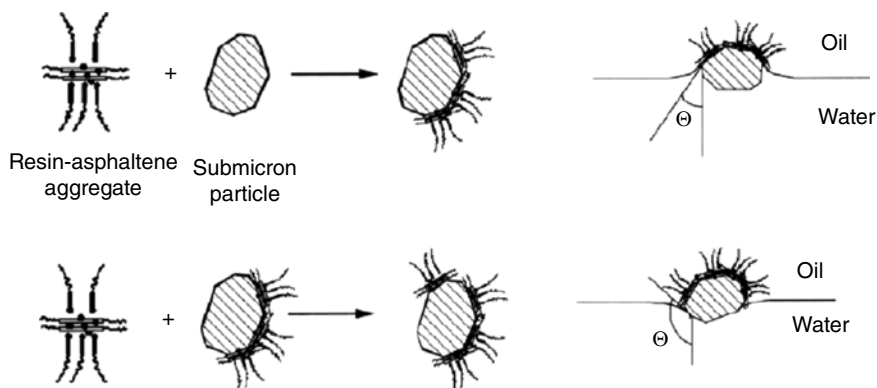


Fig. 2.49—Adsorption of resin/asphaltene aggregates to a hydrophilic particle. At low extents of adsorption, the particle is preferentially water-wet, but at high levels of adsorption, oil-wet (Sullivan and Kilpatrick 2002).

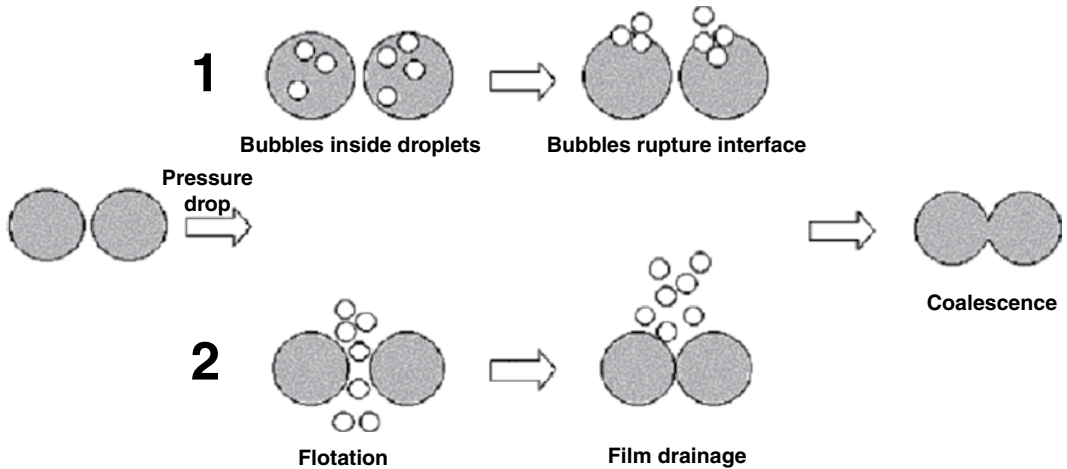


Fig. 2.50—Gas leaving solution ruptures interface film (Sjoblom et al. 2003).

The brine composition may affect the stability emulsions in complex ways. Kokal (2006) suggests that high pH and $\text{Ca}^{2+}/\text{Mg}^{2+}$ ions may degrade the interfacial films that stabilize the emulsions, but the references noted previously concerning naphthenic acids indicated that high pH and alkaline earth ions may cause solids to form that may then stabilize the emulsions. It is important to know the brine chemistry, but direct correlations may not be possible.

Turner and Smith (2005) describe a best practice for control of organic soaps and solids (and, thus, possibly emulsions). Suggestions include

1. Using a riser and a manifold line that enters the main fluid processor.
2. This unit operation is followed by a first-stage heater to heat the fluids and to break any emulsions.
3. The fluids may then be processed through one or two main separators, with possibly a second process heater followed by an electrostatic-treatment unit and coalescer for the oil.
4. A water-handling facility (including hydrocyclones, degassers, and gas-flotation units) is used to treat the water. At each stage, the fluids experience pressure drops and undergo shear, which are both known to promote soap formation; increases in temperature may generate soaps and actually impair oil/water separation.
5. Electrostatic treatment may help to concentrate the soaps and additionally impair dehydration.

In view of the influence that physical parameters have on soap/solids generation, Turner and Smith (2005) claim that care must be taken in designing the process. Any process design must be considered carefully, beyond the conventional design wisdom that a design that reduces soap generation may result in significant OPEX savings (including deferred oil). Operating parameters in existing systems can also be optimized to minimize soap generation.

The next sections (2.4.3 and 2.4.4) describe mechanical and chemical methods (including test procedures) for assessing emulsions as well as for resolving or preventing emulsion damage. Various types of mechanical and/or chemical separation can be performed at the wellsite or on the surface for an offshore installation. Some crude oil/water emulsions may resolve just by setting in a tank as the heavier water drains out of the mixture. Mechanical and chemical methods are not used independently because even with the addition of a demulsifier, mechanical separation will be required.

2.4.3 Mechanical Methods for Resolving Emulsions. Kim et al. (2002) state that mechanical methods include

- Sedimentation (settling)
- Thermal (heat) breaking methods

- Electrostatic methods
- Centrifugation

In many commercial treatment setups, all of these methods are in use to resolve emulsions. Hansen (2005) describes a separation process in petroleum production that involves a number of equipment units. The process is composed of a number of separation steps in which the pressure is stepwise reduced and gas flashed off.

A first step in oil, gas, water, and sand separation usually is based on differences in density of the fluids and most separators are gravity separators (sedimentation). They use the acceleration of gravity, in huge pressurized vessels. An example is seen in Fig. 2.51 that has a series of steps to separate three phases of water, oil, and gas. Any remaining emulsion is resolved in later steps.

Kokal (2006) and Kelland (2009) note that application of *heat* promotes oil/water separation and accelerates the treating process. An increase in temperature has the following effects:

- Reduces the viscosity of the oil
- Increases the mobility of the water droplets
- Increases the settling rate of water droplets

Kim et al. (2002) claim that electrostatic treatment in a high-voltage field is one of the most effective and simplest demulsification methods. They explain that electrostatic forces cause the coalescence of the dispersed water droplets (that also contain salts) and their growth to larger drops, which then separate because of electric forces or gravity. These forces increase dramatically as the distance between the dispersed water droplet becomes smaller. This demulsification process can be achieved with both direct current (DC) and alternating current (AC) fields. In DC fields, the electrophoretic droplet motion enhances the probability of coalescence, whereas in AC fields, the motion in the bulk fluids is necessary to increase the coalescence. These investigators found that in an AC electrostatic desalter, demulsification was enhanced with an increase in frequency of the current, and usually an optimum frequency was reported according to experimental conditions.

A process train is seen in Fig. 2.52 in which several different separation methods are seen described previously are used to provide more complete separation as well as dehydration of the gas to a desired dewpoint.

Kokal (2006) has prepared a drawing (Fig. 2.53) of a three-phase (gas, water, oil) separator that includes a heaters section, wash water, a filter section, a coalescing or stabilizing section, and electrostatic grids. Note that chemicals also may be used to speed dehydration/separation before the emulsion entering the separation equipment.

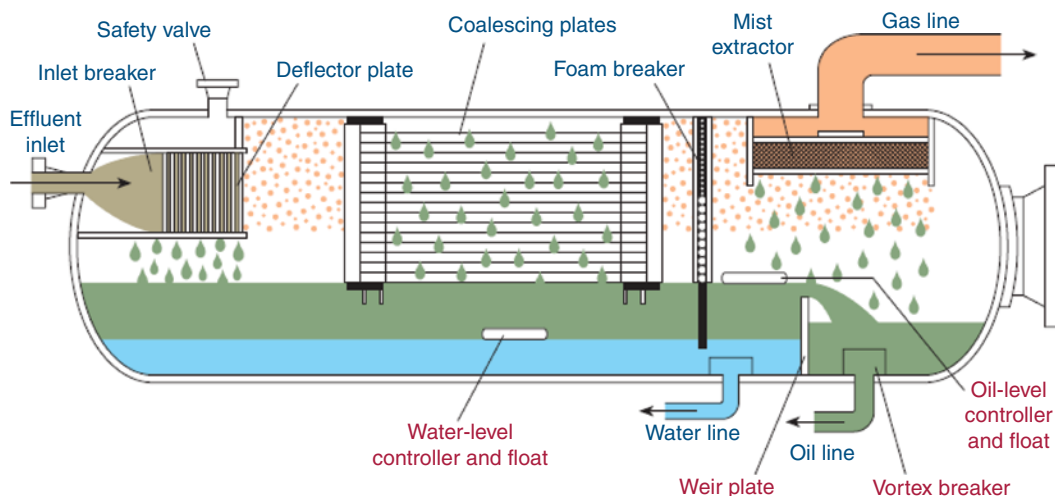


Fig. 2.51—Gravity settler (Sims 2010).

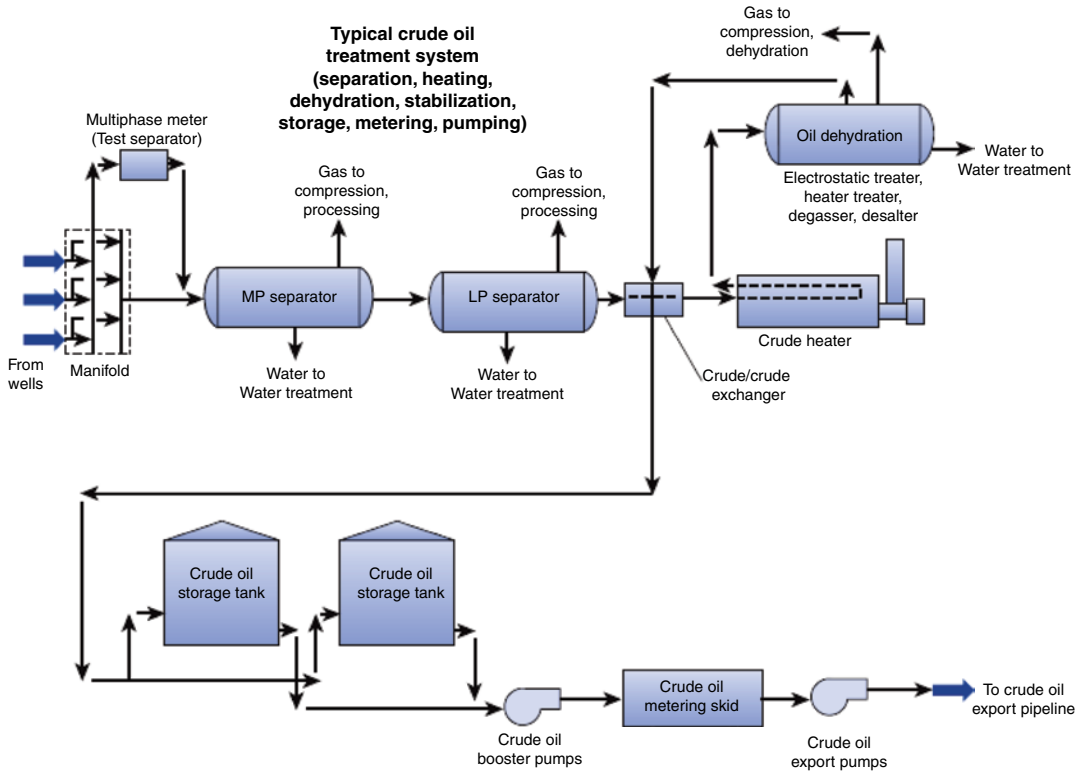


Fig. 2.52—EFP separator (Schlumberger 2010a).

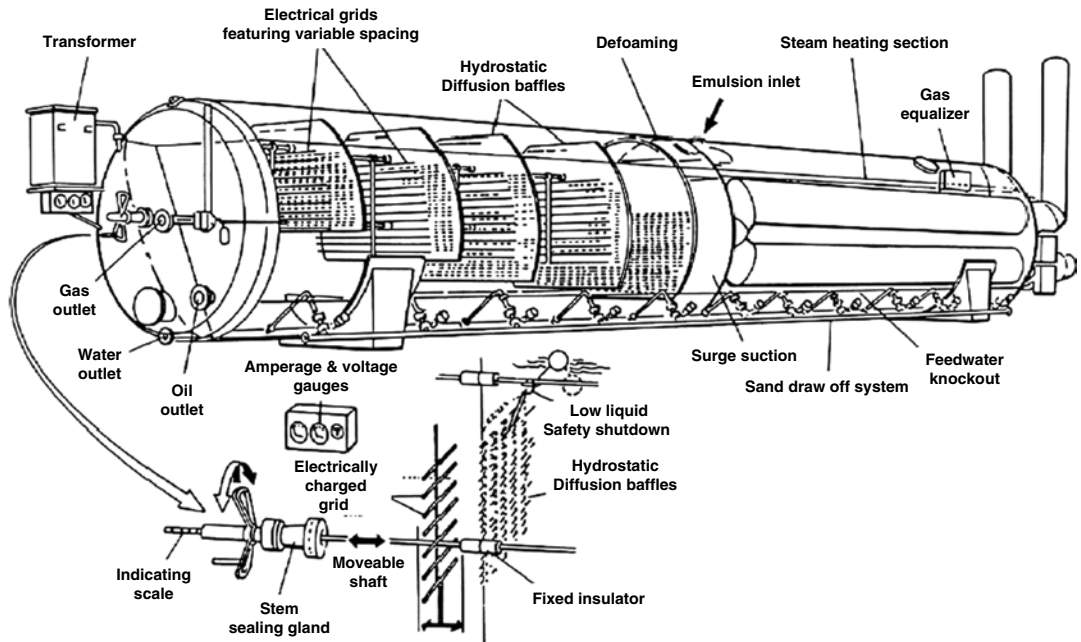


Fig. 2.53—Three-phase separator (Kokal 2006).

2.4.4 Chemical Methods of Demulsification. This section describes the test methods, mechanisms of action, and types of chemical DMs in use for treating water-oil emulsions.

Test Methods of Emulsions and Demulsifier Chemicals. There are simple as well as complex methods for testing (especially the effects of demulsifier chemicals) the stability of oilfield emulsions.

A bottle method (*API MPMS 10.4* 1988) has been described by Manning and Thompson (1995) as the API bottle test. The procedures are as follows:

1. Obtain a representative fresh sample of the fluid that contains other treating chemicals (see Section 6.3.1).
2. Drain off free water (preserve the emulsion).
3. Shake the collection container and determine percent sediment and water using *ASTM D96-88(1988)* (1988).
4. Prepare several 8 oz graduated bottles for the tests.
5. Add 100 ml of emulsion to bottles. Add the test breakers and cap the bottles loosely.
6. Place in a shaker horizontally set at 150 cycles/min.
7. Place the shaker in a heating enclosure.
8. At specific times, determine the break out volume.
9. Sample the oil layer at the 80 ml level and determine sediment and water.
10. Also sample the water layer and determine the oil content if needed.

Kokal (2006) [based on Kokal and Wingrove (2000)] has developed an emulsion separation index (ESI) test. He claims that this bottle test is a quantitative method for demulsifier testing and involves the following procedure.

1. The crude oil emulsion sample is tested as soon as possible after it is received in the laboratory. The pressurized method for sampling the emulsion is recommended. The samples are remixed with a standard bottle shaker for approximately a minute. The same amount of shaking should be used in all tests.
2. The mixed emulsion sample is added to 100-ml standard centrifuge tubes.
3. The centrifuge tubes are placed in a water bath for a minimum of 30 minutes to reach the desired temperature.
4. The required dosage of the chemical is added to the centrifuge tubes. The amount of chemical is based on the total amount of emulsion (oil and water).
5. The tubes are shaken by hand a given number of times (approximately 20 shakes) and placed in the water bath at the desired temperature.
6. The amount of water separated is measured with time (5, 10, 15, and 20 minutes).
7. After 20 minutes, the tubes are centrifuged for another 20 minutes at the desired temperature and the final amounts of water and emulsion or rag layer are measured.
8. Generally, these experiments should be done in sets to investigate the effect of certain variables. All efforts should be made to keep all the variables constant except the one under investigation. Duplicate tests can be run to improve reliability.
9. The ESI is then calculated from the measured oil/water separation data.

$$ESI = \frac{\sum W}{\sum n} \dots\dots\dots (2.14)$$

Here, *W* = water separation at a given demulsifier concentration/time as a percentage of basic sediment and water, and *n* = number of experiments in a particular set. This then gives an average ESI.

Kelland (2009) describes a test value called the relative solubility number (RSN) that was developed by Greenwald et al. (1956) as a method for describing nonionic surfactants. He notes that this is also known as the water number and has been used by suppliers to describe DM. It is associated with the

hydrophilic/lipophilic balance (HLB) of the surfactant (see equations in this section). Kelland (2009) describes how to determine the RSN:

1. 1.0 g of the DM product is weighed into a beaker containing 30 ml of a standard solution (2.6% toluene and 97.4% ethylene glycol dimethyl ether) and the product is dissolved.
2. Water is added until cloudiness indicates the endpoint. The RSN is the ml of water added. According to this author, DMs with high numbers (very hydrophilic) are usually not effective. This value as well as other metrics (Eq. 2.14) may be useful for establishing structure/activity relationships for similar crude oil/water combinations.

Sjoblom et al. (2003) have produced a very extensive review of methods for studying and classifying crude oil/water emulsions. Many advanced tests are described. Details are in this publication and include

- Microscopy/video microscopy
- NMR
- Acoustic and electro acoustic methods
- Properties in an electrostatic field
- High-pressure flow loops

Chemical DMs and Mechanisms. Because of the great complexity of the different combinations of oil, brine, solids, natural surfactants, and shear conditions possible, an equally complex set of chemicals has been developed to help the demulsification process. These chemicals are usually injected to aid the resolution and separation of the various emulsions. Kelland (2009) claims that injection of chemicals (if needed) frequently is done just before the separator units (noted in Figs. 2.51 and 2.52). However, he suggests injecting the demulsifier as far upstream as practical to make use of the heat of the fluid and the mixing of the flow. Anti-emulsifiers may be added in some of the treating fluids (such as matrix treatments: Sections 3.4 and 3.6.2) to prevent formation of emulsions. Both classes of chemicals act to allow one phase to drain by disrupting the stabilizing film.

Many of the types of tests described in the previous section have been used to evaluate them. Kokal (2006) claims that the only clear generalization regarding DMs is that they have a high molecular weight (about the same as natural surfactants) and, when used as demulsifying agents, they tend to establish an emulsion opposite in type to that stabilized by natural surfactants. This author shows a drawing (Fig. 2.54) where the DMs displace the natural stabilizers present in the interfacial film around the water droplets. This displacement is brought about by the adsorption of the demulsifier at the interface and influences the coalescence of water droplets through enhanced film drainage. The structure of the chemical must be such that it can compete with the emulsifying chemicals but must also destabilize the film so that gravity will start the draining process. This requires a specific chemical characteristic that depends on the oil chemistry as well as the water chemistry. Thus, there is a difficulty of finding universal DMs.

Fink (2003), Fink (2011), and Kelland (2009) have major sections in their books where they review the large number of demulsifier chemicals proposed or in use. Major divisions of the types of chemicals include small anionic surfactants such as dodecylbenzyl sulfonic acid as well as polymers made

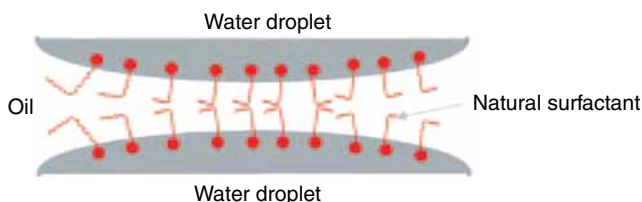


Fig. 2.54—Demulsifier mechanism (Kokal 2006).

from polyethylene or polypropylene oxide. Fink (2003) also has tables that list materials that have been recommended for W/O emulsions and those that may work with O/W emulsions.

Kelland (2009), Fink (2011), and Fink (2003) list materials that contain

- Polyalkoxylate block copolymers and ester derivatives
- Alkyl phenol-aldehyde resin alkoxyates
- Polyalkoxylate polyamines
- Vinyl polymers
- Polysilicones as boosters (these are also antifoaming agents)
- Cationic amide-ether esters
- Polyamines
- Polyamides
- Alkoxylated fatty oils
- Biopolymers
- Nonionic and anionic surfactants

The structures of several small molecules DMs are seen in [Fig. 2.55](#).

Biodegradability can be a major issue for the use of DMs (see Section 6.2). Kelland (2009) specifically notes that many of the polymers have polyether linkages and claims that those made from ethylene oxide are more biodegradable than those made from propylene oxide or butylenes oxide. He also recommends the possibility of making epoxide fatty esters from soya oil as biodegradable DMs. Feng et al. (2008) described the use of a nontoxic and biodegradable polymer, ethyl cellulose, that were used to break up emulsified water from naphtha-diluted bitumen. It was found that the ethyl cellulose polymer at 130 ppm dosage removed up to 90% of the emulsified water in the diluted bitumen by gravity settling after 1 hour at 80°C. The tests, extended to bitumen froth containing about 10% solids

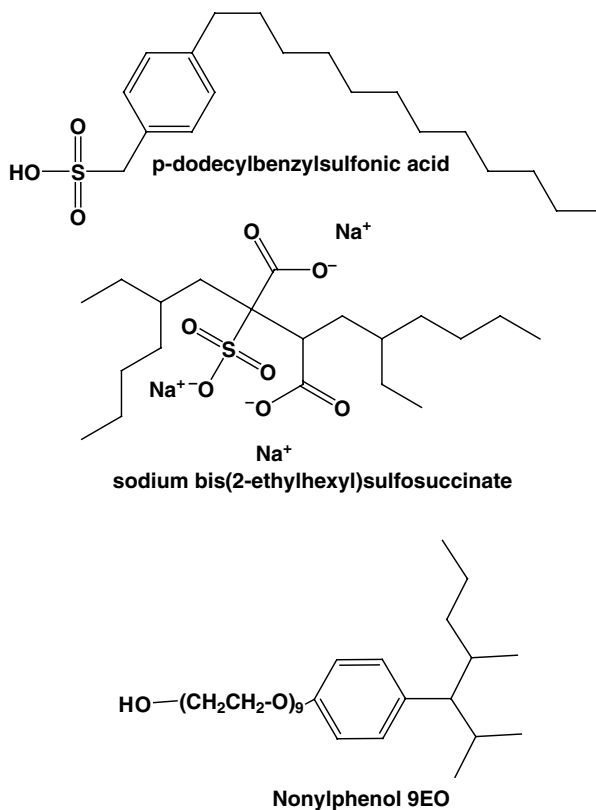


Fig. 2.55—Small molecule demulsifiers.

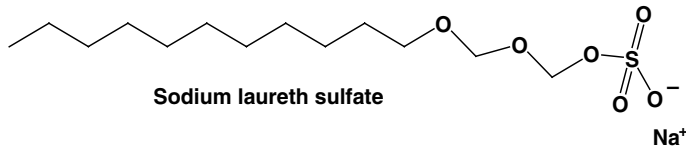


Fig. 2.56—Sodium laureth sulfate.

by weight, showed a 90% removal of the water in the diluted bitumen froth. The addition of ethyl cellulose also assisted the removal of fine solids with the water. However, for bitumen froths containing 30% or more solids, the efficiency of water removal by ethyl cellulose addition was found to be less effective. Micrographic images revealed that ethyl cellulose broke up the water-in-bitumen emulsions by flocculation and coalescence.

The HLB concept is a way of classifying surfactants and is one way to choose a correct demulsifier for the crude/water couple. It usually is applied to nonionic surfactants but may also be applied to charged molecules. Dobos (2009) notes that Griffin (1954) developed a way to streamline the selection of surfactants by using the ratio of the hydrophobic to the hydrophilic portion of the molecule. In this technique, a typical nonionic emulsifier (e.g., Laureth-4) that contains an ethylene oxide groups or polyhydric alcohol hydrophilic portions with a fatty alcohol hydrophobic portion, was analyzed (see Fig. 2.56).

The HLB for a nonionic surfactant can be calculated as follows (Griffin 1954):

$$\text{HLB} = \frac{\text{wt\% Hydrophile}}{5} \dots \dots \dots (2.15)$$

The author gives an example of the HLB calculation for Laureth-4.

- Molecular weight of ethoxylate (hydrophile) portion = 176
- Molecular weight of lauryl alcohol = 186
- Wt% Hydrophile = $[176/(176+186)] \times 100 = 48.6\%$
- HLB = $48.6/5 = 9.7$

Surfactants with high HLB values will be more water soluble and those with low HLB values are more oil soluble. The HLB can also be calculated by a method suggested by Davies (1957) that is based on calculating a value for the chemical groups of the molecule. The advantage of this method is that it takes into account the effect of strongly and less strongly hydrophilic groups. The method works as follows:

$$\text{HLB} = \sum m(H_h) - n(H_l) + 7 \dots \dots \dots (2.16)$$

with m = number of hydrophilic groups in the molecule, H_h = value of the hydrophilic groups, n = number of lipophilic groups in the molecule, and H_l = value of the lipophilic groups.

This method may give more accurate and consistent values of the HLB. The value numbers are listed in the paper by Davies (1957) and are in Table 2.3.

Using these methods, HLB numbers of mostly nonionic surfactants and been calculated. See Table 2.4 for typical uses of different classes of nonionic surfactants.

Because the use of a particular chemical depends on the composition of the crude oil as well as the brine content, several investigators have attempted to systematize the testing of DMs. Their papers are abstracted in this section.

Fan et al. (2009) describe the destabilization of crude oil emulsions by polyoxyethylene nonyl-phenol that have been investigated at a water-to-oil volume ratio of 1:1 as a function of the HLB and concentration. The results show that the stability of crude oil emulsion begins to level off after a critical surfactant concentration, which seems to correspond to their CMC. A stability minimum was

| TABLE 2.3—HLB GROUP NUMBERS (DAVIES 1957) | |
|---|--------------------|
| Hydrophilic Groups | H_h Group Number |
| –SO ₄ [–] Na ⁺ | 38.7 |
| –COO [–] K ⁺ | 21.1 |
| COO [–] Na ⁺ | 19.1 |
| N (tertiary amine) | 9.4 |
| Ester (sorbitan ring) | 6.8 |
| Ester (free) | 2.4 |
| –COOH | 2.1 |
| –OH (free) | 1.9 |
| –O– | 1.3 |
| –OH (sorbitan ring) | 0.5 |
| Lipophilic Groups | H_l Group Number |
| –CH–, –CH ₂ –, CH ₃ , =CH– | 0.475 |
| Derived Groups | Group Number |
| –(CH ₂ – CH ₂ –O)– | 0.33 |
| –(CH ₂ – CH ₂ –CH ₂ –O)– | 0.15 |

| TABLE 2.4—HLB RANGE OF SURFACTANTS | |
|------------------------------------|-----------|
| Surfactant Application | HLB Range |
| Water in oil emulsion formers | 4–6 |
| Wetting agents | 7–9 |
| Oil in water emulsion formers | 8–18 |
| Detergents | 13–15 |
| Solubilizers | 10–18 |

found after the stability plateau region, which corresponds to the inversion of emulsion from W/O to O/W. Furthermore, the chemical with HLB = 14.2 (in the same range as detergents) has the highest efficiency for demulsification with the highest separation rate and the lowest inversion point, whereas inhibitors with higher HLB are less effective, which may be because of the network formation by their very long oxyethyl head groups and interactions with indigenous components of the crude oil. Specific examples are abstracted as part of a literature review.

Goldszal and Bourrel (2000) note that the emulsification conditions and thus the optimal demulsifier may change as the conditions in the reservoir changes as the field matures and, thus, different production conditions are in place. They also claim that they have found that the rate of phase separation is maximum when a particular three-phase behavior, namely, a microemulsion phase in equilibrium with both excess water and oil phases, is observed when the system has reached its final state. They also point out that commercial DMs are generally complex mixtures, the precise chemical structures of which are not easy to figure out. The test materials are listed as nonionic surfactants and contain various amounts of ethylene oxide and propylene oxide. According to their HLB, they can be ranked as $R_1 > R_2 > R_3 > R_4$, R_1 being the more hydrophilic species. Molecular weights are in the range 4000–5000. Ethoxylated nonylphenols have been used as representatives of more conventional surfactants.

Bhardwaja and Hartlanda (1993) claim that low molecular weight surfactants were found to be completely *ineffective* as DMs. Three higher MW surfactants were effective DMs, exhibited good interfacial activity, surface adsorption and surface pressure. The performance of the DMs changed with change in salinity of aqueous phase. Surfactants effective as DMs reduced surface tension of water by more than 25 dynes-cm⁻¹. For a given crude oil-water system, the surfactant that developed surface pressure in excess of 15 dynes-cm⁻¹ was found to be good demulsifier for that system.

Hamadi and Mahmood (2010) tested commercial DMs as well as a polyacrylamide polymer using an Al-Basrah field crude oil and water. The experimental results (bottle tests at 65°C) were compared and related with the demulsifier performance. The following conclusions could be summarized:

1. Water separation efficiency increases with increasing separation time for all types of DMs, where highest separation obtained at (120 minutes).
2. Water separation efficiency increases with increasing dose of DMs where highest separation for water obtained at (80 ppm) for all types of DMs.
3. Two types of commercial DMs has been used (unknown commercial and a nonionic oil soluble surfactants, which gave (87.5%) and (72.2%) water separation efficiency, respectively). The prepared demulsifier gave water separation efficiency of (75%).

Kim and Wasan (1996) described experiments using both model W/O and water-in-crude oil emulsion systems with DMs with different chemical structures, the effects of demulsifier partitioning on the interfacial and film rheological properties were studied. There was a one-to-one correlation between the performance of demulsifier and the interfacial activity of the partitioned demulsifier; the partitioned demulsifier components exhibit an increase in static and dynamic interfacial activity, low dynamic interfacial and film tension, and a low film dilatational modulus with a high adsorption rate/low interfacial tension gradient (Marangoni-Gibbs stabilizing effect) and have excellent demulsification performance.

Dalmazzone et al. (2005) claim that formulations based on polysiloxane molecules were selected as effective nontoxic products to enhance the oil/water phase separation. Establishing the relation between the efficiency of formulations and the interfacial properties of silicone molecules is the objective of this study. They found that the coalescence of water droplets leading to the destabilization of emulsions and consequently to the oil/water separation efficiency can be related to the rheological properties of water/crude-oil interface. Therefore, such comprehensive study based on a specific methodology can lead to a strict and effective selection of emulsion breaker additives in relation with the oil composition.

Krawczyk et al. (1991) described the factors affecting the coalescence and interfacial behavior of water-in-crude-oil emulsions in the presence of oil-soluble DMs. They note that the velocity of thinning is dependent upon the balance of forces acting at the interface of the approaching fluid particles. The emulsion-breaking characteristics and interfacial properties of East Texas Crude and a model system (model crude oil system consists of 1.9 g of asphaltenes derived from East Texas Crude per liter of an alkane-aromatic solution of 70% heptane and 30% toluene) were compared.

The categories of demulsifier studied were alkoxyated polyol, alkoxyated resin, ethoxyated polyol, and a blend of phenol resins. The variation of interfacial tension with demulsifier concentration for the model system was determined by measuring the interfacial tensions between the oil and water phase. Interfacial activity, adsorption kinetics, and partitioning between the oil and aqueous phases were shown to be the most important parameters governing demulsifier performance. Important chemical conclusions of the study are

- The demulsifier should be able to partition into the water phase.
- The concentration of the demulsifier in the droplet must be sufficient to ensure a high enough diffusion flux to the interface.
- The interfacial activity of the demulsifier must be high enough to suppress the interfacial tension gradient, thus, accelerating the rate of *film* drainage and hence promoting coalescence.

Several patents are abstracted that show demulsifier chemistries. Berkhof et al. (1992) claim demulsifiers that contain R-O-Zn-O-(AO)_xH wherein R is a linear or branched, saturated, or unsaturated C₁₈ alkyl radical, Zn is an oligoglycosyl radical with *n* = 1 to 5 hexose or pentose units or mixtures thereof. Here AO is an ethylene oxide, propylene oxide, or butylene oxide radical or mixtures thereof, and *x* is 1 to 100 and useful for breaking water-in-oil petroleum emulsions. Such DMs have a low specificity and biodegradable.

Leinweber et al. (2010) describe the invention that relates to the use of alkoxyated crosslinked polyglycerols for demulsifying oil/water emulsions in amounts of from 0.0001 to 5% by weight, based on the oil content of the emulsion to be demulsified. The alkoxyated crosslinked polyglycerols of the invention is crosslinked with multifunctional electrophilic compounds having a molecular weight from 1,000 to 100,000 units and that comprise 5 to 100 glycerol units that are alkoxyated with C₂-C₄-alkylene oxide groups or a mixture of such alkylene oxide groups so that the crosslinked alkoxyated polyglycerols have a degree of alkoxylation of from 1 to 100 alkylene oxide units per free OH group.

Aveyard et al. (1990) tested the of demulsification of water-in-crude oil emulsions using a series of octylphenyl-polyethoxylates and sodium bis(2-ethylhexyl)sulfosuccinate [a.k.a Aerosol® OT—an OT type of surfactant (AOT)] as DMs. The HLB of the surfactant systems was varied systematically by changing the number of ethoxy groups in the case of the nonionic surfactants and by changing the concentration of added NaCl in the case of AOT. For all surfactants and conditions, the demulsification rate increased with surfactant concentration up to the onset of surfactant aggregation in the oil, the water, or a third, surfactant-rich phase. The highest rate reached is estimated to be close to the diffusion controlled value.

This type of mechanism implies specificity for certain chemicals based on the crude oil and the brine content. If oil is spilled into a body of water, surface active agents will then be used to disperse the oil in attempt to lessen the impact. These technologies share many aspects of the formation of the emulsions described in this section and will be discussed in Section 6.4.

2.5 Flow Enhancers

Chemicals that affect the drag of flowing hydrocarbon or emulsions are in use to reduce the pressure drop and thus increase flow rate of various fluids. Faust and Weathers (2011) note that viscous crude oils as well as other fluids (such as fracturing fluids), often result in significant pressure drops across the production system and are the source of a number of significant issues during production. These occur anywhere starting from the base of the production tubing all the way to the separation equipment. A large pressure drop can result in increased expenditures to lift the oil, through upgraded pump equipment, the use of heat to lower viscosity or through the injection of diluents to thin the oil and facilitate flow. In certain instances, viscous oils contain unstable paraffin or asphaltene fractions that may deposit and further inhibit efficient oil production. The end result of the pressure drop is a loss of production and other potential indirect effects including equipment wear, increased intervention rates, and higher production costs.

The authors report that formation of a O/W emulsion is formed, the viscosity of the fluid is reduced and the flow is enhanced. They found a pair of two polymeric surfactants that made this type of emulsion using a Canadian heavy oil. They also report that the droplet size of the oil phases are approximately 50 μm and that the emulsion is stable only under high shear, flowing conditions and will resolve when the fluid remains still.

Kelland (2009) has a whole chapter (Chapter 17) on drag reducing agents (DRAs) that are used in various oilfield applications. Fink (2011) also has a chapter (Chapter 12) that contains many structures and references. Examples include oil soluble polymers such as polyalkylenes and polyolefins are used to reduce the drag in various pipelines. In addition to the polyacrylamide polymer materials, water soluble DRA polymers include polyethylene oxides, polyvinyl alcohols, and various polysaccharides such as the guar and CMC and hydroxyl ethyl cellulose. Surfactants such as some of the betaines also may act as DRAs. Details are in Section 4.7.1.

Production chemical type DRAs target very specific components of the crude oil, or specific flow characteristics of the system to improve flow conditions in upstream pipelines. Kelland (2009) reviewed a theory of the mechanism of DRAs using (Fig. 2.57), as an example Jubran et al. (2005). In this figure, the flow is from the left and three zones are seen. There is a turbulent core, a buffer region and the laminar sublayer. In this theory, energy bursts move from the laminar sublayer into the turbulent core, this expending energy. DRAs are thought to suppress the energy bursts and thus reduce the pumping energy needed to maintain flow.

Drag reducers modify the internal drag generated by turbulent flow in crude oil pipelines (see Fig. 2.57), making their application limited to systems operating under turbulent as opposed to laminar conditions. The constraints on flow type also prevent drag reducers from being used with most viscous heavy oils, which tend to experience laminar flow. Paraffin wax inhibitors modify wax crystal structure

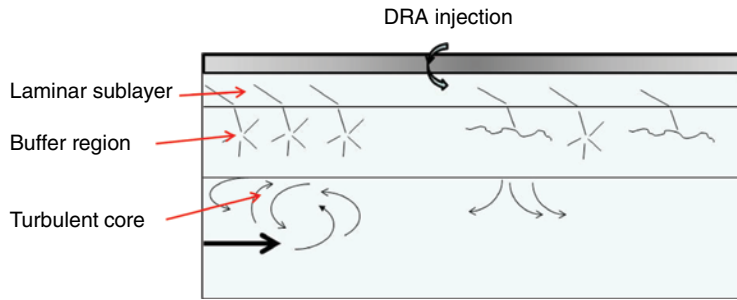


Fig. 2.57—DRA mechanism (adapted from Kelland 2009).

to lower the pour point or wax appearance temperature (wax crystal modifiers) and/or interfere with the flocculation of wax crystals (wax dispersants). See Section 6.4 of Frenier et al. (2010). Similarly, asphaltene inhibitors prevent asphaltene deposition by interacting with the asphaltene particles to delay flocculation, a process that will slow and potentially prevent precipitation and deposition. Finally, demulsifier chemicals, which disrupt interfacial oil/water films facilitating droplet coalescence, are generally used to break W/O emulsions but if applied properly will increase the droplet size of the water internal phase, reducing the apparent viscosity of the produced emulsion.

Faust and Weathers (2011) have described biphasic viscosity reducer chemicals that target the bulk fluid properties of the crude oil, regardless of the source of viscosity, by dispersing oil into free water, creating a highly flowable, low apparent viscosity, water external emulsion. Screening tests confirmed the capacity of certain polymers to emulsify heavy oils, with API gravities well below 20, as well as waxy crudes from different locations around the world into 20–25% water solutions, creating stable, water external emulsions. In all cases the emulsion exhibited significant levels of apparent viscosity reduction, generating improved flowability in a bench-top flow loop, as well as emulsion resolution under standard field separation conditions including heat and traditional emulsion breaking chemicals. The top-performing products were assessed in a full-scale field trial on a high wax crude oil, where the biphasic viscosity reducer chemical resulted in efficient pressure maintenance for the topsides flow lines over the span of the field trial, significantly reducing operating costs associated with pressure buildup in these lines. Throughout the period of chemical injection, no adverse effects on water quality or oil/water separation were observed at the separation battery.

The process of dehydrating a crude oil stream also can act as a flow enhancer. Shepherd et al. (2012) have shown that the water content can affect the viscosity of the fluid, especially at low temperatures. Fig. 2.58 shows the benefit of using the dehydration/demulsification methods described in Section 2.4.4 on the viscosity of a heavy crude oil stream.

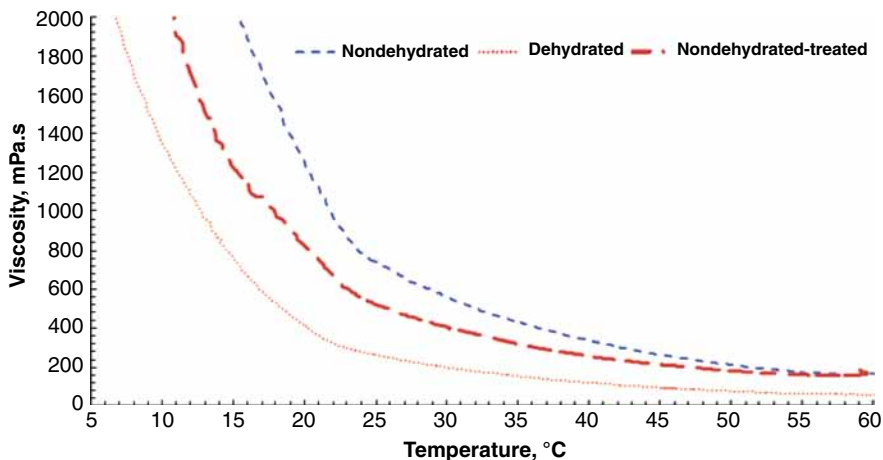


Fig. 2.58—Effect of dehydration on viscosity of heavy crude oil (Shepherd et al. 2012).

2.6 Case Histories and Best Practices for Use of Production Chemicals

This section contains case histories or best practices that illustrate the use of production chemicals for controlling corrosion and for resolving emulsion problems. Details of specific chemicals used in these operations were described in the earlier sections of this chapter (Sections 2.2.3 and 2.4.4). All of the papers cited in this and the other sections (3.9, 4.12, and 5.8) of Case Histories/Best Practices are available from SPE or associated libraries and have been reproduced with minor edits.

2.6.1 Corrosion Mitigation Chemicals. A paper by Havlik et al. (2007) note that particularly severe environments are encountered in the production and transport of wet natural gas containing corrosive components, such as hydrogen sulphide and carbon dioxide. It is, therefore, a prerequisite to take into account the corrosivity of the respective fluids in all stages of the field development, material selection, field layout, and facilities design. In preparation of the subsequent production phase, reliable corrosion monitoring programs have to be selected, established, and implemented as necessary. This paper gives a comprehensive overview of these considerations regarding four different gas fields, two in Austria and two in Pakistan, which were successfully developed and brought on-stream between 1967 and 2003.

Sour Gas Field Schoenkirchen Tief. The downhole temperatures at 6000 m are approximately 176°C and the corrosive gas composition is 2% H₂S with 12% CO₂. The control methods consist of using inhibitor squeeze treatments on the carbon steel downhole components. The method used a mixture of diesel fuel and an oil-soluble inhibitor was able to control the corrosion rates to 0.004 mm/yr.

Gas-Condensate Field Hoeflein. This is a “sweet” field with 16% CO₂ and no H₂S but at 78°C with 33,000 ppm total dissolved solids. The use of 13% Cr steel as well as a different inhibitor dissolved in condensate or methanol is introduced using a small “macaroni” string.

Sour Gas Field Miano. This is a very hot (177°C) wellhead (cooled to 110°C) before entering the flow lines. The fluid contains 12% CO₂ and 100-ppm H₂S. C-steel flowlines were protected with an environmentally friendly CI (Naraghi and Obeyesekere 2002; Obeyesekere et al. 2004). The Naraghi and Obeyesekere (2002) patent claims a composition claims possibly used in this study. It is claimed that the corrosion protection of the flowlines was effective (CR <0.02 mm/yr). The downhole equipment was protected using 22% Cr steel.

Sour Gas Field Sawan. This hot field (wellhead temperature 177°C, cooled to 93°C at the lines) also has 10% CO₂ and 100 ppm H₂S. Because of short length of the gathering lines, 22% Cr steel was used for all of the components, and inhibitors were not used.

2.6.2 Scale Inhibitor Improvements. Jordan et al. (2010) note that over the years environmental legislation has forced changes in the types of scale inhibitor molecule that can be deployed in certain regions of the world. These regulations have results in changes from phosphonate scale inhibitor to polymer-based chemistry particularly in the Norwegian and UK continental shelf where phosphonates have either been on the substitution list or phased out for many applications. Over the past 10 years significant improvements in inhibitor properties of the so called “green” scale [some are polymers made from biodegradable materials such as polyaspartate acid (Kohler et al. 2004)] inhibitors have been made. For one particular operator, the squeeze application of this green scale inhibitor resulted in poorer than expected treatment lifetimes and significant operating cost because of the frequency of retreatment. To overcome the increasing operating cost, an evaluation was made of the current treatment chemicals vs. the older more established phosphonate scale inhibitors. The results for the laboratory evaluation suggested that the older chemistry would extend treatment life and reduce operating cost. A case was made to the legislative authority and field applications started. The squeeze lifetimes for the red (phosphonate –diethylenetetraaminepentamethylenephosphonic acid) chemistry were shown to be better than the “yellow/green” inhibitors.

Conclusions.

1. Downhole scale control in challenging reservoirs/fields requires unique and individual solutions that may require the application of chemistries that are not always the most environmentally acceptable.

- For this field's scale tendency (brine composition), the phosphonates diethylenetetraaminepentamethylenephosphonic acid have similar/improved efficiency to the different polymer-based scale inhibitors previously applied. For this field's reservoir rock, the phosphonate scale inhibitor shows much better chemical retention/release characteristics in both coreflood and field application than any polymer evaluated.

2.6.3 Demulsification Case History. Wylde et al. (2010) describe the continual improvement cycle for the fluid-separation process of a heavy-oil/oil-sands production facility in northern Alberta over a period of 3 years. The major challenge posed by the operator of this 13 to 16°API crude oil was to move away from injection of two separate demulsifier formulations to injection of a single product.

A bottle testing method was developed and used to simulate the field conditions as accurately as possible. Details are given on the chemistry of the individual components of the demulsifier determined to be so crucial to adequate performance and how this was optimized in the field after being identified from the bottle tests. Fig. 2.59 shows the schematic of the treatment/demulsification process. The DMs (blend of ethylene oxide/propylene oxide block copolymers and alkoxyated amines) were added before the mixture reached the inclined two phase separator and the treaters are heated to $>100^{\circ}\text{C}$. The bottle tests allowed development of the most efficient blend/concentration of the DMs. They also found that CIs caused separation problems and entrained gas caused foaming, requiring a defoamer. Pigging operations of the pipelines removed slugs of solids, but also brought more water and solids into the treatment plant. A schematic of the process is in Fig. 2.58.

2.6.4 Multichemical Application Case History. This paper (Shepherd et al. 2012) describes the production chemistry management process undertaken during the design, commissioning, and startup phases of the Schoonebeek redevelopment. Challenging separation issues, and saline water, together with a multitude of other process conditions, resulted in complex but robust application portfolio. This was established during the design stages of the project. Early involvement of the production chemistry discipline aided this process. Chemical selection was conducted in adherence to health, safety, and security environment directives and focusing on unique produced fluid properties. Since startup, the success of chemical performance has been because of the availability of chemical treatment programs and surveillance/sampling plans. No contingency chemicals have so far been needed at the facilities since startup. Export oil and water key performance indicators have been for the majority of the time met. Further optimization of chemical applications is an ongoing process that will follow the life of the field.

Fig. 2.60 shows an overview of the types and locations of chemical treatments required to maintain flow and reliability in the plant. These chemical types are described in detail in Sections 2.4.4, 4.7.3, 4.7.4, and 4.7.5.

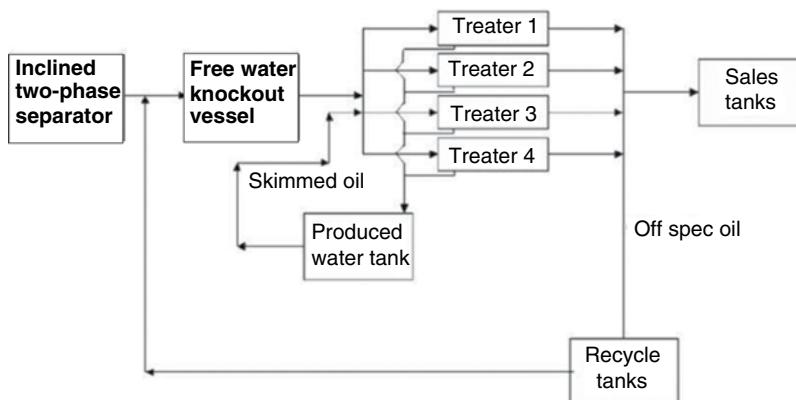


Fig. 2.59—Schematic of demulsification treatment of heavy oil (Wylde et al. 2010).

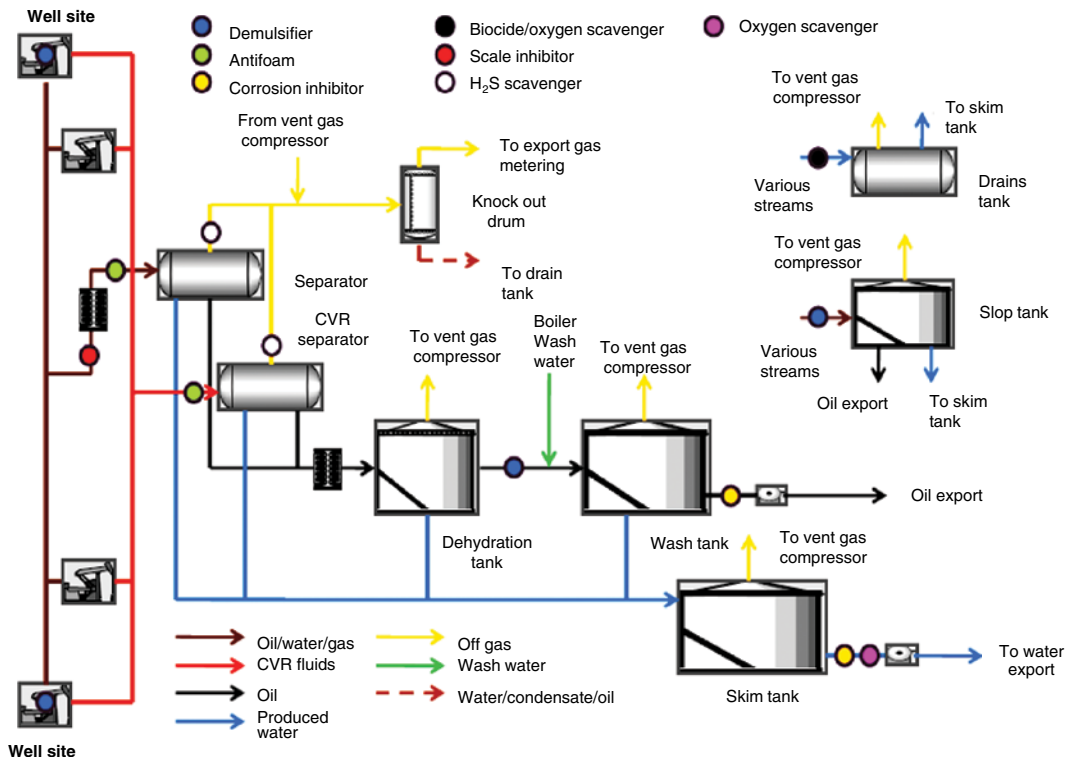


Fig. 2.60—Overview of chemical usages at the central fluid treatment facility (Shepherd et al. 2012).

2.7 Things to Think About

- The formation of fouling deposits such as inorganic scales, naphthenates, waxes, and asphaltenes is very important for understanding the other subjects that are described in this chapter including formation damage and the formation of emulsions.
- The other common and underlying technology involves the operation of various surface active agents (nonionic, cationic, anionic, and amphoteric surfactants). The natural and manufactured agents are at the center of a very large number and quantity of production enhancement procedures now in use. Surfactants are also the causative agents of many production problems. Therefore, a thorough understanding of the basic principles have been emphasized and should be reviewed because they are also at the center of many of the processes described in subsequent chapters of this book.
- New technology in the use of production CIs involves greener chemicals as well as the use of microemulsions for deployment of the chemicals in more efficient technologies. Mixed inhibitors for control of wax, asphaltenes, scales, corrosion, and hydrates simultaneously also are being tested and are in commercial operations. Inhibitors for FeS also are in use.
- Many methods for resolving production-caused water/oil emulsions are in use and contribute to safer and more efficient oil production. As noted above, the mechanisms of formation and chemicals in use are common to many other production enhancement processes and at the root of some problems.

Chapter 3

Formation Stimulation With Reactive Chemicals

Formation stimulation, in general, is performed to enhance the property value of the well by causing a faster delivery of the petroleum fluid and/or to increase ultimate economic productivity. These type of treatments can be performed with fluids that *react* with the formation (the current Chapter 3) or using *essentially nonreactive* fluids containing solids (propped fracturing: Chapter 4). Reactive stimulation (also widely called acidizing) usually is performed to remove formation damage and blockages (Section 2.3) in the tubing; however, production of a negative skin (S) (see Eq. 1.8) sometimes is possible.

Two different types of reactive fluid stimulation treatments that depend on the pressure applied to the receiving formation are discussed in this chapter. At low pumping rates (**Fig. 3.1**), the fluid enters and reacts with the formation without fracturing it. At pumping rates that produce pressures above the fracture pressure (Section 1.6.3), the fluid cracks the rock and flows into the fracture channel (note change in slope in Fig. 3.1) where it will also dissolve some of the rock. This is called fracture acidizing and is currently employed only for carbonate formations. More details of the different types of treatments are described in Sections 3.3, 3.5, and 3.8.1.

Many details of the reactions, additives, and the very important issue of fluid placement are reviewed in the various sections of this chapter. In additions, the initial discussions of fracture acidizing (Section 3.8) provides a prequel to the discussions of propped fracturing in Chapter 4.

3.1 Introduction to Stimulation Using Reactive Chemicals

Matrix stimulation is performed by pumping reactive chemicals into the near-wellbore area to remove or bypass damage caused by scale, organic deposits, or formation fines (see Sections 1.2, 2.3, and 2.2). To achieve only flow of the fluids into the tubing and the formation matrix spaces, the treatment is pumped at a rate that produces a pressure that is *less* than the fracture pressure for the formation being treated. See Section 1.6.3 for a discussion on methods for determining the fracture gradient and the fracture pressure. Fig. 3.1 shows the effects of pumping pressure on rate and the change that occurs at the fracture pressure. This process is performed on both sandstone and carbonate formations. Only carbonates are treated with high-pressure (fracturing) fluids. The treatment of carbonates as compared with sandstone (silicate) formations requires very different techniques and fluids because of the radically different chemical and physical characteristics of these strata.

Fig. 3.2 provides a radial (overhead) view of treating fluids flowing into sandstone or carbonate formations and demonstrates some of the differences. This figure notes that damage is *dissolved* by sandstone stimulation, but the damage is *bypassed* when treating carbonates. The areas of damage (brown), bypassed (red) and dissolution of damage (sandstone) (gray) are noted by the different colors in Fig. 3.2.

The carbonates formations such as limestone (CaCO_3) and dolomite [$\text{CaMg}(\text{CO}_3)_2$] are almost completely soluble in acid. The dissolution reaction with HCl, which is by far the most common acid used for stimulation are

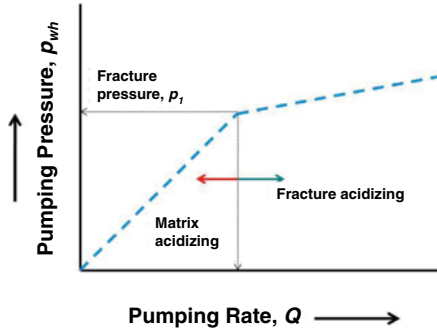
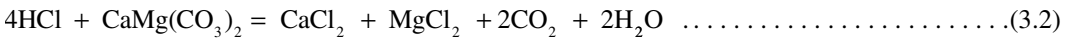
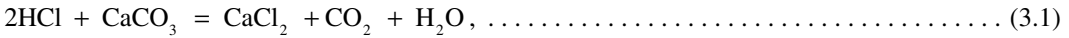


Fig. 3.1—Pumping rate and well pressure.



Because of the high-acid solubility of the carbonate minerals during matrix stimulation (low-pressure injection), the rapidly reacting acids can penetrate the formation and may cause high permeability-channels called wormholes [X-ray tomographic images in Fig. 3.3 by McDuff et al. (2010)]. Note the tree branch or fractal-like structures [described by Daccord and Lenormand (1987)] proceeding from the wellbore as well as the larger (dominant) wormholes.

If higher pressures and flow rates are employed, then the formation rock will fracture (Fig. 3.1) and dissolution of the carbonate will occur on the fracture face (Fig. 3.4). The etch on the fracture face will prevent the fracture from closing completely, allowing a conductive path for the hydrocarbons fluids.

Conversely, the silicates are mostly hydrochloric acid (HCl) *insoluble* and much more complex in structure. Because the silicate portions of the rock are soluble *only* in hydrofluoric acid (HF) containing solvents, various permutations of HCl/HF fluids [called mud acids (MAs)] have been used in the matrix mode to clean these formations. Fig. 3.5 shows visual details of a sandstone matrix

Acidizing Treatments in Sandstones and Carbonate Reservoirs

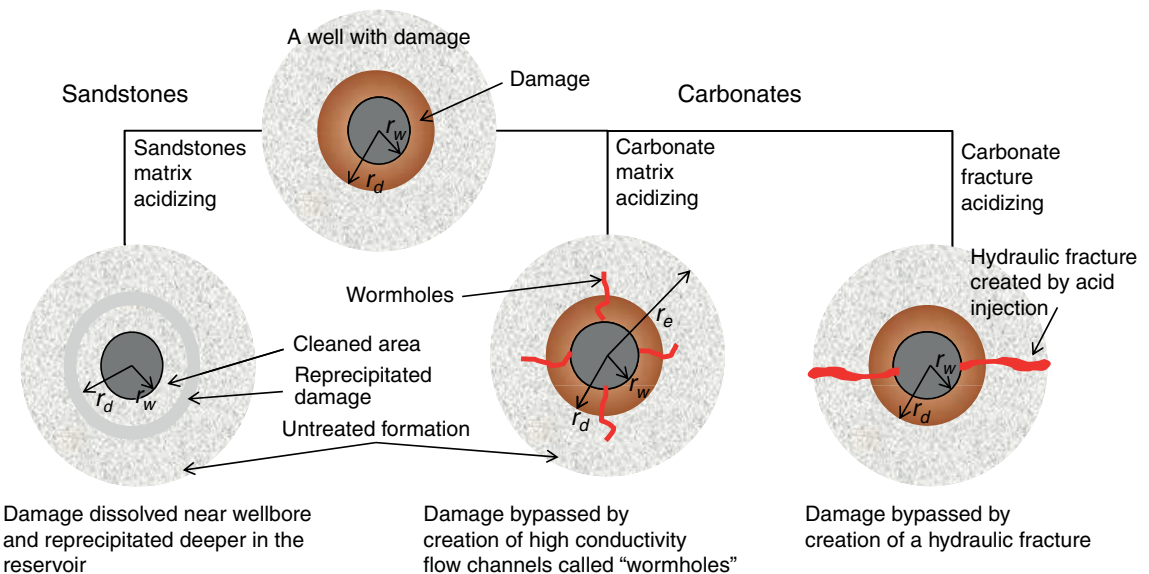


Fig. 3.2—Radial view of differences in sandstone and carbonate treatment methods, showing wellbore, damage, and untreated formation.

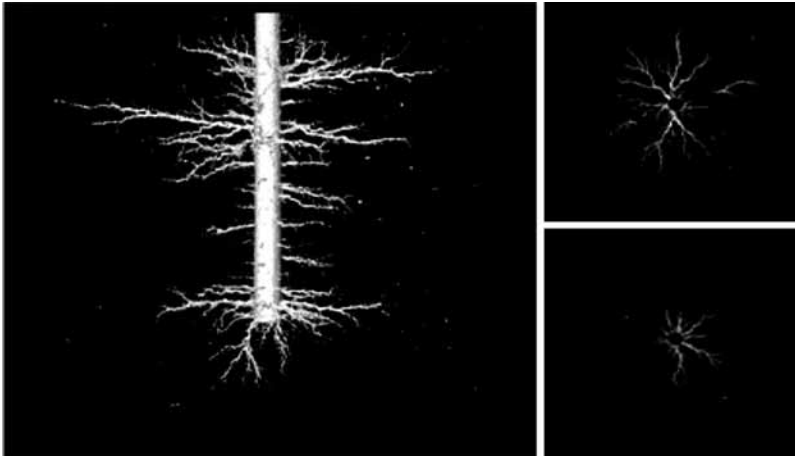


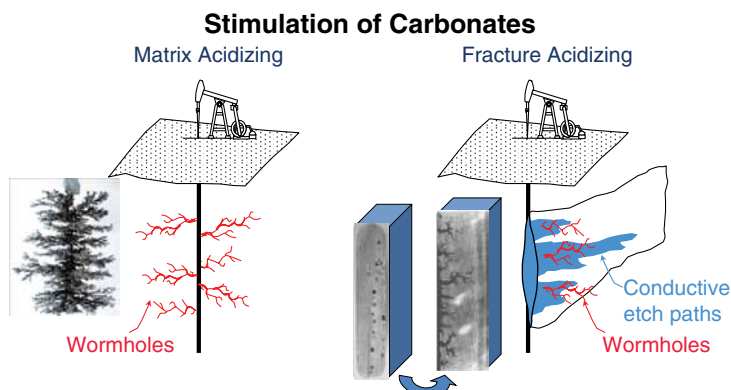
Fig. 3.3—Top and side views of wormhole structures by X-ray tomography (McDuff et al. 2010).

(Al-Harthy et al. 2008) and also shows a micrographic detail of a sandstone matrix with carbonates, silica, and clays. The complex reactions to dissolve silica and clays are described in much detail in Section 3.5.

In all cases, the steel well goods will come in contact with corrosive fluids and must be protected by appropriate corrosion inhibitors (CIs) (Section 3.6.1). More details of the carbonate and silicate formation compositions that affect stimulation and formation penetration using reactive chemicals are considered in Sections 3.3 and 3.5.

The matrix process may reduce the skin factor [see discussion by Economides and Boney (2001) and in Section 2.3.1 as well as Eq. 1.8] and, thus, restore production to expected levels. In some cases of the use of chemicals to bypass damage in carbonate reservoirs, stimulation (negative skin values) may be possible. This type of stimulation is designed to penetrate 1–2 m (radially) into the rock matrix.

An increase in the productivity index (PI) (Eq. 1.17) is the goal of the matrix treatment and Fig. 3.6 is a diagram of the effectiveness of various treatments (see details in Sections 3.3 and 3.5). This diagram shows various scenarios with the ratios of final or damaged permeability (k_D) to permeability (k) plotted against the depth of the damaged zones. Because matrix stimulation of sandstones usually can only remove damage, a final ratio of 1 (brown line) is the best possible outcome. However, for a very badly damaged well (green and purple lines), this would be an excellent outcome. The sidebar (right) uses the same color coding as Fig. 3.2.



- The injection of acids into carbonate reservoirs leads to the formation of highly conductive flow channels.
- Fluid types: gelled, emulsified, VES and plain acid.

Fig. 3.4—Matrix and fracture acidizing of carbonates.

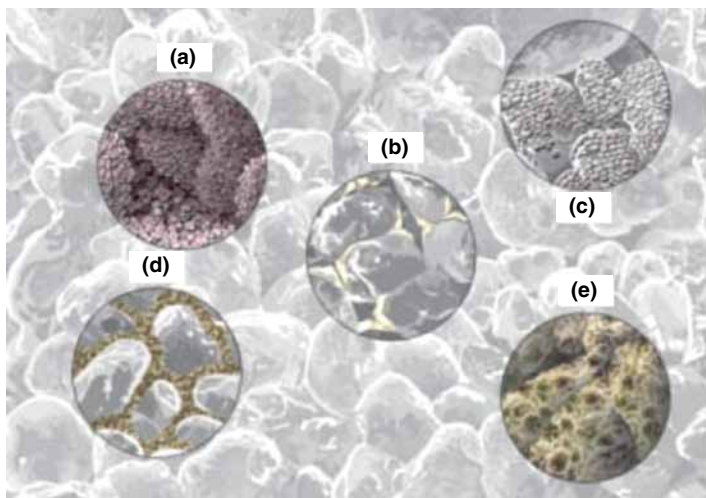


Fig. 3.5—Sandstone matrix showing overgrowth of (a) carbonates, (b) quartz, and (c) feldspar. Porosity reduction occurs from pore-filling clays such as (d) kaolinite and (e) pore-lining illite (Al-Harthy et al. 2008).

Carbonate formations can actually be stimulated because of wormhole formation; however, the maximum possible improvement is about 20% over the base line (blue and orange lines).

Hydraulic fracturing treatments that use large volumes of fluids at high pressures to fracture the rock and penetrate more deeply can increase production above expected levels and also may produce negative skin. Reactive fluids that dissolve part of the fracture face and, thus, keep the fracture open by producing nonuniform etch can be used on some carbonate formations but currently not for sandstones. The essentially nonreactive fluids containing suspended solids (proppants) to keep the fractures open are used to stimulate both sandstones and carbonates formations [see Economides and Nolte (2000) and Jones and Britt (2009)]. The reactive fracturing processes are described in Section 3.8 and propped fracturing chemistry is detailed in Chapter 4.

The use of reactive fluids to stimulate or clean oil and gas formations represent some of the first enhancement methods employed after the beginning of the modern hydrocarbon production industry and usually are called acidizing processes. This term has been widely used since HCl was employed as

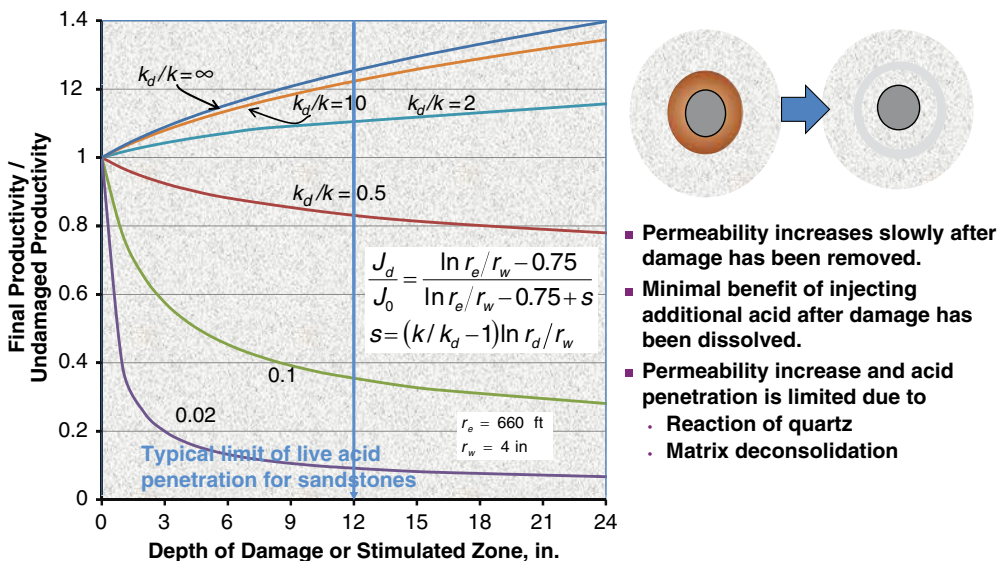


Fig. 3.6—Productivity increase from matrix stimulation.

early as 1895 to attempt to clean out an oil well. The authors of this book are using the more encompassing term reactive chemistry because many weak or nonacids are also in use for formation stimulation and cleaning treatments. This chapter will describe the chemistry and application of reactive fluids during both matrix and fracturing treatments.

The steel well tubing also can be cleaned to remove inorganic and organic solids that foul the flow paths. This is an important part of flow assurance (FA). The next three short sections (3.1.1–3.1.3) summarize the features of carbonate, sandstone, and tube-cleaning treatments.

3.1.1 Salient Features of Carbonate Stimulation Treatments.

1. Carbonate minerals are highly soluble in acid and react rapidly with most acids. Common minerals found in carbonate reservoirs are limestone (CaCO_3) and dolomite [$\text{CaMg}(\text{CaCO}_3)_2$]. Many carbonate formations are almost entirely composed of limestone, while others have varying degrees of dolomites present. Other minerals found in carbonate formations are anhydrites (CaSO_4) and siderite (FeCO_3).
2. HCl is used most often because the byproducts are soluble. See Eqs. 3.1 and 3.2 for the basic reactions.
3. HF is not used because of CaF_2 precipitate.
4. Treatment will bypass damage rather than dissolve damage.
5. Natural fractures are acidized and may take flow.
6. Competent rock formations, long horizontal wells, and many openhole completions are acidized.

3.1.2 Salient Features of Sandstone Stimulation Treatments. Compared with carbonate formations, most of the matrix is not soluble in HCl and the damage-causing agents include clays and fines that are soluble only in HF-containing fluids.

1. The goal is to *remove* damage and to reduce the skin (S ; see Eq. 1.8) to near 0.
2. Stimulation is not expected.
3. Fracture stimulation is currently not feasible.
4. The treatments require multiple stages of HCl (to remove calcite) and MA (HCl/HF) as well as flush stages.

3.1.3 Salient Features of Tubing Cleanout Treatments. Many reactive chemical treatments are pumped (at least partially) to clean out production, injection, and connecting piping.

1. They may use almost any of the matrix or fracturing base chemicals but usually not HF.
2. The may be pumped into the matrix but should be returned to the surface because it will be highly contaminated.
3. The treatment frequently will contain or be preceded by a solvent that can dissolve organic deposits (see Section 2.2.4).

3.1.4 Development of “Acidizing” as a Stimulation Method. This section provides a short review of the history of the use of the reactive method for well stimulation. Also see the histories of matrix acidizing by Thomas and Morgenthaler (2001), Al-Harthy et al. (2008), and Portier et al. (2007). Additional sections in Economides and Nolte (2000) (Chapter 13) and Kalfayan (2008) (Chapter 1) give more details of various aspects of the historical use of acids for stimulation.

Table 3.1 summarizes some of the significant dates in the development of reactive chemical stimulation processes. Some of the key technical innovations such as CIs, sandstone acidizing fluids, fracture acidizing, and diversion are still being used and are the subject of continued research and development efforts.

Details of matrix stimulation of carbonates follow in Sections 3.3 and 3.4. Matrix stimulation of sandstones is described in Section 3.5. Fracture acidizing is reviewed in Section 3.8. Generic tests used by many labs to study matrix reactive stimulation are described in the next section (3.2).

TABLE 3.1—HISTORY OF ACIDIZING (REACTIVE STIMULATION)

| <u>Date</u> | <u>Development</u> | <u>Reference</u> |
|-------------|---|------------------------------|
| 1895/1896 | Ohio Oil Company acidized both oil and gas wells with significant increases in production; however, the casing was severely corroded and the process became unpopular. A patent described the use of HCl in wells with limestone formations but did not address the corrosion problem. | Frasch (1896) |
| 1928 | Dr. Herbert Dow (founder of Dow Chemical Co.) lowered bottles of acid into brine wells for the purpose of increasing their production. However, the results were not satisfactory, largely because of the corrosion incurred and the expensive materials required to protect the metal equipment. Thus, the Dow Chemical Co. initiated a project to develop the first acid corrosion inhibitor. | |
| 1932/1935 | John Grebe of Dow discovered that arsenic acid acted as a corrosion inhibitor. Later, copper salts were used with arsenic to avoid the formation of calcium arsenate precipitate, and soon organic inhibitors were found to be far superior. | Grebe (1935) |
| 1932/1935 | Five hundred gallons of inhibited HCl were siphoned into the well, resulting in a previously "dead" well flowing 16 BOPD. Thus, acidizing was reborn, and Dow formed the Dow Well Services Group that soon evolved into Dowell. Three years later, the Halliburton Oil Well Cementing Co. in Duncan, Oklahoma, also began commercial acidizing service. | |
| 1933 | Sandstone acidizing with HF was practiced in Texas in 1933 following the issuance of a patent to the Standard Oil Company; however, the field tests were not successful because of plugging of the formation. | |
| 1935 | First fracture acidizing treatments proposed and performed. | Grebe and Stoesser (1935) |
| 1940 | Commercial application of HF acidizing of sandstones occurred in the Gulf Coast of Mexico in 1940, when Dowell introduced mud acid, a mixture of HCl and HF. Research indicated that the HCl helped maintain a low pH and decreased the precipitation of damaging solids. | |
| 1956 | Diversion of fluids with mechanical methods including foam. | Harrison (1972) |
| 1957 | Improved techniques for acid fracturing of carbonates. | Williams and Nierode (1972) |
| 1961 | Organic acids (acetic, formic) used as stimulation agents in hot wells. | Harris (1961) |
| 1965 | Understanding of sandstone stimulation and use of HCl preflush. | Smith et al. (1965) |
| 1982 | Alternate chemicals such as chelating agents used for well cleanout. | Shaughnessy and Kline (1983) |
| 2003 | Use of VES materials for diversion. | Chang et al. (2003) |

3.2 Laboratory Test Methods for Matrix Reactive Fluid Treatments

3.2.1 Methods for Carbonates. This section describes test methods that have been used to study and elucidate mechanisms of the complex geochemical reactions of fluids with producing formations. Sections 1.5.1 and 1.5.7 previewed some of the thermodynamic and kinetic equations and laws that control the reactions at a solid surface. They have been used especially for carbonates, but some also are applicable to sandstone rocks. Rates of reactions and reaction mechanisms that include the surface reaction rate (SRR) and any effects of mass transport must be investigated. Experimental tests to determine the kinetic parameters for dissolution of solids that are of interest in stimulating oil and gas formations are described in this section. This includes dissolution of calcite and dolomite as well as constituents of sandstone formations. Use of the rotating disk (RD) methods and techniques for determining the extent of wormhole formation using coreflood tests are also described in this section. In addition, the use of slurry reactors is described. Some of these methods are useful for studying both carbonate and sandstone formations and the reactive stimulation of them and apply directly to matrix stimulation; however, basic dissolution rate data also is used in fracture acidizing models (Section 3.8).

RD Methods. The RD apparatus consists of a disk of rock spinning in a volume of reactive fluid at a constant angular velocity, ω (Levich 1962). The concentrations of the products or reactants in the bulk

- Hydrodynamics are well defined
- Disk surface is uniformly accessible

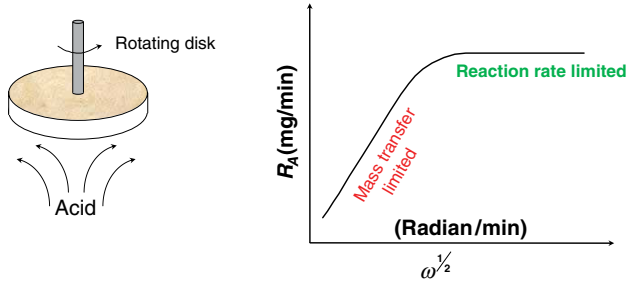


Fig. 3.7—Description of rotating disk.

are measured at various time intervals while the disk is rotating at a fixed ω . The global reaction rate at a given ω is computed from the change in concentration vs. time. The experiment is then repeated at different angular velocities to obtain the dissolution rate as a function of ω . The reaction rate data is then plotted against $\sqrt{\omega}$ to identify the reaction and diffusion limited regimes (Fig. 3.7). Additional experiments at different temperatures or different reactant concentrations are often required to obtain the full rate law for the reaction system. The method has been successfully used to measure reaction kinetics of many reaction systems important to matrix stimulation treatments (Lund et al. 1973; Fogler and Lund 1975). There are several advantages of this system of studying reactions between fluid and solid surface over the traditional system of the fluid flowing over a flat plate (Litt and Serad 1964), a flow tunnel is not required because the fluid motion is induced by the disk in addition to the following:

- Large fluid volumes are not required
- End effects are minor, whereas with a flat plate they can be a major factor
- A disk rotating in a infinite fluid volume represents a 3D flow system for which there exists an exact solution to the Navier Stokes equations
- The heat and mass transfer coefficients are constant over the surface of the disk, whereas they decrease down the flat plate

Levich (1962) provided an analytical solution for mass flux (j) of a solute from a fluid to the surface of the RD under laminar conditions as

$$j = 0.62D^{2/3}\nu^{-1/6}\omega^{1/2}C_0 \text{ gmol/cm}^2 - \text{s}, \dots\dots\dots (3.3)$$

where D is the diffusion coefficient of the solute (cm^2/s), ν is the fluid kinematic viscosity (cm^2/s), ω is the angular velocity of the disk (radians/s), and C_0 is the solute concentration (gmole/cm^3). This relation can be used to calculate mass transfer coefficient, k_m , and the diffusional boundary layer thickness (δ), as follows

$$k_m = 0.62D^{2/3}\nu^{-1/6}\omega^{1/2} \text{ cm/s}, \dots\dots\dots (3.4)$$

$$\delta \approx \frac{DC_0}{j} = 1.61\left(\frac{D}{\nu}\right)^{1/3}\left(\frac{\nu}{\omega}\right)^{1/2} \text{ cm} \dots\dots\dots (3.5)$$

The previously mentioned equations only apply when the flow in the vicinity of the disk is laminar. The theory also assumes an infinite disk spinning in an infinite fluid volume in the derivation of the equations. In practice, the disk diameter must be larger than the thickness of the boundary layer and the vessel diameter has to be at least twice the disk diameter for the observed transport rate to be almost independent of the vessel diameter (Gregory and Riddiford 1956).

Generally the reactions are studied at a high enough angular velocity, such that the rate of reaction is controlled completely by the surface reaction (Fig. 3.7). In this case, the SRR constant, k_r , can be calculated directly from the measured overall reaction rate (Lund et al. 1973; Fogler and Lund 1976)

$$\text{Measured Reaction Rate} = k_r C_0 \dots \dots \dots (3.6)$$

However, for many fast reactions, it may be difficult to achieve an angular velocity where both the reaction is surface reaction limited and the flow near the disk is laminar. For many fast reactions, the flow near the disk turn turbulent before the reaction becomes surface reaction limited and above relationship for mass transfer cannot be used. The rate of surface reaction generally slows down much more rapidly with temperature than the diffusion rate, and therefore, in some cases, it is possible to measure the kinetics at a lower temperature and then extrapolate to the temperature of interest. For example, Lund et al. (1973) lowered the reaction temperature to measure the kinetics of the calcite-HCl system. However, for aqueous systems, the freezing point of the solution sets the limit to which the temperature can be lowered. If the reaction rate cannot be made to be completely under surface reaction control, an accurate model for diffusion coefficients may be necessary to estimate the contribution of the surface reaction.

Fig. 3.8 shows a suite of equipment that has been used in RD tests (Frenier et al. 2000). It consists of a reaction chamber (modified Parr Instrument 1-L Hastelloy reactor), a heated transfer flask

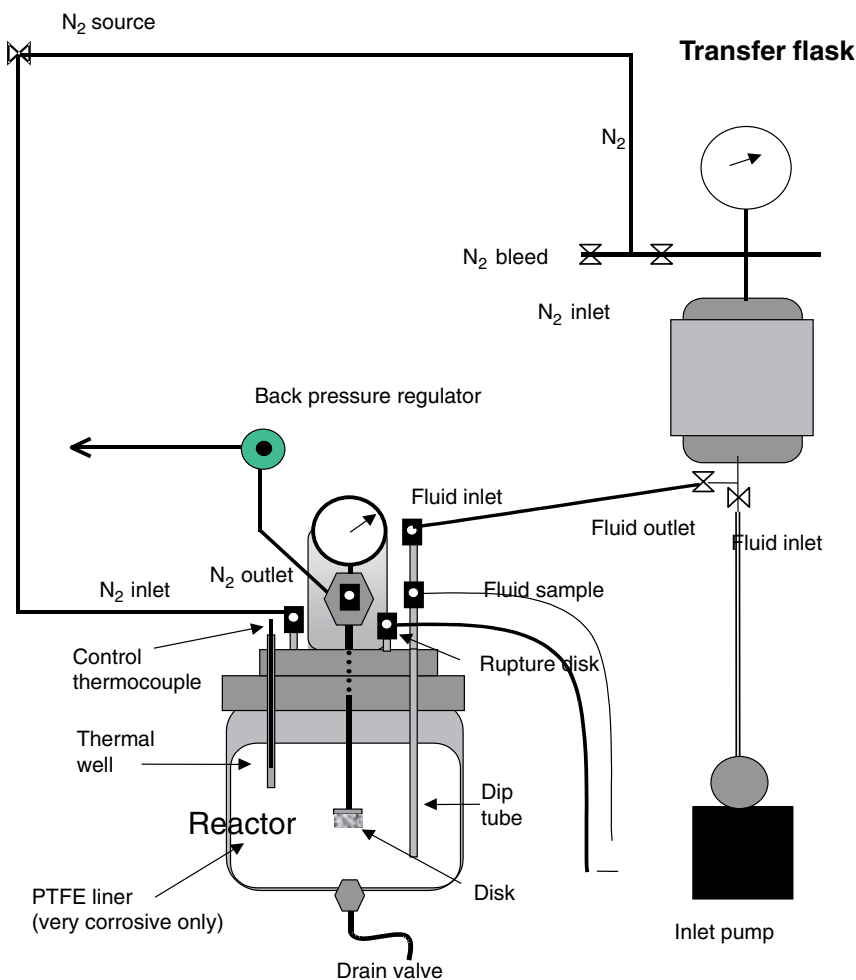


Fig. 3.8—HP reactor and RDE showing schematic of fluid flow.

for the reagents and necessary transfer piping. A spindle terminates with a 1-in. diameter disk [316 stainless steel (SS) or Hastelloy, 0.25 in. thick] that extends into the chamber. The tests were performed by the authors (Frenier et al. 2000) using Carrara marble disks or dolomite disks from outcrops (1-in.-diameter) mounted on the metallic disk. Other minerals such as gypsum or iron mineral also can be investigated using this type of equipment (Ford et al. 1992).

To perform the test, a disk is mounted on the spindle, the rotation rate (rev/min) set, and rotation started. The reactor is closed and heated to the test temperature. The test fluid (usually 850 mL) is loaded into the transfer flask and heated to the test temperature. When both vessels were at the same temperature, the test fluid is pushed into the test vessel using nitrogen pressure.

The back pressure regulator was usually set at 600 psig and the test was started. Samples are taken at intervals, and the rate of reaction determined from the slope of the [Ca] or [Mg] vs. time plot. The [metal] was determined using atomic absorption spectrophotometry or inductively coupled plasma optical emission spectrophotometry (ICPOES). Other mineral tests and corrosion studies can be performed using similar equipment and the sample can be a disk or a cylinder (Silverman 1990).

The equipment seen in Fig. 3.8 can be converted and used as a slurry reactor by removing the RD and using an appropriate impeller. The RD methodologies also can be used with glass reactors at temperatures below about 90°C.

This type of versatile high-pressure reactor also can be used for CI tests that are important for developing useful well treating fluids. These tests also can be conducted with high temperature or unstirred autoclaves (Frenier et al. 2000). See the discussion of acidizing CIs in Frenier and Ziauddin (2008) as well as in Section 3.6.1 of this book.

Coreflood Tests. Dynamic core flood tests can be run using the equipment such as is shown in Fig. 3.9. In the case of the equipment depicted, the limestone, dolomite, or various sandstone cores (1.0-in. diameter and approximately 6 in. long) were placed in a Hassler sleeve (Hassler 1944) before being placed in the heated test chamber. The temperature of the tests was maintained at values from 65–195°C. Various flow rates were used. A backpressure of 1000 psig was maintained to keep CO₂ in solution. The pore volume to breakthrough (PVTB) was determined from the onset of dramatic permeability increase, indicating that the acid had completely penetrated the core. This value has been related to the effectiveness of the treatments (Fredd and Fogler 1998b). See Section 3.3.2 for more details. The authors of this book note that many other modifications of this type of coreflood apparatus are in use, but the set-ups are similar [for example Siddiqui et al. (2006)].

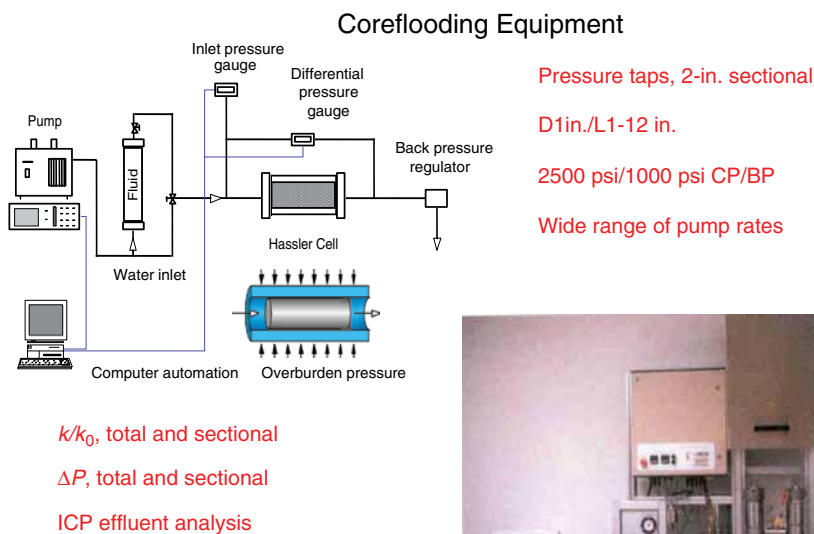


Fig. 3.9—Coreflood tester showing schematic and a photo.

Samples of the effluent were collected at 10-mL intervals and sent for chemical analyses (Fe and Ca) using atomic absorption spectrophotometry or ICPOES methods. The cores were photographed and reweighed after the test was completed.

The cores also could be imaged using computed tomography (CT) X-ray scans (Bazin and Abdulahad 1999). In one case (Frenier et al. 2000), the scans were run at 130 KV on dry cores. See Section 3.4 for test results. Additional results of X-ray imaging (2D and 3D) (Siddiqui et al. 2006) have also been used to study the fine structure of the wormhole process.

Short core and long core tests (Furui et al. 2010) also have been run. The data then can be converted to radial flow predictions using numerical models (Frick et al. 1994; Glasbergen et al. 2009).

Radial Flow Experiments. McDuff et al. (2010) have developed a larger-scale test system that includes radial flow injection tests that include (1) acidizing experiments on carbonate rock samples up to 14 ft³ in volume, (2) high-resolution nondestructive imaging and analysis, and (3) computational modeling to extend the results of experiments to field applications.

In these experiments, large-scale acidizing experiments were conducted on rock samples up to 14 ft³ in volume, weighing approximately 1 ton, and providing more than 2,000 times the rock volume of a traditional core plug sample. To establish flow rates to be used in these large block tests, wormhole efficiency curves were determined from a series of linear core-acidizing tests on 1.5×6-in. core plugs. Also, core plugs for each tested rock type are characterized by X-ray diffraction (XRD) and pre-acidizing CT scans.

Smaller blocks (0.8 ft³) also were tested to compare limestone with dolomite. In all cases, 15% HCl was used as the stimulation fluid at ambient temperature conditions, but with the blocks placed in large triaxial cells with a confining back pressure.

In the experiment described by McDuff et al. (2010), after pumping approximately 2.5 L of 15% HCl, a wormhole broke through the sidewall of the block and acid pumping was stopped. The flow conditions of the experiment are claimed by the authors to correspond to approximate field conditions of pumping 50 bbl/min into 1,000 ft of completion interval and generating 10- to 25-ft wormholes into the formation. On the basis of imaging results, wormholes grew nearly symmetrically along the entire completion interval. Wormhole branches were generated in all directions, extending radially toward the edges of the block. Note that the program used to make the predictions of the optimal rate was not described.

McDuff et al. (2010) show tests that compared limestone and dolomite. Two slices of X-ray images are seen. The dolomite tests were pumped at twice the acid rate into the limestone rock but did not achieve optimal dissolution fluxes because the dissolution patterns were very different and 10 times as much acid was needed to achieve breakthrough as the limestone tests. Note from Lund et al. (1975) that dolomite is much less reactive than limestone and at the temperatures of the test, the reactions rates may be in the SRR area not the mass transfer limited (MTL) rate regime based on these data. The discussions in Sections 3.3.2 and 3.4 by Hill and Schechter (2001) also imply that these are ramified wormholes and the rate of pumping was too high for the reaction conditions.

The authors (McDuff et al. 2010) claim that the characteristics and effects of wormholes may change during the life cycle of a well (e.g., caused by wormhole collapse, plugging, and other factors), resulting in changes to the well's connectivity to the reservoir. Incorporating detailed information on wormhole structures into well performance models enables exploring a variety of additional scenarios. These simulations, calibrated to results of the experiments, may be extended to parameter ranges outside the scope of laboratory experiments and scaled to field dimensions. An example of the output from these types of tests is seen in Fig. 3.10 (top view of borehole and wormholes) and Fig. 3.11 (side view of both limestone and dolomite showing different patterns—more details in Section 3.3.1). Note the fractal pattern that is similar to Fig. 3.3.

3.2.2 Test Methods for Silicate Formations. The reactor system (Fig. 3.8) used in the RD tests also can be used to study the dissolution chemistries of silicate formations. In this mode, it is called a slurry batch reactor. Harman et al. (2006) show details in Fig. 3.12. Either an atmospheric pressure (a) or a high-pressure reactor (b) can be used for determining the reaction rates of powdered solids, such as individual clays or prepared formation rocks. Samples removed from reactor frequently are acidified

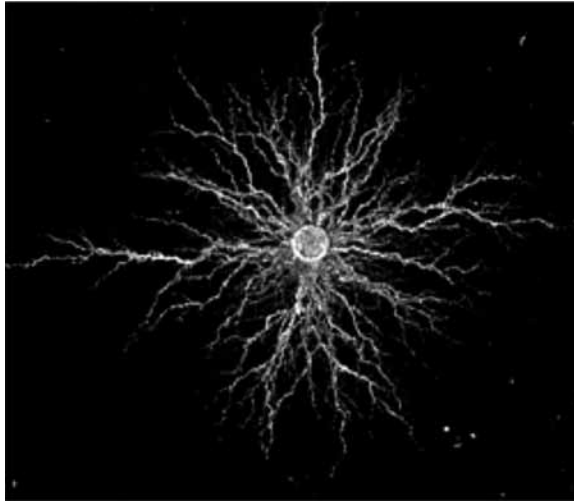


Fig. 3.10—X-ray tomography top view of large limestone block optimal pumping.

to preserve slow-precipitating solids, and then rapidly analyzed using initial circulating pressure (ICP) methods. This figure also shows the controlling equations (c) and typical output data curves (d), where concentrations of sandstone elements (Si and Al) are plotted vs. time. Examples of experimental output data for various aluminosilicates are seen in Section 3.5.2.

Coreflood tests of sandstone formation rocks also are used to elucidate the mechanisms of treating solutions to stimulate this type of reservoir. The metals dissolved are determined as a function of time (and temperature and flow rate). The permeability (k) is also determined before and after the treatment to assess removal of skin or formation of damage.

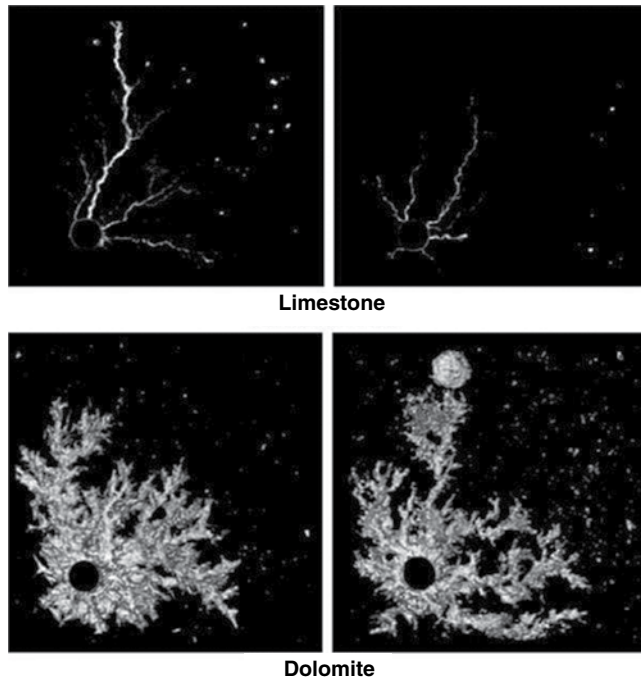


Fig. 3.11—X-ray tomography top view of small blocks showing near optimal pump rate for limestone and dolomite.

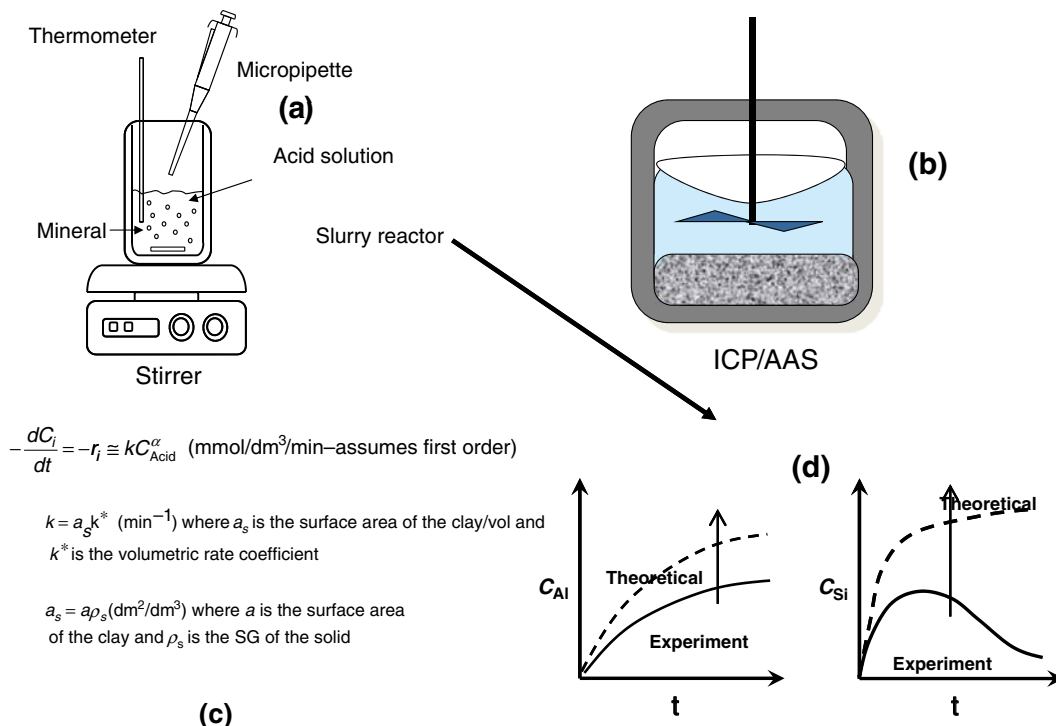


Fig. 3.12—Slurry batch reactor (a and b) used in the experiments with data output curves showing experimental and theoretical curves (d). Controlling equations are in section (c). The rate equation assumes first order, and the two lower equations convert and account for volumetric and mass rates.

3.3 Matrix Stimulation of Carbonate Formations

This section provides a mostly physical description of wormhole formation in carbonate rocks, while Section 3.4 reviews the wide range of chemical formulations available to achieve the most efficient stimulation of these formations.

Approximately 1/3 of the oil and gas production worldwide is from predominantly carbonate rocks. The remaining 2/3 of the production is from sandstones and shales (Schlumberger 2004b). However, carbonate reservoirs contain 60% of the proven reserves (Schlumberger 2008). Thus, these are very important reservoirs. There are two distinctly different carbonate formations (based on chemistry): limestone based (mostly calcite- CaCO_3) and dolomites [$\text{CaMg}(\text{CaCO}_3)_2$]. Fig. 3.13 shows some of the photos of these two formation rock types. Note that visually they are not distinguishable from each other or from many sandstone rocks.

Several different types of mostly limestone (calcite) formations are present in the earth (see Fig. 3.13). They have these properties that may affect acid stimulation:

- Oolite (small spherical sand-like grains)
 - Structures similar to sandstone
 - May have good porosity and is a good reservoir rock
- Chalk
 - A very fine-grained limestone
 - Very low primary porosity
- Ancient reefs and atolls
 - Burried mounds of shells
 - May have good primary porosity

Al-Awadi et al. (2009) note that dolomites are metastable carbonates and the mode of formation can affect the morphology and, thus, the methods and conditions used to stimulate them. Additional

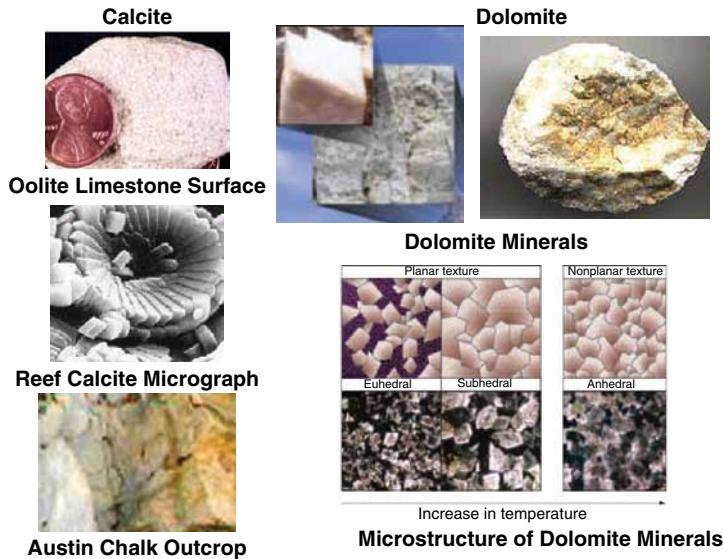


Fig. 3.13—Carbonate formation rocks (Al-Awadi et al. 2009).

studies of carbonates were described by Al-Marzouqi et al. (2010) who claim that the carbonates were formed from mostly biological organisms and are very complex when the macro- and microstructures are considered. As will be explained in a subsequent section (3.3.1), the reaction chemistries of limestone and dolomite rocks are markedly different.

The key goal of matrix stimulation of carbonates is the penetration of the near-wellbore region by conductive wormholes (Hendrickson 1972). See the photos in Hill and Schechter (2001) and Figs. 3.3, 3.10, and 3.11. If the reaction rates of the acid in the particular formation is not adjusted for the temperatures and flow rates attainable, optimal wormhole formation may not be achieved (Fredd 2000b).

Ming and El-Rabaa (2001) note that studies (Fredd 2000a) of the wormholing process in carbonate acidizing have shown that the dissolution pattern created by the flowing acid can be characterized as one of three types:

1. Compact dissolution in which most of the acid is spent near the rock face.
2. Wormholing, in which the dissolution advances more rapidly at the tips of a small number of highly conductive microchannels (i.e., wormholes, than at the surrounding walls).
3. Uniform dissolution, in which many pores are enlarged, as typically occurs in sandstone acidizing. Compact dissolution occurs when acid spends on the face of the formation. In this case, the live acid penetration is limited to within centimeters of the wellbore.

Uniform dissolution occurs when the acid reacts under the laws of fluid flow through porous media. In this case, the live acid penetration will be, at most, equal to the volumetric penetration of the injected acid. The objectives of the acidizing process are met most efficiently when near-wellbore permeability is enhanced to the *greatest* depth with the *smallest* volume of acid. This occurs when a wormholing pattern develops. See Fig. 3.14, which shows a demonstration of acid penetration in radial flow. The wormhole pattern is from a casting of Wood's metal poured into the core, and then the matrix is removed using dissolution in HCl (Hoefner and Fogler 1988). Additional details of wormhole formation and mechanisms will be described in Sections 3.3.1 and 3.3.2 and other photos have been seen as Figs. 3.10 and 3.11.

Additional challenges for carbonate wells include wellbore coverage, long horizontal wells, multi-laterals, and heterogeneous intervals. Planning and design of treatments to consider these issues are described in Section 3.3.3.

In fracture acidizing, formation of wormholes is *undesirable* because loss of fluid to the formation (called leakoff) restricts the amount of acid available to etch the fracture surfaces. Much of the

Wormhole Structure From Radial Flow

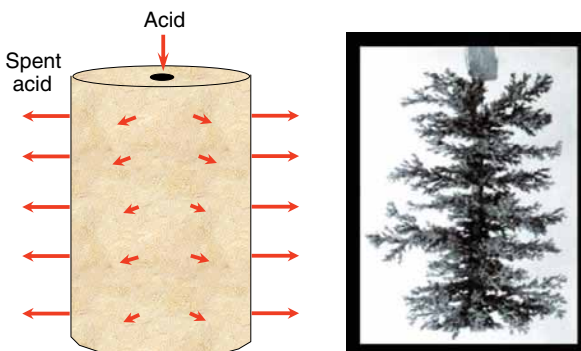


Fig. 3.14—Wormhole structure in radial flow.

technologies developed in recent years have been directed to controlling these factors and are discussed in detail in subsequent sections.

3.3.1 Distinctive Features of Reaction of Acids With Carbonate Rocks. Carbonate rocks typically have a wide range of interconnected pores. When an acid (in this section it always is dilute 5–15% HCl) is injected in a carbonate rock, more acid enters the larger pores than the smaller pores because of the lower resistance to flow in the larger pores. As the larger pores receive more acid they tend to enlarge more rapidly than the smaller ones. This results in them receiving even more acid and causing them to enlarge even more. This unstable process leads to formation of dominant fluid flow channels through the rock known as wormholes.

A typical response of carbonate core to acid injection (see coreflood tests in Section 3.2) is shown in Fig. 3.15. The pressure drop across the core is plotted against the pore volumes of acid injected. Note that after about 0.12 pore volumes, the pressure falls almost linearly until breakthrough at 0.44 pore volumes. The breakthrough occurs when the pressure drop across the core is minimal, and this usually occurs when the wormhole extends the full length of the core. The ratio of the volume of acid injected until breakthrough to the void volume of the core is referred to as PVBT. The initial 0.12 pore

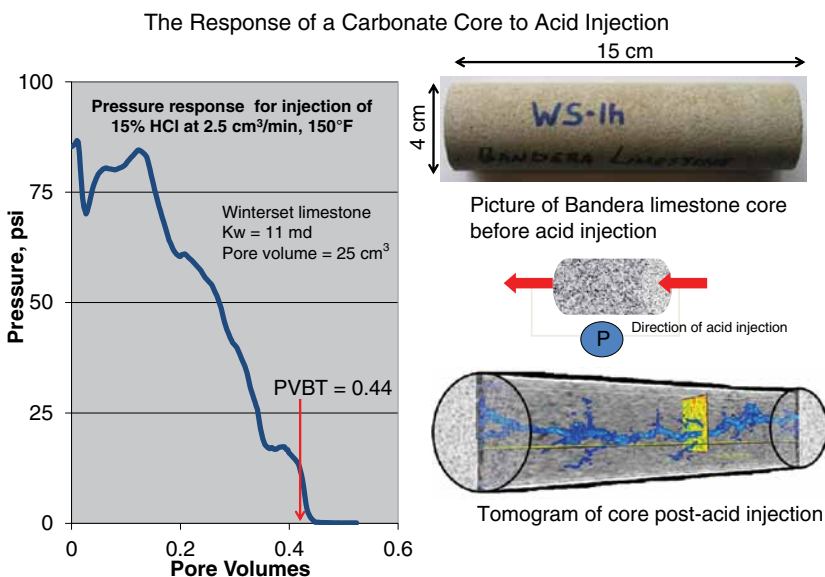


Fig. 3.15—Response of carbonate core to acid injection using 15% HCl.

volumes could be considered as the initiation phase of the wormhole and the remainder as the propagation phase. The tomogram (Siddiqui et al. 2006) of the core after acid injection shows the structure of the wormhole formed in the core in blue. Note that the diameter of the central channel remains fairly constant through the core. This is because when the diameter becomes sufficiently large, the reaction rate at the wall slows down because of diffusion limitations. The wormhole then grows axially rather than radially. Typically, once the effective wormhole radius reaches a few mm, then long wormhole lengths up to several meters are possible (Schechter 1992). The axial growth of the wormhole is limited by fluid loss and wormhole branching.

Several critical factors in wormhole development are the injection rate, rock type, and fluid saturation.

Effect of Injection Rate. When a series of coreflood experiments are carried out as described previously but at different injection rates, a relationship (Fig. 3.16) is developed that shows the PVBT value as a function of injection velocities. Note that a dominant wormhole only forms above a critical injection rate. The injection rate at which a minimum volume of acid is required to breakthrough the core is referred to as the optimum rate. The wormhole formed at the optimum rate has minimal branching. The number of branches from the main channel increase as the injection rate is increased above the optimum. This occurs because at higher injection rates, the acid leaking off from the main wormhole channel is not fully spent. This causes further rock dissolution as the acid leaks off from the main channel and creates branches.

Any unspent acid that leaks off before reaching the tip of the wormhole does not advance the wormhole forward, and therefore, a larger volume of acid is required to break through the core. As the injection rate is increased further, density of branching increase to such an extent that a dominant channel is no longer visible, and a ramified dissolution pattern is observed. Further increase in the injection rate causes the acid to flow uniformly through the core without any channeling. The dissolution pattern formed under these conditions is called the uniform dissolution pattern. Conical wormholes are observed at injection rates lower than the optimum rate. In conical wormholes, the acid is spent enlarging the wormhole at the base and by the time it reaches the tip of the wormhole it is mostly spent. At injection rates lower than that for conical wormholes, face dissolution is observed. Under face dissolution no visible wormhole is observed and improved permeability front advances by dissolving the whole rock.

Effect of Rock Type. Ziauddin and Bize (2007) have studied and classified carbonates into six categories called rock reservoir types (RRT) based on chemistry and porosity. These are

- RRT 1—A consolidated granular limestone in which dominant porosity is interparticle and is well connected. For example: Winterset limestone, and Indiana limestones I and II.
- RRT 2—Chalky microgranular limestones with both inter- and intraparticle porosity. For example: Austin chalk.

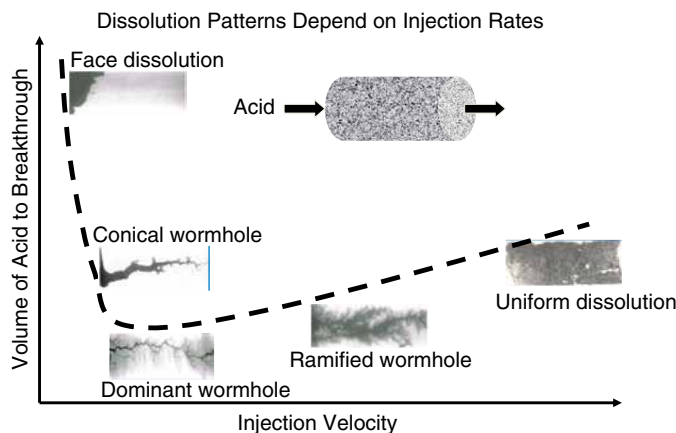


Fig. 3.16—Dependence of dissolution pattern on injection rate.

- RRT 3—Poorly sorted limestones with a predominantly grain-stone texture but with micritic matrix and moldic porosity in some areas. For example: Laune Monton limestone.
- RRT 4—Large biomoldic or oomoldic limestones in a tight crystalline matrix. For example: Savonniere I and II, limestones.
- RRT 5—Mud-dominated limestones with intercrystalline porosity. For example: Khuff Mudstone I.
- RRT 6—Mud-dominated dolostones (dolomite) with intercrystalline porosity. For example: Khuff Mudstone II.

RRT 5 and 6 have similar rock fabrics (i.e., mudstones) but are classified differently because of the difference in their chemical composition. Both of these RRTs would form poor petroleum reservoir rock but are stimulated using fracture acidizing (see Section 3.8).

These authors have used these types of classifications to interpret the acidizing properties using coreflood tests. Fig. 3.17 shows the PVBT vs. injection rate for different carbonate rock types (Ziauddin and Bize 2007) in 15% HCl at 150°F. The data in the figure are plotted against the interstitial velocity, which is simply qA/ϕ , where q is the volumetric injection rate, A is the surface of the face of the core, and ϕ is the total porosity (if data on effective porosities is available, it may better to use it instead of the total porosity). Interstitial velocity represents the velocity of the fluid front through the core if there is no channeling. It helps in normalizing data from rocks of different porosities. Fig. 3.18 shows the same data as Fig. 3.17 but instead of PVBT, the wormhole velocity is used as the ordinate axis. The wormhole velocity is a measure of the velocity of the improved permeability or the wormhole front in the core. It is approximated as the ratio of the core length to the breakthrough time. The dotted line on the plot marks the point of equality between the interstitial and the wormhole velocities. The departure of the data points from the dotted line is indicative of the degree of channeling. As expected, rock types further away from this line are more heterogeneous at the pore scale than those close to the line. Therefore, the growth rate of wormholes is expected to be faster in rocks with a greater degree of pore scale heterogeneity.

In some cases, rock types with similar wormhole velocities have different dissolution patterns. Fig. 3.19 shows the post-acid CT scans of Austin chalk (RRT 2) and Winterset limestone (RRT 1) for different injection rates. The dissolution pattern in Austin chalk is much more branched than that of the Winterset limestone at the same injection rate. A possible explanation could be postulated from the

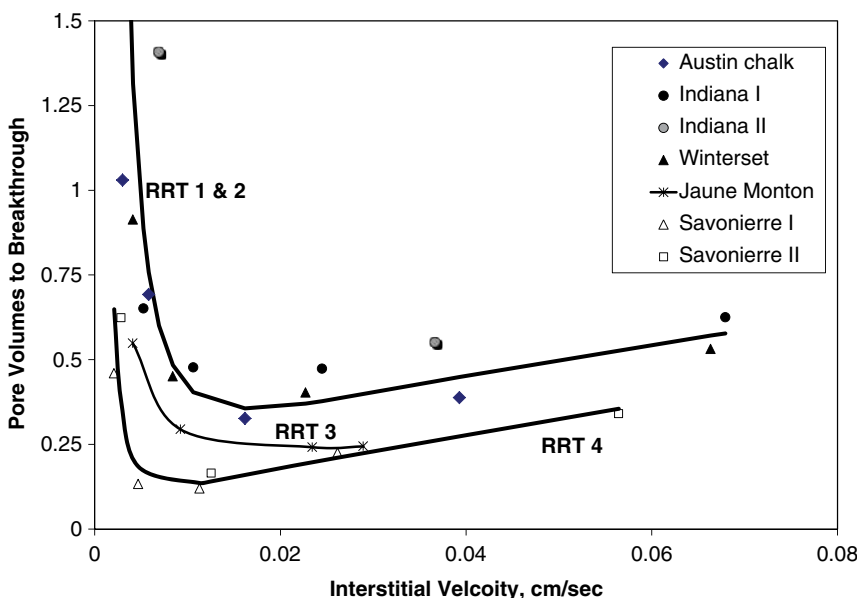


Fig. 3.17—Effect of rock reservoir type (RRT) data from Ziauddin and Bize (2007).

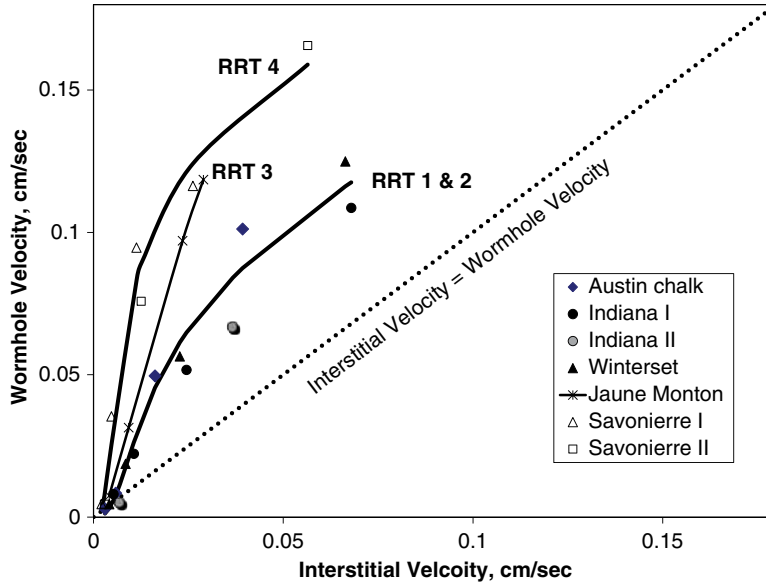


Fig. 3.18—Plot of wormhole velocity vs. interstitial velocity (Ziauddin and Bize 2007).

relationship of permeability and porosity ($k-\phi$) in these rocks. Fig. 3.20 shows that the permeability in Austin chalk increases much less rapidly with porosity than that in Winterset limestone. This suggests that the permeability contrast between the stimulated and unstimulated in the region ahead of the wormhole tip in Austin chalk is much less pronounced than in Winterset limestone. This limits the positive feedback and allows the acid at the tip to explore multiple paths resulting in a more branched dissolution pattern.

Effect of Fluid Saturations. Shukla et al. (2006) investigated the effect of having gas or oil present in the carbonate rock before the injection of acid. They found that gas injection before acid injection significantly reduced the volume of acid required to propagate wormholes through cores. The volume of acid required to wormhole was reduced by almost a factor of 3 in some cases. Furthermore, the wormholes created were narrower and less branched than in the case of water-saturated cores. The presence of oil saturation at residual water saturation had a similar effect on wormhole propagation. However, oil present at residual saturation had little effect on the acidizing process. It is believed that

Effect of Pore Scale Heterogeneity on Wormhole Shape

| Injection Rate (cm ³ /min) | Austin Chalk | Winterset Limestone |
|---------------------------------------|--------------|---------------------|
| 0.5 | | |
| 1 | | |
| 2.5 | | |
| 6.75 | | |

Fig. 3.19—Comparison of wormhole development in chalk and limestone data (Ziauddin and Bize 2007).

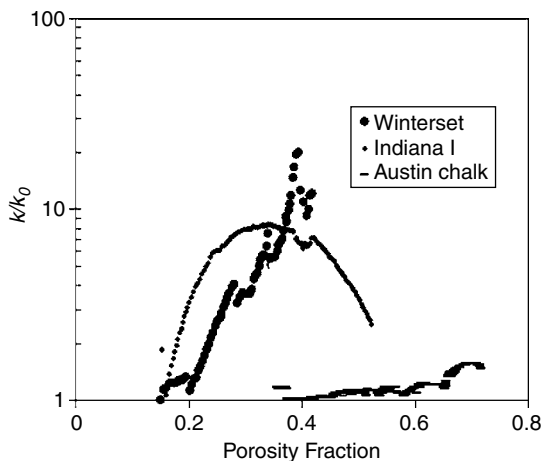


Fig. 3.20—The various processes occurring during the growth phase of the wormhole. Data from Ziauddin and Bize (2007).

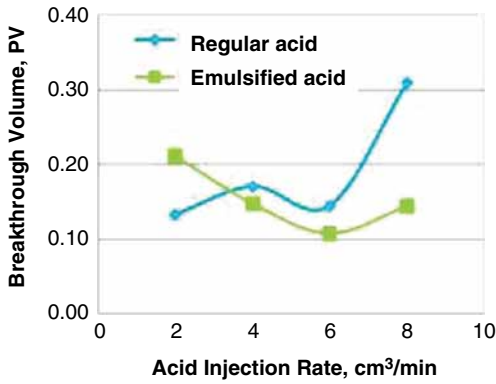
presence of an immiscible gas or oil phase reduces the relative permeability to water-based acids. This reduces the fluid loss from the main wormhole and allows for deeper penetration of wormholes for a given volume of acid.

Al-Mutairi et al. (2012) describe the effect of tar and crudes of varying API gravities on wormhole formation. Experiments included acid (HCl and an HCl inner phase emulsion described in Section 3.4.2) flooding of core plugs that were saturated with different API gravities. These tests were conducted at 200°F. The extreme case included flooding the acid through tar-saturated plugs. The wormholes were characterized by CT scanning. Differential pressures, number and sizes of wormholes, and breakthrough volumes were all measured for each experiment. The tests involved regular HCl and emulsified acids. This study showed that regular and emulsified acids produced comparable wormhole penetration in tar.

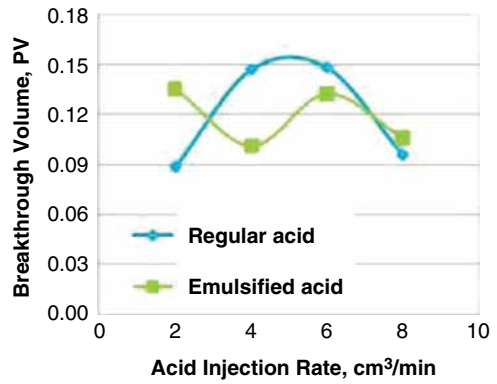
The data indicated that tarred formations were difficult to exhibit dissolution on the face of the cores (face dissolution) even at extremely low-injection rates. In general, it was noticed that penetration and, hence, benefit from emulsified acid is reduced when higher API oil saturated the rock. The wormhole breakthrough volume in a rock saturated with intermediate oil was less than that of a rock saturated with condensate oil. Condensate might have allowed better diffusion of acid droplets to react with the rock. See Fig. 3.21 for the comparison of breakthrough volumes vs. pumping rates.

This paper is the only one identified by the authors of this book to look at the effects of oil/gas (O/G) in the matrix on acid effectiveness that compared straight and emulsified acid. However, Sayed et al. (2012) investigated oil saturations of cores using (exclusively) emulsified acids at 300°F. More details are described in Sections 3.4.2 and 3.8.3. A conclusion of the authors of this book is that unless the rock surfaces have been precleaned with a solvent, these physicochemical conditions will be common and the processes deserve more scrutiny.

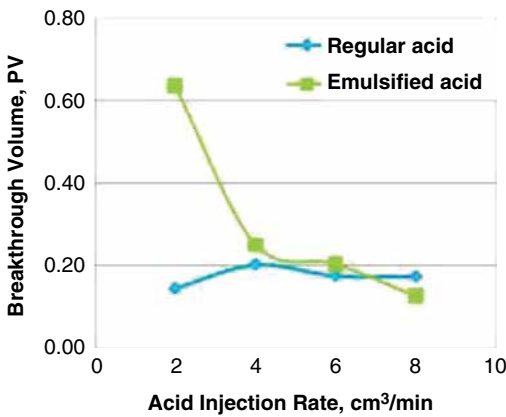
3.3.2 Summary of the Physics of Wormhole Formation. Consider a channel in a porous medium as illustrated in Fig. 3.22. The acid enters the channel at a flow rate of q_0 and a concentration of C_0 . As the acid travels through the wellbore, it leaks off into the surrounding rock (fluid loss) and also reacts with the channel walls. Assume that the flow rate of acid at the tip of the channel is q_{end} and the concentration at the tip is C_{end} . Dissolution of the rock at the tip of the channel advances the channel in the axial direction, while acid leakoff and dissolution near the walls enlarge the channel in the radial direction. The primary variables controlling the dissolution rate at the tip are q_{end} and C_{end} . The dissolution rate at the tip increases with increase in these variables. Key variables controlling the growth in the radial direction are the rate of surface reaction and acid flux to the wall. Acid is transported to the wall by both convective and diffusive mechanisms.



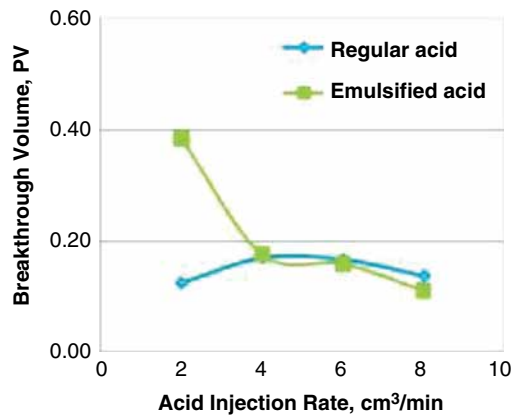
Breakthrough of regular and emulsified acids in clean plugs



Breakthrough of regular and emulsified acids in core plugs saturated with intermediate oil



Breakthrough of regular and emulsified acids in tar-bearing plugs



Breakthrough of regular and emulsified acids in core plugs saturated with condensate oil

Fig. 3.21—Comparison of core breakthrough volumes for clean and hydrocarbon soaked cores at 200°F (Al-Mutairi et al. 2012).

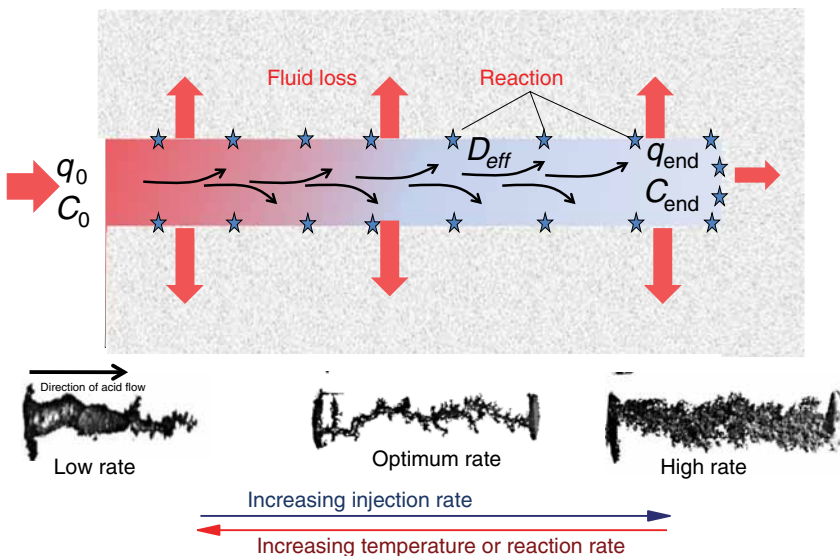


Fig. 3.22—Key processes involved in wormhole formation in carbonates.

A long thin wormhole is formed when the growth in the axial direction is faster than in the radial direction. Optimum wormhole growth occurs when q_{end} and C_{end} are close to q_0 and C_0 , respectively. This occurs for low-acid leakoff from the walls and when there is minimal acid consumption along the channel, such as in a diffusion limited reaction condition. When the reaction rate is much faster than the flow rate, then a conical wormhole pattern is observed (right picture in Fig. 3.22). On the other hand, when the reaction is slow compared to the flow rate, the acid is not fully spent when it leaks off and a branched wormhole pattern is observed (left picture in Fig. 3.22).

Several researches have proposed models for wormhole growth under various limiting conditions.

Fredd and Miller (2000) provide a critical review of these efforts. **Table 3.2** categorizes the models and lists their key limitations.

It is useful to examine further the analytical models under diffusion limited (Daccord et al. 1989) and fluid-loss limited conditions (Schechter 1992). The model for wormhole length L_w in radial flow, under diffusion-limited conditions is given by the equation:

$$L_w = \left[fb \frac{V_A X}{(2(1-\varphi)\pi h)} \left[\frac{Dh}{q} \right]^{1/3} \right]^{1/f} \dots \dots \dots (3.7)$$

where f is the fractal dimension, D is the acid diffusivity, X is the dissolving power, V_A is the volume of acid, h is the formation height, q is the injection rate, and b is a constant. Note that the model predicts that for a given acid volume, higher injection rates will yield *shorter* wormhole lengths. If the fluid loss from the wormhole (leakoff) is the dominant mechanism for the transport of the acid to the wall, the wormhole length is given by

$$L_w = \frac{(qV_A)^{1/2}}{2\pi^2 RC_R} \dots \dots \dots (3.8)$$

where C_R is the leakoff coefficient [a measure of the fluid loss tested (Section 3.8.2) or estimated], and R represents the wormhole radius. Note that the model predicts that for a given acid volume, higher injection rates will yield *longer* wormhole lengths. Therefore, care must be exercised in selecting the appropriate model for the wormholing conditions of interest. Generally, when the fluid loss does not contribute significantly to the transport of acid to the wall, such as in low to medium permeability formations, and for moderate injection rates above the optimum, the diffusion limited model provides a reasonable estimate for wormhole growth. However, it breaks down at extremely high injection rates as the acid reaction is then controlled by surface kinetics and is no longer limited by diffusion.

3.3.3 Numerical Acidizing Models. The analytical models described in Section 3.3.2 are useful for developing a conceptual understanding of the wormholing phenomena. However, they are only valid under limiting conditions. For a wide range of treatment conditions, numerical acidizing models are used instead.

Panga et al. (2002) have described that the development of an averaged/continuum model is presented for simulation of wormhole formation during matrix stimulation of carbonates. They use two concentration variables to account for the local gradients at the pore level caused by the coupling between the flow, species diffusion, and chemical reaction. Their model accounts for pore level physics by coupling the local pore scale phenomena to the macroscopic variables (Darcy velocity, pressure, and reactant cup-mixing concentration) through the structure-property relationships (permeability-porosity, average pore size-porosity, and interfacial area-porosity) and the dependence of the fluid-solid mass transfer coefficient and fluid phase dispersion coefficient on the evolving pore scale variables (average pore size and local Reynolds and Schmidt numbers).

Thomas and Nasr-El-Din (2003) claim that, historically, design engineers have used a rule-of-thumb based on field experience to quantify the design parameters for a candidate well. However, each well is different and this generic approach for treatment design can result in under- or overtreatment. The paper is directed at matrix acidizing of vertical water injection wells completed in a heterogeneous carbonate

| TABLE 3.2—WORMHOLE THEORIES AND MODEL CHARACTERISTICS (ADAPTED FROM FREDD AND MILLER 2000) | | | | | |
|---|--|-------------------------------|--------------------------|-------------------------------|---|
| <u>Model</u> | <u>References</u> | <u>Prediction</u> | | | <u>Limitations</u> |
| | | <u>Axial Worm-hole Growth</u> | <u>Optimal Flow Rate</u> | <u>Dissolution Pattern</u> | |
| Peclet | Daccord et al. (1993), Daccord et al. (1989) | X | | Optimum and ramified | Wormhole (WH) growth model applies only to MTL systems |
| | Frick et al. (1994) | X | | Face dissolution and ramified | WH growth model applies only to MTL systems |
| Transition pore model | Wang et al. (1993), Schechter (1992) | | X | | Theory cannot be applied to skin evolution and requires microscopic pore description |
| | Huang et al. (1997) | | X | | Theory cannot be applied to skin evolution and requires microscopic pore description |
| Damköhler number | Fredd and Fogler (1998a, 1999) | | X | All | Requires WH density and WH dimensions. Cannot be applied for skin |
| | Hoefner and Fogler (1988) | | X | All | Requires WH density and WH dimensions. Only applies for surface reaction. Cannot be applied for skin |
| | Fredd (2000a, 2000b) | | X | All | Requires WH density and WH dimensions |
| Capillary tube | | X | | Optimum WH | Requires microscopic pore description. Is applicable at optimum N_{Da} in MTL systems. Requires WH density and some scaling of acid transition to field scale efficiency |
| | Hung et al. (1989) | | X | Optimum ramified | Is not predictive of skin of WH geometry (l and w). Requires WH density to be scaled to field scale. |
| | Buijse (1997) | X | X | Optimum WH | Requires scaling of acid efficiency for transition to field scale. The initial conditions of the model and assumptions biases the results to indicate propagation length independent of rate, diffusivity (because WHs always exist and grow). Only applies at optimum N_{Da} , for MTL systems |
| Network | Gdanski (1999) | | | | |
| | Hoefner and Fogler (1988) | | X | All | The 2D network model does not readily scale to field or lab experiments |
| Two-scale continuum model | Fredd and Fogler (1998a) | X | X | All | The PNR model requires high computational power to translate to field or lab scale. |
| | Panga et al. (2005) | X | X | All | Requires high computational power to translate to field or lab scale |

reservoir (Arab-D) in Saudi Arabia with focus on field validation of a commercial matrix acidizing design simulator. The validation process allows the production engineer to calibrate the simulator for his specific field and to use it with confidence to improve treatment designs.

In this field study, three matrix-acidized injection wells were used for validation of a carbonate acidizing model. The wells were completed in 150- to 200-ft openhole intervals in a reservoir composed of a variety of limestone-dolomite mixtures. Treatments were performed using HCl along with particulate diverter stages, which was bullheaded down casing. The post-treatment model validation process consisted of simulation of the actual treatment using various values of acidizing efficiency to yield an acceptable match with the final skin. Subsequently, a comparison of the simulated and actual surface treating pressure and the prepost-treatment wellhead pressure during seawater injection was made. A detailed description of the validation process and the supporting well data are presented.

Oliveira et al. (2012) present the development of a methodology to numerically represent the acid treatment in a test plug, as well as to reproduce the different existing dissolution patterns and to obtain the corresponding values of PVBT. The numerical simulation is performed in a commercial computational fluid dynamics package that uses finite volume method. The modeling includes the effect of heterogeneous porosity/permeability and the presence of different types of minerals that impact the PVBT value because they have different reaction rates at usual operation temperatures. Through these considerations, the formation of preferential channels, which are characteristics of the various patterns of wormhole, is captured by the numerical simulation. The goal of this development is the extraction of the characteristic PVBT curves for any pair formation/acid by numerical simulation. It is possible through the use of measured data during drilling, such as average porosity and range of variation, rock mineralogy, etc., and through the knowledge of reaction rates for each pair formation/acid. Using these data, the simulation is able to extract PVBT curves for different numerical test plugs, making it possible to prepare a statistical analysis that has greater significance than just a few experimental tests.

The results show that PVBT curves obtained numerically are in good agreement with the physical behavior expected when compared to experiments. The variation range of the heterogeneous porosity and the presence of different minerals, which have distinct reactivity with acid, significantly change the behavior of the process for the same operating condition.

3.4 Chemical Formulations for Stimulation of Carbonate Reservoirs

To accommodate the wide range of formation types and conditions described in Section 3.3, a large number of different reactive fluids are in use in the oil and gas fields around the Earth. These include mineral acids (HCl- Section 3.4.1), simple organic acids (formic and acetic, Section 3.4.2), and more complex organic acids referred to as chelating agents (Section 3.4.3). The next sections (3.4.1–3.4.3) will describe the applications and mechanism of actions of these chemicals. They are being reviewed for the carbonate matrix treatments in Section 3.4, but they are all also used as part of matrix stimulation of sandstone (Section 3.5), cleaning tubing, and as a spearhead for hydraulic fracturing (Chapter 4), and some are employed for carbonate fracture acidizing (Section 3.8).

3.4.1 HCl. This widely produced chemical can be used at concentrations from about 5–28% for matrix stimulation and acid fracturing (Section 3.8). This solvent is also widely employed as part of the breakdown fluids during most HF treatments. At the time of the publication of this book, this may be the primary use of HCl in North America. This application is a formation cleanup process that is similar to matrix acidizing. Most of the data on carbonate dissolution mechanisms referenced in Section 3.3 were conducted using dilute (1–2 N) HCl solutions, so only a few additional aspects of this solvent are reviewed in this section (3.4.1). HCl solutions also are used to clean the tubing and the completions.

Hill and Schechter (2001) note that carbonate acidizing with HCl is not complicated by a tendency for precipitates to form, as is the case for sandstone acidization. The reaction products CO_2 , CaCl_2 , and MgCl_2 are all quite water soluble (the chlorides are about 50% soluble in water). Therefore, the formation of a precipitate or a separate CO_2 -rich phase is generally not a problem. Even if CaCl_2 precipitates

or a CO₂ phase separates, these phases are readily dissolved when oil (or gas) and water production is resumed. Eqs. 3.1 and 3.2 show the basic reactions of HCl for calcite and dolomite.

The initiation of wormholes (see Section 3.3) occurs when live acid penetrates into the pores present in the native rock. Hill and Schechter (2001) claim that these pores are distributed in size and shape; therefore, the amount of acid flowing through each of the pores differs. The rate at which a given pore is enlarged by the acid depends on the amount of acid entering that pore and the fraction of the acid reacted at the walls of the pore before the acid exits and then enters other pores located downstream.

Hill and Schechter (2001) also note that even at the pore level, the processes that contribute to the creation of an etch pattern are complex, involving convection, diffusion, and chemical reactions within each of the invaded pores. They contend that it has not been proved practical to consider these processes in a single pore and then attempt to consider the collective behavior to derive a macroscopic etch pattern. Schechter and Gidley (1969) used this approach, but to make progress using their results requires knowing in advance the entire distribution of pore sizes, permeability, and porosity of the native rock to be acidized.

While HCl is the primary acidizing chemical in use now, there are limits, including the effective use of HCl based on the achievable pumping rates because of the high reactivity with limestone (note Fig. 3.16), as well as the possible corrosion issues at temperatures of about 300°F (inhibitors are described in Section 3.6.1). On some occasions (especially when cooldown can be achieved) inhibitor schedules have been extended to about 350°F (Jasinski et al. 1988).

Various strengths of HCl (about 5–28%) are in use for both fracture acidizing as well as matrix stimulation for limestone and as part of matrix stimulation of sandstone formations (see Section 3.5). HCl solutions are also used for stimulation of chalk formations [especially in the North Sea area (see Achour et al. 2012 and Van domelen et al. 2011)]. Note that chalk (Fig. 3.13) is a soft form of limestone that frequently has low porosities and can be difficult to stimulate without rapid loss of fluid flow after treatment (Achour et al. 2012; Van Domelen et al. 2011).

To provide efficient penetration without excessive flowback of stimulation water, 28% HCl (especially when retarded as an inner phase emulsion) has been used extensively in the Middle East and North Sea areas for stimulation of the hot carbonate fields (see Section 3.8.3). Corrosion and inhibition (Section 3.6.1) is especially critical when using high-strength acids as well as the job pumping design to assure that live acid will not flow back (Achour et al. 2012; Huizinga and Like 1994).

While the majority of work described in this book has been focused on limestone rocks, O/G bearing formations composed of dolomitic rocks are also very important. Sun (1995) and Al-Awadi et al. (2009) claim that as much as 50–80% of the carbonate formations in North America contain dolomite, and some very important Middle East formation (such as Arab-D in Saudi Arabia) contain substantial amounts of this mineral. A significant reason for the low number of dolomite studies is the heterogenic nature of this mineral (Al-Awadi et al. 2009) and difficulties in obtaining reproducible specimens for lab studies on which the various models are based. However, some information is reviewed.

The reaction rate of HCl with dolomite is much lower than that with calcite [see Table 16-4 of Hill and Schechter (2001)]. At low temperatures, unless the acid flux is reduced, many of the native pores may not be candidates for wormhole initiation. Thus, according to Hill and Schechter (2001), the closely spaced multiple wormholes are likely to form, producing a highly ramified structure that is inefficient in developing an etch pattern consisting of a few dominant wormholes. It is expected (according to the authors) that corresponding to a substantial decrease in the reaction rate, there must be an associated decrease in the acid injection rate to remain at optimum. Hoefner and Fogler (1988) also studied the acid reactions of dolomite cores and found results similar to those described above. A comparison of the relative reactions of limestone and dolomite in 1N (3.6 %) HCl are in [Fig. 3.23](#). The PVBt vs. injection rate plots demonstrates that the dolomite takes much more acid for core breakthrough than the limestone and process become more effective at higher temperatures where the reaction rates are higher.

Thus, at higher temperatures (> approximately 180°F), dolomites may be good candidates for HCl stimulation by wormhole formation or acid fracturing. The mechanistic reasons for the low reactivity of HCl with dolomite have been examined by Lund et al. (1975), Wang et al. (1993), and Lund et al. (1973). These authors have used the rotating disk electrode (RDE) methods described in Fig. 3.7 and

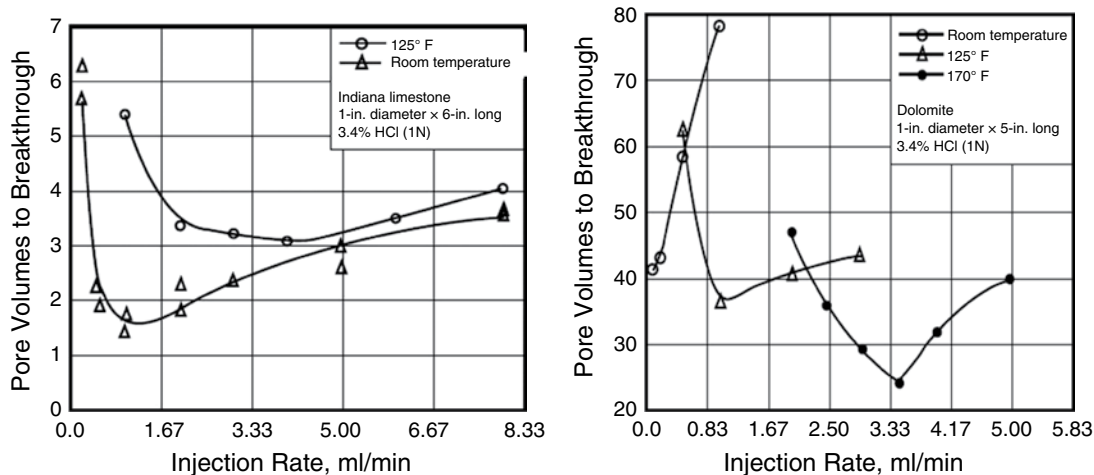


Fig. 3.23—Comparison of limestone and dolomite reactions in HCl. PVBT vs. injection rate (Wang et al. 1993).

Eqs. 3.4 and 3.5 to explore the calcite and dolomite reactions. Comparing the reaction rates of calcite and dolomite they found that calcite became mass transport limited at temperatures above 0°C while dolomite is SRR limited until at least 100°C. Adsorption data as well as the RDE information indicates that the rate determining step is the surface reaction between adsorbed H⁺ and the metal-O bond. The authors (Lund et al. 1975; Lund et al. 1973) attribute the large difference between the two minerals to the bond structures of the Mg-O bonds and the Ca-O bonds in the crystal lattice.

They propose additional details including that the chemical formula of the carbonates does not reflect their 3D structure. Because of the complicated crystal structure, the release of a cation to the solution will also be a complex process. Owing to the high dissolution rate of calcite, the Ca-O bonds in dolomite are probably broken easily and the rate determining step is the rate of breakage of the Mg-O bonds. Because the bicarbonate and chloride compounds of either calcium or magnesium are highly soluble, they claim it is plausible that the breakage of the first of the 6 Mg-O bonds is rate determining.

In addition to HCl alone as the fluid, several other HCl-based formulations have been considered for use. Cheng et al. (2011) has described a well field in China that has deep, hot dolomitic reservoirs (150°C, 110 Mpa and >6000 m). The formation was deeply damaged with the heavy mud, and the matrix acidizing has not been able to effectively eliminate the skin (because of lack of penetration of the zone). In addition, the authors claim that acid fracturing treatment cannot be carried because the surface pressure exceeds the working pressure capability of conventional 15,000 psi fracturing equipment. To effectively decrease the surface treating pressure, they have developed a high-density acid. Its density is adjustable within the range of 1.25–1.55 g/cm³.

To provide the needed densities and reactivates, HCl was mixed with the calcium chloride and some calcium bromide. The density of weighted acid was adjusted between 1.25 and 1.55 g/cm³ by regulating the type and quantity of brine. For example, the maximal density the 15% HCl can be up to 1.28 g/cm³ with the CaCl₂ as the weighting agent in the laboratory conditions. Extensive laboratory tests were conducted to evaluate its corrosion inhibition capacity, stability, and rheological properties. The tests showed that HCl weighted with CaCl₂ had dissolution capacities for the actual formation rock that was similar to unweighted HCl; however, these fluids were very difficult to effectively inhibit at 130°C. Additional tests revealed that the corrosion of HCl weighted with NaBr could be controlled at this temperature to acceptable values. See Section 3.6.1 for CI selections.

The authors of this paper (Cheng et al. 2011) described two case histories where the weighted acid was used to successfully remove mud damage at depths to 6389 m where normal HCl would not penetrate the formation. The authors of this book note that CIs containing bromide salts (Frenier 2003) can be effective for some fluids and the bromide salt may act as an inhibitor aid (Jasinski et al. 1988). However, the acid CI used in this paper was not described.

The reactivity and viscosity of HCl solutions can be changed by additives that cause the formation of gelled acids, emulsified acids (Section 3.4.2) as well as viscoelastic-based fluids [viscoelastic surfactants (VESs)]. These can be used as the main fluid in an effort to reduce the reaction rates or to reduce leakoff in the production of wormholes. The use of these chemicals as diverters is discussed in Section 3.7.2 and for fracture acidizing in Section 3.8.

While not specifically considered a reactive stimulation, substantial amounts of HCl are pumped as one of the first stages in HF treatments (Arthur et al. 2008) to clean up the tubing, perforations, and the near-wellbore area. Note the short discussion of well cleaning fluids in Section 3.1.3 as well as the much more extensive discussions of scale removal in Frenier and Ziauddin (2008). At the time of the publication of this book, this application may consume most of the acid pumped in well stimulations in North America. Details of the frac fluid formulations are in Section 3.8 and Chapter 4.

The following sections (3.4.2–3.4.4) describe the use of various formulations with lower reaction rates compared with HCl. Also, at temperatures above about 280°F, corrosion inhibition of oilfield steels in HCl requires up to 4% of an inhibitor/aid mixture (see Section 3.6.1), so alternative chemicals may be useful for corrosion control.

3.4.2 Emulsified/Gelled Acids for Matrix Stimulation. The organic acids and chelating agents described in Sections 3.4.3 and 3.4.4 may be needed (especially at high temperatures) for reducing the reaction rate of HCl with carbonates to allow efficient wormhole formation. The organic materials are also much easier to inhibit using lower volumes of CIs. These aspects of stimulation fluids will be described in Section 3.6.1.

Emulsified acids (Navarrete et al. 1998a; Al-Mutairi et al. 2008) also can be used to reduce the overall diffusion rate of the protons in HCl by sequestering the acid in an oil outer phase [water-in-oil (W/O)] emulsion, and, thus, the effective reaction rate VESs (Section 3.7.2) also can be used for this application. More discussions of gelled and emulsified acids are in Section 3.8.3. Uses of emulsified acid for wormhole control are noted in this current section.

These emulsions may contain as much as 70–80 vol% aqueous HCl and about 30% oil phase and have to be made using a specific technique. For example, Salathiel et al. (1980) claim that a specialized oil soluble surfactant (2-hydroxy isopropyl dodecylbenzene sulfonate) is blended into the oil phase, and then the inner (HCl) phase. Then, emulsification is accomplished by slowly pouring the aqueous component into the surfactant-hydrocarbon blend while intensive blending (shear) is applied.

Siddiqui et al. (2006) examined alternate ways to evaluate the performance of emulsified acids by using a nondestructive visual-based technique. Using what is claimed to be advanced image processing software and techniques, the authors note that it was possible to examine the dissolution patterns created by emulsified acids at different operating conditions. CT was successful in monitoring wormhole initiation and growth inside carbonate core plugs during the injection of emulsified acid. The authors of the paper claim that the emulsified acid systems used were successful in creating a barrier for the acid allowing its slow release away from the injection face. The reaction appeared to take place simultaneously at different places inside the core resulting in channels, which later joined together to form a continuous wormhole between the inlet and outlet ends of the core plug. The presence of natural channels (vugs, stylolites, etc.) and higher concentrations of calcite may help faster wormhole initiation. Injection rate appeared to be the most important factor affecting emulsified acid performance in terms of wormhole initiation and growth (faster injection caused faster wormhole initiation and, consequently, its growth).

All of these cores were acidized with 20 wt% HCl emulsified acid. The acid contained 0.2 vol% CI, while the diesel phase contained 1 vol% emulsifier. The acid to diesel volume ratio was 70:30. Only the acid injection rate and the rock samples were varied in these tests. The brine was doped with 10 wt% NaI to aid the X-ray analysis and the core plug inside a special core holder (X-ray transparent).

Based on the coreflood tests performed in brine-saturated plugs, the propagation of emulsified acid appeared to take place without any immiscible front movement. The wormholes appeared to develop independently as small individual channels that later joined with the others to form a continuous wormhole from one end of the plug to the other.

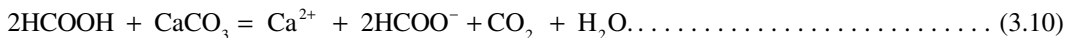
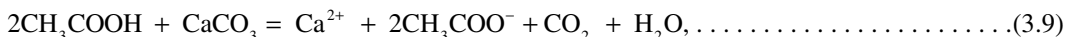
The conclusions of the authors of the report are that the initiating of the wormhole with the emulsified acid is an in-situ process. Once the already injected acid reacts with sufficient amount of rock, an elongated channel is created (can be anywhere and not necessarily initiating at the core inlet), the subsequent acid displacement then connects the different channels to form a continuous wormhole.

Sayed et al. (2012) present a study of the effect of oil saturation in the formation on the flow of emulsified acids in carbonate cores and assess the performance of emulsified acid. 15% HCl emulsified using 30 vol% diesel oil was used at 300°F in stimulating carbonate formation cores. The effect of the presence of crude oil on the volume of acid to breakthrough was studied. Also, the size, number, and distribution of the wormholes were determined using CT images. Cores that were fully saturated with water, fully saturated with crude oil, and cores saturated with crude oil at irreducible water saturation were used. The authors of this report noted that there was no optimum injection rate for emulsified acids when they were injected into Indiana limestone. For cores fully saturated with crude oil, the volume of emulsified acid to achieve breakthrough was two to three times more than those required to achieve breakthrough in cores fully saturated with water. The increase in emulsified acid volume refers to the increase in the volume of the continuous phase resulted from mixing of the crude oil and diesel. As a result, more acid was consumed to create wormhole and achieve the breakthrough. However, the emulsified acid system was effective in stimulating limestone cores, even these cores were saturated with water, oil, or oil at irreducible water saturation. Note that this result was contrasted with the tests by Al-Mutairi et al. (2012) who did find an optimal pumping rate for emulsified acid at 200°F.

As noted earlier in this section, other aspects of using emulsified acids (and theories of action) are described in Sections 3.8.3.

3.4.3 Organic Acids Including Acetic and Formic Acid (FA). Organic acids can be used instead of HCl when high bottomhole temperatures prevent efficient protection against corrosion (above about 325°F) or the HCl cannot be pumped at high enough rates to provide efficient wormhole formation. The two main types of organic acids used in the O/G fields are acetic acid and FA (Robert and Crowe 2001). Also see the extensive reference list in Li et al. (2008b). Because acetic acid is a weaker acid (Table 3.3) than FA, it may be easier to inhibit (Section 3.6.1) than FA and is used more often than FA. Acetic acid also may be considered to be a natural product.

As weak acids, they do not totally dissociate in water, the equilibrium reaction is expressed by the pK_a value (Table 3.3). This table also shows the stability (equilibrium-log*K*) constants for complexation of the acids with metals important in O/G production. Acetic and FAs react with CaCO₃ to form calcium acetate and formate, respectively:



Calcium acetate is highly soluble in spent acid (374 g/L at 75°F). High concentrations of acid, up to 20% to 25%, can be used without any precipitation problem, although concentrations above 10% are generally not used because the reactions do not go to completion (see Hill and Schechter 2001). In static conditions, the degree of completion of the reaction depends on the concentration of CO₂ in solution. For instance, at high-pressure conditions (typically above 1000 psi), only one-half of 10% acetic acid reacts with limestone at 150°F. In similar conditions, 80% of 10% FA reacts. Although some live acid remains once the reaction reaches equilibrium, a low pH is not maintained because of buffering by the reaction products (Robert and Crowe 2001). Calcium formate and magnesium formate are less soluble (162 and 140 g/L at 75°F, respectively) than the acetates. Thus, FA strength usually is limited to 9% to 10% to avoid calcium formate reprecipitation.

Mechanistic studies of acetic and FAs have been undertaken by several investigators. Using RD methods, Fredd and Fogler (1998a) have shown that the dissolution in acids is influenced by the rate of

TABLE 3.3—CHARACTERISTICS OF REACTIVE CHEMICALS [DATA FROM MARTELL AND SMITH (1978) AND JONES AND WILLIAMS (2001)]

| Compound | Sol. Water, pH 2 or less (wt%) | MW | | pKa Values | | | | | LogK Equilibrium Constant | | | |
|---|--------------------------------|------|---------|-----------------|-----------------|-----------------|-----------------|-----------------|---------------------------|---------|---------|----------|
| | | Acid | Na salt | pK ₁ | pK ₂ | pK ₃ | pK ₄ | pK ₅ | Fe (III) | Ca (II) | Ba (II) | Al (III) |
| HCl | v. | 36.5 | | -7 | | | | | | | | |
| HF | v. | 20 | | 3.2 | | | | | | | | |
| Formic acid | v. | 46 | | 3.75 | | | | | 3.1 | 1.43 | 1.38 | 1.36 |
| Acetic acid | v. | 60 | | 4.8 | | | | | 3.4 | 1.18 | 1.07 | 1.5 |
| Citric acid | 50 | 192 | 258 | 5.7 | 4.4 | 2.9 | | | 11.5 | 3.5 | 2.6 | 8.0 |
| NTA—nitrilotriacetic acid | 0.15 | 191 | 257 | 9.7 | 2.5 | 1.8 | | | 15.9 | 6.4 | 4.8 | 11.4 |
| HEDTA—hydroxyethyl ethylenediamine-triacetic acid | 10 | 278 | 344 | 9.8 | 5.4 | 2.6 | | | 19.8 | 8.4 | 6.2 | 14.4 |
| EDTA—ethylenediaminetetraacetic acid | 0.1 | 292 | 380 | 10.2 | 6.1 | 2.7 | 2.0 | | 25.0 | 10.7 | 7.8 | 16.5 |
| DTPA—diethylenetriaminepenta-acetic acid | 0.5 | 393 | 503 | 10.5 | 8.5 | 4.3 | 2.6 | 1.8 | 28.0 | 10.9 | 8.9 | 18.7 |
| HEIDA—hydroxyethyliminodiacetic acid | 15??? | 177 | 221 | 8.7 | 2.2 | | | | 11.6 | 4.8 | 2.8 | 7.8 |
| GLDA-L-glutamic acid, N,N-diacetic acid | 40 | 263 | 351 | 9.36 | 5.0 | 3.5 | 2.6 | | 11.7 (est.) | 5.9 | | |
| EDDS—ethylenediamine disuccinic Acid | | 292 | | 9.8 | 6.8 | 3.9 | 2.4 | | 22 | 4.6 | | |
| IDS—iminodisuccinic acid | | 249 | | 10.1 | 4.8 | 3.8 | 3 | | 15.2 | 4.3 | | |
| MGDA—methylglycine diacetic acid | Sol? | 157 | | 10 | 2.5 | 1.6 | | | 16.5 | 7 | | |
| HEDP—hydroxyethylidene diphosphonic acid | 17 | 206 | | | | | | | | | | |
| Vinylidene diphosphonic acid | | | | | | | | | | | | |
| DETPA—diethylenetriamine pentamethylene phosphonic acid | Miscible | 573 | | | | | | | | | | |

transport of reactants to the surface, the kinetics of the reversible surface reaction, and the rate of transport of products away from the surface (see Fig. 3.7). Below about pH 2.9, the dissolution is influenced by the transport of both reactants and products, while above about pH 3.7, the dissolution is influenced predominantly by the kinetics of the surface reaction. A general model was developed to account for the combined effects of transport and reaction on the rate of dissolution. The effect of acetate ions on the rate of dissolution was investigated in alkaline solutions (pH 8.2 to 14) to eliminate the effects of hydrogen ion attack. The presence of acetate ions was found to have no significant effect on the rate of dissolution when compared to results in potassium chloride and sodium chloride solutions.

There have been several additional studies that describe the reaction rate of solvents (such as acetic acid and FA) for calcite in relation to stimulation of calcite formations [see Hill and Schechter (2001), Lund et al. (1975), and Fredd and Fogler (1998a)]. The SRR coefficients for 0.5 M acid at 25°C are reported by these authors to be

- 2×10^{-1} cm/s for HCl
- 4.5×10^{-3} cm/s for acetic acid ($\text{CH}_3\text{-CO}_2\text{H}$)
- 5.0×10^{-3} cm/s for FA (HCO_2H)

Li et al. (2008b) claim that different mathematical models were developed to describe reaction of organic acids (both simple organic acids and polycarboxylic acids) with calcite. The authors contend that association reactions of acetate ion with calcium ion are important for reactions of acetic acid with calcite and also contend that this cannot be ignored even at low acetic acid concentrations. In addition they conclude that strong inorganic acid HCl can increase the conversion of organic acids. These authors also dispute the conclusions of Fredd and Fogler (1998a) that the formation of a calcium complex with 2 moles of acetate $[\text{Ca}(\text{AC})_2]$ is *not* important.

They do agree that proton attack controls the reaction rate of complexing agent acids with calcite at low pH values. Ligand attack controls the rate of dissolution at high pH, while water attack can influence the calcite dissolution at extremely low concentration. The combination of these two dissolution mechanisms affects the reaction rate at moderate pH values. This paper (Li et al. 2008b) has many references and provides more details of the organic acid dissolution mechanism than can be described here.

Ultimately, these acids must be used to promote wormhole formation in limestone or dolomite formations. Huang et al. (2000) presented an experimental study of the wormholing process in carbonate acidizing with acetic acid. Carbonate rock samples were acidized, and the effectiveness of the process and the optimal injection rate were studied by measuring the acid volume needed to propagate wormholes through the cores and by making castings of the wormhole structures after acidizing. A group of wormhole castings was produced by the authors. They demonstrated that as the injection rate increases, the wormhole radii at lower injection rates are larger than that of the third one, which is at the optimal injection rate. As injection rate continues to increase, the wormhole radii are getting larger and small branches more meandrous. Experiments exhibit a clear minimum acid volume, illustrating the optimal acid injection rate for wormhole propagation. The experimental results from the study confirmed

1. The optimal injection flux of acetic acid is lower than that of HCl for the same reservoir conditions.
2. Larger wormholes are created by acetic acid at the optimal flux than that by HCl at the optimal rate.
3. Wormholes of 0.1 mm radius are sufficient to give a skin factor of zero if they extend through the damaged zone.
4. While acetic acid may have benefit over HCl at elevated temperature, at low temperature HCl is the preferred acid.

Huang et al. (2000) also showed from the castings that the radius of wormholes created by acetic acid at the optimal rate is larger than that created by HCl at the optimal rate. They then demonstrated how these results can be used to determine the optimal acid system and injection schedule for field application. The conclusion that HCl is more effective at low temperatures, but acetic acid may be preferred at high temperatures.

Additional tests using chelating agents as well as organic acids (acetic and FAs) are described in the next section (3.4.4), including several additional wormhole formation studies.

Chang et al. (2008) describe the use of mixtures of HCl and organic acids (also see Section 3.4.1). The authors contend that organic acids become viable material for matrix acidizing to alleviate the two problems of too high reaction rates at high temperatures and corrosivity. Though organic acids provide the benefit of retardation and low corrosivity, their low dissolving capacity may still limit the wormhole penetration leading to insufficient stimulation of the formation. Therefore, the authors of this paper contend that opportunity exists to mix HCl with an organic acid to achieve productivity enhancement by optimizing the wormhole penetration and profile. They claim that their experiments indicate

that mixtures of HCl with either acetic acid or FA will dissolve more calcite than the individual acids alone, will provide deeper penetration of the formation, and will be less corrosive.

Qiu et al. (2009) filed a patent application that relates to a composition including a mixture of HCl and a carboxylic acid or a precursor of a carboxylic acid for use in subterranean reservoirs, particularly reservoirs with a large proportion of carbonate rocks. They claim that the carboxylic acid is prevented from dissociating in HCl because of the high hydrogen ion concentration, which the HCl provides. It is claimed that the HCl, in turn, reacts fast to dissolve the rock near the wellbore, thus creating wide channels that help to reduce the pressure gradient during production. The theory proposed by these authors is that as the HCl is spent, its hydrogen ions are depleted and the carboxylic acid begins to dissociate. This is claimed to result in further acidizing from the tip of the acid front, thus increasing the penetration of the composition.

They also claim that the precursor of the carboxylic acid can be used in place of the carboxylic acid itself to further delay the reaction. Using a precursor, an additional hydrolysis reaction, which is triggered by the higher temperature in the formation, is required to convert the precursor into the carboxylic acid. All three components, HCl, carboxylic acid, and the precursor of the carboxylic acid, can be mixed into a single composition that reacts in three stages with the formation rock. The precursors claimed include lactic acid, malic acid, and polymers that are hydrolyzed to form these acids in acidic water.

Metcalf et al. (2006) describe a method for removing or dissolving calcareous materials in a subterranean formation or in a wellbore consisting of two basic steps. In the first step, an aqueous acid solution is injected into the formation or wellbore. The aqueous acid solution contains between from approximately 15 to approximately 99 wt% of an organic acid selected from FA, acetic acid, or a mixture of FA and acetic acid. Water or brine is then injected into the formation or wellbore. The amount of water or brine injected into the formation or wellbore is an amount sufficient to reduce the concentration of organic acid in the formation or wellbore to no greater than 10 wt%.

3.4.4 Chelating Agents. An alternate to simple organics to overcome some of the problems with the use of HCl and HCl/HF as the primary formation stimulation agents are carboxylic acid and phosphonic-acid-based chelating agents. This section summarizes a large amount of research to test the advantages of these more complex chemicals (compared with simpler organic acids) for a segment of the acidizing stimulation market. The following two subsections also present studies that compare HCl and organic acids with different chelating agent formulations and are useful for clarifying mechanisms based on studies using the same sets of methods and materials.

The structures and chemical characteristics and chemical structures of most of the materials used in reactive chemical fluid are described in Table 3.3, **Fig. 3.24** (carboxylate chelating agents), and **Fig. 3.25** (phosphonate chelating agents). Eqs. 3.1 and 3.2 show the reactions for HCl with calcite and dolomite, respectively. All of the acids (except HCl) form 1:1 complexes with Ca^{2+} in aqueous solution; however, 2 moles of protons (H^+) are required to dissolve each mole of calcite. The data in Table 3.3 is particularly important because it shows the solubilities of acidic forms of the materials, which may limit the range of use of the chemical.

The balanced chemical equations for acidic formulations of chelating agents with calcite and dolomite can be written that are analogous to Eqs. 3.1, 3.2, 3.9, and 3.10. However, the alkaline solutions of ethylenediaminetetraacetic acid (EDTA), hydroxyethyl ethylenediaminetriacetic acid (HEDTA), nitrilotriacetic acid (NTA) and diethylenetriaminepentaacetic acid (DTPA), hydroxyethyliminodiacetic acid (HEIDA), and glutamic acid, N,N diacetic acid (GLDA) also will dissolve calcite at high temperatures (>approximately 90°C), and the reaction for EDTA (in an aqueous solution) is an example:



Here, the overall stoichiometries for the alkaline chelating agents are 1:1, while the simple organic acids, acidic chelating agents, and HCl are 2:1 acid/calcite. Note that the alkaline dissolution of calcite (with Na_4EDTA) has a long history of importance in the industrial cleaning industry (Frenier 2001b), and the Bersworth (1960) invention was instrumental to the use of chelating agents in industry.

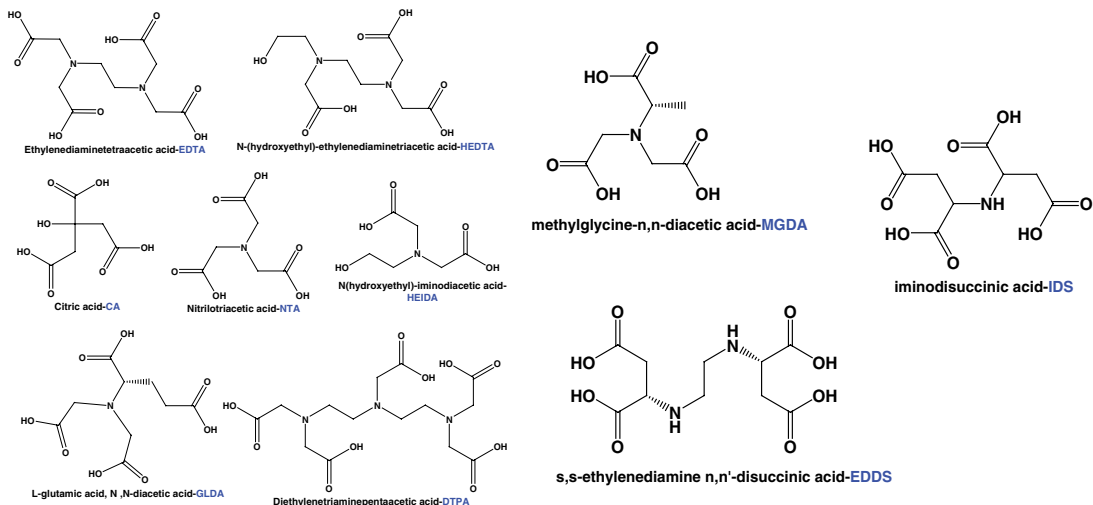


Fig. 3.24—Carboxylic acid chelating agents.

For the acidic formulations of any of the chelating agents, the reaction equations can be more complex. Thus, for dissolution comparison purposes, the capacity of any solvent for calcite or dolomite (or any other mineral) is the critical value. It depends on the ratio of the mud weight (MW) solvent molecules/MW calcite (dolomite), as well as the final solubility of the salts in the solvent at equilibrium. Table 3.4 shows experimentally (Frenier 2001a) determined solubility capacities of calcite in

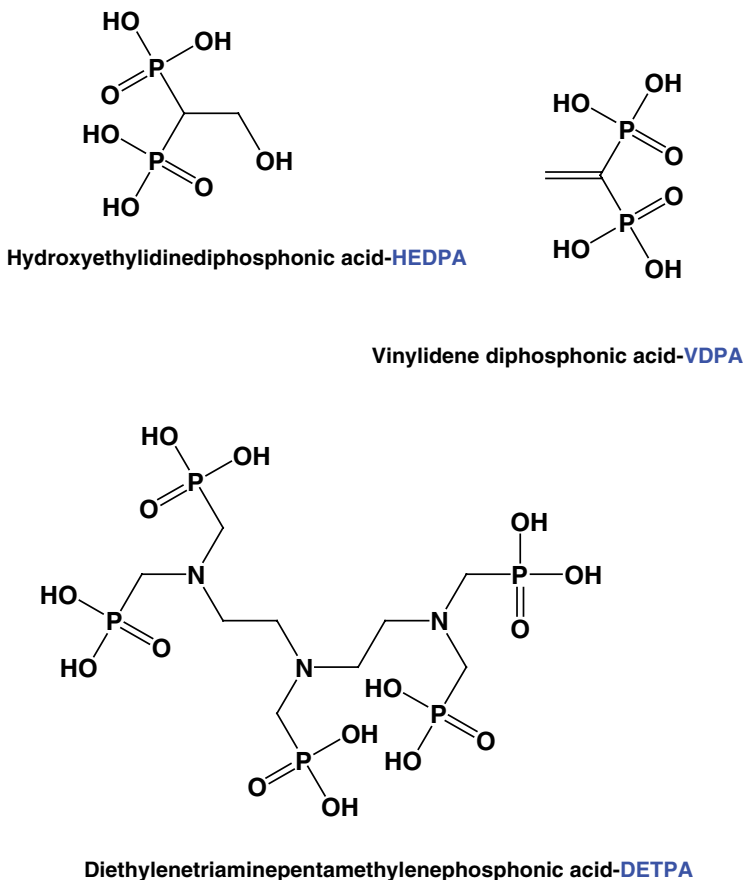


Fig. 3.25—Phosphonate acid chelating agents.

| Dissolver | CaCO ₃ dissolved (lb/1000 gal) |
|-------------------------------|---|
| 20% Trisodium HEDTA (pH 2.5) | 738@ |
| 20% Tetrasodium EDTA (pH 12) | 520@ |
| 21% Diammonium EDTA (pH 4.5) | 735@ |
| 20% Disodium HEIDA (pH 2.5) | 250@ |
| 20% Tetrasodium GLDA (pH 1.5) | 1600# |
| 15% HCl | 1833@ |
| 10% Formic acid | 845@ |
| 5% Citric acid | 5@ |
| 20% Trisodium NTA (pH 4) | 5@ |
| 10% Acetic acid | 422@ |
| @ Frenier (2001a) | # LePage et al. (2009) |

a number of different solvents that were measured at atmospheric pressure. The tests all were run to metal saturation with excess reactants in static tests in a water bath at 65°C.

Note that HCl has the highest capacity because of the very high solubility of CaCl₂ and the low MW ratios even though it takes 2 moles of HCl for each mole of calcite. The higher capacities of acidic HEDTA and GLDA are because of some acid dissolution as well as chelate dissolution. Thus, the acid solubilities of the commercial fluids may be important for practical use of the material. The poor performance of citric acid and Na₃NTA reflect low solubility of the reaction products as well as possible kinetic issues. Thus, mixed mineral acid/organic acid formulations may benefit from both acid and complexer reactions (see the formulations in Section 3.4.2).

All of the organic acids have low-toxicity values [see Frenier (1996) for a discussion] and citric and acetic acids could be considered to be food based. However, some of these chemicals are more biodegradable [there are many different tests, so this means different things in different articles; see the discussions in CLEAR (2011) and Kelland (2009)] in the environment than other ones, and this is becoming an important consideration in some sectors of the world market. Also see the more detailed discussions of toxicity and environmental issues in Frenier (1996), Kelland (2009), and in Section 6.2. The next two subsections provide details of the use and testing of this important new class of stimulation agents.

Traditional Chelating Agents. Chelating agents are materials that can be used to control undesirable reactions of metal ions. In oilfield chemical treatments, chelating agents (Frenier et al. 2000) are frequently added to stimulation acids to prevent precipitation of solids as the acid spends on the formation being treated (Section 3.6.2). Also see references by Frenier (2001a) and Frenier et al. (2001) for more detailed reviews. The materials, which were evaluated and described in this section, include hydroxy-aminopolycarboxylic acids such as HEDTA and HEIDA as well as other types of organic acids and chelating agents such as EDTA and NTA. Formulations containing GLDA (LePage et al. 2009; DeWolf et al. 2010) have also been proposed and will be described later in the next subsection. HEIDA and GLDA are also much more biodegradable than EDTA, HEDTA, or DTPA (LePage et al. 2009). This may make disposal of the used chelating agent fluids easier in some environments.

Disodium EDTA (Na₂H₂EDTA) has been used as a scale-removal agent in the Prudhoe Bay field of Alaska (Shaughnessy and Kline 1983). In this application, calcium carbonate (CaCO₃) scale had precipitated in the perforation tunnels and in the near-wellbore region of a sandstone formation. Huang et al. (2000) also have described the uses of organic acid formulations for removal of scale and fines at high temperatures.

Fredd and Fogler (1998b) and Fredd and Fogler (1998a) have proposed additional uses for EDTA-type chelating agents. This application uses the chelating agents as the primary dissolution agent in matrix acidizing of carbonate formations. Because HCl reacts so rapidly on most carbonate surfaces, diverting agents, ball sealers, and foams are used to direct some of the acid flow away from large

channels formed by the acid. Because of this high rate, the wormholes that may form initially take all the subsequent acid volume (see Section 3.7). These authors (Fredd Fogler 1998b) concluded that by adjusting the flow rate and pH of the fluid, it may be possible to tailor the slower-reacting chelate solutions to the well conditions and achieve maximum wormhole formation with a minimum amount of solvent (see detailed discussions in Section 3.3.1).

There are a large range of different types of formulations that can be produced by changing the pH with addition of acids or bases. The most common commercial base fluids available are tetrasodium EDTA and trisodium HEDTA that have pH values of approximately 12. Na_3NTA also is a commercial chemical and has been employed as an iron control additive (Section 3.6.3), but not as a matrix stimulation fluid. Diammonium EDTA (DAE) and disodium EDTA solutions with a base pH of about 4.5 also are available on the commercial market and have been employed in some commercial solvent formulations (Shaughnessy and Kline 1983; Frenier et al. 2012).

Table 3.3 shows the pK_a values for the carboxylate groups in these molecules. These values also define the buffer points because the buffer power is at a maximum when $\text{pH} = pK_a$. Many different formulations (usually proprietary) can be produced by addition of mineral acids or organic acids to sodium EDTA, sodium HEDTA, or sodium GLDA (next subsection) to make acidic fluids that are quite aggressive for dissolving calcite. Based on the pK_a values, HEDTA would buffer strongly at pH 2.6 and 5.4 (measured at 25°C), while EDTA could buffer at pH 2.0, 2.7, and 6.1. However, only HEDTA fluids can actually be produced as formulation with pH values < 5.0 due to the much higher solubility of HEDTA compared with EDTA.

Frenier et al. (2001) have used RD tests (see Section 3.2) with Carrara marble to study the kinetics of reaction of alkaline chelating fluids containing EDTA and HEDTA (0.25 M, pH 12). Fig. 3.26 shows a plot of the calculated reaction rates vs. the square root of the angular velocity ($\omega^{1/2}$). The plateau portions of the plots indicate that there is some degree of surface reaction controlled kinetics (as compared to only mass transport) at this temperature (20°C) and that the reaction rates are the same for the two chelating agents. Similar studies with acetic acid were reviewed in Section 3.4.2.

The kinetic data by Frenier et al. (2001) for sodium EDTA is similar to the data reported by Fredd and Fogler (1998a) (triangles in Fig. 3.26). This was done to validate the methods. To elucidate the kinetics and mechanisms, a number of additional tests were run on marble.

The reaction rates for the low pH solutions are also shown in Fig. 3.27. At pH 4, sodium HEDTA (0.25 M) had a dissolution rate of 1.2×10^{-8} mol Ca/cm²/s, compared with 3×10^{-8} mol Ca/cm²/s reported (Fredd and Fogler 1998a, 1998b) for sodium EDTA at pH 4. HEDTA acid has a pH value of 2.4–2.5, depending on concentration. The reaction rate at a concentration of 0.001 M HEDTA acid was measured at 1.8×10^{-8} mol Ca/cm²/s. This value is about four times higher than the same concentration of the pH 12 sodium salt. The calculated diffusion coefficient (6.5×10^{-5} cm²/s) is higher than the values reported for acetic (1×10^{-5} cm²/s) or FA (3×10^{-5} cm²/s). The diffusion coefficient for 0.001

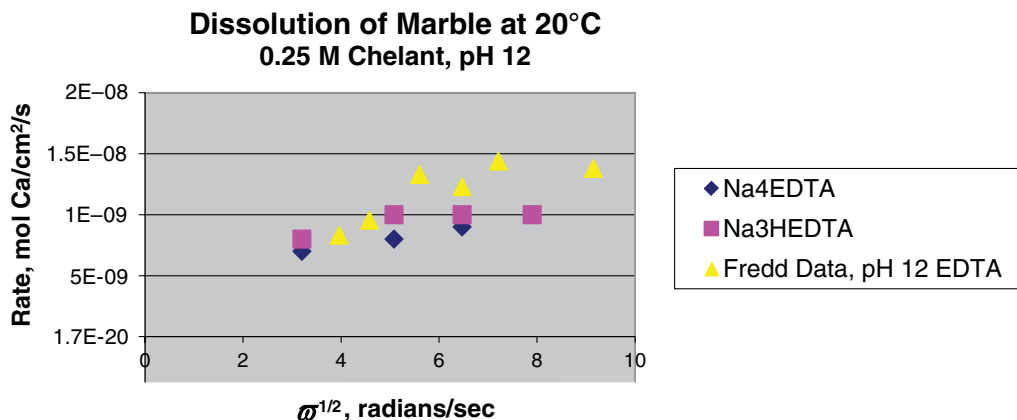


Fig. 3.26—Reaction rates from rotating disk tests with marble disks in 0.25 M sodium EDTA or sodium HEDTA, pH 12, 20°C (Frenier et al. 2001).

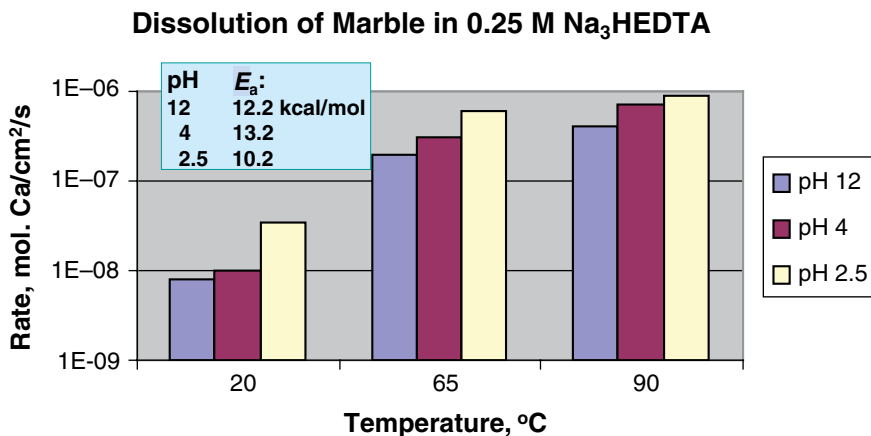


Fig. 3.27—Temperature dependency of marble dissolution rates in 0.25 M Na₃HEDTA (Frenier et al. 2001).

M sodium HEDTA, pH 4 was estimated to be 3.4×10^{-5} cm/s. This value is consistent for diffusion coefficients for hydrogen ions and indicates that a percentage of the reaction is caused by acid attack. Additional reaction rate parameters (for 0.65 M solutions) that can be used to predict optimal flow rates are described later in this book.

Fig. 3.27 shows the reaction rates for marble (rotated at 600 rev/min) as a function of temperature in 0.25 M HEDTA at three pH values. The calculated activation energy (E_a) values were 10.2–13.2 kcal/mol. The lowest value (for the pH 2.5 solvent) is in the transition range between surface reaction control and diffusion redaction control, while the other values are in the surface reaction control range. The activation energy values are consistent with data reported for sodium EDTA, in which there is comparable data (Fredd and Fogler 1998a).

Several groups have developed models of wormhole formation (see the detailed discussions in Sections 3.3.1, 3.3.2, and in Table 3.2). Hung et al. (1989) note that when acid is injected into a carbonate, the acid flows preferentially into the highest-permeability regions, that is, the largest pores, vugs, or natural fractures. The rapid dissolution of the matrix material enlarges these initial flow paths so that the acid has soon formed large, highly conductive flow channels, called wormholes. These discussions explain that wormholes are likely to occur in both matrix acidizing and fracture acidizing in carbonate formations. This section (3.4.4) applies these ideas to stimulation using organic acids and chelating agents.

Nierode and Williams (1971) developed a model to predict the length of a wormhole, but the number of wormholes and their sizes were not addressed. Hoefner and Fogler (1989) used a network model to simulate the growth of wormholes in matrix acidizing. This model illustrates the relationship between reaction rate and diffusion rate in the formation of wormholes but does not account for fluid loss through the walls of the wormholes, which can be the controlling factor limiting their length.

To describe the physical process of this wormholing phenomenon, a mathematical model that accounts for the chemical kinetics and fluid hydrodynamics in a wormhole and the initial distribution of large pores was developed. Results from the model confirm that wormholes result from the heterogeneity of carbonate rock and reaction kinetics between HCl and carbonates. Wormhole characteristics are controlled by injection, diffusion, and fluid-loss rates. While these models have been used for HCl (Hoefner and Fogler 1989) as well as for acetic acid (Fredd and Fogler 1998a), they had not been applied to chelating agent formulations.

Fredd and Fogler (1998b) used these theories to show that there exists an optimum injection rate for different types of reactant (see Figs. 3.15, 3.16, and 3.28). These were based on coreflood tests that show the dependence of the PVBT vs. injection rate for a variety of fluid in limestone systems. The figure includes data from linear coreflood experiments with 0.25 M EDTA (pH = 4 and 13), 0.5 M acetic acid and 0.5 M HCl. All the fluids exhibit an optimum injection rate at which the number of PVBT is minimized and dominant wormhole channels are formed. The number of PVBT

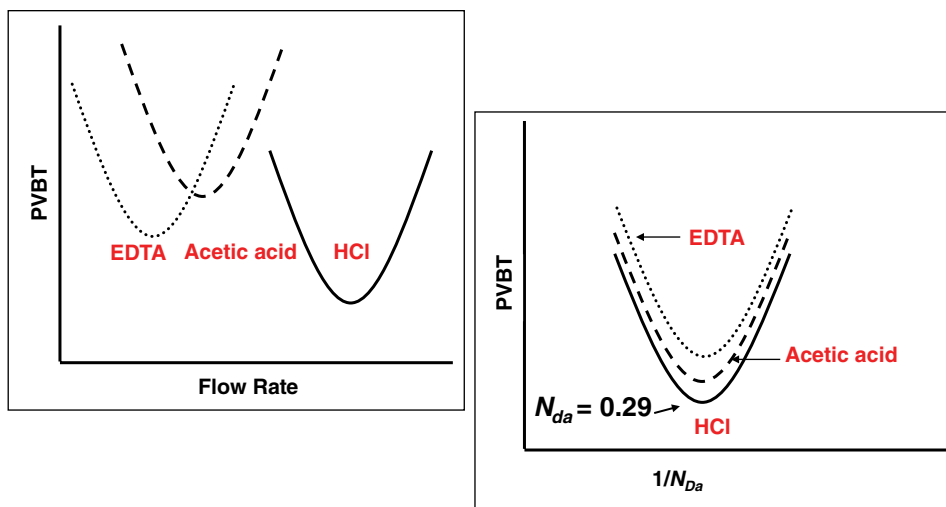


Fig. 3.28—Core breakthrough/pump rate relationships (Fredd and Fogler 1998b). Conical wormhole in limestone after 15% HCl at 5 mL/min., 65°C (150°F) (Frenier et al. 2001).

increases to the left and right of the minimum owing to the formation of conical dissolution channels and ramified wormholes, respectively. Note that the dimensionless relationship called Damköhler number (N_{Da}) that is defined as the ratio of the rate of reaction (either forward or reverse) to fluid velocity has been used in analyses of efficiencies of acid treatments. Fredd and Fogler (1998b, 1999) propose that the optimal Damköhler number is approximately 0.29 (Fig. 3.28) for a large number of solvents.

Based on these types of data, Ming and El-Rabaa (2001) claim a method for optimizing the rate at which a given acid should be injected into a carbonate-containing rock formation during an acid injection process, comprising the following steps:

- (A) Calculating the Damköhler numbers (N_{Da}) (Fredd and Fogler 1998b) for regimes in which kinematic force, diffusion rate, and reaction rate control.
- (B) Using the Damköhler numbers calculated in Step A to calculate the rate of growth of the wormholes as function of flux, said function taking into account compact dissolution, wormholing, and uniform dissolution.
- (C) Using the function calculated in Step B to calculate an optimum flux for the formation.

Also using these ideas, Frenier et al. (2001) and Frenier et al. (2004) have employed coreflood tests and X-ray (CT scans) to examine chemistry and flow rate on the formation of wormholes in limestone cores that were performed with various chelating agents and acid systems. All of the chelant-based fluids stimulated the cores at 65°C (150°F); some produced as much as 400-fold increases in permeability. For comparison, a photo of a core after exposure to 15% HCl is displayed in Fig. 3.29. The initial “conical-shaped” wormhole (note CT radiograph) implies that the pumping rate was not high enough to provide optimal spending of the acid. At 5 mL/min, the highly reactive HCl fluids were being pumped at a rate below the optimal flow-rate range for ideal wormhole formation. Fig. 3.30 shows plots of the flow rate vs. the PVBT values. These tests included four HEDTA fluids as well as FA. The shapes of the curves are similar to those described by Fredd and Fogler (1998a) for other organic acid or chelating agent formulations. The low-breakthrough volumes observed for the more acidic solvent used at 0.3–0.5 mL/min demonstrated that optimal flow rates were achieved. These data suggest that a low pH Na_3HEDTA could produce efficient solvents at 65°C (150°F).

However, this rate was too high for the chelant solutions and organic acids, which formed ramified (many branched) wormholes at 5 mL/min. This observation is based on the uniform dissolution of

15% HCl, 0.2% Inhibitor, 150°F, 5 mL/min

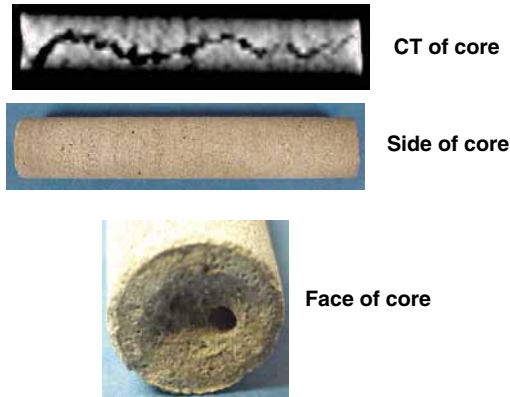


Fig. 3.29—Conical wormhole in limestone after 15% HCl at 5 mL/min., 65°C (150°F) (Frenier et al. 2001).

the core and the appearance of the cores after the test. In addition, the weight loss of the core was as high as 10% of its initial weight. There was evidence of uniform dissolution of the core with the pH 12 Na₃HEDTA.

This supposition was confirmed by the CT-radiographic images (not shown). An examination of the [Ca] vs. time data (Frenier et al. 2001) shows that the maximum in the calcium concentration or a plateau occurs at about the same time as the breakthrough. Note that Na₃HEDTA/formic held almost 60,000 ppm Ca (almost equivalent to 15% HCl).

The data for 0.5 mL/min flow rate (at 65°C) is summarized in Table 3.5. FA produced significant face dissolution, indicating that the flow rate was below the optimal pump rate for this relatively aggressive solvent. The sodium HEDTA solution at pH 2.5 also caused some face dissolution (flow rate below optimum), but from Fig. 3.30, the optimal flow rate was about 0.8 mL/min.

Figs. 3.31 through 3.33 show data from tests run at higher temperatures [121°C (250°F)]. All of these tests were conducted with 20% Na₃HEDTA formulations. Fig. 3.31 displays data for PVBT vs. flow rate. The minimums in the curves were at about 2.0 mL/min for all solvents except pH 12. As expected, the optimal injection rates increased with increasing temperature (from about 0.3 mL/min at 65°C to about 2 mL/min at 121°C). The pH 12 solvent displayed a much steeper slope at higher pump

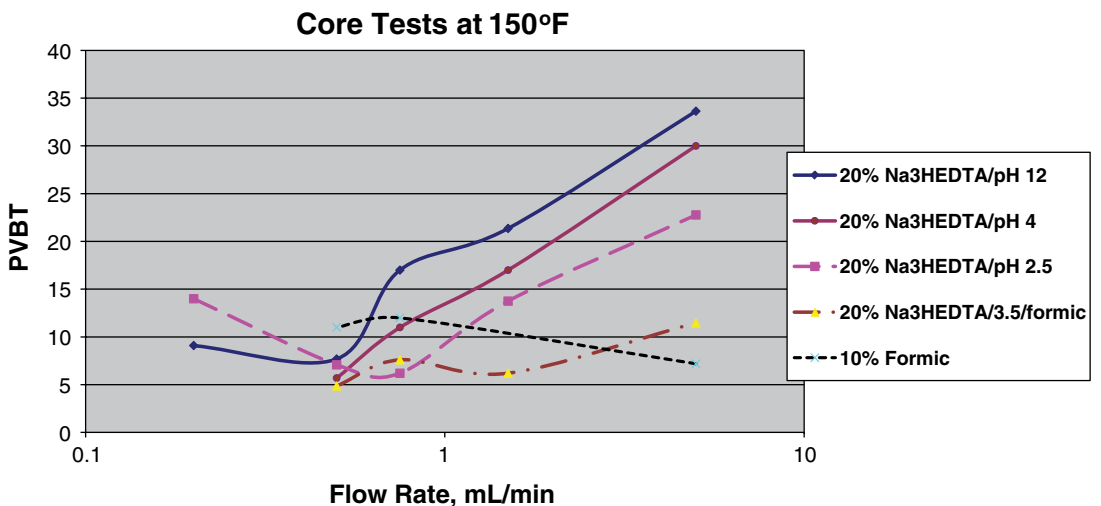


Fig. 3.30—Pore volume to breakthrough (PVBT) values for five solvents at 65°C (150°F) vs. flow rate during coreflood test (Frenier et al. 2001).

TABLE 3.5—COREFLOOD DATA AT 65°C (150°F), 0.5 mL/MIN

| Solvent | Core Length (cm) | Pore Volume (mL) | Initial Perm (md) | Total Fluid (mL) | V Bt (mL) | PVBT | Core Weight Loss (g) |
|---|------------------|------------------|-------------------|------------------|-----------|------|----------------------|
| 20% Na ₃ HEDTA, pH 12 | 15.0 | 10.4 | 16.5 | 100 | 80 | 7.7 | 2.0 |
| 0.25 M Na ₃ HEDTA, pH 12 | 15 | 9.9 | 32 | 155 | 150 | 15 | 2.2 |
| 20% Na ₃ HEDTA, pH 4 | 15.4 | 10.5 | 58 | 78 | 60 | 5.7 | 2.2 |
| 20% Na ₃ HEDTA, pH 2.5 | 15.4 | 11.3 | 14 | 100 | 80 | 7.0 | 6.6 |
| 20% Na ₃ HEDTA, pH 3.5, formic | 15.0 | 11.6 | 19 | 70 | 55 | 4.7 | 5.6 |
| 20% Na ₄ EDTA, pH 12 | 15.0 | 10.4 | 14 | 120 | 80 | 7.8 | 5.1 |
| 0.25 M Na ₄ EDTA, pH 12 | 14.6 | 9.9 | 12 | 108 | 108 | 10.1 | 2.5 |
| 10% Na ₂ HEIDA pH 2.5/HCl | 15.4 | 11.5 | 17 | 100 | 100 | 8.7 | 1.0 |
| 10% Acetic acid | 15.4 | 11.0 | 25 | 80 | 80 | 7.2 | 1.9 |
| 10% Formic acid | 15.4 | 11.0 | 28 | 87 | 70 | 6.4 | 5.9 |

rates than the low pH solvents. The CT scans and inlet photographs of the wormholes for tests run at 2.0 mL/min are shown in (Fig. 3.32). Wormholes were observed to penetrate the entire length of the cores for all pH values. The diameter of the wormhole formed with the aggressive HEDTA pH 3.5/FA fluid was much larger than the wormholes formed with the other HEDTA fluids.

The Damköhler number for a cylindrical wormhole can be calculated using Eqs. 3.3–3.6. Using the proposed optimal Damköhler number of approximately 0.29 (Fig. 3.28) (Fredd and Fogler 1998b), an average wormhole diameter of 0.16 cm, the optimal flow rates for pH 12, 4, and pH 2.5 Na₃HEDTA fluids were calculated and displayed as a function of temperature and flow rate. See Fig. 3.33. This figure predicts that the optimal injection rates should increase with increasing temperature. The experimental values of optimal flow rates from these coreflood tests were consistent with this trend and were close to the rates predicted in Fig. 3.33 from the Damköhler number calculations in Frenier et al. (2004).

Several high-temperature fluid formulations containing HEDTA were tested (Frenier et al. 2004) at 350°F (177°C). In addition, 10% acetic acid was used to stimulate the limestone core. This acid was tested because it is currently one of the few materials that are used at these high temperatures. A computational procedure was then used to relate the laboratory core flow data to radial flow in a limestone formation. The procedure relied on previous work performed by Fredd and Fogler (1998c),

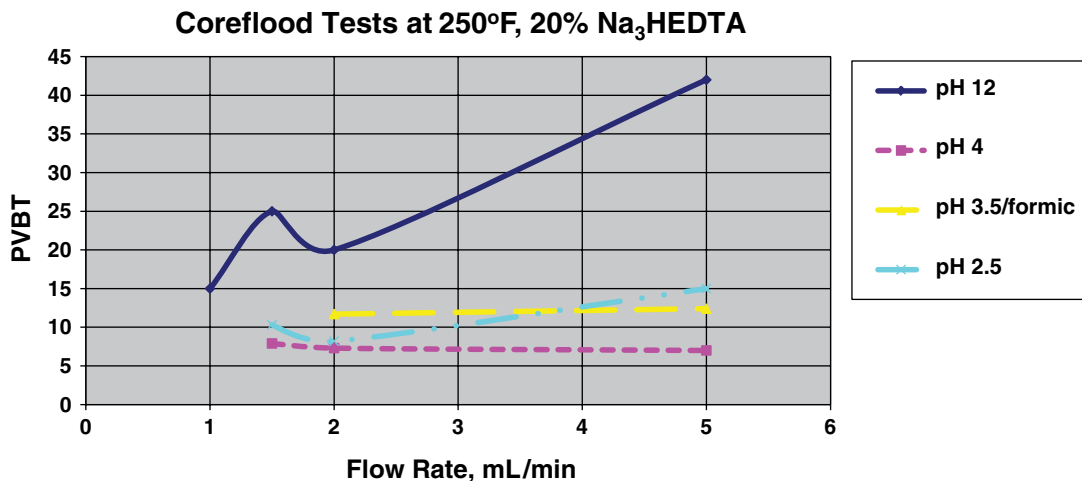


Fig. 3.31—Pore volume to breakthrough (PV BT) values for 20% Na₃HEDTA 121°C (250°F) vs. flow rate (Frenier et al. 2001).

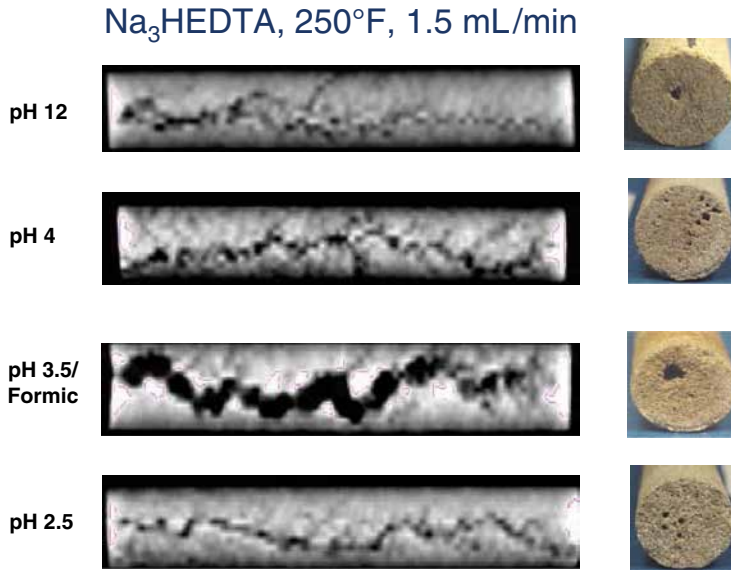


Fig. 3.32—Limestone cores after coreflood tests of four Na₃HEDTA formulations at 121°C (250°F), 2 mL/min (Frenier et al. 2001).

who normalized the wormhole formation phenomenon with a single 3D surface. The kinetic and equilibrium constants measured for HEDTA were incorporated into this model. In addition, computational fluid dynamics simulations were performed with a commercial simulator to investigate the effects of the pressure and velocity fields on the wormhole density in radial flow.

Fig. 3.34 shows how the amount of flow going through the well face decreases with the number of wormholes, effectively limiting the maximum number of dominant radial wormholes to between five and seven. Adding these results to the previous model enabled scale up from laboratory experiments to radial flow field conditions.

Fig. 3.35 shows a summary of the 350°F (177°C) data projections. In these tests, the calculated PVBT is defined as the efficiency. Acetic acid was less efficient than low-pH HEDTA at this temperature and flow rate. The low-pH chelant fluid fulfills the criteria for ideal high-temperature stimulation fluids for carbonates because the corrosion rates can be adequately controlled (Frenier 2004) to 400°F. In addition, the reduced dissolution rates allow fluid pumping to be controlled in the range to achieve maximum efficient use of the fluid and avoid fractures in the formation.

Field trials (Parkinson et al. 2010; Husen et al. 2002) in high-temperature carbonates as well as a campaign (Jimenez-Bueno et al. 2012) of the continuing use of an HEDTA-based, pH 4 chelating

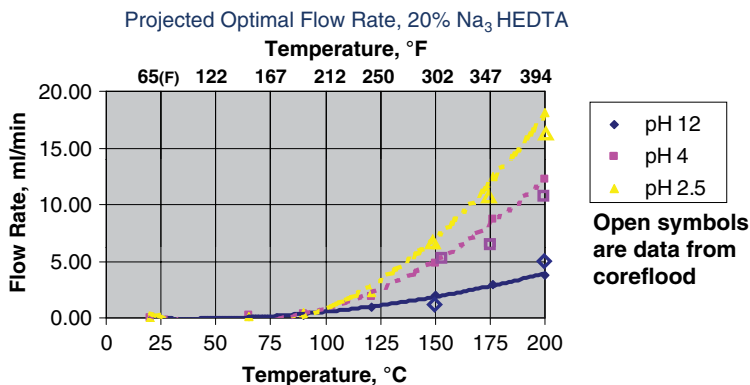


Fig. 3.33—Projected optimal flow rates at $N_{Da} = 0.29$ (Frenier et al. 2004).

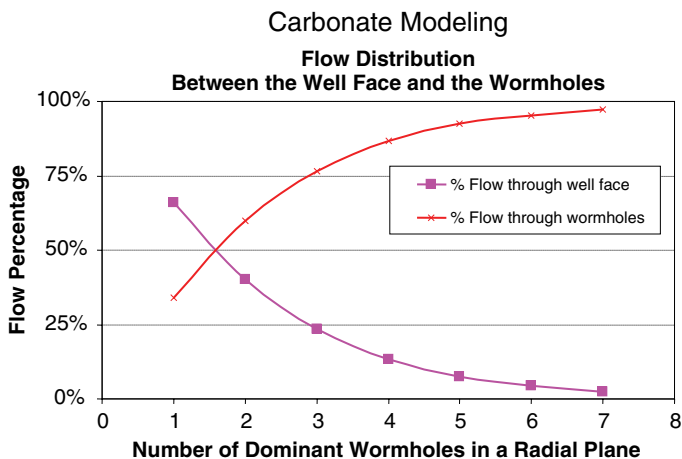


Fig. 3.34—Flow distribution between the wormholes and the well face based on radial flow simulations performed with the CFD code (Frenier et al. 2004).

formulation for stimulation of very hot (up to 350°F) carbonates in Mexico have been conducted. The formations contain a mixture of calcite and dolomite. The authors (Jimenez-Bueno et al. 2012) report that a number of wells were stimulated under matrix conditions, and the results were more favorable than offsets that were treated with HCl.

The authors (Jimenez-Bueno et al. 2012) report

- The chelating agent products were more efficient (based on the available pumping rates) and allowed the wells to return to production much faster.
- No neutralization post-treatment was needed.
- No testing surface equipment was required.

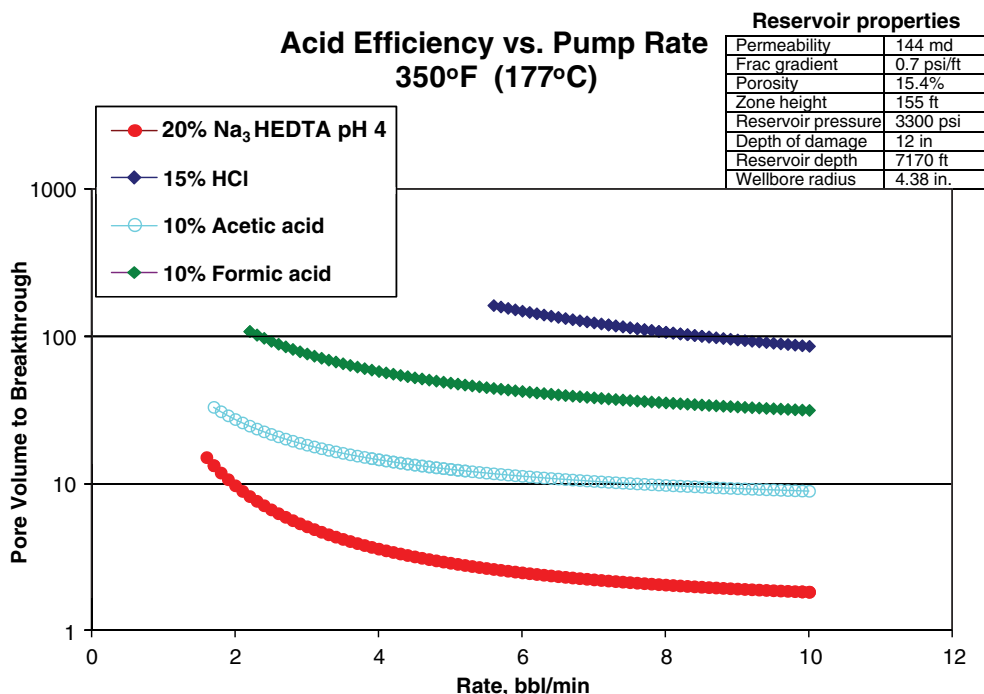


Fig. 3.35—Efficiency of stimulation (PVT) vs. pump rate for four acids at 350°F (177°C) (Frenier et al. 2004).

Emerging Chelating Agent Technologies. The following paragraphs review information on chemicals that have not been well known in the production chemical industry but may have significant uses in the future because of improved biodegradable characteristics, compared with EDTA-type chemicals. These materials are iminodisuccinate (IDS), GLDA, methylglycine N,N diacetic acid (MGDA), HEIDA, and ethylenediamine N,N disuccinic acid (EDDS) (see Fig. 3.24 and Table 3.3). The biodegradable chelating agents, citric acid, and NTA have been in use for several years along with nonbiodegradable phosphonates and EDTA, HEDTA, and DTPA. Uses of some of these chelating agents for scale removal have been described in Frenier and Ziauddin (2008).

Bayer (2001) claims that sodium IDS belongs to the aminocarboxylate class of chelating agents and that all aminocarboxylates in use today are acetic acid derivatives produced from amines, formaldehyde, sodium hydroxide, and hydrogen cyanide. In contrast, they claim that sodium IDS can be produced from maleic anhydride water, sodium hydroxide, and ammonia. The only solvent used in the production process is claimed to be water, and the only side product formed, ammonia dissolved in water, is recycled back into IDS production or used in other Bayer processes. They claim that because sodium IDS is a readily biodegradable, nontoxic, and nonpolluting alternative to other chelating agents, it can be used in a variety of applications that employ chelating agents. For example, it can be used as a builder and bleach stabilizer in laundry and dishwashing detergents to extend and improve the cleaning properties of the eight billion pounds of these products that are used annually.

GLDA is described by AkzoNobel (2009) as being based on the food-approved natural amino acid salt, monosodium L-glutamate. This report also claims that GLDA, when compared with a variety of alternative chelating agents, is the most environmentally benign chelating agent. Uses for GLDA in stimulation treatments are demonstrated later in this section.

Al-Mayouf (2006) claims that pressure is mounting for the removal and replacement of nonbiodegradable chelating agents with alternative, readily biodegradable chelates. Such an alternative (MGDA) and GLDA are claimed to possess a good ecological and toxicological profiles. The authors (Al-Mayouf 2006) claim that MGDA and GLDA meet all of requirements and, thus, can be applied as new effective and environmental friendly chelating agents. They also note that MGDA is a strong chelating agent. See the stability constants in Table 3.3.

HEIDA also has been shown to be readily biodegradable (Dow 2007b, 2007a). Dow (2007b) also has found that the potassium salts of HEIDA were more effective in removing calcium scale compared with the sodium salts.

Tandy et al. (2003) contend that EDTA and phosphonates are nonbiodegradable chelants that are used extensively in domestic and industrial applications. They claim that an environmental concern is that once the chemical is in river systems, the chelants can extract heavy toxic metals from mud and sediment and cause remobilization of the metals in the environment that may have adverse long-term effects. EDDS is claimed to be readily biodegradable and is completely mineralized in the environment. EDDS, therefore, cannot remobilize heavy metals as it has biodegraded before discharge into river systems. EDDS is classified as nonhazardous.

Charkhutian et al. (2004) investigated the biodegradable chelating agents EDDS, IDS, MGDA, and NTA as potential alternatives and compare them with EDTA for effectiveness for extracting metals from soils. Table 3.3 shows some stability data from their paper.

Saito et al. (2000) studied the galvanic coupling between magnetite and iron in EDDS solutions both with and without added iron(II) ions have been studied using electrochemical methods. The galvanic coupling accelerates the corrosion of iron because of the small shift in its potential in the anodic direction. At the same time, the potential of magnetite is cathodically polarized away from the potential range where the only faradic process—the RD of magnetite—takes place and results in a considerable decrease in its dissolution. Magnetite dissolves faster at the galvanic potential when $[EDDS] \geq [Fe^{2+}]$, whereas iron is affected to a much lesser extent. The ratio between the rates of dissolution of magnetite at the galvanic potential to that at its steady-state potential tends to decrease at higher temperatures and at higher EDDS and Fe^{2+} concentrations. This study shows that temperature plays a decisive role in the dissolution of magnetite coupled to iron. To completely remove it from the iron surface, high temperatures should be used. CIs have to be considered when high losses of the base metal cannot be

tolerated. They suggest that EDDS is a promising substitute for EDTA in the nuclear energy industry because of its composite chelating power.

Crump and Wilson (2009) made preliminary investigations into the replacement of widely used chelating agents for industrial cleansing of radionuclide-contaminated items using readily biodegradable alternatives that have equivalent effectiveness. The chelation of radionuclide cations by [S,S']-EDDS has been compared with traditional decontamination agents, EDTA, and citrate. Models indicate that in many respects, [S,S']-EDDS compares favorably with EDTA.

Wilson and Crump (1999) tested the dissolution of iron with EDDS. A sample (1.0 g) of EDDS was dissolved in deionized water, and sufficient aqueous ammonia solution is added to obtain a pH of 9.0. Deionized water is added to obtain a 5 wt% EDDS solution. The resulting solution is heated at 100°C for 3 hours with 0.2 g of iron oxide (Fe_3O_4) and cooled to room temperature. The amount of soluble iron is then determined by inductively coupled plasma spectroscopy. After 3 hours, approximately 31 wt% of the iron is dissolved in a similar experiment an EDDS solution is adjusted to a pH of 4.5 with an aqueous ammonia solution. After 3 hours at reflux, approximately 70 wt% of the iron oxide has dissolved. This data shows that ammoniated polyamino disuccinic acids are effective in dissolving iron oxide scales.

LePage et al. (2009), Boonstra et al. (2009), Charkhutian et al. (2004), Mahmoud et al. (2011a), and Rabie et al. (2011) have described extensive evaluations of the use of Na_4GLDA solutions. This chemical is a commercial raw material (AkzoNobel 2006), and the data show it to be soluble in several fluids of interest in reactive stimulation. Included are HCl (15 and 28%), acetic acid (15 and 28%), and FA (15 and 28%). The authors of these documents report that the material also shows high biodegradation values.

The authors (LePage et al. 2009; Mahmoud et al. 2010a) describe calcite dissolution tests using GLDA and other chelants over a large range of pH values (Fig. 3.36) where the pH was adjusted by adding HCl. In this figure from their paper, the EDTA and HEDTA values overlap and the “square” symbol represents data from Frenier et al. (2000). The high-dissolution values are attributed to the acid reaction of the added HCl (Eq. 3.1) as well as a chelate-type reaction such as Eq. 3.7.

Rabie et al. (2011) has performed kinetic dissolutions tests using the RDE method (see Fig. 3.7 of this book). Table 3.6 from their report indicates there is mixed kinetics for the SRR of mixtures of sodium GLDA with HCl at pH 3.8. This would be expected based on the high capacity of this solvent type (see Table 3.3).

Using coreflood methods that are similar to those proposed by Frenier et al. (2001), Mahmoud et al. (2011a) have described laboratory investigations of GLDA in carbonate matrix stimulation fluids.

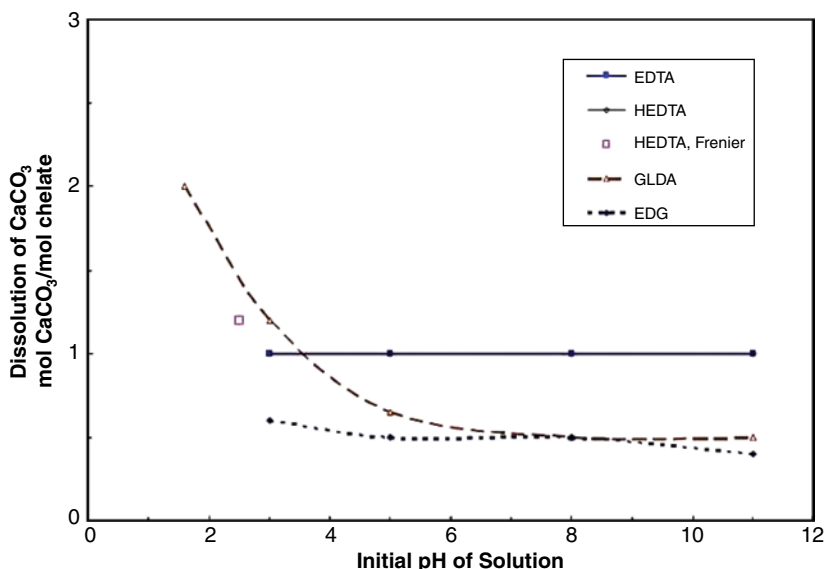


Fig. 3.36—Capacity of solvents to dissolve calcite vs. pH (LePage et al. 2009).

| Temperature (°F) | Rate of H+ Reaction (g-mol/cm ² ·s) | Rate of Chelate Reaction (g-mol/cm ² ·s) | Complexation (%) |
|------------------|--|---|------------------|
| 150 | 1.65E-06 | 3.36E-06 | 67.1 |
| 200 | 3.75E-06 | 3.82E-06 | 50.5 |
| 250 | 4.83E-06 | 5.29E-06 | 52.3 |
| 300 | 7.67E-06 | 6.06E-06 | 44.1 |

The experiments demonstrated the ability to produce wormholes in limestone cores at temperatures from 200–220°F. See [Fig 3.37](#) for a 3D CT-X-ray representation of a full-penetration wormhole. The fluids contained 20% GLDA at pH 1.7/HCl.

Mahmoud et al. (2010) claim that GLDA was introduced as alternative for HCl for stimulating deep carbonate reservoirs at which HCl will cause corrosion and face dissolution problems. In this study, calcite cores, 1.5-in. diameter with 6- and 20-in. length, were used to determine the optimum conditions where the GLDA can break through the core and form wormholes. GLDA solutions with pH values of 1.7, 3, and 3.8 were used. The optimum conditions of flow rate and pH were determined using the coreflood experiments. CT scan was used to determine the wormholes length and diameter to determine of optimum Damköhler number. GLDA was compared with chelates that are used in the oil industry such as EDTA and HEDTA. GLDA also was used to stimulate parallel cores with different permeability ratios (up to 6.25) to assess its behavior under diversion conditions.

The authors of this report (Mahmoud et al. 2010b) also claim that GLDA was found to be very effective in creating wormholes at pH = 1.7, 3, and 3.8 at different injection rates at temperatures of 180, 250, and 300°F. Increasing the temperature increased the reaction rate and less amount of GLDA was required to break through the core and form wormholes. Unlike HCl and EDTA, there was no face dissolution or washout in the cores even at very low rates. Also, an optimum flow rate and Damköhler number were found at which the pore volume required to create wormholes was the minimal. GLDA

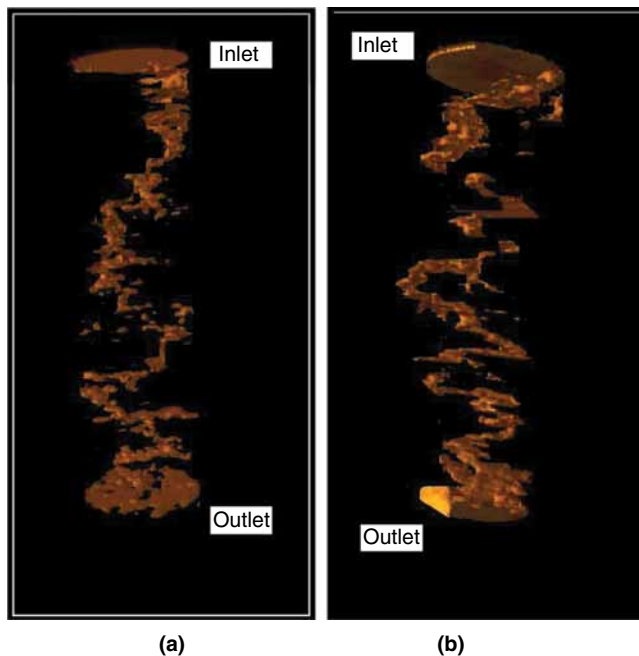


Fig. 3.37—3D CT-X-ray after (a) coreflood at 200°F and (b) 220°F (Mahmoud et al. 2010).

at pH 1.7 and 3 created wormholes with a small number of pore volumes. Compared with acetic acid, the volume of GLDA at pH 3 required to create wormholes was less than that required with acetic acid for the same conditions. GLDA was found to be effective in stimulating parallel cores with different permeabilities.

Conclusions proposed by the authors from the kinetic and coreflood studies with sodium GLDA formulations with HCl are summarized (Mahmoud et al. 2010; Rabie et al. 2011).

- Reaction of low pH GLDA with calcite is an MTL up to 1800 rev/min.
- Increasing temperature significantly increased the dissolution rate. The rate of dissolution at pH 3.8, 1000 rev/min, and 80°F increased 6 times when the temperature was increased to 200°F.
- 0.6 M GLDA reacted faster at pH of 1.7. At this pH, GLDA reacts as a polyprotic acid and the dominant mechanism is hydrogen ion attack.
- The reaction at pH 3.8 and 13 became less dependent on the disk rotational speed, which indicated that at these pH values the kinetics of the surface reaction play a key role in the overall rate.
- Increasing temperature increased both the rate of chelation and hydrogen attack reactions with a reduction in the influence of the chelation.
- Increasing the disk rotational speed did not have a significant effect on the rate of the chelation reaction.
- The values of the diffusion coefficients from the reaction study of 0.6 M GLDA was combined with coreflood data to determine the Damköhler number. In all experiments, there was an optimum Damköhler number that corresponded to a minimum pore volume required to break through the core.
- In coreflood study, increasing temperature or decreasing the pH increased the optimum Damköhler number with a reduction in the minimum pore volume required to break through.

The different chelating agent formulations that are becoming available offer opportunities for a variety of innovative fluids that may be useful in high temperature and environmentally sensitive environments where the alternative acids may not be appropriate or acceptable.

A field use of the biodegradable GLDA formulations have been reported by Stanitzek et al. (2012). The authors claim that extensive laboratory studies were conducted before the treatment was pumped that included: corrosion tests, coreflood experiments, compatibility tests with reservoir fluids, and reaction rate measurements using an RD apparatus. The details of the stimulation of a hot (300°F, sour carbonate formation) included a preflush of mutual solvent and water wetting surfactant, followed by the main stage consisting of 20 wt% GLDA with a low concentration of a proper (for organic acids) CI.

Following the treatment, the authors claim that the well was put on production, and samples of flowback fluids were collected. The concentrations of various ions were determined using ICP. Various analytical techniques were used to determine the concentration of GLDA and other organic compounds in the flowback samples. The treatment was applied in the field without encountering any operational problems. A significant increase in gas production that exceeded operator expectations was achieved. Unlike previous treatments where HCl or other chelates were used, the concentrations of iron, chrome, nickel, and molybdenum in the flowback samples were negligible, confirming low corrosion of well tubulars. Improved productivity and longer term performance results confirm the effectiveness of the new chelate as a versatile stimulation fluid.

3.4.5 Summary of Chemistries for Matrix Stimulation of Carbonates. The previous sections (3.4.1–3.4.4) describe a wide range of chemicals for matrix stimulation of carbonates. The data on the various solvents for bypassing damage in carbonates proves that the theories of wormhole formation (Section 3.3) can be applied to produce fluids that will be effective and *efficient* over a wide range of temperatures and operating conditions. The next major section (3.5), describes an equally wide variety of chemistries for removing formation damage from the infinitely variable sandstone formations.

3.5 Sandstone Matrix Stimulation

Some of the physical principles of matrix stimulation of sandstone formations are the same as for carbonates. Of great importance is that the processes fluid is pumped at rates that do not intentionally fracture the rock and the acid must penetrate the pore spaces. In addition, HCl as well as organic acids and chelating agents described in Section 3.4 also are part of many sandstone stimulation fluids. However, because the reaction rates for the *silicon* containing minerals are much lower (Hill and Schechter 2001) than any acid reacting with a carbonate, wormhole formation will not take place unless there is a streak of carbonate or a very localized clay pocket. Thus, the sandstone acids must *dissolve* the damage in the pore spaces and on any other surface, not *bypass it*. Because the damage (Section 2.3) is varied in location and chemistry, solvents that can react with calcite, silica, clays, and organic foulants must be employed.

3.5.1 Challenges for Stimulation of Sandstone Formations. Stimulation of sandstone formations is inherently more complex than carbonate stimulation because of the heterogeneous and ever-changing nature of the sandstone matrix. Fig. 3.38 shows a diagram of the constituents of a sandstone formation, and Fig. 3.39 is a photomicrograph of a Berea sandstone core showing the matrix as well as possibly fouling deposits. Fig. 3.40 lists the compositions of some of the clays (phyllosilicates) and other aluminosilicates (called tectosilicates) that are in many sandstone formations. Some discussions of the aluminosilicates were in Fig. 1.29 and Section 1.5.6.

While the carbonate portion of the sandstone rock is soluble in acid (HCl or organic), the clays and silicates require some source of HF to be dissolved. However, as compared with the relatively clean

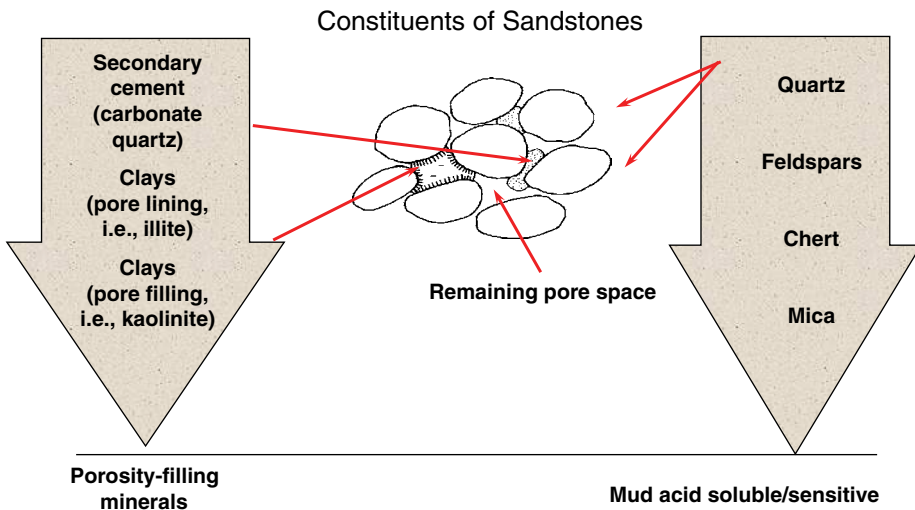


Fig. 3.38—Constituents of a sandstone matrix.

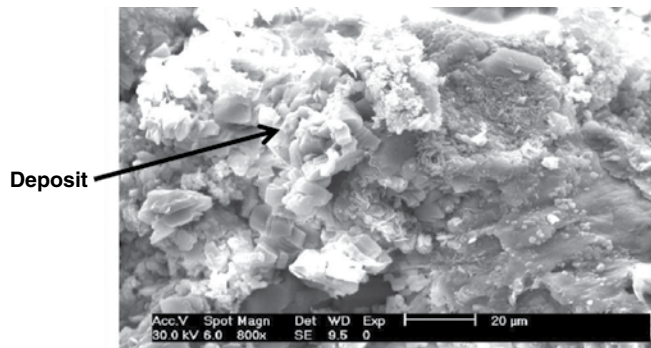


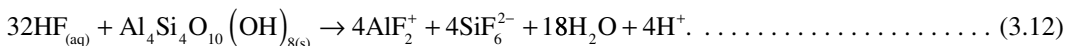
Fig. 3.39—Micrograph of a Berea sandstone core with deposits.

| | | Silicates | |
|-----------------|-----------|---|--|
| | Chemical | Minerals | Composition |
| Tectosilicates | Quartz | Quartz | SiO ₂ |
| | Feldspars | Orthoclase | Si ₃ AlO ₈ K |
| | | Microcline | KAlSi ₃ O ₈ |
| | | Albite | Si ₃ AlO ₃ KNa |
| | | Plagioclase | Si ₂₋₃ Al ₁₋₂ O ₃ (Na,Ca) |
| | Biotite | (AlSi ₃ O ₁₀) K(Mg, Fe) ₃ (OH) ₂ | |
| Phyllosilicates | Micas | Muscovite | (AlSi ₃ O ₁₀) K(Al) ₂ (OH) ₂ |
| | Clays | Kaolinite | Al ₂ (Si ₄ O ₁₀)(OH) ₂ |
| | | Illite | Si _{4-c} Al _c O ₁₀ (OH) ₂ K _c Al ₂ |
| | | Smectite | (AlSi ₃ O ₁₀)Mg ₅ (Al,Fe)(OH) ₈ |
| | | Mixed-layer | Kaolinite,illite or chlorite with smectite |

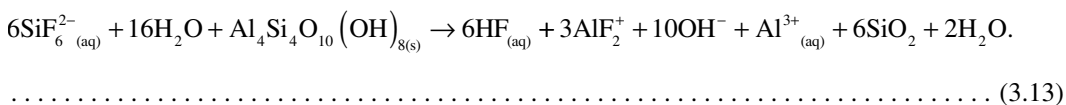
Fig. 3.40—Silicate compositions in sandstones.

reaction of HCl with calcite (Eqs. 3.1 and 3.2), the HF reactions with the silicates and aluminosilicates produce a large variety of secondary reactions. These can cause damaging solids to form that may negate the effects of dissolving the minerals and can cause the matrix to exhibit flow reductions.

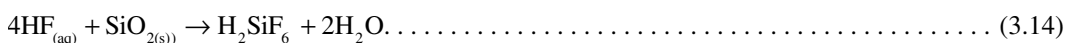
For example, the primary reaction of HF with kaolinite clay is



While the secondary reactions produce solid hydrated silica:



For silica, the primary reaction is



In addition, if the calcite has not been removed using a preliminary wash with HCl or an organic acid, fluorite (CaF₂) also will precipitate as the acid spends. Therefore, early in the development of sandstone acidizing fluids of HCl with HF called MA were produced to reduce the precipitation reactions. As long as the pH of the fluid in the matrix remains low, precipitation is inhibited; however, this is difficult to control in real formations, especially at high temperatures and in the presence of sensitive clays such as zeolites (Hartman et al. 2006).

A summary of challenges that have been addressed by the industry (and described in more detail in Section 3.5.2) are

- How to manage precipitation and the reaction of quartz?
- Address observations that permeability increases slowly after damage has been removed. Thus, there is minimal benefit of injecting additional acid after damage has been dissolved.

3.5.2 Mechanisms of Dissolution of Sandstone Minerals. Sections 3.1.1 and 3.1.2 described the differences between predominantly carbonate and sandstone formations and the challenges for stimulating those minerals using reactive chemicals. As noted in Figs. 3.2, 3.5, and 3.38, sandstones are

inherently heterogeneous and vary greatly from formation to formation. In addition, Ali et al. (2010) note that following deposition, the sediments are shaped by a variety of physical and chemical processes that significantly influence rock properties. The authors also describe these diagenetic processes and their impacts on reservoir quality. This includes the minerals present as well as the native permeability (*k*). These factors can (Sections 3.1.1 and 3.1.2) also greatly affect the reactivity with stimulation acids.

With the exception of any carbonate phases, the reaction rates of the components of sandstones with stimulation chemicals are several orders of magnitude *lower* (Hill and Schechter 2001) than carbonate reactions at the same temperatures. Therefore, the reactions take place within the formation matrix and do not form conductive wormholes (Xie et al. 2005). The only way to form pseudowormholes would be where streaks of calcite or very soluble clays occurred in a heterogeneous sandstone formation (observation of the book’s authors).

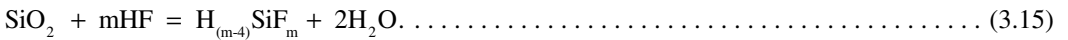
The major reason for reactive stimulations of sandstones is to remove damaging skin that has reduced the effective permeability (and thus the hydrocarbon production) of the formation. It would be very desirable to be able to reduce the skin factor to negative values, but this usually is not possible with current technology.

Analysis of the *damage* is an important aspect for selecting a stimulation solvent, because a different solvent may be needed to remove carbonate or alkaline earth (Ca/Ba sulfates) scales as compared with clay fines or organic damage. See the discussions of formation damage in Section 2.3 of this book as well as in Hill et al. (2001). Also see the discussions of scale removal (Frenier and Ziauddin 2008) and organic damage (Frenier et al. 2010) removal. However, any realistic solvent for sandstone damage must contend with three types of minerals during reactive stimulation and dissolve the damage without disturbing the remainder of the matrix. These are

- Carbonates
- Layered phyllosilicates (aka clays)
- Tectosilicates such as feldspars, zeolites, and silica (SiO₂)

As noted in the first paragraph of this section, the carbonate component of a sandstone formation is readily soluble in all types of reactive stimulation chemicals; however, the cations (Ca²⁺ and Mg²⁺) may interfere with other components of the stimulation fluid.

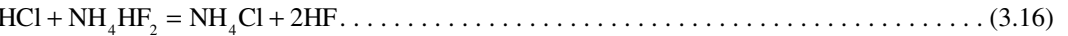
For the stimulation of sandstones, the challenge is to dissolve the damage, which usually involves calcite scale and clay fines without redamaging the formation with additional precipitates. The reader is urged to review Sections 1.5.6 and 3.5.1, in which the chemistries of clays and other aluminosilicates as well as sandstones are described. The major chemical issue is that the only successful chemicals available to dissolve the clay/silica portion of damage contain HF. Eq. 3.12 shows the primary dissolution process for the clay mineral kaolinite (all of the other minerals have similar reaction equations). The generalized reaction with silica is



Note that this equation allows for a more generalized stoichiometry compared with Eq. 3.14 since the concentration of HF may vary.

Despite much research (Iler 1979), fluoride is the only ligand available that produces a useful and soluble reaction product with Si⁴⁺ ions. Sedeh et al. (1993) tested compounds related to l-DOPA [(*S*)-2-amino-3-(3,4-dihydroxyphenyl) propionic acid] and other 1,2-dihydroxybenzene derivatives, which will form complexes with Si⁴⁺ ions, but they were not effective in dissolving large amounts of silica. NaOH will extract silicon ions from clay, but it also will precipitate a solid [Al(OH)₃].

For safety reasons, the HF frequently is produced in situ by the reaction of HCl with ammonium bifluoride (ABF):



Additional fluoride sources such as ammonium fluoride, polyvinyl ammonium fluoride, polyvinyl pyridinium fluoride, pyridinium fluoride, imidazolium fluoride, sodium tetrafluoroborate, or ammonium tetrafluoroborate are possible (Frenier et al. 2012), but not usually employed in practice.

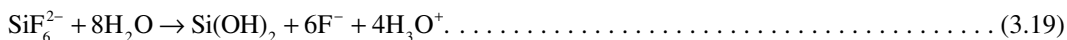
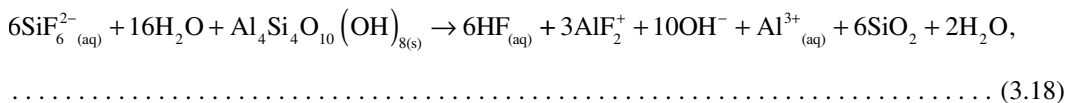
Note from Table 3.3 that HF is a weak acid and only slightly ionized in water. In HCl fluids, the HF would be essentially unionized. Mixtures of HCl with aqueous HF also can be prepared; however, concentrated HF formulations are very toxic and dangerous to handle. The production of a soluble product is a necessary consequence for dissolution of any mineral. As noted in Section 3.1.2, the reactions of clays and silicates are slow compared with the reactions of acids with calcite. The other factor that affects the overall reaction kinetics is the effective surface area of the mineral.

The layered clays have relatively high surface areas compared with most tectosilicates, so these materials dissolve slower than the clays. Thus, the overall effective rate involves the specific reaction rate for the mineral and the effective surface area. For these surface reaction-limited processes, the rate equation for the surface reaction (q_s) is

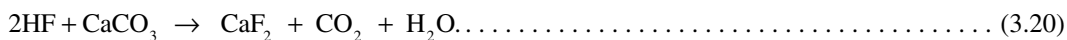
$$q_s = \kappa_j AC^m \dots \dots \dots (3.17)$$

Here κ_j is the reaction rate coefficient for the mineral, A is the surface area, C is the concentration of the solvent, and m is the order of the reaction. This is illustrated in Fig. 3.41.

For the reactions with the clays/tectosilicates, the Al removal reactions are also important (see Eq. 3.12–3.14). Unfortunately, many secondary reactions occur as the dissolution process proceeds. For kaolinite, the secondary reactions involving HF include:



These reactions produce various amounts of hydrated silica (also called silica acid). Depending on the other minerals present in the formation, a large number of additional secondary precipitates are possible. Table 3.7 shows the solubilities of some of these materials. Unless calcite has been removed by an acid wash, fluorite will be a significant precipitate.



3.5.3 Reactions and Reaction Rates for Stimulation of Sandstone Formations. Much of the technology developed over the past 40 years has attempted to reduce or delay the formation of unwanted precipitates while still dissolving the damaging minerals (Table 3.7). The standard treatment for comparison has been a multistage process in which the first stage uses 5–15% HCl (or an organic acid) pumped to dissolve calcite followed by various strengths of HCl/HF, MA, stages to dissolve clays and other silica/silicate minerals. These processes may be repeated for each zone to be treated.

Reaction Rate—Factors

- Mineral composition and surface area
- Dominant factor → surface area

| Mineral | Specific Area |
|-----------|------------------------|
| Quartz | Few cm ² /g |
| Feldspar | Few cm ² /g |
| Clays: | |
| Kaolinite | 22 m ² /g |
| Illite | 113 m ² /g |
| Smectite | 82 m ² /g |

- Reaction rate: Calcite >>>clays > feldspars > quartz
- $$q_s = r_s = \kappa_j AC^m$$

Fig. 3.41—Sandstone components relative reaction rates.

| Solid | Formula | Solubility (g/100 mL) |
|--------------------------|-----------------|-----------------------|
| Orthosilicic acid | H_4SiO_4 | 0.015 |
| Calcium fluoride | CaF_2 | 0.0016 |
| Sodium fluorosilicate | Na_2SiF_6 | 0.65 |
| Sodium fluoroaluminate | Na_3AlF_6 | Slightly soluble |
| Potassium fluorosilicate | K_2SiF_6 | 0.12 |
| Calcium fluorosilicate | $CaSiF_6$ | Slightly soluble |
| Ammonium fluorosilicate | $(NH_4)_2SiF_6$ | 18.6 |
| Aluminum fluoride | AlF_3 | 0.60 |
| Aluminum hydroxide | $Al(OH)_3$ | Insoluble |

See Fig. 3.42 for a depiction of the conventional sequences of fluids being pushed into the matrix, and that includes the over-flush fluids (frequently composed of NH_4Cl solutions).

To determine more information about the dissolution of clay-type minerals of interest in sandstone stimulation, various lab tests have been conducted. These are presumed to constitute much of the noncarbonate damage. Hartman et al. (2006) have performed a systematic examination of the reaction rates of several aluminosilicates in HCl and MA. Slurry reactor tests were performed using the equipment described in Fig. 3.12. The mineral compositions were followed using ICPOES and the data was analyzed using the method of initial rates (also in Fig. 3.12). The tests included analcime (a zeolite) kaolinite, chlorite, and illite. Additional tests were also performed on ground Berea sandstone. The characteristics of the test aluminosilicates are in Tables 3.8 and 3.9.

Results for the four minerals in HCl and 9/1 MA are described in the following paragraphs and the data help to illustrate important reaction and kinetic characteristics of these minerals.

Kaolinite. It was shown in a previous study (Ziauddin et al. 2002b) that Al is preferentially leached during the dissolution of kaolinite in HCl. Furthermore, the crystalline structures of many types of clay, such as kaolinite, are layered (or made up of sheets) in which acid attacks preferentially at the edges or planar surfaces (Kline 1980). The dissolution of kaolinite in 15 wt% HCl at 25°C illustrates that Al may have been leached from the mineral structure (Fig. 3.43a). One could also argue that Si precipitated from solution. If the precipitation of Si or preferential leaching of Al did not occur, then the concentration of Si would have been stoichiometric (Si:Al = 1:1 in kaolinite). The concentration of Al was greater than that of Si for both 25 and 100°C, demonstrating nonstoichiometric dissolution.

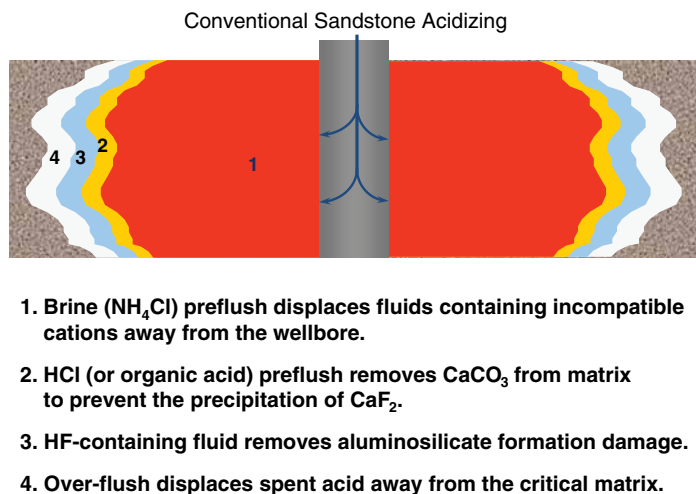


Fig. 3.42—Conventional sandstone stimulation.

| Mineral | Formula | Si:Al | Group | S.G. | Surface Area (m ² /g)* | Cation Exchange Capacity (meq/g) |
|----------|--|-------|-----------|------|-----------------------------------|----------------------------------|
| Analcime | Na ₂ Al ₂ Si ₄ O ₁₂ ·2H ₂ O | 2 | Zeolites | 2.27 | 0.59 | 4.5 |
| Kaolin | Al ₂ Si ₂ O ₅ (OH) ₄ | 1 | Clays | 2.59 | 8.0 | 0 |
| Chlorite | (Fe, Mg, Al)6(Si, Al)4O ₁₀ (OH)8H ₂ O | 2 | Chlorites | 2.95 | 7.7 | 0.2 |
| Illite | (K, H)Al ₂ (Si, Al)4O ₁₀ (OH)2-xH ₂ O | 2 | Mica | 2.72 | 21 | 0.2 |

*Surface areas were determined using N₂ BET.

| Mineral | Molar Ratio | | | | | |
|----------|-------------|------|------|------|------|------|
| | Al | Si | Na | Mg | Ca | Fe |
| Analcime | 1.00 | 1.91 | 1.00 | | 0.02 | 0.00 |
| Kaolin | 1.00 | 1.00 | | | | |
| Chlorite | 1.00 | 1.93 | | 1.56 | 0.05 | 0.04 |
| Illite | 1.00 | 1.98 | | 0.13 | 0.04 | 0.16 |

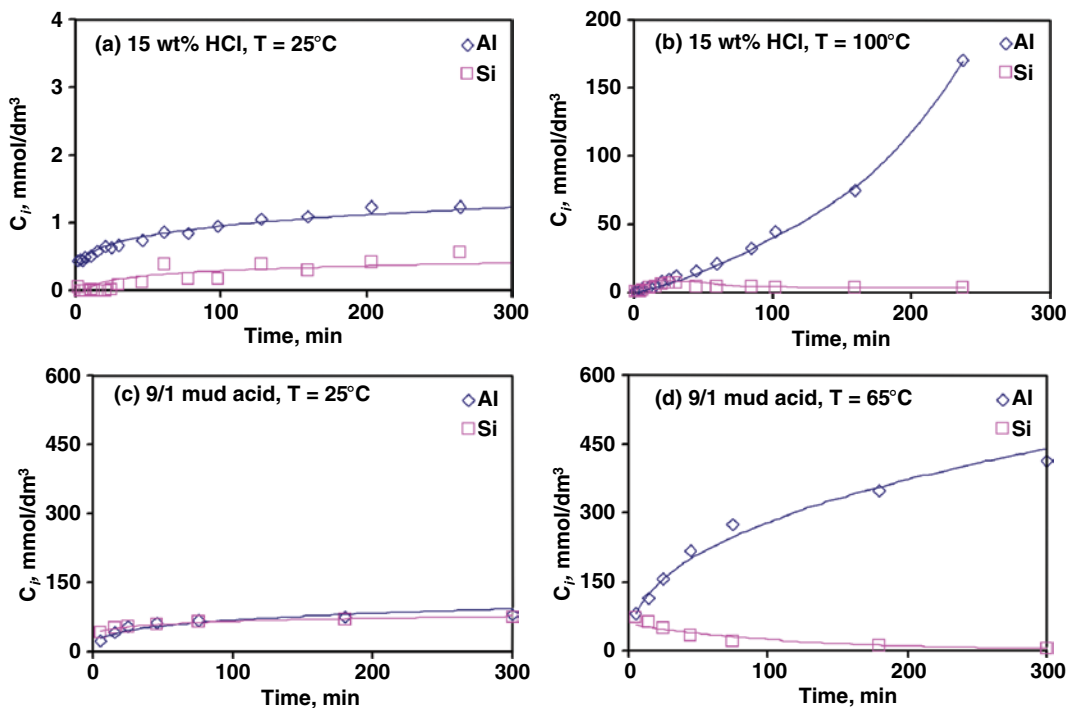


Fig. 3.43—Elemental concentration of Al, Si for the dissolution of kaolinite in 15 wt% HCl (25 and 100°C) and 9/1 mud acid (at 25 and 65°C).

At low temperature, 9/1 MA dissolves Al and Si quite stoichiometrically; however, only approximately 8.5% of the clay was dissolved in 5 hours of contact. Because there are equimolar amounts of Al and Si, we presume that only the primary reactions are occurring. At 65°C, 46% of the clay was dissolved, based on Al in solution, but Si had precipitated (Fig. 3.43d). The continual leaching of Al and precipitation of Si may be because of the secondary reaction of silicon fluoride with kaolinite and tertiary reactions that regenerate HF as the hydrated silica is precipitated (reactions Figs. 3.24 and 3.25). An XRD analysis of the undissolved kaolinite recovered at 300 minutes showed a small amount of crystalline silica, but no other identifiable crystalline species.

Tests (such as Fig. 3.44) with ground Berea sandstone stirred in 9/1 MA at 85°C show a pattern similar to kaolin clay. The data from this test show that Al was dissolved, Si dissolved and then precipitated, and Ca dissolves and remained in solution.

Analcime. Tests in HCl are seen in Fig. 3.45a, where the initial dissolution rate of Si is greater than Al and Na dissolution rates at 25°C. By 25 minutes, however, the Si concentration approaches a plateau while Al and Na continue to dissolve from the zeolite. If the Si in the zeolite had continued to dissolve, then the final Si:Al ratio would have been stoichiometric (e.g., Si:Al \approx 2:1). Nonstoichiometric dissolution may occur when precipitation takes place. One readily observes in Fig. 3.45b that silicon had already precipitated from solution even as the initial samples were taken during analcime dissolution at 100°C. It should be noted that the curves reported in Figs. 3.43 through 3.45 represent trends and not model predictions. As a result, the kinetic parameters are not reported in this study.

Chlorite. The structure of chlorite is shown schematically in Fig. 1.29, and the nature of acid attack on chlorite has been shown to be on the external mineral surface (Gdanski 1995). Data (Fig. 3.45c) indicate that both Mg and Al could have been leached from the crystalline lattice during dissolution in 15 wt% HCl at 25 and 100°C. The concentration of Si appeared to reach a maximum before decreasing analogous to analcime, indicating Si precipitation. Mass balance calculations on the data in Fig. 3.45c show that only approximately 2% of the Al present in the chlorite has been leached out, suggesting that most of the chlorite present in the reactor is left intact after 5 hours of reaction. In comparison, Wehunt et al. (1993) reported that 30% of the chlorite was destroyed after 5 hours of contact with HCl 15% at the same temperature. They also reported that chlorite is entirely destroyed after 3 hours at 82°C (Wehunt et al. 1993). The difference in reactivity can be attributed to differences in chlorite structure and composition. The oxide composition reported by Wehunt et al. (1993) indicates a Si/Al ratio of approximately 1.14, whereas that measured in the present study was found to be 2. As a result, the structure of the chlorite used in this study was more stable in HCl because H⁺ is known to preferentially attack and remove Al. Also, the amount of Fe and Mg in chlorite samples used by Simon and Anderson (1990) differ significantly from the samples used in the present study. Whereas Simon and Anderson use samples containing approximately 19% Fe and 10% Mg, samples used in the present study contain 1.6% Fe and 31% Mg. This difference in Fe and Mg content may lead to a higher stability of the chlorite, as observed by Ross (1969), who reported that the rate of chlorite dissolution decreased with decreasing Fe and increasing Mg content (Gdanski 1985).

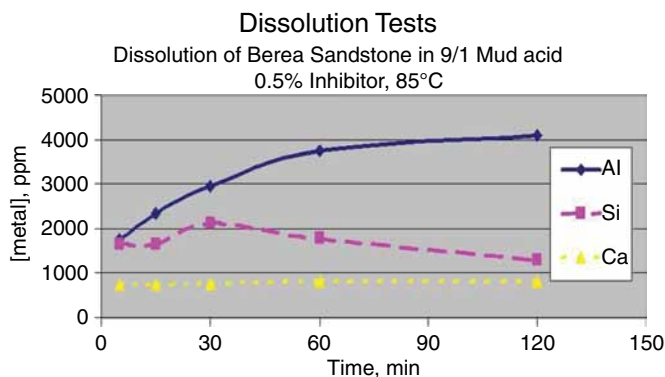


Fig. 3.44—Dissolution of Berea sandstone in 9/1 MA 85°C.

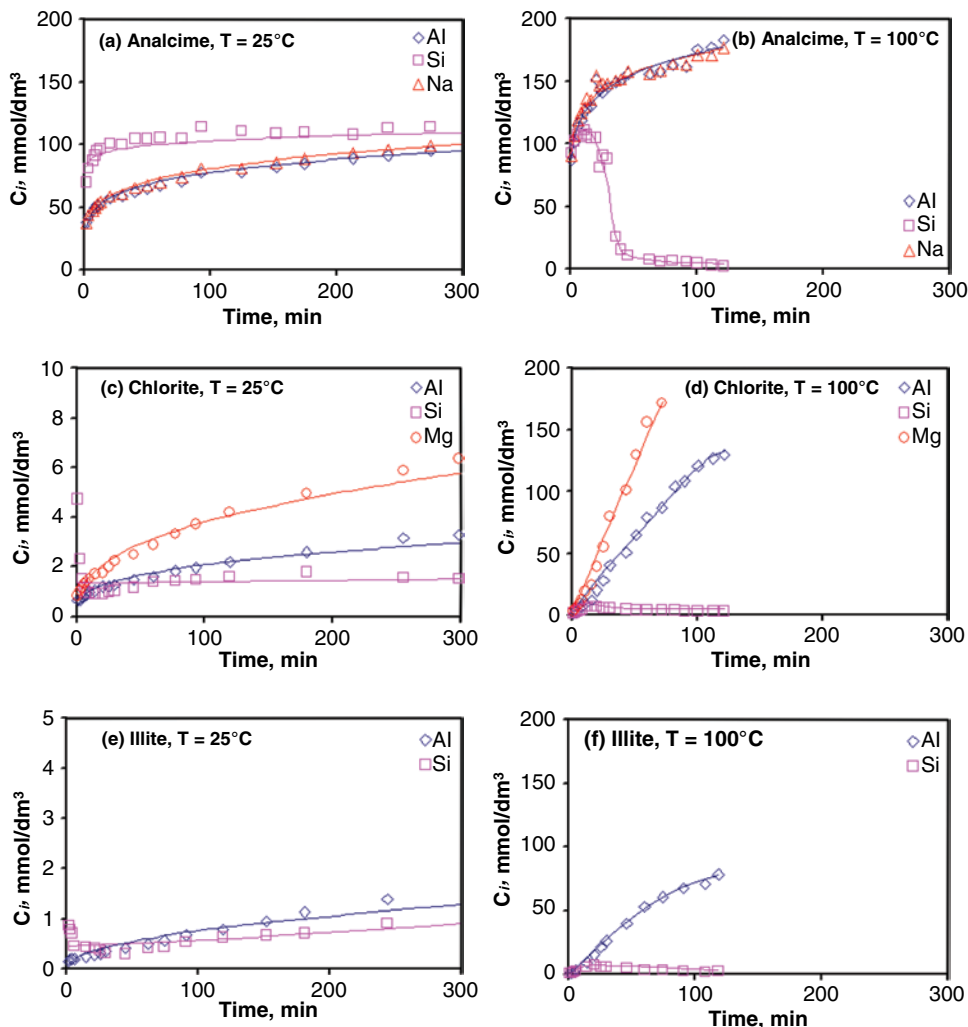


Fig. 3.45—Elemental concentration of Al, Si, Na, and Mg for the dissolution of analcime, chlorite, and illite in 15 wt% HCl (4.7 M) at 25 and 100°C.

Illite. The crystalline structure is similar to kaolin and chlorite, the dissolution of illite has previously been shown to take place at the external surface of the mineral (Gdanski 1995). At 25°C, the dissolution of illite in 15 wt% HCl resulted in either the precipitation of Si or the leaching of Al (Fig. 3.45e). For the dissolution at 100°C (Fig. 3.45f), concentration of Si reached a maximum and decreased thereafter, suggesting that precipitation occurred. The percentage of Al and Si dissolved at 300 minutes in HCl and 9/1 MA for analcime, kaolinite, chlorite, and illite were compared. See Fig. 3.46. At 25°C, nearly 45%, 1.4%, 0.4%, and 0.8% Al were dissolved for the case of analcime, chlorite, kaolin, or illite at 300 minutes (Fig. 3.46a), respectively. Roughly 33% Si was dissolved from analcime. Less than 1% Si was dissolved for the case of chlorite, kaolin, or illite (Fig. 3.46a). If no precipitation occurred, then the % Si and Al dissolved would have been stoichiometric.

Zeolites and clays are both aluminosilicates. However, analcime, a zeolite, used in the present study dissolved at a faster rate than the clays, even though the measured external surface area was an order of magnitude less than the clays (Table 3.8). This difference in reactivity could be explained by the difference in the crystalline structures of the two forms of aluminosilicates. The complex nature of zeolite structures is inherently more unstable to acid than typical layered aluminosilicates. The lattice structure of zeolites consists of a network of interconnected tunnels and cages, providing multiple internal sites for acid attack, whereas acid attack on layered aluminosilicates occurs only at the planar

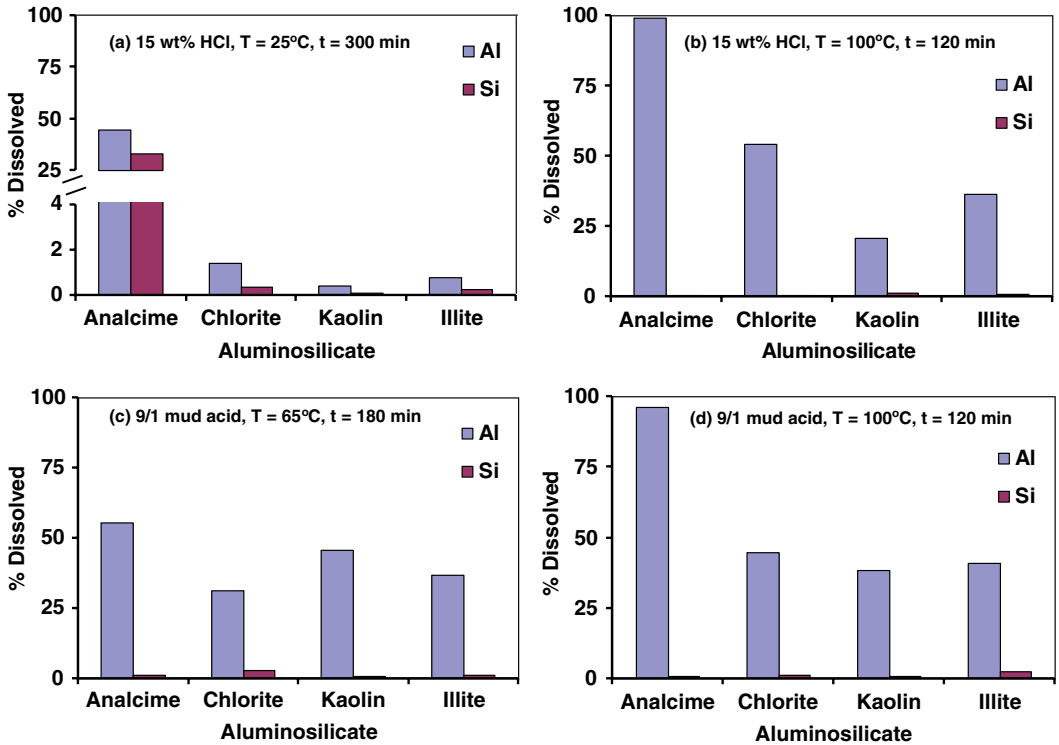


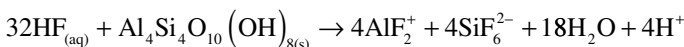
Fig. 3.46—The % dissolved of Al and Si in 15 wt% HCl at 25°C (300 min) and 100°C (120 min), and 9/1 mud acid at 65°C (180 min) and 100°C (120 min) for different aluminosilicates.

surfaces and edges. As a result, the true reactive surface area of zeolites may not be represented by nitrogen adsorption based on the Brunauer-Emmett-Teller theory (Brunauer et al. 1938), which aims to explain the physical adsorption of gas molecules. This could explain the high reactivity of analcime toward acids.

At 100°C and 120 minutes, approximately 99% Al and 0.5% Si were dissolved in the case of analcime (Fig. 3.46b). Roughly 54%, 21%, and 36% Al were dissolved for the dissolutions of chlorite, kaolinite, and illite under the same conditions, respectively (Fig. 3.46b). 9/1 MA tests were compared. The % Si and Al dissolved from analcime, kaolinite, chlorite, and illite were compared at 65°C and 180 minutes (Figs. 3.46b and 3.46c). Roughly 56%, 31%, 46%, and 37% Al were dissolved in the case of analcime, chlorite, kaolin, and illite, respectively (Fig. 3.46b and 3.46c). Less than 3% Si was dissolved for the case of all minerals. At 100°C and 120 minutes, approximately 96%, 45%, 38%, and 41% Al were dissolved during the reaction of analcime, chlorite, kaolin, and illite, respectively (Fig. 3.46d). Less than 2% Si remained in solution in each case. Similar to the dissolution in HCl, the results illustrate that a greater percentage of analcime was dissolved in the same reaction time in 9/1 MA compared to the other clays, demonstrating an inherent instability of zeolites when treated with acid formulations.

The batch reactor experimental data presented earlier were used to validate the reaction kinetics of the dissolution of kaolinite, illite, analcime, and chlorite. Reaction rate laws were obtained for each mineral and incorporated into a geochemical simulator. For example for kaolinite (Fig. 3.47), the following rate laws were used:

Primary reaction:



$$-d[\text{Al}_4\text{Si}_4\text{O}_{10}(\text{OH})_{8(s)}] / dt = A_s M_w [\text{Min}] \kappa_0' e^{(-E_a/RT)} (1 + K_0 e^{(c/T)} [\text{H}^+]^1) [\text{HF}]^1 \dots \dots \dots (3.21)$$

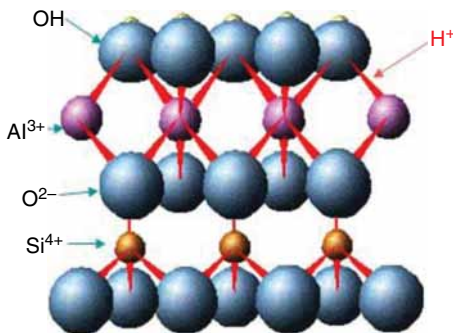
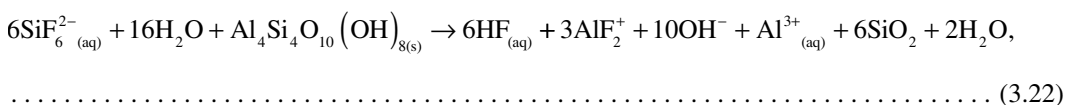


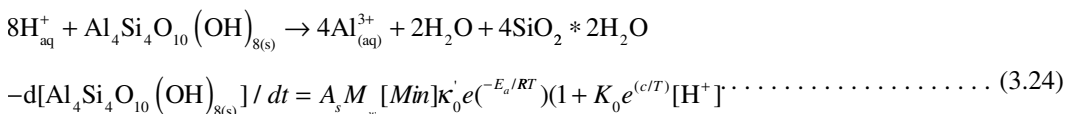
Fig. 3.47—Kaolinite structure.

Secondary reaction:

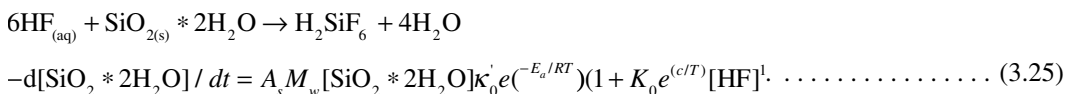


$$-d[\text{Al}_4\text{Si}_4\text{O}_{10}(\text{OH})_{8(\text{s})}] / dt = A_s M_w [\text{Min}] \kappa_0' e^{(-E_a/RT)} (1 + K_0 e^{(c/T)} [\text{H}^+]^1) [\text{SiF}_6^{2-}]^1. \dots \dots \dots (3.23)$$

Aluminum leaching reaction (see Fig. 3.47):



Amorphous silica HF reaction:



The primary reaction in the model was assumed to be catalyzed by H⁺ (Eq. 3.21). This is consistent with results by Kline and Fogler (1981). The tertiary reactions of aluminosilicates as suggested by Gdanski (1998) are not explicitly required because the equilibrium algorithm accounts them for adequately. Gdanski used a kinetic-only model for clay dissolution, and therefore, the conversion of higher aluminum fluorides to lower aluminum fluorides had to be accounted for by a separate reaction in his model. In this model, the equilibrium algorithm automatically converts the higher aluminum fluorides to lower aluminum fluorides as the solution composition changes with more clay dissolution. In this model, the conversion of higher aluminum fluorides to lower aluminum fluorides liberates HF, which reacts with the clay. Therefore, no separate tertiary reaction is required to model this phenomenon. Also, note that the authors do not include any term to reflect reaction slowdown because of silica precipitation on clay surface suggested by Gdanski (1998). Although a good match between the experimental element concentrations and the geochemical outputs suggests that the minerals reactive surface areas are not altered by amorphous silica deposition, it does not necessarily establish the validity of the argument that amorphous silica has no impact on the reaction rate of the minerals. More information is required before drawing any definite conclusion about the effects of amorphous silica on mineral dissolution kinetics.

In addition, to the experiments presented previously, a model (Hartman et al. 2006) was validated against experimental data over a wide range of temperature, pH, and acid concentrations and types. For accurate determination of the kinetics of the secondary reaction, most of the tests used in the

model validation were conducted at high clay to acid ratios. XRD analysis of the residues was used to validate the precipitation of crystalline minerals predicted by the model.

After the dissolution and precipitation of various minerals is computed, a porosity-permeability relation is required to compute the changes to permeability and, hence, the skin for the treatment. The function used to compute permeability from porosity changes in the model is

$$\frac{k}{k_0} = \prod_{i=1}^{i=N} \left[\frac{\phi_0 + M_{0,i} - M_i}{\phi_0} \right]^{\delta_i} \dots\dots\dots (3.26)$$

In this equation, k_0 , k = initial and final permeability (md), $M_{0,i}$, M_i = initial and final volume fractions of mineral, i (m^3/m^3), N = total number of minerals, δ_i = Labrid parameter for mineral i , and ϕ_0 = initial porosity.

The functional form of the porosity-permeability relationship used in the model is similar to the one proposed by Labrid (1975). However, there is one important difference. The parameter δ_i in the model is specific to each mineral and allows the mineral identity to impact the permeability, whereas the form suggested by Labrid is independent of mineral identity. In the model, the higher the value of δ_i for a mineral, the stronger the impact its dissolution or precipitation will have on the permeability. Individual values of δ_i for each mineral were determined from various core tests.

In addition to the production of secondary precipitates, problems related to the use of MA to remove damage in sandstone formations include the following:

- Rapid spending provides only a short penetration, especially at high temperatures (maximum depth about 12 in.).
- Fines, composed of either mostly quartz or mostly clay minerals, can be generated during the acid reaction and can migrate with the fluid flow. The destabilization of fines can lead to a quick production decline after treatment. Gravel-packed gas wells can exhibit a 50% productivity reduction.
- The high-dissolving power of MA destroys rock integrity at the formation face. New sandstone acidizing systems are designed to alleviate these shortcomings.

3.5.4 Sandstone Acidizing Models. Several sandstone acidizing models with varying degrees of complexity have been presented in the literature. Some of the data for these models were presented in Section 3.5.3.

Model Types. Several types of geochemical models are described in this section.

Two-Mineral Models. Two-mineral models have been presented by Hill et al. (1981), Hekim et al. (1982), and Taha et al. (1989) and have also been reviewed by Schechter (1992). In this modeling approach, the complex mineralogy of sandstones is lumped into a fast-reacting and a slow-reacting group. Schechter (1992) categorizes feldspars, autogenic clays, and amorphous silica as fast reacting and detrital clay particles, quartz grains as slow-reacting minerals and presents an analytical solution under some limiting conditions. Key learning about sandstone acidizing from this model is that there is a limit to the depth surrounding the wellbore from which damage can be removed by the acid treatment. This limit is set by the slow-reacting minerals. The acid penetration depth can only be increased by either increasing the injection rate or by reducing the reaction rate further with the slow-reacting minerals. The reaction rate can be reduced by retarding the acid formulation or by cooling down the formation.

Two-Acid, Three-Mineral Models. One of the drawbacks of the two-mineral model is that it does not account for precipitation reactions. Bryant (1991), da Motta et al. (1993), and Rodoplu et al. (2003) have shown that elevated temperatures where silica precipitation is significant, two-mineral model does not adequately describe the process. They have proposed a three-mineral model where the third mineral accounts amorphous silica precipitation. Fluosilicic acid is added as the second acid and formed by the reaction of HF with sandstone minerals. Fluosilicic acid in turn reacts with the fast-reacting minerals to produce amorphous silica, which represents the third mineral.

Geochemical Models With Kinetic-Controlled Reactions. Gdanski (2001) describes a geochemical model for sandstone acidizing in which a kinetic reaction is used to describe the reaction of the acid with each significant mineral in the sandstone. The model was used to analyze spent acidizing fluids. The model has been tuned to match the published ionic returns profiles of several HF acidizing treatments. Magnitude of fluid mixing within the matrix was also estimated from the model. It was shown that approximately two treatment volumes of aqueous production are required to recover most of the original treating fluid. The impact of mixing and ion exchange on lowering produced fluid pH long-term after acidizing treatments was also demonstrated.

Geochemical Models With Kinetic and Equilibrium-Controlled Reactions. A drawback of the geochemical models with kinetic only reactions is that the reaction rates are empirically determined and typically a large set of reaction rate parameters need to be tuned to match the data, and it is difficult to apply these parameters measured on one rock type to another. Ziauddin et al. (2002b) describe a geochemical model in which the reaction chemistry is modeled with both kinetic- and equilibrium-controlled reactions. This greatly reduces the parameters that need to be tuned empirically. They propose an equilibrium and kinetic reaction model, in which the equilibrium reactions are described by standard thermodynamic constants. Their method requires using short reservoir cores, which are much more easily available than long reservoir cores used in traditional methods. The effectiveness of the treatment design with the new technique was evaluated with a case study on a well in the Heidrun field. The author's claim that compared to alternative approaches, the new technique provides a simpler, faster, and more cost-effective method for treatment design. Furthermore, they note that the new technique also provides a more accurate scaleup to reservoir flow conditions than other design alternatives. The improved accuracy results from more precise accounting for reservoir and damage mineralogy and radial flow. Heidrun is a heterogeneous reservoir with high clay content. They found that these effects were more practical to examine with a validated simulator than with specially designed laboratory experiments. The model was also successfully applied to many other field scenarios (Ali et al. 2004).

Permeability Response. To predict the response of a formation to acidizing, it is necessary to predict the change in permeability as acid dissolves some of the formation minerals and other minerals precipitate. Generally, permeability change because of acidizing is difficult to predict, and there is no satisfactory model that applies to all rock types. However, several correlations have been proposed that provide a reasonable approximation to the change in permeability under a limited set of conditions (Labrid 1975; Lund and Fogler 1976; Lambert 1981. Panda and Lake (1995) have presented a permeability model that provides a quantitative connection among bulk physical properties of the interconnected pore system (e.g., porosity and tortuosity), the statistics of the particle size distribution, and the effects of cementing material on the permeability estimation. In addition, Quinn et al. (1997) have used this model as a part of a geochemical simulator of the acidizing process.

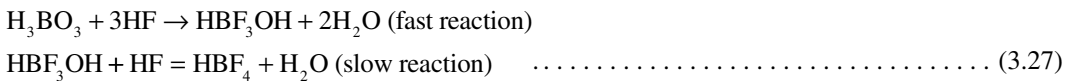
3.5.5 Acid Formulations for Matrix Stimulation of Sandstone Reservoirs. The wide variety of formation types and conditions require a number of different dissolution fluids that will remove the formation damage. The following subsections describe the base fluids that are in current (or proposed) field usage. Unless a single stage fluid is used (Section 3.5.6) an HCl or organic acid prestage is used to remove carbonates. These chemicals were reviewed in Sections 3.4.1 and 3.4.3. Note that all of these fluids will be staged with other materials and will be formulated using the chemicals described in Section 3.6.

MA. This term refers to mixtures of HCl with HF originally designed to remove drilling mud. Much of the theoretical investigations in Section 3.5.3 used MA or HCl. Hill and Schechter (2001) note that for years, the standard sandstone acidizing formulation consisted of a 12% HCl–3% HF mixture, preceded by a 15% HCl preflush. In fact, the 12% HCl–3% HF mixture has been so common that it is referred to generically as regular MA (RMA). In recent years, however, the trend has been toward the use of lower strength HF solutions such as 9% HCl +1% HF because this type of formulation reduces the possibilities of some precipitates because the pH always remains low. Figs. 3.43 through 3.46 show some dissolution tests in 9/1 MA (9% HCl + 1% HF) that were used to derive the models described in Sections 3.5.3 and 3.5.4.

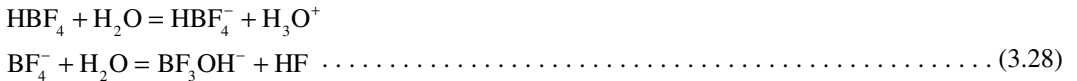
Organic MAs (where all or some of the HCl is replaced with formic or acidic acids) also are in use where the formation may be sensitive to HCl. These also have a reduced reaction rate because of relatively high pH values (compared with MA). See Al-Harbi et al. (2012) and Ziauddin et al. (2002a) for examples of tests with organic MA formulations. Additional details of formulations modified by adding organic acids or chelating agents are in Section 3.5.5. Most of the alternative formulations (Sections 3.5.5 and 3.5.6) are designed to reduce the formation of precipitates and/or the number of stages needed (Fig. 3.42).

Retarded Acid Containing Fluoboric Acid (FBA). While RMA will dissolve damage, high reaction rates, and precipitation of solids can cause problems in field use. A number of different systems have been proposed and used in the field to reduce the effects of the precipitates that occur during the use of HF-based sandstone fluids.

FBA (FBA-HBF₄) has been recommended by Thomas and Crowe (1981) as an alternative to MA. This is a retarded acid system that generates HF continually, as the equilibrium concentration of HF is consumed by the clays or silica. The total dissolving power is comparable to a 2% MA solution. In the field, FBA is prepared by mixing boric acid (H₃BO₃), ABF (NH₄F-HF), and HCl. See Eq. 3.16. FBA is formed as a reaction product of boric acid with HF:



Hydroxy FBA (HBF₃OH) may not exist in aqueous solutions unless it is in equilibrium with FBA (Wamser 1948). The slow reaction is of an order equal to unity with respect to both HF and HBF₃OH (McLeod and Norman 2001). For this reaction, equilibrium is attained at room temperature after nearly 40 minutes for a resulting 1 M HBF₄ solution. Because the equilibrium constant at 75°F is $K = 2.3 \times 10^{-3}$ (Wamser 1948), only about 6% (molar) HBF₄ is converted into HBF₃OH at equilibrium for a 1 M HBF₄ solution. These equilibrium considerations mean that at any given time and place, there is only between 0.1% and 0.2% (weight) of free HF at ambient temperature and 212°F (100°C), respectively. The dissolving power of FBA results from the generation of HF through its hydrolysis:



The hydrolysis reaction kinetics of fluoborate ions is affected by

- Concentration of the FBA ions
- Fluid pH, which has a catalyzing effect (reaction is proportional to the proton concentration)
- Temperature, through the usual activation energy term

The claim of Thomas and Crowe (1981) is that the slow release of the HF enables the acid to penetrate the matrix deeper than MA (especially at temperatures >65°C) before it is consumed by the clay and silica reactions. Because there is deeper penetration (in radial flow this converts to a much higher pour volume exposed to the acid), any effect of production of hydrated silica also is diluted.

Thomas (1979) and Thomas and Crowe (1981) also claim that the borate becomes incorporated into a “borosilicate glass” that is formed from the dissolution of the clays, and this substance acts to cement clay particles in the matrix and, thus, prevents further migration of them. This process is claimed to prevent a decrease in production that frequently is seen after an MA treatment because of clay migration. The authors show scanning electron microscope (SEM) pictures of cemented clay particles after coreflood treatments with the FBA fluid and data from the reaction of FBA with silica glass slides where boron was found as part of the surface after the reaction.

They claim also that swelling clays are desensitized by FBA, and there is a large decrease in the cation exchange capacity [e.g., a 93% decrease after 18 hours in FBA at 150°F for a Wyoming bentonite was observed by Thomas and Crowe (1981)]. Because after an FBA treatment, migrating clays

and other fines are claimed to be stabilized as a result of the rock's exposure to acid, a shut-in time is recommended in FBA treatments. Thomas and Crowe (1981) propose that during injection and while the acid spends normally, cores treated only with FBA exhibit a normal increase in permeability. However, no long-term stabilization occurs after treatment because only a portion of the clay was dissolved and the remainder did not have time to stabilize. Additional shut-in time allows this stabilization. Frequently the FBA treatment is used as a preflush to stabilize clays before an MA treatment. Because the reaction rate of HF increases with temperature and the production of HF from the FBA increases with temperature as well with $[H^+]$, the effectiveness of retarded acids is reduced as the reaction temperatures increase. Several versions of FBA acids diluted with organic acids (acetic acid and citric acid) have been used to treat some high-temperature sandstone wells. Jaramillo et al. (2010) report that more than 130 successful treatments, especially in wells with high clay content have been conducted with an organic FBA.

To provide quantitative information on the relative effects of MA and FBA, the authors of the book (Ziauddin 2012) conducted a lab test and then modeled the effects using coreflood tests of RMA and a retarded FBA (explained in the previous paragraphs) to simulate deep penetration of the acid. A short core plug represents a small part of a treatment volume in a formation. At the length scale of a short core, the permeability appears to improve after a 12% HCl and 3% HF MA treatment, but precipitation damages formation permeability just beyond that length. See Fig. 3.48, where the retarded acid (FBA) results in better permeability over the treatment volume extending 0.9 m (3 ft) or more. Permeability (k) is plotted as a ratio permeability at any location to the far-field, undamaged permeability (k_0), which is shown for comparison with the treated permeabilities (dashed line in the figure) (Ali et al. 2004).

Additional Antiprecipitation and Retarded Formulations. Several additional retarded HF acids also have been proposed and examined to reduce precipitation during sandstone acidizing.

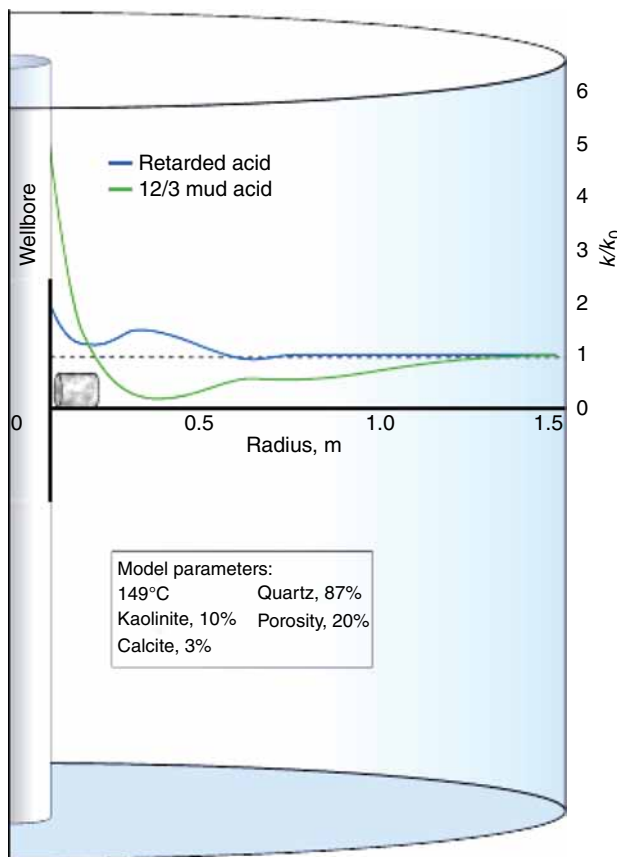
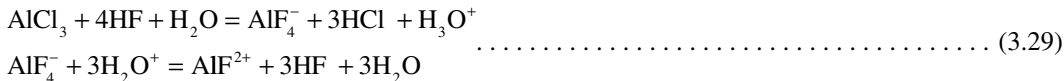


Fig. 3.48—Acid cleanup in core and near-well formation.

An acidizing system to retard HF-mineral reactions has been proposed in which aluminum chloride (AlCl_3) is added to MA formulations to complex some of the fluoride ions in the injected mixture, according to the reactions (Gdanski 1985). The retardation reactions are



This procedure is equivalent to adding dissolution reaction products to the mixture before the reactions occur (i.e., the injection of spent acid). In theory, this should slow the rates. However, the authors of this book propose that the retardation of clay dissolution has not been proved experimentally because of the prime importance of the high surface area on clay reactivity, which is much more important than a slight depletion of acid at high temperatures. The risk of early precipitation of damaging products, such as AlF_3 or fluoaluminates, is probably increased by the use of an acid that already contains aluminum ions before reaction. However, Guichard-III et al. (1996) claim an improved performance was achieved because of careful attention to reducing chemical incompatibilities. Separation of the HF fluids from the potassium chloride workover fluids and the proper choice of HCl-HF concentrations for the Wilcox formation mineralogy dramatically reduced secondary plugging from the HF treatment. The paper discusses Wilcox formation mineralogy and its susceptibility to formation damage. In addition, the paper compares conventional acid treatments to slow-reacting HF acid treatments.

Al-Harbi et al. (2012) have studied the precipitation of solids in organic MA, especially when containing organic acids and various ratios of HF. The researchers examined various solutions of different organic-HF acids, namely FA, acetic, and citric acid, that contained HF concentrations of 0.5, 1, and 1.5 wt%. Aluminum chloride or iron chloride were added separately to each organic-HF acid solution to contain 1,000, 5,000, or 10,000 mg/L of aluminum or iron (III) ions, respectively. The acid mixtures were neutralized by adding sodium hydroxide. Filtered solutions were analyzed using ICP to assess the ability of used acids to hold Al and Fe (III) dissolved ions, while formed solid precipitates were analyzed by XRD.

They found that the type and amount of precipitates were mainly dependent on solution pH, organic-HF type, and initial free fluoride concentration. All live organic-HF acids containing dissolved iron (III) showed no precipitation even after iron (III) level reached 10,000 mg/L. However, when solution pH value was raised, none of the tested organic-HF acids were able to prevent iron fluoride precipitation. On the other hand, the main factor that controlled the aluminum-fluoride precipitation was found to be F/Al ratio. It was found that there is a critical F/Al ratio, above which the aluminum fluoride precipitation occurred.

Yang et al. (2012) have also examined sandstone acid formulations containing HF and FA. In this work, FA was used to remove carbonate minerals as a preflush and with the main HF stage. A series of FA and HF mixtures with different ratios and concentrations were tested. Sandstone cores featured by different mineralogies with dimensions of 1.5 in. \times 6 in. were used in the coreflood experiments, which were run at a flow rate of 5 cm^3/min and temperatures from 77 to 350°F.

The cores were analyzed by CT scan before and after the acidizing to investigate the effect of the acid. The core effluent samples were analyzed to determine concentrations of Ca, Mg, Fe, Si, and Al by ICP. ^{19}F nuclear magnetic resonance was used to follow the reaction kinetics and products. Zeta potentials of clay particles (kaolinite, illite, and chlorite) were measured in various acid solutions.

The authors found that 9 wt% FA damaged sandstone cores. Zeta potential measurements indicated that FA can trigger fines flocculation. Addition of 5 wt% ammonium chloride helps to shield negative charges on clay surface. Analysis of core effluent samples indicated that there was CaF_2 precipitate in the core when a small volume of preflush was used. Coreflood tests highlighted that FA/HF caused loss of core permeability. The work studied the detailed chemical reactions that occurred within cores and that were followed by chemical analysis of core effluent samples and ^{19}F NMR. They determined that secondary reaction between clay minerals and HF became faster at higher temperature and decreased the ratio of Si/Al. It was also found that different clay minerals react with HF offering very different concentrations of Al and Si in spent acid. Note that similar reactions occur with MA (see Fig. 3.45).

Chang et al. (2005) claim an invention for treating a subterranean formation comprising an aqueous acidic solution, a fluoride ion source; a boron source; and an acid, or mixture of acids, which chelate aluminum ions and aluminum fluoride species, or an ammonium or potassium salt or salts of such acids. They claim that the fluoride ion source is selected from ABF and ammonium fluoride, and mixtures and the boron source is boric acid. The patent also claims that the acid that chelates aluminum ions and aluminum fluoride species can be selected from polycarboxylic acids, polyamino polycarboxylic acids, and monoamino polycarboxylic acids. A specific example is a fluoride ion from ABF, the boron source is boric acid, and the acid that chelates aluminum ions and aluminum fluoride species is selected from citric acid, malic acid, 2-hydroxyethyliminodiacetic acid, N-(2-hydroxyethyl) ethylenediaminetriacetic acid, and mixtures of them.

Di Lullo and Rae (1996) and Malate et al. (1998) propose a system that is based on acids, an HF source and phosphonates (see Fig. 3.25) that they claim can completely replace HCl in HCl:HF mixtures. The authors have compared this system with available HF acid systems and note that the new HF acid has lower reaction rate and limited solubility with clays, but higher reaction rate and dissolving power with quartz. The technology is described in a patent by Di Lullo Arias and Ahmad (1996). In this patent, the phosphonates group consists of 1-hydroxyethylidene-1,1-diphosphonic acid, diethylene triamine penta (methylene phosphonic acid), and aminotri (methylene phosphonic acid), and the HF is generated by hydrolysis of an HF precursor such as described in Eq. 3.16 using a variety of acids.

The mechanism proposed is that the mixture of the HF and the phosphonates preferentially dissolve quartz (SiO_2) grains while the clays become coated with a silica-phosphonate gel [SEM photos in Di Lullo and Rae (1996)]. Solubility tests were run to determine the effects of various acids (the method for determining solubility was not described in this document). Note that in Fig. 3.49 (Di Lullo and Rae 1996), RMA = 3% of a (12/3 HCl/HF mixture). In the paper, "RSA" is defined as "twenty gallons of HV (a solution of DETPA—Fig. 3.25) acid per 1,000 gallons of water are required to react with approximately 123 pounds of ABF to produce a 1% HF acid solution." The other fluids have HCl or acetic acid added to decrease the pH.

In the tests described in this report, the solubility of smectite was much higher in RMA than in the HV acids, and the solubility of quartz reached a plateau in the RMA and continued to increase in the HV acids. Note that the total solubility of the smectite is higher than quartz, which is in line with other data from other authors (Hill and Schechter 2001).

Malate et al. (1998) claim that the HV acid fluid, when titrated with sodium silicate, did not produce a precipitate, and the same test with RMA produced a precipitate at 12000 ppm Si. The assertion is that this fluid does not produce unwanted precipitates, even in the presence of calcite. Because part of the formulation is a powerful chelating agent for Ca, this is a reasonable expectation. Kume et al. (1999) claim the HF acid system (Di Lullo and Rae 1996) has been successfully applied on more than 30 wells over the last 2 1/2 years. Field results using the described HF acid system are claimed to demonstrate a significant increase (according to the authors) in the success ratio (greater than 400%) over conventional MA formulations.

They also claim that a consistent extension in the time to return to pretreatment production rates has been observed. An increase of 350% in the incremental hydrocarbon production, using described HF system, has been recorded over results with RMA on the same drainage points. Uchendu et al. (2006) report that this system can be applied in one-step without a preflush. The authors of the paper note that this system can be applied to sandstone formations with very low calcite concentrations. In the case histories described, the damage was formation fines in the gravel pack.

While HF acids are widely used for cleaning/removing damage from sandstone formations, Trehan et al. (2012) claim that HF acidizing in the Monterey shale has had a long history of success, dating back to a case study performed in 1999 (Rowe et al. 2004). The authors claim that the Monterey shale intervals commonly reach 1,500 to 2,000 ft in vertical height. To further complicate downhole work, intervals are not homogeneous; there are differences in natural fractures, permeability, and porosity. The authors report that with the use of various diversion methods (see Section 3.7.2) including ball sealers, foam, and benzoic acid solid diversion, large volumes of an HF acid (not identified) can be placed yielding stimulation of the formation.

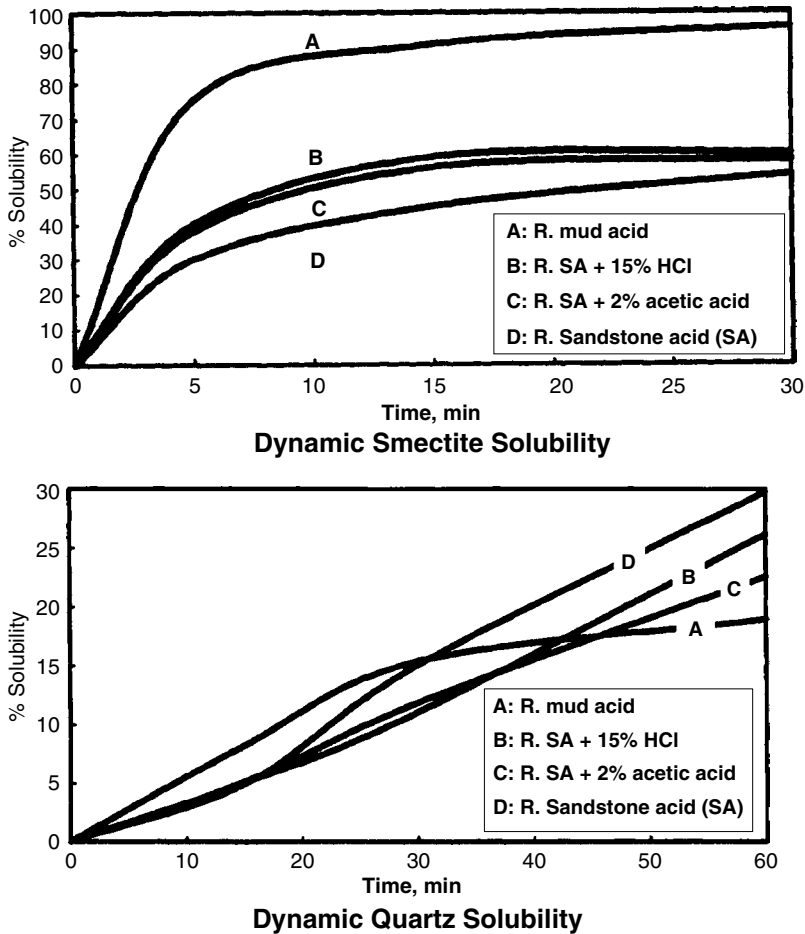


Fig. 3.49—Dissolution of smectite and quartz in HV acids (Di Lullo and Rae 1996).

3.5.6 Systems for Reducing the Number of Acid Stages. While the retarded systems described in Section 3.5.5 offer some improvements in stimulation effectiveness, sandstone acidizing still requires a multistage process. Fig. 3.42 shows the stages of a conventional four-step acid sequence that is the industry standard. Performing the process in one stage may offer significant advantages. It is possible that less fluid will be used, there is less rig time with many stages, and most importantly, all of the fluid goes into the same zone (see discussions of placement in Section 3.7). In the conventional treatments, the first fluids may alter the permeability and cause subsequent fluids to penetrate different zones. Fig. 3.50 shows a diagram of the requirements (from the authors of this book) for a single-stage sandstone fluid (SSF) that was proposed by Frenier et al. (2009a). Several different fluids including some that contain HF-containing chemicals as well as all-chelate fluids are reviewed in this section. The HF fluids are required only if clays/fines are causing the damage. It is possible to stimulate/clean some HT sandstones only by a chelate wash if carbonate scale is the damage-causing mineral.

Patents/applications by Frenier et al. (2007), Frenier et al. (2009a), Frenier et al. (2009b), and Frenier et al. (2012) teach that by predicting the formation of possible precipitates, *chelating agent* (see Section 3.4.3) formulations can be produced that may greatly minimize the formation of the major problem minerals. They claim that the formation of CaF_2 , hydrated silica, and aluminate salts can be minimized, while still maintaining the ability stimulate sensitive sandstone formations.

The key elements of the formulations cited are chemicals to provide a balance between the pH, the HF concentration, chelate concentration (and type), clay stabilizing ions such as K^+ or NH_4^+ , and other retarding agents such as borate. For example, the pH influences the reaction rate of HF with aluminosilicates and with calcite. The amount and type of the chelate affects the stability of Al salts

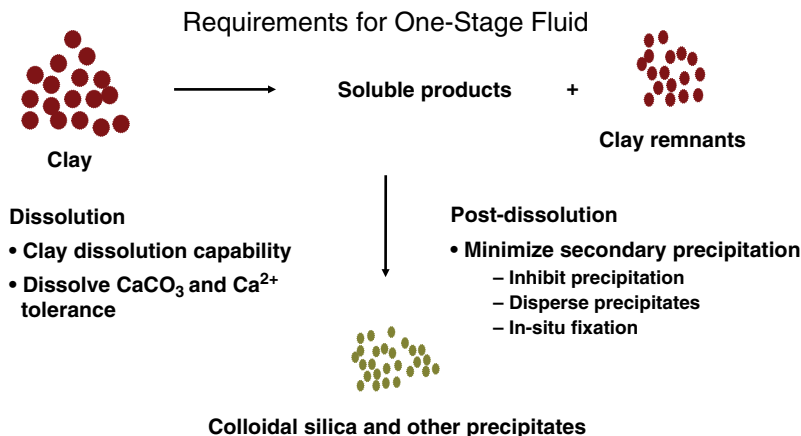


Fig. 3.50—SSF Requirements.

and the capacity to dissolve calcite. The amount of HF-forming compounds affects the rate as well as the time before silica starts to reprecipitate. Using the slurry reactor-type tests described by Hartman et al. (2006), Fig. 3.51 shows dissolution of kaolinite in DAE (see Table 3.3) as a function of ABF and how it affects the metals in solution that indicates there are optimal concentrations from some clay dissolution.

Coreflood tests were run with Berea cores and DAE at pH 6.5 with 2, 3, and 5 wt% ABF (and with 2 wt% ammonium fluoride and with/without 2 wt% boric acid). For each composition, with increasing temperature, the amount of aluminum removed and in solution increased and the amount of silicon removed and in solution decreased. The amount of calcium removed and in solution was substantial in all cases. With 5% ABF, the core permeabilities were decreased at each temperature; with 3% ABF, permeability was increased at the lower two temperatures but slightly decreased at the highest temperature. With 2% ABF, the permeabilities were closer to unchanged than with other compositions. With 2% ABF and 2% boric acid, the permeabilities were all increased, sometimes substantially, and the amounts of aluminum and silicon removed and in solution were decreased.

Tuedor et al. (2006) and Al-Harthy et al. (2008) report on tests with a chelant-containing SSF, based on the technology in Frenier et al. (2007), Frenier et al. (2009b). This fluid has been effective in stimulating Berea sandstone and field cores to temperatures as high as 375°F. Three HF-containing fluids were compared: HFS-2, an organic acid-based HF acid, HFS-3, boric acid/HF system (Thomas and Crowe 1981), and the chelate-based SSF system. Fig. 3.52 shows results of tests on damaged field cores (damaged using process) tested at 250°F. Only the new SSF stimulated the core. Fig. 3.53 shows

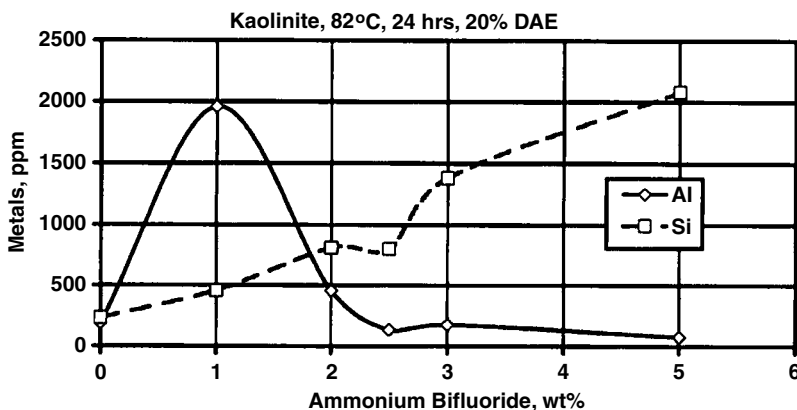


Fig. 3.51—Dissolution of kaolinite with DAE and ABF.

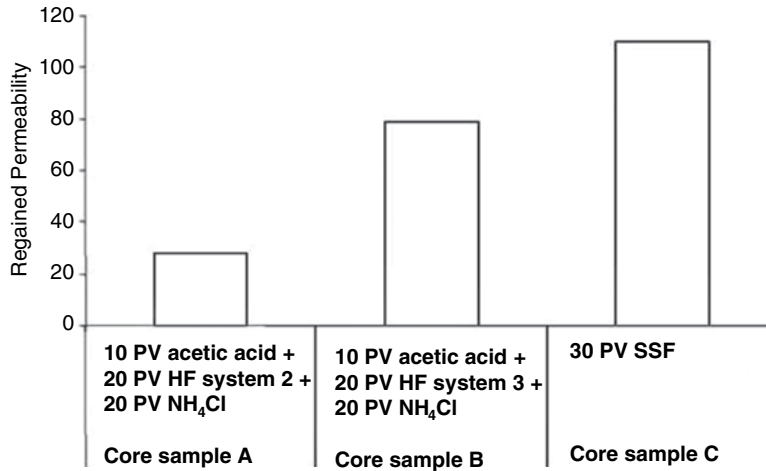


Fig. 3.52—Tests on damage field cores at 250°F (Al-Harthy et al. 2008).

the physical conditions of Berea cores stimulated by 9/1 MA and SSF at 250°F. The SSF maintained the core integrity while the MA treated core disintegrated.

Melo et al. (2012) and Rae and Lullo (2007) report that a single-stage sandstone acid that is composed of phosphonates and HF [based on the technology described previously by Di Lullo and Rae (1996) and Malate et al. (1998)] can be used without a preflush because the fluid does not precipitate CaF_2 during sandstone acidizing. Similar systems were noted in Section 3.5.5 as a way to retard damaging precipitates during sandstone acidizing. The authors also claim that this system has been used worldwide and also may limit injection damage in high-tortuosity hydraulic fractured wells.

If the formation damage consists mostly of carbonate salts (calcite/dolomite) organic acids or chelating agents may be used as a non-HF SSF. Frenier et al. (2004) has shown that HEDTA-containing fluids can stimulate Berea cores at temperatures as high as 350°F without deconsolidating the rocks. This paper also described the successful treatment of a high-temperature sandstone formulation using a pH 3 fluid.

Ali et al. (2008) report that linear coreflood test data show dramatic increases in the formation permeability after treatment with a pH 4 HEDTA chelating agent-based fluid. The improvement in permeability is ascribed to the removal of carbonate minerals and soluble clays, without secondary metal precipitation. Slurry reactor tests elucidated the kinetics of mineral dissolution in mechanically ground field samples. Treatment with acidic chelant fluids generated high levels of dissolved calcium, silicon, and aluminum that remained in solution over time. For comparison, conventional mineral acid

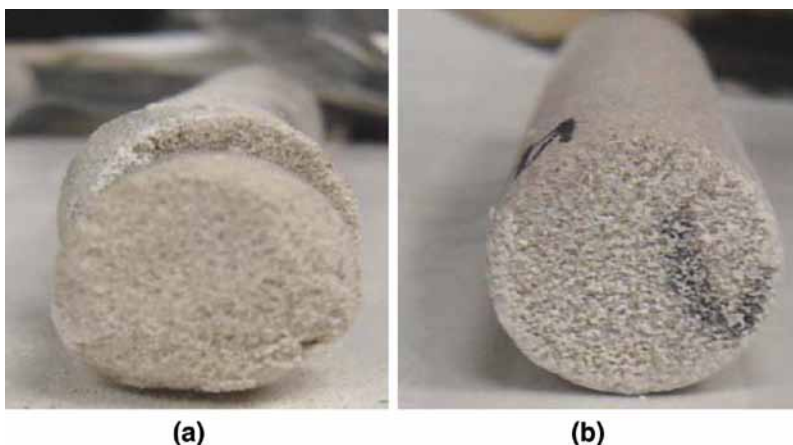


Fig. 3.53—(a) Berea core treated with 9/1 MA 250°F and (b) new SSF at 250°F.

treatment of the field samples generated high levels of metals in solution that declined over the same period of time, which is indicative of secondary precipitation. The effectiveness of the chelant fluid for stimulation of this high-temperature formation (coreflood at 300°F) was confirmed through increased formation permeability and high levels of dissolved minerals. SEM pictures (Fig. 3.54) confirm that dolomite and also some K-feldspar was removed.

Parkinson et al. (2010) note that matrix stimulation of high-temperature sandstones using HCl is difficult to achieve because of its fast reaction, possible sand deconsolidation, clays destabilization, and tubular corrosion. These problems are common in stimulating wells completed across the Pinda formation in West Africa. This formation is a multilayered formation with a wide range of carbonate content (varying from 2% to nearly 100%) and bottomhole temperatures (BHTs) in the range of 300°F. In addition, most of the wells have up to 1,500 ft of perforated intervals producing together from different layers. Stimulation treatments in the area historically have been performed using 7.5% HCl pumped through coiled tubing and using foam diversion.

They have described (Parkinson et al. 2010) a different approach that was taken to stimulate producing zones across this formation, using a low-pH chelant (pH 4) as the main stimulation fluid (without HF) and straddle or inflatable packers for mechanical diversion whenever applicable. Six wells were

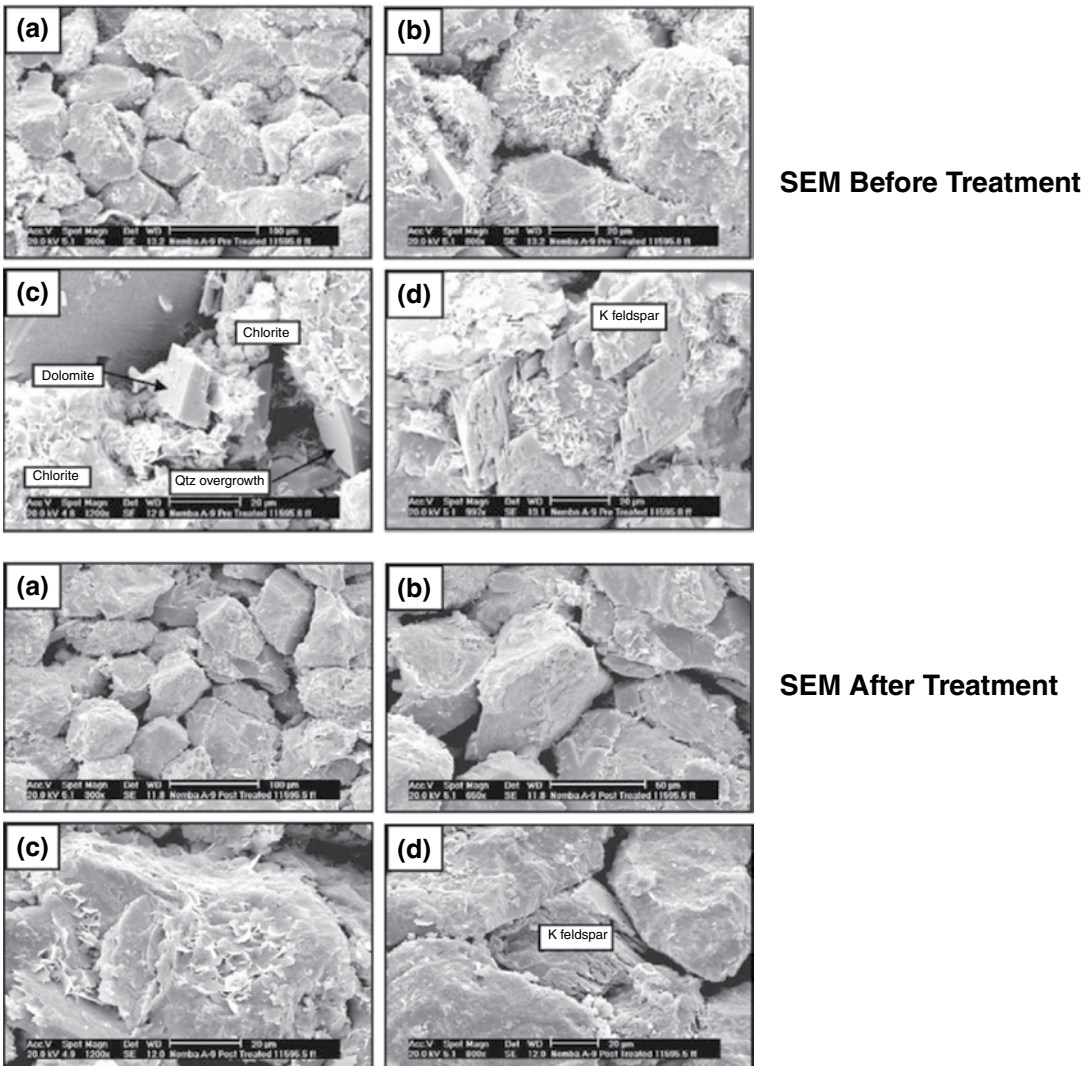


Fig. 3.54—SEM of field cores before and after treated with HEDTA fluids (Ali et al. 2008).

treated in a stimulation campaign using the chelant (based on NaHEDTA) solution. Mechanical diversion was used in three of the six wells treated; two were treated with a mechanical straddle packer and one with an inflatable packer. Low bottomhole pressure or wellbore configuration precluded the use of mechanical diversion for the other three wells; foam diversion was used instead. The results of these stimulations were encouraging, with the combined production of all six wells almost doubling. The good post-job results confirm the effectiveness of low-pH chelant in stimulating carbonate and carbonate-rich sandstones at high temperature, with the added value of low corrosion rates and reduced risk of sand deconsolidation and clays destabilization.

GLDA-based fluids (see Section 3.4.3) have also been proposed as HF-free sandstone stimulation fluids, if calcite is the major damage agents. Mahmoud et al. (2011b) describe coreflood experiments that were run at temperatures of 200 to 300°F and the concentration of GLDA was determined after the treatment. The effects of injection rate, volume of GLDA, temperature, and GLDA initial pH value were investigated on the Berea sandstone cores in the coreflood experiments. Different correlations were used to determine the core permeability after the treatment, and the correlation that gave the minimum error was determined.

GLDA showed a strong ability in chelating calcium, iron, magnesium, and it chelated small amounts of aluminum ions from the sandstone cores. At 300°F, GLDA at different pH values was able to enhance the core permeability. Decreasing the injection rate from 5 to 2 cm³/min increased the contact time between the fluid and the rock and increased the amount of dissolved ions. X-ray CT scan showed a porosity increase after the treatments at different conditions. The concentration of GLDA after the coreflood experiment was almost the same before the treatment, showing a high thermal stability up to 300°F in the coreflood experiment. The Labrid treatment (Labrid 1975) was found to be the best correlation to predict for the core permeability after treating Berea sandstone cores by 20 wt% GLDA solutions. The results of permeability tests comparing HEDTA, HCl, and GLDA are in Fig. 3.55. The data for the HEDTA are quite similar to values shown in Table 3 of Frenier et al. (2004). The new material (GLDA) appears to be the superior solvent in these tests. The actual amounts of metals removed were not shown, and a theory for the effects of the chelating agents was not proposed. However, the usefulness of these types of fluids for formation damage removal that does not require HF seems to be proven.

3.5.7 Summary of Sandstone Treatment Systems. Reduction of the skin factor in sandstone formations still requires an HF source if the damage is a clay or formation fines containing a silica or silicate.

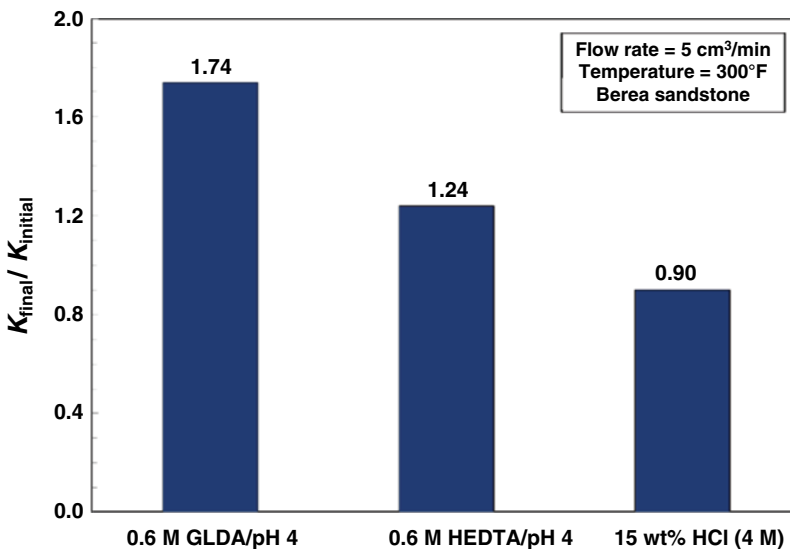


Fig. 3.55—Comparison of 0.6 M GLDA, 0.6 M HEDTA, and 4 M HCl at 300°F for stimulating Berea sandstone (Mahmoud et al. 2011b).

MA (any HCl/HF) fluid will dissolve silica and clay, but precipitates will always form and that may negate the treatment. The technologies developed and reviewed in this book have been partially successful in improving the matrix cleaning process. Improvements include

- Retarded HF acids (organic HF, FBA, Al salts)
- Reducing the number of stages using chelating agent based fluids
- High temperature (chelating) acids that will not damage a sandstone formation
- Improved diverting systems (Section 3.7)
- A solvent that does not contain HF would still be preferred but is not yet available

3.6 Additives—What Is in the Reactive Fluid?

The reactive stimulation fluid (for carbonate, sandstone, matrix, and fracturing applications) contains the chemicals that *react* (dissolve) the formation or the damage plus a number of “additives” that aid or improve the process in various ways. This section will describe the functions and mechanisms of these additives. For more details (especially of the individual chemicals) refer to Ali and Hinkel (2001), Kalfayan (2008), Kelland (2009), Fink (2003), and Fink (2011). The agent types that are discussed in this section are

- CIs
- Surfactants—wetting agents, dispersants, and foaming agents
- Water-soluble organic solvents—simple alcohols and mutual solvents
- Iron/sulfide control agents—complexers and reducing agents
- Clay stabilizers
- Water-insoluble solvents—hydrocarbons used in emulsions
- Diverting agents—described in more detail in Section 3.7.2
- Various miscellaneous additives including scale inhibitors
- Emulsions for frac acid or reaction control—described in detail in Section 3.8.3

Each reactive stimulation fluid and job will have some of these components but usually not all of them. Various computer-aided planning systems help plan the fluids and pumping rates, taking into account the chemistries described in this chapter. See stimulation models and planning aids in Sections 3.3.3 and 3.6.5.

Table 3.10 shows a list of typical components in stimulation fluids formulations and their concentrations. Details of the specific chemicals are in Sections 3.6.1–3.6.4.

CIs are listed first (after the active solvent) because (as an opinion of authors of this book) they are a requirement for a successful treatment. Thus, while essentially all reactive fluids will contain a significant amount (up to 5 vol%) of a CI formulation and usually a wetting agent, the importance of the

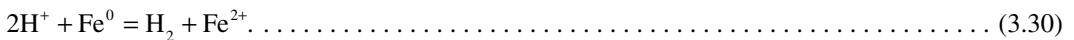
| <u>Component</u> | <u>Chemical Types</u> | <u>Concentration Range</u> |
|-----------------------------------|---|----------------------------|
| Active chemical dissolution agent | HCl, chelating agents, acetic acid, HF, other solvent molecules | 0.5–28 wt% |
| Corrosion inhibitor | Surface filming formulation | 0.5–2 vol% |
| Inhibitor aids | KI, formic acid, metal salts | 0.5–2 wt% |
| Wetting/foaming agents | IST reducing agents | 0.2–2 vol% |
| Demulsifiers | Retard O/W emulsions | 0.5–2 vol% |
| Mutual solvents | Alcohols and glycol ethers | 0–20 vol% |
| Iron control agents | Reducing and chelating agents | 0.5–2 wt% |
| Clay control agent | Clay stabilizing/adsorbing | 0–1 wt% |
| Diverting agent | Polymer, VES, solids | 0.5–2 vol% |
| Emulsifier/hydrocarbon | Acid emulsion (frac acid or rate control) | 20–30 vol% |

other additives depends on many factors. These include the formation to be treated, the temperature of the well, well construction metallurgy, the location and type of the completion and the chemistry of reactive fluid. Some of these additives may significantly increase the cost of the treatment, and affect the stability of the formulation as well as the functioning (see choice of the CI). Therefore, the selection requires significant analyses.

3.6.1 CIs for Reactive Fluids. Inhibitors for control of corrosion during most production operations were described in Section 2.2.3. However, essentially all of the solvents employed for reactive stimulation and scale removal, as well as some of the solvents for organic deposits, are corrosive to some metals of construction. Note, also, that significant amounts of HCl are used as the spearhead/break-down fluid for many hydraulic fracturing operations (see Section 4.10.1). The majority of downhole equipment requiring treatment and through which the fluid flows into the formation will be constructed of iron-based alloys. These include carbon and alloy steels. Copper-based alloys are less likely to be encountered in the downhole environment but may exist as part of a surface instillation. These metals will be attacked by the aggressive solvents (mineral acids, organic acids, and chelating agents), unless the reactive fluids contain CIs. An uninhibited solvent would damage the equipment being cleaned and the corrosion would consume the expensive solvent. This is true even for neutral or less acidic (pH 4) solvents. Thus, without the use of CIs, most chemical descaling and reactive stimulation operations should not be performed.

This section will provide a short review of the technology required to protect oilfield equipment from devastating attack during application of reactive fluids. Chemicals (these are generally different than the production inhibitors described in Section 2.2.3) are currently available to protect downhole metal to temperatures approaching 400°F, but the time of contact, the type of the fluid, as well as metallurgy have to be carefully considered before selecting the treatment details.

Reactive Fluid Inhibitor Mechanisms. In most oilfield operations, the corrosion reaction that the inhibitor must minimize is acid attack of some type. The electrochemical equation is



This type of acid attack takes place in HCl, organic acids, and chelating agents, including formulations that have pH values as high as approximately 9, especially if they contain ammonium (NH_4^+) ions. The rate of corrosions can vary by several orders of magnitude depending on the acid strength and temperature. In very general terms, the amount of damage potential increases with acidity and temperature, but most chemical stimulation agents are corrosive and require use of CIs. The review references cited below give much more information about corrosion in general. Other types of corrosion such as pitting and stress corrosion cracking also may occur but usually are initiated by acid attack.

An inhibitor formulation that is actually used in a well treatment has a number of components including

- The active ingredient that provides most of the inhibitor protection
- A surfactant to help disperse the inhibitor
- Solvents to make a one-component mixture
- Inhibitor aids to improve performance in special conditions (such as high-temperature or high-alloy steel)

These components affect the use range (such as acid strength and temperature) as well as the overall impact of the inhibitor on the environment. The other components of the formulation especially the surfactants and the solvents can significantly influence (usually negatively) protection values and must be tested as part of inhibitor selection.

A brief review of reactive chemical inhibitors is presented in this book to compliment the dissolution chemistry presented. For more details see Frenier and Ziauddin (2008), the review by Riggs (1973), and applications to chemical cleaning processes by Oakes (1972), and Frenier (2001b). Also refer to the excellent reviews in *Corrosion Inhibitors*, which is from Kuron (1995). Additional information

on inhibitors is included in the compilations of Robinson (1979), Rozenfeld (1981), and Frenier and Growcock (1989).

The mechanisms, by which many CIs function, were elucidated over the past 50 years. The reader is referred to the treatise by Damaskin et al. (1971) for an introduction to this subject. The cartoon in Fig. 3.56 shows a generic mechanism where two different types of inhibitors are protecting steel in the solution containing HCl, which include an acetylenic alcohol (ethyl octynol) and a pyridinium quat. In this case, there is no iron salt present, and the surface is covered in adsorbed Cl⁻ ions. The inhibitors are attracted to this anionic surface and, thus, adsorb. The interaction of these materials with the iron surface produces an adherent film that may include polymers (Growcock et al. 1985). These may be on the surface formed by the electro reduction of the unsaturated alcohol.

The most successful inhibitor formulations for organic acids and chelating agents require different chemistries from those needed in the mineral acids. They frequently contain amines, reduced sulfur compounds, or combinations of a nitrogen compound (amine, quats, or polyfunctional compound) and a sulfur compound. The only major exceptions are the sulfonium compounds (Frenier and Settineri 1973).

Jofa (1965) investigated the mechanism of mixtures of quaternary ammonium or alkyl ammonium compounds used with sulfur compounds, such as thiourea. He concluded that the sulfur compounds form HS⁻ ions in solution. These adsorb onto the iron surface, thus attracting the cationic amine inhibitor.



The author of this book believes that the nitrogen/sulfur inhibitors function in a similar manner in the chemical dissolution solvents. The sulfur-containing inhibitors may be required to protect some of the special alloys found in nuclear steam generators (Hausler 1983). Currently, there is no complete explanation for the specificity of these metals for the nitrogen/sulfur combination.

CI Chemistries for HCl. An examination of the references described reveals that HCl solvents usually require quaternary nitrogen or amine-based formulations plus an unsaturated oxygen compound. The other (non-HCl) reactive formulations require a nitrogen compound plus sulfur-containing molecules. Virtually, all commercial scale cleaning/formation stimulating inhibitor formulations currently contain these active ingredients. However, more environmentally acceptable materials also may be in use.

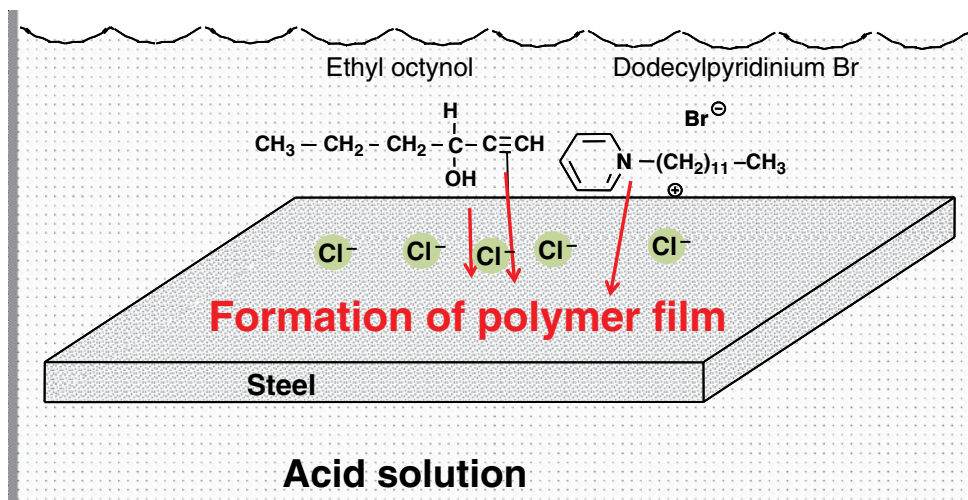


Fig. 3.56—Formation of polymer film in HCl from acetylenic alcohol and quat.

This short section involves chemistry that is a variation on the themes described by Frenier and Ziauddin (2008), but inhibitors specially developed for oil field use are highlighted. Many commercial acid inhibitors used in well acidizing services were based on the Mannich condensation reactions introduced by Saukaitis and Gardner (1956). See also Mansfield et al. (1959) and Monroe et al. (1963). This process uses formaldehyde, an amine, and a ketone to produce a “Mannich base” (Fig. 3.57). Because this reaction rarely goes to completion, some formaldehyde will remain in the reaction product that is formulated as the commercial inhibitor. Formaldehyde has been shown to be an animal carcinogen and appears on the OSHA Specifically Regulated Substance List and the National Toxicity Program Source List 9C (compilation of carcinogens). Therefore, it is desirable to remove this substance from inhibitor formulations.

Research has shown that some of the active ingredients in the Mannich reactions are phenyl ketones (Fig. 3.58). See Growcock and Lopp (1988), Frenier et al. (1988), and Frenier et al. (1991).

In addition to a condensation reaction product, commercial acid inhibitor formulations frequently contain *acetylenic alcohols* (Beale and Kucera 1966) such as propargyl alcohol, hexynol, or ethyl octynol. While these materials can produce excellent CI packages, many acetylenic alcohols are quite toxic to mammals and the lower alcohols (propargyl alcohol and hexynol) are readily absorbed through the skin. For these reasons, there is a growing necessity to produce CIs that are less toxic than current formulations.

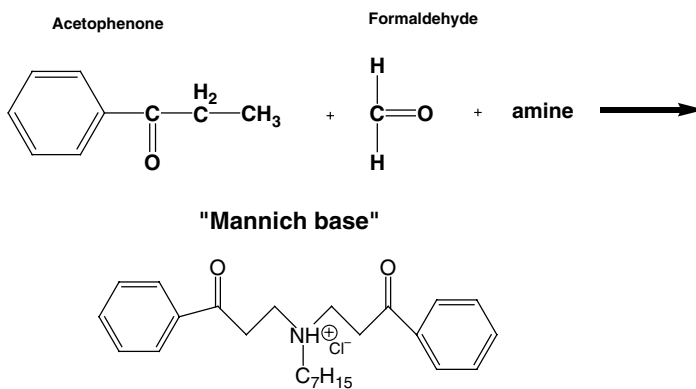


Fig. 3.57—Mannich inhibitor.

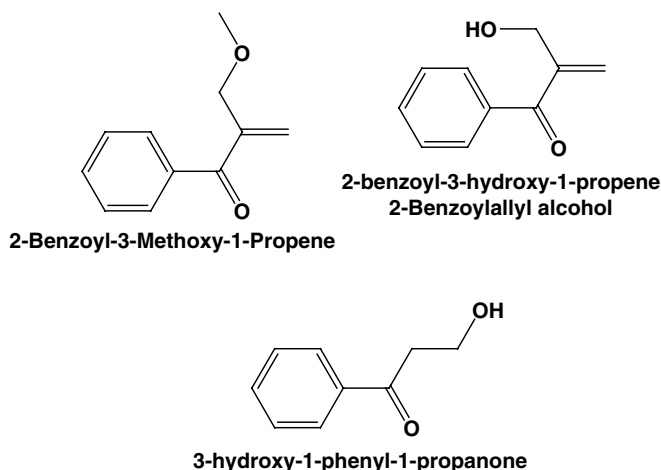


Fig. 3.58—Phenyl ketone inhibitors.

Frenier and Growcock (1988) described formulations of α,β -unsaturated aldehydes with surfactants that were shown to be effective CIs for steel in HCl. Based on this technology, the aromatic compound trans-cinnamaldehyde (also a natural product) was proposed as an ingredient in low-toxicity inhibitor formulations (Frenier and Growcock 1990). According to Growcock et al. (1989), this aldehyde adsorbs onto the surface of the steel, and then forms a low-molecular-weight polymer film that enhances the corrosion protection. A low-toxicity commercial inhibitor (Frenier 1996) formulation based on cinnamaldehyde was developed for use in HCl-based cleaning formulations. It is suitable for use in solvents containing HCl or HCl containing ABF. The inhibitor protects a variety of steel alloys as well or better than currently used commercial acid inhibitors. Various oxygen containing inhibitors are in **Fig. 3.59**.

Corrosion rates for the low-toxicity formulations (Frenier 1996) were compared with a classic Mannich-based inhibitor that contains formaldehyde and hexynol. In most of the tests, the low-toxicity inhibitor provided similar or superior inhibition compared to the classic acid inhibitor.

A very large number of nitrogen quats are also used in acid inhibitor formulations. These include (Voderbruggen and Williams 2000) alkyl pyridine quaternary salt, chloromethyl naphthalene quaternary salt, alkyl pyridine-N-methyl chloride quaternary salt, alkyl pyridine-N-benzyl chloride quaternary salt, quinoline-N-methyl chloride quaternary salt, quinoline-N-benzyl chloride quaternary salt, quinoline-N-(chloro-benzyl chloride) quaternary salt, isoquinoline quaternary salt, benzoquinoline quaternary salt, chloromethyl naphthalene quaternary salt, and mixtures thereof. The nitrogen quat (usually aromatic, such as pyridine or quinoline) are thought (Schmitt and Olbertz 1980) to adsorb by interaction with the Cl⁻ coated iron surface and through the aromatic electrons in the ring. The exact mechanism of the positive interaction between the quat and the oxygen compound is not known.

Several parts of the formulation may contribute to toxicity or environmental problems. Quaternary ammonium salts usually are synthesized in a polar solvent such as isopropyl alcohol. While this chemical is an excellent solvent for the reactants and the final formulation, the inhibitor will have a flash point <140°F and, thus, will be labeled as flammable. Therefore, one of the goals (Frenier 2003) was to eliminate this alcohol from the formulation. Duffin (1964) has shown that the solvent can drastically affect the kinetics of a quaternization reaction, so it was not clear that a different solvent would allow the reaction to proceed to completion. **Fig. 3.60** shows many of the quats in use and their synthesis.

The reaction of pyridine with an alkyl bromide (bromododecane in this case) is known as the Menshutkin reaction. It was used as the model reaction to determine the affect of the reaction solvent on the production of a pyridinium bromide salt that could then be formulated to produce some of the test inhibitors. The dodecylbenzylpyridinium bromide reaction was run using equimolar amounts of

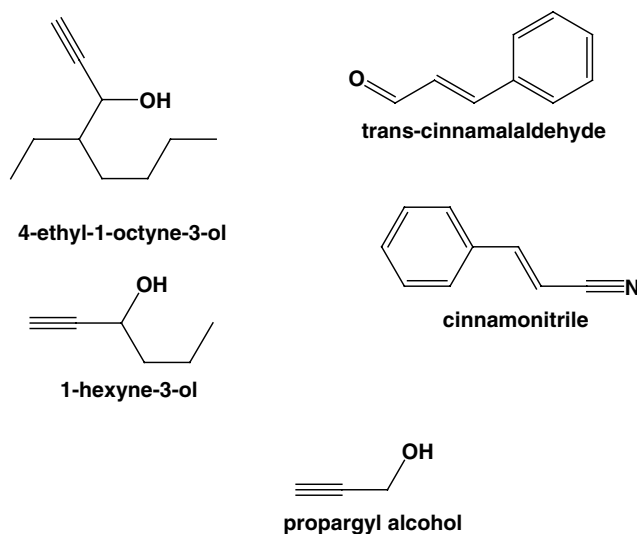


Fig. 3.59—HCl fluid oxygen containing inhibitors.

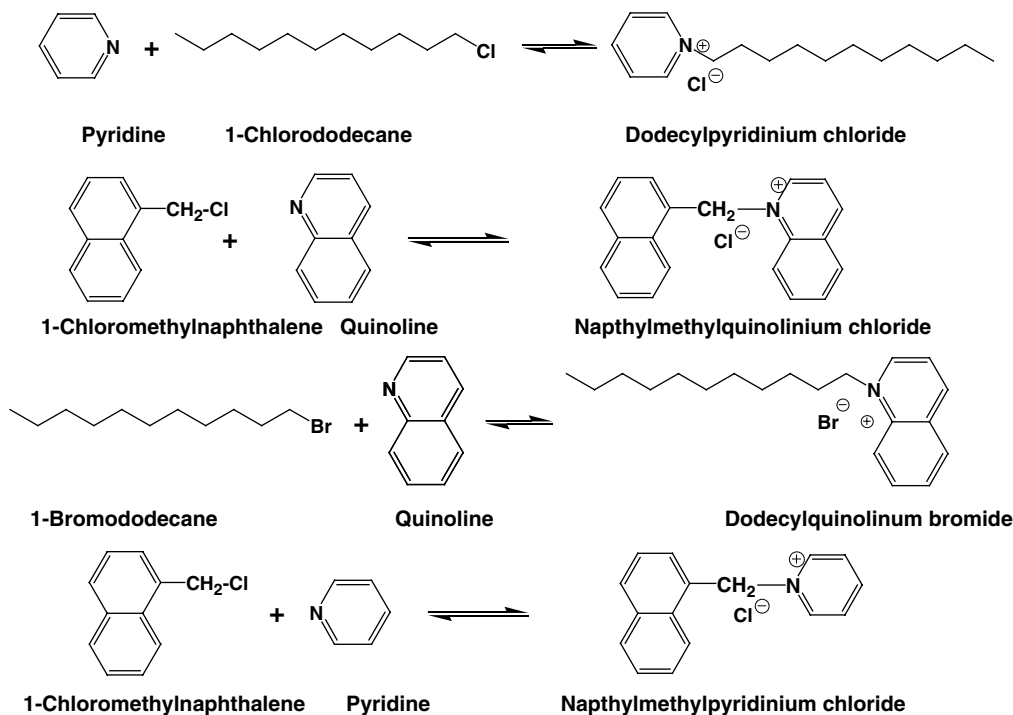


Fig. 3.60—Nitrogen quats corrosion inhibitor components and synthesis.

pyridine and bromododecane in 43 wt% solvent at 200°F. This process has been used to produce less hazardous commercial inhibitor products (Frenier 2003).

The need for greener and less toxic acid inhibitors has lead to some localities to request materials that do not contain quaternary ammonium salts. Note that some quinolone-based compounds are on the Priority Pollutant List (USEPA 2011b). While oxygen-based acid CIs are also in commercial use (see Figs. 3.57, 3.58, and 3.59), they are usually formulated in conjunction with quats (Fig. 3.56).

Sitz et al. (2012) discuss successful efforts in developing new all oxygen-based acid CIs that are biodegradable, nonbioaccumulating, and low in toxicity that meet industry standards for protection of carbon steel oilfield tubing up to 120°C. These are environmentally acceptable inhibitors with the appropriate dispensability and performance characteristics needed for critical applications in environmentally sensitive areas. The goal was to formulate an inhibitor that contained only environmentally acceptable components. The final formulations (Sitz et al. 2012) contain no propargyl alcohol, pyridine, or quinoline quats, US EPA Priority Pollutants, BTEX, methanol, ethylene glycol, or ethylene glycol monobutyl ether (EGMBE).

Usually derivatives of imidazolines are used effectively as production inhibitors in acidic *well fluids* [see Frenier and Ziauddin (2008), and Chapter 4 and Fig. 2.10 of this book]. However, Fan et al. (2012) have claimed the reaction product of Tung oil (contains eleosteric acid) with diethylenetriamine to give a substituted imidazoline amine. The material (Fig. 3.61) was found to be an effective inhibitor in 1N HCl at temperatures up to at least 90°C.

Because of the very high temperatures found in oil and gas wells, inhibitor aids frequently must be used (Frenier 1989; Frenier 1992; Jasinski et al. 1988; and Jasinski and Frenier 1992). The aids include FA, copper salts as well as antimony compounds. Jasinski and Frenier (1992) claimed formulations containing naphthylmethyl quinolinium chloride and antimony chloride as an inhibitor. Williams et al. (1992) and Williams et al. (1993a) claim inhibitor formulations containing antimony salts and quaternary compound such as quinoline-N-benzyl chloride to be less toxic than inhibitors that contain acetylenic alcohol. Williams et al. (1993b) then claim formulizations containing bismuth (such as BiOCl) and quaternary compounds such as claimed to be less toxic than the antimony and

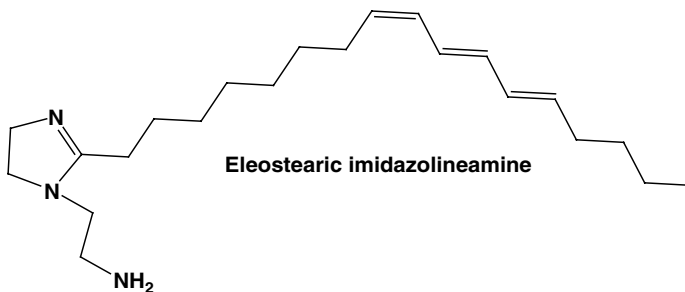


Fig. 3.61—Eleosteric imidazolineamine.

acetylenic-containing formulations. Brezinski and Desai (1997) have claimed a lowered toxicity acid inhibitor aid system for high temperature HCl. It consists of a mixture of KI and FA. Both of these materials have been used for many years (individually) as acid CI intensifiers (aids).

CIs for Organic Acids and Chelating Agents. As noted in previous paragraphs and **Table 3.11** (which gives a short review of corrosion inhibition requirements and the use of different types of inhibitors for different metals, solvents, and temperatures), the compositions needed to protect steel in HCl differ from those needed for organic acid fluids because of different surface chemistries present (Eqs. 3.31–3.33). A lower hazard CIs for use in the organic acid and chelating agent cleaning formulations were developed by Frenier (1997). This material also was shown to inhibit sulfuric acid containing solvents. This formulation does not contain formaldehyde, ethylene glycol derivatives, or any known carcinogenic materials. Through the use of a new synthetic procedure (Frenier 1998), it also does not contain isopropyl alcohol. Thus, the resulting formulation has a flash point that is >200°F. It contains quaternary nitrogen salts, an organic sulfur compound, and a nonionic surfactant.

Jenkins (2011a) has claimed an environmentally friendly CI formulation for chelating agents and organic acids that have a composition including an acid, water, and an effective amount of a CI composition (including at least one mercapto compound and at least one alkoxyated acetylenic alcohol). Examples of the mercapto compounds are 2-mercaptoethanol and the alkoxyated acetylenic alcohol includes prop-2-yn-1-ol.

CIs for use in stimulation fluids must be rigorously tested using high-pressure equipment and the actual metals that may be found in the treatment path. Unfortunately, there is no standard method for evaluation of inhibitors and fluids. Each vendor uses slightly different procedures. Hill et al. (2003) described some of the procedures required for development of inhibitors that include a number of ecological and toxicity characteristics as well as safety-related issues such as flash point and mammalian toxicity.

TABLE 3.11—INHIBITOR SELECTION FOR OILFIELD SCALE REMOVAL FLUIDS

| Fluid | Temperature Maximum (°F) | Metallurgy | Generic Inhibitor Type | Inhibitor Aid |
|------------------|--------------------------|-----------------|---|----------------------------------|
| HCl/HF | 250 | All | Ammonium quat and unsaturated oxygen compound or all oxygen chemicals | None |
| HCl/HF | 350 | Carbon steel | Ammonium quat and unsaturated oxygen compound | Formic acid or KI |
| HCl/HF | 350 | Chromium steels | Ammonium quat and unsaturated oxygen compound | Formic acid Antimony chloride |
| Organic acids | 200 | All | Ammonium compound and reduced sulfur compound | None |
| Organic acids | 400 | All | Ammonium compound and reduced sulfur compound | None or KI of CuI |
| Chelating agents | 400 | All | Ammonium compound and reduced sulfur compound | None |

Many of the additional acidizing additives are used to remove/prevent various damage types or to affect wetting of the formation during fluid placement. Ali and Hinkel (2001) have provided a chart (Fig. 3.62) to show how many additives are related to the damage present or to a formation characteristic.

3.6.2 Surface Active Agent Additives (Surfactants, Mutual Solvents, Alcohols). The reader may review the discussion of surfactants in Section 1.4.2. Ali and Hinkel (2001) note that surface-active agents are used in acidizing to break undesirable emulsions, reduce interfacial tension (IST), alter wettability, speed cleanup, disperse additives, and prevent sludge formation. The use of surfactants requires careful selection of an appropriate molecule. It is the opinion of the authors of this book that during the design of many well treatments, surfactants are selected with little or no laboratory data to support the choice and sometimes without full knowledge of their properties at the conditions in which they will be applied. Improper surfactant selection can lead to results contrary to those intended and may be detrimental to the success of the treatment.

The three major types of surfactants include anionic, cationic, and nonionic chemicals. The anionic and cationic surfactants have a formal negative (anionic) positive (cationic) charge on the organic part of the molecule that is balanced by the opposite cation or anion. These usually are simple ions such as Cl^- , Na^+ , or a nitrogen cation such as NH_4^+ . Fig. 1.8 shows simple structures that include the three basic types of surfactants: cationic, anionic, and nonionic. The use of these materials is to lower the IST and allow the surfactant (acting as a detergent) to remove hydrocarbons and, thus, to wet the mineral surfaces by the active dissolution molecules. Tests by the authors of this book have shown that various surfactants including amphoteric alkyl amines, ethoxylated sulfates, alkyl ethoxylate, alkylphenylethoxylates, and fluoro quat surfactants may lower the water/air IST from approximately 65 dynes/cm^2 to $< 30 \text{ dynes/cm}^2$. Note (Section 3.6.1) that different and possibly several surfactants are part of an acid CI package.

The use of surfactants to resolve production oilfield emulsions was described in Section 2.4.4 and some structures of small molecule surfactant DMs are seen in Fig. 2.56. Some of these types could also be used in acids. The role of surfactants and mutual solvents in reactive stimulation should affect the wetting properties of the aqueous fluids, or to change an oil/water/solid interface. Abdallah et al. (2007), in Section 1.5.3, Fig. 1.34, describe a mineral surface that has an oil drop on it. The forces that

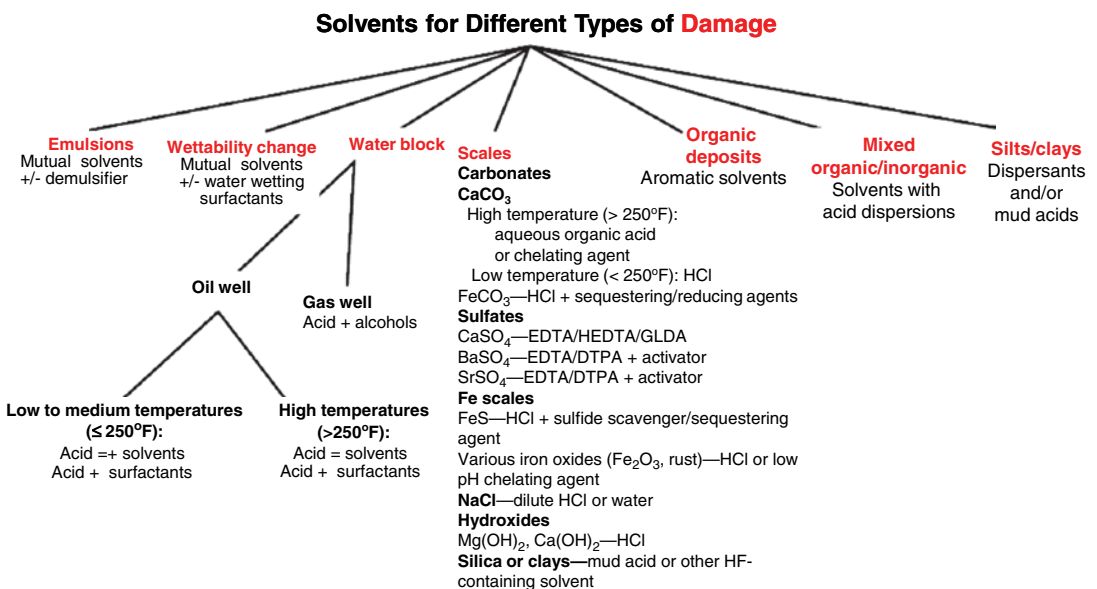


Fig. 3.62—Damage types and solvents.

cause the surface to be either oil-wet or water-wet on the intermediate cases are defined by the balance of forces described by the surface forces (tensions-ST) of the surface-oil (γ_{so}), oil-water (γ_{ow}) and the surface-water (γ_{sw}). See Fig. 1.36 with the caution about the different conventions for defining wetting. In Fig. 1.34, θ is the contact angle between two of the phases. The function of the surfactants and the mutual solvents is to reduce the surface tension of the surface and the water so the solution can water-wet the interface. This affects removal of any oil phase and allows the reactive chemicals to dissolve the mineral. A mutual solvent also will dissolve or disperse all or some of the oil or an organic foulant such as wax or asphaltene (see Frenier et al. 2010). Some surfactants also will disperse an organic solid or phase.

Fig. 3.63 shows some of the common mutual solvents. They are frequently used at high (10% or more) concentrations to help keep the entire acid mixture dispersed as well as to affect solubility of some organic molecules (Dabbousi et al. 1999). All of these materials can be effective in different acid formulations; however, Wylde and O'Neil (2011) note that 2-butoxyethanol (EGMBE) has come under scrutiny in North America [e.g., prompting Environment and Health Canada to add it to the Schedule 1 of the Canadian Environmental Protection Act-HealthCanada (2011)]. Precautions need to be taken when working with 2-butoxyethanol because of toxicity concerns. Exposure to high levels has led to reported nose and eye irritation, headaches, and vomiting. These authors recommend a replacement (identified as an alkoxyated solvent). The authors of this report (Wylde and O'Neil 2011) claim that propylene glycol-based solvents generally are less toxic than EGMBE (Frenier and Brady 2008).

Comparing the two figures, (Figs. 1.8 and 3.63), it is seen that the mutual solvents are essentially very short-chain nonionic surfactants.

Methods to determine properties of wetting angles are in Section 1.5.3. Another use for surfactants is to create a foam (usually of nitrogen or carbon dioxide) to energize the fluid (see Sections 1.4.4 and 3.7.2 on foams and foam diversion). The gas pressure enables the fluid to be more easily removed from the formation after the job is finished and also may act as a diverting agent. Because a foaming agent does lower the gas/water surface tension, it also may act to water-wet the mineral surface and usually only one surfactant will be present, but a mutual solvent also may also be added.

Dabbousi et al. (1999) conducted a comprehensive study of a number of the additives described in this section to determine the effects on the IST (and thus the water-wetting) of HCl fluids. A Krüss

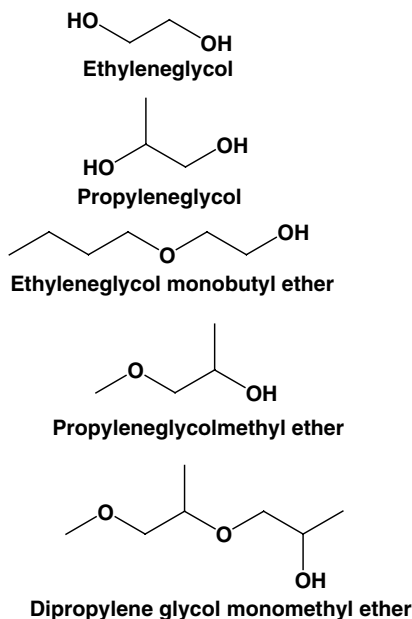


Fig. 3.63—Mutual solvents.

tensiometer (Model K-12) was used to conduct surface tension measurements, the fluids these authors examined included HCl, acetic, citric, formic, and combinations of these acids. Stimulation additives tested were mutual solvent, short-chain alcohols, CIs, hydrogen sulfide scavengers, iron-control agents, and clay stabilizers. In addition, the effects of three classes of surfactants (nonionic, cationic, and anionic) on surface tension of acid solutions also were investigated.

Significant conclusions observed include

- Acetic and FAs had lower surface tension values than HCl, especially at high acid concentrations.
- The surface tension of HCl can be reduced by mixing with acetic acid.
- Ionic surfactants reduced surface tension of HCl more than the two nonionic surfactants tested.
- The three CIs examined reduced surface tension up to a critical concentration beyond which they had no effect on surface tension.
- EGMBE lowered the surface tension of acetic, formic, and HCl acids up to 10 wt%. Increasing the concentration of EGMBE above 10 wt% had no significant effect on the surface tension of these acids.
- Short-chain alcohols reduced the surface tension of 15 wt% HCl, with the greatest reduction obtained for n-butanol.
- Citric and erythorbic acids (EAs), which are usually used as iron control agents, significantly reduced the surface tension of 15 wt% HCl. Clay stabilizers did not reduce the IST.

See the additional discussions in Ali and Hinkel (2001) and Kam et al. (2007) and simple structures (Fig. 1.8).

Simple alcohols (predominantly isopropyl alcohol and methanol) are used in acidizing fluids to remove water blocks, enhance fluid recovery, retard acid reactivity, and decrease water content. Especially in gas reservoirs, the high surface tension of water or acid solutions hinders their penetration and recovery. Conventional surfactants help, although they lose much of their activity by adsorption. The addition of alcohol to acid solutions also reduces their IST. The concentration of alcohol normally used for this purpose is sufficient so that loss by adsorption is not a problem. Note that as much as 20% alcohol is needed for some of the beneficial effects, so this can greatly increase the cost of the treatment and affect corrosion inhibition.

Alcohols and mutual solvents also can be added to various acids and chelating agents to produce a solvent that may dissolve organic as well as inorganic damage. Frenier and Brady (2008) have proposed a mixture of several types of glycols with chelating agents and other solvents and surfactants that were effective for removing inorganic and organic deposits from the near wellbore area of the formation. The fluids were a single phase and could be used with various CIs at high temperatures and in high-salt content fluids.

Many types of surfactants can be added to acids or chelating agents to help the fluid penetrate the mixed deposit. Note that ether-alcohols are essentially short-chain nonionic surfactants and a very large variety of materials are custom-blended depending on the individual usage. Wang et al. (2004) describe an alcoholic acid formulation that contains 20% methanol and either HCl or 9/1 MA for removing fracturing agent polymer damage from wells in China. The formation as well as the propped fractures was treated using a diverted acid.

A single-stage acid microemulsion fluid that is formulated with acid, aromatic solvents, surfactants, and cosurfactants was claimed by Smith et al. (2011a). The patent describes the details of the surfactants (consisting of fatty alcohol alkoxyates, fatty alcohol ethoxyates, nonylphenol ethoxyates, nonylphenol alkoxyates, block copolymers, reverse block copolymers, tetrols, and reverse tetrols), low MW alcohols, and organic solvent (10–20 vol% aromatic chemical). The formulation was claimed by Boswood and Kreh (2011) to be more effective than xylene for dissolving paraffin wax.

Another (and possibly contradictory) class of antiemulsifiers or antisludging agents also may be added to acid formulations to prevent emulsions (see Section 2.4.4) that form when the acid/reaction products come in contact with crude oil. Cassidy et al. (2006) claim that these compositions may contain dodecylbenzene sulfonic acid (an anionic surfactant) that may not be compatible with cationic acid CIs. These authors then describe a conjugate ion pair of a dimethyl coco alkylamine oxide

surfactant and a dodecyl sodium sulfate surfactant that does not react with the cationic CI and reduces the formation of sludge and emulsions resulting from the acid solution contacting the formation oil.

These surfactant mixtures may affect wetting; however, Saneifar et al. (2011) have tested the IST values (using a pendant drop method described in the report) of spent HCl (i.e., CaCl_2) at low and high temperatures and found similar effects to the study of Dabbousi et al. (1999). The conclusion is that the additives may positively or negatively affect oil and gas production and should be rigorously tested.

To summarize: As many as three–four individual surface active agents may be added to a matrix acidizing fluid and include a wetting agent, anti-emulsifier, and a cosolvent or alcohol. Therefore, the CIs must be chosen to be compatible with the other surface active additives. The CIs are designed to adsorb/film onto a steel surface, so the other surface active chemicals should not remove so much inhibitor film to render it inoperative. Thus, corrosion testing as well as stability testing must be conducted using the entire stimulation fluid. Note the discussions in Cassidy et al. (2006).

3.6.3 Iron and Sulfide Control Agents. Different chemical agents are in use to control iron precipitation as well as sulfide fouling during reactive stimulation treatments. The sources of the iron (dissolved) and sulfide (as H_2S) include iron corrosion products (see Section 2.2.3), the formation and products from a soured or connecting formation. Details of control agents are in the next sections.

Iron Control Agents. Iron compounds can exist in rock formations as the mineral hematite (Fe_2O_3), as various iron sulfides (Fe_xS_y) and in some clay minerals such as chlorites. During production operations, especially acid stimulations, additional iron can be forced into the formation if the acid dissolves rust (FeOOH) from a tank, from the tubulars or from siderite or iron sulfide on piping. If the iron is in the 3+ oxidation state, ferric hydroxide [$\text{Fe}(\text{OH})_3$] will precipitate as the acid is spent on the formation carbonates. This chemical reaction produces a gelatinous mass that can cause formation damage. This precipitation of ferric iron occurs at a pH > approximately 2.0. The precipitation of ferrous iron (II) hydroxides does not occur until the pH is above 7.0. Returned spent acids seldom have a pH this high. However, if H_2S is present, then ferrous sulfide (FeS) may precipitate. Because the major fear is the less soluble $\text{Fe}(\text{OH})_3$, the use of reducing agents to produce Fe(II) ions from the Fe(III) ions as well as chelating agents have been employed to control possible damage. Pickling the tubing and rigorous quality control of the injected acid and the acid tankers also will control iron damage, but many operators insist that an iron control agent be present in the fluid as an insurance against possible problems.

Reducing agents convert ferric [Fe(III)] to ferrous [Fe(II)] iron. EA and sodium erythorbate are commonly used as reducing agents. EA is preferred over sodium erythorbate in sandstone acidizing because the addition of sodium salts of either sequestering or reducing agents to MA can lead to the precipitation of insoluble sodium hexafluosilicate. EA is an isomer of ascorbic acid (vitamin C, Fig. 3.64).

Hall and Dill (1988) reported that EA is unstable in hot HCl and decomposes to form an insoluble precipitate. Although this is true, the decomposition process is slow and the acid normally spends long before precipitation can occur (Crowe 1984). EA or the sodium salt is used frequently because it is very efficient. See Ali and Hinkel (2001). Alternate reducing agents based in hydroxylamine, hydrazine compounds, semicarbohydrazide or ketoxamines (Hill 2005) to reduce Fe(III) ions in gel systems (Section “Self-Generated Gel Diversion and Emulsified Acids”); however, the use in this current application is not clear to the authors of this book.

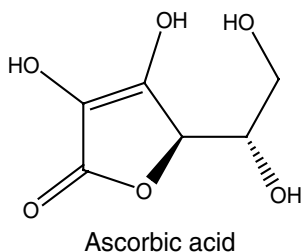


Fig. 3.64—Ascorbic acid.

Frenier et al. (2000) have described the use of chelating agents (sequesterants) as iron control agents. EDTA, in particular, is used to stabilize iron in spent HCl. These are the same materials that can be used as primary formation stimulation agents. See Section 3.4.4, Table 3.3, and Fig. 3.24. Crowe (1987) reviewed the use of chelating agents and reducing agents for iron control. According to this author, EDTA will control precipitation of ferric and ferrous hydroxide up to 350°F. Above 250°F, its efficiency actually improves because it then acts as a reducing agent (Crowe 1987). It works better than citric acid/acetic acid (Smith et al. 1969) because CaEDTA is more soluble than calcium citrate (see Section 3.4.4). Mixtures of citric acid and levulinic acid (Dill and Knox 1979) and citric acid with 5-sulfosalicylic acid (Street-Jr. 1979) have been developed to get around the shortcomings of citric acid, a biodegradable material. Taylor et al. (1998) teach the use of citric/acetic acid mixtures as compared with EDTA or NTA. Taylor et al. (1998) claim that EDTA is not soluble (enough) in 15% HCl to control significant amounts of Fe(III) ions.

This assertion is contrary to the practice of the authors of this book who note that > 3% tetrasodium EDTA (expressed as the 100% salt) is routinely used in acidizing formulations (though they agree that HCl formulations with >3% sodium EDTA are not stable if left for more than a few hours). Gouglar et al. (1985) advocate cleaning the tubulars before acidizing the formation to reduce the iron load introduced into the formation. Chelates also are used with EA (Crowe and Maddin 1986) to stabilize iron and prevent precipitation of sulfur in sour acid and with aldehydes (Dill and Walker 1989) for the same purpose (the carbonyls react with the sulfide ions). This patent recommended NTA, aldol, and ethylene glycol monobutyl alcohol to control both the iron and the sulfides. However, Brezinski (1999) claims that EDTA and NTA are not stable as iron control agents in HCl/carbonate spending tests. He suggests using sulfide control chemicals. A major use for chelating agents in oilfield services consists of stabilizing iron during and after the acidizing treatments of carbonate formations. See literature cited previously.

Frenier et al. (2000) have conducted tests to simulate this application of chelating agents as iron control agents. These tests were designed to test materials that are more soluble than EDTA in strong HCl. The tests used EDTA, HEIDA, NTA as well as HEDTA. A sample containing 100 g of HCl was contaminated with various amounts of Fe(III) as FeCl_3 . Iron control agents were added at equimolar amounts, based on the amount of iron added. The solutions were neutralized to pH 3.5–3.8 using powdered CaCO_3 . The sample was split into two portions. One portion was put into a water bath (or oven) at 150°F and the other sample was stored at lab temperature (about 70°F). Tests at 190°F were conducted by placing a sample of the neutralized solution into an oven. A final sample containing one chelant (Na_3HEDTA) was put in a corrosion autoclave at 310°F. After the test period (6 to 72 hours of exposure), a small sample was filtered and analyzed using ICP spectroscopy. Iron recovery was most consistently high for the solutions containing the stronger complex formers, EDTA, and HEDTA. The recovery values were usually > 80%, even at 150°F. Fig. 3.65 shows the data for room temperatures. HEIDA was effective with about 3000 ppm Fe(III) in solution.

Using a similar test, LePage et al. (2009) have reported very high iron retention values using GLDA. See Table 3.3 for the chelating agent characteristics. An advantage claimed for GLDA is that it is much

Iron at Room Temperature, Spent HCl, pH 3.5

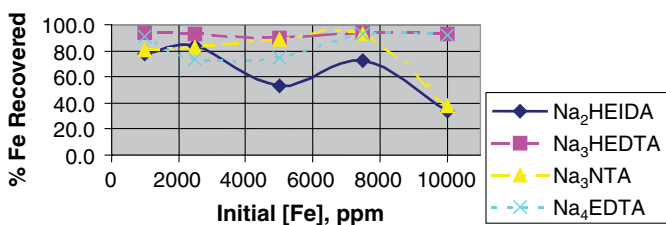


Fig. 3.65—Recovery of ferric iron from 15% HCl, spent with CaCO_3 . Samples contained equimolar (based on iron concentration) of the chelating agent. Solution aged at room temperature (68–70°F) for 72 hours. (Frenier et al. 2000).

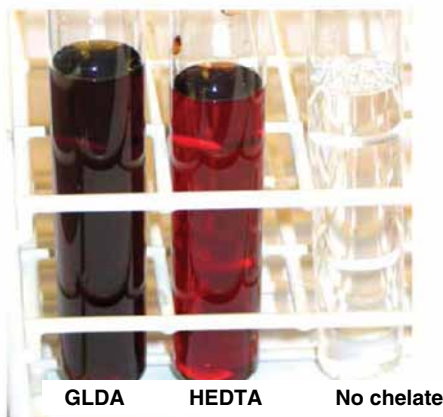


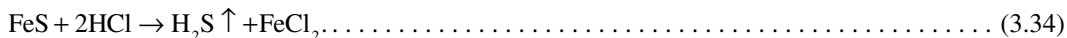
Fig. 3.66—Filtrate tests of neutralized HCl (with calcite) containing 2500 ppm Fe³⁺ iron with and without GLDA or HEDTA.

more soluble than EDTA or HEDTA in very high concentrations of HCl and is more effective than HEIDA. GLDA also is much more biodegradable than EDTA, as is HEIDA [as reported by Frenier et al. (2000)]. Fig. 3.66 shows the filtrates of HCl spent with calcite in the presence of 2500 ppm Fe³⁺ iron. The color of the complexed iron indicates that the presence of the complex, while the clear blank (no chelating agent) indicates the absence of dissolved Fe³⁺ iron. Both GLDA and HEDTA were very effective.

While the chelating agents described in this section are used primarily for control of iron depositions in the current application, most of them (Figs. 3.24 and 3.25) also will control calcium deposition. The first uses of chelating agents in scale control was for dissolution and control of these deposits (Bersworth 1960)). Because it may be important to use seawater instead of fresh water to make up an acid formulation, control of alkaline earth ions may be necessary. Berry et al. (2012) have described tests of HCl fluids. The tests are claimed to demonstrate that calcium sulfate does precipitate from conventional acidizing fluid systems mixed with seawaters containing high levels of sulfate. Also this precipitate decreases the solubility/stimulation of carbonate rock. They then developed the use of chelating agent-based chemical methods to treat seawater-mixed acid systems to effectively minimize or prevent the precipitation of calcium sulfate solids during carbonate acid stimulation treatments.

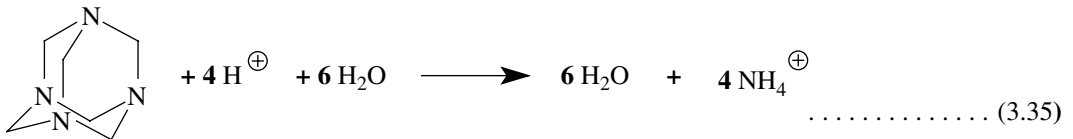
Sulfide Control Chemicals for Reactive Stimulation. Details of general control of iron sulfide precipitation are in Section 2.2.3. This current section relates to control of sulfide precipitation as well as the effects of H₂S on corrosion during acidizing operations.

HCl can be used to dissolve iron sulfide deposits with varying degrees of success. In general, iron sulfide deposits with low sulfur content have higher solubility in acids (Ford et al. 1992). Acid reaction with iron sulfide produces hydrogen sulfide, as shown in Eq. 3.34.



This may be the object of the acidizing treatment or may happen inadvertently. Removing iron sulfide scale is a difficult task for several reasons. Depending on the well type, iron sulfide scale can be coated with oil, condensate, or biomass. These materials act as a diffusion barrier that will inhibit acid reaction with the scale. Another important factor is aging of the scale. Continuous exposure of FeS to hydrogen sulfide will result in the formation in iron sulfide species that are rich in sulfur. The presence of H₂S greatly increases the *corrosivity* of the acid (Schmitt and Bedbur 1985) as well as being very toxic. In addition, if sulfides are present at the end of the treatment any Fe(II) iron present in the spent acid can reprecipitate as FeS, possibly causing formation damage. Therefore, various sulfide control technologies are in use. Note that several sulfide control chemicals are claimed in the previous section.

Several additional different suppression technologies are reviewed in the current section. Note that some of these chemicals are also used in nonacidic applications (Section 2.2.3, Figs. 2.14, and 2.15). Ball and Frenier (1984), Buske (1981), and Frenier (1982) developed suppression agents that contain aldehydes. The most efficient agent is formaldehyde that reacts stoichiometrically with hydrogen sulfide to produce trithiane, a very insoluble material. Sometimes, a backup scrubber system also is used to ensure complete removal of sulfide gas. Because of concerns about formaldehyde, this chemical was replaced by glyoxal or aldol [3-hydroxybutanal (Kalfayan 2008)]. The chemical, glyoxylic acid (Buske 1981) also can be used with HCl and sulfuric acid. Formaldehyde can also be generated in-situ by adding hexamethylenetetramine to strong acid.



Hexamethylenetetramine

Nasr-El-Din et al. (2000b) and Nasr-El-Din et al. (2000c) made extensive studies of sulfide scavengers and other acidizing additives on the dissolution of oilfield FeS (Eq. 3.34). Many of the scavengers caused a retardation of the dissolution reaction. Several hydrogen sulfide scavengers were tested at various concentrations up to 10 wt%. Dissolution of FeS by the acid in the presence an aromatic type chemical scavenger is shown in Fig. 3.67. This scavenger interfered with the acid reaction with FeS at high scavenger concentrations. A white polymeric material was noted on the surface of FeS particles. It is believed that this material acted as a diffusion barrier and stopped the acid reaction with the FeS scale. Fig. 3.67 shows that the acid concentration in the supernatant did increase somewhat in the presence of a test scavenger (called “D” in the paper). This result further confirmed the adverse effect of this scavenger on acid reaction with iron sulfide. The results shown in Fig. 3.67 indicate that hydrogen sulfide scavengers, which are needed to prevent reprecipitation of iron sulfide scale, can inhibit the acid reaction with the scale. These chemicals should be thoroughly tested to determine the optimal dosage to affect scale removal and CI.

Frenier and Hill (2002) developed a scavenger system that did not significantly inhibit FeS dissolution that contained glyoxylic acid and an unsaturated aldehyde. This system uses glyoxal or preferably glyoxylic acid and cinnamaldehyde (Fig. 3.68) to dissolve FeS, capture the H₂S, and lower the corrosion rate to an acceptable value.

This is the chemistry of the scavengers described by Nasr-el-Din and Al-Hamaidan (2000) previously. Additional tests (Fig. 3.69) describe dissolution tests where glyoxal (Scavenger A in the plot)

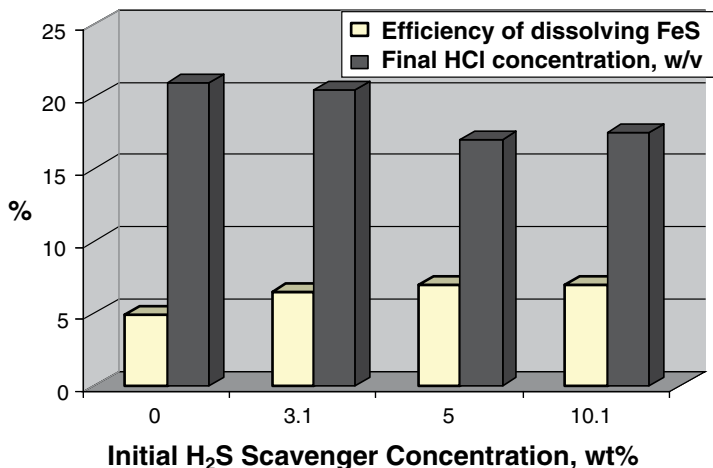


Fig. 3.67—Effects of additives on FeS dissolution (Nasr-El-Din et al. 2000b, 2000c).

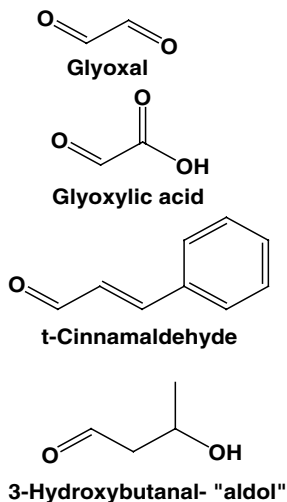


Fig. 3.68—Aldehyde H₂S control agents.

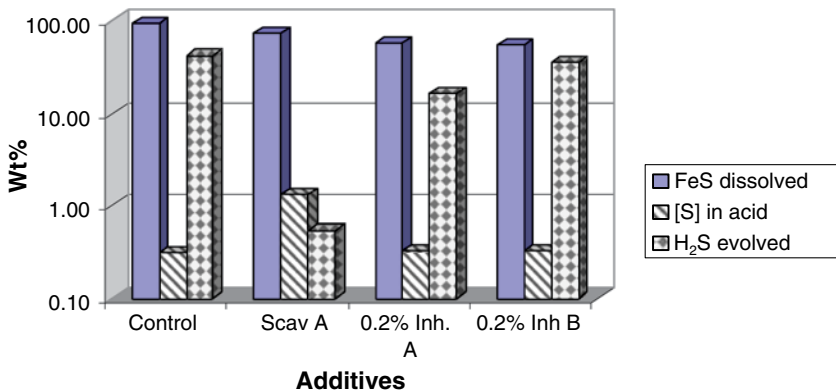


Fig. 3.69—Effect of hydrogen sulfide scavengers on FeS dissolution and H₂S formation at 150°F (Nasr-El-Din 2000b, 2000c).

controlled the H₂S. In the two tests on mixed scavengers, the right side of Fig. 3.69 shows the materials called “Inh. A” and “Inh. B” (which contain glyoxylic acid). This formulation allowed more dissolution of the FeS to occur than the other combinations.

Nasr-El-Din et al. (2007b) claim that research and development work has led to the use of a new generation of hydrogen sulfide scavengers (mixture of aldehydes) for use in acidizing treatments (Nasr-El-Din et al. 2000b). They also claim that a drawback of this scavenger in acidizing treatments is the formation of oily material, which may adversely affect the performance of water injectors. This paper discusses a scavenger that is based on hydroxyalkyl triaziane (see 2.2.3 and Fig. 2.18). Laboratory work included compatibility of the old and new hydrogen sulfide scavenger with live acids. The impact of the new scavenger on corrosion of low-carbon steel was also addressed. They claim that based on encouraging results from the laboratory, field trials were conducted on a number of wells. Post acidizing flowback samples were collected and analyzed to confirm laboratory results. Finally, injectivity results from the field trial were compared with offset well performance to validate the technical benefits of the new hydrogen sulfide scavenger.

The studies described above presume that the iron sulfide deposit is predominantly an FeS mineral such as Mackinawite. However, there are a number of other iron sulfide minerals (Frenier and Ziauddin 2008) that include additional amounts of sulfur in the crystal structure and end the form of FeS₂. These minerals are not readily soluble in acids and must be removed using mechanical means.

3.6.4 Clay Control Chemicals (CCCs) as Additives. Section 3.5.5 describes various methods including FBA-containing (Thomas 1979) HF acids and phosphonate-containing (Di Lullo and Rae 1996) HF acids that are thought to control the migration of clay and clay fines during acid dissolution treatments. Some of the other chelate-based fluids are also designed to reduce production of damaging fines by *not* disrupting the clay molecules in the formation.

In addition to use of these specific formulations, a number of CCCs have been prescribed for addition to acid stimulation fluids when high clay content (or very water sensitive) formations are treated. Generally, it is most effective to add the CCC to every fluid in an acidizing treatment (Ali and Hinkel 2001); however, a post-flush of the chemical also may be useful. Many of these additives (especially simple salts such as KCl and NH₄Cl) also are used in frac fluids (see Section 4.7.5). Some aspects associated with clay stability and fines migration and formation damage also were described in Sections 1.5.6, 2.3.3, and 2.3.4 of this book.

Ali and Hinkel (2001) have reviewed the use of CCCs, and they note that these materials act to stabilize clays and fines function by being adsorbed, usually by electrostatic attraction or ion exchange, on the minerals to be stabilized. See the structures in Figs. 3.40 and 1.29. Fink (2003) and Fink (2011) have provided an entire chapter (Chapter 3 in both books) on clay control. The emphasis is on drilling in water sensitive formations, but the principles apply to acidizing and fracturing. This author describes the macrostructure of clays (Section 1.5.6 of the current book, Fig. 1.29, and Fig. 1.32) and in Fig. 3.70 as a “house of cards.” The consequences of the charges on the clay particles is that water may adsorb on them and a change of charge on the particle may cause them to disperse.

This author (Fink 2003) also notes that clays can swell because of adsorption of water or by osmotic swelling where the concentration of the cations are higher *between* the layers than in the bulk. Then water will migrate into the layers to equalize the chemical potential. Note in Fig. 3.70 that the cations on the surface may be exchangeable with the cations in the bulk, and KCl frequently used in well fluids may prevent the exchange. Zhou and Law (1998) provide more insight into the mechanisms of clay control. They note that the structural layers are always deficient in positive charges because of cation substitution, and interlayer cations are required to balance the negative layer charge. Interlayer cations are exchangeable and the exchange is reversible for simple cations. They claim that when the exchangeable cations are hydrated and water molecules enter the space between the structural layers, the distance between two structure layers [i.e., (001) d-spacing] increases and volume of the clay

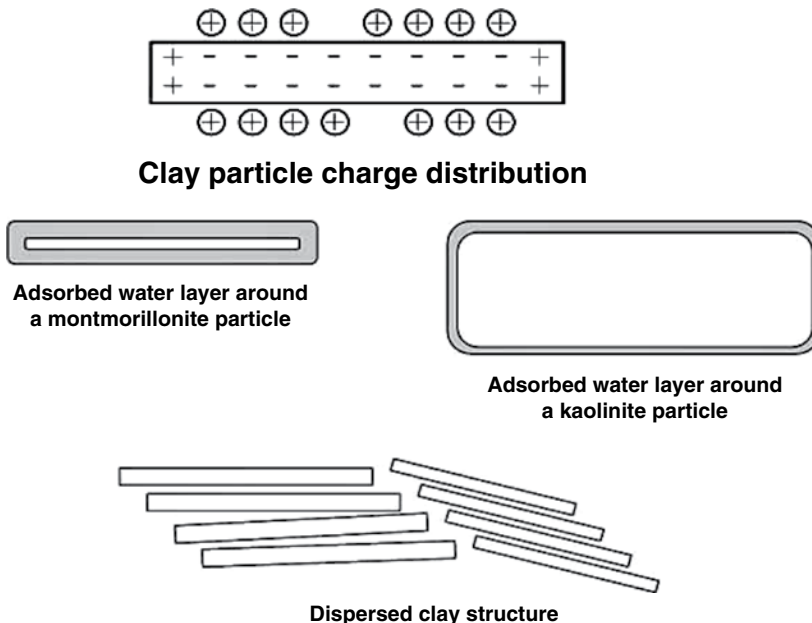


Fig. 3.70—Clay house of cards macrostructure.

expands. This is clay swelling. In severe cases, the clays can disperse and cause plugging and formation damage.

Zaltoun and Berton (1992) describe mechanisms of clay stabilization. According to these authors, clay can be stabilized three ways: ion exchange, coating of clay particles, or modification of surface affinity toward water. These mechanisms are described in more detail in the following subsections. Methods for testing of CCCs are in the next subsection.

Testing of CCCs. These types of tests may be appropriate for acidizing and prop fracturing fluids. Himes and Vinson (1989) and Fink (2011) have described the testing of CCCs using the Hassler-type coreflood instruments shown in Section 3.2.1. Formulation with and without the control agent are flowed through sandstone cores and changes in permeability are used to evaluate the effectiveness. El-Monier and Nasr-El-Din (2011a) describe coreflood tests to evaluate CCCs. The type of cores (6-in. length and 1.5-in. diameter) that were used is Berea sandstone of 60–85 md mainly contained 5 wt% kaolinite. Various coreflood experiments were performed to assess the effectiveness of three stabilizers at 200 and 300°F. ICP was used to analyze the core effluent to measure the concentrations of key cations. Zeta potential ($-\zeta$ an indirect measure of the charge on a particle—see Section 1.6.1 and Fig. 1.32) methods (Malvern 2003) have been used to determine electrophoretic mobility of particles and, thus, the potential for them to disperse in a fluid.

Smith et al. (2006) have advocated a test of effectiveness of various clay stabilizers based on a capillary suction time (CST) test (Scholz and Tapp 2005). In the CST apparatus application procedure described in this document, a slurry of a test material is poured into a small open funnel (circular tube) resting on a piece of paper. Filtrate is extracted by capillary suction and a cake is formed at the bottom of the funnel. The time taken for the waterfront to pass between these two electrodes constitutes the CST. This time can be related to a pressure drop (and thus the permeability) of the test solids.

Hill (1982) claims that determining the concentration of polymer required to adequately stabilize clays is dependent upon many factors including the clay content of the reservoir, the natural wettability of the reservoir, and the adsorbed cations in equilibrium with the formation. The authors claimed that the most important is the cation exchange capacity of the reservoir rock. This may be determined in the laboratory and used to predict the required concentration of the cationic additive to obtain stabilization. Details of the tests are in the reference. Various clay control mechanisms and chemical formulations are described in the next sections.

Ion Exchange Control Mechanisms. Because clay swelling and destabilization are enhanced when Na^+ is the clay counter-ion, (it is easily exchanged) its replacement by other monovalent positive ions (such as NH_4^+ , H^+ , or K^+) is an effective way to increase clay stability. Zhou and Law (1998) note that the magnitude of clay swelling depends on the nature (type) of the exchangeable cations, composition of the solution, and the clay compositions, and that swelling is most severe in fresh water. As salinity increases, the potential of clay swelling decreases; however, with salinity being the same, the potential of clay swelling is largely influenced by the nature of exchangeable cations. Among the monovalent cations, swelling potential *decreases* in the order $\text{Li}^+ < \text{Na}^+ < \text{K}^+$, $\text{NH}_4^+ < \text{Cs}^+$. Because the charges are the same, the effect of the protection is related to the relative stability constants for the ion exchange reactions of the various salts, as well as the activities of the fluids. Note that this order is associated with the radius of the ions because the smallest ion will be the most acidic (Cotton et al. 1999). See the discussions in Section 1.5.1 and in Chapter 2 of Frenier and Ziauddin (2008).

Potassium salts are used most extensively because of their efficiency, low cost, and excellent brine compatibility. NH_4Cl brines are used extensively in sandstone acidizing treatments because potassium salts of possible reaction products are less soluble than ammonium compounds. See Section 3.5.5. Monovalent ions (and divalent ions), however, are known to have a temporary effect when exposed to dilute solutions. In the presence of brines with high NaCl concentrations, the stabilizing effect disappears progressively by the same ion-exchange process that leads to the replacement of K^+ by Na^+ ions. See Fig. 3.71.

Based on these ideas, Gijtenbeek et al. (2006) have found using ion exchange tests that 2% KCl loses about 0.5% of its ions to the formation, and, thus, it was decided to use 7% KCl as a temporary clay control additive in HF acidizing and with water-based fracturing fluids for treatments in western Siberia. One-molar salt solutions have been used for all the treatments performed during the last

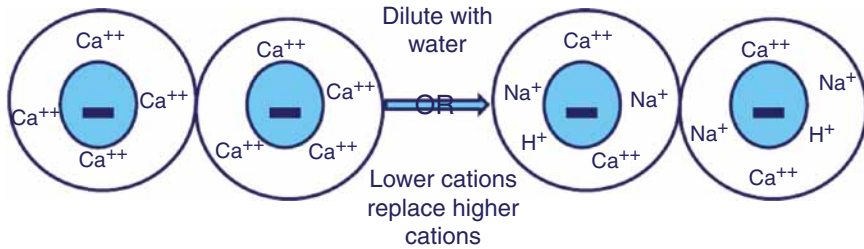


Fig. 3.71—Cation exchange in dilute water or salt brine (EI-Monier and Nasr-EI-Din 2011c).

4 years with good results for preventing fines migration. Small, positively charged organic quats such as tetramethylammonium chloride (TMAC) (See Fig. 3.72) also are thought to protect the clay by this mechanism (Ali and Hinkel 2001).

More permanent effects are obtained with cations having higher valences, such as Ca^{2+} , Al^{3+} , or Zr^{4+} . The high positive charge of these ions makes them more strongly bonded (higher ion exchange stability constants) to clay and not easily removable by other ions. Zhou et al. (1995) call the Al materials cationic inorganic polymers (CIP) and list an empirical structure as $[\text{Al}_x(\text{OH})_y(\text{H}_2\text{O})_{6x-2y}]^{(3x-y)+}$. These authors also note that the disadvantage of CIP-Al is that they can be applied only in a limited pH range. For Al, the polymerization pH is 3.5–6. In very acid solution ($\text{pH} < .5$), Al will not polymerize; in neutral and alkaline solutions ($\text{pH} > 6$), Al will precipitate as a hydroxide. Thus, the use is limited in the near-wellbore region, especially as a post-acid treatment. The carrier solution has to be strongly buffered for CIPs to be effective.

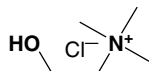
The effect of the high charge is nonlinear and the higher charged ions are much more effective than the monovalent ions [possibly many thousands (Veley 1969)]. This is because of the surface charges provided by an individual ion that is proportional to the log of the charge on the ion. See the discussions



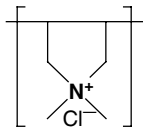
Zirconium oxychloride



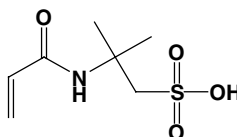
Tetramethylammonium chloride- TMAC



Choline chloride



Dimethyldiallylammonium chloride polymer



2-acrylamido-2-methylpropanesulfonic acid

Fig. 3.72—Clay control compounds.

of surface potential in El-Monier and Nasr-El-Din (2011c) and Masliyah and Bhattacharjee (2006). Specific examples of clay control by Zaltoun and Berton (1992) are noted in the following paragraphs.

Coating of Clay Particles as a Control Mechanism. Zaltoun and Berton (1992) claim that adsorption of high-molecular-weight polymers is known to prevent fine migration. The mechanism involved is the formation of polymer bridges that maintain clay particles linked together on the rock surface. Moreover, polymer particles may be linked together on the rock surface and polymer adsorption is almost irreversible, so it produces a long-term effect. Anionic or nonionic polymers have been among the first to be used: polyacrylamides with different ionic sites, polyacrylates, CMC, carboxymethyl hydroxyethylcellulose, etc. Cationic organic polymers, such as polyquaternary amines, have been shown to be used as clay control agents and (Fink 2011) have been shown to be excellent clay stabilizers. The authors (Zaltoun and Berton 1992) also include in this category inorganic polymers, such as hydroxyl aluminum, which like the cationic organic polymers, combines a coating effect with the ionic effect of aluminum ions.

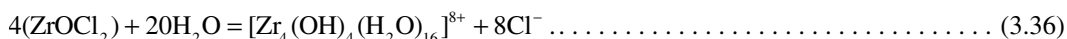
Modification of Surface Affinity Toward Water. Zaltoun and Berton (1992) claim that the adsorption of lipophilic additives on a clay surface makes this surface less water-wet while decreasing its hydration tendency. This category of additives includes oil-wetting surfactants, asphaltenes, and petroleum-heavy ends. As shown for the case of hydroxyl aluminum, some additives stabilize clays by a combination of different effects. The same effects may be obtained with mixtures of clay stabilizers. For example, KCl/polymer systems are commonly used in drilling fluids. Some additives combine clay stabilization with other properties. Potassium hydroxide slugs are known to improve well injectivity both by clay stabilization from the K^+ ion and by decreasing residual oil saturation caused by caustic flush. Their paper (Zaltoun and Berton 1992) investigates the stabilizing effect provided by high-molecular-weight polymer adsorption on montmorillonite clay dispersed in a sand matrix. All the polymers used in this investigation were either nonionic or anionic; thus, the only phenomenon involved is the coating of clay particles by adsorbed phenomenon involved in the coating of clay particles by adsorbed polymer molecules.

The authors claim these polymers have several advantages, such as excellent compatibility with most brines and good propagation properties through reservoir rocks because of their moderate adsorption level. Indeed, because of their strong adsorption tendency, injectivity of high-molecular-weight cationic polymers may be rather questionable, especially in low-permeability reservoirs.

Details of the Types of Clay Control Compounds. As this is a very “substance rich” field, some additional details of individual formulations are included in this section. Some of them are thought to work by more than one mechanism described in the previous sections. Because silicates exist in some fluids in a state above their point of zero charge values, the crystals will have a negative charge. Thus, the most effective stabilizer has a positive charge (cationic). Common clay stabilizers are highly charged cations, quaternary surfactants, polyamines, polyquaternary amines, and organosilane. As noted in the previous paragraphs, metal salts, such as KCl, are used as temporary fines stabilizers.

In addition, soluble Al oxides and $ZrOCl_2$, which are Lewis acids, have been used in the past (Ali and Hinkel 2001) as a more permanent clay stabilizers. These two materials have polycharged cations and are more effective than monocations to stabilize the charges on the clay particles. They also form inorganic polymers at certain pH ranges that may cause a physical coating to form (Zaltoun and Berton 1992). However, the Al polymers may be soluble in acid, and Hollenbeak and Brown-Jr (1985) claim that the $ZrOCl_2$ also can be removed by acid (under circumstances not defined by this author).

Ali and Hinkel (2001) have reviewed the chemistries of these materials and claim that zirconium oxychloride rapidly hydrolyzes in water followed by hydration, thus resulting in polynuclear cations with high cationic charge. The reaction is



Hydroxy-aluminum is also a polynuclear cation with high cationic charge (Veley 1969). The structure is $[Al_6(OH)_{12}]^{6+}$. Stabilization occurs with these polycations by masking many anionic sites, thereby reducing the probability of exchange with other monovalent or divalent cations. This polyvalent cationic charge also reduces the counter-ion environment around the clays, maintaining them in their flocculated state.

Veley (1969) claims that hydrolysable metal compounds, such as zirconium oxychloride, have improved acid treatments in several south Texas acid-sensitive formations. The large nuclear ions attach to the released clay particles, hasten their flocculation, and interfere with their rearrangement. However, the hydroxy-aluminum clay complex is destroyed by acid.

El-Monier and Nasr-El-Din (2010) claim that Al and Zr compounds in current use as well as cationic polymers have several drawbacks. Al and Zr compounds are claimed to be removed by acids. Cationic polymers are claimed to cause formation damage in some cases, and their environmental impact is questionable [cationic compounds may kill fish and may not be biodegradable (Kelland 2009; Frenier 1996)].

The authors (El-Monier and Nasr-El-Din 2010) report on laboratory studies that were conducted on a newly developed polymeric Al compound (also identified as an Al/Zr formulation, “A”—[Table 3.12](#)). The liquid has a pH of 2.9, a viscosity of 96 cp at 25°C and 12.6% Al/wt and 0.37% Zr. Zeta potential and particle size measurements were used to determine surface charge of four types of clays, kaolinite, illite, montmorillonite, and chlorite, and to optimize clay stabilizer concentration. Coreflood experiments were conducted on Berea sandstone cores (1.5-in. diameter and 6.0-in. length) to assess the effectiveness of the new compound and determine the impact of acids on its performance. Atomic absorption was used to measure the concentrations of Al, Mg, Ca, and Fe in the coreflood effluent.

The authors claim that the Al/Zr-based clay stabilizer was very effective in mitigating fines migration. Zeta potential indicated that the isoelectric point (see Section 1.5.6) at which complete shields of surface charge of clay particles was achieved at a stabilizer concentration of 0.2 wt%. Coreflood tests showed that this new chemical was effective, and unlike previous Al compounds, it did not dissolve in acids. In addition, it is claimed to be an environmentally friendly compound and also worked very well at 200°F. The behavior of the new stabilizer was much better when it was prepared in deionized water than in brine. The authors did not provide comparisons with other stabilizers in these tests.

El-Monier and Nasr-El-Din (2011a) reported on the testing of an Al/Zr-based fluid [claimed to be the same fluid (A) described by El-Monier and Nasr-El-Din (2010)] and that also is reported to be a 100% inorganic polymer. Comparative tests (coreflood—water shock) were performed with Al/Zr, TMAC, and choline (see Fig. 3.72 and [Table 3.12](#)). Their data showed that the inorganic polymer was as effective as TMAC or choline in the water-shock test and was not removed by HCl rinses, indicating that it was more permanent than the amine-based materials. Results of coreflood tests done at 200°F demonstrated the Al/Zr polymer solution was able to suppress fines migration more effectively than the two nitrogen quats.

The authors of this book note that octaaluminum zirconium octachloride icosahydroxide, (CAS # 98106-55-9) is listed as an antiperspirant agent and has an Al/Zr ratio similar to those seen in the El-Monier and Nasr-El-Din (2010) publication. A patent by Carrillo et al. (2003) gives information on the preparation of Al/Zr mixtures. Also see more discussions of Al/Zn clay stabilizers in Section 4.7.5.

A number of structures of organic clay stabilizers are described in the report by Ali and Hinkel (2001), as well as those by Fink (2003), Fink (2011), and Kelland (2009). Ali and Hinkel (2001) recommend that during the acidizing, a water sensitive formation with HF, clay stabilizer should be used if possible. If it is not possible to put clay stabilizer in all fluids, it should be used in the overflush, which should be over displaced with fluid that contains no clay stabilizer to ensure that no unadsorbed clay stabilizer is left at the wellbore. A normal concentration of polyquaternary amine for applications

**TABLE 3.12—CHARACTERISTICS OF TEST CLAY STABILIZERS
(EL-MONIER AND NASR-EL-DIN 2011b)**

| Stabilizer | pH | Viscosity (cp at 77°F) | Density (g/cm ³ at 77°F) | Al (ppm) | Zr (ppm) |
|----------------------|-----|---------------------------|---|----------|-------------|
| A (Al/Zr polymer) | 2.9 | 96 | 1.5 | 125,560 | 37,270 |
| TMAC | 8.9 | 16 | 1.02 | | |
| Choline Cl | 7.5 | 7.5 | 1.09 | | |

in HF treatments is 5 gal/1000 gal of active polymer in all fluids or 7½ gal/1000 gal of clay stabilizer in 200 gal of overflush. A large number of additional clay stabilizers are listed in Fink (2003); however, the polyquat amines are used frequently in stimulation treatments to control clay migration that can cause permeability losses.

Examples of quats and polyquats are described in a patent by Himes and Vinson (1989). Some specific examples are an additive that can comprise N-alkylpyridinium halides; N,N,N-trialkylphenylammonium halides; N,N,N-trialkylbenzylammonium halides; N,N-dialkylmorpholinium halides; alkyl quaternary ammonium salt of 2 mole oligomer of epihalohydrin.

Hollenbeak and Brown-Jr (1985) describe a water-soluble clay stabilizing agent comprised of a copolymer of diallyldimethylammonium chloride and sulfur dioxide to prevent or reduce clay swelling and fines migration in permeable subterranean formations. The method of use is carried out by contacting swellable clays and migratable fines or combinations thereof with an effective amount of the aforesaid copolymer having a molecular weight in the range from about 1000 to about 100,000, and preferably from about 3000 to about 20,000, having a nitrogen-to-sulfur mole ratio of about 1.

Smith et al. (2006) and Smith et al. (2010) have claimed a clay control formulation that includes a polyquaternary amine having a high to very high charge density is added along with lower molecular weight amine salts to substantially permanently exchange cations with the clay in the formation. Several types of CCCs are shown in Fig. 3.72.

Hongkun et al. (1998) report on evaluations of clay control agents that can be used in steam floods at 200°C. The clay control and antiswelling agents are described as cycloparaffinic hydrocarbon cationic polymers containing nitrogen. They are water soluble. They are not only a good anticlay swell agent under high temperature (decreasing the expansion ratio of montmorillonite by 66.7%). Duplicate experiments were conducted to measure the expansion ratio in a reaction tower at 250°C. The tests found the content of montmorillonite decreased by 19%, quartz and plagioclase (nonclay mineral) increased by 13% and 76%, respectively. This is an important idea because the metallic agents described next also are claimed to be effective at high temperatures.

3.6.5 Summary of Reactive Fluid Additives and Selection

Summary. Because as many as five (or more) additives may be present in a reactive fluid, compatibility in the fluid and especially the effects of them on the corrosion characteristics of the entire fluid must be determined for individual additives as well as mixtures. This is especially true of the “surface active” additives (surfactants, clay stabilizer, mutual solvents, and alcohols). All or any of these materials may remove the inhibitor film or may interfere with the inhibitor in other ways. In addition to the additives reviewed, nitrogen gas frequently is injected to energize the fluid and improve cleanup. Nitrogen also may be injected to affect foam diversion described in Section 3.7. Nitrogen is inert as long as it is of high purity. Liquid nitrogen, which is available in populated areas, and especially on land operations, will be of high purity. An issue is that nitrogen also can be produced by membrane separation of ambient air (Baker et al. 1991) and may contain residual O₂. Injection of oxygen into any acid will cause corrosion that cannot be controlled by any CIs. Quality control of the injected gases is critical. Additional diversion/placement agents also will be described in Section 3.7.

Physical and Chemical Attributes. The choice of a particular chemical for a specific application and wellsite locations are very important issues. Jordan and Feasey (2008) provide a summary of petroleum industry chemical additives. Fig. 3.73 shows the principle factors that have an impact on the selection of suitable additives, according to these authors. These also include chemical and physical properties of importance summarized in Table 3.13. Additional details are described in Section 3.7.3 on wellsite delivery.

Environmental compliance also is a very major issue that was reviewed in some detail in our earlier book, Frenier and Ziauddin (2008). Hill et al. (2003) also describe the development of more environmentally acceptable product as a process that requires working with regulatory agencies, clients, and chemical suppliers to achieve regulatory compliance for material safety data sheets, labels, and environmental testing protocol. The paper recognizes that international environmental statutes and guidelines combined with clear corporate goals to minimize environmental impact are key requirements in regulating industrial use and discharge of environmentally harmful chemicals. The development of

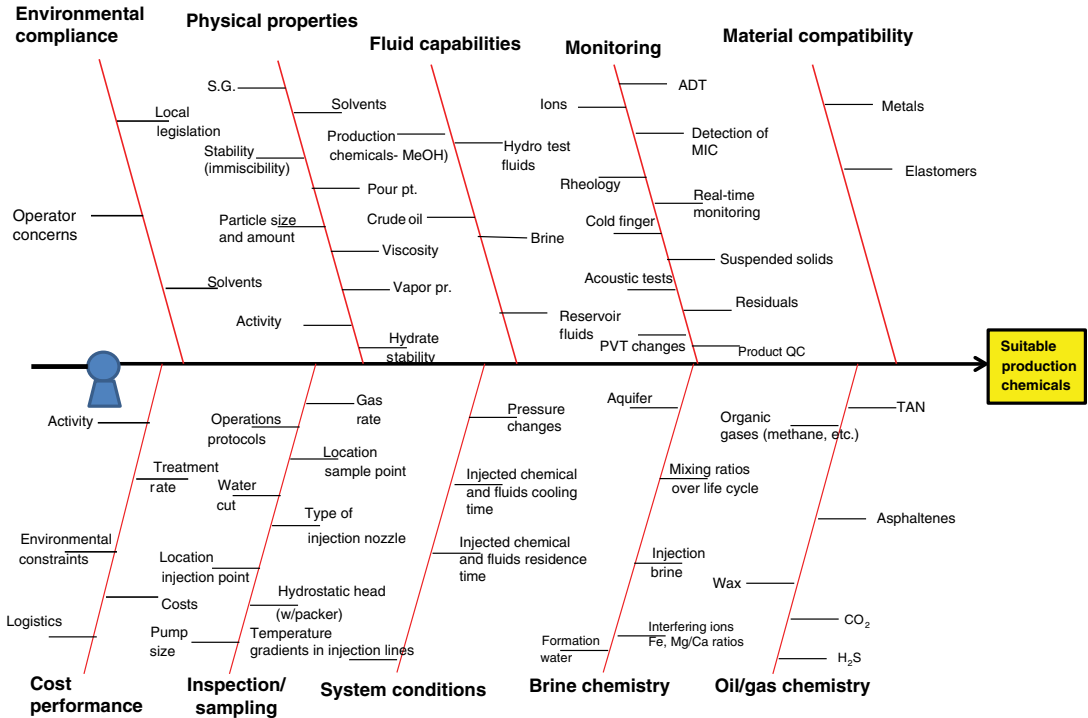


Fig. 3.73—Additive selection properties (Jordan and Feasey 2008).

more environmentally acceptable products requires a thorough screening of environmental fitness and status of compliance with relevant laws and regulations. The critical impact of health, safety, environment (HSE) activities and considerations are present in each step of the product development process. See Fig. 3.74.

Oilfield chemicals have primary active ingredients that may be harmful if discharged to the environment. Improving the characteristics of these products to reduce risk or damage to marine life requires changes in previously acceptable products, such as elimination of restricted materials and incorporation of components with improved ecotoxicity values. Note that HSE issues are a major concern for

| TABLE 3.13—PROPERTIES OF OILFIELD CHEMICAL ADDITIVES | |
|---|--|
| Property | Importance |
| Physical properties | Appropriate for wellsite conditions of temperature and storage (shelf-life) |
| Fluid compatibility | Will the chemical be stable in the aqueous phase and not cause problems (emulsions, downstream) with the hydrocarbon product? |
| Material compatibility, including corrosion of metals | Is the additive compatible with the CI and all other additives, and will it affect the stability of well, delivery, and storage materials of construction? |
| Ability to monitor | This may or may not be an issue. However, scale inhibitors require monitoring, but most other additives are not measured once pumped. |
| Cost/performance characteristics | The best additive may not fit in the budge of the treatment |
| Application, including onsite handling and injection | The additive must be pumpable/mixable under all sell-site conditions, from about -10°F to about 150°F and possibly in inclement weather |
| HSE compliance | See Chapter 6 |

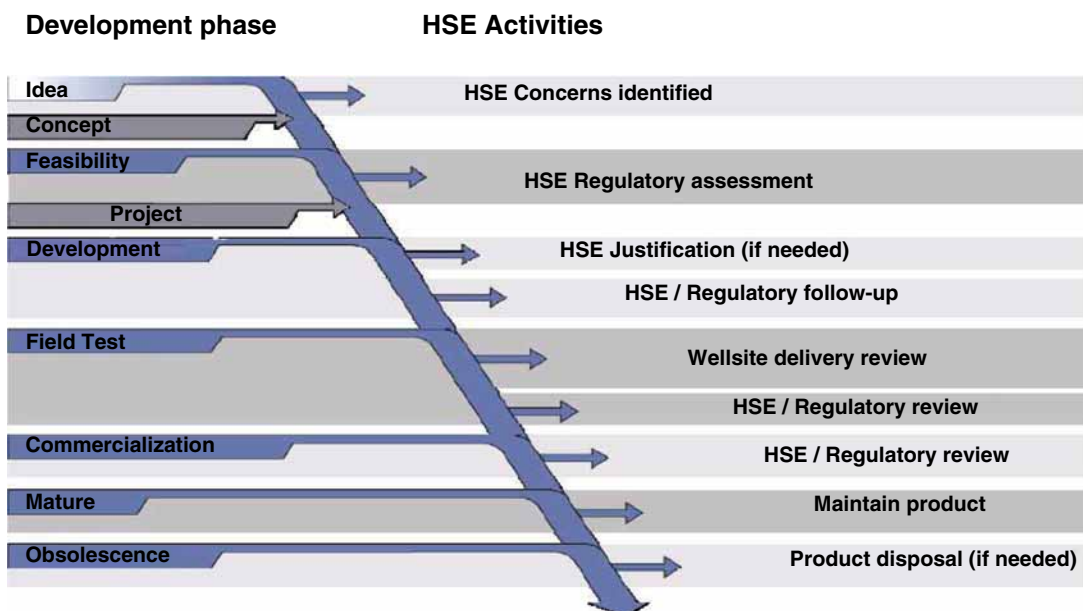


Fig. 3.74—HSE considerations during product development (Hill et al. 2003).

the use of inhibitors, surfactants, and iron control chemicals, especially in the North Sea operations area. More general discussions of HSE in the oil and gas production industry are provided in Chapter 6.

3.7 Placement of Matrix Fluids

Previous sections (3.4–3.6) have described the complex stimulation fluid mixtures for both carbonates and silicate formations. This section describes placement of the fluids, which the authors of the book contend is possibly more important than the individual chemistries. The best chemistry has limited use if it goes into the wrong zone.

Typical sequences of steps for a matrix treatment are listed; however, there may be many of the modifications/combinations in chemistries described in Sections 3.4, 3.5.5, and 3.6.

1. Select treatment flow path (coiled tubing, bullhead through tubing, etc.)
 - a. Tube pickling
 - b. 15% HCl + Surfactants + Iron Stabilizer
 - i. 50–100 gal/1,000 ft of tubing at 0.5–2 bbl/min
2. Preacid preflush (optional)
 - a. 3–6% NH_4Cl (for sandstones) and/or mutual solvent or organic solvent (diesel oil)
3. Damage removal/bypass system
 - a. Sandstones (damage removal) (see Fig. 3.42)
 - i. Brine preflush: 3–6% NH_4Cl
 - ii. Acid preflush: 10–15 % HCl or organic acid
 - iii. Main fluid: HF-based fluid (MA, organic MA), 25–150 gal/ft
 - iv. Post flush: 3–6% NH_4Cl
 1. With a SSF, i, ii, and iii may be combined
 - b. Carbonates (damage bypass)
 - i. Main fluid: 10–28% HCl, organic acid, or chelant
 1. Straight, emulsified, foamed or gelled
4. Diverter stage (1 stage for each 20 to 30 ft of formation)
 - a. Chemical/bridging agents: foam, fibers, benzoic acid flakes, self diverting acids
 - b. Mechanical: ball sealers, packers
5. Repeat 3 (damage removal/bypass) and 4 (diverter) based on zone thickness (1 stage for each 20 to 30 ft of formation)

6. Flush to top of perforations (KCl, NH₄Cl, N₂, or crude)
7. Flowback (for production wells)

In this typical treatment sequence, the use of diversion (placement) is seen in a number of the steps. Because there are wide varieties of well completion methods, only general methods are described in this section.

However, if the reactive fluids do not penetrate and stimulate the target zone or if all of the fluid penetrates only a high permeability zone and a lower permeability formation area is not stimulated, then the treatment may not achieve the goals. In a worse case, a high water content zone may be stimulated instead of a hydrocarbon formation, possibly causing severe economic loss. Correct placement is especially important for stimulating sandstone formations if multiple fluids (see Fig. 3.42) are used and the first fluid (or subsequent fluids) causes an unwanted change that reduces stimulation of the target formation.

Robert and Rossen (2001) note that matrix stimulation is almost always performed in multilayer reservoirs containing zones and likely with wide injectivity contrasts, caused either by different permeabilities or by uneven severity of damage. Other phenomena causing vertical heterogeneities within a completion interval include permeability gradients in thick reservoirs and selective damage in some perforations. The natural trend of stimulation fluids is to follow the path of least resistance (i.e., to invade the most permeable or least damaged zones). To optimize treatment results, most of the open interval must be treated, and, thus, treating fluids must also be injected in significant volumes into the least permeable and most damaged zones.

In an example from Robert and Rossen (2001), a three-layer formation is described in [Table 3.14](#). These authors have calculated that the three zones could be treated using 15,000 gal of acid if there were the same amount of acid placed in each zone. However, because of the differences in permeability and skin, more than 40,000 gal of acid would be required to treat all of the layers and some would be overtreated and possibly damaged by excessive amounts of acid (especially if MA was used on a sandstone formation).

Correct fluid placement is also very important when treating deviated or horizontal wells and those with openhole completions. The goal of placement is to uniformly treat all zones while minimizing the amount of fluid pumped as well as the flow rates needed. The authors of this book note that the terms diversion and placement are used in reactive stimulation but describe the same physical phenomena as “mobility control” used to depict fluid movement in improved oil recovery (see Sections 1.6.4 and 5.2.1). Placement of matrix fluids also applies to the scale inhibitor squeeze treatments where the inhibitors are adsorbed or precipitated into the near-wellbore area. See Section 2.2.3 as well as Frenier and Ziauddin (2008).

Correct placement can be accomplished using mechanical as well as chemical methods.

Mechanical methods include

- Specific pumping strategies
- Ball sealers
- Mechanical tools

Chemical methods (frequently called diversion) include

- Various particulates
- Foam
- Viscous diverters

**TABLE 3.14—EXAMPLE OF THREE-LAYER FORMATION
(ROBERT AND ROSSEN 2001)**

| Layer | Permeability (md) | Thickness (ft) | Skin (s) |
|-------|-------------------|----------------|----------|
| 1 | 50 | 50 | 10 |
| 2 | 500 | 10 | 5 |
| 3 | 100 | 40 | 10 |

This following sections will describe and compare the various types of placement method in use or proposed. Some diversion/diversion methods can be used for sandstone or carbonate formations and some have been applied only in specific formation types.

3.7.1 Mechanical Placement Methods. This chapter is primarily about chemical methods for reactive stimulation, but placement is such an important issue that a short review of mechanical methods is included. See more complete treatments in Kalfayan (2008) and Robert and Rossen (2001).

The Maximum Pressure Differential and Injection Rates (MAPDIR) Technique. This method was introduced by Paccaloni and Tambini (1993) and Paccaloni (1995). In this method, the fluids are pumped at the maximum pressure possible without fracturing the formation. The authors (Paccaloni and Tambini 1993) claim that it maximizes use of the fluids; however, Robert and Rossen (2001) contend that this is *not* a diversion method because it does not change the permeability or the placement of the fluid. In addition, the pumping rate may not be the optimal value based of the reactivity of the fluids (see Fig. 3.15).

Ball Sealers. These devices have been in use since the 1950s (Robert and Rossen 2001) to seal the perforations taking the highest flow rates, thus allowing fluid to go into other zones. Small spheres are made of various rubber and elastomers (see Fig. 3.75). Wang et al. (2012b) note that ball sealers have different specific gravity values so that they are buoyant or sink in the fluids. Also see Fig. 3.76 for a drawing of a ball sealer in a perforation where it deforms and blocks the perfs.

Ball sealers are incorporated into the treatment fluid and pumped with it. The effectiveness of this type of mechanical diversion requires keeping the balls in place and is strongly dependent on the differential pressure across the perforation and the geometry of the perforation itself.

Initially, nonbuoyant ball sealers were used, and these frequently had fit problems and were held in place only during steady pumping. They then fell into the well's rathole. Robert and Rossen (2001) describe the use of buoyant ball sealers instead of conventional nonbuoyant ones (Erbstoesser 1980). As shown in Fig. 3.77, when a buoyant ball sealer is transported to the perforations, it either seals an upper perforation or is carried to the lowest one that is accepting fluid. However, because of its buoyancy, it does not remain in the quiescent fluid in the rathole. In comparison with chemical diverters, ball sealers seated on the perforations facing a high-permeability interval effectively stop fluid entry and direct the entire flow to areas with lower injectivity. The density of buoyant ball sealers must be compatible with the density of the carrying fluid to allow transport downhole while prohibiting settling in the rathole. Therefore, there are many different sizes and compositions. Kalfayan (2008) notes that rubber-coated neoprene are the most common type and are available depending on the size of the perforations, the temperatures of the well and the composition of the fluids. Kalfayan (2008) states

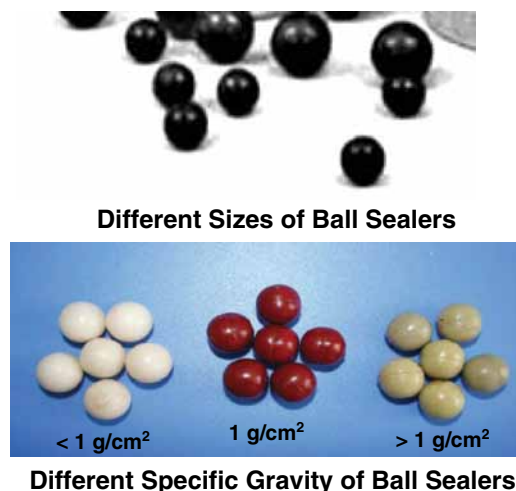


Fig. 3.75—Ball sealers sizes and densities (Wang et al. 2012b).

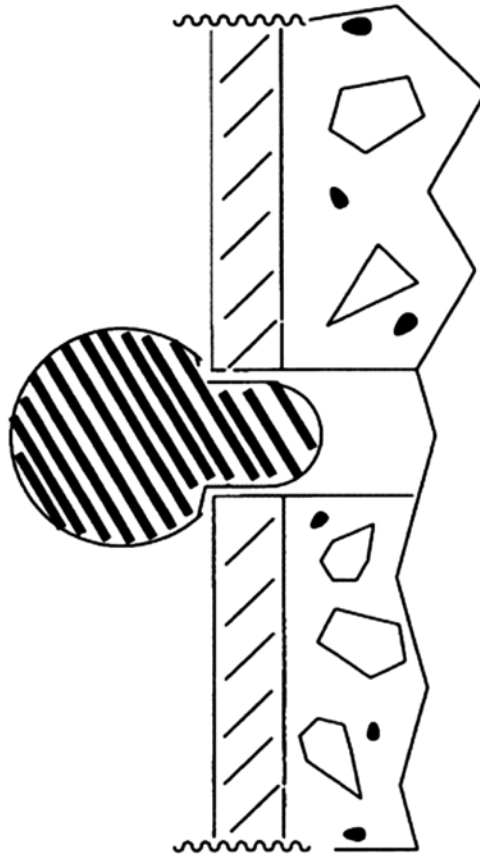


Fig. 3.76—Ball in a perforation (Akbar et al. 2010).

that while ball sealers range in size from $\frac{5}{8}$ – $1\frac{1}{4}$ in., most are $\frac{7}{8}$ in. in diameter and are most effective in newer wells where there has been less damage to the formation and the perforations.

Bale (1984) reports that acid treatments in Saudi Arabia are performed primarily to remove the perforation damage and to establish a flow path through the formation damage near the wellbore.

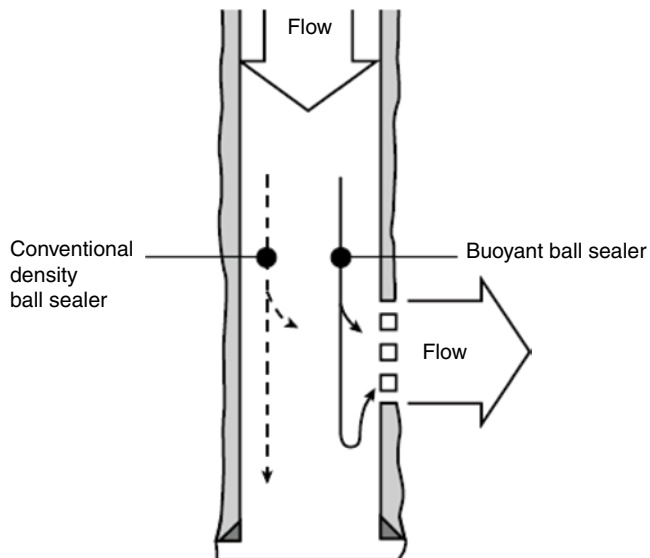


Fig. 3.77—Two ball sealer seating processes (Erbstoesser 1980).

Completion intervals in the carbonate reservoirs may be either openhole or perforations. Intervals will vary from 10 to 90 m (30 to 300 ft) or more in thickness with diverse porosities and permeabilities. The authors report that high-density ball sealers, 1.3 g/cm³ have been used, especially whenever high injection rates are maintained.

Baser et al. (2009) claim a multilayered ball sealer having a deformable layer. The multilayered ball sealer has an outer or intermediate layer that is deformable under pressure. In the former, the deformable layer may be water-soluble or hydrolysable. In the latter, the outer layer is a sheath that contains the deformable layer and adapts to its shape. A multilayered ball sealer may be used as a diversion agent by being suspended in a fluid injected into a wellbore and applying pressure to deform the shape of the intermediate layer such that the multilayered ball sealer adapts to the shape of a perforation opening on which the multilayered ball sealer has seated.

Akbar et al. (2010) claim an oil-degradable ball sealer for use in the oil and gas production. The ball seal comprises a particular composition including ethylene and one or more alpha-olefins, prepared by an injection molding technique to provide a ball sealer that will dissolve in stimulation or wellbore fluids after stimulation operations are complete. The composition, when dissolved into wellbore fluids, is claimed not to pose a hazard or problem to aqueous wellbore fluids or further wellbore stimulations.

Packers and CT as Placement Devices and for Temperature Sensing. Packers and plugs are elastomers (rubber)-based devices that are placed in the wellbore to hydraulically isolate the sections above and below the packer and to provide a mechanical anchor to prevent the packer from sliding inside the wellbore. When in place, they isolate the zone that is to be stimulated. See Fig. 3.78, which shows tubing (a) and CT (c) packers as well as a packer in the well (b).

Robert and Rossen (2001) note that retrievable packers have been developed that use various techniques for setting and retrieving. Tension-set packers are particularly suitable for matrix acidizing

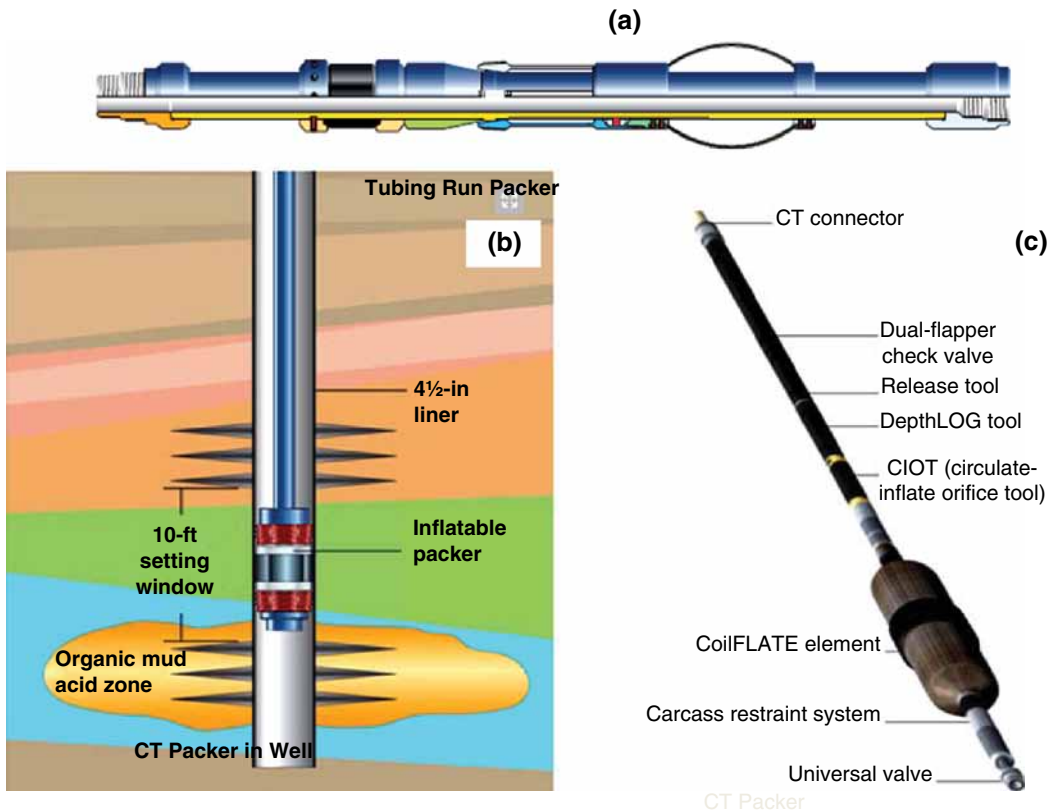


Fig. 3.78—(a) Tubing packer, (b) packer in well, and (c) CT packers (Schlumberger 2010a).

operations. They are initially set by pulling tension on the tubing and held in place by the pressure differential between the tubing and the annulus above the packer.

Additional techniques have been developed to convey packers with CT. Inflatable straddle packers can provide zonal isolation during matrix treatment. Before packer setting, the treating fluid can be circulated down the CT above the packers. Setting of the packer is affected by picking up on the CT and applying pump pressure to inflate the packer elements. Treating fluid can then be directed to the interval between the packers by slacking off weight on the toolstring. In CT completion applications, the packer also holds the CT string in place. Packers are set mechanically, hydraulically, or on wireline. The mechanical-set packer is set by applying either tension or compression on the packer. The hydraulic-set packer is activated by hydraulic pressure.

The variety of packers on CT includes a range of packers and plugs used in wellbore treatments, selective stimulation, water conformance jobs, tubing integrity testing, CT completions, straddle repair installations, temporary or permanent well abandonment, and more.

Kalfayan (2008) notes that there are several advantages and disadvantages with CT packers. The advantages include ease of operation and ability to move the packer from zone to zone. In addition, various tools can be attached to the CT for improved cleaning or circulation. Disadvantages include smaller diameters than the production tubing, so there is higher pressure drops and possible problems with particulate diversion materials. Another significant concern is the corrosion of the CT. While the metallurgy is very similar to production tubing from a general corrosion standpoint and the same acid inhibitors usually can be used as those used to protect the production tubing, residual acid left in the CT may cause disastrous after-job corrosion. Special CT CIs have been developed for this purpose (Arnham et al. 2000).

Swellable packers (Kleverlaan et al. 2005) also may be used to isolate zones in wells so that only some specific areas are acidized. These devices are made of a tubing segment that is lined (on the outside diameter) with an elastomer that swells in contact with water. Al-Yami et al. (2010) claim that, currently, cementing is the only method used in Saudi fields to provide zonal isolation. However, in horizontal sections, cementing becomes a challenge and excessive water production can occur because of channeling. They claim that another method for zonal isolation is to use a rubber elastomer bonded onto a base pipe. The rubber swells in water and provides a seal between the base pipe and the openhole.

Use of another CT-based method is called real-time distributed temperature sensing (DTS) that may help improve the real-time decision process of fluid placement and temporary plugging placement. Several different applications of the methodologies are described. Tardy and Chang (2011) note that DTS involves use of a fiber-optic technology that provides continuous temperature profiles along the length of a wellbore. Inside a CT, installed as a retrievable or permanent cable, the DTS can be used to monitor the temperature evolution during a matrix treatment. Reyes et al. (2011) explain that the fiber-optic cable uses a laser pulse that causes a Raman back-scatter effect that is temperature-sensitive (Grattan and Meggitt 2000). The method uses changes in the temperature of the well fluids at the total depth to analyze placement of the stimulation fluids.

Al-Najim et al. (2012) describe the combination of a smart fluid described as a temporary water-blocking gel and a VES-based self-diverting acid (see Section 3.7.2) in an acid stimulation treatment pumped through CT. It is claimed by the authors that the real-time DTS technology helped improve the real-time decision process of fluid placement, temporary plugging placement, and treatment efficiency evaluation. During CT placement with DTS, the CT tools were moved from zone to zone to place an acidizing fluid, and the temperature log during shut-in is compared with the expected temperatures (based on the known temperature/depth relationship) along the CT string. Various anomalous temperature changes that may include heating because of reaction of carbonate with acid or cooling because of gas expansion or loss to the formation.

Al-Najim et al. (2012) note that the DTS also was used to translate the actual temperature profiles into fluid invasion profiles across the horizontal openhole section of the well. Additionally, a full-scale acid placement and thermal modeling was proposed to perform an in-depth post-treatment evaluation. The authors claim that the bottomhole data evaluation further confirmed the benefits of using a smart fluid. Following the treatment, the well produced at a rate of 1500 bbl/day with 17% water cut, which is well below the field average of approximately 50%.

Reyes et al. (2011) have used the laser-based DST method. The authors claim that the effectiveness of many acid jobs are dictated by how effective the fluid is placed into all zones. Concerns related to the acid treatments included where the acid was placed in the well, if the acid went where it was supposed to, and if the acid went into the first least-resistive zone and subsequent zones went untreated.

They also claim that historically, on acid jobs, surface readings for pressure and rate were the only indicators to judge the effectiveness of the treatment. The paper claims that the operator attempted the previously mentioned acid treatments and also monitored the treatment using DTS, and it was observed that what is seen at the surface can be misleading. This is because surface pressure can be masked by friction and is therefore not a valid indicator for what occurred downhole, and because diversion can take place without surface indication. DTS allowed for practical adjustment to the diversion strategy for the well that was being treated.

Various types of packers are used with fracturing techniques, including the acid fracturing described in Section 3.8 and Chapter 4. The use of ball-operated packers and stimulation ports have also been developed for use in matrix acidizing of horizontal wells. See PackersPlus (2011a). The operation is similar to the fracturing system described in Section 3.8 of this book.

3.7.2 Chemical Diversion Methods. Chemical diversion methods can be used along with some of the mechanical techniques described in Section 3.7.1, or as the primary method in the treatments if the mechanical equipment is not appropriate to the well environments.

Nasr-El-Din et al. (2007) have reviewed some of the chemical diversion methods in current use. They note that mechanical control of treating fluid placement (described above) can be accomplished by coiled tubing with an inflatable packer, or with conventional straddle packers or ball sealers (see Section 3.7.1 of this book). Although mechanical techniques are very effective, they may be more expensive and time consuming than chemical techniques, and they are often not applicable or not effective in wells with openhole completion.

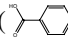
These authors (Nasr-El-Din et al. 2007), note that mechanical techniques divert treatment fluids from the *wellbore*; however, there is no control once the fluid enters the *formation*. Chemical diversion can be achieved through placing a viscous fluid, foam, or gel to lower the penetration of treatment fluid in the created wormholes and/or the surrounding matrix. In addition, particulates in a carrying fluid, which creates a filter cake on the surface of the formation or wormhole, also may be an effective diversion method. The goal usually is to alter the permeability (temporarily) of the formation to cause a more even distribution of the fluid. Thus, a filter cake results in temporary *skin* effect (see Eq. 1.8), which alters the injection profile. Gelled and foamed acids are also being used as a means of improving acid placement by combining stimulation and diversion in one step, and all of the techniques can be used in both carbonate and sandstone formations; however not every specific chemical can be used in every treatment.

Understanding how chemical diverters interact with the formation rock and fluid is the key to selecting the proper product for a specific treatment. It is the intent of this section to provide a technical overview of the chemical diverters used in the reactive stimulation industry. The various mechanisms by which these chemicals to achieve acid diversion, their application histories, and their limitations are presented. Some of the same chemicals are also used in enhanced oil recovery (EOR) (Chapter 5) for permeability modification during various chemical floods. This section (3.7.2) will describe chemical diversion using

- Solids (particles)
- Foams
- Viscous gels

Solid Diverting Agents. Many of these agents were reviewed by Robert and Rossen (2001). They describe the very wide range of particulate agents that can be pumped with reactive fluids to physically block high-permeability flow paths. This is essentially the same mechanism as particle fluid loss agents that form a filter cake during fracture treatments. See Section 4.6. Included are Ca-soap

solutions that would precipitate a solid, various naphthalenes, crushed limestone, oyster shells (also calcium carbonate), paraformaldehyde, and “chicken feed.” All of these materials have some solubility in the acid or in the returned fluids; however, Robert and Rossen (2001) report that formation damage frequently results.

Additional materials that have been more successful are specially sized rock salt (NaCl), benzoic acid () and various oil-soluble resins that can block some of the pores (produce a filter cake) that would be redissolved as the higher pH fluid is produced (Crowe 1971).

Robert and Rossen (2001) classify the particulates as bridging agents that are large sized—10/20 to 100 mesh and very small particles (below 0.004-in. diameter). Note that some of the same types of solids are in use as fracture fluid loss agents. See Section 4.6. The particles must be sized for the formation to be treated. Problems with the various particle diverters are that they may have some solubility in the acidic fluids (and change the characteristics), that they may block the wrong zones, and also may cause permanent formation damage. In addition to these issues, Chang et al. (2008) note that any diverter must be able to perform at the bottomhole temperature of the well. This would be a significant issue for some resins have low melting points and benzoic acid melts at 42°C. Rock salt has been used very successfully in HCl because it has no compatibility issues; however, it cannot be used in HF solutions because of possible precipitation issues with some aluminosilicate reaction products (see Section 3.5.2). Therefore it cannot be used in all of the fluids used in sandstone stimulation treatments.

Solid diverting agents that are claimed to be biodegradable have been described by Halliburton (2011a) and Denney (2011). These authors explain that the products contain a combination of particle sizes (Fig. 3.79) that are quickly and efficiently block flow paths of varying widths temporarily, resulting in redirecting fluid flow for maximum effectiveness. The material will self-degrade over time at temperature, eliminating use of remedial removal techniques. The material claimed to be applicable from 180 to 320°F.

While the composition of the products is not described, a patent application assigned to Halliburton Services (Fulton et al. 2010) claims biodegradable diverting particles that comprises at least one substance selected from the group consisting of a chitin, a chitosan; a protein, an aliphatic polyester a poly(lactide), a poly(lactic acid); a poly(glycolide), a poly(epsilon-caprolactones), a poly(hydroxybutyrate), a poly(anhydride), an aliphatic polycarbonate; a poly(orthoester), a poly(amino acid), a poly(ethylene oxide), a polyphosphazene, and a derivative thereof. The author and Halliburton (2011a) and Denney (2011) also claim that the particle diverters can be used in hydraulic fracturing applications (Section 4.6).

Various fibers can be used as diverting agents. Jauregui et al. (2010) describe the use of these type of solids in the acid diversion fluids. These materials are useful when there is a very large permeability difference or when the formation is naturally fractured. The authors claim that they can be pumped with common acid types. Cohen et al. (2010) report the use of a fiber-laden, self-diverting,



Fig. 3.79—Biodegradable particle diverting agent (Denney 2011).

and viscoelastic acid has been successfully used for matrix acidizing of highly heterogeneous carbonate formations. The fibers have been designed to be inert under surface and pumping conditions, and their geometry allows them to form strong and stable fiber networks that can effectively bridge across natural fractures, wormholes, and perforation tunnels. Eventually, the fibers hydrolyze into a water-soluble organic liquid that is produced back to the surface during flowback. An example of these types of fibers (also used in fracturing—Section 4.9.6) are in the patent by Hoefer et al. (2008). In the case of perforated wells, their experiments suggest that diversion with fibers operates in three phases.

- First, as the early volumes of fiber-laden acid reach the perforations, the acid penetrates the reservoir as if no fibers were present.
- Second, as the fibers bridge, they accumulate inside the perforations and form a fiber cake.
- Third, the fibers plug the perforation, and the injectivity decreases locally, promoting diversion into other perforations.

Foam Diversion. This type of fluid can aid acid well stimulation by diverting the fluid into damaged or low-permeability layers near the wellbore (Ettinger and Radke 1992; Gdanski 1993; Thompson and Gdanski 1993). See Section 1.4.4 for an introduction to foams and the differences between bulk foams and foams in a formation.

This is a powerful and useful technique because surfactants are already employed in acid formulations and nitrogen (the usual foam gas for acidizing) is inert and acts as an energizing agent that improves cleanup. Thus, in some cases, the surfactants already in the formulation can support foam formation. A possible downside is availability and gas purity if nitrogen is used as the gas. The authors of this book report that in some markets, nitrogen is produced using membrane technologies (Mulder 1996). If the separation is not complete, oxygen can be pumped into the acid and can cause significant corrosion. CO₂ also can be used as the inert gas for producing the foam; however, the choice of a surfactant may be different from those used with N₂. Untreated (not deoxygenated) air should *never* be used with any reactive fluid.

Kam et al. (2007) reviewed the flow characteristics of foam in porous media. Here (that is in the formation), the liquid films, or *lamellae*, between bubbles in foam greatly restrict the mobility of gas. Therefore, the number of these lamellae (the bubble size) governs the mobility reduction with foam (Falls et al. 1988). Thus foam mobility depends on various processes that create or destroy lamellae, as well as other processes that mobilize or trap bubbles. The backpressure created as the foam propagates is the major diversion mechanism for subsequent volumes of the foamed solvent.

Kam et al. (2007) note that it is useful to distinguish between strong foam and weak foam, although the distinction between strong and weak foam is not always quantified in the literature and in any case varies among studies. Strong foams reduce gas mobility greatly, by factors of 10,000 to 1,000,000 at the same water saturation (by smaller factors if comparisons are made at the same foam quality). Weak foams reduce gas mobility by smaller factors. Foam generation is a transformation, often abrupt, from a state of high gas mobility (weak foam or no foam) to one of low mobility (strong foam) (Rossen and Gauglitz 1990; Kam and Rossen 2003).

Foam generation is a process where lamella creation greatly exceeds the rate of lamella destruction. Thus, what one observes as foam generation in the laboratory is a result of both lamella creation and the stability of lamellae that are created. Separating these two factors can be difficult. Rossen and Gauglitz (1990) argue that in steady flow in homogeneous porous media foam generation results from mobilization of a small population of lamellae present initially. Foam mobilization and generation depends on exceeding a minimum pressure gradient that depends on injected gas volume fraction, surfactant formulation, the properties of the porous medium, and other factors. Once strong foam is created, it can exist and advance through the porous medium at a lower injection rate (though not necessarily at lower pressure gradient) than that required to create the foam (Kam and Rossen 2003).

An example is shown in **Fig. 3.80**. Here foam generation (creating low-mobility strong foam out of weak or coarse foam) requires *exceeding* a minimum interstitial velocity of about 2000 ft/day (7.06×10^{-3} m/s). If gas and liquid are injected at fixed rates, there is an abrupt increase in pressure gradient at this threshold by a factor of about 100. Once strong foam is created, however, the injection

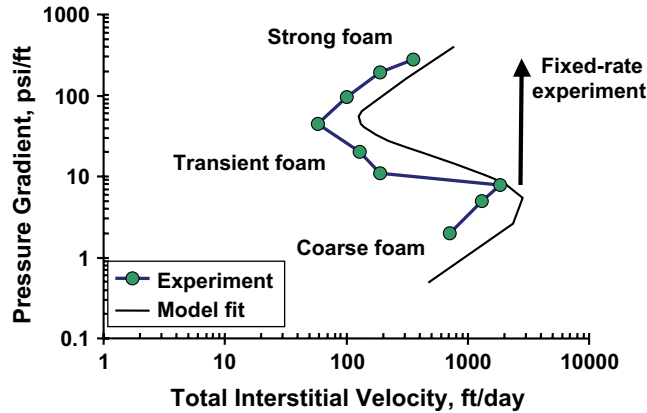


Fig. 3.80—Foam generation experiment of Gauglitz et al. (2002) for 90% quality foam in 7.1-darcy ($7.1 \times 10\text{-}12\text{ m}^2$) Boise sandstone, and model fit to data by Kam and Rossen (2003). In an experiment with fixed injection rates, pressure gradient would increase abruptly.

rate can be reduced substantially and still maintain strong foam. This indicates that observing foam strong at a given injection rate can be affected by hysteresis. Careful studies at fixed pressure gradient rather than fixed injection rates find an unstable transient regime between the strong and coarse foams. Various studies support these findings (Rossen and Gauglitz 1990; Kam and Rossen 2003).

Kam et al. (2007) claim that foam generation is favored by high pressure gradients (or high injection rates), low injected gas volume fractions (low foam qualities—that is more liquid and surfactant), injecting alternating slugs of gas and liquid, and other factors that stabilize foam lamellae, such as relatively low temperature and high surfactant concentration (Rossen and Gauglitz 1990; Kam and Rossen 2003). The first three factors are thought to favor the creation of lamellae, and the other factors to favor survival of the lamellae once created.

Success in the field depends on both foam generation and foam advance, or propagation. It is not clear to what extent foam advances by the movement of bubbles and by creation of new bubbles ahead of the foam front—in other words, to what extent foam propagation is a separate issue from foam generation (Friedmann and Jensen 1986). Foam can propagate at injection rates too low for foam generation, just as strong foam can be maintained at injection rates too low for foam generation (Fig. 3.80). On the other hand, the conditions that favor foam generation also favor foam propagation (Friedmann and Jensen 1986).

The pattern of strong-foam regimes is observed with a variety of surfactant formulations and gases, in porous media varying from consolidated cores to sand packs and bead packs, and over a wide range of injection rates (Osterloh and Jante 1992; Rong 2002). The difference between these two regimes is important because their rheology and ability to divert flow between layers differing in permeability is very different. There is only one study of these regimes at elevated temperature: that of Osterloh and Jante (1992) at 150°C (302°F), and no studies of the two flow regimes for foam with acid. Parlar et al. (1995) described the results of a series of dual (diversion) and single core foam experiments followed by liquid injection in unfired Berea sandstone cores.

Surfactant type, preflush, and foam slug sizes are identified as critical parameters for subsequent liquid diversion into low-permeability regions. In contrast to EOR processes (Section 5.7.3), surfactant adsorption is shown to be *beneficial* for diversion. At low liquid rates, and high foam qualities relevant to EOR, foam at steady-state is found to behave as a Newtonian fluid with respect to liquid rate provided that the gas rate is above a critical rate. At high liquid rates and low qualities, a shear-thinning behavior is observed. Pressure gradient during post-foam liquid injection is found to be independent of both foam and subsequent liquid rates and to depend only on permeability for fixed surfactant chemistry. The entrance effects noted in foam literature are found to be more pronounced at high permeabilities and intermediate injection rates. Potential mechanisms as to why foam diversion in matrix acidizing works in the field are also discussed.

TABLE 3.15—DESCRIPTION OF SURFACTANTS FOR HT TESTS (KAM ET AL. 2007)

| Surfactant | Type |
|------------|---|
| A | Amphoteric alkyl amine |
| B | Blend of ethoxylated alcohols |
| C | Blend of ammonium alcohol, ethoxysulfate and ethoxylated alcohols |
| D | Formulated amphoteric alkyl amine |

Parlar et al. (1995) found that a strongly adsorbing surfactant *may* promote diversion of foamed-acid into low permeability (damaged) regions where the cation exchange capacity (of the formation clays) may be higher, or alternatively, it may improve the tolerable foam slug size that can still yield diversion of subsequent liquid (acid). Although small foam slugs followed by liquid can divert much larger fractions of the liquid into low permeability regions compared to acid foam, they are also likely to be more difficult to control in the field. Destabilizing effects of oil may be beneficial in controlling the size of foam slugs following surfactant preflush. Foamed acid at low foam qualities may be a better alternative to foam slugs followed by acid injection because foam itself is diverted into low permeability regions, although this may not be desired in wells with high water or gas-cut problems.

Kam et al. (2007) conducted a study that examined four surfactant formulations at room temperature, 104°C and 204°C with and without acid and CI. The surfactants included amphoteric as well as nonionic foaming agents. See [Table 3.15](#) for the chemical descriptions. The acid formulation was a mixture of an HEDTA chelating agent and HCl, with the pH of approximately 4. Formulations were tested at all three temperatures for foaming with N₂ gas (80% quality foam) at backpressure of 4.1 MPa in sand packs and for bulk-foam stability in a pressure cell. Foam was created in most cases at 24°C without acid or CI. Creating foam with acid and CI at 204°C was more difficult, requiring higher injection rates and lower foam quality. Once formed, strong foam had higher mobility at elevated temperatures than at room temperature. Addition of CI was more adverse to foaming than acid itself. At 204°C foam propagation was slower, and steady-state pressure gradient was lower than at 24°C. The two steady-state strong-foam regimes reported elsewhere were present at 104°C and in the presence of acid. The pressure gradient at 104°C was lower in both high-quality and low-quality foam regimes.

Experiments conducted in this study comprise two parts: bulk-foam stability tests in a high-pressure visual cell, and flow experiments in sand packs. In both cases, temperature ranges from room temperature (about 24°C) to 204°C. The bulk foam cell ([Fig. 3.81](#)) and the sand pack apparatus are seen as [Fig. 3.82](#). Foaming tests were run in KCl as well as in the acidic chelating agent formulation.

The bulk foam stability tests without acid or CI at room temperature 104°C and 204°C. The tests indicated that surfactant A was the most stable at the higher temperature (204°C), compared with the other materials. In all cases, bulk-foam stability decreased significantly with increasing temperature. In two separate tests, it appears surfactant degraded chemically when tested at 204°C, also in agreement with previous studies.

The bulk-foam stability results agree qualitatively with the sand pack results, but quantitative relationships between the two tests are hard to draw. Bulk foams made with surfactants C and D all collapsed quickly at 104°C, but those same surfactants were capable of creating strong foam at high injection rates in sand packs. Surfactant stabilized bulk foams the best of those tested at all temperatures but was not always markedly better in foaming in sand packs. In all cases tested in the sand packs, increasing injection rates and decreasing foam quality help foam propagate through the sand pack. These results also suggest that these surfactants may degrade over a period of time, for example, a couple of hours at 204°C. Residence time in the heated sand pack, therefore, should be properly accounted for in design of experiments. These results are consistent with decreasing foam stability at higher temperature, adverse interactions between foaming surfactant and CI, and easier form generation at higher velocity and lower foam quality. The chemical structures of the surfactants are critical to foam propagation, especially at high temperature.

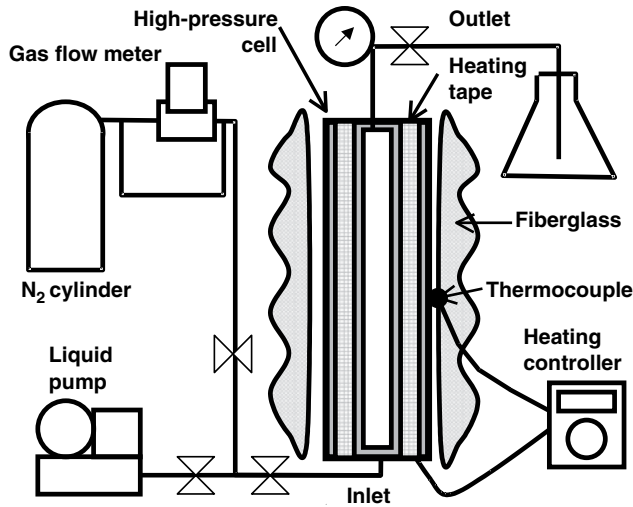


Fig. 3.81—Schematic of bulk-foam stability-test apparatus (Kam et al. 2007).

Cheng et al. (2001) have claimed a simulator that accounts for the effects of gas trapping on gas mobility in foam and in liquid injected after foam, and for the effects of pressure gradient on gas trapping. The foam model fits steady-state foam behavior in both high- and low-quality flow regimes and steady-state liquid mobility after foam.

The dynamics in the transition period are found to be complex. For instance, they (Cheng et al. 2001) explain that simulations indicate that most of the core experiences a period of drier flow at the start of liquid injection, because of expansion of gas already in the core. Simulations and new laboratory results suggest that a dead volume present upstream of the core in previous studies strongly affects the transition period seen in those experiments. Simulations and data agree that the transition is faster

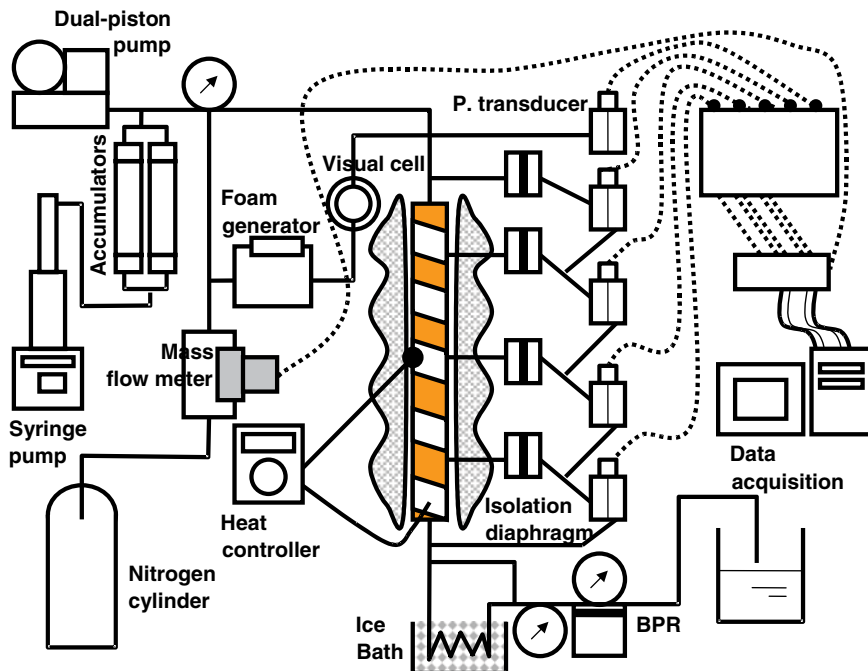


Fig. 3.82—Schematic of laboratory sand pack apparatus and data-acquisition system (Kam et al. 2007).

at higher pressure (with lower gas compressibility) and that response to a shut-in period depends on how much gas escapes during the shut-in (i.e., on how long the shut-in lasts). Extended to radial flow, the simulator suggests that the transition period may not be so crucial to field application as it first appeared from laboratory corefloods. In the cases examined, injection-well pressure approaches its steady-state value within about 15 minutes or less of the start of liquid after foam.

Siddiqui et al. (2003) described the results from several dual-core experiments using 11- and 22-in. (27.9- and 55.9-cm) long and 1.5-in. (3.8-cm) diameter fired Berea sandstone cores (permeability range: 10–1000 md) in which parameters such as foam quality, total injection rate, foam slug size, etc., are varied systematically for different permeability contrasts. The authors tested an anionic as well as a nonionic foaming surfactant (a lauryl amine oxide).

Major conclusions from Siddiqui et al. (2003) are

- The permeability of the cores dominated the diversion performance and a linear relationship was observed between the permeability ratio and the diversion performance.
- The effect of foam quality on the diversion performance seemed to depend on surfactant type, permeability range, and in some cases (with Surfactant 8), a range of 65–75% gave better results and in some other cases (with Surfactant 3) a quality of 85% gave better results.
- It appears that the absence of surfactant preflush, the addition of surfactant in the post-foam fluid, and use of a higher backpressure helps foam diversion.

A summary of foam diversion mechanisms from the reviewed literature in this section are

- The major mechanism is large increase in pressure because of trapped gas.
- Generation of foam happens by shear in matrix and in tubulars.
- The stability of foam (time) is critical and depends on the surfactant and the temperature.

Crowe et al. (1992) note that foam diversion can be more effective if a surfactant-laden slug is injected before the foam stage and then the foaming agent is added to every acid stage. This ensures that the formation is saturated with surfactant and improves the time that the diversion backpressure is effective (Zerhobu et al. 1994).

Self-Generated Gel Diversion and Emulsified Acids. Several different types of *in-situ gelled acids* have been shown to improve acid placement in carbonate reservoirs (limestone and dolomite). Some systems also are claimed to be useful in sandstone formations and will be described in this section. The large issue is that most of the gelled acid diverters require a pH change that may not occur during sandstone treatments. The difference between an *in-situ gelled acid* and external gelled acid (such as acid gelled with polyvinyl alcohol) or other diverting agents is that the external gelled acids or diverting agents are already activated on surface. Thus, when they reach the formation face, the viscosity is the same for the high-permeability and low-permeability formations. The proportion of fluid entering each zone is simply determined by Darcy's law (Eq. 1.2). The *in-situ gelled acid* offers the benefit of increasing viscosity *inside* the formation; therefore, when acid enters the high-permeability zone (or wormhole), it will have higher viscosity than the acid still in the wellbore. This extra resistance helps direct incoming acid into the low-permeability zone.

Jennings (1993) claims a solidifiable viscous gel containing gel breakers is injected into the higher permeability zone. The gel enters the wormholes and forms a solid gel, thus precluding entry of additional acid while displacing the acid further into the formation. Jennings recommends hydroxypropyl guar but does not describe the *in-situ gelling* mechanism.

Another type of *in-situ gelled acid* diversion formulation [self-gelling acid diversion (SGAD)] is prepared by gelling the HCl acid with a polymer along with adding a crosslinker and an internal breaker (Mukherjee and Cudney 1993). This is a complex system. When the acid spends upon dissolving carbonate, the increase of pH causes the crosslinker to activate and the gelled acid becomes crosslinked. This crosslinked gel temporarily blocks the wormholes being created and diverts acid elsewhere. Any further increase of pH by complete spending of the acid causes the breaker to activate, and the *in-situ gelled acid* hence breaks down to near water-like viscosity to assist easy flowback.

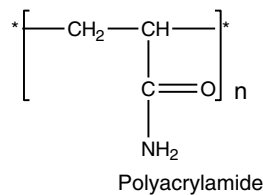
Because the system contains polymers, and when the bulk fluid viscosity is dramatically reduced, there still may be a *polymer residue* (Mohamed et al. 1999) that can plug the face of the wormholes.

The exact chemistries of the SGAD (Mohamed et al. 1999) systems were not revealed; however, a patent by (Hill 2005) of a SGAD of the type described previously consists of HCl mixed with a polyacrylamide or a cationic polyacrylamide copolymer. The mixture is crosslinked using FeCl_3 as the pH rises to about 2 and, thus, thickens in the wormhole and diverts acid. The mixture also contains a reducing agent (a hydrazine compound or sodium erythorbate) that is activated at higher pH values. This agent then reduces the Fe(III) to Fe(II) and the gel brakes and the viscosity is reduced. **Fig. 3.83** is the mechanism proposed.

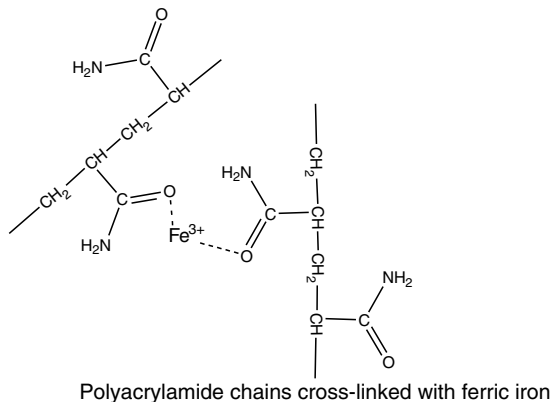
The patent (Hill 2005) also lists alternative reducing agents that also may be useful in this and other redox processes.

The effectiveness of a SGAD was evaluated by Bazin et al. (1999). This system crosslinks when the acid spends in the formation and the pH increases at a value of about 2. The crosslinked gel effectively stops any further invasion and diverts the subsequent acid stage from the path of least resistance. The crosslinked gel is claimed to break upon further spending at a value of about 3 to 4, and the viscosity of the fluid will return to its original value. In particular, the effects of the acid strength in both the diverter stage and the neat acid stage are scrutinized. This diversion system was used as a prestage and was followed with ungelled HCl.

The diverting effect was also analyzed with a multicore flow apparatus (similar to **Fig. 3.84**) specially designed to reproduce downhole injection conditions in horizontal wells. The study demonstrated that when 3% SGAD was injected first, followed by 7% HCl, a better equalization of the flow rates and a longer breakthrough time in the high-permeability core were observed. However, the stimulation of a limestone was also considerably reduced because wormholing occurred over 2 cm only. The authors conclude that the SGAD method is effective to delay wormhole propagation in the high-permeability core and to stimulate the low-permeability limestone. However, high neat acid concentrations are required.



In acid, amide and acetate groups are protonated. As pH reaches about 2, ferric iron crosslinks PAA chains.



As the pH reaches about 4, the reducing agent is activated and iron is reduced:

$$\text{Fe}^{3+} + \text{e}^- \longrightarrow \text{Fe}^{2+}$$

Fig. 3.83—PAA gel crosslink mechanism.

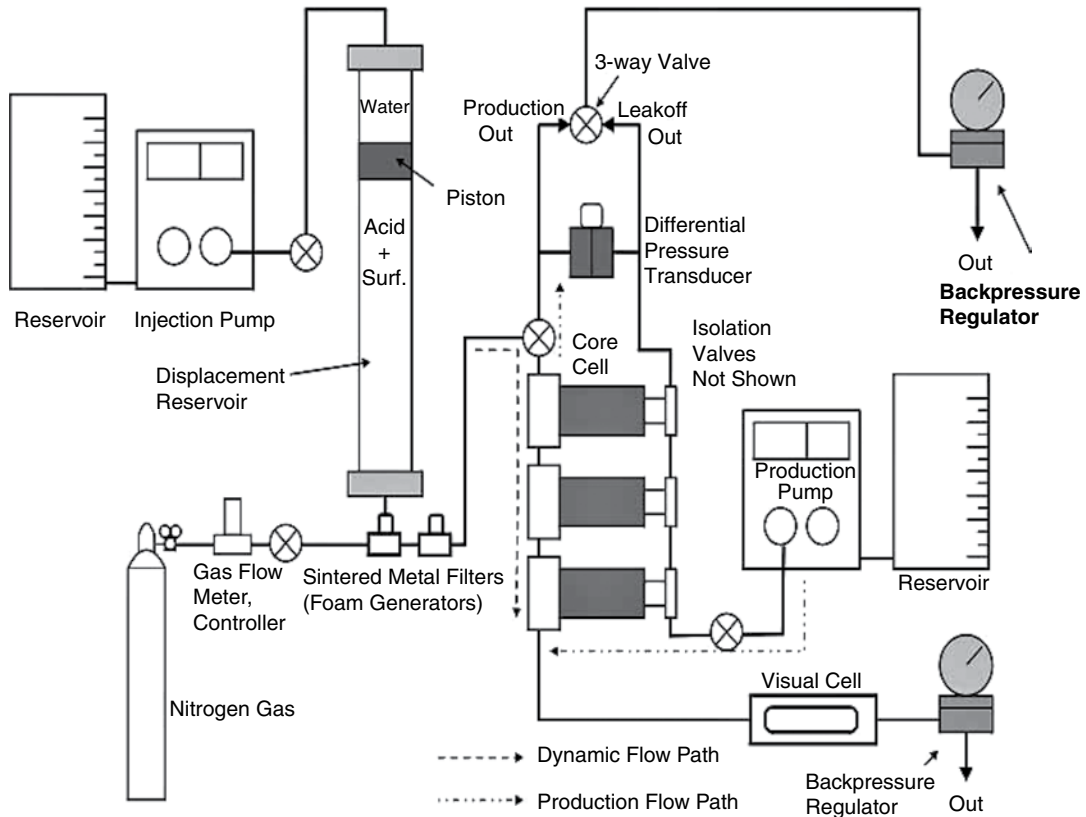
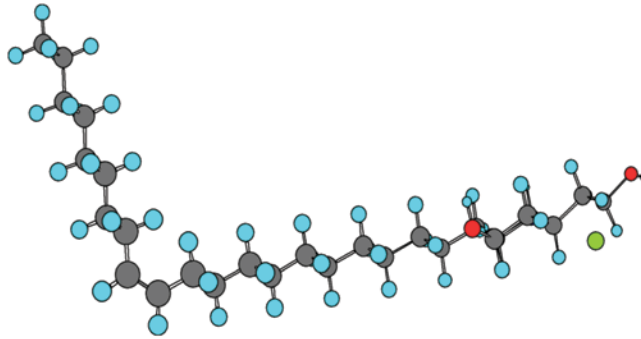


Fig. 3.84—Multicore system for diversion studies (Chang et al. 2001a).

Gomaa and Nasr-El-Din (2010) and Gomaa et al. (2011) studied the apparent viscosity of the SGAD and claim that the polymer plays a key role in diversion because it creates a viscosity differential in treated and untreated zones. An extensive literature survey and field data showed that there is no agreement on the effectiveness of this acid system. Therefore, a study was conducted to better understand this acid system and determine factors that impact its viscosity buildup. Three commercially available in-situ acids were examined.

The effect of salts and [Fe(III)] contamination on the apparent viscosity of these acids was examined in detail. Several new findings were identified, including that polymer and other additives were separated out of the acid when these acids were prepared in high-salinity brines. Preparing the in-situ gelled acid with saline waters decreased the viscosity of the acid in live and partially neutralized conditions. Concentrated HCl solutions produced high concentrations of calcium ion that reduced the viscosity of the in-situ-gelled acid system. Therefore, in-situ-gelled acids that are based on polymers should be used at low HCl concentrations (3 to 5 wt% HCl). They also concluded that this acid system caused damage in some cases.

Forming an emulsion [acid in oil (W/O) of oil in acid (O/W)] will cause the viscosity of the overall fluid to be increased and an O/W emulsion will have reduced reactivity with the carbonates. Increasing the viscosity slows down the penetration rate allowing deeper penetration of the formation. See Sections 1.4.4 and 2.4.2 on the various types of emulsions. Navarrete et al. (1998a) claim that these types of fluids also reduce the *dissolution rate* of the acid on carbonates. This can also improve penetration of some limestone formations because a retarded rate-acid system allows the operator to pump at a lower rate to achieve the optimum ratio of reaction rate to convection and allow better wormhole penetration. Bustos et al. (2011) claim that the addition of small particles to the acid/oil/surfactant system improves the stability of the emulsions. The authors claim the use of nutmeg, mustard, or guar and oil-seed particulates (preferably powder). The effect of solids (especially asphaltenes) had been shown to



Erucyl bis(2-hydroxyethyl)methyl ammonium chloride.

Fig. 3.85—A VES surfactant molecule.

stabilize unwanted production emulsions (see Section 2.4.2). Also see discussions of emulsion-based acid systems in Section 3.4.2.

Reaction rate retardation is a very useful property at high temperatures and will be explored more fully in Section 3.8.3 on fracture acidizing. Also see Salathiel and et al. (1980).

VES Gelled Acid for Carbonates. Another gelled acid diversion system is based on VESs that are similar to those used in hydraulic fracturing (Norman et al. 1995; Chase et al. 1997; Samuel et al. 1997; Tibbles et al. 2003). See Section 4.4.2.

One cationic surfactant described in these documents is erucyl bis(2-hydroxyethyl)methyl ammonium chloride (**Fig. 3.85**). According to the discussion in Chase et al. (1997), these materials can form viscous gels when the fluid contains various salts or other species that cause the individual molecules to self-associate to form rod-like micelles (**Fig. 3.85**). Then, as the process continues, the rod-like micelles form a gel structure (**Fig. 3.86**) in which the rod clusters overlap to form the gel that behaves like a polymer. However, these gels can be thinned by shear (**Fig. 3.87**), thus reducing the viscosity of the fluid.

Chang et al. (2001a) described an in-situ gelled acid diversion system based on VES chemicals. Chang et al. (2003) also claim a formulation that contains amphoteric betaine surfactants such as

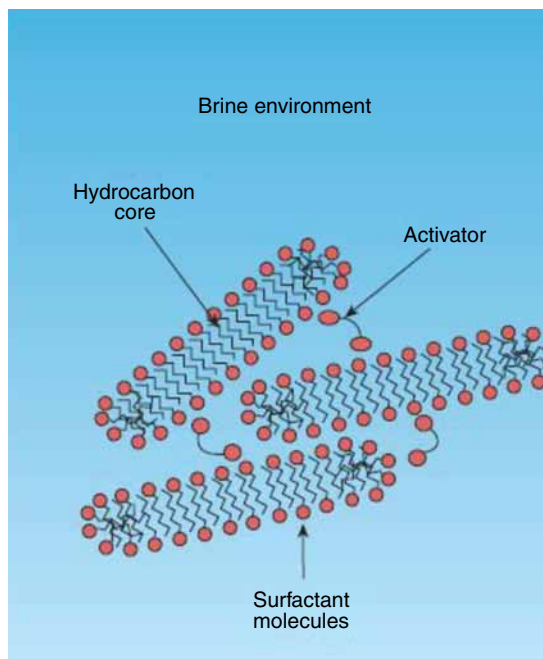


Fig. 3.86—VES association to rod-like micelles (Chase et al. 1997).

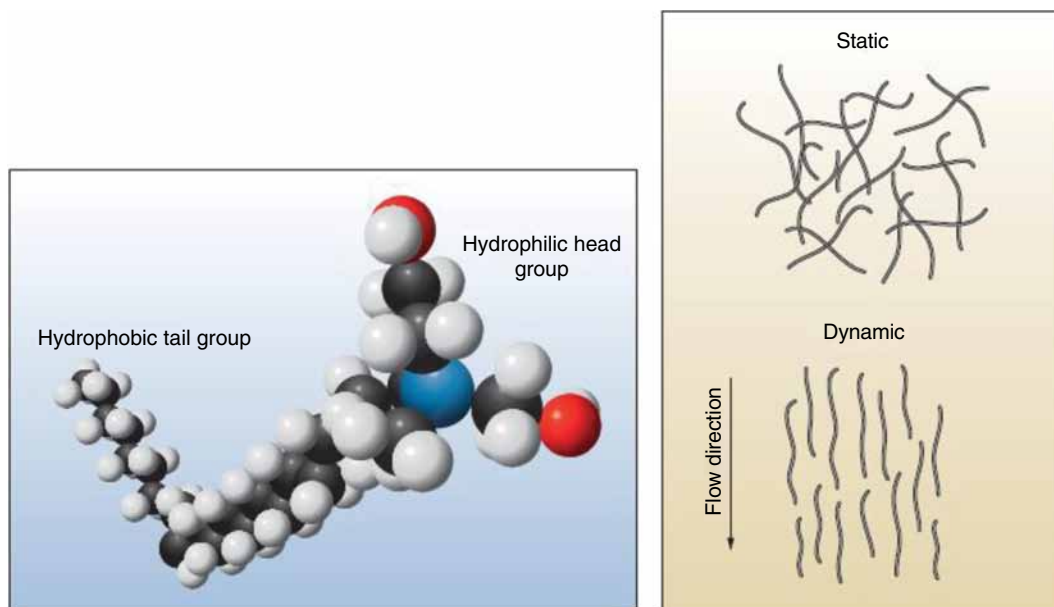


Fig. 3.87—Reversible VES gel (Kefi et al. 2004).

those seen in Fig. 3.88. The formulation also is claimed to have a cosurfactant such as para-sodium dodecyl benzene sulfonate. The mechanism of activation involves a change in pH that affects the formation of the wormlike micelles that takes place as the acid spends on the carbonate formation. A rheology test was performed by Chang et al. (2001a) to investigate the effect of pH on the gellation. A 24% CaCl_2 solution was used to simulate spent 15% HCl. The gelling agent was added into the simulated spent acid and the pH was adjusted by adding a small amount of HCl. The viscosity profile as a function of pH was obtained. The second series of rheology testing was to measure spent gelled acid viscosity as a function of temperature. The gelling agent was added into the acid. After the solution was well mixed, CaCO_3 was slowly added to spend the acid until the pH value of the fluid reached 4 to 4.5. The gel was then loaded into a Fann 50 viscometer and the viscosity was measured at elevated temperatures.

The viscosity increased significantly when the pH increased above 2 (Fig. 3.89). When the acid was spent upon reacting with CaCO_3 , the pH increases and Ca^{2+} ions are released into the solution.

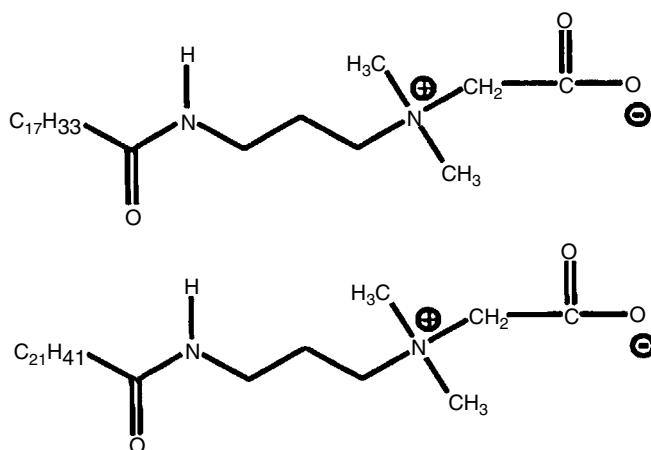


Fig. 3.88—Amphoteric betaine surfactants (Chang et al. 2003).

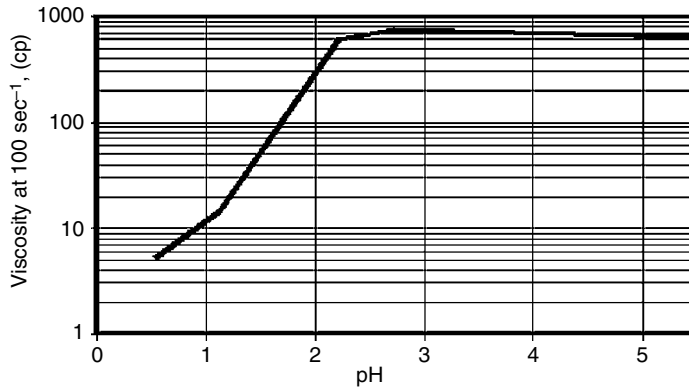


Fig. 3.89—Viscosity profile of the VES-based in-situ gelled acid as a function of pH at 75°F during acid spending (Chang et al. 2003).

This causes the surfactant molecules to form rod-like micelles, and the tangled rod-like micelles cause the fluid to exhibit viscoelastic behavior. As the acid spends in the formation, the ambient pH will naturally increase, resulting in gelling inside the formation. In the acid diversion process, this in-situ gelling phenomenon creates extra resistance in the zone in which acid has entered. Therefore, the acid that is still in the wellbore (which has low viscosity) will be forced to enter the untreated zones. See [Fig. 3.90](#) for a possible mechanism. This figure shows the monomers of the surfactant reacting with the Ca^{2+} ions as well as the increased pH (which changes the charge structure of the surfactant) to form a worm-like micelle. The figure also shows the produced hydrocarbon disrupting the micelle structure, thus reducing the viscosity. The authors of this book claim that VES-based gels and the SGAD gels (prior subsection) both are initiated (at least partially) by an increase in pH and salinity; however, the actual gels are different (a permanent polymer or a virtual VES polymer).

Because the VES surfactants also may support foam, addition diversion potential may be used. Chatriwala et al. (2005) describe tests with a different VES chemical that was used to form stable foam during matrix stimulation of a seawater injector. The length of the target zone was 1,500 ft, and the average permeability of the carbonate was 700 md. A 1.75-in. CT was used to better distribute the acid in the openhole section (6.125 in. in diameter). They note that the surfactant molecules form structures in solution in the presence of salts. These structures enhance the viscosity of solution significantly and can be broken by dilution with injection water or by adding mutual solvent (3–5 vol%) to the preflush/post-flush stages. One of the authors (Cawiezel and Dawson 2009) lists a VES diversion system based on amidoamine oxide surfactants such as seen in [Fig. 3.91](#). This patent claims that a self-diverting fluid is generated in situ by spending of the acid and generation of the calcium chloride, which, in turn, increases the viscosity of the fluid. The gelled or thickened diverting agent diverts a portion of the acid (and subsequent acid stages) from the more permeable zones of the formation to the less permeable zones. This is a similar mechanism as that described by Chang et al. (2001a).

To provide greater understanding of the process, Chang et al. (2003) performed multiple (3) core-flood tests (using equipment seen in [Fig. 3.84](#)) to test the ability of 15% HCl containing formulations

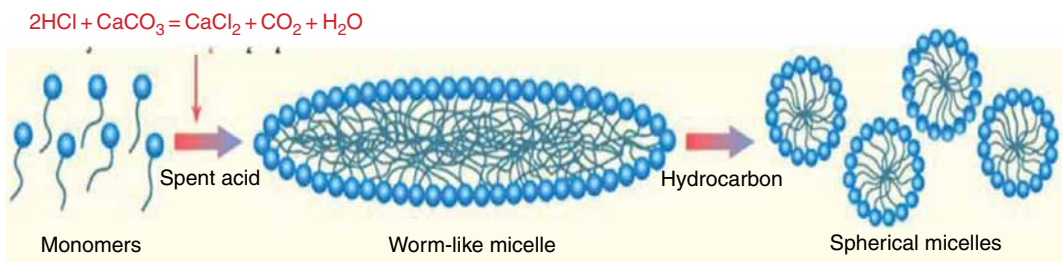
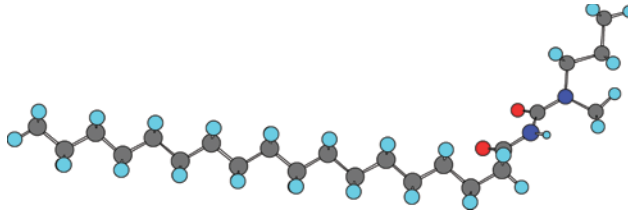


Fig. 3.90—VES diversion mechanism (Al-Anzi et al. 2003).



stearyl amidopropyl dimethylamine oxide

Fig. 3.91—Amidoamine oxide VES surfactant.

to divert fluids. **Fig. 3.92** presents results of a study in which the VES-based in-situ gelled acid was injected into the multiple cores. In this particular study, the three cores had initial permeabilities of (from left to right) 35.0, 48.7, and 32.1 md. The pressure profile behavior as a function of pore volume injected shows that the acid starts to viscosify upon spending, as it enters the high-permeability core.

As evidenced by the CT scan images in Fig. 3.92, the VES-based in-situ gelled acid (in contrast to 15% straight HCl solution the baseline system), produces wormholes in all three cores, rather than just a single dominant flow channel in the high-permeability core. The regained permeability measurement showed dramatic stimulation in the low-permeability rocks. A control test using ungelled 15% HCl did not show any stimulation of the low-permeability cores.

Nasr-El-Din et al. (2011) and Nasr-El-Din et al. (2009b) have provided additional information on surfactant-based acid systems (VES) that were developed for diversion and to overcome the problems caused by polymer residue and crosslinker precipitate after polymer-based system treatments during matrix and fracture acidizing.

Two types of VESs have been used: amphoteric and cationic surfactants. The authors state that the surfactant molecules can form rod-like micelles and significantly increase the viscosity in the presence of salts. After acid treatments, the surfactant gel can be broken by mixing with hydrocarbons, external breakers, internal breakers, or by reducing the concentration of salts and or surfactant through

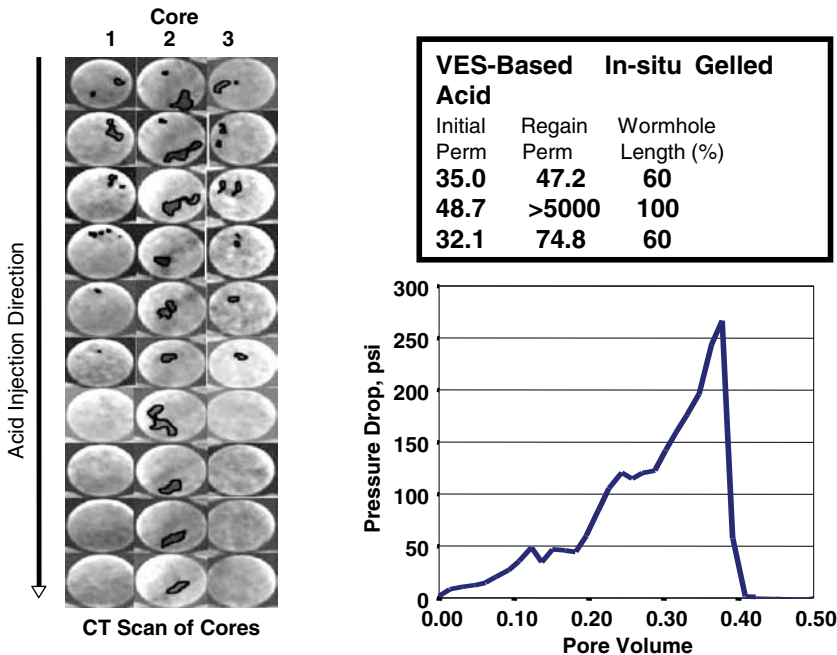


Fig. 3.92—Multicore flow study of VES- based in-situ gelled acid at 150°F (Chang et al. 2003).

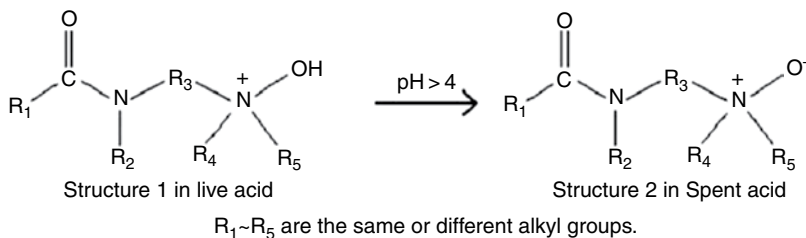


Fig. 3.93—Amine oxide structures (Li et al. 2010).

dilution with water. This paper describes tests with viscoelastic-amphoteric surfactant (amine oxide) seen in **Figs. 3.91 and 3.93**. Note that it carries a positive charge in live HCl acids. The effects of acid additives and Fe(III) contamination were examined on its rheological properties. Measurements were made at temperatures from 75 to 220°F and 300 psi at various shear rates from 0.01 to 935 sec⁻¹. Acid additives included CIs, a mutual solvent, a nonemulsifying surfactant, iron-control agents, and a hydrogen-sulfide scavenger.

The authors (Nasr-El-Din et al. 2011; Nasr-El-Din et al. 2009b) report that the apparent viscosity of surfactant solutions prepared in deionized water, live acid, and spent acid was found to be a function of temperature. Apparent viscosity of live surfactant-based acids was also found to be a function of HCl concentration. Fe(III) contamination caused enhancement of apparent viscosity, then two immiscible liquids, and finally precipitation of surfactant/Fe complex. A demulsifier and mutual solvent decreased the apparent viscosity at all temperatures examined. Multiple iron-control agents were tested and found to reduce the apparent viscosity of this surfactant-based acid. Only up to 1 wt% methanol could be used with this spent-acid system at temperatures below 175°F. Hydroxy chelating agents such as HEIDA and GLDA decreased the viscosity, so more concentrated surfactants are recommended with these additives.

Nasr-El-Din et al. (2009b) and Ahmad et al. (2010) describe the evaluation and field use of cationic surfactant-based VES fluids that were compatible with CIs and were successfully tested in lab and field treatments. The particular cationic surfactant and the CI type were not identified in this paper but the reference to more than 100 successful applications attests to the maturity of this type of diversion technology.

Lungwitz et al. (2007) describe results of a self-diverting-acid based on VES chemicals. They state that the system has been successfully used during numerous stimulation treatments of carbonate formations in various fields. The decrease of acid concentration during the spending process viscosifies the fluid through the transformation from spherical micelles to an entangled worm-like micellar structure while penetrating the carbonate rock. The highly viscous fluid acts as a temporary barrier and diverts the fluid into the remaining lower-permeability treating zones. After treatment, the VES barrier breaks when contacted either by formation hydrocarbons or pre- and post-flush fluids. Quantifying diversion, fluid efficiency, and cleanup are important factors for successful candidate selection and job design. Laboratory tests defining these key factors are presented in this paper.

This paper is claimed by the authors to demonstrate the diverting ability of the acid as a function of permeability, characterized by introducing the concept of maximum pressure ratio in coreflood tests (dP_{\max}/dP_0) supported by core-flow and acid conductivity tests using limestone and dolomite cores. In this ratio, dP_{\max} is the maximum pressure seen in the coreflood test (see Fig. 3.92) and dP_0 is the maximal pressure seen in the control without the diverter. The results are claimed to demonstrate high dP_{\max}/dP_0 in high-permeability cores and low dP_{\max}/dP_0 in low-permeability cores. In addition, retained permeability results indicate that VES systems clean up easily and that it provides higher regained permeability than conventional gelled acid systems.

Al-Ghamdi et al. (2011) have conducted a series of experiments using 20 in limestone cores (most other data is collected with 6-in. long cores) and 15% HCl with or without 7.5% of an amphoteric VES (not identified). The data that included pumping test conducted to core breakthrough as well as X-ray studies of the cores. There data indicate that there may be an optimal pumping rate for use of VES

diversion based on the core permeability. The reaction rates of the VES/acid fluid was not described; however, this factor may be important for some formations.

As noted in the paper by Nasr-El-Din et al. (2009b) different cationic VES materials are in use as acid diverting agents. A patent by Colaco et al. (2007) reviews the many types of VES materials that may be used in various oilfield applications. The authors list cationic surfactants, amines, amphoteric surfactants as well as anionic surfactants that may form VES structures in some fluids. These materials would not necessarily all be effective in acid diversion, but may be useful in other applications such as fracturing (described in Section 4.4.2) and will provide a useful guide for development of new fluids.

Madyanova et al. (2012) describe the application of a high temperature, highly retarded emulsified acid system that slows the reaction times by a factor of 5 to 15 compared to conventional HCl systems. This has been applied in a very high-temperature carbonate (to 350°F and calcite and dolomite). The emulsified acid system (see Section 3.4.2) combined with a self-diverting VES-based acid (Chang et al. 2003) . The compositions of the fluids are in **Table 3.16**.

The VES-diversion system was claimed to be able to achieve complete stimulation of a 197-ft long perforated interval without the need of CT. A pressure buildup test showed a post-stimulation skin value of -3.3 and the production log analysis demonstrated complete and uniform zonal coverage with the upper zones contributing with 53% of the total well production and the lower zone with 47%.

Jauregui et al. (2010) describe a fiber-laden polymer-free self-diverting acid system that was introduced in Saudi Aramco to improve zonal coverage across the entire interval of interest in vertical and highly slanted wells during stimulation treatments. This diversion system combines fiber and a self-diverting acid, which uses a VES fluid that gels as the acid spends. The combination of the self-diverting acid and fiber enhances the diversion process by combining the aspects of both particulate and viscosity-based diversion techniques. The fluid system is claimed to offer an advantage in that it does not contribute to reservoir damage as the VES will break down upon contact with hydrocarbons, and the fiber will dissolve with time and temperature. The initial results indicated substantial pressure responses and excellent gas production performance. More details are in the paper by Cohen et al. (2010).

**TABLE 3.16—EMULSIFIED ACID/VDA COMPOSITIONS
(CHANG ET AL. 2003)**

| Emulsified Acid | | |
|----------------------------|---------------|---------------|
| Additive | Concentration | Unit |
| Diesel | 300 | gal/1,000 gal |
| Fresh water | 246 | gal/1,000 gal |
| Surfactant emulsifier | 6 | gal/1,000 gal |
| HT corrosion inhibitor | 15 | gal/1,000 gal |
| HT corrosion inhibitor aid | 30 | gal/1,000 gal |
| Chelating agent | 50 | lb/1,000 gal |
| Iron control agent | 10 | lb/1,000 gal |
| 32% HCl | 403 | gal/1,000 gal |
| VES SDA | | |
| Additive | Concentration | Unit |
| Fresh water | 442 | gal/1,000 gal |
| VES surfactant | 75 | gal/1,000 gal |
| HT corrosion inhibitor | 10 | gal/1,000 gal |
| HT corrosion inhibitor aid | 30 | gal/1,000 gal |
| Chelating agent | 50 | lb/1,000 gal |
| Iron control agent | 10 | lb/1,000 gal |
| Methanol | 10 | gal/1,000 gal |
| 32% HCl | 443 | gal/1,000 gal |

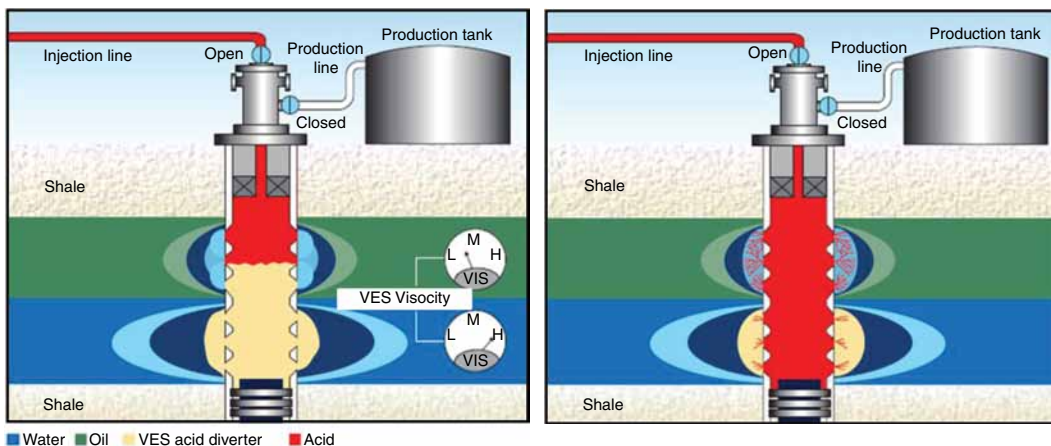


Fig. 3.94—VES acid diverter process (Kefi et al. 2004).

VES Gelled Acid for Sandstone Formations. Some usage of VES diversion for sandstone matrices also have been proposed and the following paragraphs abstract pertinent references.

Chang et al. (2001b) have proposed using VES formulations to divert acidizing fluids away from high water cut zones so that the oil-bearing zones are stimulated. This process uses a VES prestage to preferentially block the high permeability-water zone [tan in Fig. 3.94 from Kefi et al. (2004)]. Stages of acid (red in the figure) (the process is effective for sandstone and carbonate) then stimulate the oil zone (green) more than the water zone (blue).

In the Chang et al. (2001b) report, a 3,800-ft 165°F sandstone well was stimulated using the following sequence of chemicals:

- Xylene 48 bbl
- 5-staged acid treatment
 - Preflush 110 bbl 15% HCl
 - Main fluid 110 bbl 9/1 MA
 - Overflush 110 bbl 3% NH₄Cl
 - Diverter 3.5% VES-diverter 4 Pills 500 gal each
 - Displace at maximum rates below frac pressure

Additional VES Diversion Methods. Proposed diversion and production enhancement are reported in the following paragraphs.

A patent by Fuller et al. (2009) describes a method for self-initiated diversion in both sandstone and carbonate formations. They claim to have found that certain VES fluid systems may be used at initial surfactant concentrations much lower than would previously have been thought possible. This is an unusual claim since other sandstone diversion systems use separate stages.

They define the initial concentration or the initial fluid as the concentration or fluid that is pumped into the wellbore. They claim that at the concentrations used in the initial fluids, the surfactant system is unable to form a 3D structure that increases the viscosity of the fluid. The VES in the initial fluid may or may not form micelles; if micelles are formed, they are not of the proper size, shape, or concentration to create viscosifying structure, and so the initial fluid has an essentially water-like viscosity. However, as the fluid flows through the formation, the concentration of surfactant in the fluid at some location, for example at or near a wormhole tip, increases because of interactions between the formation and the fluid and its components. As the localized surfactant concentration increases, micelles are formed, or micelle shape or size or concentration increases, and the fluid viscosity increases because of aggregation of VES structures. Still not to be limited by theory, but formation of carbon dioxide by the dissolution of formation carbonate may be a factor in the viscosity increase. They claim that a suitable cationic VES is erucyl bis(2-hydroxyethyl)methyl ammonium chloride.

They (Fuller et al. 2009) claim that a sandstone core was stimulated and diversion was carried out using solutions of a polyaminopolycarboxylic acid and a hydrogen fluoride source. Here a mixture of diammonium ethylenediaminetetraacetate (“DAE” in this example) and acidic ABF is the primary formation-dissolution agent. These fluids also have added brine (potassium chloride or ammonium chloride) to increase the overall ionic strength. The solutions are held at a more neutral pH than conventional sandstone acidizing fluids in these examples. The surfactants (BET O-30 and BET E-40) were used as received.

Fu (2010) claims a fluid that is self-diverting and nondamaging when it is injected into sandstones. On reaction with the small amount of acid-soluble material found in sandstones, it forms a gel that is viscous enough and stable enough to divert mud-acid (or any other matrix stimulation fluid) and that then decomposes after the mud-acid treatment. The author claims that preferably, the self-diverting preflush sandstone acid should be stable under downhole conditions for at least 2 hours but should decompose within about 1 to 3 hours after shut-in at the completion of the job. The fluid contains water, a selected surfactant (such as BET-E-40 betaine—Fig. 3.88), an inorganic acid, and a selected organic acid. It preferably contains a CI and optionally contains an alcohol such as methanol. Most importantly, it is strongly acidic, gels when only a small amount of the acid has been spent, is safe for use in easily damaged sandstone formations, and cleans up readily.

Additional types of surfactant-based diversion systems are claimed by Welton et al. (2007) with a fluid based on methyestersulfonate surfactant with an alkyl chain from about 16 carbon atoms to about 22 carbon atoms. It is a palm-oil derivative commercially available from Halliburton Energy Services, Inc., Duncan, Oklahoma, under the trade name EFS.TM.-4 surfactant.

Alleman et al. (2003) claim a new fluid was developed by incorporating a polyelectrolyte with the surfactant to facilitate the vesicle formation, to reduce surfactant concentration, and to enhance thermal stability of the fluid. The rheological properties of the fluid can be adjusted by fluid pH, surfactant concentration, and properties of polyelectrolyte and temperature. An internal breaker package was developed to break the surfactant gel and reduce the fluid viscosity to that of water at the desired time and temperature. This system does not require contact with formation fluids, brines, or acids for clean up to provide optimum production.

Eoff et al. (2005) describe the use of associative polymer technology (APT) (aka VES materials) to achieve fluid diversion during an acid stimulation treatment. In this case, the author of this paper claims that the APT involves the use of a very low viscosity aqueous-polymer solution. It is claimed to react immediately with the formation surface to significantly reduce the ability of subsequent aqueous fluids to flow into high-permeability portions of the rock. The first stage containing the APT predominately will enter the most permeable area, diverting the following acid stage(s) to less-permeable sections of the rock. APT is claimed to have little or no effect on the flow of subsequent hydrocarbon production. Furthermore, in rock containing significant proportions of sandstone-type lithology, the water permeability of the treated zone is decreased permanently, resulting in post-treatment reduced water production from the treated zone. This technology is similar to that described by Chang et al. (2001b).

A patent application by Welton et al. (2009) claims a polymer diversion system of a relative permeability modifier comprises a reaction product of a reaction comprising a hydrophilic polymer and a hydrophobic compound or a polymerization reaction product of a polymerization reaction comprising a hydrophilic monomer and a hydrophobically modified hydrophilic monomer.

Francini et al. (2006) claim that acids are diverted with an agent that is an energized or foamed acidic VES system that contains a VES that gels and increases in viscosity when the acid in the foamed acidic VES system is spent. The method provides a synergistic combination of the diverting capabilities of foams and the diverting capabilities of viscoelastic gel systems. The resistance to flow of the gelled foamed VES system is greater than expected from a foam or a viscoelastic gel system alone.

3.7.3 Matrix Acidizing Planning, Fluid Selection, and Wellsite Delivery.

Planning and Fluid Selection. Integrating the massive amount of chemistry presented in Sections 3.1–3.7 as well as the references cited, into a treatment plan will usually require computer-aided

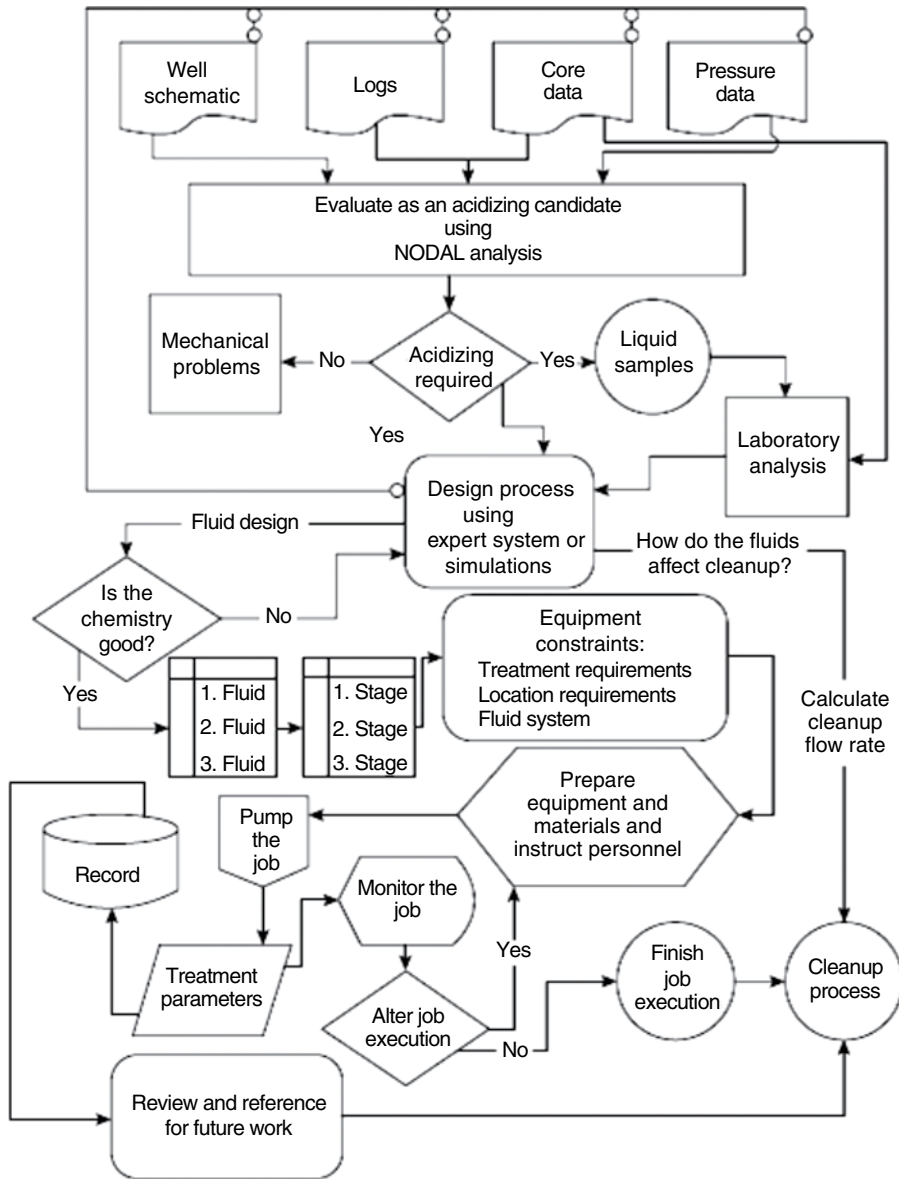


Fig. 3.95—Acid treatment plan (McLeod and Norman 2001).

design programs that include geomechanics, geochemical reactions, as well as knowledge of logistics, environmental compliance, and cost/benefit analyses. It is beyond the scope of this book to review the commercial programs available; however, Section 3.3.3 discusses numerical acidizing models. This section will provide qualitative selection guides based on the text above (Sections 3.1–3.7) as well as those in Robert and Crowe (2001), McLeod and Norman (2001) (Fig. 3.95), Hill et al. (2001), and Kalfayan (2008).

A generalized workflow diagram that can apply to both sandstone and carbonate treatments was provided by McLeod and Norman (2001).

The key elements include

- Determining if the damage can be removed/bypassed by chemical treatments
- Designing the process (described in next paragraphs)
- Determine equipment needs (see Section 1.7)

- Plan for flowback and disposal (see Section 6.3)
- Execution
- Disposal of the flowback
- Re-evaluation of the well after execution

Actual fluid selection will be different for carbonate compared with sandstone formations.

Carbonate Fluid Selection. See the discussions in Robert and Crowe (2001). Items keyed to this book include

- HCl compared with organic acids or chelating agents (Sections 3.4.1, 3.4.2, and 3.4.3). These selections depend largely on formation composition and temperature
- Inhibitor selection based on chemistry (3.6.1)
- In-situ or ex-situ diversion/placement (3.7)
- Surface active additives and solvents (3.6.2)
- Other additives depending on formation conditions (3.6.3 and 3.6.4)
- Testing of the final package for compatibility and effectiveness

Sandstone Formations. See the discussions in McLeod and Norman (2001). Items keyed to this book are very similar to those for carbonates, *except* that a carbonate removal prestage will be needed if one of the single stage formulations (3.5.6) is not used. The prestage, if required, can be HCl or an organic acid. The main stage (as well as the acid prestage) may include

- MA (HCl/HF) or a retarded MA (3.5.5 and 3.5.6) these selections depend largely on formation composition and temperature. This only applies to the main silica/clay removal stage
- Inhibitor selection based on chemistry (3.6.1)
- In-situ or ex-situ diversion/placement (3.7)
- Surface active additives and solvents (3.6.2)
- Other additives depending on formation conditions (3.6.3 and 3.6.4). Clay control may be especially important for sandstone acidizing (3.6.4)
- Testing of the final package for compatibility and effectiveness

Geochemical models to predict the formation responses of various stimulation fluids are an integral part of the planning process and were described in Section 3.3.3 for carbonates and in Section 3.5.4 for sandstone formations. These models can be used to test [virtually—Ali et al. (2004)] the formations response to various formulations before the final selection.

Wellsite Delivery of All Oilfield Chemicals. This section has been placed in the reactive fluids section because of the large number of additives (see Sections 3.6.1–3.6.4) that are usually in the final fluid. However, wellsite delivery also applies to frac fluid additives (Sections 4.4, 4.6, and 4.7), direct use of CIs and scale inhibitors (Sections 2.2.3, 2.4.4, and 2.5) as well as the EOR chemicals in Sections 5.4, 5.5, and 5.6.

In planning the delivery of production enhancement chemicals to the wellsite for injection into a well, the developer must be aware of all of the information reviewed in Table 3.13 and Figs. 3.73 and 3.74, as well as the delivery, storage, and pumping devices seen in Section 1.7. The chemicals must be usable from arctic to desert and rain forest environments where they will be exposed to this full range of weather conditions for long periods of storage. This means that *each* chemical that is present at the wellsite may require *special formulation* for specific conditions. Thus, a number of specific requirements must be met by the oilfield formulations and verified by an appropriate test.

Liquid Products. *Pour point* (flow from the storage container)—a winterized version may be needed. *Viscosity* (flow in the transfer lines)—a winterized version may be needed. *Flash point*—high vapor pressure materials may cause a container to bulge at high storage temperatures. *Physical stability*—test for separation during long storage times. Test freeze/thaw cycles. *Shelf life*—test for separation of solids and activity reduction after storage at low and high temperatures. *Reactivity* with metals and elastomers—determine reactivity with storage containers and wellsite equipment.

Solid Products. *Melting point*—at high temperatures, will the product melt or become sticky. *Pour/move ability*—can the product be handled and moved to the well at all temperatures. *Shelf life*—test for activity reduction after storage at low and high temperatures. *Affected* by moisture and freezing. *Changes* in/or reactions with other onsite chemicals. If a container breaks, will solids be hazardous.

All Products. Available, economical, and transportable to the wellsite (on-shore, off-shore, remote) anywhere in world. Compatible with blending and mixing equipment at different and specific wellsites.

3.8 Fracture Stimulation of Carbonates and Sandstone Using Reactive Fluids

To this point, most of the discussion in this chapter has been about the use of reactive chemicals during *matrix stimulations* conducted at flow rates below the fracturing pressures of the formation rock. Many carbonate formations and potentially some sandstone wells can also be stimulated using reactive chemicals injected at pressures high enough to cause the rock to *fracture* (see the cartoon in Fig. 3.4). This is a large market for acids (especially HCl) because thousands of gallons of acid may be pumped into some carbonate formations, as compared with possibly just hundreds of gallons of a fluid for a small matrix treatment or well cleanout operation. However, the process is more complex and expensive because high pressure frac pumps will be needed to place the fluid at a rate above the frac pressure. See Sections 1.6.3 and 1.7 for some frac pressure calculations.

Hydraulic fracturing is a procedure by which fluids are pumped at rates and pressures sufficient to break the rock, hopefully forming a fracture with two wings of equal length on either side of the borehole (especially for a conventional vertical well). More details on complex wells are in Section 4.1.2. When the pumping has stopped, the fluids will leak off into the formation and the fracture will close if not supported in some manner. This can be done with an *acid etch* or solid *proppants*.

Smith and Shlyapobersky (2001) note that hydraulic fracturing is one of the primary engineering tools for improving well productivity. This is achieved by

- Placing a *conductive channel* through near-wellbore damage, then bypassing this crucial damage zone.
- Extending the channel to a significant length into the reservoir to further increase productivity.
- Placing the channel such that fluid flow in the reservoir is altered.

The authors of this book compare fracturing to building a superhighway for oil and gas production and, thus, avoiding the back roads. Once the formation has been broken down because of the application of the stress from the injected fluids, the frac must propagate. Fig. 3.96 (Brady et al. 1992)

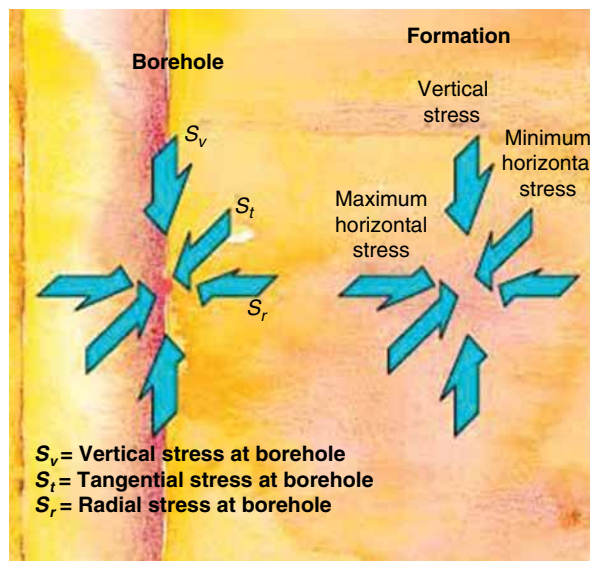


Fig. 3.96—Stresses from the earth at borehole and in the formation (Brady et al. 1992).

describes the stresses from the earth that will act on the fracture in a vertically drilled well. The diagram notes the terms for the stress in the 3 principal directions at the borehole and in the deeper formation. Because the vertical stresses are usually greater than the horizontal stress in a vertical well, the fluid will flow into the formation in the horizontal direction and the fracture will orient vertically. Also see the discussions of geomechanics in Section 1.6.3.

Using a similar description (Smith and Shlyapobersky 2001), Fig. 3.97 shows a cartoon of a fracture propagating and the wiggly lines represent leakoff of the fluid to the formation. Note that in this picture, the fracture wings appear to be larger in the vertical direction than in the horizontal direction. This happens because the fracture wings form at 90° (normal) to the applied stress (through the wellbore horizontally in a vertically drilled well). Also, they are constrained vertically by a layer of rock that can accept more stress than the formation rock. In this drawing (Fig. 3.97), fluid loss is one of the factors that may limit the fracture length in both propped and reactive fluid fracture stimulation.

The effectiveness of the treatment depends mostly on the length of the fracture and the conductivity, which are a function of the width and the permeability of the fracture. The dimensional fracture conductivity (C_D) is defined as

$$C_D = k_f w \dots \dots \dots (3.37)$$

Here, k_f is the fracture permeability and w is the fracture width. The units are md-ft. This equation applies to both a propped fracture as well as an acidized fracture (a dimensionless conductivity number will be described in Chapter 4). In a propped fracture, the polymer fluid that carries the prop may remain in the fracture and reduce the frac permeability. In acid fracture, it is related to the etch pattern and the compression of the etched surface by the closure stress. The other important factor for increased productivity is the fracture half-length (penetration) x_f . The frac fluid chemistry is used to enhance x_f when this is a goal of the treatment plan.

If a solid proppant is present (see discussions in Chapter 4) as well as in Smith and Shlyapobersky (2001), this material will keep the fracture open once the stress is removed (pumping stopped) and provide a high permeability pathway. However, for an acid fracked well, the conductive paths must be held open by small pillars of undissolved formation (such as the coal pillars that hold open a coal mine). See Fig. 3.98 for a drawing that illustrates the differences between the two propping methods.

This section (3.8) will discuss methods to provide the conductive paths with a reactive fluid. While the physics of producing the initial fracture is the same in etched and propped fracturing, the *fluid chemistry* needed to produce the conductive paths are quite different. Leakoff of fluids are important

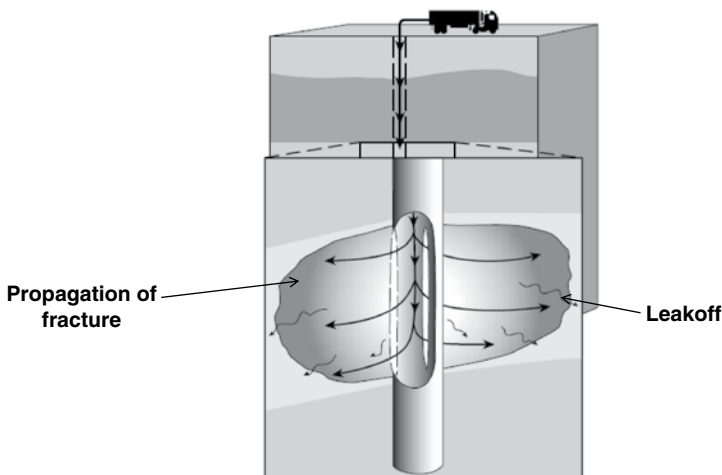


Fig. 3.97—Fracture propagation (Smith and Shlyapobersky 2001).

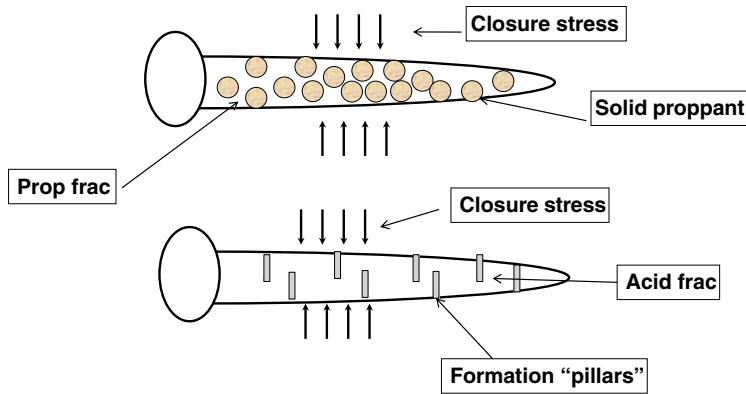


Fig. 3.98—Frac support in proppant and acid fracs.

in each case, but frequently different chemistry applies because almost all reactive fracturing is performed in carbonates while prop fracturing is performed in sandstone and shale as well as in some carbonates. Smith and Shlyapobersky (2001) also note that the fracture propagation rate and fluid flow rate inside the fracture become important. They are dominated by fluid-loss behavior. See Eq. 3.38.

In Eq. 3.38, the fluid-loss rate q_L from a fracture can be expressed as a function of the C_L (the fluid-loss coefficient), A is an element of the fracture area (i.e., increased in-flow area), t is time measured from the start of pumping, and τ is the time when each small area element of a fracture is created or opened. As a direct consequence of this relation, the highest rate of fluid loss is always at the fracture tip.

$$q_L \approx \frac{2C_L A}{\sqrt{t - \tau}} \dots \dots \dots (3.38)$$

The fluid loss rate can affect the fracture penetration in both propped and acid fracturing and, thus, the overall production potential.

3.8.1 Fracture Acidizing of Carbonates. Hydraulic fracturing of limestones or dolomites with acid (usually HCl, but also with other reactive fluids) is an alternative to propped fractures in acid-soluble formations. The major difference between acid and propped fractures is that *conductivity* is obtained by etching the fracture faces instead of by using a proppant to prevent the fracture from closing (Fig. 3.98). The chemical reactions needed to dissolve the rock are the same as those that happen for matrix stimulation of carbonates. See Eqs. 3.1 and 3.2. The reaction kinetics is also the same; however, here the goal is the production of a nonuniform acid that etches on the face of the fractured surface, and wormholes lead to undesirable fluid loss. Therefore, the pumping strategies and some of the additives that will affect wormhole formation must be modified to fit different goals of this treatment.

Acid fracturing may be preferred operationally because the potential for unintended proppant bridging and proppant flowback is avoided. However, designing and controlling the depth of penetration of the live acid into the formation and the etched conductivity may be more difficult than controlling proppant placement (Mack and Warpinski 2001).

In acid fracturing treatment, a viscous pad fluid and acid are injected in sequence using high-pressure pumps at a high rate. This raises the bottomhole pressure higher than the formation fracture breakdown pressure (Section 1.6.2 and 1.6.3) and, thus, creates fractures in the target zone. Acid is then transported through these fractures and penetrates further into formation rocks (Fig. 3.99). During the same time, acid reacts with carbonate rocks on fracture surfaces and also creates wormholes into the formation. Because of rock heterogeneity and the random characteristic of chemical reactions, the reaction rates are *not* uniform along fracture surfaces. Thus, the acid etches the fracture surfaces *unevenly*. After the treatment is finished, the fractures close under formation stress. However, there is

Acid fracturing

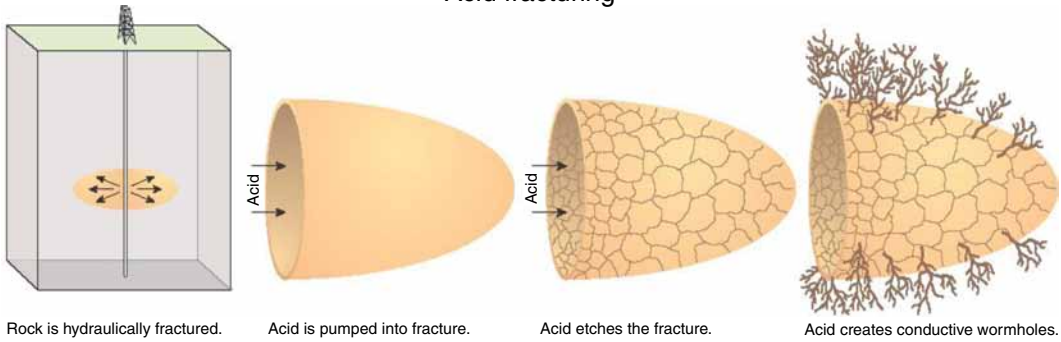


Fig. 3.99—Acid fracturing process.

remaining conductivity in closed fractures because of the unevenness on fractures surfaces. The fracture is then supported by the remaining unetched surfaces (Fig. 3.98).

Nierode and Kruk (1973) note that when acid is used without a pad fluid, the fracture will generally be short and narrow because the rate of fluid loss for acid is high (the acid reacts too fast). If a viscous pad fluid is used, the long, wide fracture that is formed will begin to close as acid is injected and will approach the geometry expected if acid alone had been used. The authors claim that this decrease in fracture volume occurs because the acid wormholes through the region invaded by the viscous fluid and thereby increases the rate of fluid loss. Thus, the viscous pad provides some degree of wormhole control. Other methods are described later in this section (3.8.3).

The stimulation obtained in an acid fracturing treatment is controlled by the length of the fracture that is *effectively* acidized, not by the induced fracture length. The distance that the reactive acid moves along the fracture (the acid penetration distance) is governed by the acid flow rate along the fracture, the rate of acid transfer to the fracture wall, and the reaction rate at the rock surface. Under most circumstances, the reaction rate between acid and rock is very fast (if concentrated HCl is the reactant), and the rate of mass transfer to the rock face (not the SRR) controls the overall acid reaction rate.

The major points are

- The reactive fluid (usually following a viscous pad—a water-based gel such as hydroxypropyl guar (Gulbis and Hodge 2001) is injected above fracturing pressure.
 - A hydraulic fracture is created.
 - Fracture faces are dissolved/etched.
 - Conductive channels are created (that is, wormholes—Fig. 3.3).
- Effectiveness is determined by
 - Effective fracture length (x_f), which depends on reactivity and leakoff.
 - Fracture conductivity (C_D), which depends on the embedment strength and the heterogeneous etch.

The chemistry of the process and its success are controlled by (see Fig. 3.100)

- Acid type, strength, and volume (the reaction rate and mechanism)
- Acid leakoff (wormholes are bad)
- Acid viscosity
- Injection rate
- Formation type

The leakoff can be controlled by the viscosity, which may be increased by special additives (described later—Section 3.8.3). The reaction rate can be controlled by the choice of reactive fluid (strength of HCl or with organic acids) as well as by using other additives or by emulsifying the acid. The

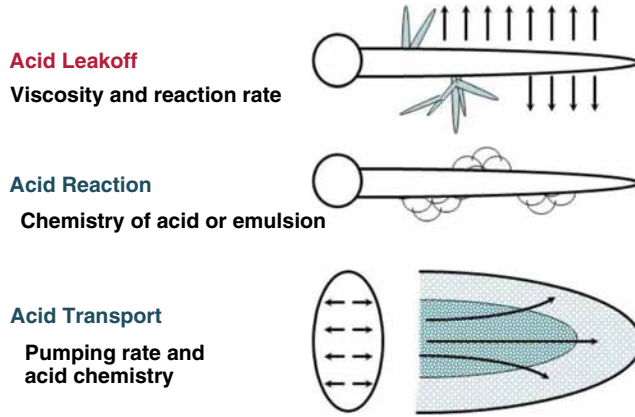


Fig. 3.100—Acid frac mechanics.

acid transport is affected by the leakoff as well as by the viscosity and pumping rate. Ultimately, the conductivity and the fracture length (which control the ultimate productivity) are controlled by the effectiveness of production of a nonuniform etch over as long a distance as possible. This section will describe chemicals and methods to achieve the productivity goals of the treatment.

An important factor affecting the conductivity is (β) the *capacity* of the fluid to dissolve limestone or dolomite. For 100% HCl, 1.37 g of limestone can be dissolved for each gram of acid. The various dilutions are just the fraction of this amount. Other acids (Tables 3.3 and 3.4) would have lower values of capacity based on the ratios of the molecular weights and solution concentration to the mineral molecular weights. However, they may be desirable because of reactivity factors at high temperatures.

Mack and Warpinski (2001) state that the dissolving power (X_c) must be converted to volume values to be used in fracture models, thus the acid volume capacity is

$$X_c = \frac{\rho_c \beta C}{\rho_{CaCO_3}} \dots \dots \dots (3.39)$$

Here ρ_c and ρ_{CaCO_3} are the densities of the acid solution and calcium carbonate, respectively, and C is the weight-fraction concentration (e.g., 0.28 for 28% acid). β is the ratio of the molecular weight of the rock to that of HCl and for limestone is 1.37. From this relationship, the maximum volume of the etched area (ΔE_{ich}) can be calculated.

The reactivity of an acid and various other fluids with carbonates were discussed in Section 3.4. Mack and Warpinski (2001) note that detailed modeling of the reaction in terms of the activities is not required for a hydraulic fracture simulator because of the large amount of uncertainty in the other parameters. Instead, the reaction rate can be assumed to be governed by the simple equation for the rate of acid consumption r (Settari 1993):

$$r = \frac{\partial M_{acid}}{\partial t} = -K_r (C_{wall} - C_{eqm})^m \dots \dots \dots (3.40)$$

The authors claim that the concentration at equilibrium (C_{eqm}) is assumed to be 0, so the acid concentration at the wall of the fracture is the controlling factor. In flowing fluids, this equation is no longer valid because acid transport is by convection rather than diffusion. For acid fracture modeling, Eq. 3.40 is replaced by

$$r = \frac{\partial M_{acid}}{\partial t} = -(K_g + \mu_L)(C_{av} - C_{eqm}), \dots \dots \dots (3.41)$$

where the mass-transfer coefficient is

$$K_g = D_{\text{eff}} N_{\text{Sh}} / w \dots \dots \dots (3.42)$$

Here D_{eff} is the effective acid diffusion coefficient and N_{Sh} is the Sherwood number (ratio of conduction to diffusion). For HCl, the reaction with calcite is mass-transport limited and the D_{eff} value is needed in the fracture models. Depending on the temperature and the alternative reactive fluid, the reaction could also be SRR limited, or there could be mixed kinetics.

Mack and Warpinski (2001) state that acid fracture conductivity is much more poorly understood than propped fracture conductivity. For laminar flow (the general case for flow inside hydraulic fractures), the pressure drop (Δp_{net}) along some length Δx of the slit is

$$\frac{\Delta p_{\text{net}}}{\Delta x} = \frac{12\mu q}{h_f w^3} \dots \dots \dots (3.43)$$

Fortunately, claims Mack and Warpinski (2001), the acid etches the rock surface in a nonuniform manner because of rock heterogeneity and fingering of the acid through the wider previously etched channels. This results in numerous horizontal pillars supporting the channels between them, for which Eq. 3.43 could be used with the fixed fracture height h_f replaced by the distance between the pillars. They claim that it is not practical to model this in detail because the pattern is not generally known. Because conductivity is higher in formations where numerous small channels occur supported by numerous pillars, uniform etching is not desirable. If, however, the pillars lack the strength to support the additional load required to keep the channels open, some of the pillars will collapse, reducing the conductivity. Fracture conductivity is, thus, dependent not only on the etching pattern, but also on the rock strength and closure stress. More studies of acid frac conductivity patterns are in Section 3.8.2.

The amount of formation dissolved is used to calculate a uniform (ideal) etched width. The ideal conductivity for a uniform open fracture with a width of 0.1 in. is about 4.5E+6 md-ft. The empirical correlation for zero closure stress reduces this by almost 3 orders of magnitude to about 6.5×10^3 md-ft (Mack and Warpinski 2001). Further reductions are made as closure stress and embedment strength effects are considered. They claim that this correlation is a conservative estimate, and calibration with other tests was recommended by Nerode and Kruk (1973).

Kalfayan (2007) has reviewed recent trends in acid fracturing and concludes that acid fracturing has benefits over prop fracturing when

- The carbonate formation is naturally fractured and could lead to propped fracture complications
- The formation is heterogeneous and is conducive to a high degree of differential etching
- The zone of interest is near a water zone that is not separated by a stress barrier
- The formation permeability is high and/or there is formation damage
- The well will not accept a proppant for mechanical reasons

3.8.2 Lab Studies of Conductivity and Reactivity. Since the *conductivity* of a fracture as well as the reaction rates and leakoff control the effectiveness, methods have been developed to understand and measure these properties. This section will review several test methods that are used to produce data for acid frac models.

Several test setups have been proposed including Malik and Hill (1989), Navarrete et al. (1998b), and Navarrete et al. (2000). Zou (2006) also has developed testing equipment and methods for determining acid fracture conductivity using a modified API cell and a flow system for exposing samples to various acids. This thesis is being abstracted because of the details of the procedures that are described.

Fig. 3.101 shows the a modified API cell and **Fig. 3.102** shows the flow system used by this investigator. Note from the size of the tanks that acid frac conductivity tests require large volumes of acid to produce useable data. One of the major issues with acid frac lab simulators is the need for using very expensive materials of construction (such as high Ni-containing alloys) for all wetted surfaces. Materials



Fig. 3.101—Modified API cell for acid frac conductivity tests (Zou 2006).

such as 57% Ni, 16% Cr, 16% Mo, and 5% Fe alloys have been used by the authors of this book to test HCl solutions. Also note that large test specimens (called platens) in these figures (Figs. 3.102 and 3.103). This equipment is similar to prop frac conductivity (Section 4.2.2) measurement devices but is more robust because the conductivity must be formed by the acid dissolution of the platens.

Included in the system are brine and acid storage, heaters to raise the temperature to the test temperature, and a method for confining the fluid and for putting the core platens under appropriate stress. The flow system also has to have an adjustable leak-off system to simulate loss of fluid to the formation. See details in the thesis referenced (Zou 2006).

The overall process includes the following:

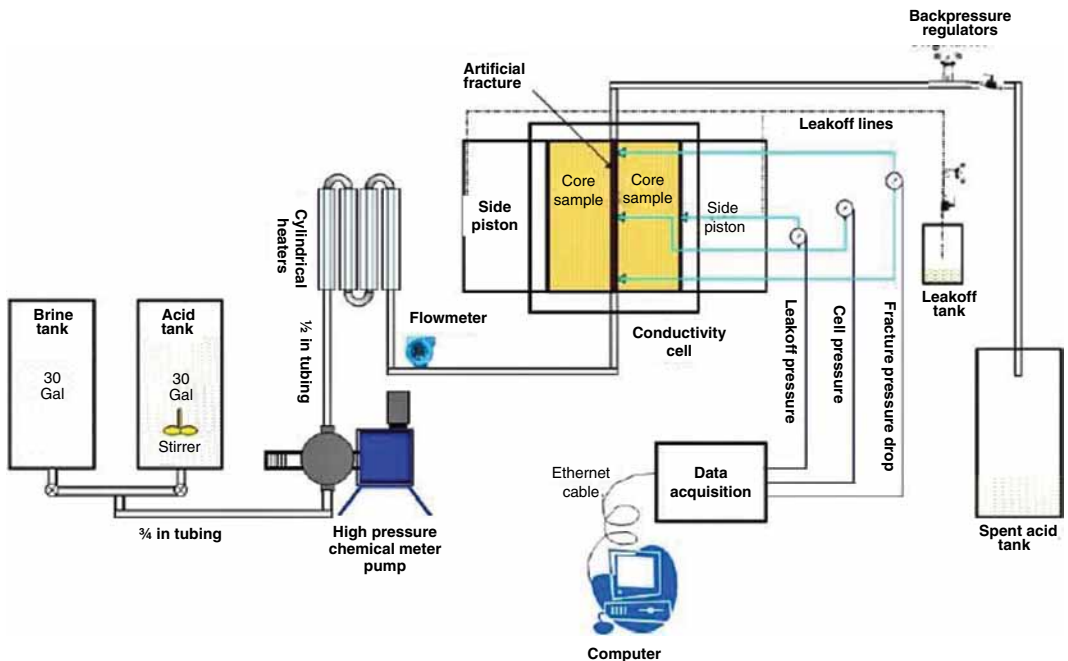


Fig. 3.102—Acid frac conductivity flow system (Zou 2006).

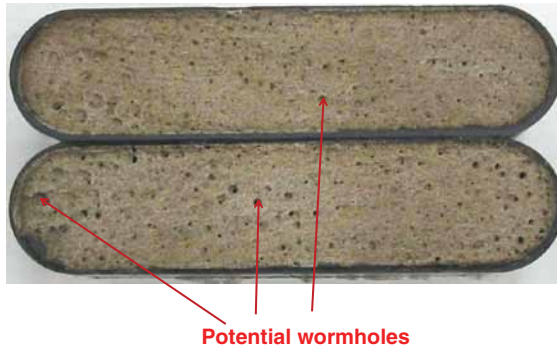


Fig. 3.103—15% HCl 200°F, 30 min contact, etched platen (Zou 2006).

Acid etching procedure:

- Prepare core samples
- Saturate core samples with brine
- Prepare acid and brine
- Assemble core samples into conductivity cell and set at desired fracture width
- Pump heated acid in between rock samples to etch the fracture surfaces
- Switch the pump suction to water tank and flush the rock samples
- Disassemble the unit and clean up

Fracture conductivity measurement procedure:

- Prepare and load acid etched core samples into conductivity cell
- Place conductivity cell in load frame and connect flowlines
- Apply desired overburden pressure on core samples and let stabilize
- Flow nitrogen and record data at different flow rate
- Increase overburden pressure and repeat last two steps
- Process data and calculate the conductivity

The fracture conductivity is calculated from Eq. 3.37 (the unknown is the fracture permeability κ). Zou (2006) used the method developed by Pursell (1987), which employs the Philipp Forchheimer (1852–1933) equation as it is applied for high-rate nitrogen flow in porous media to determine the pressure drop:

$$\frac{p_1^2 - p_2^2}{L} = \frac{2ZRT\mu\rho v}{M\kappa} + \frac{2ZRT\beta(\rho v)^2}{M}, \dots \dots \dots (3.44)$$

where β = the inertial flow coefficient (when the inertial flow term is small, Forchheimer’s equation reduces to Darcy’s law); p_1 = upstream pressure (psi); p_2 = downstream pressure (psi); L = distance between upstream and downstream ports (ft); Z = nitrogen factor; R = gas constant parameter; T = nitrogen temperature (°F); M = molecular mass (g/mole); and κ = fracture permeability.

For straight 15% HCl, Zou (2006) found that the longer the acid remains on the surface, the more rock is dissolved. In the case tested, the carbonate limestone was dissolved heterogeneously at the platen surfaces. The wormholes were distributed randomly in the material. See Fig. 3.103, which shows rock platens that have been etched. Potential wormholes also are noted.

Because the reactions are assumed to be MTL, *diffusion* is the controlling element. De Rozieres et al. (1994) compared diffusion coefficients obtained by two different techniques. The first technique uses a diaphragm diffusion cell, and these results are compared to values obtained from a RD device (see Section 3.2.1) and the discussion associated with it. The authors note that the diaphragm diffusion

cells can be used to measure the diffusivity of organic molecules in solvents and of ions in electrolyte solutions. The diffusion cell contained two chambers separated by a porous diaphragm. The cell and the diaphragm are constructed of Pyrex™ glass. The pore size of the diaphragm is in the range of 2 to 5 μ . In each chamber, there is a stirrer that is made of iron wire sealed in soft glass. The densities of the stirrers are adjusted by the inclusion of air in the soft glass seals so that the upper stirrer has a higher density than the solution, and the lower stirrer has a lower density than the solution. The chambers are connected to capillary legs made of Pyrex glass. The inside diameter of the capillary tubes is 0.75 mm. The capillary legs are fitted with Teflon plug valves, which serve the purpose of filling and emptying the chambers. The experiments are run by allowing fluids to diffuse through the cell and then measuring the concentrations of the acid as well as Ca^{2+} or Mg^{2+} ions by titration or by AA. The D_{eff} values are calculated:

$$D_{\text{eff}}\beta t = \ln \frac{C_{lo} - C_{uo}}{C_{of} - C_{uf}} \dots \dots \dots (3.45)$$

Here, β = a cell constant determined using a standardized fluid; t = time, seconds; C_{lo} = original concentration in the lower cell; C_{uo} = original concentration in the upper cell; C_{of} = final concentration in the lower cell; and C_{uf} = final concentration in the upper cell.

They also used a RD procedure (see Section 3.2.1) to calculate the diffusion coefficients. The procedures are covered in the literature (Fredd and Fogler 1998c). They report that at 85°F the diffusion coefficient measured by the diaphragm cell is 2.70×10^{-5} cm^2/s when fresh 15% HCl diffuses to totally spent acid (2.41 mole/L of calcium ions). The result from the RD test is 2.13×10^{-5} cm^2/s under the same conditions. These values are fairly close. The diaphragm cell could not be used for emulsified acid (Section 3.8.3).

Nieto et al. (2008) contend that despite the critical role of differential etching in the creation of fracture conductivity, little is known about the texture of the fracture surface created during acid fracturing or about the dependence of this texture on the acidizing conditions. To study this important aspect of the acid-fracturing process, they used a surface profilometer to measure the surface profile of a rock sample accurately and rapidly and used the instrument to characterize fracture surfaces after acidizing.

The profilometer measures the distance to the rock surface with a laser device that measures distance with an accuracy of 0.001 in. Experimental details are in the paper.

They have measured the etched-fracture-surface profile for a wide range of acidizing conditions. The etched-surface characteristics depend strongly on the acidizing conditions, including acid type and strength, velocity in the fracture, leakoff rate, and rock type.

Conclusions of the study include

- Limestone (3 md) was acidized at 200°F with 15% HCl/viscosified with a surfactant, and the fracture surface exhibited much higher attack at the entrance side of the fracture and a wedge-shaped pattern. Note that this is similar to the wormhole in a matrix test where the rate of reaction is too high for the flow rate. However, much more rock was removed than the dolomite, so the conductivity was higher at low closure pressures.
- Dolomite (40 md), also was acidized at 200°F with 15% HCl/viscosified with a surfactant and had a very rough surface with long wormhole patterns and pits and the etching was uniform from inlet to outlet. This reflects the much lower reaction rate of dolomite with HCl compared with limestone, but less rock was removed.
- Chalk (a low permeability—2 md soft calcite) was treated with straight 28% HCl at 100°F and had very deep channels resulting in essentially infinite conductivity at low closure stresses.

Details of systems for managing the reactivity and leakoff of the fluids are described in the next section (3.8.3).

Neumann et al. (2012) have studied the development of conductivity on small-scale carbonate samples with sawn faces, from both outcrops and well cores, to reconfirm the existence of three main acid

patterns, namely uniform, channels, and roughness. The design of the experimental investigation used the following procedures to generate acid conductivity. Experimental details are in the paper. They found that the acid etching patterns determine different conductivity behavior under different confining stress, and the surface mismatch provides the conductivity.

3.8.3 Methods for Managing Reactivity and Leakoff. Because of the very high reactivity of HCl with limestone, the rates may be too high for effective acid usage, except at temperatures below about 200°F. There are several methods for reducing the reactivity of the acid at high temperatures, thus, allowing deeper acid penetration. These include adding organic acids and using gelled acids and emulsified acids. Several methods for reducing leakoff that include different plugging agents also are described. Some of these methods are claimed to reduce leakoff and also affect the reaction rates.

Retardation of the Reaction Rates. Several methods are reviewed in this section.

Organic Acids and Chelating Agents. These are chemicals that exhibit much lower reaction rates than HCl for limestone because of much higher pK_a values and lower acid concentration. See the discussions in Section 3.4. Buijse et al. (2004) discuss the use of organic acids as a stimulation fluid in carbonate formations. Organic acids, such as acetic acid or FA, have been used for many years as alternatives to HCl because of the retarded reaction rate, low corrosivity, and reduced tendency to form acid/oil sludge in asphaltene-rich crudes. Frenier and Ziauddin (2008) also report on the use of organic acids and chelating agents as alternatives to HCl at high temperatures.

In Venezuela, Buijse et al. (2004) report that organic acids were pumped in acid-fracturing treatments in deep, hot (280°F) limestone formations. A model (described in the report) for acid spending is proposed in this paper that can be used for strong (HCl) and weak (organic) acids as well as acid mixtures. Compared to existing (HCl) models, the only new element is the acid dissociation constant that describes the differences between strong and weak acids.

The process uses organic acid stages as well as gelled organic acid stages. The authors note that while the reaction rates of the organic acids are significantly lower than HCl at the high temperatures, the capacity is low due to the solubility of the Ca salts and the equilibrium coefficients (see Table 3.3 and Fig. 3.24). These characteristics did allow the acid frac lengths to be longer than HCl at a similar temperature.

Welton and Domelen (2008) describe a combination of HCl and organic acids that have been used because of their high dissolving power and relatively low rates of corrosion at elevated temperatures. In extreme cases, combinations of organic acids are used. While HCl/FA blends have been used in the past, the unique rheological properties of these blends have not been fully explored. The chemistry and rheology of gelled and in-situ crosslinked HCl/FA blends equivalent to 28% HCl are described and compared with traditional gelled acid and in-situ crosslinked acid (ICA).

The benefits claimed for HCl/FA blends are

- Less corrosion than HCl
- Can be crosslinked for fluid loss and reaction control and more robust viscosity compared with HCl

Chang et al. (2008) also describe how organic acids have been used in stimulating carbonate formations. These include FA, acetic, and more recently, citric and lactic acids. Selecting a suitable organic acid for a specific acidizing treatment is more difficult because the reactions between organic acids and carbonate are less understood than those of HCl with carbonate rocks. They also note that organic acid/carbonate systems are complicated because of the presence of CO₂, organic ligands, and potential precipitation of the reaction products—the organic salts of calcium and magnesium. Therefore, more testing and modeling are needed to better understand these reactions. This paper discusses the required information to properly design an organic acid or HCl plus organic acid treatment. In addition to reaction kinetics, data such as carbonate dissolving capacity at reservoir temperature and pressure, solubility of reaction products, and the effect of HCl to organic acid ratio are needed to better design field treatments. Recommendations are given on what and how laboratory evaluation should be carried out to obtain this information.

Nasr-El-Din et al. (2009a) describe an acid system that is an ester of an organic acid in the form of solid beads. The ester reacts with water (hydrolyzes) at BHT and produces lactic acid, which reacts with carbonate minerals and etches the surface of the fracture. The system was examined in the laboratory and showed promising results.

This system may be related to a patent by Still et al. (2007) who claim an acid fracturing method is provided in which the acid is generated in the fracture by hydrolysis of a solid acid precursor selected from one or more than one of lactide, glycolide, polylactic acid, polyglycolic acid, a copolymer of polylactic acid and polyglycolic acid, a copolymer of glycolic acid with other hydroxy-, carboxylic acid-, or hydroxycarboxylic acid-containing moieties, and a copolymer of lactic acid with other hydroxy-, carboxylic acid, or hydroxycarboxylic acid-containing moieties. The solid acid-precursor may be mixed with a solid acid-reactive material to accelerate the hydrolysis and/or coated to slow the hydrolysis. Water-soluble liquid compounds are also given that accelerate the hydrolysis.

Nasr-El-Din et al. (2009a) claim that the treatment with the esters was conducted in the field without encountering operational problems. After successful placement of the solid beads in the fracture, the well was shut in for 24 hours to give ample time for the ester to hydrolyze and for the generated acid to react with the formation rock. The well was allowed to flow, and samples of the fluids produced were collected to understand chemical reactions that occurred during the treatment. The treatment has resulted in a slight increase in gas production, and no significant improvement was noted over a 9-month period. Consequently, the well was matrix acidized with 28 wt% HCl and responded positively to the treatment.

Gelled Acids. Robert and Crowe (2001) claim that gelled acids were developed primarily for fracturing but have found some applications in matrix acidizing. They are used in acid fracturing to increase the viscosity and decrease the leakoff rate. Under mild conditions, the increased viscosity, because of the gelation, can also decrease the diffusion rate and possibly improve the fracture length.

In the design of gelled acid treatments, the stability of the gelling agent at BHTs must be checked carefully. Several types of gelling agents are used. Xanthan gums (see discussions of various polymers in Section 4.4) are claimed by the authors (Robert and Crowe 2001) to be adequate for moderate conditions [i.e., temperatures up to 230°F (110°C)], with the acid strength limited to 15% (Crowe et al. 1981). Kelland (2009) states that acid gelling formulations containing polyacrylamides also can be crosslinked using Zr(IV), Ti(IV), and Al(III) salts as the pH raises and the acid spends. All of these salts will coordinate with the acrylate groups.

The same gelled acids described by Hill (2005) are used to reduce leakoff. These are the in-situ gelled acids of the type described previously (Section 3.7.2) and consist of HCl mixed with a polyacrylamide or a cationic polyacrylamide copolymer. The mixture is crosslinked using FeCl₃ as the pH rises to approximately 2 and, thus, thickens in the wormhole and diverts acid. The mixture also contains a reducing agent (a hydrazine compound or sodium erythorbate) that is activated at higher pH values. This agent then reduces the Fe(III) to Fe(II) and the gel brakes and the viscosity is reduced. Under more severe conditions, synthetic polymers may be more appropriate for use up to 400° to 450°F [205° to 230°C].

However, Crowe et al. (1990) showed that under dynamic conditions gelled HCl exhibits the same reaction rate with limestones as ungelled acid. In some cases, reaction rates are accelerated. The reaction rate measured is the rate of calcite consumption. It is the overall reaction rate, determined by the limiting step, which is acid transport by diffusion. It is claimed (Muhr and Blanshard 1982) that the rate of diffusion depends on the solvent viscosity and is *not* modified by the presence of polymers, at least as long as the distance between the polymer chains is large compared with the size of the ions in solution.

Crowe et al. (1990) also claim that the interaction between polymer chains and the rock surface can affect the overall reaction rate and live acid penetration. Thus, if the gel exhibits a non-Newtonian behavior, the shear rate at the rock surface can be modified, which may increase the mass transfer and result in a higher reaction rate. Also they claim that the polymer can plug the smaller pores, acting as a fluid-loss agent. This effect was studied by Nierode and Kruk (1973), who found that the growth rate of wormholes is at a maximum for a small concentration of fluid-loss agent. HCl is usually the acid

| Acid | Temperature (°F) | D_{eff} (cm ² /s) |
|---------------------------|------------------|--------------------------------|
| 15% HCl, straight | 40 | 1.31×10^{-6} |
| 15% HCl, straight | 84 | 2.3×10^{-5} |
| 15% HCl, gelled (PAA) | 84 | 7.9×10^{-6} |
| 15% HCl, gelled | 112 | 7.9×10^{-6} |
| 15% HCl, gelled | 145 | 9.6×10^{-5} |
| 15% HCl, emulsified (W/O) | 83 | 2.6×10^{-8} |
| 15% HCl, emulsified | 109 | 24.3×10^{-8} |
| 15% HCl, emulsified | 147 | 4.6×10^{-8} |

component of gelled mixtures. Acid strength varies typically from 5 to 28%. Some results of tests are described in the next section on W/O emulsions (**Table 3.17**).

Metcalf et al. (2000) have noted that gelling of acids has been accomplished for years using emulsions to facilitate the addition of polymer to acid to achieve good hydration. They claim a new emulsion system and polymer were the micelles of this new polymer emulsion are approximately 1/15 the size of those previously applied. The polymer emulsion is claimed to use a highly specific external activator to initiate and promote hydration, dramatically reducing the formation of fisheyes. In addition, it allows for continuous mix operations on location. Production results are presented from three wells, showing a 34% improvement in production in which the new polymer system has been used. The chemistry was not described.

Oil Outer Phase Emulsions (W/O). These materials are formed by using a surfactant, diesel fuel (or other applicable oil phases that may be available), and an acid (usually HCl) (see general discussions of emulsions in Section 1.4.4 and 3.4.2). These systems control the reaction rate by *greatly* reducing the diffusion of the acid to the surface. **Fig. 3.104** shows a cartoon of the acid in the oil phase and diffusion to the surface impeded by the oil phase.

De Rozières et al. (1994) measured the D_{eff} values for regular, gelled, and emulsified acids and found that the gel reduced the diffusion reaction compared with ungelled acid and the emulsified acid was even more effective. The rates were essentially comparable to Brownian motion. The diffusion coefficients calculated using the RDE are in Table 3.17. The emulsified acid had diffusion rates 2–3

Retardation Mechanism

- Emulsified acid is an internal acid phase (HCl) and an external oil phase (diesel)
- H^+ transport is dominated by Brownian diffusion of acid droplets

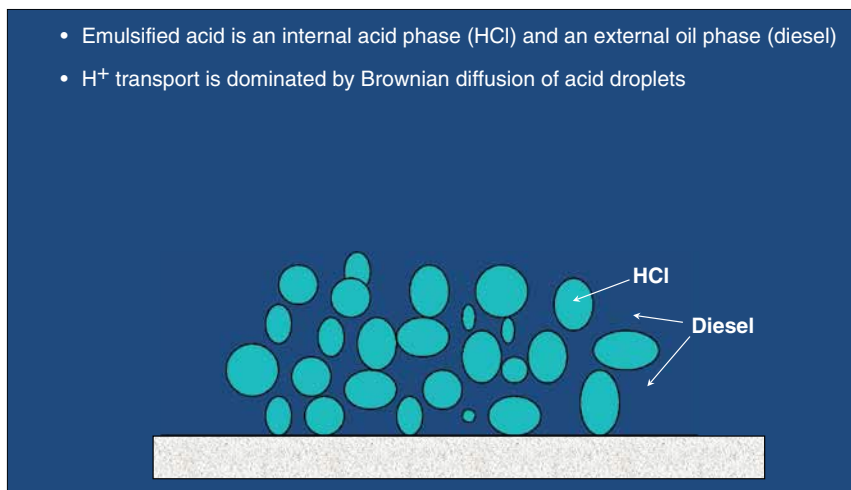


Fig. 3.104—Emulsion retards reaction rate.

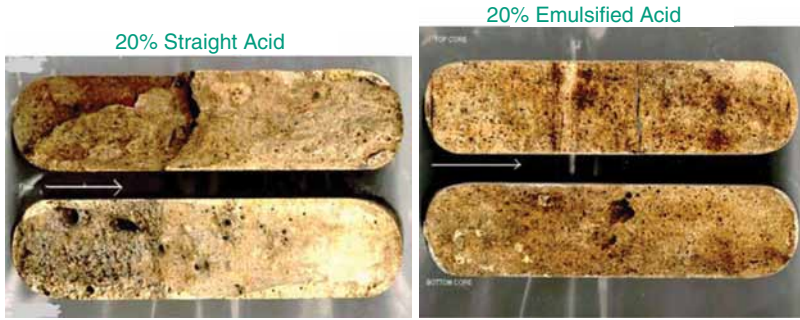


Fig. 3.105—Acid etched surfaces, 320°F (Navarrete et al. 1998b).

orders of magnitude lower than straight HCl and also much lower than gelled acid. Fig. 3.105 shows the physical results of acid conductivity tests run at 320°F [using equipment similar to those described by Zou (2006)]. The straight acid consumed the front end of the core while the emulsified acid allowed an even etch of the limestone.

Navarrete et al. (1998b) conducted acid conductivity experiments using limestone samples designed to simulate this complex process. Special emphasis was placed on scaling the processes described. Two different acid systems were compared: inhibited 28% HCl and emulsified 28% HCl at 130°F and 215°F. Results show that emulsified acid is 8.5 times more retarded than straight acid and that emulsified acid provides a more efficient use of the acid capacity, allowing for longer fracture length without sacrificing fracture conductivity.

These data are based on a “retardation factor” that was calculated from the diffusion coefficients (D_{eff}) and $[H^+]_b$ is the bulk acid concentration:

$$RF = \left(\frac{D_{eff}^{HCl}}{D_{eff}^{Emul}} \right)^{2/3} \left(\frac{[H^+]_b^{HCl}}{[H^+]_b^{Emul}} \right) \dots \dots \dots (3.46)$$

An acid fracturing simulator was used to illustrate the effect of acid retardation on the resulting etched fracture. The simulator computes many operating parameters, which enables the systems to be compared under realistic field conditions. The emulsified acid is most beneficial at high temperatures, where it generates greater etched half-lengths than HCl even at substantially lower injection rates.

Sayed and Nasr-El-Din (2012) have used viscometric and RDE tests to determine the kinetics of the dissolution of dolomite in the presence of an emulsified acid fluid. The experimental fluids contained diesel oil as the organic phase, 28% HCl, commercial CIs and two different cationic surfactants that acted as the emulsifier. They claim that rheological measurements indicated that emulsified acid systems behaved as a non-Newtonian shear-thinning fluid, and this behavior can be represented by a power law model. They claim that the emulsifier concentration and temperature affect greatly the viscosity of emulsified acids. They also found that the emulsified acid–dolomite reaction was MTL at low emulsifier concentration. The behavior was in the middle region between MTL and surface reaction limited for higher emulsifier concentrations. At high emulsifier concentration, the reaction appears to be surface reaction limited. This paper has an excellent review of the equations that describe the kinetics of emulsified acid systems.

Al-Mutairi et al. (2008) claim that experiments were carried out by the authors at 25, 50, and 85°C, under 1,000 psi pressure, and disk rotational speeds from 100 to 1,000 rpm. Samples of the reacting acid were collected and analyzed for calcium concentration. The effects of droplet size on the overall reaction rate were significant. The effective diffusion coefficient of emulsified acid was found to increase linearly with the average droplet size of the acid. Emulsions with low emulsifier concentrations (1 gpt) have average droplet sizes of nearly 13 μm. These emulsions were found to have high effective diffusion coefficients ($5.093 \times 10^{-9} \text{ cm}^2/\text{s}$) and low retardation. On the other hand, emulsions

with high emulsifier concentrations (10 gpt) have smaller average droplet sizes (nearly 6 μm) and found to have low effective diffusion coefficients ($4.905 \times 10^{-11} \text{ cm}^2/\text{s}$) and high retardations.

Conclusions of the experiments are listed:

- Diffusion rate of acid droplets to the surface of the disk decreased with increasing emulsifier concentration because of higher viscosities and smaller droplet sizes.
- Effective diffusion coefficient of emulsified acid was found to increase linearly with the average droplet size of emulsified acid.
- Weight loss results can assist in predicting the effective diffusion coefficient.
- Brownian diffusion cannot be used to explain the diffusion rate of emulsified acid.
- The effect of temperature on the diffusion coefficient did not follow the Arrhenius law.

Zou (2006) used fluids with different viscosities and found that the viscosity affects acid transport and heat transfer. He also found that the different types of acid fluids create different surface etching result:

- Straight acid reacts fast and remove the most carbonate from the cores.
- Emulsified acid react the slowest.
- Gelled acids create the most wormholes in the cores.

The authors of this book note that the industry has used these observations to adapt the fluids to many different operating conditions.

Many different acid/surfactant/oil phase formulations have been described (frequently in the patent literature). Several examples are abstracted to show the range of formulations and approaches to making the emulsions. Kirkpatrick et al. (1965) claim a system using emulsifying agents that contain one or both of the following: (1) a 9-18 carbon monocarboxylic fatty acid salt of a partial amide of a polyalkylene polyamine with 2-6 carbon alkylene groups and 3-5 amino nitrogen in which at least 2 amino groups are acidified with 9-18 carbon monocarboxylic fatty acids and wherein there is at least one nonacidified amino group forming a salt with the acid; (2) a polyamide of an alkylene polyamine with 2-6 carbon alkylene groups and 2-5 amino nitrogen and a 9-18 carbon monocarboxylic fatty acid. The water phase of the W/O emulsion contains 5 to 25% by weight of HCl and various percentage mixtures of the emulsifiers.

Kiel (1974) claims a system that used alkyl and alkylaryl sulfonates, quaternary ammonium compounds such as long-chain quaternary ammonium chloride, and nonionic emulsifying agents. Dodecylbenzene sulfonic acid was a preferred emulsifying agent. This author specifies that the oil phase can be crude oil, a gas condensate, or a virgin or refined petroleum fraction such as kerosene, gasoline, diesel oil, gas oil, liquefied petroleum gases, or the like. They claim that crude oil or gas condensate produced from the formation to be treated are preferred because of their availability and because of their compatibility with the formation. The authors of this book note that using liquefied petroleum gas produces a significant surface fire risk. The authors of the report show a chart that describes the dissolution rate reduction regimes of acid/outer phase and acid/inner phase. Both forms cause retardation in the mass transfer rate, with the acid/inner phase having the lowest MT rate.

Navarrete et al. (1998a) discuss two acid systems that were used in tests: an inhibited HCl and an inhibited emulsified HCl. Three acid strengths were used: 15%, 20%, and 28%. All fluids were batch mixed and all acid systems contained a CI. The emulsified acid contained a high-temperature emulsifier surfactant mixture. The emulsified acid system consisted of an oil external emulsion formed by a 70:30 HCl-to-oil ratio stabilized by a high-temperature emulsifier. The emulsion was prepared by separately mixing the oil phase (diesel) and acid phase. In one bucket, the emulsifier was added to the diesel phase. In a second bucket, the CI was added to the acid phase. The acid phase was added to the diesel phase 500 mL at a time under intense agitation to form the emulsion. The phase mixing process took about 1 hour. Emulsions prepared this way were stable for 4 to 5 days at ambient temperature and had a viscosity of 70 cp at 170 sec^{-1} .

Nasr-El-Din et al. (1999) described the use of an emulsified acid that consisted of 70 vol% of 15 wt% HCl, 30 vol% diesel and an emulsifier (a cationic surfactant). Nasr-El-Din et al. (2008) describe

the use of an emulsified acid that was developed and used to acid fracture over 10 wells in a deep gas reservoir in Saudi Arabia. The formation is predominantly limestone and dolomite with streaks of anhydrite. The acid fracturing practices consist of pumping 28 wt% emulsified acid (acid to diesel volume ratio = 70:30), a pad and in-situ gelled acid to create long conductive fractures.

Salathiel et al. (1980) described the details of a method for formation of W/O emulsion: No. 2 diesel oil and surfactant ENJ 3029 is added in a ratio of 3:1 to form a hydrocarbon/surfactant mixture. Water was slowly added to the hydrocarbon-surfactant mixture while vigorous mixing was applied by a blender until the water-to-oil ratio was about 9:1 by weight. The W/O emulsion formed by the blending operation was then homogenized to form an extremely fine grained W/O emulsion. This patent mentions a number of surfactants as well as a range of hydrocarbon oils.

To produce a less toxic formulation, Bustos et al. (2011) claim that the oil phase also may be made up of vegetable oils and white oils such as MultiTherm PG-1® (described as a high-quality food grade mineral oil) as well as those noted by Kiel (1974) and provided this procedure:

- Acid: 15% HCl solution: 69.5% or 695 gpt
- CI: 1 gpt
- Oil: 30% or 300 gpt
- AQUET 942 Emulsifier: 4 gpt

The acid containing the CI is added in drops to the oil containing the emulsifier in a Waring blender. The fluid is blended for 5 min at low speed and measuring the viscosity on a Fann 35 viscometer.

Pauls et al. (1995) claim an emulsifying system with an oleic diethanol amide and an emulsion viscosity reducing agent comprising a fatty ammonium salt of a fatty acid. A second patent (Pauls et al. 1994) describe a mixture of fatty alkanol amides and a blend of an amphoteric amine salt, a phosphate ester, an ethoxylated dialkyl phenol and a propylene glycol ether. These fluids retard the dissolution of the carbonated by reducing the effective diffusion coefficient of the acid to the surface of the fracture.

Acid emulsions also were described by Appicciutoli et al. (2010) in which asphaltenes were a problem. The authors note that during production, asphaltenes form and are deposited in the well, making it even more difficult to distribute the acid evenly. Because the field is located in an environmentally sensitive area, all fluids need to be mixed and pumped using a zero operational-risk philosophy. Some of the matrix-stimulation challenges were overcome as a result of the development of a novel emulsified acid that combines the practiced asphaltene-dissolving technique with proven acid-diversion technology. The environmental challenges are claimed to be overcome by creating an oil-external/acid-internal emulsion, on-the-fly, just before the fluid is pumped downhole. A number of environmental challenges with stimulation methods including the toxicity of the diesel oil as well as onsite issues are described in Chapter 6.

Methods To Reduce Leakoff (Fluid Loss). Even if the reaction rate of the acid can be reduced for use at high temperatures, leakoff by formation of wormholes causes a significant loss in acid volume that could be used to produce a more effective fracture length. A number of methods have been proposed to control leakoff of the acid during acid fracturing. Some of these also may affect the acid reactivity, so there is some overlap with the previous section.

Elbel and Britt (2000) state that the use of a water-base or gelled-water viscous pad preceding the acid stage is commonly used to initiate the fracture and deposit a filter cake that can act as a barrier to acid leakoff. The actual ability of the pad fluid to control fluid loss in this manner is questionable. Studies by Nierode and Kruk (1973), Coulter et al. (1976), as well as Crowe et al. (1989) have shown that the filter cake deposited by the pad is quickly penetrated by wormholes resulting from acid leak-off. Once this occurs, acid fluid loss can be the same as if no pad were used. Multiple stages of gelled pads have been used to control acid fluid loss (Coulter et al. 1976). In this technique, the fracture is initially created by a pad, after which alternating stages of acid and pad are pumped. These additional pad stages enter and seal wormholes created by the preceding acid. The sequential pad and acid stages are effective for controlling the leakoff of acid into wormholes and enlarged natural fractures. They note that the pad has other useful functions. Cooling effects decrease acid reaction within the tubulars and on the formation face, whereas the relatively large viscosity increases width, which can improve

etched penetration. A wider fracture reduces the areal reaction rate by reducing the surface area relative to the transported acid volume. Viscous pads also promote acid fingering for improved conductivity. Particles, foams, and gels also will be reviewed in this section.

Particulate Diverters (See Section 3.7.2) and Foam. These materials are also used for matrix treatments and are in use for leakoff control during acid fracturing. Messina (2004) claims that a liquid slurry of oil soluble resin used as a fluid loss additive for HCl, HCl/HF, and acetic acids. In acid fracturing, this nonionic product is claimed to be an effective fluid loss control material that is compatible with acid inhibitors in both live and spent acid. Returning acid has no effect on the material, while producing crude solubilizes the product, allowing for easy cleanup. The product is claimed to be effective to 200°F, with the typical loading of 10 gpt of acid. A 100-mesh powdered oil soluble resinous fluid loss additive is also claimed to be effective in all HCl and HCl/HF acid treatments.

Scherubel and Crowe (1978) discuss the use of *foamed acid* (also used as a matrix diverter) for frac acid fluid-loss control. They state that it is further enhanced by the use of a viscous pad preceding the foamed acid. However, foaming the acid reduces the effective amount of acid available for etching because less acid is present per unit volume injected. As a result, they recommend that 28% HCl should be used in preparing the foamed acid to maximize the amount of acid available for fracture etching. The non-Newtonian flow properties obtained by foaming or emulsifying acid can promote fingering of the fluid during fracturing to enhance channels on the fracture face. Volz (1977) claim that acid containing and then foamed can be an effective fluid for fracture acidizing. Francini et al. (2006) described using foamed VES fluids (next section) for fracturing/acidizing carbonates. The claim is that the viscosity is higher than for unfoamed VES fluids and there is improved leakoff control

The same *gelled acids* described by Hill (2005) are used to reduce leakoff. These are in-situ gelled acid of the type described above consists of HCl mixed with a polyacrylamide or a cationic polyacrylamide copolymer. The mixture is crosslinked using FeCl_3 as the pH rises to approximately 2 and, thus, thickens in the wormhole and diverts acid. The mixture also contains a reducing agent (a hydrazine compound or sodium erythorbate) that is activated at higher pH values. This agent then reduces the Fe(III) to Fe(II), the gel brakes, and the viscosity is reduced. Other gelled acids described by Kelland (2009) also can be used. VES-based fluids are now also employed for fluid loss control and to increase the viscosity of the acid and to partially affect the reaction rates.

VES Materials. These chemicals were described in Section 3.7.2 as diverting agents. Lungwitz et al. (2007) tested 15% HCl and 15% HCl containing a VES chemical using an acid conductivity apparatus similar to those described by Zou (2006). The tests were run at 240°F using Edwards's limestone cores. Photos of the cores are seen as [Fig. 3.106](#). The acid conductivity test with the straight 15% HCl showed a conductivity of 137 md-ft at a closure stress of psi, but a significant decrease at 2500 psi, indicating a crushing of the fracture surfaces. In addition, there was a deep wormhole in the first 2.5 in. In contrast, the core acidized with the HCl/VES fluid had a deep differential etch over the whole core (indicating good leakoff control). The conductivity was 1426 md-ft at 2000 psi and 147 md-ft at 4500 psi.

Hill et al. (2007) conducted a series of acid fracture conductivity tests using a protocol that are claimed to mimic the fluid flow in a hydraulic fracture, both in the main flow direction along the fracture, and in the fluid loss direction. In the tests, the injection rate into the fracture is much higher than in many previous tests, and the fluid loss flux is controlled to match field fluid loss rates. They studied three commonly used acid fracturing fluids—an acid viscosified with a polymer, an emulsified acid system, and an acid viscosified with surfactants—at elevated temperatures of 200°F and 275°F. The acid fracture conductivity apparatus is similar to a standard API fracture conductivity cell ([Fig. 3.101](#)), but with a capacity to hold core samples that are 3 in. long in the leakoff direction. The *long cores* allow for better control of leakoff as the acid creates wormholes into the core samples.

In these tests, acid was pumped through the fracture for contact times ranging from 15 to 60 min. After the fracture surfaces were characterized with a surface profilometer (see Section 3.8.2), the fracture conductivity was measured at increments of closure stress, up to a maximum closure stress of 6,000 psi.

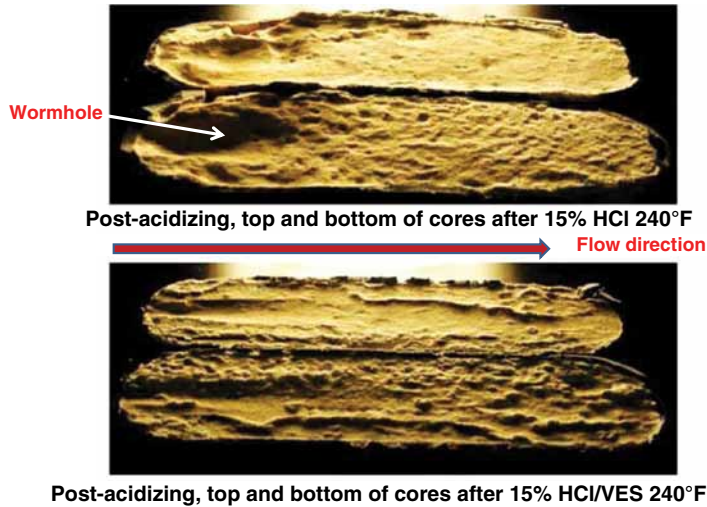


Fig. 3.106—Limestone cores with and without VES in 15% HCl 240°F (Lungwitz et al. 2007).

In this paper, they presented the results obtained from a series of experiments with these fluids using Indiana limestone and dolomite core samples. Among the findings:

1. The fracture conductivity created did not show a general increase with acid contact time, and in fact decreased at higher contact times with some fluid systems. This suggests that optimal times of acid exposure in acid fracturing treatments exist.
2. There were large differences in the conductivity created with the three acid systems tested. At 200°F, the acids viscosified with polymer or surfactants created much higher conductivity than the emulsified acid system.
3. The laboratory-scale acid fracture conductivities measured in these experiments do not agree with the predictions of the Nierode-Kruk correlation.

Jauregui et al. (2011) describe the use of a fiber laden polymer-free self-diverting acid system that was introduced in Saudi Aramco as an acid fracturing diverter to control fluid leakoff and enhance the diversion process by combining the aspects of both particulate and viscosity-based diversion techniques. The fluid system has a distinct advantage in that it does not contribute to formation damage because the VES will break down upon contact with hydrocarbons, and the fiber (an ester-) will degrade with time and temperature.

Pournik et al. (2010) also conducted a series of acid fracture conductivity tests using four commonly used acid fracturing fluids—gelled, in-situ gelled, emulsified, surfactant-based acid. Detailed rheological properties were measured to explain trends noted with conductivity data. Acid system influences the degree of etching and the etching pattern because of differences in chemical and physical properties of acid systems. Under the experimental conditions, viscoelastic acid generated the greatest degree of etching and best etching pattern. Majority of experiments showed differences in conductivity among acid systems tested with most optimal acid system depending on the closure stress. While viscoelastic acid generated the highest conductivity at low closure stress, emulsified acid resulted in the largest retained conductivity at higher loads for our experimental conditions. See [Fig. 3.107](#). Furthermore, Pournik et al. (2010) claim that effluent analysis on both the leakoff and fracture flow showed that most of the fracture face etching is the result of leaked acid into the formation with minimal etching from the fracture flow acid.

Conclusions. The authors (Pournik et al. 2010) claim that the success of acid fracturing depends on the conductivity created and retained under closure stress in addition to the length of conductive fracture. The majority of acid-fracturing treatments show a sharp decline in conductivity with increasing closure stress, with almost no significant conductivity after a short production time.

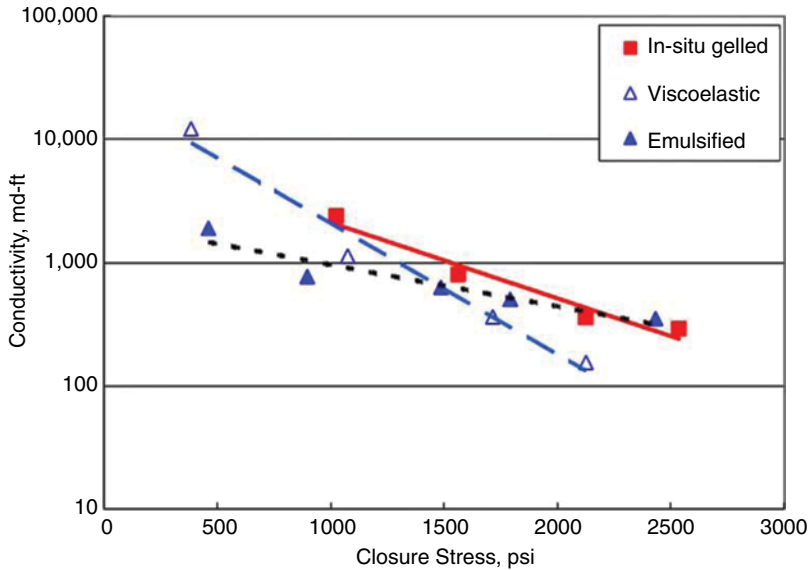


Fig. 3.107—Conductivity vs. closure stress (Pournik et al. 2010).

As a result, many wells are refractured to restore them to the original productivity after the initial fracture.

The authors of this book also note that the design of the experiment (such as long cores vs. short cores) can affect the perception of the final results and must be carefully examined and used with the geochemical models described in Sections 3.3.3 and 3.8.5 to make field recommendations.

Additional Technologies for Carbonate Acid Fracturing. Pournik et al. (2011) have described what they claim is a new approach to overcome productivity decline of acid-fractured wells, which is to perform closed-fracture acidizing (CFA) at the appropriate time in the life of the well to keep fractures conductive. In this process, the acid fracture is reacidized without opening the fracture.

An experimental study was conducted to investigate the effect of CFA on already acid-fractured cores exposed to a certain level of closure stress. Indiana limestone cores were acidized with a typical acid system of 15 wt% HCl viscosified with a polymer under typical field conditions. After the first acidizing process, conductivity measurements were conducted on acid-etched core faces up to a certain closure stress. While the fracture was kept under the closure stress, a CFA treatment was conducted under the same conditions as the initial acidizing. The re-etched fractures were once again placed under different levels of closure stress, and conductivity measurements were taken at each stress. Experiments were conducted under different conditions of leakoff, polymer concentration, and closure stress after the first acidizing to determine the influence of these parameters on the refracturing conductivity.

In the cases examined, CFA enhanced fracture-face etching, while it significantly increased fracture conductivity under closure stress. However, leakoff, polymer concentration, and closure stress did influence the degree of success of CFA.

The use of self-hydrolyzing particles and fibers has been claimed by Still et al. (2007). They state that an acid fracturing method is provided in which the acid is generated in the fracture by hydrolysis of a solid acid-precursor selected from one or more than one of lactide, glycolide, polylactic acid, polyglycolic acid, a copolymer of polylactic acid and polyglycolic acid, a copolymer of glycolic acid with other hydroxy-, carboxylic acid-, or hydroxycarboxylic acid-containing moieties, and a copolymer of lactic acid with other hydroxy-, carboxylic acid or hydroxycarboxylic acid-containing moieties. Thus, as the acid spends, more acid (such as lactic acid or glycolic acid) will be generated in situ and, thus, provides a continuing stimulation to the formation and the method ensures that the acid contacts fracture faces far from the wellbore.

Summary of Fracture Acidizing Chemistry. HCl (frequently 28%) is used for most treatments because it is economical and has a high capacity for dissolving the carbonate. The amount of rock

TABLE 3.18—PUMPING SCHEDULE FOR MULTIFRACK TREATMENT (AL-NAIMI ET AL. 2008)

| Stage | Stage Name | Slurry Vol. (bbl) | Pump Rate (bbl/min) | Pump Time (min) | Fluid Name | Fluid Vol. (gal) |
|-------|-----------------|-------------------|---------------------|-----------------|-----------------|------------------|
| 1 | Open frack port | 50.0 | 5.0 | 10.0 | Water | 2100 |
| 2 | Shutdown | 5.0 | 5.0 | 1.0 | Water | 210 |
| 3 | Hole fill | 357 | 35.0 | 10.2 | Linear gel | 15000 |
| 4 | Inject. test | 185 | 35.0 | 5.3 | Linear gel | 7770 |
| 5 | Pad | 119 | 35.0 | 3.4 | Crosslinked gel | 5000 |
| 6 | Acid | 381 | 35.0 | 10.9 | Emulsified acid | 16000 |
| 7 | Pad | 119 | 35.0 | 3.4 | Diverter acid | 5000 |
| 8 | Acid | 381 | 35.0 | 10.9 | Emulsified acid | 16000 |
| 9 | Pad | 119 | 35.0 | 3.4 | Crosslinked gel | 5000 |
| 10 | Acid | 429 | 35.0 | 12.2 | Diverter acid | 18000 |
| 11 | Flush | 349 | 35.0 | 10.0 | Linear gel | 14658 |

dissolved is important for determining the success of a treatment. Organic acids also have been used in very hot wells to control reactivity and corrosion, however, the capacity will always be lower than with HCl. The most effective way for controlling reactivity is production of an HCl inner phase emulsion in a suitable oil. This method has been employed in carbonate fields in both the East and the West. **Table 3.18** in Section 3.8.4 shows one pumping schedule.

Control of acid leakoff frequently is accomplished using stages of gelled acid (several types) with stages of emulsified acid. The oil phase may be an issue in some markets and can be managed by using low toxicity (but more expensive) oils. The low durability of the acid frac conductivity surface may require refracturing in high closure pressure fields.

3.8.4 Mechanical Placement for Fracture Acidizing. Placement of the fracture in open hole/deviated wells can be controlled by the use of mechanical packers. Al-Jubran et al. (2010) claim that horizontal wellbores have enabled significant increases in productive zone contact areas. However, even with these increased contact areas, the expected long-term production increases were not initially realized with conventional stimulation techniques. They claim that the use of multistage fracturing systems have resulted in long-term production improvements, but the deployment of these assemblies into deep and long reach horizontal wells was initially problematic. This placement requires a mechanical system for allowing multistage fractures.

A description of an openhole packer system (from Baumgarten and Bobrosky 2009) is seen in **Fig. 3.108**. These authors report that use of multiple mechanical isolation points has demonstrated average initial production increases of 77 to 102% and final production increases of 12 to 28% compared to historical wells. The micro to very fine crystalline dolomite of the Crossfield member in Canada has average permeability ranges from 0.1 and 0.3 md; therefore, acid stimulation is required to economically extract the resource.

The multistage fracturing systems (in **Fig. 3.108**) consists of ball-actuated or hydraulically actuated sliding sleeve packers that are operated in sequence starting from the toe of the well to the heel. After the treatments, the balls are flowed back to the surface. In this figure (**Fig. 3.108**), the authors note that the multiple fractures can help connect “sweet spots” in the oil-bearing reservoir (A in the figure). Details of the activation system are in B. These types of systems also can be used in sandstone formations for propped fracturing see Section 4.11.4, and in matrix acidizing (PackersPlus 2011a).

Al-Naimi et al. (2008) describe fracture acidizing treatments of a sour carbonate field in Saudi Arabia. Seven acid stimulation stages were pumped in a continuous operation. The case history describes the use of a total of 330,000 gals of 28% HCl acid was mixed and pumped downhole. The treatment design for each interval was made based on fracture model simulation. A high temperature acid-in diesel emulsified acid was chosen as the main acid fluid to achieve deep penetration and better etched fracture conductivity; a polymer-based leakoff control acid was selected as the chemical diverter to

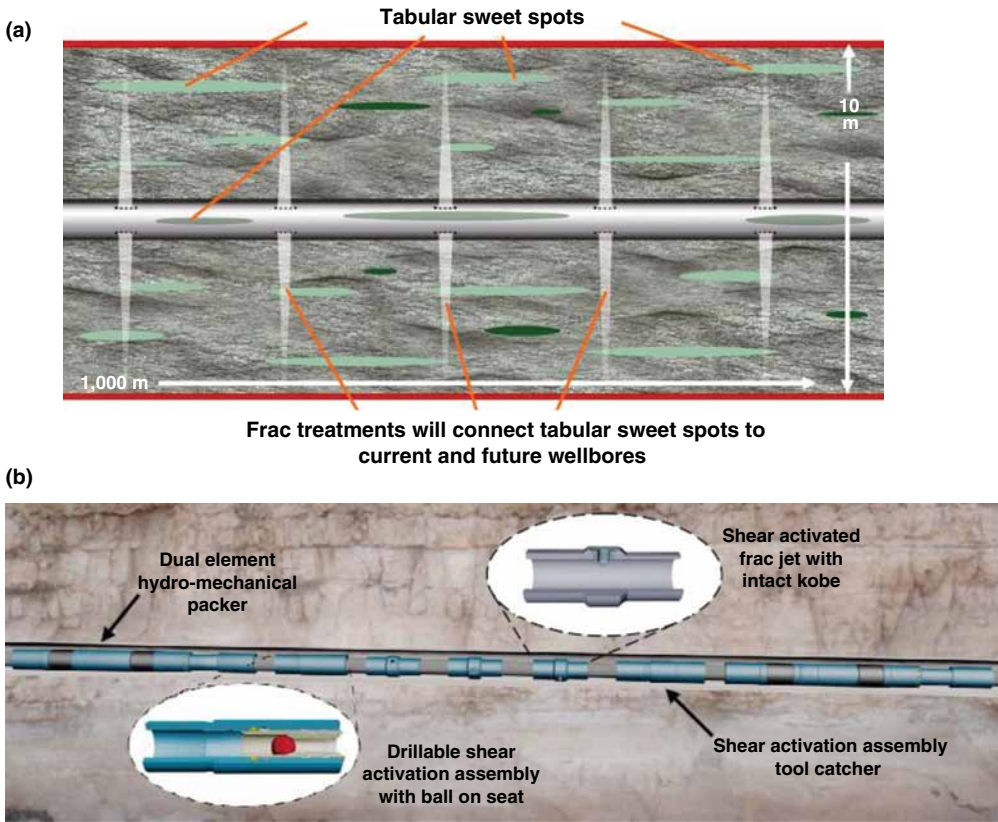


Fig. 3.108—Openhole MFS system (Baumgarten and Bobrosky 2009).

ensure good zonal coverage in each stimulation compartment. The treatment was pumped whereby alternating stages of crosslinked guar polymer and acid was pumped to achieve deeper acid penetration. Table 3.18 provides an example of a pumping schedule used during the stimulation stages. Mechanical packers also were in use.

During the treatment, different treatment pressures were observed during each stage, compared with the previous one, indicating that all of the packers were set and sealing properly. The results initially showed a 3-fold increase in the production index of this oil well after the treatment and this was sustained at 2-fold (compared with an offset well) after two months.

3.8.5 Carbonate Acid Frac Models. A number of authors have proposed various approaches for modeling carbonate acid fracturing (Settari 1993; Williams and Nierode 1972; Elbel and Britt 2000; Settari et al. 2001). The key design parameters that carbonate acid frac models predict are fracture geometry during the treatment, the conductive fracture length and the fracture conductivity created by acid reaction. The models for fracture geometry for acid fractures are similar to propped fractures and are reviewed in Section 4.11. The models for conductive fracture length and fracture conductivity are described below.

Mou et al. (2010) describe the acid-fracturing process, where the fracture conductivity created by acid etching of the fracture walls is because of the surface roughness created by the acid’s nonuniform dissolution of the fracture surfaces. The acid-fracture conductivity is dependent on surface etching patterns, which are determined by permeability and mineralogy distributions. That is, the spatial distribution of fracture roughness affects the fracture conductivity, which cannot be considered in laboratory measurements of acid-fracture conductivity, which use core samples that are too small to observe such macroscale heterogeneities, or in typical acid-fracture simulators, in which the gridblock size is much larger than the scale of local heterogeneities.

An accurate prediction of acid-fracture conductivity necessitates the detailed description of the acid etching profiles on the fracture surfaces, which depend on acid transport in the fracture, leak off because of local permeability, and acid/rock reactions. Mou et al. (2010) develop a 3D intermediate-scale acid-fracture model with gridblock sizes small enough (gridblock sizes comparable to the core-sample size in experiments) and total dimensions large enough (the total dimensions comparable to a gridblock size in an acid-fracture simulator) to capture local and macroscale heterogeneity characteristics. The model predicts the pressure field, the flow field, acid concentration profiles, and fracture-surface profiles as functions of acid injection volume. They use a front-fixing method (Crank 1984) to handle the irregular, moving boundaries in numerical simulation. Spatially correlated permeability and mineralogy distributions were generated by using a semivariogram model.

The model was validated by comparing simulation results with experimental results from an acid-fracture conductivity cell. With the model, by extensive numerical simulation, they analyzed the relationship among fracture-surface-etching patterns, conductivities, and the distributions of permeability and mineralogy. They also illustrate the formation characteristics necessary for acid to create channel-caused high acid-fracture conductivity. They found that a fracture segment with channels extending from the inlet to the outlet of the segment has high conductivity because fluid flow in deep channels causes a very small pressure drop. Such long and highly conductive channels can be created by acids if the formation has heterogeneities in either permeability or mineralogy or both, with high correlation length in the main flow direction, which is the case in laminated formations.

Deng et al. (2011) show that the conductivity of acid-etched fractures depends on spaces along the fracture created by uneven etching of the fracture walls remaining open after fracture closure. They have modeled the deformation of the irregular fracture surfaces created by acid etching and the resulting fracture conductivity as closure stress is applied to the fracture.

These authors (Deng et al. 2011) have modeled the dissolution of the fracture surfaces in a formation having small-scale heterogeneities in both permeability and mineralogy. This model yielded the geometry of the etched fracture at zero closure stress. Beginning with this profile of fracture width, they have modeled the deformation of the fracture surfaces as closure stress is applied to the fracture.

At any cross section along the fracture, they approximate the fracture shape as being a series of elliptical openings. Assuming elastic behavior of the rock, they calculate how many elliptical gaps remain open and their sizes as a function of the applied stress. The sections of the fracture that are closed are assigned a conductivity value because of small-scale roughness features using a correlation obtained from laboratory measurements of acid-fracture conductivity as a function of closure stress. The overall conductivity of the fracture is then obtained by numerically modeling the flow through this heterogeneous system. They have determined how the channels in acid fracturing remain open as closure stress is applied. Their model predicts the rock characteristics that are necessary for acid-fracture conductivity to be sustainable under high closure stress.

Mou et al. (2010) claim that in the acid-fracturing process, the fracture conductivity created by acid etching of the fracture walls is because of the surface roughness created by the acid's nonuniform dissolution of the fracture surfaces. The acid-fracture conductivity is dependent on surface etching patterns, which are determined by permeability and mineralogy distributions. That is, the spatial distribution of fracture roughness affects the fracture conductivity, which cannot be considered in laboratory measurements of acid-fracture conductivity, which use core samples that are too small to observe such macroscale heterogeneities, or in typical acid-fracture simulators, in which the gridblock size is much larger than the scale of local heterogeneities.

An accurate prediction of acid-fracture conductivity necessitates the detailed description of the acid etching profiles on the fracture surfaces, which depend on acid transport in the fracture, leakoff because of local permeability, and acid/rock reactions. In this paper, we developed a 3D intermediate-scale acid-fracture model with gridblock sizes small enough (gridblock sizes comparable to the core-sample size in experiments) and total dimensions large enough (the total dimensions comparable to a gridblock size in an acid-fracture simulator) to capture local and macroscale heterogeneity characteristics. The model predicts the pressure field, the flow field, acid concentration profiles, and fracture-surface profiles as functions of acid injection volume. In the model, we use a front-fixing method (Crank 1984)

to handle the irregular, moving boundaries in numerical simulation. Spatially correlated permeability and mineralogy distributions were generated by using a semivariogram model.

The model was validated by comparing simulation results with experimental results from an acid-fracture conductivity cell. With the model, by extensive numerical simulation, we analyzed the relationship among fracture-surface-etching patterns, conductivities, and the distributions of permeability and mineralogy. We also illustrated the formation characteristics necessary for acid to create channel-caused high acid-fracture conductivity. We found that a fracture segment with channels extending from the inlet to the outlet of the segment has high conductivity because fluid flow in deep channels causes a very small pressure drop. Such long and highly conductive channels can be created by acids if the formation has heterogeneities in either permeability or mineralogy or both, with high correlation length in the main flow direction, which is the case in laminated formations.

3.8.6 Sandstone Fracture Acidizing. Currently, there are no sandstone fracture acidizing systems that have proven to be successful in field use. However, several experimental systems have been described in the patent literature. An important issue for fracture acidizing of sandstone formations is the *capacity* of any fluid. These are based on HF (the only known solvent for silica and clays) that must dissolve a significant amount of a sandstone fracture face. The dissolution equations (Eqs. 3.1, 3.1, 3.12, and **Table 3.19**) show that the most favorable theoretical molar relationships are low compared with carbonate and HCl. Real solvents are even more unfavorable because of solubility and concentration issues. However, because the reactions will probably preferentially dissolve clays, possibly silica pillars or sand particles may provide some fracture conductivity.

The patents abstracted in this section propose methods to address these problems.

Qu and Wang (2010) claim a method of acid fracturing a subterranean sandstone formation of a well to stimulate production of hydrocarbons, the method comprising the steps of: (1) injecting into the formation an acid fracturing fluid at a pressure sufficient to form fractures within the formation, the acid fracturing fluid comprising a sulfonate ester, a fluoride salt, a proppant, and water, the sulfonate ester being hydrolyzed to produce sulfonic acid, and (2) producing HF in situ in the formation by reacting the sulfonic acid with the fluoride salt subsequent to injection of the acid fracturing fluid into the formation. The reaction of the ester and fluoride salt is delayed so that HF is produced in situ. In one example, a stable O/W emulsion acid fracturing fluid composition is provided. Similar to other embodiments described herein, the acid fracturing fluid composition comprises about 1 vol% to about 20 vol% sulfonate ester, approximately 1 lb to approximately 400 lb fluoride salt per 1000 gal fracturing fluid, partial monolayers of proppant (20/40 mesh) at a loading of about 0.01 lb/ft²-about 0.4 lb/ft², and about 60 vol% to about 99 vol% water.

In an aspect, the composition further includes about 1 vol% to about 6 vol% 1-hydroxyethylidene-1, 1-diphosphonic acid. In another aspect, the composition comprises about 1 vol% to about 20 vol% sulfonate ester, approximately 200 lb fluoride salt per 1000 gal acid fracturing fluid, partial monolayers of proppant (20/40 mesh) at a loading of about 0.01 lb/ft² to approximately 0.4 lb/ft², and approximately 60 wt% to about 99 vol% water.

Brown et al. (2008) proposed a dry solid composition is disclosed that, when added to an aqueous liquid, provides a slurry that can be used in sandstone acid fracturing. The slurry generates HF

TABLE 3.19—STOICHIOMETRIC CONSTANTS (SCHECHTER 1992)

| <u>Solvent</u> | <u>Mineral</u> | β (lbm mineral/lbm 100% <u>solvent</u>) |
|----------------|--|---|
| HCl | Calcite | 1.37 |
| HCl | Dolomite | 1.27 |
| Formic acid | Calcite | 1.09 |
| Formic acid | Dolomite | 1.00 |
| HF | SiO ₂ | 0.75 |
| HF | Albite (NaAlSi ₂ O ₈) | 0.40 |

downhole to etch the sandstone fracture faces created. The chemical and physical properties of the composition result in very uneven etching of the fracture faces, enhancing the fluid conductivity of the final fracture. Optionally, inert masking materials may be included in the dry composition, or added to the slurry, to increase in homogeneity of the etching and further increase the fluid conductivity. The ideas for the use of an inert masking agent are illustrated in Fig. 3.109 from the patent. Part A shows the results of a core flow experiment that was conducted with an inert masking material, while part B is a projection of the possible etch pattern that would result. Data from conductivity measurement did show an improvement with the use of a polyacrylates mixed with an HF generator compared with the use of a standard MA formulation.

Kalfayan (2007) claims that research (undocumented) shows that some formulations of “high pH–high HF” fluids may be able to etch a sandstone surface if the HF is released slowly. In addition, this paper suggests that placing deformable beads could help form an etch pattern.

3.9 Best Practices and Case Histories of Use of Reactive Chemicals for Stimulation

Several examples of the successful application of reactive chemicals in different formulations and situations are abstracted to illustrate some of the processes described in previous sections.

3.9.1 Diversion/Fluid Loss. Buijse et al. (2000) describe the matrix acidizing treatment ICA as the diverting agent. The high-pressure high-temperature (HPHT) Trecate-Villafortuna well discussed in this paper produces oil from a naturally fractured dolomite reservoir at a depth of 6000 m. In this well, a new horizontal 220-m section was drilled and completed as openhole. The goal of the acid treatment was to remove the near-wellbore mud damage and to improve the permeability of the horizontal drain. The high pressure at 6000 m and the bottomhole static temperature of 182°C, classify the acid treatment as HPHT.

The treatment is unique because it represents the highest temperature application ever attempted for such a system and falls under the definition of HPHT.

Major design issues:

- High acid-rock reaction rate
- Crosslinking chemistry

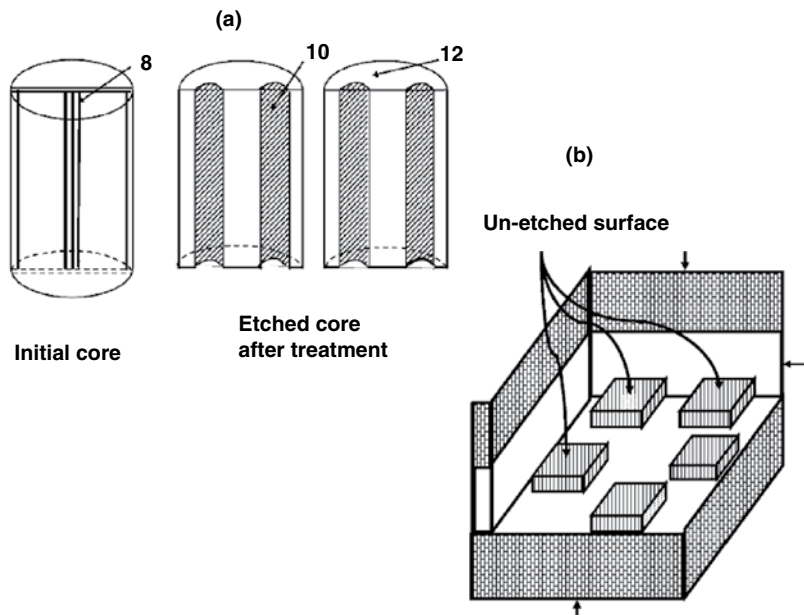


Fig. 3.109—Illustration of use of an inert masking agent (Brown et al. 2008).

- Corrosion of tubular surfaces
- Proper diversion and optimal zonal coverage of 220-m pay zone

The design process included temperature simulations, detailed laboratory testing, and a review of acid formulations that were used successfully in the Trecate-Villafortuna Field and elsewhere. Temperature simulations indicated that cooldown from the BHT of 180°C to at least 150°C could be achieved despite the high treating pressures that limited injection rates. Even after cooldown, serious concerns about corrosion and the effectiveness of the ICA system still existed. Laboratory support included fluid optimization for high-temperature application of the ICA. The flow tests enabled the selection of the most appropriate base acid systems and demonstrated that the ICA system would indeed function at the predicted high temperatures.

Solutions:

- Acid reaction rate control and corrosion control achieved with a mixture of 13% HCl/11% acetic acid.
- Diversion achieved with combination of in-situ crosslinked acid (5% HCl with polymer and crosslinker—see Section 3.7.2) and MAPDIR (Paccaloni 1995) (fast pump rate—see Section 3.7.1).

The treatment was bullheaded at a rate from 1–22 bbl/min and the PI increased from 0.11 m³/day/bar to 14 m³/day/bar.

Metcalf et al. (2007) note that stimulation of carbonate reservoirs is typically used to restore or enhance production to an economic level. Horizontal openhole wellbores in carbonate formations have become an everyday occurrence to improve production economics. Carbonate formations are typically stimulated by using HCl. An acid treatment in the well configuration described provides a significant challenge in diversion to accomplish complete stimulation of the lateral. Various techniques have been employed to overcome this problem. These include preperforated or slotted liners, specialty treating fluids, solid diverting materials and tools. All have had some successes in various regions of the world. Presented are three case histories in which openhole packers and sliding sleeves have been employed with and without the aid of specialty treating fluids.

Devonian [True Vertical Depth (TVD) 10,400 ft]. These are openhole wells and control of acid placement is by use of openhole packers and sliding sleeves operated by use of phenolics balls. Several different treatment schedules included slickwater (low concentrations of polyacrylamide polymer) followed by emulsified acid of 15% HCl. In some cases VES acids were used for diversion.

Devonian (TVD 8,800 ft). These are also openhole horizontal completions and placement is by use of openhole packers and sliding sleeves. Slick (polyacrylamide polymer) HCl, crosslinked gelled HCl and linear gelled HCl fluids were used in the stimulation as well as for diversion stages. Note these may be similar to the ICA described in the previous case history.

San Andres (TVD 5,700 ft). This well was initially completed as a vertical well drilled, perforated, and hydraulically fracture stimulated with 43,000 lb of 16/30-mesh white sand. Lower than expected production resulted. Recompletion using a horizontal wellbore drilled in the center of the vertical pay zone and a large acid job performed in four stages was carried out. The treatment that was pumped using slick water VES acid and HCl. Openhole packers and sliding sleeves were used to control placement of treatment stages to effectively treat 400- to 600-ft intervals of the horizontal wellbore. With every diversion stage a significant pressure increase was observed, indicating diversion of treating fluids in new intervals. A viscoelastic acid system was used to effect this diversion.

Nasr-El-Din and Samuel (2007) claim that VES-based acid systems have been used in Saudi Arabian fields in matrix acid stimulation, and in leakoff control acids during acid-fracturing treatments. These surfactants were used to provide diversion during acidizing of vertical, long horizontal, and multilateral wells. They were used in sour environments where hydrogen sulfide levels reached nearly 10 mol%. They were also used in gas wells to reduce acid leakoff and create deep fractures in dolomitic carbonate reservoirs (250 to 275°F). In addition, they were successfully employed to stimulate seawater injectors and disposal wells where the BHT was in the range of 100 to 150°F.

More than 250 wells (oil, gas, water injectors, and disposal wells) were treated with VES-based acid systems. The acid was placed either by bullheading, by using CT with or without a tractor. In some cases, these treatments included stages of emulsified or regular acids. All these wells responded positively to the treatment. There were no operational problems encountered during pumping these acids even when low-permeability reservoirs were treated. Because these acid systems do not contain polymers, there was no need to flow back water injectors. The spent acid in oil and gas wells was lifted from the treated wells in a very short period of time. Finally, wells treated with surfactant-based acid systems showed sustained performance for longer times than those treated with other acid systems.

Case histories described in the paper include

- Matrix acidizing of seawater injectors
- Matrix stimulation of horizontal wells with openhole completions
- Matrix stimulation of water disposal wells
- Stimulation of extended reach wells
- Acid fracturing of water injectors
- Acid fracturing of deep sour wells

3.9.2 Carbonate Stimulation. The Middle East has a large number of very productive carbonate wells (calcite and or dolomite) and many new reactive stimulation processes have been applied in these formations.

Al-Anazi et al. (1998) describe optimization of an emulsified acid system to stimulate deep, sour gas reservoirs. High temperatures encountered in deep wells have a tendency to destabilize emulsified acid and, as a result, this acid may lose its retardation effect. In addition, some of the commonly used acid additives were found to adversely affect the stability of the emulsified acid. Therefore, extensive experimental studies were performed to evaluate the influence of temperature on emulsion stability and retardation effect. In addition, the effects of various acid additives on emulsion stability were examined in detail.

Results, Observations, Conclusions. An acid-in-diesel emulsified acid was evaluated to stimulate deep, sour reservoirs in Saudi Arabia. The acid (28 wt% HCl) to diesel volume ratio is 70:30. Experimental results indicate that the emulsified acid is stable for more than two days at ambient conditions and more than 4 hours at 250°F. The retardation factor of the emulsified acid was found to be greater than ten times that of the conventional acid systems. Coreflood tests using tight carbonate plugs (dolomite cores) indicated that the emulsified acid could be injected into tight cores (permeability less than 10 md) without encountering any injectivity problems. The acid created deep wormholes, which significantly increased the permeability of the treated cores.

Emulsified acid can be effectively used to stimulate deep sour, gas wells. The stability criteria developed in this study enhances the performance of emulsified acids, especially for high temperature wells. Emulsified acids require minimum amounts of additives and maintain the integrity of well tubulars. Field results indicated conclusively that emulsified acid is a cost effective option to stimulate deep wells. They also suggest that this acid can be used to stimulate wells completed with special types of tubing.

Nasr-El-Din et al. (2000a) describe the stimulation of two wastewater disposal wells in a carbonate reservoir in Saudi Arabia that suffered loss of injectivity because of severe formation damage. A thorough experimental study was conducted to evaluate the use of acid-in-diesel emulsions to stimulate these wells, which had several tight zones. The emulsified acid consisted of 70 vol% of 15 wt% HCl, 30 vol% diesel, and an emulsifier. This is the first time emulsified acid has been used to stimulate disposal wells. Experimental results indicated that the acid-in-diesel emulsion behaved as a shear-thinning fluid. The stability and reaction rate of the acid with reservoir rocks were found to be a function of emulsifier concentration. Coreflood results showed that the emulsified acid formed wormholes in tight carbonate cores. The treatment was very successful and the injectivity of both wells has significantly increased. Field data indicated that longer soaking times were needed to stimulate disposal wells. This is to ensure complete acid spending.

Abou-Sayed et al. (2007) note that previously, an oil company had undertaken a multidisciplinary approach to develop and integrate the required technologies for design, implementation, and evaluation of acid treatments in thick heterogeneous carbonate reservoirs. The developers of the reservoirs have customized the technologies and integrated methodology for application in a major field in the Middle East with a high level of success.

Important steps in the integrated methodology developed and implemented for matrix acidizing include

1. Determine the stimulation requirements given the well/reservoir objectives
2. Characterize the various rock types present in the formation
3. Develop an integrated perforation/stimulation strategy
4. Conduct appropriate laboratory tests with representative field core plugs
5. Model the stimulation process with tools calibrated to the formation of interest
6. Develop field procedures and implement the treatments as per design
7. Evaluate stimulation effectiveness
8. Optimize treatments based on post-stimulation performance and operational constraints

Kabir et al. (2011) described lessons learned during several acid fracturing and then refracturing of a tight gas/HP carbonate reservoir in North Kuwait.

The results showed that PI (J^*) increased by 2.5 folds during the post treatment production test. However, after 3 months of continuous production, the PI declined down to 1.2 folds despite the pressure build up performed indicated fracture conductive behavior.

One of the biggest challenges is the bottomhole static temperature is 275°F. The treatments used various combinations of emulsified acids and VES.

Conclusions.

- Acid refracturing was designed and executed successfully. Designed frac half-length of 250 ft is fairly consistent with the PBU test interpretation of 214 ft.
- The initial PI of the well after perforation and stimulation was -0.13 bbl/psi vs. PI to date of 0.45 bbl/psi (max at 0.98 bbl/psi immediately after acid refrac).
- The case study clearly shows the effort of extending the well life by maximizing reservoir contact and conductivity. Further improvement needs to be done to extend the fracture half-length beyond what has currently achieved which is required for very low permeability formation. However, this is a very big challenge to be achieved by acid fracturing, given the fact that acid tend to spend very fast at high temperature. Therefore, even if we can hydraulically open the fracture deep into formation, the conductivity contributed by acid etching effect towards the tip of the fracture becomes less.
- Hydraulic proppant fracturing may be a more viable option as fast acid spending at high temperature will not be an issue anymore.
- The authors of this book suggest that alternates such as organic acids and chelating agents and solid acids described in Section 3.4.2 also should be investigated because there are also significant difficulties with high temperature prop fracturing.

Bustos et al. (2007) describe a combination of technologies, which has recently been applied successfully in the Strawn formation in Terrell County, Texas.

The goal of an acid fracture treatment is to generate a highly conductive pathway of sufficient length from the reservoir to the wellbore. Depth of penetration of live acid is the critical factor in determining the success of an acid-fracturing treatment. Depth of penetration is controlled by the acid reaction rate, leakoff, and stimulation rate. Acid reaction rate is a function of several factors, the most important of which is the reservoir temperature. Yet another concern, in acid fracturing in long carbonate intervals, is attaining the necessary diversion to ensure that multiple sets of perforations are adequately stimulated. There has been a large number of highly successful acid fracture treatments in the Permian Basin incorporating a combination of new polymer-free self-diverting acid combined with an existing acid-oil emulsion technology.

3.10 Things to Think About

- The earliest and in many ways the simplest stimulation/enhancement method for oil and gas wells has been expanded from just pumping HCl to the use of a large number of sophisticated “reactive fluids” that can be used at temperatures up to 400°F in a wide variety of formation types.
- The chemistry and physics of the reactions of the various acids and chelating agents with carbonates has been investigated in enough detail that the fluids can be tailored to the well conditions and can be used with a significant amount of predictability.
- A very large amount of information on the reactions of acids and chelating agents with sandstone formations and their very complex constituents has been produced. There also has been progress in developing single-stage treatment fluids. However, HF-producing chemicals still must be used if clays and the silica components of the sandstones must be dissolved. Wormholing of sandstones (a hallmark of carbonate stimulation) usually is not achieved in most cases. The HF components are also still not ideal because of safety and reactivity issues.
- Acid fracturing is an important process that is used in a number of carbonate reservoirs in mono-ethanolamine as well as in North America. Most of the issues with reactivity and leakoff can be controlled using W/O emulsions and VES materials. Replacement of diesel oil as the oil phase is required for a “greener” process. Fracture acidizing of sandstone formations is not usually effective at this time.
- The final fluid formulations will contain a large number of additives, the most important of which is the CI. The inhibitor schedule must include all of the other additives as well as the temperatures experienced and the metallurgy of the components to be contacted for the maximum time of the treatment.
- In the opinion of the authors of this book, placement and design of the treatments are the major controlling factors for success or failure of a reactive stimulation treatment. The use of a treatment plan based on a robust geochemical simulator is a requirement for success.

Chapter 4

Propped Fracturing Chemistry and Applications

Formation stimulation using predominantly *nonreactive fluids*, where the fracture conductivity is maintained by an inert proppant, is an immensely important technique. Both carbonate and silicate-type formations can be stimulated using propped fracturing. Because of high reactivity, some carbonates can also be effectively treated using both matrix and acid fracturing, while most of the stimulation of silicates with reactive fluids involves low-pressure matrix treatments for near-wellbore cleanup. See Chapter 3.

4.1 Introduction to Propped Fracturing Processes

This chapter will describe the fluids and solids used in propped (prop) fracturing technologies. Mechanistic interpretations will be provided where understanding has been developed. Many of the important concepts and equations of hydraulic fracturing (HF) were introduced in Section 3.8, which describes HF using reactive fluids (for carbonates). Therefore, there will be significant references to that section and the reader is encouraged to review the contents.

While the basic chemistries of sandstone matrices have been reviewed in Section 3.5, Ali et al. (2010) note that while siliciclastic formations are mostly the product of erosion from a parent source of rock, the diagenetic processes that then take place have a great effect on the final permeability as well as the final chemistry. The lesson is that sandstones are almost infinitely variable. Also, as noted in Sections 3.3 and 3.8, carbonate formations show great variations in the physical properties even though the basic chemistry may be more uniform than silicate formations. While the authors of this book contend that carbonates and silicate formations can and are treated using prop fracture methods, the actual geochemistry of each formation will have a significant influence on the choice and use of the fracturing chemistry and pumping methods. Prop fracturing is a more “mechanical” process than acidizing; however, the formation matrix *cannot* be thought of as being inert.

Webber (1994) estimates that more than 50% of all oil and gas wells in the US will be treated by fracturing methods during their life cycle. The use of this method has also materially increased the availability of natural gas and oil, especially from tight shale formations (API 2008; GWPC 2011). This new technology for producing gas and oil requires that most of these wells be fractured in multiple sections using horizontal completions. Thus, more than 50% of wells may be fracture treated in the future.

Fracture acidizing uses many of the same steps as prop fracturing, but proppant usually is not used. This procedure was described in Section 3.8. Acid fracturing generally has lower risk (no screenout). However, it is only applicable to carbonates (with some future use in silicates, see Section 3.8.6) and not suitable in high-stress environments. Acid fracs in softer carbonates such as chalks may not have a long treatment life (the fracture may heal and not support the conductivity).

Prop fracturing frequently starts with an HCl stage to clean the perforations. Then, most fracturing treatments use thickened fluids, pumped in stages. The first frac stage (called a pad) usually

is a mixture of water, a polymer, and other additives. This is the breakdown fluid that initiates the fracture. This type of pad fluid also is used to initiate a reactive fluid (acid) fracture treatment (Section 3.8).

The next stage is the *slurry* (a more viscous polymer, surfactant or oil-gelled oil fluid) that contains the proppant (frequently sand). Different concentrations of slurry and proppant are used in the subsequent stages as the fracture propagates. A final *wash* stage usually ends the treatment to flush the proppant from the equipment and the wellbore. After a calculated shut-in time, additives in the fluids (and heat) may cause the viscosity to be reduced, and the well is *flowed back* and production can commence.

Hopefully, a very permeable frac pack is left that will improve production. Harris and Sabhapondit (2009) note that fluids for commercial fracturing applications contain viscosity causing agents [polymers or viscoelastic surfactants (VES)], crosslinking agents, surfactants, clay-protective agents, and viscosity breakers. All of these chemicals must be balanced to provide the physical properties required to place the proppants at elevated temperatures and pressures without damaging the proppant pack or rock formation. The complex chemistry must be carefully controlled on a large scale and in a hostile environment for the fracturing process to be successful. The authors of this book note that some jobs are being pumped in shale formations without a proppant being present. A discussion of shale and tight gas (TG) fracturing is in Sections 4.1.1 and 4.10.1.

A typical (but not exclusive) sequence of steps (tasks) is described by Arthur et al. (2009) for conducting a fracture treatment and is shown in Fig. 4.1. The 11 tasks are noted with the section of the book where they are explained in more detail.

1. Drilling and data collection—See brief description of geochemistry and mechanics in Sections 1.5.6 and 1.6.3, needed for models.
2. Model simulation—Section 4.11.1.
3. Frac equipment brought to site—Section 1.7.
4. Bring fluids to site safely and mix—Sections 6.1 and 4.2.
5. Rig up safely—Section 6.1.

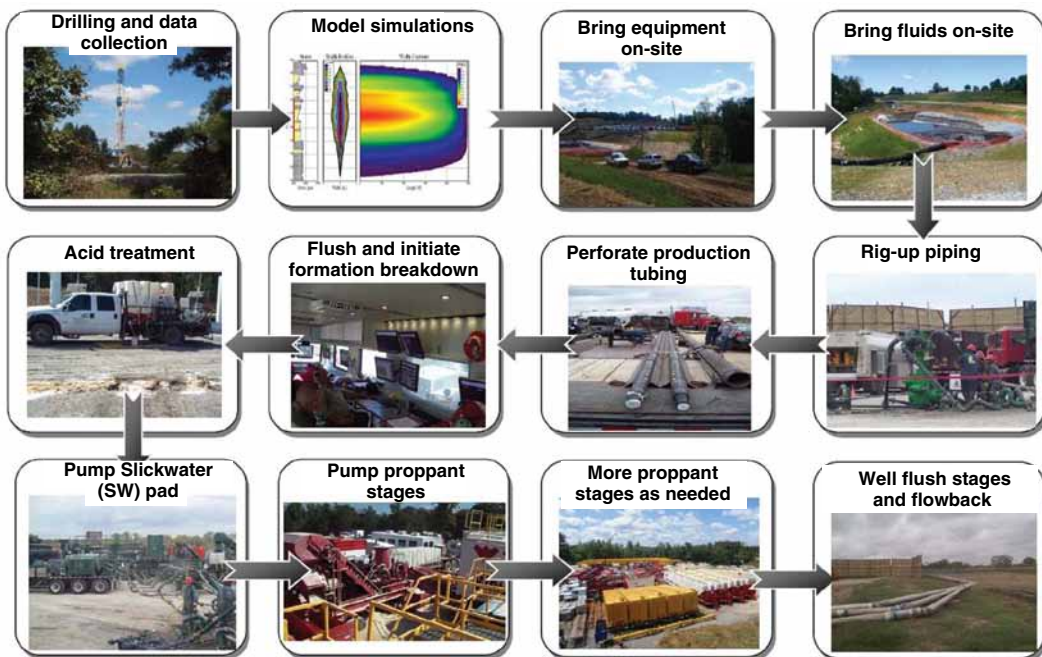


Fig. 4.1—Process flow diagram for a hydraulic fracture treatment.

6. Perforate tubing—not described in this book (but look at Section 4.11.3 for some innovative systems).
7. Flush and initiate breakdown—Section 4.3.1.
8. Acid treatment to clean perforations—Section 3.4.1.
9. Pump slickwater (SW) pad (if needed)—Section 4.7.1.
10. Pump fluid with prop stages—Sections 4.4, 4.5, 4.6, 4.7, 4.8, and 4.9.
11. Flowback well, flush, and disposal of liquids and solids—Sections 6.3 and 6.4.

Vast varieties of chemicals are in use. GWPC (2011) provides a generalized description of the fracturing process as well as a long list of specific chemicals (with Chemical Abstract Service numbers) that have been used in actual formulations. However, any particular job may use only some of these chemicals, and they will be described in more detail in Sections 4.4 through 4.7 of this book.

4.1.1 Application Areas for HF. This section will describe how HF contributes to the reservoir producibility in different reservoir types. A typical design criterion for a treatment in each reservoir type is included in these preliminary descriptions. Many more details of fracturing selection methods are included in Sections 4.10 and 4.11.

An improvement in the productivity index (Eq. 1.17) is used to justify many fracturing treatments in oil and gas wells including TG, shale, and unconsolidated reservoirs. However, prop fracturing is *not applicable* in all reservoir types. Problem areas include

- Water or gas zone (for oil) nearby
- Generally high-permeability reservoirs (exceptions: frac and pack where the goal is to provide sand control) (Baycroft et al. 2005; Morales et al. 2003)
- High-stress areas (too difficult to fracture)
- Where proscribed by environmental or governmental considerations

Conventional Reservoirs of Oil and Gas. Conventional reservoirs include those drilled, completed, and stimulated using the tools and chemicals that have been used and developed in the past 100 years. Many of the most important techniques reviewed in this book were developed for use in these types of plays. They exist in carbonate and sandstone formations. The stimulation methods include acidizing as well as fracturing using proppants. By exception, they are not unconventional (described later in this section). They also may include consolidated and unconsolidated reservoirs. Selection rules are described in Section 4.10.

Consolidated Reservoirs. Usually a sandstone (or a carbonate) formation is cemented together to form a mass (see Fig. 3.39). Thus, consolidated limestone and sandstone will have high compressive strengths and can be used as primary building materials. A diagram of conventional planar hydraulic fracture in a consolidated reservoir is seen in Fig. 3.97 as well as in Section 4.1.2. If filled with a conductive proppant, it will provide enhanced permeability and may improve connections within the reservoir. Lack of connections either aerially or vertically is a major reason for bypassed hydrocarbons. See the discussions in Section 5.2.1.

Unconsolidated Reservoirs. Soft unconsolidated sand formations exist and frequently have high permeabilities but still may be improved through HF. Specific fracturing requirements for these plays include

1. Conductivity of proppant pack is important to increase J^*
2. Length of fracture is not as important
3. Typical frac and pack designs may apply (Morales et al. 2003) to control sand production

Unconventional Reservoirs of Oil and Gas. According to Holditch et al. (2007), this term usually applies to a low-permeability reservoir (< 0.1 md) that produces mainly dry natural gas. Many of the low-permeability reservoirs that have been developed in the past are sandstone, but significant quantities of gas are also produced from low-permeability carbonates as well as shales and coalbed deposits. Liquid hydrocarbons also have been produced from some shale formations (RRC 2011).

| Region | Coalbed Methane (P50) | Tight Sands Gas (P50) | Shale Gas (P50) | Total (TCF) (P50) |
|------------------------------------|--------------------------|--------------------------|--------------------|----------------------|
| Austral-Asia | 1,348 | 6,253 | 2,690 | 10,291 |
| North America | 1,629 | 10,784 | 5,905 | 18,318 |
| Commonwealth of Independent States | 859 | 28,604 | 15,880 | 45,343 |
| Latin America | 13 | 3,366 | 3,742 | 7,122 |
| Middle East | 9 | 15,447 | 15,416 | 30,872 |
| Europe | 176 | 3,525 | 2,194 | 5,895 |
| Africa | 18 | 4,000 | 3,882 | 7,901 |
| World | 4,052 | 71,981 | 49,709 | 125,742 |

Fig. 4.2—Geographic distribution of unconventional original gas in place in TCF.

Fig. 4.2 describes the geographic distribution of unconventional original gas in place (Dong et al. 2011) for various sections of the Earth. Note that TG sands are currently the largest known source of future gas; however, development of shale gas may change these estimates as these frequently produce wet gas as well as other hydrocarbon liquids. At the time of the publication of this book, the estimates are in flux as new technologies develop.

Cramer (2008) has reviewed the stimulation of the unconventional reservoir, and he notes that this term has different meanings to different people. Certain reservoirs that are termed unconventional have a rock matrix consisting of interparticle pore networks with very small pore connections imparting very poor fluid-flow characteristics. The author claims that abundant volumes of oil or gas can be stored in these rocks, and often the rock is high in *organic content* [such as kerogen—an immature product from the degradation of ancient biomaterials (McCarthy et al. 2011)]—and the source of the hydrocarbon. However, because of marginal rock-matrix quality, these reservoirs generally require both natural and induced fracture networks to enable economic recovery of the hydrocarbon. Rock types in this class include shale and coalbed methane (CBM). He notes that the term shale is a catch-all for any rock consisting of extremely small framework particles with minute pores charged with hydrocarbon and includes carbonate and quartz-rich rocks. Cramer (2008) claims that another type of unconventional reservoir is the stacked pay unit, that exhibiting somewhat better pore characteristics than is the case outlined previously but with the individual units tending to be lenticular in shape and having an extremely small size or volume. These two classes of unconventional reservoirs are amenable to well stimulation.

When the above rock types become commercially exploited, they are known as *resource plays*. Once a low priority, the depletion of conventional reservoirs and improving price for oil and gas has driven unconventional reservoirs to an important place in the oil and gas industry. In some regions (i.e., Rocky Mountain province), unconventional reservoirs represent the primary target of current activity and remaining hydrocarbon development. Cramer (2008) claims that given their unique petrophysical properties, each type of unconventional reservoir requires a unique approach to well stimulation, with often differing objectives than exist with conventional reservoir types. The paper reviews the characteristics of the basic unconventional reservoir types, lessons learned, and successful stimulation practices developed in completing these reservoirs, and areas for improvement in treatment and reservoir characterization and treatment design.

HF has contributed greatly to the economic producibility of these reservoirs. Natural gas production from shallow, fractured shale formations in the Appalachian and Michigan basins in the US has been underway for decades. What changed the game was the recognition that one could create a permeable reservoir and high rates of gas (and/or oil) production by intensely stimulating horizontal wells by

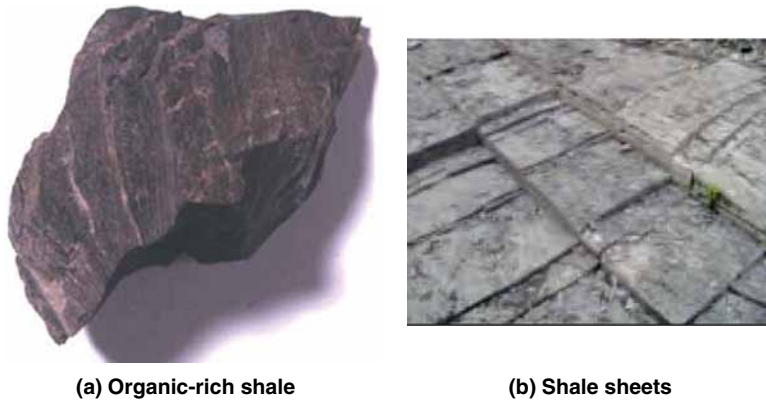


Fig. 4.3—Shale rocks shale (USGOV.jpg; Boyer et al. 2011).

multistage fracturing. Sections 4.10.1 and 4.11.3 directly describe some of these advances. Details of several important unconventional reservoirs are in subsequent sections.

Shale Gas and Oil Reservoirs. A very important type of predominately *silicate* formation that contains shale beds are now being frequently treated using propped fracturing methods. Shale is the most common sedimentary formation on earth (Boyer et al. 2011) but is quite different from sandstones that contain sand grains mixed with clays and other minerals (Figs. 3.38, 3.39, and 3.40). Shale (Wikipedia 2010b) is defined as a fine-grained clastic sedimentary rock that was formed from a clay mud that was compacted over time. As such, the major minerals represented are largely kaolinite, montmorillonite and illite. This report notes that clay minerals of late Tertiary mudstones contain expandable smectites while in older rocks especially in mid to early Paleozoic shales, illite clays predominate. The shales may be very dark (black) in color because of the presences of *unoxidized carbon* compounds as well as iron oxides. Fig. 4.3 shows a photo of a chunk of organic shale as well as an outcrop of a shale bed with sheets arranged like a stair step. The shales that are of interest to the petroleum industry are known as organic-rich shales. Some shale formations, such as the Haynesville (Buller 2010) also may contain calcite and dolomite and may have a HCl solubility up to 15%.

Akrad et al. (2011) also calls these formations prospective shales because the clay content is usually less than 50%. They note that the high carbonate content of some of these rocks makes them soft (low E) and, thus, may require different frac fluids/proppants for stimulation.

Shale has long been considered to be a source rock (McCarthy et al. 2011; Cramer 2008) as well as a barrier trap for migrating hydrocarbons. Fracturing of shale now makes it a viable producing formation, and these are now called resource rocks plays (Cramer 2008).

The trapped carbon is the source of the methane/liquids that is the object of the fracture stimulation treatments. Shales also can be called *slates*. The major physical attributes are very thin lamella or parallel bands (see Fig. 4.3 and Fig. 4.4) less than 1 cm thick that are called *fissility*. The shale beds have *very low primary permeabilities*.

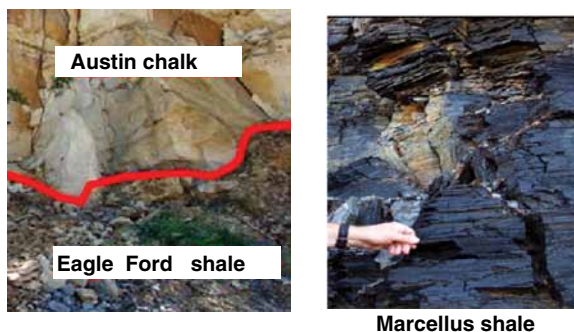


Fig. 4.4—Outcrops of Austin chalk, Eagle Ford shale (Wikipedia 2011b), and Marcellus shale (Arthur et al. 2009).

Soeder (1988) examined a Marcellus shale that was free of a mobile liquid phase and had a measured gas porosity of approximately 10% under stress with a fairly strong adsorption component. Permeability to gas (k) was highly stress dependent, ranging from about 20 μd at a net stress of 3000 psi down to approximately 5 μd at a net stress of 6000 psi (note that most conventional oil and gas producing sandstones have permeability values in the 1–1000 md range). These properties make extraction of gas from shales very difficult unless they have been fracture treated. Kaufman et al. (2008) report that shale gas formations also have microfractures and cleats that provide access to the gas. In this characteristic, they share similarities with coalbeds that also can be fractured to produce methane. Very important fields of gas producing shale include the Barnett shale in central Texas and the Marcellus group that underlies parts of New York, Pennsylvania, Ohio, and West Virginia.

Another important formation is the Eagle Ford shale group of Texas that runs from the Mexican border to about Dallas. According to the RRC (2011) the lower section of the Eagle Ford consists of organic-rich, pyritic, and fossiliferous marine shales. Also, a small part of the Eagle Ford consists of a thin limestone unit between the shales, and this part is especially amenable to HF. The wells in the deeper part of the play deliver a dry gas, but moving northeastward (and with an updip), the wells produce more liquids. See the discussion in Boyer et al. (2011) and McCarthy et al. (2011). One of the fields is actually an oil field [Eagleview (Eagle Ford)]. Even though the conditions are severe

- 6 to 10% porosity
- 200 to 600 nD
- 7,000 to 10,000 psi bottomhole pressure
- 2.0 to 4.5 Mpsi Young's modulus
- Bottomhole static temperature 270–300°F

More than 5,000,000 bbl of oil have been produced in 2 years (RRC 2011) from this reservoir. The field ends in the vicinity of Dallas, where an outcrop of Austin chalk over the shale can be seen (Fig. 4.4). Thus, it runs for almost 400 miles (width about 50 miles) and with a maximum thickness of about 250 ft (RRC 2011). Fig. 4.4 also shows the layers of the Marcellus shale, which is a very important gas play that covers several eastern US states.

See **Fig. 4.5** for location of major shale oil and gas plays in North America. Note that other shale formations such as the Bakken in North Dakota and the Utica in Ohio (Wickstrom et al. 2012) also are producing (or have potential of) significant volumes of liquid hydrocarbons. **Fig. 4.6** describes the properties of the major shale basins. Note that the landscape and potentials are continually changing as new plays are evaluated.

Directional drilling and HF are vital technologies that have allowed these resources to be developed [see Arthur et al. (2009) and King (2010)]. Details of fluids and treatment methods specifically for shale are in Sections 4.12.1 and “Fluids for High Carbon Shales” under Section 4.10.1. Design criteria are described in “Fluids for High Carbon Shales” in Section 4.10.1 and in Section 4.12.1.

A diagram showing the placement of multiple fractures is in **Fig. 4.7** (PackersPlus 2011b).

The key features of fracture treatments of shale plays include

- Large stimulation treatments
- Long laterals
 - 1500 to 3000 m
- Multiple hydraulic fractures to 40 frac stages (see **Fig. 4.8** for a wellsite picture of a massive HF treatment). This photo also illustrates the equipment requirements and possible health, safety, and environment issues (Chapter 6).
- Large water volumes
 - Vertical well 2000 to 4000 m³
 - Horizontal well 7500 to 23000 m³
 - Managing water key (sources, reuse, disposal, Sections 6.2 and 6.3)

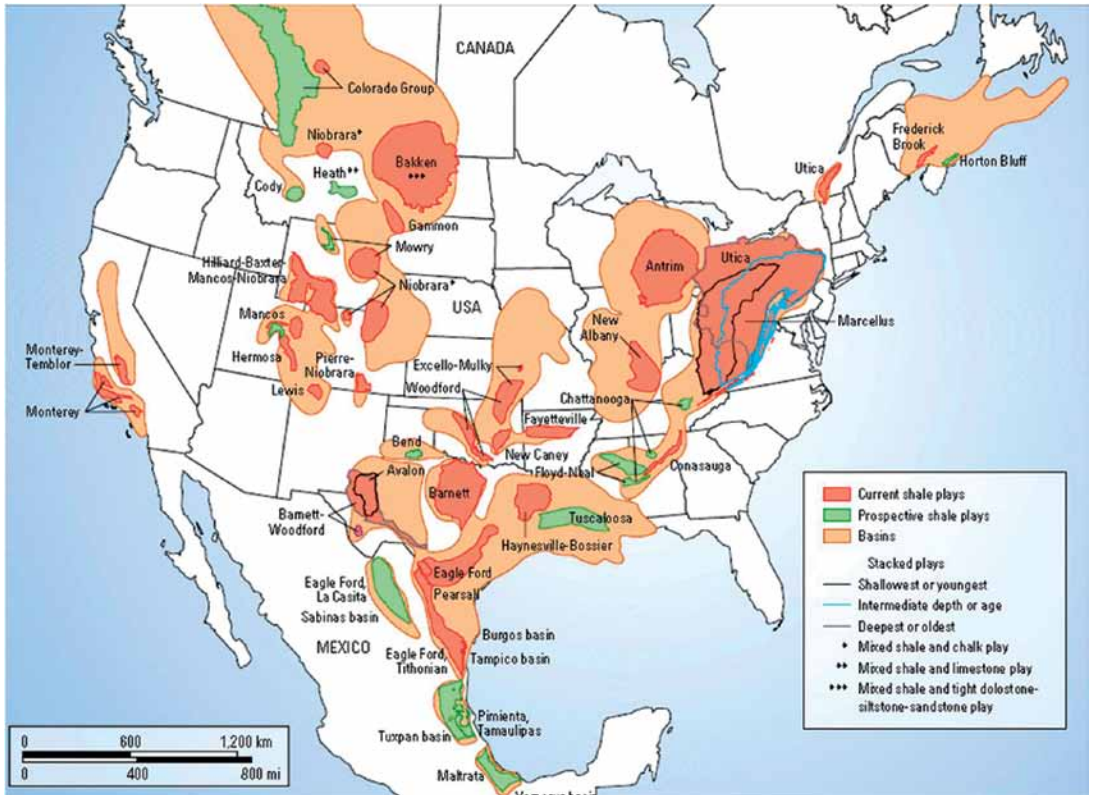


Fig. 4.5—Shale gas and shale oil plays (Boyer et al. 2011).

- Large proppant volumes
 - 0.5 to 1 lbm/gal
 - Vertical well: 225k to 450k kg
 - Horizontal well: 1,300k to 4,500k kg
 - Small mesh: 100, 40/70, 30/50
 - Non-API standards
- Type of fracturing treatments for these types of nonconventional wells include
 - Simultaneous fracturing more than one zone or well
 - Tri-fracs—Three fracs pumped at the same time, which lead to the rock between the wells being cracked more effectively
 - 4 to 5 stages/well
 - 15,000 bbl/stage
 - 3mm lbm sand/well
 - Chevron tri-frac: Three parallel horizontal, one higher in pay zone
 - Quad-fracs (four fracs pumped at the same time)
 - Zipper fracs [adjacent fracs treated without bleedoff—see Ghiselin (2009)]

TG. Deep (hot), *TG* has been a major focus of fracking and has led to the development of many of the chemistries described in Sections 4.4, 4.5, 4.6, and 4.7. Some *TG* carbonates also can be stimulated using acid fracs. [See Section 3.8.1, and Bustos et al. (2007).]

Key points in proppant frac design of *TG* include

1. Conductivity of proppant is not important because it will always be much higher than the formation
2. Length of fracture is key to provide contact with the formation

Comparison of Data for Gas Shales in US

| Gas Shale Basin | Barnett | Fayetteville | Haynesville | Marcellus | Woodford | Atrium | New Albany |
|--|-------------|--------------|---------------|-------------|--------------|-----------|------------|
| Estimated area, square miles | 5,000 | 9,000 | 9,000 | 95,000 | 11,000 | 12,000 | 43,500 |
| Depth, ft | 6,500–8,500 | 1,000–7000 | 10500–13,500 | 4,000–8,500 | 6,000–11,000 | 600–2,200 | 500–2,000 |
| Net thickness, ft | 100–600 | 20–200 | 200–300 | 50–200 | 120–220 | 70–120 | 50–100 |
| Depth to base of treatable water, ft | ~1200 | ~500 | ~400 | ~850 | ~400 | ~300 | ~400 |
| Rock column thickness between top of pay and bottom of treatable water, ft | 5,300–7,300 | 500–6,500 | 10,100–13,000 | 2,125–7,650 | 5,600–10,600 | 300–1,900 | 100–1,600 |
| Total organic carbon, % | 4.5 | 4.0–9.8 | 0.5–4.0 | 3–12 | 1–14 | 1–20 | 1–25 |
| Total porosity, % | 4–5 | 2–8 | 8–9 | 10 | 3–9 | 9 | 10–14 |
| Gas content, scf/ton | 3–350 | 60–220 | 100–300 | 60–100 | 200–300 | 40–100 | 40–80 |
| Water production, bb/day | N/A | N/A | N/A | N/A | N/A | 5–500 | 5–5,000 |
| Well spacing, acres | 60–160 | 80–160 | 40–560 | 40–160 | 640 | 40–160 | 80 |
| Original gas in place, tcf | 327 | 52 | 717 | 1,500 | 23 | 76 | 160 |
| Technically recoverable resources, tcf | 44 | 41.6 | 215 | 262 | 11.4 | 20 | 19.2 |
| References to various values are in the referenced paper | | | | | | | |

Fig. 4.6—Properties of key shale gas basins in US (Kell 2009).

- They usually are hot (>200°F), so fluid selection to accommodate the reactivity of the fluids is critical. See Sections 4.10.1 and 4.12.1

CBM. Coal also is a low-permeability solid (Wikipedia 2010e). Almost all the permeability of a coalbed is usually considered to be because of fractures, which in coal are in the form of cleats. The permeability of the coal matrix is negligible by comparison. Coal cleats (natural fractures) are of two types: butt cleats

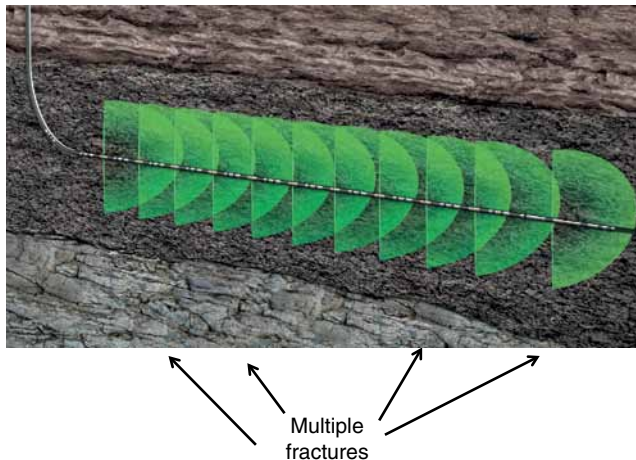


Fig. 4.7—Stimulation of a shale bed with multiple fractures (Packers Plus 2011b).

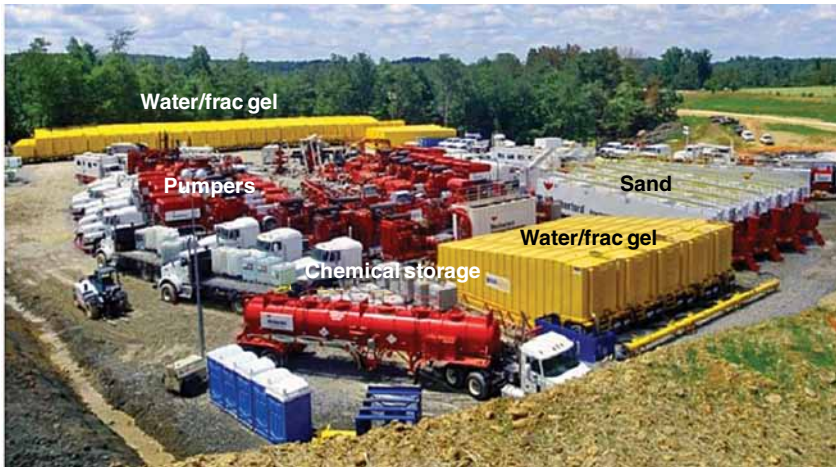


Fig. 4.8—Wellsite organization for a massive hydraulic frac.

and face cleats, which occur at nearly right angles to each other. The face cleats are continuous and provide paths of higher permeability while butt cleats are noncontinuous and end at face cleats. This article claims that, on a small scale, fluid flow through CBM reservoirs usually follows rectangular paths. The ratio of permeabilities in the face cleat direction over the butt cleat direction may range from 1:1 to 17:1. Because of this anisotropic permeability, drainage areas around CBM wells are often elliptical in shape. Fracturing treatments as well as the use of chemicals to drain the water are in use and will be described in this chapter.

Many higher-permeability sandstone and carbonate formations also may benefit from fracture stimulation treatments. In fact, there is a commonly held belief (especially by vendors of fracturing technologies) that the best wells are also the best fracture candidates because they will then produce more hydrocarbons than poor wells (opinion of this book's authors).

4.1.2 Key Concepts and Parameters for Fracturing. This chapter will describe how some very complex chemistry is used to maximize the final conductivity, areal contact, and fracture length so as much oil and gas can be produced as possible. Fracturing is essentially a *mechanical* (physical) technique for improving the overall permeability of the formation. If it were possible to inject proppant directly into a fracture without a viscous fluid, that would be preferable, but it is not practical in most cases [however, foams and CO_2 have been used as the carrier (Kubala and Mackay 2010)]. Thus, the fracturing fluid is a very important key to producing successful fracture treatments. In this chapter, most of the discussion is about the chemistry of the fracturing fluids and not about the reactions with the formation. If the fluid is chosen properly, the reactions with the formation will be minimal, however this factor always must be considered in the selection and modeling processes (Sections 4.8 and 4.10.1) because unwanted reactions do occur.

Key mechanical parameters that are highly dependent on the fluid chemistries are fracture conductivity, fluid efficiency (including leakoff) and proppant transport. These can greatly affect the fracture geometries in different formation types. The next sections discuss these concepts.

Fracture Conductivity. This very important parameter (dimensional conductivity, C_D -units: md-ft) is defined in Eq. 3.37, where k_f is the fracture permeability and w is the fracture width. This equation applies to both a propped fracture as well as an acidized fracture. Factors that may affect C_D include

- Proppant characteristics and packing
- Residual polymer residue

For steady-state flow, Prats (1961) and Cinco-Ley et al. (1978) showed that a fracture affects productivity (J^* , Eq. 1.17) through the equivalent wellbore radius r_w' , and that r_w' is related to the productive fracture half-length or penetration (x_f) by the dimensionless fracture conductivity (C_{fD}):

$$r'_w \approx \frac{2}{\pi} x_f \dots \dots \dots (4.1)$$

$$C_D = \frac{k_f w}{k x_f} \dots \dots \dots (4.2)$$

Here, k_f (md) is the proppant-pack permeability, w (ft) is the average fracture width, k (md) is the formation permeability, and x_f (ft) is the productive fracture half-length. The idea is that the new fracture provides a superhighway that increases the equivalent wellbore radius, r'_w , and, thus, the productivity index. However, note that the flow in the frac pack (C_D) is balanced by the permeability of the formation and fracture half-length (Eq. 4.2), so very low-permeability formations will require more than just a permeable frac pack including more frac length and contact surface area for increased production.

C_D for known or new formulations are measured in the elaborate conductivity cells described in Section 4.2.2. A significant amount of chemistry including breakers (Section 4.6) as well as solid additives (4.9.6) have been designed to increase or modify C_D . Akrad et al. (2011) note that Young’s modulus (the stiffness, E , Eq. 1.39) of the formation may have an effect on embedment of the proppant into the rock face. The degree of embedment may then have an influence on κ_f and, thus, fracture conductivity. They (Akrad et al. 2011) have studied the effects of the frac fluid and the reservoir rock. More details are given in Section 4.10.1 on fluids/systems for shale formations.

Fluid Efficiency and Fluid Leakoff. According to Smith and Shlyapobersky (2001), a major equation for determining fracturing control is the *material balance*. This relationship says that during fracturing, a certain volume of fluid is pumped into the earth. Some part of that fluid is lost to the formation during pumping, and the remainder creates fracture volume (length, width, and height). The volume (V_i) of fluids pumped is

$$V_i = q_i \cdot t_p \dots \dots \dots (4.3)$$

A major role of the fluid additives is to *maximize the volume* of the fluid that creates the fracture. This defines the *efficiency* of the treatment. Another important relationship is the fracture half-length (Smith and Shlyapobersky 2001) that is estimated from

$$L \cong \frac{q_i t_p}{6C_L h_L \sqrt{t_p} + 4h_L S_p + \bar{w} h_f} \dots \dots \dots (4.4)$$

In these equations, q_i is the pump rate, t_p is the pumping time, C_L is the fluid-loss (FL) coefficient, h_L is the FL height, and S_p is the spurt loss; h_f is called the average gross fracture height, and \bar{w} is the average fracture width.

This author (Smith and Shlyapobersky 2001) also notes that the productive fracture half-length, x_f , may be less than the created (or the created and propped) half-length, L , because of many factors. For example, he claims that the fracture width near the tip of a fracture may be too narrow to allow adequate propped width. The authors of this book note that some of the factors can be estimated using laboratory tests (some described in Section 4.2.2), while others are determined only after a treatment when a model (Section 4.11.1) is compared with production results.

Fluid and additive properties are very important because the amount of fluid that can be pumped at a given pressure is a function of the viscosity (Eq. 1.2), and the FL as well as the carrying capacity for proppants are also a function of the chemistry of the fluids. The *productivity* of the treatment depends on the fracture volume (length, height, and width) as well as the *conductivity* (Eqs. 3.37 and 4.2). Also see Section 4.2.2 for laboratory test methods.

Fracture Geometry. Fracture length and width are key parameters for fracture geometry. Parameters that control the length include FL as well as proppant carrying characteristics. Areas that must be considered in the models (Section 4.11.1) include

- For low-permeability reservoirs: long fractures are required.
- For high-permeability reservoirs: short but wide fractures [frac and pack; see Moreno et al. (2009)]
- To treat the complex fractures for shales and coalbeds: maximize reservoir contact area
- Consider the conductive and propped fracture length vs. total length

Details of different fracture types are described in the next sections.

Transverse and Longitudinal Fractures. Transverse fractures are those in which the direction of the fracture runs perpendicular to the wellbore. They are created by drilling the well in the direction of the minimum horizontal stress. Longitudinal fractures are parallel to the wellbore and result from fracturing wells drilled in the direction of maximum horizontal stress. Transverse fractures are usually better for reservoir drainage; however, drilling in the direction of the minimum horizontal stress is more challenging because of wellbore integrity issues. See Fig. 4.9 that depicts the orientation of longitudinal (light green) and transverse fractures (light blue).

Planar, Nonplanar, and Complex Fractures. A planar fracture is where the fracture geometry is contained in a single plane. Generally, planar fractures are observed in homogeneous rocks where there are no interactions with other fractures or heterogeneities. The stress field for planar fractures is typically homogeneous and the propagation path of the fracture is perpendicular to the minimum in-situ stress (see Fig. 3.97). Fractures that are not contained within a single plane are referred to as nonplanar fractures. Nonplanar fractures generally result when the stress direction changes over the length of the fracture. This can occur when the initial fracture plane is misaligned with the far-field stress direction because of near-wellbore conditions.

In the case where multiple fractures intersect each other, the fracture system is considered complex. Complex-fracture growth can occur in both lateral and vertical directions. Cipolla et al. (2010) divide the lateral hydraulic fracture growth in into four categories: (1) planar growth (simple fracture), (2) complex growth (planar), (3) complex growth with fissure opening, and (4) complex network growth. See Fig. 4.10 (Cipolla et al. 2010). Complex-fracture growth in lateral direction typically occurs because of interaction with natural fractures or pre-existing hydraulic fractures.

Complex growth in the vertical direction typically occurs because of the fracture interacting with various geological layers or laminations with different rock properties and stresses. Fig. 4.11 shows three possible scenarios for vertical fracture growth. The fracture on the left side of the figures shows the classical mechanism of fracture height confinement caused by increased closure stresses in the layers above and below the target zone. The middle picture shows the case where interface slippage

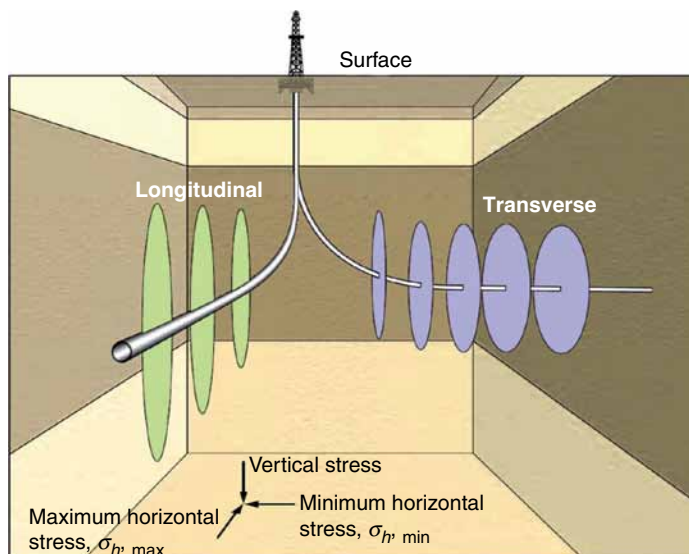


Fig. 4.9—Transverse and longitudinal fractures (Al-Matar et al. 2008).

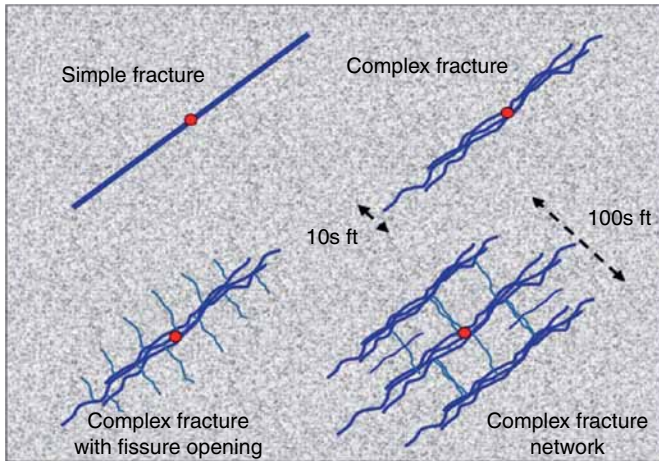


Fig. 4.10—Fracture growth and complexity scenarios.

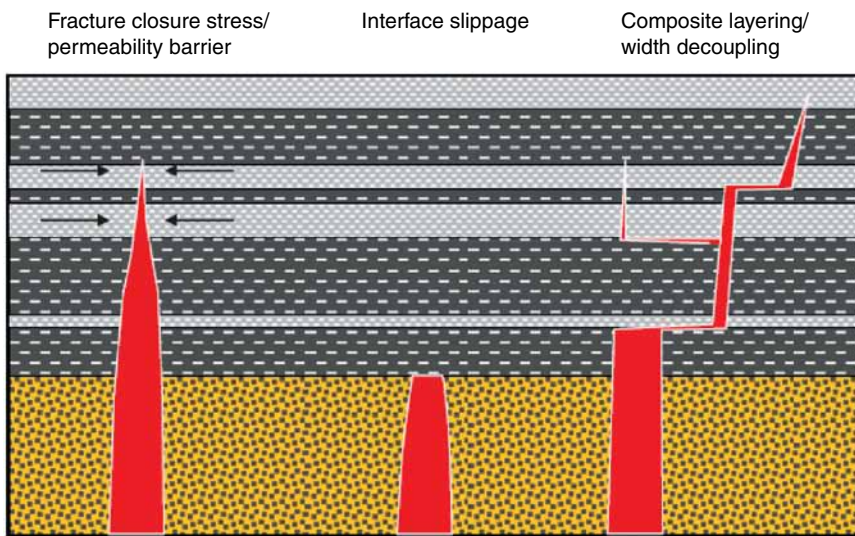


Fig. 4.11—Fracture growth complexities in the vertical direction.

results in perfect confinement at a layer interface. The picture on the right shows composite layering effect caused by partial debonding of layer interfaces (Cipolla et al. 2010).

Large-scale fracture complexity can be measured using microseismic and/or tilt meter fracture mapping or fracture pressure analysis. Direct observations of hydraulic fracture complexity from mineback experiments and cores of hydraulic fractures have also been attempted. The observation area of these direct techniques is small, but it provides useful insight into complexities in the fracture geometry. **Fig. 4.12** shows photo of mineback of complex fracture initiated by a crosslinked-gel frac treatment at high-treating pressures. The main fracture on the right looks curved, but it is a vertical fracture that is cut by a curved mineback face. Note the horizontal component running off to the left in the photograph, and the four separate strands at the bottom and the double strands in the center (Cipolla et al. 2010).

Reservoir Contact Area. One of the strategies used today to produce from low-permeability reservoirs is to greatly enhance the wellbore contact with the formation and so improve drainage and increase production rates per well. HF treatment when combined with extended reach wells and multi-zone completions can increase the reservoir contact area by about three orders of magnitude. **Fig. 4.13** illustrates this concept. In the drawing, a 100-ft, 8.5-in. vertical wellbore results in about 222 ft² of

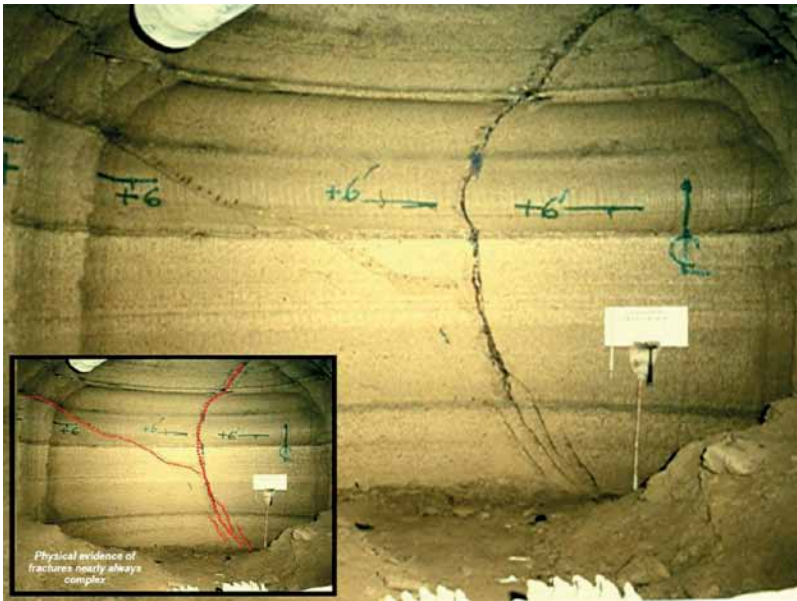


Fig. 4.12—Mineback photograph of crosslinked gel sand fracture with multiple stands and a near horizontal component (Cipolla et al. 2010).

formation contact, a 2,000-ft horizontal wellbore increases formation contact 20 times the vertical. A 150-ft fracture in the vertical well increases contact 270 times over that of the untreated vertical well and 13.5 times that of the 2,000-ft untreated horizontal well. When the 2,000-ft horizontal is treated with ten 75-ft long fractures, formation contact increases 1,013 times that of the untreated vertical well and 50 times that of the untreated horizontal well. Note in Fig. 4.10 that microfractures (called fissures in this figure) also may open, and Wu et al. (2013) point out that this complexity may greatly increase the available contact area and then may take some of the fluid flow from the fracture process.

The next Sections (4.2–4.8) describe the wide variety of materials need to treat these situations.

4.2 Characteristics of Fracturing Fluids, Additives, and Proppants

A very large variety of propped fracturing fluids and proppant materials are in use to serve the wide range of applications of this powerful technique. There is no typical fracture fluid; however, thickeners

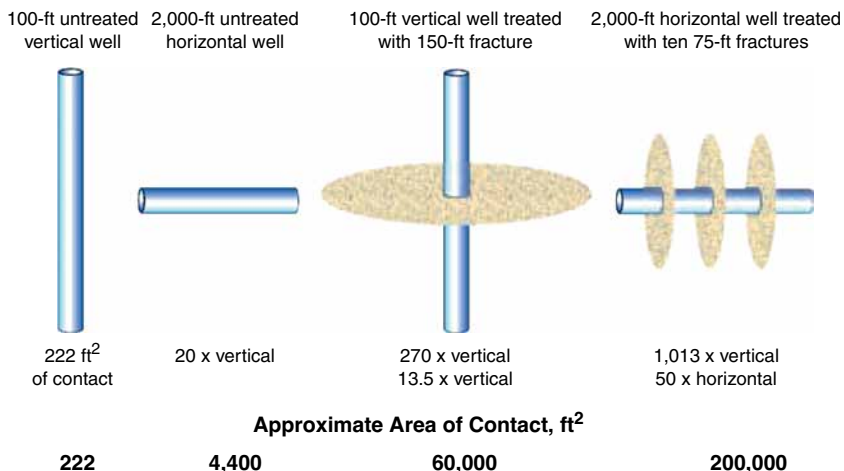
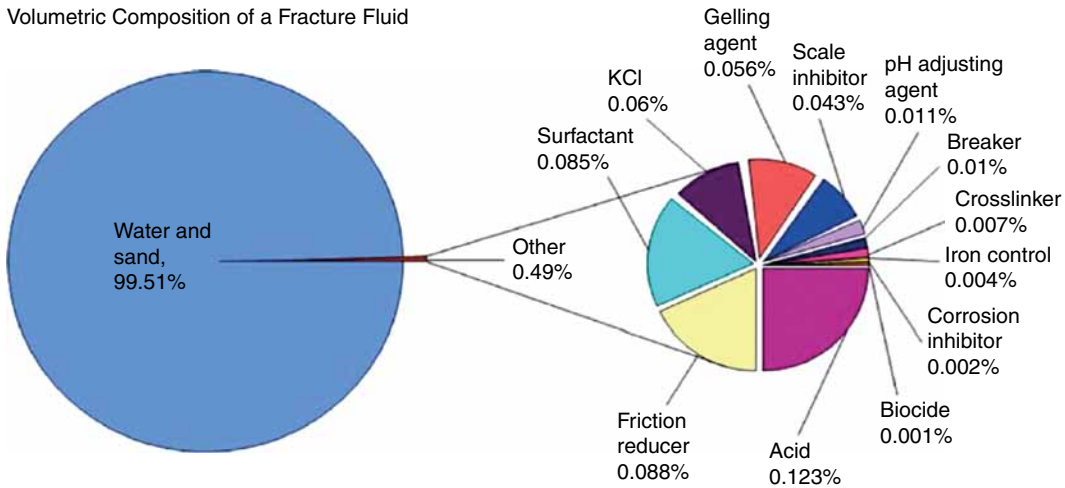


Fig. 4.13—Hydraulic fracturing greatly improves reservoir contact.

Volumetric Composition of a Fracture Fluid



Source: ALL Consulting based on data from a fracture operation in the Fayetteville Shale, 2008

Fig. 4.14—Composition of a proppant-laden fracture fluid for shale (courtesy of ALL Consulting).

as well as a solid proppant usually are present. A list of chemicals for treating some shale plays is in [Fig. 4.14](#). The pie chart estimates the weight % of each component family that may be used in a fracture treatment. In this illustration, most of the fluid is water and sand (proppant). Note that not all of these chemicals are in each phase of the treatment. The chart illustrates the idea that the other chemicals are minor components; however, because as much as 50,000,000 lbm of total fluid may be pumped, the absolute amounts are significant.

The major fluid that supports the proppant placement can be based on water, foam, or gelled hydrocarbons. In some cases (some shale fracs) proppant is not added. This section introduces the chemicals and processes as well as methods for testing frac fluids.

4.2.1 Introduction to Fracture Fluid Chemicals. A review of the important chemistries of frac fluids are in Sections 4.3–4.7 and more details are in Gulbis and Hodge (2001). Methods for fluid selection are considered in Section 4.10, and acid fracturing fluids were described in Section 3.8.

The major categories of the propped frac base fluids are

- *Carbohydrate*-based water-soluble polymers such as guar, modified guar [such as hydroxypropyl guar (HPG)], hydroxyethyl cellulose (HEC), and xanthans. These materials are crosslinked (to increase the viscosity) using metals such as borate, titanium, and zirconium salts. Usually they are broken with oxidizers or enzymes
- *Synthetic polymers* such as partially hydrolyzed polyacrylamides (HPAAs). These materials are usually employed as friction reducers (FRs) but can be crosslinked with metals (for acid diversion—Section 3.7.2, and conformance control—Section 5.7.2) and may be used as the only polymer in SW treatments for fracturing TG formations
- *VES* water-based fluids (see Section 3.7.3 and 4.4.2). These surfactant-containing fluids will become viscous in response to various salts in the fluids (such as KCl) but can be viscosified more effectively in the presence of certain cosurfactants. Because these materials are not polymers, conventional breakers are not used. If needed, certain additives (frequently called VES breakers) are used to improve cleanup
- *Oil-based gels*—These materials represent some of the first fracturing fluids used and consist of gelled aluminum phosphate esters. Slowly dissolving acids or bases are added on the fly to achieve a viscosity reduction. They also break readily at higher temperatures > 150°F
- *Emulsions* of oils in a brine outer phase that are formed using various surfactants
- *Foams* are generally made using a polymer fluid (previously mentioned) by injecting either N₂ or CO₂ in the presence of an appropriate surfactant. They increase proppant suspension and

flowback, and reduce water sensitivity and the liquid volume needed. They can be crosslinked, but the agent must be compatible with the pH

- *Alcohols* including methanol and IPA
- *Carbon dioxide*-based fluids

The major types of *proppants* are (ranked by crush resistance)

- Lightweight proppants (LWPs) including polymers and hollow beads
- Various types and varieties of sand
- Resin-coated proppant (RCP) (usually coated sand)
- Ceramics
- Sintered bauxite
- *Fibers*—added with the proppant to prevent flowback of the solids and to delay proppant settling

There are important materials that are *added* depending on the fluid type, formation, temperature, and friction pressure expected to improve the functioning.

- *Crosslinkers*—The choice of borate, titanate, zirconate, or aluminates for the carbohydrate fluids depends on the pH, base polymer, and the temperature. Various delay agents include coatings, pH controllers, and complexers. Cosurfactants may be added to VES chemicals to also improve the viscosity formation.
- *Stabilizers* such as methanol and thiosulfates (reducing agents) help preserve the carbohydrate polymer viscosity at high temperatures.
- *Buffers and delay agents* are used to control the rate of crosslinking.
- *Breakers* must degrade the polymer chain and enable cleanup to happen. Without them, the frac conductivity would be very low. Major categories of breakers include oxidizers such as persulfates, organic, and inorganic peroxides as well as enzymes. For some fluids, a pH change may improve the break. Many of these chemicals have been encapsulated to control the rate of the reactions. Cleanup agents (aka VES breakers) for VES fluids include unsaturated fatty acids (Crews and Huang 2008) polyols and oxidizing agents (Li et al. 2008a).
- *FRs*—Polyacrylamides or hydrocarbons are added to reduce the friction pressure. They may be the only polymer in some slick-frac fluids.
- *FL agents*—Oil-based resins, silica flower, and dispersions of oils are in use to reduce FL to the formation.
- *Biocides* are critical for use with the polysaccharide polymers. Materials such as glutaraldehyde, chlorophenates, quaternary amines, and isothiazoline are used to control bacteria (Ruseska et al. 1982). Usually the materials kill the bacteria, but they do not always inactivate the enzymes they have produced that are responsible for breaking down the polysaccharides. For this reason, it is common practice to add bactericide to fracture tanks before the water is added to ensure that the bacterial enzyme level is kept low. These materials also help prevent sulfate-reducing bacterias (SRBs) from producing H₂S from the polymer residues in the frac pack.
- *Surfactants and clay stabilizers* also may be added to reduce surface tension, cause foam to form, increase flowback rate, and to protect water-sensitive formations. Some of these types of chemicals are also used in reactive fluids and are described in Section 3.6.

A list of examples of specific types of additives is in **Table 4.1**. This table shows the generic chemical, the use in fracturing, and other common applications for that category of material. Many more details are in Sections 4.4 through 4.7.

While reactive stimulation is a *chemical* method where the formation is partially dissolved, fracturing is primarily a *physical* method of increasing useful permeability. Here, physics rules and the chemistry must support it. Webber (1994) notes that for the stimulation to be successful, the fracturing fluid must possess the number of characteristics that were described by Gidley et al. (1989), which control many of the variables in Eqs. 4.2, 3.37, and 3.42. The characteristics are listed below.

TABLE 4.1—FRACTURING FLUID ADDITIVES, CHEMISTRY, AND COMMON USES

| Additive Type | Typical Main Compound(s) | Purpose in Fracturing | Common Usages Outside Frac Industry |
|---------------------|---|---|--|
| Diluted acid (15%) | Hydrochloric acid (HCl) | Dissolves carbonate rock and clean fracture | Swimming pool chemical and cleaners |
| Biocide | Glutaraldehyde | Kills bacteria in water that may affect frac gels and cause corrosion | Disinfectant used in industry |
| Breaker | Ammonium persulfate | Causes breakdown of polymer gel to allow clean up | Bleaching agent in detergents and household products |
| Corrosion inhibitor | Different amines and quaternary compounds | Prevents corrosion of piping during use of acids | Used in many industrial products |
| Crosslinker | Borate salts | Increase viscosity of frac gel | Laundry detergent and cleaning agents |
| Friction reducer | Polyacrylamide | Reduces friction of flowing fluids | Water treatment and soil conditioner |
| Frac gel | Guar gum or cellulose compounds | Thickens water to support proppant | Cosmetics and various foods |
| Iron control | Citric acid and EDTA | Prevents precipitation of iron compounds | Food and agricultural additives |
| KCl | Potassium chloride | Basic component in brine frac fluid | Low sodium table salt substitute |
| Oxygen scavenger | Ammonium bisulfate | Removes oxygen from water to reduce corrosion and gel degradation | Cosmetics and water treatment |
| pH adjusting agent | Sodium or potassium carbonate | Maintain effectiveness of gels and crosslinkers | Washing soda, detergents |
| Proppant | Silica sand | Allows fracture to remain open after pumping ends | Drinking water filtration, major component in concrete |
| Scale inhibitor | Organic phosphonates | Prevent scale deposits in fractures and pipes | Additive in cleaning agents |
| Surfactants | Anionic and cationic organic compounds | Viscosifying agent and wetting agents | Cleaners and detergents |

Compatible With the Formation Material. Compatibility with the formation material is a very important characteristic. If the chemistry of the fluid causes clay swelling or blocking of pores, then the treatment will be unsuccessful. Similarly, the treatment will fail if the fracturing fluid dissolves the material cementing the grains together. Therefore, a very active chemical mixture must appear to be inert as far as the formation is concerned.

Compatible With the Formation Fluids. If the fracturing fluid causes fines and/or clays to migrate, then the treatment will not be successful. Also, if the fracturing fluid creates emulsions and/or sludging of the crude oil then plugging rather than stimulation will occur (Gidley et al. 1989).

Capable of Suspending Proppants and Transporting Them Deep Into the Fracture. A critically important characteristic of a fracturing fluid is its ability to transport proppant from the surface through the perforations and deep into the fracture.

Capable of Developing the Necessary Fracture Width To Accept Proppants. If the fluid is not sufficiently viscous, then the created fracture width will be too small to allow proppants to be transported far into the fracture. Note that this is somewhat in opposition to being able to pump large volumes because viscosity affects the pressure drop in a pipe.

Have Low FL (Eqs. 3.38 and 4.1). The fracturing fluid must be *efficient*, meaning that the proportion lost to the formation is small. Fluid efficiency is normally achieved by the addition of FL additives (FLAs) to the highly viscous fluid. Common FLAs include plugging agents, bridging agent, and microemulsions (MEs). If most of the fluid leaks off into the formation, then the fluid will be incapable of creating the desired fracture geometry or of transporting the proppant. Note Eq. 4.2.

Easy To Remove From the Fracture. This happens when the treatment is complete (i.e., it should be easy to break and should leave little residue). A fracturing fluid must be capable of changing rapidly from high viscosity to low viscosity once the treatment is complete. This is necessary so that the fluid can be easily *removed* from the formation. The viscosity is normally reduced by thermal degradation, in high-temperature wells, or by controlled fluid degradation. Breaking agents such as enzymes, oxidizers, or weak acids are used in controlled degradation. Much of the most recent technology is involved in the controlled breaking and FL control. Note that even the most efficient breakers will impair the pack permeability, so this impairment must be part of the fracture model.

Have Low-Friction Properties. FRs as well as the choice of the fluid itself will affect the friction pressure, which affects the horsepower needed to pump the job. If the fluid cannot be pumped easily down the tubulars, then it is usually unacceptable as a fracturing fluid.

Retain Its Viscosity Throughout the Treatment. A fracturing fluid should also be capable of retaining its viscosity throughout the treatment. If a fluid loses viscosity because of thermal thinning or shear degradation, then it cannot be used to fracture high-temperature wells.

Easy To Prepare in the Field. Much of the technology developed in the last 15 years has been designed to improve the efficiency of field preparation.

Cost Effective. A fluid that has all of the above qualities but is not *cost effective* may not be acceptable.

Fig. 4.15 shows a cartoon (API 2008) of a frac job setup. In this example, the fluid flows from storage tanks (or is mixed on the fly) to a blender where additional chemicals are added. It is then mixed with proppant and pressurized. There are several ways of accomplishing the pressurization and mixing (see equipment discussion in Section 1.7). The slurry of proppant and fluid enters the wellhead, and then flows down the tubing to the perforations. It enters the initial fractures and propagates the fracture. The pumping stops, the fracture closes. On flowback, the viscosity degrades and the broken fluid returns to the surface for disposal or reuse.

This figure also shows (in red) the *viscosity* requirements as well as the *shear and temperature* conditions that will exist in each section of the treatment. See Fig. 4.16 (Constein et al. 2000) and Fig. 4.17 (Constein et al. 2000) for more quantitative shear and temperature estimates during various stages for one case of a borate-crosslinked HPG fluid. The conditions of the fracture model (Geertsma and de Klerk 1969) (aka KGD) (Section 4.11.2) simulation are in the report cited. The frac fluid chemistry developers see these conditions as both a *challenge* as well as *opportunities* to cause needed chemical reactions to happen in a sequence that enhances the proppant placement, fracture length, and the final

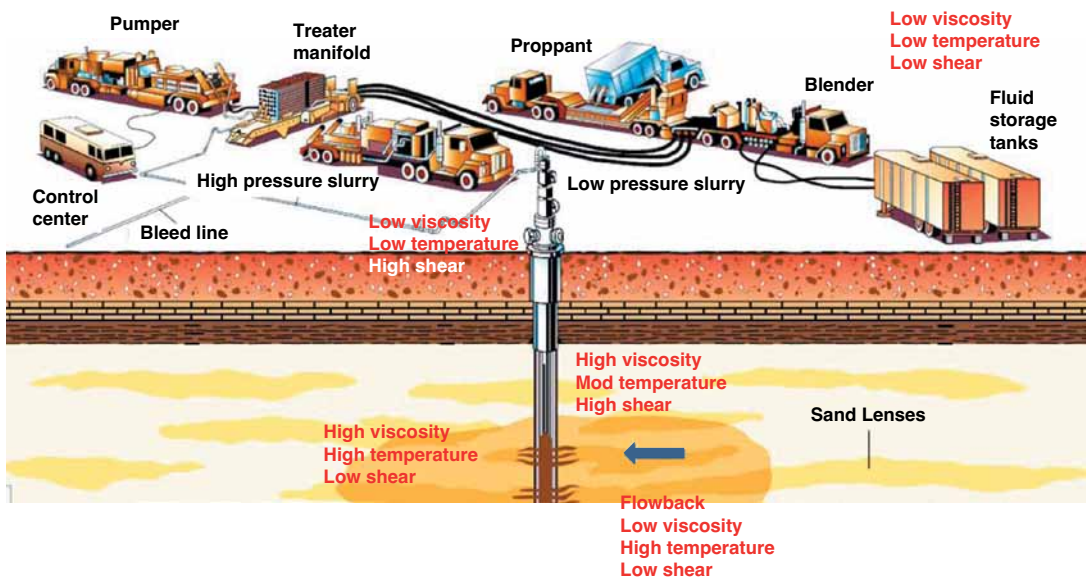


Fig. 4.15—Frac site layout with fluid requirements (after API 2008).

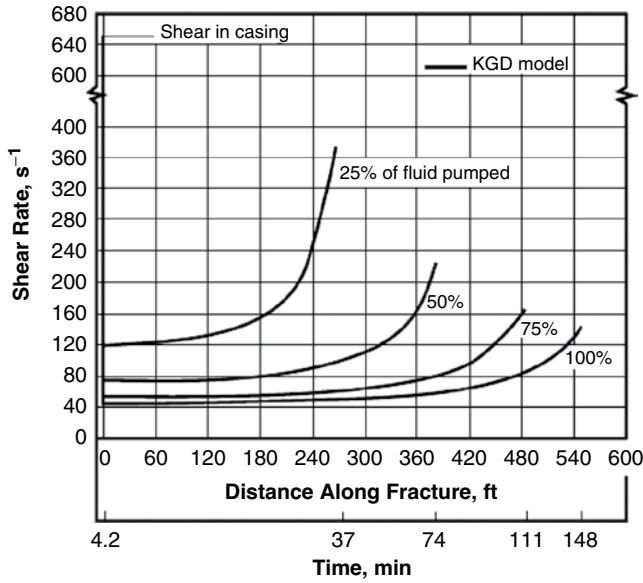


Fig. 4.16—Shear rate in fracture calculated by KGD model (Constein et al. 2000).

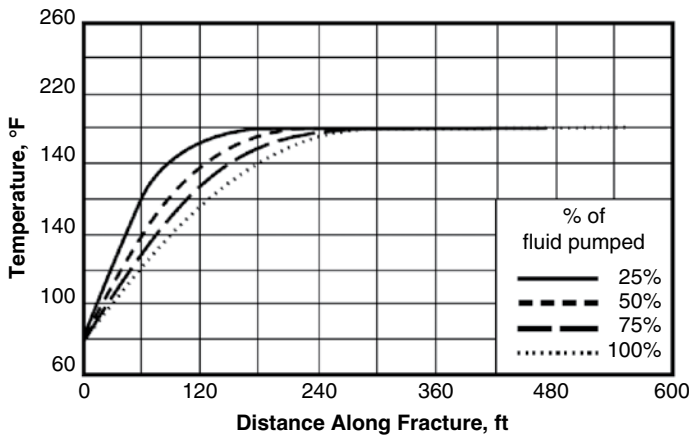


Fig. 4.17—Temperature profile in fracture for 200°F reservoir calculated with the KGD model (Constein et al. 2000).

pack conductivity. The next subsections describe testing of frac fluids as well as the general chemistries that accomplish the tasks in each stage of a treatment. Sections 4.3, 4.4, and 4.5, then, describe additional details of specific fluid chemistry and mechanisms.

4.2.2 Characterization Methods for Fracturing Fluids. To develop frac models that predict the formulations needed as well as the pumping schedules, various tests of potential fluids must be performed. These include base fluid rheology, slurry rheology, FL tests, breaker tests, and fracture conductivity. Basic information is provided in this text, while more detailed information is in Gulbis and Hodge (2001) and Constein et al. (2000). These authors suggest that whatever fluid system is used, a set of data describing the fluid rheology, FL, pipe friction, fracture conductivity, and possible formation damage should be determined before the fluid system is used in field operations.

Base Fluid Rheology. An introduction to viscosity and rheological testing was given in Section 1.5.3. Also see Figs. 1.25, 1.27, and 1.28, as well as Eqs. 1.44, 1.47, and 1.48.

Constein et al. (2000) note that fracturing-fluid rheology data are usually determined under laminar flow conditions in a rotational concentric cylinder viscometer (Fig. 1.25) and reported in terms of the power-law parameters n and K . However, K is dependent on the flow geometry for concentric cylinder devices and is referred to as the viscometer consistency index K_v . For a power-law fluid, the shear rate depends on the value of n in addition to the flow rate and conduit dimension. As a result, determination of the shear rate (Eq. 1.44) is coupled to the determination of n from the flow data. Tests also are performed using a reciprocating capillary viscometer, seen as Fig. 4.18. In this equipment, the rheology is studied by measuring the ΔP across a stainless steel tube where the viscosity can be measured using a flow relationship such as Eq. 1.16. Because the fluid will encounter a range of shear and temperature conditions, the *shear history* is important for characterizing polymer-based fluids. Crosslinked fracturing fluids fall into two distinct categories: gels with reversible crosslinks and gels with irreversible crosslinks. Both types of gels may look equally solid or liquid in bulk, but the reversibility of the crosslink sites make profound differences between the flow properties and microstructures of the gels. Fig. 4.19 shows equipment designed to test the effects of shear and time at temperature on the fluid. Note that this equipment incorporates a reciprocating capillary viscometer to determine the viscosity before and after shear.

This technique maintains the fluid under flowing conditions from the time the crosslinker is added until the test is complete. The test procedure subjects the fluid to a high-shear environment to simulate flow down the tubing or casing followed by a reduced shear rate and increased temperature to simulate fracture conditions. A crosslinker is continuously metered into the fluid at the start of the high-shear conditioning. The equipment for conducting the experiment varies from small laboratory devices to large coiled-tubing devices connected to slot-flow viscometers.

Slurry Rheology and Friction Pressure. While the rheology of the base fluids can be determined with the devices described previously, the rheology of fluids that contain proppants requires large slot-flow devices, wiped disk concentric viscometers, and wide-gap concentric viscometers. Using devices such as these, Gardner and Eikerts (1982) found that the apparent viscosity was increased 2.3–2.7 times the base viscosity of a crosslinked polymer (with 6 lbm/gal-ppg sand) depending on the shear

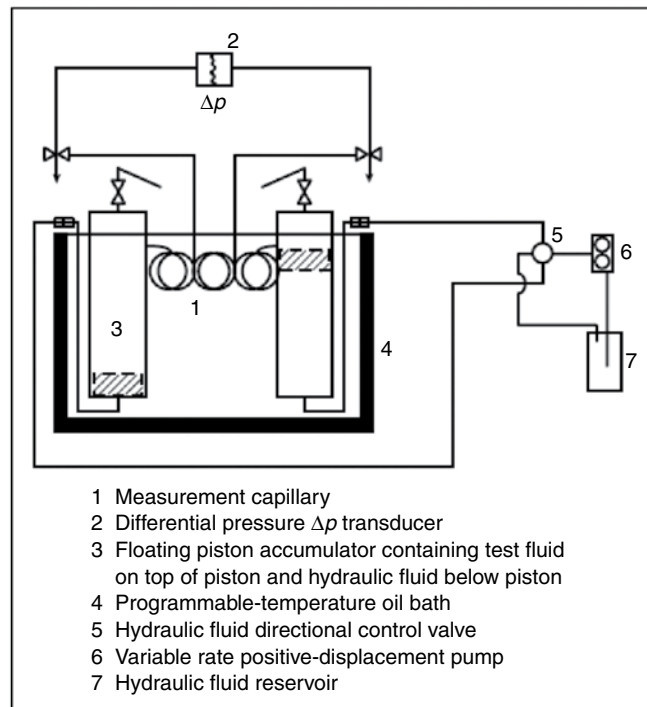


Fig. 4.18—Reciprocating capillary viscometer (Constein et al. 2000).

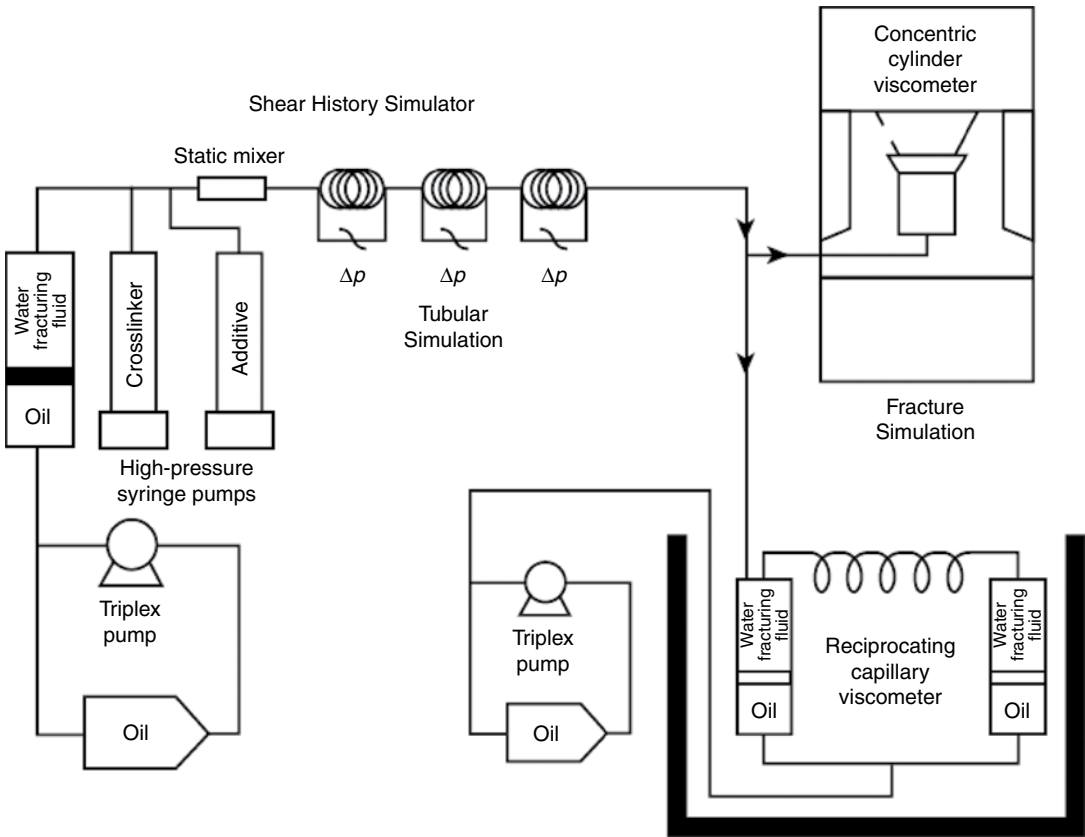


Fig. 4.19—Shear history simulator with RCV (Constein et al. 2001).

rate. The additional viscosity affects the pressure drop in the tubing during pumping of the slurry, as well as in the fracture.

For Newtonian fluids, the pressure drop in a pipe is given by

$$\Delta P = \frac{2L}{D} \cdot f \rho u^2 \dots \dots \dots (4.5)$$

Here, L is the length of the pipe, D is the pipe diameter, ρ is the fluid density, f is the friction factor, and u is the average fluid velocity. This is defined as $u = 4q / (\pi D^2)$, where q is the volumetric flow rate. For laminar flow, the friction factor is defined as $f = 16/Re$, where Re is the Reynolds number. For turbulent flow in a smooth pipe, $f = 0.079/Re^{0.25}$. Note that the definition of the Reynolds number is

$$Re = \frac{\rho u D}{\mu}, \dots \dots \dots (4.6)$$

where μ is the fluid viscosity. Note from Eq. 4.5 and the discussion in the subsequent paragraph that going from laminar flow to turbulent flow at the same Re increases the pressure drop by as much as 40%.

The friction factor and, thus, the pressure drop because of it is much more difficult to calculate for power-law (and other non-Newtonian) fluids. Shah and Lee (1986) studied the relation of friction pressure to proppant concentration and size in four different HPG base fluids in different pipe sizes and correlated the laboratory predictions with field measurements. The study illustrates the complexity of characterizing slurry rheology. The friction pressure of fluids containing proppant was found to increase with increasing proppant concentration. The predicted amount of friction pressure increase

diminished with turbulent flow rates (e.g., >12 bbl/min). A relation for the increase in friction pressure in turbulent flow resulting from the presence of proppant is

$$\Delta p_{\text{friction}} = (\mu_r)^m (\rho_r)^{(1-m)}, \dots \dots \dots (4.7)$$

where $\Delta p_{\text{friction}}$ is the friction pressure ratio with and without solids, μ_r is the ratio of the apparent slurry viscosity to the apparent fluid viscosity, ρ_r is the ratio of the slurry density to the fluid density, and m is the log-log slope of the friction plotted vs. the Reynolds number. The effect of sand concentration on 40 lbm HPG/1,000 gal fluid at various flow rates is seen in Fig. 4.20 in which the friction pressure increases by a factor of about 4 from 2–8 lbm/gal of sand.

Kamel and Shah (2008) studied a VES, Aromox APA-T (more details of VES fluids are in Section 4.4.2), using a full-scale flow loop that consisted of a 50 bbl fluid mixing tank; a centrifugal feeder pump is used to feed the Triplex pump that is used to pump the fluid. It can deliver fluid at 200 gal/min at 5000 psi. A 200-ft straight test section of flow conduit is in the system. Using this method, they studied the rheological behavior in a straight pipe, found surfactant-based fluids exhibit a significant degree of drag reduction, and drag reduction increases with concentration. They showed better drag reduction than conventional polymers (Keck et al. 1992). Also see the discussion by Cipolla et al. (2010) of the effect of proppant in different scenarios.

Proppant Transport. Constein et al. (2000) note that most of the experimental studies to characterize proppant-transport properties use one or more of the following three approaches:

- Measuring the rheological properties of clean fluid and using these as the basis for predicting the transport properties.
- Measuring proppant-settling velocities in stagnant fluids.
- Observing proppant transport in slot-flow devices, flow loops, or concentric cylinder devices.

Particle settling velocities have been measured in a variety of experimental devices. Babcock et al. (1967) studied the flow and deposition of sand slurries in a vertical slot-flow model. Schols

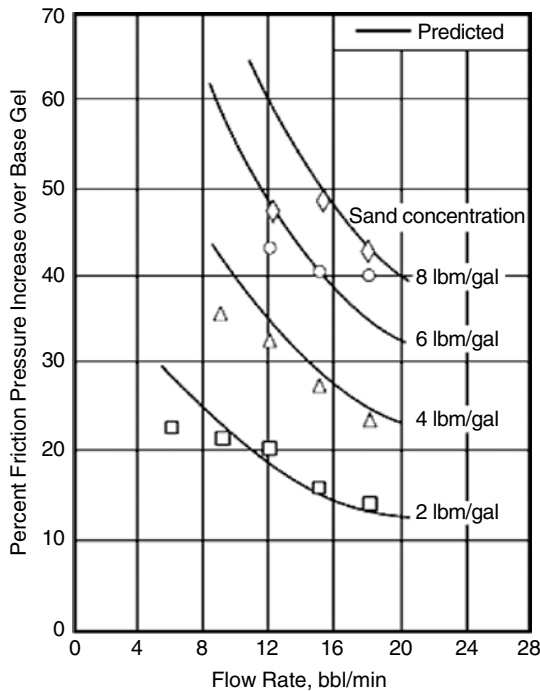


Fig. 4.20—Effect of sand concentration on 40 lb HPG/1,000 gal fluid friction pressures at various flow rates (Constein et al. 2000).

and Visser (1974) also used a vertical slot-flow model to develop equations for both the height and length of deposition beds. See the detailed discussion in Constein et al. (2000). This author notes that when using appropriate drag coefficients, described by Acharya (1986), and Meyer (1986), proppant-settling rates can be predicted from rheological measurements. They also note that the more generalized power-law equation (Eq. 1.47) should be used instead of Eq. 1.44.

Proppant settling is described by Stokes law:

$$V = \frac{(2gr^2)(d_1 - d_2)}{9\mu}, \dots\dots\dots (4.8)$$

where V is the particle velocity (cm/s), g is the acceleration caused by gravity (cm/s²), r is the equivalent particle radius (cm), d_1 is the particle density (g/cm³), d_2 is the fluid density, and μ is the viscosity (dyne-s/cm²).

Bivins et al. (2005) point out that fluid viscosity in the fracture is a complex balance. As fluid viscosity increases, fracture height also increases, and this may cause the fracture to extend outside of the pay zone (see Fig. 4.21). However, the proppant settling rate also may be affected by the viscosity. Low viscosity or low flow rates may cause proppant drop out before completion of the treatment (Fig. 4.22). Proppant settling may result in the entire pack being at the bottom of the fracture before the fracture closes. Proppant settling can be reduced by higher viscosity (more polymer or crosslinks), but there is a cost to this approach. More details of the effect of fluid chemistry on proppant transport are described in Section 4.4.3.

FL. FL is very important to fluid efficiency. See Eq. 4.2. Depending on the formation and the type of fluid and the additives, FL is controlled by compressibility, viscosity, and/or filter-cake building. This control mechanism is most effective when the reservoir fluids have high viscosities and are not greatly

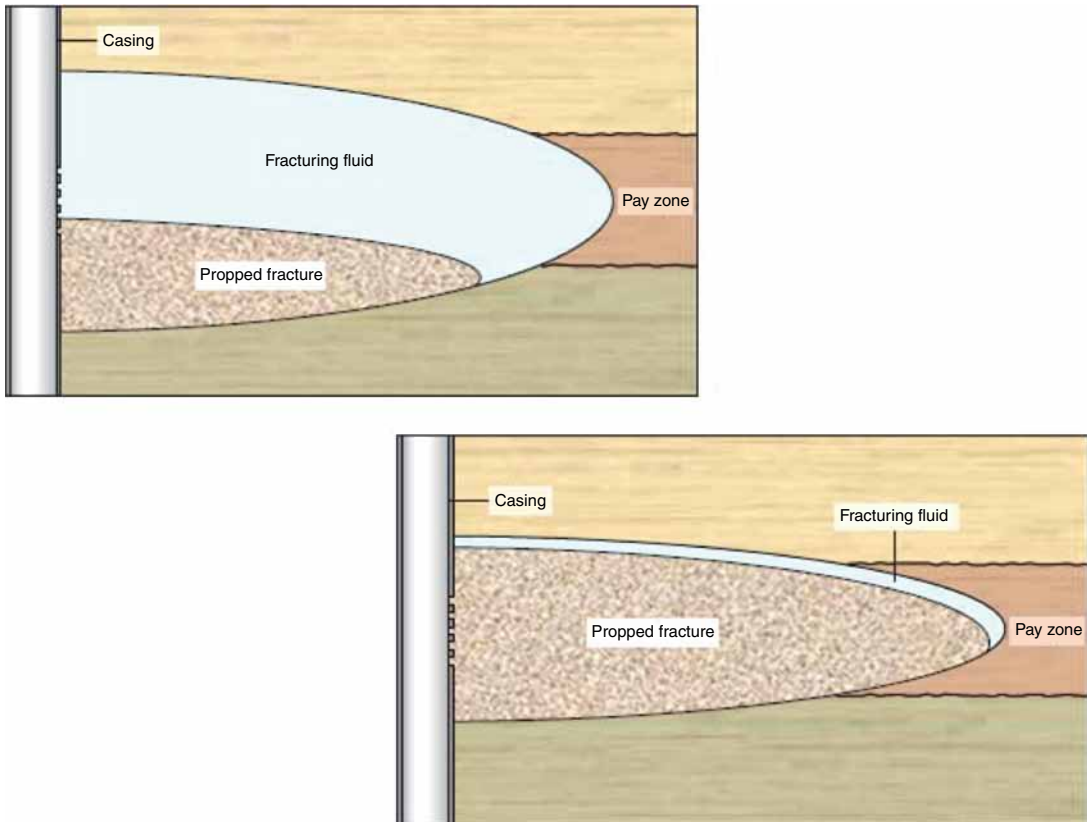


Fig. 4.21—Effect of viscosity on frac geometry (Bivins et al. 2005).

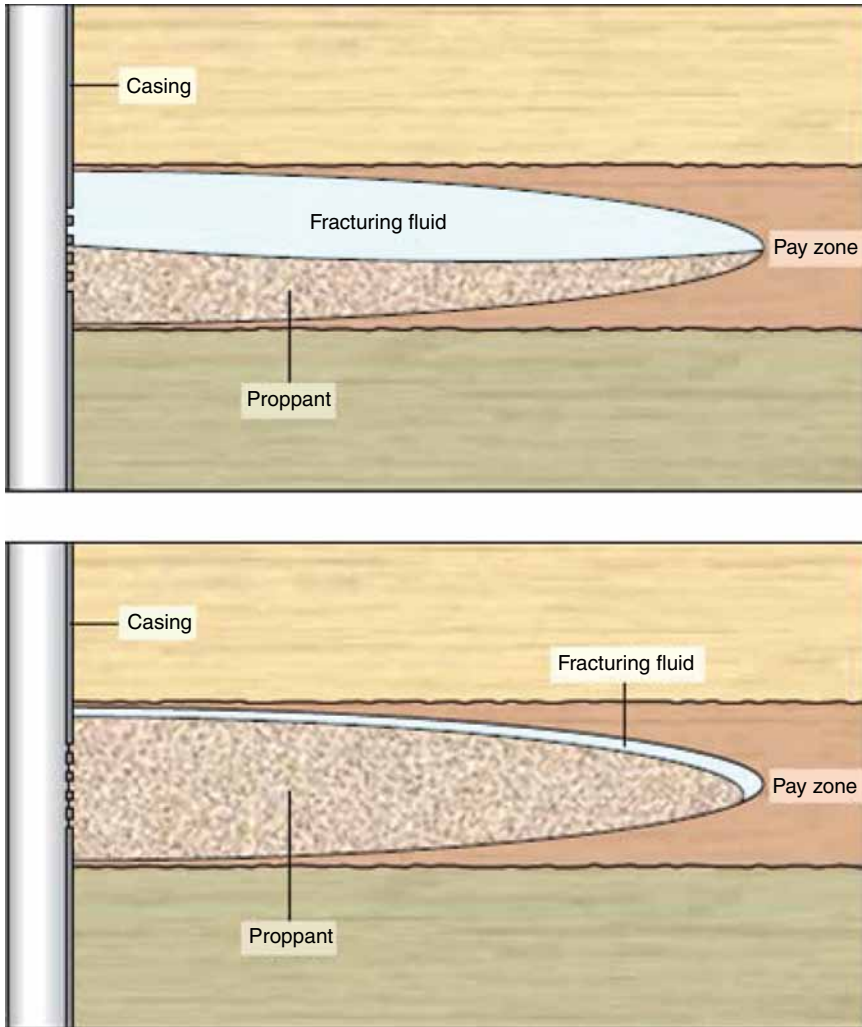


Fig. 4.22—Effect of proppant settling velocities (Bivins et al. 2005).

compressible (e.g., heavy oil). The reservoir-controlled (or compressibility-controlled) FL coefficient (C_c) is calculated as follows (Constein et al. 2000):

$$C_c = 0.00118 \Delta p_i \sqrt{\frac{\kappa_r \phi c_r}{\mu_r}}, \dots \dots \dots (4.9)$$

where k_r is the reservoir permeability, c_r the compressibility of the reservoir in psi^{-1} , and μ_r is the viscosity of the reservoir fluid in cp.

Constein et al. (2000) note that filtrate viscosity and relative permeability can control FL when their ratio is greater than that for the reservoir fluid. The filtrate-controlled (or viscosity-controlled) FL coefficient (C_v) in $\text{ft}/\text{min}^{1/2}$ is described by

$$C_v = 0.0469 \sqrt{\frac{\kappa_{fi} \Delta p_i \phi}{\mu_{fi}}}, \dots \dots \dots (4.10)$$

where k_{fi} is the filtrate permeability in md into the saturated reservoir, Δp_i is the total differential pressure between the fluid in the fracture and the initial reservoir pressure in psi, ϕ is the formation porosity

(fraction), and μ_{fi} is the apparent viscosity in cp of the filtrate flowing into the formation. The filtrate control mechanism is most likely in effect when a gas reservoir is fractured with a nonwall-building, high-viscosity fluid or for a formation at irreducible water saturation.

Because it is possible for both filtrate and reservoir effects to be factors in controlling FL, it is common practice [according to Constein et al. (2000)] to combine the two coefficients:

$$C_{cv} = \frac{2C_v C_c}{C_v + (C_v^2 + 4C_c^2)^{1/2}} \dots \dots \dots (4.11)$$

For many polymer fluids, especially those with added FLAs, filter-cake wall building is the major mechanism for control/loss of the fluids. Static FL tests are run using equipment such as seen in Fig. 4.23.

Constein et al. (2000) describe the process for testing wall-building fluids. Static FL for fracturing fluids are tested using the methods of Howard and Fast (1970). A simple schematic of a static FL test is shown in Fig. 4.23a. In static FL tests, fluid is heated to the test temperature, a differential pressure is applied across the core (usually 1000 psi), and the rate of filtrate volume forced through the core is measured vs. time. For wall-building fluids, the filter cake continues to grow with time and the FL rate decreases. For an ideal wall-building fluid, a plot of the filtrate volume vs. the square root of time results in a straight line. The slope of the straight line is used to calculate the wall-building coefficient C_w , and the intercept is used to calculate the spurt loss S_p .

The value of C_w is directly proportional to the leakoff velocity through the established filter cake. The *spurt* value represents the fluid that leaks off *during* the formation of an effective filter cake.

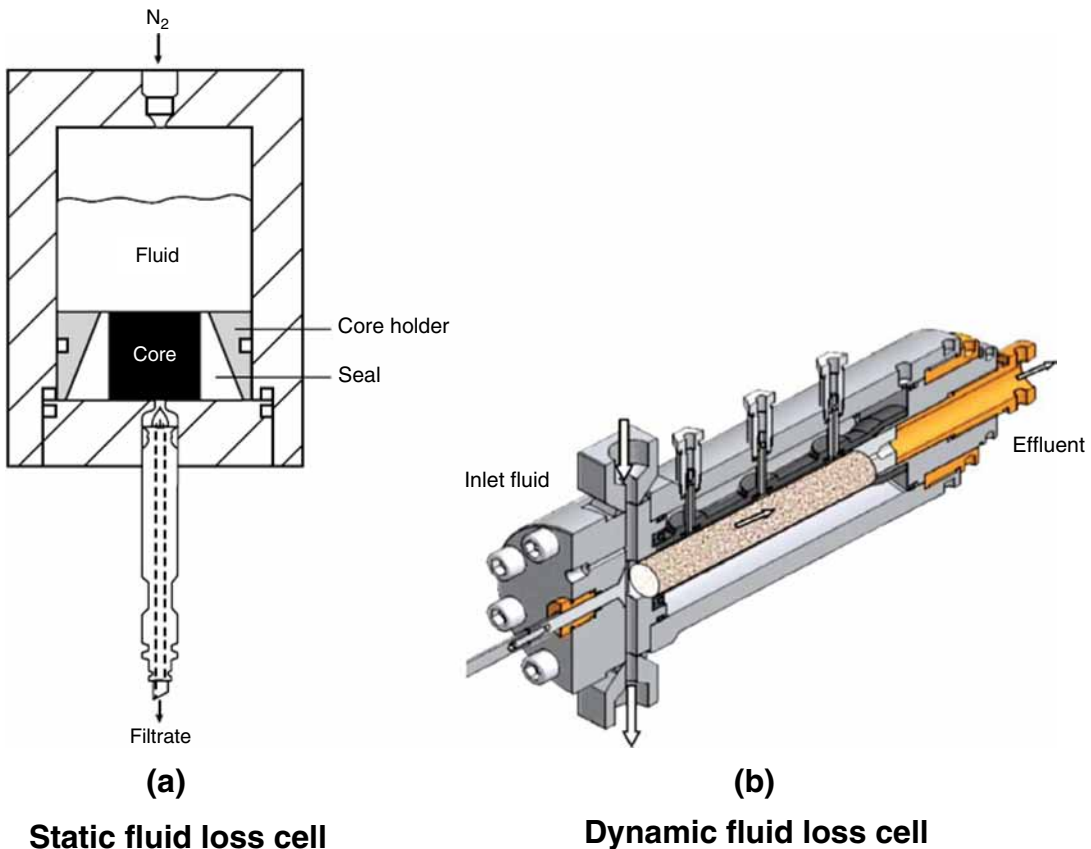


Fig. 4.23—(a) Static fluid loss cell (Constein et al. 2000) and (b) dynamic fluid loss cell.

By using the intercept to calculate spurt, the assumption is made that the filter cake is instantaneously established. However, because a finite time or volume is required for an effective filter cake to form, calculated values of spurt only approximate the FL behavior during filter-cake formation. C_w is calculated in ft-min^{1/2} as

$$C_w = \frac{0.0164 m}{A}, \dots \dots \dots (4.12)$$

where m is the slope of the leakoff plot in ml/ft-min^{1/2} and A is the area in cm² of core exposed to fluid. The authors of this report (Constein et al. 2000) then note that from the y -axis intercept b , the spurt value is determined in gal/100 ft². The spurt loss (S_p) is

$$S_p = \frac{24.4b}{A}. \dots \dots \dots (4.13)$$

Ribeiro and Sharma (2012) describe a dynamic FL cell (Fig. 4.23b) that has been used for testing foamed fluids. In this equipment, the fluid flows through a 1-ft core (either sandstone or carbonate) and leakoff can be measured at several points along the core.

Armstrong et al. (1995) describe tests using dynamic FL methods and claim that the dynamic FL method described produces more accurate results; however, the equipment and testing is much more expensive than the static method.

Fracture Conductivity. The dimensional fracture conductivity (C_D) is defined by Eq. 3.37 as fracture permeability (κ) \times fracture width (w). Thus, determining the fracture pack permeability (κ) is the critical laboratory process. The equipment is similar to that described in Section 3.8.1. The method of Brannon and Pulsinelli (1990) and Gulbis et al. (1992) is described. An API cell, modified for flow injection and leakoff is used with a hydraulic press as seen in Fig. 4.24. The system allows for precise closure pressure as well as for heating the fluids and leakoff control. Thus, tests with and without

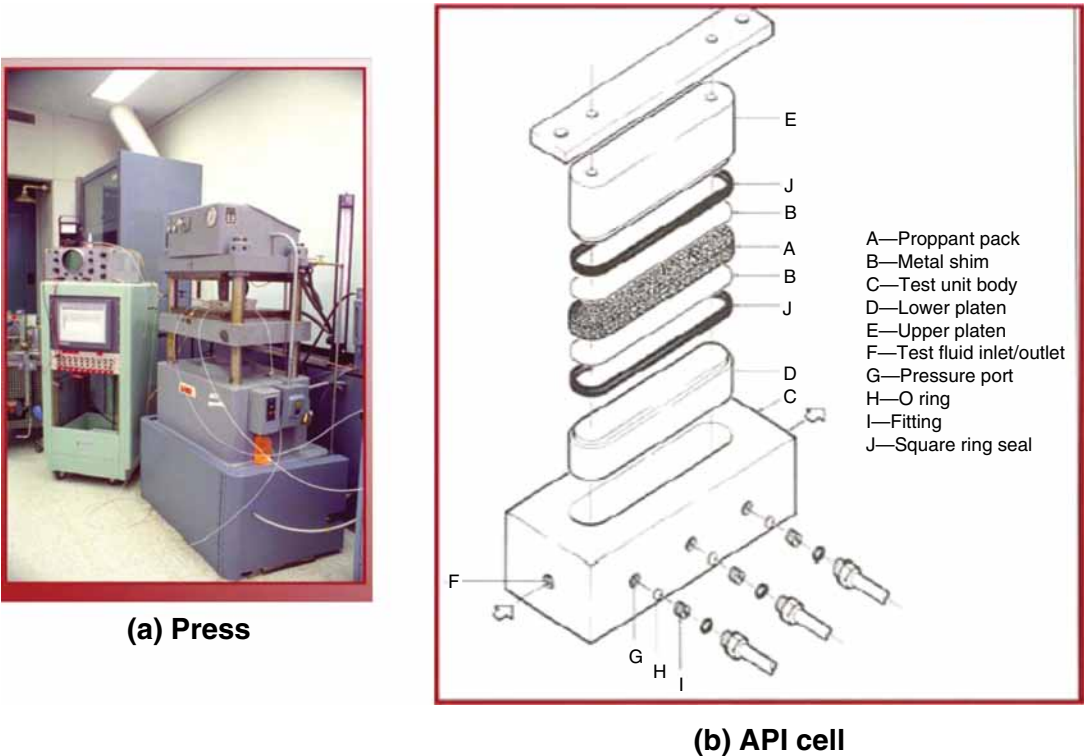


Fig. 4.24—API conductivity cell (a) is the assembled press and (b) is the breakdown of the cell.

leakoff are possible. Pressure transducers are used to determine the Δp across the pack. A sand/proppant pack is assembled and a fracturing fluid to be tested is carefully added (without disturbing the sand pack). The cell is assembled and carefully closed and heat up is started. If a leakoff is desired, 500 psi is added to cause leakoff (and concentration of the polymer if desired). Various tests are possible, but at the end, a cleanup fluid is passed through the pack until the Δp is stable. Then, permeability, κ , is determined using Darcy's law (Eq. 1.2). Note that this is similar to the equipment used to determine acid frac conductivity (Section 3.8.2).

A very comprehensive compilation of rheological test methods is provided by USDOE (2000) that details the development and use of a high-pressure fracture simulator.

4.3 Introduction to Fracture Fluid/Proppant Chemistry Using HPG as an Example

The next four sections (4.3.1–4.3.4) will introduce the chemistry that is used in each stage during a fracture treatment. This initial example will use a HPG-based aqueous fluid, which is crosslinked using a delayed borate. The proppant is silica sand. The fluid also contains an encapsulated ammonium persulfate breaker and silica flower as a FLA. The bottomhole static temperature (BHST) is 180°F and the formation is sandstone with 10% clays and 5% calcite with an initial permeability of 20 md. This type of fluid has been chosen as a base case because significant research has been performed on it, and this type of fluid has been used in thousands of treatments over more than 30 years (opinion of the authors of this book).

In Sections 4.4–4.7, various *additional* fluids will be described and more detailed mechanism will be discussed, and the HPG case will be used as a comparison. The working conditions in this example are keyed to Fig. 4.15. More details of the chemistry of guar and guar derivatives are in Section 4.4.1.

4.3.1 Preparation and Mixing of the Fluids and Proppants. Working conditions: ambient temperature on surface can be very cold to 140°F. There is relatively low shear (from the mixers). The viscosity is produced from both the polymers and added proppant.

In this example, the linear gel is made up of HPG (Fig. 4.25 shows a monomer unit) dissolved in a KCl brine. This type of polymer will have mw values of $1\text{--}2.5 \times 10^6$ daltons (based on the measurement method and source). The KCl is a clay stabilizer (see Sections 3.6.4 and 4.7.4). The mix water has been analyzed and is free of species that may affect the formation or the fluid performance.

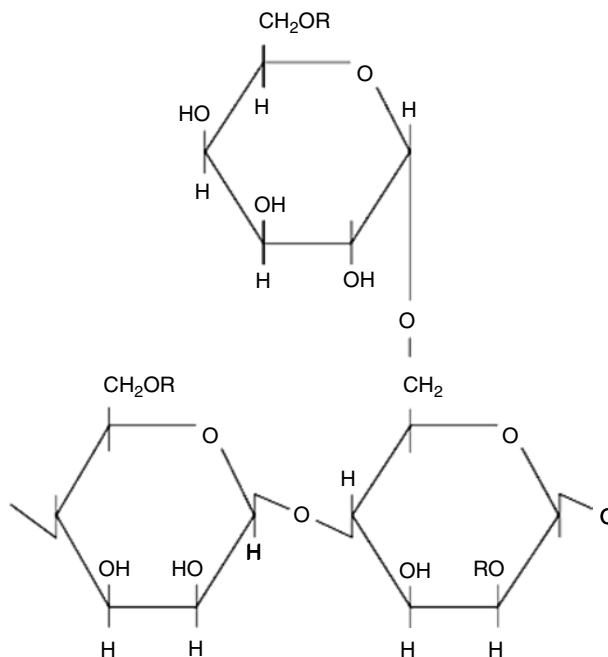


Fig. 4.25—Drawing of the HPG monomer unit: $R = \text{CH}_2 - \text{CH}(\text{OH}) - \text{CH}_3$.

A boric acid crosslinker will be used and an encapsulated ammonium peroxydisulfate (APS) breaker also must be added. HPG is a derivative guar (a polysaccharide with a mannose backbone and galactose substituents). Because guar is a natural product, derived from a bean that grows in Asia, the exact composition will vary. The hydroxypropyl groups provide addition stability at higher temperatures, and because it is the result of a chemical reaction (with propylene oxide), the base material has been cleaned and subjected to quality control. The guar polymer has a high affinity for water. When the powder is added to water, the guar particles swell and hydrate, which means the polymer molecules become associated with many water molecules and unfold and extend out into the solution. The guar solution on the molecular level can be pictured as bloated strands suspended in water. The strands tend to overlap (at a concentration called C^*) and hinder motion, which increases the viscosity of the solution.

One method that has been used on the surface is to prepare the base gel solution before a job by adding the polymer powder to a circulating stream of water and the salts, allowing them to hydrate until the polymer is dissolved, and the initial viscosity of the linear fluid is attained. Because these are large molecules, full hydration is difficult to attain and lumps of polymers can form (called fish-eyes). This prehydration requires a crew to arrive early and prepare the gel in the large frac tanks (Fig. 4.8). Hydration is slower in cold water and in warm conditions; the attack by bacteria is increased. Biocides are usually added to any guar-based fluid. If the job is postponed, a whole batch can be lost. In addition, a fraction of the frac tank always is unusable.

An improved method is to hydrate the polymers at the time of pumping using a slurry or a solution of a concentrated polymer. Diesel fuel has been frequently used in lieu of water to dissolve the guar powder because its carrying capacity per unit volume is much higher. Diesel does not enhance the efficiency of the fracturing fluid; it is merely a component of the delivery system. Using a diesel slurry (or solution) instead of just water minimizes the number of transport vehicles needed to carry the liquid gel to the site. Brannon (1988) claimed a hydrophobic solvent (diesel), a suspending agent such as organophillic clay, a surfactant (nonylphenol ethylene oxide or sorbitan monooleate) and HPG.

Other greener hydrocarbon fluids also can be used to make a concentrated polymer solution. Harris Jr. (1999) claims a mixture of carbohydrate polymers and polyethylene glycol as a liquid delivery fluid. Nondiesel hydrocarbon fluids such as a white mineral oil also can be employed (observation of the authors of this book).

Using these fluids, direct on-site liquid mixing equipment (see Schlumberger 2004a) can be used. Brown et al. (2000) note that to ensure that a continuous-mix operation goes smoothly, several requirements must be observed. The polymers should be of a liquid or a slurried variety to ensure that they can be added at precise concentrations. They claim that these polymers produce an improved, quicker hydration, especially when mixed with process-controlled equipment. Specialized mixing and hydration units provide the metering capabilities, proper shear environment, and sufficient residence time for proper hydration. The hydration process is related to time and shear, and this has proven to be extremely important for continuous-mix treatments. If the base fluid has not progressed sufficiently in the hydration process before the fluid is crosslinked, the fluid may experience stability problems. Other solid and liquid additives such as crosslinkers and breakers must be added as the fluid is mixed with the proppant.

Process-controlled proppant blenders use computers to meter precise proppant-to-fluid ratios throughout the treatment. This precision-blending capability is perfect for ramping proppant, which is considered the ideal for optimum proppant placement. The blenders accurately mix and meter proppant, dry additives, liquid additives, and fracturing fluid together at a specified density in a pre-programmed, automatic mode. The proppant concentration can be precisely and safely controlled at concentrations higher than 22 lbm/gal added for sand or 32 lbm/gal added for high-strength proppant. The overall proppant/liquid ratio is constantly monitored and controlled in a range of $\pm 0.5\%$ according to Brown et al. (2000).

4.3.2 Pumping Through the Tubing. Working conditions: High shear, low temperature to high temperature, delayed crosslinking, moderate to high viscosity and friction pressure.

The linear gel containing a boric acid (H_3BO_3) crosslinker, delaying chemicals, an encapsulated breaker, sand, and a FL agent (and other additives described in Section 4.7) is being pumped into the formation through several thousand feet of steel tubing. In this example, the temperature at the surface is approximately 60°F, and the bottomhole standard temperature (BHST) is 180°F. The flow is in the turbulent regime and the shear rates are high. To avoid excessively high-friction pressures (Pandey 2001) (that is pressure drops) and possible degradation (shear) of the polymer, the action of the borate has been delayed so that crosslinking is achieved as the fluid approaches the perforations. An HPAAs polymer also could be added as an additional FR.

Fig. 4.26 shows a proposed (Menjivar 1986) mechanism of crosslinking that includes the $B(OH)_4^-$ ion complexing with hydroxyl groups on two of the guar molecules, thus, increasing the effective molecular size and the viscosity. The borate anion is generated by the hydrolysis of boric acid or sodium borate ($Na_2B_4O_7$) and requires a high pH (>10) to be effective. Fig. 4.26a shows the initial complex with the borate, and Fig. 4.26b shows a link to another guar molecule.

The borate ion is generated at high pH (about 10.0) (Fig. 4.27), so one possible delay method is to add a species that generates hydroxyl ions slowly. Using MgO as the base source will affect a delay because it is sparingly soluble in water (86 mg/L at 65°F). Additional delay at high temperature can be achieved by adding materials that compete with the guar for the borate ion.

These types of materials include the polyols (such as ethylene glycol or sodium gluconate) (Nelson et al. 1995). Some amount of delay is also achieved by encapsulating the boric acid in polymers such

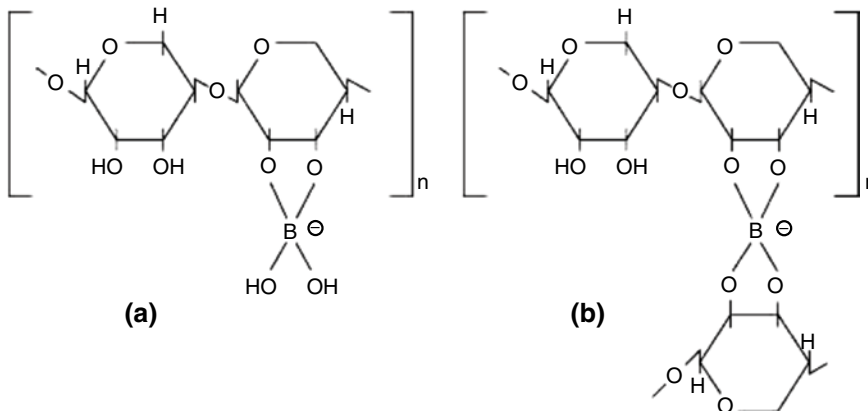
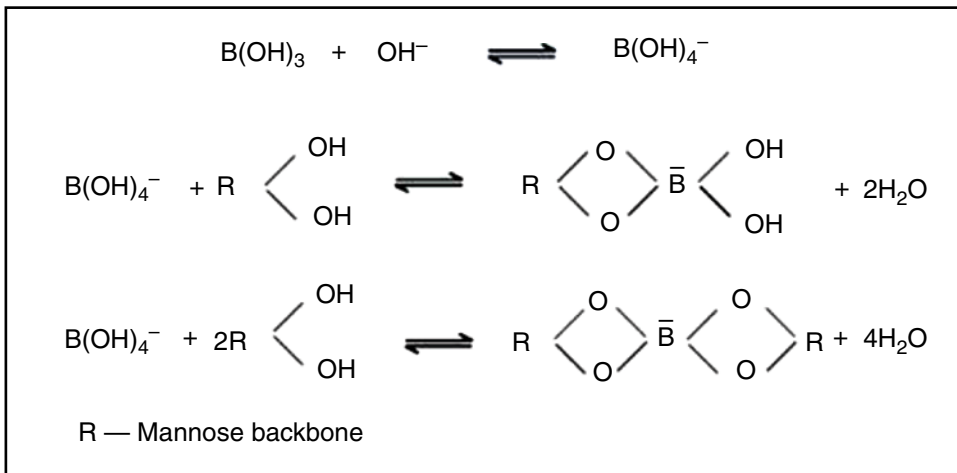


Fig. 4.26—Proposed borate crosslinking mechanism show the initial complex and crosslink forming (Gulbis and Hodge 2001).

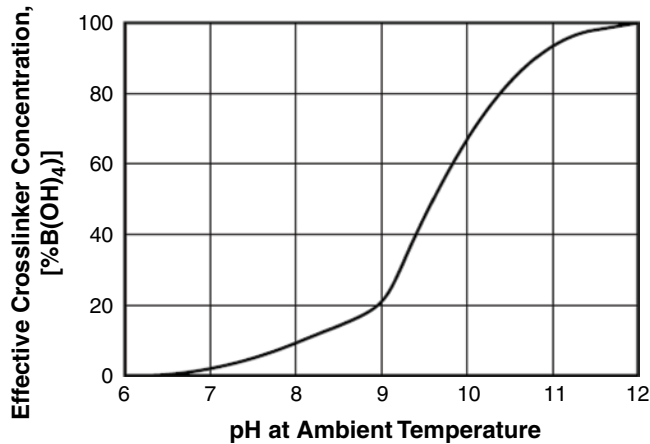


Fig. 4.27—Borate ion concentration as function of pH (Gulbis and Hodge 2001).

as Ethocel. However, a patent by Nelson et al. (1995) shows that addition of the polyol (sodium gluconate) much improves the maintenance of viscosity at 300°F by delaying the crosslink process. This has been shown to improve the strength of the gel. More details are in Section 4.4.1.

4.3.3 Propagation of the Fracture. Conditions: Moderate to high shear, formation temperatures, and maximum viscosity. This is one of the most important stages where the proper fracture height (h_f) and half-length (x_f) required by the frac plan/model is achieved.

As the fluid containing proppants enter the fracture, the combination of proper viscosity and flow rate must propagate the fracture as far as possible in the zone of interest and still support the proppant. FL also must be controlled, or the fracture may screen out too soon to achieve the required fracture length. Also, see the discussion in Section 4.2.2, 4.6.1, and Figs. 4.21 and 4.22.

Card et al. (1994), and Card et al. (1995) have proposed the addition of fibers to control proppant settling as well as flowback, and that application will be described in the next section. Many different types of fibers are in use, with the major criterion of being stable and nondamaging in the proppant slurry and pack (Card et al. 2001; Card et al. 1994). According to Bivins et al. (2005), the fibers are claimed to be effective and allow lower-viscosity fluids to be employed because they disrupt the settling process by forming a network in the fluid. They claim that conventional fracturing fluids proppant slurries settle in accordance with Stokes' law (Eq. 4.6), while the proppant slurries with the fibers of correct length display Kynch (Tiler 1981) settling behavior. This is illustrated by the example seen as Fig. 4.28 that shows fluids with proppants with and without fibers.

Additives, as well as the fluid itself must provide control of loss of the liquid to the formation. This is one of the major variables that control the material balance and, thus, the efficiency of the treatment. Based on Eqs. 4.9–4.13, Gulbis and Hodge (2001) describe leakoff into the rock matrix of the fluid as it enters the pore spaces of the rock. They note that some polymers, such as guar and HPG, are filtered out on the surface of low-permeability rocks. Fluids containing these polymers are called wall-building fluids because of the layer of polymer and particulates that builds up on the rock (Fig. 4.29).

Smith and Shlyapobersky (2001) claim that for fluid to leak off from the fracture fluid, the reservoir fluid must be displaced. This sets up some resistance to FL, and this reservoir effect is characterized by the compressibility coefficient C_c . The parameter for this calculation is governed by a pressure difference p between the pressure inside the fracture (i.e., closure pressure + p_{net}) and the reservoir pressure, permeability to the movable formation fluid k , total system compressibility for the reservoir ct , and the viscosity of the reservoir fluid (gas or oil) μ . This parameter is claimed by the authors of the report to be more important for a liquid-saturated reservoir (low compressibility and relatively high reservoir fluid viscosity) and when a filter cake does not develop. Each of these three mechanisms provides some resistance to FL, and all three act as resistors in series (although the fluid-loss coefficient itself is defined in terms of conductance or the inverse of resistance). The three mechanisms variously combine

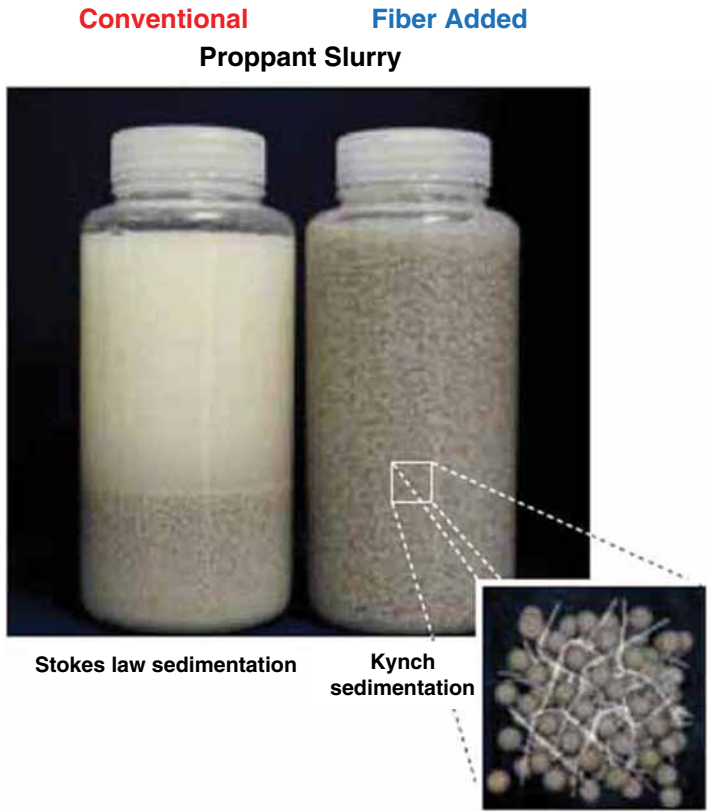


Fig. 4.28—Stokes' law and Kynch sedimentation of proppant slurries (Bivins et al. 2005).

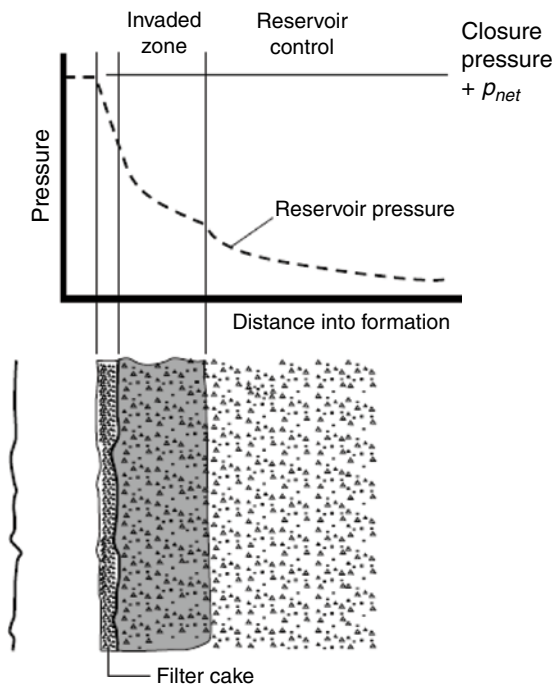


Fig. 4.29—Three zones of fluid loss (Smith and Shlyapobersky 2001).

in different situations to form the total or combined FL coefficient C_L , which is used for fracture design (see Section 4.11).

The filter cake is generally much less permeable than the formation. If the fluid contains particulates of the proper size, these particulates tend to plug the pore spaces and enhance the formation of filter cake. The fluid volume lost before an effective cake forms is called spurt loss (see Eq. 4.13) and can cause a large loss of fluid. Pore-size distribution for the rock matrix varies from formation to formation. Generally, lower-permeability formations have smaller pore openings.

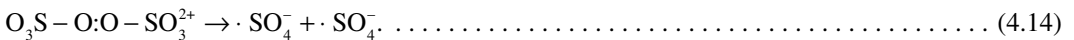
A 0.1-md rock may have an average pore diameter of less than 1.0 μm , whereas a 500-md rock may have an average pore diameter of 20 μm . The range of pore size may be quite large, which makes it beneficial for FL additives to have a wide range of particle sizes so that all pore spaces can be bridged. In high-permeability formations, polymer and additives may be able to penetrate most pore throats and form an internal filter cake. Smith and Shlyapobersky (2001) claim that in this case, most of the resistance to leakoff, and therefore pressure drop, occurs inside the rock, leaving only a small fraction of the total pressure drop in the external cake. The formation also may be damaged if the particles of polymer infiltrate into the formation spaces as seen in **Figs. 4.30 and 4.31**.

Depending on the permeability of the formation, additional FL agents such as silica flower, deformable polymer particles, or oil-soluble resins may be added. In high-permeability formations, polymer and additives may be able to penetrate most pore throats and form an internal filter cake. In this case, most of the resistance to leakoff, and therefore, pressure drop, occurs inside the rock, leaving only a small fraction of the total pressure drop in the external cake (Armstrong et al. 1995). More details on other FL additives are given in Section 4.6.

4.3.4 Flowback and Cleanup. Conditions: Formation temperature, low shear, lower viscosity.

After the pumping has ceased and the fracture is allowed to close on the proppant pack, the HPG fluid must degrade to allow the fluid to be removed and the permeability of the formation and the pack to improve and reach the values described in the frac model.

In the example we are considering, the BHST is 180°F, an encapsulated APS breaker is in the fluid. This oxidizing agent (**Fig. 4.32**) can generate very reactive sulfate radicals:



These radicals attack and degrade the polymer backbone, thus reducing the viscosity. Gulbis and Hodge (2001) note that the free radicals produce a chain reaction that increases breaker efficiency. Decomposition of persulfate, and therefore, reactivity, is very temperature dependent, as is typical of chemical reactions. At temperatures of about 150°F, the half-life of the persulfate is too short to produce the viscosity break in the fracture, instead of in the tubing. Coated (encapsulated APS) products were developed to delay the break time. **Fig. 4.33** shows a microphotograph of particles of APS coated with a polymer.

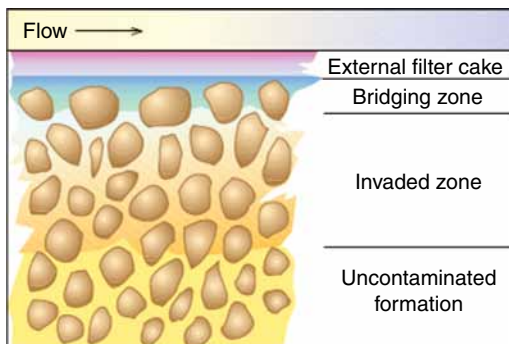


Fig. 4.30—Filter cake leakoff effects (Armstrong et al. 1995).

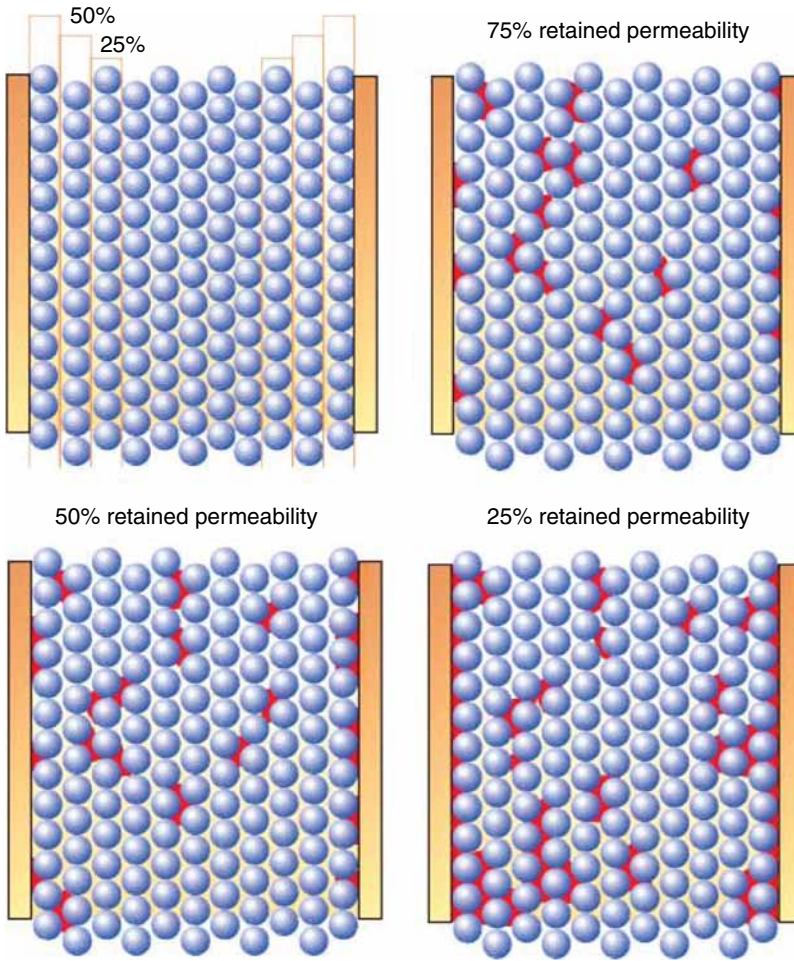


Fig. 4.31—Infiltration of particles into the matrix (Armstrong et al. 1995).

Gulbis et al. (1992) claim that many types of coatings are possible, and the material is customized for the temperature conditions of the various well environments. These authors speculate that the release mechanism is a combination of crushing by the closing pack and diffusion of water into the coated particles. The data in this report demonstrates that a coated breaker delays the viscosity degradation and greatly improves the sand-pack conductivity compared with uncoated APS. Breaking the polymer gel is very important since the filtration of water into the formation concentrates the polymer gel and this may greatly increase the viscosity. More details of the guar chemistries are described in Section 4.4.1. Howard et al. (2010) also recommend the addition of certain surfactants that may improve cleanup of the fracture pack. See Section 4.7.2.

Proppant pack sand flowback can be a significant problem because sand flowing into the wellbore will damage upstream components as well as degrading the fracture conductivity. Several solutions include RCP as well as fibers. The curable-RCPs are mixed and pumped in the later stages of the

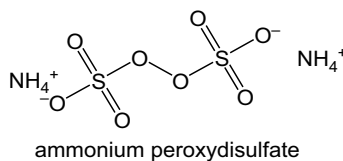


Fig. 4.32—Ammonium peroxydisulfate.

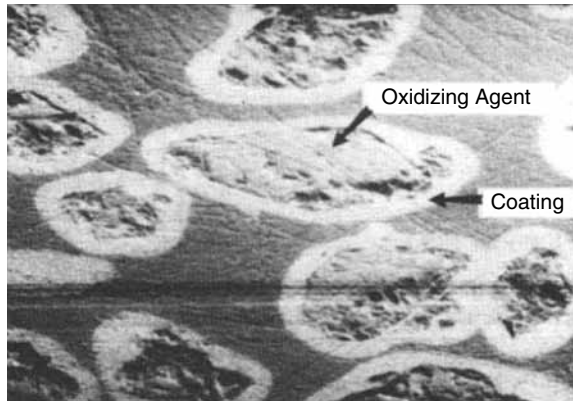


Fig. 4.33—Microphotograph of coated APS particles (Gulbis et al. 1992).

treatment, and the well is shut in for a period to allow the resin to bind the proppant particles together. Theoretically, the RCP cures into a consolidated, but permeable, filter near the wellbore. Card et al. (1994) describe using fibers to delay/reduce flowback of proppant because of the network formed with the fibers and the proppant particles. Additional details of RCP and fibers are in Section 4.9.

At the end of the flowback, the fluids must be treated, possibly reused, or sent for permanent disposal. Details are in Section 6.3.

4.3.5 How Various Fluids and Additives Fulfill the Requirements of the Physics. Sections 4.3.1–4.3.4 describe *one case* of the use of a borate-crosslinked HPG fluid that was broken with APS, as the fluids went through the four major phases of a fracture treatment. In this case, silica sand was the proppant. There are hundreds (probably thousands) of other combinations of fluids, crosslinkers, proppants, and breakers. The different combinations of fluids and proppants reflect the great diversity of formation, temperatures, and well conditions that may require treatments. Note the short descriptions of different fracture requirements for different reservoirs that were described in Section 4.1.1.

Additional fluids will be described along with the other additives (Sections 4.6 and 4.7) necessary to accommodate the many requirements of the prop fracture technique. Where applicable, the authors of the book will compare them with the base case mentioned previously. Reviews of pertinent mechanistic studies also will be provided where appropriate. Subsequent sections (4.4–4.7) provide most of the information on the frac fluid chemistry, while Section 4.9 discusses the proppants. Sections 4.10 and 4.11 will tie the chemistry with the proppants using selection guides and computer models to design the fracture treatment based on geology, engineering, and chemistry.

The major divisions of frac fluids are water-based (aqueous—Section 4.4) and nonaqueous (or low water—Section 4.5) systems. Within the category of aqueous-based fluids, there are those containing polymers and those containing VES-type chemicals. These form association polymers in solution, and may be called micellar fluids or live polymers. A third (gaseous) phase may be added to the aqueous/nonaqueous fluids to form *foamed fluids* (Section 4.7.2). The various types of formulations require different types of crosslinkers and breakers and possibly different proppants.

4.4 Water-Based Fluids

These fluids provide the basis of the majority of the frac jobs pumped. The nomenclature of the fracturing-fluid business (Malpani 2006) includes

- Linear fluids (no crosslinker added or active)
- Crosslinked fluids that have additional viscosity
- Water frac (WF)—a name given to fracture treatments that use minimum amounts of chemicals and also may include SW formulations that only contain a FR (with other additives)
- VES fluids are linear micelles under high shear and have characteristics of crosslinked polymers at low shear

Palisch et al. (2010b) claim that SW fracs may contain HPAA or small amounts of linear uncross-linked carbohydrate gels. Grieser et al. (2003) define WF as “a low-viscosity (10 cp or less), water-based fracturing fluid.” Proppant concentrations in WFs average 0.5 lbm/gal or less (sometimes no proppant is used). Guar gel concentrations vary between 0.5–20 lbm/1,000 gal and are mainly used to reduce friction, not transport proppant. Other additives include long-chained polymer FRs at lower concentrations than guar gel, surfactants, biocides, and clay stabilizers. In the low chemical fracs, the shear from the high pumping rate supports the proppant.

Hybrid treatments may have stages of linear gels and crosslinked fluids. The frac fluids, in general, can be made up using fresh water, seawater, or reprocessed flowback water (see Section 6.3). The freshwater fluids usually also contain KCl to act as a clay/formation stabilizer.

Seawater (or possibly formation brines) can be used. However, Harris and Batenburg (1999) note that the chemical factors that operators must address to successfully substitute seawater for fresh water in borate-crosslinked guar fracturing fluids. They claim that seawater contains cations and anions that affect the performance of the fracturing fluid’s components, as well as the fluid’s interaction with the formation. Because seawater has high ionic strength, it lowers the viscosity obtained from borate-crosslinked guar. High magnesium in the water consumes hydroxide ions and affects pH control, which in turn affects the equilibrium borate-ion concentration. Note that Mg^{2+} is actually used as a borate delay agent (see Section 4.4.1). A number of different polymers are in use to provide the viscosity necessary to cause a fracture and to place proppant.

Special fluids, complexes, and other additives will be described later in this section as well in Sections 4.6 and 4.7 to deal with various factors, as well as the interfering ions. However, tests with the actual mix water are always necessary.

4.4.1 Carbohydrates. These materials are literally “hydrates of carbon” and make up a large part of the thickening agent chemicals used in HF. These include the guar (and derivatives), cellulose, and biopolymers such as xanthan. An example of the use of HPG was given in Section 4.3.

One of the most abundant (but not the simplest) carbohydrate in nature is glucose. This chemical is basic to most life on earth and provides the energy for most processes in the human body. Glucose is described chemically as an aldohexose because it is a six-carbon aldehyde. In aqueous solution, however, it is converted to a cyclic hemiacetal called glucopyranose. Fig. 4.34 shows an example of the equilibrium that takes place in solution. This equilibrium is important because most depictions of

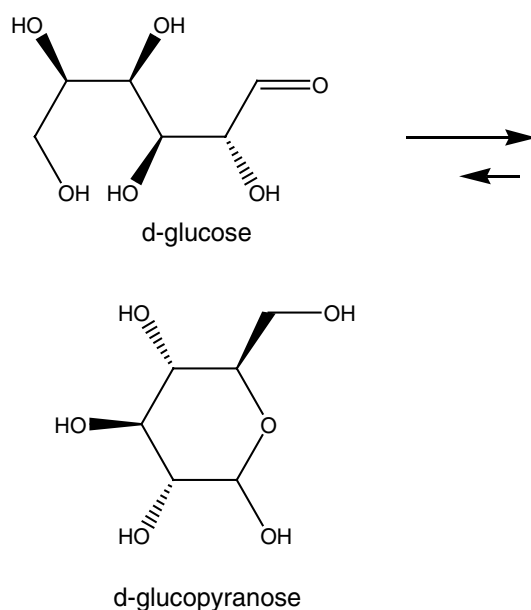


Fig. 4.34—Glucose equilibrium in solution.

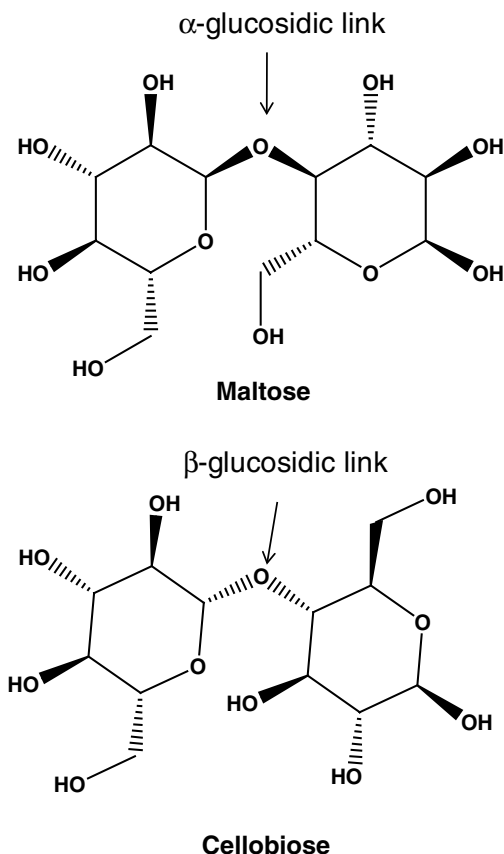


Fig. 4.35—Dicarbohydrate links that may control water solubility.

carbohydrates in fracturing literature show the cyclic ring structure, and it does affect the reactions needed for the use as a fracturing chemical. Glucose is a monosaccharide (single sugar), however di- and polycarbohydrates are much more common in nature.

Fig. 4.35 shows two dicarbohydrates, maltose and cellobiose, that are derived from glucose. They both have two six-member rings that are connected by a *glucoside* (ether) link. There is a difference in the *orientation* of the link that is very important when the carbohydrates are metabolized by biological organisms. For the glucose to be used by the organism, an enzyme catalyzes the hydrolysis of the glucoside link and different enzymes (α and β glucosidases) are required for the two orientations. This type of difference defines two large groups of polycarbohydrates, the polyglycans that have an α -1,4-glucose link and the cellulotics that have the β -1,4-glucose link. In addition, these two classes of carbohydrates may have very different solubilities in water that also may affect the use as a thickening agent; however, this is a complex issue that also depends on the different carbohydrates in the particular compound.

Guar-based frac fluids, xanthans, and other biopolymers are polysaccharides that have natural water solubility, but the cellulose-based materials must be modified by addition of a carboxy-methyl (or hydroxyethyl) group to form chemicals [such as carboxymethylcellulose (CMC)] to be water-soluble. The guar polymers are much more susceptible to some types of biological degradation than CMC-type polymers but have other desirable characteristics that will be discussed in later paragraphs of this section.

Further details of carbohydrate chemistry are beyond the scope of the book and the reader is referred to basic books on organic chemistry such as Solomons (1992a).

Guar-Based Polymers. This chemical family composes a large portion of the fluids used in fracturing. Beckwith (2012b) has reviewed some of the chemistry as the supply chain for this very important chemical family.

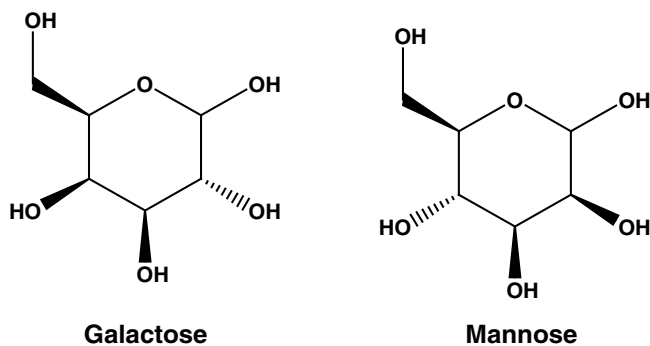


Fig. 4.36—Galactose and mannose monomers.

This polymer is made up of galactose and mannose units (Fig. 4.36).

The structure of guar gum consists of a linear backbone of $\beta(1,4)$ -linked D-mannose units with various amounts of $\alpha(1,6)$ -linked D-galactose side chains. The ratio of mannose to galactose is 1.5–2:1. See the structure in Fig. 4.37 that shows only two repeat units in a compound that may have a molecular weight (MW) in excess of 10^6 daltons.

The guar polymer is an economical thickener and stabilizer. Because guar is used in many foods (such as ice cream), it usually is considered as very safe to use (Sciencelab 2012). It easily hydrates in cold water to give a highly viscous solution. Section 4.3 described some initial information of the chemistry of HPG.

Additional details have been described by Constein et al. (2000) (and others in the following paragraphs) who claim that guar and other polysaccharides are conformationally mobile in dilute solution and adopt disordered or random-coil geometries (see Fig. 1.11). Viscosity—MW relations for several guar samples were determined by Robinson et al. (1982) using dilute solution viscometric and light-scattering measurements. They also concluded that guar acts as a random-coil polymer and that the methods commonly used to study synthetic polymers could be used to determine information such as intrinsic chain flexibility. Various viscometric parameters were described by Constein et al. (2000) that are used to study the properties of these polymers in solution and characterize the frac fluid.

The intrinsic viscosity μ_i is an index of the size or hydrodynamic volume of isolated polymer coils in solution. For random-coil polymer solutions, μ_i can be expressed as a function of the end-to-end distance of a random-coil polymer and the MW. An experimental determination of the intrinsic viscosity is obtained with

$$\mu_i = \left(\frac{\ln \mu / \mu_0}{C} \right)_{C=0} = \left(\frac{\ln \mu_r}{C} \right)_{C=0} \dots \dots \dots (4.15)$$

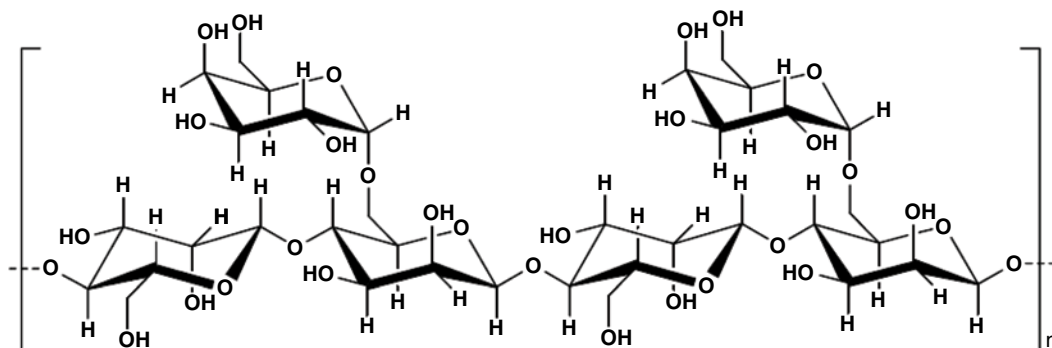


Fig. 4.37—Guar structure showing two repeat units.

In this equation, μ is the solution viscosity, μ_r is the relative viscosity, μ_0 is the zero shear viscosity, and C is the concentration of the polymer. More information is found by using the Mark-Houwink equation, which provides a close approximation of the variation of μ_i with MW (thus, allowing an estimation of the MW of the polymers in solution):

$$\mu_i = KM_v^a \dots \dots \dots (4.16)$$

In this equation, K = proportionality constant (aka Mark-Houwink coefficient), M_v = viscosity average MW of the polymer, and a = shape factor.

Constein et al. (2000) note that the Mark-Houwink (Wagner 1985) coefficient K (in dl/g) and the exponent a are experimentally determined constants for a polymer-solvent system at a specific temperature. The value of a provides an indication of the degree of coiling or extension of the polymer chains. For spheres, $a = 0$; for rigid rods, $a = 2$; and for random chains, $a \approx 1$. For guar, values of a typically have been reported between 0.72 (Robinson et al. 1982).

Venugopal and Abhilash (2010) have used these concepts to study the hydration of guar using viscometric methods described in Section 4.2.2. The most interesting information from this paper (Venugopal and Abhilash 2010)) is that the apparent MW (and thus possibly effectiveness) changed with pH. On moving away from neutral pH, there is a decline in the values of intrinsic viscosity (and thus the MW). The authors suggest that this could be attributed to partial hydrolysis of polysaccharides by acid/alkali and because of the variation in the dielectric constant of solvents resulting in an apparent decrease in the MW.

These authors also studied the hydration time of different guar concentration. The time to reach a plateau in Fig. 4.38 (indicating maximum hydration) was seen to be concentration dependent.

Constein et al. (2000) say that the interaction of concentration and the molecular size or weight of the gelling agent is important for understanding the critical concentrations necessary for crosslinking and the shear stability of dilute crosslinked fracturing fluids. As the concentration C of the gelling agent in solution is increased, the polymer coils begin to interact at a concentration called the critical overlap concentration (C^*). The value of C^* is determined by measuring the solution viscosity as a function of concentration. The results are plotted as the log specific viscosity μ_{sp} ($= \mu_r - 1$) vs. log polymer concentration. The specific viscosity is used to remove the contribution of the solvent to the bulk viscosity. This number is important since C^* is the theoretical minimum concentration at which intermolecular crosslinking is possible

Additional details of the interactions of the polymers in solution are given by Lei and Clark (2004) who claim that as more and more molecules are added to the solution, a concentration is reached when

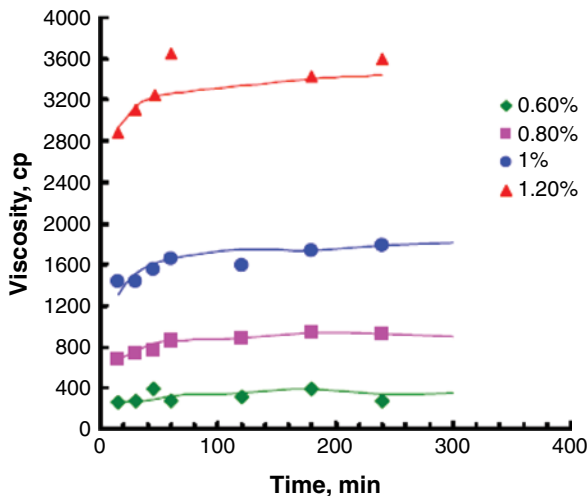


Fig. 4.38—Hydration of guar at 30°C measured at 0.5 s⁻¹ (Venugopal and Abhilash 2010).

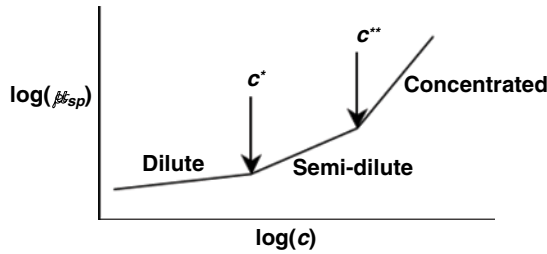


Fig. 4.39—Change in specific viscosity with concentration of a polymer showing two critical concentration values.

the polymer molecules begin to *weakly interact* and the slope of the viscosity—concentration curve changes (Fig. 4.39). This change is not abrupt, but it can be seen when the log of the specific viscosity is plotted against the log of the concentration. Addition of more polymer molecules is accompanied by an increase in polymer—polymer interactions and a decrease in the volume of space occupied by each polymer molecule. Eventually, the polymer molecules reach a point where further contraction is not possible and the only way to make room for additional polymer is for the molecules to begin to interpenetrate strongly.

This point is marked by *another* slope change and labeled C^{**} . Below C^* , it is not possible to form chemical crosslinks because the polymer molecules are too far apart. Reaction of the crosslinker below C^* results predominantly in intrapolymer crosslinks but not interpolymer crosslinks. Lei and Clark (2004) also claim that the effectiveness of crosslinking between C^* and C^{**} increases dramatically as the concentration increases. Somewhere between C^* and C^{**} there is a critical crosslinking concentration that indicates the minimum concentration needed for a full 3D crosslinked structure to develop. The authors claim that this concentration is probably not enough for use in fracturing, but it does form a lower bound for crosslinking concentration.

Determining a value for the critical crosslinking concentration, also referred to as the gel point, presents some problems. The gel point or sol-gel transition occurs when a 3D network pervades the whole solution and the effective MW approaches infinity.

Additional information on the structure of guar-type polymers as well as the gel point can be obtained using a dynamic oscillatory rheometer (DOR) (Fig. 1.28). Weitz et al. (2007) explain that this is done by inducing a sinusoidal shear deformation in the sample and measuring the resultant stress response. In a typical experiment, the sample is placed between two plates. While the top plate remains stationary, a motor rotates the bottom plate, thereby imposing a time-dependent strain (γ), on the sample.

$$\gamma(t) = \gamma \cdot \sin(\omega t) \dots \dots \dots (4.17),$$

Simultaneously, the time-dependent stress $\sigma(t)$ is quantified by measuring the torque that the sample imposes on the top plate. Solutions of polymers including guar exhibit viscoelastic behavior and DOR studies can help characterize the polymer structure. The viscoelastic behavior of the system at a certain frequency (ω) of rotation is characterized by the storage modulus, $G'(\omega)$, and the loss modulus, $G''(\omega)$, which respectively characterize the solid-like and fluid-like contributions to the measured stress response (Fig. 1.26). Constein et al. (2000) note that DOR can help determine whether the fluid is behaving as a liquid or more like a solid. More details will be given in the section on crosslinkers in Section 4.4.2.

The major characteristic of these polymer solutions is *shear thinning*. When the fluid is at rest, the overlapping polymer chains produce the viscosity; however, when the fluid is sheared, the number of entangled coils that are entangled is reduced. The apparent viscosity at any shear rate is a function of the rate that the coils tangle and untangle. Fig. 4.40 shows plots of several concentrations of HPG as a function of shear-rate values and the dramatic change in the apparent viscosities of different concentrations of HPG. As noted in Section 4.2.2 and Fig. 4.19, it is important to test fracturing fluids using a shear history simulator because under extreme shear conditions (with some crosslinkers), shear degradation of the polymer may be permanent.

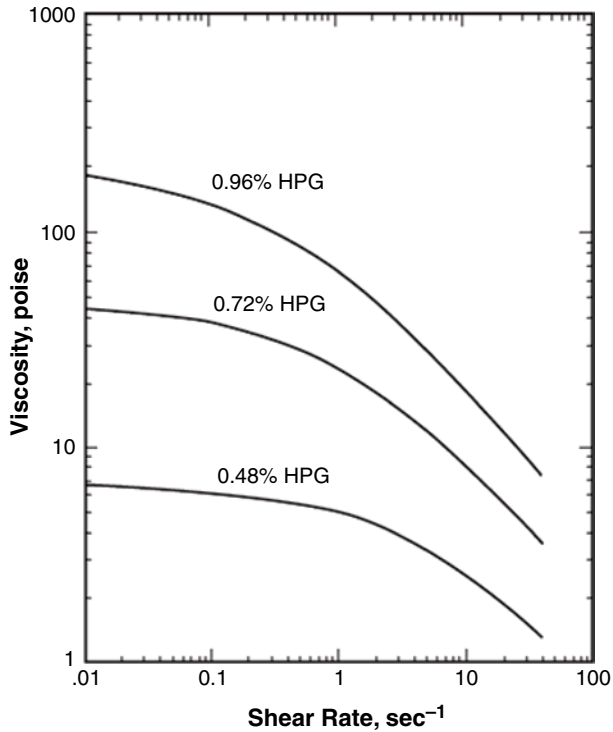


Fig. 4.40—HPG viscosity as function of concentration and shear rate (Aqualon 2007).

Frequently, guar is derivitized to produce HPG (see Fig. 4.25) or other analogs. As noted by Gulbis and Hodge (2001), guar can be reacted with propylene oxide to produce the HPG. This process cleans up the polymer and makes the crosslinking process less rapid because some of the hydroxyl groups are removed. The derivation process is claimed to produce a fluid that has less residue than guar. These are very desirable properties for high-temperature fracturing processes and the cleaner fluids may produce less formation damage. Another guar derivative used in recent years is carboxymethyl HPG (CMHPG). This double-derivitized guar contains the hydroxypropyl functionality of HPG as well as a carboxylic acid substituent. CMHPG was first used for low-temperature wells (Almond and Garvin 1984).

Aqualon (2007) claim that HPG hydrates efficiently in many salt solutions at 80°F and also develops viscosity at 40°F. They claim that with adequate shear, excellent viscosity is formed in 10 minutes. The most effective pH range is 5–6. HPG can also be hydrated in 50:50 methanol (while guar cannot tolerate this much methanol). This author also notes the CMHPG can be hydrated in most salt solutions.

For these applications, CMHPG may be crosslinked with Al(III) through the carboxyl groups. This is claimed to produce a less expensive fluid than HPG crosslinked with Ti and Zr complexes. More recently, CMHPG has been crosslinked with a Zr crosslinker to produce fluids with higher viscosity at high temperatures than those made with comparable amounts of HPG (Hunter and Walker 1991). While the derivitized guar has less residue by weight than guar, Rae and di Lullo (1996) claim that the *volume* of residue is similar to the unreacted guar implying that the expense for the derivitized material is unwarranted.

Biopolymers. These types of polymers includes *xanthan gum*, which is a polysaccharide used as a food additive and rheology modifier. It is produced by fermentation of glucose or sucrose by the *xanthomonas campestris* bacterium. After a fermentation period, the polysaccharide is precipitated from a growth medium with isopropyl alcohol, dried, and ground into a fine powder. See Fig. 4.41 that shows a very complex backbone-repeating unit for this chemical. Gulbis and Hodge (2001) found that xanthan solutions behave as power-law fluids even at low shear rates (Kirkby and Rockefeller 1985), whereas HPG solutions become Newtonian at low shear rates. Clark et al. (1985) showed that at shear

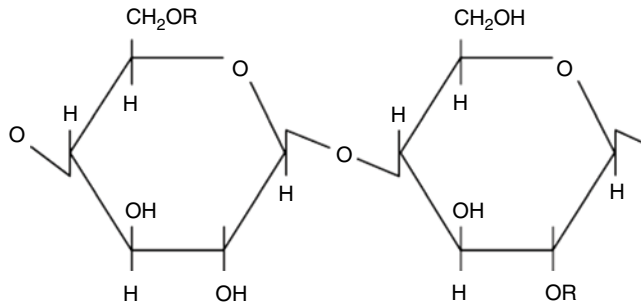


Fig. 4.43—HEC repeat unit (Gulbis and Hodge 2001).

water. Since this feasibility project was completed, the applicable temperature range and conditions have been expanded, and this fluid system is now a commercial product. Note that the Walters et al. (2008) patent teaches that the biopolymers are to be mixed with a guar-type polymer to provide a crosslinked fluid.

Cellulose Derivatives. These are also a type of carbohydrate that have been used in fracturing-fluid formulations. Cellulose itself is not water soluble because of strong intermolecular hydrogen bonding; however, it can be derivitized to make it water-soluble. These modifications include adding hydroxyethyl groups. Fig. 4.43 shows the repeat unit for HEC. It is claimed (Dow 2006) that HEC fluids leave less damaging byproducts in the frac pack after the treatment compared with guar-type fluids. Fluids based on CMC also have been proposed. Lord et al. (2005) and Rae and di Lullo (1996) claim that HEC can be used successfully in a proportion of frac packs (a gravel placement method). *Hydroxypropylcellulose* and *carboxymethylhydroxyethylcellulose* (CMHEC) have also been used as clean fracturing fluids, but this use may be limited by their high cost and restrictive use range. When the carbohydrate or other fluids are added to appropriate brine at the proper pH value, a viscous fluid is produced. This is the liner gel where the increase in fluid viscosity is associated with the entanglement of the polymer chains.

These materials can be crosslinked with a zirconate (Section 4.4.2). Trabelsi and Kakadjian (2013) claim to have tested the properties of CMC and compared it to guar fluids; however, C^* was higher with CMC. The authors also claimed that CMC may be economically favorable when guar supplies are tight and have been regularly used by their company. See Beckwith (2012a) for more information on guar supplies.

4.4.2 Crosslinking of Carbohydrate Fluids. This section describes metallic crosslinker chemistries as well as additional mechanisms that apply to guar-type polymers.

Crosslinking With Metallic Compounds. For some well conditions, linear gels may provide enough viscosity to support proppant, especially if the fluid is pumped at high rates. Fig. 4.44 (Gulbis and Hodge 2001) shows that the viscosity of three HPG fluids varies as a function of temperature. The viscosity increases with HPG concentration but drops significantly with temperature. However, a lower concentration of borate-crosslinked HPG produces much higher viscosity values that are not significantly degraded up to 200°F. The uses of HPG fluids were prefaced in Section 4.3. This section will discuss the use of several different types of crosslinking agents.

These materials usually are employed to link the carbohydrate type of polymer fracturing fluids and include borates (Na_2BO_7 or H_3BO_3), aluminates [Al(III): AlCl_3], titanates [Ti(IV):2-propanol , titanium(4+) salt, titanium lactate], and zirconates [Zr(IV) such as tetra-triethanolamine zirconate]. The carbohydrate polymers have several hydroxyl ($-\text{OH}$) groups (as well as carboxylate for some) on each chain (recall that these are high MW polymers, usually more than 10^6 daltons).

In the aqueous solution, the polymer chains will entangle (see discussion in the previous Section 4.4.1). This entanglement (resulting in net increases in effective MW) causes the initial increase in viscosity as the polymers hydrate (a chemical reaction where the polymer molecules are surrounded with water molecules; see Fig. 4.38). Hydrogen bonding provides some of the mechanism for the

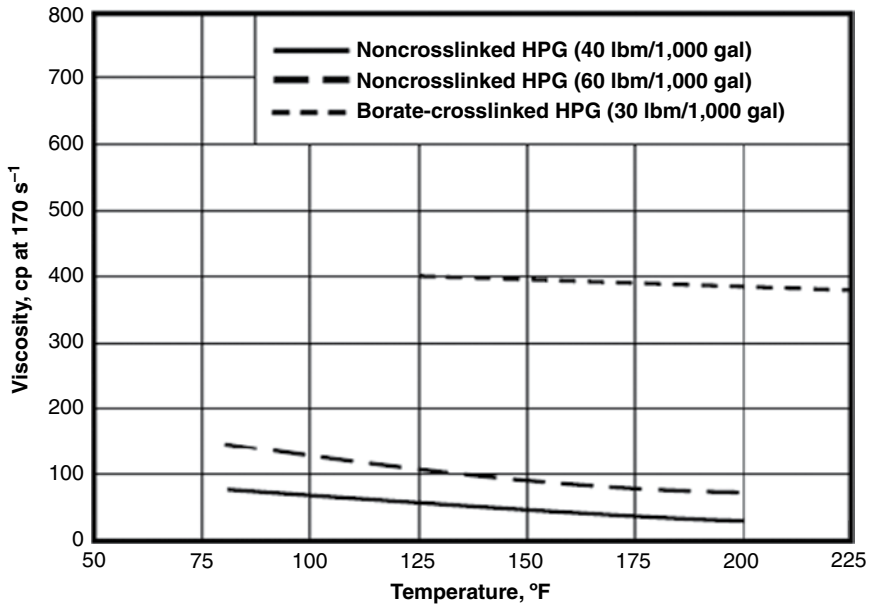
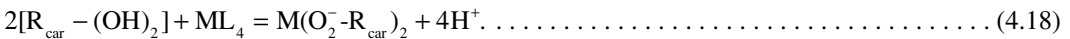


Fig. 4.44—Effect of concentration, temperature, and crosslinker on viscosity of HPG (Gulbis and Hodge 2001).

viscosity. Cheng et al. (2002) described concentrated arrays of guar galactomannan macromolecules and HPG that were examined using the osmotic stress method combined with X-ray scattering. The studies show a liquid crystalline structure with packing free energies that are very similar for guar and HPG and are well described by the entropic steric repulsion between chains. Hydroxypropyl substitution of galactomannan hydroxyl groups causes steric interference that decreases the stability of this hydrogen-bonded crystalline structure. Some details of liquid concentrates that aid hydration are described in Section 4.3.1. To further increase the effective MW and, thus, the viscosity, the chains are linked.

The crosslink reactions are ligand exchange processes (Section 1.5.7) and one generic reaction is



Here $R_{\text{car}} - (\text{OH})_2$ represents the carbohydrate polymer, and L is a ligand associated with the metallic crosslinker. An equilibrium coefficient, K_{eq} , will describe the extent of the reaction and a kinetic coefficient can describe the rate of crosslinking. Many factors can affect both of these properties. These include the relative equilibrium coefficient for each polymer and metal. In addition, the rate at which the reaction occurs depends on the individual reactions, concentrations of reactants, and temperatures. Putzig and St. Clair (2007) note that diffusion as well as steric hindrance may affect the rate of crosslinking. Usually, a high pH drives the reaction to the right (Eq. 4.18) as the protons are reacted to form water. However, low-pH crosslinking in the presence of CO₂ is possible if some Ti or Zr compounds are used.

The initial crosslinking mechanisms for borate were seen and discussed with Figs. 4.26 and 4.27. Note that the cis (same side) the $-\text{O}^-$ groups form coordinate bonds with the B³⁺, and then with the oxygen groups of another carbohydrate molecule, thus forming the crosslink.

Initially, the alcohol groups are protonated and must lose the proton to form the bond with the boron ion. Because boron forms relatively weak coordinate bonds with the sugar, the pH must be raised (Figs. 4.26 and 4.27) before the metal can react. Titanium and zirconium form 6-coordinate octahedral complexes with some ligands in solution, while boron forms 4-coordinate tetrahedral complexes.

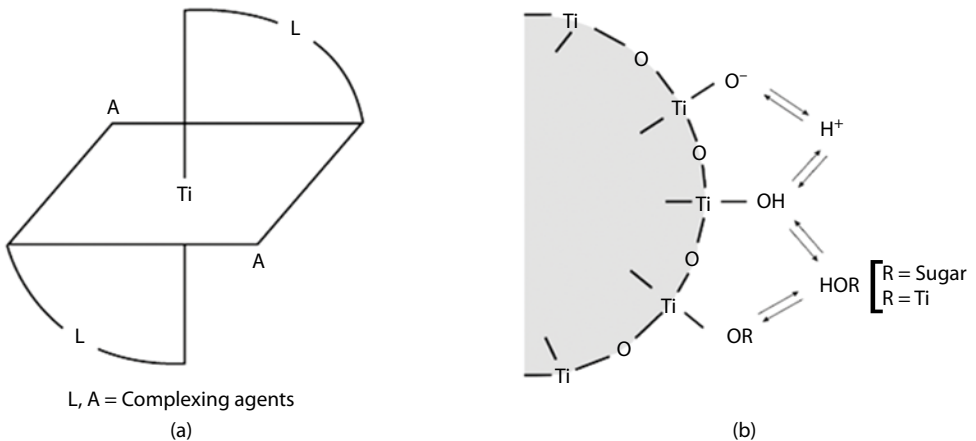


Fig. 4.45—Metal cross linking mechanisms (Gulbis and Hodge 2001).

Fig. 4.26 shows a metal crosslinking mechanism that involves the metal forming bonds with two carbohydrate molecules. Except at low temperatures, these reactions are fast. To accommodate higher fracturing temperatures, a large part of the technology developed includes the use of various *delay* strategies to change the rate enough to allow the fluid to pass through most of the tubing before the crosslinking takes place. As noted in Sections 4.3.2 and 3.1.4, the ideal fracturing system will have low-friction pressure but will support the proppants in the fracture.

A number of techniques can be used to control the reaction rate of the metal ion and polymer. For example, many different organic molecules (ligands) are capable of reacting with the metal ion (cross-linker), which can strongly affect the properties of the complex and will delay the crosslink by reducing the effective metal concentration in solution.

Gulbis and Hodge (2001) describe a hypothetical titanium complex with two ligands (*L*) capable of binding at two sites (bidentate) and two ligands (*A*) capable of binding at one site (monodentate) is illustrated in Fig. 4.45a. On addition to water, complexes of titanium (and zirconium) form colloidal particles (Fig. 4.45b) (Prud'homme et al. 1989). For crosslinking to occur, polymer molecules must displace the organic compounds at the coordination sites on the surface of the colloidal particles. If the ligands are easy to displace, crosslinking occurs rapidly. If the organic compounds are difficult to displace or are present in a high concentration, crosslinking occurs more slowly.

Because it is critical that the frac fluid can flow into the well with minimal friction pressure, many delay strategies are employed. Hodge (1989) claimed a crosslinking delay agent for titanate cross-linkers that includes an organic hydroxycarboxylic acid, preferably hydroxyacetic acid. The pH of the composition is preferably less than 5. The pH of the composition is adjusted when a sufficient amount

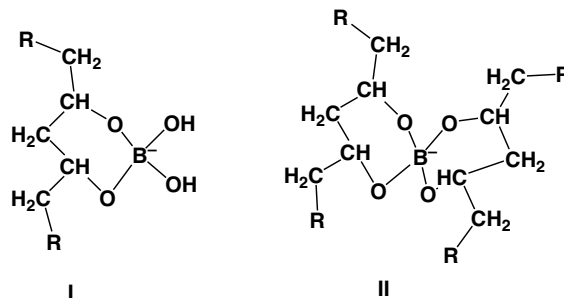


Fig. 4.46—Borate complexes with polyols.

of composition is added to an aqueous polymer solution to result in delayed crosslinking of the polymer; the composition produces a pH in the resulting gel solution, of about 3 to about 4.5.

These materials would be useful for fracturing fluids that contained CO₂. Note that the borate fluids require a high pH to be effective. As noted in Section 4.3.2, borate crosslinking can be delayed by using a slowly dissolving base (MgO) or an encapsulated base. Dawson (1992) claims a delay additive (such as glyoxal), which is effective within a selected pH range, to chemically bond with both boric acid and the borate ions produced by the crosslinking additive to thereby limit the number of borate ions initially available in solution for subsequent crosslinking of the hydratable polysaccharide.

Harris and Batenburg (1999) address the problems and provide guidelines for borate fluid formulation to offset seawater characteristics for temperatures as high as 300°F. They claim that borate fluids from seawater can control FL as well as freshwater borate fluids. Chemical gel breakers for offshore environments are claimed to have been developed to help control the viscosity reductions in fracturing fluids. Conductivity values are claimed with seawater fluids that are equal to or better than freshwater fluids. The presence of divalent cations in the seawater fluid caused no harm to the FL properties or the retained conductivity with borate seawater fluids.

Several additional publications and options for crosslinking formulations are abstracted.

Putzig and St. Clair (2007) describe a delay agent that has hybrid functionality. It delays viscosity development in fracturing fluids based on guar derivatives crosslinked with a variety of common zirconate and titanate crosslinkers under a wide range of pH. The titanium complex contains a lactic acid chelate that competes with the carbohydrate for the complexing site on the metal and, thus, delays the complexing reaction. Putzig (2009) also claims a delayed system of contacting a zirconium complex with an alkanolamine and ethylene glycol wherein the mole ratio of alkanolamine to zirconium is 2:1 to 4:1, and the mole ratio of ethylene glycol to zirconium is 1:1 to 10:1. Lord et al. (2005) claim the use of with ammonium titanyl citrate as a crosslinker for a number of carbohydrate polymers in seawater fluids.

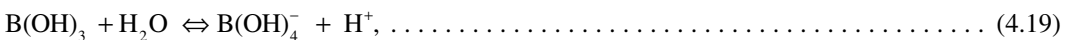
Trabelsi and Kakadjian (2013) claim that they have crosslinked CMC (25 lb/1000 gal) using a zirconate salt with an acetate buffer at pH 4.75.

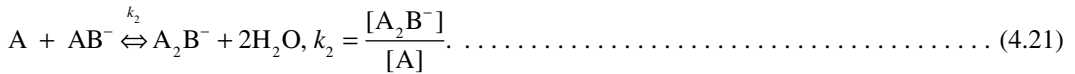
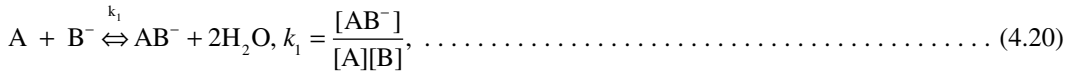
Lord et al. (2005) claim a seawater-delayed crosslinking system that contains guar-type polymers and the crosslinking agent used in the invention is capable of causing delayed crosslinking of the gelling agent for pipe transit times greater than 5 minutes. Thus, the delay in crosslinking exhibited by compositions of the present invention is about 5 minutes or more. Suitable delayed crosslinking agents include but are not limited to ammonium titanyl citrate, ammonium titanyl tartarate, ammonium titanyl gluconate, and mixtures thereof. Of these, ammonium titanyl citrate, the coordination compound ammonium dicitratotitanate, is preferred by the authors.

Viscosity Building Mechanism of Guar-Based Fluids. Because of the importance of this group of fluids, details of studies of the mechanism by which viscosity is built and maintained are reviewed. This is considered to be an expert section.

Because guar polymers are polyalcohols, a model compound, poly(vinyl alcohol) (PVA) cross-linked with borate was studied. Schultz and Myers (1969) used a rotating cylinder viscometer to determine the thermodynamic parameters for the crosslinked fluids. The enthalpy for the crosslinking reaction was determined to be of the order of -5 kcal/mol. The activation energy for breaking individual crosslinks was 6 kcal/mol. The activation energy for viscoelastic flow was determined to be (from the horizontal shift) 10 kcal/mol. The chemical relaxation time at room temperature was 0.33 seconds. These types of data can be used in modeling reactions. Some initial information on the borate crosslinking is seen in Fig. 4.26. To provide more mechanistic information, Sinton (1987) also performed experiments with PVA and small diols to determine information about the reactions with borates. Borate hydrolyzes according to Eq. 4.19 and complexes with polyols in a two-step process (Eqs. 4.20 and 4.21). Two structures (I) and (II) that develop from these reactions are described in Fig. 4.46.

In these equations, A is a polyol and B is boron.





Using ^{11}B nuclear magnetic resonance (NMR) methods, Sinton (1987) determined that the reaction enthalpies are on the order of -3 and -7 kcal/mol for 1:1 and 2:1 complexation was found for the 2,4-propylene diol. These figures are claimed by the author to compare reasonably well because the authors expect about equal enthalpy changes for each step in the formation of 2:1 complexes. The PVA system has a slightly larger enthalpy of formation for crosslinks. Structure II was confirmed for these crosslinks by comparing diol/styrene-butadiene polymer and PVA/styrene-butadiene polymer spectra. Relaxation data indicate that if there are two types of crosslinks, they experience different local molecular motions.

Pezron et al. (1988) described a study that showed the crosslinking mechanism involved the formation of reversible gels in galactomannan-borax systems. They studied interactions between borate ion and guar and/or (hydroxypropyl) guar. They found that borate ions can form several types of complexes with the various % hydroxyl groups of the sugar units. This is similar to the reactions with polyols. To elucidate the structure of the involved complexes, glycoside compounds were used as models. Evidence of the existence of five-member and six-member ring monodiol- and didiol-borate complexes has been obtained by ^{11}B NMR studies. Complex formation constants were determined at four temperatures from ^{11}B NMR spectra. In addition, the thermodynamic functions ΔH and ΔS are reported. For guar and (hydroxypropyl) guar, it was possible to detect monodiol-borate complexes whose formation constant was calculated from dialysis. This is similar to the tests done by Sinton (1987) using low MW diols.

Pezron et al. (1988) have found that the mechanism of formation of crosslinks in this system is governed by complexation equilibrium between borate ions and hydroxyl groups of galactomannan sugar unit. The number of crosslinks may be well controlled by borate and polymer concentrations and temperature. Under suitable conditions, in 1 M NaCl solutions, they observe a striking effect of perfectly reversible demixing into polymer dilute and concentrated phases, even though they are far from ideal conditions. Such a phase transition is not observed in a low ionic strength medium. The demixing can be induced by increasing the number of crosslink.

Pezron et al. (1989) studied the influence of the polymer concentration on complex formation for polyols and galactomannans. In their analyses, the number of multicoordinated complexes per polymer site should be independent of the global monomer concentration in the solution. In the semidilute regime, the number of multicoordinated complexes per polymer site should vary with the polymer site concentration since interchain complexes are formed.

Aqualon (2007) has shown that the amount of the polymer as well as the amount of the crosslinker has an effect on the measured elastic modulus (G'). See Section 1.5.3 and Fig. 1.28. According to these authors, an increase in G' reflects an increase in the number of entanglements of the polymer chains that is reflected in the plots in Fig. 4.47. The data noted that both increased polymer as well as the crosslinker increased the entanglements.

Lei and Clark (2004) also have used DOR methods for studying the formation of gels in crosslinked polymer solutions. They studied guar, HPG, CMHPG, carboxymethyl guar (CMG), and GUAR-3 (a specially processed guar was used). The two guar polymers and HPG were crosslinked with borate, while CMHPG and CMG were crosslinked with a zirconium chelate.

For the uncrosslinked solutions, they found that intrinsic viscosity is indicative of the molecular size in solution. For the polymers, they studied the intrinsic viscosity increase in the order HPG, guar, CMHPG, GUAR-3, and CMG. Both CMG and CMHPG are charged species in solution. Their measurements with the uncrosslinked fluids indicated the crossover frequency of G' and G'' correlates with the gel formation. This is similar to the data of Walters et al. (2009).

Crosslinking radically modifies the properties of water-soluble polymer solutions. These solutions go from weakly viscoelastic fluids to strongly viscoelastic gels. In this study (Lei and Clark

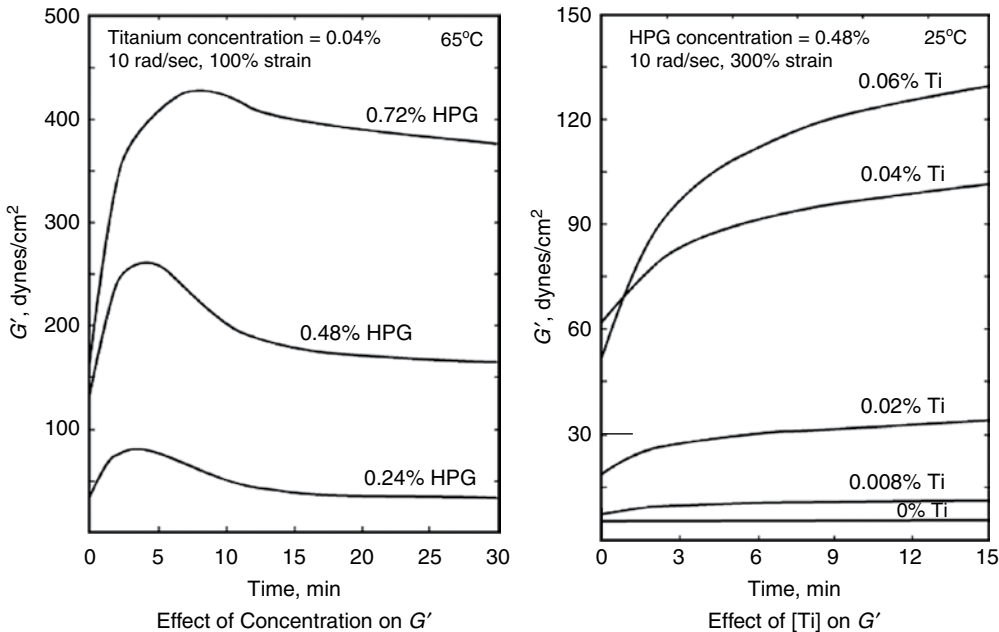


Fig. 4.47—Effects of polymer (HPG) and Ti on G' (Aqualon 2007).

2004), guar, GUAR-3, and HPG were crosslinked with boric acid, and CMG and CMHPG were crosslinked with a zirconium chelate. Data indicated the change in the dynamic (oscillatory) measurements upon crosslinking a 0.5 wt% guar solution with borate. Values for the storage modulus increase dramatically, and the dependence on angular velocity almost disappears while the loss modulus decreases below that found in the noncrosslinked fluid. They also conclude that the critical crosslinking concentration is strong function of polymer properties and only a weak function of crosslinker.

Summary of Understanding of Polymer Chemistry in Carbohydrate Frac Fluids. The initial viscosity is caused by the entanglement of the random coils of the high MW water-soluble polymer molecules.

- At a critical concentration (C^*), there is enough overlap to allow crosslinking if an agent is present.
- Crosslinking involves a ligand exchange reaction between two or more strands through the cis-hydroxyl groups.
- Viscosity and building of effective MW can be studied using oscillation rheology methods that measure G' and G'' .

Chemical Problems With Carbohydrate Viscosity Modifiers. Several chemical/biological stability problems have been mentioned in previous sections (4.3.1 and 4.4.1). Because of the importance of degradation of the fluid, several additional points are considered.

Because guar and guar derivatives and the other polysaccharides (sugar polymers) used to thicken water are an excellent food source for bacteria (Gulbis and Hodge 2001), degradation is likely if the microorganisms are present. Bacteria not only ruin gel by reducing the MW of the polymer, but some can turn the reservoir fluids sour. Once introduced into the reservoir, some bacteria can survive and reduce sulfate ions to hydrogen sulfide (H_2S). Biocides are described in Section 4.7.3 and are used in most frac treatments.

Some metal ions will react with the sugar and acrylamide polymers. Borate, zirconium, and titanium salts will crosslink the sugar polymers, while magnesium salts may be a delay agent. Checking water quality and then testing the fluids with the frac water is a basic requirement. Fe(III) and Cr(III) salts will crosslink the polyacrylamide polymers.

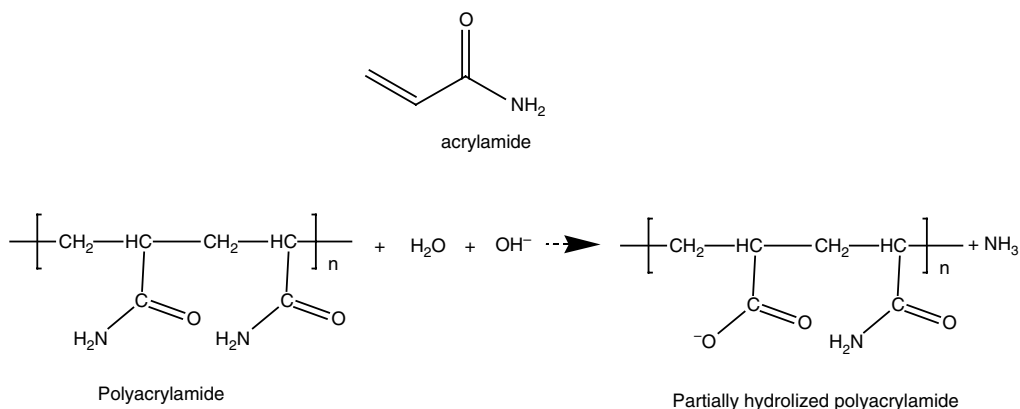


Fig. 4.48—Partially hydrolyzed PAA.

4.4.3 SW Fracturing Fluids and Use of Synthetic Polymers. This is a process that replaces cross-linked carbohydrate polymer gel fracs with 1 to 3+ million gallons of water. Depending on the exact application, small amounts (<1000 ppm) of a synthetic polymer such as HPAA or linear carbohydrate gels, may be added (thus the slick designation). These polymers also can be used as FRs in crosslinked fracturing formulations. Fig. 4.48 shows a structure. The HPAA materials are also used as diverting agents for acid placement and in improved-oil-recovery polymer floods. See Fig. 3.83 as well as details in Sections 4.7.1, 4.10.1, and 5.5.3.

They are also used at higher concentrations (50–80 lbm/1,000 gal) to form SW fracturing fluids that can be employed in stimulation of some gas formations (Sharma et al. 2004). The lower viscosity may create improvements in shale stimulation including less polymer damage and increased penetration of small microcracks in the shale. However, proppant-carrying capacity also will be reduced. See Palisch et al. (2010b) and Section 4.10.1. Wu et al. (2013) claim that the friction reduction during pumping SW treatments may exceed 30% in the tubing, but if the fluid penetrates microcracks, the FR effects are less because the fluid is no longer flowing in the turbulent regime. These authors also report that the HPAA is introduced into the frac fluid “on the fly,” while dispersed in a hydrocarbon solvent such as diesel oil. In the aqueous fluid, the emulsion inverts and the polymer must hydrate in a manner similar to guar (Sections 4.3.1 and 4.4.1).

These polymers can be produced by polymerizing acrylamide and then partially hydrolyzing it to produce a desired amount of carboxylate groups. This type of polymer also can be produced by copolymerizing acrylic acid with acrylamide. Each process will produce a water-soluble polymer with different properties. Compositions that may be useful include homopolymer of acrylamide or methacrylamide and copolymers of acrylamide or methacrylamide with each other or with one or more of the following: acrylic acid, sodium acrylate, potassium acrylate, sodium ethylene sulfonate, potassium ethylene sulfonate. The final polymer’s MW can exceed 2×10^6 daltons. See more information in Section 4.10, the discussion in Section 5.5.3, and the review from Thomas et al. (2012).

Sun et al. (2013) have determined the size distribution of the HPAA gels in SW solutions and claim the distribution is from 0.07–1.6 μm and the peak at 0.55 μm . The authors claim that this is in the range of the microcracks induced in some shale formation, so formation damage is possible. Note that formation damage from guar-type polymers also is expected (Constein et al. 2000) because FL caused the gels to form a filter cake (Section 4.6.1).

An additional synthetic polymer is described by Carman and Gupta (2011). They claim a high-temperature synthetic low-pH crosslinked fluid system has been developed to avoid pitfalls of high temperatures fracturing systems that include the hydrolysis of the polymers. The system employs a synthetic copolymer in an environmentally compliant oil-based emulsion that hydrates very rapidly with excellent fluid rheology properties. Proppant pack regain conductivity using encapsulated oxidizers has also shown very good cleanup at these temperatures. The system uses exceedingly low polymer concentrations (18 to 40 pptg) compared to others (60 to 100 pptg) at temperatures from 350 to

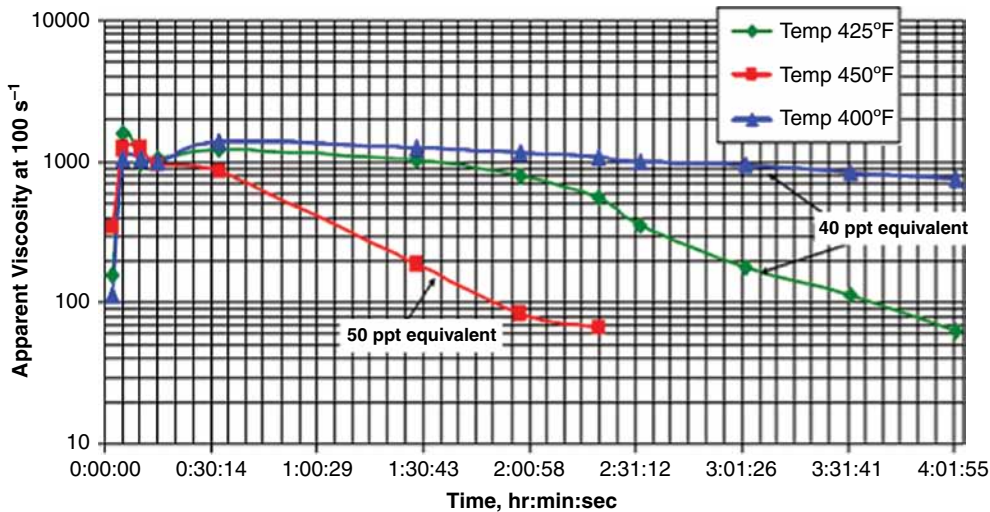


Fig. 4.49—AMPS polymer viscosity at high temperatures.

over 450°F. The fluid can also be energized with nitrogen or carbon dioxide or foam if needed. It is claimed that operationally, fracturing with this fluid can be performed with conventional equipment without any modifications.

According to this article, the chemistry is based on an acrylamide-methyl propane sulfonate polymer with a small amount of vinyl phosphonate in the chain to aid crosslinking. The liquid additive mixed on the surface is an invert emulsion that hydrates very rapidly and is crosslinked with chelated zirconium. It is claimed to provide good viscosity at temperatures >400°F. See Fig. 4.49 that shows the viscosity profiles at high temperatures vs. time.

4.4.4 VES Fracturing Fluids. Thickened fluids based on VESs were described in Section 3.7.2 as chemicals that can be used as diverting agents in various acidizing formulations. As noted in that section, these materials were first characterized as having been developed as potentially nondamaging hydraulic prop fracturing fluids (Norman et al. 1995; Chase et al. 1997; Samuel et al. 1997; Tibbles et al. 2003). A number of different surfactants including cationic, amphoteric, and anionic surfactant types are in use or have been proposed. Figs. 3.85, 3.86, 3.87, and 3.88 show some of the structures that have been used. The mechanism of formation of viscosity is illustrated in Fig. 3.87. When blended with appropriate salt solutions (and surfactant “aids” that act somewhat like a crosslinkers), the VES molecules form rod-shaped micelles that then become entangled under static conditions.

Chemistry of VES Viscosity Modification. In addition to the VES chemicals described in the previous paragraph and in Section 3.7.2, Welton et al. (2007) claim a VES system that contains a methyl ester sulfonate (MES) surfactant and a betaine. Chang et al. (2001a) described an in-situ gelled acid system based on VES chemicals. Chang et al. (2003) also claim a formulation that contains amphoteric surfactants such as those seen in Fig. 3.88. The formulation also is claimed to have a cosurfactant such as para-sodium dodecylbenzene sulfonate. Therefore, a large number of VES-producing chemicals are in use or proposed.

The next paragraphs describe the current understanding of the chemistry of the use of these materials in fracturing-fluid formulations.

Kefi et al. (2004) note that a chemo-mechanical effect produces the initial viscosity of a VES fluid. However, when shear is applied to the system, the micelles untangle and the viscosity is reduced. These associations are electrostatic in character; therefore, VES fluids are *not* as sensitive to *shear history* as polymer-based fluids. If the micelles are disrupted during shear, they will quickly re-aggregate and recover viscosity when shear ceases. Similar to polymer-based fluids, the performance of VES fluids is sensitive to temperature; thus, the surfactant concentration (and in some cases, the salt concentration) must be adjusted accordingly. See the comparison with HEC in Fig. 4.50 that shows the

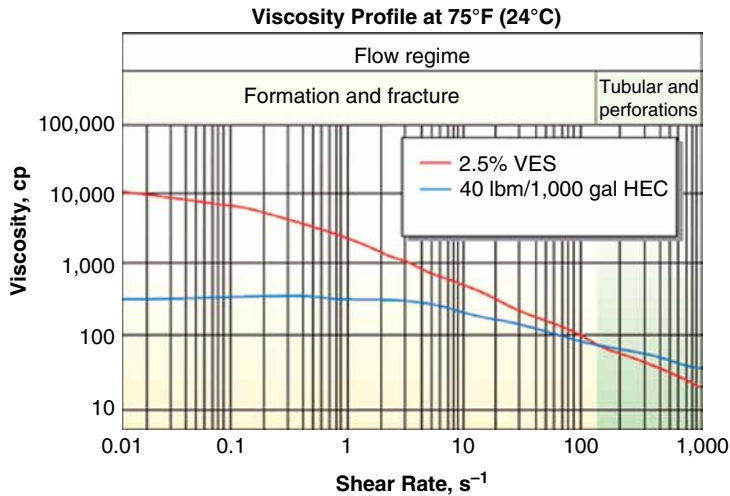


Fig. 4.50—VES and HEC viscosity profiles as a function of shear rates (Kefi et al. 2004).

effects of shear; here, the VES fluid has higher low shear behavior than HEC, but lower values at very high shear than the HEC-gelled fluid. This type of behavior is very useful in fracturing because the flowing viscosity (and thus the friction pressure) is reduced, but the fluid can support proppants when the shear is reduced because it exhibits very high low shear viscosity.

Kefi et al. (2004) have demonstrated the effects of temperature on two different concentrations of a VES fluid in Fig. 4.51. The data show that the VES fluids have sufficient viscosity (about 100 cp) to support proppant up to about 275°F (note the spikes are artifacts of the measurement method). These authors claim that VES fracturing fluids support proppant as effectively as/or more effectively than polymer fluids because the shear thinning is quickly recovered when the shear stress is removed.

The properties of Aromox APA-T (tallow amidopropyl dimethylamine oxide in glycol), a VES used as a gelling agent in aqueous- and brine-based fluids, was investigated by Kamel and Shah (2010).

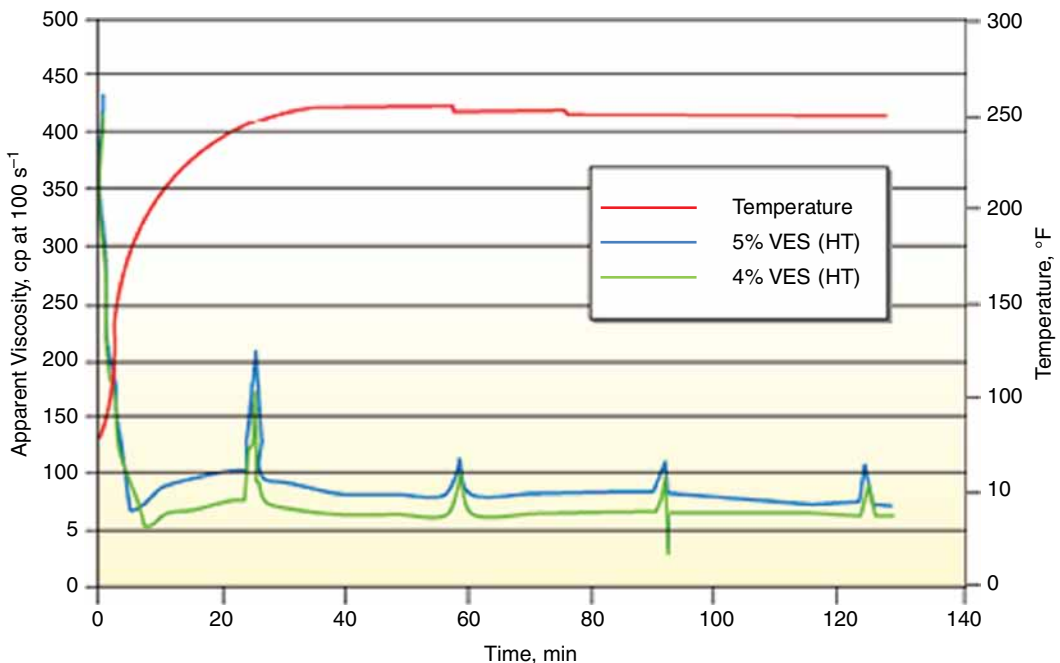


Fig. 4.51—Viscosity over time (temperature spikes are artifacts) (Kefi et al. 2004).

Rheological measurements are conducted using a Bohlin rheometer for VES fluid concentration of 1.5, 2, 3, and 4 vol%. Flow data were gathered using 1/2, 1 1/2, 2 3/8, and 2 7/8-in. outside diameter coiled tubing (CT) with various curvature ratios.

Kamel and Shah (2010) describe results that show that VES fluids exhibit non-Newtonian pseudoplastic behavior. Elastic and viscous properties of VES fluids are very sensitive to surfactant concentration.

The role of the cosurfactant in VES formulations can be very significant and has been explored by several investigators. Castro Dantas et al. (2003) contend that a cosurfactant is largely responsible for their stability, mainly in systems formed by ionic surfactants. In the work described by these authors, ethyl and isoamyl alcohols were used as cosurfactants in microemulsified systems to evaluate their influence in obtaining anionic surfactant-based gels. Steady and oscillatory shear experiments were carried out to study and compare rheological properties of specific systems. From the obtained results, they claim that ethyl and isoamyl alcohols influence gel structure and this can be verified through rheological analysis.

Couillet et al. (2004) described the structural and dynamic properties of micellar solutions of erucyl bis(hydroxyethyl)methyl ammonium chloride blended with 2-propanol, in the presence of KCl. The chemicals were investigated by means of light scattering and rheological experiments. In the dilute regime, the micellar growth was found to be larger than expected from mean-field or scaling models. The results obtained near the overlap concentration (C^*) suggests the presence of large aggregates, with size >100 nm, possibly micellar rings or microgels. In the semidilute regime, the relationship between the zero shear viscosity and the surfactant concentration is described by a power law. The authors of this book note that some of the alcohols describe also are used to form MEs in enhanced-oil-recovery fluids (Section 5.5.5).

Chen et al. (2012) claim a VES fluid mixture having rheological properties wherein the mixture exhibits shear-thickening behavior when the shear rate is increased from a first shear rate to a second higher shear rate because a shear activation additive interacts with the VES to facilitate the shear-thickening behavior and the shear activation additive is a delayed shear activation additive so that shear activation is delayed. Examples of these additives include a polyvinyl ester, a polyvinyl acetate, a polyacrylate, a polyvinyl alcohol, an aromatic sulfonate, mutual solvents, ABA copolymers (a class of block copolymer arranged A-B-A), and combinations of these chemicals.

Wattebled and Laschewsky (2007) discuss the effects of tests with a series of aromatic anions (also called hydrotropes) on characteristic solution properties of a family of ammonium gemini surfactants with dodecyl chains (that show VES behavior). They claim that the stoichiometric addition of the organic salts to the gemini materials can result in clear solutions or in phase separation/precipitation, depending on the detailed nature of the added counter ions and on the spacer group of the gemini surfactant. They note that many organic anions induce synergistic effects, strongly reducing the CMC and the surface tension at the CMC. They found that a number of combinations of organic anions and gemini exhibit thickening of their aqueous solutions. The effects of the added salts were shown to be strongly enhanced for the gemini surfactants compared to the monomeric analog *N*-dodecyl-*N,N,N*-trimethylammonium chloride. The authors claim that even anions such as benzoate may be effective for thickening, and viscoelastic solutions can be obtained with salicylate despite the relatively short alkyl chains. See Fig. 4.52 that illustrates the arrangement of the aromatic groups.

The authors claim that the added organic salts are preferentially located at the interface. They concluded that the aromatic anions are located among the dimethylammonium groups and the first few methylenes of the dodecyl chains and the spacer groups, all near the surfactant head groups at the interface. There are implications for the effects of similar anions (such as salicylic acid anions) that are used to enhance the formation of rod-like micelles with monomeric VES cations.

Sharma et al. (2009) have studied the formation, structure, and rheological behavior of viscoelastic wormlike micelles in the mixed system of long polyoxyethylene chain phytosterol (PhyEO₃₀) and polyoxyethylene dodecyl ether (C₁₂EO_{*n,n*} = 3 and 4) surfactants in water. The effect of the cosurfactant was confirmed in this study. Addition of short polyoxyethylene chain nonionic surfactant (C₁₂EO_{*n,n*} = 3 and 4) to the dilute aqueous solution of PhyEO₃₀ dramatically increases the viscosity by several

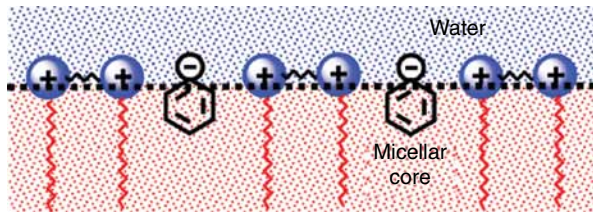


Fig. 4.52—VES and hydrotrope (figure from the abstract online) (Wattebled and Laschewsky 2007).

orders and forms very long wormlike micelles, which entangle in a network and show viscoelastic characteristics.

Shashkina et al. (2005) note that the viscoelastic behavior of VES is similar to that of polymers in semidilute or concentrated solutions. However, in contrast to polymer macromolecules, the surfactant micelles incessantly break and recombine, which makes viscoelastic properties of VES highly responsive to the variation of external conditions (e.g., temperature, hydrophobic additives). For instance, in contact with hydrocarbons the viscosity of VES can drop by several orders of magnitude as a result of transformation of cylindrical micelles into spherical ones. The responsiveness to hydrocarbons makes VES very promising for the use in fracturing fluids, especially at the stage when the porous space between proppant particles should be cleaned up from the residuals of the viscous fluid to allow oil to drain to the wellbore. However, one of the weak points of VES viscosifies in comparison to the conventional polymers is a significant deterioration of their rheological characteristics at elevated temperatures.

They studied cationic VES fluids [Erucyl Bis(hydroxyethyl) methyl ammonium chloride (EHAC)—Fig. 3.85] and mixtures with HPAA (Couillet and Hughes 2008). Dynamic and steady-state rheological measurements were made. They found that the viscosity of the VES fluids alone increased slowly until a critical concentration (C^*) was reached where the rod-like micelles started to entangle (similar behavior is found for polymer solutions). They also found that the temperature dramatically affected the viscosity, but the addition of HPAA significantly decreased the temperature degradation of the viscosity. These authors proposed that the HPAA formed a network (somewhat like a crosslinker) with the VES strands. See Fig. 4.53.

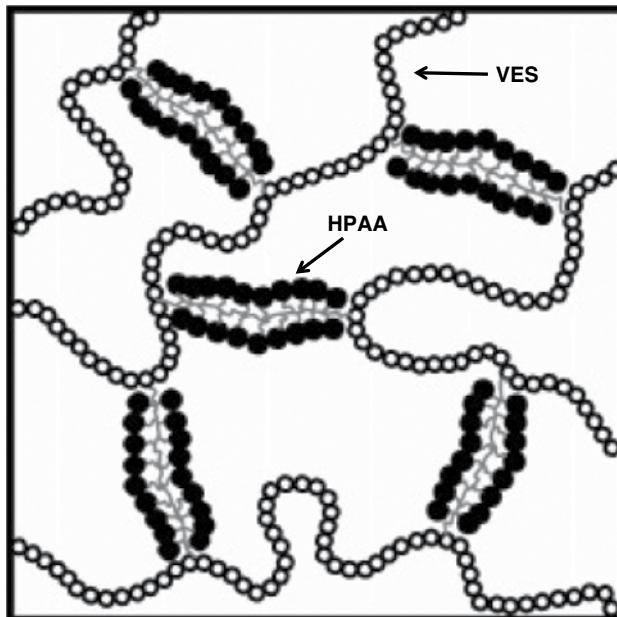


Fig. 4.53—VES-HPAA network (Shashkina et al. 2005).

They also studied the addition of hydrocarbons (which act as breakers for VES fluids—see Section 4.6.3). The addition of a hydrocarbon still broke the fluid by interfering with the VES/polymer network and changing the micelle configurations. Molchanov et al. (2006) has found that VES fluids containing anionic surfactants and polymers (HPAA) can form wormlike micelles, and the addition of hydrocarbons causes the networks to be converted to spherical micelles and the network collapses.

Malhotra and Sharma (2011) claim that one of the most important advantages of VES fluid systems is to minimize damage to the proppant pack and to transport efficiently proppants into fractures. This paper presents an experimental study that investigates the impact of fluid elasticity and fracture width and presents a general correlation for proppant settling in VES fluids. An experimental correlation was presented to quantify the settling velocity of proppants in VES fluids as a function of the fluid rheology and proppant size. It was shown that the VES fluids should be designed such that the relaxation time is greater than the critical relaxation time (T_{crit}). These correlations can be directly used in fracture simulators for proppant selection and for the design of fracturing fluids.

Conclusions on Mechanisms of VES Viscosified Fluids. VES fluids are thickened using surfactants (cationic, anionic, mixed, and amphoteric) that have a correct hydrophilic lipophilic balance as well as the ability to form rod-like (wormlike) micelles. At the C^* concentration, the elongated micelles start to interact and form the larger structure that gives rise to living polymer structures and increased viscosities.

These fluids (especially the cationic and amphoteric materials usually contain a cosurfactant (of the opposite charge or a short chain alcohol) that orients at the water/micelle interface and helps to sustain the rod/wormlike shape. These structures are shear thinning but reassemble after the shear is released. They are broken using hydrocarbons, hydrocarbon-like materials, or some oxidizing chemicals. The temperature limit can be extended by crosslinking the structures using some types of polymers. They are claimed to be less damaging to the frac pack than carbohydrate polymers but may be limited in usefulness in high-permeability formations because of high FL (see Section 4.6.2 for VES FLAs).

4.4.5 Chemistry of Proppant Transport in the Fluid. An important goal of the fracture fluid chemistry is the effective transport of the proppant particles and placement in the fracture. This will apply to all of the fluids including carbohydrates, HPAA, and VES chemicals. Smith and Shlyapobersky (2001) says that single-particle settling that is governed by Stokes law (Eq. 4.8). For the particle falling through a liquid medium, the velocity is given by

$$v_{fall} = 1.15 \times 10^3 \frac{d_{prop}^2}{\mu} (\gamma_{prop} - \gamma_{fluid}) \dots \dots \dots (4.22)$$

In Eq. 4.22, v_{fall} is the settling rate in ft/sec, d_{prop} , the average proppant particle diameter (d) is in inches, μ is the fluid viscosity in cp, and γ_{prop} and γ_{fluid} are the specific gravity (SG) of the proppant and the fluid, respectively. Based on this relationship, the settling rate, and thus the efficiency with which proppant can be transported into the fracture, is directly related to the fluid *viscosity*. These authors, thus, contend that usually the main consideration is how much viscosity is required for a fracture treatment. However, there are additional considerations for calculating settling following Stokes law. Smith and Shlyapobersky (2001) also contend that at low-proppant concentrations (e.g., less than 1 or 2 ppg) particles may clump, producing an apparent diameter greater than the actual particle diameter and accelerating settling. Higher particle concentrations act to increase the slurry viscosity and retard settling (also known as hindered settling). The pump rate is also an important parameter controlling proppant transport for simple settling by Stokes law. Some fracturing fluids for TG sands use dilute polymer solutions and are designed to transport the proppant mostly by using a high pump rate.

They (Smith and Shlyapobersky 2001) note that for a Newtonian fluid, the distance that a proppant particle is transported into a fracture and before that particle can fall from the top of fracture can be calculated using Stokes law and Eq. 4.22. However, it is known from all previous discussions (see Sections 0 and 0) of fracturing fluids that these are *not* necessarily Newtonian fluids, but they are viscoelastic and the shear rates as well as other fluid properties are important. Bivens et al. (2005) claim that at 100 s⁻¹ shear rates, 100 cp viscosity values are required for transportation of the proppant during

the production of the frac pack and unless this value (or other means) are employed, the particles will not fill the entire fracture. See Fig. 4.22. As the fluid-flow rate slows and the shear rate is reduced, some materials (such as VES fluids) very rapidly recover the viscosity that is needed to prevent proppant settling.

de Kruijf et al. (1993) contend that proppant transport can be understood using a fundamental knowledge of the relation between fluid chemistry (as a function of borate crosslinker, pH, and polymer/crosslinker concentration) and its physical properties (proppant-carrying capacity, viscoelasticity, and the temperature stability of the resulting crosslinked structure). These authors have used a helical screw viscometer, as well as the DOR methods and static settling tests to probe these fluids (HPG/borate). A DOR (Fig. 1.28) can generate signals to identify separately the elastic property of fluids. The elastic response is given by the G' storage modulus, and the viscous response is reflected in the G'' loss modulus. These investigators have found based on their tests that a plot combining the measured values of G' of a borate gel as a function of pH and the calculated concentrations of accessible borate show the sites available for crosslinking.

Harris et al. (2009) claim that the elastic character of a fluid is also an important component of viscoelastic fluids and their ability to transport proppant (Harris and Walters 2000; Geol and Shah 2001) and note that elastic character is not reflected in typical steady-shear rate viscosity measurements (see the methods described in Section 4.2.2 that describe different measurement). Also, review the discussions of viscosity (see Section 1.5.3).

The relative magnitudes of G' and G'' vs. oscillation frequency produce a crossover frequency (where the two curves cross) that can be used to infer an ability to support and transport particles, even though particles are not a part of the measurement. Using DOR measurements, they have plotted the change of G' and G'' vs. frequency (ω) for two different biopolymer fluids (Walters et al. 2008; Walters et al. 2009). The results shown in Fig. 4.54 are interpreted by implying that polymer B is more elastic than polymer A.

The conclusions of these authors was that the proppant-carrying properties of the uncrosslinked fluids (as measured by settling times) can be correlated best with the crossover frequencies as compared with steady-state viscosity measurements. More discussions of frac proppant transport are presented in Sections 4.9 and 4.10.

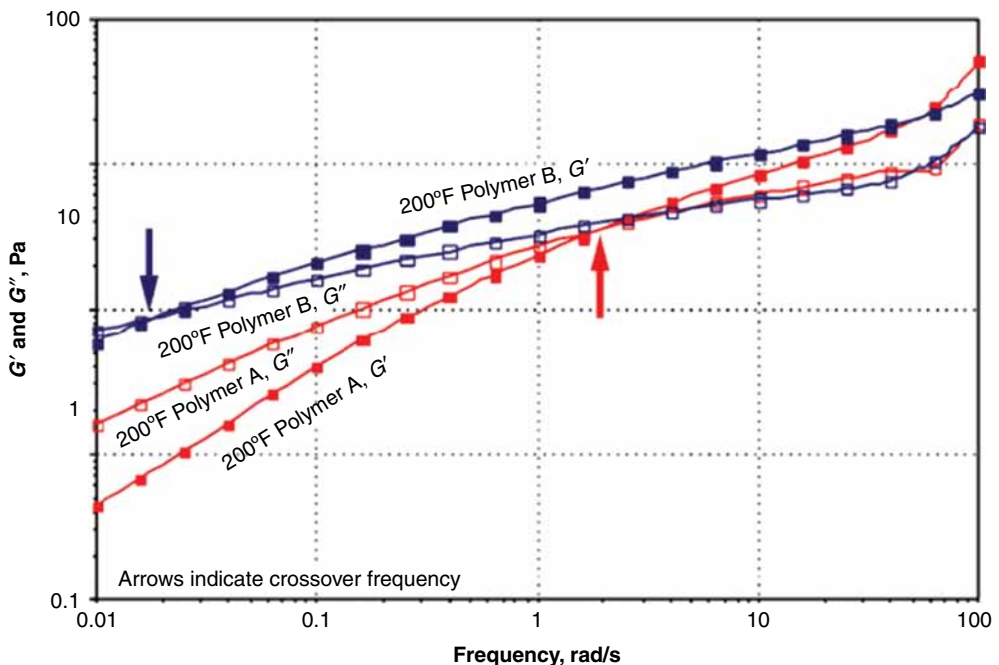


Fig. 4.54—Crossover plot (Harris et al. 2009).

4.5 Nonwater-Based Fluids

The fluids described previously are considered to be systems that are suitable for formations that are compatible with water. While many formations can be treated with aqueous fluids containing clay stabilizers or foams that limit the amount of water present, nonaqueous fluids such as gelled oil, methanol, or mixtures of methanol and water or emulsions have been used, according to Ely (1989b). This section includes fluids made wholly or partially from hydrocarbons, alcohols, or other materials. Usually these materials are required for extremely water-sensitive formations (this means that the clays will migrate and plug the formation).

4.5.1 Gelled Oil. Gulbis and Hodge (2001) describe the chemistry of oil-based fracturing fluids. They note that aluminum phosphate ester chemistry remains the preferred method of gelling hydrocarbons for fracturing purposes. Both methods of thickening oil rely on an “associative” mechanism (Baker et al. 1970). As suggested in Fig. 4.55, interactions between the aluminum complexes and phosphate ester molecules produce a long polymer chain. The R groups shown in Fig. 4.55 are hydrocarbon chains that must be soluble in the oil to be gelled. The soluble R groups keep the aluminum phosphate ester polymer in solution. Generally, the R groups are hydrocarbon chains containing 1 to 18 carbon atoms (Crawford et al. 1973). The R groups have a high affinity for oils such as kerosene and diesel that comprise 12- to 18-carbon (and somewhat higher) chains. Syrinek and Huddleston (1988) describe a system of 57–73 wt% primary branched chain C_{10} – C_{22} alcohols (classified as fatty alcohols) and 29–41 wt% of mixed long-chain Al phosphate esters (C_{18} – C_{33} ester; C_{18} – C_{22} ether) that are used as crosslinkers. These types of fluids are used only when the formation is too sensitive to aqueous fluids. Note that gelled-oil fluids also can be foamed or energized if necessary.

4.5.2 CO_2 as the Carrier. Kubala and Mackay (2010) describe a method of treating a shale-containing subterranean formation penetrated by a wellbore that is accomplished by forming a carbon dioxide treatment fluid having a viscosity of less than about 10 mPa·s at a shear rate of about 100 s^{-1} . The carbon dioxide treatment fluid is introduced into the formation through the wellbore at a pressure above the fracture pressure of the formation. The treatment fluid may comprise from about 90% to 100% by weight carbon dioxide and may contain a proppant. The authors claim that the formation being treated may have a permeability of less than 1 md.

4.5.3 Alcohols. Gidley et al. (1989) mention the use of methanol and isopropyl alcohol as the basis of fracturing fluids, and the authors claim that HPG can be added to as much as 60% methanol to form a fracturing gel. Gupta et al. (2007) report on the use of a high-quality emulsion of carbon dioxide (CO_2) in aqueous alcohol-based gel (CO_2 emulsion), which was introduced into the Western Canadian Sedimentary Basin as a fracturing fluid in 1981. Since that time, the use of the fluid has been very successful, particularly in low-pressure, TG applications. The fluid is claimed to have all the advantages of

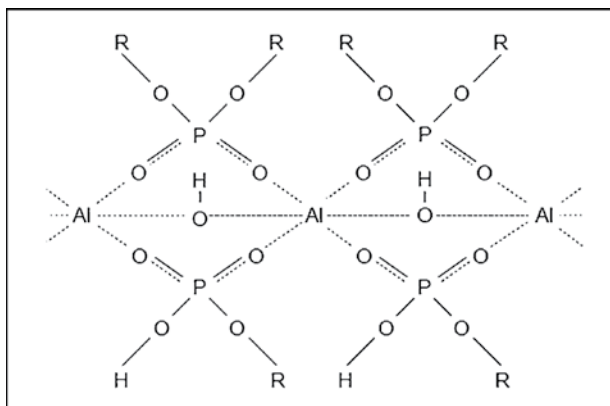


Fig. 4.55—Phosphate ester crosslinking of oil (Gulbis and Hodge 2001).

conventional high-quality CO₂ foams/emulsions, with the added advantage of minimizing the amount of water introduced into the well.

Malone et al. (2004) state that crosslinked methanol has been available as a stimulation fluid since the late 1980s. They claim that crosslinked methanol will never take the place of standard water-based fracture fluid systems because of their wide application range and relative low cost. They do also claim that in some Morrow formations (New Mexico) that exhibit certain reservoir characteristics, cross-linked methanol has found success, and that reservoir parameters should always be the driving force behind fracture stimulation design and subsequent fluid selection. They note that another application of methanol is to prevent the introduction of water to supposed water-sensitive formations during stimulation or workover operations.

Litt et al. (2006) claim a method of fracturing a formation comprising the following: (a) providing a first fluid containing a liquid carrier and a crosslinkable polymer, (b) combining a preformed borate ester present in an organic solvent (methanol) to the first fluid to form a formation treating fluid, and (c) pumping the formation treating fluid into the formation.

4.5.4 Emulsions. Kakadjian et al. (2009) claim an invention for fracturing gas wells that relates to an ME system for rapid cleanup and enhanced production of hydrocarbon-containing fluids in fractured tight subterranean formations. In the invention, the ME system includes a surfactant subsystem including one monoalkyl branched propoxy sulfate or a plurality of monoalkyl branched propoxy sulfates, a solvent subsystem and a cosolvent subsystem. The reference also includes methods for making and using the ME systems. They claim that ME systems of this invention are adapted to be added to fracturing fluids for low-permeability formations in concentrations between about 1 gal/Mgal (gallons per thousand gallons) and about 5 gal/Mgal. At this concentration range, the systems are claimed to improve removal of water block (speeds up the removal of water blocks), thereby improving gas production. Kakadjian et al. (2001) describe a crosslinked oil-in-water emulsion system has been developed for HF treatments. The external phase contains polysaccharide, which acts as thickening agent. Different polymers have been evaluated to obtain a stable emulsion. The oil phase contains a refined petroleum fraction such as gas oil or paraffin oil. A mixture of surfactants has been used to provide a stable emulsion in the preferred volume ratios of the oil and water phases.

The system is claimed to be broken using conventional oxidizer breakers, lowering the viscosity below 40 cp at 170 s⁻¹/140°F after 2.5 hours of rheological evaluation. This fluid is claimed to fulfill the requirements of fracturing fluids having good FL control during fracturing and being capable of suspending and transporting proppant for better fracture packing.

4.5.5 Foamed Fluids. These will be described in Section 4.7. Additional gases (usually CO₂ or N₂) can be added to water-based and nonwater-based frac fluids to reduce the water contact, to improve cleanup and possibly to reduce materials and costs.

4.6 Fluid Loss Agents and Breakers

This section describes two very important classes of additives that are frequently vital for producing efficient and effective fracture treatments. See the discussions of FL tests in Section 4.2.2 and a general discussion in Section 4.1.2. FL to the formation can greatly affect proppant transport and fracture length.

4.6.1 FL Agents for Carbohydrate Fluids. Materials used in addition to the filter cake produced by the polymer fluids may be needed for high-permeability formations and also when VES fluids are used. The rate of fluid leakoff to the matrix during a HF treatment is one of the most critical factors affecting fracture geometry and treatment performance. The filtration rate during a fracturing treatment will affect the designed treatment size, optimal proppant schedule, and resulting proppant distribution within the fracture.

The filtration of the frac polymer should provide the primary FL control; however, the filtration process also may cause damage. Xu et al. (2011) note that guar gum and its derivatives have been the most commonly used polymers to increase the viscosity of fracturing fluids. In this study, they experimentally evaluated two important aspects of the gel damage/filtration process—the thickness of the

polymer gel filter cake that is created as fracture fluid filtrate leaks off into the formation, and the yield stress of the concentrated polymer gel that accumulates in the fracture. The thickness of the filter cake created during the leakoff process was measured as a function of the polymer loading and the volume of leakoff. They claim that the filter cake is created following the procedure described by Ayoub et al. (2006), and then they measured the filter-cake thickness with a precise laser profilometer. They found that the filter-cake thickness varied linearly with *leakoff volume*, meaning that the gel concentration factor is constant for this guar polymer fluid.

The authors Xu et al. (2011) claim that the concentrated polymer filter cakes created by leakoff behave rheologically as Herschel-Bulkley (Herschel and Bulkley 1926) fluids having a yield stress. The yield stress of this material is a critical parameter influencing whether or not the gel can be removed from the fracture. The yield stresses of the polymer filter cakes were found to depend strongly on the concentration of both polymer and breaker. Thus, if the filter cake does not provide needed leak-off control, then some of the materials described in this section may be needed as additives. If the gel is too damaging, then alternative fluids such as the VES formulations also may have advantages (see Section 4.4.4).

In addition to the lab tests described in Section 4.2.2, field tests (commonly termed minifrac) may be required before each main treatment that provide estimates of average filtration rates. Uribe (2006) describes minifrac injection tests (also called calibration treatments or injection tests) that have been developed to diagnose features including interpretation of near-wellbore tortuosity and perforation friction, fracture height growth or confinement, pressure-dependent leakoff, fracture closure, and transmissibility and permeability. The author notes that a calibration treatment is a test done right before a main stimulation treatment. The short fracture created in this test allows the connection between the undamaged formation and the wellbore. Accurate analysis of the minifrac data requires a good understanding of the filtration process, because leakoff may differ significantly with injection volume. Additionally, the ability to use minifrac data to estimate filtration rates in other situations (i.e., other fluids, additives, and/or well conditions) requires a comprehensive understanding of the factors affecting FL. If the tests described in Section 4.2.2 indicate that the fluid has unacceptable FL rates on the intended formation rock, then additional materials may be added to reduce that loss rate.

The type of added material will depend on the formation type and permeability as well as on the fluid composition. During leakoff into the rock matrix, fluid enters the pore spaces of the rock. Some polymers, such as guar and HPG, are filtered out on the surface of low-permeability formation. The polymer is filtered out by passing into the porous rock and forms a filter cake. The filtration time to the formation of the cake is the cause of the spurt *loss* (S) described in Eq. 4.11. The range of pore size of the formation may be quite large, which makes it beneficial for FL additives to have a wide range of particle sizes so that all pore spaces can be bridged. In high-permeability formations, polymer and additives may be able to penetrate most pore throats and form an internal filter cake. In this case, most of the resistance to leakoff, and therefore, pressure drop, occurs inside the rock, leaving only a small fraction of the total pressure drop in the external cake. See Figs. 4.29, 4.30, and 4.31. The size, shape, and size distribution are important considerations. FL additives of the past and present include bridging materials such as 100-mesh sand, 100-mesh soluble resin, and silica flour, or plastering materials such as starch blends, talc silica flour, and clay (Ely 1985).

McGowen and Vitthal (1997) have found that each FL additive has an optimum performance range that depends on the fluid type and core permeability. Several different types of FLAs are in current use. These include inorganic solids, hydrocarbon resins, and various polymers.

Inorganic Solids (Silica Flour). This is a finely ground (nominally 200-mesh) inorganic particulate (ground SiO_2), which is inherently temperature stable. While these inert particles are very stable and effective if sized properly, they may damage the formation if they do not flow out when the well is produced. Sized calcite (CaCO_3) also has been used (Fink 2003). This material may slowly dissolve as the formation water is produced.

Resin Hydrocarbon. The resins are hydrocarbon soluble FLA that are designed for use in water- or acid-based fracturing fluids. Various types of hydrocarbon resin have been ground to a nominal 100-mesh size, however, to ensure effectiveness. Products can be ground to mesh sizes within the following

ranges: coarse (10–70 mesh), medium (70–140 mesh), fine (170–325 mesh), or can be ground to a specific (controlled) mesh size. Gilsonite (a natural asphalt) is one type of hydrocarbon soluble FLA that is designed to be removed by the oil flow. Cleanup of these materials depend on their solubility in the produced liquid hydrocarbons.

McGowen and Vitthal (1997) note that hydrocarbon (nonparticulate) FLAs, even at low concentrations (0.5% by volume), were found to be effective in reducing the filter-cake permeability of cross-linked-gel systems in low-permeability cores (less than 10 md). Unless effective *particulate* FLAs were also used, hydrocarbon additives were ineffective in reducing the spurt loss or the filter-cake permeability in higher-permeability cores. Because hydrocarbon additives principally work on reducing the filter-cake permeability, they exhibited more shear-rate sensitivity than neat fluids. However, in contrast to the pressure-independent behavior of neat fluids, the FL coefficients with hydrocarbon additives increase with pressure. Lignosulfonates are another type of FLA (Fink 2003).

McGowen and Vitthal (1997) claim that particulate FL additives were very effective in reducing spurt loss, especially for low-viscosity fluids. Inert and oil-soluble materials outperformed most water-soluble particulates, particularly in higher-permeability formations. These authors also claim that an investigation of the particulate particle size indicated that the optimum particulate size distribution must incorporate particles one to two times larger than the peak core pore size. The spurt loss with inert particulate additives was relatively independent of pressure, in contrast to the pressure-dependent spurt loss of neat fluids.

Deformable/Degradable Polymers. Gallus (1969) claims that a mixture of wax and polymer becomes a highly effective diverting agent for reducing FL to formations during hydraulic pressure treatment of wells. The key to its effectiveness is its plastic deformability. In addition, the material must be completely soluble in the produced oil or condensate liquid so that it can be removed readily; it must not cause formation damage. Based on initial tests of strength and hardness, several blends of wax and polymer were selected for extensive testing in the laboratory and the field. These compounds have congealing temperatures ranging from 140 to 190°F; they are insoluble in water and soluble in oil. They (Gallus 1969) claim that laboratory and field tests were conducted using these wax-polymer materials to demonstrate that the use of a deformable diverting agent can significantly improve fluid diverting performance.

Todd et al. (2005) describe specific examples of FL polymers that include homopolymers, random, block, graft, and star- and hyper-branched aliphatic polyesters. The polymers may be prepared by polycondensation reactions, ring-opening polymerizations, free-radical polymerizations, anionic polymerizations, carbocationic polymerizations, coordinative ring-opening polymerizations. Examples of polymers suitable for use include polysaccharides such as dextran or cellulose, chitin, chitosan, proteins, aliphatic polyesters, poly (lactide), poly (glycolide), poly (s-caprolactone), poly (hydroxybutyrate), poly (anhydrides), aliphatic polycarbonates, poly (orthoesters), poly (amino acids), poly (ethylene oxide), and polyphosphazenes. In certain cases, the deformable, degradable material is a degradable polymer, such as an aliphatic polyester or a polyanhydride.

Williamson and Allenson (1989) claim the use of blends of natural and modified starches, which can be employed as effective particulate FLAs. They claim that the blends are significantly more effective in lowering the spurt FL values by and controlling the leakoff more effectively than any of the individual starches. The idea is that starches are similar to the frac fluids and will be degraded by the same breakers that are used to degrade the polymer fluids. The size, shape, and water absorbing properties are important in determining a starch's usefulness as an FLA. As mentioned earlier, the starch source and type of substitution will change these properties. The particle size varies from approximately 3 to 100 microns, and the shape varies from round to polygonal. Starch absorption of water varies from less than 10% to several times its volume.

Le et al. (2001) claim a method for reducing FL while using oil-based fracturing fluids that uses water swellable particles comprising synthetic polymers that are crosslinked so that they are water insoluble, but capable of *swelling* in the presence of relatively small amounts of water. When used with treatment fluids containing at least a small amount of water, the particles swell and reduce FL to the formation during the treatment. When used during an HF treatment of a hydrocarbon bearing formation, the particles may also reduce or eliminate water production following the fracturing treatment by

restricting the extension of a fracture into water-bearing formations, and/or by restricting the flow of fluids from water-bearing areas.

Hutchins et al. (2011) have described mixtures of acrylic copolymers, polyvinyl alcohols, polyvinyl acetates, polyvinyl acetates, butyl maleates, and polyvinyl pyrrolidones (Hutchins et al. 2010) that can act as a drag reducer (DR) for inclusion in fracturing fluids for TG (0.001 to 0.5 md). This mixture was able to decrease leakoff as well as improve the efficiency of a guar/borate fracturing fluid in lab tests as well as in single fracture field tests. The cleanup time as well as the gas production rate were increased when the additive was used compared with the offset.

4.6.2 FL for VES Fluids. Wood (2008) claims that water-soluble uncrosslinked polysaccharide FL control agents may be used for VES fluids and include guar gum and derivatives thereof; cellulose and derivatives thereof; propylene glycol alginate; salts (e.g., sodium, potassium, and calcium salts) of iota, kappa, and lambda carrageenan; agar-agar; and xanthan gum as FL agents for VES fluids.

Huang and Crews (2007) describe technology for controlling the FL of VES fluids up to about 300°F. The FL control agents (Huang and Crews 2007) are slowly water-soluble particles that are used at relatively low concentrations. According to the authors, the particles will be dissolved and/or flowed back with the producing fluid. The rate of the pseudofilter-cake cleanup is enhanced by use of internal VES breakers. The results of rheology, leakoff, and core flow tests will be presented for the VES fluid systems at temperatures 150°F and 250°F. Huang et al. (2009) were issued a patent for alkaline earth metal compounds that may act as FLAs for VES. The FL control agents may include oxides and hydroxides of alkaline earth metal, and in one case, magnesium oxide in which the particle size of the magnesium oxide is between 1 nm to 0.4 mm. The FL agent appears to associate with the VES micelles and together form a novel pseudofilter-cake crosslinked-like viscous fluid layer that limits further VES fluid flow into the porous media. Thus, use of VES reduces the amount of fluid needed to convey the proppant into the fracture.

4.6.3 Viscosity Breakers for Carbohydrate Frac Fluids. Chemicals that can reduce the viscosity and remove polymer/surfactant residues are needed to provide a more permeable frac pack after the fracture has closed. Because filtration of a carbohydrate type of fracturing fluid is one of the FL mechanisms, the polymers will concentrate in the fracture pack. Gulbis and Hodge (2001) and Penny (1987) cite data that suggest that the concentration of the polymers may increase by 10–20 times compared with the surface concentration. The increased polymer concentration causes a major increase in viscosity. For example, the viscosity of an unbroken guar fluid containing polymer at 400 lbm/100 gal (40 lbm/1,000 gal gel concentrated 10 times because of FL on fracture closure) has been estimated to be in excess of 1000 poise.

All of the natural polymers used to provide viscosity will naturally degrade over time, depending on the temperature. However, materials that attack the polymer backbone and structure have long been employed and usually are pumped simultaneously with the fracturing fluids to improve cleanup. Ideally, a gel breaker put into the fluid at the surface should have minimal effect on the gel until pumping ceases (and the fracture closes), and then should react rapidly with the gel. The viscosity of the gel and the MW of the polymer should be significantly reduced to allow rapid cleanup of the sand pack. The broad categories of internal breakers (those pumped with the fluid) are *oxidizing agents* and *enzymes*. Occasionally, an acid overflush may also be pumped to help clear out the polymer, but this usually is not a desirable procedure. Because acids do degrade guar polymers, the release must be controlled, because fracturing fluids for high-temperature formations generally are high pH to achieve the desired stability. Examples of the various types of gel/viscosity breakers for carbohydrate fluids are described in the next sections. Breakers for VES fluids are discussed later in this section.

Acidic Breakers. A combination breaker/FLA was developed using an acid condensation product (Cantu and Boyd 1988). It was claimed that the additive (hydroxyacetic acid monomers and dimmers) (Cantu et al. 1989) slowly degraded into water-soluble monomeric units at temperatures greater than 150°F after fracture stimulation experiments. The high-acid-content degradation product then claimed to act as an excellent HPG gel breaker and effectively cleaned the proppant packs.

As a FL-control additive, the measured wall-building coefficients were as good as, or better than, those of silica flour in crosslinked-gel systems. This paper summarizes a 2-year study of the evaluation and application of this new product in fracturing-fluid systems. Still et al. (2007) also have proposed the use of an acid that can be produced as the fracture pack is affected by the heat and water content of the degrading fluids. High concentrations of acid are typically required to reduce the pH of the fracturing fluid sufficiently for conductivity improvement, so this type of breaker has not been widely used.

Oxidizing Agent Breakers. This is one of the two classes of chemicals that are added to most carbohydrate HF treatments (enzymes are the other major class). These materials can be used for both guar and CMC-type polymers (Trabelsi and Kakadjian 2013). The use of APS as an oxidizing breaker was described briefly in Section 4.3.4 and the basic mechanism was shown in Eq. 4.14. Additional oxidizing breakers include potassium persulfate, as well as calcium peroxide (CaO_2), and potassium, sodium, or ammonium salts of peroxymonosulfate and a tetra-n-alkylammonium peroxymonosulfate. Hutchins et al. (2009) have described unsymmetrical persulfates that are claimed to be more stable than APS at higher temperatures.

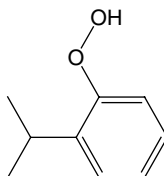
Le and Dawson (1995) indicate that various *organic* peroxides can be used as breakers. Included are cumene hydroperoxide; t-butyl cumyl peroxide; di-t-butyl peroxide; di-(2-t-butylperoxyisopropyl) benzene; 2,5-dimethyl-2,5-di(t-butylperoxy) hexane; di-isopropyl benzene monohydroperoxide; di-cumyl peroxide; 2,2-di-(t-butyl peroxy) butane, t-amyl hydroperoxide, benzoyl peroxide. Dawson and Le (1995) claim a breaker system that includes the use of a slightly water soluble, organic peroxide in a water immiscible, nonoxidizable organic solvent. The preferred peroxide in this invention is cumene hydroperoxide (Fig. 4.56).

They claim that the system has several advantages. The breaker system remains active at both alkaline and acid pH 4.5 levels. The higher pH levels strengthen the crosslinks in the gel, allowing for better fracturing and contribute to better proppant transport. Yet, the breaker system also works at acid pHs. The breaker system is active at moderate to high temperatures commonly found in subterranean formations. In addition, the fracturing fluid and method allow a delayed reduction in viscosity of the fracturing fluid so that the gelled fluid breaks at the conclusion of the pumping operations. Oxidation breakers act to reduce viscosity by cleaving the polymer into smaller MW fragments.

Still et al. (2003) and Weaver et al. (2003) note that guar (see Fig. 4.25) is a linear polymer with a backbone composed of mannose connected by β -1,4 acetal linkages. This backbone has single-unit branches of galactose connected by α -1,6 acetal linkages. The ratio of mannose to galactose has been shown to influence the solubility of the guar gum. As the galactose content is reduced, the solubility of the polymer in water decreases dramatically.

Concerning the oxidative breaking mechanism, these authors then claim the following:

- The free radicals generated by the breakdown of the peroxides seek electrons to balance an unpaired electron.
- The free-radical oxidation of hemiacetals is a chain reaction.
- The process begins when sulfate free radicals are generated. See Eq. 4.12.
- The sulfate free radicals extract a hydrogen atom from the polymer by attacking the 1-4 β -glycoside linkages of the mannose backbone and the 1-6 α -glycoside linkages to the pendant galactose substituents. See Figs. 4.25, 4.34, and 4.35.



cumene hydroperoxide

Fig. 4.56—Cumene hydroperoxide.

- Breaking these linkages reduces the polymer MW.
- It is also possible to break the carbon-oxygen bond in the cyclic hemiacetal structure, although that reaction is less favorable.
- The free-radical attack on the polymer turns the polymer into a free-radical molecule.
- These unstable free-radical species then split into two smaller molecules, one of which remains a free radical.
- That free-radical segment can either extract hydrogen from another polymer molecule or fragment into smaller molecular segments, creating another free radical.
- This ongoing process is referred to as fragmentation and propagation.
- The process ends when two free radicals combine, enabling the unpaired electrons to become paired and returning the molecule to a low-energy state (termination step).

The result of oxidative polymer degradation is viscosity and MW reduction. Aqualon (2007) has discussed the mechanism of degradation of guar-type polymers that happens through temperature as well as with oxidizers. Two chemical pathways for degradation include hydrolysis of the glycoside linkage that results in a breakage of the polysaccharide chain. The other is oxidative/reductive depolymerization. Acid hydrolysis also is possible (see Section 4.6.3). Radical oxidation, such as described in the prior paragraphs also was noted.

Gall (1985) notes that the decrease in HPG MW using ammonium persulfate breaker is most rapid during the first few hours of reaction time (3 to 10 hours depending on temperature), then more gradual for the next 24 to 48 hours. The fast reaction is caused by a free-radical chain reaction initiated by the breaker.

The slow reaction may be caused by thermal degradation or other reactions were not identified (Gall 1985). The conclusions of this report are as follows:

- Temperature increases the rate of HPG MW degradation caused by the breaker. The rate increases by a factor of 2 for an increase in temperature of 10°C for an initial breaker concentration of 0.005%.
- The rate of HPG MW reduction does not appear to depend on the initial amount of breaker in solution. Adjusting breaker concentration to control the rate of MW degradation should be ineffective.
- The extent of MW decrease caused by the breaker depends on the square root of the breaker concentration. The total MW degradation depends on the temperature and the APS concentration.

As noted in Section 4.3.4, it frequently is desirable to *delay* the crosslinking reaction (however, accelerating the reactions at low temperatures also is needed). The use of various delayed encapsulated breaker systems also are in use because a premature viscosity degradation may result in a premature screen out of the proppant and, thus, a lowering of the frac length. See Gulbis et al. (1992).

Complexed breakers have been disclosed to allow a controlled breaking rate. Brannon and Ault (1991) claim a guar-based fluid utilizing an organically complexed borate crosslinking system. Laboratory evaluations of this system were claimed to demonstrate superior rheological properties at temperatures exceeding 300°F. Tjon-Joe-Pin et al. (2001) describe a breaker-crosslinker-polymer complex and a method for using the complex in a fracturing fluid to fracture a subterranean formation that surrounds a wellbore by pumping the fluid to a desired location within the wellbore under sufficient pressure to fracture the surrounding subterranean formation. The complex may be maintained in a substantially nonreactive state by maintaining specific conditions of pH and temperature, until a time at which the fluid is in place in the wellbore and the desired fracture is completed. Once the fracture is completed, the specific conditions at which the complex is inactive are no longer maintained. When the conditions change sufficiently, the complex becomes active and the breaker begins to catalyze polymer degradation causing the fracturing fluid to become sufficiently fluid to be pumped from the subterranean formation to the well surface.

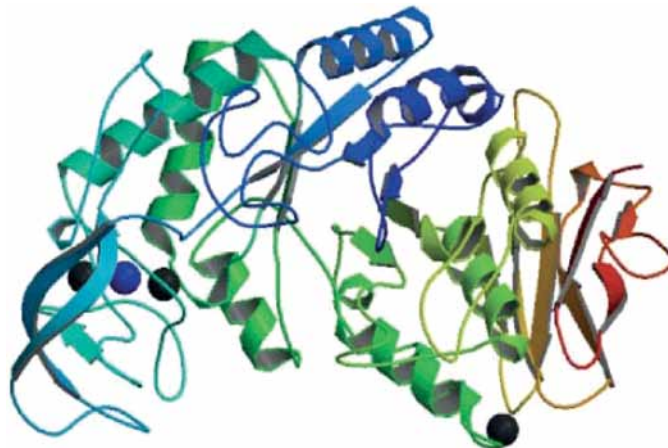
One of the key claims is the following:

A method of fracturing a subterranean formation that surrounds a wellbore: comprising the steps of forming a gellable fracturing fluid: comprising a breaker-crosslinker-polymer complex, comprising a matrix of compounds, said compounds each including a breaker component comprising guar-specific enzyme, a crosslinker component comprising zirconium, and a polymer component comprising CMHPG maintaining said breaker-crosslinker-polymer-complex at about pH 9.3 to about pH 10.4 at about 200°F to about 250°F, wherein said complex is substantially nonreactive; pumping the breaker-crosslinker-polymer complex to a desired location within the wellbore under sufficient pressure to fracture the surrounding subterranean formations; ceasing to maintain said breaker-crosslinker-polymer complex at a condition at which the breaker molecule is substantially nonreactive; and allowing the breaker to catalyze polymer degradation causing the fracturing fluid to become less viscous, whereby the fracturing fluid can be pumped from the subterranean formation to the well surface.

Breakers also may be needed to reduce the viscosity of HPAA gels used in SW fracs. Carman and Cawiezel (2007) report on a study of several conventional oxidizers (see earlier in this section) that were chosen and screened to determine if they could effectively reduce the viscosity of the polyacrylamide polymer. The MW degradation of the polymer was then measured using a MW cutoff filtration technique to determine the size and percentage of polymer fragments. They found that most of the breakers tested showed some reduction in viscosity and in MW. Additional laboratory testing was then conducted to ensure that the addition of breaker to the FR did not adversely affect polymer hydration or friction-reduction performance. The major conclusion was that persulfate breakers were more effective than other oxidative breakers.

Enzyme Breakers. Enzymes also have been used to clean up frac packs containing carbohydrate fluids. Gulbis and Hodge (2001) note that enzyme breakers of the class of hemicellulase have been used to reduce the viscosity of water-based fluids. Enzymes have been in use for some time, but before 1994, their use was thought to be limited to a relatively mild environment: pH range of about 3.5 to 8 and temperatures less than about 150°F. Because they are active at ambient temperature, enzymes begin to degrade the polymer immediately upon mixing and under some conditions can be too reactive, like persulfates. Higher temperature enzyme breakers as well as knowledge that is more mechanistic have been developed since that time.

Samuel et al. (2009) note that enzymes are proteins that have active sites that can act as catalysts for certain reactions. In the cases of degradation of carbohydrates, they act to increase the reaction rates that cause the scission (usually hydrolysis) of C-O bonds. A 3D drawing of an α -amylase enzyme is in Fig. 4.57.



3D structure of α -amylase (from *Bacillus licheniformis*). Ca ions (●) stabilize the secondary structure and are responsible for the HT stability. (●) denote chloride ions

Fig. 4.57—Drawing of an amylase enzyme (Samuel et al. 2009).

The report by Samuel et al. (2009) claims that the reactions catalyzed by the hydrozylate enzymes are affected greatly by both pH and temperature. Each type of enzyme (there are many) is active only in a specific pH range and will attack only specific bond sites. Increase in temperature may also increase the reaction rate of degradation of the carbohydrate (this may be useful or not useful) but at some temperatures, the high-temperature denatures (unfolds) the protein structure of the enzyme, rendering it ineffective. The activity also may be modified by the specific salt content as well as the presence of cations such as Ca^{2+} . Enzymes are much more specific catalysts for particular carbohydrates as compared with chemical oxidizing agents because they fit into specific regions of the polymers to facilitate the chemical reactions that break up the structure. In the papers abstracted below, very specific enzymes are described. The Samuel et al. (2009) paper gives a review of enzymes in use in the oilfield production environment.

Cheng and Prud'homme (2000) have probed the enzymatic degradation of guar galactomannan using gel permeation chromatography and steady shear viscometry. They found that in very dilute polymer solutions, the reaction rate increases with first-order kinetics with substrate concentration. In the intermediate concentration regime, the enzyme/polymer binding saturates, and the degradation kinetics is zero order. However, as the solution increases in concentration, the reaction rate decreases, and the enzyme diffusion through the concentrated polymer gel becomes a limiting factor. A reaction-diffusion model was presented by the authors to explain the competition between enzyme reaction and diffusion. The influence of polymer derivatization on the degradation kinetics was also explored. The degradation rate was shown by the authors to be greatly affected by the type of substituent groups as well as the degree of substitution. Several specific examples of enzyme breakers are abstracted.

Tjon-Joe-Pin (1993) describes a method of fracturing a subterranean formation in the presence of a polymeric gel viscosifier and an *enzyme* breaker that is allowed to degrade the crosslinked polymer with time to reduce the viscosity of the fluid so that the fluid can be pumped from the formation back to the well surface. The particular *enzyme* breaker used has an activity in the range of 2.0 to 11.0 and is effective to attack only specific linkages in the crosslinked polymer gel. The claimed breaker is a 1:2 solution of 1,6- α -D-galactosidase and mannanendo-1,4- β -mannosidase.

Brannon and Tjon-Joe-Pin (1996) claim that the preferred enzymes are galactomannan hydrolases collectively called galactomannanase, and they specifically hydrolyze the 1,6- α -D-galactomannosidic and the 1,4- β -D-mannosidic linkages between the monosaccharide units in the guar backbone, respectively. The preferred galactomannanase is commercially available from Novo Nordisk of Norway as Gammanase 1.5L. The preferred concentration of galactomannanase is a 1:2 (weight/weight [w/w]) solution of 1,6- α -D-galactosidase and mannan endo-1,4- β -D-mannosidase, the galactomannanase being present in the range from about 0.001 to 0.004% by weight, based on the total weight of aqueous fluid.

Gupta and Prasek (1995) claim an encapsulated enzyme breaker. The encapsulated enzyme breaker is allowed to degrade the crosslinked polymer with time to reduce the viscosity of the fluid so that the fluid can be pumped from the formation back to the well surface. The particular enzyme breaker uses open cellular encapsulation to protect and delay the action of the enzyme. The encapsulated enzyme breaker of the invention is comprised of a breaker enclosed within an inert open cell microporous matrix, which is permeable to the enzyme breaker such that upon sufficient contact with fracturing fluid or a fluid in the formation, the enzyme breaker is controllably released over time by diffusion through the matrix into the fracturing fluid. The invention also provides an encapsulated enzyme breaker that is capable of functioning in an aqueous-based fluid at low temperatures, from about 40.0°F. to about 200.0°F, without premature release of the enzyme breaker into the fracturing fluid.

Barati et al. (2011) have proposed and tested a system for using a commercial enzyme loaded into polyelectrolyte nanoparticles as a method for delaying and also protecting the enzyme breakers at high temperatures. They claim that the entrapment method was originally developed for drug delivery applications (Tiyaboonchai et al. 2003) using a polyethyleneimine (PEI)-dextran sulfate to form polyelectrolyte complex nanoparticles. The nanoparticles were formed by mixing the PEI and dextran sulfate and then slowly adding the enzymes and were measured (using zeta potential techniques

described in the paper) to be approximately 450 nm in hydrodynamic diameter. Berkland et al. (2008) list a large number of polycations and the polyanions that can be mixed to form nanoparticles that can then be used for encapsulating oilfield chemicals.

Barati et al. (2011a) note that the particles formed in this system ranged from about 230–450 nm in diameter, which is outside of the generally accepted size of nanotechnology materials (2–100 nm) (NNI 2011). The enzyme used is a 25% pectinase from *Aspergillus aculaceatus*. In this study, the test frac fluids were borate-crosslinked guar formulations. In these tests, they found that the nanoparticles encapsulated breaker was delayed up to 11 hours, compared to about 3 hours for equivalent systems where the enzyme mixture was not entrapped. Polyelectrolyte complex nanoparticles also protected both enzymes from denaturation at an elevated temperature and pH. Part of the mechanism is thought to be because entrapment of enzymes within the nanoparticles confers protection from the pH of the bulk solution, presumably by a local buffering effect by the PEI, which dominates the pH of the nanoparticle preparations. They also claimed that the nanoparticles were insensitive to shear forces expected during fracturing.

Samuel et al. (2009) describe enzymes that can be used to degrade starch and xanthan polymers. The major limitation of enzymes is their inability to stay active at temperatures greater than 200°F. The activity of enzymes at 207°F was less than 10% of their activity at 200°F.

The authors claim that previous studies to increase the stability enzymes were aimed at (1) changing salinity, (2) changing the source of the enzymes, (3) using additives that alter the conformation of enzymes, or (4) modifying the enzymes chemically. These techniques did not maintain the activity of the enzymes at 200°F. For filter-cake removal, enzymes have been used globally at higher temperatures, though their activity is known to be much less than 2%.

The chemicals were not described; however, a patent application by Rimassa, Samuel et al. (2009) claims that water-soluble amphoteric surfactants at low concentration can thermostabilize enzymes in brine. The thermostabilized enzyme compositions can be used in a method to digest polymers at temperatures and/or salinities at which the enzyme is normally inactivated and/or coagulated without the surfactant. Functionally, this idea may be similar to the nanoparticle process described by Berkland et al. (2008) and Barati et al. (2011).

Breakers for VES Fluids. Because VES fluids form association polymers from the coordination of vesicles in solution and do not have a polymer backbone, different types of breakers and formation cleanup agents are required. These are claimed to be necessary because the VES fluids may enter the pores of the formation and, thus, may be more difficult to clean up. The authors of this book note that chemicals that act as FLAs (Section 0) also can help prevent the VES micelles from entering the formation.

Crews and Huang (2007) note that VES fluids will usually break when the fluid comes in contact with hydrocarbon fluids. Kefi et al. (2004) show a diagram (Fig. 4.58) of the effect of the hydrocarbons on the viscosity of a VES fluid. The theory is that the hydrocarbons convert the tangled wormlike micelles into spherical micelles that produce much less viscosity. However, to produce more hydrocarbons during the cleanup time (possibly as many as 90 days), internal breakers that mimic (or provide) hydrocarbons are being used to speed the process. Kefi et al. (2004) (Fig. 4.59) show a chart of the viscosity of a VES fluid with and without a breaker (several compounds are described later in this section)

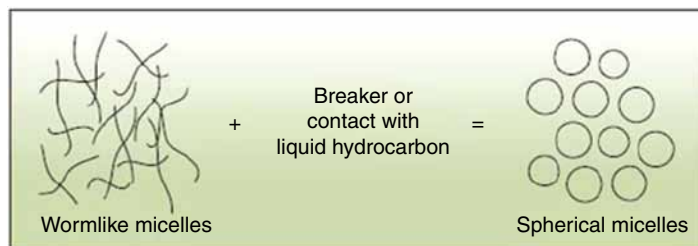


Fig. 4.58—Effect of hydrocarbons or breakers on VES (Kefi et al. 2004).

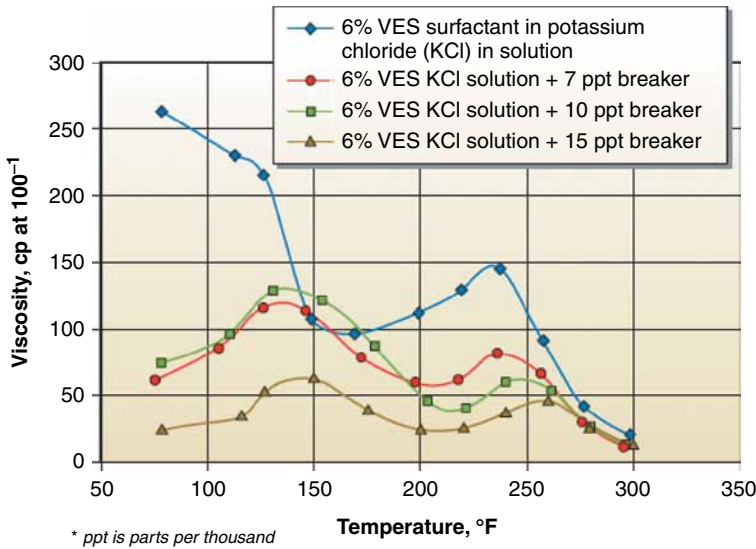


Fig. 4.59—Effect of breakers used at various concentrations on viscosity of VES fluids (Kefi et al. 2004).

and contend that field tests show more oil is produced when a breaker is included with the fluid. The figure shows that without a breaker, the viscosity stays high until the temperature reaches about 150°F.

Crews and Huang (2007) claim that internal breakers are compounds placed within the VES fluid during surface mixing that will (1) go wherever the fluid goes, (2) ensure the VES fluid breaks, and (3) break the VES fluid into an easily producible fluid. From this point of view, using internal breaker is like adding the required amount of reservoir hydrocarbons to the VES fluid at the surface, ahead of time, so complete break in VES fluid viscosity will occur over time at reservoir temperature without the need for contacting reservoir hydrocarbons.

The use of internal breakers should also improve (1) the rate and ease of VES fluid cleanup, and (2) prevent viscous emulsions from forming when problematic reservoir hydrocarbons contact, mix with, and break VES-laden fluid in the reservoir. Compounds that have been proposed as breakers for VES fluids include unsaturated fatty acids and mineral oil. Crews and Huang (2008) claim specific compounds such as linoleic acid, omega-3 fatty acids, omega-6 fatty acids, stearidonic acid, eleostearic acid, eicosadienoic acid, eicosatrienoic acid, arachidonic acid, or eicosatetraenoic acid. These materials have fatty (hydrocarbon) functions that act like produced hydrocarbons but are faster to reduce the VES viscosity.

Li et al. (2008a) have filed a patent application for breakers for VES fluids that are polyols, for example, natural and synthetic sugars, monoalcohols, and mixtures of the two. The sugars also may be ketones and aldehydes. The sugars are also claimed to be breaker aides for oxidizing agents that may be included to help break the fluids and include sorbitol, fructose, sucrose, lactose, dextrose, maltodextrin, and sucralose.

Lin et al. (2008) also claim a bromate oxidizing agent and a breaking activator for the bromate oxidizing agent, selected from the group consisting of acid-generating breaking activators, oxidizing or reducing sulfur containing breaking activators, and reducing agent breaking activators. The activators claimed are persulfates, thiosulfates, thiosulfites, dithionites, dithionates, tetrathionates, hyposulfites, bisulfites, metabisulfites, and aldehydes.

4.7 Additional Frac Additives

A large number of additional chemicals are being mixed with the fracturing fluids to enhance the performance of the treatment in particular situations. Included in this section are friction/drag-reducing agents (DRAs), foamers, biocides, and formation/fluid stabilizers. Table 4.1 shows a list of common additives. Subsequent sections (4.7.2–4.7.5) describe details of the chemical and chemistries of action of these additional chemicals. Note that some of these chemicals were also used as additives (and mostly for the same reasons) in reactive stimulation fluids (Section 3.6).

4.7.1 FR/DR Agents. Partially HPAAs are commonly used as FR/DR agents during fracture treatments. Fig. 4.48 shows a structure. Section 4.4.3 describes the chemistry of these synthetic polymers. These polymers can be used at low loading (less than 10 lbm/1,000 gal) to reduce the horsepower required to pump water at high rates. In fracturing, various HPAAs are the most prevalent friction-reducing agents (FRAs). However, Kelland (2009) has a whole chapter (Chapter 17) on DRAs that are used in various oilfield applications. Oil-soluble polymers such as polyalkylenes and polyolefins are used to reduce the drag in various pipelines. In addition to the HPAAs materials, water-soluble DRA polymers include polyethyleneoxides, polyvinylalcohols, and various polysaccharides such as the guar and CMC and HEC. Surfactants such as some of the betaines also may act as DRAs.

In SW formulations, biocides, KCl, and clay control agents are mixed with low concentrations of HPAAs. (Kaufman et al. 2008). These authors have tested various types of HPAAs polymers. They note that nonionic, anionic, and cationic HPAAs are available. The nonionic and anionic varieties can be made by partial hydrolysis of the PAA, but the cationic materials must be produced as a copolymer of anti-agglomeration inhibitor with a cationic monomer such as an vinyl quat ($-\text{CH}=\text{C}[-\text{CONH}-\text{RN}^+(\text{CH}_3)_3]-$). The authors of this paper recommend testing to determine the most effective FRAs for the specific fluid in use.

Sun et al. (2011) claim that FRs used in SW fracturing can cause damage to the formation and, especially, to natural fractures because of their chemical nature as high MW polyacrylamides and because of the large volumes injected during a typical treatment. They claim that such concerns can be addressed with two approaches:

1. Developing more effective FRs with (a) more efficient polymers and/or (b) faster hydration to shorten the dormant period before FRs are fully hydrated, considering the fact that fluids typically travel from surface to perforation within only 3 minutes.
2. Developing breakable FRs, which are effective during pumping but degrade under downhole conditions, leaving little residue. The authors of the report to have developed less damaging chemicals, but did not describe the chemistries. As noted in Section 4.6.3, HPAAs fluids also may require external breakers based on known oxidizers for good cleanup.

Kelland (2009) and Chesapeake (2010) also note that hydrocarbons have also been used as FRs in some deep shale treatments. However, the use of hydrocarbon fluids such as diesel oil (a toxic fluid) is being restricted in some states where shale gas formations are being fractured (Rehm 2011).

Shah and Vyas (2010) discuss an experimental study of two commonly used DRs, HPAAs—ASP-700 and ASP-820—flowing through CT with different salinities and temperatures. Both small-scale and large-scale flow loops were used in this study. The small-scale flow loop included a 1/2-in.-outside diameter smooth CT, while the large-scale flow loop included 2 3/8-in. rough CT. Elevated temperature tests and salinity tests are conducted using optimum concentrations of DRs in fresh water, 2% KCl, and synthetic seawater. The flow data gathered were analyzed and used to develop correlations that can predict drag reduction at different salinities and temperatures. The developed correlations show reasonable agreement with experimental data.

The following conclusions were reached:

- They claim that ASP-700 and ASP-820 polymers are found to be equally effective in exhibiting adequate drag-reducing properties under various conditions of elevated temperature and increased salinity that will be encountered in many industrial applications. Drag reduction in the range of 30 to 65% is reported.
- The chemical degradation of polymers has been observed. Because of the differences in the synthesis process of ASP-700 and ASP-820 polymers, ASP-700 was found by Shah and Vyas (2010) to be more resistant to chemical degradation at elevated temperature and increased salinity. This indicates its superior performance under such conditions.
- In case of ASP-820, the authors of the report claim that the effect of increased salinity is more pronounced at low Reynolds numbers.

4.7.2 Surfactant Type Foaming Agents and Flowback Aids. Surface active chemicals are used in most fracturing fluids and provide several important functions including control of surface wetting, producing foams, and as flowback agents (FBAs). Because surface wetting was described in Sections 1.4.2 and 3.6.2 and will be the subject of further discussion in Section 5.9, foams and FBAs are described in this section.

Foams and Foaming Agents. These types of chemicals were described in Section 1.4.4 and are used as diverting agents in matrix acidizing treatment (Section 3.7.2) as well as in enhanced oil recovery (Section 5.6.2 and 5.8.3). Table 3.15 also gave a description of various types of surfactants that can be used to produce foams. These foamed/energized fluids have value in fracturing when the formation is water sensitive. In addition, they may be less expensive as the amount of liquid may be reduced compared with a liquid fluid. Gulbis and Hodge (2001) note that foams used for fracturing include a liquid phase (aqueous) and a gas phase that may include N_2 , natural gas, or CO_2 . Nitrogen and carbon dioxide are the usual gases.

The fluid can be made up entirely of a brine (KCl or possibly seawater) and surfactants; however, Gulbis and Hodge (2001) claim that viscosifying the liquid phase with a polymer is an effective method for increasing the stability of foams (Wendorff and Ainley 1981). The thicker the continuous phase, the more difficult it is for the gas bubbles to move together and coalesce. Guar, HPG, and xanthan gum have been used as stabilizer. A further improvement in foam stability can be achieved by crosslinking the polymer in the aqueous phase (Watkins et al. 1983). The liquid phase then becomes viscous enough to maintain dispersion of the gas bubbles, even at foam quality less than 40%. Thickening the liquid phase also improves foam rheology and FL control. Proppant concentrations in the foamed fluid are generally lower than the concentration achieved with single-phase, liquid treatments. Therefore, a larger volume of foam may be required to place the desired amount of proppant. CO_2 as a foam or as an energizing agent has been used extensively because the foam may be more stable (Gulbis and Hodge 2001), but then metallic crosslinkers may be needed because the pH is too low for use of borates.

Lin et al. (2009) note that foamed fluids have been used in HF since the 1970s (Chambers 1994). Among many benefits foamed fluids offer over nonfoamed fracturing fluids, one is that they have stored compressed gas for quick cleanup, efficiently returning the injected fracturing fluid to the surface. Thus, foamed fluids are particularly suitable for depleted or underpressured gas wells. Foams also minimize the amount of water injected into a well while providing superior rheology (Reidenbach et al. 1986), making them excellent treatment fluids in water-sensitive formations. Furthermore, foams provide good FL control, improving the fluid efficiency. In addition to applications in HF, foams can also be used as diverting agents (Burman and Hall 1986) and employed in wellbore cleanout applications (Ozbayoglu et al. 2003). These authors claim that for optimal performance, the foam must remain stable throughout the treatment.

Pena, Salamat et al. (2009) list a number of nonionic, ionic, and amphoteric surfactants that can be used to form fracturing foams. A few examples include nonionic surfactants, which include, but are not limited to, alkyl alcohol ethoxylates, alkyl phenol ethoxylates, alkyl acid ethoxylates, alkyl amine ethoxylates, sorbitan alkanates, and ethoxylated sorbitan alkanates. Ionic surfactants include, but are not limited to, 60 anionic surfactants such as alkyl carboxylates, alkyl ether carboxylates, alkyl sulfates, alkyl ether sulfates, alkyl sulfonates, α -olefin sulfonates, alkyl ether sulfates, alkyl phosphates, and alkyl ether phosphates. Cationic surfactants include those such as alkyl amines, alkyl diamines, alkyl ether amines, alkyl quaternary ammonium, dialkyl quaternary ammonium, and ester quaternary ammonium compounds.

Using the equipment seen in Fig. 4.60, Lin et al. (2009) have tested several factors that affect foam stability, including the viscosity of the base fluid, the type and concentration of the foaming agent or foamers, the formation temperature, and the type and volume percentage of the gas phase. As noted by Chambers (1994), improved stability can be achieved by using linear polymer fluids or cross-linked gels. As temperature increases, the drainage of the liquid phase in the foam structure accelerates because of thermal thinning of the liquid, leading to reduced foam stability. For this reason, maintaining the foam stability becomes increasingly challenging at high temperatures. Selecting foaming agents is critical in formulating stable foams, especially at elevated temperatures. These investigators have used a high-pressure/temperature foam rheometer to perform some of the evaluation tests.



Fig. 4.60—Schlumberger-Chandler foam rheometer (Lin et al. 2009).

To do a test, the base fluids and gas were introduced simultaneously until the desired density was reached. After the desired temperature was reached and stabilized, the fluid was recirculated through the loop (Fig. 4.60). The apparent viscosity was determined from the pressure drop along the loop at various shear rates. The base fluids were 50 lbm guar/1,000 gal fluid with various foaming agents. Using these tests, the investigators identified improved foamers that were stable in the presence of CO₂ and at temperatures up to 275°F. A patent by Pena et al. (2009) identifies a special additive as an organoamino compound that is selected from the group consisting of tetraethylenepentamine, triethylenetetramine, pentaethylenhexamine, triethanolamine. These are used with polysaccharides as well as zwitterions-type surfactants and may act as pH stabilizers. Note that Kam et al. (2007) also found that foaming procedures conducted at high temperatures may require different surfactants compared with low-temperature operations, and testing at high temperatures is required.

Ribeiro and Sharma (2012) have developed innovative dynamic FL cells (see the article) to test foamed polymer containing frac fluids. They describe a laboratory apparatus that has been specifically designed and built for measuring the leakoff rates for both gas and liquid phases under dynamic FL conditions. This paper provides experimental leakoff results for linear guar gels and for N₂ guar foam-based fracturing fluids under a wide range of fracturing conditions. In particular, the effects of the rock permeability, the foam quality, and the pressure drop are investigated. Analysis of dynamic leakoff data provides an understanding of the complex mechanisms of viscous invasion and filter-cake formation occurring at the pore scale.

This study presents data supporting the superior FL behavior of foams, which exhibit minor liquid invasion and limited damage. It also shows direct measurements of the ability of the gas component to leak off into the invaded zone, thereby increasing the gas saturation around the fracture and enhancing the gas productivity during flowback.

Flowback Aids. Howard et al. (2010) describe the importance of using FBAs in fracturing treatments that include various surfactants and/or cosolvents. These chemicals are added to stimulation treatments to reduce capillary pressure and water blocks (see formation damage because of water blocks in Section 0).

These materials also may be used with fracturing fluids to speed cleanup. The authors note that as the stimulated gas reservoirs become tighter, the perceived value of these additives has grown. Also note from the Trabelsi and Kakadjian (2013) article, formation damage from SW HPAA gels may require cleanup chemicals (including oxidizing breakers) to remove the gel residues from the frac pack and the microcracks formed in the shale beds.

However, Howard et al. (2010) claim that this value must be balanced with the cost of the additives, which can be significant in SW fracturing treatments. There is a range of different flowback additives

containing water-wetting nonionic to amphoteric, ME, and oil-wetting components. Determining the best additive for a specific reservoir is not a simple matter for the end user, and the existing literature is full of conflicting claims as to which one is most appropriate.

The paper compares four different flowback aids: An ME, two water-wetting flowback additives, and an oil-wetting additive. Fig. 4.61 shows the structures of several different flowback aid chemicals that are based on the work of Hinkel and England (2001), Nimerick and Hinkel (1993), and Pursley et al. (2008). Laboratory testing was conducted to evaluate surface tension and contact angle for each flowback aid, using the recommended concentrations. Imbibition and drainage tests were performed that allowed calculation of the capillary pressures for the three additives.

Howard et al. (2010) report that drainage tests were performed on 1- to 3-md and 0.1-md cores. See Eqs. 1.25 through 1.29. Capillary-tube-rise testing was also conducted as a check of the coreflood testing capillary pressures. This provided several different methods to determine capillary forces for the flowback aids. In addition, fluid-loss testing was conducted to determine if the flowback additives could improve FL. See some structures in Fig. 4.61. All the flowback aids demonstrated low surface tension (approximately 30 mN/m), but each was different in terms of surface wettability and adsorption in the rock. In all cases, the flowback aids reduced capillary pressure to similar levels 70% lower than water alone. The authors note that one of the water-wetting additives had much stronger

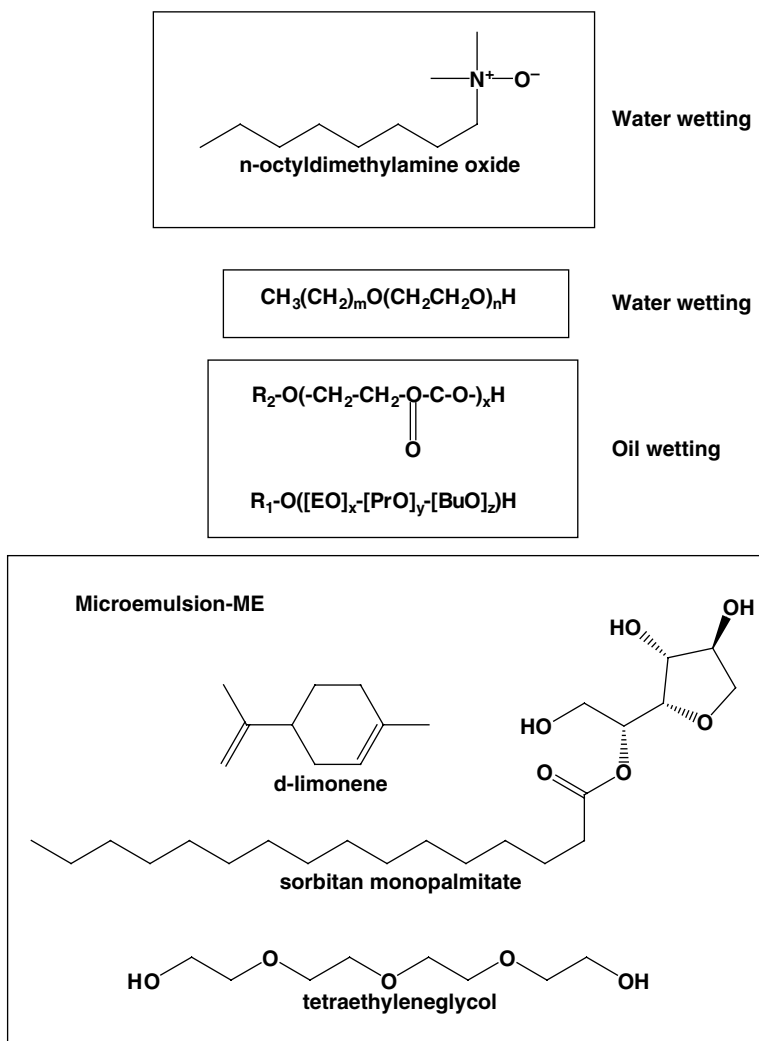


Fig. 4.61—Flowback additives.

adsorption in the core material than the other additives. The ME and the oil-wetting additive had improved FL in a fully formulated fracturing fluid. In spite of the low capillary pressures, the additives had little effect on cleanup or return permeability on cores greater than 1 md. Some other conclusions from Howard et al. (2010) were the following:

1. Drainage results in cores *greater* than 1 md did not show an improvement because of the flowback additives.
2. The amine oxide and the ME did show a cleanup advantage in the 0.1md cores.

Another conclusion was that FL studies and return permeabilities in 1-md Berea cores indicated that the additives decrease the FL coefficient, with the hydrophobic ME and isoalkyl alcohol having the greatest improvement. The linear ethoxylated alcohol lowered surface tension and reduced FL in a fully formulated fracturing fluid. The amine oxide left the water-wet surfaces with a higher contact angle than the other additives and was strongly adsorbing to the surfaces.

Luo et al. (2011) claim a flowback aid for fracturing that consists of a green surfactant (fatty acid MES) and a biodiesel fuel. The effects of NaCl and n-butanol mass concentrations, the type of alcohols on the ME phase behavior, and the optimal salinity and the salinity length were investigated. Lab test results showed that the ME phase state changed from Winsor I to Winsor III and then to Winsor II with the increase of salt and alcohol mass concentrations. The optimal salinity and the salinity length of the middle phase ME decreased with the increase of alcohol carbon chain length (see discussions in Section 5.5.5 for use of MEs in enhanced oil recovery). Luo et al. (2011) describe the basic formula of green fracturing cleanup additive as 0.5% MES nano-emulsion +0.0075% FC-006 + 0.015% Span80. Laboratory evaluation showed that the cleanup rate of MES middle phase ME was 87.07%, which was increased by 16%, compared to the cleanup additive CF-1. The permeability recovery ratio of reservoir was enhanced by about 2 times with the use of MES middle phase ME, which verified the potential application of an environment-friendly middle phase ME in improving fracturing cleanup effect.

As noted in other sections (4.1.1 and 4.10.1), fracture treatments in organic-containing shale deposits are an increasingly common process. Xu and Fu (2012) note that it is not an easy task to recover oil and gas from these low-permeability unconventional reservoirs. To enhance initial production (IP) and minimize production problems, surfactants, FRs, scale inhibitors (SIs), biocides, and sometimes clay stabilizers are typically pumped together with the frac fluids. The surfactant used in a completion procedure is just one component, but it can be crucial to enhancing IP in the unconventional oil and gas formations. These authors have tested a number of surfactants with various shale oils to produce a weak emulsion that will be easily broken after the fluids have been returned to the surface.

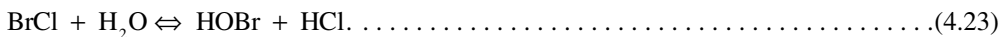
The authors (Xu and Fu 2012) used emulsion tests that also are used to evaluate enhanced-oil-recovery fluids, and the tests are described in Section 5.3.2 of this book. An important conclusion was that very low concentrations (< 1 gal/1,000 gal) could simply be adsorbed; however, when the weakly formed emulsions described in the paper were employed, more oil was recovered compared with offset wells. The tests showed that the CMC was about 1700 ppm/surfactant, so that amount is required.

4.7.3 Biocides. These materials are added to the frac water used to prepare polysaccharide-based fracturing fluids to prevent the action of bacteria from reducing the viscosity of the fluids. They also are added to enhanced-oil-recovery water and floodwater to prevent souring of the reservoir (Section 5.5.4).

Because many of the frac materials are sugars, fermentation types of reactions can happen readily, especially at the temperatures that of fluids in many areas. The use of mixing on the fly reduces the needs to some extent, because the frac fluid may not spend hours in a frac tank. However, these reactions may still happen downhole and may not be controlled. In addition, SRB may also be present, and these materials can multiply in the formation and turn it sour. Two different types of biocides are described by Kelland (2009). The two major classes are the following:

1. Oxidation chemicals such as chlorine, chlorine dioxide, bromine chloride, and various peroxides are in wide use. These materials are very effective for killing microorganisms and may be used to sterilize injection water.

Carpenter and Nalepa (2005) review information on the family of bromine-based biocides and discuss the basics of their chemistries and properties. They focus on a new stabilized bromine-chloride-based biocide that has been demonstrated in a SW fracturing-fluid field trial. See Eq. 4.23.



Here, excellent microbiological control was claimed to be maintained cost effectively with relatively low biocide residuals. These materials kill the bacteria by disrupting their cell membranes. The use of ozone, especially generated on-site has been described by McGuire and Jakhete (2010) as a more environmentally acceptable way to treat frac water. Some of these materials may also act as surfactants.

2. The nonoxidizing biocides are recommended for carbohydrate-based frac fluids because they are less likely to destroy viscosity as well as the bacteria. These include aldehydes (glutaraldehyde), chlorophnates, and quaternary amines. Additional chemicals mentioned by Kelland (2009) include triazines and dithiocarbamates. Note that comparability with the frac fluids as well as with environmental laws must be considered.

Kaufman et al. (2008) also describe tetrakis-hydroxymethylphosphonium sulfate, as well as relative newcomer to the oilfield applications: tetrahydro-3,5-dimethyl-1,3,5-thiadiazinane-2-thione. This biocide (called thione) has been shown not to interfere with FR, is extremely effective in killing acid producing bacteria as well as SRB, and is a broad spectrum biocide. A discussion of similar chemicals is in Section 0.

4.7.4 Oxygen Scavengers/Reducing Agents. These materials are used to protect the polymers from oxidative attack (or pipelines from corrosion). Various reducing agents, especially sulfites, bisulfites, and metabisulfites are in current use to control the amount of O₂ in a fluid. Here, the reaction with a sulfite is



The authors of this book note that this reaction is slow at low temperatures (<100°C) and various metal salts [Fe(III), Mn(II)] are in use to act as catalysts.

Reducing agents such as sodium thiosulfate as well as methanol (not a strong reducing agent) are added to stabilize polymeric fluids to reduce the chance of premature reduction in viscosity because of free radicals. Gulbis and Hodge (2001) note that sodium thiosulfate is generally used at 10 to 20 lbm/1,000 gal. Sodium thiosulfate is the more effective of the two, increasing the viscosity at elevated temperatures by a factor of 2 to 10, depending on the temperature and time of exposure to temperature (Elbel and Thomas 1980). The mechanism for these stabilizers is not fully understood. It is believed that they act as oxygen scavengers and prevent the rapid gel degradation caused by dissolved oxygen. Walker et al. (1995) studied several oxygen scavengers and found sodium thiosulfate to be the most effective at maintaining gel stability. However, other reducing agents such as sodium erythorbate are not effective compared with thiosulfates.

Kelland (2009) also lists several other chemical types (see Chapter 16 of his book) including

- Dithionite salts
- Hydrazines
- Oximes

This author also lists nonchemical processes that [such as MINOX—Henriksen et al. (1984)] are used to strip O₂ for oilfield waters before use.

TABLE 4.2—COMMON BUFFER SOLUTIONS

| Buffer | pK_a |
|---|--------|
| Sulfamic acid/sulfamate | 1.0 |
| Fumaric acid/hydrogen fumarate | 3.0 |
| Formic acid/formate | 3.8 |
| Benzoic acid/benzoate | 4.2 |
| Acetic acid/acetate | 4.7 |
| Dihydrogen phosphate/hydrogen phosphate | 7.1 |
| Ammonium/ammonia | 9.3 |
| Bicarbonate/carbonate | 10.4 |

4.7.5 Fluid Stabilizers, Formation Stabilizers, and SIs. This section describes additional classes of fracturing additives that help to stabilize the formation being treated or prevent formation damage.

Buffers. These types of additives are used to stabilize the pH, especially as the temperature increases. Common materials in use are various carbonates and phosphate salts. **Table 4.2** from Fink (2003) shows the pK_a values of various buffer solutions. Chelating agents such as ethylenediaminetetraacetic acid or hydroxyethyl ethylenediaminetriacetic acid can be added to some fluids to control the effects of Ca^{2+} or Mg^{2+} ions if seawater or formation water is used to mix a gelling agent. Any gelling agent containing a carboxylic or sulfonic acid group (CMHEC, CMC, HPAA, amphoteric/anionic VES agents, as well as amphoteric/anionic foaming agents) will have some sensitivity. Crews (2006) notes that various types of chelating agents including ethylenediaminetetraacetic acid, hydroxyethyl ethylenediaminetriacetic acid, hydroxyethyl iminodiacetic acid, and other organic acids can be added to aid/retard crosslinking reactions.

Clay Control Chemicals. To stabilize the formation and to prevent fines migrations that will damage the formation of the pack, these types of chemicals are frequently used with frac fluids. The mechanisms are seen in Figs. 1.31, 3.70, 3.71, and 3.72, and some of these materials were described in detail in Section 3.6.4.

Chemicals that are used routinely in fracturing fluids include KCl, which is used in most water-based fluids. Recent improvements for frac fluids are abstracted.

El-Monier and Nasr-El-Din (2011b) and El-Monier and Nasr-El-Din (2011c) describe the testing of all *inorganic* clay control agents that contain polymerized Al and Zr compounds. Coreflood and zeta potential testing have shown the formation (Berea sandstone) treated with these metal polymers to be resistant to high pH (12) fluids and resisted clay production and loss of permeability. The authors claim that the lab results indicated that the new clay stabilizer worked effectively up to 300°F. No reduction in permeability was noted in any of the coreflood tests using sandstone cores of various mineralogies and initial permeabilities. The concentrations of various cations were found to be a function of core mineralogy. In parallel tests, tetramethylammonium chloride and choline chloride (Fig. 3.72) was not effective when followed by fresh water and incompatible with the high pH fluids. Data on the new stabilizer is claimed by the authors to lower toxicity values compared with the nitrogen quats, but because they are inorganic compounds, they are not biodegradable and would persist in the environment. They are claimed to be useful in HF and alkaline-based chemical enhanced-oil-recovery methods to mitigate clay-related problems.

Huang et al. (2010) claim a fracturing fluid, gravel-pack fluid, and/or frac-pack fluid containing particles such as proppants, gravel, and/or sand may contain an effective amount of a nanosized particulate additive to fixate or reduce fines migration. The particulate additive is an alkaline earth metal oxide, alkaline earth metal hydroxide, alkali metal oxides, alkali metal hydroxides, transition metal oxides, transition metal hydroxides, post-transition metal oxides, post-transition metal hydroxides piezoelectric crystals, and piezoelectric crystals. The nanosized particulate additive is bound to the particles with a coating agent such as an oil. The particle size of the magnesium oxide or other agent may be nanometer scale, which may provide unique particle charges that help fixate the formation fines. The carrier fluid used in the treating fluid may be aqueous, brine, alcoholic, or hydrocarbon based.

Belcher et al. (2010) describe nanoparticle technology based on Huang et al. (2010) and was applied in conjunction with HF to combat the fines migration issue. The particular case in this paper is focused on the Gulf of Mexico. The use of nanotechnology in a hydraulic fracture allowed the operator to achieve near-IP rate without producing fines particles. The postponement of fines entering the near-wellbore region will also protect the investments made in the downhole assembly and fracture as well as surface equipment, while extending the production life of the well and minimizing the frequency of intervention.

SIs. These materials may be needed if the fracturing fluid dissolves enough soluble materials (calcite, dolomite) to exceed the scaling index of the fluid, and then as the pH changes, mineral scales may form. In addition, contact between the frac water and formation brines also may form scale. The formation of mineral scale and the use of SI materials are described by Frenier and Ziauddin (2008) and an abstract is in Section 2.2 of this book. Frenier and Ziauddin (2008) also note that SIs can be delivered using fracturing-fluid treatments. Additional new information on the use of proppant-containing SIs was described in Section 2.2.3 of this book.

The current trend of using HF to stimulate gas and oil-shale formations (very low permeability) with millions of gallons of aqueous fluids (Section 4.10.1) requires operators to be aware of the changing nature of the fluids flowing back from the wells (more details in Sections 4.8.1 and 6.3). Szymczak et al. (2012) have described possible scale-related conditions in the Bakken play in North Dakota and note that significant, but variable quantities of calcium, magnesium, strontium, and iron are present in the waters recovered from the wells. The amount of calcium present in the waters ranges from approximately 10,000 to 15,000 mg/L. Bicarbonate levels commonly fall in the 350 to 600 mg/L range but can be over 800 mg/L. The pH monitored in the water is from about 5.5 to 6.5. In a few cases, pH has been above 7.0. These conditions could produce significant scaling problems. These authors also claim that conventional phosphonate SIs are in use and residual were measured routinely by the chemical vendor with an inductively coupled plasma instrument. However, production results indicated that 7 of 20 *failed wells* for which data was available showed SI residuals in the ranges from 50 to 100 ppm while 9 of 20 showed less than 50 ppm. Moreover, they note that the calcium carbonate scaling tendency at the time of the water sampling was moderate to heavy. Thus, even with residual samples that showed the presence of excess inhibitor, there were well failures.

To solve this problem, Gupta et al. (2010) and Szymczak et al. (2012) describe the use of solid chemical SIs placed in the formation during HF, which are claimed to have provided inhibition protection for up to 5 years. According to the authors, the longest documented treatment has been in the ground for over 5 years. Placing a solid chemical inhibitor into the formation via the fracturing process requires a product that is compatible with the fracturing fluid, is claimed not to adversely affect conductivity, and provides long-term inhibition through the controlled release of the inhibitor into the produced fluid. The solid inhibitor is added to the fracturing proppant. The goal is to maximize the inhibitor loading, minimize the chemical release rate without negatively impacting the stimulation. The authors claim that the use of the SI-loaded-proppant additives has helped more than 160 wells remain free of damaging scale for several years.

Adams (2002), Willberg et al. (2006), and Bourne et al. (2000) also have described SI impregnated solid proppants that can place the SI chemicals deep into the frac pack for long-term water treatment. More details are described by Frenier and Ziauddin (2008).

Shen et al. (2012) claim that special SIs are needed in high Fe-containing shale flowback waters to protect these wells from failure because of formation of scale (calcite as well as barite) in the near-wellbore area as well as the frac pack, tubulars, and gathering lines. Because the shale formations have very low natural permeability scale in these critical areas, it could kill the well. See Section 4.8.1 for details as to the reactions of the frac fluids with the formation and discussions of solutions by Shen, Shcolnik et al. (2012).

Summary of Fracturing-Fluid Additives. This section has described additives that include surfactants for producing foam or are used as flowback aids to improve frac-pack cleanup. Various other surface active materials may be added to control scale or organic deposits. Buffers also may be added to control the pH during viscosity formation of during breaking. While the additional materials may

play an important role, rigorous testing must be performed to ensure that the primary role of the fluid that is proppant placement is not degraded.

The next section reviews some possibly undesirable reactions between the fluids and the formation or the produced fluids that may require the addition of chemicals described in Section 4.7.

4.8 Reactions of Fracturing Fluids With Formations and Well Fluids

Fracturing fluids are designed to be inert to the formation minerals and to the well and formation fluids. The first two fluid/proppant selection criteria in Section 4.10 are compatibility with the formation and with the formation fluids. This section will explore possible reactions that may require a modification of the process by the use of additional chemicals or use of a different fluid. Many of these interactions were reviewed in Sections 2.3 and 2.4 because these problems cause formation damage and emulsions. The additives described in Section 4.7.5 help to eliminate some of these effects.

4.8.1 Reactions With Formation Minerals. This section includes interactions that are in addition to polymer-cake damage described in Section 4.6.3.

These types of reactions include the dissolution of easily water-soluble minerals such as halite (NaCl) and acid soluble minerals including calcite, dolomite, FeS, and some iron oxides. Clays and feldspars should not be soluble in any aqueous fracturing formulation that was not intended for such a purpose, and these were described in Section 3.8.6. However, silicate minerals can be dispersed, flocculated, or swollen by aqueous fluids. Organic solids associated with shales, coal seams as well as asphaltenes in oil wells could be affected by both aqueous and oil-based fracturing fluids. Finally, components of the fracturing fluids will adsorb and then precipitate on mineral surfaces during a treatment. This is part of the FL process as well as a consequence of fracture fluid breakdown and cleanup.

Specific known reactions that may produce undesirable products could include the use of HCl as part of an initial breakdown fluid. As noted in Eqs. 3.1 and 3.2, dissolution of any calcite or dolomite will produce large amounts of Ca^{2+} and Mg^{2+} ions. In addition, reactions with acid sensitive clays can produce Al^{3+} ions as well as possibly precipitate hydrous silica (Hartman et al. 2003). These materials may interfere with crosslinking or produce formation damage. Kaufman et al. (2008) recommend using SIs (see Section 4.7) because some water-based frac fluids also may dissolve carbonates. CO_2 -containing fluids have low pH values and could dissolve these types of minerals.

Shen et al. (2012) have been investigating the minerals dissolved by the fracturing water during shale gas production. The authors note that in contrast with conventional reservoirs, shale gas reservoirs like the Marcellus formation do not produce water naturally. The composition of the water recovered during production is a function of the frac water source and the chemical reaction that occurs with the shale. Also, view the overall discussions of handling flowback water in Section 6.3.

The reactions that take place during the fracturing process occur through the contact of the frac water with the fracture face over time. The first water produced from the wells is described as flowback water and is characterized by gradually increasing total dissolved solids over time. Eventually the total dissolved solids level plateaus. Significant but variable quantities of calcium, barium, strontium, and iron are present in the waters recovered from the wells. The amount of calcium present in the waters ranges from approximately 10,000 to 25,000 mg/L.

Shen et al. (2012) claim that the barium present will range from 3,000 mg/L in West Virginia and southwestern Pennsylvania to 17,000 mg/L in northeastern Pennsylvania. Strontium commonly falls in the 3,000 to 6,000 mg/L range but can run over 10,000 mg/L. Dissolved iron is present in the waters from about 50 to 300 mg/L. Theoretical analyses of these waters indicate a propensity toward the formation of calcium carbonate, barium sulfate, strontium sulfate, and iron-related scales. To date, Shen et al. (2012) claim the scale deposits analyzed have comprised calcium carbonate, iron-related scales, and sodium chloride. The saturation indices calculated for barium sulfate scales in various parts of the play can be in the hundreds or thousands, thereby potentially overloading the SI. At the same time, a high level of dissolved iron (200 ppm) commonly present in the water may be reducing the SI performance.

As noted in Section 4.7.5 (above), SI are commonly used in frac fluids to combat scaling and loss of well productivity. However Shen et al. (2012) describe studies that show that the high level

of dissolved iron commonly present in the water adversely affects the ability of the current SIs to inhibit calcium carbonate scale. Under these conditions, they claim that two new chemicals (not identified) were able to control calcium carbonate scale effectively in the presence of dissolved iron up to 200 ppm, whereas the performance of polycarboxylic acid, amino tri(methylene phosphonic) acid, and carboxymethyl inulin dropped sharply even in the presence of small amounts of Fe^{2+} (5 ppm). The inclusion of iron-sequestering agents with these chemicals and the effect of iron upon calcium sulfate inhibition are also discussed in this paper. Sections 2.2.4 and 2.2.3 of this book discuss recent new applications of SIs and corrosion inhibitors to supplement the material in Frenier and Ziauddin (2008).

The swelling and migration of some clay types as well as unidentified formation fines is well documented (Fink 2003). This author has devoted a significant part of a chapter in his book to the discussion of clay control chemicals. The chemicals are described in Sections 3.6.4 and 4.7.

4.8.2 Reactions With Well Fluids. Formation brines contain a wide variety of cations and anions that may react with the various aqueous and nonaqueous frac fluids. Ca^{2+} and Mg^{2+} ions will complex and or precipitate gelling agents such as HPAA, CMC, and CMHEC. These ions also may affect both crosslinkers and breakers. The pH changes in the presence of the ions may cause scale (calcite) to form. Cenegy et al. (2011) have produced a detailed study of the effects of the high bicarbonate content (caused by the alkaline frac fluid flowback mixing with formation water) on scaling. Also, see Section 4.7.5. A mixing water simulation (Cenegy et al. 2011) was run from zero to 100% formation water mixed with the simulated fracturing fluid (with two different alkalinity levels—red 1000 mg/L and blue 600 mg/L in Fig. 4.62), at 235°F and 600 psi. The results are shown in Fig. 4.62 and indicate that blending of formation water into frac water increases the calcite scaling potential and represents the quantity of calcium carbonate scale that could form as the water composition ranges from no formation water to 100% formation water. The largest quantity of scale deposited occurs at about 15% formation water (for both alkalinity concentrations of frac water), after which further dilution of the simulated fracturing-fluid aqueous phase by produced water only serves to reduce the available alkalinity and lower the pH (and thus less scale). The authors have shown a direct relationship between the total amount of produced water and onset of pump scaling.

The high ionic strength of some well brines may affect polymer stability. These dissolved salts also may greatly affect VES fluids. Liquid hydrocarbons may be emulsified by various fracturing fluids and these fluids may actually be breakers for some fracturing fluids such as some VES materials.

Fracturing fluids, especially those with surfactants, can form emulsions described in Section 2.4. The next subsections (in 4.9) describe properties and chemistries of the solid proppants that must keep the frac open after the fluids have placed them, then flow back to the surface.

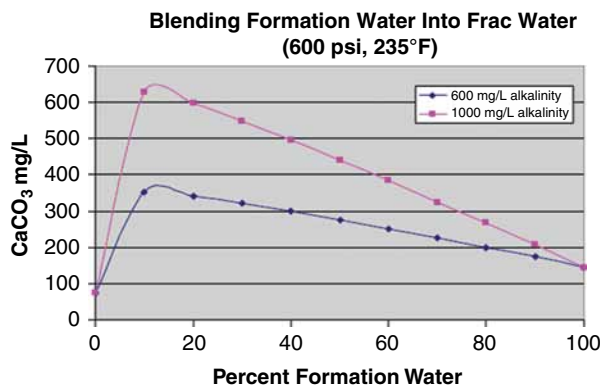


Fig. 4.62—Blending of formation water into frac water that gives a calcite scaling potential (Cenegy et al. 2011).

4.9 Proppants and Proppant Aids

Sections 4.4 and 4.5 gave detailed descriptions of various fluids that are needed to cause the fracture to form and to support the proppants during placement. Various proppant materials are needed to keep the fracture open and provide the highly permeable path for production of the hydrocarbons that are critical to the success of this type of treatment. This section (4.9) provides details of the solid proppant materials. A general list of proppant types was provided in Section 4.2. Gulbis and Hodge (2001) note that proppant selection significantly affects the final results of the procedure. Characteristics that are important include

- The physical composition and processing that determines the
 - Proppant strength
 - Grain size and size distribution
 - Quantity of fines
 - Roundness and sphericity
 - Density
- Coating on the proppant
- Movement in the fracture
- Flowback

This section will review the types and characteristics of the various proppants as well as the methods to stabilize the frac pack for long-term production. The sequence of proppants described in the following is listed by toleration to increasing fracture closure pressure, and the conditions where they are recommended (Gulbis and Hodge 2001) are

- LWPs < 5000 psi, SG < 2.0, including lightweight (lt.wt) ceramic, SG = 2.75
- Sand for closure stress < 6000 psi, SG = 2.65
- RCP—closure stress up to 8000 psi, SG = 2.65
- Intermediate strength proppant (ISP) to 10,000 psi, SG ≈ 3
- High-strength proppant (HSP) to >10,000 psi, SG = 3.4–3.7

Because the proppant crush strength as well as the *products* from crushing the proppant has consequences for the pack permeability, stability, and particle production, a discussion of testing is required.

The authors refer to *ISO 13503-2* (2006) that provides standard testing procedures for evaluating proppants used in HF and gravel-packing operations. The objective of the standard is to provide a consistent methodology for testing performed on HF and/or gravel-packing proppants. A specific crush test is in *API RP 56* (1995).

Palisch et al. (2010a) also have reviewed the crush tests (*ISO 13503-2* 2006; *API RP 56* 1995) and have made a number of conclusions:

- Crush-test procedures are standardized and described in *ISO 13503-2* (2006) that replaced the testing procedures contained in *API RP 56* (1995) *API RP 60* (1989a).
- While crush testing plays a valuable role in proppant identification and in manufacturing quality control, caution must be exercised when using the results of these tests for proppant selection in fracture designs.

Some of the pitfalls and misconceptions associated with crush testing and crush results include the following:

- Many aspects of the crush test do not mimic actual fracture conditions.
 - Crush-test results are extremely sensitive to the loading technique employed during the procedure.
 - Applying crush results from wide fractures to typical narrow fractures is invalid because the narrower fractures result in elevated crush.

- Crush percent typically increases as proppant sieve size increases, but larger particles actually have higher-individual-grain-strength than smaller particles.
- Crush percent does not indicate how much proppant has been damaged.
- Resin coating does not improve the strength of individual proppant grains.
- Not all proppants crush in the same manner.
- Different proppant packs are affected differently by fines.
- Caution must be exercised when modifying the crush test to be more realistic.
- It is inadvisable to make direct, quantitative correlations between crush and conductivity. Rather, conductivity tests should be run at realistic conditions to measure directly the conductivity that will inherently include the effects of crush, fines, temperature, fluids, etc.
- Care should be taken when comparing the crush of two proppants, as there are many things that can be done to reduce crush that either do not change the proppant-pack conductivity or more often reduce it.

Despite the opinions and cautions of Palisch et al. (2010a), the crush strength test is usually the first criterion of choice depending on the closure pressure of the well. Fig. 4.63 shows a chart with typical closure strength for some proppants and the amount of permeability seen at various closure pressures. Note that the crush strength is not a specific number, but a range of usability.

There are other selection criteria and Gulbis and Hodge (2001) describe several additional general considerations about proppants.

- Proppants with larger grain sizes provide a more permeable pack because permeability increases as the square of the grain diameter increases; however, their use must be evaluated in relation to the formation that is propped and the increased difficulties that occur in proppant transport and placement.
- Larger grain sizes can be less effective in deeper wells because of greater susceptibility to crushing resulting from higher closure stresses (as grain size increases, strength decreases). Larger proppants have more placement problems. These include that a wider fracture is required for the larger grains, and the particle settling rate increases with increasing size.
- The roundness and sphericity of a proppant grain can have a significant effect on fracture conductivity.

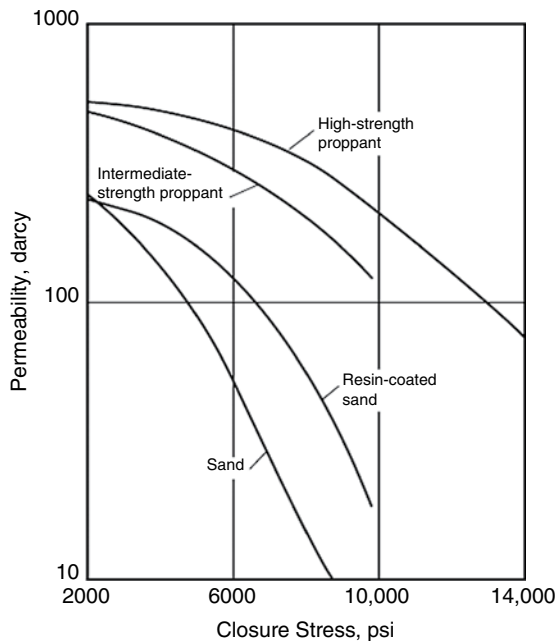


Fig. 4.63—Proppant conductivity and closure stress (Gulbis and Hodge 2001).

- Proppant density has an influence on proppant transport because the settling rate increases linearly with density. Therefore, high-density proppants are more difficult to suspend in the fracturing fluid and to transport to the top of the fracture.
- Cost is always a factor and must be part of the selection process. Generally, the more highly processed proppants are more costly.

The next sections (4.9.1–4.9.6) describe more details of the characteristics of proppants and proppant aids in current use. Section 4.10.2 describes more selection guides.

4.9.1 LWP. This category includes material such as polymeric proppants, resin-coated walnut hulls, and low-density ceramics. Mohanty (2009) has tested some of these types of materials for use in fracturing shale formations (such as the Barnett shale). Because the fracture length in these horizontal wells may be quite long, a dense proppant such as Ottawa sand ($SG = 2.5$) may not be suitable (because it may settle too fast, especially if SW is used). The types of materials described by the author have specific gravities that range from 1.08–1.75 and have bulk density (g/cm^3) from 0.66 to 1.2. This author has tested the crush resistance of these materials at the pressures of the Barnett shales and has claimed they are acceptable; however, some of these produce significant amounts of fines, so conductivity tests were recommended. If acceptable to operators, these materials could be used with SW fracs and foam frac fluids.

Kulkarni (2008) has reviewed the use of LWPs and has determined the crush characteristics of coated/impregnated walnut hulls. He concluded that walnut hulls offer realistic potential to be adopted as proppants. Polymer-coated walnut hulls have displayed significant improvement in resisting high-closure stresses at the downhole conditions in industrial laboratory tests. He noted that the addition of a resin coat introduces stiffening in the response of the walnut hull, but the increase is marginal. The maximum force applied was 100 N (4,500 lbf).

Hollow ceramic spheres also have been proposed as LWPs. A hollow spherical solid may have the strength of a ceramic material with the SG of a much lighter material because of the internal void. If the proppant could have neutral buoyancy (SG same as the fluid), proppant placement may be greatly improved, and simpler fluids (without polymers) may be employed. Cutler et al. (1981) and Jones and Cutler (1985) have described the manufacture of hollow ceramic particles that could be used as proppants.

The authors contend that spray drying into a fluidized bed appears to be a viable method for producing both porous and hollow proppants. The details are that the hollow proppants are made from a fine ceramic powder that is preferably produced by dry milling or a like process, which is then well dispersed in an aqueous slurry. They claim that the slurry is pumped through a nozzle into a spray dryer and the spray drying parameters, thereof, are controlled to make hollow spheres, preferably in the 600–1000- μm diameter range. The ceramic spheres are then sintered in air at an appropriate temperature so as to retain the small grain size, with a permitted shrinkage in the 125–2250 mm in diameter range, preferably in the 400–800 mm range. The authors claim that the SG of the particles were 2.25–3.35 and had acceptable crush characteristics at 10,000 psi.

Barron (2005), Smith et al. (2008), and Barron (2009) claim methods for producing lightweight ceramic spheres based on nanosized alumina particles. The processes start with hollow template particles (various polymers, glass spheres, or ceramic spheres) that are contacted with carboxy alumoxane. This is produced by the reaction:



The process is outlined in **Fig. 4.64**, where photos of the spherical particles are seen.

An application by Smith et al. (2011b) claims the methods of this invention are aimed at the fabrication of proppants that exhibit neutral buoyancy, high crush strength, high sphericity, narrow size distribution, and/or high smoothness. These materials, thus, may have the ability to materially reduce and/or possibly eliminate the need to employ expensive and reservoir permeability-destroying polymer

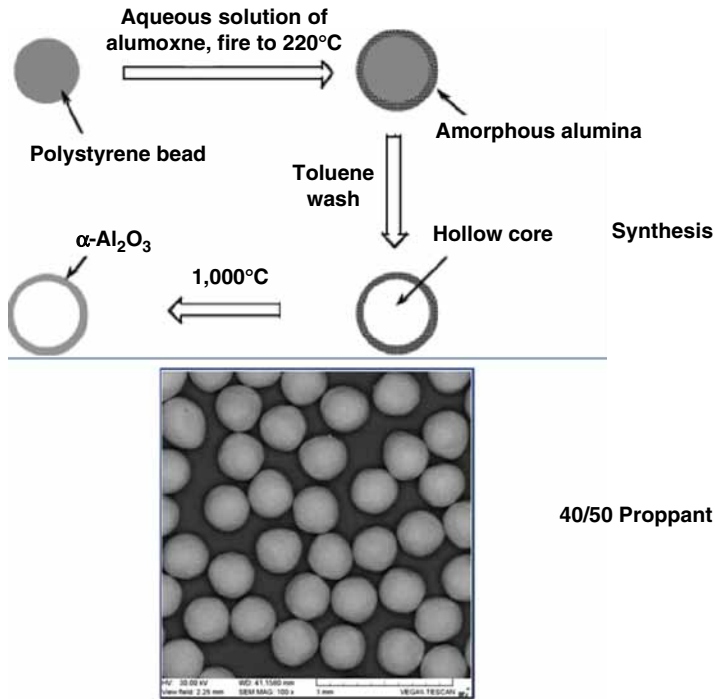


Fig. 4.64—Synthesis method and photos of hollow ceramic proppants (Barron 2009).

carrier gels. The authors of this book note that these would be very important characteristics; however, the fluids described in Section 4.3.5 of this book must have a very large range of properties to fit many thousands of different well fluid/formation requirements.

The authors (Barron 2009) report that particles with an SG of approximately 2 can be made and are able to provide satisfactory crush resistance at 5,000 psi.

4.9.2 Sand. This common mineral is the least expensive and most common fracturing proppant. Chemically, sand is composed mostly crystalline SiO_2 (quartz). The actual chemical composition can vary greatly and also may contain chert (mostly silica) and igneous rock. The brown color usually indicates the presence of iron. Several different types of frac sand include northern white sand, Texas brown sand, and several varieties of silica sand. Frac sand (see Fig. 4.65 for an example) is generally available in sizes from 12/20 to 40/70 mesh sizes. Mesh size refers to the particle size distribution of proppant grains. Mesh size is notated with a fraction, which increases as grain diameter decreases. For example, 12/20 proppant is smaller in diameter than 20/40 proppant. *API RP 56* (1995) specifies that 90 wt% of the sand must fall within a specified size range for a particular product. The generally defined frac sand products are 12/20, 20/40, 40/70, and 70/140. For example, to meet the requirements of a 20/40 product, 90 wt% must be $-20 + 40$ mesh. This can be achieved through high-efficiency screening. Silica sand has been deslimed to remove -100 mesh fines. The more highly colored sand products will contain some amount of iron as Fe_2O_3 .

WDNR (2012) notes that not all silica sands can be used for HF procedures. To meet the industry specifications [see discussions by Palisch et al. (2010a) and Gulbis and Hodge (2001)], frac sand needs to be nearly pure quartz, very well rounded, and must meet tight size gradation standards. As noted in Fig. 4.63 the sand must also have a high compressive strength, generally between 6,000 psi and 14,000 psi. The report says that sands that meet these specifications are mined from poorly cemented Cambrian and Ordovician sandstones and from unconsolidated alluvial sands locally derived from these sandstones. This report claims that sands derived from Quaternary glacial deposits, and most beach and riverbank sands are too impure and too angular to be used as frac sand. The report also describes the permitting, mining, cleaning, and shipping of frac sand to the wellsite operations.



Fig. 4.65—Frac sand (Halliburton 2005b).

Outotec (2008) lists the significant parts of the *API RP 56* (1995) specs for sand:

1. Grain size: *API RP 56* (1995) specifies that 90 wt% of the sand must fall within a specific size range for a particular product. The generally defined frac sand products are 12/20, 20/40, 40/70, and 70/140. (E.g., to meet the requirements of a 20/40 product, 90 wt% must be $-20 + 40$ mesh.) This can be achieved through high-efficiency screening.
2. Sphericity and roundness: Round or spherical quartz grains are a result of the deposition of the quartz deposit. Most deposits containing these preferred grains are geologically very old because over time the quartz grains have been rounded and nonquartz-type minerals removed. From a practical standpoint, there is no processing route that can change the grain shape.
3. Crush resistance: The resistance to crushing is a key consideration as it relates to the amount of fines generated after a product is subjected to a particular pressure, as defined by API. “Good crush deposits” tend to be older geologically because aging allows for the creation of the more pure quartz that is void of other, softer minerals. There are some processing routes that can improve the crush results by removing the majority of the softer minerals.
4. Acid solubility: For a product to have low-acid solubility, it must be primarily quartz with little to no other minerals present. There are some processing routes that can improve the acid solubility.
5. Turbidity: The amount of silt and clay-sized particulate matter is also important. Some deposits are naturally low in fines, but when they are present, there are processing routes that can improve these criteria.
6. Clusters or agglomerated grains: There are some processing routes that can improve the number of agglomerates; however, very tightly bound agglomerates or deposits with many agglomerated grains cannot be economically processed to meet the API specification, which is $< 1\%$ clusters.

Casto (2009) has claimed that for fracture treatments in Marcellus shale, the *choice* of the proppant can greatly affect the amount of proppant required as well as the final fracture conductivity. The author of this report relied on data from Arnold (Arnold, Zach. Completions Engineer with Chesapeake

Energy in West Virginia. Provided rock property data commonly used in Marcellus shale fracture simulations. Phone Conversation with Casto 2009) and simulation software (Meyer & Associates Inc. 2008) to determine that the results would have been much improved if 20/40 sand had been used compared with 100-mesh sand.

4.9.3 RCP. To make RCP, white sand (usually) is coated with a polymer. It may then be precured so that it will be stable, or some of the curing may take place in the pack so that the proppant will stick together. Hexion (2008) describes three types of RCP products:

1. **Precured resin coatings:** A precured resin coating is designed to increase the strength of the individual proppant grains. Hexion (2008) claims it does this by putting a thin deformable coating on an otherwise rigid surface. This deformable coat allows for an increased area of grain-to-grain contact to distribute more evenly the point stresses. Fig. 4.66 is a drawing that claims to show that RCP also have the ability to encapsulate any fines that are generated because of grain failure. Fines that are not encapsulated are likely to migrate through the proppant pack and reduce fracture flow capacity.
2. **Partially cured or curable-resin coating:** Partially cured and curable-resin coatings are different but are claimed by the company to exhibit all of the same properties except one. This type of RCP has added benefits [according to Hexion (2008)] compared to a precured resin coating.
3. **Curable proppants:** These only require temperature to start the bonding process. However, bonding that occurs in the wellbore could cause costly cleanouts that require drilling or acid treatments to remove the proppant from the wellbore. “Stress-to-bond” proppants left in the wellbore can normally be flowed out or washed out with coil tubing.

Gulbis and Hodge (2001) claim that resin-coated sand is stronger than conventional sand and may be used at closure stresses less than 8,000 psi, depending on the type of resin-coated sand. However, the document from Palisch et al. (2010a) questions if this is an accurate observation. At closure stresses greater than 4,000 psi and without adverse fluid effects on the resin, resin-coated sand may have higher conductivity than conventional sand. In addition Hexion (2008) claims that the resin helps spread the stress over a larger area of the sand grain and reduces the point loading. When grains crush, the resin coating helps encapsulate the crushed portions of the grains and prevents them from migrating and plugging the flow channel. Another claimed advantage of RCP is that at higher temperatures, the resin grains will become sticky and help prevent the proppant from migrating in the pack and possibly migrating into the wellbore.

It is claimed by Hexion (2008) that because of its ability to bond, there is a greater reduction in fines generation because the surface area of grain-to-grain contact is larger. Instead of just a single grain making contact with another grain, there are multiple grains bonded together in a network of deformable surfaces. The authors note that this unified proppant pack increases the distribution of stress on the proppants within the fracture, decreasing the stress on each individual grain. The ability to bond

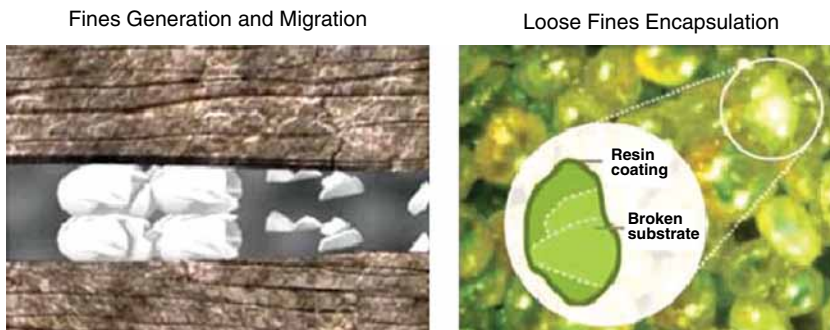


Fig. 4.66—Curable RCP comparing fines migration between sand and RCP (Hexion 2008).

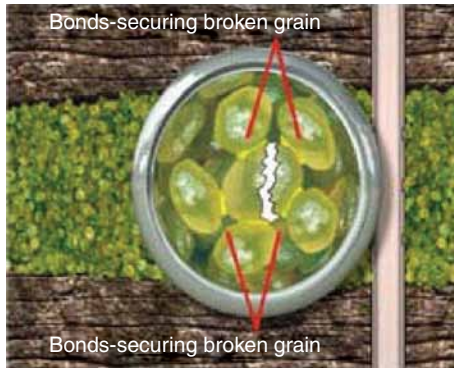


Fig. 4.67—Curable RCP shown to hold grains together (Hexion 2008).

not only reduces the amount of fines generated, it also reduces the amount of loose fines that are able to migrate through the proppant pack. When grain failure occurs with a precured RCP and the resin fails, loose fines are generated. These fines are then mobile and can plug the pore spaces of the proppant pack. See Fig. 4.67.

The resins used with these materials include (Youngman et al. 2002) any formulation that is capable of being coated on the substrate and then being cured to a higher degree of polymerization. Examples of such resins include phenol-aldehydes of the resole and novolac type, urea-aldehyde resins, melamine-aldehyde resins, epoxy resins and furfuryl alcohol resins and copolymers of such resins. The resins must form a solid nontacky coating at ambient temperatures. This is required so that the coated particles remain free flowing and so that they do not agglomerate under normal storage. Youngman et al. (2002) claim the preferred resins are the phenol-formaldehyde resins. These resins include true thermosetting phenolic resins of the resole type and phenolic novolac resins that may be rendered heat reactive by the addition of catalyst and formaldehyde. Such resins with softening points of 185°F to 290°F are acceptable.

An example of a resin molecular cluster is depicted in Fig. 4.68.

Because of the chemistry of these chemicals (Fig. 4.68), it can be seen that they contain components such as multiple hydroxyl groups that are also in the carbohydrates and which are needed to form links with the various crosslinking metals. Possibly undesirable interactions have been reported by Dewprashad et al. (1993) and Nimerick et al. (1992). These authors claim that the resins on the RCP may interfere with the crosslinking of metallic crosslinkers, suppress fracturing-fluid cleanup by consuming oxidative breakers, and compromise proppant-pack bonding, leading to reduced permeability, proppant flowback, and increased proppant crushing. Gulbis and Hodge (2001) lists several ways of avoiding the problems when using RCP.

- Minimize the amount of RCP. If proppant flowback control is required, consider alternate materials for addressing the problem. Card et al. (1995) described the incorporation of fibers in the proppant pack as a means to prevent flowback.
- Use precured-RCPs. These materials are cured (at least partially) and are typically less reactive with fracturing-fluid additives than fully curable-resin coated proppants.
- Avoid using curable-RCPs in conjunction with high concentrations of oxidative breakers.

4.9.4 ISP. These materials are usually made of a fused-ceramic (low-density) or sintered-bauxite (medium-density) material. The sintered-bauxite ISP is processed from bauxite ore [usually containing boehmite- γ -AlO(OH)] containing large amounts of mullite ($Al_{4.5}Si_{1.5}O_{9.75}$). This is in contrast to a HSP, which is processed from bauxite ore high in corundum (Al_2O_3). ISP is generally used at closure stresses greater than 5,000 psi, but less than 10,000 psi. The SG of ISP ranges from 2.7 to 3.3. It is produced in 16/30, 20/40, 30/60, and 40/70 mesh sizes. A photo of the highly spherical material is seen in Fig. 4.69. Both the ISP and HSP are heated to very high temperatures to produce the two types of solids.

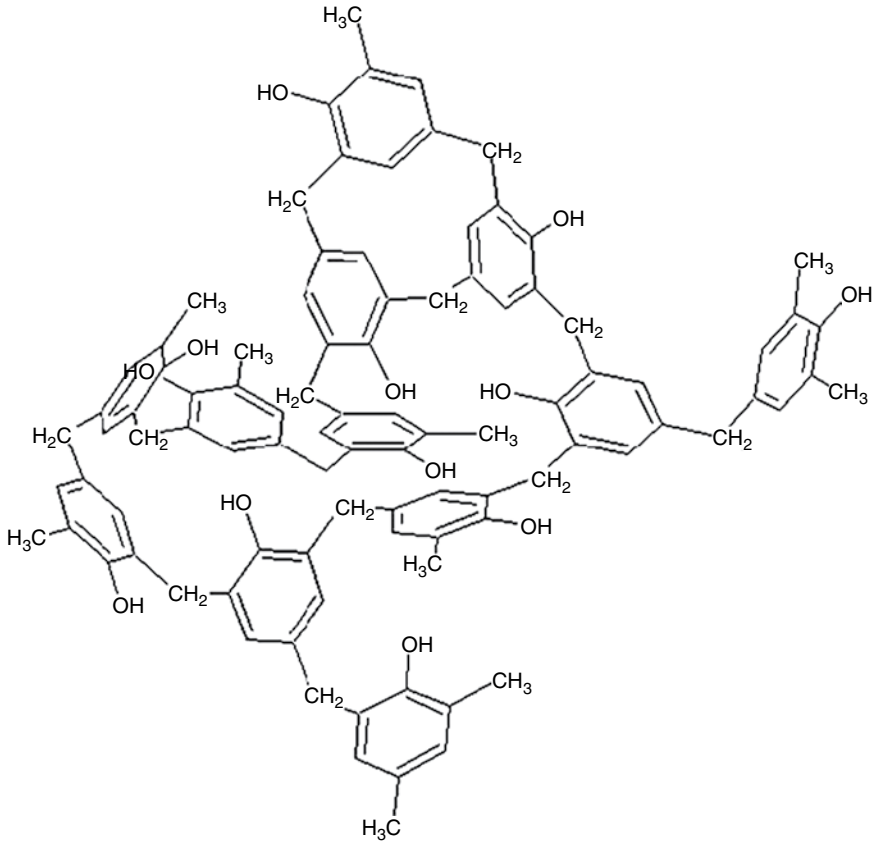


Fig. 4.68—Phenol-formaldehyde resin (Wikipedia 2010c).

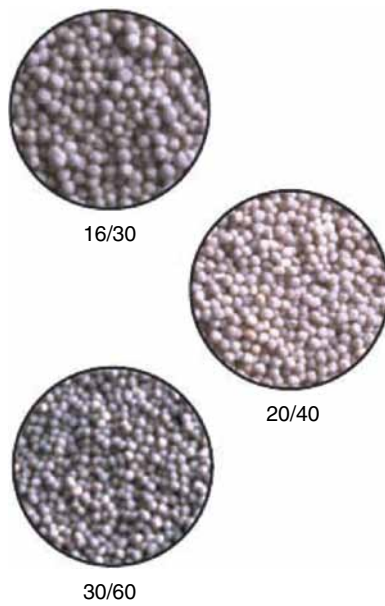


Fig. 4.69—Highly spherical ISP (Carbo 2010).

Usually ISPs have high densities (see previous); however, Rickards et al. (2003) claim that recent research on material properties has led to the development of an ultralightweight (ULW) material with particle strength more than sufficient for most HF applications. The current ULW proppants have apparent SG of 1.25 and 1.75 g/cm³. Laboratory tests are claimed to have demonstrated exceptional fracture conductivity at stresses up to 8,000 psi. They also claim two different avenues for production of ULW particles. The first is a porous ceramic that uses a resin technology to coat the outside of the particle without invading the porosity to encapsulate effectively the air within the porosity of the particle. Encapsulation of the air provides preservation of the ULW character of the particles once placed in the transport fluid. Additionally, the resin coating significantly increases the strength and crush resistance of the ULW ceramic particle. In the case of natural sands, the resin coat protects the particle from crushing, helps resist embedment, and prevents the liberation of fines.

The second avenue of research was directed toward an even lighter particle that may be described as a resin-impregnated and then coated cellulosic particle. The cellulosic substrate is sized ground walnut hull. The low SG of this particle allows near neutrally buoyancy behavior in flowing streams of SW-type fluid. The application benefits of the ULW proppant are further enhanced beyond those discussed previously. Resin impregnation and coating provide significantly enhanced strength beyond that afforded by the unaltered walnut hulls alone. Also see the work by Kulkarni (2008).

4.9.5 HSP. The highest strength materials may be required if the closure stress is greater than 10,000 psi. San-Miguel et al. (2010) claim that proppants may be made from either a naturally occurring material, such as sand, or from compositions that have been produced via a manufacturing process. An example of a composition used to manufacture proppants is a combination of metal oxides, such as bauxite, that has been mixed with various additives, formed into a plurality of generally spherical balls and then sintered to form a plurality of ceramic proppants. While the exact chemical composition of bauxite may vary depending upon the location of the mine from which the bauxite is removed, most bauxite includes between 60 and 90 wt% Al₂O₃. Another example of a composition that may be used to manufacture proppants is commonly known as red mud, which is a byproduct of a process for refining aluminum (Wikipedia 2011c). This waste product typically contains oxidized iron, titanium, sodium, silica, and other impurities. These authors claim an improvement relates to a process for making a particle comprising a sintered ceramic material. Sintering the precursor and then heating the precursor and exerting an externally applied compressive force on the precursor thereby forming a sintered ceramic particle. The density of this HSP is in excess of 3.5 g/cm³.

4.9.6 Proppant Aids. Aids to the placement and consolidation of the prop pack as well as methods for preventing flowback of proppant are in use. There are several different methods of addressing proppant flowback. RCP, which was described in Section 4.9.3 and in Figs. 4.66 and 4.67, has also been employed to consolidate the proppant pack. The resin can become sticky and, thus, resists movement in the frac pack. RCP is not always effective because there is some difficulty in placing it uniformly within the fractures and, additionally, the resin coating can have a deleterious effect on fracture conductivity. RCP also interacts chemically with common fracturing-fluid cross-linking systems such as guar or hydroxypropylguar with organometallics or borate. This interaction results in altered crosslinking and/or break times for the fluids thereby affecting placement. Additionally, these chemicals can dissolve the coating on the RCP making their use ineffective despite their high cost.

Vreeburg et al. (1994) conducted a laboratory study to help clarify the effect of curing temperature, water production rate, proppant size, and stress cycling on the integrity of RCP packs. The experiments confirmed the field experience that stress cycling has a dramatic effect on proppant back production of commercial RCP packs. The number of applied stress cycles (i.e., the number of times the well is shut in) and the initial RCP pack strength appear to be the dominant factors that govern proppant back production. Dedicated experiments, therefore, are required to evaluate the use of RCPs to eliminate proppant back production for a particular field application.

Another method of limiting proppant flowback [disclosed by Rickards et al. (2000)] is mixing the proppant with *deformable particulate* material, especially in the form of bead-shaped particles.

The deformable particles are made of polymer materials and are in the shape of one or more than one of beaded, cubic, bar-shaped, cylindrical, and shapes with a maximal length-based aspect ratio equal to or less than 5. The deformable particles may also be in the form of plastic balls or composite particles made of a nondeformable core and a deformable coating. Typically, the nondeformable core is 50 to 95% of the overall particle size; usually the nondeformable core is made of quartz, cristobalite, graphite, gypsum, or talc. In another embodiment the core consists of deformable materials and may include ground or crushed nut and seed shells, ground or crushed fruit pits, and processed wood.

For limiting proppant flowback, proppant may also be mixed with adhesive polymeric materials [as disclosed by Caveny et al. (1996)]. The adhesive compounds interact mechanically with proppant particles and coat them to produce a thin and sticky layer. As a result, proppant particles stick to one another and to produced sand and crushed proppant particles, thus at least largely preventing particle flowback.

Armstrong et al. (1995) have shown that *fibers* can help reduce flowback as well as proppant settling when they are added to the proppant as it flows into the fracture. See Fig. 4.30 for an example of the slurries of fiber and sand. A chart from Bivins et al. (2005) (Fig. 4.70) demonstrated that the settling rate of a proppant (20/40 sand) slurry is reduced by one order of magnitude compared with the slurry without the fibers. Also, as the figure demonstrates, the fluid has higher effective viscosity than a fluid without the fibers.

Card et al. (1994, 1995) have also proposed the addition of fibrous materials in mixture with particulates for fracturing and gravel packing. It is claimed to decrease or eliminate the flowback of proppant and/or formation fines while stabilizing the sand pack and lowering the demand for high polymer loadings in the placement fluids. The preferred fibers in this patent include glass, aramide, nylon, and other natural and synthetic organic and inorganic fibers and metal filaments. Using a laboratory

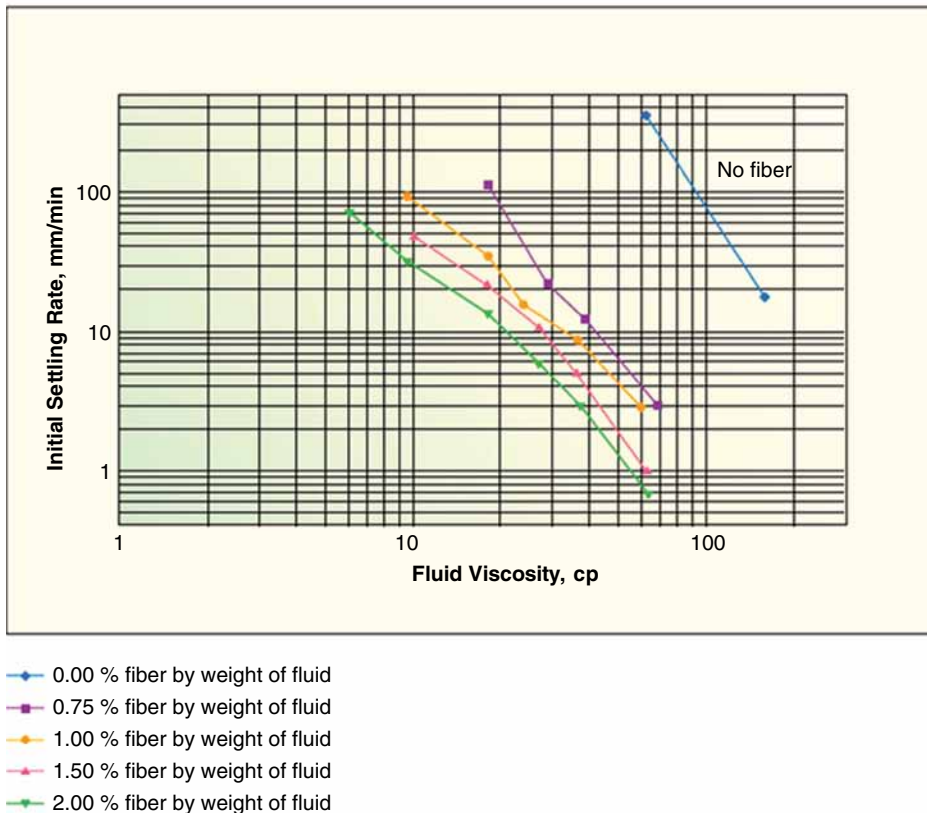


Fig. 4.70—Proppant settling rates of 20/40 slurry with and without fibers (Bivins et al. 2005).



Fig. 4.71—Micrograph of proppant entangled by fibers (Bivins et al. 2005).

test, the authors have tested the effects of using fibers to control sand-pack flowback. A photo from Bivins et al. (2005) (Fig. 4.71) shows proppant entangled by fibers. Hoefler et al. (2008) also claim fibers made of a hydrolyzable but partially crystalline polyvinyl alcohol polymers as suitable for use in hydraulic fracturing treatments.

In an example from this paper, a fibers stabilized sand-pack treatment was described: A 30 lbm/1,000 gal uncrosslinked guar solution was made. Glass fibers were mixed with of 20/40 proppant sand added to the mixture. The resulting mixture was poured into a vertical glass column 12 mm in diameter with a “T” section at the bottom. Next, the water flowed left to right across the “T.” The process washed the sand and fiber from the “T” section. The sand/fiber pack in the column section remained stable. A pressure drop was created across the sand/fiber pack, and no screen prevented the sand from moving with the flow. The pressure drop was increased (by increasing the flow rate) until the sand/fiber pack failed and flowed out of the vertical section of the column. The pressure drop across the sand/fiber pack required to do this was in excess of 275 kPa (40 psi). They found that almost none of the sand in the sand/fiber pack flowed out of the vertical section of the column.

Bulova et al. (2006) claim that most of the low-permeability TG market that is treated by low-viscosity SW fracturing treatments results in ineffective propped fractures because of rapid proppant settling. They say that currently hybrid fracturing and ULW proppants are employed for improving performance of SW treatments. The hybrid fracturing methodology uses a combination of linear and crosslinked gels to improve proppant placement. The disadvantages of existing lightweight proppants are their high cost and applicability only to reservoirs characterized by low closure stresses.

The paper describes the use of a fiber-laden low-viscosity fluid technology, which has been developed to improve proppant transport for HF in low-temperature TG formations. The system creates a fiber-based network within the fracturing fluid that decouples proppant settling from fluid viscosity. This network entangles proppant, dramatically reduces proppant settling, and provides a mechanical means to transport and place the proppant at greater distances from the wellbore. An additional advantage of the new system lies in fiber degradability, which leads to a nondamaged fracture conductivity with time.

As compared with the frequent use of fiber-laden low-viscosity fluids in TG fields, Oussoltsev et al. (2008) and Sitdikov et al. (2009) report on the successful field use of HPG-borate frac fluids using large mesh (16/20 and 12/18) proppants in western Siberian oil fields. The support and placement of these large proppants was materially improved by employing *hydrolysable fibers* [see Hoefler et al. (2008) for one example]. Characteristics such as leakoff behavior, viscosity development, settling rate for large-sized proppants, and fiber degradation in static and dynamic conditions were determined in

various laboratory tests. This engineering work allowed fiber-based fluids technology to be extended to moderate permeable oil reservoirs (1–20 md) and relatively cool formations (76–95°C), in which fracturing treatments are regularly designed for tip-screen out treatments requiring fracture geometry control maximizing proppant-pack permeability by increasing mesh size and proppant concentration. The benefits realized included

- Enhanced proppant support
- Proppant antisettling
- Fracture containment
- Less damage to the frac pack because the fibers degrade and hydrolyze with time
- J^* increased by up to 9% compared to offset wells

A different proppant aid was described by McDaniel et al. (2010). This paper describes a proppant that was developed to improve the final fracture conductivity achievable with high-strength spherical proppants currently available in the market place. This product is an elongated rod-shaped, high-strength particle with integrated proppant flowback control. A comparison of the shape and the porosity of a pack of cylindrical and spherical proppant are in Fig. 4.72. The rods are produced by extruding ceramic materials to the desired shape.

A possible risk with use of the product stemmed from the tendency of the rods to align with the flow. It was feared that this would reduce conductivity; however, as shows Fig. 4.73, the rods settle in a random fashion to allow good conductivity.

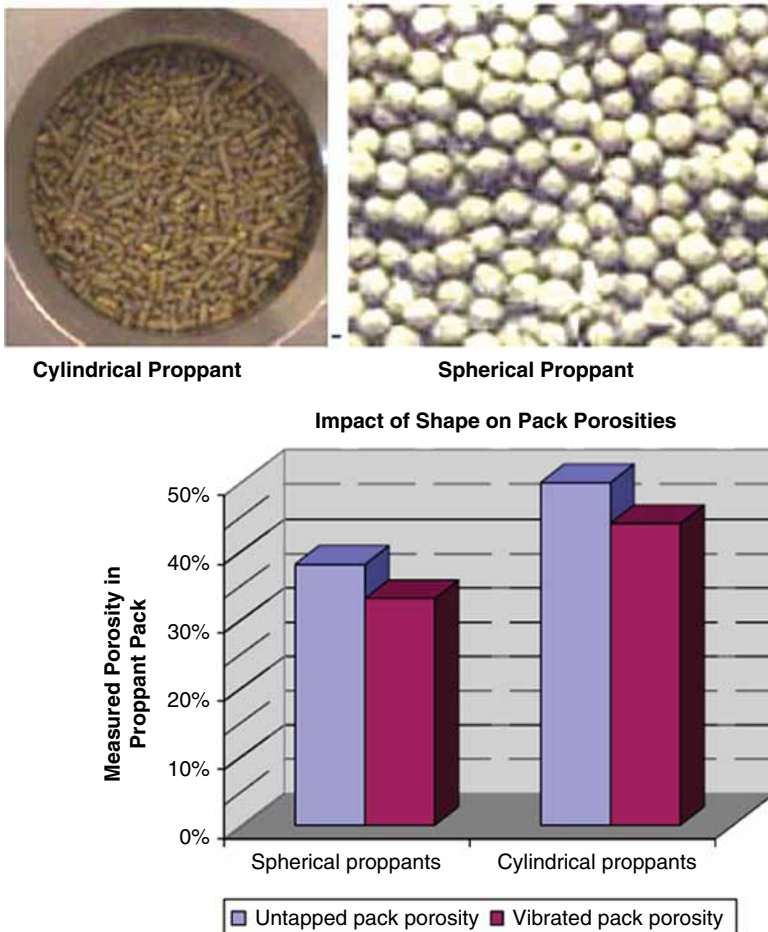


Fig. 4.72—Comparison of cylindrical and spherical proppants (McDaniel et al. 2010).



Fig. 4.73—Views of random alignment of rods after settling in a slot (McDaniel et al. 2010).

Initial field testing of the product was conducted in moderate permeability formations where production from previous fracture treatments indicated lower-than-optimum fracture conductivity. Production results from these field tests confirmed that substantial increases in fracture conductivity can be achieved. The large improvement seen in fracture conductivity can be attributed to increased porosity of the proppant pack and to reduced fracture conductivity losses because of non-Darcy and multiphase flow effects. Completely changing the typical geometry of proppants used in HF is a viable option for improving the conductivity of hydraulic fractures to a point not currently obtainable with spherical proppants.

4.10 Fluid Selection/Proppant Selection

Based on the information in Sections 4.3, 4.3.5, and 4.9, there clearly are thousands of combinations of chemicals and proppants that may be needed to produce the preferred fracturing fluid/proppant slurry for an individual well condition. Fluid selection/proppant selection is the application of all of the information described in the previous section and requires a consideration of all of the factors described in Sections 4.2, 4.3, and 4.3.5.

The considerations include

- Compatible with the formation (water sensitivity or clays)
- Compatible with the formation fluids
- Capable of suspending proppants and transporting them deep into the fracture
- Capable of developing the necessary fracture width to accept proppants
- Have low FL
- Easy to remove from the formation
- Have low-friction properties
- Retain its viscosity throughout the treatment
- Easy to prepare in the field
- Can be handled using known flowback and disposal methods
- Cost effective

In the field practice, many of these decisions are made using the fracture models and computer aids reviewed in Section 4.11. This current section (4.10) will describe some of the *qualitative* methods that can help to choose the correct fluid and proppant using various graphical selection guides. These qualitative methods may enable the engineer to better understand and judge the recommendations of the computer models.

4.10.1 Fracturing-Fluid Selection. To produce an optimal result from an HF treatment, the correct fluid, proppant, and pumping strategies must be selected. This section describes various *qualitative* fluid selection processes for sandstone and carbonate, and it has subsections on coal seams and shale plays. Computer-aided designs (CADs) that produce quantitative models are discussed in Section 4.11.

Ely (1989b) provides selection guides that are seen in Appendix B of the (Gidley et al. 1989) Monograph 12 (Ely 1989a). These guides consist of four very detailed charts as well as lists of “yes/no”

| TABLE 4.3—FLUID SELECTION GUIDE (ELY 1989b) | |
|---|---|
| Nonaqueous | Aqueous |
| Refined oil (no friction reducer) | Linear gel (guar, HPG, cellulose based) |
| Gelled oil (phosphate ester) L.T. | L.T. crosslinked gel (low, neutral, high pH, guar, HPG, CMHPG, CMHEC) |
| Water external emulsion (2/3 oil) | H.T. delayed crosslinked gel with HPG |
| Oil-based foam | Linear gel with secondary gel system (“hybrid frac”) |
| Gelled oil (phosphate ester) H.T. | Foamed water |
| Gelled methanol/water | Crosslinked foam |
| Foamed methanol | HCl is the only acid listed for acid fracturing carbonates |
| Foamed methanol/water | |
| Crosslinked methanol/water | |

questions that cover sandstone and carbonate formations. The first question is “have water-based fluids been used before in this formation?” It then leads to other questions to determine if water-based or nonwater-based fluids are required, and then to the specific type. Once the general fluid type is determined based on water sensitivity, then very detailed charts lead the reader through a selection process for each formation type (sandstone or carbonate) based on permeability, pressure, interval length, and temperature. For carbonates, acid fracturing fluids are offered as options. Table 4.3 lists the specific fluid types used in this guide. Note that this monograph was written in 1989, so many more recent developments such as VES fluids are not listed. However, the detailed approach as well as the things that must be considered are noteworthy and can be emulated for other graphical and computer-aided guides.

Elbel and Britt (2000) have provided Fig. 4.74, a general graphical guideline for fluid selection starting with a distinction between oil and gas wells. They claim that experience has shown that both water- and oil-based fluids have been used successfully in oil and gas wells. The greatest concern is the use of oil-based fluids in dry gas wells; however, they have been used in gas condensate wells. The major selection criteria are the formation pressure, permeability, water sensitivity, and the temperature. This

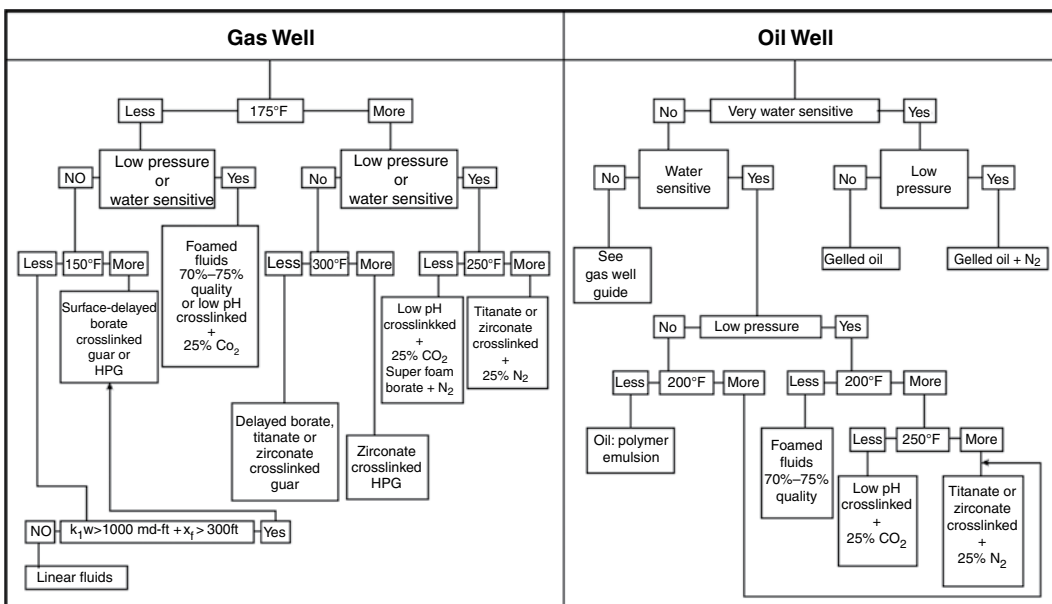


Fig. 4.74—Fluid selection chart the major division for oil or gas wells (Elbel and Britt 2000).

chart also was produced before the various VES fluids were developed (see Sections 3.7.2 and 4.4.4). Flowback and cleanup considerations may favor these materials depending on the reservoir conditions and the ability to provide FL control. VES fluids were not a part of the older selection guides but are included in the CADs described in Section 4.11 and in this section in which there is adequate information. Frequently, these materials can be used in the place of the polymer fluids subject to the limitations described in Section 4.4.1.

McGowen et al. (1993) claim that the fracturing treatments being applied to high-permeability formations (k greater than 10 md) may lead to an increase production (the goal) but also may produce formation fines. Fluid selections for these treatments range from gravel-pack fluids to typical HF fluids. To determine guidelines for fluid selection, detailed measurements of FL, core damage, and fracture conductivity were performed under realistic fracturing conditions on cores with liquid permeabilities ranging from 10 md to 1000 md. The bulk of the data presented is based on Berea sandstone ranging from 200 md to 400 md. Results of these tests indicate the relative effectiveness of these treatment fluids for fracturing high-permeability formations based on FL, formation permeability damage, and fracture conductivity. Treatment and production simulations are provided stressing the difference in performance between systems.

Several specific formation types including coal seams, shale, and TG formations are given more detail in the following subsections.

Frac Fluids for Treating Coal Seams. An EPA/USDOE (2004) paper provided another general format (Fig. 4.75) with some specific guidelines for fracturing coal seams to produce CBM. This document also notes that the fluid choice is only one part of the treatment design that includes roughly in order of importance

1. The *in-situ* stress profile
2. Formation permeability
3. FL characteristics
4. Total fluid volume pumped
5. Propping agent type and amount

| Base Fluid | Fluid Type | Main Composition | Used For |
|-------------|--------------------------|--|--|
| Water based | Linear fluids | Gelled water, Guar < HPG, HEC, CMHPG | Short fractures, low temperatures |
| | Crosslinked fluids | Crosslinker + Guar, HPG, CMHEC, CMHPG | Long fractures, high temperatures |
| Foam based | Water based foam | Water and foamer + N ₂ or CO ₂ | Low pressure formations |
| | Acid based foam | Acid and foamer + N ₂ | Low pressure or water sensitive formations |
| | Alcohol based foams | Methanol and foamer + N ₂ | Low pressure formations with water blocking problems |
| Oil based | Linear fluids | Oil, gelled oil | Water sensitive formations, short fractures |
| | Crosslinked fluids | Phosphate ester oil gels | Water sensitive formations, long fractures |
| | Water external emulsions | Water + oil and emulsifier | Good for fluid loss control |

Fig. 4.75—DOE CBM fracturing fluid selection guide (USDOE 2004).

6. Pad volume
7. Fracture fluid viscosity
8. Injection rate
9. Formation modulus (Young's)

Details of some these fluids are described in Section 4.2.2 and will be included in selection guides for other formations.

For treating coal seams, USDOE (2004) notes that the productive coal reservoirs are usually less than 5,000 ft deep. The permeability in highly cleated coal seams decreases with increasing depth and overburden stress. At depths greater than about 5,000 ft, in most cases, the coal seam does not have enough permeability to be economical. Because most productive coal seams are shallow, low-temperature reservoirs, then the choice of fracturing fluid (according to Fig. 4.75) will be

1. N₂ foam for low-pressure reservoirs
2. Linear water-based fluids if all you need is a short, low-conductivity fracture
3. Crosslinked gel if the formation needs a wide or long fracture

Holditch et al. (1989) discussed the criteria for selecting a fracturing fluid in the Gas Research Institute's Coal Seam Stimulation Manual (GRI 1990). For thick highly cleated coals, a crosslinked fluid was recommended to create wide fractures and place as much proppant as possible in the fractures close to the wellbore. The authors claim that the purpose of the treatment is to link up the cleats to the wellbore using the hydraulic fracture and the proppant. They also claim that the fluid should use the minimum amount of gel possible and breaker should be used to minimize damage to the fracture and to assist in cleanup.

Kefi et al. (2004) claim that for some coalbeds, the use of a VES fluid may provide more retained permeability (an important consideration), compared with guar-based fluids. Lab data on measured retained permeability are described in Fig. 4.76.

Roza et al. (2007) described a system designed to eliminate the fracture face skin created during the fracture treatment using a treatment incorporating a prepad of acid viscosified with a solids-free VES. By incorporating this stage into the fracturing treatments, the retained matrix permeability was seen to increase to +/- 30%, resulting in a negligible fracture face skin. The productivity of fracturing treatments performed using this technique resulted in negative skin factors and production ratios that exceeded expectations.

Fluids for High Carbon Shales. Fracturing the various gas- and oil-containing shale plays have greatly increased the availability of natural gas supplies in the US according to HFF (2010) and Kell

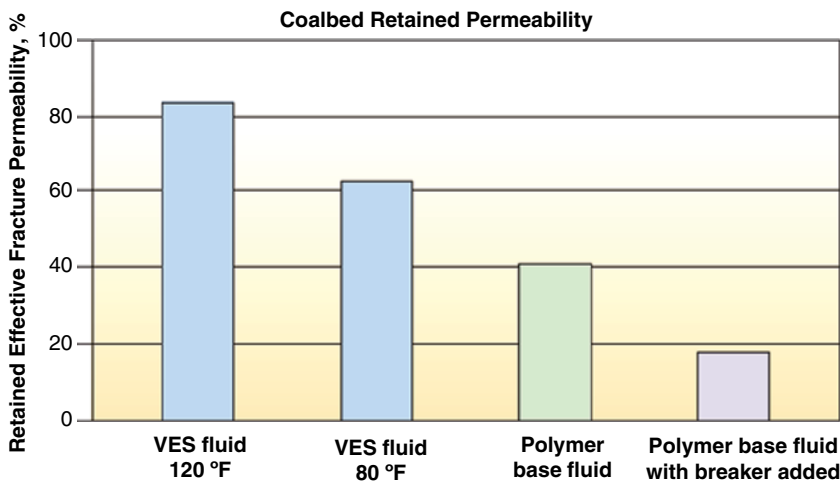


Fig. 4.76—Laboratory retained permeability for coalbed (Kefi et al. 2004).

(2009). In addition, several of the shale plays (Brakken and Eagle Ford) also are producing significant (Hlidek and Rieb 2011) amounts of liquid hydrocarbons.

King (2010), Arthur et al. (2008), and Arthur et al. (2009) have provided reviews of the technologies for fracturing shale gas formations based on 30 years of experiences (with a lengthy reference list). These include discussions of the significant environmental implications of fracturing shale oil and gas formations. These subjects also will be reviewed in Section 6.3.

Examples of fluid/proppants selection for fracturing shale formations that include SW-type uncross-linked (Section 4.4.3) and/or foamed fluids (Section 4.5.5) with LWP for some Barnett shale (6,000–8,000 ft) are provided by Mohanty (2009). Crosslinked-guar-type and VES formulations also are in use.

Cramer (2008) has reviewed literature on the frac fluids and proppants used in shale as well as coal-gas seams. He notes that given their unique petrophysical properties, each type of unconventional reservoir requires a unique approach to well stimulation, with often differing objectives than exist with conventional reservoir types. The paper reviews the characteristics of the basic unconventional reservoir types, lessons learned, and successful stimulation practices developed in completing these reservoirs, and areas for improvement in treatment and reservoir characterization and treatment design.

Kaufman et al. (2008) consider the use of a typical SW stimulation for the Marcellus. In this paper they describe proppant selection and placement, using 587,500 lbm of proppants in 545,000 gal of 5 ppt SW at a 50 BPM rate, in which he uses 17% (100,000 lbm) 80/100 mesh, 60% (350,000 lbm) 30/50 mesh, and 23% (137,500 lbm) 20/40 mesh. A biocide also was added at a loading of 0.25 gpt and an ME at 2 gpt. This treatment was considered successful. They recommend that sand proppants with an SG of around 2.6 and small diameters should work in a SW fractures. They claim that the smaller the size of proppant, the greater the transport, assuming all other parameters are the same. For treating deep Haynesville shale, Chesapeake (2010) recommends borate-crosslinked guar or HEC and silica sand as the proppants.

Schlumberger (2010d) has provided a complete formulation list for fracturing fluids designed for treating TG formations such as shale gas reservoirs. See [Table 4.4](#). The fluid is designed to give a low-friction fluid pressure as well as being capable of supporting proppant. The acrylamide polymer and the amphoteric alkylamine surfactants will provide the necessary viscosity in the presences of the specific salt package seen in the product list. The authors claim that the fluid will have minimal environmental impact because of the low concentrations of chemical ingredients. Chesapeake (2010) has provided similar information on fluids used in the Haynesville shale play. Additional information on the discussions of TG fracturing fluid control and disposal are described in Sections 6.3.1 and 6.3.2 of this book.

TABLE 4.4—CHEMICAL COMPOSITION OF CROSSLINKED FRACTURING FORTNIGHT GAS FORMATIONS (SCHLUMBERGER 2010b)

| Chemical | Wt% |
|---|---------|
| Water | 99.57 |
| NaCl | < 0.16 |
| MgCl ₂ | < 0.08 |
| Amphoteric alkylamine | < 0.08 |
| NaCaMgPO ₄ | < 0.05 |
| 2-propanol | < 0.04 |
| Acrylamide copolymer | < 0.03 |
| (NH ₄) ₂ SO ₄ | < 0.03 |
| Na ₂ SO ₄ | < 0.02 |
| KCl | < 0.02 |
| Urea | < 0.01 |
| Noncrystalline silica | < 0.002 |
| Dimethylsilixanes and silicones | < 0.001 |

Waters (2011) claims that frac fluids for sensitive shale formations, including the acid spearhead, SW, and linear polymer gel and crosslinked-gel systems, are being produced that are

- Fully functional, fully formulated and fully disclosed
- Designed with additives that avoid the use of *Priority Pollutants (USA)* and contaminants listed on the *National Primary Drinking Water Standard*
- In continual improvement in formulations to reduce trace contaminants and to minimize priority pollutants

Kell (2009) has authored a report (for the US Department of Energy) on shale gas production that contains significant information of the fracturing fluids used in the various reservoirs across the continental US. The report notes that shale gas has been located in the highly organic shales in approximately 21 states (see Fig. 4.5) and accounts for more than 50% of new gas production. A key element in the emergence of shale gas production has been the refinement of cost effective horizontal drilling and HF technologies. A frac design described in this report had 14 stages of propped fluids that included from 5,000 to 100,000 gal of liquid and slurry, including the pad and the HCl prestage. While the report notes that 1,000,000 to 2,000,000 gal of fluids may be pumped, more than 99.50% is water (brine) and sand. For the 2,000,000 gal treatment, the other additives (Fig. 4.14) amount to approximately 1,000 gal. An explanation of the function of the components for a low-solids (SW) formulation used in the Fayetteville shale fields are in Section 4.4.3.

FTS (2011) claims a green SW formulation that includes

- FR
- Biocide
- Oxygen scavenger
- Clay control
- SI

Details of the individual chemicals were not provided by this reference.

As noted in the paper by Malpani (2006), crosslinked gels are also in use as well as the low-solids SW fluids. To find the effectiveness of various fluids, Cipolla et al. (2009) presented a paper on production evaluation criteria that can be used to compare the overall stimulation effectiveness in unconventional gas reservoirs. The authors claim that because of the uncertainty in matrix permeability and network fracture spacing (i.e., complexity), it is difficult to find unique solutions when modeling production data in unconventional gas reservoirs. However, it may be sufficient to identify qualitative behaviors that can distinguish between key production mechanisms.

This paper claims to use numerical reservoir simulation combined with advanced decline curve analyses to identify expected production signatures that can be used to evaluate stimulation effectiveness in unconventional gas reservoirs. The paper (Cipolla et al. 2009) concludes with the evaluation of production data from 41 Barnett shale fracture treatments, including fracture and refracture treatments. The dataset included vertical and horizontal wells stimulated using WFs and crosslinked-gel treatment designs. Significant conclusions were

1. Although the initial crosslinked-gel treatments showed production signatures indicating higher fracture conductivity than the subsequent water-frac refracs, all of the water-frac refracs significantly improved gas production
2. The water-frac treatments in the horizontal wells appear to provide better relative fracture conductivity on average than the vertical well-WFs.

An article by Beckwith (2012b) claims that approximately 50% of shale gas treatments use a guar-based fluid (including the modified guar; see Section 4.4.1) and the other 50% depend on synthetic SW formulations (Section 4.4.3) and other formulations. The authors note that the use of guar as the thickening agent reduces the amount of fluid necessary because the higher viscosity allows more

proppant per volume of the fluids. Thus, this article notes the very high dependence of the supply of guar for North American shale fracturing treatments, with the majority of the supplies originating in India or Pakistan.

To improve cleanup of TG formations, Hinkel et al. (2005) claim a fluid that contains small but sufficient amounts of certain amine oxides to aid in the removal of the fracturing fluid from the formation. By facilitating the removal of fluid from the invaded zones, the amount of damage to the fracture faces in the formation is thereby minimized. The amine oxides are added to the fracturing fluids in small but sufficient amounts to promote rapid cleanup. Normally, they are added as an aqueous solution in amounts from about 0.01 to about 1 wt% of amine oxide, weight-by-weight basis (w/w), and preferably from about 0.006 to about 0.024 wt%. The amine oxides can be added “on the fly” to the fracturing fluid as it is being pumped into the wellbore or the amine oxides can be added to the so-called frac tank, which holds the mix water for the fracturing fluid.

A specific example fluid (Hinkel et al. 2005) is an aqueous polymer solution of a guar derivative (CMHPG at 35 lbm of polymer per 1,000 gal of fracture fluid), containing a zirconate crosslinker, a high-temperature gel stabilizer, a clay stabilizer, and a breaker for the gelled polymer addition of n-decyl-N,N-dimethylamine oxide so that each modified fluid contained the amine oxide at a concentration of 0.1 %, weight-by-weight basis. In most cases, this corresponds to adding the surfactant at a ratio of between 1 and 2 gal/1,000 gal. For additional discussions of cleanup chemicals, see Howard et al. (2010).

Akrad et al. (2011) have tested four different shale formation rocks to determine the effects of different frac fluids on Young’s modulus (E) and, thus, on embedment of the frac proppant into the rock (see Sections 1.5.3 and 4.1.1). Their tests indicated that the rock composition (high carbonate, quartz, or clay) affects embedment. The most sensitive formations are the high carbonates that are softer than the clay/quartz rocks and are not protected by the KCl in most frac fluids as the harder formations. This factor may affect proppant embedment and, thus, fracture conductivity.

King (2010) contends that the great complexity of the shale gas formations requires an individualized approach to selecting the proper fluids and fracturing design.

He also contends that four factors have allowed the rapid development of this energy source.

- SW (low levels of polymer additives—see Section 4.4.3) have replaced heavier gels, gas, and foams. This has reduced costs, and formation damage, but also has reduced proppant placement effectiveness (Britt et al. 2006).
- Horizontal wells have replaced vertical wells. Toe-up lengths of 750 m over 1600 m enable more of the formation to be contacted.
- 10–20 (or more) frac stages are used to contact more of the formation (see Section 4.11.3).
- Simultaneous or sequential fracturing uses real-time stress changes detected in an offset well to divert the fracs into unprocessed rock (see Section 4.1.2 of this book).

Fluids for TG. As noted by Cramer (2008) and Holditch et al. (2007) in Section 4.1.1, gas from tight sandstones and carbonates (< 0.1 md) can be described as unconventional, but they are fundamentally different from shale and CBM plays. These TG sources frequently come from deep, hot formations that require complex fracturing fluids.

Malpani (2006) has provided (Fig. 4.77) a selection guide for TG fracturing of these reservoirs. He notes that the development of optimal fracturing procedures has a large impact on the long-term economic viability of the wells. This study takes into account various parameters such as the type of formation, the presence of natural fractures, reservoir properties, economics, and the experience of experts we have surveyed. This work is claimed to provide a guide to operators concerning the selection of an appropriate type of fracture fluid for a specific set of conditions for a TG reservoir.

Fluids considered include

- Crosslinked-gel fracture treatments
- Water fracture treatments (including SW)
- Hybrid fracture treatments: gelled water pad followed by crosslinked gel with proppant

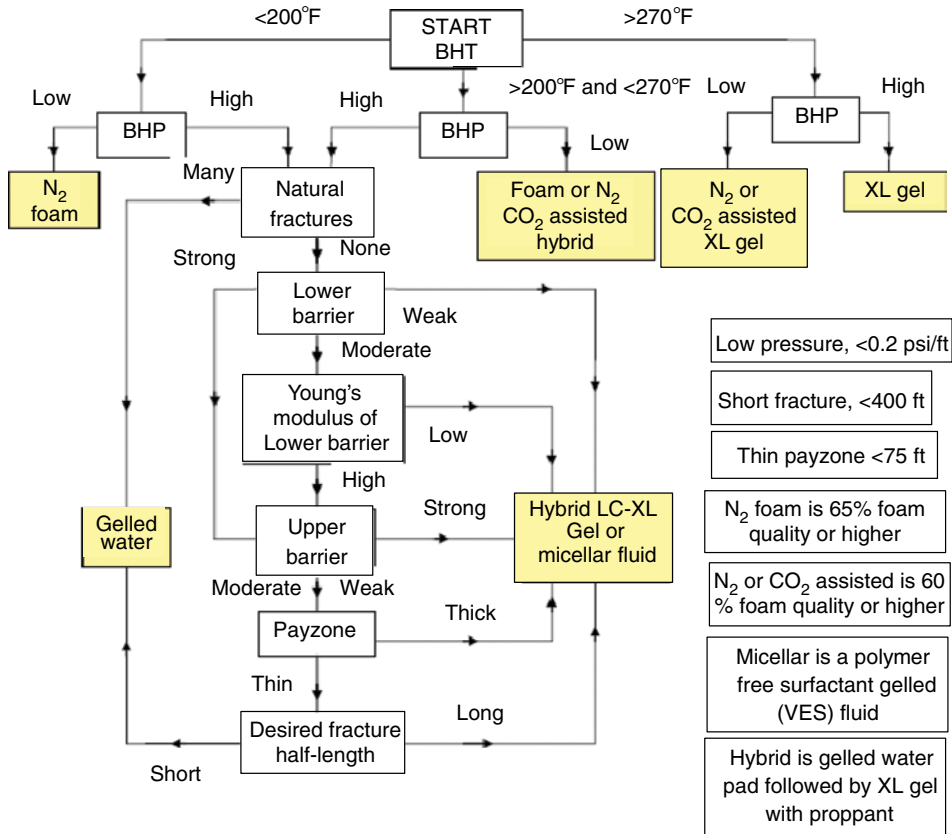


Fig. 4.77—Tight gas fluid selection guide (Malpani 2006).

- Foam fracture treatments
- Micellar fracture treatments: Polymer-free, surfactant gelled fluid (VES)

4.10.2 Proppant Selection. Elbel and Britt (2000) claim that proppant selection consists of optimizing permeability or conductivity vs. the associated cost and benefit. Fig. 4.78 shows two charts that describe the relative volume required of different types of proppant (a) and the relative cost

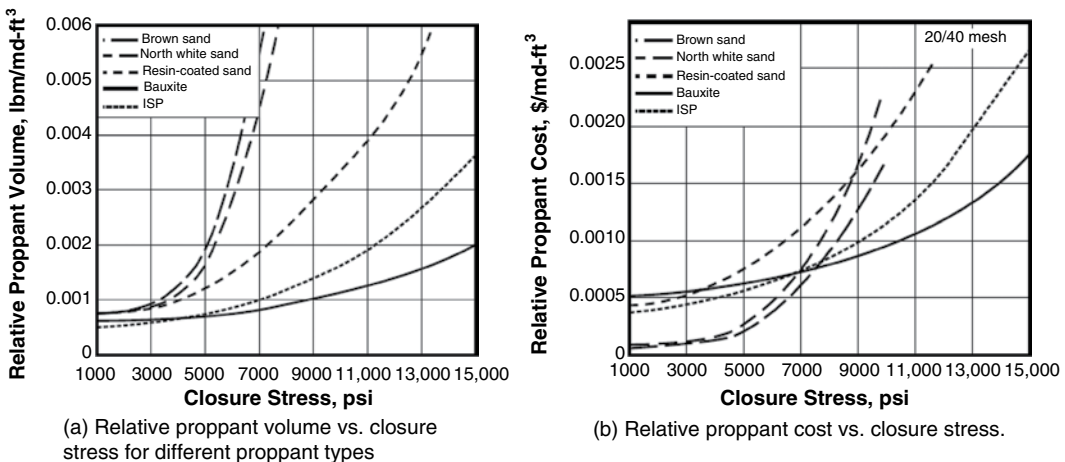


Fig. 4.78—Proppant selection (Elbel and Britt 2000).

effectiveness to achieve long-term pack conductivity (b). The conclusions are that at the higher closure pressures, the higher-strength (and initial higher cost) proppants provide long-term value.

Mohanty (2009) has tested several different LWP types to determine possible applicability for their use in shale frac operations in which minimal amounts of chemicals are added in SW treatments. The report found that all three materials with bulk density values from 0.1–1.2 g/cm³ had sufficient crush resistance to support the stresses in Barnett shale, but some of them produced significant amounts of fines. The report recommended conductivity tests be run to evaluate the effect of fines on productivity.

Palisch et al. (2010a) have some selection rules for choosing a proppant that include that following:

- Proppant should not be selected based on the results of crush tests alone. Selecting a proppant solely by investigation of crush, sieve size, mean particle diameter, density, price, or any other single parameter will rarely provide an optimal solution.
- With the exception of price, an *ISO 13503-2* (2006) conductivity test will take most of these parameters into account. Optimizing proppant selection is a complex problem and requires more than a simplistic rule of thumb or crush threshold to achieve the ideal economic selection.
- Second, the conductivity of each potential proppant must be measured in the laboratory and then corrected for downhole or realistic conditions.
- Production must be predicted for each proppant and an economic comparison performed, leading to the economically optimized frac design. This analysis generally requires the use of a fracture/production model.
- Analyze the field results after the frac has been performed to check the assumptions and the frac model. In general, the authors have found that hydraulic fractures are conductivity limited, meaning that efforts to increase the conductivity of a fracture usually increase production.
- A primary challenge is to determine the most cost-effective manner to improve the fracture conductivity.

4.11 Fracture Planning and Models: Combining Chemistry and Engineering

This section describes the use of interactive and computer systems and fracture models to help plan the jobs as well as innovative pumping strategies that combine chemistry and mechanical technology to produce improved outcomes.

4.11.1 Interactive Selection Systems. Pandey (2004) has patented a Wellbore Treatment Fluid Selection Interactive Computer System. This process claims to be an interactive computer system, user friendly, to aid an engineer in selecting a proper treatment fluid for a particular situation. The authors also claim that the desired fluid properties are obtained through a combination of additives such as polymeric additives used for controlling the viscosity. This system is claimed to take the user through a series of screens that answer yes/no questions (such as described in Figs. 4.74 and 4.77).

4.11.2 Fracture Models. Before a fracture stimulation treatment can be pumped, a very large amount of chemical and mechanical information must be combined to form a treatment plan. Decisions on the exact chemistry needed (that is described in Sections 4.3, 4.3.5, and 4.10) are linked, and then applied using the equipment described in Section 1.7. Some of these selections may be done using the rules noted in Sections 4.10.1 and 4.10.2; however, complex CAD programs are usually employed.

The major elements in the plan include reservoir/geomechanical calculations, fluid and proppant selection, and then development of the pumping schedule. A chart (Fig. 4.79) illustrates the major elements required.

Details of the design elements that the programs should supply include the following:

- Candidate selection—How to recognize wells/fields/formations as good fracture candidates including the consideration of complex factors such as multifractured wells, non-Darcy, and multiphase flow.
- Hydraulic fracture rock mechanics/fracture geometry—Understand the basic physics of the HF process, and based on this, estimate the parameters required for preliminary treatment designs, preliminary planning, etc.

Elements of a Fracture Treatment Design

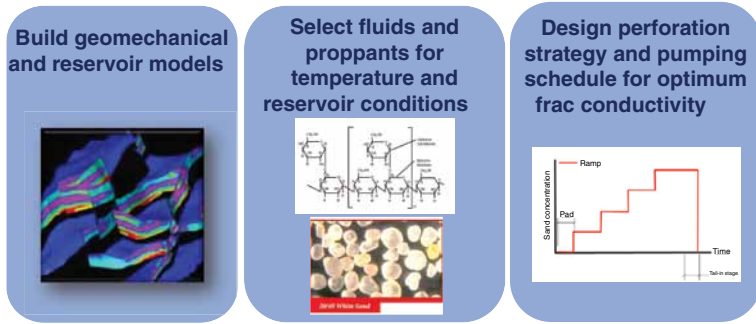


Fig. 4.79—Elements of fracture treatment design.

- Fracturing pressure analysis—Using fracturing pressure analysis and net pressure history matching to refine the input variables and optimize treatments.
- Economics—Fracturing is an expensive treatment, and the geometry model should be coupled with a reservoir model to allow comparison of treatment designs, based on economic considerations (see Section 1.3).
- Materials/execution—Select the appropriate proppant and fluid for a treatment, field application, and quality control.
- Treatment design—Use the refined geologic parameters to generate the final pumping schedule.
- Post-frac analysis—Reservoir modeling for post-frac production analysis.

Commercial design programs for doing these processes include MFrac® (Meyer 2010), StimPlan® (NSI 2011), and FracCADE® (Schlumberger 2009b). An output of a fracture geometry simulation based on one of the computer programs in commercial use was provided by Arthur et al. (2009). This diagram, **Fig. 4.80**, shows the projected width (in.) as a function of length (ft).

Note that the authors of this book do not endorse any commercial program, and this is for information only. In addition, the material in this chapter has been provided to allow the engineers an

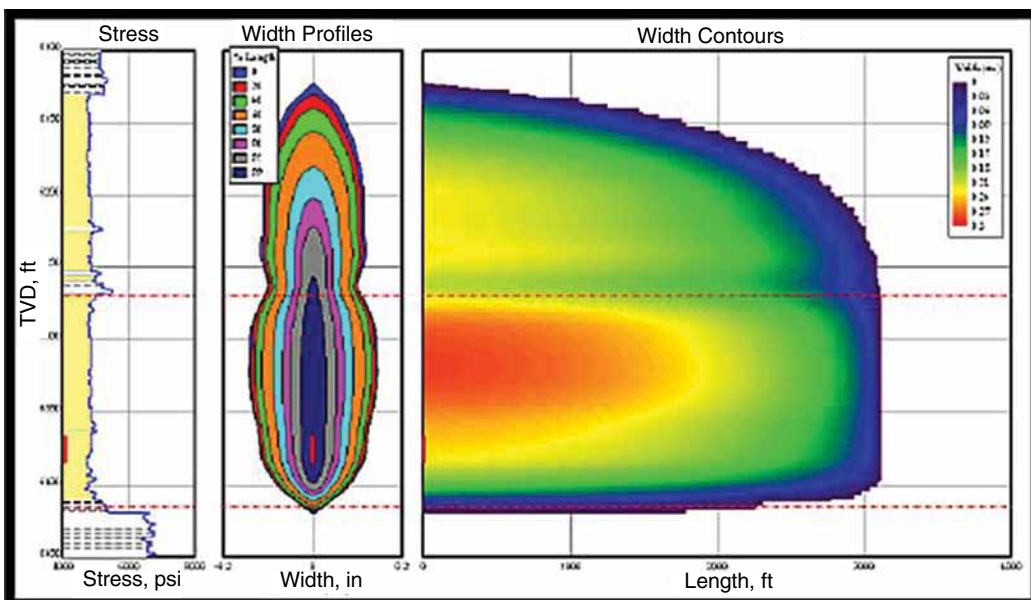


Fig. 4.80—Frac geometry simulation (Arthur et al. 2009).

understanding of the chemistries and physics of the fracturing process, so that they may be able to fact-check the input and output of the various CAD programs.

General Methods for Modeling of Hydraulic Fractures. Several families of models are available for describing the geometry of hydraulic fractures. These include 2D, pseudo-3D, planar-3D, and fully 3D models. More recently, for complex fractures formed in unconventional reservoirs, wire-mesh and unconventional fracture models have been introduced. Detailed reviews of these models are available in the literature and only a brief description is provided here; see Economides and Nolte (2000), Weng et al. (2011), Adachi et al. (2007), Meyer and Bazan (2011), and Nagel et al. (2011) for more details.

2D models were developed from 1950 to 1970 and laid the foundation of modern hydraulic fracture modeling. These models allow analytical solutions, provided some limiting assumptions are made in the coupled solid mechanics and fluid-flow equations. One common limiting case is when the fracture length is that when the fracture length is much greater than the height ($x_f \ll h_f$). In such cases the model by Perkins and Kern (1961) and Nordgren (1972) provides a reasonable approximation and is commonly referred to as the PKN model after the developers (Fig. 4.81). However, when the fracture height is much greater than the length, (i.e., $x_f \ll h_f$), the model developed by Khristianovich and Zheltov (1955) and Geertsma and de Klerk (1969) and is referred to as the KGD model is more appropriate (Fig. 4.82).

In the KGD model, the assumption that $x_f \ll h_f$ implies that the fracture width changes slowly vertically along the fracture face from any point on the face than it does horizontally. This approximation allows one to assume that all horizontal cross sections are identical, which effectively converts the 3D problem into a 2D plane-strain problem. The fracture tip region plays an important role and the net pressure is governed by fracture mechanics. The fluid pressure gradients are approximated. On the other hand, in the PKN model, as $x_f \gg h_f$, it is assumed that each vertical section acts independently. Fracture mechanics and the effect of the fracture tip are not considered; fluid flow in the fracture dominates the pressure gradients.

Both the PKN and KGD models assume that the fracture is planar. They assume that the fluid flow is 1D along the length of the fracture. The rock in which the fracture propagates is assumed to be a continuous, homogeneous, isotropic linear elastic solid. The models were initially developed for Newtonian fluids but later extended to include power-law fluids. Furthermore, no consideration is given to the layers surrounding the fractured zone. A significant limitation in the simple 2D models is that they

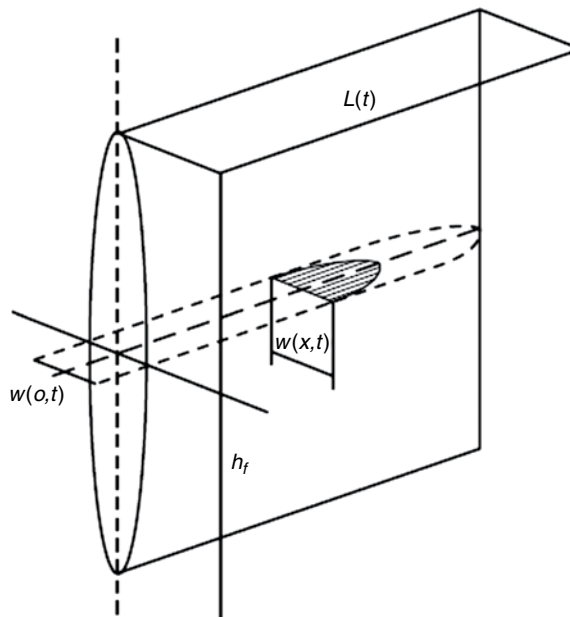


Fig. 4.81—PKN fracture (Mack and Warpinski 2001).

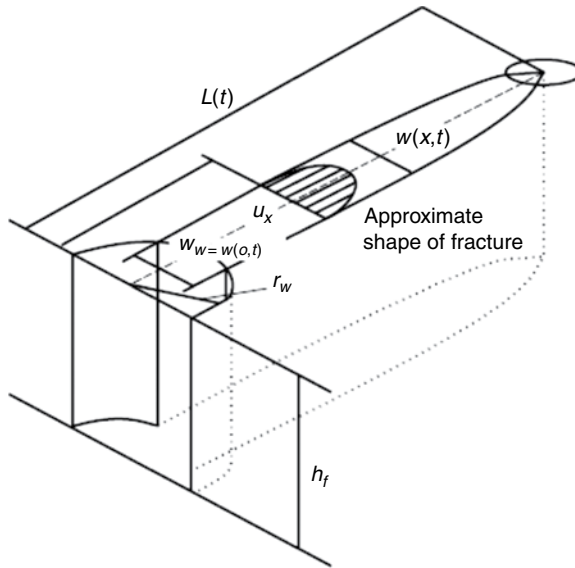


Fig. 4.82—KGD fracture (Mack and Warpinski 2001).

assume that the fracture is of a fixed height or completely confined in a given layer. It is not always obvious from logs and other data where or whether the fracture will be contained. Pseudo-3D, planar-3D, and 3D models were developed to address this limitation.

General 3D fracture models make no assumptions about the orientation of the fracture. Factors such as the wellbore orientation or perforation pattern may cause the fracture to initiate in a particular direction before turning perpendicular to the far-field minimum in-situ stress. Simulators incorporating such general 3D models are computationally intensive and require data that are not easily available. This limits their use to research studies and special problems (Morales et al. 1993).

Planar-3D models are based on the assumption that the fracture is planar and oriented perpendicular to the far-field minimum in-situ stress (Economides and Nolte 2000). No attempt is made to account for complexities that result in deviations from this planar behavior. Simulators based on such models are still too computationally demanding for routine commercial applications. They should be used where a significant portion of the fracture volume is outside the zone where the fracture initiates or where there is more vertical than horizontal fluid flow. Such cases typically arise when the stress in the layers around the pay zone is similar to or lower than that within the pay.

Pseudo-3D models attempt to capture the significant behavior of planar models without the computational complexity (Economides and Nolte 2000). In the lumped pseudo-3D models the vertical profile of the fracture is assumed to consist of two half-ellipses joined with their centers in the fracture length direction (Fig. 4.83). The horizontal length and wellbore vertical tip extensions are calculated at each timestep, and the assumed shape is matched to these positions. These models assume that the fluid flow is along streamlines from the perforations to the edge of the ellipse and that the streamlines have a particular shape derived from simple analytical solutions. An alternative to this approach is the cell-based pseudo-3D models in which the fracture is treated as a series of connected cells. The approach is similar to planar models, except that only one dimension is discretized instead of two. Fluid flow is assumed to be essentially horizontal along the length of the fracture, and the solid mechanics is typically simplified by assuming plane strain at any cross section. As in the PKN model, these assumptions make these models suitable for reasonably contained fractures, which are long relative to their height.

For many commercial treatments, the pressure history during treatment is the only data available to validate the model. Even in these cases, the quality of the data is questionable, especially if the bottomhole pressure is inferred from the surface pressure. Even when the bottomhole pressure is available, it is also not sufficient to determine uniquely the fracture geometry. Additional data from tilt meter and microseismic surveys are required to constrain the geometry; however, these data are generally not

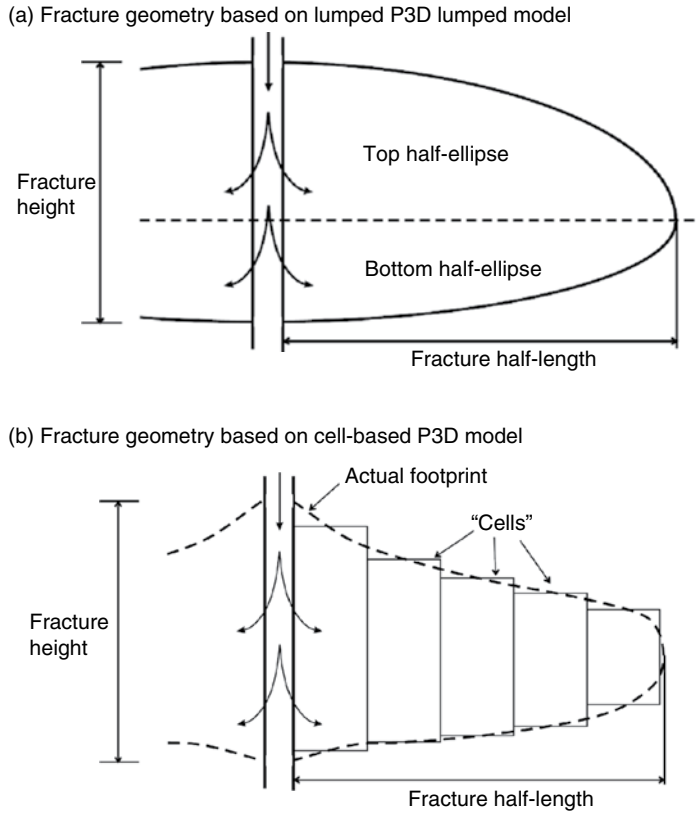


Fig. 4.83—(a) Fracture geometry for lumped and (b) cell-based P3D models (Adachi et al. 2007).

available for most treatments. Therefore, the sophistication of the model should be matched with the required input data available for validation.

Modeling of Hydraulic Fractures in Unconventional Reservoirs. HF in unconventional reservoirs often results in complex-fracture networks. Complexity is frequently associated with the interaction of the hydraulic fracture with a pre-existing rock-fabric heterogeneity, such as natural fractures, fissures, or cleats (see Fig. 4.10 and Fig. 4.84) (Warpinski and Teufel 1987; Fisher et al. 2005; Daniels et al. 2007; Cipolla et al. 2010; Weng et al. 2011). Depending on the intensity of heterogeneity and

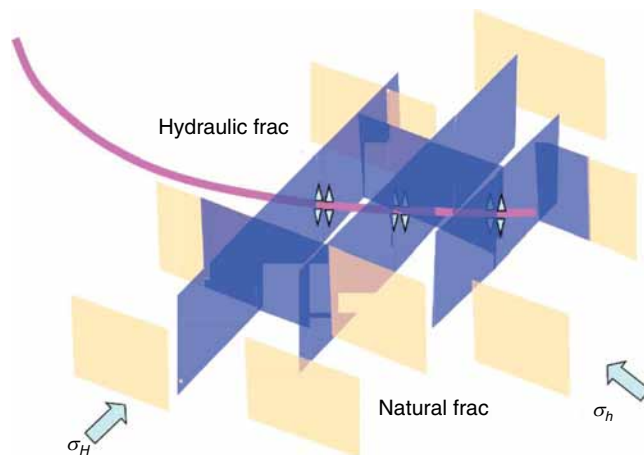


Fig. 4.84—Conceptual diagram of a complex fracture network formed due to the interaction of hydraulic fractures with pre-existing natural fractures.

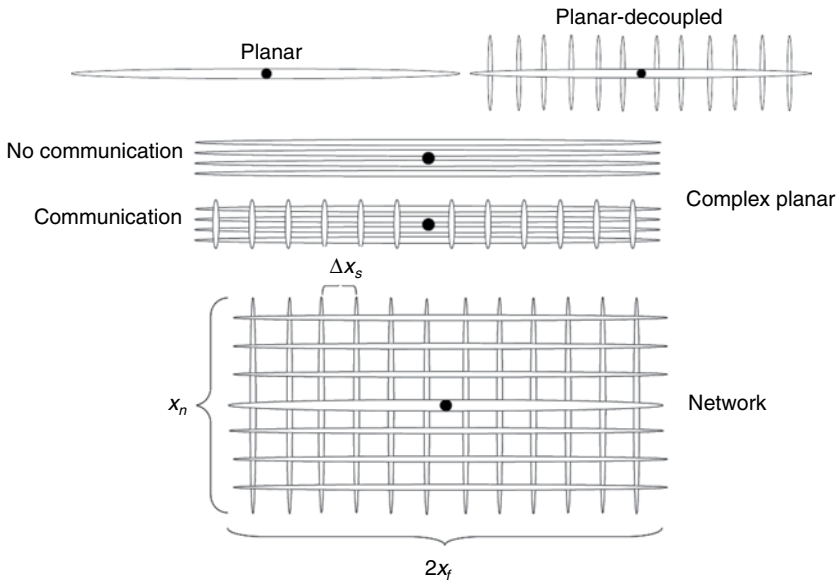


Fig. 4.85—Fracture-growth and complexity scenarios (Cipolla et al. 2010).

treatment conditions, several levels of complexity are possible (Fig. 4.85). Conventional planar fracture models discussed above are inadequate for simulating these complex-fracture networks.

Furthermore, proppant transport in complex-fracture networks is also not well understood. Low-viscosity fracturing fluids used to promote fracture complexity generally have poor proppant-transport properties. Therefore, large portions of complex fractures can remain unpropped. Cipolla et al. (2010) have studied proppant distribution scenarios in complex-fracture networks for three limiting scenarios (Fig. 4.86). In Case 1, the proppant is evenly distributed throughout the complex-fracture system, in Case 2, the proppant is concentrated in a dominant planar fracture with an unpropped complex-fracture system accepting fluid only; in Case 3, the proppant settles and forms pillars that are evenly

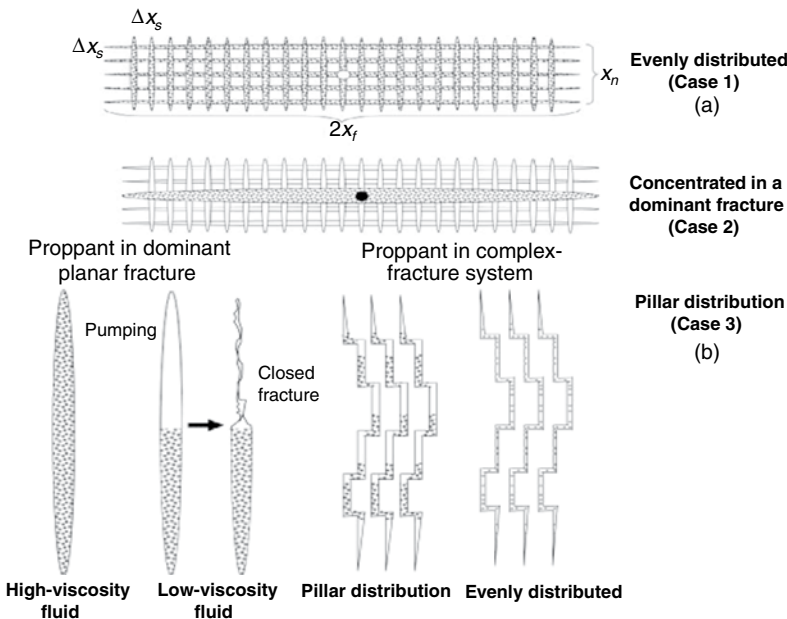


Fig. 4.86—(a) Proppant-transport scenarios planar view and (b) side view (Cipolla et al. 2010).

distributed within the complex-fracture system. They argue that in Case 1 the proppant concentration would be too low to be effective, and unpropped fracture conductivity would likely dominate well productivity. In Case 3, a very small percentage of the total fracture area is propped, and it would likely be insufficient to support the closure stress and resist fracture closure. Case 2 appears to be the best of three limiting cases as it provides a much higher conductivity connection to the wellbore.

Two main modeling approaches have been proposed to overcome the limitation of the conventional fracture models in modeling complex-fracture networks. In the wire-mesh approach (Xu et al. 2010; Meyer and Bazan 2011), the hydraulic fracture network of the complex fracture is represented by an elliptical volume of the stimulated formation (Fig. 4.87). It approximates the growth of a complex network by modeling the growth of two perpendicular sets of vertical planar fractures, while accounting for mechanical interactions among themselves and the injected fluid volume. Proppant placement is simulated using the advective transport of proppant by the flow injected fluid and hindered settling of proppants relative to the fluid. Once the model is calibrated, it can be used to provide an estimate of the fracture network dimensions and proppant placement in the network.

A limitation of the wire-mesh model is that the fracture network pattern cannot be directly linked to the pre-existing natural fractures (Weng et al. 2011). The network geometry is assumed to be symmetric with respect to the injection point, and the shape is elliptical, which limits the ability to match microseismic data that show significant asymmetry or irregular shape in the stimulated region. Furthermore, the model assumes fixed fracture spacing, and any effect of treating parameters on the resulting fracture network pattern is not taken into account. If the reservoir characteristics and pumping parameters change significantly, calibration against one set of microseismic data cannot be used in other wells or even other stages in the same well.

Another modeling approach for complex fractures is to explicitly model the growth of a hydraulic fracture in an existing network of natural fractures (Weng et al. 2011; Nagel et al. 2011; Fu et al. 2011). In the unconventional fracture model proposed by Weng et al. (2011), the branching of the hydraulic fracture at the intersection with the natural fracture gives rise to the development of a nonplanar, complex-fracture pattern (Fig. 4.88). The approach is similar to the pseudo-3D models, but instead of solving the problem for a single planar fracture, they solve the equations for the complex-fracture network. At each intersection, a decision is made whether the hydraulic fracture is propagated through or is arrested by the natural fracture. A three-layer proppant-transport model consisting of a proppant bank at the bottom, a slurry layer in the middle, and clean fluid at the top is adopted for simulating proppant transport in the fracture network. In the distinct element method (3D) proposed by Nagel et al. (2011), the rock mass is modeled as 3D assemblage of rigid or deformable blocks. The size, shape, and orientation of the blocks are defined by a discrete fracture network. Discontinuities are regarded as distinct boundary interactions between these blocks; joint behavior is prescribed for these interactions. The natural fracture aperture is affected by shear displacement and fracture fluid pressure.

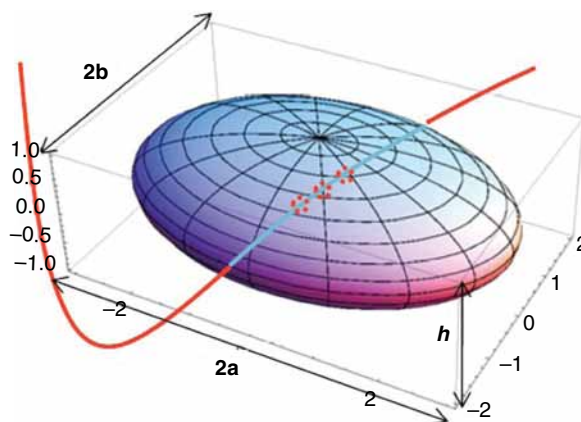


Fig. 4.87—Ellipsoidal representation of a stimulated reservoir formation in a wire-mesh fracture model for complex fracture network.

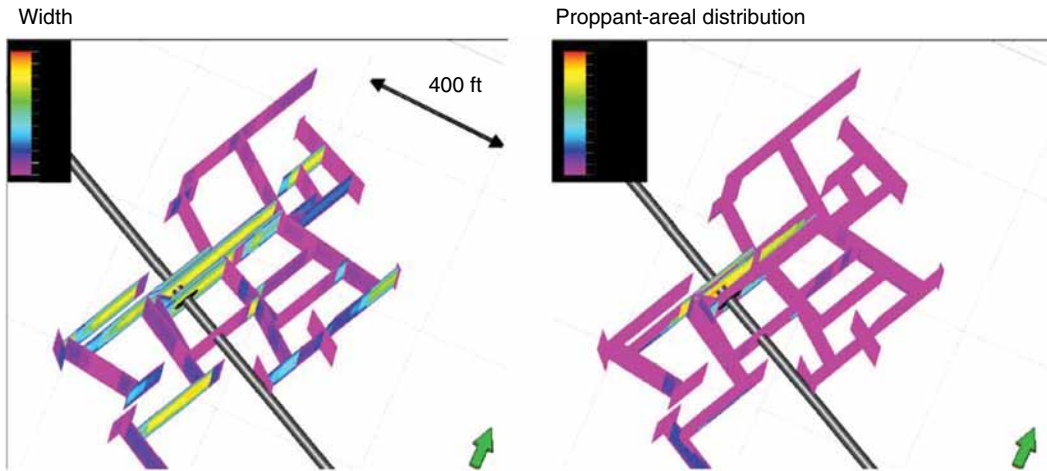


Fig. 4.88—Innovative pumping, drilling, and placement strategies.

Several innovative drilling, pumping, and placement strategies have been developed to overcome geological obstacles to the efficient introduction of proppants into the fracture and to enable greater drainage of the zone.

4.11.3 Improved Proppant Placement Methods. This section reviews new technologies to improve proppant placement and to boost proppant pack conductivity in new and older wells. Discussed are use of ball sealers, a channel-forming method to open up the frac pack and comparisons with SW with propped treatments in shale wells. Details of drilling and mechanical completion methods in long-reach shale wells are described in Section 4.11.4.

Wang et al. (2012b) contend that in many parts of the world, frac stimulation employs mechanical zonal isolation or sand and polymer plugs to control proppant placement. The authors claim these technologies are used by them in a number of reservoirs, but they depend on the presence of newly targeted and intentionally perforated sections of horizontal wells that are not already perforated. However, because most horizontal wells in the mature Huabei oil field have been producing for a very long time and the perforations are all along the horizontal sections, it is practically impossible to use these technologies.

To prevent multiple-fracture initiation in a given section, sealing-ball staged fracturing has been developed and used successfully in horizontal wells of the Huabei field. Three kinds of sealing balls (Fig. 3.73) shows general examples of ball sealers that are also used in acidizing—with densities of < 1 , 1 , and > 1 g/cm³ respectively—are pumped between stages of fracturing. They can seal perforations 360° around the horizontal well section. Higher-permeability zones are sealed off preferentially. Because staged fracturing can be carried out effectively without stopping the pumps while running ball sealers downhole, the process can be accomplished in a significantly shorter period of time than other techniques. These authors also claim that because these sealing balls are made of *wax*, they can be dissolved and removed later by the oil produced from the formations.

As noted in Fig. 4.80 as well as Sections 4.1.2 and 4.2, frac conductivity has been the subject of major efforts to improve the ability to flow fluids through a porous proppant pack. The industry has extended significant efforts toward the goal of increasing proppant-pack permeability through the development of less damaging carrier fluids, higher-strength man-made proppants, more efficient fracturing-fluid breakers. See the discussions in Sections 4.3.4, 4.6.3, and 4.9.

However, Gillard et al. (2010) contend that well testing frequently indicates disappointingly shorter or less conductive fractures than designed and that proppant-pack retained permeability is often a small fraction of the maximum expected value. The authors describe a technique that is based on the creation of a network of *open channels* inside the fracture to provide greatly improved pack conductivity. They

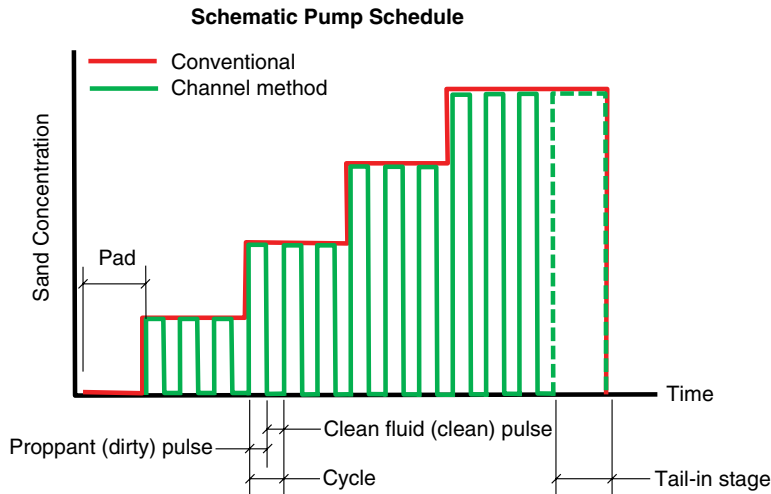


Fig. 4.89—Channel creation pumping schedule.

claim in this paper that modeling and experimental work indicates that this technique can deliver conductivities in excess of 10 times those obtained from conventional fracture treatments.

Work by Willberg et al. (2009), Gillard et al. (2010), and Medvedev et al. (2013) supported the development of a multistage process that starts with a pad, and then Gillard et al. (2010) describe a pumping schedule that consists of “short pulses” of clean fluid followed by propped-laden fluid. **Fig. 4.89** shows an example of this type of pumping schedule that compares a conventional (red) and the channel process (green). Here the usual increase in sand concentration is accomplished in small steps in which the clear fluid (no prop) is cycled with the proppant substages, but the prop concentrations are also increased as in the conventional treatments.

The *final stage* of the process (Gillard et al. 2010) terminates injection of proppant-containing fracturing fluid to tail-in the proppant to ensure a stable and reliable connection between the channels and the wellbore. This process forms channels in the proppant that fills the fracture and, thus, divides the proppant into discrete clusters (pillars), as illustrated by the graphic drawing in **Fig. 4.90**, that compares the proppant distribution using the normal process (see Section 4.3.3) with the pulsed (channel-forming) method.

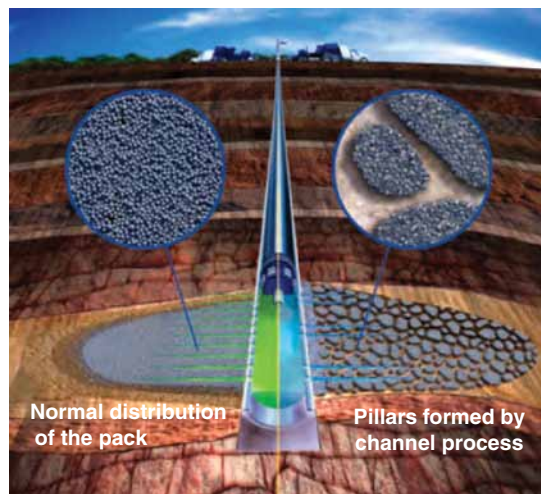


Fig. 4.90—Channeled frac pack (d'Huteau et al. 2011).

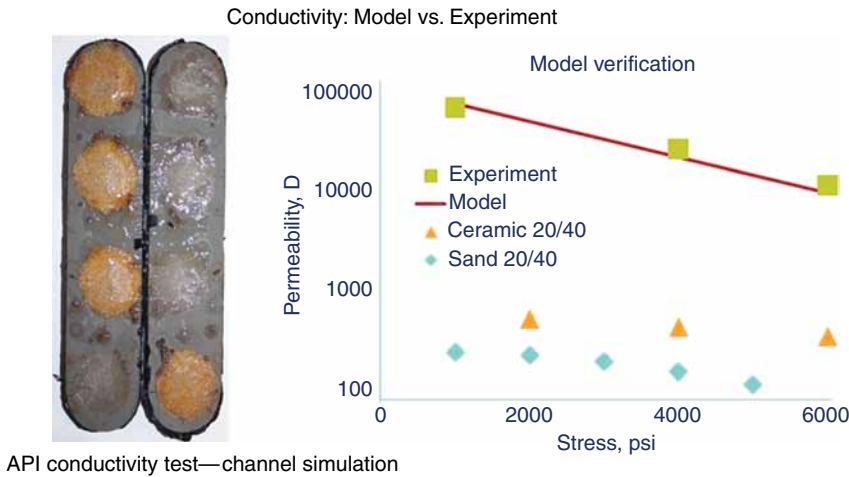


Fig. 4.91—Permeability vs. model for channel formation (Gillard et al. 2010).

Gillard et al. (2010) and Medvedev et al. (2013) report that extensive lab-, yard-, and field-scale experiments combined with theoretical work allowed creating the framework that describes the physical processes occurring during the application of this new technique. One of the experiments was a fracture conductive test done using groups of proppant that were used to simulate the “pillars” thought to be formed by the pulsed pumping method. A model was established to estimate the pack conductivity in a heterogeneous structure in which an open channel is maintained. An *API RP 61* (1989b) conductivity method was used to validate the model. **Fig. 4.91** shows that the experiment layout with the “pillars” compares well with the model and the conductivity is much higher than sand or ceramics.

The effect of adding fibers were also tested by Gillard et al. (2010) who performed proppant settling experiments using a 0.3-in. translucent slot. Gillard et al. (2010) also note that various types of solids, including fibers, may be added to the fluids. These fibers could be modified to have an adhesive coating alone or an adhesive coating coated by a layer of nonadhesive substance dissolvable in the fracturing fluid as it passes through the fracture. Medvedev et al. (2013) claim that *degradable fibers* [example: Hoefler et al. (2008)] are also being employed during this pulsed fracturing process and hydrolyze in the fluid to produce an organic acid. Both the fibers and the RCPs were described in Section 4.9.

Samples of proppant-laden fluid were injected at the top of the slot. Settling of the slugs was monitored over time and also assessed qualitatively by visual inspection. **Fig. 4.92** shows the position of a given proppant slug (dark brown blob) at the beginning of the test (left panel). This figure also shows the position of a proppant slug with fibers (center panel) and without fibers (right panel) after the same elapsed time after slug injection. It is seen that the proppant sample that contained fibers exhibited a significantly smaller settling rate and maintained better integrity when compared to the proppant sample without fibers. These results demonstrate that fibers not only reduce the settling rate, which is critical to preserve the distribution of pillars and channels across the fracture height, but also reduce the dispersion of sand slugs, which allows maximizing the volume within the open channels and therefore, increase the overall fracture conductivity.

The authors (Gillard et al. 2010) claim that significant improvements claimed are less frac water required and less proppants needed because there are clear areas where little proppant is present. In the time period of the publication of this book, the availability of large volumes of appropriate frac water as well as proppant have become major challenges to expansion of the frac method. See Section 6.3 for additional discussions of frac water use and reuse. These authors also claim that a 15-well field study, selected from over 50 treatments, performed up to date with this technique, show post treatment results with significant gains in well production, and expected ultimate recovery with respect to offset wells treated with conventional fracturing methods. The exact details of the fracture fluids were not provided.

Rhine et al. (2011) have studied fracture treatments in the Eagle Ford formation (true vertical depth: 10,900–11,500 ft) in the Hawkville field near Cotulla, Texas. See Fig. 4.5. This section of the play

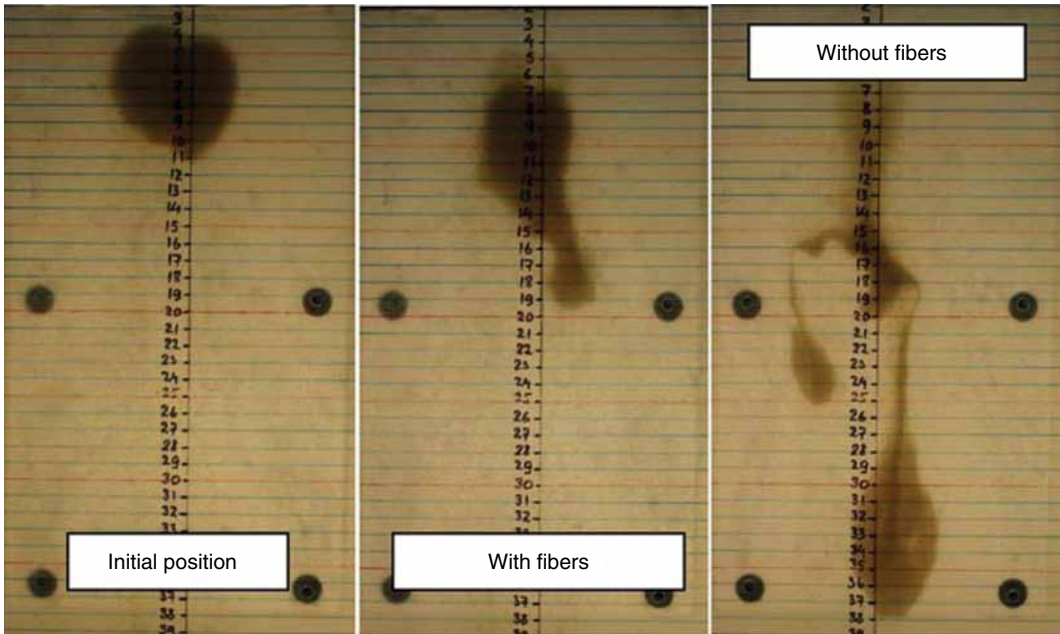


Fig. 4.92—Impact of fibers on proppant slug settling and consolidation (Gillard et al. 2010).

comprises mainly limestone with 100 to 600 nD permeability and 7 to 10% total porosity. The formation requires horizontal laterals with multistage HF for economic production. The authors data claim that the channel-fracturing technique (Gillard et al. 2010) was evaluated in 12 horizontal wells. Results from 38 offset wells treated with conventional techniques (SW or hybrid-type treatments) are also reported to compare performance. Non-normalized data from this sample of 50 wells showed hydrocarbon production increases ranging between 32 and 68% in favor of the channel-fracturing technique. Another important observation was that the amount of water and proppant used was significantly less than that required from the offset wells. Water savings are especially significant in the south Texas counties that hold the Eagle Ford oil/gas plays.

The authors of this book also note that some fracturing treatments in many low-permeability formations in North America have been pumped using low-viscosity hydraulic fracture fluids that were proppant-free or with only a small amount of proppant. This method has several names, the most common of which is referred to as a WF or SW (see Section 4.3). Some fractures created by the SW process may be practically proppant-free. However, the created fracture surfaces shift relative to each other during fracture creation and propagation. The resulting misalignment of irregular surface features (asperities) prevents the two fracture faces from forming a tight seal upon closure. However, because of poor transport, the proppant tends to accumulate below the casing perforations, most likely along the base of the created hydraulic fracture. This accumulation occurs because of a high rate of proppant settling in the fracturing fluid along a narrow hydraulic fracture, and insufficient proppant-transport ability, (both because of low-fracturing-fluid viscosity). When fracturing-fluid injection stops at the end of a WF, the fracture immediately shortens in length and height. This procedure slightly compacts the proppant, which remains as a dune at the fracture base near the wellbore. Because of the dune's limited length, width, and typically, strength (often low-strength sand is used), WFs are usually characterized by short, low-conductivity fractures (Fredd et al. 2000).

This discussion illustrates that WFs result from the passage of formation fluid flowing through the network of narrow channels created inside of the fracture because of incomplete closure caused by surface rock imperfections (i.e., the SW process results in low-conductivity fractures).

4.11.4 Drilling and Mechanical Frac Placement for Long, Deviated Wells. King (2010) notes the development of long horizontal wells has contributed materially to the improvement in production

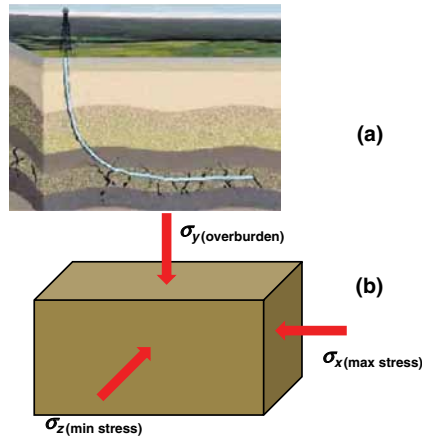


Fig. 4.93—(a) Directional drilling illustration and (b) direction of the stress field.

from shale formations. The direction of the drilling process relative to the stress field also can affect the final fracture effectiveness. Fig. 4.93 shows a drawing of directional drilling into a horizontal reservoir (a). Part (b) of the drawing shows the stress field on this formation. Drillers would normally place the horizontal part of the hole in the same direction as the minimum stress (z axis in this drawing) because it takes less force in that direction. However, then the fractures would then propagate in the same direction and not necessarily give a good stimulation. However, if the well is drilled in the x axis (maximum stress), the fractures would propagate at 90° to σ_{\max} , and thus, possibly increase the drainage field. When coupled with the multiple-fracture methods described in the next paragraphs, the productivity of a TG formation may be increased greatly.

Several processes have been developed to produce the multiple fractures needed to stimulate a TG formation. Halliburton (2005a) has developed a staged fracturing process to treat horizontal wells. As seen in an illustration (Fig. 4.94) of the process, sand-laden fluid is pumped through a hydraulic jetting tool. The fluid impinges on the formation thus creating a cavity. As the cavity is formed, pressure on the bottom of the cavity increases, eventually initiating a fracture in the formation. The annular fluid is pulled into the fracture, helping to extend it. Using a coil tubing rig, multiple fractures can be started. The author notes that the process can also be used to produce acid fractures in carbonate formations. This article also claims that an openhole horizontal well had 5½-in. casing, depth 3,821 ft, with a 4¾-in., 1,600-ft openhole horizontal section. 2⅞-in. CT was used to rapidly deploy the multiple fracturing service assembly into the openhole section. Eight fractures were successfully placed within a 5-hour period. The treatment was claimed to have resulted in an eightfold production increase.

A multiple-stage fracturing process (PackersPlus 2011b) has been implemented using a system that places multiple rock packers in the drilled hole (see Figs. 3.108 and 4.7). The article claims that the hardware components for the services are typically installed in a single-well operation, and stimulation fluid placement is performed in one continuous pumping operation, providing claimed excellent operational efficiency. In addition, there is no requirement for a drilling rig while the stimulation fluids are being pumped. As noted in this illustration, ball actuators are run to open each segment starting with the toe of the well. The article also claims that VES fluids are the preferred chemistry for these operations (see Section 4.4.4).

Al-Naimi et al. (2008), Baumgarten and Bobrosky (2009), and Al-Jubran et al. (2010) have given more details of the multifracture system described in previous paragraphs. They note that horizontal wellbores have enabled significant increases in productive zone contact areas. However, even with these increased contact areas, the expected long-term production increases were not initially realized with conventional stimulation techniques. Multistage fracturing systems have resulted in impressive long-term production improvements.

Al-Naimi et al. (2008) explain that the completion is now run as part of an uncemented liner, and components are spaced out based on the required number of stages. Once in place, the openhole

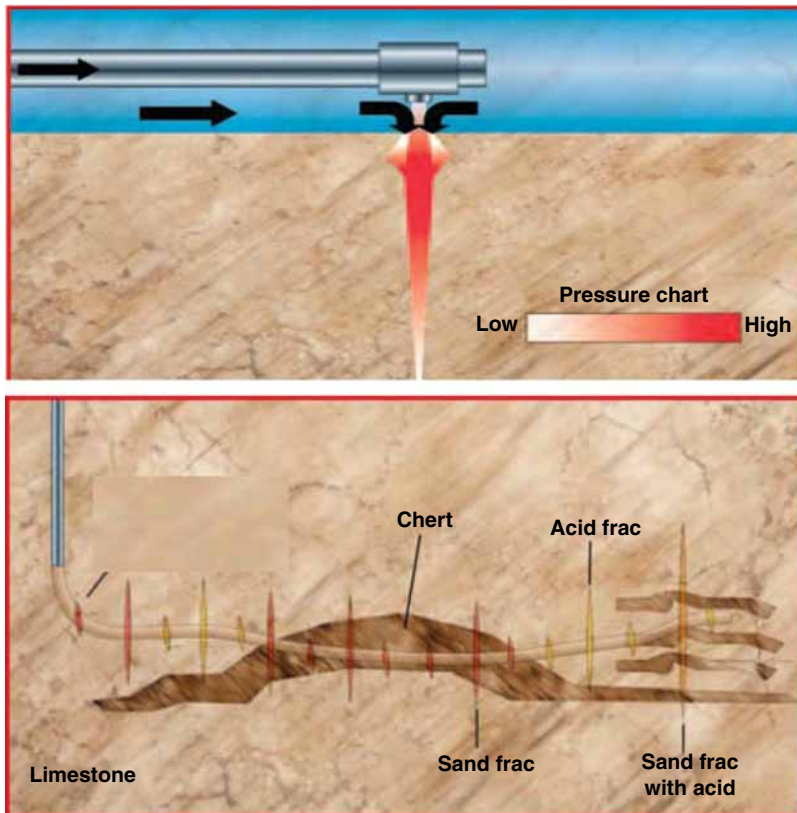


Fig. 4.94—Multiple fractures with jet (Halliburton 2005a).

packers are hydraulically set. Ball-activated frac ports (FPs) are placed between a set of two openhole packers with spacing between the packers varying from 100 ft to 1,000 ft. A maximum of nine FPs (Fig. 4.7) can be run in the openhole in this type of liner. Initially, all FPs are closed. Starting from the toe section of the well, each FP is opened by dropping a ball from the surface and the ball isolates the horizontal section below each FP, thus ensuring that at any given time only one zone is being treated.

With the implementation of these well preparation and deployment techniques, several multistage fracturing assemblies have been successfully installed, allowing proper placement of multiple fracturing jobs, which have in turn resulted in continued production improvements from TG formations.

Seale (2007) describes a fracturing system for sandstone wells that uses multiple FPs. Initial layouts for the FP designed for the maximum flow area the system required, while retaining the desired tensile and compressive strengths as the standard parent liner for the size in question. For example, they claim that in 8½-in. openhole, the standard completion is 7 in. or 5½ in., so the mechanical properties of the FP were designed to exceed liner properties.

Halliburton (2012) describes a multiple fracturing and multiple zone system based on swellable packers as well as balls that open FPs to allow the proper placement of the fluid and proppant. The sequence of tools is run into the target zone before pumping the fluids. Fig. 4.95 shows a screen print from a film clip that describes the use of the tools.

The reference claims the following benefits:

- Alternative to plug and perforate process
- Helps eliminate the necessity of wireline intervention and its associated risks
- Reduces stimulation cycle time from weeks to days or from days to hours with continuous pumping
- Helps prevent issues associated with pumping tools into place

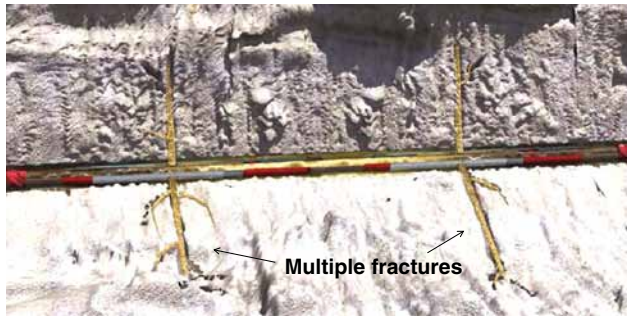


Fig. 4.95—Multiple fracturing system showing a simulation of the process (Halliburton 2012).

- Reduces water requirements when compared to pumping plugs and guns on depth
- Number of flow ports and sleeve may be tailored to flow regimen

Westenhaus (2012) claims that this multifracturing system as well as the channeled frac processes described in Section 4.11.3 (Gillard et al. 2010) constitute super-frac technologies that will be used in millions of wells worldwide.

4.12 Case Histories and Best Practices for Proppant Fracturing

These papers document some case histories and best practices in recent applications of hydraulic proppant fracturing treatments.

4.12.1 TG and Shale Gas. Rahim et al. (2002) report that as part of gas production enhancement and quick recovery of reserves initiative, HF campaign was initiated in 1998 to treat the sandstone and carbonate formations in the Ghawar gas fields in Saudi Arabia. To date, numerous wells have been matrix acidized, acid fractured, and proppant fractured. Many different procedures and fracturing techniques have been adopted as part of a learning process to optimize candidate selection, perforation strategy, fracture design, and implementation. The incremental production from the Khuff carbonate gas ascertains the success of the acid fracturing treatments.

For the pre-Khuff sandstone reservoirs, because of the unconsolidated nature of some high-potential sandstone layers, indirect fracturing technique has been adopted where the consolidated, low-porosity section is perforated and from where the induced fracture is initiated. This procedure curtails the risk of sand production. Very recently, fracturing wells with frac-pack technique and completing them with mechanical screen are being implemented. Successes on these pre-Khuff treatments are usually judged by sand-free production rate and conditions and by comparing post-fracture production increase with simulated, prefracture production based on reservoir properties calibrated by post-fracture production match. In most cases, this gain is significant to justify the expenses of the fracture treatment. However, the priority in Saudi Aramco is to recover the required volume of gas to feed its giant gas plants.

A frac-pack screens completion although more expensive does not limit drawdown pressure. Fast recovery can be with high-drawdown pressures. Sand production models were used for prediction purposes.

Cramer (2008) has reviewed the stimulation the unconventional reservoir, which has different meanings to different people. Certain reservoirs termed unconventional have a rock matrix consisting of interparticle pore networks with very small pore connections imparting very poor fluid-flow characteristics. Abundant volumes of oil or gas can be stored in these rocks, and often the rock is high in organic content and the source of the hydrocarbon. Yet because of marginal rock-matrix quality, these reservoirs generally require both natural and induced fracture networks to enable economic recovery of the hydrocarbon.

Rock types in this class include shale and CBM. The term shale is a catchall for any rock consisting of extremely small framework particles with minute pores charged with hydrocarbon and includes carbonate and quartz-rich rocks. Another type of unconventional reservoir is stacked pay units exhibiting

somewhat better pore characteristics than in the case outlined above but with the individual units tending to be lenticular in shape and having an extremely small size or volume. These two classes of unconventional reservoirs are amenable to well stimulation and will be the focus of this paper.

The above rock types, when commercially exploited, are known as resource plays. Once a low priority, the depletion of conventional reservoirs and improving price for oil and gas has driven unconventional reservoirs to an important place in the oil and gas industry. In some regions (i.e., Rocky Mountain province), unconventional reservoirs represent the primary target of current activity and remaining hydrocarbon development. Given their unique petrophysical properties, each type of unconventional reservoir requires a unique approach to well stimulation, with often differing objectives than exist with conventional reservoir types. This paper reviews the characteristics of the basic unconventional reservoir types, lessons learned, and successful stimulation practices developed in completing these reservoirs, and areas for improvement in treatment and reservoir characterization and treatment design.

LaFollette and Holcomb (2011) documents a data-mining study of well, hydraulic fracture treatment, and production parameters for horizontal wells in the north Texas Barnett shale play. In this study, the authors have analyzed well and production data from more than 13,400 producing Barnett wells. A subsample of over 3,300 horizontal wells was characterized with respect to detailed well architecture data such as drift direction and angle, lateral length, perforations, etc. The study uses pattern-recognition techniques in conjunction with more traditional statistical techniques to interpret hidden trends in otherwise scattered datasets. This work provides a case study in the practical use of data-mining techniques to address questions of best practices in shale gas reservoirs

Hlidek and Rieb (2011) summarize fracture stimulation treatment best practices determined by a 3-year study of production results of several thousand fracture treatments in more than 460 wells in the Bakken Shale formation in Saskatchewan, Canada. Treatment variables include proppant type, proppant concentration, fracturing-fluid formulation, treatment size, wellbore azimuth, and lateral frac density. Treatment effectiveness is based on 4-month cumulative production comparisons that include: oil, water, and total fluid.

The Bakken is a low-permeability oil and water-producing formation at a depth of about 1500 m (4,900 ft). The study area covers about 390,000 hectares (1500 mile²) in the northern region of the Williston Basin. Wells in this region require propped fracture stimulations for economic production. All wells in this study are drilled horizontally, normally completed openhole in the Middle Bakken. Most completions consist of isolated multistage treatments. One of the significant challenges encountered during fracture treatment design is the presence of an overlying water aquifer, known as the Lodge pole. Fracture treatments that breach the Lodge pole aquifer are considered less than optimum because of excess water production.

Crosslinked fluids (borate as well as Zr) were used in most of the treatments. **Fig. 4.96** shows a plot of water and oil production for wells fracked with both fluids. The authors conclude that there were no statistically significant differences. The sand concentration correlated with water production but not with oil production. That is, lower sand concentrations improved the oil-in-water ratio.

4.12.2 Horizontal Completions. Daneshy (2011) notes that the unparalleled spread and variety of completions in use by the industry have clouded the selection of suitable completion and best fracturing strategies for optimizing productivity of hydraulically fractured horizontal wells. There also exists a gap in our understanding of the mechanics of fracture initiation and extension in horizontal wells. This has resulted in uncertainty in our response to large variations observed within and between different fracturing stages in the same horizontal well and, in fact, within the reservoir.

This paper is based on review of many horizontal well hydraulic fractures. It includes a discussion of multiple completion options for both open and cased holes. It shows that in openhole completions there is strong tendency for fractures to initially grow axially (longitudinally) before reorienting to become perpendicular to the least in-situ principal stress. This can cause fracture extension across openhole packers and possibility of randomly located transverse fractures (well orientation permitting). Infrequent screenouts usually occur within the openhole section itself. There is evidence indicating that the sealing balls used for separating different fracturing stages may sometimes break during

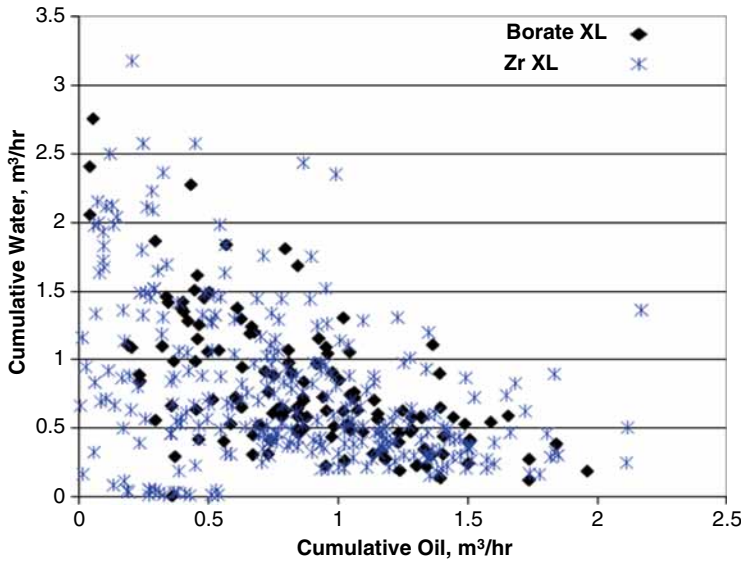


Fig. 4.96—Water and oil production from Brakken fracture treatments as function of crosslinker (Hlidek and Rieb 2011).

the treatment. This may prohibit fracturing all well segments and may also interfere with production. In cases of openhole fractures created by hydrojetting techniques, one of the issues is propensity to proppant flowback. In cased-hole completions, the tendency for axial initiation and early growth still exists. One of the popular techniques is creation of multiple closely spaced limited entry fractures within each isolated wellbore interval. Treatment data shows that many of these fractures soon join and coalesce toward a single fracture.

Furthermore, proppant and fluid have different distributions between various perforations. The issues with techniques based on hydrojetting include inadequate perforations, hardware problems, and tendency for proppant flowback.

4.12.3 Frac Pack. Morales et al. (2003) note that as the frac-pack technology continues to evolve, there are a number of topics that need more understanding and improvement. Some of these are the estimation of correct closure pressure, which in turn leads to evaluation of the correct fluid efficiency, and ultimately leads to the design of the slurry schedule. In addition, a proper fluid selection criterion is critical to the placement of highly conductive propped fracture wings via tip screenout.

Special attention is given to skin data from buildup tests showing skin increasing with increase in k_r . In essence, the paper shows effective ways to lower the skin, and consequently increase production. This goal is accomplished by adjusting the design of the frac-pack slurry schedule to observation from field data and to numerical modeling of the fracturing process and, also, by considering the issues stated above. As a consequence, the paper shows that important steps to minimize the skin are to

- Design the fracturing fluids to suit the character of the fractures in soft formations where cool down, fluid velocities, and fluid exposure time are important.
- Use equilibrium method to fine-tune the closure pressure (and fluid efficiency) evaluation.
- Clean and pack the perforations not aligned with the fracture.
- Use diversion techniques to pack the entire reservoir.
- Evaluate the packing efficiency with bottomhole gauge data (temperature and pressure) and/or radioactive tracers.

When these steps are meticulously followed, fracture performances with lower skins can be obtained as demonstrated in the case history. A case history illustrates these principles. The wells in the Camben Hills area of the Gulf of Mexico are frac-packed to prevent fracture propagation into wet

sand. The designed fracture length was 20–30 ft/1 in. propped width. The pumping schedule that was successful was

- Pumped 50 gal/ft 10% HCl to clean the perforations
- Equilibrium step rate test using a linear gel
- Calibration treatment using a crosslinked gel
- Frac pack with rates ranging from 20–30 bpm
- The leakoff coefficient was 0.01–0.032 ft/min^{1/2}
- Skin ranged from 1 to 4

4.12.4 VES Fluids. Bustos et al. (2007b) claim that CO₂-based fluids are commonly used to fracture-stimulate formations with low-reservoir pressure as well as formations that are more sensitive to water treatments (high capillary pressure, swelling clays, etc.). In particular, the Frontier formation located in Bighorn Basin, Wyoming, has seen a variety of stimulation fluids used over the past years with varying degrees of success. When dealing with water-sensitive formations, a common practice has been to use oil-based fluids. However, fluids of this nature can have detrimental effects on gas zones with low-reservoir pressure, and this might be the reason for erratic well performance of previously treated Frontier completions. It has also been determined that oil-based fluids can alter the reservoir wettability and hence cause formation damage. With this in mind and considering the environmental and economical benefits of using a water-based fracturing fluid, a VES based, CO₂-compatible, high foam quality (>60%) fluid was proposed as the main fracturing fluid.

The fluid is based on a patent by Chen et al. (2010b) that describes an aqueous VES fluid foamed or energized with carbon dioxide, in which the VES is more compatible with the carbon dioxide, is made by the addition of one or more than one synergistic cosurfactant. The synergist cosurfactant includes quaternary amines and ethoxylated carboxylates having a hydrophobic chain shorter than the hydrophobic chain of the VES.

The case study was in the Big Horn field in Wyoming, clean sandstone with a bottomhole temperature of 160°F. The treatment used a 70% quality CO₂ foam with the VES. After the pad, 5 VES/CO₂ stages were pumped with the proppant ramped from 2,000 to 25,000 lbm and 1–5 PPA. The well has produced 1100 Mcf/D for 7 months.

4.13 Things to Think About

- HF (propped frac as well as acid fracturing described in Section 3.8) encompasses a very wide range of stimulation enhancements methods that are applied to sandstone, carbonate as well as to shale-type formations. Because of the wide variety of applications, an equally wide variety of fluids and proppants must be tailored to the differing well and placement conditions. This chapter has described how the chemistry of the fluids must support the goals of the treatment. Usually the goal is to place a highly permeable frac pack with as little FL as possible. The degraded viscous fluids must then be quickly returned to the surface. Many new advances in chemistry as well as understanding of the physical chemical principles have been reviewed.
- Major advances in the chemistries start with the use of polymer concentrates including solutions/suspensions of guar-type polymers in organic fluids. These fluids are hydrated in the surface mixers, then metered precisely, and then mixed with the proppant before insertion into the well. This advance has reduced the needs for prehydration of the linear gel.
- A new type of viscous polymer fluid based on VES gels is being applied in many wells. These fluids are shear thinning when stressed and then reform into the gel when the stress is removed. They thus have good friction pressure characteristics and do not require a polymer-type breaker. However, they can be more expensive than conventional gactomannans polymers, require different FL agents and a different type of cleanup aid (frequently called a VES breaker). The use of N₂ and CO₂ to cause foams of polymers and VES fluids to form allow for improved FL characteristics as well as reduced water requirements.

- Many fundamental investigations of the chemistry of the fluids during the various parts of treatments have used new equipment such as reciprocating and oscillating viscometers.
- Different delay mechanisms have been developed to precisely control the rate of crosslinking as well as the rate of fluid viscosity reduction to aid the proper placement of proppant as well as to control the friction pressure. Included are a range of encapsulated additives that include the crosslinkers and the breakers.
- New proppants including very high-strength ceramics, rod-like ceramics for high-pressure reservoirs were developed. For the emerging TG applications, ultralow density proppants that include hollow spheres and those made from natural products are in use. To prevent flowback of proppants, sticky coatings and fibers that trap the sand can be employed.
- The application of fracturing methods to various types of TG formations has materially increased the availability of gas supplies in the US. This has not come without some controversy because thousands of gallons of fluids are needed and there are concerns with the use and disposal of these fluids. Various methods to treat and to reuse the fluids are described in Chapter 6.

Improved Oil Recovery Chemical Applications

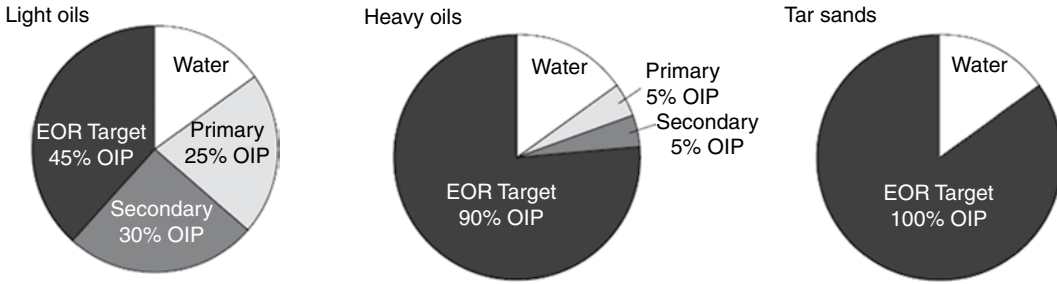
Improved oil recovery (IOR) and enhanced oil recovery (EOR) encompass processes designed to produce more oil and gas than simply letting a well flow naturally until it is uneconomical. Sheng (2011) provides a review of the definitions used in the literature for IOR and EOR. Unfortunately, the terms are often used interchangeably. Generally, IOR activities occur in the secondary and tertiary production phases (described in Chapter 1) and are considered to include EOR as well as conformance control, immiscible gases injections, water injection, and stimulation processes. EOR is generally limited to those processes that aim to reduce residual oil saturation in the reservoir. These activities generally occur during the tertiary production phase and primarily include thermal recovery methods, miscible floods, and chemical floods (polymer, surfactant, combination processes).

Typical improved recovery from IOR is about 5 to 30% oil in place (OIP), depending on the technology, the oil, and the reservoir (NETL 2001). Thomas (2008) shows EOR recovery targets based on the gross oil viscosity. **Fig. 5.1** shows the estimated average amount of OIP for three oil types after primary and secondary methods have been applied, and thus the amount that is the target of EOR processes. Note that EOR accounts for most of the production of OIP from heavy oils and tar sands.

This chapter will focus on the application of IOR using chemical methods. Both conformance control as well as the chemically related EOR methods will be described. **Fig. 5.2** lists thermal and non-thermal IOR methods that are in use or are being developed (Thomas 2008). This chapter will focus primarily on the nonthermal processes (blue box in the figure) and especially on the chemical methods. There is a large amount of published literature already on IOR and hence this chapter will provide only limited coverage of IOR fundamentals and will instead focus on highlighting current trends and emphasizing the links between chemical processes in IOR with chemical processes described in Chapters 2 through 4. The reader should consult the books by Green and Willhite (1998) and by Lake (2010) for detailed description of EOR and the books by Willhite (1986) and Sheng (2011) for a description of waterflooding and chemical EOR methods, respectively.

Thermal methods primarily improve production by using heat to reduce oil viscosity of the oil. Approximately 60% of the world's production of oil from IOR involves thermal methods (Chekhonin et al. 2012). Thermal methods include the more common steam injection (steamflooding) and the less commonly applied in-situ combustion, in which a portion of the oil is burned within the reservoir to produce heat. Steam injection may be considered a part of an IOR/EOR process (or as part of primary production for very heavy oils). While, steamflooding is not classified as a chemical method, there is lot of chemistry involved in the process as the hot water dissolves minerals in the rock as well as the interactions with crude. Thus, examination of the topics of scale control and corrosion (Section 2.2.3) as well as emulsions (Section 2.4) are necessary for maintaining flow and production. Please consult Lindley (2001a) and Lake (2010) for detailed description of thermal methods.

The physical/chemical procedures described in this chapter have been introduced and used in other processes described in previous chapters. For example, chemical diversion methods are employed in



(Assuming $S_{oi}=85\%$ PV and $S_w=15\%$ PV)

Fig. 5.1—EOR targets (Thomas 2008).

acidizing (Section 3.7.2) to direct chemicals to different zones where they will dissolve the rock or damage. In EOR, the same diversion chemicals [hydrolyzed polyacrylamide polymer (HPAA), viscoelastic surfactants (VESs)] provided water cutoff and mobility control. Also surfactants are widely used in acidizing and fracturing to produce foams, form or prevent emulsions, and to remove hydrocarbons from mineral surfaces. The surfactant EOR methods perform many of the same functions.

Other areas of commonality with the processes discussed in Chapters 2 and 3 include the need for flow assurance (FA) activities, including corrosion and scale control/removal and organic deposit suppression. When IOR processes (including waterflooding) commence, the number of active wells may jump by a factor of 5 (or more), along with a forest of connecting lines, flowlines, and pipelines. The EOR activities can greatly increase the water/oil (W/O) ratio, and processes such as CO₂ injection will alter the pH and change the scaling/corrosion conditions. Therefore, operators require a holistic approach to the integration of all of these chemistries to maintain/enhance production.

This chapter will emphasize the use of the chemical IOR/EOR methods highlighted in Fig. 5.2 and that are depicted in Fig. 5.3 and include polymer, alkaline, surfactant, miscible, and micellar polymer

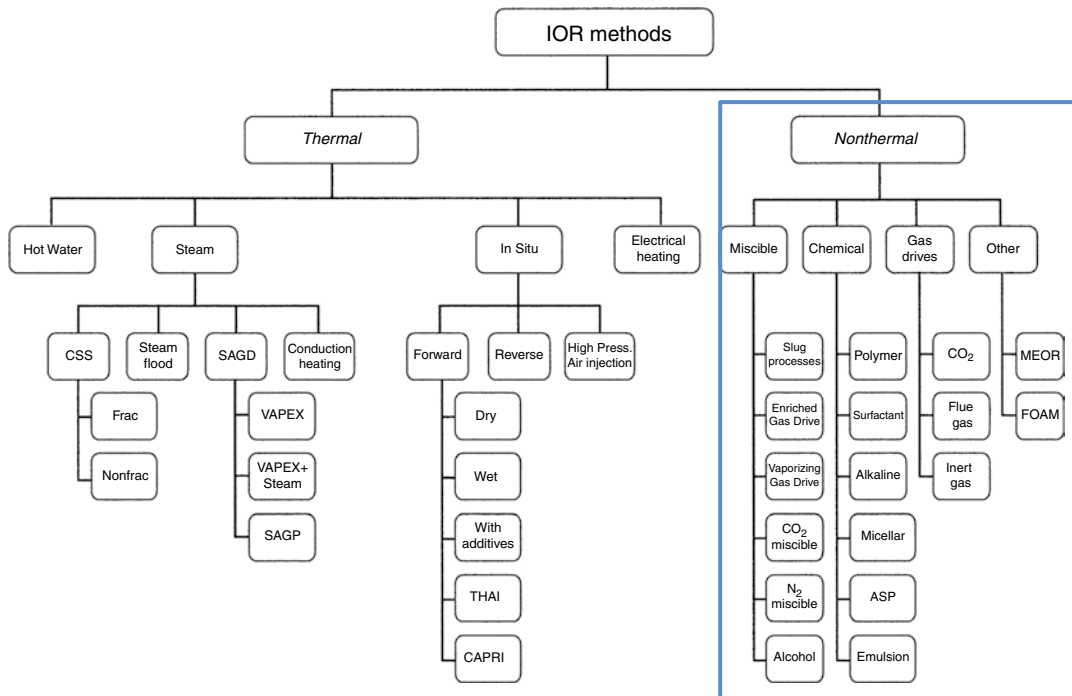


Fig. 5.2—Summary of IOR treatment methods (Thomas 2008). Chemical methods in blue box.

Recovery methods in this category may include surfactant, polymer, and alkaline flooding. After a reservoir is conditioned by a water preflush, specific chemicals are injected to reduce interfacial tension (help release oil), and/or improve mobility control (reduce channeling). This action is followed by injecting a driving fluid (water) to move the chemicals and resulting oil bank to production well.

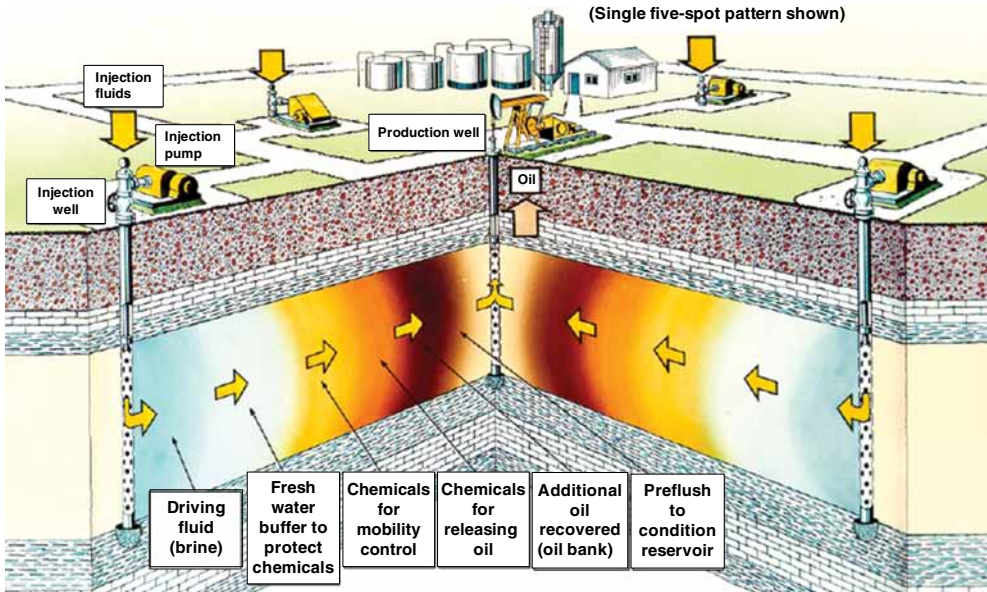


Fig. 5.3—Chemical recovery EOR methods (Lindley 2001a).

(MP) as well as mixed methods such as alkaline-surfactant polymer (ASP). These methods use several different strategies but can be summarized as ones that

- Increase the *volume* of the reservoir that is contacted by a displacing fluid including water or a gas. This is accomplished by using diverting agents that direct flow to areas not being swept.
- Improve the removal efficiency of the displacing fluid. This is accomplished by changing the wetting characteristics of the three phases to allow the displacing phase to wet the surface. The oil is then dissolved or dispersed by the fluid. This same process takes place in removing any oily fluid (such as a food residue) from a hard surface by adding a surfactant to water.

In this chapter, Section 5.1 introduces the basic chemical and physical principles that will control the enhanced recovery of liquid hydrocarbons (HCs). Section 5.2 describes various selection criteria for IOR projects, while Section 5.3 describes test methods for deterring properties of the well fluids and EOR fluids. Sections 5.4 and 5.5 discuss the details of the use of many different chemicals used to achieve the enhanced production of oil through the application of these principles. Section 5.6 describes methods (in addition to polymer floods) to improve sweep efficiency and to reduce excess water or gas production (conformance control). Section 5.7 provides a review of the use of chemical tracers in various EOR-related applications.

5.1 Basic Principles of IOR

An important question is why is there so much oil that *cannot* be recovered by primary and secondary methods, even for low-viscosity oil? One set of major reasons is that the reservoirs are very heterogeneous, and there are not necessarily connections between various sections of the reservoir either vertically or horizontally. Creek et al. (2009) note that the reservoir may be compartmentalized so that there are no connections to allow the fluids to reach the production tubing. EOR treatments usually *cannot* affect these types of disconnections; however, hydraulic fracturing (HF) (Chapter 4) may be able to connect some zones.

Production methods that involve directional drilling and perforations into unconnected pockets also may improve ultimate recovery. Even in reservoirs where there are physical connections, the permeability and porosity as well as mineralogy may differ greatly from zone to zone, and these factors can affect the flow of oil as it is swept by the primary and secondary processes. Another group of reasons for oil remaining in place is because of the relative W/O wetting characterizations of the formation. A drawing from Abdallah et al. (2007) (Fig. 5.4) shows various possibilities of the fluid/surface wetting in the pore spaces of a formation. A water-wet formation (a) allows the oil to move with less friction, because most of the oil is *not* adsorbed on the mineral surfaces, while mixed-wet (b) and oil-wet formations (c) would impede the flow of the oil phase as it is displaced by water or gas. As the reservoir matures and various processes have been applied, these factors may change the initial wetting characteristics. Oil also may be bypassed because of permeability differences in which the sweep fluid goes preferentially into the higher permeability sections and lower permeability sections are bypassed.

Thomas (2008) and Lake (2010) describe two very important factors that can control recovery of some of this residual oil using EOR methods. These include *increasing* the capillary number (N_c) and *reducing* the mobility ratio (M), defined below. Using these concepts, EOR methods may be designed to affect the total sweep efficiency of the reservoir as well as the oil in the individual pores of the reservoir. N_c is associated with the micropore level chemistry and M is associated with both microreservoir as well as the macroreservoir flow characteristics. These are discussed in Sections 5.1.1 and 5.1.2. The definitions are in Eq. 5.1 and 5.2. The capillary number is defined as

$$N_c = \frac{v\mu}{\gamma} \dots\dots\dots (5.1)$$

Here, v is the Darcy velocity (m/s) of fluid flow, μ is the displacing fluid viscosity (Pa·s), and γ is the interfacial surface tension (IST) (N/m) between the *two* fluids (displacing and the oil). The most effective way of improving displacement and for increasing N_c is by reducing γ through the application a surfactant or by heat. Note that in the theoretical plot in Fig. 5.5, the capillary number must be increased by several orders of magnitude to affect a significant improvement in oil saturation. Increasing the viscosity of the displacing fluid also increases N_c . Thus, making the fluids more miscible is a requirement for improvement. The mobility ratio is defined as

$$M = \frac{\lambda_{ing}}{\lambda_{ed}}, \lambda = \frac{\kappa}{\mu} \dots\dots\dots (5.2)$$

Here, λ_{ing} is the mobility of the displacing fluid (water or mixture) and λ_{ed} is the mobility of the displaced fluid (oil), κ is the effective permeability of the formation (md) to the fluid, and μ is the

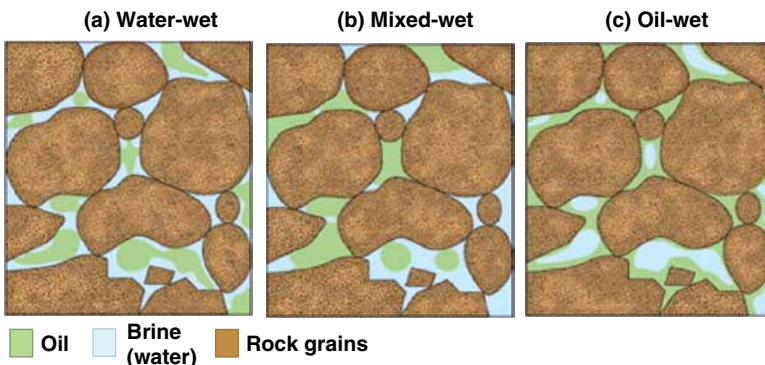


Fig. 5.4—Oil and water wetting of formation particles (Abdallah et al. 2007).

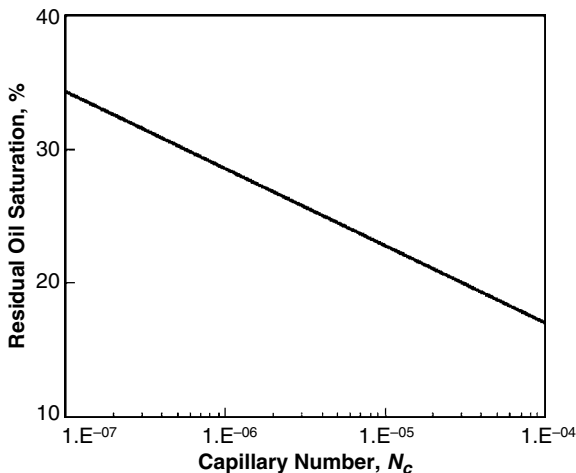


Fig. 5.5—Effect of capillary number on residual oil saturation (Thomas 2008).

viscosity of the fluid concerned. The author (Thomas 2008) claims that when $M > 1$, this is an *unfavorable* situation and may indicate more or a different fluid is needed. This is a measured property and the permeability will be affected by the oil/water (O/W) wetting characteristics of the formation. Fig. 5.6 shows the effect of the mobility ratio on the amount of displaceable oil when 1, 2, and 3 pore volume (PV) of sweep fluid has been injected. At high M values, little oil can be displaced. The author (Thomas 2008) notes that these calculations are based on the Buckley-Leverett theory of waterflooding (Buckley and Leverett 1942).

Much of the technology described in subsequent sections of this chapter will consider methods to affect these values and thus remove more of the OIP. The various EOR methods, and especially the chemical strategies, have to affect the microscopic forces that take place at the pore structure level of the matrix as well as improving the ability of the fluids to sweep a higher percentage of the volume of the reservoir space.

5.1.1 Macroscopic Displacement of Fluids. In displacement processes, the fluid initially present in the pores of the reservoir rock is removed and replaced by a second fluid, with which it is not miscible.

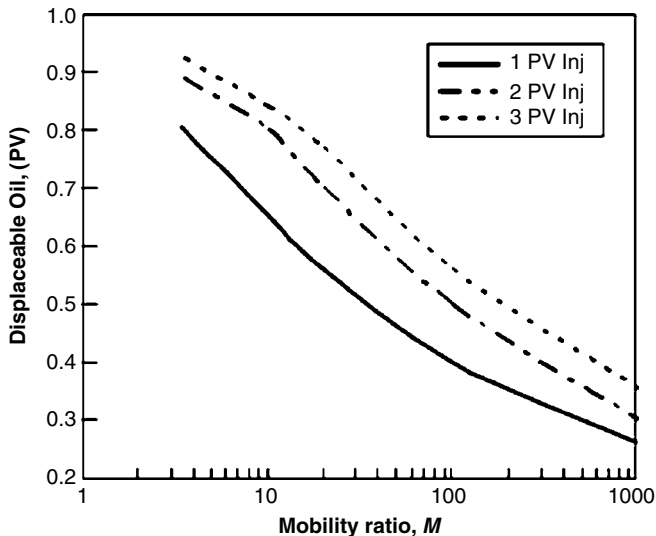


Fig. 5.6—Effect of mobility ratio on displaceable oil (Thomas 2008).

A displacement process can take place either naturally (e.g., when the connate water, which is present since the formation of the rock, or the gas cap invades the oil-bearing zone following a decline in pressure caused by production), or by means of injection from the surface of either water, steam, or gas. In oil fields (not including heavy oil), water drive is the mechanism that results in the highest recovery factor (Lake 2010) in the reservoir. When the reservoir lacks a natural aquifer maintaining reservoir pressure, injecting water frequently is the preferred method both to maintain the pressure of the reservoir at a value equal to or slightly higher than saturation pressure, and to sweep the oil toward the production wells. At the scale of interwell distances (macroscopic), oil is bypassed because of lateral or vertical formation heterogeneity, well pattern inefficiencies, or low-viscosity injection fluids. Improving sweep efficiency is typically one of the goals of reservoir engineering, modeling, and IOR efforts.

This applies to all types of IOR that uses fluids different from the crude oil. In the processes of *immiscible displacement*, the composition of the displacement fluid (e.g., water) and the displaced fluid (oil) remains unaltered and a separation interface is maintained throughout the entire process; water and oil constitute two completely distinct fluid phases.

Lake (2010) describes the efficiency of recovery of a species (the oil, *i*) E_{Ri} (Eq. 5.3) using two components, the displacement efficiency (E_{Di}), and the volumetric sweep efficiency (E_{Vi}).

$$E_{Ri} = E_{Di} E_{Vi} \dots \dots \dots (5.3)$$

The components of Eq. 5.3 are

$$E_{Di} = \frac{\text{Amount of } i \text{ displaced}}{\text{Amount of } i \text{ contacted}} \dots \dots \dots (5.4)$$

$$E_{Vi} = \frac{\text{Amount of } i \text{ contacted}}{\text{Amount of } i \text{ in place}} \dots \dots \dots (5.5)$$

These quantities in turn are specified independently: E_{Di} is as a function of time and fluid viscosities, relative permeabilities, and capillary pressures, and this is controlled primarily by surface chemistry factors that were described in Section 5.4.

E_{Vi} is a function of time, viscosities, well arrangements, heterogeneity, gravity, and capillary forces and is a combination of areal (V_a) as well as the vertical sweep efficiency (V_v). Fig. 5.7 shows a graphical illustration of the two volumetric factors. This figure shows some zones that are contacted and those that are not contacted in the areal and vertical dimensions. Part (a) indicates that the areal sweep misses oil and part (b) shows that vertically arrayed zones are not completely contacted.

Cherian (2002) explains that the Buckley-Leverett model (Buckley and Leverett 1942) is the fundamental theory that governs immiscible displacement in one dimension. According to this model, oil displaced by water in a rock is like a *leaky piston*, this is, it pushes, but some fluid *escapes*. Based on the concept of relative permeability, they (Buckley and Leverett 1942) developed the physical conditions where the pressure drop is constant, and the fluids are immiscible. The assumptions made by this model are

- A flood front exists, with only oil moving ahead of the front. Oil and water (or an immiscible gas) move behind the front.
- The displacement is in a single homogenous layer.
- The cross-sectional area to flow is constant.
- Darcy’s law applies for linear, steady-state flow.
- Capillary and gravity effects are negligible.

An example of a displacement wave is seen as Fig. 5.8. This shows the local fraction of water (f_w), which must range between zero and one, in practice variable between S_{wc} (saturation in connate water) and $1-S_{or}$ (maximum saturation in water, corresponding to the residual saturation in oil). It is dependent on relative function of the medium’s water saturation (S_w) in which the displacement takes place and

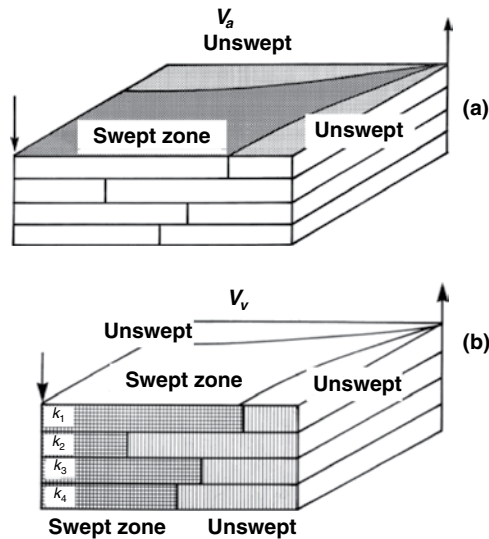


Fig. 5.7—Graphical illustration of volumetric sweep factors (Lake 2007).

is also dependent on the permeabilities and the capillary pressure. If the characteristics of the fluids and the porous medium are equal, it is a function of the medium's water saturation (S_w) in which the displacement takes place (Verga 2009). Fig. 5.9 shows a depiction of a flow front displacing the oil and is a demonstration of E_{vai} .

A typical arrangement of injection and production wells is a “five-spot” pattern, in which four injection wells are located at the corners of a square (see Fig 5.10; however, the exact shape of the flood and number of wells depends on the reservoir dimensions) (Chang 2010; Singh and Kiel 1982). Usually the production well is placed in the center of the square. The injection fluid, which is normally water (brine), steam, or gas, is pumped (or injected) simultaneously through the four injection wells to displace the oil toward the central production well (Schlumberger 2010c). See Otott (2007) for one description of this layout and by Singh and Kiel (1982) that shows a number of different plans based on the reservoir characteristics.

Viscous Fingering. This phenomenon is a common issue reducing areal sweep efficiency (Al-Mjeni et al. 2010). If the displacing fluid—typically water—is significantly less viscous than the oil it is displacing, the flood front can become unstable. Rather than being linear or radially symmetric, the leading edge of the front forms waves that transition to fingers extending farther into the oil. Eventually,

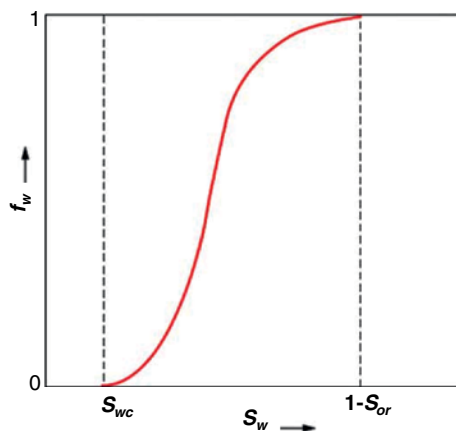


Fig. 5.8—Displacement front water fraction (f_w) vs. water saturation (S_w) (Verga 2009).

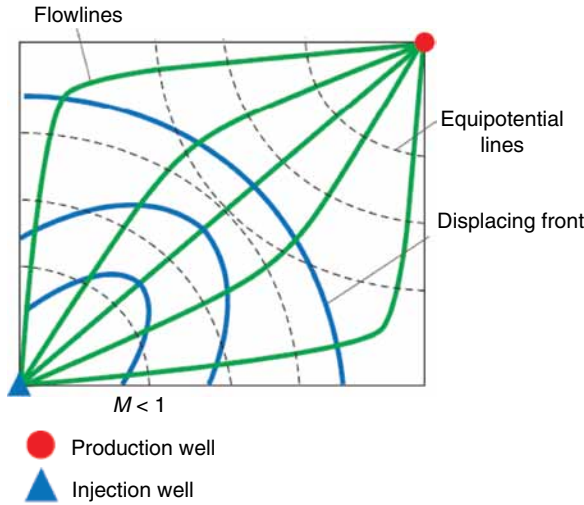


Fig. 5.9—Macroscopic sweep efficiency (E_{va}) (Verga 2009).

water fingers reach the producing well. At that point, additional injected water will preferentially follow the water-filled paths. Fig. 5.11 (Lake 2007) shows an illustration of the aqueous fluid only contacting a portion of the zone being swept. Note that viscous fingering reduces macroscopic displacement efficiency.

Heterogeneity and Vertical Sweep. Lake (2007) notes that E_{Vv} is quite complex and depends on heterogeneity, gravity, mobility ratio, and capillary forces. Fig. 5.12 shows the effect of heterogeneity on E_{Vv} . Verga (2009) claims that this is the parameter that describes multilayer reservoirs (i.e., those in which the HC levels present different petrophysical characteristics and are totally or partially separate

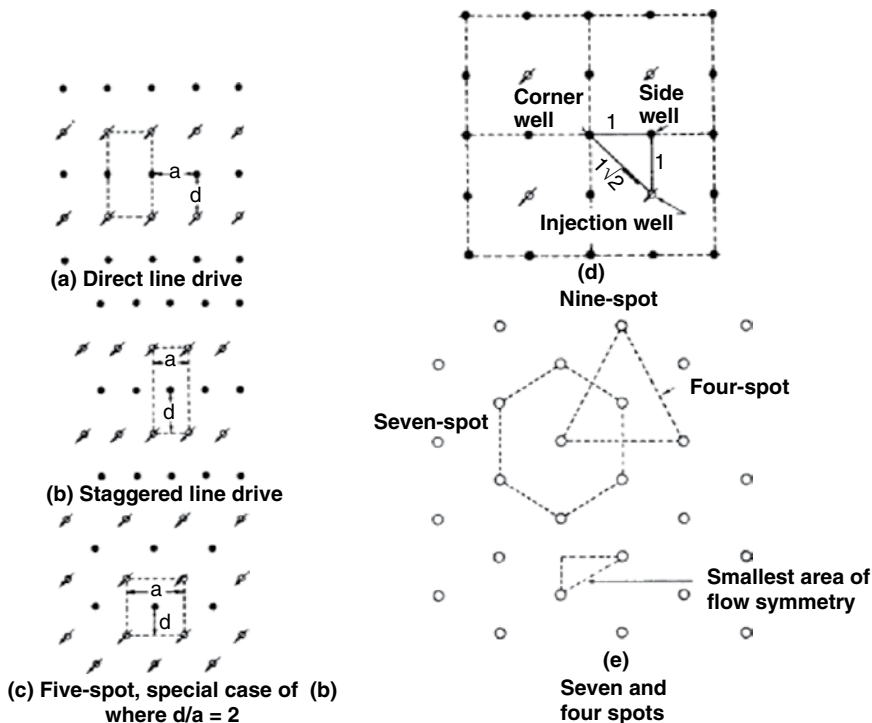


Fig. 5.10—Injection/producer patterns (Singh and Kiel 1982).

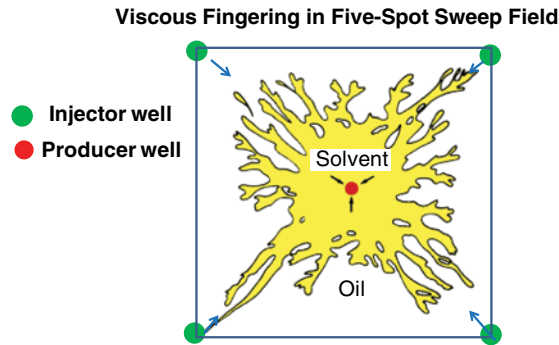


Fig. 5.11—Viscous fingering (Lake 2007).

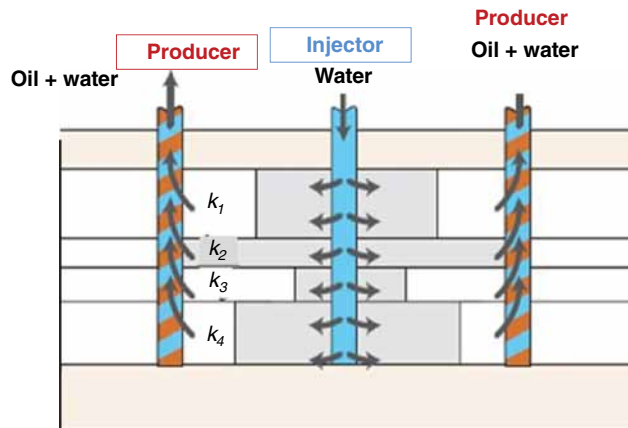


Fig. 5.12—Effect of heterogeneity on volume sweep efficiency. More fluid flows through the higher permeability (k) and thicker zones (Verga 2009).

from one another). In this case, a mobility ratio of less than one indicates a favorable condition [also see Thomas (2008)]. Verga (2009) claims that if the velocity with which the water front flows along each level tends to diminish progressively as the front itself advances toward the production well, the different fronts, relative to the different layers, in time tend to become uniform and to constitute a single front that reaches the production well compactly.

Gravity effects (that is the Bond number— B_g) will be quite important when there is good communication between the zones and the gravity forces are strong compared with the viscous forces. Thus, lighter fluid will “tongue over” the more dense fluid and not move it to the producing well. Mobility ratios and capillary forces were described previously [Thomas (2008), Eqs. 5.1 and 5.2].

The next section (5.1.2) describes microscopic characteristics of the formations that control displacement of the well and injected fluids.

5.1.2 Microscopic Displacement of Fluids. Waterflooding (Anderson 1987; Willhite 1986) is a frequently used secondary recovery method in which brine or water is injected into the reservoir, displacing the oil in front of it. Assuming that the reservoir is initially at the initial water saturation (IWS), only oil is produced until breakthrough (the time when water first appears at the production well). After breakthrough, increasing amounts of water and decreasing amounts of oil are produced. The process continues until the water to oil ratio is so high that the well becomes uneconomical to produce. Waterflooding is actually a part of most EOR processes because a water bank follows most chemical treatments and the use of a polymer (only) flood affects only the sweep efficiency, not the capillary number, so the effect of wetting is critical in all EOR floods. However, Lake (2010) contends that the

initial use of water sweeps does not constitute an EOR method [unless additional chemicals are added, but it is a part of IOR according the definitions of Sheng (2011)].

Willhite (1986) provides an understanding of the displacement of oil at the reservoir pore level (this affects E_d in Eq. 5.4). Chapter 2 of his book gives details of the process of immiscible displacement of oil (usually by water brine). Some of these factors are reviewed in this section because the addition of EOR chemicals will be shown to *modify* the various interactions (Section 5.4 and 5.5). The fundamental ideas described by Willhite (1986) for *miscible displacement* include IST, and wettability of surfaces and capillary pressure (P_c). Note that some surface chemical properties including wettability and IST were described in Section 1.6.1 of this book and wettability/wetting of surfaces also has applications in acidizing (3.6.4) and HF (4.7.2).

Fig. 5.4 and Fig. 5.13 show depictions of oil and water in the pore spaces. The drawing in Fig. 5.13 indicates that the pores have different sizes and are connected by pore throats and contain both oil and water phases. This drawing can apply to both sandstone or carbonate formations; however, the wetting conditions will be controlled by the chemistries of the surfaces as well as by the chemistries of the oil and water phases. The silicate surfaces will have a point of zero charge (PZC) in the acid range (approximately pH 2.4–7) because of the clay minerals (Appel et al. 2003), while the PZC of a carbonate will be much more alkaline (>pH 8) (Salinas-Nolascoa et al. 2004). The PZC is determined by the adsorption of either H^+ or OH^- ions as well as the other brine ions and chemicals. These differences in surface chemistries will affect the surfactants and polymers used in EOR and may require different chemicals to help remove the residual oil, as well as affecting the relative surface wetting characteristics. Fig. 5.13 (Lake 2010) shows that the nonflowing phase (either oil or water) can be trapped, and it depends on which phase the wetting phase is on as to what fluid will be displaced. In the chemical EOR examples, it is assumed that water (brine) is the flowing phase.

During waterflooding and other IOR/EOR activities, the main technical goal is moving trapped oil from these pores. These are affected by the physical/chemical properties of the reservoir including IST, wetting, and capillary pressure.

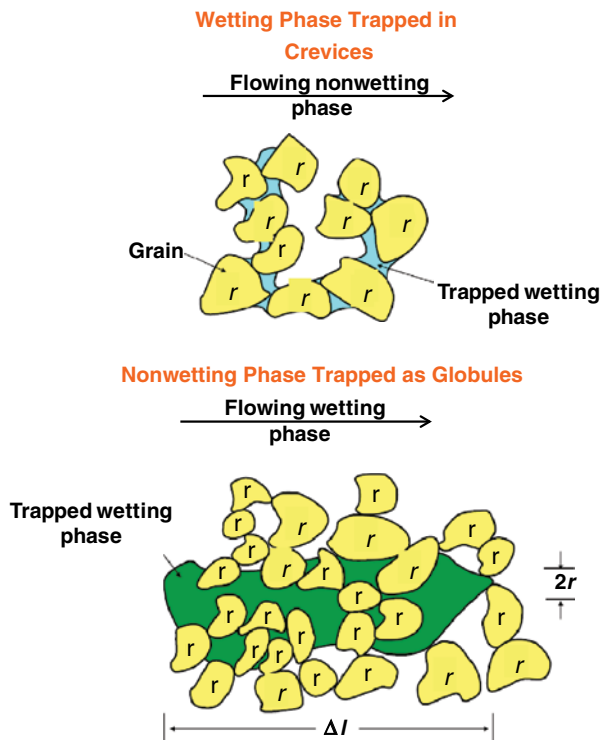


Fig. 5.13—Trapped oil showing movement of fluids depending on the surface wetting phase (Lake 2010).

IST. Willhite (1986) describes the interface between two phases as a region of limited solubility, which is, at most, a few molecules thick. It may be visualized as a phase boundary that occurs because the attractive forces between molecules in the same phase are much larger than those that exist between molecules in different phases. The IST is a fundamental thermodynamic property of an interface. It is defined as the energy required to increase the area of the interface by one unit. See further discussion of IST in Section 1.6.1 of this book.

Wettability. The contact angle and, thus, the capillary pore pressure (Eq. 1.56) are very important to the fluid flow in the matrix. Anderson (1986) notes that the wettability of a rock/fluid system is important because it is a major factor controlling the location, flow, and distribution of fluids in a reservoir. In general, one of the fluids in a porous medium of uniform wettability that contains at least two immiscible fluids will be the wetting fluid (see Fig. 1.35). When the system is in equilibrium, the wetting fluid will completely occupy the smallest pores and be in contact with a majority of the rock surface (assuming, of course, that the saturation of the wetting fluid is sufficiently high). The *nonwetting fluid* will occupy the centers of the larger pores and form globules that extend over several pores (Fig. 5.4). Contact-angle measurements were described in Section 1.5.3; however, Abdallah, Buckley et al. (2007) also note that the apparent contact angle measured from the average surface plane can differ significantly from the real surface (Fig. 5.14) because of the asperities of the surface and an O/W double layer.

Capillary Pressure. This has been described in Section 1.6.1; however, because it applies to EOR, more details are described here. The bulk properties of the matrix are defined by the porosity, ϕ , which is the fraction of open volume and the permeability (κ) that can be defined by the Darcy equation (Eq. 1.2) for the whole matrix. However, the *permeability* in a capillary tube is described (Eq. 5.6) by

$$k = \frac{r^2 \phi}{8\tau} \dots \dots \dots (5.6)$$

Here r is the radius of the pores and τ is the tortuosity, which is related to an average pore length and usually is in the range of 2–5 (Lake 2010) for many petroleum formations. Note, however, that the permeability is not uniform throughout any formation or even within a single core, and thus, the heterogeneities of the formations described in Chapter 3 also affect flow during EOR activities.

Fig. 5.15 illustrates single-phase laminar flow in a capillary tube (a) as well as two-phase flow (b) in which there is a wetting phase and a nonwetting phase.

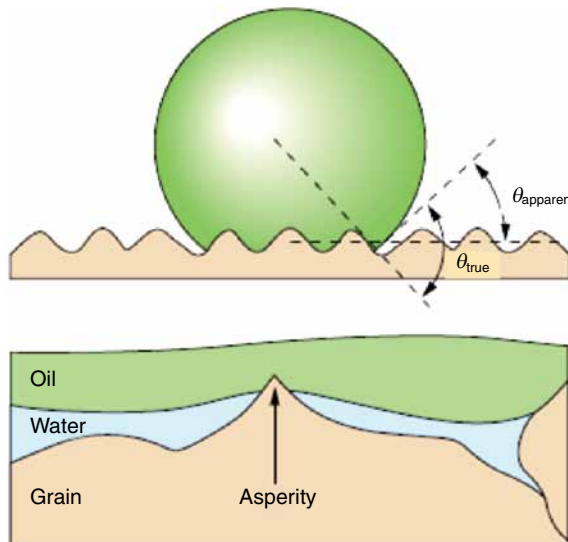


Fig. 5.14—Effect of surface roughness on contact angle (Abdallah et al. 2007).

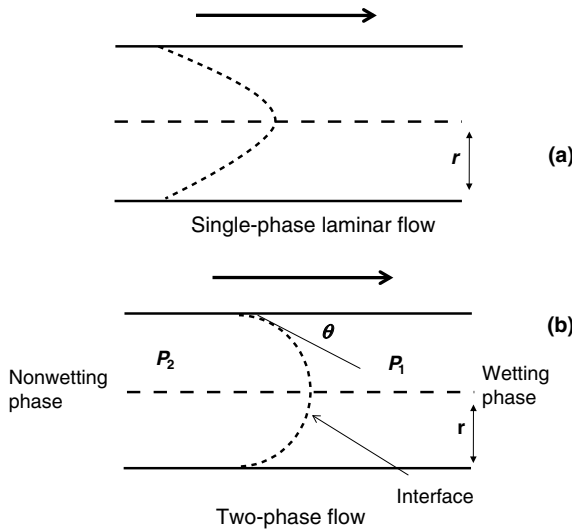


Fig. 5.15—Flow in capillary tubes.

Because of difference in wetting (see Eqs. 1.56 and 1.60, it is related to the contact angle), a two-phase flow (Fig. 5.15b) in a capillary tube results in the capillary pressure P_c that equals $P_2 - P_1$. This results in a backpressure that can keep the oil from exiting the pore space, or water from entering to displace it (this is also called imbibition, which is defined as the displacement of one fluid by another *immiscible* fluid). At complete wetting ($\theta = 0$), P_c is 0, and there is only single-phase flow. As long as there are two phases present in the pore spaces, the oil may be trapped (Figs. 5.4 and 5.13) unless the pressure is *increased* or the contact angle is *reduced* by adding a surfactant (that forms an emulsion) or a miscible fluid. The miscible fluid will cause single-phase flow to take place after the oil is dissolved and the surfactant is added to reduce the contact angle.

The effect of capillary pressure on water penetration of the pores (which must happen to displace the oil) is shown in Fig. 5.15. Here a water-wet surface allows water to enter, while an oil-wet surface excludes the water phase. Therefore, waterfloods in water-wet and oil-wet systems are known (Nutting 1925) to behave very differently. For uniformly wetted systems, it is generally recognized (Lake 2007) that a waterflood in a water-wet reservoir is more efficient than one in an oil-wet reservoir. In an example from Anderson (1987) (see Fig. 5.16), steady-state O/W relative permeabilities were measured in an outcrop of Torpedo sandstone using NaCl brine and a 1.7-cp [1.7-mPa·s] refined mineral oil. The wettability of the system was controlled by adding either (1) various amounts of barium dinonyl naphthalene sulfonate to the oil, which made the system more oil-wet, or (2) Orvus K TM liquid (a detergent) to the brine to achieve a strongly water-wet system with a contact angle of 0° in the brine.

Wettability in this experiment was monitored by contact-angle measurements on a quartz crystal. In Fig. 5.16, the water breakthrough is the point at which each curve first becomes nonlinear. Anderson (1987) contends that this figure demonstrates that earlier water breakthrough and less efficient oil recovery occur as the system becomes more oil-wet. For example, this author contends that 8% less oil will be produced at a water to oil ratio of 25 if the contact angle is 138° rather than 47° .

Waterflood recovery is controlled by the oil and water relative permeabilities of the system and by the W/O viscosity ratio. A simplified form of the fractional flow equation [e.g., see Craig (1971)] is

$$f_w(S_w) = \frac{1}{1 + \frac{\mu_w \kappa_{ro}}{\mu_o \kappa_{rw}}}, \dots \dots \dots (5.7)$$

where f_w = fractional flow of water, S_w = water saturation, μ_o , μ_w = oil and water viscosities, respectively, cp, and κ_{ro} , κ_{rw} = oil and water relative permeabilities, respectively.

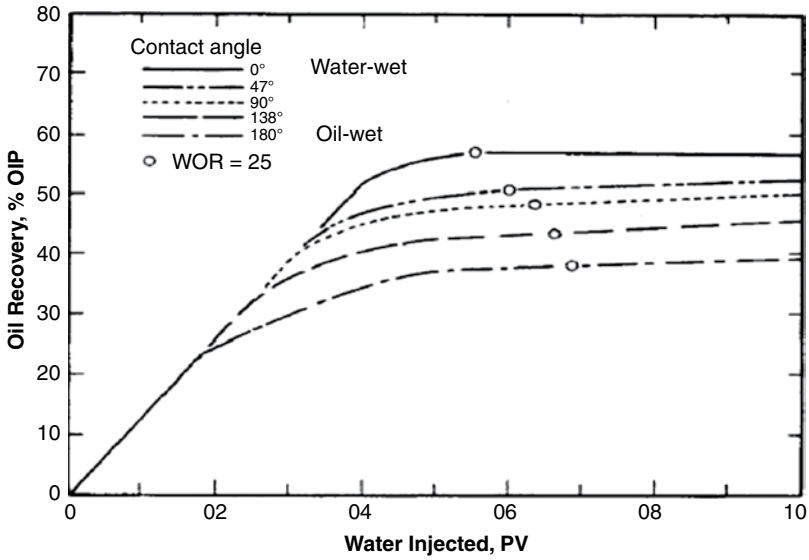


Fig. 5.16—Effects of wettability on waterfrac performance (calculations) (Anderson 1987).

This equation (Eq. 5.7) shows that the fractional flow of water at a given saturation is increased when the W/O viscosity ratio is decreased. Decreasing the W/O viscosity ratio will cause earlier breakthrough and less efficient oil production. Similar effects will occur when the W/O relative permeability ratio is increased. This author also notes that the oil and water relative permeabilities are explicit functions of the water saturation. They are also affected by pore geometry, wettability, fluid distribution, and saturation history. The use of polymers (and surfactants) is designed to increase this ratio.

Alshehri et al. (2009) claim that waterflooding typically recovers < 50% of the OIP, leaving much oil in the reservoir. They also state that recovery efficiency in fractured reservoirs can be dramatically lower in comparison to conventional reservoirs because water channels selectively from injector to producer, leaving considerable oil within the matrix and uncontacted by injected water. An enhanced recovery process is needed to access such oil held in the reservoir matrix. Addition of aqueous surfactants (Section 5.6.2) to injection water dramatically reduces O/W IST, and surfactant may adsorb to oil-wet rock surfaces inducing a shift in wettability that improves the imbibition of water. At the pore level, capillary forces are responsible for oil trapping and generally dominate over viscous and gravitational forces. Because of the reduction in IST between oil and water with the addition of surfactant, the role of capillary forces on fluid flow can be minimized.

When gravity parameters are large enough to give a Bond number (ratio of gravity to capillary forces— B_o) greater than 10, gravitational forces become more dominant, and oil held with rock matrix by capillarity may be released because of buoyancy. The definition of the Bond number is given:

$$B_o = \frac{\Delta\rho g d^2}{\gamma} \dots\dots\dots (5.8)$$

Here, $\Delta\rho$ is the difference in the density of the two phases, g is the acceleration caused by gravity, and d is the mean pore diameter. In this work (Alshehri et al. 2009), they use experiments conducted in 2D micromodels to investigate the effect of gravity at low IST. The micromodels have the geometrical and topological characteristics of sandstone and the network is etched into silicon. Pore-level mechanics were observed directly by means of a reflected-light microscope. A screening study of sulfonate and sulfate surfactants was conducted to choose an appropriate system compatible with the light crude oil (27° API).

Surfactants and solvents described in Sections 1.4.2 and 3.6.2 are injected during many EOR processes to change the water-wetting characteristics of the surfaces as well as the viscosities of the oil

phases to affect more efficient displacement of the HCs. These materials can change both N_c and M to improve oil removal. Descriptions are in Section 5.5.

5.2 Selection Criteria for IOR Treatments

The choice of an IOR/EOR treatment will depend on a number of different criteria that include the reservoir change needed, cost, and the reservoir conditions. Several general selection guides are presented in this section. Details of the methods used are discussed in Sections 5.4 and 5.5, and modeling programs are listed in Sections 5.6.2 and 5.6.4.

Al-Mjeni et al. (2010) have produced a chart (Fig. 5.17) of the various EOR methods and an indication of which parameter (including Eqs. 5.1 and 5.2) each changes and the relative recovery expected. These authors as well as Lake (2007) note that various combinations of the chemical methods are in use such as surfactant with polymers (SP) or ASP. These combinations are described in Section 5.5. These authors (Al-Mjeni et al. 2010) categorize the processes slightly different than Thomas (2008) and NETL (2001, 2008); however, the current chapter will describe all processes that are in scope of this book.

Table 5.1 (Lake 2007) shows the initial oil recovery values expected of different chemical processes and proposes that the various methods differ significantly in initial oil recovered as well as in the amount of chemicals required to accomplish the recovery. These values will help determine the economic viability of the method in a particular reservoir situation.

Taber et al. (1997) described screening criteria that have been proposed for all IOR methods. Data from EOR projects around the world have been examined and the optimum reservoir/oil characteristics for successful projects have been noted. The oil gravity ranges of the oils of current EOR methods have been compiled, and the results are presented graphically (Fig. 5.18). The proposed screening criteria are based on both field results and oil recovery mechanisms. The current state of the art for all methods is presented briefly, and relationships between them are described. Steamflooding is still the dominant IOR method. At the time of this report (1997), all chemical flooding had been declining, but polymers and gels are being used successfully for sweep improvement and water shutoff. Only CO₂ flooding activity has increased continuously, while at the publication of the current book, some of the other chemical processes also are in commercial use.

Table 5.2 shows a selection guide based on a number of different criteria. The chemical methods generally have been recommended for the intermediate-lighter oils, moderate depths, and temperatures.

| EOR Method | | Pressure Support | Sweep Improvement | IFT Reduction | Wettability Alteration | Viscosity Reduction | Oil Swelling | Hydrocarbon Single Phase | Compositional Change ¹ | Incremental Recovery Factor |
|----------------------|----------------------|------------------|-------------------|---------------|------------------------|---------------------|--------------|--------------------------|-----------------------------------|-----------------------------|
| Waterflood | Waterflood | | | | | | | | | Base case ² |
| | Engineered water | | | | | | | | | Low |
| Gasflood: immiscible | Hydrocarbon | | | | | | | | | Moderate |
| | CO ₂ | | | | | | | | | High |
| | Nitrogen or flue gas | | | | | | | 3 | 3 | Moderate |
| Gasflood: miscible | Hydrocarbon | | | | | | | | 4 | High |
| | Hydrocarbon WAG | | | | | | | | 4 | Very High |
| | CO ₂ | | | | | | | | | High |
| | CO ₂ WAG | | | | | | | | | Highest |
| Thermal | Steam | | | | | | | | | High |
| | High-pressure air | | | | | | | | | High |
| Chemical | Polymer | | | | | | | | | Low |
| | Surfactant | | | | | | | | | Moderate |
| | ASP | | | | | | | | | High |

- IFT = Interfacial tension**
- WAG = Water alternating gas**
- ASP = Alkaline-surfactant-polymer**
- 1 = Change of composition of liquid hydrocarbons**
- 2 = Waterflooding provide the base case**
- 3 = Oil stripping occurs as miscibility develops**
- 4 = Condensing and vaporization exchange**

Fig. 5.17—Different EOR methods and properties that are changed (Al-Mjeni et al. 2011).

TABLE 5.1—OOIP RECOVERY BY METHOD (LAKE 2007)

| Process | Typical IOR (% OOIP) | Typical Agent Utilization/ Incremental (bbl) |
|--------------------|----------------------|--|
| Polymer | 5 | 1 lbm polymer |
| Micellar/polymer | 15 | 15–25 lb surfactant |
| Alkaline/polymer | 5 | 35–46 lb chemical |
| Miscible solvent | 10–15 | 10 Mcf |
| Immiscible solvent | 5–10 | 10 Mcf |

Taber et al. (1997) note that the goal of the many chemical methods is to reduce the IST between oil and water, generally to displace discontinuous trapped oil (remaining oil saturation, S_{or}) that remains after a waterflood. Because it is approximately 10 times more difficult to replace trapped oil than continuous oil, the surfactant slugs for these chemical processes must be very efficient. The oil-displacement mechanics are well understood, and many formulations have been devised to give very high recoveries in laboratory experiments with actual reservoir rocks and fluids. Fig. 5.19 shows the effect of the price of oil on the use of chemical floods.

They note that there have been some technical successes for surfactant floods in the field (Maerker and Gale 1992); however, there have been fewer economic successes because the cost of the fluids is too high. Therefore, there has been an effort to lower the fluid cost by adding more alkali and less surfactant or cosolvent to these mixtures and are often called ASP processes (Section 5.5.5), and very large slugs can be injected because the cost is low compared with the classic micellar/polymer formulations. The alkali costs much less than the surfactant or cosolvent, and it helps to lower the IST and reduce adsorption of the surfactant on the rock. In one case, workers were able to reduce surfactant concentration by 10 times by adding low-cost alkali, and the formulation still provided very good oil recovery (Yang 1995). The ASP process has also been tested in the field. A fieldwide project in Wyoming reports costs of USD 1.60 to USD 3.50/bbl of oil [at the time of the Yang (1995) report] recovered using an ASP process.

Yang (1995) claims that over 35 years, a large number of polymer floods have been applied over a remarkably wide range of conditions with reservoir temperatures from 46 to 235°F; average reservoir

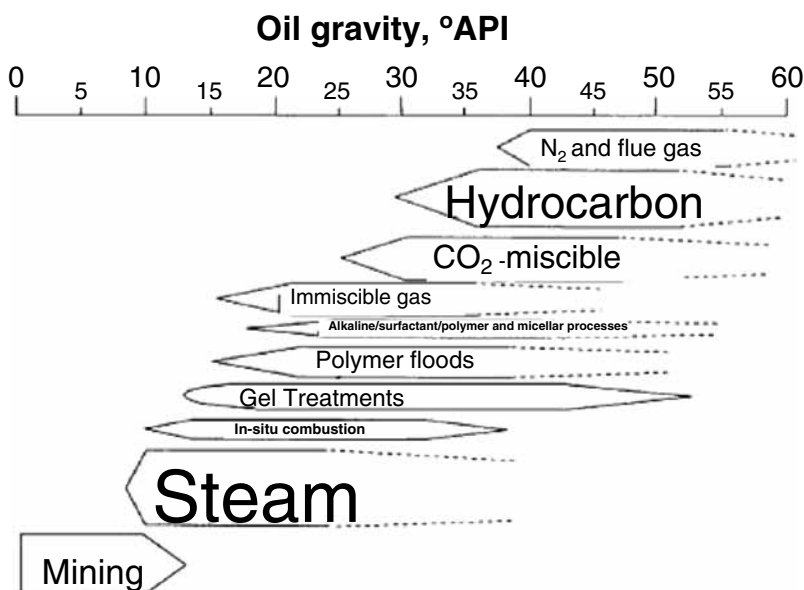


Fig. 5.18—IOR selection based on API gravity (Taber et al. 1997).

TABLE 5.2—SELECTION GUIDE FOR ALL EOR PROCESSES (TABER ET AL. 1997)

| EOR Method | Gravity (°API) | Viscosity (cp) | Oil Composition | Oil Saturation (% PV) | Formation Type | Net Thickness (ft) | Average Permability (md) | Depth (ft) | T (°F) |
|-----------------------------------|----------------|----------------|---|-----------------------|---------------------------|---------------------|--------------------------|-------------|----------|
| N ₂ /flue gas | > 35–48 | < 0.4–0.2 | High % C ₁ –C ₇ | > 40–75 | SS or Carbonate | Thin unless dipping | N.C. | > 6000 | N.C. |
| Hydrocarbon | > 23–41 | < 0.3–0.5 | High % C ₂ –C ₇ | > 30–80 | SS or Carbonate | Thin unless dipping | N.C. | > 4000 | N.C. |
| CO ₂ | > 22–36 | 1.5–< 10 | High % C ₅ –C ₁₂ | > 20–55 | SS or Carbonate | Wide range | N.C. | > 2500 | N.C. |
| Immiscible gases | > 12 | < 600 | N.C. | > 35–70 | N.C. | N.C. if dipping | N.C. | > 1800 | N.C. |
| Micellar/polymer/ASP and alkaline | > 20–35 | 13–<35 | Light intermediate and some organic acid for alkaline | > 33–53 | SS preferred | N.C. | > 10–450 | 3250–>9000 | 80–>200 |
| Polymer flood | > 15 | > 10–150 | N.C. | >50–80 | SS preforations | N.C. | >10–800 | 3500–<11500 | 140–>200 |
| Combustion | > 10–16? | 1200–<5000 | Some asphaltic compound | > 50–72 | High porosity SS or Carb. | > 10 | 50 | 1500–<4500 | >100–135 |
| Steam | >8–13.5? | 4700–<200000 | N.C. | >40–66 | High porosity SS or Carb. | >20 | >200–2500 | | N.C. |
| Surface mining | 7–11 | 0 cold flow | N.C. | >8% wt. sand | Mineable sand | >10 | N.C. | | N.C. |

permeabilities from 0.6 to 15,000 md; oil viscosities from 0.01 to 1,494 cp; net-pay from 4 to 432 ft; and resident brine salinities from 0.3 to 21.3% total dissolved solids (TDSs). At project startup, the percent of OOIP ranged from 36 to 97.1%, and the producing W/O ratio ranged from 0 to 100. The four successful floods had a number of features in common. These characteristics may be useful as screening criteria for today’s economic environment. First, the floods were applied in high-permeability (> 0.87 d) sands and low-temperature (86 to 136°F) reservoirs. High oil saturations (71 to 92% OOIP) were present at project startup, and the O/W viscosity ratios (15 to 114) at reservoir temperature were relatively high. The injected polymer solutions contained relatively high HPAA concentrations (900 to 1,500 ppm) in low-salinity waters, and large quantities of polymer (162- to 520-lbm polymer/

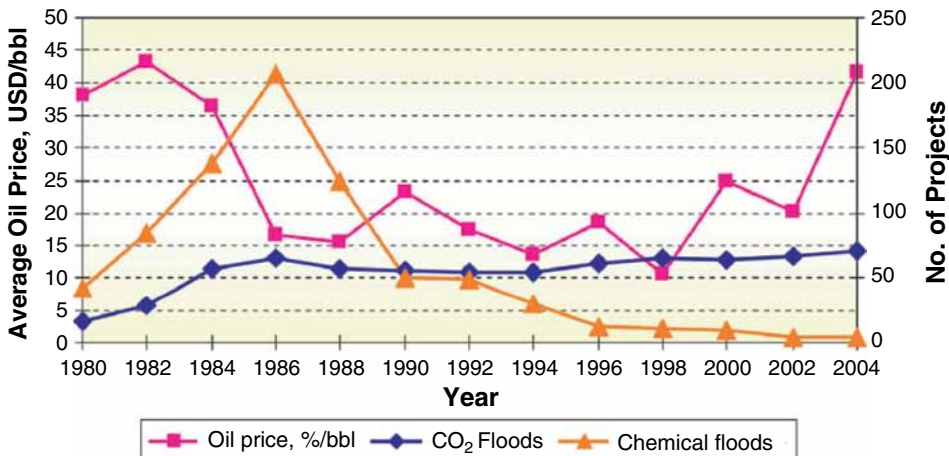


Fig. 5.19—Evolution of chemical and CO₂ EOR projects in US vs. oil prices (Taber et al. 1997).

acre-ft) were injected. Finally, the incremental oil recoveries (11 to 30% OOIP or 155- to 499-bbl oil/acre-ft) were high.

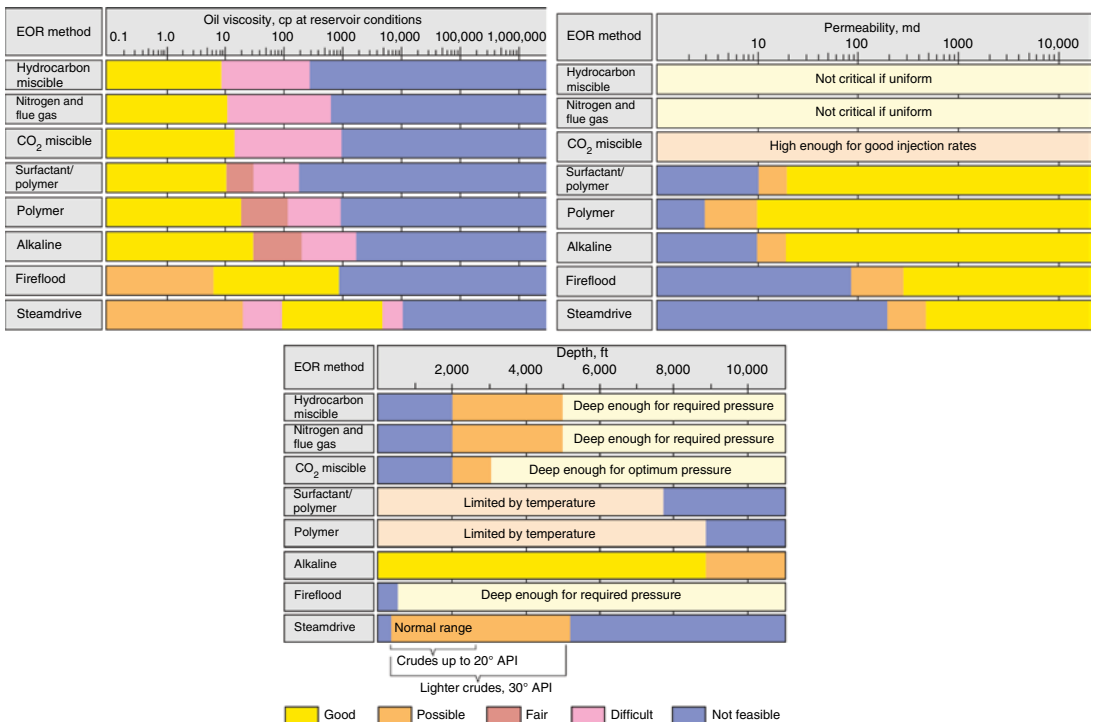
Lake (2007) has provided a selection guide (Fig. 5.20) based on formation and oil properties. This author also notes that the cost/bbl oil recovered can be as much as USD 50/bbl (in 1992 dollars) but also may recover as much as 70% of the oil still in place.

Lake et al. (1992) also have estimated the amount of IOR-produced oil in 1992 (Table 5.3).

Al-Mjeni et al. (2010) outline a general philosophy of selection. It starts with the reservoir properties, combines lab testing of fluids for removal efficiency, and finally leads to a pilot scale test. These may be single well tests or a more complex pattern, the most important aspect is to obtain data quickly. See Fig. 5.21.

Manrique et al. (2007) note that a considerable portion of the world’s HC endowment is in carbonate reservoirs. Carbonate reservoirs usually exhibit low porosity and may be fractured. These two characteristics along with oil-to-mixed wet-rock properties usually result in lowered HC recovery rates. When EOR strategies are pursued, the injected fluids will likely flow through the fracture network and bypass the oil in the rock matrix. The high permeability in the fracture network and the low equivalent porous volume result in early breakthrough of the injected fluids. Infill drilling programs and well conformance strategies—mostly gas and water shutoff—have been effectively used to mitigate the early breakthrough and increase oil recovery. In most cases, however, 40 to 50% of the original oil in place (OOIP) is not produced.

A large number of EOR field projects in carbonate reservoirs have been referenced in the literature since the early 1970s. These field projects demonstrate the technical feasibility of various EOR methods in carbonate reservoirs. However, because of the collapse in oil prices, most of the aforementioned project plans have been abandoned. This paper presents a comprehensive compilation of EOR (gas, chemical, and thermal methods) field experiences in carbonate reservoirs within the US, as an attempt to identify key variables and project design parameters for future evaluation and revitalization of mature carbonate reservoirs.



Selection of EOR techniques by oil viscosity, permeability, and depth

Fig. 5.20—IOR selection guide (Lake 2007).

TABLE 5.3—IOR OIL 1992 BY TYPE AND REGION (LAKE ET AL. 1992)

Estimated Annual Worldwide EOR Produced Oil (B/D × 1000) in 1992

| Country | Thermal | Miscible | Chemical | EOR Total | % |
|---------------------|------------|------------|-------------|---------------|------------|
| USA | 454 | 191 | 11.9 | 659.9 | 42 |
| Canada | 8 | 127 | 17.2 | 152.2 | 10 |
| Europe | 14 | 3 | — | 17 | 1 |
| Venezuela | 108 | 11 | — | 119 | 7 |
| Other South America | 2 | NA | NA | 17 | 1 |
| USSR | 20 | 90 | 50 | 160 | 10 |
| Other (estimate) | 171* | 280** | 1.5 | 452.5 | 29 |
| Total | 777 | 702 | 80.6 | 1574.6 | 100 |

*Mainly Duri field (Indonesia).
 ** Mainly Hassi-Messaoud (Algeria) and Intisar (Libya).

Carbon dioxide flooding [continuous or water-alternating gas (WAG)] is the dominant EOR process used in the US. This is because of the high availability of low-cost CO₂. In addition, EOR represents the logical first step toward viable geologic carbon storage and sequestration. EOR chemical methods in carbonate reservoirs, especially polymer flooding, have been widely tested in US carbonate reservoirs. However, EOR chemical methods have made a marginal contribution, relatively, in terms of total oil recovered. These authors note that most of the chemical floods in carbonates have been the use of polymers [usually partially HPAAs (PHPAAs)] that were added early in a waterflood to increase mobility ratios and thus ultimate recovery. Some micellar surfactant/polymer (S/P) floods have also been done in carbonates. These were considered pilot tests that lasted about 60 days and were considered successful.

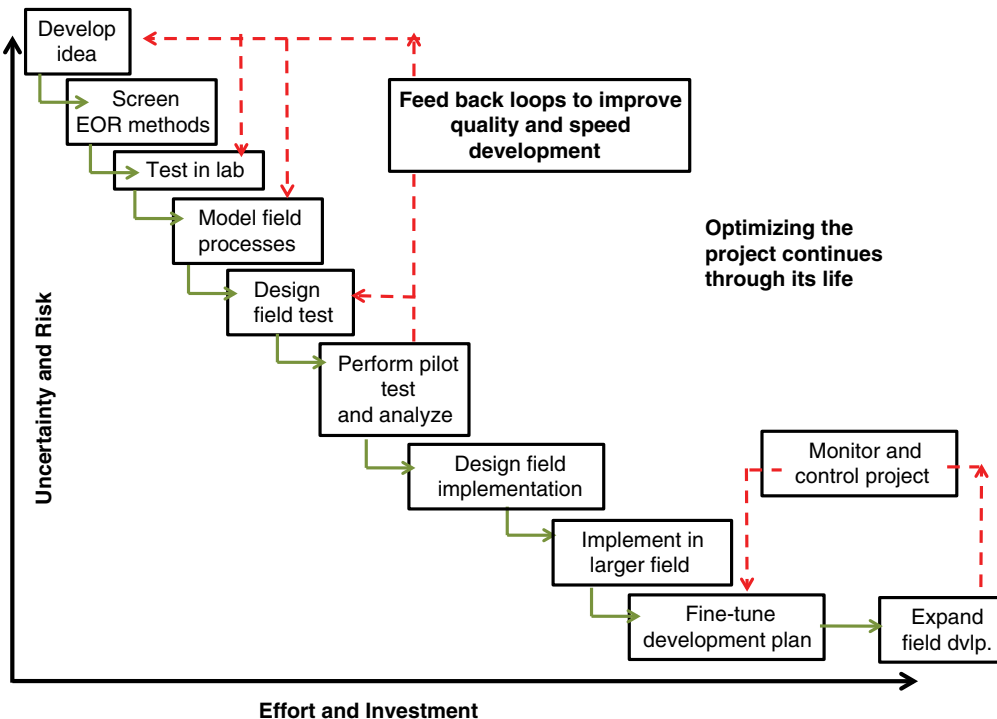


Fig. 5.21—IOR Plan (Al-Mjeni et al. 2010).

Awan et al. (2008) have provided a summary and a guide of the EOR technologies initiated in the North Sea in the period from 1975 until the beginning of 2005. The five EOR technologies that have been initiated in this region are HC miscible gas injection, WAG injection, simultaneous water-and-gas (SWAG) injection, foam-assisted WAG (FAWAG) injection, and microbial EOR. Each EOR technology that has been initiated in the North Sea was identified with its respective maturity level and/or maturation time frame, technology use restrictions, and process efficiency based on incremental oil.

Apart from WAG at Ekofisk and FAWAG at Snorre central fault block, all technologies have been applied successfully (i.e., positive in economic terms) to the associated fields. HC miscible gas injection and WAG injection can be considered mature technologies in the North Sea. The most commonly used EOR technology in the North Sea has been WAG, and it is recognized as the most successful EOR technology.

The main problems experienced were injectivity (WAG, SWAG, and FAWAG projects), injection system monitoring, and reservoir heterogeneities (HC miscible gas injection, WAG, SWAG, and FAWAG projects). Approximately 63% of all the reported EOR field applications have been initiated on the Norwegian continental shelf, 32% on the UK continental shelf, and the remainder on the Danish continental shelf. Statoil has been the leader in conducting EOR field applications in the North Sea. While the majority of future research will concentrate on microbial processes, CO₂ injection, and WAG (including SWAG) injection schemes, large polymer floods also are in use. Statoil (2009) notes that polymers are being evaluated for the Dalia field offshore Angola.

5.3 Testing Methods for IOR Processes

This section describes methods for testing and evaluating fluids and interactions before starting IOR applications. Specific testing methods can be applied to the well fluids, proposed EOR fluids and to the reservoir rock to select the most appropriate treating fluid or method. Because EOR operations may require massive amounts of chemicals and the treatments may last for several years, economic considerations frequently are the major factor in the decision-making process. Refer to Section 1.3 of this book as well as to Lake and Walsh (2008) and Lake (2010).

The microscopic (pore-level) chemistry and physics of the retention of oil is affected by the capillary number. The macroscopic factors define the ability to contact (sweep) the reservoir PV using the fluids that are injected and thus mobilize as much oil as possible and replace it with water or another fluid. If it were possible to contact the entire PV with a fluid that would remove all of the oil, the process would be 100% efficient. This is rarely possible even with an individual core in the lab and is much harder in a volume of many thousands of m³ of pore space. However, this is essentially the same problem faced by the designers of matrix stimulation treatments described in Section 3.7 and similar methods are employed.

This is summarized (Lake 2007) by the basic oil recovery equation:

$$N_p = \frac{E_v E_D S_o V_p}{B_o} \dots \dots \dots (5.9)$$

In this equation, N_p = cumulative oil recovery, E_v = volumetric sweep efficiency = (E_A , areal efficiency) (E_v , vertical efficiency), E_D = local displacement efficiency, S_o = initial oil saturation, V_p = PV, and B_o = oil formation volume factor at abandonment.

5.3.1 Reservoir Fluid Properties. As noted by Thomas (2008), the viscosity and API gravity of the reservoir fluids are a prime determinant of the selection of EOR treatments and OIP. In Chapter 3 of Frenier et al. (2010), the authors describe a number of test methods for determining fluid properties that include

- Compositional tests such as chromatographic, physical, spectrographic, and saturate aromatic resins asphaltene analyses
- Physical tests such as pore volume temperature (PVT), rheology, and surface analyses (also see Section 1.4 of this current book)

Lim et al. (2008) document the design and initial results of EOR and FA fluid studies to be used in evaluation of the feasibility of nitrogen gas injection for recovery of substantial incremental oil over pressure depletion. They note that conventional EOR laboratory studies were complicated by the need for FA considerations because of the deepwater offshore environment and high asphaltene content of the main producing horizon EOR target oil zone. Also, it became important for laboratory testing to thoroughly evaluate the EOR process mechanisms and provide rigorous data for reliable reservoir modeling and simulation.

Results of the laboratory work (Lim et al. 2008) revealed different ideas to suggest novel directions in how fluid studies and FA issues should be addressed in evaluating an EOR process for deepwater offshore application. They conclude from the findings the following:

1. Surface separator fluid samples can be successfully recombined to obtain representative reservoir fluids for PVT, EOR, and FA work.
2. Asphaltene stability tests resulted in a substantial increase in the asphaltene onset pressure with increase in the solution gas/oil ratio and a greater effect for HC vs. nitrogen gas.
3. Improved procedures for experimental slimtube tests can provide more representative determinations of miscibility pressures. A comprehensive strategy and program for fluid sampling and laboratory fluids testing has been prepared and is being implemented.

The authors (Lim et al. 2008) concluded that ideas for planning fluid sampling and lab testing programs aid operators to evaluate the reservoirs for gas injection EOR and other processes in deepwater offshore environments.

5.3.2 Properties of the EOR Fluids. Polymers and surfactants dissolved in brines make up the majority of the EOR fluids that are described in Sections 5.4 and 5.5. Pope (2007a) suggests that polymer fluids should be tested for the following:

- Rheological characteristics that include viscosity under shear (see Section 4.2.2 of this book).
- Filterability to reduce formation damage.
- Thermal stability. The fracturing fluids described in Chapter 4 require similar tests.
- Stability and rheology in the presence of the brine to be used. The brine chemistry also should be evaluated. See Davies and Scott (2006) for a very comprehensive description of oilfield water tests.

Some testing of surfactant fluids was described in Sections 1.5.6 and 1.4.2. The basic tests are described for determining the critical micelle concentration (CMC) (especially in the presence of the brine) and the effect on the IST and wetting characteristics of different surfaces. Emulsion tests are described in Section 5.5.5 as well in Section 2.4.4.

Wu et al. (2009) presented a screening method to study the long-term thermal stability of water-soluble polymers in the absence of oxygen. Viscosity measurements were performed for a matrix of conditions of temperature and salinity.

The viscosity measurements were conducted at three temperatures (25°C, 50°C, and 90°C) using a Brookfield DV-I+ viscometer. Later tests were done to include temperatures of 90 and 120°C, and salinities ranging from low-salinity case (TDS <3000 mg/L), to synthetic seawater (TDS ≈ 35,000 mg/L), to a so-called high-salinity case (TDS about 180,000 mg/L). Results show that some products at dilute concentration can create substantial initial viscosity even at temperatures as high as 90°C.

Not surprisingly, they claim, the viscosity performance is generally much better in the low-salinity brines than the higher-salt brines. The better products attain a target viscosity (approximately 10–20 cp at a shear rate of several sec^{-1} at 90°C) with polymer concentrations of less than 3,000 ppm. The best product for efficiency in creating solution viscosity differs depending on the temperature and the brine salinity.

Levitt and Pope (2008) have reviewed the testing of polymer solutions to determine chemical and thermal stability. The detailed test methods are in this paper, and included

- Filtration
- Polymer and surfactant compatibility
- Viscosity measurements
- Ca^{2+} tolerance
- Thermal stability
- Chemical stability, including adding iron compounds (they note that H_2 gas must be added with FeCl_2 to maintain the oxidation state)

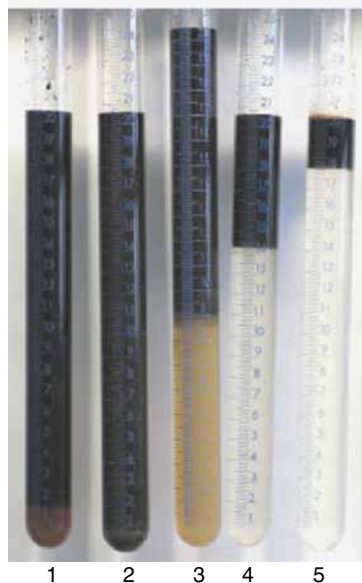
5.3.3 Properties of the Mixture of the EOR Fluid and the Oil. Several chemical EOR methods (alkaline, surfactant, and ASP) are designed to form miscible fluids from the oil and the displacing fluid. Thus, temporary emulsions will result. Tests to determine the correct concentrations of chemicals in the treating brine are needed. Examples of a lab test to form emulsions are seen in Fig. 5.22 (Stoll et al. 2010). Mixtures of the oil and the test fluid were mixed together and then allowed to separate. In this example where a variable is the amount of alkaline material added, the tube No. 2 is the optimal fluid balance to displace the oil because more oil is emulsified (very little water is seen at the bottom of the tube). Additional specific emulsion tests for surfactant-based EOR methods are described in Section 5.5.3, and details of the alkaline EOR methods are in Section 5.5.4. Note that these emulsions must then be resolved as the oil is produced. See Sections 1.4.4 and 2.4.1.

Pope (2007a) suggests the following fluid tests:

- Fluids screening
- Viscosity and cost for feasible salinity options
- Filtration and quality control
- Thermal stability

5.3.4 Rock/Fluid Interactions. Several tests are described.

Wettability and Imbibition Tests. The relative wetting of rock surfaces is of paramount importance for mobility of oil. Imbibition is the process of absorbing a wetting phase into a porous rock. Imbibition is important in a water drive reservoir because it can advance or hinder water movement, affecting



Mixtures of crude oil and brine with different concentrations of alkaline agents

Fig. 5.22—Crude oil emulsion tests (Stoll et al. 2010).

areal sweep (see Section 5.4). Spontaneous imbibition refers to the process of absorption with *no external pressure* driving the phase into the rock. It is possible for the same rock to imbibe both water and oil, with water imbibing at low in-situ water saturation, displacing excess oil from the surface of the rock grains, and oil imbibing at low in-situ oil saturation, displacing excess water. An imbibition test is a comparison of the imbibition potential of water and oil into a rock. The wettability of the rock is determined by which phase imbibes more. See Fig. 5.23. Abdallah et al. (2007) show an example of this process. In this figure, the pressures (P) are only the capillary pressures (usually denoted P_c). In the water-wet core (reservoir), water rises (imbibes) into the core and the rock/water contact angle (θ) = 0° . In the oil-wet core, the oil displaces the water and the rock/water contact angle (θ) = 140° . The text below the two figures shows one equation for the capillary pressure (P_c) that is equivalent (but expanded) in Eqs. 1.56–1.60.

Ma et al. (1999) claim that the most common methods used to test imbibition are the Amott test (Amott 1959) and the US Bureau of Mines (USBM) test. These authors also claim that the Amott test does not discriminate adequately between systems that give high values of wettability index to water and are collectively described as very strongly water-wet. In addition, the USBM test does not recognize systems that achieve residual oil saturation by spontaneous imbibition. Therefore, both methods as well as variations are described in this section.

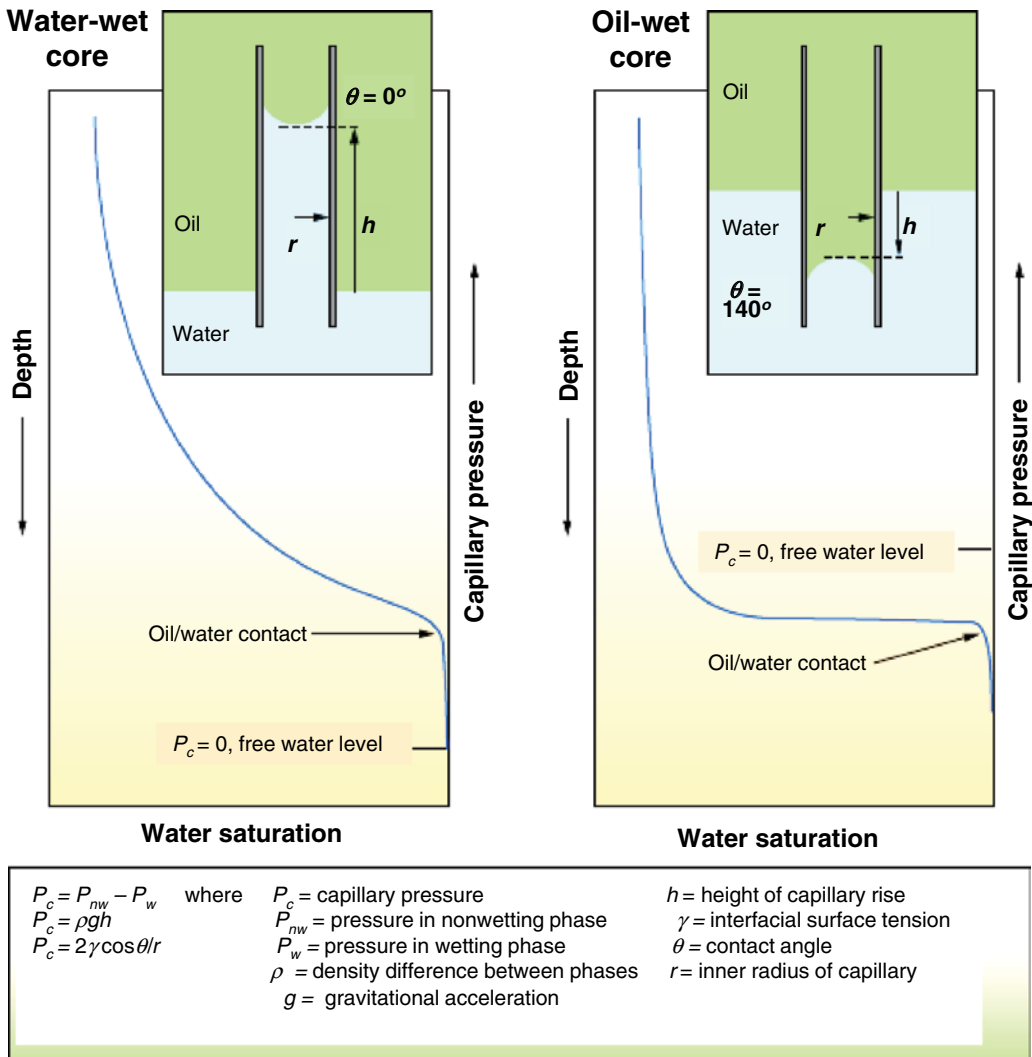


Fig. 5.23—Effect of capillary pressure on water (imbibition) invasion of the pores (Abdallah et al. 2007).

Amott-Harvey Index and Test. The Amott test (Amott 1959) defines two different indices: the Amott water index (I_w) and the Amott oil index (I_o). The two Amott indices are often combined to give the Amott–Harvey index. It is a number between 0 and 1 describing wettability of a rock in drainage processes. It is defined as

$$AI = I_w - I_o \dots \dots \dots (5.10)$$

These two indices are obtained from coreflood tests using equipment as seen in Fig. 5.24 [instructions in Wang, Butler et al. (2012)] and then by plotting the capillary pressure curve as a function of the water saturation as shown on Fig. 5.25. The calculations are Eqs. 5.11 and 5.12.

$$I_w = \frac{S_w - S_{wr}}{1 - S_{wr} - S_{or}} \dots \dots \dots (5.11)$$

Here (Eq. 5.11), S_w is the water saturation for a zero capillary pressure during the imbibition process, S_{wr} is the irreducible water saturation, and S_{or} is the residual oil saturation after imbibition.

$$I_o = \frac{S_o - S_{or}}{1 - S_{wr} - S_{or}} \dots \dots \dots (5.12)$$

In Eq. 5.12, S_o is the oil saturation for a zero capillary pressure during the secondary drainage process, S_{wr} is the irreducible water saturation, and S_{or} is the residual nonwetting phase saturation after imbibition.

Using this test, a rock is defined as

- Water-wet when the Amott–Harvey index is between 0.3 and 1
- Weakly water-wet when the Amott–Harvey index is between 0 and 0.3
- Weakly oil-wet when the Amott–Harvey index is between –0.3 and 0
- Oil-wet when the Amott–Harvey index is between –1 and –0.3

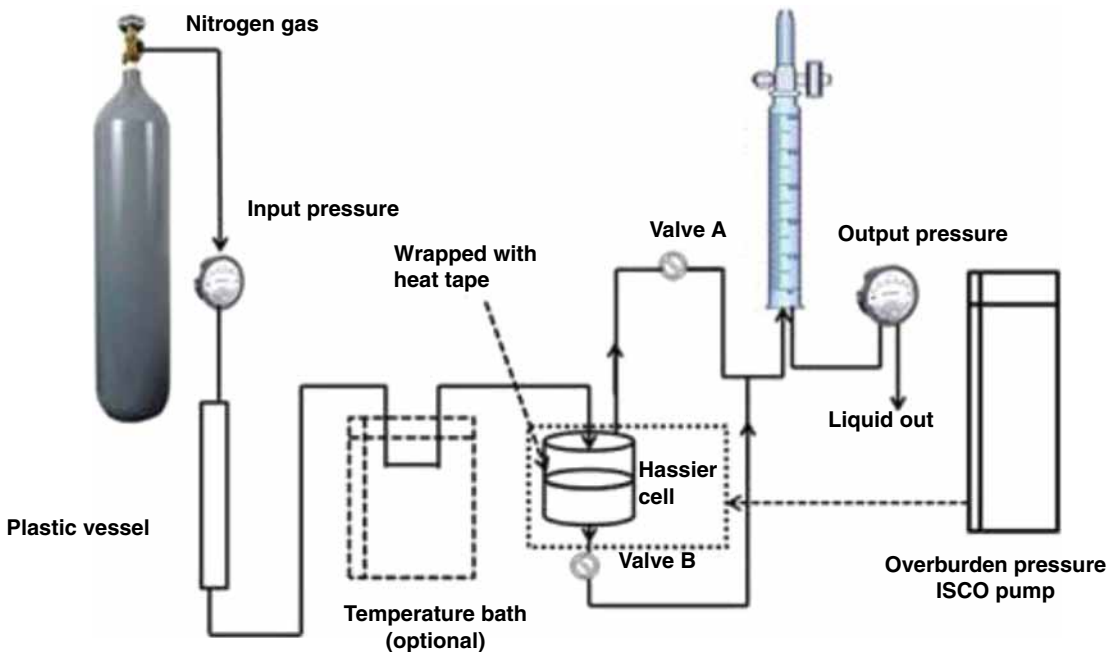


Fig. 5.24—Test setup for spontaneous and forced imbibition (Wang et al. 2012a).

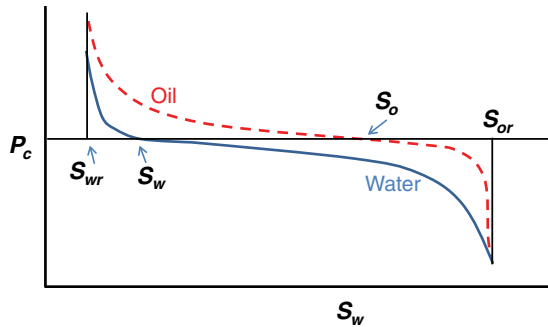


Fig. 5.25—Amott–Harvey index number calculation.

Wang et al. (2012a) have proposed several modifications of the Amott test for evaluation of wetting in the Bakken shale fields. This paper also shows various coreflood setups for determining wetting/imbibition properties of reservoir cores.

USBM Test. Donaldson et al. (1969) describe a quantitative method for measuring the wettability of porous media containing brine and crude oil that has been developed by the USBM using capillary pressure curves determined with a centrifuge. The USBM method for determining wettability is based on a correlation between the degree of wetting and the areas under the capillary pressure curves. The method employs the two areas under the capillary pressure curves (Fig. 5.25).

These measurements are claimed to be reproducible within a standard deviation of 8.2%. The determination of fractional wettability has been compared with a method involving a combination of imbibition and displacement. Results are claimed to be in agreement qualitatively as to whether a sample was water-wet or oil-wet. When tested with outcrop cores of Torpedo sandstone, wetting tendencies of oils from widely different fields range from highly water-wet to almost neutral. Silicone-treated cores vary in extent of wettability in a predictable manner, becoming more oil-wet as the concentration of silicone used in core preparation is increased.

Reactions With the Rock Matrix Minerals. Section 4.8 of this book describes reactions of frac fluids with reservoir rock. Also, as noted as follows, a coreflood test may reveal an interaction between EOR chemicals and the formation minerals. The details of such interactions may be tested using kinetic/analytical tests with individual minerals, as well as with mixtures. Mohnot et al. (1987) have tested the effects of various alkaline chemicals on various minerals and more details of reactions with the formation are in Section 5.5.4. Additional information on kinetic tests on minerals are in Sections 3.5.2 and Figs. 3.43 and 3.45 of this book for acidizing chemicals, but the basic methods are similar to tests with EOR fluids. The main ideas are to determine the effects of the fluids on the stability of clays and alkaline earth minerals as well as the effect of the reaction products on subsequent formation damage. Adsorption of polymers and surfactants also must be determined and the type of the adsorption isotherm should be modeled. See Fig. 1.9.

Coreflood Tests (CFTs). These are used in many different situations to determine the effects of various fluids on reservoir rock. The methods used are described in Frenier and Ziauddin (2008) and results of CFTs are also described in Section 2.3 and Fig. 2.36 of this book. Pope (2007a) suggests that CFTs should include

- Reservoir conditions and fluids
- Pressure taps on core to determine changes with penetration
- Wide range of variables of temperature and pressure

Problems include

- Polymer behavior not uniform along core
- Steady state never reached

Many different variations in CFT are employed in EOR applications. Stoll, Shureqi et al. (2010) showed an example of the use of CFTs to examine the use of an ASP flood to displace oil as well as describing undesirable effects. The authors were able to obtain a 30 cm/5 cm core from a surface outcrop of a sandstone formation that may be the subject of an EOR treatment. Fig. 5.26 shows the core pressures, oil recovered, and the oil cut. The data are shown along with a simulation (lines black, red, and blue). The ASP was injected after a waterflood and removed almost all of the oil, but an increase in pressure (right axis) indicates possible formation damage, probably from adsorption of the polymer.

Lake et al. (1992) note that these are small, 1D tests; however, if a process is not successful using a CFT, it probably will not be successful in field operations, so they are very important as part of the evaluation.

5.4 Immiscible Displacement Processes

The driving phase and the reservoir fluids (usually oil) are not soluble in each other (immiscible) in these operations.

5.4.1 Waterflooding. Waterflooding (Willhite 1986) has been used successfully for decades; however, the design and operation of the flood must be appropriate; otherwise, failures may occur. There are many factors to consider when designing a successful waterflood, including (Pope 2007a)

- Reservoir permeability (both absolute and relative)
- Beginning and ending fluid saturations (oil, water, and gas)
- Reservoir heterogeneity
- Oil gravity and viscosity
- Water source and compatibility
- Formation clay content
- Depth and lifting costs

The water for injection and flooding frequently come from produced water from the same field or from seawater. See Fig. 5.27 for one recycle setup using water from the same well field. *Formation damage* because of injected water (either connate, seawater, or mixtures) as well as corrosion is a major cause of well problems and some of the mechanisms are described in Section 2.3.3. Thus, there must be analyses of the injection water and plans for dealing with the interactions such as scale, emulsions, and corrosion.

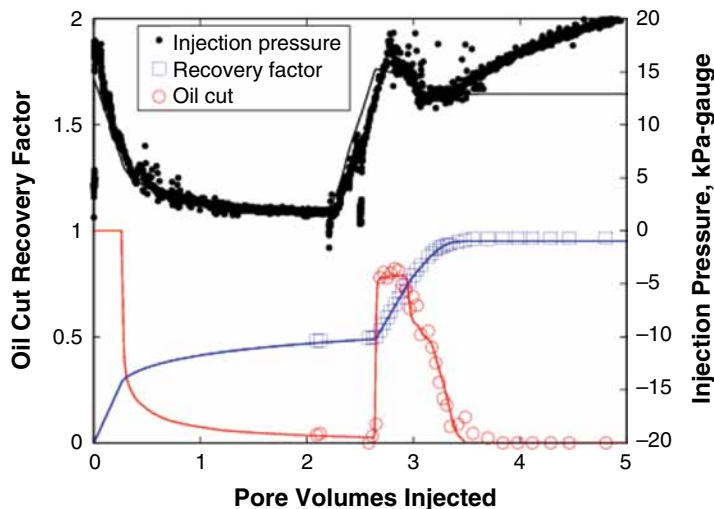


Fig. 5.26—Coreflood results for sandstone core and ASP treatment (Stoll et al. 2010).

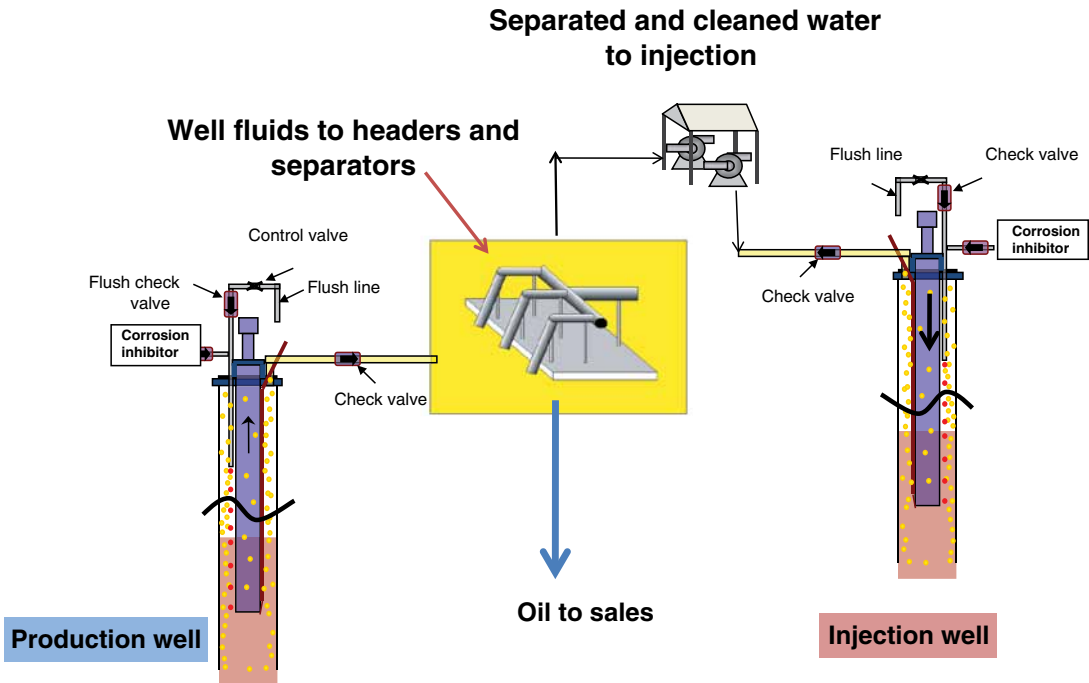


Fig. 5.27—The water cycle in EOR showing the source, treatment, and re-injection.

These issues also apply to waterfloods augmented by the use of polymers. According to a course by PDHengineer (2004), basic rock properties including porosity (ϕ), permeability, and the relative permeability of the oil phase and the water are key parameters that must be evaluated. These are determined by examining core samples (Corelab 2011). The viscosity of the oil phase is the key oil parameter that must be known. They (PDHengineer 2004) note that the waterflood performance can be analyzed using the fractional flow equation (Eq. 5.13) along with the frontal advance equations:

$$L = \frac{W_i}{A\phi} \left(\frac{df_w}{dS_w} \right) \dots \dots \dots (5.13)$$

Here, L = total distance that a specified water saturation plane has moved, W_i = cumulative volume of injected water (also the volume of the displaced oil), A = cross-sectional area perpendicular to the direction of the frontal advance, and df_w/dS_w = slope of the fractional flow plot of fractional flow vs. water saturation.

The time to breakthrough (t_b) equation also is used:

$$t_b = AL\phi \frac{(S_{wf} - S_{wi})}{q_i} \dots \dots \dots (5.14)$$

Here, S_{wf} = the water saturation at breakthrough, and q_i = injection rate.

These are used to produce a simulation of the movement of the waterflood front using the Buckley-Leverett method, and one example of a 900-day flood is seen in Fig. 5.28. The figures show the piston-like movement of 100% water saturation as a function of time.

Singh and Kiel (1982) note that waterflooding was first used over 100 years ago, but it was not until the 1950s that it gained popularity when field applications increased at a rapid rate. At the time of this book’s publication, waterflooding is so well regarded as a reliable and economic oil recovery technique that almost every field that does not have natural water drive is being or soon will be waterflooded. Because this type of enhancement requires approximately 3–4 injection wells for each producing well,

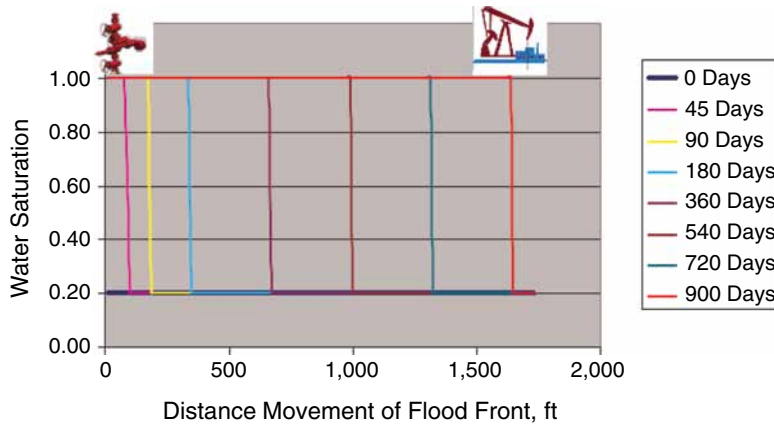


Fig. 5.28—Buckley-Leverett simulation of movement of the flood front (PDHengineer 2004).

the number of sites that may require treatment and stimulation could be greatly increased. According to Singh and Kiel (1982), there are two basic classifications of water injection projects:

- (i) Waterflooding—those which displace oil from semidepleted and depleted reservoirs, that is increasing recovery through the more efficient displacement process.
- (ii) Pressure maintenance—those which maintain a pressure in new or partially depleted reservoirs for sustaining the production rate.

Also Singh and Kiel (1982) contend that the main difference between secondary recovery (waterflooding) and pressure maintenance operations is the amount of reservoir pressure existing at the time the operations are begun. If the reservoir pressure is fairly high, the operation is called *pressure maintenance*, but if the pressure has been substantially depleted, the operation is called *secondary recovery*. Both operations should increase ultimate recovery from the affected reservoir. Under normal circumstances, pressure maintenance operations will not bring about the rate increase that a waterflood will achieve because it is installed when the reservoir-producing rate is at a higher level.

The factors controlling offshore waterfloods are

1. Reservoir geology and method of deposition
2. Primary production mechanisms and stage of depletion
3. Reservoir and fluid properties
4. Reservoir pressure
5. Well spacing and possible waterflood patterns

Design factors include

1. The rate of injection
2. Pattern
3. Estimation of producing rates and expected oil recovery

A large number of patterns are described by these authors (Singh and Kiel 1982). An evaluation of each type of pattern with literature citations is in the paper (Singh and Kiel 1982). See Fig. 5.10 for examples of well injection/production patterns.

Injection of brine (water) for pressure maintenance and to sweep additional oil from the reservoir is a characteristic of some secondary recovery processes (Thomas 2008) and some aspects were described in Section 5.2. Chemically related modifications to a waterflood process that are in commercial/pilot use or in research and development will be described in this section (5.4). These include

processes that include control of the salinity, addition of polymers for mobility control, and additions of specific microorganisms that may improve oil returns.

- *Salinity control* including low-salinity enhancement (LSE) (Morrow and Buckley 2011) are waterflood procedures that may change the wetting characteristics for some formations and thus release more oil from the pores. This process does not inject additional chemicals but may involve selection of a special water source or modification of available water sources. Details are in Section 5.4.2.
- *Polymer flooding* is used under many reservoir conditions that lower the efficiency of a regular waterflood, such as fractures or high-permeability regions that channel or redirect the flow of injected water, or heavy oil that is resistant to flow. Adding a water-soluble polymer to the waterflood allows the brine to move through more of the reservoir rock, resulting in a larger percentage of oil recovery. Polymer gels are also used to shut off high-permeability zones (Needham et al. 1974). See the discussion of these methods in Section 5.7.2. In these cases, the polymers are crosslinked using metal ions. This use of polymers also is similar to the use of chemical diverters that were described in Section 3.6.2. Pope (2007a) notes that the objective of polymer flooding as a mobility control agent is to provide better displacement and volumetric sweep efficiencies during a waterflood.

Because polymer flooding has been used for many years and is one of the more mature technologies in the EOR processes, it is treated as a distinct section and details are in Section 5.4.3. Additional diversion methods such as foam are described briefly in Section 5.6.3.

5.4.2 Low-Salinity Waterflooding. The use of injected water usually does not change the wetting mechanisms of the rock surfaces and thus usually do not change the capillary number. However, some *specific* saline solutions appear to alter the wettability under some select conditions.

Morrow and Buckley (2011) have reviewed the LSE applications and claim that improved recovery of crude oil by low-salinity waterflooding (LSWF), with only modest increase in resistance to flow, was seen by Tang and Morrow (1997) and Tang and Morrow (1999).

A process termed “smart water” (SW) was claimed by RezaeiDoust et al. (2009) who assert that waterflooding has for a long time been regarded as a secondary oil recovery method. However, the authors claim that the *composition* of the injected water can change wetting properties of the reservoir during a waterflood in a favorable way to improve oil recovery. Thus, injection of SW with a correct composition and salinity may act as a tertiary recovery method. Examples described by the author of SW injections include treatment of both carbonates and sandstones. Included are

1. Injection of seawater into *high-temperature* chalk reservoirs
2. Injection of *low-salinity floods* in sandstone reservoirs and some carbonates

There are different mechanisms for carbonates and sandstones. Note that desorption of clay using low-salinity water may also cause formation damage if the clay particles clog the near-wellbore area of the formation. See Section 2.3.3.

Henthorne and Wodehouse (2012) address one of the more important issues with low-salinity floods. What is the source for the LSWF? Various membrane methods have been in long usage to remove various ions from brine and surface water (Burke 2011; Henthorne and Wodehouse 2012):

- Offshore treatment of seawater to remove sulfate ions for waterflooding. More than 50 sulfate removal packages are collectively installed in the North Sea, Gulf of Mexico, Brazil, and West African waters.
- Process water production in water-scarce regions such as the Middle East. For instance, Saudi Aramco is known to have more than 30 brackish and seawater reverse osmosis and electro dialysis reversal plants in operation (IDA 2006).

- Deionized water used for power production.
- Desalinated water for drinking water offshore.
- Wash water production for desalting crude.

Morrow and Buckley (2011) have provided a summary of LSE results and issues:

- To date, improved recovery by LSE has targeted mobilization of remaining oil for reservoirs that are producing at W/O ratios that press economic limits. Increased oil-production rates would provide direct evidence of successful low salinity water application.
- The authors claim that, as with many recovery processes, much greater overall improvement in recovery would derive from application of LSE at the outset of reservoir development. However, interpretation of field results for evidence of success will involve much more ambiguity than for LSWF at S_{or} . Confidence in the LSWF processes continues to depend on laboratory observations and on improvements in understanding the mechanisms by which brine compositions affect oil recovery.
- The LSE has been reported for brine compositions of up to 5,000 ppm. For LSWF at S_{or} , injection waters with compositions in the range of 2,000 to 3,000 ppm have been used in field tests.
- If LSWF is not readily available, such as in offshore operations, desalinization will be a major component of the cost of a project. The authors of this book note that at the time of publication, the availability of LSWF (and possibly most sources of water) is a major economic and environmental issue for producers.

Carbonates. Strand et al. (2008) claim that seawater can be described as an EOR fluid for hot, fractured chalk oil reservoirs because it may be able to *modify the wetting* conditions and improve the displacement of oil. Austad (2010) claims that there are ongoing pilot projects for carbonates:

- BP—limestone in Abu Dhabi
- Maersk/UiS—limestone in Qatar
- Total/NFR—outcrop limestone
- Saudi Aramco—limestone

The reason proposed is that the carbonate rock is neutral to preferentially oil-wet and often highly fractured. It is claimed that *carboxylic compounds* (such as the naphthenic acids described in Section 0) in some crude oil adsorb strongly onto the carbonate surface and makes it partly oil-wet. Because of the negative capillary pressure in oil-wet rock, water will not imbibe into the matrix blocks to displace the oil. The water will only displace the oil present in the fractures, and less than 5% recovery is therefore expected in some cases when the oil reservoir is highly undersaturated and contains a large aquifer for pressure support.

When seawater is injected into hot carbonates, a wettability alteration is claimed in that Ca^{2+} , Mg^{2+} , and SO_4^{2-} play an important role because of their reactivity toward the chalk surface. The theory is that the interaction between SO_4^{2-} , Ca^{2+} , and Mg^{2+} , which are all components of seawater, will *remove* some of the carboxylic (natural acids, see Section 2.4.2) material from the chalk surface, change the wetting angles and thereby increase the capillary forces to promote spontaneous imbibition of water into the matrix blocks. The mechanism is schematically shown in [Fig. 5.29](#).

Chalk, which is purely biogenic CaCO_3 (Strand et al. 2008), consists of fragmentary parts of calcite skeletons produced by plankton algae known as coccolithophorids, and it is believed to have a more reactive surface than ordinary limestone. To validate seawater as an EOR fluid also for limestone and dolomite, the affinities of these ions toward the rock surfaces must be evaluated (according to the authors of this report).

Austad (2010) describes some preliminary experimental studies of the affinity of SO_4^{2-} , Ca^{2+} , and Mg^{2+} toward the surface of reservoir limestone cores at temperatures ranging from room temperature to 130°C. The results of core tests indicate that the ions had interacted with the rock surface and that

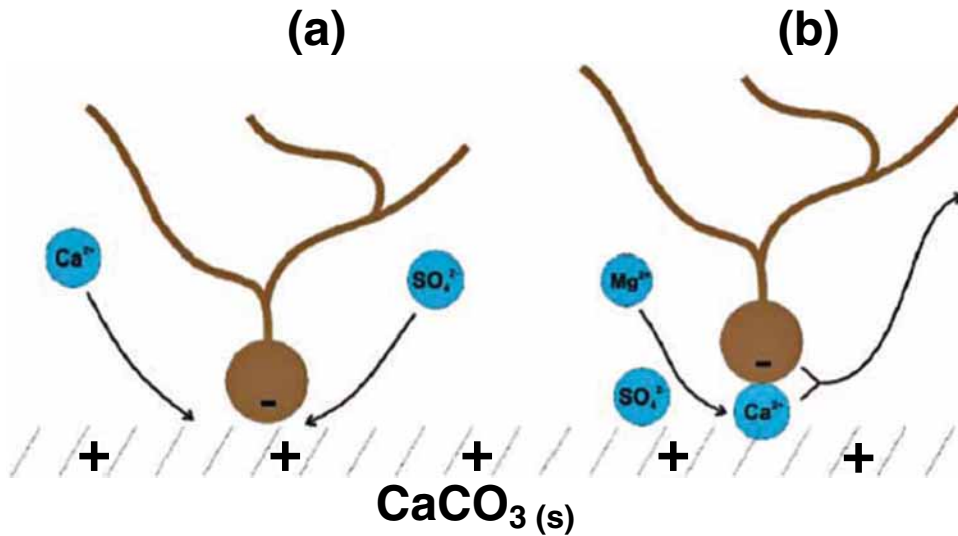


Fig. 5.29—Seawater wettability mechanism. (a) Ca^{2+} and SO_4^{2-} displace hydrocarbon and (b) Mg^{2+} and SO_4^{2-} displace hydrocarbons (Strand et al. 2008).

the established chemical equilibrium was sensitive to the relative concentrations of the ions. It was also observed that the adsorption of Ca^{2+} and Mg^{2+} from a NaCl solution onto the limestone surface was quite similar at room temperature but that Mg^{2+} adsorbed more strongly at higher temperatures. At high temperatures (130°C), Mg^{2+} in seawater was able to substitute Ca^{2+} on the surface but the reactivity was less than for chalk. These findings indicate that seawater will act as an EOR fluid in limestone as well, but its potential is probably smaller than for chalk. This was also confirmed by spontaneous imbibition tests performed at 120°C .

Yousef et al. (2012) claim that substantial oil recovery beyond conventional waterflooding can be achieved by optimizing the *ionic composition* of field injection brine in *carbonate* formations at low temperatures (tests at $< 70^\circ\text{C}$). They also contend that research confirmed that the driving mechanism is wettability alteration. In this paper, they present the results of new reservoir condition laboratory coreflooding studies, conducted using composite rock samples from different carbonate reservoir, to investigate the impact of ionic content on oil recovery at both secondary and tertiary recovery modes.

The paper reports results of a range of laboratory studies addressing the role of water ions. In addition, they briefly disclose the results of first-ever field application conducted in a carbonate reservoir to demonstrate the SW potential. The experimental results revealed that substantial tertiary oil recovery beyond conventional waterflooding can be achieved by altering the ionic content of field injection water. Fig. 5.30 shows coreflood data for oil removal from a carbonate core and the effects of *reducing* the salinity of the flood fluids.

Yousef et al. (2012) note that experimental results are claimed to confirm that wettability (reduction in IST as much as 12–14 units) alteration is the main cause for the substantial increase in oil recovery. Compared to previous reported work (Strand et al. 2008), the variation in oil recovery from two different carbonate reservoirs is attributed by Yousef et al. (2012) to the variations in reservoir temperature and also the chemistry of initial formation water. For field application, two field trials confirmed that injection of low-salinity flood achieved approximately 7 saturation units' reductions in residual oil beyond conventional seawater flooding.

Sandstone. Lager et al. (2008) state that for over 10 years, research has been carried out on the impact of low-salinity waterflooding on oil recovery. Data derived from corefloods, single well tests, and log-inject-log tests have shown that injecting low-salinity water into an oil reservoir should result in a substantial increase in oil recovery in many cases. The results varied from 2 to 40% increases in waterflood efficiency depending upon the reservoir and composition of the brine.

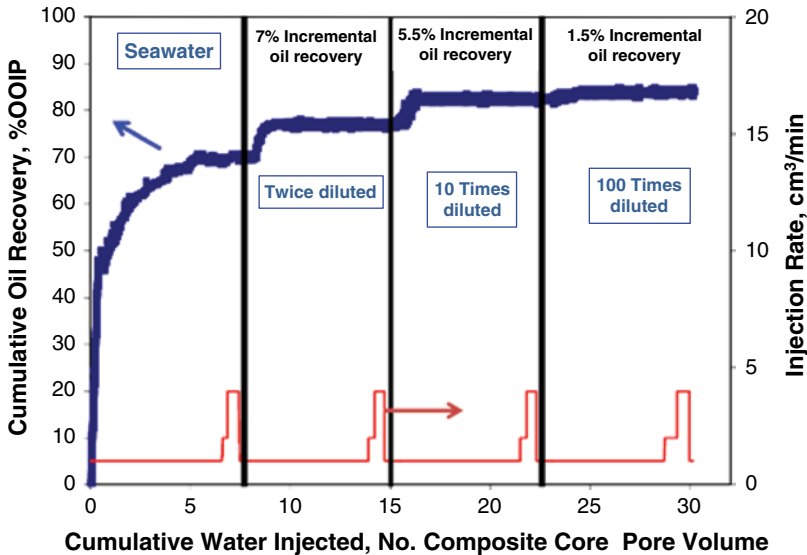


Fig. 5.30—Effects of seawater dilution on oil recovery from carbonate core (Yousef et al. 2012).

In 2005, a hydraulic unit was converted to inject low-salinity brine into an Alaskan reservoir, by switching a single injection pad to low-salinity water from high-salinity produced water. A surveillance program was devised that included capturing produced water samples at regular intervals for ion analysis and the capturing of production data. Detailed analysis of the production data and the chemical composition of the produced water demonstrated an increase in oil production and provided direct field evidence of the effectiveness of a low-salinity flush at interwell scales. Additionally, the response of the reservoir to low-salinity water injection was confirmed by single well tracer test (SWTT) (see Section 5.7.2).

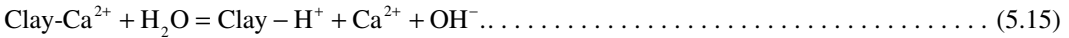
Parallel laboratory studies (Lager et al. 2008) are claimed to have led to mechanistic understanding of low salinity in terms of multiple-component ionic exchange between adsorbed crude oil components, cations in the in-situ brine, and clay mineral surfaces. The results show that the enhanced oil production and associated water chemistry response was consistent with the multiple-component ionic exchange mechanism proposed.

Austad (2010) and Austad et al. (2010) contend that EOR can be conducted for sandstone reservoirs by performing a tertiary *low-saline* (1000–2000 ppm) waterflood. However, because of the complexity of the crude oil-brine-rock interactions, the mechanism behind the low-saline EOR process has not been confirmed. They contend that at reservoir conditions, the pH of formation water is about 5 because of dissolved acidic gases like CO_2 and H_2S . At this pH, the clay minerals, which act as cation exchange material, are absorbed by acidic and protonated basic components from the crude oil, and cations, especially divalent cations from the formation water, like Ca^{2+} . Injection of a low-saline fluid, which promotes desorption of Ca^{2+} , will create a local increase in pH close to the brine-clay interface because Ca^{2+} is substituted by H^+ from the water. A fast reaction between OH^- and the adsorbed acidic and protonated basic material will cause desorption of organic material from the clay. The water wetness of the rock is improved, and increased oil recovery is observed. They cite work by Lager et al. (2007) and Lager et al. (2008).

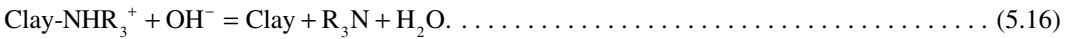
To observe low-salinity EOR effects in sandstones, a balanced initial adsorption of organic components from the crude oil (see Section 2.2.4) and Ca^{2+} onto the clay is required. Both the adsorption capacity and the pH-window for adsorption/desorption of organic material is different for various types of clay minerals. A detailed knowledge of the chemical mechanism behind the low-saline EOR process together with information on formation brine composition, oil properties, and type of clay material present, will make it possible to evaluate the potential for increase in oil recovery by a low-salinity waterflood. Various individual organic materials such as quinoline and carboxylic acids (t-butylbenzoic acid) were used.

Conclusions claimed by Austad (2010), and Austad et al. (2010) for sandstone mechanism are

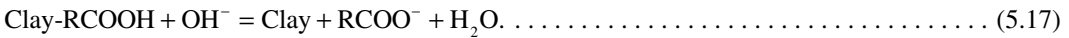
- Desorption of cations by low salt water:



- Wettability alteration
 - Basic material



- Acidic material



It is claimed (Austad et al. 2010) that the oil (must have absorbable organics), the brine (cations needed) as well as the low-salinity injected fluid are important (but the oil and the brine) are more important for the oil recovery affects. However, desorption of the ions from the clays as the low-salinity water is added is the key factor.

Fjelde et al. (2012) conducted laboratory and computational studies of sandstone rocks with high clay content. The high-salinity waterflood with formation water was found to give close to piston-like displacement, while the oil was produced over much longer periods in LSWF. They contend that higher concentrations of polar oil components can then be bonded to the clay surfaces by the divalent cations and make them less water-wet. It is concluded that the low-salinity water altered the wetting state of the rock. The direction of alteration can be explained by ion exchange taking place on the clay surface. The low-salinity water potential for improving recovery should be considered on a case-by-case basis based on the interactions between the formation brine, injected brines, oil components, and rock type.

5.4.3 Polymer Floods. The next two subsections describe processes that are most frequently called “polymer floods” in that additional and frequently large amounts of *synthetic polymeric* chemical are injected into the reservoirs for long periods of time. Very significant amounts of research and development time and money have been expended on the synthetic chemical processes; however, they currently represent a small amount of EOR-produced oil to date (Lake and Walsh 2008). That trend may be changing. Surkalo (2012) list the numbers of chemical EOR projects initiated since 1985:

- Polymer-27
- Alkaline/polymer-9
- S/P-6
- ASP-33

Mechanisms for Polymer Floods. The reason for adding polymers to waterfloods (as essentially the only active chemical) is to enhance the areal and vertical sweep efficiencies of the immiscible fluid. Thus, the chemical acts as a diversion agent and is similar in intent to the processes described in Section 3.7.2. The big difference is that it is applied to an *entire* reservoir section instead of just a few meters from a production wellbore. The reader may also view the information in Section 5.6.2 in which similar polymers are used for water shutoff.

Lake and Walsh (2008) and Lake (2010) report that polymer methods consist of injecting an aqueous phase (water or brine) into which has been dissolved a small amount of a polymeric thickening agent. The chemical increases water *viscosity* and in some cases lowers the permeability of that phase to bring about the lowered *mobility ratio* (Eq. 5.2). However, polymer methods *do not* increase the *capillary number* (Eq. 5.1). Thus, the irreducible oil saturation does not decrease, but the remaining oil saturation does decrease.

Lake (2010) and Zaitoun (2009) have described additional details of how polymers function to improve the efficiency of what is essentially an enhanced waterflood. **Fig. 5.31** is a depiction of the

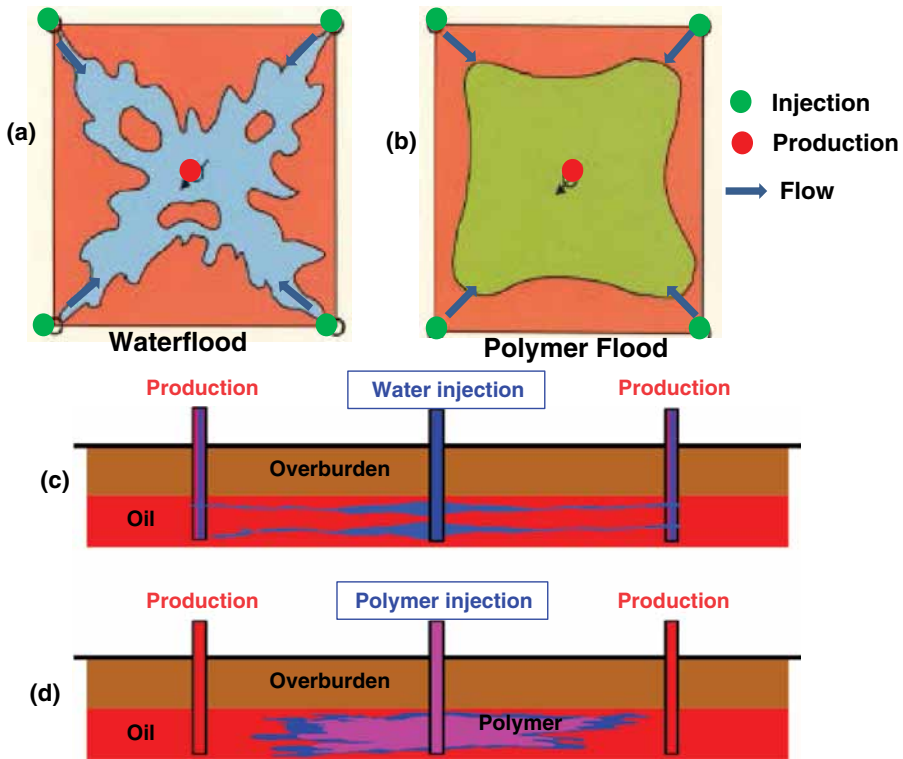


Fig. 5.31—Improvements in areal sweep efficiency by mobility control (Zaitoun 2009).

increase in sweep efficiency of a polymer flood compared with a waterflood. The figure shows two views (overhead A-B and side views C-D) of that indicates that the water normally would be channeled (see discussion of fingering in Section 0) through the most permeable zones to the production wells in this five-spot flood. The bottom half of the (C-D) figure shows that the water may breakthrough to the production wells rapidly without the polymer. By increasing the viscosity of the water, more portions of the reservoir are contacted by the water and the mobile oil (Fig. 5.31) is moved to the production well.

The mechanism described by Lake (2010) is that in addition to the increase in *viscosity* that slows the water penetration into higher permeability areas, the *adsorption* of the polymer also reduces the *permeability* of all of the water-wet zones. Also because the adsorption of the polymers follows a Langmuir-type process and the polymer and the connate water are miscible, the polymer front is piston-like.

Lake and Walsh (2008) claim that because of its relatively low cost [and favorable mass ratio/oil recovered (Table 5.1)] there have been more polymer floods done than any other type of synthetic chemical EOR process in the US. However, he notes that in the past (1980s), these have taken advantage of an artificial taxing policy in the US and were not designed to recover much incremental oil. With the lapsing of the policy and the collapse of the oil price in the mid-1980s, these projects virtually disappeared, giving way to a variation of the process based on polymer gels. With the restoration of the oil price, interest has picked up, especially because of the significant reported successes in the Chinese Daqing field (Pu et al. 2008). Polymer processes have historically recovered about 5% of the OIP and taken about 1 lbm of polymer/bbl of oil.

Pope (2007b) notes that the cost of HPAA (the most used polymer) has actually decreased in price in real terms since the 1980s) and 1 bbl of initial oil can be produced for USD 1–2 of polymer (as of the time of the publication of this book). Details of the current technologies are reviewed in this section. The process uses dilute aqueous solutions of water-soluble polymers that have the ability to *reduce* the mobility of water in a reservoir, thereby improving the efficiency of the flood. This is accomplished by

increasing the viscosity of the aqueous phase and thus slowing the progress through the matrix. Also, note Eq. 1.2 and Eq. 5.2.

While a large number of polymer types have been proposed [see Kelland (2009), Fink (2003), and Fink (2011)], PHPAA and xanthan gum polymers have been used in most commercial operations. These chemicals have been described in Sections 4.4.1, 4.7.1. Also, Fig. 4.46 shows the structure of the HPAA molecule that is also used in HF. The degree of hydrolysis as well as the final MW can be modified over a very wide range to accommodate particular requirements, such as salinity of the brine.

Thomas et al. (2012) have reviewed a number of aspects of the use of HPAA polymers for use in waterfloods. They note that a typical polymer flood project involves mixing and injecting polymer over several months for surfactant slugs and several years for polymer alone at concentrations ranging from 300 to 3,000 ppm, until 30% or more reservoir PVs have been affected. This concentration of polymer is somewhat lower than the amounts used in SW fracturing (about 5,000 ppm). Important characteristics of the HPAA include loss of viscosity as a function of salinity, Ca²⁺ ions and degradation processes are described later in this section.

Reservoirs that are good candidates can be recognized by poor volumetric efficiency (Green and Willhite 1998) and selected if the conditions respect the polymer tolerance limits (temperature approximately < 130°C, salinity < 250,000 TDS and reservoir permeability > 40 md).

Lake (2010) claims that copolymers based on acrylamide polymerized with 2-acrylamido-2-methyl propane sulfonate (AM/AMPS) (Fig. 5.32) and hydroxyethyl cellulose (Fig. 4.41) are the only additional materials that have been used in commercial polymer floods; however, a range of alternate polymers have been proposed and tested.

The reduction in permeability to water that is achieved with HPAA solution may be permanent while the permeability to oil can remain relatively unchanged. The resistance factor (R_f) is a term that is used to indicate the resistance to flow that is encountered by a polymer solution as compared to the flow of plain water. Three equations describe the effects:

$$R_f = \frac{\text{Flow rate with polymer}}{\text{Water flow rate}} \dots\dots\dots (5.18)$$

The residual resistance factor is

$$R_{rf} = \frac{\text{Water flow rate before polymer}}{\text{Water flow rate after polymer}} \dots\dots\dots (5.19)$$

The permeability reduction is

$$R_k = \frac{\text{Permeability to water}}{\text{Permeability to polymer}} \dots\dots\dots (5.20)$$

Eqs. 5.18 and 5.19 are equivalent to pressure drops in the matrix. When a fluid penetrates a porous medium with different relative permeability values, it penetrates the higher zone first and then as the resistance (ΔP) because of the polymer develops in that zone; it then penetrates the lower-permeability zone.

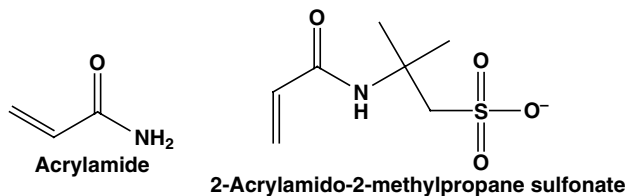


Fig. 5.32—Structure of AM and AMPS monomers.

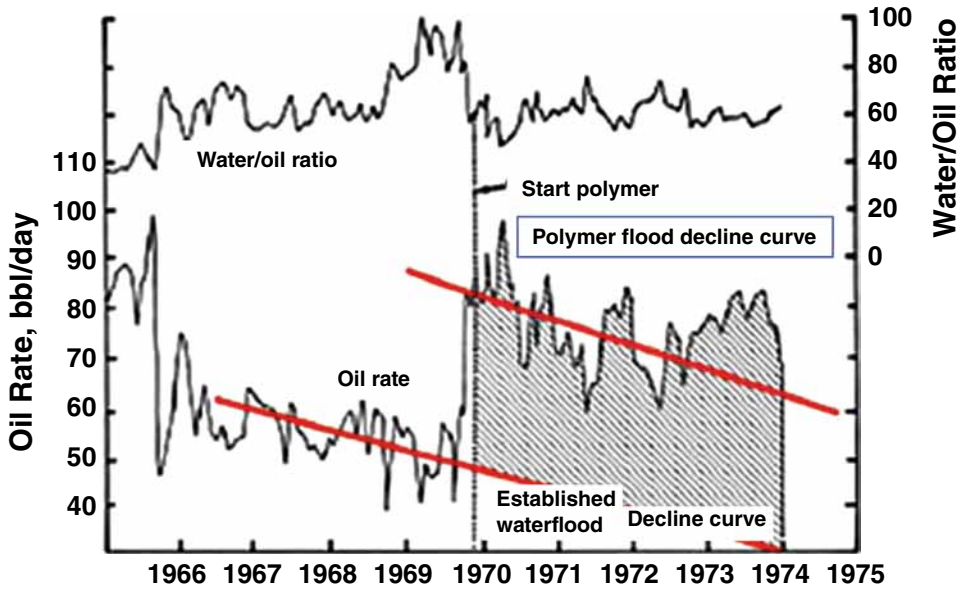


Fig. 5.33—Polymer EOR results North Burbank unit (Clampitt and Reid 1975).

A successful treatment using polymer injection during the 1970s time frame is shown in Fig. 5.33 that was performed in the North Burbank unit, Osage, Oklahoma (Clampitt and Reid 1975). The shaded portion is the incremental oil recovery.

Information on more recent large polymer floods is described in the next subsection. The technology of polymer floods is continuing to develop and several recent new technologies are abstracted. Reichenbach-Klinke et al. (2011) claim that a new thickener based on associative properties (aka VES) is being developed. They also claim that this fluid thickener consists of an anionic, water-soluble copolymer containing pendant associative groups. Note the discussion of VES (monomeric surfactants that associate) materials in Sections 3.7.2 and 4.4.4, which also can form larger association polymer in some brine solutions.

A patent application by Reichenbach-Klinke et al. (2010) claims water-soluble, hydrophobically associating copolymers, which comprise types of hydrophobically associating monomers. The monomers comprise an ethylenically unsaturated group and a polyether group with block structure comprising a hydrophilic polyalkylene oxide block, which consists essentially of ethylene oxide (EO) groups, and a terminal, hydrophobic polyalkylene oxide block, which consists of alkylene oxides with at least four, preferably at least five carbon atoms. VES materials are also discussed in Section 5.6.4 on alternative “diversion” technologies for EOR. Details of adsorptive problems with EOR polymers are discussed in Section 5.4.4. The authors (Reichenbach-Klinke et al. 2011) report that the associative polymer shows good resistance to shear during injection.

Seright et al. (2011) have investigated the behavior of a new associative polymer in porous media. The tetra-polymer has low hydrophobic-monomer content (0.025–0.25 mol%) and a molecular weight (MW) of 12–17 million g/mol. Total anionic content is 15–25 mol%, including a few percent of a sulfonic monomer. Compared with HPAA, the new polymer is claimed to have a significantly higher level of shear thinning at low fluxes and a lower degree of shear thickening at high fluxes.

Recent Large Polymer Projects. The higher price of oil since 2005 has improved the economic viability of polymer floods in some markets. Tielong et al. (1998) conducted a pilot test of polymer flooding in the Shuanghe reservoir located in the southeast Henan oil field, China. The target reservoir has a net thickness of 15.56 m (50 ft), an average permeability of 420 md, and a temperature of 75°C (167°F). The polymers used are two types of modified partially HPAAs, named S525 and S625, which have MWs of 16,700,000 and 19,670,000 daltons, respectively. The objective of this pilot

test was to investigate the feasibility of polymer flooding for improving oil recovery in an elevated-temperature reservoir. The polymer flooding started in February 1994. Through December 1995, a total of 246 tons (about 0.5×10^6 lbm) of dry polymer had been used with an injection concentration of 900 to 1,100 ppm. The PV injected reached 0.2164. As a result, oil production increased by 22,000 tons (184,000 bbl) and water production decreased by 153,000 tons (962,000 bbl), which accounts for the incremental oil recovery of 3.8% and water-cut reduction of 5.6% in the test block. The key improvement was the addition of thiourea to retard the degradation of the polymer from oxygen attack (see next section).

They estimate that, by the end of this project, the ultimate increase in oil production will exceed 63,000 tons (528,000 bbl) with the EOR going up to 9.8%. The yield is 0.2 tons more oil produced per kilogram of polymer injected or 0.7 barrel of oil produced per pound of polymer. They attribute the success of the pilot test to the techniques used during the implementation of the flooding, including prevention of polymer-thermal degradation, good reservoir description, and the profile modification carried out before and after the polymer injection. This pilot test illustrates a case where polymers with extra-high MW are successfully injected in an elevated-temperature reservoir to control the mobility ratio and modify the permeability profile.

Cheng et al. (2010) report on the results of the very extensive polymer flooding in the Daqing (China) oil field. A large-scale commercial application of polymer flooding has been proceeding in the Daqing oil field since 1996, and its yearly oil-production rate by polymer process has continuously reached 10 million tons for 8 years. To date, polymer injection has become the leading technology to control oil-production decline in Daqing oil field. The field practice indicates that the viscosity and elasticity (viscoelasticity) of polymer solution can greatly enlarge swept volume and enhance oil recovery efficiency, resulting in oil recovery by polymer injection in major reservoirs 10% higher than that of waterflooding, but there are still about 50% crude oil remained underground after polymer injection.

The authors company performed analyses based on well log interpretation and core studies before and after polymer flooding in three fields. This was called a macro analyses. These macro results indicate that swept thickness of the reservoir increased 21.4% from 68.6% of waterflooding to 90% of polymer flooding, and oil saturation reduced 11.9% from 52.8% to 40.9%, and displacement efficiency went up 7.6%. The residual oil distribution after polymer flooding is scattered in horizontal direction, while it is interleaved in vertical direction. Following polymer flooding, 10.6% unswept thickness is mainly distributed in thick oil layers, and most of the remaining oil within thick oil layers lies in the interlayers and at the top of thick oil layers, with its effective thickness close to 80%. From the macro analyses point, remaining oil is mainly located in distribution lines or some places where injection and production relation is imperfect or the phase is changed, and oil saturation located in the distribution line is 4.4% higher than that along the mainstream line. The micro analysis (core membrane fluorescence) to determine the oil remaining in individual cores shows that the behavior of remaining oil distribution is similar to waterflooding, which is mainly controlled by capillary force. These data illustrate the discussion of sweep control described in Sections 5.1.1 and 5.4.1.

For large polymer floods, many thousands of pounds of polymers may be needed. The polymers usually are provided as a powder that must be mixed and hydrated (see the discussion of polymer hydration in Section 4.3.1). Morel et al. (2010) describe a very large polymer injection project on the Dalia field, one of the main fields of Block 17 in deep offshore Angola, is a world first for both surface and subsurface aspects. The injection of polymers is intended to be started early in the waterflood instead of later during a typical EOR flood.

An in-depth integrated geosciences and architecture study culminated, in January 2009, in the start of polymer injection in one of the Dalia water injection wells. Dalia field is a high-permeability sandstone reservoir (> 1 D on average) and contains medium viscosity oil (1 to 11 cp under reservoir conditions).

The key challenges of the project were to start polymer injection

- Very early in the field development because first oil was in December 2006
- With much wider well spacing than in any other project

- Under high-salinity conditions (>25g/L)
- With the specific logistics of a remote deep offshore area

After a positive single well injectivity test early in 2009, additional single well injectivity tests were performed at the end of 2009 on three Dalia wells in various configurations. They demonstrated an injectivity of the polymer solution that satisfies the field development requirements in terms of the voidage replacement, as defined in the water injection base case. During this testing period, the capacity of the logistics and surface facilities (capacity of 7 t/D) to successfully prepare the polymer solution on board the floating, production, storage, and offloading unit have been demonstrated after specific difficulties and issues were identified and fixed. Based on these positive results, a Phase 1 project was sanctioned and started on 8 February 2010 on the Camelia complex. Viscosified water is injected in one of the four injection lines of Dalia field (average base, sediment, and water of 20% on the associated producers at beginning of Phase 1 polymer injection). By mid-June 2010, more than 3 million bbl of cumulative of polymer solution have been injected in the Camelia reservoir.

The specificities of the Dalia field (large well spacing and low base, sediment, and water at polymer injection startup) mean that a late response will be noted if the usual EOR monitoring techniques are applied. Various monitoring options were considered to verify the injected polymer solution properties in situ, and accelerate the sanction for a full-field development. The studies concluded on a recommendation to drill a well to sample in situ the injected viscosified water. Locations of the sampler well at a distance of 100 m from an injector and best timing to drill the well were based on 4D seismic data history match and waterflood performance forecast.

Pope (2007b) lists the criteria for successful polymer floods:

- High remaining oil saturation
- Low waterflood residual oil saturation
- High-permeability and porosity
- Sufficient vertical permeability to allow polymer to induce crossflow in reservoir and good geological continuity
- High polymer concentration and slug size
- High injectivity because of favorable combination of high permeability, wells, or injection of parting pressure
- Fresh water and/or soft water
- Reservoir temperatures less than 250°F

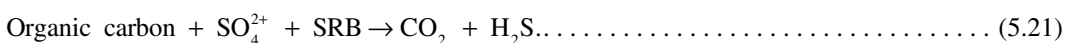
Lake (2007) adds more information on favorable conditions for the use of polymer flooding:

- Large water-oil mobility ratio (< 50)
- Large mobile oil saturation (> 0.1)
- Good reservoir continuity

Additional information on the chemical effects on polymer floods is in Section 0.

5.4.4 Chemical Issues With Immiscible Floods. Chemically related problems associated with injecting water and other chemicals into a producing reservoir include the possibility of producing H₂S (souring) as well as other unwanted chemical interactions with the rock and reservoir fluids.

Reservoir Souring. Schofield and Stott (2012) have reviewed the problems and solutions of reservoir souring that can take place with any water-based flood including polymer as well as the surfactant fluids described in Section 5.5.3. In the presence of sulfate ions, organic carbon is oxidized [catalyzed by sulfate-reducing bacteria (SRB)], producing carbon dioxide and hydrogen sulfide:



The authors claim that the reduction of sulfate may occur deep in the reservoir by contact with biofilms in (a) or (b) near the injection wellbore and then *migrates* to the producing well. See Fig. 5.34.

In either case, the production of the sour gas affects corrosion as well as production of iron scales (see Section 2.2.2 and 2.2.3).

Details about SRB (Seagraves 2007) are

- They reduce sulfate ions to sulfide ions
- Colonize areas of stagnation
- Associated with sand, silt, scale, etc.
- Accelerate corrosion by depolarizing the cathode by hydrogen removal
- Sulfide ions react with soluble metal ions to form metal sulfides, an excellent plugging agent
- Infestation of 100 colonies/mL are significant

Work by Augustinovic et al. (2012), Larsen et al. (2009), and Larsen et al. (2010) highlights the use of molecular microbiology methods to unveil the complex distribution of microorganisms in oilfield systems. These are techniques based on characterization of DNA and/or RNA content in the samples

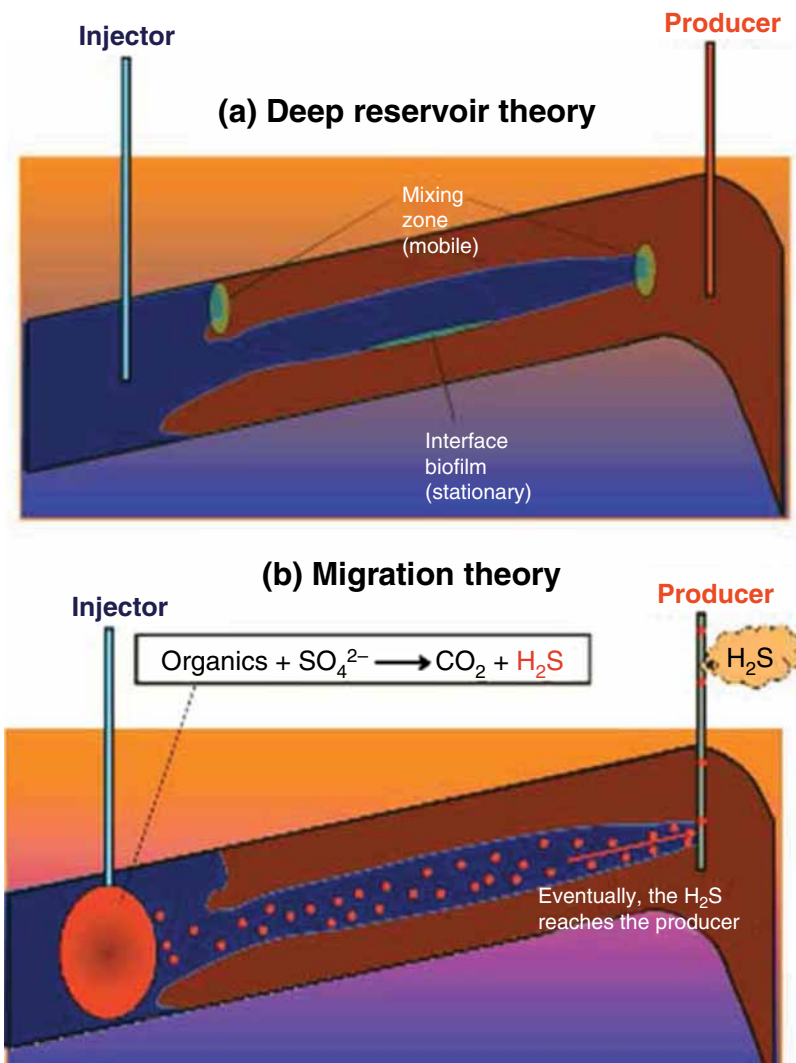


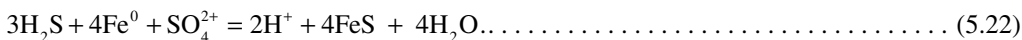
Fig. 5.34—Theories of reservoir souring (Schofield and Stott 2012).

of water rather than on viable counts of some microorganisms. These authors have used the designation of Prokaryotes for both SRBs as well as a group of *Archaea* (called sulfate-reducing *Archaea*) that have been seen as being part of the problem microorganisms in oilfield waters. Note that *Archaea* are a separate branch on the Earth’s tree of life that also includes bacteria and more complex organisms (including mammals). The molecular microbiology methods described are beyond the scope of this book and the reader is directed to the references in the cited papers.

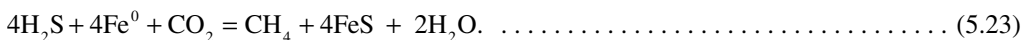
The claim of the authors (Augustinovic et al. 2012) is that previously used methods of identification of microorganisms (using culturing) only identify 10% of the possibly problem-causing micro species. The expanded mechanism is seen as Fig. 5.35.

The net reactions

- Sulfate reduction



- Methane production



The effects of the production of H₂S on corrosion and scale may be reduced by removing sulfate from the injection water or by using biocides, which are discussed in Section 4.7.3. However, Schofield and Stott (2012) claim that Ca²⁺ or Na⁺ nitrates have been used as biocides. These authors observe that the nitrates stimulate nitrate-reducing bacteria that then compete with the SRB. Thorstenson et al. (2002) describe tests comparing glutaraldehyde with nitrate injection to prevent formation souring (and thus production of H₂S). These authors conclude that nitrate was more effective than glutaraldehyde, and this was an effective method in the reservoirs being treated.

They found

- Nitrate injection led to reduction in SRB numbers and activity and a concomitant enrichment of nitrate reducing bacteria
- The effect of nitrate injection was evident 4 months after start of injection
- Corrosion measurements on metal coupons showed a decrease in weight loss from 0.7 mm/year before nitrate addition to 0.2 mm/year with nitrate treatment

Several trials have been conducted. See Hubert et al. (2004), Jack et al. (2009), Sunde et al. (2004), and Youssef et al. (2009) for more details.

Additional Unwanted Chemical Interactions in the Reservoir. Possible unwanted chemical interactions with the use of polymers include the adsorption/reaction of the polymers with the rock matrix

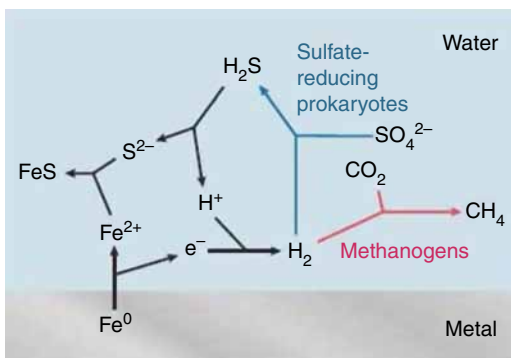


Fig. 5.35—Sulfate reactions (Augustinovic et al. 2012).

minerals, oxidative degradation, shear degradation, and polymer/fluid reactions. Water quality is also a major concern for polymer floods as well as for other use of chemicals including the surfactants described in Sections 5.5.3 and 5.5.5. Application of fresh water or water with low Ca²⁺ content (soft) water may be necessary for some polymer formulations because HPAAs-type polymers that contain carboxylate groups can complex with the cations and reduce the viscosity (and thus the effectiveness) of the polymer.

The selection of the amount of hydrolysis affects the charge ratio of the polymer as well as the reaction to the ions in the water. Higher amounts carboxylate (–COO[–]) increased water solubility while the amide groups [–C(O)HN₂] groups are unaffected by Ca²⁺ ions, which complex and can precipitate the polymer. Thomas et al. (2012) describe the characteristics of various HPAAs polymers.

The addition of the AMPS structure in the AM/AMPS copolymer reduces the effects of the calcium ions on viscosity, as well as improving the viscosity at temperatures to 225°F according to Pope (2007b), Tielong et al. (1998), and Thomas et al. (2012). These AM-type polymers are claimed to be very efficient and 500–2000 ppm is usually sufficient for the diversion effects needed. A description of the mechanisms of polymer viscosity enhancement is in Section 4.4.1. The relationship between the viscosity and the concentration and the MW is complex but can be described by the intrinsic viscosity (Eq. 1.44) as well as the Flory equation:

$$MW = \frac{2RTT_{max}}{H(T_{max} - T)} \dots \dots \dots (5.24)$$

Here *R* is the gas constant, *T* is the temperature of the test, *T*_{max} is the maximum melting temperature, and *H* is the enthalpy of melting. In addition, in the flowing fluids, these polymer fluids act as viscoelastic materials that can be described by the power-law equation (Eq. 1.31). An example of the effect of shear rate as a function of solution salinity for an AMPS polymer is seen in Fig. 5.36. Note that in highly saline water, even the initial viscosity (and thus the diverting utility) is low. The other HPAAs polymers are also sensitive to the shear rate and salinity (Thomas et al. 2012).

For injection water quality requirements, it is noted that not all of the water used for EOR needs to be fresh. The use of *treated* produced water can significantly reduce the quantities of fresh water that would be sought from other sources. Royce et al. (1984) claim that at the time of this report, no major

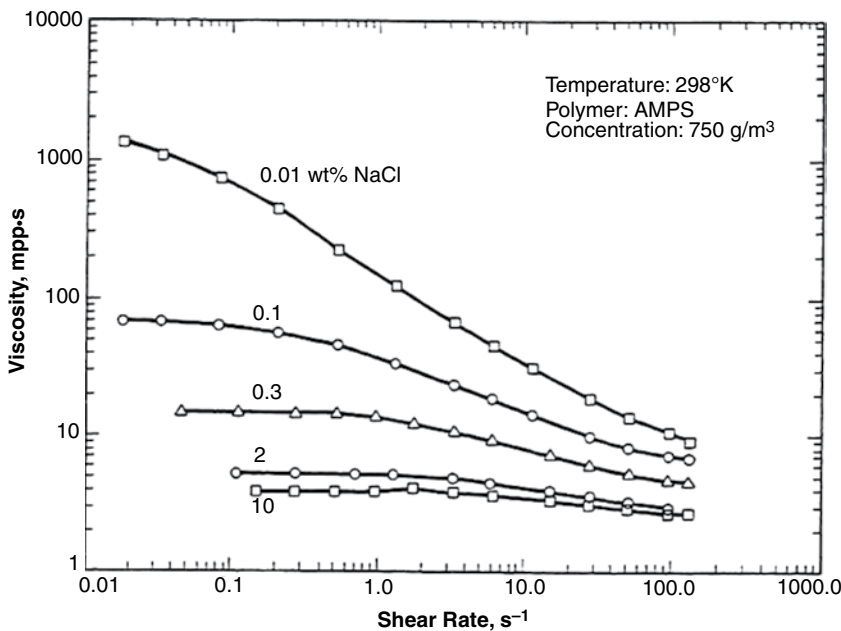
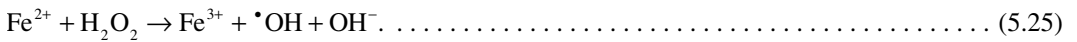


Fig. 5.36—AMPS polymer solution viscosity vs. shear rate (Lake 2010).

EOE project to date has been abandoned because of water supply problems, competing regional uses for water, drought situations, and scarcity of high quality (e.g., low TDSs, surface water, and ground water could be impediments to certain projects in the near future). However, in the time of the publication of this book, the high rate of water use for HF (see Sections 4.10.1 and 6.3.2 also may affect waterflood and EOR water use).

Dissolved iron may also be present at very low concentrations from natural minerals, corrosion of piping or from acidizing treatments. Shiau et al. (2012) have reported 24 mg/L of iron (and 4000 mg/l Ca^{2+}) in Oklahoma brine where EOR treatments were contemplated. Iron (III) will complex and gel HPAA in the acid range (Hill 2005) and has been used as a gelling agent [similar to use of Cr(III)]. However, the concentration of Fe(III) iron is extremely low at EOR pH values because of the very low solubility of the oxides (Frenier and Ziauddin 2008). Thus, the iron should be in the 2+ oxidation state unless oxygen is present. The concern with dissolved iron is not direct complexation with the polymer at possible brine concentrations, but the possibility that the iron will catalyze the hydroxyl radical degradation of the polymer. This is called the Fenton reaction and is a known degradation mechanism for many organic molecules in aqueous solution including chelating agents and polyacrylamides (Motekaitis et al. 1980; Grollmann and Schnabel 1982; Levitt and Pope 2008).

The production of the hydroxyl radicals is as follows:



While removal of small amounts of iron is not usually possible, use of oxygen scavengers as well as radical scavengers [see Gaillard et al. (2010) for a short review] will reduce the possibility of this type of degradation. The authors of this book note that in the time frame of the publication, the cost/availability of oilfield water as well as the quality are major technical and economic issues. See the reports by Burnett and Vavra (2006), Burnett (2011), and the patent application by Weerasooriya and Pope (2011b).

Interactions with the rock minerals will cause a loss of the polymer from solution (which will cause a reduction in viscosity) and a permanent reduction in permeability. All polymers experience retention in permeable media because of adsorption onto solid surfaces or trapping within small pores. Polymer retention varies with polymer type, MW, rock composition, brine salinity, brine hardness, flow rate, and temperature. Field-measured values of retention range from 7 to 150 μg polymer/ cm^3 of bulk volume, with a desirable retention level being less than about 20 $\mu\text{g}/\text{cm}^3$ (Lake 2010).

Retention causes the loss of polymer from solution, which can also cause the mobility control effect to be lost, especially at low polymer concentrations. Polymer retention also causes a delay in the rate of the polymer and generated oil bank propagation. The polymer adsorption can be described using the Langmuir isotherm equation (Fig. 1.9 and Eq. 1.22). However, Lake (2010) notes that the slope is high, and this may indicate that less than one monolayer of coverage is achieved. There also will be a loss in permeability (called a resistance factor, R_f , Eqs. 5.12 and 5.13) that will depend on the polymer, temperature, and salinity. All of the factors affect the sweep efficiency of the polymer and must be evaluated to determine the economic impact on the proposed treatment.

Lorenz and Tham (1981) have shown that Ca^{2+} , generated by dissolution of the formation rock by a brine may be enough to affect both the behavior of an HPAA (if there was calcium from the brine) as well as some surfactants in a P/S slug. Chemical, mechanical, and biological degradation of the polymer also must be addressed. These factors also affect the use of polymers for HF (see Section 4.4).

Seright, Campbell et al. (2010) note that at elevated temperatures in aqueous solution, partially HPAAAs experience hydrolysis of amide side groups. However, in the absence of dissolved oxygen and divalent cations, the polymer backbone can remain stable so that HPAA solutions were projected to maintain at least half their original viscosity for more than 8 years at 100°C and for approximately 2 years at 120°C. Within their experimental error, HPAA stability was the same with and without oil (decane). An acrylamide-AMPS copolymer (with 25% AMPS) showed similar stability to that for HPAA. Their results may offer assurances for use of HPAA polymers in EOR at temperatures up to 120°C if contact with dissolved oxygen and divalent cations can be minimized.

Seright et al. (2010) also have performed calculations considering oxygen reaction with oil and pyrite revealed that dissolved oxygen will be removed quickly from injected waters and will not propagate very far into porous reservoir rock. These findings indicate that dissolved oxygen that entered the reservoir before polymer injection will have been consumed and will not aggravate polymer degradation. Second, if an oxygen leak (in the surface facilities or piping) develops during the course of polymer injection, that oxygen will not compromise the stability of the polymer that was injected before the leak developed or the polymer that is injected after the leak is fixed. However, polymer that is injected while a leak is active will be susceptible to oxidative degradation. Maintaining dissolved oxygen at undetectable levels is thus necessary to maximize polymer stability.

Shear degradation as well as chemical effects have also been investigated. Zaitoun et al. (2012) conducted an experimental study of shear stability of several high-molecular-weight polymers used as mobility control agents in EOR projects has been performed in well-controlled conditions.

The shearing can occur at different stages of handling and injection process such as

1. Use of shearing device for polymer dissolution in makeup water
2. Recirculation with centrifugal pump
3. Flow through chokes under high differential pressure
4. Flow through downhole valves
5. High rate flow through perforations and sand face

They claim that usually, the operator accepts a viscosity loss of 10–20%, but higher values may compromise the project itself. The shearing device of the current study (Zaitoun et al. 2012) was made of a capillary tube with inside diameter of 125 μm , through which polymer solution was injected at controlled rate. The setup enables a precise measurement of the shear rate to which the polymer macromolecule is submitted. The degradation rate was measured by the viscosity loss induced by the passage into the capillary tube. The shear rate was gradually increased up to 106 sec^{-1} while checking degradation rate at each stage.

Different commercial EOR polymer products were submitted to the test with polyacrylamide backbone and different substitution monomer groups. All macromolecules behave as flexible coils in solution. The parameters investigated were

- MW (between 6 and 20×10^6)
- Nature of substitution group [acrylate, 2-acrylamido-tertbutylsulfonic acid (ATBS)/sulfonate, *N*-vinyl-pyrrolidone (*N*-VP)]
- Salinity

Zaitoun et al. (2012) found that polymer shear degradation increases with MW and salinity but decreases with the presence of acrylate, ATBS, and *N*-VP. All results can be interpreted in terms of chain flexibility. The highly flexible polyacrylamide homopolymer is the most sensitive to shear degradation. Introduction of acrylate groups in the polymer chain induces some stability because of the rigidity provided by charge repulsion, which vanishes in the presence of high salinity (because of the screening of acrylate negative charges). ATBS and VP groups, which are larger in size, provide significant chain rigidity thus better shear stability. It is also shown that some very high MW polymers, after passing the shearing device, attain a final viscosity lower than lower-MW products with the same chemical composition. This factor has to be taken into account in the final choice of a polymer for a given field application. As a comparison, although less popular today than two decades ago, xanthan gum, which behaves like a semirigid rod, is shown to be much less sensitive to the shear degradation test than the coiled polyacrylamides.

Kulawardana et al. (2012) have investigated polymers that are claimed to be stable in harsh environments (high salinity/hardness and high temperature). They note that commonly used partially HPAAs have been successfully used in the field for decades, but they hydrolyze at high temperature and eventually precipitate in the presence of high concentrations of divalent cations. This paper mainly focuses on rheology and transport behavior of scleroglucan (nonionic polysaccharide is also proposed for HF;

see the “Biopolymers” subsection under Section 4.4.1) and *N*-VP-polyacrylamide copolymer. The authors claim that the rigid, rodlike, triple helical structure of scleroglucan imparts exceptional stability, and its nonionic functionality makes it insensitive to salinity and hardness. They have proposed a different mechanism for *N*-VP in modified HPAA in that it protects the polymer’s amide group against thermal hydrolysis (i.e., by sterically hindering the amide group). This allows maintaining high viscosity even in high-salinity brines at high temperature.

They conclude that both scleroglucan and *N*-VP co- or ter-polymers show good filterability and transport properties in sandstone and carbonate cores at high temperature and in brine with high salinity and hardness. Therefore, both polymers are promising candidates for polymer flooding, SP flooding, and alkali-surfactant-polymer flooding in hard brine at high temperature (about 85–100°C). Neither material has been used in field trials or pilot tests.

Mohammadi and Jerauld (2012) claim that while polymer flooding is a proven technology that improves waterflood recovery efficiency by increasing the water-oil viscosity ratio, low-salinity EOR is an emerging technology, which enhances the displacement efficiency by changing wettability (see Section 5.2.2). The authors suggest that the combined EOR processes are additive because they target different things. The authors of this book and Henthorne and Wodehouse (2012) note that RO has been used for many years to condition EOR water because the HPAA widely used in chemical EOR hydrolyze at high temperatures and precipitate if calcium concentration is above 200 ppm (see previous). The authors of this report (Mohammadi and Jerauld 2012) thus claim that the use of low-salinity EOR can make the use of polyacrylamide polymers feasible up to reservoir temperatures of at least 100°C or enable the use of polymers with larger degrees of hydrolysis. Polyacrylamide solution viscosity increases as salinity decreases so operation expenditure will reduce because of lower required polymer concentration. One third or less of polymer is required with low-salinity waterflooding EOR compared to conventional waterflooding.

They also claim (based on the modeling described in the paper) that they have demonstrated that addition of polymer enhances recovery efficiency and timing of LSWF. The incremental oil recovery between the homogeneous and heterogeneous cases is close, especially for more viscous oil. At high oil viscosity, combination of low-salinity injection water and polymer gives incremental oil recovery about equal or better than the summation of each if used separately. We demonstrate that both secondary and tertiary combined processes are effective but secondary gives better timing. Synergistic behavior of combined processes is more effective in tertiary flood than the secondary cases. Chemical cost comparison of the cases studied shows that a five-time reduction in chemical cost per bbl of oil recovered can be expected when polymer is added to low salinity. We show that operational constraints in field application can limit the synergy between these combined processes.

Summary of Degradation/Failure Modes. Thomas et al. (2012) conclude that studies (including this author and the papers described in the current section) indicate that the types of degradation include

- Chemical degradation
- Mechanical degradation
- Thermal degradation

Pope (2007a) summarizes a number of possible *failure* routes for polymer flooding:

- Do not inject enough polymer
- Open up high mobility paths by injecting water for a long time before polymer
- Shear degrade the polymer
- Plug the rock with low quality solution or polymer too large for small pores
- Use biodegradable polymer such as xanthan gum without effective biocide
- Inject polymer in wells without geological testing

The addition of polymers to a waterflood does not affect the capillary number and thus, does not affect the microscopic properties of the matrix. Section 5.5 describes methods that do affect the surface chemical factors of EOR processes. Polymer pusher stages frequently follow these types of treatments.

5.5 Miscible Displacement Processes

The term miscible generally means *soluble in all proportions*. Thus, water and ethanol (as well as some other alcohols) are miscible. These fluids are then considered thermodynamically stable. Various HC fluids also can be miscible. When applied to EOR methods, miscible displacement processes involve injecting a chemical (solvent) that forms a stable mixture with the oil and also reduces its viscosity (Stalkup-Jr. 1992). Short summaries of these processes are described in this section. Thomas (2008) shows a drawing (Fig. 5.37) of the mixing zone of a solvent contacting the oil phase and the miscible zone enlarging as time (t_1 and t_2) and the sweep proceeds. A narrow transition zone (mixing zone) develops between the displacing fluid and the reservoir oil, inducing a piston-like displacement. The mixing zone and the solvent profile spread as the flood advances. Because the fluids are miscible, in that zone, the N_c will approach ∞ and the displacement efficiency is very high if the mobility ratio is < 1 .

Section 5.5.2 describes (briefly) the use of CO_2 to displace the trapped crude oil using dissolution processes. Sections 5.5.3, 5.5.4, and 5.5.5 consider the applications of three different types of surfactant-based methods to emulsify the oil as well as to change the wetting characteristics of the oil/rock surfaces to aid the release of the oil. Various diversion methods (such as polymers and foams) also may be employed with many of these treatments, so there is overlap in many of the applied chemistries.

Solvents that are in use as miscible drive materials include low MW HCs (natural gas, propane, C_4 – C_6 liquids, and other petroleum gases), N_2 , and CO_2 . Under correct reservoir conditions of temperature and pressures, these materials form fluids that are miscible with the oil. Miscible displacement is used to increase the production value of formations containing light crude oils that will be soluble in the flood solvents. The mechanism is recovery of oil by mass transfer. For some processes, the mass transfer of intermediate HC components is from the crude to the solvent [vaporizing gas drive (VGD)] and for others the transfer is from the solvent to the crude (condensing or rich gas drives). CO_2 , nitrogen, or flue gas comprises the VGDs and HC miscible drives are the latter. In all cases, it is the intermediate component (the *s*-shaped area in Fig. 5.37), that is doing the transferring, that is the key to the process.

Verga (2009) says that for the miscible displacement processes to be effective, the displacement fluid is, or becomes, miscible with the oil under the reservoir's pressure and temperature conditions. This type of displacement is characterized by a progressive change in composition of both the displacement fluid and the displaced fluid, until the two fluids in contact form a single phase. In miscible processes, the displacement fluid is also referred to as the *solvent*; it dissolves in the oil, reducing its viscosity and increasing its volume, and ensures greater mobility toward the production wells.

The CO_2 miscible method has been gaining prominence in recent years, partly because of the possibility of CO_2 sequestration as well as the abundance and relatively low cost. Verga (2009) also notes that in addition to the environmental objectives, CO_2 is a unique displacing agent because it has relatively low minimum miscibility pressures (MMPs) with a wide range of crude oils. CO_2 extracts heavier fractions (C_5 – C_{30}) from the reservoir oil and develops miscibility after multiple contacts (MCs). The process is applicable to light and medium light oils ($>30^\circ$ API) in shallow reservoirs at low temperatures. CO_2 requirement is of the order of 500–1500 sm^3/sm^3 oil, depending on the reservoir and oil characteristics. Many injection schemes are in use for this method. These will be described in Section 5.5.2.

5.5.1 Types of Miscible Gas Drives (Except CO_2). A temperature/vapor pressure chart is seen as Fig. 5.38. This shows that CO_2 and other gases will be a supercritical fluid with liquid-like properties

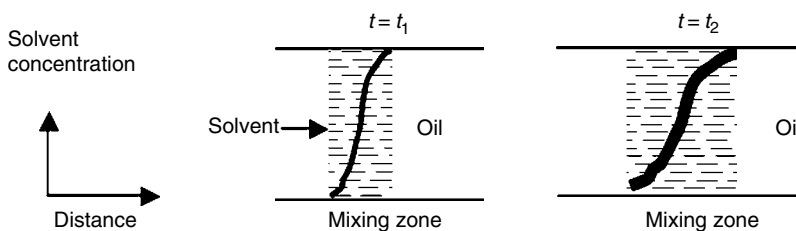


Fig. 5.37—Solvent mixing zone at different times in the sweep (Thomas 2008).

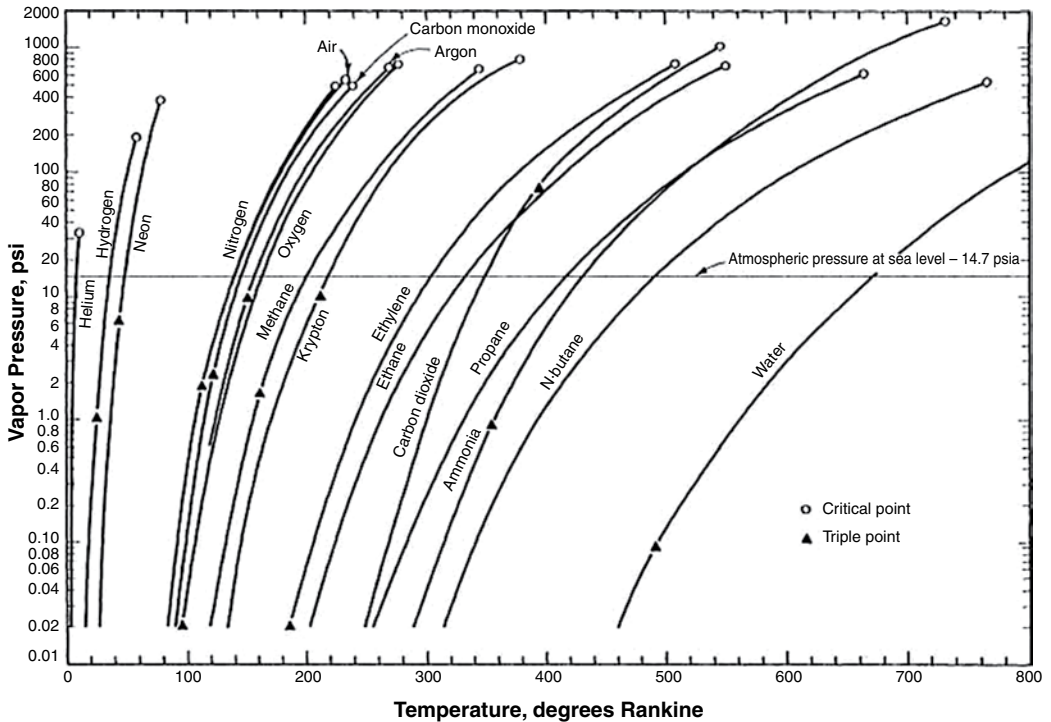


Fig. 5.38—Vapor pressure curves for various fluids.

at most reservoir conditions. Lake (2010) also notes that even though it takes more CO_2 to fill a specific reservoir volume than air or N_2 it has a much higher viscosity, and thus a lower mobility ratio so the sweep efficiency will be higher. CO_2 drives are described in Section 5.5.2.

Single Miscible Contact Slug. These processes are described by Thomas (2008). These include several different processes that involve the HC fluids. One process is termed a single miscible contact slug. This involves the higher HC liquids (C_3 – C_6) that are pushed as a single slug by natural gas, N_2 , or water. The major drawback (other than availability) is gravity segregation, and it is claimed by this author to work best in carbonate reef formations.

Enriched Gas Drive. These use miscible gases in the C_2 – C_4 (flue gas, with nitrogen or natural gas with some higher components) range and are injected at moderately high pressures (8–12 MPa). The gases condense and through MCs dissolve in the crude oil phase and provide the reduced viscosity needed to move the fluids.

VGDs. Thomas (2008) describes this also as a MC-type process and involves the continuous injection of natural gas, flue gas, or nitrogen under high pressure (10–15 MPa). When these conditions exist, the C_2 – C_6 fractions are vaporized from the oil into the injected gas. A transition zone develops and miscibility is achieved after MCs. A limiting condition is that the oil must have sufficiently high C_2 – C_6 fractions to develop miscibility. Also, the injection pressure must be lower than the reservoir saturation pressure to allow vaporization of the fractions. Applicability is limited to reservoirs that can withstand high pressures.

Sharma (1995) states that the availability of HC gases (solvents) on the Alaska North Slope make the HC miscible solvent injection process an important consideration for the EOR project in Schrader Bluff reservoir. Because HC solvents are costly, a miscible solvent slug injection process rather than continuous solvent injection is considered appropriate.

Ogbe and Zhu (2002) performed experimental and numerical studies of vapor extraction (VAPEX) process (VGD) in West Sak and Ugnu. VAPEX is a nonthermal recovery method that uses horizontal well to inject (low MWs) vapors close to their dewpoint into a heavy-oil reservoir. See Fig. 5.39.

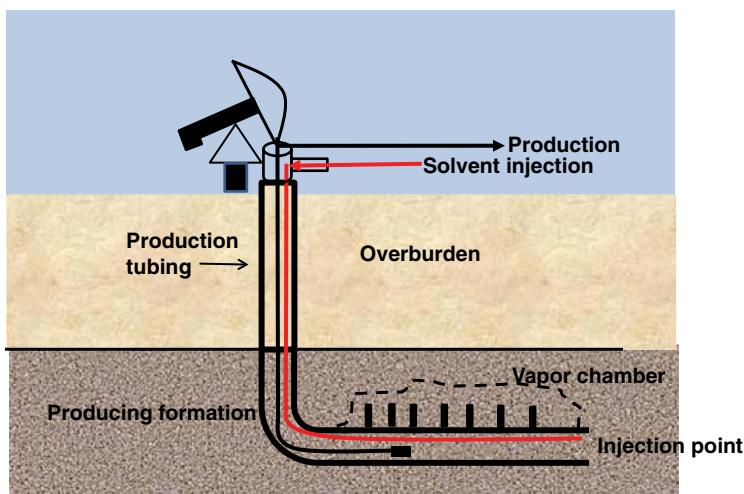


Fig. 5.39—VAPEX process horizontal well (Source: Alberta Research Council, <http://www.arc.ab.ca>) (Alberta 2011).

Numerical simulation study of VAPEX was initiated during the first year. The vapor dissolves the heavy oil and reduces its viscosity, allowing the diluted oil to drain by gravity to the production well.

Analysis of the experimental data obtained from VAPEX study indicated that all experiments resulted in significant recovery of oil. In a scaled sense, the study predicted that 15 to 20% of the original oil could be recovered in a time equivalent to 15 years at field scale.

At the time of the assembly of this book, the production of oil from shale beds had become an important source of liquid HCs in North America. According to Hoffman (2012), the Bakken shale in north central US and Canada may have >4 billion bbl of recoverable oil. Directional drilling and multiple hydraulic fractures are needed to produce any oil (see Section 4.11), but the primary recovery is only 10–15% OOIP. Hoffman (2012) has conducted a study of the possibilities of using immiscible miscible gas injection to improve OOIP recoveries. A 4-section area of the Elm Coulee field in eastern Montana was used to study the impact of different gas injection schemes: carbon dioxide, immiscible HC, and miscible HC. This paper examines the difference in total recovery, production rate, and efficiency using a flow simulation model (Shoib and Hoffman 2009). Recovery efficiency was similar for both miscible HC gases and carbon dioxide with recoveries increasing from 6% on primary production to around 20% with gas injection.

They claim that while the increased recovery is encouraging, both methods have some practical limitations. Carbon dioxide is currently unavailable in many basins, and while HC gases are available in most oil fields, they are rarely used as injectants because they are marketable. The authors of the report performed a cost-benefit analysis of selling the HC gas vs. using it to increase oil production.

5.5.2 CO₂ Miscible Floods. EOR methods using CO₂ injection are currently the most often used of the chemical addition method (NETL 2010; Lake and Walsh 2008) because the gas is generally less expensive than other chemical treatments and may be available from on-site production steams. In addition (Sweatman et al. 2009) note that use of CO₂ EOR can be used as a part of capture and sequestration of the gas. Lake (2010) notes that many solvents will become miscible with crude oil under the right conditions, but all of the solvents of commercial interest are *immiscible* to an aqueous phase. CO₂ can be an agent in a miscible flood.

Fig. 5.40 (NETL 2011) shows a diagram of this type of chemical flood. When CO₂ is injected into an oil reservoir, it becomes mutually soluble with the residual crude oil as light HCs from the oil dissolve in the CO₂ and CO₂ dissolves in the oil. This occurs most readily when the CO₂ density is high (when it is compressed) and when the oil contains a significant volume of light (i.e., lower carbon) HCs (typically a low-density crude oil). Fig. 5.40 shows the CO₂ being delivered by a tanker truck as

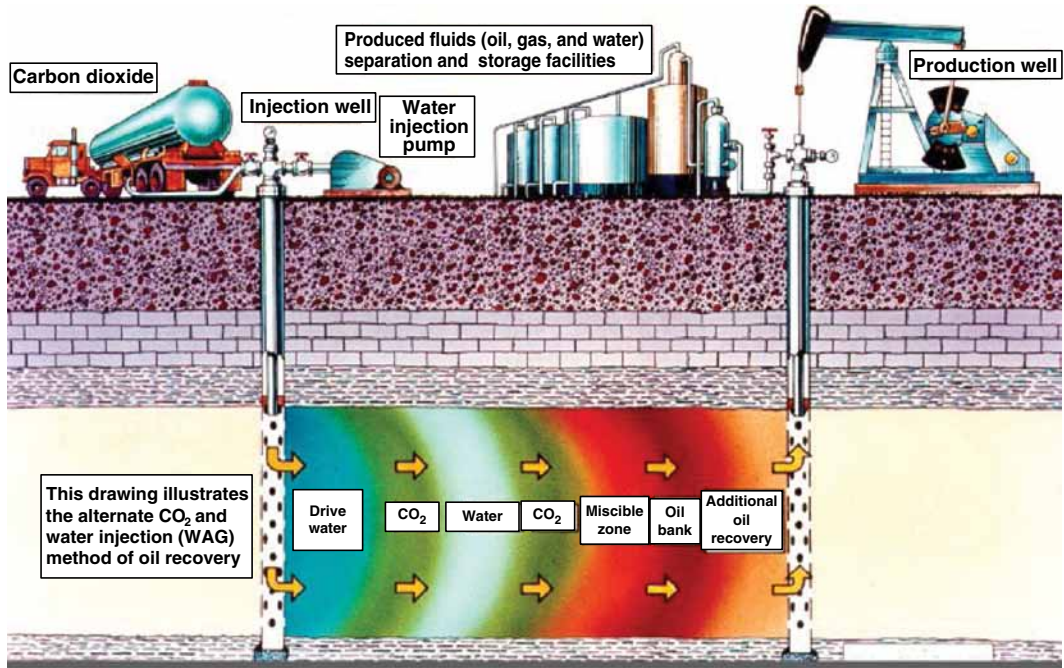


Fig. 5.40—Miscible CO₂ EOR showing the formation of a miscible zone (NETL 2010).

liquefied or compressed gas, but frequently the fluid comes from a nearby production well or industrial facility. The lack of readily available and inexpensive gas is a major controlling factor on the use of this method (Jarrell et al. 2002).

Below the MMP, CO₂ and oil will not form a solution. As the temperature increases (and the CO₂ density decreases), or as the oil density increases (as the light HC fraction decreases), the minimum pressure needed to attain miscibility changes. Then, the operators must consider the pressure of a depleted oil reservoir when evaluating its suitability for CO₂ EOR. Low pressured reservoirs may need to be repressurized by injecting water. When the injected CO₂ and residual oil are miscible, the physical forces holding the two phases apart (IST, see Section 1.6.1) effectively disappears. This enables the CO₂ to displace the oil from the rock.

Lake (2010) states that while this diagram seems simple, it does not reflect the complexity of a CO₂ flood because the solubility of CO₂ in a particular crude oil depends on the composition of the oil [see the discussions of solubility parameters in Section 4.2 of Frenier et al. (2010) and Section 1.5.2 of the current book] as well as the temperature and pressures. If the solvent is completely (first-contact) miscible with the oil, the process has a very high ultimate displacement efficiency because there can be no residual phases. If the solvent is *only* partially miscible with the crude, the total composition in the mixing zone (miscible zone infix) between the solvent and the oil can change to generate or develop miscibility in situ. The author (Lake 2010) concludes that regardless of whether the displacement is developed or first-contact miscible, the solvent must *immiscibly* displace any mobile water present with the resident fluids.

Note that a waterflood (described in Section 5.4.1), is an *immiscible* flood for the crude oil. The author (Lake 2010) notes that in the chase of fluid, N₂, water, and dry natural gas may seem to be the most common choices, but may not itself be a good solvent. However, it is selected to be compatible with the solvent and because it is available in large quantities. A temperature/vapor pressure chart is seen as Fig. 5.38 and a larger view of the CO₂ phase diagram is in Fig. 5.41.

At temperatures and pressures above the critical point, the fluid behaves like an organic solvent. Mungan (1981) claims that CO₂ may not be miscible at first contact, but it still will act as an EOR agent. The different effects include

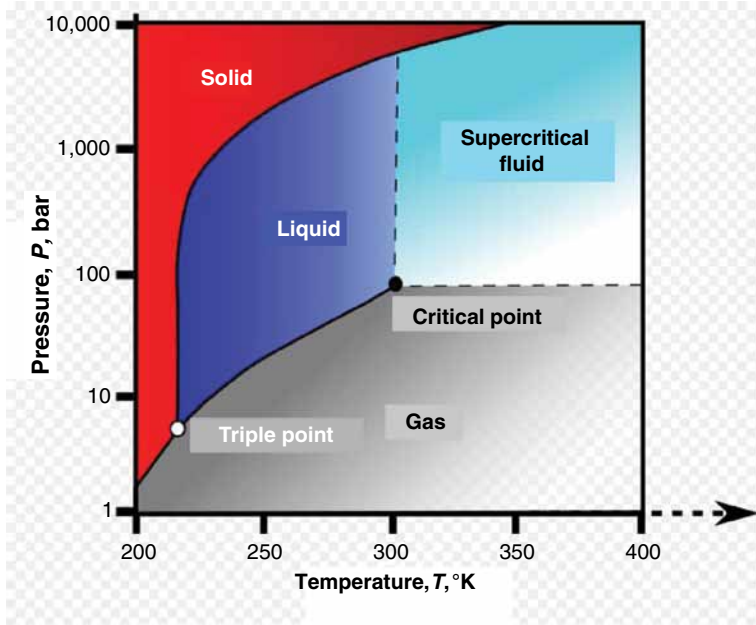


Fig. 5.41—CO₂ phase diagram (Wikipedia 2011a).

- Reduction of crude oil viscosity
- Swelling of crude oil
- Miscibility effects
- Increase of injectivity
- Internal solution gas drive

The miscible CO₂ mechanism is illustrated in Fig. 5.42 (NETL 2010), which shows the pore-level process of CO₂ entering the pores, mixing with the oil and flowing from the formation.

The major calculation needed for a CO₂ flood is the determination of the MMP that is defined as the lowest pressure where the CO₂ containing fluid will form some miscibility with the crude oil. The authors (Mungan 1981) suggests this test:

The measurement may be made in either a conventional PVT cell or using slimtube displacement tests. The latter offers distinct advantages. To start with, carbon dioxide is not

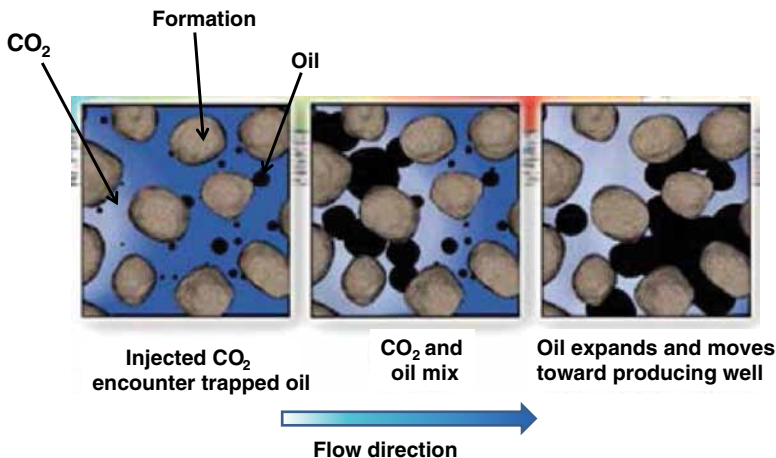


Fig. 5.42—CO₂ EOR mechanism (NETL 2010).

miscible with most reservoir crude oils on a first-contact basis. Miscibility develops upon multicontacts much in the same way that HC miscible displacement operates in reservoirs. A slim tube consists of a tube 0.5 to 1.0 cm in internal diameter and from 10 to 40 m in length. The tube is packed with sand or actual crushed formation material. It is coiled to fit easily into a constant temperature bath. A visual observation cell is mounted on the outflow end of the tube. The tube is saturated with crude oil having a composition and a saturation pressure representative of the reservoir crude oil. The entire displacement system is maintained at reservoir temperature. A fluid containing CO₂ and having the exact composition of the fluid, which is planned for use in the field is injected on a continuous basis into the slim tube. Miscibility is assumed to have been achieved if the following criteria are met in the displacement experiment: (a) A minimum of 85% recovery of the OIP at breakthrough of the injected fluid with 95–98% oil recovery at 1.2 PV of injection. (b) Absence of fluid interfaces in the visual cell. What should generally be observed is a gradual and continuous change in the color of the fluid.

Holm and Josendal (1974) investigated the use of CO₂ as a solvent for residual HCs. The extraction of C₅ to C₃₀ HCs by CO₂ at these pressures promotes a displacement efficiency approaching 100%. However, Holm and Josendal (1974) suggest that there are various mechanisms by which it can displace oil from porous media. The mechanisms include

- Solution gas drive
- Immiscible CO₂ drive
- HC-CO₂ miscible drive
- HC vaporization
- Direct miscible CO₂ drive
- Multiple-contact dynamic miscible drive

These are essentially the same processes as those proposed by Mungan (1981). They note that some of these processes also may reduce the IST. These authors performed displacement tests using long slim tubes packed with sand and in Berea and Boise consolidated sandstone systems of various lengths. Fluids were injected into the cores at constant rates, or at rates that were varied to maintain constant average pressure during flooding. Produced fluids were collected in graduated containers, and standard gas meters were used to measure produced gas. The compositions of produced fluids were measured by chromatographic techniques.

The conclusions from Holm and Josendal (1974) from the study of CO₂ flooding of crude oils:

- CO₂ can enhance the recovery of oil from porous rock by (a) solution gas drive, (b) swelling of oil and reduction of its viscosity, and (c) miscible effects through extraction of HCs from the oil in the porous rock.
- The extraction of HCs (C₅ to C₃₀) from the crude OIP by CO₂ promotes a displacement efficiency approaching 100%.
- Unlike liquefied petroleum gas, CO₂ does not achieve direct miscible displacement at practical reservoir pressures (for this crude oil). Also, unlike the high-pressure gas-miscible process, the displacement of oil by CO₂ does not depend upon the presence of light HCs (C₂–C₄) in the reservoir oil. The CO₂ process is applicable to reservoirs in which the oil has been depleted of its gas and liquefied petroleum gas components.
- A simple correlation [based on the Benham et al. (1960) method] was used to determine the optimum displacement pressure for CO₂ floods.
- The presence of methane in the reservoir oil does not appreciably change the optimum displacement pressure, but it does reduce the overall recovery efficiency of the displacement process.
- More favorable mobility relationships with resultant improved conformance may be achieved at flood pressures somewhat below the optimum displacement pressure. Longer transition zones and higher residual oil saturations are developed at these lower pressures.

Malik and Islam (2000) describe a billion-dollar CO₂ injection project has been launched to increase oil recovery in the Heyburn field of Canada. Initially, the project will use 5,000 tons of CO₂ daily in 19 patterns. The background economic calculations use the assumption that miscibility will be achieved and a steady supply of CO₂ at a cost of USD 35/ton will be available. This paper provides detailed results of a comprehensive reservoir simulation study using a fully compositional model to optimize the pattern and injection/production strategies.

Zhou et al. (2012) claim that the treatment of the SACROC unit (Kelly-Snyder field of west Texas, a Pennsylvanian carbonate) by CO₂ injection was the first large-scale CO₂-EOR project in the world (Crameik and Plassey 1972). They also claim that as of the date of the article, there are more than 100 CO₂ injection projects producing more than 250,000 bbl of oil per day in the US. They note that recent growth of CO₂-EOR projects has been in the area along the Gulf of Mexico coast because of CO₂ availability from Jackson Dome. However, availability of economic CO₂ has become a limiting factor in many areas.

A report by Lake and Walsh (2008) gives a very comprehensive bibliography of current EOR processes. This was developed under contract with the Danish Energy Agency and is particularly directed to North Sea operations. One example described by these authors was in the Colorado Rangley Weber Sand Unit. The net result was that the produced oil cut increased significantly but the oil rate did not. Fig. 5.43 shows the oil cut response, as reported by the operators. The oil cut increased from about 5.8% to a peak cut of almost 9%. This peak oil cut is claimed by Lake and Walsh (2008) to be typical for most successful miscible floods; however, the rate response is atypical.

The authors of this book note that a 70% loss of injectivity is seen frequently after CO₂ floods. This is caused by gas being trapped and thus acting like a foam-diverting agent. An unpublished report (Ken Waugh, Chaparral Energy, 2010, Oklahoma City, Oklahoma to Tulsa NACE meeting) found that using a slug of a microemulsion (ME) prior to a CO₂ flood increases water injectivity. The mechanism is not known, but it is possible that the ME is dissolving the CO₂. Various scaling processes exist when carbon dioxide is injected, including the production of calcite, thus injection wells are frequently stimulated/cleaned using reactive fluids (see Chapter 3), and all of the benefits and problems with this technique must be addressed and made part of the overall FA plan (see Fig. 2.2). The addition of a surfactant to the CO₂ to cause gas diversion to happen is an important development and will be described in Section 5.6.3.

Several different application methods and problems with CO₂ floods are in the following subsections.

WAG. These methods include the injection of cycles of CO₂ and water in WAG (Langston et al. 1988). This technique forms sequential banks of fluids in the reservoir rock: oil, CO₂, and water that

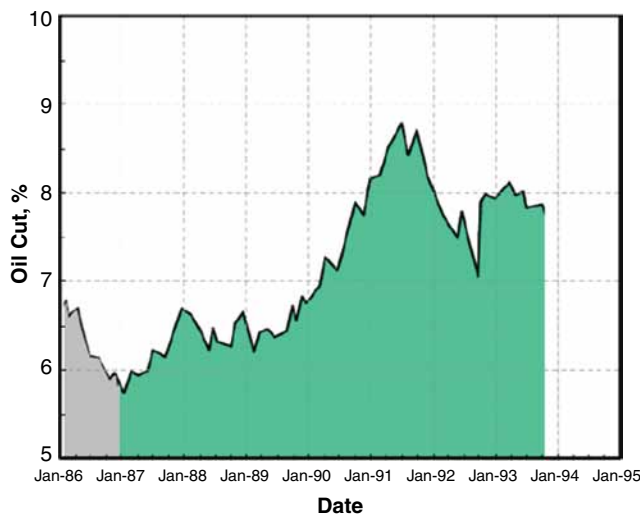


Fig. 5.43—Rangley Weber Sand Unit oil cut history. The gray-shaded region is the waterflood and the green-shaded region is the CO₂ flood (Lake and Walsh 2008).

migrate from the injection to the production wells. Enick et al. (2012) have reviewed the use of WAG and claim that 90% of tertiary CO₂ floods use some form of WAG for conformance control; they note that the water stages increase the water saturation and reduce the CO₂ saturation but do not change the viscosity of the solvent phase. They also claim that WAG is considered to be state of the art, but may leave 35–65% OOIP.

The water is being injected behind a slug of CO₂ that creates a miscible zone, which helps release oil that had previously been trapped when using only water. The frequency of alternating the working fluid in a WAG process can vary considerably from a few days to several months: it very much depends on the oil reservoir, injection and production volumes, well location, and residual oil. A useful rule of thumb (Langston et al. 1988) is based upon when the volume of breakthrough gas or water cut suddenly increases compared with the volume oil that is produced.

Foamed CO₂/Brine. Adding foaming agents such as ethoxylated and/or unethoxylated species, fluoroacrylate-styrene copolymers, lignosulfonates, etc., to CO₂ (or the water phase to form stable foams) will increase its viscosity without compromising its efficacy (Bernard et al. 1980). These authors contend that the viscous foams facilitate formation of oil and CO₂ banks, which migrate from injector to producer while suppressing adverse hydrodynamic instabilities, such as fingering, which lead to vertical fluid stratification and reduced oil recovery.

The use of foam as a diversion method in chemical matrix stimulations was described in Section 3.7.2, and the same principles apply to the use of foam in EOR because the foam is being generated and propagated in a porous medium and is not bulk foam. See Fig. 3.78 for a test foam generator. Note also that because surfactants are used to generate the foam, the use of foam also may provide some of the benefits of surfactant floods described in Section 5.6.3, including IST modification and partial increase in solubility in an aqueous phase. If CO₂ foam is generated, the assumption is that the CO₂ would be acting as a miscible displacement agent and will decrease the fluid/gas IST to cause foam to form. Some portion of the fluid must act as a trapped gas to allow the diversion to occur. Several examples of the use and development of foamed CO₂ EOR are abstracted.

Tsau and Heller (1992) note that in recent years, the application of CO₂ foam in mobility control has gained more interest among surfactant-based EOR processes. This is because the mobility-controlled CO₂ flood can mitigate the problems of frontal instability as well as the preferential flow of CO₂ in a heterogeneous reservoir, which otherwise induces the early breakthrough of CO₂. They claim that earlier laboratory results indicate that the changes of flow and displacement behavior of CO₂ foam can reduce the mobility of CO₂ alone and increase the displacement efficiency.

They tested the effectiveness of surfactants for CO₂-foam mobility control in dolomite limestone formations and evaluated the surfactants at concentrations below their (CMC). The candidate surfactants are commonly used formants, which are either nonionic or anionic types of surfactants. The evaluation procedures include the determination of formability of surfactants and foam durability of CO₂ foam, the measurements of adsorption parameters of surfactant onto reservoir core samples, and the measurements of CO₂-foam mobility in reservoir rock samples (see Sections 3.7.2 and 4.5.5 examples of the use of foams in other services). All of the experiments except the adsorption measurements were conducted at reservoir conditions. Adsorption of surfactant onto reservoir rocks was measured using a modified drop-weight method in a direct flow-through measurement at ambient conditions.

Tsau and Heller (1992) found that the CO₂-foam activities were affected by the presence of crude oil in the foam durability test. However, CO₂-foam mobilities were still reduced effectively inside the rock samples containing some residual oil. It was also found that an additional amount of surfactant over the surfactant concentration required for CO₂-foam propagation is needed to satisfy the permanent adsorption. At surfactant concentrations below the CMC, the effectiveness of mobility reduction of CO₂ foam as well as the amount of surfactant adsorption varies with the type of surfactant and its concentration in reservoir brine. The candidate surfactants include commonly used anionic and nonionic types of foaming agents. In the dolomite cores tested, a nonionic surfactant had the lowest amount of adsorption on the Ca/Mg carbonate mineral, yet it reduced the mobility (good diversion) at 500 ppm.

Chang and Grigg (1996) developed a CO₂-foam model based on the foam resistance factor that has been incorporated into two reservoir simulators. Moradi-Araghi et al. (1997) performed laboratory experiments in South Cowden Unit (west Texas) cores to select a suitable surfactant for possible

CO₂-foam application in the South Cowden Unit. The reservoir contains different dolomite formations with anhydrite. Thus, some dissolution by the CO₂ was expected. Four surfactants designated 1045, 1050, 25 and 128 were evaluated for their foaming ability in synthetic Cowden brine (78000 TDS). These surfactants were tested in co-injection as well as a surfactant-alternating gas (SAG) processes at various frontal velocities. The resulting foams exhibited selective permeability reduction (higher resistance factor in higher permeability zones) as well as shear-thinning behavior. The authors claim that the foams produced by co-injection of surfactant and CO₂ produced the better results than those made by the SAG process.

McLendon et al. (2012) claim that the addition of CO₂-soluble, brine-soluble surfactants to the high-pressure CO₂ may facilitate the in-situ generation of CO₂-in-brine foams for conformance and/or mobility control. The series of surfactants claimed included branched nonylphenol ethoxylates, containing an average of 12 or 15 EO repeat units (Fig. 5.44) and were selected for mobility and coiled-tubing studies detailed in this paper.

Transient mobility measurements were conducted using a water-wet Berea core (104 md), a water-wet Bentheimer sandstone core (approximately 1500 md, and several mixed wettability SACROC carbonate cores (3.6 and 8.9 md).

McLendon et al. (2012) state that regardless of what phase the surfactant was dissolved in, in-situ foam generation in the relatively high-permeability sandstone was evidenced by total pressure-drop values that were 2 to 3 times greater than the test with no surfactant. The mobility reduction was more modest (20–50% increases in pressure drop) in the lower-permeability SACROC cores (3.6 and 8.9 md) when the surfactant was dissolved in the CO₂. When the surfactant was dissolved in the brine, the pressure drops increased by a factor of 1.5–3 for the 8.9 md core.

Syahputra et al. (2000) note that a possible advantage of SAG over WAG for mobility improvement is that it can consist of higher gas saturation, 85 to 95% gas. In addition, Syahputra et al. (2000) showed that lignosulfonates were compatible with most of the tested surfactants in generating high-pressure CO₂ foam. Lignosulfonates are a weak foam former by themselves; however, they may become a good foaming agent when mixed with another surfactant. Using such a mixture system in coreflooding experiments resulted in a significant improvement in oil recovery with a smaller amount of more expensive foaming agents and foam volume. Diversion into the high-permeability section was proven and more oil was removed with the foam stabilized with lignosulfonates.

Additional tests were conducted by Yin et al. (2009) to address three carbon dioxide (CO₂) foam flooding parameters:

- Optimum gas fractional flow
- Surfactant adsorption behavior
- Oil recovery vs. CO₂/aqueous phase injection methodologies

They confirmed that the mobility decreased as the fractional gas flow increases. This is similar to the conclusions of Kam et al. (2007) and Rossen (2005). The CO₂-foam flow behavior in the absence and presence of oil and the optimum oil recovery methodologies associated with different stages are described in this paper.

This study (Yin et al. 2009) demonstrates that, with similar residual oil in the core, CO₂ foam had higher oil recovery than CO₂-brine co-injection. Additional oil was recovered with CO₂-foam injection

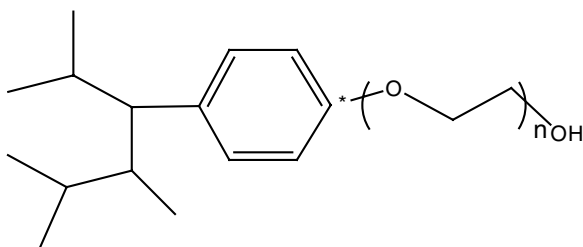


Fig. 5.44—Branched Nonylphenol ethoxylates, containing an average of 12 or 15 EO.

following CO₂-brine co-injection. However, no additional oil was recovered if CO₂-foam injection was applied first. The surfactant adsorption equilibrium was characterized by the occurrence of foam. More information on foams as diverting agents in other EOR treatments such as ASP is in Section 5.6.4.

Thickeners. Rousseau et al. (2012) claim that CO₂-dissolved polymers could be used as mobility control agents for CO₂ EOR. They also claim that unlike classical CO₂ mobility control techniques, using polymers would involve a single thermodynamically stable CO₂ phase and would not require water injection, which would eliminate difficulties linked to well acidification.

According to these investigators, developing an industrial CO₂-polymer EOR method implies three challenges:

1. Suitable polymers must be evaluated in terms of solubility in CO₂ under reservoir conditions and thickening ability.
2. Polymer-oil and polymer-rock interactions must be understood. Their consequences in terms of effective polymer transport far from the injection wells and potential mobility or permeability impairment must be physically modeled.
3. Reservoir scale simulations must be carried out to determine an economically optimal scenario (with parameters such as viscous slug size and polymer concentration).

Their work has investigated polymer-oil and polymer-rock interactions from coreflood experiments involving polymer-thickened CO₂. They claim that polydimethylsiloxane-based model systems whose solubility in CO₂ and viscosity enhancement ability have been previously evaluated in the literature.

Enick et al. (2012) also reviewed the use of polymers as well as small molecules (such as tributyl lithium fluoride) to increase the viscosity of CO₂. However, they note that because of the expense, no field applications have happened as the date of the current publication.

Scale, Corrosion, and Inhibitor Issues in CO₂ Floods. Despite the importance of CO₂ as an EOR fluid, operators must be concerned about and plan for possible problems that include corrosion of any steel structures in the well train, stimulation of scale (especially calcite) formation, and reactions with the geological minerals. If CO₂ is being sequestered, then the geological reactions may be useful, but it also could cause changes in a producing formation. The mobility and sweep efficiency also must be considered.

Because CO₂ is an acidic gas, it can cause sweet corrosion of carbon steel and if H₂S is also present, the partial pressures of the two gases will determine if carbonate scale, iron sulfide scale, or mixtures of these may form. See the discussions in Section 2.2.3. Therefore, injection of scale and/or corrosion inhibitors may be needed for protecting the injection and the production wells. Further discussions of corrosion and scale inhibitors (SIs) for production gases are in Frenier and Ziauddin (2008). The API (Meyer 2007) also has produced a technical examination of CO₂/EOR activities that includes information on steel corrosion as well as the suitability of casing cement.

Sweatman et al. (2009) note that the CO₂ dissolved in the brine may solubilize ions such as Mg²⁺ and Ca²⁺ or may precipitate salts of these minerals, depending on the pH and acid activities. These reactions may open up the formation or cause formation damage.

Mineral scale can be an FA problem in any producing well and some information was provided in Section 0 of this book and in Frenier and Ziauddin (2008) and Frenier et al. (2010). In addition, Morgenthaler et al. (1993) note that mineral scale deposition may become more severe as producing wells respond to CO₂ injection. Carbon dioxide reduces brine pH and enhances mineral dissolution at reservoir conditions, increasing brine scaling tendency in the wellbore. The lowered pH (as low as approximately 3.3) may dissolve calcite from carbonate formations. When the pressure is released, flash scaling of calcite may occur (see Frenier and Ziauddin 2008).

In wells where sulfate and alkaline earth ions become present because of mixing of different flow streams, gypsum (CaSO₄·H₂O) and barite (BaSO₄) can form. This mineral is especially troublesome because it is very difficult to dissolve (Frenier and Ziauddin 2008). Both the sulfates and carbonates can be inhibited using the technologies reviewed in Section 2.2.3. However, the very low pH values may limit the effectiveness of some of the SIs.

Reports from Graham et al. (2003), Laing et al. (2003), and Sorbie and Laing (2004) have found that the chemical structures (Fig. 2.20) of the inhibitors limit their use to certain pH ranges:

- Phosphonates to pH > about 5 (for threshold inhibition)
- Polyphosphonoarboxylic acid, to pH > about 4 (for threshold inhibition)
- P polyvinyl sulfonate < pH 4 for dispersant-inhibitor action

According to these authors, the mechanisms are based on the pKa of the acid groups in the SIs. Ramsey and Cenegy (1985) also have proposed a theory linking an SI's effectiveness at low pH to its dissociation constant. Chesnut et al. (1987) reached the same type of conclusion on the pH and the pKa values of the acid groups in the SIs and also described the testing needed for SIs in CO₂ fluids. Some SI tests are simple jar tests [see for review of SI tests Frenier and Ziauddin (2008)], but more predictive tube-blocking tests may require a pressurized system to retain CO₂. The pH can be simulated by adding an appropriate amount of HCl, but this does not necessarily simulate all of the effects of increased partial pressures of CO₂.

CO₂ Summary and Challenges. Ziauddin (2011) has summarized some of the benefits and challenges with CO₂ floods.

Economic challenges are

- CO₂ EOR project are capital intensive
 - CO₂ recycle plant
 - Corrosion resistant field infrastructure
 - CO₂ gathering and transportation lines
- Large operating costs
 - Purchase of CO₂ (approximately USD 2/Mcf)
 - Historically largest cost
 - Carbon capture and sequestration initiatives may change that
 - Recycle costs: approximately USD 0.7/Mcf to 15 Mcf of CO₂/bbl of oil
- These costs must be paid well in advance of the onset of incremental production
 - Payout time can be long with risk of fluctuations in oil price
 - 0.5 to 2 years for initial response and 6 years to peak oil recovery

The summary of cost from this author is based on estimates from the estimate from DOE-National Energy Technology Laboratory, March 2011 (NETL 2011). See Fig. 5.45.

- The *technical* challenges include (Ziauddin 2011)

Illustrative Costs and Economics of a CO₂ EOR Project

| | |
|--|---------------------|
| Oil price, USD/bbl | \$70 |
| Gravity/basis differentials, royalties and production taxes | (\$15) |
| Net wellhead revenues, USD/bbl | \$55 |
| Capital cost amortization | (\$5 to \$10) |
| CO₂ costs (at USD 2/Mcf for purchase; USD 0.7 Mcf for recycle) | (\$15) |
| Well/lease operations and maintenance | (\$10 to \$15) |
| Economic margin, pre-tax, %/bbl | \$15 to \$25 |

Estimate from DOE-National Energy Technology Laboratory, March 2010

Fig. 5.45—EOR costs (NETL 2011).

- Sweep
 - Density contrast
 - Viscosity contrast
 - Heterogeneity
- Methods for improving sweep
 - WAG, SWAG
- FA
 - Asphaltene precipitation (see Section 2.2.5)
 - Wax and hydrates
 - Scales (see Section 2.3.3)
 - Reactions of carbonic acid
 - Wellbore integrity

API (Meyer 2007) also notes that because the viscosity of CO_2 at reservoir conditions is much lower than that of most oils, viscous instability may limit the sweep efficiency of the displacement and, therefore, oil recovery. The API author and Enick et al. (2012) claim that *mobility control* by several means are recommended. These are WAG, foamed CO_2 with brine, and various thickeners (viscosity increases). Note that polymers and foam are also used with waterfloods to improve reservoir coverage (Sections 5.4.3 and 5.6.3). Waterfloods (Section 5.4.1) also have limitations because of viscosity differences. In addition, reservoir rock is extremely heterogeneous, exhibiting zones of high permeability in close proximity to those of low permeability. These permeability differences may be innate, which is caused by differences in pore structure at the time of geological deposition, or a product of fractures, natural or man-made. Reservoir heterogeneity and the adverse effects of CO_2 viscosity must be addressed to optimize oil recovery.

5.5.3 Surfactant Floods. Additional miscible chemical oil recovery methods include surfactant, S/P (this subsection) alkaline/caustic (Section 5.5.4), and ASP (Section 5.5.5) floods. These are the methods where a lot of the production chemistry is applied and is thus a major subject of this current book. They are designed to modify the capillary number (Eq. 5.1) or/and the mobility (Eq. 5.2) of the fluids to affect an increase in oil production.

Variations in the terminology used to describe these methods include micellar-polymer, ME, or low-tension waterflooding, flooding, and ASP flooding. Lake (2010) refers to *all* of these processes as MP processes because surfactant fluids that may involve micelles are present and polymers usually are also involved as part of the surfactant slug and as part of a water sweep. A description of a MP flood is in Fig. 5.46. Note that the chemical slug may include several chemicals and a mobility buffer with a polymer follows the chemical *slug*. In the drawing V_{pf} = the floodable PV of the volume treated.

Surfactants are effective in lowering the IST between oil, water, as well as a solid surface such as the rock surfaces of the formation. This can reduce the capillary pressure (and increase the N_v)

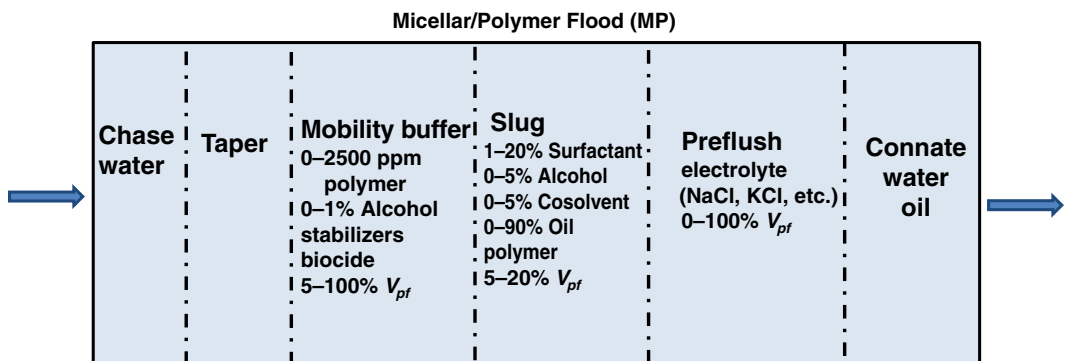


Fig. 5.46—Micellar/polymer flood sequence (Lake 2010).

and allow the aqueous phase to displace the oil. All of these methods involve mixing chemicals in water before injection. Therefore, these processes require conditions that are very favorable for water injection: low-to-moderate oil viscosities, and moderate-to-high permeabilities. Thus, chemical flooding is most applicable for oils that are more viscous than those oils recovered by gas injection methods but less viscous than oils that can be economically recovered by thermal methods.

Reservoir permeabilities for chemical flood conditions need to be higher than for the gas injection methods, but not as high as for thermal methods (Thomas 2008). Because lower mobility fluids are usually injected in chemical floods, adequate injectivity is required (see the discussion of injection wells in Section 5.1.1).

The surfactant-based methods employ ideas that are familiar to almost everyone. An oil is on a surface and is removed using a surface-active chemical that reduces the IST, allowing the water to displace it and also to emulsify it and prevent redeposition. In the case of crude oil in very small pores, the viscosity of the emulsified product is critical for removal. Delshad et al. (2007) have studied and modeled the use of surfactants in EOR processes. They note that surfactant solutions have two important effects on the rock/fluid system. The first effect is reduction of IST between the trapped oil and injected aqueous phase and therefore, solubilization and mobilization of trapped oil. The second effect is the alteration of the wettability of the matrix rock toward more water-wet conditions, which would increase the brine imbibition rates. These ideas were described in Section 5.1.2 and these sections (5.5.3–5.5.6) will describe all of these types of processes.

A source for pre-1980 technical information on surfactant floods is in the dissertation by Salager (1977). This investigator notes that a chemical flooding surfactant formulation must exhibit the following properties:

- Good displacement efficiency (i.e., it must produce a low tension against crude oil).
- Low adsorption on reservoir rocks and clays to reduce the surfactant losses.
- Good compatibility with reservoir fluids, especially tolerance to divalent cations such as Ca^{++} and Mg^{++} .

Those characteristics also must apply to chemicals developed since the report by Salager (1977). This dissertation also has many references as well as structures of chemicals available at that time.

Surfactant Evaluation Methods. Evaluation tools include laboratory models that simulate sandstone and various wet methods for testing surfactant flood processes are described in this section. Also, see Section 5.3 of this book for more general EOR evaluation tests.

Phase-behavior tests as well as CFTs have been described by Hirasaki et al. (2006) and Shiao et al. (2012) to evaluate surfactants and the specific crude oil to be removed. Along with the capillary number (Eq. 5.1), Hirasaki et al. (2006) have used the Bond number (B_o) (Eq. 5.8) as a determinant of effectiveness. When gravity parameters are large enough to give a Bond number (ratio of gravity to capillary forces) greater than 10, gravitational forces become more dominant, and oil held within a rock matrix by capillarity may be released because of buoyancy. In this work, they used experiments conducted in 2D micromodels to investigate the effect of gravity at low IST.

Micromodels of sandstone formations produced by Hirasaki et al. (2006) are claimed to have the geometrical and topological characteristics of sandstone and the network is etched into silicon. Using these micromodels, a screening study of sulfonate and sulfate surfactants was conducted to choose an appropriate system compatible with the light crude oil (27°API). A variety of flow behavior through the microscope is investigated including forced and spontaneous imbibition. Results are illustrated via pore-level photo and image analysis of microscopic pictures of the micromodel. Forced displacements are claimed to be conducted at realistic flow rates to maintain a 1 m/day Darcy velocity and at surfactant concentrations of 0.9% to 1.25%. Forced displacement with a horizontal or vertical positioning of the micromodel yields dramatic improvement of recovery for surfactant injection cases. Most of the oil retained after a waterflood was recovered by tertiary injection of surfactant solution. In comparison, about 25% oil saturation remained after a waterflood.

Levitt et al. (2009) report results of evaluations of a number of EOR surfactants, based upon a laboratory screening process that is claimed to be fast and highly effective in selecting the best surfactants to use with different crude oils. Initial selection of surfactants was based upon desirable surfactant structure (details in Section 5.5.5). Phase-behavior screening was then used to quickly identify favorable surfactant formulations. They claim that salinity scans are conducted to observe equilibration times, ME viscosity, oil and water-solubilization ratios, and IST. Cosurfactants and cosolvents are included to minimize gels, liquid crystals, and macroemulsions and to promote rapid equilibration to low-viscosity MEs.

These authors (Levitt et al. 2009) as well as Weerasooriya et al. (2011) describe details of the test that determine some of the physicochemical attributes needed for surfactant-based EOR fluids. Mixtures of oil and water containing various surfactants and cosolvents were allowed to equilibrate in calibrated thin tubes and examined visually in Fig. 5.47. The values read from the calibrations were used to determine the solubilization ratios (σ) of the volume of the oil in the ME phase (V_o) to the volume of the surfactant (V_s), as well as the ratio of the volume of the water in the ME phase (V_w) to V_s . Details are in Levitt et al. (2009).

These values are plotted vs. several variables that can be used to assess the efficiency of the surfactants. One of the most important is the salinity of the water [based on salt (Na_2CO_2 used in this example) concentrations]. The intersection of these two plots (Fig. 5.48) is the optimal solubilization ratio (σ^*) (Huh 1979) that is related this to the IST (γ) by

$$\gamma = \frac{C}{(\sigma^*)^2} \dots \dots \dots (5.26)$$

Levitt et al. (2009) claim that the Huh equation (in Eq. 5.26, C is a constant) can be used to calculate the IST for many different combinations more efficiently than by using a spinning drop method (Wikipedia 2010d). The experiments are conducted in calibrated pipettes and observed visually to estimate the different phases needed to calculate the IST. See Fig. 5.47. The oil solubilization ratio is defined as the volume of oil solubilized divided by the volume of surfactant in ME. All the surfactant is presumed to be in the emulsion phase.

$$\sigma_o = \frac{V_o}{V_s} \dots \dots \dots (5.27)$$

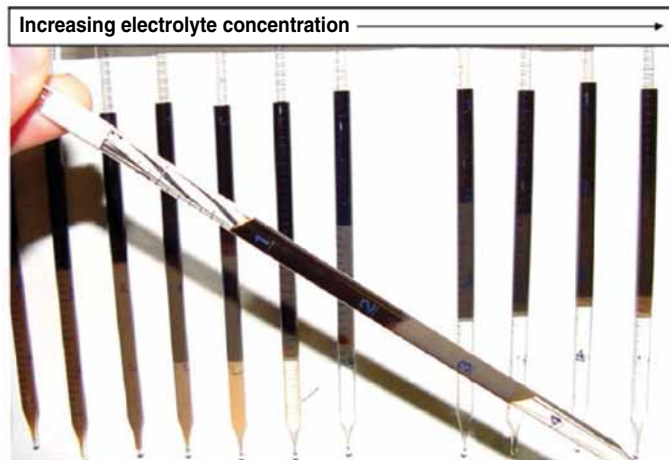


Fig. 5.47—Qualitative observation of phase behavior (amount solubilized), interface fluidity, and viscosity by tilting pipettes (Levitt et al. 2009).

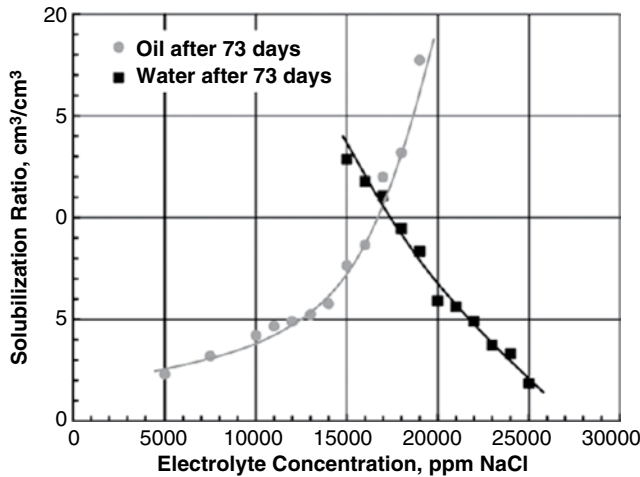


Fig. 5.48—Solubilization phase behavior for a surfactant system and WT crude oil at 38°C (Levitt et al. 2009).

In Eq. 5.27 σ_o = oil solubilization ratio, V_o = volume of oil solubilized, and V_s = the volume of the surfactant. The water-solubilization ratio is defined as the volume of water solubilized divided by the volume of surfactant in ME. All the surfactant is presumed to be in the emulsion phase.

$$\sigma_w = \frac{V_w}{V_s} \dots \dots \dots (5.28)$$

In Eq. 5.28, σ_w = water-solubilization ratio, and V_w = volume of water solubilized. In Eq. 5.26, σ^* is determined by the intersection of the two plots in Fig. 5.48. More details on this method is described in the patent application of Weerasooriya et al. (2011).

These types of ME tests also have been used by Mohammadi et al. (2009) to evaluate models for ASP floods as well as the development of new surfactants by Weerasooriya and Pope (2011b) and Pope et al. (2011).

Shiau et al. (2012) have developed surfactant testing for high-salinity reservoirs. Beside divalent ions, Ca^{2+} , and Mg^{2+} , presence of iron in the brine can be a challenging issue. Different surfactant formulations were evaluated and incorporate cosurfactants and cosolvents, which minimize viscous macroemulsions, promote rapid coalescence under Winsor Type III conditions (see Section 2.4.2 and Fig. 1.18), and stabilize the chemical solution by reducing precipitation and phase separation. The optimal surfactant formulations were further evaluated in 1D sandpacks and CFTs using Berea sandstone, reservoir oils, and brines at reservoir temperatures. Specific tests included (described in the publication):

- Phase behavior
- IST
- Column tests
- CFTs

Sasol (2012) has described a more detailed method to fit surfactant structures to the oil and salinity conditions of the reservoir. The method is based on the hydrophilic-lipophilic deviation (HLD) equation from Salager (1977):

$$HLD = \ln(S) - \kappa(EACN) - f(A) - \alpha_T \Delta T + C_c \dots \dots \dots (5.29)$$

In this equation, the best combination of components for a given oil produces an HLD value of 0, so that the various solubility forces are balanced to produce the lowest possible IST. At this balance point, the surfactant is equally soluble in oil and water, and it is also at this point that bicontinuous

MEs (Winsor Type III) (Winsor 1954; Huh 1979) form. In this equation, S = salinity, EACN = equivalent alkane carbon number (the oil characteristic), $f(A)$ = cosolvent contribution, C_c = characteristic curvature, which is the surfactant's hydrophobic contribution and ability to form micelles, and ΔT = temperature difference from 25°C.

EACN can be estimated for a simple HC by counting the carbon atoms. For more complex pure (or known) materials, it can be calculated

$$\text{EACN} = n_c - 2n_r - \frac{4}{3}n_{db} \dots \dots \dots (5.30)$$

In this equation (Cayias et al. 1976), n_c = number of carbon atoms, n_r = number of rings, and n_{db} are the number of double bonds. This equation is based on the ideas that both rings and double bonds make the oil less alkane and thus easier to emulsify. For crude oil, an estimate can be made based on the analyses described in Frenier et al. (2010), and an average of about 8 can be used for this equation (Eq. 5.30).

The values $f(A)$, the contribution of adding a low MW alcohol, has to be performed experimentally for each surfactant by plotting the IST vs. the salinity in the presence of the surfactants and an added alcohol. See Salager (1977). The fitting constants are the slopes of plots of the variables (i.e., S vs. concentration of alcohol to give a clear solution).

C_c can be determined for a surfactant by evaluating the shift in optimal electrolyte concentration as a function of the mole fraction of the test surfactant in a *mixture* with a reference surfactant, such as sodium dihexyl sulfosuccinate and applying the appropriate an HLD equation (such as Eq. 5.29) for ionic surfactant mixtures to determine C_c . See the discussion in Acosta et al. (2008) for more information on the thermodynamic significance of HLD and the C_c of individual surfactants.

Simple equipment (DuNoys ring and Wilhemly plate) for determining the IST have been described in Section 1.6.1. Additional equipment called the spinning drop tensiometer is in use for determining ultralow IST values. The measurements are carried out in a rotating horizontal tube, which contains a dense fluid. To do a measurement, a drop of a less dense liquid or a gas bubble is placed inside the fluid. Because the rotation of the horizontal tube creates a centrifugal force toward the tube walls, the liquid drop will start to deform into an elongated shape; this elongation stops when the IST and centrifugal forces are balanced. The surface tension between the two liquids (for bubbles: between the fluid and the gas) can then be derived from the shape of the drop at this equilibrium point. See Salager (2005).

The concept of the hydrophilic/hydrophobic balance (HLB) was described in Section 2.4.4 and the HLB of surfactants can be determined by the method of Davies (1957) using Eq. 2.16. For selecting EOR surfactants. Barnes et al. (2010) studied internal olefin sulfonates (IOSs) surfactants for use in chemical flooding. Surfactant structure was characterized by an in-house developed liquid chromatography mass spectrometry technique and properties focused on O/W ME phase behavior. Such relationships are important to match the surfactant formulation to particular reservoir conditions (temperature, salinity, and crude oil). The relationship between IOS structure (by liquid chromatography mass spectrometry) and optimal salinity (by phase tests) has been modeled by the empirical HLB number and by a semiempirical molecular model.

Synthetic Surfactant (SS) Processes (MP/SP). The uses of surfactants are important in various types and combinations of EOR operations. Natural-soap surfactants are the basis of the alkaline flood [Section 5.6.4 and SSs are also needed to produce diversion foams (Section 5.7.3)]. SS may be required in EOR processes when there are not enough soap-forming chemicals in the crude oil for the alkaline process to be effective, or if the alkaline solvents are not compatible with the reservoir.

The current section provides more details of synthetic S/P flood method as well as micellar processes that form MEs with a surfactant and cosurfactant and an oil phase. The nomenclature in the literature is not consistent. Lake (2010) refers to all of these processes as MP processes because surfactant fluids that involve micelles and polymers usually are also involved. This author has provided Fig. 5.46 to summarize the sequence of pumping slugs for an MP flood. However, he notes that these processes are also called detergent, surfactant, micellar, and just chemical methods. This section will

describe the various permutations of the use of Ss to improve oil recovery, with the exception of ASP that is described in more detail in Section 5.5.5 (although overlap with some ASP technologies are unavoidable because these terms are used interchangeably in some publications).

Arf et al. (1987) define a micellar solution as one that has slightly more surfactant than the CMC (see Fig. 1.11) and an MEs (Section 1.4.4) as one that also contains oil [an ME usually also has an alcohol (aka the cosolvent) that promotes formation of nanosized droplets]. The authors of this book have noted in other sections (Sections 1.4.4 and 2.2.3) that macroemulsions and sometimes MEs can cause big problems in some production operations. An emulsion block in the near-wellbore formation is a cause of formation damage and emulsions in the topside equipment can also lead to severe production problems. In EOR processes, the goal is to produce stable, low-viscosity (nongelling) MEs. This frequently requires the use of cosurfactants in addition to the high-shear conditions that cause nanosize droplets to form.

Investigators (Lake 2010; Levitt et al. 2009) have used the ideas of Winsor (1954) and Huh (1979) to describe the ideal surfactant-based fluids. They explain that MEs can be Winsor Type I (O/W), Type II (W/O), or Type III (bicontinuous oil in water in a middle-phase ME). They contend that the IST will be at the lowest value for a Type III ME. They also contend that this type of ME also will produce the lowest viscosity and that this will allow the most effective removal of the oil from the rock. They also contend that MEs based on anionic surfactants (such as sulfonates) will transition between these phases, depending on the salinity and other solution and oil-phase variables. A discussion of the Winsor system was presented in Section 1.4.4 as well as Section 5.4.1, and a diagram from Paul and Moulik (2001) is seen as Fig. 1.18.

Surfactant Chemistry. An aqueous surfactant slug (possibly containing a small amount of a polymer and a cosolvent) usually is followed with a polymer slug [for conformance (mobility) control], and the two chemical slugs are driven by brine or a gas. A very large number of different surfactants have been proposed. These may be used for an S/P flood or the ASP process described in Section 5.5.5. Fink (2003) devotes a whole chapter (Chapter 16 and Table 16-2) to EOR chemicals. A majority of surfactants listed are sulfates ($-R-OSO_3H$) or sulfonates ($R-SO_3H$) as well as some carboxylate and a few cationic surfactants. Because some anionic surfactants, especially sulfates will be sensitive to the calcium content of the brine, compatibility with the brine as well as the oil phases is the major testing criterion. The efficiency of the surfactant including the losses to the rock matrix also is critical parameters in determining the cost effectiveness of a treatment.

Note from Table 5.1 that the surfactant requirements can be high compared with polymer treatments. Examples of surfactant structures are seen in Figs. 1.8 and 2.57, and **Figs. 5.49 and 5.50** [that show an alkyl propoxide sulfonate (APS)]. Table 9.2 in the Lake (2010) book shows a long list of surfactants that are used or proposed and includes mostly alkylaryl sulfonates, laurel sulfonates, linear alkyl xylene sulfonates, and alpha olefin sulfonates (AOSs). The dissertation by Salager (1977) also has a long list of possible surfactants. Petroleum sulfonates are some of the most mature surfactant classes and frequently are the least expensive. There were a number of surfactant floods in the past, but [according to Welton and Domelen (2008)] they were largely ineffective, mainly because of excessive surfactant loss to the porous medium. Surfactant adsorption and reactions with the rock minerals (Somasingh and Hanna 1979).

To improve the efficiency of surfactant floods, Arf et al. (1987) describe the synthesis and testing of a large number of alkaline petroleum sulfonate surfactants that were produced from C_{19} , C_{22} , and C_{26} feedstocks and evaluated in core tests for their ability to enhance oil recovery. They claim that conventional petroleum sulfonates are produced from aromatic crude oil fractions of suitable boiling-point range. These have been the most frequently considered surfactants for EOR by chemical flooding. Because they are also in demand as lubricant additives and for other uses, their supply is not adequate for large-scale EOR projects. All three feedstocks for the new sulfonates were composed predominantly of saturated paraffinic and naphthenic HCs. The C_{19} feedstock includes about 12% aromatics. The HCs were vapor-phase oxidized at low temperatures to provide cyclic ethers, which subsequently were sulfonated to form a product mixture of mono-, di-, and trisulfonates. Corefloods were conducted with both sulfonates developed by the authors as well as commercial sulfonates in Berea sandstone cores.

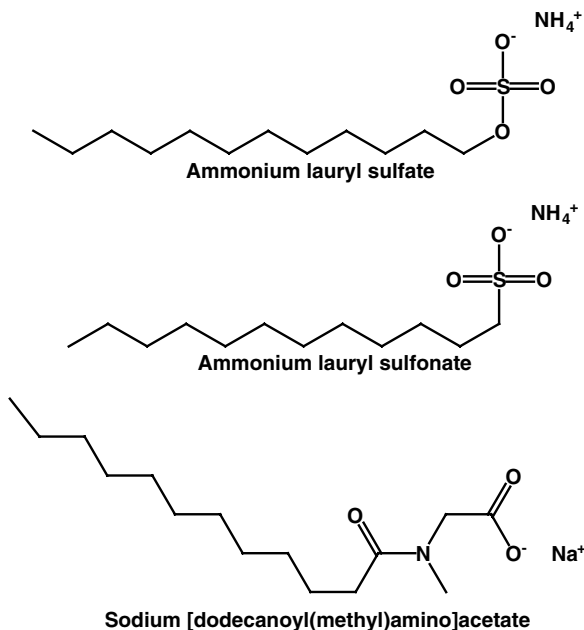


Fig. 5.49—Model types of EOR anionic surfactants.

Arf et al. (1987) claim that the production performances have been related to recovery and the interfacial activity of the sulfonates. The core tests show that the optimum use sulfonates synthesized by the authors for oil recovery is in the form of dilute slugs. High oil recovery efficiencies were realized when the sulfonates are used without cosurfactants to form dilute chemical slugs.

Specifically, the EORs obtained with C₂₂ sulfonates were significantly larger than those obtained with the C₁₉ and C₂₆ sulfonates. This is consistent with the O/W IST and phase behavior of the three types of sulfonates. Furthermore, EOR results and core-effluent analysis studies indicate that sodium carbonate (Na₂CO₃) in low concentrations is an effective sacrificial agent for some sulfonates, thus preventing adsorption and loss.

The authors (Arf et al. 1987) claim that the average equivalent weight of the surfactants, and the type and concentration of cosurfactants and electrolytes are varied to minimize IST or to maximize the amounts of oil and water solubilized in a middle-phase ME (Winsor III). In this study, a procedure based on these methods has been applied to nonaromatic sulfonates and conventional aromatic

Example of Branched PO Sulfate N67-7PO-SO₄

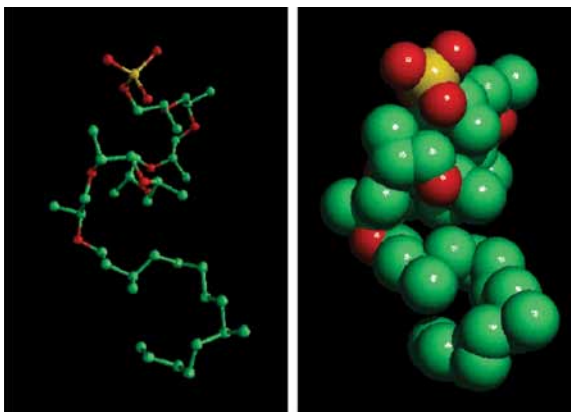


Fig. 5.50—Branched PO sulfonate (Lake 2007).

sulfonates. The connection between the molecular structures of the sulfonates, their interfacial activity, and their ability to displace oil in corefloods was explored. They claim that a very simple system of NaCl, Na₂CO₃, and a strongly water-soluble sulfonate had a high-solubilization capacity and very low IST characteristics. They also note that the sodium carbonate reduces the adsorption of the sulfonate on the rock (Berea sandstone) when applied in dilute slugs.

Gogarty and Tosch (1968) and Thomas et al. (1986) claim that ME-based EOR has been more successful (Welton and Domelen 2008) in the field than other chemical flooding processes. The main components of this method are an ME slug (also known as a micellar slug) and a polymer slug. These two slugs are driven using brine.

Hirasaki et al. (2011) have described a number of different alcohol-based cosolvents used to make the MEs. They claim that the alcohol will partition between the aqueous and oil phase and will make the phases less rigid and will increase the rate of equilibrium. Short chain (isopropyl alcohol) and longer chain alcohols (2-butanol, pentanol or hexanol) have been used as well. Careful testing must be done because the optimal salinity also may be affected.

Hirasaki et al. (2004) and Hirasaki et al. (2006) described tests with 24 surfactants that were compared for their efficacy for oil recovery by surfactant flooding. These were mostly synthetic sulfonates as well as olefin sulfonates with various amounts of EO. These tests were done because surfactant structure-performance relationships are needed for applications with a specified crude oil composition, brine salinity, reservoir temperature, formation mineralogy, and recovery mechanism. The surfactants were characterized by the optimal salinity for given oil, the level of IST at optimal conditions, and whether it forms viscous gel or liquid crystalline phases.

The authors claimed that an ASP flood was being developed (Section 5.5.5) for enhanced spontaneous imbibition in a fractured, oil-wet, carbonate formation. The importance of the carbonate ion of sodium carbonate (part of the brine phase) acts as a potential determining ion in carbonate formations such as calcite and dolomite. Alteration of the mineral surface to a negative charge aids in the wettability alteration and makes a dramatic reduction in the adsorption of anionic surfactants.

They argued that capillarity, governed by wettability and IST, is responsible for retaining oil in the oil-wet matrix when a fractured, carbonate formation is waterflooded. This is demonstrated by observations with a calcite plate, either in a horizontal configuration or in a narrow, vertical gap. Replacement of brine with alkaline-surfactant solution results in mobilization of oil by buoyancy or gravity drainage. Spontaneous imbibition did not occur when partially oil saturated dolomite core samples were placed in an imbibition cell filled with brine. Spontaneous imbibition occurred when the brine was replaced with alkaline-surfactant solution. Scaling of the rate of recovery indicated that dominant mechanism for recovery was gravity drainage.

The authors of this book note that the use of a high-pH material (sodium carbonate) described in this paper as well as the work of Arf et al. (1987) show the overlap with the ASP processes described in Section 5.6.4. In these papers, the alkalinity is mainly for surface charge control. Frequently small amounts of a polymer are present in the surfactant slug for viscosity enhancement. Further examples of different surfactants and applications are abstracted.

Mohanty (2003) claims that there are many carbonate reservoirs in the US (and the world) with light oil and fracture pressure below its MMP (or reservoir may be naturally fractured). Many carbonate reservoirs are naturally fractured. This author (Mohanty 2003) tested a number of surfactants including: 2 alkyl aryl sulfonates, a Gemini surfactant (oil chem technology surfactant 422) and an ethoxy sulfonate (Stepan Polystep B-27). The author acquired field oil and core samples and field brine compositions and has conducted preliminary adsorption and wettability studies. He found that addition of Na₂CO₃ decreases anionic surfactant adsorption on calcite surface, thus improving efficiencies; however, the different surfactants affected surface wetting and IST values differently, requiring more complex testing. Arf et al. (1987) also have recommended using Na₂CO₃ for decreasing adsorption of the surfactants on carbonates.

Steinbrenner et al. (2009) have claimed a method that uses of a surfactant mixture comprising an iso-C₁₆-oleosulfonate and in formulation, 16.7% by weight of the cosurfactants various cosurfactants such as a mixture of C₁₃-E07 and C₁₃-E09. The idea is to form an ME that will remove the oil, but then will break when the O/W mixture is produced. This mixture also is stable in the presence of CaCl₂.

| (a) CANDIDATE SURFACTANTS TESTED FOR EOR | |
|--|---|
| Descriptive Name | Abbreviated Chemical Formula* |
| C ₁₁₋₁₃ Alkyl Benzene Sulfonate (ABS) | $bC_{11-13}(C_6H_5)-SO_3^-$ |
| C ₁₆ o-Xylene Sulfonate | $C_{16}-(C_8H_{12})-SO_3^-$ where C_8H_{12} = o-Xylene |
| Secondary Alkane Sulfonate (SAS) | $R-CH(SO_3^-)-R'$ where $R + R' = C_{14}-C_{17}$ |
| C ₁₄ AOS | $bC_{11}-CH(OH)-CH_2-CH_2-SO_3^-$ (≈75%) $bC_{11}-CH=CH-CH_2-SO_3^-$ (≈25%) |
| C ₁₆₋₁₈ AOS | $bC_{13-15}-CH(OH)-CH_2-CH_2-SO_3^-$ (≈75%) $bC_{13-15}-CH=CH-CH_2-SO_3^-$ (≈25%) |
| C ₂₀₋₂₄ AOS | $bC_{17-21}-CH(OH)-CH_2-CH_2-SO_3^-$ (≈75%) $bC_{17-21}-CH=CH-CH_2-SO_3^-$ (≈25%) |
| C ₁₅₋₁₈ IOS | $R-CH(OH)-CH_2-CH(SO_3^-)-R'$ (≈75%) $R-CH=CH-CH(SO_3^-)-R'$ (≈25%), where $R+R = C_{12,15}$ |
| C ₁₆₋₁₇ Alcohol 3-Propoxy Sulfate (C ₁₆₋₁₇ -(PO) ₃ -SO ₄) | $bC_{16-17}-O-[CH_2(CH_3)CH-O]_3-SO_3^-$ |
| C ₁₆₋₁₇ Alcohol 5-Propoxy Sulfate (C ₁₆₋₁₇ -(PO) ₅ -SO ₄) | $bC_{16-17}-O-[CH_2(CH_3)CH-O]_5-SO_3^-$ |
| C ₁₆₋₁₈ Alcohol 5.7-Propoxy Sulfate (C ₁₆₋₁₈ -(PO) _{5.7} -SO ₄) | $C_{16-18}-O-[CH_2(CH_3)CH-O]_{5.7}-SO_3^-$ |
| C ₁₆₋₁₇ Alcohol 7-Propoxy Sulfate (C ₁₆₋₁₇ -(PO) ₇ -SO ₄) | $bC_{16-17}-O-[CH_2(CH_3)CH-O]_7-SO_3^-$ |

* b = Branching in the carbon chain.

| (b) SOME FORMULATIONS SCREENED WITH WT CRUDE OIL AT 38°C | | | |
|---|--------------------------------|------------------------------|---------------------------------|
| Surfactant Formulation | Optimum Salinity S* (ppm NaCl) | Optimum Sol. Ratio, σ(cc/cc) | Equilibration Time at S* (days) |
| 2% $bC_{12}-(PO)_3-SO_4$, 2% TDA-(PO) ₃ -SO ₄ , 1% dihexyl-sulfosuccinate | 75,000 | 3.5 | <2 |
| 4% C ₂₀₋₂₄ AOS, 8% SBA | 25,000 | 6 | 5 |
| 1.5% C ₁₆₋₁₇ -(PO) ₇ -SO ₄ , 0.5% C ₁₅₋₁₈ IOS | Viscous/slow equil. | – | – |
| 0.75% C ₁₆₋₁₇ -(PO) ₇ -SO ₄ , 0.25% C ₂₀₋₂₄ AOS, 2% SBA | 17,000 | 11 | 73 |
| 1.5% C ₁₆₋₁₇ -(PO) ₇ -SO ₄ , 0.5% C ₁₅₋₁₈ IOS, 1% SBA, 1% Na ₂ CO ₃ | 38,000 | 6 | <1 |
| 0.375% C ₁₆₋₁₇ -(PO) ₇ -SO ₄ , 0.125% C ₁₅₋₁₈ IOS, 0.5% SBA, | Viscous/slow equil. | – | – |
| 0.75% C ₁₆₋₁₇ -(PO) ₇ -SO ₄ , 0.25% C ₁₅₋₁₈ IOS, 2% SBA, 1% Na ₂ CO ₃ | 33,000 | 14 | <1 |
| 1.5% C ₁₆₋₁₇ -(PO) ₇ -SO ₄ , 0.5% C ₁₅₋₁₈ IOS, 1% Na ₂ CO ₃ | 35,000 | 12 | 2 |
| 0.75% C ₁₆₋₁₇ -(PO) ₇ -SO ₄ , 0.25% C ₁₅₋₁₈ IOS, 2% SBA, 1375 ppm CaCl ₂ | 45,000 | 12 | 14 |

Fig. 5.51—Surfactants tested for EOR (Levitt et al. 2009).

Levitt et al. (2009) report results of tests based on phase-behavior testing. Branched alkyl propoxy sulfates (Fig. 5.50), IOSs, and branched AOSs have been identified as good EOR surfactants using this screening process. This long list shows many (Fig. 5.51a) structures. The optimal salinity and solution ratios are also seen in Fig. 5.51b for a number of combinations as well as ratios with crude oils that provide optimal removal. These surfactants are claimed to be compatible with both polymers and alkali, such as sodium carbonate and, thus, are good candidates for both SP and ASP EOR processes. The best formulations were tested in both sandstone and dolomite cores and found to give excellent oil recovery and low surfactant retention with a west Texas crude oil. Fig. 5.51 shows the surfactants

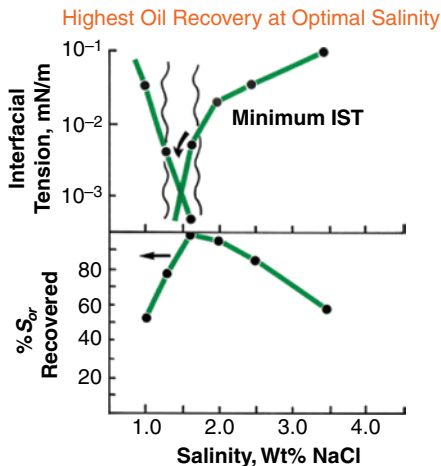


Fig. 5.52—Optimal microemulsion formulation (Lake 2007).

tested as well as the characteristics with the west Texas oil (which will be explained in the subsequent paragraphs). These tests illustrate an application of the methods described in Section 5.3.1.

Using these methods, the authors (Levitt et al. 2009; Mohammadi et al. 2009) tested APS mixtures, as well as cosurfactants and alcohols to optimize EOR fluids. CFTs of optimized systems were then tested in sandstone and dolomite cores. Several conclusions include

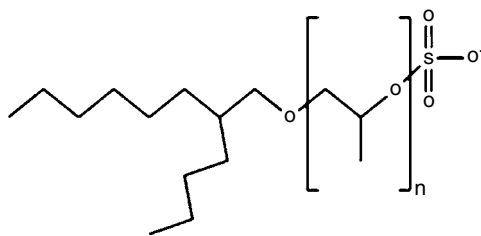
- Surfactant structures with branched hydrophobes seem to be most appropriate for EOR because they tend to form low-viscosity emulsions.
- Adding propylene oxide (PO) to the structure improves performance.
- Adding sodium carbonate speeded coalescence of the emulsions and reduced adsorption of the sulfonates on the carbonate surfaces and on the sandstones.

Certain alkalis as well as the overall salinity have a dramatic effect on the ionic environment, which affects both surfactant activity and optimal partitioning between phases and polymer hydrolysis, stability, and phases and polymer hydrolysis, stability, and viscosity. Also, alkalis can modify mineral surfaces leading to reduced adsorption of the more expensive chemical components. These observations correlate well with coreflood performance where the various chemicals are used either together or in successive slugs of various combinations. In general, at low concentrations, most of these chemicals are compatible with each other and appear to enhance overall performance when used together. Lake (2007) has summarized the optimization of the formulation in Fig. 5.52. The information in this figure also reflects the methods and techniques described in Section 5.4.3 for developing optimal oil recovery formulations in which the minimum in the IST vs. salinity plot of the fluid provide the preferred emulsification conditions.

Additional optimization methods also are in current use. Using the Salager (1977) HLD method (Eq. 5.29), Sasol (2012) describes the development of anionic (sulfate) surfactant mixtures based on a large number of long-chain alcohols and various amounts of EO or PO. Fig. 5.53 for the base structure. The authors claim that by using Eqs. 5.29 and 5.30, it is possible to design a very low IST (<10 dyn/cm) ME fluid without adding a coalcohol.

Weerasooriya and Pope (2011b), Weerasooriya and Pope (2011a), Pope et al. (2011), Weerasooriya et al. (2011), Kulawardana et al. (2012), and Adkins et al. (2012) have claimed the development of dialkyl and large hydrophobic surfactants for uses in EOR applications in which they are used for solubilization and mobilization of oil. Fig. 5.54 shows some of the structural types described by these authors.

The authors claim that these surfactants are less affected by the brine strength and the calcium content of the brine compared with other surfactants. One patent application (Weerasooriya and Pope 2011b) claims the improved surfactant system plus the addition of a chelant such as ethylenediaminetetraacetic acid to complex the alkaline earth metals that may precipitate the surfactant. These systems frequently are claimed to contain a high MW surfactant as well as a cosurfactant system consisting of a C_{20-24} IOS, and triethylene glycol mono butyl ether.



Vary the hydrophobe length and degree of branching as well as the PO and EO number

Fig. 5.53—Sasol surfactant (sulfates) (Sasol 2012).

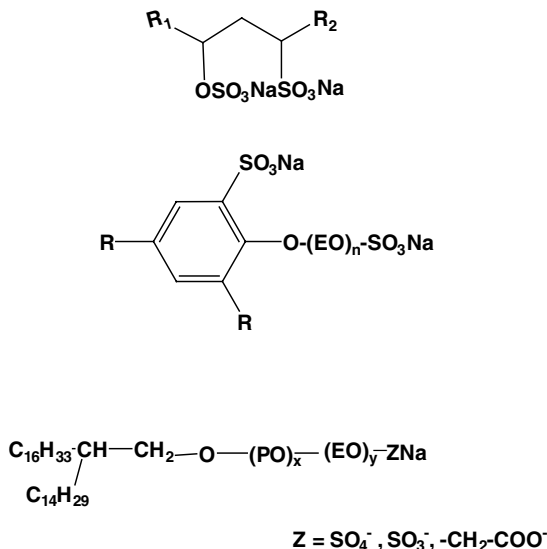


Fig. 5.54—Large hydrophobe surfactants (Weerasooriya and Pope 2011a).

In addition, Solairaj et al. (2012) claim that SS *retention* is one of the most important variables affecting the economics of chemical flooding and varies widely depending on the surfactant structure, mineralogy, salinity, pH, Eh, ME viscosity, crude oil, cosolvent, and mobility control among other variables. The authors have conducted a large number of dynamic surfactant retention measurements over a wide range of conditions using a variety of surfactants with and without a cosolvent to recover crude oils from both sandstone and carbonate cores. The list contains more than 25 formulations that give the chemical details.

They found that surfactant retention values for both SP and ASP floods were measured and correlated with pH, total acid number of the oil, temperature, cosolvent concentration, salinity of the polymer drive, mobility ratio, and MW of the surfactant. Surfactant retention values ranged from 0.01 to 0.37 mg/g of rock. SP and ASP formulations included mixtures of anionic and nonionic surfactants with and without cosolvents. The retention of anionic surfactants of all types was found to be similar on both sandstones and carbonate rocks.

Krumrine and Falcone Jr (1983) note that these were severe and in some cases of undesirable interactions between surfactants and oils or the matrix. Treatment and disposal of emulsions were also of concern. Surfactants, polymers, and alkaline chemicals are the major components of any chemical flooding process. Interactions of these chemicals can be a problem and are extremely important to the final outcome of field trials because the desired effect of each chemical may be enhanced or degraded as the various chemical slugs become mixed in the reservoir. In some instances, it may be desirable to inject these various chemicals together in the same.

A short summary of findings of the search for improved surfactants are that three important factors are increasing pH (that decreased retention of SSs), optimal surfactant structure for the oil, and the reactivity of the oil (which produces more soap natural surfactant). Balancing the salinity to achieve a Winsor Type III ME also will optimize oil removal.

Modeling and Field Applications of Surfactant Floods. Success of a surfactant flood include a large number of factors including [according to Hirasaki et al. (2004)] the capillarity of the formation with the current oil and water phases, that is governed by wettability and IST, and which is responsible for retaining oil in the oil-wet matrix. These forces are overcome by adding alkalinity and surface-active chemicals (surfactants and possibly cosolvents and polymers). They must for the correct types of MEs to allow the brine sweep pressure to push out a plug of oil. This complexity requires mathematical models that can assign values to grouped factors that cannot be measured and integrated individually so that the processes can be scaled up for field applications.

Delshad et al. (2007) used the data from Hirasaki et al. (2004) and a chemical flooding simulator that was adapted to model IOR processes involving wettability alteration using surfactants. Multiple relative permeability and capillary pressure curves corresponding to different wetting states are used to model the wettability alteration. The authors state the base correlations involve changes in relative permeability and capillary pressure. The relative permeability of the oil and aqueous phases were calculated using an exponential function described in their text. This includes the IST, which is calculated using a dimensionless number called the trapping number—a combination of N_c and B_o .

Simulations were then performed to better understand and predict EOR as a function of wettability alteration, and to investigate the impact of uncertainties in the fracture and matrix properties, reservoir heterogeneity, matrix diffusion, buoyancy-driven flow, IWS, and formation wettability. The proposed wettability-alteration model and its implementation were successfully validated against laboratory experiments. Up-scaled simulations indicated the importance of matrix properties on the rate of imbibition. The oil recovery increases with an increase in matrix permeability and a decrease in matrix IWS. The target was naturally fractured carbonates such as dolomite.

The Berryhill MP Project, located in the south central portion of the Glennpool Field, Oklahoma, is described by Crawford and Crawford (1985) to be an example of a successful field application of an S/P flood. A steamflood pilot project, located in the southwest quadrant of the Berryhill lease, was activated in 1976 and shut down in 1978 because of economics, before the viability of the project was established. In 1978, polymer and sulfonate injectivity tests were conducted in the northwest quadrant of the lease. Because of these tests, an 18-acre MP pilot was initiated in the same area. The pilot, started in 1977, consisted of nine producers and four injectors open in the Upper Glenn producers and four injectors open in the Upper Glenn sand. In 1981, two pilot observation wells showed excellent response to the process. The two wells, 130 and 220 ft away from an injection well, showed reduction in W/O ratios from over 100 to less than 2. This reduction confirmed that waterflood residual oil was being displaced and that a large oil bank had been formed.

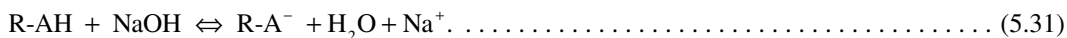
S/P floods also have been investigated and found by Manrique et al. (2007) to be effective. They claim that these have been the second most employed process for EOR treatment of carbonate fields in the US for light crude oil. They report that the surfactants were petroleum sulfonates as well as alkyl sulfonates and the polymers employed consisted of water-soluble HPAA's and a few biopolymers.

Lake and Walsh (2008) claim that micellar-polymer process virtually disappeared in the low-price environment of the 1980s but is experiencing revitalization, though as yet there are no current field projects. MP processes recover about 15% of the OOIP, but they are not economical at oil prices less than about USD 30/bbl.

5.5.4 Alkaline Flooding. This method as well as other surfactant processes (described in Sections 5.5.3 and 5.5.5) are used to reduce the capillary number and to help release the oil from the rock. These materials also may affect the viscosity and relative permeability and, thus may change the mobility ratio.

Alkaline flooding requires the injection of high-pH chemicals (frequently caustic soda-NaOH solutions, or KOH) into a reservoir, where it then reacts with petroleum-based acids to form surfactants. Other alkaline materials that have been used include soda ash (Na_2CO_3) and sodium orthosilicate (Na_4SiO_4). The natural surfactants in some crude oils (generic: R-AH) are described in Section 2.4.1 and include the naphthenic acids. See Fig. 2.42. The *amount* of natural acid surfactant present in the oil is described by the *acid number*, which is measured by titrating the 1 g of crude oil with KOH to pH 7. An acid number from 0.2 mg/g to about 0.5 mg/g are considered to be optimal (Lake 2010) to generate enough natural surfactant to reduce the surface tension and, thus, the contact angle and to affect oil removal.

NaOH (up to 5% w/w) can be added to the brine. As it contacts the acidic surfactants in the crude oil, the reaction to produce the natural surfactant is

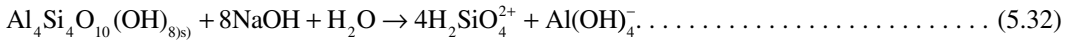


The natural surfactants are a very diverse group and while Eq. 5.31 shows a monoacid reaction, polyacids also may be present. As noted in Frenier et al. (2010) and in Section 2.4, these can act as the natural surfactant (frequently called the soap), but also can form solids (calcium naphthenates). See Eqs. 2.10, 2.11, and 2.12. Therefore, these materials may cause formation damage as well as stabilizing emulsions, which can result in fouling of surface equipment. Because the type and amount of the natural acids vary greatly, employing the testing methods (described in Sections 5.4 and 5.5.3) are critical.

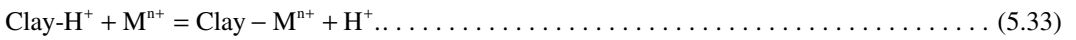
Note that this is essentially the same reaction used to make natural washing soaps in which the organic fatty acid is derived from either animal fat or a vegetable agent (such as palm oil) and the alkaline material may be NaOH or even wood ashes that contain KOH. These reactions have been used by various human populations for thousands of years (Willcox 2000).

When an adequate amount of natural surfactant is available and calcium naphthenates formation conditions [Section 4.4 of Frenier et al. (2010)] are not present, alkaline flooding can be an economical process and the oil can then be more easily moved through the reservoir to production wells. A demonstration of the effectiveness of an alkaline flood was claimed by Graue and Johnson Jr. (1974). See Fig. 5.55. These authors report that more than 55,000 ft³/month of oil was recovered. This graph also demonstrates the length of the treatment (approximately 1 year) as well as the time to recover the additional fluids. Water injection (including the caustic flood) was required for 10 years.

While a caustic flood may be an economical process, several reactions with the formation may cause damage as well as loss of the alkalinity. This then allows reaction (Eq. 5.31) to reverse. Major possible adverse reactions include dissolution of clays (a generic reaction with kaolinite is shown in Eq. 5.32) with extraction of silica and formation of aluminum hydroxide:



Cation exchange also takes place (Eq. 5.33).



Extensive investigations have been conducted to elucidate these important reactions. Bunge and Radke (1985) found that hydroxide consumption falls into three broad categories:

1. Reversible rock adsorption or ion exchange
2. Congruent and incongruent mineral dissolution
3. Precipitation of insoluble hydroxides

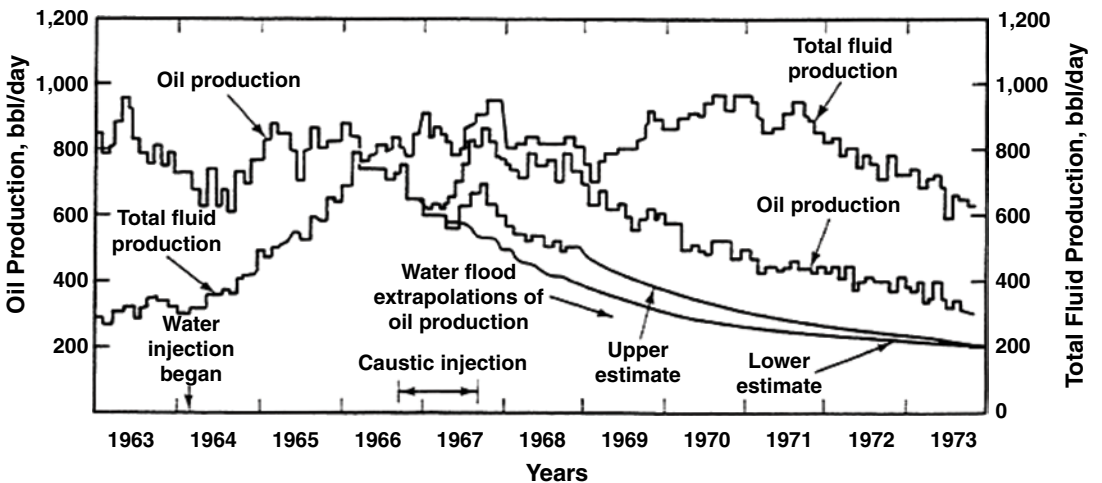


Fig. 5.55—Effect of a caustic flood (Graue and Johnson 1974).

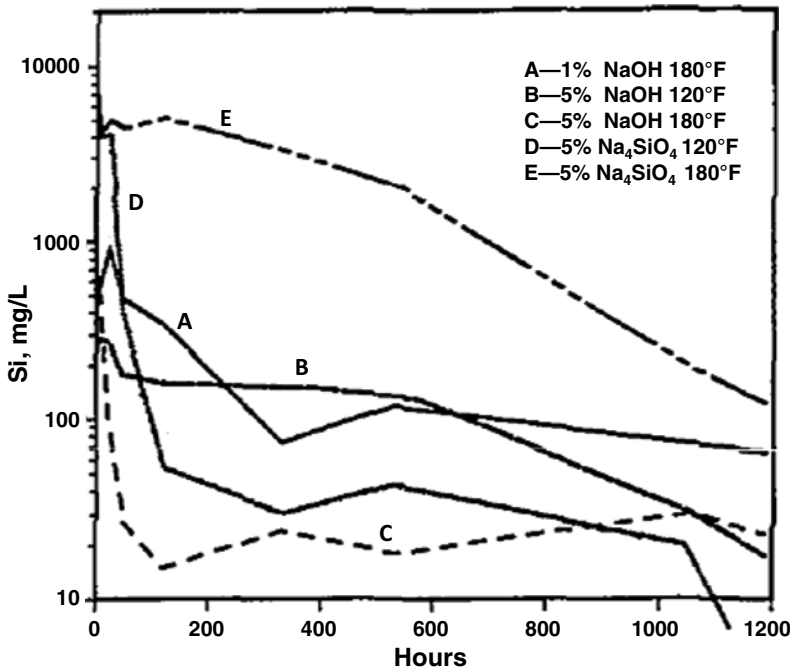
Mohnot et al. (1987) performed static dissolution tests with high concentrations of NaOH and orthosilicate solutions placed in the presence of several minerals (montmorillonite, kaolinite, illite, and quartz sand). The reaction time varied from 10 minutes to 2 months. Solutions were analyzed for hydroxide, Si, and Al, and solids were analyzed by X-ray diffraction and other spectroscopic techniques. The loss of useful alkalinity was the highest with kaolinite and the least with quartz sand for high-alkali concentration (5 wt%) or temperature [180°F (82°C)]. A detailed study of kaolinite/alkali reaction kinetics and quartz/alkali equilibrium showed that a small amount of immediate alkalinity loss by ion exchange was observed.

At high temperature, the irreversible alkali consumption by kaolinite was very fast for about 100 hours and slowed later. Neither hydroxide consumption nor production of dissolved Si or Al followed simple kinetic models of a single irreversible reaction. The kaolinite/alkali reaction (at 180°F [82°C] and/or 5% NaOH) proceeded incongruently, forming new minerals and consuming previously forming new minerals and consuming dissolved Si along with hydroxide ions. Therefore, after long-term reaction, the Si concentration dropped to a negligible value even if the initial alkali contained high-Si concentration. Under specific conditions of slow reaction, however, [e.g., 120°F (49°C) and 1% NaOH] the alkali consumption could be described by a single first-order reaction; see Figs. 5.56 and 5.57 that show kinetic curves for Si and Al for various alkaline solvents.

Specific conclusions from Mohnot et al. (1987) are

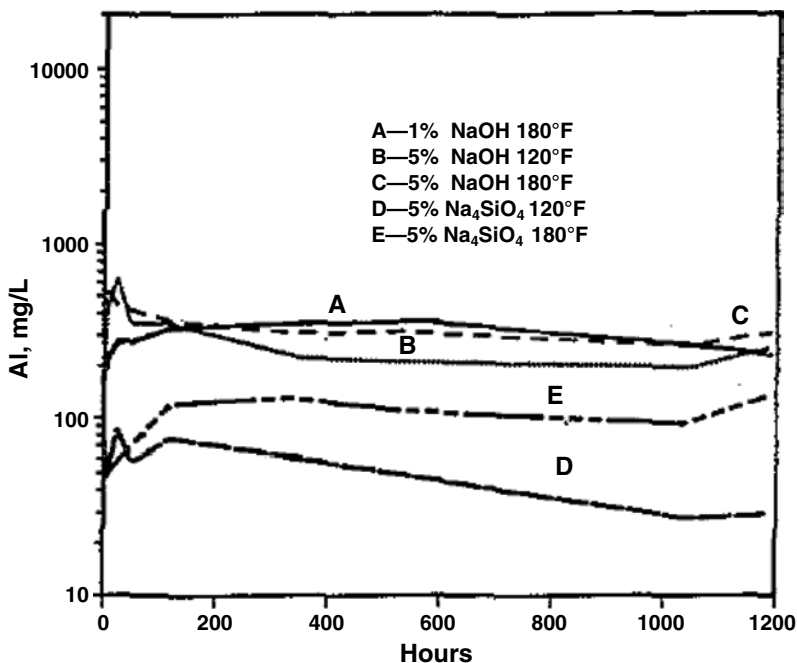
- Kaolinite is much more reactive and consumes more alkali than the other clays tested.
- The reactions are complex and include precipitation of various crystalline and amorphous solids, including possibly zeolites.
- Other alkalis such as sodium orthosilicate are not more effective, in that they also form various reaction products.
- There is less dissolution with orthosilicate (a weaker base).

A comparison can be made with the complex clay dissolution chemistries in HF-containing fluids described in Section 3.5.2. These reactions also readily extract Al and Si from the clays and then



Silicon Concentrations vs. Time for Dissolution of Kaolinite

Fig. 5.56—Si concentration dissolution of kaolinite by alkali (Mohnot et al. 1987).



Aluminum Concentrations vs. Time for Dissolution of Kaolinite

Fig. 5.57—Al concentration dissolution of kaolinite by alkali (Mohnot et al. 1987).

precipitate hydrated silica as well as various clay fragments and solids. An analysis of these types of reactions with the minerals in a proposed alkaline flood candidate will be a requirement.

The alkaline flood was used during the 1970–1990 time period but has been supplanted largely by MP and ASP methods described in the next two sections.

5.5.5 ASP Floods. If sufficient natural surfactants are in the crude oil, a modification of the MP (SP) process [according to Welton and Domelen (2008)] is the addition of alkali to the fluids, giving rise to an ASP EOR method that may be a less costly form of MP flooding. Note that an alkaline flood is essentially a surfactant flood using in-situ generated surfactants as well as SSs; see Section 5.5.3. Also, when the oil does *not* have the necessary chemicals in the mix (or the use of the concentrated caustic is not desirable), SSs can also be used.

ASP may use lower amounts of each component than the *individual* EOR systems. Stoll et al. (2010) claim that the concentrations are typically 1% alkaline material, 0.3% SS, and 0.1% polymer. *Conventional alkaline* processes may use up to 5% alkali, and surfactant floods use > 1% surfactant. The practical difference between this method and the MP/SP methods described in Section 5.5.3 is that there must be enough natural surfactants present and thus enough alkali to generate them, to offset the lower amounts of SSs used. So, while the processes are essentially the same (chemically), there is the additional unknown of the IST alterations and the production of the correct ME from an essentially unknowable natural surfactant. See discussions of the naphthenic acids in Section 2.4.2 and the references in that section.

The ASP processes are a combination of the chemistries described in Sections 5.5.3 and 5.5.4, so all of the advantages and potential problems must be considered. Some additional mechanistic information and use examples are presented in the current section.

Srivastava et al. (2009) describe some typical SSs as including a (C₁₆₋₁₇) alcohol propoxy sulfate and C₁₅₋₁₈-olefin sulfonate with a twin-tailed hydrophobe, which can be used with ASP formulations. With these SSs, it is claimed that lower amount of alkali will reduce formation damage and the process may be further tuned for the particular crude oil and matrix properties.

These authors also note that while the previously known chemical flooding processes had suffered from inherent disadvantages (significant adsorptive surfactant loss in a plain surfactant flood; long duration of a dilute alkaline flood), the ASP process promises to mitigate these through the combined chemical phase behavior of the injected surfactant and the in-situ generated natural surfactant known as petroleum soaps. Augmented by an internal polymer, and suitably adjusted to the oil viscosity, the ASP process may reduce oil saturation to zero in laboratory corefloods. Srivastava et al. (2009) claim that the range of applicability of ASP is largely determined by stability criteria for the involved chemicals and by economic constraints include

- A reservoir temperature below 90°C to prevent polymer degradation
- A formation water salinity below 20 wt% to limit the necessary polymer concentration
- A sufficiently high permeability greater than a few tens of millidarcies to allow the polymer molecules propagating
- An oil viscosity not exceeding a few hundreds of centipoises to warrant sufficient injectivity of the ASP slug

Thomas and Ali (2001) describe and compare the results for two methods, micellar flooding (MP/SP) and ASP flooding processes. Both of these methods have been tested successfully in the field, notably micellar flooding. Laboratory results are described for micellar floods in consolidated sandstone cores as well as in unconsolidated sandpacks, including a 3D model, equipped with horizontal or vertical wells. Floods were also carried out in unconsolidated cores using combinations of an ASP. Individual slugs were injected sequentially in some of the experiments, while the three components were mixed and injected as a single slug in other experiments. Oil recoveries in the two cases were similar.

These authors claim that while the results for the two processes are compared and contrasted, showing that on the basis of oil volume recovered per unit mass of the chemical used, the two processes are similar. However, based on total oil recovery, micellar flooding was the superior process, with oil recoveries ranging from 50 to 80% of the oil left in the porous medium after a waterflood. The other references shown below claim that ASP is preferred in some cases, requiring careful calculation and optimization of each project to be viable economically.

Nieuwerf (2009) has provided a visual illustration (see [Fig. 5.58](#) with a video at the reference) of an ASP flood showing the macro push (a) with the emulsified oil being pushed by the water/polymer flush as well as the ME of the oil in the pore (b) and the push from the pore (c).

Lau (2005) reports on a successfully implemented ASP flood technology in Canada to extend the production life of the Taber South Mannville B Pool, in the Warner field. He claims that the successful implementation of the ASP technique means that a significant number of reservoirs in Alberta may benefit from the knowledge gained from this technology.

Li et al. (2008c) note that the development of ASP technology in the Daqing (China) field was in three stages.

- First stage is laboratory experiments stage. This oil has a low acid number and high wax content. However, in 1988, formulations were screened that achieved an ultralow IST with Daqing oil. Physical simulation experiments indicated that the final oil recovery achieved to 20% OOIP over that of waterflooding.
- Second stage is pilot field tests stage. Daqing oil fields had completed 5 ASP flooding pilot field tests since 1994. All have gotten high displacement efficiency according to the laboratory results.
- Third stage was industrial pilot tests stage. Daqing implemented the development and production of alkyl benzene sulfonate (adapt to strong base and weak base). Since year 2000, several industrial ASP flooding tests have been carried out successively, which have shown a satisfied effect of higher oil production and lower water cut. The field test scale is from 1 injector-4 producers to 6 injectors-12 producers. It is claimed that large-scale industrial field application is ongoing in Daqing oil fields.

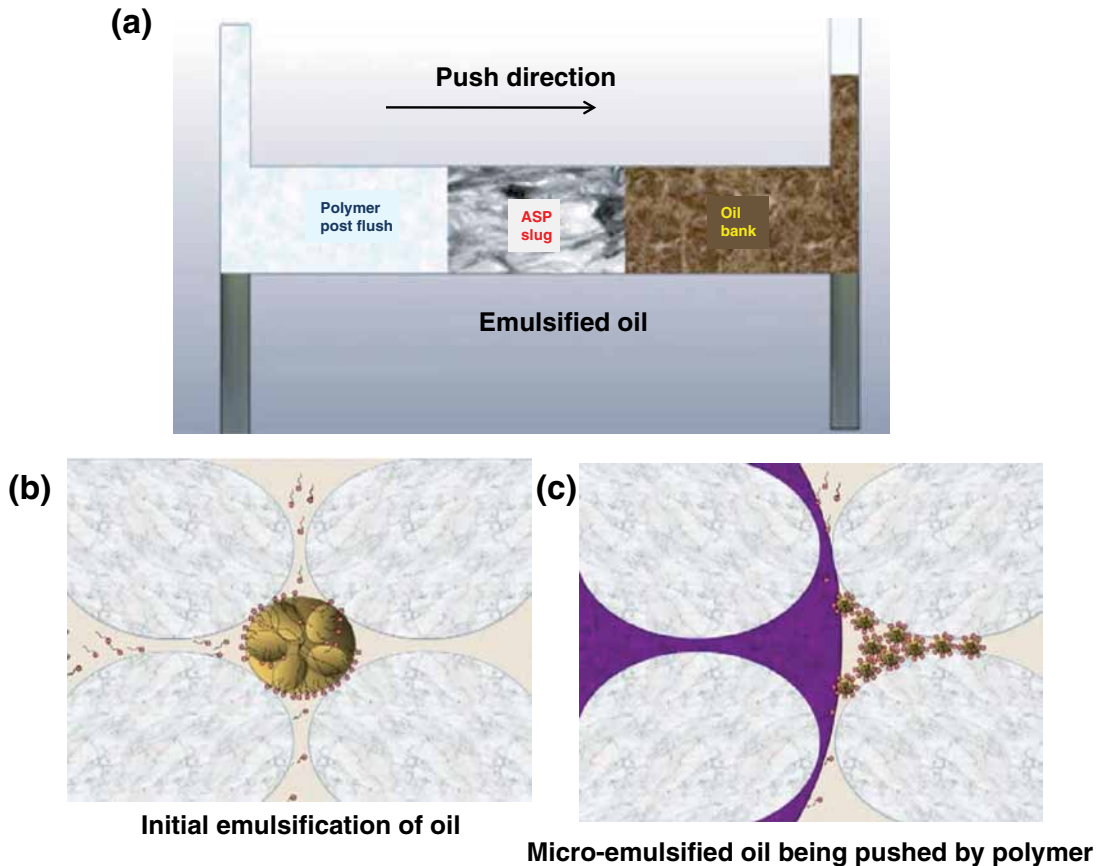


Fig. 5.58—ASP flood illustration showing (a) macro push, (b) emulsification, and (c) microview of polymer push (Nieuwerf 2009).

Srivastava et al. (2009) report that while ASP flooding is an attractive EOR method, some reservoir conditions are not favorable for the use of polymers or their use would not be economically attractive because of low permeability or other unfavorable conditions. Then, foam (Section 5.6.3) can be an alternative to polymer for improving the displacement efficiency in chemical EOR process. The use of foam as a mobility control agent by co-injection or alternate injection of gas and chemical slug is termed, here, as alkaline-surfactant gas.

In this process, foam reduces the relative permeability of the injected chemical slug that forms ME at ultralow oil-water IST and generates sufficient viscous pressure gradient to drive the foamed chemical slug. The use of foam in chemical EOR can reduce the technical disadvantages associated with polymer in low-permeability and fractured reservoirs.

Improvements to ASP are also described by Karazincir et al. (2011) who report on work to identify complexing agents and commercial SIs that can prevent scale formation in field brine during an ASP flood. Scaling (especially CaCO_3) is likely if there is dissolved calcium in the water and the pH is raised. See Frenier and Ziauddin (2008), Chapter 3.

Karazincir et al. (2011) report that the original field brine in this test has about 1,000 ppm $\text{Ca}^{++}/\text{Mg}^{++}$ and 450 ppm HCO_3^- at pH 6 (scale index = 0 at reservoir conditions). During ASP flooding, when the pH is increased to above 9, CaCO_3 and MgCO_3 scale occurs (scale index = 2.36). To prevent scaling during an ASP flood, divalent cations can be captured by addition of agents that form water-soluble complexes with metal ions in brine. With this purpose, six organic and two inorganic complexing agents as well as six different commercially available complexing agent brands have been tested. Addition of 200 to 500 ppm of phosphonate or polyvinyl sulfonate-based SI helps drop the complexing agent concentration needed to prevent scale formation down to 5,500 ppm at pH values of 10.3 or

less. Sodium ethylenediaminetetraacetic acid was selected as the complexer and a polyvinyl sulfonate was the most effective SI in this operation. See Frenier and Ziauddin (2008), Chapters 4 and 5.

Liu et al. (2010) claim that the design of ASP process requires knowledge of the amount of soap formed under alkaline conditions from naphthenic acids in the crude oil. They also claim that for several crude oils that when substantial acid is present, the acid number determined by nonaqueous-phase titration is approximately twice that found by hyamine titration of a highly alkaline aqueous phase used to extract soaps from the crude oil. This acid number by soap extraction should provide a better estimate than nonaqueous-phase titration because the extracted soap interacts with the injected surfactant to form surfactant films and ME droplets during an ASP process.

Here, an ASP simulator has been used by Liu et al. (2010) for various acid contents, injected-surfactant concentrations, slug sizes, and salinities to show that high recoveries of waterflood residual oil (> 90%) can be expected for a wide range of near-optimal (Winsor III) and under-optimum (Winsor I) conditions for a constant-salinity process, even with relatively small slug sizes.

The authors claim that a key factor leading to this good performance is development of a gradient in soap/surfactant ratio, which ensures that a displacement front with ultralow IST forms and propagates through the formation. Conclusions from this study are

- A soap/surfactant gradient is generated that helps in the profile passing through the optimal conditions of IST and makes the process more robust because the surfactant ahead into the soap-dominated region ahead of the surfactant bank.
- There is a wide optimal region for constant-salinity ASP.
- The best process and recovery occurs when there is a large ASP slug. Small slugs may cause a failure.

Modeling ASP. Because this process is even more complex than MP (aka SP) described in Section 5.5.3, computational modeling is even more important. Mohammadi et al. (2009) point out that if the consumption of the injected alkaline materials is not too large and the alkali can be propagated at the same rate as the SS and polymer, the process can be productive. However, the process is complex, so the authors contend that it is important that new candidates for ASP be selected taking into account the numerous chemical reactions that occur in the reservoir. The reaction of acid and alkali to generate soap (Section 5.6.3) and its subsequent effect on phase behavior is the most crucial for crude oils containing naphthenic acids. Mechanistic simulation of the ASP flood considering the chemical reactions, alkali consumption, and soap generation and the effect on the phase behavior is the key to success of future field operations.

The key features of the ASP model that must be considered (Mohammadi et al. 2009) are listed below with the references to details described in this book or other references:

1. In-situ generation of soap by reaction with the acid in crude oil—Sections 2.2.4 and 5.5.4.
2. Phase behavior as a function of soap and surfactant concentrations—Section 5.5.3, as well as in this section.
3. IST reduction as a function of soap (natural surfactant) and SS concentrations—Sections 5.3.3 and 5.5.5.
4. Reduction of surfactants' adsorption with increasing pH—Section 5.5.3.
5. Ion exchange reactions with clays in the rock—Sections 1.5.6 and 3.5.2.
6. Aqueous chemical reactions—Section 1.5.7 and Frenier and Ziauddin (2008).
7. Dissolution/precipitation reactions—Section 2.2.2 and Frenier and Ziauddin (2008).

The authors then showed that when using numerical models (UTCHEM-Delshad et al. 1998; Saad 1989), the process can be designed and optimized to ensure the proper propagation of alkali and effective soap and surfactant concentrations to promote low IST and a favorable salinity gradient. An important assumption of this model is that of local thermodynamic equilibrium, wherein it is assumed that the fluid and solid surfaces are in equilibrium wherever and whenever they are in contact.

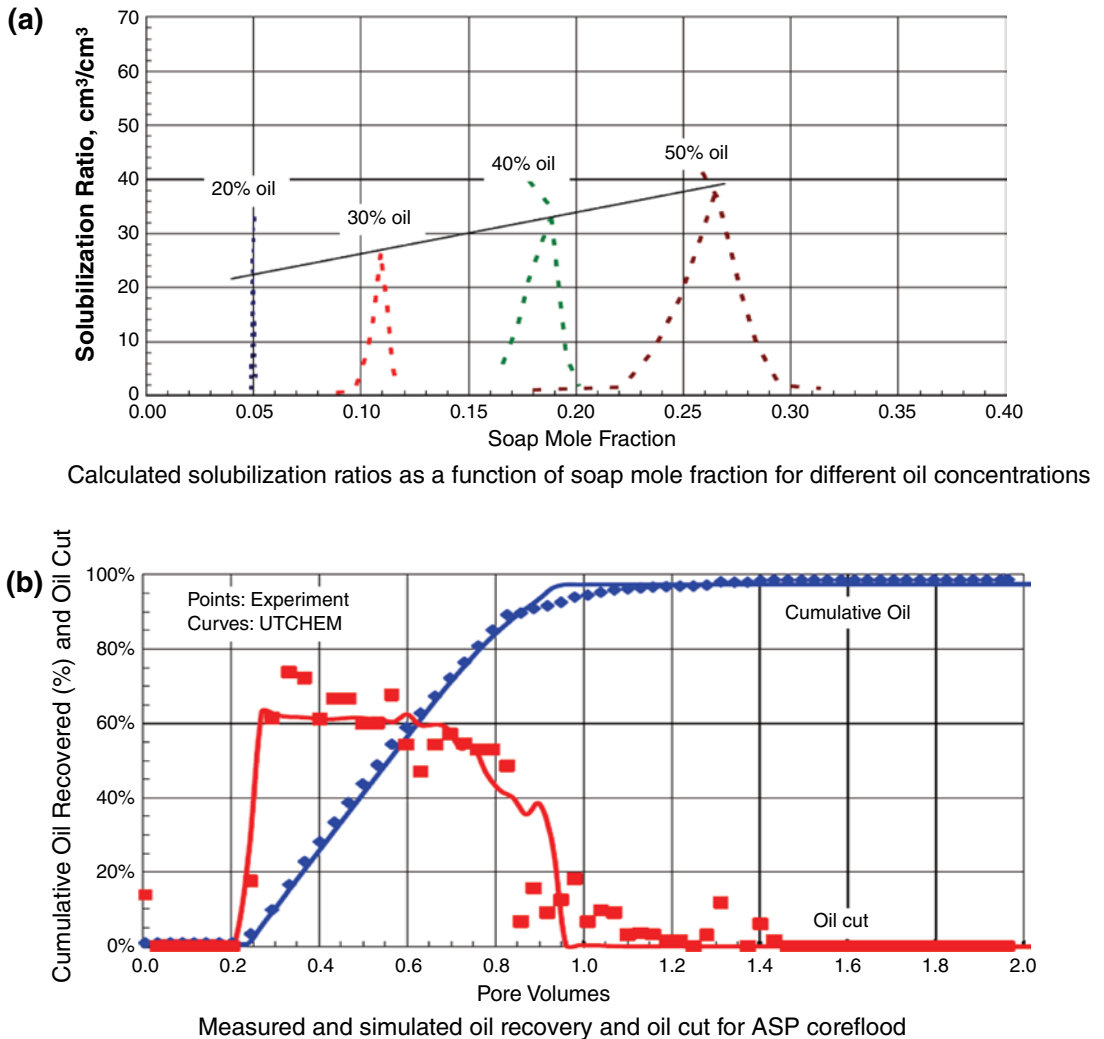


Fig. 5.59—Calculated and measured predictions from UTCHEM-ASP model (Mohammadi et al. 2009).

This means that kinetic calculations are not made. Bhuyan (1989) and Bhuyan et al. (1991) claim that this assumption probably is not true in most cases, but the models still have high levels of prediction.

The phase-behavior calculation (item 2 in the list above) is thought to be a critical factor and is based on the idea that there is an optimal salinity value of the combination of oil, soap, sodium carbonate, and SS to form a Type III ME (that provides optimal oil mobilization). A nonlinear mixing rule (Bhuyan 1989) was used to calculate the optimal salinity. See details in the current publication (Mohammadi et al. 2009).

An example of the predictions is in Fig. 5.59. The test parameters are listed in Table 5.4. Details of the type of surfactants used are in the publication. Part A of Fig. 5.59 shows the calculated solubilization ratios for the test oil for different concentrations and part B shows measured and predicted oil removal (based on CFTs) values.

Several conclusion of the report (Mohammadi et al. 2009) are

- The ME phase behavior is the key phenomenon in both SP and ASP floods.
- The optimal salinity for formation of the ME followed a log-mixing rule for the salinities of the SS and the soap.
- The model was successful in predicting the effects on the rock/solution and oil interactions.

| <u>Property</u> | <u>Core and Fluid Data Value</u> | |
|--------------------------------------|---|------------------|
| Berea core porosity | 0.17 | |
| Brine permeability | 683 md | |
| Waterflood residual oil saturation | 0.4 | |
| Residual water saturation | 0.32 | |
| Oil endpoint relative permeability | 0.6 | |
| Water endpoint relative permeability | 0.05 | |
| Acidic crude oil viscosity | 19 cp | |
| Water viscosity | 0.5 cp | |
| <u>Slug Pumped</u> | <u>Chemical composition of ASP</u> | <u>Viscosity</u> |
| ASP slug (0.3 PV) | 0.2 wt% surfactant, 1% cosolvent, 0.3% polymer, 2.75% Na ₂ CO ₃ | 28 cp |
| Polymer drive (approx. 2 PV) | 0.2% polymer in 0.6 wt% NaCl/ water brine | 33 cp |

- The soap/SS concentration gradient acts as a salinity gradient and is partially responsible for the success of an ASP flood.

5.5.6 Summary of Surfactant Method Technologies. Hirasaki et al. (2011) have reviewed progress in the use of surfactant methods for EOR. They claim that the technology of surfactant flooding has advanced to overcome many of the past causes of failures and to reduce the amount of surfactant required. These developments/understandings include

1. Surfactant adsorption can be significantly reduced in sandstone and carbonate formations by injection of an alkali such as sodium carbonate. This alkali also sequesters divalent ions. The reduced adsorption permits lower surfactant concentrations.
2. A wide selection of surfactant structures is now available to meet requirements for specific applications. (a) Branched alcohol alkoxy sulfate and sulfonates are tolerant of divalent ions. Ethoxylation increases optimal salinity; propoxylation decreases optimal salinity. In both cases, EO or PO, the optimal salinity decreases with increasing temperature. They note that alkyloxylated glycidyl ether sulfonate is more expensive than sulfate but is stable at elevated temperatures. Low-cost, double-tailed surfactants also are in development. Structures of SSs are in Figs. 5.49, 5.50, and 5.51.
3. Aqueous solutions of a blend of N67-7PO sulfate and IOS 15-18 with alkali have a larger single-phase region extending to higher salinities and calcium-ion concentrations than either alone. This blend, without alcohol, can form a single phase for injection with polymer but can form MEs with crude oil without forming a gel.
4. Soap generated in situ by the alkali acts as a cosurfactant that can change the phase behavior of the injected-surfactant solution from lower- to middle- to upper-phase MEs. It is lower phase when injected, middle phase at the displacement front, and upper phase ahead of the displacement front.
5. Injection of the surfactant and polymer at salinity that is under optimum with respect to the injected surfactant avoids S/P phase separation and ME trapping. The soap generated in situ by the alkali causes a middle layer to form and coexist with the lower-phase ME, which results in ultralow IST over a wide range of salinity.

6. Anionic surfactants and sodium carbonate can alter wettability for either sandstone or carbonate formations. Spontaneous oil displacement can occur by gravity drainage.
7. Foam can be used as the drive of the alkaline/surfactant process in place of the polymer drive. Foam can efficiently sweep layered and fractured systems.

Kalra et al. (2012) have studied the effect of surfactants on the rheology of W/O emulsions by making two different types of emulsions: (1) native-brine W/O emulsions without surfactants to provide a baseline and (2) brine W/O emulsions with surfactants used in ASP injections. This way, the impact of ASP injections on emulsion rheology can easily be quantified. A new correlation was developed, based on historical experimental data, to describe rheology of emulsions without surfactants. The important factors are the shear rate, API gravity (and composition of the oil), water cut, temperature, and additional surfactant.

Further, to understand the effect of ASP injections, new experimental measurements were made by adding surfactants to brine solutions. The addition of surfactants resulted in different rheology as compared with emulsions formed by brine solutions. These differences have been attributed to the W/O IST, and IST was added to modify the original correlation.

5.6 Chemical Methods for Improving Sweep Efficiency (Mobility Control)

Mobility control (or mobility ratio control) involves processes that cause the oil and water phases to flow in ways that optimize the production of the HCs. These are methods to address mostly the macroscopic issues described in Section 5.1.1. This section addresses specifically the use of chemicals for water (or gas) shutoff in *selected problem areas* of the formation, but NOT as an additive to a *reservoir-wide* EOR flood. Those types of mobility control issues are addressed in Section 5.4.3.

As in many of the areas of production enhancements described in this book, the nomenclature of the individual authors cited are not consistent. *Mobility control* can refer to water shutoff as well as to a segment of an EOR flood (here it may be called a permeability modifier). The term *conformance control* is used for the same processes. A gel treatment usually refers to water shutoff, but various polymer gels also can be used in EOR floods and the base chemicals may be identical. The authors of this book will attempt to clarify the chemistry and how it applies to each application.

Zaitoun et al. (1999) claim that water-flow paths in the reservoir, especially close to the wellbore, are irregular thus bypassing large HC-saturated zones and inducing undesirable high water-cut levels.

The production of excessive water is also considered to be one of the SPE's five grand research and development challenges (SPE 2011). In such situations, this is considered undesirable *water*, as opposed to good water produced under normal conditions. There are several causes of excessive water production. Seright (1997) proposed the following list, whose order corresponds to increasing difficulty of treatment using chemical gels:

1. Tubing/casing/packer leaks
2. Flow behind pipe
3. Layered reservoirs with vertical flow barriers
4. Individual fractures between injectors and producers
5. 2D coning through fractures
6. Channeling through naturally fractured reservoirs
7. 3D coning or cusping
8. Layered reservoirs without vertical flow barriers
9. Breakthrough from old wells
10. Waterflood breakthrough

Zaitoun et al. (1999) note that in this list, cases 1 and 2 correspond to completion failures and are workover problems. Case 3 is frequently encountered in field situations and is difficult to solve. However, when the different layers are clearly separated and workover costs are acceptable, water shutoff treatments that aim at sealing off the watered-out layer with strong gels (described in Section 5.6.2) may be placed by mechanical tools (coil tubing, packers, etc.). Nevertheless, they claim that in

practice, bullheading (any pumping procedure in which fluid is pumped into the well against pressure) is often the only option for the operator because of several problems like poor identification of the different zones surrounding the wellbore, multilayered production, unfavorable completion (gravel pack, slotted liners, etc.), or excessive workover costs (offshore wells, marginal wells). The other cases may also be addressed using chemical blocking or mechanical plugs and some of the processes described in Sections 5.6.1 and 5.6.2 will address them.

Kelland (2009) also claims that water shutoff operations may be performed as a zone starts to water out (breakthrough) and then other zones are perforated. Gels and cement may be used to reduce water for these operations. The authors of this book note that the excess and sometimes unexpected water, mixing from several zones (including breakthrough from old wells), may be particularly problematic because this can become sources of unplanned scale and corrosion (see Section 2.3.3 of this book as well as Frenier and Ziauddin 2008).

Mobility control as part of a waterflood/EOR operation as described in Sections 5.4.3. These operations also frequently are accomplished using polymers or sometimes with foams (Section 5.6.3). Taber et al. (1997) claim that the technical objective of a gel treatment (that is use of gels for water cutoff) is very different from that of a *polymer* flood. In most cases, the objective of a gel treatment is to prevent channeling of fluid (usually water) without damaging HC productivity. However, gels also can be used to shut off a high gas flow region (Zhang and Bai 2010). An example of the use of a polymer plug to divert flow from a high permeability thief zone is seen in Fig. 5.60. This figure applies directly to an injector (or to treatment of a production well), but the same effects apply to plugging a high-water zone or unwanted gas production.

The objectives of the use of polymers (and foams) during EOR is much different because the polymers must be part of the entire sweep and penetrate all the way to the producer well. In contrast, water shutoff gels (and other blocking materials) should only penetrate the higher permeability water-producing zones and not affect the permeability of the oil producing areas of the formation. Thus, precise placement of a water cutoff technology is critical. When possible, coil tubing using packers or packers without CT can be used to permanently (or temporarily) block a water-producing zone. In Section 3.7, the importance of correct placement of reactive stimulation fluids was described and various mechanical and chemical methods were discussed. Included was an oil seeker technology that selectively stimulated the oil producing zones instead of the water-producing zones. Thus, the developments of smart chemicals that seek out specific parts of the formation are a continuing goal in the production industry.

Zaitoun (2009) describes two strategies for water shutoff (not directly associated with a polymer EOR sweep) that include

1. Relative permeability polymers (RPM)
2. Sealing gels (Zhang and Bai 2010) calls these in-situ gels

He claims that

- Sealing gels block a water-producing interval.
- Sealing gels compete with cements or packers and are *placed* using packers/CT.

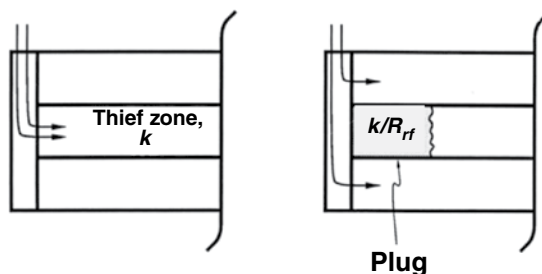


Fig. 5.60—Plugging a thief zone with a gel (Lake 2007).

Water Shutoff by Relative Permeability Polymers

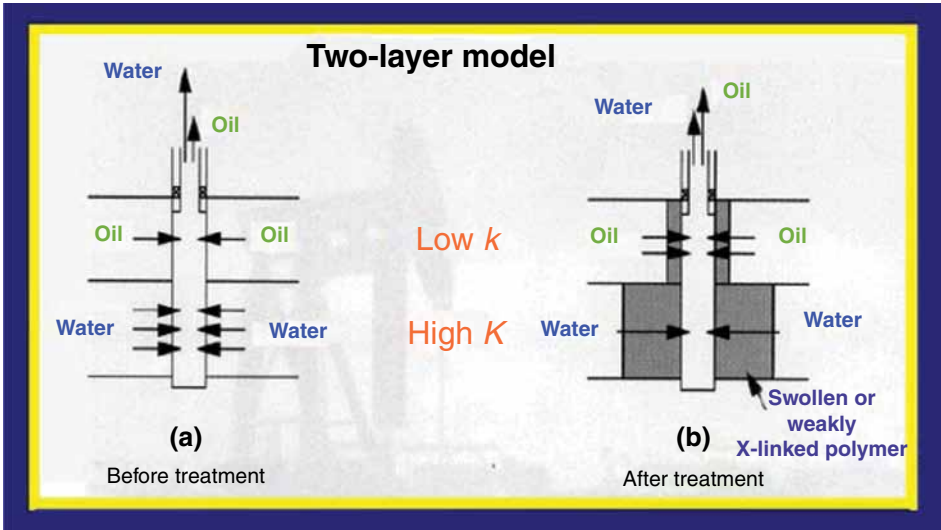


Fig. 5.61—Use of RP polymers for water shutoff. The number of arrows show relative flow before and after treatment (Zaitoun 2009).

- RPMs are *weak* polymers/gels (including microgels) that are designed to affect only *water* permeability and are temporary blocking agents.
- The RPMs are usually bullhead-injected into the whole open interval.

The next two sections describe the use of RPM and in situ formed strong sealing gels.

Additional methods to control the relative movement of the oil and water phases during EOR activities include foams as well as particulates. Both of these methods are also used in matrix stimulation diversion as well as fluid loss processes during HF, so the reader is referred to Sections 3.7.2 and 4.6 for a review of similar chemicals in those technologies.

5.6.1 RPM Type Water Shutoff Chemicals. Zaitoun (2009) describes the use of RPM chemicals. Fig. 5.61 shows the placement of *swollen* or *weakly crosslinked* polymer in the high permeability part of the formation (presumably the water zone). Zaitoun et al. (1999) use Fig. 5.62 to demonstrate the

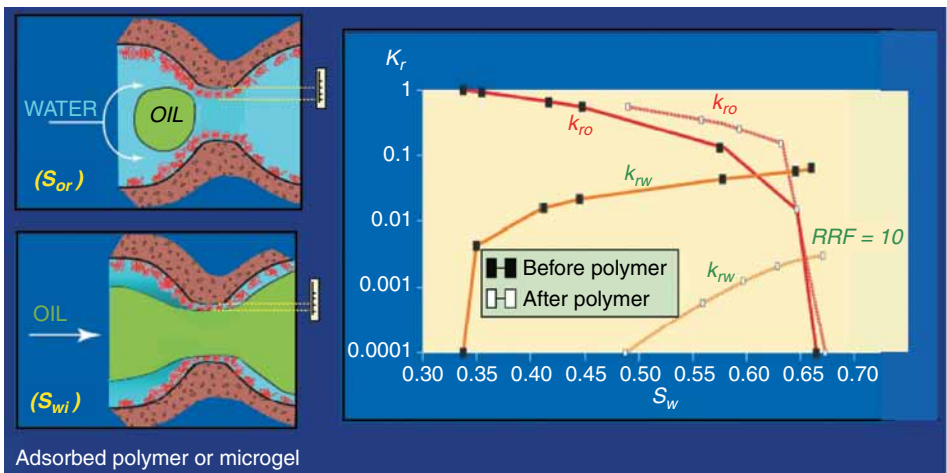


Fig. 5.62—Principle of RP polymers (Zaitoun 2009).

author's description of the action of the polymer or microgel to block water penetration of a pore channel. Note that in this drawing, the gels affect the *surfaces* more than the entire pore.

The authors claim that one theory is based on fluid partitioning, whereas the other relies on wall effects. The fluid partitioning theory claims that there are segregated flow paths for oil and for water inside the porous medium, and the gel tends to invade water-flow paths, thus reducing water mobility preferentially (Liang et al. 1995). They note that results from an experiment with an oil-based gel suggest that segregation of oil and water pathways through a porous medium may play the dominant role in causing the disproportionate permeability reduction. In the wall effect theory, the basic assumption of the authors is that after gel injection, a film covers the pore walls and changes dramatically two-phase flow properties by wettability, steric, and lubrication effects.

The RPM materials are thus claimed to maintain oil *permeability* and *reduce* water permeability. Kelland (2009) uses the term disproportionate permeability reducers to describe some chemicals such as rosin wood derivatives and emulsified gels that are called disproportionate permeability reducers but produce the same effect as the chemicals called relative permeability modifiers (RPMs). His book has an entire section on the wide variety of chemicals claimed for this purpose with more than 200 references. The authors of this current book note that while many chemicals have been proposed, various HPAAs formulations form the basis for most of the commercial systems.

Zaitoun et al. (1999) provide more details of water shutoff technology that is based on the use of RPMs. The technique consisted of bullhead injection of polymer solutions into existing completions, usually without zone isolation. The polymer can be swelled or weakly crosslinked in-situ to increase permeability reduction to water. Microgels also can be preformed. The chemistry of the different processes is explained. Each process covers a specific domain of temperature and salinity. All systems are designed to affect oil or gas relative permeability only slightly.

Process A. These are claimed to be applicable in low-salinity, low-temperature matricial reservoirs. HPAAs are injected in high-salinity brines. After production release, low-salinity formation water replaces progressively injection brine and swells the polymer adsorbed on pore walls. Advantages claimed are a low viscosity during injection, a large adsorption and a high-permeability reduction to water without the risk of well impairment by gels. More details are given in Zaitoun et al. (1991).

Process B. Depending on produced brine salinity, nonionic polyacrylamides are injected with either a caustic swelling agent (that hydrolyzes the polymer in situ) or an organic crosslinker (glyoxal). For higher temperatures, acrylamide copolymers can be crosslinked by zirconium lactate. A process description with different options is given in Zaitoun et al. (1991).

Process C. This is claimed to be applicable in high-temperature matricial reservoirs. It uses scleroglucan, (a polysaccharide) with strong shear-thinning rheology and excellent thermal stability. Polymer swelling can be simply obtained by the release of shear forces between high injection rates and low production rates. The polymer can be weakly crosslinked by zirconium lactate.

The authors (Zaitoun et al. 1999) review typical field cases (i.e., water shutoff in gas storage wells, heavy-oil horizontal wells, offshore gravel-packed wells, and multilayer-waterflooded wells) in both sandstone and limestone reservoirs. Several guidelines are presented, dealing with candidate well selection, process design, operational aspects, and treatment evaluation. Crucial for a successful treatment is the placement of the chemicals.

Chauveteau et al. (2000) have studied the formation of stable *preformed* microgels as RPMs to reduce water production and as a procedure to minimize the risk of formation plugging and consequently of inefficiency of in-depth treatments. This paper describes the results of theoretical and experimental investigations carried out to show how to control both size and conformation of microgels formed under constant shear flow. **Fig. 5.63** (Zaitoun et al. 2007) shows the comparison of a linear polymer and several microgels. These are polymer species with internal crosslinks that make them more rigid. The polymers are claimed to be flexible and about 0.3 μm in diameter and the microgels can range from 0.3–2 μm , but the internal crosslinking makes them more rigid and thus better attuned for temporary plugging of the flow spaces than the polymers (according to this author). Additional details of proposed mechanisms are in the report by Chauveteau et al. (2000).

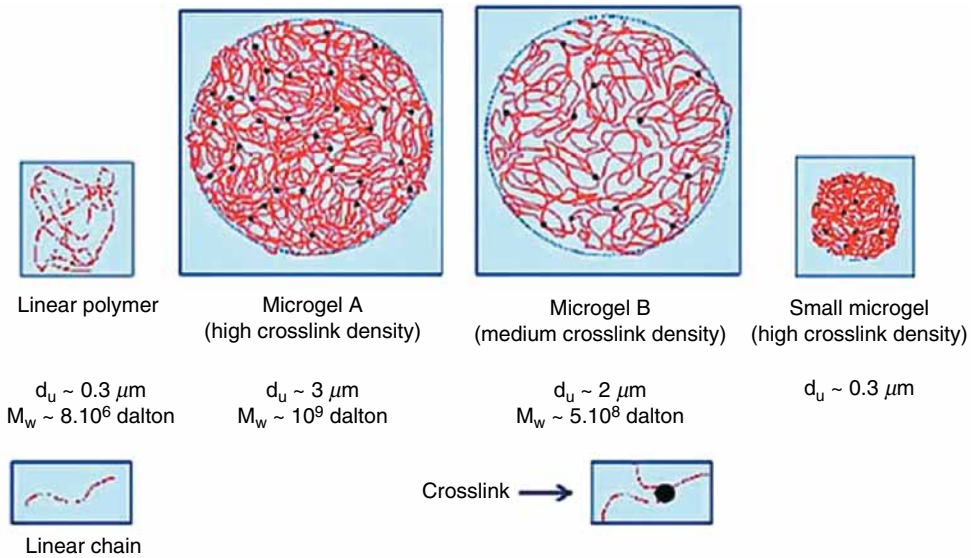


Fig. 5.63—Comparison of polymers and microgels showing various proposed gel and crosslinking structures (Zaitoun et al. 2007; Zaitoun 2009).

Kelland (2009) proposes that various VES-type fluids have been considered as temporary water shutoff materials that would be permeable to oil. This author also summarizes the wide variety of claimed RPM chemicals that include

- PHPAA
- Xanthan
- Scleroglucan
- Cationic PAA
- Other cation modified natural polymers such as starches
- Acrylamide/AMPS copolymers
- Vinyl sulfonate/acrylamide copolymers

Some of these types of polymers are also described as permeability modifiers for use in polymer waterfloods (see Section 5.4.3).

5.6.2 Permanent or Semipermanent Water Shutoff Chemicals. More traditional water shutoff processes use polymers (and sometimes monomers) that are pumped with a crosslinker into the water zone to be closed. The authors of this book will note that many of the same types of chemicals described as RPMs are used in the more permanent water shutoff treatments. These frequently are placed using CT or tubing packers to isolate that zone.

Kelland (2009) notes that various strong gels are available for pumping into the zone that are to be closed and does point out that these materials will stop both water and oil production from these areas. Shutoff chemicals also can be employed to block excessive gas production zones.

According to Fink (2003), the gel type of water shutoff chemicals typically includes a water-soluble polymer that has carboxy and/or carboxy amine pendant groups. Thus, examples are PHPAA, carboxycelluloses polymers, and hydrolyzed polyacrylonitriles. The root mechanisms are that the polymers are pumped into the well mixed with a crosslinker and possibly a delay agent and do not form a gel plug until they are in the high permeability water zone.

The structure of PHPAA is seen in Fig. 4.48. Because various transition metals (Fe, Cr, and Co) will form coordinate bonds with carboxylate and amine groups, these metals can form crosslinks with the gel-forming polymers and the metal complexing reaction can be delayed by adding chelating agents

to the mixture or by adding complexed metals. These reactions are very similar to those described in the reactive fluids section (Section 3.7) and the fracture fluid section (4.10.1), where the mechanisms of polymer crosslinking as well as chemical diversion methods are described.

Kelland (2009) lists a number of different types of permanent blocking agents including

- Resins—phenolics, epoxies, and furfural alcohols
- Inorganic gels—silicates
- Crosslinked organic polymers

The Kelland (2009) list includes the use of sodium silicate solutions as water and gas blocking agents. This author notes that the silicates are not compatible with most formation brines and must be pumped behind a freshwater spacer into the zone to be blocked. A spacer separates an activator (such as ammonium sulfate or CO_2), which will cause the gel to form. However, various other slow-release activators such as acid esters that generate the acid in-situ have been proposed.

Islam and Farouq (1993) describe 13 large-model experiments that were conducted using silica gel, to study the effect of oil-to-water zone permeability contrast and thickness ratio, oil viscosity, and CO_2 injection. A qualitative comparison is made to show the relative merit of CO_2 -activated silica gel injection among other mobility control agents. Several runs were conducted to study silica gel rheology both in presence and in absence of CO_2 .

Seright and Liang (1994) describe results of a study that demonstrates that gel treatments have been applied over a wide range of conditions. Unfortunately, the success rates for these projects have been very inconsistent. The analysis indicates that the producing W/O ratio was usually the only criterion used to select candidate wells.

They claim that to improve the success rate for future gel applications, *the source and nature* of the water production problem must be adequately identified. Results from interwell tracer studies (see Section 5.7) and simple injectivity and productivity calculations can be especially useful in this diagnosis. Recovery calculations should indicate that considerable mobile oil remains that could be recovered more cost effectively if a blocking agent could be realistically placed in the proper location. Improvements are needed in the methods used for sizing gel treatments. They claim that the method of sizing should be tailored to the type of channeling problem encountered. Two studies indicated that less than 45% of the gel treatments were successful. The uses of silicates also are described.

Examples of organic gel-type water shutoff chemicals include those described by Fink (2003) as well as in Taber et al. (1997) and Kelland (2009) have been noted previously. Specific additional examples and methods (some from patents) are abstracted and include metal crosslinked systems and those using nonmetals.

Chromium (III) crosslinked HPAA systems are in current use. Marty et al. (1991) provide data on the gelation of a polyacrylamide/thiourea/Cr(VI) gel system in unconsolidated sandpacks. This system produces Cr(III) ions by the reduction of Cr(VI) using the thiourea. The idea is to delay the crosslinking mechanism until the chemicals are in the water zone. Southard et al. (1984) have studied the kinetics of the reaction and found that there is a first-order dependence on chromium(VI) concentration on thiourea and on pH. Additional results of the thiourea study show that a constant amount of chromium(VI) is consumed at gelation regardless of the initial concentration of that species, indicating that the Cr(VI) reduction reaction may be the rate-determining step in gelation.

Marty et al. (1991) claim that at these low rates, in-situ gelation during flow was characterized by an abrupt increase in flow resistance that occurred over a short distance at a specific location along the sandpack. The location of this region was a function of now raw, and its distance from the inlet increased as flow rate increased. Filtration of gel aggregates appears to be the mechanism causing this behavior.

Chen et al. (2010a) note that commonly used systems consist of HPAA with a chromium (III) crosslinker. Transport of these chemicals through the reservoir rock is essential for a successful treatment. In carbonate reservoirs, dissolution of the carbonate raises the pH of the gellant to levels where chromium precipitates, robbing the gellant of crosslinker. The transport of chromium acetate solutions through dolomite rock material was studied by injecting various solutions through short cores and

measuring Cr, Mg, and Ca concentrations and pH in the effluent. Chromium retention in the cores caused by precipitation was a rate-controlled process. A mathematical model was developed that described convection, dispersion, kinetic reactions of carbonate dissolution and chromium precipitation, and chemical equilibrium for reactions between aqueous components. Experimental data from this work and taken from literature were simulated by the model. One rate equation with one set of parameters described the steady-state values of chromium concentration exiting the cores after the breakthrough of the injected solutions.

Dovan and Hutchins (1994) describe a polymer treatment process that has been developed for selectively reducing water permeability in gas wells. Three field treatments are discussed. The most notable treatment was performed on an offshore gas well that previously was loaded up with water. The treatment returned gas production to the well, averaging 1.9 MMcf/D gas for almost 3 years. The water production was reduced from a high of almost 600 to < 50 B/D.

The chemistry is in the patent by Hutchins and Doan (1995) and claims that the most widely practiced production well gel technology for water control employs cation-crosslinked (Fe^{3+} , Cr^{3+}) polyacrylamide gels. However, they claim that there are a number of problems that limit universal use of existing gel technologies. To resolve these issues the authors claim the use of *visible gels* (employs an organic crosslinking agent that creates a covalently bonded gel structure) that are formed by mixing an inorganic crosslinking agent with a low-viscosity aqueous solution having a low-polyacrylamide concentration and devoid of polymers containing a vicinal diol pendant group. The visible gels are employed to reduce the water/HC permeability ratio of subterranean formations. This is compared with microgels that the authors claim will permanently reduce the oil permeability.

Caili et al. (2011) describe the development and use of polymer gels with different gelation time for water coning control in a horizontal well located in Weizhou offshore oil field in China. The selected horizontal well was shut in with zero oil production and 100% water cut before treatment. This paper also reports the detailed information about the treatment, including production history of this horizontal well, gallants formulas with different gelation time optimization, operational procedure, and reservoir performance after treatment. In addition, a method is built up to control water coning for horizontal well in offshore oil field. The gallants formulas are 0.30% HPAA + 0.60% phenol formaldehyde resin, 0.40% HPAA + 0.10% $\text{Na}_2\text{Cr}_2\text{O}_7$ + 0.20% thiourea, and 0.40% HPAA + 0.20% $\text{Na}_2\text{Cr}_2\text{O}_7$ + 0.40% (thiourea, with corresponding gelation time of 3.5 day, 2.0 day, and 1.0 day separately at 75°C). The authors claim that the gellants were successively injected with injection volumes of 384 m³, 256 m³, and 128 m³. The overdisplacing fluid was used to displace gellant away from percolation area. Then, the well was shut in for 4 days to form gel that could be used as packer between oil-water interfaces to control water coning. At the same time, real-time monitoring data about injection pressure and rate were also recorded. The treatment resulted in an oil increase of approximately 16.3–27.4 t/d and average water cut decrease of 6% \approx 9% in 1 year after treatment. This paper provides a good description of the chemistry and the placement of the gel. However, the use of *toxic* Cr(VI) compounds as well as toxic thiourea, noted here and by Marty et al. (1991) may limit this type of chemistry in most markets.

A number of systems that use *nonheavy metal* systems also have been proposed.

Zaitoun and Kohler (1989) claim a process that comprises injecting a non-HPAA or copolymer into the producing formation and producing hydrolysis in situ by subsequent injection of an alkali metal basic compound. It is claimed that it is then possible to restart the well in oil or gas production. It is claimed that using the non-HPAA is an improvement because it is not ionic and thus less likely to be adsorbed onto the matrix. The invention then assumes that a *caustic* overflush will go into the target zone and hydrolyze the PAA. The preferred polymer according to the invention is a non-HPAA of high MW or a nonhydrolyzed nonionic copolymer of acrylamide, preferably in a proportion lower than 50%, with one or more comonomers, also nonionic, preferably in a proportion higher than 50%, such as N-VP, as well as various vinyl ethers or esters, such as butyl methacrylate, methyl and glycidyl acrylate, vinyl acetate, etc.

Kohler and Zaitoun (1992) describe a process for selectively reducing permeability to water in an underground formation producing oil and/or gas by injecting into the formation a composition comprising water, at least one water-soluble *aldehyde* compound at a concentration (by weight) of 180

to 20,000 ppm and at least one nonionic polysaccharide at a concentration (by weight) of 200 to 5000 ppm, the concentration of aldehyde compound being higher than that of polysaccharide. Examples of the aldehydes compounds according to the invention include formaldehyde and dialdehydes of the general formula, $(\text{OHCCR})_n\text{CHO}$ in which $n = 0$ to 6, preferably 0 to 3, and R is a divalent HC radical with 1 to 4 carbon atoms (such as glyoxal or glutaraldehyde), are preferable for economic reasons.

Berkland et al. (2008) claim in a patent application that crosslinking of polymers such as HPAAs can be *delayed* by making nanoparticles of them. In an example, a water-soluble organic polymer (acrylamide-co-acrylic acid) was mixed with polyethyleneimine (PEI) aqueous solution, 9,997 ppm, and dextran sulfate (DS) aqueous solution, 9,991 ppm. First, a solution comprising 9,997 ppm PEI (100.63 g) was formed, and a separate solution comprising the 9,991 ppm DS (46.94 g) was formed. The polyelectrolyte complex solution was prepared by mixing the two solutions together to form the nanoparticles and then the HPAAs were added. The authors claim that the PEI slowly dissociates from the polyelectrolyte complex, and then crosslinks the HPAAs. The gelation can be controlled to occur after 7, 8, 9, 10, 11, 12, or more days. This same type of use of chemicals encapsulated using nanoparticles also was described by Barati et al. (2011) (in Section 4.6) as a method to delay enzyme degradation of guar-fracturing fluids. The current application claims a large number of polycations (such as chitosan) that can be mixed with a polyanion to form the nanoparticles.

A polyethyleneimine (PEI)-nanoparticle system also has been proposed by Jayakumar and Lane (2012) as being effective in blocking water zones in fractured tight-gas formations. Fig. 5.64 shows a depiction of the problem where various microfractures go into an aquifer that then adds a lot of water to the flow to the production wells. The authors claim that excessive water production (in excess of the frac water) has been seen in the Barnett shale and Cotton Valley formations.

Jayakumar and Lane (2012) have described the details of the PEI-DS nanoparticles (also see Berkland et al. 2008). They claim that the nanoparticles formed by the PEI and DS delay the crosslinking of the HPAAs that have been pumped into the water zone as a low-viscosity fluid. The authors claim that by impeding water production, the gel system developed here can be used to delay water loading and subsequent premature abandonment (or installation of expensive equipment), thereby extending life and reserves of unconventional gas wells. They propose that potential applications include the Barnett shale, where 15% of wells produce more water than injected during drilling and stimulation, presumably because of hydraulic fracture growth into underlying water zones.

The use of crosslinked HPAAs colloidal dispersion gels (CDGs) for use as water-blocking control is described by Skauge et al. (2010). They have also reviewed the field applications involving CDGs, aiming at sweep improvement in adverse mobility heterogeneous oil reservoirs. They concluded that in most cases, oil production increased and W/O mobility ratio decreased. Based on the result, they also concluded that CDGs “provide an excellent tool for in-depth control of permeability.”

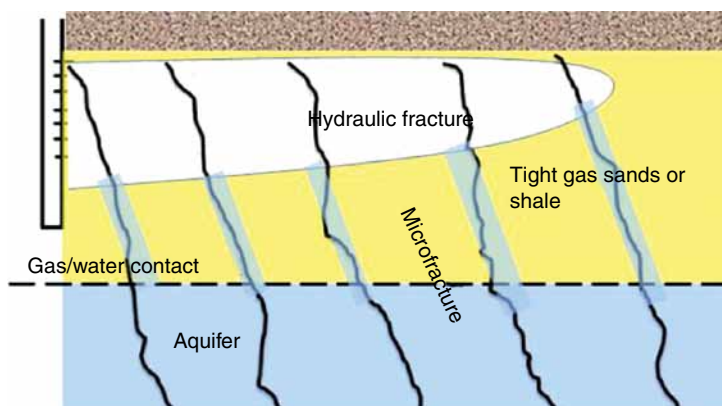


Fig. 5.64—Fractures into water zone.

The authors claim that there has been little systematic information of the detailed mechanisms of the CDG process. To improve on this situation, filter tests were performed both for selection of suitable silica particles for coreflooding experiments.

CFTs showed the following conclusions:

- Nanosized silica particles passed through the water-wet Berea sandstone cores.
- The silica particles did not produce more oil.
- Pregenerated CDG particles gave an increase in oil recovery from water-wet cores.
- The process related to log-jamming blockages is thought to be part of the mechanisms.

Details of the use of water-blocking chemicals are in a patent by Munday (2003). This type of process could be used with different chemicals. It is claimed that the present invention conveniently provides a process for reducing water flow from a HC production well comprising the following steps:

- (a) Injecting a first chemical composition that is reacted to form a polymer that is effective as a relative permeability modifier polymer into the HC and water zones of a reservoir.
- (b) Injecting a second chemical composition into the HC and water zones, the second chemical composition reacted to form a flow-blocking polymer.
- (c) Affecting a shut-in for a reaction period of the first chemical composition to form the relative permeability modifier polymer.
- (d) Producing a second polymer composition from a [noted in the patent—Munday (2003)] chemical composition out from the HC zones before reaction of the second polymer composition.
- (e) Maintaining the production of the first and second polymer compositions from the HC zones to facilitate the creation of a passage for HC flow while enabling the second polymer composition to react in the water zones to form a water shutoff.

The authors of this book note that the perfect gel-type water-blocking system is still not universally available because of several problems (Kelland 2009):

- Sineresis (collapse of the gel structure)
- Precipitation
- Chemical degradation
- Placement into the correct zone

The next two sections (5.6.3 and 5.6.4) describe additional chemicals that are designed to affect mobility during the various reservoir floods described in the chapter. These methods are used as an alternative to or with the polymers described in Section 5.4.3.

5.6.3 Foam. The use of surfactants for producing CO₂ foams were described in Section 5.5.2. The current section considers the use of N₂ foams as well as mixed systems. Foams are used in both acidizing (Section 3.7.2) and fracturing for mobility control as well as proppant transport (Section 4.5.5).

Rossen (2005) conducted a detailed study of foams for improved sweep efficiency in miscible gas, steam, and surfactant-based EOR. This is a 152-page report and only a few observations and conclusions will be abstracted. The author claims that a pore-network model for foam generation resolves two paradoxes troubling the model of foam generation by mobilization and division. First, the model shows how new lamellae are created near the inlet of the porous medium to replace those mobilized and transported downstream.

A series of sandpack experiments found several effective ways of enhancing foam generation, and some that were not effective. In homogeneous sandpacks, foam generation occurs at lower pressure gradient and lower gas velocity at higher liquid injection rates, lower permeability, and higher surfactant concentration. Foam generation occurred more easily in flow across sharp increases in permeability than in homogeneous packs. Temporarily increasing pressure gradient did not facilitate foam generation in homogeneous sandpacks but did trigger lasting foam generation in layered packs.

When gas was injected following a slug of liquid, or into a pack presaturated with liquid, foam generation occurred at a lower pressure gradient than with steady co-injection of liquid and gas. These results are similar to tests done in diversion of stimulation solvents (Kam and Rossen 2003; Kam et al. 2007).

Rossen (2005) also investigated the interactions of polymers and foam in search of means to stabilize and strengthen foam using polymers, especially in the presence of oil. For the polymers (xanthan and partially HPAAs), oils (decane and 37.5°API crude oil), and surfactant (AOS) that were tested, it appears from coreflood pressure gradient that the polymer *destabilizes* foam modestly, raising water saturation (S_w) and water relative permeability (k_{rw}). The increased viscosity of the aqueous phase with polymer partially compensates for the destabilization of foam. It is expected that the whole combination of oil type, surfactant type, and polymer will affect foam stability.

Li et al. (2006) report that foam is extensively applied in steamflooding (Keijzer et al. 1986) and CO₂ flooding (Yaghoobi 1994) to enhance oil production, but not as flooding technique for the conventional reservoirs. The combination system, which they claim consists of surfactant, polymer, and gas (such as N₂, CO₂, natural gas, etc.), was called polymer foam flooding. The polymer foam flooding may channel selectively through high-permeability zones, and its apparent viscosity is greater than any other displacement medium to improve sweep efficiency during flowing in porous media. Meanwhile, it also can further enhance oil production by mixing surfactant with crude oil to make emulsification to displace more remaining oil in reservoir. In field test, co-injection and liquid alternating with gas were all practiced. But for actual injection ability, only liquid alternating with gas could realize polymer foam flooding injection. Lab study and field test in Gudao oil field provided proof that polymer foam flooding is a promising technique for high heterogeneous reservoir.

Li et al. (2006) claim that the goal of the paper is to present the results of laboratory and field studies of polymer foam flooding in Gudao oil field. For polymer foam, the displacement medium is N₂ mixed with surfactant as foaming agent and polyacrylamide. Fig. 5.65 shows that the maximum resistance factor takes place at gas/liquid ratios of 1:2.

Hou et al. (2012) claim that most of the high-permeability reservoirs in Daqing oil field have been treated by waterflooding and polymer flooding. The average oil recoverable recovery has reached up to 53% after polymer flooding. Currently, the further development of such reservoirs has become a big challenge because of both serious heterogeneity reservoirs and highly dispersed residual oil. Foam flooding, as a candidate EOR technique integrating both properties of gas injection technique and chemical flooding, has been proposed. In this study, the authors describe systematic laboratory experiments on foam flooding EOR technique for Daqing reservoirs after polymer flooding have been performed.

Several operating parameters have important influences on the recovery efficiency.

1. Both the formability and stability are the key factors to ensure high performance of recovery. The foam formulas were optimized with good performance of formability and stability.

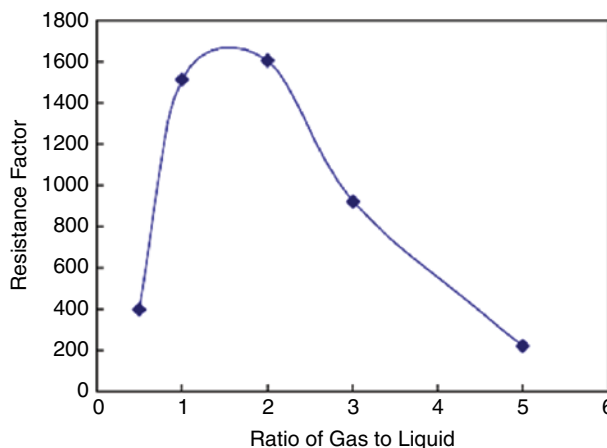


Fig. 5.65—Ratio of gas to liquid ratio and resistance factor (Li et al. 2006).

2. Injecting mode is another important factor. Three main injection modes, including co-injection of gas and solution, alternative injection of gas and solution, and direct injection of foam were compared. The direct injection of foam is the most effective mode and the alternative injection of gas and solution is the poorest.
3. The gas liquid ratio can also affect the flooding efficiencies greatly. The optimized gas liquid ratio was proposed as 3:1–4:1 for direct injection mode at the reservoirs condition. EOR effect evaluation of foam flooding after polymer flooding has been conducted upon three-layer positive rhythm sandpack cores flooding tests. Results indicate that foam flooding can contribute 12–22% OOIP recovery even if the recovery after polymer flooding is nearly 55%. The authors have used an N_2 /brine fluid stabilized using a C_{14} – C_{16} AOS/HPAA. The increasing of injection pressure during the foam flooding indicates that nitrogen foam flooding has excellent profile-control ability.

They conclude that foam flooding can block thief zones for highly heterogeneous reservoirs. It may become a promising EOR method for Daqing reservoirs after polymer flooding.

5.6.4 Particles and VES for Diversion. The use of crosslinked HPAA CDGs for use as water-blocking (mobility) control was described in Section 5.6.2. These particles also can be used for mobility control in various chemical modified water sweeps.

Another type of diversion may involve selective formation damage. In all cases, the migration of fines during water injection may affect the final result of the treatment by causing formation damage. See Section 2.3.3. Lemon et al. (2011) have reviewed fines migration and subsequent reduction in permeability that have been observed to occur during coreflood experiments as a result of decreased water salinity, increased flow velocity, and altered water pH or temperature (Khilar and Fogler 1998; Civan 2000). The authors note that the traditional view of fines migration is that it should be *avoided* because of its detrimental effect on reservoir permeability (see Section 2.3.3 of this book). However, during waterflooding, an induced reduction in the effective permeability to water of the reservoir in the water-swept zone, caused by fines migration, may be used to provide mobility control to improve the performance of the waterflood. This effect may be similar to other mobility control techniques such as polymer flooding (see Section 5.4.3). These authors (Lemon et al. 2011) suggest that the reducing the salinity of the injected water may be a practical method to implement mobility control.

A very common method of causing formation damage is to induce fines migration because of the shock to the formation with fresh water (see Section 2.3.3). This will control the release of fines are not easily changed or, in the case of velocity, affect the whole reservoir, not just the water-swept portion. Low-salinity water (if available) may be inexpensive compared to other alternatives (see earlier in Section 5.6.2).

Lemon et al. (2011) have used the (Dietz 1953) model for waterflooding in a layer-cake reservoir with a constant injection and production rate that was combined with a particle detachment model to provide a simple analytical model for the process. The application of the model to an example data set showed induced fines migration might improve sweep efficiency for a given volume of injected water.

Morvan et al. (2009) and Morvan et al. (2012) reports on an alternative approach to polymers based on VES-based fluids (see Sections 3.7.2 and 4.4.2). The technology developed is claimed to match the rheological properties of polymer solutions in a broad range of reservoir conditions (temperature and salinity) without any injectivity limitation even when considering very viscous surfactant solutions (i.e., up to 1000 cp) and low-permeability cores. The authors claim that the potential of this surfactant-based technology is illustrated through a specific reservoir case involving heavy oil. A series of coreflood experiments has been performed in reservoir cores. The surfactant slug can be combined with a conventional low-concentration polymer flooding to further improve the process. Reduction in residual oil saturation in the range of $\Delta S_w = 10$ –15% has been obtained. The authors did not reveal the specific chemistries, however a patent application (Morvan et al. 2010) claims mixtures of a phosphate and a monoalkyl ester of formula (I), a phosphate dialkyl ester of formula (II) or a mixture of the compounds of formulas (I) and (II). The proportion by weight in the final reaction mixture of the phosphate

monoalkyl ester of formula (I) to the phosphate dialkyl ester of formula (II) is generally controlled by the method of synthesis of the phosphate alkyl esters.

5.6.5 Pilot Tests and Field Evaluation. Development of new chemical processes usually require laboratory-level tests involving small amounts of chemicals and oil, and then some type of pilot plant test involving multigallon lots and the field tests. Scale up of EOR treatments are quite difficult and usually involve only computer simulations (Delshad et al. 1998; Veedu et al. 2010), and then field trials that may take several years to provide conclusive results.

Arora et al. (2010) describe an alternative for performing single well chemical EOR tests that is a variant of log-inject-log and is termed a micropilot. In this method, the remaining oil saturation and flood geometry after injecting a small volume of EOR fluid are measured across a correspondingly small flooded zone. This technique can be executed in a day or so depending on well and reservoir conditions. The pre-flood and post-flood fluid saturations are determined using wireline logs, and in the case described, a nuclear magnetic resonance and dielectric log (Schlumberger 2012b).

Anderson et al. (2006) note that the success of an SP flood depends upon the ability to propagate the surfactant and polymer, overcome chemical adsorption, and improve the sweep efficiency. In this work, an optimization study was performed to meet these three goals and maximize the oil recovery and profitability of an SP flood in a mixed-wet dolomite reservoir. The optimization study included a sensitivity analysis, which included the aforementioned parameters, and an uncertainty analysis, which was extended to other parameters such as kv/kh , capillary desaturation curves, and permeability.

The optimization and sensitivity simulations reported in this paper were performed using UTCHEM (Pope 2009), a chemical flooding simulator developed and validated for chemical processes such as SP and ASP. The results of the simulations were analyzed using discounted cash flow to determine the economic feasibility of the optimized SP flood design for a particular carbonate reservoir in the Permian Basin. (Scathe results of this study showed that chemical flooding this mixed-wet dolomite reservoir is likely to be profitable over a range of crude oil prices based upon the laboratory performance of the S/P flood and the optimum process design determined in this study.

Shiau et al. (2012) describe the EOR testing including lab and pilot tests needed to qualify an S/P flood in a high-salinity formation in Oklahoma. The authors describe how the different surfactant formulations were evaluated and incorporate cosurfactants and cosolvents, which minimize viscous macroemulsions, promote rapid coalescence under Winsor Type III conditions, and stabilize the chemical solution by reducing precipitation and phase separation. The optimal surfactant formulations were further evaluated in 1D sandpacks and CFTs using Berea sandstone, reservoir oils, and brines at reservoir temperatures.

They then described six different steps in performing a pilot test.

1. Perform a brine flood of at least 4 PV to ensure as low S_{or} that will be found at the end of a waterflood.
2. Determine the SWTT (see Section 5.7) to determine the S_o in the target zone.
3. Two-day shut-in to allow hydrolysis of the ester-type tracer.
4. Perform the injection of the optimized surfactant slug at the 0.5 PV level, flowed by 0.1 PV polymer solution.
5. Inject 3 PV of brine to chase the oil.
6. Perform another SWTT to determine the final S_o and the effectiveness of the trial.

5.7 Use of Chemical Tracers

The addition of a tracer material to an injected fluid can provide valuable information about the reservoir, the distribution of oil and water and the flow rates and productivity of the treatment. Passive and reactive tracers can be used. Passive tracers are soluble only in the aqueous or oil phase and can be used to follow that phase. Reactive tracers such as esters can be injected then partitioned into the aqueous and the oil phases based on a simple, predictable chemical reaction. Tracers are used in EOR (Chapter 5), HF (Chapters 3 and 4), and in reactive stimulation (Chapter 3).

Bjørnstad (2008) defines tracers as any substance whose atomic or molecular, physical, chemical, or biological properties provide for the identification, observation, and study of the behavior of a fluid. These can include various physical, chemical, or biological more or less complicated processes (dispersion or concentration, flow, kinetics and dynamics, chemical reactions, physiological interactions, etc.), which occur either instantaneously or in a given lapse of time. The tracers must be composed of chemicals that can be *distinguished* from the phase being traced. This author also notes that chemically, tracers can include

- Stable isotopes (^2H , ^{13}C , etc.)—they are analyzed by isotope mass spectrometry.
- Nonradioactive chemical species (esters, Co or other metallic compounds)—they are analyzed by chemical instrumental methods or other methods.
- Radioactive atoms or molecules (^3H , ^{14}C)—analyzed by nuclear detection techniques.
- The tracer must be very stable in the fluid/formation unless a reaction is part of the mechanisms.

Very sensitive analytical equipment must be available to detect the small amounts of the chemicals in the produced phases. The tracers must also contain elements or compounds that can be *easily* distinguished from the components of the water and oil-containing phases. Adsorption or reaction of the tracer with either the formation of the fluids will complicate the analyses. Tracers can be used in single well tests where a fluid is pumped into the formation and then returned to the same well. Tracers also are used in two-well tests where they are pumped from an injection well to another (production) well to chart the flow pattern. Tracers also have been used in fracturing treatments to follow the return flow from those treatments. More details of tracers in use for oil and gas activities are reviewed in Sections 5.7.1 and 5.7.2.

5.7.1 Passive Tracers. This category of chemical does not undergo a chemical reaction in the fluid. Both radioactive and nonradioactive tracers are in use (Fink 2003). Tritium (^3H) can be incorporated into water to follow only the aqueous phase. This is a relatively long half-life isotope (12.3 years). ^{14}C can be incorporated into many organic compounds and has a very long half-life (5730 years). Radioactive materials are one class of commonly used tracers.

The Schlumberger Glossary (Schlumberger 2012a) claims that the technique used is the same as for natural gamma ray spectroscopy (Blum et al. 1997) but measures the quantities of various short half-life radioactive tracers in addition to natural gamma rays. The log can be run to monitor the results of processes that can be tagged, for example, HF, gravel-pack placement, squeeze cementing, acid treatment, and lost-circulation detection. Different radioactive tracers are added at different stages of the process so that by measuring the different tracers, it is possible to track the development, for example, of a hydraulic fracture. The report claims that the most common radioactive tracers used in fracturing are ^{110}Ag (silver), ^{195}Au (gold), ^{135}I (iodine), ^{192}Ir (iridium), ^{124}Sb (antimony), and ^{46}Sc (scandium).

A report by Lockwood and Kordziel (2010) also describes the use of Sc, Sb, and Ir radioactive tracers to plot the course of an acid fracture treatment. These tracers have several drawbacks. One drawback is that they require special handling because of the danger posed to personnel and the environment. Another drawback is the alteration by the radioactive materials of the natural isotope ratio indigenous to the reservoir, thereby interfering with the analysis of the reservoir fluid characteristics.

The additional examples are from (Bjørnstad 2008) and include the energy [in electron volts (eV) and half-life ($t_{1/2}$)] of the isotopes (for β rays and γ rays):

For aqueous fluids:

- ^3H , HTO, $E\beta = 18 \text{ keV}$, $t_{1/2} = 12.32 \text{ y}$
- $^{60}\text{Co}(\text{CN})_6^{3-}$, $E\gamma = 1173 \text{ and } 1332 \text{ keV}$, $t_{1/2} = 5.2 \text{ y}$
- $^{22}\text{Na}^+$, $E\gamma = 511 \text{ and } 1274 \text{ keV}$, $t_{1/2} = 2.5 \text{ y}$
- S^{14}CN^- , $E\beta = 159 \text{ keV}$, $t_{1/2} = 5730 \text{ y}$

For HC fluids:

- n-butanol, ¹⁴C-labelled, Eβ = 159 keV, t_{1/2} = 5730 y
- Isopropyl alcohol, ¹⁴C-labelled, Eβ = 159 keV, t_{1/2} = 5730 y
- MBK, ¹⁴C-labelled, Eβ = 159 keV, t_{1/2} = 5730 y

Many other passive tracers for the oil phase include halo chemicals (containing Cl or Br) and halo HCs that would not normally be in the oil phase. Miller et al. (1993) describe water-soluble complex metal anions such as cobalt hexacyanide that are used as nonradioactive tracers in reservoir studies. Sensitive analytical procedures enable detection and measurement of very low tracer levels. An example is a reservoir targeted for carbon dioxide flooding, about 700 g of potassium cobalt hexacyanide was injected into several injection wells where the wells were on 40-acre spacing in roughly a five-spot pattern. Cobalt is easily detected at very low concentrations using inductively coupled plasma optical emission spectroscopy methods (described in detail in this patent). Nonradioactive isotopes also include ¹⁸O [and Deuterium, D, (¹H²H¹⁶O or HDO) measured as isotopic ratios (¹⁸O/¹⁶O (δ¹⁸O) and ²H/¹H (δD)] with mass-spectrometric techniques.

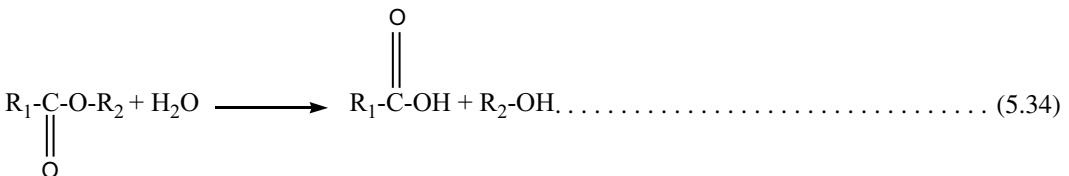
For example, Miller et al. (1993) report that the average thickness of a net-pay reservoir was 62 ft, the average porosity was 11.7%, the injection rate per well was 1,000 B/D, and the average production rate per well was 896 bbl per 30 day. A nonradioactive tracer (cobalt hexacyanide) responded in measurable and interpretable concentrations, such that reservoir characteristics could be determined without the need for radioactive tracers. The authors of this book note that Co is readily detected using inductively coupled plasma optical emission spectroscopy methods.

A patent by Hutchins and Saunders (1993) notes that organic tracers are employed to monitor the movement of subterranean fluids. These organic tracers should be

- (a) Stable at elevated temperatures
- (b) Capable of being detected at low concentrations
- (c) Not adversely affected by the makeup of at least one subterranean formation

In addition, a plurality of these tracers should be measured by a single analytical technique. The authors mention and claim various aromatic carboxylic acids as well as aromatic sulfonic acids that have solubilities in aqueous and or oil-based fluids and can be detected at concentrations to about 20 ppb using high-pressure liquid chromatography methods. Examples are of 2,4-dimethylbenzene sulfonic acid; 2,5-dimethylbenzene sulfonic acid; 1-naphthalene sulfonic acid; 2-naphthalene sulfonic acid; 2,6-naphthalenedisulfonic acid; 1,5-naphthalenedisulfonic acid; o-methylbenzoic acid; m-fluorobenzoic acid; p-methylbenzoic acid; methylbenzoic acid; 2,3-dimethylbenzoic acid; and 3,4 dimethylbenzoic acid.

5.7.2 Reactive Tracers. This category of chemical is used to determine OIP and saturation ratios of oil and water in oil and gas reservoirs to determine the needs for waterflooding and various EOR floods. Reactive tracers include *esters* that have very precisely determined hydrolysis rates (Solomons 1992b) for the reaction:



In these tests, a *partially* oil-soluble ester is added to a test oil phase and then flushed into the formation. The well is shut in so that some of the ester can hydrolyze to acid and alcohol. The shut-in time will depend on the bottomhole static temperature and the rate constant for this reaction. The ester and the water-soluble alcohol will partition (*K_i* is the partition coefficient) into the oil phase and the water phase (Fig. 5.66). When the well is then produced, the ratio of the residual ester and the new alcohol in the oil and water phases can be used to determine the amount of connate water and the *S_{or}*.

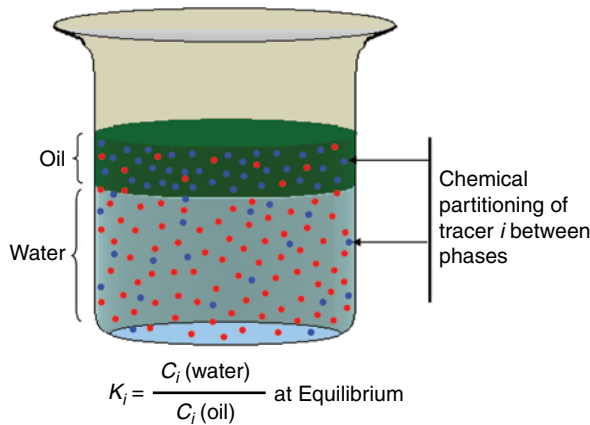


Fig. 5.66—Chemical partitioning of tracers (CTI 2007).

Ester tracers in use include ethyl formate, ethyl acetate, as well as isopropyl acetate (CTI 2007).

A set of return fluid curves are seen Fig. 5.67. From these values, the oil and water phases in the reservoir can be mapped.

Oyemade et al. (2010) describe the use of SW tracer tests in a total of five wells selected for the trial in three different fields across Oman to capture different reservoir settings. The ASP single well completion test aims to confirm the suitability of the ASP process, the potential recovery factor increase, and to mitigate some key risks, mainly injectivity and sweep. The trials are designed to evaluate the remaining oil saturation before and after injection of ASP cocktails to determine incremental oil recovery.

Various challenges were faced in planning the project. Completion challenges because of the age of existing wells/casing, well shape, type of artificial lift, need to produce/inject water, and ASP cocktail from same wells. Water source/tie-in for preliminary flooding also varied in each field. Handling of produced fluids during tests required special attention to avoid destabilizing the production station.

Treatment sequence, equipment layout, and logistic requirements were different for each field. Procedures were developed for each field incorporating chemical preparation and mixing. Fig. 5.68 shows the layout and emphasizes the amount of equipment needed for the tests.

Shiau et al. (2012) describe the use of SWTT to determine S_{or} before and after a pilot treatment using S/P slugs. The tracers include methanol and propanol as nonpartitioned tracers and ethyl formate as the partitioned tracer. Note the choice of the specific ester is determined by the oil solubility and the temperature that controls the hydrolysis rate of the ester during the shut-in time (Shiau et al. 2012).

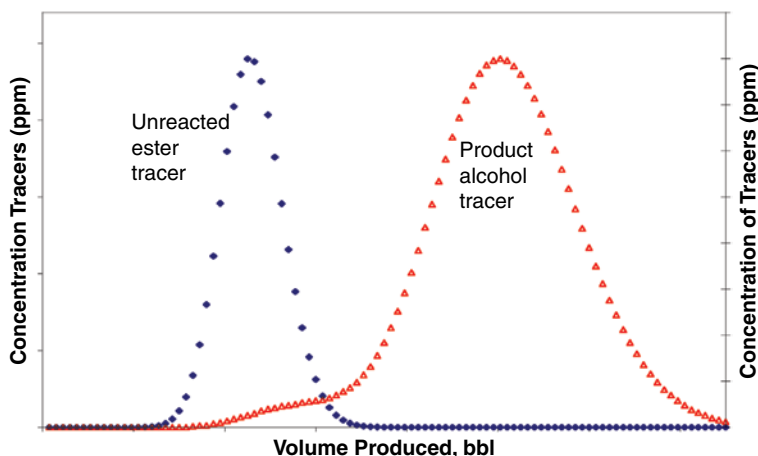


Fig. 5.67—Single well (SW) tracer return profile (CTI 2007).

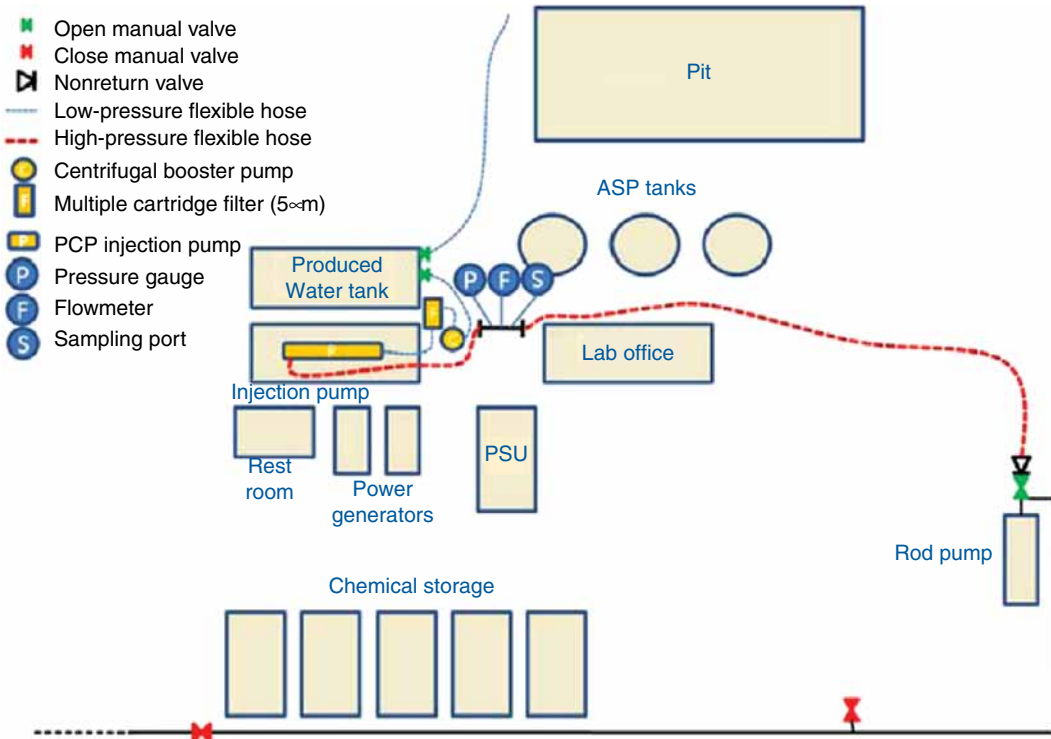


Fig. 5.68—Single well chemical tracer layout (Oyemade et al. 2010).

Fig. 5.69 shows that there was significant partitioning of the ethyl formate into the oil phase before the S/P treatment and much less (all curves together) after the treatment. This indicates that the S_{or} fell from 26–3% and a treatment of the whole reservoir section may recover commercial amounts of oil.

5.8 Case Histories and Best Practices for Chemical EOR

Alkafeef and Zaid (2007) carried out an updated investigation of EOR applications in Kuwait. The investigation employs EOR screening analysis to determine the suitability of EOR processes to mature oil reservoirs. Following the determination of the suitable EOR process, the performed incremental recovery calculations. They also performed a preliminary economic analysis to determine the economic feasibility of the EOR processes in question.

The screening analysis revealed that CO_2 and other miscible processes would have wide applications in these mature oil reservoirs. Polymer, S/P, and alkaline flooding processes would also be widely applicable. In some cases, the polymer and S/P processes were not suitable because of high reservoir temperature. Some of the important oil reservoirs have shown to be suitable for the application of thermal recovery processes, particularly steam injection.

A relatively new injection method known as steam-assisted gravity drainage appears to be viable for enhancing heavy-oil recovery from the oil reservoirs containing heavy oil. These reservoirs are thick fractured layers, which can be good candidates for drilling horizontal wells where injected steam chambers can contact large volumes of oil. The presence of fractures may present a conduit for steam to cover a large volume pore space.

The incremental recovery calculations indicated that the additional recovery is 10–12% for miscible, 4–5% for polymer, and 20–22% for S/P, all of which refer to percentage of OOIP in addition to waterflooding. The fractional recovery caused by the application of steam injection (steam-assisted gravity drainage) could be as high as 50% of the OOIP for the reservoirs containing the heavy oil. The economic analysis revealed that the oil market environment is favorable for the application of EOR processes in Kuwait where reservoirs are thick and contain huge oil volumes.

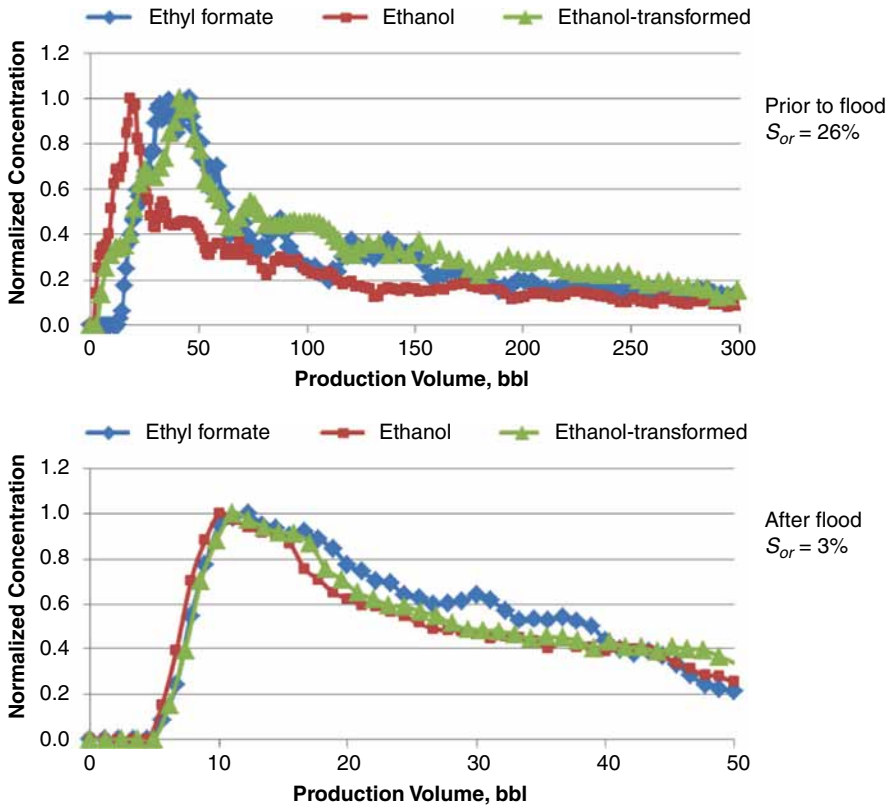


Fig. 5.69—Chromatographic data for partitioning tracers before and after S/P pilot test (Shiau et al. 2012).

Anderson et al. (2006) claim that many pilot tests and several commercial field projects have been performed over the past few decades and have shown that S/P and ASP floods can recover high percentages of residual oil saturation. However, these chemical processes are sensitive to parameters such as chemical slug size and concentrations, salinity, reservoir heterogeneity, and surfactant adsorption among other key parameters. In this study, a sensitivity analysis of these key parameters was performed to optimize a chemical flood design for a mixed-wet dolomite reservoir in the Permian Basin. The simulations were performed using the reservoir simulator UTCHEM, a multiphase, multicomponent chemical flooding simulator. The base case design was developed using a reservoir model provided by the operator, injection and production rate constraints from actual field conditions, brine and oil properties from the field, and chemical properties provided by the EOR laboratory at the University of Texas. An optimum design was selected based on net present value calculated from discounted cash flow analysis. The results of this study showed that chemical flooding this mixed-wet dolomite reservoir is likely to be profitable over a range of crude oil prices based upon the laboratory performance of the S/P flood and the optimum process design determined in this study.

Manrique et al. (2007) present a comprehensive compilation of EOR (gas, chemical, and thermal methods) field experiences in carbonate reservoirs within the US, as an attempt to identify key variables and project design parameters for future evaluation and revitalization of mature carbonate reservoirs.

Carbon dioxide flooding (continuous or WAG) is the dominant EOR process used in the US. This is because of the high availability of low-cost CO₂. CO₂ EOR in particular represents the logical first step toward viable geologic carbon storage and sequestration. EOR chemical methods in carbonate reservoirs, especially polymer flooding, have been widely tested in US carbonate reservoirs. However, EOR chemical methods have made a marginal contribution, relatively, in terms of total oil recovered.

Alvarado and Manrique (2010) claim that HC gas injection (continuous or in a WAG mode) continues to be the preferred recovery process in offshore fields, gas condensate reservoirs, or fields in

remote locations without access to gas markets. N_2 -EOR projects seem to be in decline except in the Bay of Campeche in Mexico because of the availability of vast installed N_2 -generation capacity.

CO_2 injection is getting most of the attraction as an EOR method and potentially as a sequestration strategy in recent years. However, CO_2 -EOR projects in operation are mostly concentrated in the US (especially in the Permian Basin) and associated to natural sources of CO_2 . CO_2 -EOR/sequestration projects are not expected to grow in the near future until industrial sources of CO_2 are produced at much lower costs and the proper regulatory framework is in place. Chemical EOR methods have made a relatively small contribution to the world's oil production during the last decades. China is the country with the largest oil production coming from chemical EOR projects. However, there are an increasing number of ongoing and planned SP and ASP evaluations at pilot scale, especially in Canada, and the US polymer flooding is gaining interest for heavy crude oil reservoirs (i.e., Canada) and offshore fields. However, chemical EOR is not expected to impact world's oil production for at least 2 decades, if it is ever implemented at commercial scales. The combination of conformance technologies (gel treatments) to improve injection profile and sweep efficiency with chemical EOR flooding, such as CDG, SP, or ASP, is starting to gain more interest from operators in South America and the US based on El Tordillo Field's successful experience in Argentina. Despite the growing research interest on chemically assisted methods (e.g., spontaneous imbibition, wettability modifiers, and (interfacial surface tension reductions) and SP flooding to improve oil recoveries in carbonate formations, these projects are not expected to impact global oil production in the near future.

5.9 Things to Think About

- EOR is being reborn after a long pause because of low oil prices. Building on the large legacy of technologies invented, developed, and pilot-tested during the 1970s–1990s, new technologies are being applied to give longer life to many older reservoirs that may still have 50% OOIP.
- The basic physical parameters are well understood and involve both macro- and microreservoir characteristics.
 - Volumetric sweep \times Displacement efficiency = overall oil recovery
 - Areal sweep \times Vertical sweep = volumetric sweep
 - Areal sweep depends on the fluid mobility, pattern type, heterogeneity, and total volume of fluid injected
 - Vertical sweep is governed by vertical heterogeneity, gravity segregation, fluid mobilities, and total fluid injected
 - Displacement efficiency is a function of injection rate, viscosity, density, and IST of displacing fluid
- The various physical-chemical parameters that control recovery are modified by injecting various chemicals that include physical sweep agents (gases and water) and solvents (CO_2 and various low MW HCs). Water-soluble polymers act as diverting agents, and surfactants will affect the IST and form temporary MEs to dissolve the oil. Some of these surfactants produce foams and with polymers and other diverting agents act to control the mobility of the sweep fluids. At the time of this book, CO_2 floods are the most used chemical EOR method (in North America) because of relative low cost and availability of CO_2 and possible sequestration credits.
- More complex chemical floods, especially ASP combination floods, are benefiting from the development of new surfactants as well as the physical-chemical models needed to design the floods.
- It is also understood that the injection of chemicals not naturally in the matrix (including the injection water) will fundamentally alter the chemical reactions occurring in the formations. Hopefully (with good planning), additional HCs will be extracted at an economical rate. However, the operators must plan for the unwanted consequences that include corrosion, differing scale minerals, and a dramatic decrease in the O/W ratio. The disposal of the unwanted phases must be a major part of the plan.
- Various active and passive chemical tracers are in use to determine the oil and water saturation values and to track the movement of the phases in the reservoir.

Chapter 6

Health, Ecology, and Safe Handling of Treating Chemicals and Produced Fluids

There are four interrelated issues concerning the handling and use of chemicals in the production environment that will be reviewed in this chapter. They are

1. The *health and safety* of all persons who may be exposed to the chemicals that are being used, including the reaction products and waste streams. These concerns and possible solutions are described in Section 6.1.
2. The *effects* of the chemicals and reaction/waste products on organisms in any environment, which may be impacted by the use of the chemicals. See Section 6.2.
3. The plans and techniques to *safely dispose/reuse* of the chemicals and wastes, including methods for recycling the chemicals and the water used to generate them, are described in Section 6.3.
4. *Emergency* plans/operations for control of spill also must be considered in each production phase and are described in Section 6.4.

These activities and technologies are interconnected; however, it is useful to consider them separately because they are primarily associated with different parts of most jobs.

6.1 Safety Considerations During Production Enhancement Operations

These issues are related to mechanical hazards as well as chemical hazards and are chiefly associated with human contact with chemicals and equipment during the storage, transport, and execution of a treatment. As such, contact with the treating chemicals is mostly a concern for the employees and contractors of the treating companies and the employees and contractors of the wellsite owners. Public exposure to chemical hazards also must be considered, but these issues usually are associated with waste products of the treatments and will be described in Sections 6.2 and 6.3. Chemical hazards to personnel are a result of the inherent chemistries of the individual products as well as the final formulations and the produced fluids. Methods to *plan for* and to *reduce* hazards are also considered in Sections 6.2 and 6.3.

Direct exposure to chemicals can affect people through contact with the skin, eyes, and inhalation, and by ingestion. The *toxicity* of most chemicals in use have been determined through lab-type animal tests (Frenier 1996), but the data is mostly associated with ingestion or inhalation of the chemical. At the wellsite, acute hazards caused by *contact* (chemical burns) are the most frequent source of concern, but people who handle large amounts of chemicals (such as bulk plant operators) must be concerned with long-term and delayed effects caused by periodic contacts.

Inhalation of toxic gases such as H_2S and CO_2 also must be considered, and testing equipment, breathing support, and wind direction indicators should be available at the job site and at the mix plant. H_2S may come from the well either because of FeS reacting with an acid or because of released well fluids. CO_2 could come from the well or from the treating equipment as part of a foam job, “energized” fluid treatment, or an enhanced oil recovery (EOR) treatment. This gas is not highly toxic but will exclude oxygen and may thus cause asphyxiation. Both of these gases are heavier than air and will accumulate in low spots at the site such as the mud/waste pit. N_2 liquid (a very cold fluid) or compressed gas may also be present. Very large quantities also could cause asphyxiation, but it is slightly lighter than air [density of air at standard temperature and pressure is 1.292 kg/m^3 and the density of nitrogen is 1.251 kg/m^3] and usually would not cause problems unless it entered an enclosed space such as a van or an enclosed wellsite structure.

The *reactive* hazards of some chemicals during transportation, on-site, and during and after a treatment also should be controlled. Many treating chemicals (as well as the well fluids) are flammable or combustible. The flash point (described in Section 6.2) is the major metric for determining flammability hazards. Some other oilfield chemicals contain oxidizing agents that could potentially react (explode or cause a fire) if they are exposed to organic compounds (including fuels and other organic materials on-site). Storage and handling practices must be in place to prevent this contact until the oxidizers are needed. Other chemicals, such as HCl or $NaOH$ are *corrosive* to metals, human flesh, as well as to other materials and thus, may damage them if contact is made.

Material Safety Data Sheets (MSDSs) are the major document for communicating chemical safety risks to all personnel on the rigsite or at a supplier’s area and during transit (Department of Transportation hazard placards also are required on transport vehicles). A book of MSDSs for all of the on-site chemicals or other compilations (such as digital/internet) should be available and used as part of the planning and on-site safety meeting. The first page and an interior page of a MSDS for HCl are seen as Fig. 6.1. These documents may run to as many as 10 pages, so only a small set of the data are reproduced in this figure. These documents contain health, safety, and toxicity information of every chemical on-site. An important part of the document is the list of personal safety equipment (PSE) that is needed to safely handle the chemical. A list of typical safety equipment includes

| SAFETY DATA SHEET (USA) (Complies with USA OSHA 29 CFR 1910.1200 and ANSI Z 400.1) | | | Product Code: H036 | Revision date: 09 May 2012 |
|---|-------------------|---|--|----------------------------|
| Version: 3 Revision date: 09 May 2012 | | | Hazardous polymerization: Hazardous polymerization does not occur. | |
| 1. IDENTIFICATION OF THE SUBSTANCE/PREPARATION AND THE COMPANY/UNDERTAKING | | | Shelf life - (years): 10 | |
| Product Code: H036 | | | Other Information: Gives off hydrogen by reaction with metals. | |
| Product Name: Hydrochloric Acid 36% Uninhibited H36 | | | 11. TOXICOLOGICAL INFORMATION | |
| Use of the Substance/Preparation: | | | PRODUCT TOXICOLOGICAL INFORMATION | |
| Company Identification: Your Chemical Company | | | Acute Health Hazard | |
| Emergency Telephone Number: | | | Eye contact: Corrosive. Rapidly causes pain, burns, corneal injury. May cause permanent damage and blindness. | |
| 2. HAZARDS IDENTIFICATION | | | Skin contact: Corrosive. Rapidly causes pain, burns, redness, swelling and damage to tissue. | |
| EMERGENCY OVERVIEW DANGER Main physical hazards: Corrosive to metals Main health hazards: Corrosive to tissue. Causes severe eye burns. Causes severe skin burns. Causes burns to respiratory tract. Causes burns to mouth, throat and stomach. Other Information: Gives off hydrogen by reaction with metals. Precautions: Keep away from heat. Wear suitable protective equipment. Avoid contact with eyes. Do not breathe vapors or spray mist. Do not get on skin or clothing. Wash thoroughly after handling. HMIS classification: Health: 3 Flammability: 0 Physical hazard: 1 Form: Liquid (fumes) Color: Colorless - Lightyellow Odor: Pungent Principle routes of exposure: Skin contact. Eye contact. Inhalation. | | | Ingestion: Corrosive. causes pain and severe burns to mouth, throat and stomach. | |
| | | | Inhalation: Corrosive. Short exposure can injure lungs, throat and mucous membranes. Causes pain, burns, choking and coughing. | |
| | | | Sensitization-lung: Not known to cause allergic reaction. | |
| | | | Sensitization-skin: Not known to cause allergic reaction. | |
| | | | Toxicologically synergistic Products: None known. | |
| | | | Other Information: Prolonged exposure at low concentration may cause erosion of the teeth. | |
| | | | Chronic Health Hazard | |
| | | | Carcinogenic effects: None known. | |
| | | | Mutagenic effects: Not known to cause heritable genetic damage. | |
| | | | Teratogenic effects: Not known to cause birth defects or have a deleterious effect on a developing fetus. | |
| | | | Reproductive toxicity: None known to adversely affect reproductive functions and organs. | |
| | | | Target organ effects: See COMPONENT TOXICOLOGICAL INFORMATION below. | |
| | | | COMPONENT TOXICOLOGICAL INFORMATION | |
| Component | | Target Organ effects | LD50/LC50 | |
| Hydrochloric acid | | skin, eyes, respiratory system | 3124 ppm (Inhalation LC50: Rat) 1 h 5010 mg/kg (Dermal LD50: Rabbit) 700 mg/kg (oral LC50: Rat) | |
| Component | IARC Group 1 or 2 | ACGIH-Carcinogens | OSHA Listed Carcinogens | NTP |
| Hydrochloric acid | — | A4 - Not Classifiable as a Human Carcinogen | — | — |
| | | | 12. ECOLOGICAL INFORMATION | |
| | | | PRODUCT INFORMATION | |

Fig. 6.1—MSDS HCl .

- Hard hats
- Appropriate eye protection
 - Safety glasses with side shields
 - Chemical goggles
- Face shields
- Hearing protection
- Flame/chemical-resistant clothing
- Respirators/air packs
- Steel-toe/chemical-resistant boots
- Chemical-resistant gloves

Brown et al. (2000) have provided a list of safety considerations required during hydraulic fracturing operations that also should apply to any rigsite application of chemicals. They note that at no time should the safety aspects of a treatment be compromised. Safety guidelines have been developed from experience derived from *previous incidents/accidents*. Many of these incidents have had great potential to seriously injure personnel or destroy valuable equipment. The inherent risk of dealing with high pressures can be greatly minimized by following simple safety procedures. Therefore, hydraulic fracturing and other wellsite treatments can never be considered a success if an accident results in the destruction of equipment or injury to personnel.

- PSE—each person on location should wear appropriate safety equipment to minimize the risk of personal injury. Hard hats, hard-toed shoes, and safety glasses should be the minimum level of safety equipment worn on location. Other equipment such as hearing protection, goggles, fire-retardant fabrics, and filter masks should be worn if exposure to the conditions they protect against is a possibility. Wearing safety equipment is a simple step that creates a positive safety atmosphere on location. The minimum personal PSE is noted on the MSDS (Fig. 6.1); however, individual contractors and wellsite owners may have requirements that are more comprehensive.
- Safety meeting—holding a pretreatment safety meeting ensures that all personnel on location are aware of specific dangers and required procedures relative to the treatment. Each person on location should clearly understand his or her role during the treatment as well as individual responsibility during emergencies. A head count must be taken to account for everyone on location. An escape route and meeting place should be agreed upon where all personnel will gather in the event of an emergency. Personnel who are not directly involved in the treatment should have limited location access during the actual pumping operations. Everyone should be aware of the unique dangers of each treatment. Some locations may be in an area with hydrogen sulfide (H₂S) or possibly the fluids being pumped are highly flammable. Frequently, the rigsite will have windsocks to indicate the wind direction, so people can evacuate if needed in a direction opposite to or perpendicular to the indicated wind direction.

As many of the potential safety problems or concerns as possible should be brought to the attention of everyone. Maximum pressure limits should be set at this time, and every high-pressure pump operator must be aware of these limits. Instructions for pressure testing the treating iron must also be covered. The high-pressure treating line, up to the wellhead valve, should be tested to slightly above the anticipated fracturing pressure. A properly tested line includes tests of each pump in addition to the main treating line. The pressure rating of the wellhead should be checked to make sure it exceeds the treating pressure. If the wellhead has a lower pressure rating than the anticipated treating pressure, a wellhead isolation tool (aka the tree saver) will be necessary to isolate the wellhead from this pressure level. The pretreatment safety meeting is the principal communications to all personnel. A well-organized safety meeting helps ensure that the treatment is an operational success without being a threat to human safety. The safety meeting should be a part of the preoperational planning document and should include operator personnel so all communications are in place.

- Well control at the wellhead—to ensure that well control is always maintained, the valve arrangement at the wellhead should consist of at least two valves. A frac or master valve should

be installed above the main wellhead valve. If one valve fails to hold the pressure, the other valve can quickly be closed to control the well. It is preferable to have the main wellhead valve flanged to the casing head, rather than using a threaded connection. If a threaded connection is necessary, the condition of the threads must be thoroughly inspected for thread wear and proper taper.

- Precautions for flammable fluids—Note the MSDS, as well as the company manuals handling on the well fluids. Oil-based fluids should be tested for volatility before they are accepted as a fracturing fluid. An oil is generally considered safe to pump if it has a Reid vapor pressure less than 1, API gravity less than 50°, and open-cup flash point of 10°F [−12°C]. However, even if the fluid is considered safe to pump, several additional safety rules should be followed when pumping oil. Storage tanks for flammable fluids should be diked and spotted at least 150 ft from the wellhead. Many other treating chemicals may have low flash points and may be flammable. Any fluid that contains any alcohol may be flammable. Spotting the fluids in this manner helps minimize exposing the wellhead to fire if problems occur during pumping. Also, all low-pressure hoses should be enclosed in a hose cover to prevent oil from spraying on hot engine components of the trucks, should a hose leak. Care must be taken to ensure that there is no smoking on location. It is a good idea to have all personnel check matches and lighters when they arrive on location to prevent them from unintentionally lighting up. Finally, fire-fighting equipment should be on location and ready to be operated. In this way, a small fire may be contained before it has a chance to spread and become a major disaster. To further reduce the risk for an on-location fire, equipment should be both bonded and grounded. Bonding forms an electrical conduit between vessels containing flammable fluids and the equipment that transfers this fluid and pumps it. It ensures that the electrical potential from electrostatic buildup is controlled between all of the units handling the flammable fluid. Grounding controls the electrostatic buildup between the equipment and the ground. When bonding and grounding are combined, it ensures that all points between the wellhead and each piece of equipment are all at the same potential and that any static electricity generated during the operation is dissipated without the possibility of a static discharge.
- Precautions for energized fluids—N₂ and CO₂ are the gases most commonly used in foamed and energized fluids. During flowback following a treatment, they provide an efficient source of concentrated energy to aid rapid, more complete post-treatment cleanup (see Sections 3.7.3, 4.5.5, and 5.6.3). There are potential hazards associated with the use of N₂ and CO₂. As the fluid exits the flowline during flowback, the gaseous phase expands rapidly. This rapid release of energy must be controlled to avoid a loss of flowback efficiency and to ensure personnel safety. Service companies have recommended procedures for the flowback of energized fluids. Another potential hazard that is often overlooked is asphyxiation. N₂ and CO₂ can collect in low areas, displacing breathable air. Personnel should avoid these areas and remain upwind at all times. The use of remotely operated valves will increase the margin of safety.
- Environmental considerations—fracturing and other treatment operations should be conducted using sound environmental practices to minimize the potential for contamination of air, water, and soil. All operations should comply with all applicable environmental laws and regulations. Hazardous material spills should be cleaned up quickly in accordance with a spill plan. All waste and unused materials should be handled and disposed of in accordance with locally approved regulations. More details of exotoxin management and waste disposal are in the next three major sections (6.2, 6.3, and 6.4).

The authors of this book note that these items are *not* to be used as standards, but as common sense considerations based on their experiences. The legal and regulatory aspects of safety and exotoxin managements vary by state, country, and area, and are continually evolving and beyond the scope of this book.

An *API RP 54* (1999) recommended practice is available, that covers all of the items described previously (and others such as job site setup) in significant detail. The main items in the RP Table of Contents are listed here:

1. General
2. References
3. Definitions
4. Injuries and First Aid
5. Personal Protective Equipment
6. Operations
7. Fire Prevention and Protection
8. Flammable Liquids
9. Drilling and Well Servicing Rig Equipment
10. Drilling and Well Servicing Rig Electrical Systems
11. Pumping Units
12. Special Services
13. Stripping and Snubbing
14. Drillstem Testing
15. Acidizing, Fracturing, and Hot Oil Operations
16. Cementing Operations
17. Gas, Air, or Mist Drilling Operations
18. Hot Tapping and Freezing Operations
19. Hot Work, Welding, and Flame Cutting Operations

Several articles on safety are noted. Arceneaux and DeKerlegand (2009) claim that large-volume sand control and reservoir stimulation methods in the offshore market require connecting a heavy, low-yielding flexible hose (Coflex) from the service company stimulation vessel to the drilling rig or platform. From there, it is typically connected to rigid high-pressure treating line routed to a manifold. The use of a flexible hose anchoring point pre-installed on the rig greatly reduces exposure to accidents by eliminating dangerous chaining-up methods to secure the hose to the rig. This device may remain on the rig for future pumping events. The use of a flexible hose rig-anchoring point provides an engineered solution to reduce human, hands-on interaction when securing the treatment hose to the rig before a sand control or stimulation pumping event. Pinch points for hand and foot interactions are eliminated.

Placing workers in precarious situations on the outboard of the rig's handrail, high above the water surface, is prevented by use of a "drop-in and lock-in" landing plate that supports the flexible hose and its connection flange in a vertical position. This process saves time by eliminating repositioning measures when having to secure the flexible hose to some fixed object on the outboard side of the rig such as handrail posts or mooring cleats using chains.

Mcilroy (2009) describes a program that calculates the direction/concentration of toxic gases such as H₂S that may be evolved from activities at a wellsite. This program could be used in the case of a release during production operations to warn local communities of a gas release.

6.2 Health, Safety, and Environmental (HSE) Management

Developing green, low-toxicity formulations or less hazardous chemicals has become the goal of many formulators; however, there is not total agreement (Gupta 1998) on what is green chemistry, even though many proposed green formulations are shown in Sections 2.4.4, 3.5.5, and 4.4 as well as other sections (based on their authors' assessments). Darling and Rakshpal (1998) of the US Environmental Protection Agency (EPA) defines green products as "pollution prevention at the molecular level, designed to reduce or eliminate the use or generation of chemicals that are hazardous to human health or the environment." The authors of this book will use this definition where possible, but many of the references cited define green in relationship to more limited criteria, such as a particular governmental regulation or list of regulations. Some of these are listed in Section 6.2.1, as well as in Chapter 1 of Kelland (2009).

6.2.1 Chemical Selection To Enhance HSE Compliance. Developing, achieving, and managing an effective HSE program must start at the beginning of any chemical-related project. A Department of Energy (DOE) report from an industry/government committee (Deutch et al. 2011) agrees with this

assessment and notes that two of the major recommendations for safer shale gas production includes replacing diesel oil from all fracturing formulations (Sections 4.2.1 and 4.3.1) as well as disclosing most components of the mixtures.

A major oil service company (Purinton and Manning 1996) described a quantitative assessment of HSE impacts of prospective new well production chemicals that includes four areas of concern. The program (Purinton and Manning 1996) considers the following criteria (with scores in parenthesis).

The total scores are added and the worst (with the highest scores) products are then slated for elimination or modification. The four areas of concern are listed as follows and under them are the specific items that are evaluated or tested. Note that this program was developed in the mid-1990s and some of the individual control items may have changed; however, the methodology can be used with appropriate updates. The four areas for consideration are listed.

1. Global “Restricted Use” Considerations—this consideration notes if the product and its components are listed on any of the following:

| | |
|---|-----|
| EU controlled substances | (4) |
| EU land-banned material | (4) |
| North Sea banned list | (3) |
| Organohalogens (nonpolymeric) | (4) |
| CERCLA/CWA hazardous substance table 302.4 with RQ 100 lbm or less | (3) |
| Environmental Protection Agency extremely hazardous materials | (3) |
| Carcinogenic, mutagenic or toxic to reproduction substances | (3) |
| Marine pollutants | (2) |
| Resource Conservation and Recovery Act waste code U or P | (4) |
| CA Prop 65 | (2) |
| Priority Pollutants Clean Water Act 2010 | (4) |
| Process safety management chemicals list | (4) |
| Arms Control and Disarmament Agency schedule (arms control subs) | (2) |
| US Health Department Annual Carcinogen Rep | (3) |
| Toxic metals list | (4) |
2. Physical/Chemical Properties—an assessment then gives scores for physical and chemical properties are based the following values.

Flammability based on flash point:

| | |
|----------------------|-----|
| >141°F (60.5°C) | (0) |
| 73–141°F (23–60.5°C) | (1) |
| 10–73°F (–12–23°C) | (2) |
| < 10°F (–12°C) | (3) |

If a Flammable Solid, scores (Yes = 2, No = 0)

Corrosivity:

| | |
|--------------------|-----|
| pH = < 2 or > 12.5 | (2) |
| 2–12.5 | (0) |

Reactivity: Reactivity scores are based on the material’s NFPA rating (0–4) or if the material’s product structure has an energy containing functional group. If yes, score = 3, if no, score = 0.

3. Environmental Screening—three parameters are evaluated under environmental screening: biodegradation, bioaccumulation, and toxicity. Ecotox scoring is based on the following values:

Biodegradation:

28-Day oxygen depletion test:

| | |
|---------------------------------|-----|
| Very low biodegradation (< 20%) | (3) |
| Low biodegradation (20–70%) | (2) |
| High biodegradation (> 70%) | (0) |

Bioaccumulation:

| | |
|-----------------------------------|-----|
| Log $P_{O/W}$ > 3 and MW < 600 | (2) |
| Log $P_{O/W}$ < 3 and/or MW > 600 | (0) |

Toxicity:

| | |
|----------------------------|-----|
| EC ₅₀ 1 mg/L | (4) |
| LC ₅₀ 1–10 mg/L | (3) |
| 10–100 mg/L | (2) |
| >100 mg/L | (0) |

4. Exposure Hazards—Assessed are exposure hazards using the following data sources and data provided on vendor's MSDSs. The testing procedures and nomenclature was described by Frenier (1996):

- Registry of toxic effects of chemical substances
- MDL, Haward, California MSDS database
- CCINFO MSDS database
- Other resources as applicable

Score assignments are as follows:

Inhalation:

| | | |
|---------------|---------------------|-----|
| Highly toxic: | LC50 < 0.5 mg/L | (4) |
| Toxic: | 0.5 < LC50 < 2 mg/L | (3) |
| Low-toxic: | LC50 > 2 mg/L | (0) |

Ingestion:

| | | |
|------------------|-----------------------|-----|
| Extremely toxic: | LD50 < 5 mg/kg | (4) |
| Highly toxic: | 5 < LD50 < 50 mg/kg | (3) |
| Toxic: | 50 < LD50 < 500 mg/kg | (2) |
| Low-toxic: | LD50 > 500 mg/kg | (0) |

Skin absorption:

| | | |
|---------------|-----------------------|-----|
| Highly toxic: | LD50 < 40 mg/kg | (4) |
| Toxic: | 40 < LD50 < 200 mg/kg | (3) |
| Low-toxic: | LD50 > 200 mg/kg | (0) |

Carcinogen: If the product or its components are classified, the following International Agency for Research on Cancer group rating (or equivalent rating from other agencies):

1 = 4, 2A = 3, 2B = 2, 3 or none = 0

If the product or its components is a mutagen: Yes = 2, No = 0

The assessment process will score the potential product and will attempt to produce a product with the lowest overall score. A score of zero is the goal. This initial assessment probably will not be the final consideration of toxicity. If the material is to be used in North Sea countries, or if the material is not registered in various potential use countries, additional testing may be required.

Jenkins (2011b) has provided a review of the current UK offshore regulations and the protocols for screenings. See **Fig. 6.2** for a diagram of the harmonized mandatory control scheme (HMCS). This chart takes the investigator through the steps to determine if additional data is needed before a new chemical can be introduced. The acronyms in the chart are keyed to the glossary of this book and are explained by Jenkins (2011).

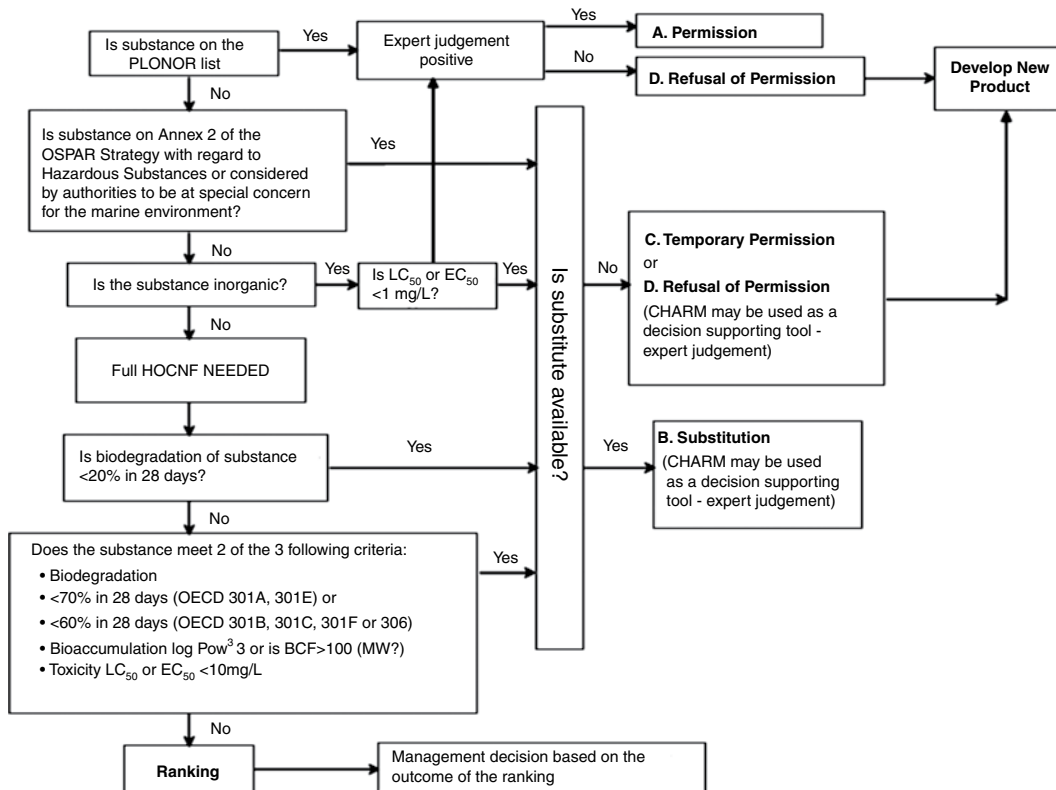


Fig. 6.2—Harmonized mandatory control scheme (HMCS).

Intense interest in green chemistry or other HSE issues is a recent phenomenon. At the European Symposium on Corrosion Inhibitors 6 in 1985, there were no papers with toxicity or green in the title (even though some described lower-toxicity materials). Also, the first NACE International Symposium considering green inhibitors was held in 1995. Since then, additional NACE symposia were held in 1998 and 1999. Likewise, many of the papers at European Symposium on Corrosion Inhibitors 7 (1990) and 8 (1995) were concerned with toxicity or environmental concerns. The patent literature also has started to describe formulations in which toxicity values or environmental improvement are the subject of the major claims of the inventors. Today, most articles or presentations involving corrosion inhibition and other oilfield chemicals have some mention of an HSE type of assessment or concern. Clearly, HSE or green concerns are hot-button issues.

Many additional HSE-related conferences have been held within the oil and gas production chemicals community (especially papers presented in the Formation Damage and Oilfield Chemical symposia) and SPE frequently holds conferences such as the SPE International Conference on HSE in Oil and Gas Exploration and Production, 12–14 April 2010, Rio de Janeiro, Brazil, that cover a wider range of HSE issues.

There are additional ways to look at development of new chemicals. Jordan and Feasey (2008) provide a summary of industry chemical activities. They contend that production chemical development should focus on the development of new chemicals that have higher activity but lower viscosity than currently used chemicals, hence allowing deployments at colder temperatures and over longer distances. HSE issues are also affected by these considerations. Fig. 3.73 shows the principle factors that have an impact on the selection of suitable scale, wax, and hydrate inhibitors for a subsea application according to these authors.

The chemical and physical properties of importance:

- Physical properties
- Fluid compatibility

- Ability to monitor
- Material compatibility, including corrosion of metals
- Cost/performance characteristics
- Application, including injection and sampling
- Effects of system conditions including temperature and viscosity
- Compatibility with brine and hydrocarbon fluids

Willmon and Edwards (2006) have reviewed chemical-injection issues and conclude that they can be safely and successfully managed in new (deepwater) projects by proper fluid characterization and risk assessment; a field-development strategy that includes design, specialty treating chemicals, and operating plans; the involvement of specialists and specialty providers; and training and communication. These functions include

- Exploration—collected bottomhole samples are used for fluid characterization and risk assessment of any flow-assurance issues. From these initial data, prevention, and mitigation strategies, including but not limited to chemical inhibition, are developed. Chemical products can be developed and/or screened for effectiveness and applicability from this initial assessment. This includes performance screening, chemical/chemical-compatibility testing, chemical/material-compatibility testing, and product stability (which are particularly important for umbilical applications).
- Facility design—Specifications for the processing system and equipment are detailed; materials of construction are screened for chemical and fluid compatibility, volume, and deliverability requirements are determined; and the chemical-injection systems are designed.
- Facility construction—Monitoring and oversight throughout the construction process are performed to maintain the integrity of the initial design.
- Operational strategies—Strategies will be developed that address initial flowback, startup, steady-state, and shut-in techniques.
- Logistic strategies—Strategies will be developed that address logistical concerns (e.g., product transfers and handovers).
- (Pre) startup commissioning and testing of equipment—Cleanliness and operability of the system are an absolute must. The chemical day tanks and injection lines are flushed to specification.

Hill et al. (2003) have provided more details on a process for development of more environmentally acceptable products. This requires working with regulatory agencies, clients, and chemical suppliers to achieve regulatory compliance for MSDS, labels, and environmental testing protocol. The paper recognizes that international environmental statutes and guidelines combined with clear corporate goals to minimize environmental impact are key requirements in regulating industrial use and discharge of environmentally harmful chemicals. The development of more environmentally acceptable products requires a thorough screening of environmental fitness and status of compliance with relevant laws and regulations.

Details are given by Hill et al. (2003) on the aggressive programs developed to address a wide range of environmental opportunities and issues. International environmental statutes and guidelines are the strongest driving force to restrict industrial use and discharge of environmentally harmful chemicals. The primary tool of environmental risk reduction is an aggressive product development program incorporating more environmentally friendly chemical solutions. The critical impact of HSE activities and considerations are present in each step of the product development process. See Fig. 3.74. This represents an update of the program developed by Purinton and Manning (1996).

The authors of this book have noted (Section 3.6) that oilfield chemicals have primary active ingredients that may be harmful if discharged into the environment, as well as other additives to an on-site formulation. Improving the characteristics of these products to reduce risk or damage to marine life requires changes in previously acceptable products, such as elimination of restricted materials and incorporation of components with improved ecotoxicity values. Note that HSE issues are a major concern for the use of kinetic hydrate inhibitor and anti-agglomeration type low-dose hydrate inhibitor chemicals, especially in the North Sea operations area. See Kelland et al. (1995) and Del Villano et al. (2008).

Kelland (2009) begins his book with a chapter on selection of chemicals and especially environmental issues associated with the European Convention for Protection of Environment regulations for use of production chemicals in the northeast Atlantic (and North Sea) region. This chapter has 54 references.

6.2.2 HSE Concerns With Tight Gas Production and Other Fracturing Processes. With the development of fracturing methods that can be applied to tight shale, the concerns about exposures to production chemicals has increased because many of the wells are now located near populated areas and could affect groundwater supplies (Kell 2009) and expose the public to other hazards (flowback, vehicle traffic). While tight gas fracking (at the time of the publication of this book) is a very public issue, the chemicals in any production enhancement technique can cause similar concerns.

Also, the amount of water used and the ultimate disposal have been major issues. This will be discussed in much more detail in Sections 6.3.1 and 6.4. An additional concern is the possible loss of methane (a powerful greenhouse gas) to the atmosphere during the drilling and production processes. Beckwith (2011b) has reviewed the issue and concluded that the major dispute between the studies' findings (reviewed in her report) revolves around the data quantifying methane emissions and the methodologies used to make emissions estimations. As stated in the study, obtaining good data presents logistical challenges. However, she also concludes that preventing gas emissions makes good economic sense.

Hess (2010) claims that concerns about the frac water include the biocides and scale control chemicals. This article also notes that nondisclosure of formulation chemicals is also one of the public issues. To try to alleviate this type of concern, Chesapeake (2010) has listed the chemical in a proposed deep Haynes shale frac fluid (see Table 4.1) along with other uses for the chemicals. Many more details of frac chemicals and additives were reviewed in Chapter 4 of this book. Table 4.4 also lists ingredients for a generic shale frac fluid from Schlumberger (2010d).

API (2009) describes environmentally sound practices, including reclamation guidelines for domestic onshore oil and gas production operations. It is intended to be applicable to contractors as well as operators. Facilities within the scope of this document include all production facilities, including produced water handling facilities. Offshore and arctic areas are beyond the scope of this document. Operational coverage begins with the design and construction of access roads and well locations, and it includes reclamation, abandonment, and restoration operations. Gas compression for transmission purposes or production operations, such as gas lift, pressure maintenance, or EOR is included. This recommended practice lists many of the hydraulic fracturing chemicals noted in Sections 4.3 and 4.3.5.

This API (2009) has sections on chemical selection as well as water selection, sources of water and site construction and well construction and design to protect groundwater. See [Fig. 6.3](#) that describes well construction with the goal that the wells are drilled below the potable water zones and isolated by impermeable formations. The well construction, especially selection of the cement formulation (Nelson and Guillot 2005) to prevent gas migration is critical because any pipe that extends into the gas zone may provide a channel for gas migration into any of the zones penetrated (energyNOW! 2011).

A report developed from Waxman et al. (2011) of the US House of Representatives was able to obtain usage data on potentially toxic chemicals that were used from 2005–2009 in some fracturing fluids in the continental US. What is significant about this report is that information was received from 14 different fracturing service providers. This included the large multinationals as well as much smaller suppliers. The companies pumped more than 2,500 hydraulic fracturing products containing 750 chemicals and other components. Overall, (the report claimed) that these companies used 780 million gallons of hydraulic fracturing products—not including water added at the wellsite. The authors of this book note that many of the products may be the same or similar, but have different company trade names. The primary source of information on the individual chemicals was obtained from the MSDS, which is not required to list all ingredients.

The toxic chemical that was identified most frequently by Waxman et al. (2011) was methanol, followed by IPA, 2-butoxyethanol, and ethanol glycol. Note that all of these chemicals are solvents or coupling agents and are part of many other formulations such as inhibitors and surfactant packages.

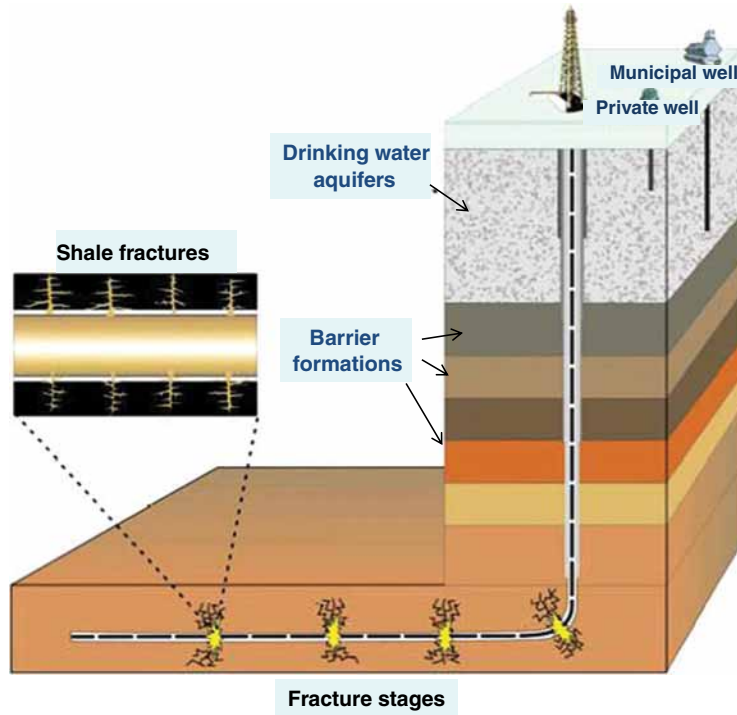


Fig. 6.3—Horizontal well in shale zone to protect ground water (HFF 2010).

Light petroleum distillates that contain benzene, toluene, or xylene also may be in the mixture of chemicals used in various stages of a treatment. These chemicals (as well as a few others) are known carcinogens. The report was not able to estimate the actual pounds of these chemicals that were pumped, so the potential for ecological damage or contamination of groundwater was not assessed. The conclusions that the formulation developers should remove toxic materials from all injected fluids are clear. This action, along with transparency of the formulations themselves may reduce public and governmental concerns with fracturing for gas and oil production.

One other observation of the report was that a significant percentage (about 15%) of the service providers who gave information, do not develop their own chemicals and thus are dependent on suppliers for all of the safety/toxicological information. The report gives the impression (conclusion of the authors of this book) that these operators may have little knowledge of the safe handling of toxic chemicals. One of the service providers is quoted that it “does not have any information in its possession about the components of such products beyond what the distributor of each product provided to—in the MSDS sheet.” The authors of this book contend that lack of adequate training on the operation of wellsite treatments as well as lack of understanding of the complex chemicals, may exacerbate the risks of the treatments.

A very detailed study by Groat and Grimshaw (2012) was performed, and it looked at hazards caused by fracturing including

- Drill pad construction and operation
- Hydraulic fracturing and flowback water management
- Groundwater contamination
- Blowouts and house explosions
- Water consumption and supply
- Spill management and surface water protection
- Atmospheric emissions
- Health effects

The following conclusions were proposed:

1. Natural gas found in water wells within some shale gas areas (e.g., Marcellus) can be traced to natural sources and probably was present before the onset of shale gas operations.
2. Although some states have been proactive in overseeing shale gas development, most regulations were written before the widespread use of hydraulic fracturing.
3. Media coverage of hydraulic fracturing is decidedly negative, and few news reports mention scientific research related to the practice.
4. Overall, surface spills of fracturing fluids pose greater risks to groundwater sources than from hydraulic fracturing itself.
5. The lack of baseline studies in areas of shale gas development makes it difficult to evaluate the long-term, cumulative effects and risks associated with hydraulic fracturing.

As the unconventional gas shale market gained momentum in the mid-2000s, individual states began adopting new rules to regulate this booming business activity. Since 2010, pumping service companies began disclosing chemical components used to formulate stimulation fluids to their oil and gas operator clients. The operator, in turn, furnishes this information, as required, to the state in which they are operating. As of June 2012, 15 states require some form of chemical disclosure ranging from as little as MSDS documents to full chemical disclosure depending on the respective state-drafted regulation.

One US state-supported media site for publicly posting stimulation chemicals used in hydraulic fracturing fluids is FracFocus (GWPC 2011), which allows operators to submit a disclosed chemical list by well name, county, state, and API number to a database. This database can be accessed by anyone to see the relative percentage of chemicals pumped in a specific well located in a specific area. Since September of 2012, eight states are currently using FracFocus for regulatory purposes. As of the date of the publication of this book, over 430 oil and gas operators are participating in the FracFocus chemical disclosure registry (Clum 2012). An additional HSE-related report is abstracted.

Taylor et al. (2004) note that since 1995, refinery distillation tower plugging has been observed in some refineries processing Canadian sweet light crude. This plugging may be associated with materials that come from the well enhancement and flowback activities. This plugging has resulted in numerous and costly unplanned refinery shutdowns and could potentially result in a devaluation of Canadian crude.

Taylor et al. (2004) claim that the Canadian Crude Quality Technical Association formed a Phosphorus Project Group to investigate and manage this problem. The group includes representatives from refineries, pipeline companies, service companies, chemical producers, and testing laboratories. The key finding of the group was that residual phosphate esters used in fracturing operations are the primary cause of plugging.

The paper describes work done to understand and solve the problem through formulation of new phosphonate ester oil gellant chemistry. As described by Taylor et al. (2002), CO₂-miscible, gelled hydrocarbon fracturing fluids may offer superior gas well stimulation.

Additional information on control and reuse of frac water is in Section 6.3.

6.2.3 Additional Means of Improved Environmental Control. Baycroft et al. (2005) contend that changes in the environmental performance of the fluid saves disposal costs, minimizes wellsite logistics, and reduces risks associated with an accidental spill to both the operator and service company. A case history of the use of the fluid in an environmentally sensitive area is discussed and how the low environmental impact fracturing fluid system enabled the operator to discharge the fluid saving on disposal costs.

DeVine et al. (2003) describe the lab and field development of an environmentally friendly liquid diesel-substitute-based (DiSub) system for completion and stimulation, with properties similar to or exceeding those achieved with diesel. The chemical evolution of the DiSub system and properties of the fluid including rheology, break and conductivity testing, and toxicity data will be presented. The DiSub is described as a blend of hydrocarbons with a high-paraffin (>92%) content that is less toxic

than diesel fluid. Gas chromatographic testing showed that the diesel has more toxic aromatic compounds than the DiSub fluid. It was gelled using a phosphate ester. Use of materials such as these may alleviate concerns about pollution by added hydrocarbons (Section 6.2.2).

Kargbo et al. (2010) suggest that intensified concerns by the public have prompted some companies to search for alternatives to hydrofracturing and, in some cases, to develop more environmentally friendly hydrofracture fluids. For example, diesel is being replaced by mineral oil, and some companies are experimenting with plant-based oils, such as palm oil and soy. EnCana reports that it stopped using 2-butoxyethanol, a solvent that has caused reproductive problems in animals. Many of the service companies are reported (Clum 2012) to have discontinued the use of fluorocarbons that are persistent environmental pollutants. While this may be good news, replacements for the discontinued chemicals are yet to be identified. One of the most effective methods of reducing exposure to contaminated waste water is to implement processes that do not generate waste water.

The authors (Kargbo et al. 2010) claim that a vendor of services is testing the use of liquefied petroleum gas (LPG), a fracturing agent that also transports the proppants into the fractures. First introduced in Marcellus shale drilling in September 2009, LPG is derived from natural gas processing and consists mainly of propane in gel form. Note, however, the use of LPG as a fracturing fluid is not an innovation. Hurst and Smith (1968) were issued a patent and LPG/CO₂ methanol-gelled fluids were used in the field. The process is claimed by them to generate no waste water because all of the LPG is recaptured back up the well. However, because of the extremely high risk of using the fluid, this stimulation technique was abandoned by some service companies in the interest of safety (information from authors of this book).

Kargbo et al. (2010) also have reviewed information on a process that uses CO₂ [see Section 4.5.2 of this book and Kubala and Mackay (2010)]. It is claimed [by Kargbo et al. (2010)] that they have had more than 1,200 successful simulations, and it has performed better than other fracturing fluids during several US DOE sponsored demonstration projects in the system using liquid CO₂ as the carrier fluid without water or any additional treatment additives. The authors describe the process whereby a pressurized CO₂ blender mixes the proppant into the CO₂ stream, thus eliminating the need for traditional carrier fluids to transport the sand. A provider performed CO₂/sand simulations on Devonian shale wells in eastern Kentucky and Devonian sandstone gas storage wells in western Pennsylvania. Results indicate that average cumulative gas production is as much as five times greater than production from conventional hydrofracture treatments. However, *ice formation* in wells resulting from the use of CO₂ is a real possibility. Consequently, the process has been optimized with the addition of N₂ gas, which not only reduces the formation of ice but also reduces the overall treatment costs.

Ainley et al. (1997) have reviewed how the control of the manufacture of oilfield chemicals can contribute to improve the safety and environmental protection. A major improvement is in the handling and recycling of production chemical storage containers. Frequently chemicals are sent to the job site in bulk containers; however, intermediate size amounts may require drums that may be difficult to recycle. Reusable totes are an improvement. See Fig. 6.4 for a diagram of the process that routes the containers from the wellsite back to the factory for reuse.

HMMG (2010) describes stainless steel intermediate bulk container totes as the original intermediate bulk container of the liquid handling industry and that they were introduced over 50 years ago as an efficient and sensible alternative to the use of 55-gal drums. They are claimed to be more durable than standard 55-gal drums, the totes help control risk to the environment. In fact, one 550-gal tote

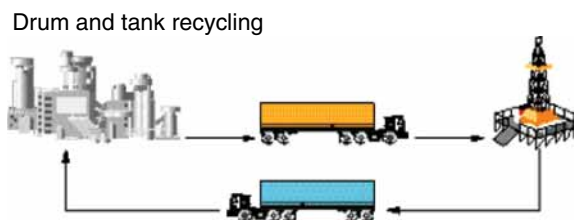


Fig. 6.4—Drum and tank recycling (Ainley et al. 1997).



Fig. 6.5—Recyclable tote (HMMG 2010).

replaces 10 drums, thereby minimizing the amount of handling required, which in turn, lowers the risk of liquid handling accidents (Fig. 6.5).

Additional information on disposal/spill remediation issues are in Sections 6.3.2 and 6.4.

6.3 Handling, Reuse, and Disposal of Flowback Fluids

Waste disposal and control of waste can start with the selection of less hazardous and toxic chemicals. See Section 6.2 and the discussions in Hill et al. (2003) and Azem et al. (2011). The next step is to design the layout of the job site to avoid spills and to control flowback. Wellsite layouts for treatments can vary greatly depending on the type of the job. According to SPE (2011) and Boschee (2012), the management of produced water is one of the “grand challenges” facing the petroleum exploration and production industry in the near future. This includes the naturally coproduced brine as well as water present in association with a stimulation treatment or EOR floods (which increases the water cut).

Section 6.3.1 describes safe handling of the produced fluids, and Section 6.3.2 discusses planned waste disposal options including examples of waste minimization using recycle. Section 6.4 reviews remediation methods and chemicals for use *after* a spill event has occurred.

6.3.1 Flowback Activities. Flowback is the process of allowing fluids to return from the well following a treatment, either in preparation for a subsequent phase of treatment or for cleanup and returning the well to production. These fluids include those returned from a reactive chemical stimulation, hydraulic fracturing, water/brine from chemical EOR activities and any other well service in which altered fluids are retrieved from a well. Fluids produced by the normal production processes (frequently called produced water) are routinely treated in three-phase separators (see Section 2.4.4). The nomenclature of these different waters have not been resolved, but from the perspective of the authors of this book, all well fluids must be treated, reused, or disposed of in some manner. Many production enhancement fluids (waterflood, EOR, frac, acid) contain chemicals and phases that can be difficult to treat using the normal separation equipment, in addition to the produced oil, gas, and brines. The total volume of the returned fluids may contain the following:

- Treatment hydrocarbons (that may be different from the reservoir produced fluids)
- Gases such as N_2 , CO_2 , and H_2S
- Acids, chelating agents, and metals
- Polymers and polymer residues
- Mixed dissolved salts, including new salts from the formation
- Solids such as proppants

The concerns of the production engineers include the following:

- Safe collection (explosive, toxic, and hot fluids including gases)
- Primary separation
- Treatment
- Reuse
- Final disposal

The change in the fluids after a well treatment can alter the ability of the producer to treat/reuse them and can contribute to additional/changed corrosion expectations for the downstream piping and facilities. See Sections 2.2.3, 2.4, and 6.2.2.

In addition to these hazards, an article by Urbina (2011) claims that the danger to the environment from hydraulic fracturing flowback fluids may be greater than previously believed in that some of the fluids contain radioactive isotopes [naturally occurring radioactive materials (NORM)] that may be returned to the surface. NORM is a widely recognized problem in many wells and the occurrence downhole on surfaces usually is related to alkaline earth deposits such as calcite, barite, and gypsum. Because Ra^{2+} is an alkaline earth element, it can be incorporated into these scales. See the discussion in Section 2.2.3 of Frenier and Ziauddin (2008) as well as in Fisher (1995). The concern of this article is that any waste water that is taken to a local waste water treatment plant may not be adequately treated because many such facilities do not have the chemistries available to reduce any radioactivity to EPA discharge limits (USEPA 2010b) before being sent to surface streams or rivers. The author (Urbina 2011) claims that “the risks are particularly severe in Pennsylvania, which has seen a sharp increase in drilling, with roughly 71,000 active gas wells, up from about 36,000 in 2000. The level of radioactivity in the waste water has sometimes been hundreds or even thousands of times the maximum allowed by the federal standard for drinking water.” Kell (2009) also has a short section that has references in NORM issues in shale gas production.

Schubert (2010) provides some additional details on the flowback of water from hydraulic fracturing in the Marcellus shale deposits in Pennsylvania, New York, and West Virginia. He notes that important quantitative points that affect the possible use/reuse of the flowback water include the following:

- 2–4 million gallons of frac water may be pumped into the formation to induce the fracture [also see Exhibit 37 in Kell (2009)].
- The flowback time is 4–15 days and eventually the well produces nearly all gas.
- While the period after completion is termed produced water, this water is *actually* still partially *frac water* produced slowly because these formations do not normally flow connate water. See [Table 6.1](#) for the produce water compositions of several shale fields.

TABLE 6.1—PRODUCED WATER FROM SHALE FORMATIONS (GE 2012)

| Content (mg/L) | Shale Formation | | |
|-------------------------------|-----------------|----------------|----------------|
| | Barnett | Haynesville | Marcellus |
| TDS | 40,000–185,000 | 40,000–205,000 | 45,000–185,000 |
| Cl ⁻ | 25,000–110,000 | 20,000–105,000 | 25,000–105,000 |
| Na ⁺ | 10,000–47,000 | 15,000–55,000 | 10,000–45,000 |
| Ca ²⁺ | 2,200–20,000 | 3,200–34,000 | 5,000–25,000 |
| Sr ²⁺ | 350–3000 | 100–3000 | 500–3000 |
| Mg ²⁺ | 200–3,000 | 600–5,200 | 500–6,000 |
| Ba ²⁺ | 30–500 | 100–2,200 | 50–6,000 |
| Fe(total) | 22–100 | 80–350 | 20–200 |
| SO ₄ ²⁺ | 15–200 | 100–400 | 100–400 |

- The water produced from flowback equals only about one-half of the frac water, and the rest is produced over the life of the well. The concern then is that the flowback water will contain chemicals not usually in the produced water.

Reports from Kell (2009), Kargbo et al. (2010), and energyNOW! (2011) also note that contact with the *formation* minerals may greatly alter the composition of the frac water and make it much more salty and thus more difficult to treat [including the NORM mentioned by Urbina (2011)]. The dissolved salts are described in a report by Blauch et al. (2009). They claim that one of the most prominent unexplained phenomena observed in the Marcellus and some other shale plays is the concentration of dissolved salts in produced waters after hydraulic stimulation. In this paper, they present both geochemical and lithology laboratory and field data to address the salt question: Is salt being dissolved from the shale, or are deep saline aquifers being breached during hydraulic fracturing?

To understand this system, Blauch et al. (2009) report that more than 100 flowback analyses were collected over 18 months from both the southwestern and northeastern regions of the Marcellus shale play. These data incorporate both cation and anion water analyses in either a full or a partial determination of the cation and anion balance. Detailed inorganic geochemical and mineralogical analyses of shale samples were integrated to help determine the presence or absence of physical evidence of minerals that may be the root cause for high salinity. This paper provides interpretations at both the regional and local scales to try to explain basal variations observed in the data. It discusses implications of the phenomenon of high-saline frac flowback fluids, along with methods being used to mitigate environmental problems associated with the post-frac flowback water geochemistry.

Flowback waters from the Marcellus wells characteristically carry high levels of total dissolved solids (TDS) in the form of soluble chloride salts (Table 6.1). Cenegy et al. (2011) also claim that the high pH of some frac water may affect scaling potential in the well. See Section 4.8.2 of this book and Frenier and Ziauddin (2008) for details of scaling and mitigation. Blauch et al. (2009) ask what to do with the post-frac flowback waters in light of scarce brine disposal facilities and substantial handling costs is an enormous burden to the economic development of the Marcellus natural gas resource? They claim that in the Commonwealth of Pennsylvania, new regulatory limits have been proposed further limiting discharges.

Boschee (2012) also has reviewed flowback and water reuse options in shale gas/oil fields in Wyoming and Texas and notes that treatment/reuse is becoming an economical option. Flowback from large acidizing treatments (see Section 3.4) also can cause significant surface problems. If the strong acids such as 15–28% HCl are completely spent on calcium carbonate from a carbonate reservoir, the flowback fluids will contain large quantities of CaCl_2 as well as other ions from the formation. The pH of the spent fluid will be in the range of approximately 4.5–6. However, if the acid is not completely spent, the pH value may be < 2 (and even lower). The concern is that the acid water now does not contain sufficient corrosion inhibitors to protect flowlines and pipelines before reaching a treatment unit.

The concern of the presence of live acid in well flowback was raised by Huizinga and Liek (1994). Meanwhile, typical inhibited live acid, based on 15% hydrochloric acid (HCl), was not unacceptably aggressive toward 13% Cr steel. It was shown that severe damage from locally initiated acid attack in back-produced spent acid, with a reduced inhibitor content but still highly acidic, could be avoided by limiting the contact time with the tubular steel. In typical chloride (Cl)-containing brines, 13% Cr steel repassivated after acidization within some hours. A risk of pitting corrosion existed only at very high Cl levels at elevated temperatures. A similar work was done later by Morgenthaler et al. (1997). Their experimental work was done on acidizing of sandstone rocks by HCl/HF acid. Simulated and real spent acids were used to test their effects on low-carbon steel (L-80) and stainless steel (super Cr-13). Both studies agree that spent acid could be corrosive and may adversely affect the integrity of well tubulars. The extent of the problem can be addressed by a thorough understanding of the composition of the spent acid and its effect on various types of tubing (Al-Mutairi et al. 2005).

In addition, Achour et al. (2012) report on acid flowback from HCl treatments of chalk-formation wells in the North Sea. They note that chemicals as well as the low pH have adversely affected the efficiency of the corrosion inhibition as well as scale inhibitor programs. The results of lab studies

have shown that continuously injected corrosion and scale inhibitors can at times fail to overcome the adverse effects of acid flowback even at high dosage. Moreover, low pH and the presence of traces of certain metals (Fe, Ni, Cr, and Al) can also hinder the efficiency of these inhibitors. The results can be high corrosion rates in pipelines (as seen by corrosion coupons) as well as mineral scale in the water separators. Note that high Fe concentrations have also been reported (Shen et al. 2012) to interfere with scale control in Marcellus hydraulic fracturing flowback fluids.

6.3.2 Planned Waste Disposal Options for Flowback Fluids. API (2010) is a guidance document that identifies and describes many of the current industry best practices used to minimize environmental and societal impacts associated with the acquisition, use, management, treatment, and disposal of water and other fluids associated with the process of hydraulic fracturing and other well treatments. While this document focuses primarily on issues associated with hydraulic fracturing pursued in deep shale gas development, it also describes the important distinctions related to hydraulic fracturing, EOR, and in other applications. The options for disposal also can apply to any other type of production waste. In general, well permits will specify that all fluids, including fracture fluids and flowback water, must be removed from the wellsite. In addition, any temporary storage pits used for fracturing fluids must be removed as part of reclamation. Water used in the hydraulic fracturing and other processes is usually managed and disposed of in one of three ways:

1. Injected in permitted disposal wells under an underground injection control regulatory program.
2. Delivered to water treatment facilities depending on permitting (in certain regions of the country, the water is actually treated to remove pollutants and achieve all regulated specifications and then surface discharged).
3. Reused/recycled.

A document by Deutch et al. (2011) describes these options and also notes that direct discharge to any water course is strictly prohibited. Disposal options are dependent on a variety of factors, including the availability of suitable injection zones and the possibility of obtaining permits for injection into these zones, the capacity of commercial and/or municipal water treatment facilities, and the ability of either operators or such plants to successfully obtain surface water discharge permits for treated water.

Veil (2009) has reviewed methods for reducing the amount of water that enters the wellbore and the surface as well as processes for dealing with the volumes of produced water. This author lists methods for reducing water entry that include

- Mechanical devices
 - Plugs
 - Packers
 - Cement
- Water shutoff chemicals

All of these methods were reviewed in Section 5.7.2 of this book. Veil (2009) also notes that various onshore and subsea separation methods are in use to reduce the amount of brine that enters the product streams.

For all well fluids, initial separations will then be required. Fig. 6.6 diagrams a simple onshore initial gas/liquid separator system and a depiction of a subsea separator as seen in a reference by Veil (2009).

A website from the US DOE (2007) includes a fact sheet with various references on where and how produced water [including frac water flowback and water from coalbed methane (CBM)] should be managed. This document notes that in the US, discharge activities are subject to all applicable regulatory controls required by the US EPA and the state agencies. The EPA's national discharge standards—the effluent limitation guidelines for the oil and gas extraction point source category—include five subcategories. These are further described in the produced water management information system. This can be accessed through the US DOE (2007). It lists different sub categories that include (a) onshore, (b) offshore, (c) costal, and (d) CBM.

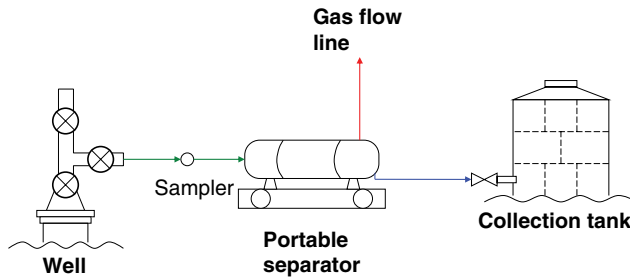


Fig. 6.6—Portable gas/liquid separation and collection system. Note the tank also could provide some oil/water separation.

In addition, the EPA provides subcategories of some of these. This document notes that produced water management typically differs between onshore and offshore facilities. This is partly because of the space and weight restrictions at most offshore sites. Also, the primary contaminant of concern is typically different between onshore discharges (salt content) and offshore discharges (oil and grease level).

Onshore-produced water faces different options depending on where in the country the well is located and whether the water comes from an oil or gas well or from coalbed natural gas (methane or CBM) production.

This very comprehensive website also lists the various disposal/treatment technologies that are available. As produced fluids are brought to the surface, the first step in managing produced water is *basic separation of fluids* (oil, gas, water) solids from one another. See Section 2.4.4 as well as Fig. 6.6.

Once the materials have been separated, companies can use a variety of technologies and practices to manage the water. The management technologies and practices can be grouped into three major categories: water minimization, recycle/reuse, and treatment/disposal. However, the categories overlap somewhat. For example, many of the reuse opportunities require that the produced water be treated before it can be used for another purpose.

The options and subcategories are listed and the links on the website (USDOE 2007) provide details of the methods. On the website (USDOE 2007), each method is connected to a fact sheet that describes the method and gives references. The categories of methods are listed.

Water minimization

Practices that can reduce the volume of produced water entering the well.

Mechanical blocking devices

Water shutoff chemicals

Practices that can reduce the volume of produced water managed at the surface.

Downhole separation

Seafloor separation

Recycle/reuse

Practices that find another use for produced water.

Underground injection for increasing oil recovery

Underground injection for future water use

Recycle on-site (especially frac water)

Injection for hydrological purposes

 Subsidence control

 Stream flow augmentation

Agricultural use

 Irrigation

 Livestock watering

 Wildlife watering

 Managed wetlands

Industrial use

- Dust control
- Use in drilling fluids or hydraulic fracturing fluids
- Cooling water makeup
- Other

Domestic Use

Treatment/disposal

Practices to dispose of produced water.

Discharge

Underground injection for disposal

Evaporation

Off-site commercial disposal

Practices to remove salt and other inorganic from produced water.

Membrane processes

- Reverse osmosis
- Filtration
- Electrodialysis

Ion exchange

Capacitive deionization

Thermal distillation

Practices to remove oil and grease and other organics from produced water.

Physical separation

- Hydrocyclones
- Centrifuge
- Filtration

Coalescence

Flotation

Combined physical and chemical processes

Solvent extraction

Adsorption

Oxidation/combustion

The European Commission (EC 2003) has issued a general waste control guide that is very comprehensive and also has contact information on the waste control bodies in the individual countries of the EU. Vehlow et al. (2007) state that in the EU, waste management is almost totally regulated by EU directives, which supply a framework for national regulations. The main target in view of sustainability is the prevention of direct disposal of reactive waste in landfills. The tools to comply with these principles are recycling and material recovery as well as waste incineration with energy recovery for final disposal. The adaptation of the principles laid down in EU directives is an ongoing process. A number of countries have already enacted respective national regulations and their realization shows that recycling and incineration are not in competition but are both essential parts of integrated waste management systems.

Kell (2009) has summarized water management for the various shale gas basins. This report has more than 300 references on various aspects of shale gas production including wastewater disposal. See [Table 6.2](#). However, Rassenfoss (2011a) claims that in Pennsylvania, recycling water from wells in the Marcellus shale has been transformed from a trend to an essential skill. He notes that the tipping point came in mid-April in a notice from the state's Department of Environmental Protection telling 15 public water treatment plants to stop handling waste water from wells in the this shale trend.

The authors of this book note that the subject of tight gas production is a scientific, economic, and political issue, and regulations will change with time and the production engineers will have to adapt.

Details of treatment and reuse of fracture water are in subsequent sections. Note that there may be some overlap in the articles described.

TABLE 6.2—CURRENT PRODUCED WATER MANAGEMENT IN SHALE GAS BASINS (KELL 2009)

| <u>Basin</u> | <u>Major States</u> | <u>Waste Management Technology</u> | <u>Availability</u> | <u>Comments</u> |
|--------------|---|---|---|--|
| Bakken | Wyoming, North Dakota | Recycling | On-site, pipeline | For reuse in subsequent fracturing jobs |
| Barnett | Texas | Class II injection wells | Commercial and noncommercial | Disposal into the Barnett and underlying Ellenberger Group 304 |
| Barnett | Texas | Recycling | On-site | For reuse in subsequent fracturing jobs |
| Barnett | Texas | Class II injection wells | Noncommercial | Water is transported to two injection wells owned and operated by a single producing company |
| Fayetteville | Arkansas | Recycling | On-site | For reuse in subsequent fracturing jobs |
| Haynesville | Texas, Louisiana | Class II injection wells (Burnett and Vavra 2006) | Commercial and noncommercial | |
| Haynesville | Texas, Louisiana | Class II injection wells | Commercial and noncommercial | Limited use of Class II injection wells |
| Eagle Ford | South Texas | Recycling | On-site | For reuse in subsequent fracturing jobs |
| Marcellus | New York, Pennsylvania, Ohio, Maryland, West Virginia | Treatment and Discharge | Municipal waste water treatment facilities, commercial facilities reportedly contemplated | Primarily in Pennsylvania |
| Marcellus | New York, Pennsylvania, Ohio, Maryland, West Virginia | Recycling | On-site | Future frac jobs |
| Marcellus | New York, Pennsylvania, Ohio, Maryland, West Virginia | Class II injection wells | Commercial | Disposal into multiple confining formations |
| Woodford | Oklahoma | Land farming | Commercial | Permit from Oklahoma Corp. Commission |
| Woodford | Oklahoma | Recycling | Noncommercial | Water recycling and storage facilities at a central location |
| Antrim | Michigan | Class II injection wells | Commercial and noncommercial | |
| New Albany | Illinois, Indiana | Class II injection wells | Commercial and noncommercial | |

General Treatment and Recycle Methods. These processes are intertwined in many well treatment situations and are described in this section. They apply to the treatment and reuse of water for hydraulic fracturing as well as water from acid stimulation and EOR activities. However, depending on the chemical additives needed for the reused water, specifications may vary with the location and geologic formation. Operating and well-service companies have approached the problem of renewable water supply by separating, filtering, and even distilling produced formation waters and frac-fluid flowback waters for future use or surface discharge. The salinity of the produced water as well as the proposed



Fig. 6.7—Frac pit for flowback fluid collection (Tinto And Solomon 2010).

reuse will determine the treatments required. Some of the shale waters (Table 6.1) have very high salt loads while some western plays in Wyoming and Colorado are not as salty (Bomgardner 2012).

In general, the first step in treatment or reuse is separation of the various phases. A simplified separation system for well fluids before other activities is seen in Fig. 6.6. Any toxic or flammable gases will be treated by chemical methods or by flaring if this is part of the well permit. This (Fig. 6.6) shows a collection tank; however, the fluids may also flow into a frac flowback pit (Tinto and Solomon 2010) that is seen as Fig. 6.7, and this may be a part of a collection/treatment process. If the water has suspended oil that is not easily removed, a separator/oil adsorber described in Fig. 6.8 may be used to produce oil-free water. These on-site and possibly temporary systems are similar in intent to more permanent facilities present on offshore rigs or large land-based operations. These pits usually are regulated by permitting from the individual states [example OERB (2000)]. See Section 2.4.4 for details of primary separators/demulsifier technologies and the chemicals used for demulsification in general oil and gas production.

A diagram (Fig. 6.9) of additional primary unit operations for treating flowback water that is being used in the Bakken fields was provided by Boschee (2012). This reviewer notes that the economics of using recycle of flowback water for large well fields include: the benefits of lower transportation and disposal costs as well as environmental benefits. Each step may remove a different potential undesirable entity. The anaerobic basin tries to remove sulfate-reducing bacteria while aeration may remove iron. Note that this process does not alter the brine chemistry by changing the ionic makeup.

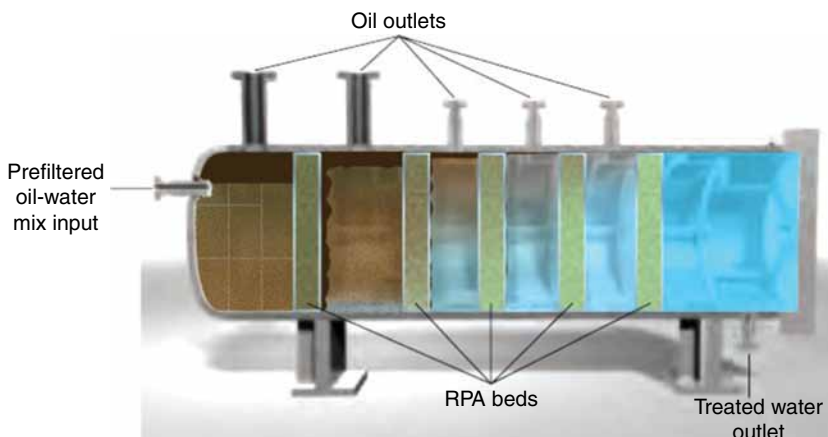


Fig. 6.8—Oil/water separator with reusable petroleum absorption (RPA) beds (Azem et al. 2011).

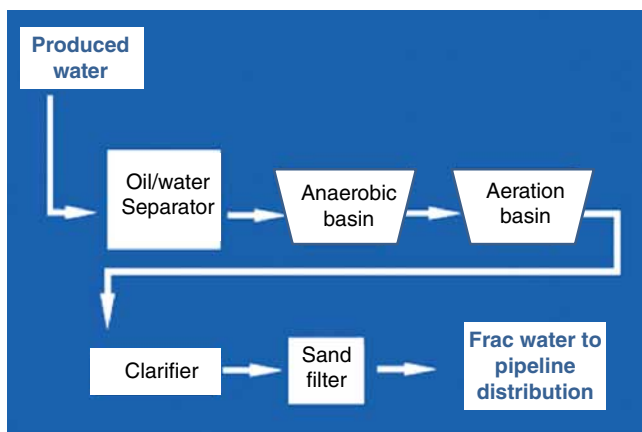


Fig. 6.9—Primary frac water treatment for recycle (Boschee 2012).

This diagram also shows the recycled water will be delivered to a pipeline system for use in other operations in the fields. Therefore, a number of flow-assurance issues (Section 2.1) must be addressed.

Arthur et al. (2008) claim that operators are using a variety of containment tanks and storage trucks to reduce the potential for exposure of fluids to the environment during the transport of chemicals to disposal locations away from the well pad (see Figs. 6.7 and 6.8). Many Marcellus operators in states like New York are actively researching options where Class II disposal wells (Burnett and Vavra 2006) and municipal and industrial treatment facilities can or cannot be used to manage flowback water.

Chemical and Mechanical Processes for Treatment and Reuse. Additional technologies are described that propose solutions. Specific solutions based on chemistry are noted, and then mechanical/chemical methods are considered.

Li et al. (2009) performed a series of laboratory experiments to optimize the viscosity profile of fracturing fluids prepared with produced water. Preparation of polysaccharide-based fracturing fluids with produced water frequently resulted in fluids with poor viscosity profiles despite the fact that the produced water was pretreated with biocide. Furthermore, the problem could not be resolved by just adding more biocide. In a number of representative cases, the guar-based fracturing fluids, prepared with produced water and regular biocide, quickly lost their viscosity after hydration, possibly because of the degradation of the guar by the bacterial enzymes in the produced water. This paper exemplifies the need for good analyses of the produced water before reuse.

Perry and Williams (2009) describe a composition and method for breaking down and denaturing friction-reducing compound (such as hydrolyzed polyacrylamide polymer) introduced into the ground during the drilling of oil wells and for destroying other contaminants and biohazards naturally present within and artificially introduced into oil wells, which are formed as a result of the drilling and pumping processes. The composition claims several species of oxidizing agent compounds that are effective in breaking down hydrogen sulfide produced by bacteria as well as the friction-reducing polymer used during drilling and several other organic compounds. Protection of the reservoir from souring is extremely important. See the discussions in EOR floods in Section 5.5.4.

Jones (2000) describes a method of reducing the concentration of metal soaps of partially esterified phosphates from a hydrocarbon flowback fluid resulting from a hydraulic fracturing fluid operation comprising adding to and mixing with the hydrocarbon flowback fluid and effective reducing amount of a hydroxide selected from the group consisting of potassium hydroxide, lithium hydroxide, sodium hydroxide cesium hydroxide, calcium hydroxide magnesium hydroxide, and mixtures of them.

Kozora (2010) notes that early flowback water will have the *lowest* TDS and other contaminants of waste water from the well. As a result, one approach being implemented is to not treat this waste water. Instead, it is blended with fresh water and reused for the next frac operation. This method is claimed to offer initial advantages of minimizing wastewater disposal and minimizing the resulting trucking and costs associated with disposing of it. However, blending only addresses the lower TDS levels that

are typical of early flowback. Early flowback water is the initial waste water from the well during, approximately, the first few weeks. Higher TDS flowback water and essentially all produced water, which is the waste water that continually surfaces months and even years after the drilling operation is complete, will require unreasonable quantities of fresh water to blend to an adequate water composition for reuse. Higher TDS waste water will still require some treatment before it can be reused.

Gupta and Hildek (2010) claim that shallow-gas fracturing is very prevalent in western Canada. Several thousand wells are typically drilled and completed in the shallow-gas fields every year. All these wells are typically hydraulically fractured; because the fluids cannot be land farmed, attempts were made to recycle the flowback fluid. The chemistry of the surfactant-gel fluid was insensitive to the water quality, which made the recycling concept successful. This paper details the chemistry of the fracturing gel, which are made from viscoelastic surfactant chemicals (see Section 4.4.4) as well field application in which the optimized recycling operation, and the details on cost advantages achieved, as well as future direction for further reduction in freshwater usage on a project basis. The details of the reuse of the frac return water from the western Canada wells is as follows:

- Flow into a tank, allow settling for 24 hours. The tank has valves at several levels. The settled water is withdrawn at the 1-m level to avoid settled solids as well as any hydrocarbons on the top of the tank.
- The fluid is filtered and then used as part of the makeup water for the next surfactant (viscoelastic surfactant) treatment. The authors claim that the anionic part of the fluid may be in the returns but the cationic portion usually remains in the formation.
- Using appropriate quality control procedures, the chemical requirements for the next job may be reduced significantly.

They (Gupta and Hildek 2010) also claim that since 1990, approximately 5,000 wells have been treated using recycled water, thus greatly reducing the frac water requirements.

Kargbo et al. (2010) report there is the potential to solve both water supply and environmental problems of frac water. However, a major problem with use of flowback water for makeup of frac water is the very high concentration of *scale forming* constituents including barium, calcium, iron, magnesium, manganese, and strontium (Ba, Ca, Fe, Mg, Mn, and Sr). These constituents readily form precipitates that rapidly block the fractures in gas-bearing formations required for economic gas production. Kargbo et al. (2010) suggest that the use of treated acid mine drainage (AMD) water may solve both water quantity and quality problems. In many Marcellus shale areas of Pennsylvania, AMD from past coal mining activities is present in large amounts, and its use could alleviate a major water quality problem. Recently, they claim, approximately 12 mL (3 million gallons) of treated AMD was obtained from the Blue Valley Fish Culture Station and used in a Marcellus completion hydraulic fracturing process.

Kaufman et al. (2008) propose that water used to treat shale formations can be recycled using the following procedures in the Haynesville shale wells:

- Step 1: Oxidation to remove iron, kill bacteria, and break polymers. Oxidizers such as hydrogen peroxide or hypochlorite can be used.
- Step 2: Flocculation of solids. Use classic water treatment chemistry to remove suspended solids and scale by precipitation.
- Step 3: Filter to 25 μm .
- Optional: Add scale inhibitor to maintain water compatibility.

Tinto and Solomon (2010) have investigated the use of thermal evaporation of frac well flowback and have tested (lab and pilot plant) an evaporation system for simulated frac water. Scaling is a major issue and must be treated with scale inhibitors. A system for treating 1.0 million gal/D of frac water flowback and produced waters can provide a treatment cost to the producers of less than USD 5.00/bbl of water brought to the facility. The facility operator is envisioned to be independent of the natural gas producers, though the operator would contract with the producers for specific treatment volumes. Note the other methods described in the USDOE (2007) fact sheet on produced water.

Devon Energy Corporation (Devon) reports that it is currently using water distillation units at centralized locations within the Barnett shale play to treat produced water from hydraulic fracture stimulations (Ewing 2008). The report notes that as of early 2008, Devon had hydraulically fractured 50 wells using recycled water and reports that the program is still in its testing and development stages.

Blauch et al. (2009) note that the Pennsylvania Department of Environmental Protection announced that all industrial discharges will be limited to 500 mg/L TDS as of 1 January 2011. They claim that there are currently no facilities in the state that can treat flowback fluids to this level. The options for an economic solution are few for operators in dealing with these saline flowback fluids. They contend that evaporation/crystallization is the only established technology for treatment of the produced waters that can achieve the newly proposed TDS limit and produce a very highly concentrated brine solution or large volumes of crystalline salt cake that still must be disposed. The paper claims that a 1 million gal/D crystallization plant will generate approximately 400 tons/D of salt waste. Unless some beneficial use for these residues can be found, they will require disposal in a secure solid waste facility, in addition an evaporation/crystallization plant is very energy intensive and thus has the potential for increased air quality impact and greenhouse gas emissions in addition to its cost of operation. However, Bomgardner (2012) claims that the salt-cake produce from the evaporator (40% of the water) may be used as a road salt (details and regulations in the various states was not addressed by this author).

Some operators are using large fixed-site treatment operations. Boschee (2012) has described a fixed-site system in use in the Pinedale Anticline (Bakken, Wyoming play) that shows a coagulant and flocculation tanks with a clarifier (Fig. 6.10) next to a collection lagoon with aerobic (aeration) treatments.

Portable operations also are in use. Halliburton (2011b) has introduced a portable water treatment/recycle system called CleanWave™. Specifics of the system are

- Electrical charge coagulates suspended matter (electrocoagulation precipitation)
- Containerized unit with 100 kVA generator
- Scalable—can handle total flow in real time
- 99% reduction in total suspended solids
- Coagulates particles < 1 μm
- Reduces turbidity to < 10 NTU
- Nonpolymer-based water treatment contributes up to 75% reduction in sludge generation
- Breaks emulsions
- Removal of some divalent and heavy metals (total removal requires chemical treatment or other methods)
- Handles wide variety of source waters (*TDS range = 100 to 300,000 mg/L*)



Fig. 6.10—Frac water lagoon and treatment plant (Boschee 2012).

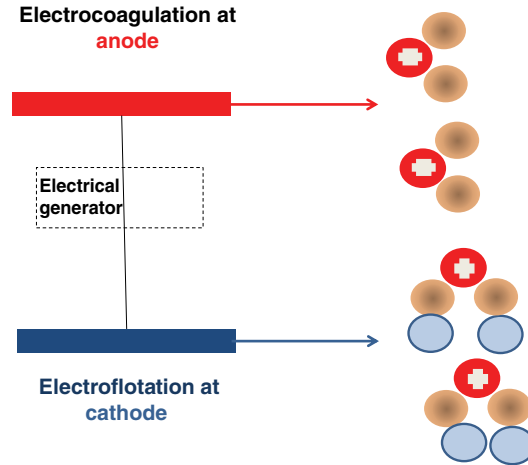


Fig. 6.11—Electrocoagulation/flotation.

This process is claimed (Halliburton 2011b) to be based on *electrocoagulation/flotation* (Rodriguez et al. 2007). These types of units are electrochemical cells in which positive ions (Fig. 6.11), possibly Al^{3+} or Fe^{3+} , are generated at the anode and a gas (H_2 or O_2 depending on the pH) is generated at the cathode to help float the lighter particles. The heavier clumps of the solids are settled and then removed. Disruption of emulsions also can be accomplished using *electrostatic* processes as seen in Section 2.4.4.

Mobile waste treatment plants are described by GE (2012) and include mobile evaporators as well as equipment and technologies to remove ions by reverse osmosis, specialized membranes to remove frac chemicals and to reduce the need for biocides. On-site chemical treatment also can be used depending on the original water quality. Waters (2011) has summarized mobile and fixed-site water management methods and has described the cost trends in Fig. 6.12.

Summary of Water Reuse. Flowback water can be used (or reused) for several different treatments including waterflooding, EOR and HF. Fig. 6.13 shows some of the steps in a water cycle [also see

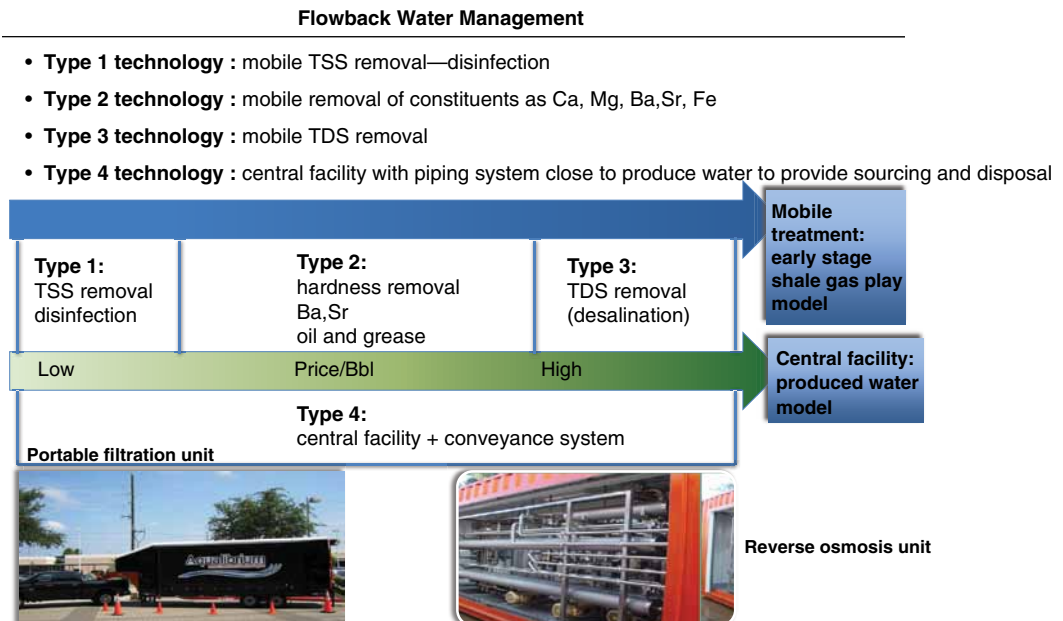


Fig. 6.12—Water management options (Waters 2011).

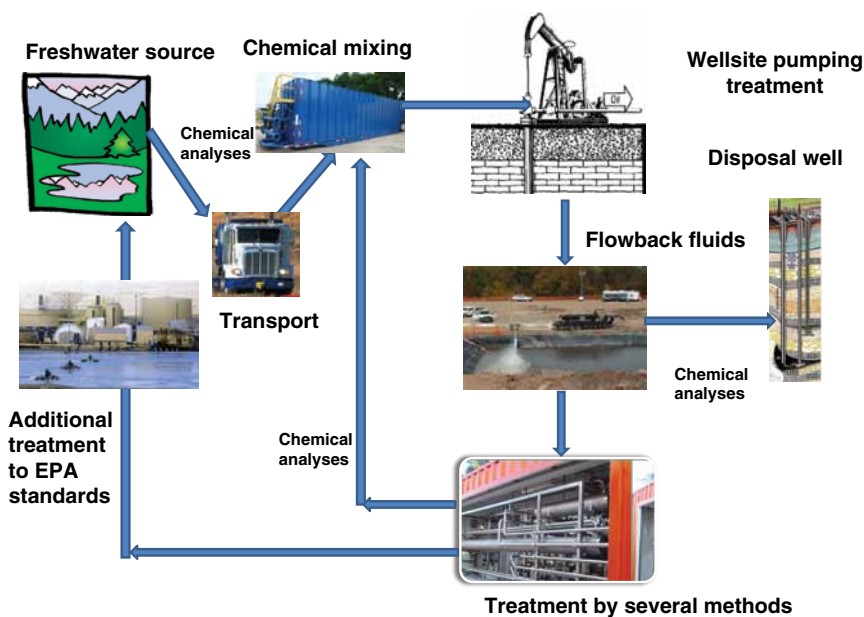


Fig. 6.13—Well treatment water cycle.

Bomgardner (2012)]. Here, fresh water is transported and mixed with chemicals and used in a treatment. The flowback fluids are stored, and then treated or disposed of by injection. Treated water (several methods) is transported to another wellsite for reuse or to additional treatment facilities for return to a freshwater source. Chemical analyses are performed at several stages to comply with use or disposal standards.

Disposal in Injection Wells or Surface Streams. Even if frac water and EOR water is recycled or used several times, an ultimate disposal of the contaminated fluids will be required. Use of a Class II injection well will be the preferred solution in many cases (see Table 6.2). USEPA (2011a) describes these wells as those licensed to inject brines and other fluids associated with the production of oil and natural gas or natural gas storage operations. They note that when oil and gas are produced, brine is also brought to the surface. The brine is segregated from the oil and is then injected into the same underground formation or a similar formation. Class II disposal wells can *only* be used to dispose of fluids associated with oil and gas production. Disposal wells represent about 20% of the approximately 140,000 Class II wells in the US. A diagram of the layout of a Class II well is in Fig. 6.14. Note the requirement for isolation from the producing formation and sources of drinking water.

Properly drilled, completed, and maintained, these wells should provide permanent disposal and isolation of the well fluids. However, there have been claims that injection of fluids into the disposal formations have contributed to earthquakes. A documented (van Poollen and Hoover 1970) case involved aqueous wastes injected into pre-Cambrian formations northwest of Denver, Colorado. The authors note that since injection started into the 12,000-ft well, earthquakes were observed in the area. Earthquake activities also have been noted after initiation of the disposal of frac water in Ohio in 2011. Niiler (2012) has reported and quoted (Art McGarr, a geophysicist with the US Geological Survey in Menlo Park, California) that “it’s reasonably clear that these Youngstown earthquakes are being caused by the disposal well activities the earthquakes started in March of last year. That’s about the same period that the major injection activities started.” The article also claims that geophysicists are working on a model to predict which areas near drilling sites will be susceptible to earthquakes, although there’s still no way to accurately predict their size and strength.

In some cases, the water can be treated to meet surface discharge requirements. Fig. 6.15 (Boschee 2012) shows the types of operations that would provide water of a quality equivalent to a municipal wastewater treatment plant.

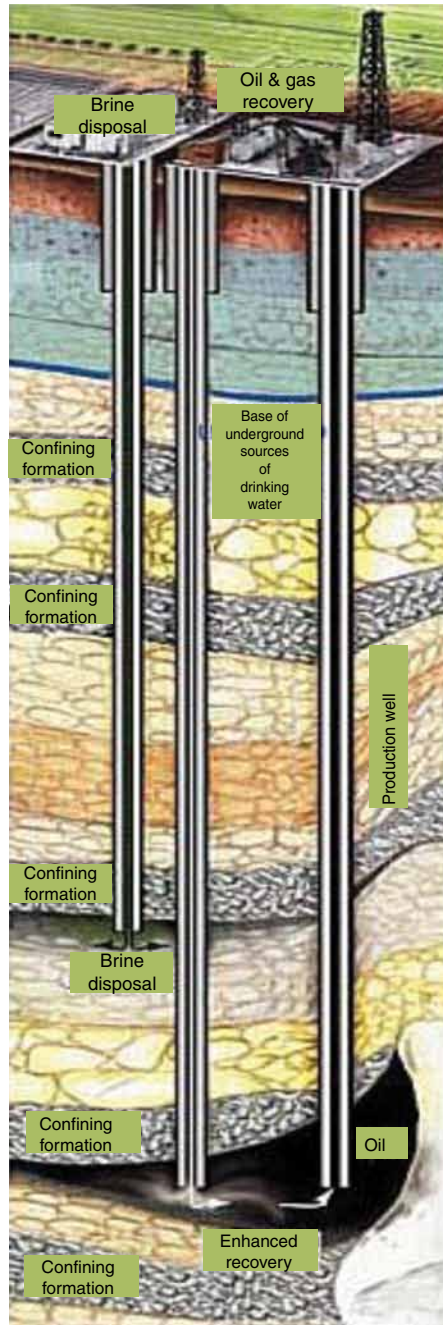


Fig. 6.14—Diagram of a Class II injection well (USEPA 2011a).

6.4 Control and Remediation of Spills in Water Bodies and on Land

Spills of oil (crude or products) as well as various stimulation fluids (frac fluids, acids, flowback fluids as well as produced water) can occur in every part of the oil and gas production process. This section describes methods used for containment/treatment of spills in water bodies as well as on land.

6.4.1 Spill Control. Introduction and Planning. Notification, control, removal, and final disposal of the fluid or solid may require the cooperation and participation of multiple governmental agencies as well as commercial entities. In the US territories and waters, the first response to a spill should be the

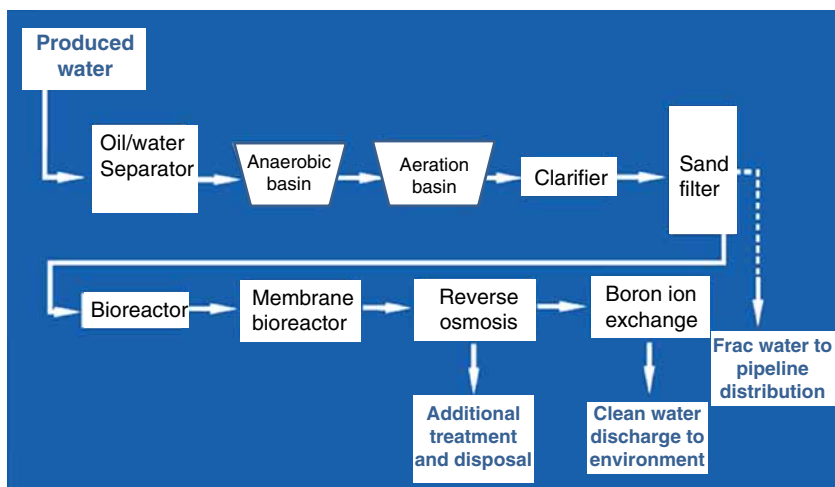


Fig. 6.15—Surface water discharge treatment operations (Boschee 2012).

National Response System (NRS) (2009). Initially, this system was focused on oil spills and selected hazardous polluting substances discharged into the environment. It has since been expanded by other legislation to include hazardous substances and wastes released to all types of media. The report claims that the NRS functions through a network of interagency and intergovernment relationships that were formally established and described in the National Oil and Hazardous Substances Pollution Contingency Plan (NCP). The website noted in the reference the emergency contact number that should be used in case of a spill. This system is a part of the National Incident Management System (NIMS 2008), a part of the US Homeland Security Department. The document cited in the reference has details of the planning and control of a spill incident. The document claims that the National Incident Management System provides a systematic, proactive approach to guide departments and agencies at all levels of government, nongovernmental organizations, and the private sector to work seamlessly to prevent, protect against, respond to, recover from, and mitigate the effects of incidents, regardless of cause, size, location, or complexity, to reduce the loss of life and property and harm to the environment.

The EMSA (2010) system provides spill response and vessels for control of spills in European waters. Individual countries may have more procedures, but the authors of this book have not accessed them.

Jermelov (2010) describes the major types of oil releases that have taken place since 1970. Included have been the washing of tanker tanks, tanker spills including 12 major ones since 1970. Fink (2003) listed 15 spills in the same time frame. In same time period, Jermelov (2010) claims there were more than 25 pipeline spills/year (rising recently to 35/year in the 2000s). There were a few (four) large blowouts, and the Ixtoc 1 in 1979 was the largest offshore spill before BP's Macondo well on Transocean's Deepwater Horizon rig (BPMTDH) 2010 (total release 4–5 million bbl (MSNBC 2010a).

SPE (2010) reports that the largest spill in US history occurred onshore in Kern, California, when 9 million barrels of oil was spilled on land in 1910 and 1911. Fink (2003) also lists the numerous fires that were set during the 1991 Gulf War as having released 11,000,000 bbl of oil to the land and the sea around Kuwait (Beckwith 2012a). That author also notes a major tank storage fire at a facility in Panama with a release of 240,000 bbl. Jermelov (2010) claims that the washing out of tanker tanks has become better regulated in recent years.

Spills of other types of oilfield fluids also have been noted and are areas of concern, especially because the surge in hydraulic fracturing activates the production of natural gas from coalbeds and from shale formations. Concerns include the toxicity of the frac fluids as well as the general problems with oilfield truck traffic in rural areas not usually associated with this activity (Jaffe 2010).

Wikipedia (2010f) lists several spills: A well blowout in Clearfield County, Pennsylvania, on 3 June 2010 sent more than 35,000 gallons of hydraulic fracturing fluids into the air and onto the surrounding landscape in a forested area. Campers were evacuated and a company has been ordered to cease all operations in the state of Pennsylvania pending investigation. The Pennsylvania Department of Environmental Protection has called this a “serious incident.”

EOR activities also may cause contamination of groundwater and the produced fluids must be handled in the same manner as any well production. Abandoned wellsites and chemical servicing camps are another source of pollution. Wellcare (2003) notes that normally groundwater flows through soil and bedrock formations, known as aquifers, which filter unhealthy organisms, minerals, and other substances. Water that enters an abandoned well bypasses this purifying action. Contaminants enter the aquifer through the unsealed well and may eventually harm the water quality in other wells nearby. Contaminants usually get into an abandoned well through the casing pipe. It may not extend high enough above the ground surface to prevent run off from washing into casing pipe, which also may be in poor condition, poorly cemented or isolated, or even nonexistent. Possibly, the well cap could be broken or in poor condition. In the US, there are many thousands of abandoned wells. The 27,000 Abandoned Oil and Gas Wells (2010) claims that there are more than 25,000 abandoned wells in the Gulf of Mexico, some going back as far as the 1940s. Zenone et al. (2002) state that more than 250,000 wells have been drilled in Pennsylvania alone. Unless the wells have been properly killed and plugged, oil and gas may leak into groundwater as well as onto surfaces. Most states have programs to reseat/eliminate the risks of old wells. In Oklahoma, the Oklahoma Energy Resources Board (OERB) restores abandoned wellsites. Since 1994, they claim to have restored more than 10,000 abandoned wellsites across the state. Currently, they restore two to three sites per day.

Abandoned treating company sites are also a source of polluting chemicals. These are locations where treating equipment for servicing wells was stored, serviced, and loaded with chemicals to perform acidizing, fracturing, and other treatments. At some sites, hundreds of barrels, and many thousands of gallons of corrosive and possibly toxic chemicals were stored. In addition, various diesel- and gasoline-powered vehicles may have operated and been cleaned. In particular, these sites usually had a “wash rack” where the vehicles were cleaned after a service and the tanks were cleaned before the next treatment. If the wash water was not properly contained and processed, the site may have been damaged.

In response to concerns about groundwater pollution from well stimulation activities, the (USEPA 2010a) notes that in its fiscal year 2010 budget report, the US House of Representatives Appropriation Conference Committee identified the need for a focused study of hydraulic fracturing. The report also notes that the EPA’s Office of Research and Development will be conducting a scientific study to investigate the possible relationships between hydraulic fracturing and drinking water. EPA will use information from the study to identify potential risks associated with hydraulic fracturing to continue protecting America’s resources and communities.

Beckwith (2011a) has reviewed the activities at the Ohmsett Oil Spill Research and Test Facility. This site also is known as the National Oil Spill Response and Renewable Energy Test Facility (NOSRRETF) and is the largest outdoor wave/tow tank facility in North America. According to the author, the facility provides a full-scale testing environment in which no oil substitutes are used. The wave/tow tank allows full-scale evaluation of containment booms and skimmers using a wide range of oil viscosities. In addition, sorbents, chemical treating agents, and dispersants, as well as pumping systems and temporary storage devices, can be reliably evaluated.

API (2009) provides a comprehensive document that gives guidance and highlights industry recommended practices for well construction and integrity for those wells that will be hydraulically fractured. The guidance provided here will help to ensure that shallow groundwater aquifers and the environment will be protected, while also enabling economically viable development of oil and natural gas resources.

The document proposed that in the event a spill occurs, it is extremely important for all responsible operating personnel to know how to respond quickly and effectively to control, contain, and clean up the spill. To ensure this capacity exists, a contingency plan should be prepared for inland areas as well

as for areas near water. The plans should provide utilization of capabilities of oil-spill cooperatives, whenever advantageous. Spill plans should address the need to advise the public about significant releases. Also review NRS (2009) earlier in this section.

The plan should include procedures to advise government officials and provide appropriate information and access to the press. Section 8.7.5, Control and Containment of API (2009) states that in the event a spill occurs

1. The source of the spill should be stopped, or reduced as much as possible, in a safe manner. The spread of the spilled substance should be controlled or contained in the smallest possible area to minimize the adverse effects. Some methods that can be used to control and contain discharged substances, particularly oil, include retaining walls or dikes around tanks and other spill-prone equipment.
2. Secondary catchment basins should be designed to prevent the spread of oil if it escapes the primary wall or dike.
3. Permanent booms in water basins should be adjoined to the facility.
4. Temporary booms should be deployed in the water after the spill occurs.
5. Special chemicals to gel or biodegrade the oil should be used to prevent the spread of oil spilled into or on water. Operators should evaluate the potential for spills and damages and use this information to determine the type and size of primary and secondary containment necessary. The type and footage of containment boom installed or stored for deployment will vary with the type, size, and location of the facility and spill potential. This information should be developed for each main area or facility and be stated in the facility contingency plan. In addition, the contingency plan should be listed where emergency equipment is located.

A very comprehensive report produced for the Bureau of Land Management by OERB (2000) provides a number of good lease practices to prevent pollution. Information is included for

- Wellhead(s) and prime moving equipment (pumping units)
- Oil/condensate tank(s)
- Saltwater tank(s)
- Production vessels
- Containment
- Tier III chemicals (toxic, environmental issues)
- Environmental concerns

Specific Actions for Spill Containment/Removal. Clayton et al. (1993) and NOAA (2005) describe four strategies to treat spills once they occur in lakes, rivers, and offshore.

1. Mechanical cleanup. This method uses booms and other containment devices to surround the oil. Then skimmer boats and other removal devices can extract the oil from the surface of the water. After the oil has been surrounded, then controlled burns can be used. Several more efficient methods of oil collection were tested in 2011 at the Ohmsett Oil Spill Research and Test Facility. See details in the article by Beckwith (2011a).
2. Burning (**Fig. 6.16**) can be used on oil that is localized. This was used extensively in the 2010 BPMTDH spill.
3. Bioremediation. Clayton et al. (1993) says that bioremediation at sea usually includes adding nutrients to the spill to aid the natural bacteria in attacking the hydrocarbons. Dispersants also use bioremediation to ultimately remove the hydrocarbons.
4. Treatment with dispersants. This is described in detail in Section 6.4.2.

6.4.2 Use of Remediation Chemicals in Bodies of Water and Proposed Mechanism of Action. NOAA (2005) described the use of chemicals to help control hydrocarbon spills in water bodies. This document notes that once oil has spilled, chemical countermeasures can be used to try to reduce the



Fig. 6.16—Spill cleanup methods (NOAA 2005).

adverse effects of spilled oil on the environment. Spills of water-based fluids in water bodies are much more difficult to remove unless the area can be diked very quickly and then removed mechanically. The MSDSs will be a major source of information for the first responders.

Dispersants are one kind of countermeasure for spills in water bodies including the ocean, rivers, and lakes. They are chemicals that are applied directly to the spilled oil to remove it from the water surface, where oil may be most harmful. When dispersants are applied to surface oil slicks, they act to break up the slicks and move the oil, in the form of tiny droplets, from the water surface down into the water column (the volume of water extending from the surface to the bottom). Dispersion of an oil into water also occurs during petroleum production if the water to oil ratio is high. This natural phenomenon was described in Section 2.4.1. In those cases, most of the consideration was the formation of water/oil (W/O) emulsions; however, oil/water (O/W) emulsions also occur. When used for remediation, mostly synthetic chemicals are used to form an O/W emulsion so that the slick will not foul the land (beaches, marshes, etc). Fig. 6.17 shows an example of a light plane spraying a dispersant onto an oil slick.



Fig. 6.17—Plane spraying a dispersant on an oil spill (NOAA 2005).

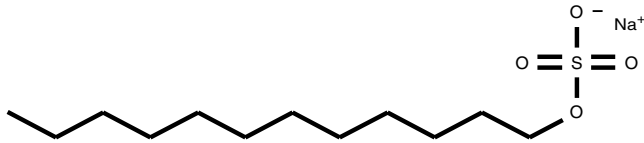


Fig. 6.18—Laurel sulfate.

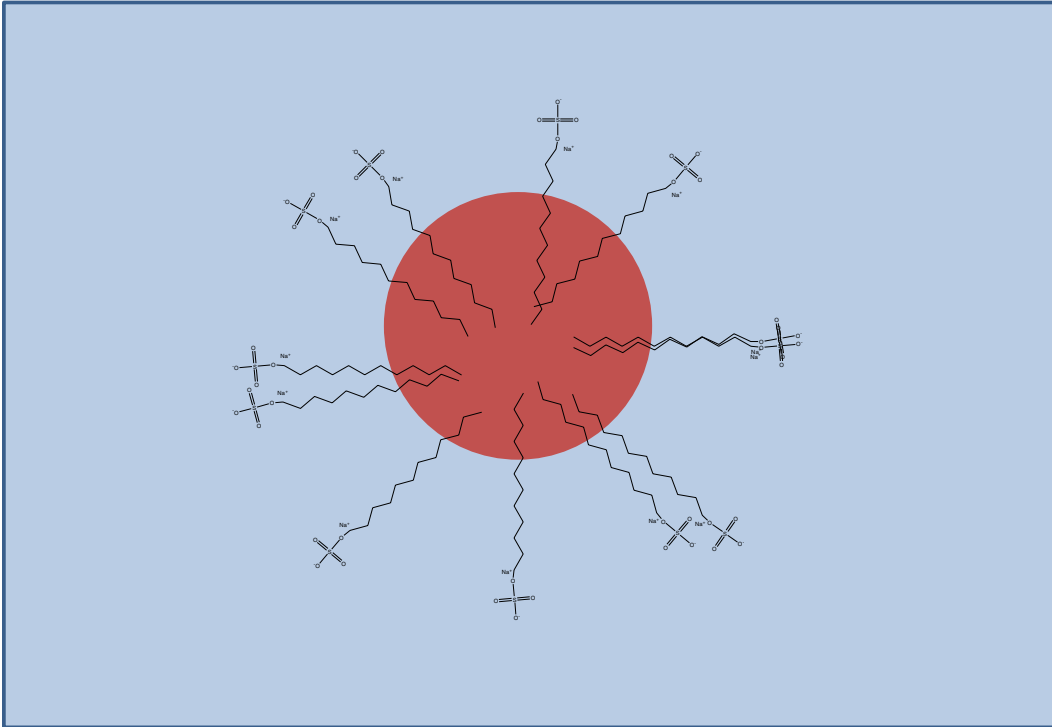


Fig. 6.19—Laurel sulfate dispersion of an oil drop in water.

In the case of the an intentional use of a dispersant, the oil droplets will be stabilized by a surfactant (such as laurel sulfate, Fig. 6.18) and the hydrocarbon ends will be in the oil and the sulfate end will be in the water. See Fig. 6.19. More details are given later in this section.

As noted by NOAA (2005) in a simplified diagram of a dispersant being sprayed on the surface (Fig. 6.20), the wave action provides the energy necessary to break the oil into small droplets and the surfactant will then associate at the O/W interface and the small droplets (5–20 μm) will be stabilized. See Fig. 6.20. Note that lighter crude oils (mostly lower molecular weight oil molecules) are easier to disperse than heavy crude. The heavy crudes are more viscous and also may contain asphaltenes and other chemicals that act as natural surfactants that may emulsify water into the mass. See Section 2.4.1 that discusses the formation of production phase emulsions. Surprisingly, very high waves may hinder dispersion by limiting contact between the oil and the chemicals. A very flat sea condition may not provide enough mixing energy to be effective.

The generalized mechanism of the action of all dispersants is described by Clayton et al. (1993). As noted in Section 2.4.1, mechanical action is needed to form an emulsion, and a surfactant is needed to then stabilize the film that forms around the droplet of the inner phase. In the case of an O/W dispersant, the surfactant lowers the interfacial tension (IST) (see the general discussion of IST in Section 1.5.3). The mixing energy (W_K) is given by

$$W_K = (\gamma_{O/W})(A_{O/W}) \dots \dots \dots (6.1)$$

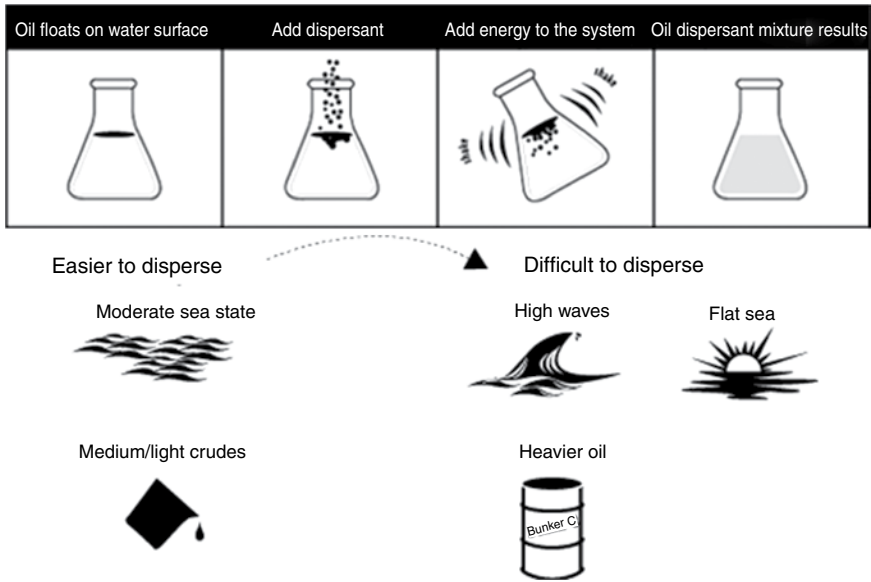


Fig. 6.20—Simplified dispersant mechanism.

Here, γ_{ow} is the O/W IST and A_{ow} is the area of contact. The surfactant allows the surface area to be larger at a given amount of mixing energy by lowering the IST. The authors (Clayton et al. 1993) have found that surfactants that lower the IST the most at the critical micelle concentration (concentration where surfactant micelles form) usually are the most effective agents. See Fig. 6.21. More details of the individual chemicals are described later in this section.

Clayton et al. (1993) also claim that five things must happen when a dispersant is applied. These ideas are in line with the description in Fig. 6.20 by NOAA (2005). They are the following:

1. The dispersant must be deposited on the surface of the oil at the correct concentration.
2. The dispersant must penetrate the oil.
3. The molecules of the dispersant must orient with the hydrophobe in the oil and the hydrophil in the water phase (see Fig. 6.19).
4. The O/W IST must decrease, thus weakening the cohesive strength of the oil phase.
5. Mixing energy must be applied to reduce the particle size so the surfactant can stabilize the droplets.

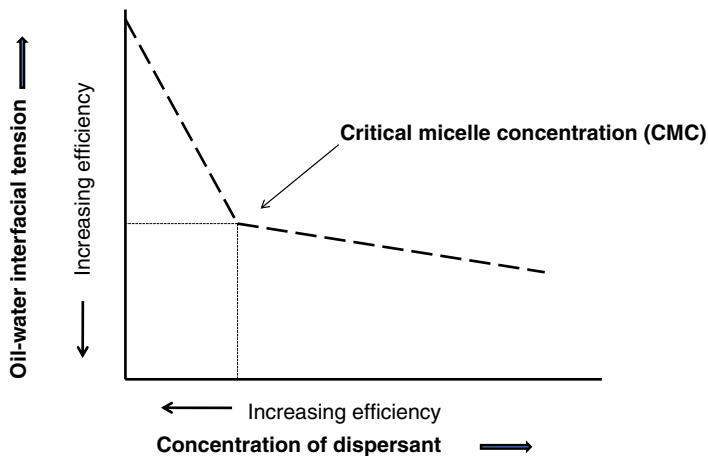


Fig. 6.21—IST and CMS for surfactants (Clayton et al. 1992).

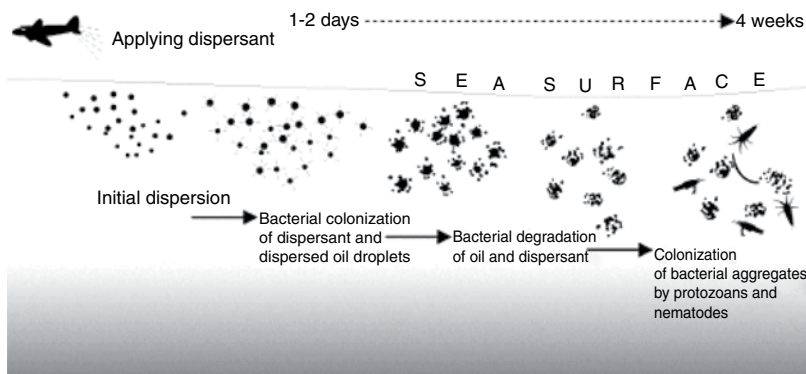


Fig. 6.22—Dispersant/oil degradation mechanism.

Fink (2003) devotes an entire chapter (19) to oil-spill treating chemicals. He notes that the particular crude oil spilled and the specific dispersant chemicals must be matched.

Once the oil is dispersed, biodegradation will then start to take place. Fig. 6.22 shows a simplified mechanism of the proposed sequence of action as the chemicals react with the oil in the water column. In this depiction, naturally occurring bacteria start to colonize the dispersed oil particles. In addition to breaking the oil slick into very small particles, this action of the dispersant chemicals also greatly increases the surface area on which the bacteria can operate and thus increase the rate of action. Daling and Lewis (2001) note that the dispersants usually work for oils that have viscosities up to about 5,000 cp; however, the actual composition is critical (note the discussion of crude oil composition in Section 2.2.5 and Fig. 2.22) and thus they will not work in all conditions. Important conditions include the temperature (viscosity usually increases with lower temperature) as well as the wave action as noted previously (NOAA 2005). Lewis (2001) also claims that studies have shown that many residual fuel oils are dispersible up to viscosities around 20,000–30,000 cp. Very heavy industrial fuel oils, cannot be dispersed because the viscosities are too high to allow small globules of oil to form. They also tend to float as very thick patches on the sea, too thick to be sprayed with dispersants. Clayton et al. (1993) discuss the effect of the composition and also note that the composition of the crude oil also greatly affects the use of the dispersants and choice of the dispersant. Several charts in their book show the effects of using different surfactants to disperse different crude oil samples and, depending on the sample, different formulations dispersed from 100% to less than 30% of the oil.

Daling and Lewis (2001) claim that once the oil has weathered at sea, it also is more difficult to disperse because the low molecular weight components have dissipated and the heavier components such as asphaltenes are more difficult to be affected by the surfactants. They claims that there is only a 12–48 hour window available until the oil is too thick to disperse. During the 2010 Gulf of Mexico spill, the authors of this book observed video showing direct injection of dispersant into the oil plume exiting the damaged blowout preventer of the well.

As described in Fig. 6.22, the bacteria then degrade the dispersed oil and then are themselves consumed by other aquatic organisms. Note that aerobic bacteria are responsible for the degradation of the oil. Thus, the process will consume dissolved oxygen from the water column and possibly produce a dead zone. Some of the pros and cons of actually using/not using dispersants will be described briefly in the section titled “Pros and Cons of Dispersant Use.”

Description and Testing of Spill Cleanup Chemicals. A list of characteristics of a preferred dispersant includes

- Low toxicity to humans
- Low toxicity to marine organisms
- Low flammability
- Biodegradable
- Highly active

- Noncorrosive
- Long shelf life
- Low viscosity
- Easy to apply from the air and at sea
- Inexpensive

There are many types of tests that are used to develop and qualify dispersants. Effectiveness tests are described by several authors. Allen (1984) shows a table that demonstrates a large variety of tests, including tank tests, shake tests, IST tests, and sea trials. Clayton et al. (1993) describe various laboratory tests. These include the Institut du Francais du Petrole tests (described as follows), tank tests, and shaker flask tests. Clayton et al. (1992) is a comprehensive book and gives many more details than can be given in this book.

Fink (2003) lists wave basin tests as well as ice tests as possible evaluation methods. In the ice test, this author claims that dispersants were tested in salt water that contained frozen ice. A moderate wave action was applied and 90% of a light crude oil was dispersed in 2 hours. Fink (2003) also lists several lab-level tests that include dispersing the oil in water, separating the phases and then extracting the aqueous phase with methylene chloride and then determining oil extracted using a colorimeter. He claims that some light oils (more paraffinic) do not have sufficient absorption in this test and it gives large errors.

Jacob and Bergman (2001) describe a test they claim is required by the US EPA (*USEPA 40 CFR 300.900 Test* 1994) and was conducted to demonstrate the criticality of their invention and its superior performance over currently approved dispersants. The document cited has been used by the EPA to qualify dispersants under the NCP product schedule.

According to Jacob and Bergman (2001) the following is the protocol for 40 CFR 300.900 testing and a dispersant must attain an effectiveness value of 45% or greater to be added to the NCP list.

1. Prepare a premixed dispersant-oil by mixing 1 part dispersant 10 parts oil (v:v).
2. Store this in glass containers.
3. Add 120±2 mL synthetic sea water to 3 each of modified 125-mL glass Erlenmeyer flasks.
4. Measure and record the water temperature.
5. Place the flasks securely into an attached slot on a shaker table. Carefully add 10.0 mL of an oil-dispersant solution onto the center of the water's surface using a positive displacement pipette.
6. Agitate the flasks for 20±1 minutes at 150±10 rev/min on the shaker table.
7. After 20±1 minutes shaking, remove the flasks from the shaker table and allow them to remain stationary for 10±1 minutes for oil droplet settling.
8. At the conclusion of the 10-minute settling period, carefully decant a 30-mL sample through the side spout of the test flasks into a 50-mL graduated cylinder.
9. Perform methylene chloride extraction and analyze using UV-spectrometer at 340, 370, and 400 nm wavelength and determine the quantity of oil.
10. Performance criterion: The dispersants tested remain in consideration for addition to the NCP product schedule if the average dispersant effectiveness, as calculated, is at least 45% (i.e., 50% ± 5%).

Fiocco et al. (1998) describe a test [see diagram in Clayton et al. (1993)].

1. The physical apparatus for the test involves a cylindrical glass container for holding a test solution and an oscillating hoop that fits inside the container. The glass container has two ports: (1) an inlet port located just below the experimental water level, and (2) an outlet port that is located near the bottom of the vessel and contains an overflow arm extending upward to determine the depth of the test solution in the container.
2. Clean seawater is introduced by a peristaltic pump into the glass container through the inlet port. Overflow water (containing oil droplets) leaves the container through the exit port and is

collected in a flask. The oscillating hoop is suspended 20–35 mm beneath the water’s surface and moves up and down with a 15-mm vertical path by an electromagnet controlled by an electronic timer. The frequency of the oscillation can be varied in the range of 6.66–20 cycles/minute.

3. For tests designed to evaluate dispersant effectiveness the following experimental protocol is followed: the glass container is filled with seawater.
4. A specified amount of oil is poured onto the water surface inside a 10-cm diameter vertical ring.
5. Dispersant is added onto the surface of the oil.
6. The oscillating hoop is started, and water flow through the peristaltic pump is started at a specified flow rate (e.g., to produce a dilution or turnover rate of 0.5/hour).
7. Outflow water is collected for specified periods of time (e.g., 0–30 minutes, 30–60 minutes, and 60–120 minutes) and analyzed for oil content.
8. Oil content in the collected samples follows the equation

$$x = x_o e^{-Dt}, \dots\dots\dots (6.2)$$

where x = oil concentration at time t , X_o = initial dispersed oil concentration in the experiment, D = dilution rate. The percentage of the washed-out oil is P at time t :

$$P = 100(1 - x/x_o) = 100(1 - e^{-Dt}) \dots\dots\dots (6.3)$$

The effectiveness (E in %) is

$$E = 100[(P_d - P_c)/P_c] \dots\dots\dots (6.4)$$

Here, P_d is the % with the dispersant, and P_c is the control without the dispersant.

Sections 6.1 and 6.2 of this book have discussed most of the ecotox issues associated with the use of production chemicals and have referenced some of the safety/ecotox test methods for qualifying production chemicals. The toxicity values for chemicals are listed on the MSDS if they are in the levels that necessitate control by the EPA. Additional guidelines are in Fink (2003) and Daling and Lewis (2001). Also see Mulkins-Phillips and Stewart (1974). This paper (Mulkins-Phillips and Stewart 1974) was concerned with the effect of the dispersants on biodegradation. They tested four dispersants and found that all of the dispersants used alone supported good growth of microorganisms, but qualitative population shifts were caused by the dispersant-oil combinations. The degrees of degradation of the n -alkane fraction of the crude oil varied depending upon the dispersant used. Under these test conditions, only one, which had the poorest emulsifying capacity, promoted n -alkane degradation compared with the values of the other materials. An additional issue with the toxicity of the dispersants is a claim by Earle et al. (2010) and other scientists that the toxicity of a dispersant to mitigate the BP MTDH spill (Gulf of Mexico 2010) + the spilled crude oil is *more* toxic to marine life than the oil itself. More discussions of the pros and cons of dispersant use are at the end of this section.

Chemistry of Dispersants. Dispersants in commercial use are usually considered to be proprietary formulations, so most of the information described next has been obtained from the patent literature as well as a few published sources. Daling and Lewis (2001) mention that in the 1970s and 1980s petroleum-based dispersants, such as petroleum sulfonates were used, and these were more toxic to marine life than the crude oil. Geraci and Aubin (1988) talk generally about dispersants and note that these are surface-active and include anionic, cationic, and nonionic chemicals. They claim that nonionic surfactants are used most frequently in dispersants. They include ethoxylated alkylphenols, such as nonylphenol-ethylene oxide, ethoxylated linear alcohols, such as oleyl alcohol, and esters formed by the reaction of fatty acids with polyhydric alcohols. Some of these compounds are shown in Fig. 2.55 and are used in many other oilfield formulations. Solvents frequently are needed to dissolve

the surfactants and these may include aliphatic and aromatic hydrocarbon mixtures, water or alcohols in water, glycols, and glycol ethers. These are similar to formulations for corrosion inhibitors [Section 3.6.1 and Frenier and Ziauddin (2008)].

Geraci and Aubin (1988) also claim that the formulations with hydrocarbon solvents tend to be more effective in treating heavy, viscous oils. They are easier to mix and apply but are more toxic than those containing water-soluble solvents. A stabilizer may also be added to adjust pH, reduce corrosiveness, and help fix the dispersion after it is formed, or counteract adverse color or odor. Dispersant stabilizers may include alkalis, phosphates, silicates, nitrates, dyes, and polymerized alkyl naphthalene sulfonates and cosolvents including glycol ethers. These are also part of formulations for heavy organic deposits described by Frenier et al. (2010).

Lumcon (2008) provides an online bibliography of dispersant information that is mostly concerned with reports on ecotox data collected about dispersants. A number of possible dispersant compounds from this database are listed. This list contains chemicals that were also described in previous paragraphs.

- Nonionic surfactants include
 - Mono-, di-, and tri-sorbitol oleate esters
 - Oxyethylene oxypropylene amine
 - Polyethylene glycol ester
 - Oxyethylene alcohol
 - Hexactoxyparanonylphenol
 - Sophorolipid biosurfactant solutions (aescin, lecithin, rhamnolipid, saponin, and tannin) (Urum et al. 2005).

A list of various additional nonionic surfactants is in [Fig. 6.23](#).

- Anionic surfactants:
 - Alkylarylsulfonate (sodium dodecyl sulphate)
 - Dialkyl sulfosuccinate
 - Fatty alcohol oxyalkyl esters
- Cationic surfactants:
 - Lauryl pyridinium chloride

Clayton et al. (1993) describe the same surfactant list seen previously and claim that for nonionic surfactants, the hydrophilic and lipophilic balance (HLB) values needed for the entire formulation should be about 15. [Fig. 6.24](#) shows the authors view of HLB values that are useful in different functions. The authors also claim that for commercial formulations, this HLB range is achieved by mixing a high HLB material (such as a sulfonate) with low HLB materials (such as a hydrotrope that would include glycol ethers). Note that there are discussion of several HLB methods in Section 2.4.4.

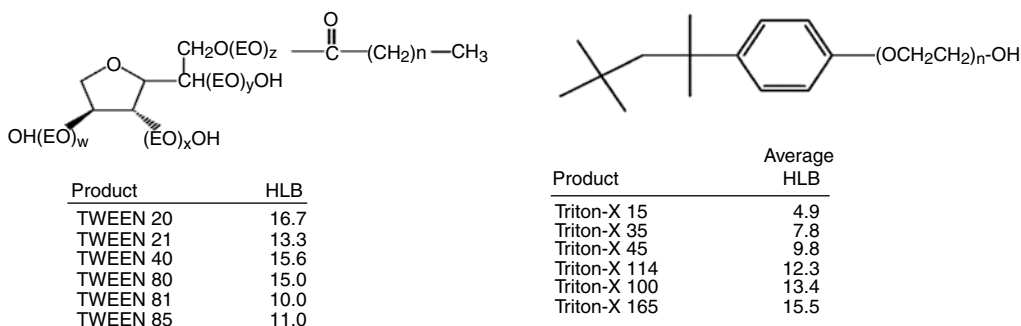


Fig. 6.23—Anionic surfactants.

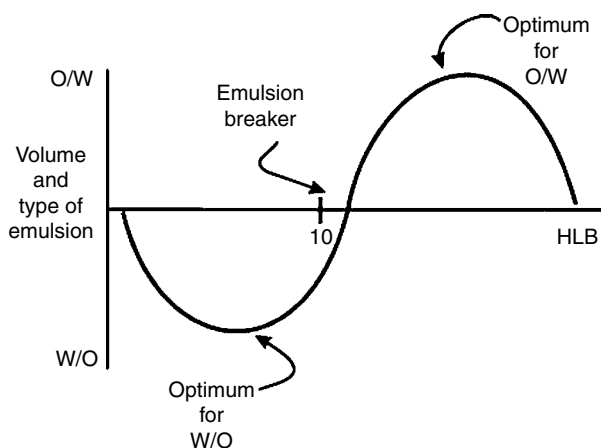


Fig. 6.24—HLB range for various applications.

the correct combination can be tailored of the specific crude oil and tested using one of the methods described previously and previously and in the books by Clayton et al. (1993) or Fink (2003). While toxicity depends on the species tested, the general trend is nonionic < anionic < cationic (Hidu 1965); however, within a series, the chain length is also important.

Several patents and other papers that describe specific dispersant chemistries are abstracted to illustrate some possible formulations.

Fiocco et al. (1998) claim formulations containing a mixture of a sorbitan monoester of an aliphatic monocarboxylic acid, a polyoxyethylene adduct of a sorbitan monoester of an aliphatic monocarboxylic acid, an alkali metal salt of a dialkyl sulfosuccinate, a polyoxyethylene adduct of a sorbitan triester or a sorbitol hexaester of an aliphatic monocarboxylic acid, and a solvent comprising at least one of a propylene glycol ether, ethylene glycol ether, water an alcohol, glycol, and a paraffinic hydrocarbon. These are claimed to produce very low IST values (to allow oil wetting and dispersion) and low toxicity.

Some of these chemicals are drawn in Fig. 6.25. This patent also reviews a large number of formulations and solvents that can be used to make various formulations. They found a synergism between various solvents, and surfactants and note that even solvents that are soluble in water can be effective dispersants when mixed with Isopar M (a hydrocarbon) in small amounts. Furthermore, at low cosolvent concentrations, there are toxicological concerns over glycol ethers containing an aromatic moiety. One formulation (seen in Fig. 6.25) has been reported (Wikipedia 2010a) to have been used in the 2010 Gulf of Mexico oil spill. This mixture contains an anionic sulfonate, ethylene glycol as a solvent, and a glycol ether as a cosolvent. These are all part of the general types of formulations described by Geraci and Aubin (1988) and Fiocco et al. (1998).

Potter and Dibble Jr (1985) claim a formulation that relates to a substantially intact proteinaceous particulate material that is effective as an oil-spill dispersant composition. In a preferred respect, the invention is a grain product (such as oats) from which lipids are removed through organic solvent extraction. The authors claim that when such compositions are applied to an oil spill, they will adsorb oil, emulsify it, and finally disperse the oil with high efficiency and are claimed to be substantially nontoxic. In preferred embodiments, the proteinaceous materials have a protein concentration of about 10% to 50%, or more preferably in the range of about 20% to 30%.

Lessard et al. (2001) describe a formulation of chemical surfactants, solvents, and inorganic salts is effective for dispersing heavy oils in both salt and fresh water. The formulation comprises a mixture of a sorbitan ester of an aliphatic monocarboxylic acid, a polyoxyethylene adduct of a sorbitan monoester of an aliphatic monocarboxylic acid, an alkali metal salt of a dialkyl sulfosuccinate, a polyoxyethylene adduct of a sorbitan triester of a monocarboxylic acid, a solvent comprising a hydrocarbon and/or a glycol ether, and an inorganic salt containing a soluble divalent cation such as calcium or magnesium.

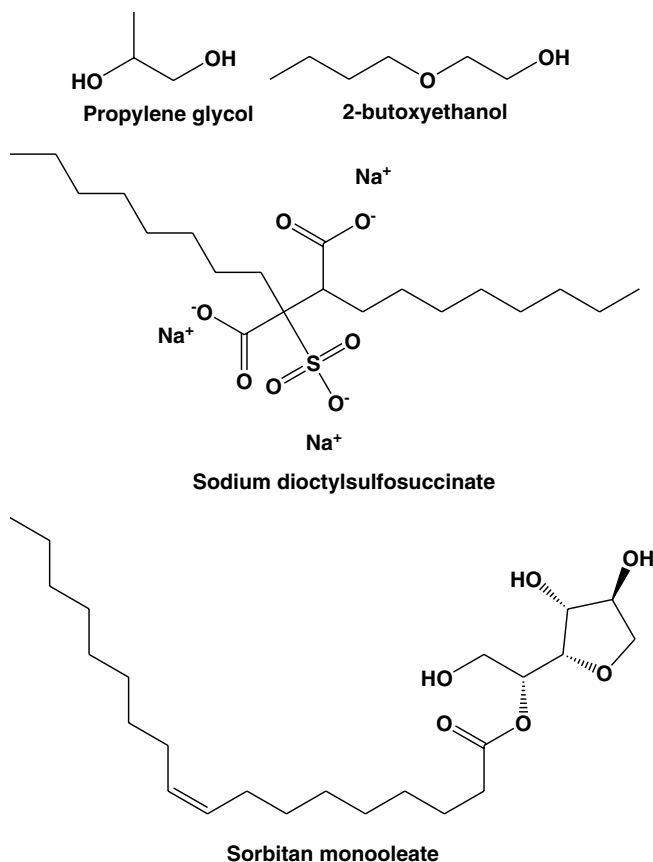


Fig. 6.25—Seawater oil dispersant chemicals.

Jacob and Bergman (2001) claim a formulation that is called ecologically friendly by the author. It includes an effective and nontoxic oil-spill dispersant that combines a predominately oil-soluble surfactant (e.g., polyethylene glycol mono-oleate) with a predominately water-soluble surfactant (e.g., cocoamide) and a cosolvent for coupling a mixture of the predominately oil-soluble surfactant and the oil spill, with the predominately water-soluble surfactant. Water is included in the combination to help increase the interaction between the predominately oil-soluble surfactant and the predominately water-soluble surfactant as well as the cosolvent.

A water-soluble component also helps reduce the viscosity of the dispersant to allow it to be pumped under pressure. These authors claim to have developed the formulations based on the HLB theory of surfactants (see Section 2.4.4 and Fig. 6.24). They note that the effectiveness of a dispersant depends on the type of surfactant or surfactant combination used in the system. If nonionic surfactants are used, the HLB value of the combined system is a vital factor in producing a stable emulsion. The HLB is applicable mostly to nonionic surfactants that are polyethoxylated. This type of system is called a W/O emulsion. The surfactant that does the emulsification or dissolution may be called as an oil-soluble emulsifier. The claim is that the complex formulations are more effective than the materials from Fiocco et al. (1998) and Potter and Dibble Jr (1985).

In addition to the chemicals noted in the previous paragraphs, Fink (2003) describes documents that claim formulations using oxyethylated fatty alcohols. These have chain lengths from about C₁₀–C₂₀ (Sulejmanov et al. 1993). Brandes and Loveless (1996) describe an invention that provides dispersants and dispersant viscosity index improvers, which include polymers of conjugated dienes that have been hydrogenated and functionalized. The dispersant substances include compositions including a copolymer of a ring substituted styrene and a conjugated diene. The polymers are selectively hydrogenated to produce polymers that have highly controlled residual amounts of aromatic unsaturation, permitting highly selective functionalization.

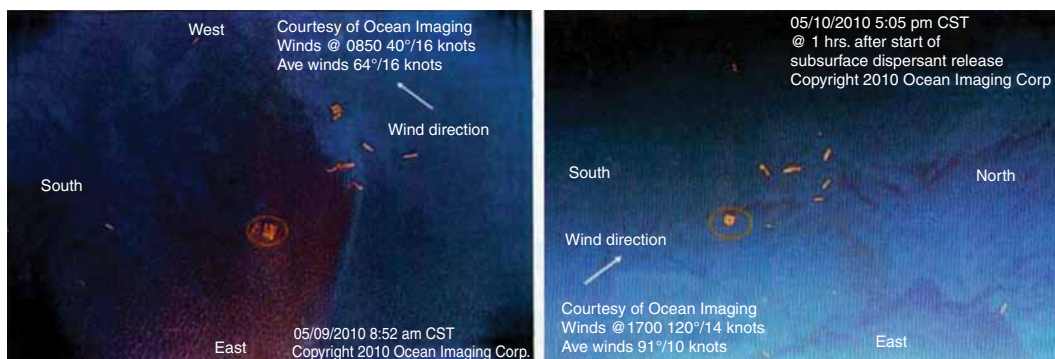


Fig. 6.26—Aerial photos of wellsite on 9 May 2010 and 11 hours later (Denney 2012; Nedwed et al. 2012).

Pros and Cons of Dispersant Use. Denney (2012) has reviewed information on the effects of the use of dispersants [based on the report of Nedwed et al. (2012)] during the BPMTDH spill. They claim that the use of 25,000 bbl of dispersants during this spill was able to keep oil from contacting the shore areas. **Fig. 6.26** shows photos of the ocean near the wellsite before and after subsea injection of dispersants. The reports quote estimates of up to 90% dispersion of the oil slick from the left photo. These authors also claim that volatile organic carbon measurements indicate that the use of the dispersants was highly successful for keeping the oil from the shore areas.

MSNBC (2010b) reports that a newly discovered type of oil-eating microbe suddenly is flourishing in the Gulf of Mexico and gobbling up the BPMTDH spill at a much faster rate than expected, scientists reported.

Scientists discovered the new microbe while studying the underwater dispersion of millions of gallons of oil spilled since the explosion of the BPMTDH drilling rig. Also, the microbe is claimed to work without significantly depleting oxygen in the water.

Daling and Lewis (2001) and NOAA (2005) note that there are pros and cons associated with the use of dispersants. The document by Daling and Lewis (2001) describes two case histories where dispersants were used to combat large spills. NOAA (2005) explains that in any particular situation, the decision to use dispersants involves balancing the potential advantages of dispersant use—removing oil from the water surface and avoiding some shoreline impacts—with the potential disadvantages, such as impacts to plankton or other water column organisms. Part of the work of planning the response to potential oil spills is the difficult task of evaluating these trade-offs, which requires careful consideration of the resources and issues. This document also notes that dispersant use will be limited in the areas where corals are present because they are very sensitive to oil and surfactant contamination. **Fig. 6.27** from Daling and Lewis (2001) shows a summary of the arguments. They note that some of these arguments describe a “birds vs. fish” controversy that is an inevitable result of competing economic and ecological interests [also see Earle et al. (2010)].

Daling and Lewis (2001) also have attempted to provide a net environmental benefit analysis (NEBA) method for determining which methods are the most useful (from an economic viewpoint). They claim that the purpose of any oil-spill response method should be to reduce the amount of damage done by an oil spill. The damage might be to ecological resources, such as sea birds and sensitive habitats, or economic damage to resources, such as fisheries or tourism. The concept of NEBA is that, in some circumstances, it might be reasonable to sustain some damage to a particular resource as the result of oil-spill response, provided the response prevents a greater degree of damage occurring to another resource. NEBA considers the overall damage that might be caused by an oil spill and does not concentrate on one particular aspect.

Efroymson et al. (2004) describe NEBA as a methodology for comparing and ranking net environmental benefits associated with multiple management alternatives. A NEBA for chemically contaminated sites typically involves comparison of several management alternatives: (1) leaving contamination in place, (2) physically, chemically, or biologically remediating the site through traditional

| Criticism | Counterargument |
|---|--|
| The best method of protecting the environment is to immediately pick up all spilled oil from the sea. The use of dispersants is the wrong approach to oil-spill response. | Mechanical containment and recovery with the use of booms and skimmers is a very useful response strategy for small spills in calm waters, but suffers from some major limitations for large spills and in rough water. |
| Dispersants push the oil into the environment rather than removing it from the environment and this is a bad strategy. | Dispersants <u>do</u> transfer the oil from the water surface into the water column. If this is done in conditions that allow rapid dilution of the dispersed oil to very low concentrations, the risk of ecological harm is small, compared to letting the oil impact the shoreline or other sensitive sites. |
| Dispersants are only used to hide oil pollution and thus to remove it from view, but the oil is not “neutralized” and will cause unseen harm. | The aim of the treatment is NOT to hide the oil, but to transfer it to the water column, where it is hoped that the damage (economic and ecological) will be minimized. |
| Addition of toxic chemicals to an already polluted environment will increase the poisoning of marine life. | Dispersants are less toxic than the oil they are used to disperse. |
| Dispersants are an unreliable method because they do not always work. Mechanical recovery should be used instead. | Dispersants <u>do</u> have limitations. They may not disperse high-viscosity oils in cold waters or disperse weathered oils. Mechanical methods of recovery also have limitations, caused by weather, amount of the oil, location and oil characteristics. |

Fig. 6.27—Arguments about dispersant use (Lewis 2001).

means, (3) improving ecological value through on-site and off-site restoration alternatives that do not directly focus on removal of chemical contamination, or (4) a combination of those alternatives.

Efroymsen et al. (2004) claim that NEBA involves activities that are common to remedial alternatives analysis for state regulations and the Comprehensive Environmental Response, Compensation, and Liability Act, post-closure and corrective action permits under the Resource Conservation and Recovery Act, evaluation of generic types of response actions pertinent to the Oil Pollution Act, and land management actions that are negotiated with regulatory agencies in flexible regulatory environments (i.e., valuing environmental services or other ecological properties, assessing adverse impacts, and evaluating remediation or restoration options). This article presents a high-level framework for NEBA at contaminated sites with subframeworks for natural attenuation (the contaminated reference state), remediation, and ecological restoration alternatives. Primary information gaps related to NEBA include nonmonetary valuation methods, exposure-response models for all stressors, the temporal dynamics of ecological recovery, and optimal strategies for ecological restoration.

The problem with this approach and any other quantitative analysis is to assign values that are agreeable to all parties, and to do it during the window of opportunity where intervention may be appropriate. Mechanical methods such as booms, skimmers, and controlled burns are also in the cleanup “tool box” according to NOAA (2005). See Fig. 6.16.

6.4.3 Cleanup of Contaminated Soil and Affected Wildlife. This section describes aspects of cleanup methods on land and water wildlife after a spill.

Cleanup on Land. If a spill of oil or a production chemical occurs on land, different cleanup methods and chemicals probably will be necessary. An OERB (2000) report (commissioned by the US Soil Conservation Service) lists a number of options.

Restoration of salt-impacted soils: This could include spills of other aqueous treating chemicals such as frac fluids. The method may depend on the exact chemicals spilled and the toxicity values include the following:

- Natural remediation—do nothing
- Pond construction—build a pond over the spill, then treat the water
- Land application—also called land farming

- Chemical amendment application—use various chemicals to leach/neutralize the chemicals
- Burial—below the root zone
- Road spreading—mix with road treatment chemicals
- Soil washing—similar to chemical amendment
- Solidification—mix with a chemical that fixes the waste
- Off-site disposal—in an approved site

Restoration of hydrocarbon impacted soils: This may require different methods compared with inorganic waste remediation.

- Natural attenuation—do nothing
- Land application—see above
- Bioremediation—use of natural soil bacteria, sometimes augmented. See Zenone et al. (2002) below
- Dilution burial—add fresh soil
- Road spreading—see above
- Solidification—see above, but probably different methods needed
- Off-site disposal—see above

Steps for restoration of salt-impacted or hydrocarbon soils:

- Gather information concerning the physical characteristics of the site. This information could include such items as soil types, proximity to surface water, slopes, vegetative cover, depth to bedrock, annual precipitation, depth to groundwater, and intended land use.
- Design a sampling plan to determine the physical extent and degree of chemical impact and subsurface conditions. The sampling plan should be sufficient to collect enough information to be able to make an informed decision on the restoration protocol.
- Collect samples in accordance with the sampling plan. The initial plan may have to be modified in the field based on additional information obtained during sampling. Evaluate sample analysis and physical characteristics of the site to determine which restoration protocol to use.
- Review local, state, and federal rules and regulations to determine if the selected restoration option is allowed. If required, submit a restoration plan with sample analysis to the appropriate regulatory agency for approval.
- If the restoration option requires additional land use, obtain approval from the surface owner.

Zenone et al. (2002) described bioremediation of oil damaged soils in Pennsylvania. Several examples were presented.

- a) As an alternative to off-site disposal, a biopod (on-site treatment area) was created to bioremediate the oil-contaminated soil. The abandoned oil wells were plugged in 1996, the oil-contaminated soil was solidified, organic matter was added, and root tilling was conducted to homogenize the oil-contaminated soil. By the end of the growing season, a vegetative cover was established and no further actions.
- b) Established after the removal of a tank in the summer of 1997. The total petroleum hydrocarbons concentrations were reduced from approximately 891,500 mg/kg to approximately 12,000 mg/kg by the end of the summer when the operations were suspended for the winter. After reconfiguration of the biopod in the spring of 1998, samples were collected in June 1998, establishing a baseline sample of approximately 8,260 mg/kg.

Fink (2003) mentions that remediation of soil can include various chemical treatments including a foamed ethanol and use of biodegradable surfactants and polyacrylamides. Urum et al. (2005) report experimental measurements on the ability of aqueous biosurfactant solutions (aescin, lecithin, rhamnolipid, saponin, and tannin) at removing Ekofisk crude oil from a laboratory-contaminated soil under

varying washing conditions. The oil removal performance of the biosurfactants was evaluated against a synthetic anionic surfactant (sodium dodecyl sulphate) using distilled water as a base case. The washing parameters and ranges tested were temperature, time, shaking speed, volume/mass ratio, and surfactant concentrations. Results indicated that washing temperature was the most influential parameter on the oil removal while washing time was the least. It was possible to obtain more than 80% oil removal at 50°C for all the surfactant solutions, except lecithin, which yielded less than 15% removal. However, saponin, lecithin, aescin, and tannin removed less than 50% crude oil when tested at a temperature of 20°C and other parameters. Soil washing was found to have considerable potential in removing crude oil from the contaminated soil; therefore, we suggest further testing be performed with weathered contaminated soils.

Augustinovic et al. (2012) have reviewed the use of microbiological colonies for cleanup of onshore and offshore wastes and note that the additions of nutrients and oxygen to oily wastes can reduce linear paraffins and diesel oil contamination by 90% in 30 days.

Cleaning of Wildlife and Birds. Various wildlife, including sea birds, turtles, and sea otters have become fouled during oil spills. Various agencies have then been contacted to try to remove the oil before the animals suffer permanent damage using chemicals. These materials are also oil dispersants but usually are more related to shampoo and dish-cleaning soaps rather than some of the components in the formulations seen in Fig. 6.25. To reduce skin irritation, the pH usually will balance in the neutral range. Some of these were developed [as described by Newman et al. (2003)]. Between 1973 and 1976, the International Bird Rescue Research Center responded to six smaller California oil spills that affected approximately 1,300 birds and tried cleaning birds with solvents and many other products sent to them by the petroleum industry.

Unfortunately, many side effects (neurological symptoms, torpor, and death) were observed in oiled birds cleaned with solvents, and rehabilitators also reported skin rashes and headaches (Berkner 1979). In 1976, with a grant from the American Petroleum Institute, the International Bird Rescue Research Center started testing detergents as cleaning products for oiled wildlife and determined that a dish-washing fluid was the most effective. Eventually, it is claimed, that additional research by Bryndza et al. (1995) determined that Dawn™ (Proctor and Gamble—Fig. 6.28 is a possible formulation) was the best cleaning detergent for oiled wildlife. Dawn™ removed oil from plumage relatively easily, did not damage the plumage, irritate the animal's skin, or cause other health problems to wildlife or to people cleaning the animals.

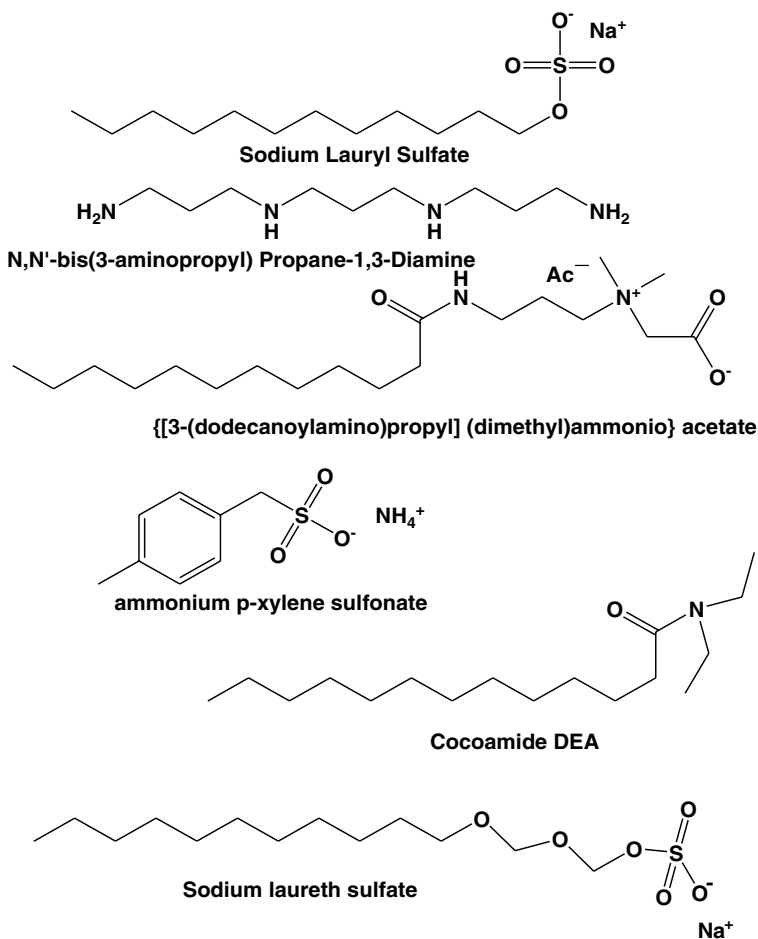
6.5 Continual Quality Improvements With Oilfield Chemistry

Through application of the production oilfield chemistry principles described in this book as well as in the many sources cited, the authors contend that continuous quality improvements can be achieved in the oil and gas sector of the world economy. The authors note that at least four of the five SPE Research and Development Grand Challenges (Judzis et al. 2011) are directly related to current or proposed oilfield chemistry processes:

1. Increasing recovery factors (current EOR—Chapter 5, and hydraulic fracturing—Section 3.8 and Chapter 4).
2. In-situ molecular manipulation (injection of chemicals—reactions in porous media described in Sections 1.6.2 and 3.3.1), heat, or microorganisms.
3. Carbon capture and sequestration (CO₂ EOR—Section 5.5.2).
4. Produced water management (reuse of water for EOR—Section 5.4.1 and/or hydraulic fracturing or other treatments, Section 6.3.2).

Several suggestions are offered for consideration as possible ways to continue the improvements.

- Accelerate the search for safer, more environmentally acceptable chemicals as well as improved application methods. This process will offer economic, environmental, and public perception benefits. As an example, if benzene-containing diesel fuel (Section 4.3.1) is not used in



(water, sodium lauryl sulfate, sodium pareth-23, sulfate C-12-14-16, dimethyl amine oxide, SD alcohol, undeceth-9, propylene glycol, cyclohexandiamine, polyacetate) = A household cleaner

Fig. 6.28—Shampoo and dish cleaners.

hydraulic fracturing treatments; these chemicals *cannot* be in groundwater supplies because of the hydraulic fractures.

- Quality also can be enhanced through an understanding of the entire petroleum product supply chain, which includes production (upstream), transportation (midstream—of multiple fluids including oil, gas, and aqueous phases and finished products) as well as refining/petrochemical (downstream) manufacturing. This book has attempted to emphasize that chemical and physical principles are the same in any environment where the conditions are also the same (Section 1.1). In addition, it must be emphasized that each phase of the supply chain affects the next, and there are also feedback loops, where one phase affects the earlier phase. For example, the quality requirements for pipeline transportation of fluids affects the well products that are needed as well as the facilities required for the treatments and separations.
- Realizing that all well fluids are potential products, NOT wastes for disposal, provides a different perspective for resources conservation. Thus the products are seen to include the hydrocarbon liquids, gases, water, and the dissolved salts. This view also includes CO₂ capture products for any sources and even problem gases like H₂S. Use of these valuable chemicals is already well underway (and described in Chapters 4 and 5) in some sectors, as gases and brines are used in EOR and hydraulic fracturing water is being recycled. With the exception of possible use of

the salt cake from evaporation of brines for road salt (Rassenfoss 2011a), the authors of this book are not aware of routine brine uses as a chemical feedstock. Veil (2009) has shown several examples of methods (including distillation and evaporation for producing the salt cakes). Detailed analyses of some brines may reveal useful amounts of rare or costly chemical species.

In other industries, fresh brines from selected formations have a long history as chemical feedstocks. For example, the Dow Chemical Company (Whitehead 1968) was founded based on extraction of bromine (and then NaOH and chlorine) from brines. There is also the example of the great overlap with the chemical/petrochemical industries that routinely use other firms' "waste streams" as their raw materials. The authors of the book do recognize that transportation of well fluids may be a limiting factor for economic reuse.

- Various standards/recommended practices are being produced by industry-related groups including *API Publications 2012 Catalog* (2012), *ISO* (2012), and *NACE* (2012) to provide quality control in various parts of the upstream/midstream petroleum environments. Specific examples of operational safety and reliability standards and recommended practices include *API RP 14E* (1991), *API RP 54* (1997), *ANSI/NACE MR 0175/ISO 15156* (2009), and *NACE ANSI/NACE SP0502* (2010). These are in use to provide reliability guidelines for corrosion control as well as safety issues at the wellsite. Many other standards are available from these organizations. If the industries involved continue to provide strong standards of performance and show that these are good business practices, less governmental oversight may be required.

Nomenclature

- α = angle of incidence, degree or other constants
- β = a cell constant
- β = the ratio of the molecular weight of the rock to that of HCl
- γ = IST, dyne/cm
- ΔG = Gibbs free energy, kJ/mol
- Δh = height difference, cm
- ΔH = enthalpy change, kJ/mol
- Δp = pressure differential, Pa
- ΔU = enthalpy of vaporization, kJ/mol
- δ = solubility parameter, (MPa)^{1/2} or labrid parameter
- ε = strain
- ε = dielectric constant- coulombs/m²
- ζ = zeta potential, mv
- η = absolute (intrinsic) viscosity, Pa-sec (kg·m⁻¹·s⁻¹)
- θ = contact angle, degree
- κ = permeability, Darcies (d)
- μ = viscosity, cP (1 cP = 0.001 Pa·s = 1 mPa·s)
- π = 3.1416
- ρ = density, g/cm³
- σ = stress, Pa
- σ^* = solubilization ratio
- τ = time when each small area element of a fracture is created or opened
- τ_y = yield stress of gel, Pa
- ν = kinematic viscosity (η/ρ)-(m²/s)
- ν = Poisson ratio, dimensionless
- ϕ = volume fraction or initial porosity of formation
- χ = Flory-Huggins interaction parameter
- ω = rotational rate, radians/sec
- ω = frequency, cycles/sec
- A = surface area, cm²

\AA = angstrom- 10^{-8} m

AI = Amott index

B = a volume factor

B_o = oil formation volume fraction at abandonment

B_o = bond number (dimensionless)

C = concentrations

C^* = critical overlap concentration

C^* = critical concentration

C_c = compression controlled fluid loss coefficient

C_D = conductivity, md-ft

C_{fd} = dimensionless fracture conductivity

C_L = fluid loss coefficient

d = diameter, cm

D_{eff} = effective diffusion coefficient, m^2/s

E = Young modulus

E_A = areal sweep efficiency

E_D = local displacement efficiency

E_R = efficiency of recovery of oil

E_v = volumetric sweep efficiency

f = friction factor, unit less

f_w = fractional flow of water, m^3/d

G = shear modulus

G' = storage modulus

G'' = loss modulus

g = gravity acceleration, m/s^2

H = enthalpy

h = height, m

I_o = Amott oil index

I_w = Amott water index

J^* = productivity index, bbl/psi

K = consistency index, $lbf \cdot s^n / ft^2$ or $kPa \cdot s^n$

K = equilibrium coefficient, mol/kg

k = permeability, d

k = a rate coefficient (units vary depending on reaction order)

keV = thousand electron volts

l = length, m

m = molality, mol/kg

M = molar mass of solvent, g/mol

M = mobility ratio, unitless

- n = refractive index, unitless
 n = power law (viscosity) coefficient
 N_c = capillary number, unitless
 N_{Da} = Damköhler number (ratio of reaction rate to convective mass transport), unitless
 N_o = Avogadro's number, $6.02 \times 10^{23}/\text{mol}$
 N_p = cumulative oil recovery, m^3
 N_{sh} = Sherwood number (ratio of convective mass transfer coefficient/diffusive mtc)
 P = poise ($1 P = 1 \text{ dyne}/\text{cm}^2$)
 p = pressure, Pa
 P_c = capillary pressure- Pa
ppt = pounds per thousand gallons
 q = volumetric flow rate, m/sec
 R = universal gas constant, $8.314 \text{ J}/^\circ\text{K}\text{-mol}$
 R = reaction rates
 r = radius, cm
 R_e = Reynolds number, unitless
 R_f = resistance factor, unitless
 S = skin
 S_o = oil saturation at $0 P_c$
 S_{or} = oil saturation
 S_p = spirit loss, cm^3
 S_w = water saturation at $0 P_c$
 S_{wr} = irreducible water saturation
 S_{wr} = irreducible oil saturation
 t = time, seconds
 $t_{1/2}$ = half-life for radioactive decay processes
 t/d = metric ton per day
 T = temperature ($^\circ\text{K}$, $^\circ\text{C}$)
 T_{wat} = wax appearance temperature
 V = volume, cm^3
 V_a = areal sweep efficiency
 v_m = molar volume, m^3/mol
 V_v = vertical sweep efficiency
 V_{pf} = floodable pore volume, m^3
 w = width, cm
 x = length, m
 X_c = dissolving power

References

- 27,000 Abandoned Oil and Gas Wells in Gulf of Mexico Ignored by Government, Industry. 2010. The Associated Press, 7 July 2010.
- Abdallah, W., Buckley, J.S., Carnegie, A. et al. 2007. Fundamentals of Wettability. *Oilfield Review* **19** (2): 44–61.
- Abdel-Aal, H.K., Aggour, M., and Fahim, M.A. 2003. *Petroleum and Gas Field Processing*. New York: Marcel Dekker.
- Abdou, M., Carnegie, A., Mathews, S.G. et al. 2011. Finding Value in Formation Water. *Oilfield Review* **23** (1): 24–35.
- Abou-Sayed, I., Shuchart, C.E., Choi, N.H. et al. 2007. Well Stimulation Technology for Thick, Middle East Carbonate Reservoirs. Presented at the International Petroleum Technology Conference, Dubai, 4–6 December. IPTC-11660-MS. <http://dx.doi.org/10.2523/11660-MS>.
- Acharya, A.R. 1986. Particle Transport in Viscous and Viscoelastic Fracturing Fluids. *SPE Prod Eng* **1** (2): 104–110. SPE-13179-PA. <http://dx.doi.org/10.2118/13179-PA>.
- Achour, M., Bredal, F., and Blumer, D. 2012. Effect of Acid Flowbacks on Corrosion Inhibition Effectiveness. Presented at the 14th Middle East Corrosion Conference and Exhibition (MEECE), Manama, Bahrain, 12–15 February. 56-CT-02.
- Acosta, E.J., Yuan, J.S., and Bhakta, A.S. 2008. The Characteristic Curvature of Ionic Surfactants. *J. Surfactants Deterg.* **11** (2): 145–158. <http://dx.doi.org/10.1007/s11743-008-1065-7>.
- Adachi, J., Seibrits, E., Peirce, A. et al. 2007. Computer simulation of hydraulic fractures. *Int. J. Rock Mech. Min. Sci. & Geomech. Abstracts* **44** (5): 739–757. <http://dx.doi.org/10.1016/j.ijrmms.2006.11.006>.
- Adams, T.A. 2002. *Scale Inhibitor Impregnated Proppant Siip, DL 11219*. Sugar Land, Texas: Schlumberger.
- Adkins, S., Arachchilage, G.P., Solairaj, S. et al. 2012. Development of Thermally and Chemically Stable Large-Hydrophobe Alkoxy Carboxylate Surfactants. Presented at the SPE Improved Oil Recovery Symposium, Tulsa, 14–18 April. SPE-154256-MS. <http://dx.doi.org/10.2118/154256-MS>.
- Ahmad, T., Beaman, D.J., and Birou, P. 2010. Viscoelastic Surfactant Diversion: An Effective Way to Acidize Low-Temperature Wells. Presented at the Abu Dhabi International Petroleum Exhibition and Conference, Abu Dhabi, UAE, 1–4 November 2010. SPE-136574-MS. <http://dx.doi.org/10.2118/136574-MS>.
- Ahmadi, M., Sharma, M.M., Pope, G. et al. 2011. Chemical Treatment To Mitigate Condensate and Water Blocking in Gas Wells in Carbonate Reservoirs. *SPE Prod & Oper* **26** (1): 67–74. SPE-133591-PA. <http://dx.doi.org/10.2118/133591-PA>.
- Ainley, B., Clouse, D., Hill, D. et al. 1997. Specialty Chemicals in the Oil Field. *Oilfield Review* **9** (1): 26–40.
- Akbar, A., Hu, X., Neville, A. et al. 2011. Flow Rate and Inhibitor Influences on Protective Scale Formed on Carbon Steel. *Mater. Performance* **50** (12): 54–59.
- Akbar, S., Okell, P.R., and Sinclair, A.R. 2010. Degradable Ball Sealers and Methods for Use in Well Treatment. US Patent No. 7,647,964.
- Akbarzadeh, K., Hammami, A., Kharrat, A. et al. 2007. Asphaltenes: Problematic but Rich in Potential. *Oilfield Review* **19** (2): 22–43.

- Akrad, O.M., Miskimins, J.L., and Prasad, M. 2011. The Effects of Fracturing Fluids on Shale Rock Mechanical Properties and Proppant Embedment. Presented at the SPE Annual Technical Conference and Exhibition, Denver, 30 October–2 November. SPE-146658-MS. <http://dx.doi.org/10.2118/146658-MS>.
- AkzoNobel. 2006. Dissolvine GL-38 Safety Data Sheet. Deventer, The Netherlands: Akzo Nobel Functional Chemicals LLC.
- AkzoNobel. 2009. Dissolvine GL Technical Brochure. Chicago, Illinois: Akzo Nobel Functional Chemicals LLC.
- Al-Abduwani, F.A.H., Shirzadi, A., van den Broek, W.M.G.T. et al. 2005. Formation Damage vs. Solid Particles Deposition Profile During Laboratory-Simulated Produced-Water Reinjection. *SPE J.* **10** (2): 138–151. SPE-82235-PA. <http://dx.doi.org/10.2118/82235-PA>.
- Al-Anazi, H.A., Nasr-El-Din, H.A., and Mohamed, S.K. 1998. Stimulation of Tight Carbonate Reservoirs Using Acid-in-Diesel Emulsions: Field Application. Presented at the SPE Formation Damage Control Conference, Lafayette, Louisiana, USA, 18–19 February. SPE-39418-MS. <http://dx.doi.org/10.2118/39418-MS>.
- Al-Anzi, E., Al-Mutawa, M., Al-Habib, N. et al. 2003. Positive Reactions in Carbonate Reservoir Stimulation. *Oilfield Review* **15** (4): 28–45.
- Al-Asmi, K., Benayan, M., and Hezar, L. 1999. Pipeline Flow of Water-Oil Mixtures. *Chem. Pet. Eng.* **35** (5): 245–249. <http://dx.doi.org/10.1007/bf02360962>.
- Al-Awadi, M., Clark, W.J., Moore, W.R. et al. 2009. Dolomite: Perspectives on a Perplexing Mineral. *Oilfield Review* **21** (3): 32–45.
- Alberta. 2011. *Vapex*. Calgary, Alberta, Canada: Alberta Research Council. www.arc.ab.ca.
- Alexander, T., Baihly, J., Boyer, C. et al. 2011. Shale Gas Revolution. *Oilfield Review* **23** (3): 40–66.
- Al-Ghamdi, A.H., Hill, D., Nasr-El-Din, H.A. et al. 2011. Acid Diversion Using Viscoelastic Surfactants: The Effects of Flow Rate and Initial Permeability Contrast. Presented at the SPE Annual Technical Conference and Exhibition, Denver, 30 October–2 November. SPE-142564-MS. <http://dx.doi.org/10.2118/142564-MS>.
- Al-Harbi, B.G., Al-Dahlan, M.N., and Khaldi, M.H. 2012. Aluminum and Iron Precipitation During Sandstone Acidizing Using Organic-HF Acids. Presented at the SPE International Symposium and Exhibition on Formation Damage Control, Lafayette, Louisiana, USA, 15–17 February. SPE-151781-MS. <http://dx.doi.org/10.2118/151781-MS>.
- Al-Harthy, S., Bustos, O.A., Samuel, M. et al. 2008. Options for High-Temperature Well Stimulation. *Oilfield Review* **20** (4): 52–62.
- Ali, S., Frenier, W.W., Lecerf, B. et al. 2004. Virtual Testing: The Key to a Stimulating Process. *Oilfield Review* **16** (1): 58–68.
- Ali, S.A. and Hinkel, J.J. 2001. Additives in Acidizing Fluids. In *Reservoir Stimulation*, third edition, M.J. Economides and K.G. Nolte. New York: John Wiley & Sons.
- Ali, S.A., Clark, W.J., Moore, W.R. et al. 2010. Diagenesis and Reservoir Quality. *Oilfield Review* **22** (2): 14–27.
- Ali, S.A., Ermel, E., Clarke, J. et al. 2008. Stimulation of High-Temperature Sandstone Formations From West Africa With Chelating Agent-Based Fluids. *SPE Prod & Oper* **23** (1): 32–38. SPE-93805-PA. <http://dx.doi.org/10.2118/93805-PA>.
- Al-Jubran, H.H., Wilson, S., and Johnston, B.B. 2010. Successful Deployment of Multistage Fracturing Systems in Multilayered Tight Gas Carbonate Formations in Saudi Arabia. Presented at the SPE Deep Gas Conference and Exhibition, Manama, Bahrain, 24–26 January. SPE-130894-MS. <http://dx.doi.org/10.2118/130894-MS>.
- Alkafeef, S.F. and Zaid, A.M. 2007. Review of and Outlook for Enhanced Oil Recovery Techniques in Kuwait Oil Reservoirs. Presented at the International Petroleum Technology Conference, Dubai, 4–6 December. IPTC-11234-MS. <http://dx.doi.org/10.2523/11234-MS>.
- Alleman, D., Qu, Q., and Keck, R. 2003. The Development and Successful Field Use of Viscoelastic Surfactant-based Diverting Agents for Acid Stimulation. Presented at the International Symposium on Oilfield Chemistry, Houston, 5–7 February. SPE-80222-MS. <http://dx.doi.org/10.2118/80222-MS>.
- Allen, T.E. 1984. *Oil Spill Chemical Dispersants: Research, Experience, and Recommendations: A Symposium*, no. 840. West Conshohocken, Pennsylvania: American Society for Testing and Materials.

- Al-Marzouqi, M., Al-Farisi, O., Al-Felasi, A. et al. 2010. Acid Effect Life Cycle in Carbonate Reservoir, Field Case. Presented at the Abu Dhabi International Petroleum Exhibition and Conference, Abu Dhabi, 1–4 November. SPE-138523-MS. <http://dx.doi.org/10.2118/138523-MS>.
- Al-Mayouf, A.M. 2006. Dissolution of Magnetite Coupled Galvanically With Iron in Environmentally Friendly Chelant Solutions. *Corros. Sci.* **48** (4): 898–912.
- Al-Mjeni, R., Arora, S., Cherukupalli, P. et al. 2010. Has the Time Come for EOR? *Oilfield Review* **22** (4): 16–35.
- Almond, S.W. and Garvin, T.R. 1984. High Efficiency Fracturing Fluids for Low Temperature Reservoirs. *Proc.*, 31st Annual Southwestern Petroleum Short Course, Texas Tech University, Lubbock, Texas, 15 April.
- Al-Mutairi, S., Al-Obied, M.A., Al-Yami, I. et al. 2012. Wormhole Propagation in Tar During Matrix Acidizing of Carbonate Formations. Presented at the SPE International Symposium and Exhibition on Formation Damage Control, Lafayette, Louisiana, USA, 15–17 February. SPE-151560-MS. <http://dx.doi.org/10.2118/151560-MS>.
- Al-Mutairi, S.H., Nasr-El-Din, H.A., Al-Driveesh, S.M. et al. 2005. Corrosion Control during Acid Fracturing of Deep Gas Wells: Lab Studies and Field Cases. Presented at the SPE International Symposium on Oilfield Corrosion, Aberdeen, 13 May. SPE-94639-MS. <http://dx.doi.org/10.2118/94639-MS>.
- Al-Mutairi, S.H., Nasr-El-Din, H.A., Hill, A.D. et al. 2008. Effect of Droplet Size on the Reaction Kinetics of Emulsified Acid With Calcite. Presented at the SPE International Symposium and Exhibition on Formation Damage Control, Lafayette, Louisiana, USA, 13–15 February. SPE-112454-MS. <http://dx.doi.org/10.2118/112454-MS>.
- Al-Naimi, K.M., Lee, B.O., Shourbagi, S.M. et al. 2008. Successful Case History of a Novel Open-Hole Horizontal Well Completion in Saudi Arabia. Presented at the SPE Asia Pacific Oil and Gas Conference and Exhibition, Perth, Australia, 20–22 October. SPE-114961-MS. <http://dx.doi.org/10.2118/114961-MS>.
- Al-Najim, A., Zahedi, A., Al-Khonaini, T. et al. 2012. A New Methodology for Stimulation of a High-Water-Cut Horizontal Oil Well through the Combination of a Smart Chemical System with Real-Time Temperature Sensing: A Case Study of South Umm Gudair Field, PZ Kuwait. Presented at the SPE/ICoTA Coiled Tubing & Well Intervention Conference and Exhibition, The Woodlands, Texas, USA, 27–28 March. SPE-154387-MS. <http://dx.doi.org/10.2118/154387-MS>.
- Alshehri, A., Sagatov, E., and Kovscek, A.R. 2009. Pore-Level Mechanics of Forced and Spontaneous Imbibition of Aqueous Surfactant Solutions in Fractured Porous Media. Presented at the SPE Annual Technical Conference and Exhibition, New Orleans, 4–7 October. SPE-124946-MS. <http://dx.doi.org/10.2118/124946-MS>.
- Alvarado, V. and Manrique, E. 2010. Enhanced Oil Recovery: An Update Review. *Energies* **3** (9): 1529–1575. <http://dx.doi.org/10.3390/en3091529>.
- Al-Yami, A., Nasr-El-Din, H.A., Al-Humaidi, A.S. et al. 2010. Effect of HCl Acid and Brines on Water-Swelling Packers. *SPE Drill & Compl* **25** (3): 322–327. SPE-114812-PA. <http://dx.doi.org/10.2118/114812-PA>.
- American Completion Tools (ACT). 2010. Treating Irons, Union Connections, Bull Plugs, Cross Over Adaptors and Swages, http://www.acthammerunion.com/ACT1/Catalog_files/act%20brochure%202011_1.pdf (downloaded 8 July 2013).
- Amott, E. 1959. Observations Relating to the Wettability of Porous Rock. *Trans.*, AIME, **216**: 156–162.
- Anderson, G.A., Delshad, M., King, C.L.B. et al. 2006. Optimization of Chemical Flooding in a Mixed-Wet Dolomite Reservoir. Presented at the SPE/DOE Symposium on Improved Oil Recovery, Tulsa, 22–26 April. SPE-100082-MS. <http://dx.doi.org/10.2118/100082-MS>.
- Anderson, W.G. 1986. Wettability Literature Survey—Part 1: Rock/Oil/Brine Interactions and the Effects of Core Handling on Wettability. *J. Pet Tech* **38** (10): 1125–1144. SPE-13932-PA. <http://dx.doi.org/10.2118/13932-PA>.
- Anderson, W.G. 1987. Wettability Literature Survey—Part 6: The Effects of Wettability on Waterflooding. *J. Pet Tech* **39** (12): 1605–1622. SPE-16471-PA. <http://dx.doi.org/10.2118/16471-PA>.

- ANSI/NACE MR0175/ISO 15156, *Petroleum and natural gas industries—Materials for Use in H2S-Containing Environments in Oil and Gas Production*, parts 1, 2, and 3. 2009. Houston, Texas: NACE International.
- API RP 61, *Recommended Practices for Evaluating Short Term Proppant Pack Conductivity*. 1989b. Washington, DC: API.
- API MPMS 10.4, *Manual of Petroleum Measurement Standards, Chapter 10: Sediment and Water—Section 4: Determination of Sediment and Water in Crude Oil by the Centrifuge Method (Field Procedure)*. 1988. Washington, DC: API.
- API Publications 2012 Catalog. 2012. Washington, DC: American Petroleum Institute.
- API RP 14E, *Recommended Practice for Design and Installation of Offshore Production Platform Piping Systems*, fifth edition. 1991. Washington, DC: API.
- API RP 54, *Recommended Practice for Occupational Safety for Oil and Gas Well Drilling and Servicing Operations*, third edition. 1999. Washington, DC: API.
- API RP 56, *Recommended Practices for Testing Sand Used in Hydraulic Fracturing Operations*. 1995. Washington, DC: API.
- API RP 60, *Recommended Practices for Testing High Strength Proppants Used in Hydraulic Fracturing Operations*. 1989a. Washington, DC: API.
- API. 2008. Hydraulic Fracturing at a Glance, http://www.api.org/policy/exploration/upload/hydraulic_fracturing_at_a_glance.pdf (downloaded 15 July 2013).
- API. 2009. Hydraulic Fracturing Operations—Well Construction and Integrity Guidelines. Guidance Document HF1, American Petroleum Institute, Washington, DC, (October 2009).
- API. 2010. Water Management Associated with Hydraulic Fracturing. Guidance Document HF2, American Petroleum Institute, Washington, DC (June 2010).
- Appel, C., Ma, L.Q., Dean Rhue, R. et al. 2003. Point of zero charge determination in soils and minerals via traditional methods and detection of electroacoustic mobility. *Geoderma* **113** (1–2): 77–93. [http://dx.doi.org/http://dx.doi.org/10.1016/S0016-7061\(02\)00316-6](http://dx.doi.org/http://dx.doi.org/10.1016/S0016-7061(02)00316-6).
- Appicciutoli, D., Maier, R.W., Strippoli, P. et al. 2010. Novel Emulsified Acid Boosts Production in a Major Carbonate Oil Field with Asphaltene Problems. Presented at the SPE Annual Technical Conference and Exhibition, Florence, Italy, 19–22 September. SPE-135076-MS. <http://dx.doi.org/10.2118/135076-MS>.
- Aqualon. 2007. Guar and Guar Derivative in Oil and Gas Field Applications, Wilmington, Delaware: Aqualon.
- Arceneaux, C. and DeKerlegand, K. 2009. Safety in Offshore Frac Hose Rig Hookups. Presented at the SPE Americas E&P Environmental and Safety Conference, San Antonio, Texas, USA, 23–25 March. SPE-120570-MS. <http://dx.doi.org/10.2118/120570-MS>.
- Arf, T.G., LaBelle, G., Klaus, E.E. et al. 1987. EOR With Penn State Surfactants. *SPE Res Eng* **2** (2): 166–176. SPE-12308-PA. <http://dx.doi.org/10.2118/12308-PA>.
- Armstrong, K., Card, R., Navarrete, R. et al. 1995. Advanced Fracturing Fluids Improve Well Economics. *Oilfield Review* **7** (3): 34–51.
- Arnab, W.D.V., T. McCoy, J.C., and Rosine, R. 2000. The Effect of Corrosion in Coiled Tubing and Its Prevention. Presented at the SPE/ICoTA Coiled Tubing Roundtable, Houston, 5–6 April 2000. SPE-60744-MS. <http://dx.doi.org/10.2118/60744-MS>.
- Arora, S.M., Horstmann, D., Cherukupalli, P.K. et al. 2010. Single-Well In-Situ Measurement of Residual Oil Saturation After an EOR Chemical Flood. Presented at the SPE EOR Conference at Oil & Gas West Asia, Muscat, Oman, 11–13 April. SPE-129069-MS. <http://dx.doi.org/10.2118/129069-MS>.
- Arthur, J.D., Bohm, B., and Layne, M. 2008. Hydraulic Fracturing Considerations for Natural Gas Wells of the Marcellus Shale. Presented at the Ground Water Protection Council 2008 Annual Forum, Cincinnati, Ohio, USA, 21–24 September.
- Arthur, J.D., Bohm, B.K., Coughlin, B.J. et al. 2009. Evaluating the Environmental Implications of Hydraulic Fracturing in Shale Gas Reservoirs. Presented at the SPE Americas E&P Environmental and Safety Conference, San Antonio, Texas, USA, 23–25 March. SPE-121038-MS. <http://dx.doi.org/10.2118/121038-MS>.

- ASTM D1133 - 10, *Standard Test Method for Kauri-Butanol Value of Hydrocarbon Solvents*. 2010. West Conshohocken, Pennsylvania: ASTM International.
- ASTM D445-04e1, *Standard Test Method for Kinematic Viscosity of Transparent and Opaque Liquids (and the Calculation of Dynamic Viscosity)*. 2004. West Conshohocken, Pennsylvania: ASTM International.
- ASTM D96-88(1998), *Standard Test Methods for Water and Sediment in Crude Oil by Centrifuge Method (Field Procedure)*. 1988. West Conshohocken, Pennsylvania: ASTM International.
- ASTM D5334-08, *Standard Test Method for Determination of Thermal Conductivity of Soil and Soft Rock by Thermal Needle Probe Procedure*. 2008. West Conshohocken, Pennsylvania: ASTM International.
- Aulfem, I.H. 2002. *Influence of Asphaltene Aggregation and Pressure on Crude Oil Emulsion Stability*. PhD thesis, Norwegian University of Science and Technology, Trondheim, Norway (June 2002).
- Augustinovic, A., Birketveit, O., Clements, K. et al. 2012. Microbes-Oilfield Enemies or Allies. *Oilfield Review* **24** (2): 4–17.
- Austad, T. 2010. Enhanced Oil Recovery: Potential by “Smart Water” from Carbonates and Sandstones. Presented at the Danish Academy of Technical Sciences, Copenhagen, Denmark, 18 March.
- Austad, T., RezaeiDoust, A., and Puntervold, T. 2010. Chemical Mechanism of Low Salinity Water Flooding in Sandstone Reservoirs. Presented at the SPE Improved Oil Recovery Symposium, Tulsa, 24–28 April. SPE-129767-MS. <http://dx.doi.org/10.2118/129767-MS>.
- Aveyard, R., Binks, B.P., Fletcher, P.D.I. et al. 1990. The Resolution of Water-in-Crude Oil Emulsions by the Addition of Low Molar Mass Demulsifiers. *J. Colloid and Interface Science* **139** (1): 128–138.
- Awan, A.R., Teigland, R., and Kleppe, J. 2008. A Survey of North Sea Enhanced-Oil-Recovery Projects Initiated During the Years 1975 to 2005. *SPE Res Eval & Eng* **11** (3): 497–512. SPE-99546-PA. <http://dx.doi.org/10.2118/99546-PA>.
- Ayello, F., Robbins, W., Richter, S. et al. 2011. Crude Oil Chemistry Effects on Inhibition of Corrosion and Phase Wetting. Presented at the NACE International CORROSION 2011, Houston, 13–17 March. NACE-11060.
- Ayoub, J.A., Hutchins, R.D., Bas, F.v.d. et al. 2006. New Findings in Fracture Cleanup Change Common Industry Perceptions. Presented at the International Symposium and Exhibition on Formation Damage Control, Lafayette, Louisiana, USA, 15–17 February. SPE-98746-MS. <http://dx.doi.org/10.2118/98746-MS>.
- Azem, W., Candler, J., Galvan, J. et al. 2011. Technology for Environmental Advances. *Oilfield Review* **23** (2): 44–52.
- Babcock, R.E., Prokop, C.L., and Kehle, R.O. 1967. Distribution of Propping Agents in Vertical Fractures. *Producers Monthly* **31** (11): 11–17.
- Bakeev, K.N., Chuang, J., Drzewinski, M.A. et al. 2000. Methods for Preventing or Retarding the Formation of Gas Hydrates. US Patent No. 6,117,929.
- Baker, H.R., Bolster, R.N., Leach, P.B. et al. 1970. Association Colloids in Nonaqueous Fluids. *Ind. Eng. Chem., Prod. Res. Develop* **9** (4): 541–547.
- Baker, R.W., Cussler, E.L., Eykamp, W. et al. 1991. *Membrane Separation Systems*. Park Ridge, New Jersey: Noyes Data Corporation.
- Bakke, J.M., Buhaug, J., and Riha, J. 2001. Hydrolysis of 1,3,5-Tris(2-hydroxyethyl)hexahydro-s-triazine and Its Reaction with H₂S. *Ind. Eng. Chem. Res.* **40** (26): 6051–6054. <http://dx.doi.org/10.1021/ie010311y>.
- Bale, G.E. 1984. Matrix Acidizing in Saudi Arabia Using Buoyant Ball Sealers. *J Pet Technol* **36** (10): 1748–1752. SPE-11500-PA. <http://dx.doi.org/10.2118/11500-PA>.
- Ball, C.L. and Frenier, W.W. 1984. Improved Solvent for Iron Sulfide Deposits. Presented at the 39th NACE International Corrosion Forum, Houston, 12–16 March. NACE-84002.
- Bang, V.S.S., Pope, G., Sharma, M.M. et al. 2010. A New Solution To Restore Productivity of Gas Wells With Condensate and Water Blocks. *SPE Res Eval & Eng* **13** (4): 323–331. <http://dx.doi.org/10.2118/116711-PA>.

- Barati, R., Johnson, S.J., McCool, S. et al. 2011. Fracturing Fluid Cleanup by Controlled Release of Enzymes From Polyelectrolyte Complex Nanoparticles. *J. Appl. Polym. Sci.* **121** (3): 1292–1298. <http://dx.doi.org/10.1002/app.33343>.
- Barnes, J.R., Dirkwager, H., Smit, J.R. et al. 2010. Application of Internal Olefin Sulfonates and Other Surfactants to EOR. Part 1: Structure—Performance Relationships for Selection at Different Reservoir Conditions. Presented at the SPE Improved Oil Recovery Symposium, Tulsa, 24–28 April. SPE-129766-MS. <http://dx.doi.org/10.2118/129766-MS>.
- Barron, A. 2005. *Commercialization of Alumoxane Nanoparticles*. Department of Chemistry, Rice University, Houston, Texas.
- Barron, A.R. 2009. *Applying Nanotechnology to the Oil and Gas Industry*. Rice University, Houston.
- Barthelmy, D. 2009. Mineralogy Database. David Barthelmy, <http://webmineral.com/>.
- Barton, A.F.M. 1983. *CRC Handbook of Solubility Parameters and Other Cohesion Parameters*. Boca Raton, Florida: CRC Press.
- Baser, B., Boney, C.L., Clum, E. et al. 2009. Multilayered Ball Sealer and Method of Use Thereof. World Application. Patent No. WO/2009/050681.
- Baumgarten, D. and Bobrosky, D. 2009. Multi-Stage Acid Stimulation Improves Production Values in Carbonate Formations in Western Canada. Presented at the SPE Saudi Arabia Section Technical Symposium, AlKhobar, Saudi Arabia, 9–11 May. SPE-126058-MS. <http://dx.doi.org/10.2118/126058-MS>.
- Baycroft, P.D., McElfresh, P.M., Crews, J.B. et al. 2005. Frac Packing with Low Environmental Impact Hydraulic Fracturing Fluid Benefits the Operator. Presented at the SPE/EPA/DOE Exploration and Production Environmental Conference, Galveston, Texas, USA, 7–9 March. SPE-94236-MS. <http://dx.doi.org/10.2118/94236-MS>.
- Bayer. 2001. An Environmentally Friendly and Readily Biodegradable Chelating Agent, 2001 Greener Synthetic Pathways Award. Munich, Germany.
- Bazin, B. and Abdulahad, G. 1999. Experimental Investigation of Some Properties of Emulsified Acid Systems for Stimulation of Carbonate Formations. Presented at the Middle East Oil Show and Conference, Bahrain, 20–23 February. SPE-53237-MS. <http://dx.doi.org/10.2118/53237-MS>.
- Bazin, B., Charbonnel, P., and Onaisi, A. 1999. Strategy Optimization for Matrix Treatments of Horizontal Drains in Carbonate Reservoirs, Use of Self-Gelling Acid Diverter. Presented at the SPE European Formation Damage Conference, The Hague, 31 May–1 June. SPE-54720-MS. <http://dx.doi.org/10.2118/54720-MS>.
- Bazin, B., Peysson, Y., Lamy, F. et al. 2010. In-Situ Water-Blocking Measurements and Interpretation Related to Fracturing Operations in Tight Gas Reservoirs. *SPE Prod & Oper* **25** (4): 431–437. SPE-121812-PA. <http://dx.doi.org/10.2118/121812-PA>.
- Beal, C. 1946a. The Viscosity of Air, Water, Natural Gas, Crude Oil and Its Associated Gases at Oil Field Temperatures and Pressures. *Trans., AIME* **165** (1): 114–115. <http://dx.doi.org/10.2118/946094-G>.
- Beal, C. 1946b. The Viscosity of Air, Water, Natural Gas, Crude Oil and Its Associated Gases at Oil Field Temperatures and Pressures. *Trans., AIME* **165** (1): 94–95. <http://dx.doi.org/10.2118/946094-G>.
- Beale, J.A.F. and Kucera, C.H. 1966. Corrosion Inhibitors for Aqueous Acids. US Patent No. 3 231 507.
- Becker, J.R. 1997. *Crude Oil, Waxes, Emulsions and Asphaltenes*. Tulsa, Oklahoma: PennWell Publishing Company.
- Becker, J.R. 1998. *Corrosion and Scale Handbook*. Tulsa: PennWell Publishing Company.
- Beckwith, R. 2011a. Quantifying the Invisible: Getting a Handle on Methane’s Climate Impact. *J. Pet Tech* **63** (11): 54–58.
- Beckwith, R. 2011b. Mitigating Disaster. *J. Pet Tech* **63** (12): 48–51.
- Beckwith, R. 2012a. Depending on Guar for Shale Oil and Gas Development. *J. Pet Tech* **64** (12): 44–55.
- Beckwith, R. 2012b. The Post-Macondo World: Two Years after the Spill. *J. Pet Tech* **64** (5): 36–47.

- Belcher, C.K., Seth, K., Hollier, R. et al. 2010. Maximizing Production Life With the Use of Nanotechnology to Prevent Fines Migration. Presented at the International Oil and Gas Conference and Exhibition in China, Beijing, 8–10 June. SPE-132152-MS. <http://dx.doi.org/10.2118/132152-MS>.
- Bell, T., Chambers, R., and Pyle, R. 2008. Overcoming the Challenges to Intelligently Pig the Unpiggable—Platform Elly to Shore Oil Pipeline Case Study. Presented at the Prevention First 2008, California Land Commission, Long Beach, California, 9–10 September.
- Benham, A.L., Dowden, W.E., and Kunzman, W.J. 1960. Miscible Fluid Displacement—Prediction of Miscibility. *Trans., AIME* **219**: 229–237.
- Bennion, B. 1999. Formation Damage—the Impairment of the Invisible, by the Inevitable and Uncontrollable, Resulting in an Indeterminate Reduction of the Unquantifiable!. *J. of Canadian Petroleum Technology* **38** (2): 12–15.
- Berg, S. 2004. Hydrated Chloride Ion Life Requires Water. Lecture notes, Winona State University, Winona, Minnesota, <http://course1.winona.edu/sberg/241f04/Lec-note/Water.htm>.
- Berkhof, R., Kwekkeboom, H., Balzer, D. et al. 1992. Demulsifiers for Breaking Petroleum Emulsions. US Patent No. 5,164,116.
- Berkland, C., Cordova, M., Liang, J.-T. et al. 2008. Polyelectrolyte Complexes as Delayed Gelling Agents for Oil and Gas Applications. US Application Patent No. 2008/0223578 A1.
- Berkner, A.B. 1979. Wildlife Rehabilitation Techniques: Past, Present, and Future. Presented at the US Fish and Wildlife Service Pollution Response Workshop, St. Petersburg, Florida, USA, 8–10 May.
- Bernard, G.C., Holm, L.W., and Harvey, C.P. 1980. Use of Surfactant to Reduce CO₂ Mobility in Oil Displacement. *Society of Petroleum Engineers Journal* **20** (4): 281–292. SPE-8370-PA. <http://dx.doi.org/10.2118/8370-PA>.
- Berry, S.L., Boles, J.L., and Smith, K.L. 2012. Cost-Effective Acid Stimulation of Carbonates Using Seawater-Based Systems Without Calcium Sulfate Precipitation. Presented at the SPE International Symposium and Exhibition on Formation Damage Control, Lafayette, Louisiana, USA, 15–17 February. SPE-149997-MS. <http://dx.doi.org/10.2118/149997-MS>.
- Bersworth, F.C. 1960. Metal Ion Control. US Patent No. 2,961,311.
- Bhardwaja, A. and Hartlanda, S. 1993. A Study of Demulsification of Water-in-Crude Oil Emulsion. *J. of Dispersion Science and Technology* **14** (5): 541–557.
- Bhuyan, D. 1989. *Development of an Alkaline/Surfactant/Polymer Compositional Reservoir Simulator*. PhD dissertation, Austin, Texas (December 1989).
- Bhuyan, D., Pope, G.A., and Lake, L.W. 1991. Simulation of High-pH Coreflood Experiments Using a Compositional Chemical Flood Simulator. Presented at the SPE International Symposium on Oilfield Chemistry, Anaheim, California, 20–22 February. SPE-21029-MS. <http://dx.doi.org/10.2118/21029-MS>.
- Bigorange. 2010. Bigorange XVIII Stimulation Vessel, Sugar Land, Texas: Schlumberger Technology Company.
- BiolinScientific. 2009. Surface Tension, <http://www.attension.com/surface-tension.aspx> (accessed 20 July 2013).
- Bivins, C.H., Boney, C., Fredd, C. et al. 2005. New Fibers for Hydraulic Fracturing. *Oilfield Review* **17** (2): 34–43.
- Bjørnstad, T. 2008. Interwell Tracer Technology. Presented at the SPE ATW on Tracer Technology, Dubai, 12–16 October.
- Blauch, M.E., Myers, R.R., Moore, T. et al. 2009. Marcellus Shale Post-Frac Flowback Waters—Where is All the Salt Coming from and What are the Implications? Presented at the SPE Eastern Regional Meeting, Charleston, West Virginia, USA, 23–25 September. SPE-125740-MS. <http://dx.doi.org/10.2118/125740-MS>.
- Blum, P., Rabaute, A., Gaudon, P. et al. 1997. Analysis of Natural Gamma-Ray Spectra Obtained from Sediment Cores with the Shipboard Scintillation Detector of the Ocean Drilling Program: Example from Leg 1561. In *Proceedings of the Ocean Drilling Program, Scientific Results*, T.H. Shipley,

- Y. Ogawa, P. Blum, and J.M. Bahr, Vol. 156, Chap. 14, 183–195. College Station, Texas: Ocean Drilling Program.
- Bockris, J.O., Ahmed, J., Singh, W.P. et al. 1995. About a Chemical Computational Approach to the Design of Green Inhibitors. Presented at the Corrosion/95, NACE International, Houston, NACE-95033.
- Boek, E.S., Ladva, H.K., Crawshaw, J.P. et al. 2008. Deposition of Colloidal Asphaltene in Capillary Flow: Experiments and Mesoscopic Simulation. *Energy Fuels* **22** (2): 805–813.
- Bomgardner, M.M. 2012. Cleaner Fracking. *C&E News* **90** (42): 13–16.
- Boonstra, T.O., Heus, M., Carstens, A. et al. 2009. Glutamic Acid N,N-Diacetic Amide, Glutamic Acid N-Acetic Amide N-Acetonitrile, Alkali Metal Salts Thereof, Process to Prepare Them and Their Use. World Application Patent No. WO/2009/024519.
- Børeng, R., Schmidt, T., Vikane, O. et al. 2003. Downhole Measurement of pH in Oil & Gas Applications by Use of a Wireline Tool. Presented at the SPE European Formation Damage Conference, The Hague, 13–14 May. SPE-82199-MS. <http://dx.doi.org/10.2118/82199-MS>.
- Boschee, P. 2012. Handling Produced Hydraulic Fracturing Water. *Oil & Gas Facilities* **1** (1): 23–26.
- Boswood, D.W. and Kreh, K.A. 2011. Fully Miscible Micellar Acidizing Solvents vs. Xylene, The Better Paraffin Solution. Presented at the SPE Production and Operations Symposium, Oklahoma City, Oklahoma, USA, 27–29 March. SPE-140128-MS. <http://dx.doi.org/10.2118/140128-MS>.
- Bourne, H.M. 1995. A Novel Scale Inhibitor Delivery System for Horizontal and Problem Wells. Presented at the IBC Scale Conference, Aberdeen, 20–21 November.
- Bourne, H.M., Heath, S.M., McKay, S. et al. 2000. Effective Treatment of Subsea Wells with a Solid Scale Inhibitor System. Presented at the International Symposium on Oilfield Scale, Aberdeen, 26–27 January. SPE-60207-MS. <http://dx.doi.org/10.2118/60207-MS>.
- Boyer, C., Clark, B., Jochen, V. et al. 2011. Shale Gas: A Global Resource. *Oilfield Review* **23** (3): 28–39.
- Brady, B., Elbel, J., Mack, M.G. et al. 1992. Cracking Rock: Progress in Fracture Treatment Design. *Oilfield Review* **4** (4): 2–17.
- Brandes, B.E. and Loveless, C.F. 1996. Dispersants and Dispersant Viscosity Index Improvers from Selectively Hydrogenated Polymers. World Patent No. WO96/40845.
- Brannon, H.D. 1988. Fracturing Fluid Concentrate and Method of Use. European Patent No. EP 280341.
- Brannon, H.D. and Ault, M.G. 1991. New, Delayed Borate-Crosslinked Fluid Provides Improved Fracture Conductivity in High-Temperature Applications. Presented at the SPE Annual Technical Conference and Exhibition, Dallas, 6–9 October. SPE-22838-MS. <http://dx.doi.org/10.2118/22838-MS>.
- Brannon, H.D. and Pulsinelli, R.J. 1990. Evaluation of the Breaker Concentrations Required To Improve the Permeability of Proppant Packs Damaged by Hydraulic Fracturing Fluids. Presented at the SPE Formation Damage Control Symposium, Lafayette, Louisiana, USA, 22–23 February. SPE-19402-MS. <http://dx.doi.org/10.2118/19402-MS>.
- Brannon, H.D. and Tjon-Joe-Pin, R. 1996. Fracturing Fluid Treatment Design to Optimize Fluid Rheology and Proppant Pack Conductivity. US Patent No. 5,562,160.
- Brezinski, M.M. 1999. Chelating Agents in Sour Well Acidizing: Methodology or Mythology. Presented at the SPE European Formation Damage Conference, The Hague, 31 May–1 June. SPE-54721-MS. <http://dx.doi.org/10.2118/54721-MS>.
- Brezinski, M.M. and Desai, B. 1997. Method and Composition for Acidizing Subterranean Formations Utilizing Corrosion Inhibitor Intensifiers. US Patent No. 5,697,443.
- Britt, L.K., Smith, M.B., Haddad, Z.A. et al. 2006. Water-Fracs: We Do Need Proppant After All. Presented at the SPE Annual Technical Conference and Exhibition, San Antonio, Texas, USA, 24–27 September. SPE-102227-MS. <http://dx.doi.org/10.2118/102227-MS>.
- Brooks, F.A. ed. 1992. *Cementing*. Richardson, Texas: SPE Reprint Series, No. 34, Society of Petroleum Engineers.

- Brown, L.D. 2002. Flow Assurance: A ? Discipline. Presented at the Offshore Technology Conference, Houston, Texas, 6–9 May 2002. OTC-14010-MS. <http://dx.doi.org/10.4043/14010-MS>.
- Brown, E., Thrasher, R.W., and Behrmann, L.A. 2000. Reservoir stimulation. In *Reservoir Stimulation*, third edition, M.J. Economides and K.G. Nolte. New York: John Wiley & Sons.
- Brown, J.E., Still, J.W., Fu, D. et al. 2008. Solid Sandstone Dissolver. US Application Patent No. 2008/0006409.
- Brunauer, S., Emmett, P.H., and Teller, E. 1938. Adsorption of Gases in Multimolecular Layers. *J. Am. Chem. Soc.* **60** (2): 309–319. <http://dx.doi.org/10.1021/ja01269a023>.
- Bryant, S.L. 1991. An Improved Model of Mud Acid/Sandstone Chemistry. Presented at the SPE Annual Technical Conference and Exhibition, Dallas, 6–9 October. SPE-22855-MS. <http://dx.doi.org/10.2118/22855-MS>.
- Bryant, S.L. and Buller, D.C. 1990. Formation Damage From Acid Treatments. *SPE Prod Eng* **5** (4): 455–460. SPE-17597-PA. <http://dx.doi.org/10.2118/17597-PA>.
- Bryndza, H.E., Foster, J.P. Jr., McCartney, J.H. et al. 1995. Methodology for Determining Surfactant Efficacy in Removal of Petrochemicals From Feathers. In *Wildlife and Oil Spills: Response, Research, and Contingency Planning*, L. Frink, K. Ball-Weir, and C. Smith, 69–86. Hanover, Pennsylvania: Sheridan Press Inc.
- Buckley, J.S. and Wang, J. 2002. Crude oil and asphaltene characterization for prediction of wetting alteration. *J. Pet. Sci. Eng.* **33** (1–3): 195–202. [http://dx.doi.org/10.1016/S0920-4105\(01\)00189-9](http://dx.doi.org/10.1016/S0920-4105(01)00189-9).
- Buckley, J.S., Wang, J., and Creek, J.L. 2007. Solubility of the Least-Soluble Asphaltenes. In *Asphaltenes, Heavy Oils and Petroleomics*, O.C. Mullins, E.Y. Sheu, A. Hammami, and A.G. Marshall, Chap. 16, 401–437. New York: Springer Science+Business Media.
- Buckley, S.E. and Leverett, M.C. 1942. Mechanism of Fluid Displacement in Sands. *Trans., AIME* **147** (1): 107–116. <http://dx.doi.org/10.2118/942107-G>.
- Buijse, M., de Boer, P., Breukel, B. et al. 2004. Organic Acids in Carbonate Acidizing. *SPE Prod & Fac* **19** (3): 128–134. SPE-82211-PA. <http://dx.doi.org/10.2118/82211-PA>.
- Buijse, M., Maier, R., Casero, A. et al. 2000. Successful High-Pressure/High-Temperature Acidizing With In-Situ Crosslinked Acid Diversion. Presented at the SPE International Symposium on Formation Damage Control, Lafayette, Louisiana, 23–24 February. SPE-58804-MS. <http://dx.doi.org/10.2118/58804-MS>.
- Buijse, M.A. 1997. Understanding Wormholing Mechanisms Can Improve Acid Treatments in Carbonate Formations. Presented at the SPE European Formation Damage Conference, The Hague, 2–3 June. SPE-38166-MS. <http://dx.doi.org/10.2118/38166-MS>.
- Buller, D. 2010. Haynesville Shale Reservoir Evaluation & Stimulation Topics. Presented at the Tulsa SPE Luncheon, Tulsa, Oklahoma, 11 March.
- Bulova, M.N., Nosova, K.E., Willberg, D.M. et al. 2006. Benefits of the Novel Fiber-Laden Low-Viscosity Fluid System in Fracturing Low-Permeability Tight Gas Formations. Presented at the SPE Annual Technical Conference and Exhibition, San Antonio, Texas, USA, 24–27 September. SPE-102956-MS. <http://dx.doi.org/10.2118/102956-MS>.
- Bunge, A.L. and Radke, C.J. 1985. The Origin of Reversible Hydroxide Uptake on Reservoir Rock. *SPE J.* **25** (5): 711–718. SPE-11798-PA. <http://dx.doi.org/10.2118/11798-PA>.
- Burke, J. 1984. Solubility Parameters: Theory and Application. In *The Book and Paper Group Annual*, Vol. 3, 1–35. Washington, DC: The American Institute of Conservation.
- Burke, P. 2011. Sustainable Solutions for a Thirsty Planet. Presented at the IDA World Congress on Desalination and Water Reuse, Perth, Australia, 4–9 September.
- Burman, J.W. and Hall, B.E. 1986. Foam as a Diverting Technique for Matrix Sandstone Stimulation. Presented at the SPE Annual Technical Conference and Exhibition, New Orleans, 5–8 October. SPE-15575-MS. <http://dx.doi.org/10.2118/15575-MS>.
- Burnett, D. 2011. Grand Challenges: Brine Management: Produced Water and Frac Flowback Brine. *J Pet Technol* **63** (10): 46–48.
- Burnett, D.B. and Vavra, C.J. 2006. Desalination of Oil Field Brine. Presented at the The Future of Desalination in Texas, Texas A&M University, College Station, Texas, 6–8 August.

- Buske, G.R. 1981. Method and Composition for Removing Sulfide-Containing Scale from Metal Surfaces. US Patent No. 4,289,639.
- Bustos, O., Samuel, M.M., Chang, F. et al. 2011. Compositions and Methods to Stabilize Acid-in-Oil Emulsions. World Application Patent No. WO 2011/058479 A2.
- Bustos, O.A., Heiken, K.R., Stewart, M.E. et al. 2007a. Case Study: Application of a Viscoelastic Surfactant-Based CO₂ Compatible Fracturing Fluid in the Frontier Formation, Big Horn Basin, Wyoming. Presented at the Rocky Mountain Oil & Gas Technology Symposium, Denver, 16–18 April. SPE-107966-MS. <http://dx.doi.org/10.2118/107966-MS>.
- Bustos, O.A., Sievert, C.J., Rodriguez, V.O. et al. 2007b. Recent Acid-Fracturing Practices on Strawn Formation in Terrell County, Texas. Presented at the SPE Annual Technical Conference and Exhibition, Anaheim, California, U.S.A., 11–14 November 2007. SPE-107978-MS. <http://dx.doi.org/10.2118/107978-MS>.
- Butler, J.N. and Cogley, D.R. 1998. *Ionic Equilibrium: Solubility and pH Calculations*. New York: John Wiley & Sons, Inc.
- Byars, H.G. 1999. *Corrosion Control in Petroleum Production*. Houston, Texas: NACE International.
- Caili, D., You, Q., Yuhong, X. et al. 2011. Case Study on Polymer Gel to Control Water Coning for Horizontal Well in Offshore Oilfield. Presented at the Offshore Technology Conference, Houston, 2–5 May. OTC-21125-MS. <http://dx.doi.org/10.4043/21125-MS>.
- Cantu, L.A. and Boyd, P.A. 1988. Laboratory and Field Evaluation of a Combined Fluid-Loss Control Additive and Gel Breaker for Fracturing Fluids. Presented at the SPE Annual Technical Conference and Exhibition, Houston, 2–5 October. SPE-18211-MS. <http://dx.doi.org/10.2118/18211-MS>.
- Cantu, L.A., McBride, E.F., and Osborne, M.W. 1989. Formation Fracturing Process. US Patent No. 4,848,467.
- Carbo. 2010. Intermediate Strength Proppants, Houston, Texas: Carbo Ceramics.
- Card, R., Howard, P.R., and Feraud, J.-P. 1994. Control of Particulate Flowback in Subterranean Wells. US Patent No. 5,330,005.
- Card, R., Howard, P.R., Feraud, J.-P. et al. 2001. Control of Particulate Flowback in Subterranean Wells. US Patent No. 6,172,001.
- Card, R.J., Howard, P.R., and Feraud, J.-P. 1995. A Novel Technology To Control Proppant Backproduction. *SPE Prod & Oper* **10** (4): 271–276. SPE-31007-PA. <http://dx.doi.org/10.2118/31007-PA>.
- Carman, P.S. and Cawiezel, K.E. 2007. Successful Breaker Optimization for Polyacrylamide Friction Reducers Used in Slickwater Fracturing. Presented at the SPE Hydraulic Fracturing Technology Conference, College Station, Texas, USA, 29–31 January. SPE-106162-MS. <http://dx.doi.org/10.2118/106162-MS>.
- Carman, P.S. and Gupta, D.V.S.V.S. 2011. Fracturing Fluid for Extreme Temperature Conditions is Just as Easy as the Rest. Presented at the SPE Hydraulic Fracturing Technology Conference, The Woodlands, Texas, USA, 24–26 January 2011. SPE-140176-MS. <http://dx.doi.org/10.2118/140176-MS>.
- Carpenter, J.F. and Nalepa, C.J. 2005. Bromine-Based Biocides for Effective Microbiological Control in the Oil Field. Presented at the SPE International Symposium on Oilfield Chemistry, The Woodlands, Texas, USA, 2–4 February. SPE-92702-MS. <http://dx.doi.org/10.2118/92702-MS>.
- Carrillo, A.L., Oryszczak, R., and Shen, Y.-F. 2003. Aluminum-Zirconium Antiperspirant Salts with High Peak 5 Al Content. US Patent No. 6,649,152.
- Cassidy, J.M., Kiser, C.E., and Lane, J.L. 2006. Methods and Aqueous Acid Solutions for Acidizing Wells Containing Sludging and Emulsifying Oil. US Application Patent No. 2006/0040831.
- Casto, W. 2009. Optimization of Proppant Size and Concentration in a Marcellus Shale Fracture Treatment. Presented at the Marietta College, Dept of Petroleum Engineering and Geology, Marietta, Ohio, USA, 6 April.
- Castro Dantas, T.N., Santanna, V.C., Dantas Neto, A.A. et al. 2003. Ethyl and Isoamyl Alcohols as Cosurfactants in Gel Systems. *Ind. Eng. Chem. Res.* **42** (23): 5809–5812. <http://dx.doi.org/10.1021/ie030346t>.

- Caveny, W.J., Weaver, J.D., and Nguyen, P.D. 1996. Control of Particulate Flowback in Subterranean Wells. US Patent No. 5,582,249.
- Cawiezal, K.E. and Dawson, J.C. 2009. Method of Acidizing a Subterranean Formation with Diverting Foam or Fluid. Patent No. 7,510,009.
- Cayias, J.L., Schechter, R.S., and Wade, W.H. 1976. Modeling Crude Oils for Low Interfacial Tension. *SPE J.* **16** (6): 351–357. SPE-5813-PA. <http://dx.doi.org/10.2118/5813-PA>.
- Cenegy, L.M., McAfee, C.A., and Kalfayan, L.J. 2011. Field Study of the Physical and Chemical Factors Affecting Downhole Scale Deposition in the North Dakota Bakken Formation. Presented at the SPE International Symposium on Oilfield Chemistry, The Woodlands, Texas, USA, 11–13 April. SPE-140977-MS. <http://dx.doi.org/10.2118/140977-MS>.
- Chambers, David J. 1994. Foams for Well Stimulation. In *Foams: Fundamentals and Applications in the Petroleum Industry*, Vol. 242, Chap. 9, 355–404. Advances in Chemistry, American Chemical Society. <http://dx.doi.org/10.1021/ba-1994-0242.ch009>.
- Chang, F., Qu, Q., and Frenier, W. 2001a. A Novel Self-Diverting-Acid Developed for Matrix Stimulation of Carbonate Reservoirs. Presented at the SPE International Symposium on Oilfield Chemistry, Houston, 13–16 February. SPE-65033-MS. <http://dx.doi.org/10.2118/65033-MS>.
- Chang, F.F., Acock, A.M., Geoghagan, A. et al. 2001b. Experience in Acid Diversion in High Permeability Deep Water Formations Using Visco-Elastic-Surfactant. Presented at the SPE European Formation Damage Conference, The Hague, 21–22 May. SPE-68919-MS. <http://dx.doi.org/10.2118/68919-MS>.
- Chang, F.F., Nasr-El-Din, H.A., Lindvig, T. et al. 2008. Matrix Acidizing of Carbonate Reservoirs Using Organic Acids and Mixture of HCl and Organic Acids. Presented at the SPE Annual Technical Conference and Exhibition, Denver, 21–24 September. SPE-116601-MS. <http://dx.doi.org/10.2118/116601-MS>.
- Chang, F.F., Qu, Q., and Miller, M.J. 2003. Fluid System Having Controllable Reversible Viscosity. US Patent No. 6,667,280.
- Chang, F.F., Thomas, R.L., Grant, W.D. et al. 2005. Composition and Method for Treating a Subterranean Formation. US Patent No. 6,924,255.
- Chang, H.L. 2010. Chemical EOR Progress in China Advances and Challenges. Presented at the Workshop for EOR, Oil and Gas Patagonia, Neuquen, Argentina, 3–5 November.
- Chang, S.-H. and Grigg, R.B. 1996. Foam Displacement Modeling in CO₂ Flooding Processes. Presented at the SPE/DOE Improved Oil Recovery Symposium, Tulsa, 21–24 April. SPE-35401-MS. <http://dx.doi.org/10.2118/35401-MS>.
- Charkhutian, K.B., Libutti, B.L., De Cordt, F.L.M. et al. 2004. Process for Inhibiting Scale and Fouling on the Metal Surfaces Exposed to an Aqueous System. US Application Patent No. 20040011743.
- Chase, B., Chmilowski, W., Marcinew, R. et al. 1997. Clear Fracturing Fluids for Increased Well Productivity. *Oilfield Review* **9** (3): 20–33.
- Chatriwala, S., Cawiezal, K.E., Nasr-El-Din, H.A. et al. 2005. A Case Study of a Successful Matrix Acid Stimulation Treatment In Horizontal Wells Using a New Diversion Surfactant in Saudi Arabia Presented at the SPE Middle East Oil and Gas Show and Conference, Kingdom of Bahrain, 12–15 March. SPE-93536-MS. <http://dx.doi.org/10.2118/93536-MS>.
- Chauveteau, G., Omari, A., Tabary, R. et al. 2000. Controlling Gelation Time and Microgel Size for Water Shutoff. Presented at the SPE/DOE Improved Oil Recovery Symposium, Tulsa, 3–5 April. SPE-59317-MS. <http://dx.doi.org/10.2118/59317-MS>.
- Chekhnin, E., Parshin, A., Pissarenko, D. et al. 2012. When Rocks Get Hot: Thermal Properties of Reservoir Rocks. *Oilfield Review* **24** (3): 20–37.
- Chen, F., McCool, C.S., Green, D.W. et al. 2010a. Experimental and Modeling Study of the Transport of Chromium Acetate Through Carbonate Rocks. *SPE J.* **15** (2): 349–367. SPE-100064-PA. <http://dx.doi.org/10.2118/100064-PA>.
- Chen, P., Vikane, O., Asheim, T.I. et al. 2006. Field Experiences in the Application of an Inhibitor/Additive Interaction Package To Extend an Inhibitor Squeeze Life. Presented at the SPE

- International Oilfield Scale Symposium, Aberdeen, 31 May–1 June. SPE-100466-MS. <http://dx.doi.org/10.2118/100466-MS>.
- Chen, T., Montgomerie, H., Chen, P. et al. 2009. Development of Environmental Friendly Iron Sulfide Inhibitors for Field Application. Presented at the SPE International Symposium on Oilfield Chemistry, The Woodlands, Texas, USA, 20–22 April. SPE-121456-MS. <http://dx.doi.org/10.2118/121456-MS>.
- Chen, Y., Bustos, O., and Sullivan, P. 2012. Shear-Activated Viscoelastic Surfactant Fluid and Method. US Patent No. 8,240,379.
- Chen, Y., Lee, J., and Pope, T.L. 2010b. Carbon Dioxide Foamed Fluids. US Patent No. 7,803,744.
- Cheng, J., Wei, J., Song, K. et al. 2010. Study on Remaining Oil Distribution After Polymer Flooding. Presented at the SPE Annual Technical Conference and Exhibition, Florence, Italy, 19–22 September. SPE-133808-MS. <http://dx.doi.org/10.2118/133808-MS>.
- Cheng, L., Kam, S.I., Delshad, M. et al. 2001. Simulation of Dynamic Foam-Acid Diversion Processes. Presented at the SPE European Formation Damage Conference, The Hague, 21–22 May. SPE-68916-MS. <http://dx.doi.org/10.2118/68916-MS>.
- Cheng, X., Li, Y., Ding, Y. et al. 2011. Study and Application of High Density Acid in HPHT Deep Well. Presented at the SPE European Formation Damage Conference, Noordwijk, The Netherlands, 7–10 June. SPE-142033-MS. <http://dx.doi.org/10.2118/142033-MS>.
- Cheng, Y. and Prud'homme, R.K. 2000. Enzymatic Degradation of Guar and Substituted Guar Galactomannans. *Biomacromolecules* **1** (4): 782–788. <http://dx.doi.org/10.1021/bm005616v>.
- Cheng, Y., Prud'homme, R.K., Chik, J. et al. 2002. Measurement of Forces between Galactomannan Polymer Chains: Effect of Hydrogen Bonding. *Macromolecules* **35** (27): 10155–10161. <http://dx.doi.org/10.1021/ma020887e>.
- Cherian, J. 2002. *Microscopic and Macroscopic Visulation of Displacment of Oil from Porous Media*. MS thesis, Texas Tech University, Lubbock, Texas.
- Chesapeake. 2010. Haynesville Shale Hydraulic Fracturing, Oklahoma City, Oklahoma: Chesapeake Energy.
- Chesnut, G.R., Chappell, G.D., and Emmons, D.H. 1987. The Development of Scale Inhibitors and Inhibitor Evaluation Techniques for Carbon Dioxide EOR Floods. Presented at the SPE International Symposium on Oilfield Chemistry, San Antonio, Texas, USA, 4–6 February. SPE-16260-MS. <http://dx.doi.org/10.2118/16260-MS>.
- Cinco-Ley, H., Samaniego-V., F., and A.N., D. 1978. Transient Pressure Behavior for a Well With a Finite-Conductivity Vertical Fracture. *SPE J.* **18** (4): 253–264. SPE-6014-PA. <http://dx.doi.org/10.2118/6014-PA>.
- Cipolla, C.L., Lolon, E.P., and Dzubin, B. 2009. Evaluating Stimulation Effectiveness in Unconventional Gas Reservoirs. Presented at the SPE Annual Technical Conference and Exhibition, New Orleans, 4–7 October. SPE-124843-MS. <http://dx.doi.org/10.2118/124843-MS>.
- Cipolla, C.L., Warpinski, N.R., Mayerhofer, M. et al. 2010. The Relationship Between Fracture Complexity, Reservoir Properties, and Fracture-Treatment Design. *SPE Prod & Oper* **25** (4): 438–452. SPE-115769-PA. <http://dx.doi.org/10.2118/115769-PA>.
- Civan, F. 2000. *Reservoir Formation Damage—Fundamentals, Modeling, Assessment, and Mitigation*. Houston, Texas: Gulf Publishing Company.
- Clampitt, R.L. and Reid, T.B. 1975. An Economic Polymerflood in the North Burbank Unit, Osage County, Oklahoma. Presented at the Fall Meeting of the Society of Petroleum Engineers of AIME, Dallas, 28 September–1 October. SPE-5552-MS. <http://dx.doi.org/10.2118/5552-MS>.
- Clark, P.E., Halvaci, M., Ghaeli, H. et al. 1985. Proppant Transport by Xanthan and Xanthan-Hydroxypropyl Guar Solutions: Alternatives to Crosslinked Fluids. Presented at the SPE/DOE Low Permeability Gas Reservoirs Symposium, Denver, 19–22 March. SPE-13907-MS. <http://dx.doi.org/10.2118/13907-MS>.
- Clayton, J.R. Jr., Payne, J.R., and Farlow, J.S. 1993. *Oil Spill Dispersants: Mechanisms of Action and Laboratory Tests*. Boca Raton, Florida: CRC Press.
- Clegg, J.D. ed. 2007. *Petroleum Engineering Handbook, Vol. IV: Production Operations Engineering*. Richardson, Texas: Society of Petroleum Engineers.

- Clewlou, P.J. 1995. Amine Adducts as Corrosion Inhibitors. US Patent No. 5,427,999.
- Clewlou, P.J., Haselgrave, J.A., Carruthers, N. et al. 1994. Corrosion Inhibitors. US Patent No. 5,300,235.
- Coffey, M.D. 1980. Corrosion Inhibitor for Aqueous Brines. G.B. Patent No. 2,027,686.
- Cohen, C.E., Tardy, P.M.J., Lesko, T.M. et al. 2010. Understanding Diversion with a Novel Fiber-Laden Acid System for Matrix Acidizing of Carbonate Formations. Presented at the SPE Annual Technical Conference and Exhibition, Florence, Italy, 19–22 September. SPE-134495-MS. <http://dx.doi.org/10.2118/134495-MS>.
- Colaco, A., Marchand, J.-P., Li, F. et al. 2007. Viscoelastic Surfactant Fluids Having Enhanced Shear Recovery, Rheology and Stability Performance. US Patent No. 7,279,446.
- Collins, I.R. and Hewartson, J.A. 2002. Extending Squeeze Lifetimes Using Miscible Displacement. Presented at the International Symposium on Oilfield Scale, Aberdeen, 30–31 January. SPE-74650-MS. <http://dx.doi.org/10.2118/74650-MS>.
- Collins, I.R. and Vervoort, I. 2003. Water-in-Oil Microemulsions Useful for Oil Field or Gas Field Applications and Methods for Using the Same. US Patent No. 6,581,687.
- Collins, I.R., Jordan, M.M., Feasey, N. et al. 2001. The Development of Emulsion-Based Production Chemical Deployment Systems. Presented at the SPE International Symposium on Oilfield Chemistry, Houston, 13–16 February. SPE-65026-MS. <http://dx.doi.org/10.2118/65026-MS>.
- Constien, V.G., Hawkins, G.W., Prud'homme, R.K. et al. 2000. Performance of Fracturing Materials. In *Reservoir Simulation*, third edition, M.J. Economides and K.G. Nolte, Chap. 8, 8-6–8-9. New York: John Wiley & Sons, Ltd.
- Corelab. 2011. Routine Rock Properties, Houston, Texas: Core Laboratories.
- Corex. 2010. A New Tool for Exploration and Appraisal: Formation Damage Analysis. Presented at the 7th European Production and Development Conference and Exhibition, Aberdeen, 12–13 May.
- Correra, S., Simoni, M.D., Bartosek, M. et al. 2010. Assessment of Asphaltene Deposition Risk in an EOR Intervention Through CO₂ Injection. Presented at the SPE Annual Technical Conference and Exhibition, Florence, Italy, 19–22 September. SPE-135001-MS. <http://dx.doi.org/10.2118/135001-MS>.
- Cotton, F.A., Wilkinson, G., Murillo, C.A. et al. 1999. *Advanced Inorganic Chemistry*, sixth edition. New York: John Wiley & Sons.
- Couillet, I. and Hughes, T. 2008. Aqueous Fracturing Fluids. US Patent No. 7,427,583.
- Couillet, I., Hughes, T., Maitland, G. et al. 2004. Growth and Scission Energy of Wormlike Micelles Formed by A Cationic Surfactant with Long Unsaturated Tails. *Langmuir* **20** (22): 9541–9550. <http://dx.doi.org/10.1021/la049046m>.
- Coulter, A.W., Crowe, C.W., Barrett, N.D. et al. 1976. Alternate Stages of Pad Fluid and Acid Provide Improved Leakoff Control for Fracture Acidizing. Presented at the SPE Annual Fall Technical Conference and Exhibition, New Orleans, 3–6 October. SPE-6124-MS. <http://dx.doi.org/10.2118/6124-MS>.
- Coviello, T., Palleschi, A., Grassi, M. et al. 2005. Scleroglucan: A Versatile Polysaccharide for Modified Drug Delivery. *Molecules* **10** (1): 6–33. <http://dx.doi.org/10.3390/10010006>.
- Cowan, J.C. and Weintritt, D.J. 2004. *Mineral & Organic Scale Deposits*. Lafayette, Louisiana: Cowan & Weintritt Publishing Company.
- Crabtree, M., et al. 1999. Fighting Scale—Removal and Prevention. *Oilfield Review* **11** (3): 30.
- Craig Jr., F.F. 1971. *The Reservoir Engineering Aspects of Waterflooding*, Vol. 3, 29–77. Richardson, Texas: Monograph Series, SPE.
- Crameik, T.D. and Plassey, J.A. 1972. Carbon Dioxide Injection Project Sacroc Unit, Scurry County, Texas. Presented at the Annual Meeting Papers, Division of Production, Houston, 6–8 March. API-72-D001.
- Cramer, D.D. 2008. Stimulating Unconventional Reservoirs: Lessons Learned, Successful Practices, Areas for Improvement. Presented at the SPE Unconventional Reservoirs Conference, Keystone, Colorado, USA, 10–12 February. SPE-114172-MS. <http://dx.doi.org/10.2118/114172-MS>.
- Crank, J. 1984. *Free and Moving Boundry Problems*. Oxford, UK: Clarendon Press.

- Crawford, C.C. and Crawford, M.E. 1985. Wm. Berryhill Micellar Polymer Project: A Case History. Presented at the SPE Annual Technical Conference and Exhibition, Las Vegas, Nevada, 22–26 September. SPE-14444-MS. <http://dx.doi.org/10.2118/14444-MS>.
- Crawford, D.L., Earl, R.B., and Monroe, R.F. 1973. Friction Reducing and Gelling Agent for Organic Liquids. US Patent No. 3,757,864.
- Creek, J., Cribbs, M., Dong, C. et al. 2009. Downhole Fluids Laboratory. *Oilfield Review* **21** (4): 38–54.
- Crews, J.B. 2006. Biodegradable Chelant Compositions for Fracturing Fluid. US Patent No. 7,078,370.
- Crews, J.B. and Huang, T. 2007. Internal Breakers for Viscoelastic Surfactant Fracturing Fluids. Presented at the International Symposium on Oilfield Chemistry, The Woodlands, Texas, USA, 28 February–2 March. SPE-106216-MS. <http://dx.doi.org/10.2118/106216-MS>.
- Crews, J.B. and Huang, T. 2008. Unsaturated Fatty Acids and Mineral Oils as Internal Breakers for Ves-Gelled Fluids. US Application Patent No. 2008/0227672.
- Crolet, J.L. and Bonis, M.R. 1985. A Tentative Method for Predicting the Corrosivity of Wells in New CO₂ Fields. Presented at the NACE International CORROSION/85, Boston, Massachusetts, 25–29 March NACE 85027.
- Crowe, C. and Maddin, C.M. 1986. Method for Preventing Precipitation of Ferric Compounds During Acid Treatment of Wells. US Patent No. 4,574,050.
- Crowe, C., Masmonteil, J., Touboul, E. et al. 1992. Trends in Matrix Acidizing. *Oilfield Review* **4** (4): 24–40.
- Crowe, C.W. 1971. Evaluation of Oil Soluble Resin Mixtures as Diverting Agents for Matrix Acidizing. Presented at the Fall Meeting of the Society of Petroleum Engineers of AIME, New Orleans, 3–6 October. SPE-3505-MS. <http://dx.doi.org/10.2118/3505-MS>.
- Crowe, C.W. 1984. Evaluation of Agents for Preventing Precipitation of Ferric Hydroxide from Spent Treating Acid. Presented at the Formation Damage Control Symposium, Bakersfield, California, 2–4 February. SPE-12497-MS. <http://dx.doi.org/10.2188/12497-MS>.
- Crowe, C.W. 1987. Method of Preventing Precipitation of Ferrous Sulfide and Sulfur During Acidizing. US Patent No. 4,633,949.
- Crowe, C.W., Hutchinson, B.H., and Trittipio, B.L. 1989. Fluid Loss Control: The Key to Successful Acid Fracturing. *SPE Prod Eng* **4** (2): 215–220; Trans., AIME, 287. SPE-16883-PA. <http://dx.doi.org/10.2118/16883-PA>.
- Crowe, C.W., Martin, R.C., and Michaelis, A.M. 1981. Evaluation of Acid-Gelling Agents for Use in Well Stimulation. *SPEJ* **21** (4): 415–424. SPE-9384-PA. <http://dx.doi.org/10.2118/9384-PA>.
- Crowe, C.W., McGowan, G.R., and Baranet, S.E. 1990. Investigation of Retarded Acids Provides Better Understanding of Their Effectiveness and Potential Benefits. *SPE Prod & Eng* **5** (2): 166–170. SPE-18222-PA. <http://dx.doi.org/10.2118/18222-PA>.
- Crump, D.K. and Wilson, D.A. 2009. Formulations with Unexpected Cleaning Performance Incorporating a Biodegradable Chelant. US Application Patent No. 2009/0099058.
- CTI. 2007. Single Well Chemical Testing Service. Laramie, Wyoming: Chemical Tracers, Inc.
- Cutler, R.A., Jones, A.H., Swanson, S.R. et al. 1981. New Proppants for Deep Gas Well Stimulation. Presented at the SPE/DOE Low Permeability Gas Reservoirs Symposium, Denver, 27–29 May. SPE-9869-MS. <http://dx.doi.org/10.2118/9869-MS>.
- CVI. 2011. Electromagnetic Viscometer. Medford, Massachusetts: Cambridge Viscosity Incorporated.
- da Motta, E.P., Plavnik, B., Schecter, R.S. et al. 1993. Accounting for Silica Precipitation in the Design of Sandstone Acidizing. *SPE Prod & Oper* **8** (2): 138–144. SPE-23802-PA. <http://dx.doi.org/10.2118/23802-PA>.
- Dabbousi, B.O., Nasr-El-Din, H.A., and Al-Muhaish, A.S. 1999. Influence of Oilfield Chemicals on the Surface Tension of Stimulating Fluids. Presented at the SPE International Symposium on Oilfield Chemistry, Houston, 16–19 February. SPE-50732-MS. <http://dx.doi.org/10.2118/50732-MS>.

- Daccord, G. and Lenormand, R. 1987. Fractal Patterns from Chemical Dissolution. *Nature* **325** (6099): 41–43.
- Daccord, G., Lenormand, R., and Liétard, O. 1993. Chemical Dissolution of a Porous Medium by a Reactive Fluid—I. Model for the “Wormholing” Phenomenon. *Chem. Eng. Sci.* **48** (1): 169–178. [http://dx.doi.org/http://dx.doi.org/10.1016/0009-2509\(93\)80293-Y](http://dx.doi.org/http://dx.doi.org/10.1016/0009-2509(93)80293-Y).
- Daccord, G., Touboul, E., and Lenormand, R. 1989. Carbonate Acidizing: Toward a Quantitative Model of the Wormholing Phenomenon. *SPE Prod Eng* **4** (1): 63–68; *Trans.*, AIME, **287**. SPE-16887-PA. <http://dx.doi.org/10.2118/16887-PA>.
- Dake, L.P. 1995. *Fundamentals of Reservoir Engineering*, 8. New York: Developments in Petroleum Science, Elsevier.
- Daling, P.S. and Lewis, A. 2001. Oil Spill Dispersants. Guidelines on the Planning and Effective Use of Oil Spill Dispersant to Minimise the Effect of Oil Spills. Report No. STF6601018, SINTEF, Trondheim, Norway
- Dalmazzone, C., Noïk, C., and Komunjer, L. 2005. Mechanism of Crude Oil/Water Interface Destabilization by Silicone Demulsifiers. *SPE J.* **10** (1): 44–53. SPE-80241-PA. <http://dx.doi.org/10.2118/80241-PA>.
- Damaskin, B.B., Petrii, O.A., and Batrakov, V.V. 1971. *Adsorption of organic compounds on electrodes*. New York: Plenum Press.
- Daneshy, A.A. 2011. Hydraulic Fracturing of Horizontal Wells: Issues and Insights. Presented at the SPE Hydraulic Fracturing Technology Conference, The Woodlands, Texas, USA, 24–26 January. SPE-140134-MS. <http://dx.doi.org/10.2118/140134-MS>.
- Daniels, J., Waters, G., Le Calvez, J. et al. 2007. Contacting More of the Barnett Shale Through an Integration of Real-Time Microseismic Monitoring, Petrophysics, and Hydraulic Fracture Design. Presented at the SPE Annual Technical Conference and Exhibition, Anaheim, California, USA, 11–14 November. SPE-110562-MS. <http://dx.doi.org/10.2118/110562-MS>.
- Darcy, H. 1857. *Recherches Expérimentales Relatives Au Mouvement De L'eau Dans Les Tuyaux*. Paris, France: Mallet-Bachelier.
- Darley, H.C.H. and Gray, G.R. 1988. *Composition and Properties of Drilling and Completion Fluids*, fifth edition. Amsterdam: Gulf Professional Printing.
- Darling, D. and Rakshpal, R. 1998. Green Chemistry Applied to Corrosion and Scale Inhibitors. Paper NACE 98207, presented at CORROSION 98, San Diego, California, 22–27 March.
- Davies, J.T. 1957. A Quantitative Kinetic Theory of Emulsion Type, I. Physical Chemistry of the Emulsifying Agent, Gas/Liquid and Liquid/Liquid Interface. In *Gas/Liquid and Liquid/Liquid Interfaces: Proceedings of 2nd International Congress on Surface Activity*, 426–438. London: Butterworth.
- Davies, M. and Scott, P.J.B. 2006. *Oilfield Water Technology*. Houston, Texas: NACE International.
- Dawson, J.C. 1992. Method for Improving the High Emperature Gel Stability of Borated Glactomannans. US Patent No. 5,145,5900.
- Dawson, J.C. and Le, H.V. 1995. Controlled Degredation of Polymer Based Aqueous Gels. US Patent No. 5,447,199.
- de Kruijf, A.S., Roodhart, L.P., and Davies, D.R. 1993. Relation Between Chemistry and Flow Mechanics of Borate-Crosslinked Fracturing Fluids. *SPE Prod & Oper* **8** (3): 165–170. SPE-25206-PA. <http://dx.doi.org/10.2118/25206-PA>.
- de Rozieres, J., Chang, F.F., and Sullivan, R.B. 1994. Measuring Diffusion Coefficients in Acid Fracturing Fluids and Their Application to Gelled and Emulsified Acids. Presented at the SPE Annual Technical Conference and Exhibition, New Orleans, 25–28 September. SPE-28552-MS. <http://dx.doi.org/10.2118/28552-MS>.
- De Wolf, C.A., Lepage, J.N., and Bemelaar, J.H. 2010. Acidic Aqueous Solution Containing a Chelating Agent and the Use Thereof. US Application Patent No. 20100276152.
- Dean, J. ed. 1961. *Lange's Handbook of Chemistry*, 10th edition. New York: McGraw-Hill.
- Del Villano, L., Kommedal, R., and Kelland, M.A. 2008. Class of Kinetic Hydrate Inhibitors With Good Biodegradability. *Energy Fuels* **22** (5): 3143–3149. <http://dx.doi.org/10.1021/ef800161z>.

- Delshad, M., Han, W., Pope, G.A. et al. 1998. Alkaline/Surfactant/Polymer Flood Predictions for the Karamay Oil Field. Presented at the SPE/DOE Improved Oil Recovery Symposium, Tulsa, 19–22 April. SPE-39610-MS. <http://dx.doi.org/10.2118/39610-MS>.
- Delshad, M., Pope, G.A., and Sepehrmoori, K. 2007. Modeling Wettability Alteration Using Chemical EOR Processes in Naturally Fractured Reservoirs. Final report, DOE No. DE-FC26-04NT15529, NETL, University of Texas, Austin, Texas (July 2007),
- Deng, J., Hill, A.D., and Zhu, D. 2011. A Theoretical Study of Acid-Fracture Conductivity Under Closure Stress. *SPE Prod & Oper* **26** (1): 9–17. SPE-124755-PA. <http://dx.doi.org/10.2118/124755-PA>.
- Denis, J. and Briant, J. 1997. *Lubricant Properties Analysis & Testing*. Paris: Editions Technip.
- Denney, D. 2011. Technology Applications: Diverter for Near-Wellbore Applications. *J. Pet Tech* **63** (8): 20.
- Denney, D. 2012. Value of Dispersants for Offshore-Oil-Spill Response. *J. Pet Tech* **64** (8): 99–102.
- Deutch, J., Holditch, S., Krupp, F. et al. 2011. Shale Gas Production Subcommittee 90-Day Report. US Department of Energy, Washington, DC.
- DeVine, C.S., Wood, W.D., Shekarchian, M. et al. 2003. New Environmentally Friendly Oil-Based Stimulation Fluids. Presented at the SPE Annual Technical Conference and Exhibition, Denver, 5–8 October. SPE-84576-MS. <http://dx.doi.org/10.2118/84576-MS>.
- Dewprashad, B., Abass, H.H., Meadows, D.L. et al. 1993. A Method To Select Resin-Coated Proppants. Presented at the SPE Annual Technical Conference and Exhibition, Houston, 3–6 October. SPE-26523-MS. <http://dx.doi.org/10.2118/26523-MS>.
- d'Huteau, E., Gillard, M., Miller, M. et al. 2011. Open-Channel Fracturing—a Fast Track to Production. *Oilfield Review* **23** (3): 4–17.
- Di Lullo Arias, G.F. and Ahmad, A.J. 1996. Acid Treatment Method for Siliceous Formations. US Patent No. 5,529,125.
- Di Lullo, G. and Rae, P. 1996. A New Acid for True Stimulation of Sandstone Reservoirs. Presented at the SPE Asia Pacific Oil and Gas Conference, Adelaide, Australia, 28–31 October. SPE-37015-MS. <http://dx.doi.org/10.2118/37015-MS>.
- Dietz, D.N. 1953. A Theoretical Approach to the Problem of Encroaching and By-Passing Edge Water. *Proc. Akad. van Wetenschappen* **56-B**: 83.
- Dill, W.R. and Knox, J.A. 1979. Acidizing Subterranean Well Formations Containing Deposits of Metal Compounds. US Patent No. 4,151,098.
- Dill, W.R. and Walker, M.L. 1989. Compositions and Method for Controlling Precipitation When Acidizing Sour Wells. US Patent No. 4,888,121.
- Dillon, E.T. 1990. Composition and Method for Sweetening Hydrocarbons. US Patent No. 4,978,512.
- Dobos, K. 2009. HLB—the Easiest Way to Create an Emulsion. *The Chemists Corner*, <http://chemistscorner.com/hlb-the-easiest-way-to-create-an-emulsion>.
- Donaldson, E.C., Thomas, R.D., and Lorenz, P.B. 1969. Wettability Determination and Its Effect on Recovery Efficiency. *SPE J.* **9** (1): 13–20. SPE-2338-PA. <http://dx.doi.org/10.2118/2338-PA>.
- Dong, Z., Holditch, S.A., McVay, D. et al. 2011. Global Unconventional Gas Resource Assessments. Presented at the Canadian Unconventional Resources Conference, Alberta, Canada, 15–17 November 2011. SPE-148365-MS. <http://dx.doi.org/10.2118/148365-MS>.
- Dovan, H.T. and Hutchins, R.D. 1994. New Polymer Technology for Water Control in Gas Wells. *SPE Prod & Oper* **9** (4): 280–286. SPE-26653-PA. <http://dx.doi.org/10.2118/26653-PA>.
- Dow. 2006. Drilling Fluids With Cellosize™ Hec, Midland, Michigan: Dow Chemical Co.
- Dow. 2007a. XUS40855.01 Developmental Chelating Agent, Midland, Michigan: Dow Chemical Co.
- Dow. 2007b. Versene™ HEIDA Chelating Agent. Technical Data Sheet, Form No. 113-01355-06-1, Midland, Michigan: Dow Chemical Co.
- Duffin, G.F. 1964. The Quaternization of Heterocyclic Compounds. In *Adv. Heterocycl. Chem.*, A.R. Katritzky, Volume 3, 1–56. Academic Press. <http://www.sciencedirect.com/science/article/pii/S0065272508605401>.

- Dunlop, A.K., Hassell, H.L., and Rhodes, P.R. 1985. Fundamental considerations in sweet gas well corrosion. In *Advances in CO₂ Corrosion: Selected Papers from the Corrosion/84 Symposium on Corrosion by CO₂ in the Oil and Gas Industry and Corrosion/85 Symposium*, P.A. Burke, A.I. Asphahani, and B.S. Wright. Houston, Texas: NACE.
- Earle, S.A., Guggenheim, D.E., Shaw, S.D. et al. 2010. Consensus Statment: Scientists Oppose the Use of Dispersant Chemicals in the Gulf of Mexico. <http://msnbcmedia.msn.com/i/TODAY/Sections/aNEWS/2010/07-July%2010/ScientistsConsensusStatement.pdf>.
- Eaton, B.A. 1969. Fracture Gradient Prediction and Its Application in Oilfield Operations. *J Pet Technol* **21** (10): 1353–1360. SPE-2163-PA. <http://dx.doi.org/10.2118/2163-PA>.
- EC. 2003. Preparing a Waste Management Plan, Brussels, Belgium: European Community.
- Economides, M.J. and Boney, C. 2001. Reservoir Stimulation in Petroleum Production. In *Reservoir Stimulation*, M.J. Economides and K.G. Nolte. New York: John Wiley & Sons.
- Economides, M.J. and Nolte, K.G., ed. 2000. *Reservoir Stimulation*, Third. New York: John Wiley & Sons.
- Economides, M.J., Hill, A.D., and Ehlig-Economides, C. 1994. *Petroleum Production Systems*, Vol. 1. New Jersey: Petroleum Engineering Series, Prentice Hall.
- Efird, K.D., Blevins, S., Smith, J.L. et al. 2004. The Crude Oil Effect on Steel Corrosion: Wettability Preference and Brine Chemistry. Presented at the CORROSION 2004, New Orleans, 28 March–1 April 2004. NACE-04366.
- Efroymsen, R.A., Nicolette, J.P., and Suter, G.W., II. 2004. A Framework for Net Environmental Benefit Analysis for Remediation or Restoration of Contaminated Sites. *Environmental Management* **34** (3): 315–331. <http://dx.doi.org/10.1007/s00267-004-0089-7>.
- Elbel, J. and Britt, L. 2000. Fracture Treatment Design. In *Reservoir Stimulation*, third, M.J. Economides and K.G. Nolte, Chap. 10. New York: John Wiley & Sons.
- Elbel, J.L. and Thomas, R.L. 1980. The Use Of Viscosity Stabilizers In High Temperature Fracturing. Presented at the SPE Rocky Mountain Regional Meeting, Casper, Wyoming, 14–16 May 1980. SPE-9036-MS. <http://dx.doi.org/10.2118/9036-MS>.
- El-Monier, E.A. and Nasr-El-Din, H.A. 2010. A New Environmentally Friendly Clay Stabilizer. Presented at the SPE Production and Operations Conference and Exhibition, Tunis, Tunisia, 8–10 June. SPE-136061-MS. <http://dx.doi.org/10.2118/136061-MS>.
- El-Monier, E.A. and Nasr-El-Din, H.A. 2011a. A Study of Several Environmentally Friendly Clay Stabilizers. Presented at the SPE Project and Facilities Challenges Conference at METS, Doha, Qatar, 13–16 February. SPE-142755-MS. <http://dx.doi.org/10.2118/142755-MS>.
- El-Monier, E.A. and Nasr-El-Din, H.A. 2011b. Mitigation of Fines Migration Using a New Clay Stabilizer: A Mechanistic Study. Presented at the SPE European Formation Damage Conference, Noordwijk, The Netherlands, 7–10 June. SPE-144180-MS. <http://dx.doi.org/10.2118/144180-MS>.
- El-Monier, E.A. and Nasr-El-Din, H.A. 2011c. A New Al-Based Stabilizer for High pH Applications. Presented at the Brasil Offshore, Macaé, Brazil, 14–17 June. SPE-143260-MS. <http://dx.doi.org/10.2118/143260-MS>.
- Ely, J.W. 1989a. Selection of Water–Non Water or Acid-Based Fracturing Fluids. In *Recent Advances in Hydraulic Fracturing*, J.L. Gidley, S.A. Holditch, D.E. Nierode, and R.W. Veatch Jr., Vol. 12, SPE Monograph, 380–388. Richardson, Texas: Society of Petroleum Engineers.
- Ely, J.W. 1989b. Fracturing Fluids and Additives. In *Recent Advances in Hydraulic Fracturing*, J.L. Gidley, S.A. Holditch, D.E. Nierode, and R.W. Veatch Jr., Vol. 12, 131–146. Richardson, Texas: SPE Monograph, Society of Petroleum Engineers.
- EMSA. 2010. Network of Stand-by Oil Spill Response. Brussels, Belgium.
- energyNOW! 2011. The Promise and Problems of Shale Gas. <http://www.energynow.com/video/2011/07/22/Promise-Problems-Shale%20Gas-07.24.2011>.
- Enick, R.M., Olsen, D.K., Ammer, J.R. et al. 2012. Mobility and Conformance Control for CO₂ EOR via Thickeners, Foams, and Gels—A Literature Review of 40 Years of Research and Pilot Tests. Presented at the SPE Improved Oil Recovery Symposium, Tulsa, 14–18 April. SPE-154122-MS. <http://dx.doi.org/10.2118/154122-MS>.

- Eoff, L.S., Dalrymple, E.D., and Reddy, B.R. 2005. Development of Associative Polymer Technology for Acid Diversion in Sandstone and Carbonate Lithology. *SPE Prod & Oper* **20** (3): 250–256. SPE-89413-PA. <http://dx.doi.org/10.2118/89413-PA>.
- Erbstoesser, S.R. 1980. Improved Ball Sealer Diversion. *J Pet Technol* **32** (11): 1903–1910. SPE-8401-PA. <http://dx.doi.org/10.2118/8401-PA>.
- Ettinger, R.A. and Radke, C.J. 1992. The Influence of Texture on Steady Foam Flow in Berea Sandstone. *SPE Res Eng* **7** (1): 83–90. SPE-19688-PA. <http://dx.doi.org/10.2118/19688-PA>.
- Ewing, J. 2008. Taking a Proactive Approach to Water Recycling in the Barnett Shale. Presented at the Fort Worth Business Press Barnett Shale Symposium, 29 February, Fort Worth, Texas. <http://www.barnettshalenews.com/documents/EwingPres.pdf>.
- Expro International Group Ltd. 2007. Multitool® a pH-Sensor System Suitable for HPHT Oil and Gas Applications, brochure. Houston, Texas: Expro International Group Ltd.
- Eylander, J.G.R., Frigo, D.M., Hartog, F.A. et al. 1998. A Novel Methodology for In-Situ Removal of NORM from E & P Production Facilities. Presented at the SPE International Conference on Health, Safety, and Environment in Oil and Gas Exploration and Production, Caracas, Venezuela, 7–10 June 1998. SPE-46791-MS. <http://dx.doi.org/10.2118/46791-MS>.
- Falls, A.H., Lawson, J.B., and Hirasaki, G.J. 1988. The Role of Noncondensable Gas in Steam Foams. *J Pet Technol* **40** (1): 95–104. SPE-15053-PA. <http://dx.doi.org/10.2118/15053-PA>.
- Fan, Y. and Llave, F.M. 1996. Chemical Removal of Formation Damage From Paraffin Deposition Part I - Solubility and Dissolution Rate. Presented at the SPE Formation Damage Control Symposium, Lafayette, Louisiana, 14–15 February 1996. SPE-31128-MS. <http://dx.doi.org/10.2118/31128-MS>.
- Fan, Y., Simon, S.b., and Sjöblom, J. 2009. Chemical Destabilization of Crude Oil Emulsions: Effect of Nonionic Surfactants as Emulsion Inhibitors. *Energy Fuels* **23** (9): 4575–4583. <http://dx.doi.org/10.1021/ef900355d>.
- Fan, Z., Zhang, H., Yin, C., Zhang, J., Wang, Y. and Liu, F. 2012. Elacostearic Imidazoline Inhibition for N80 Steel in HCl Solution. *Materials Performance* **51** (1): 52–55.
- Faust, M. and Weathers, T. 2011. Biphasic Viscosity Reducers as Production Aids for Viscous Oils. Presented at the SPE International Symposium on Oilfield Chemistry, The Woodlands, Texas, USA, 11–13 April 2011. SPE-141037-MS. <http://dx.doi.org/10.2118/141037-MS>.
- Feng, X., Xu, Z., and Masliyah, J. 2008. Biodegradable Polymer for Demulsification of Water-in-Bitumen Emulsions. *Energy Fuels* **23** (1): 451–456. <http://dx.doi.org/10.1021/ef800825n>.
- Fetkovich, M.J. 1973. The Isochronal Testing of Oil Wells. Presented at the Fall Meeting of the Society of Petroleum Engineers of AIME, Las Vegas, Nevada, 30 September–3 October 1973. SPE-4529-MS. <http://dx.doi.org/10.2118/4529-MS>.
- Fink, J.K. 2003. *Oil Field Chemicals*. Burlington, Massachusetts: Gulf Professional Publishing Elsevier.
- Fink, J.K. 2011. *Petroleum Engineer's Guide to Oil Field Chemicals and Fluids*. Waltham, Massachusetts: Gulf Professional Publishing Elsevier.
- Fiocco, R.J., Becker, K.W., Canevari, G.P. and Lessard, R.R. 1998. Chemical Dispersants for Oil Spills. US Patent No. 5,728,320.
- Fischer, E.R. and Parker III, J.E. 1997. Technical Note: Tall Oil Fatty Acid Anhydrides as Corrosion Inhibitor Intermediates. *Corrosion* **53** (1). NACE-97010062.
- Fisher, M.K., Wright, C.A., Davidson, B.M. et al. 2005. Integrating Fracture-Mapping Technologies To Improve Stimulations in the Barnett Shale. *SPE Prod & Fac* **20** (2): 85–93. SPE-77441-PA. <http://dx.doi.org/10.2118/77441-PA>.
- Fisher, R.S., 1995. Naturally Occurring Radioactive Materials (NORM) in Produced Water and Scale from Texas Oil, Gas and Geochemical Wells: Geographic, Geologic and Geochemical Controls, Geological Circular 95-3. Austin, Texas: Bureau of Economic Geology, University of Texas.
- Fjelde, I., Asen, S.M., and Omekeh, A.V. 2012. Low Salinity Water Flooding Experiments and Interpretation by Simulations. Presented at the SPE Improved Oil Recovery Symposium, Tulsa, Oklahoma, USA, 14–18 April 2012. SPE-154142-MS. <http://dx.doi.org/10.2118/154142-MS>.

- Fontana, M.G. 1986. *Corrosion Engineering*, third edition. Boston, Massachusetts: McGraw-Hill.
- Ford, W.G.F., Walker, M.L., Halterman, M.P. et al. 1992. Removing a Typical Iron Sulfide Scale: The Scientific Approach. Presented at the SPE Rocky Mountain Regional Meeting, Casper, Wyoming, 18–21 May 1992. SPE-24327-MS. <http://dx.doi.org/10.2118/24327-MS>.
- Førde, H., Nodland, E., Sjöblom, J. et al. 1995. A Multivariate Analysis of W/O Emulsions in High External Electric Fields as Studied by Means of Dielectric Time Domain Spectroscopy. *J. Colloid Interface Sci.* **173** (2): 396–405. <http://dx.doi.org/http://dx.doi.org/10.1006/jcis.1995.1340>.
- Francini, P.-A., Chan, K., Brady, M. and Fredd, C. 2006. Self-Diverting Foamed System. US Patent No. 7,148,184.
- Frasch, H. 1896. Increasing the Flow of Oil in Wells. US Patent No. 556,669.
- Fredd, C.N. 2000a. Dynamic Model of Wormhole Formation Demonstrates Conditions for Effective Skin Reduction During Carbonate Matrix Acidizing. Presented at the SPE Permian Basin Oil and Gas Recovery Conference, Midland, Texas, 21–23 March 2000. SPE-59537-MS. <http://dx.doi.org/10.2118/59537-MS>.
- Fredd, C.N. 2000b. Advances in Understanding and Predicting Wormhole Formation. In *Appendix in Reservoir Stimulation*, third edition, ed. M. J. Economides and K. G. Nolte, A16 1–18. New York: John Wiley & Sons.
- Fredd, C.N. and Fogler, H.S. 1998a. The influence of chelating agents on the kinetics of calcite dissolution. *J. Colloid Interface Sci.* **204** (1): 187–197. <http://dx.doi.org/10.1006/jcis.1998.5535>.
- Fredd, C.N. and Fogler, H.S. 1998b. The Influence of Transport and Reaction on Wormhole Formation in Porous Media. *AIChE J.* **44** (9): 1933–1949. <http://dx.doi.org/10.1002/aic.690440902>.
- Fredd, C.N. and Fogler, H.S. 1998c. The Kinetics of Calcite Dissolution in Acetic Acid Solutions. *Chem. Eng. Sci.* **53** (2): 3863–3874. <http://dx.doi.org/10.1016/j.physletb.2003.10.071>.
- Fredd, C.N. and Fogler, H.S. 1999. Optimum Conditions for Wormhole Formation in Carbonate Porous Media: Influence of Transport and Reaction. *SPE J.* **4** (3): 196–205. SPE-56995-PA. <http://dx.doi.org/10.2118/56995-PA>.
- Fredd, C.N. and Miller, M.J. 2000. Validation of Carbonate Matrix Stimulation Models. Presented at the SPE International Symposium on Formation Damage Control, Lafayette, Louisiana, USA, 23–24 February. SPE-58713-MS. <http://dx.doi.org/10.2118/58713-MS>.
- Fredd, C.N., McConnell, S.B., Boney, C.L. et al. 2000. Experimental Study of Hydraulic Fracture Conductivity Demonstrates the Benefits of Using Proppants. Presented at the SPE Rocky Mountain Regional/Low-Permeability Reservoirs Symposium and Exhibition, Denver, 12–15 March. SPE-60326-MS. <http://dx.doi.org/10.2118/60326-MS>.
- Freedoniagroup, 2008. World Oilfield Chemicals to 2012. Cleveland, Ohio: Freedoniagroup.
- Frenier, W., Ziauddin, M., Davies, S. and Chang, F. 2007. Composition and Method for Treating a Subterranean Formation. US Patent No. 7,192,908.
- Frenier, W.W. 1982. Method and Composition for Removing Sulfide-Containing Scale from Metal Surfaces. US Patent No. 4,310,435.
- Frenier, W.W. 1989. Acidizing Fluids Used to Stimulate High Temperature Wells Can Be Inhibited Using Organic Chemicals. Presented at the SPE International Symposium on Oilfield Chemistry, Houston, Texas, 8–10 February 1989. SPE-18468-MS. <http://dx.doi.org/10.2118/18468-MS>.
- Frenier, W.W. 1992. Process and Composition for Inhibiting High-Temperature Iron and Steel Corrosion. US Patent No. 5,096,681.
- Frenier, W.W. 1996. Introduction to Toxicity Testing. Paper NACE 96154 presented at NACE International Corrosion 1996, Denver, 24–29 March.
- Frenier, W.W. 1997. Development and Testing of a Low Hazard Corrosion Inhibitor for Use in Organic Acid and Chelant-Based Cleaning Solvents. Paper IWC-97-43 presented at the Engineers' Soc. of West. Pennsylvania, Pittsburgh, Pennsylvania, 10–11 November.
- Frenier, W.W. 1998. Strategies for Formulating Low Hazard Corrosion Inhibitors for Use in Chemical Cleaning Solvents. Paper NACE 98214 presented at Corrosion 1998, San Diego, California, 22–27 March.

- Frenier, W.W. 2001a. Novel Scale Removers Are Developed for Dissolving Alkaline Earth Deposits. Presented at the SPE International Symposium on Oilfield Chemistry, Houston, Texas, 13–16 February. SPE-65027-MS. <http://dx.doi.org/10.2118/65027-MS>.
- Frenier, W.W. 2001b. *Technology for Chemical Cleaning of Industrial Equipment*. Houston: NACE International.
- Frenier, W.W. 2003. Low Hazard Corrosion Inhibitors and Cleaning Solutions Using Quaternary Ammonium Salts. US Patent No. 6,521,028.
- Frenier, W.W. and Brady, M. 2008. Treating Composition. US Patent No. 7,427,584.
- Frenier, W.W. and Garcia, M. 2004. Development of a Scale Inhibitor for Use in Matrix Acidizing. Schlumberger Technology Company.
- Frenier, W.W. and Growcock, F.B. 1988. Mixtures of Unsaturated Aldehydes and Surface Active Agents Used as Corrosion Inhibitors in Aqueous Fluids. US Patent No. 4,734,259.
- Frenier, W.W. and Growcock, F.B. 1989. Corrosion Inhibitors for Chemical Cleaning Solvents; a Review of Recent Literature. Paper NACE 440 presented at Corrosion 1989, NACE International, Houston, TX.
- Frenier, W.W. and Growcock, F.B. 1990. Cinnamaldehyde--A Low Toxicity Acid Corrosion Inhibitor. Presented at the 7th European Symposium on Corrosion Inhibitors, Ferrara, Italy, 17–21 September.
- Frenier, W.W. and Hill, D.G. 2002. Well Treatment Fluids Comprising Mixed Aldehydes. US Patent No. 6,399,547.
- Frenier, W.W. and Kennedy, W.C. 1986. Passivation of Steel in Ammonium Ethylenediaminetetraacetic Acid Solutions. *Corrosion* **42** (10): 613–622. <http://dx.doi.org/10.5006/1.3583032>.
- Frenier, W.W. and Settineri, W.J. 1973. Sulfonium Compound as a Corrosion Inhibitor in Aqueous Acid. US Patent No. 3,764,543.
- Frenier, W.W. and Ziauddin, M. 2008. *Formation, Removal and Inhibition of Inorganic Scale in the Oilfield Environment*. Richardson, Texas: Society of Petroleum Engineers.
- Frenier, W.W. and Ziauddin, M. 2010. A Multifaceted Approach for Controlling Complex Deposits in Oil and Gas Production. Presented at the SPE Annual Technical Conference and Exhibition, Florence, Italy, 19–22 September 2010. SPE-132707-MS. <http://dx.doi.org/10.2118/132707-MS>.
- Frenier, W.W., Brady, M., Al-Harthy, S. et al. 2004. Hot Oil and Gas Wells Can Be Stimulated Without Acids. *SPE Prod & Fac* **19** (4): 189–199. SPE-86522-PA. <http://dx.doi.org/10.2118/86522-PA>.
- Frenier, W.W., Fredd, C.N., and Chang, F. 2001. Hydroxyaminocarboxylic Acids Produce Superior Formulations for Matrix Stimulation of Carbonates. Presented at the SPE European Formation Damage Conference, The Hague, The Netherlands, 21–22 May. SPE-68924-MS. <http://dx.doi.org/10.2118/68924-MS>.
- Frenier, W.W., Fu, D., Davies, S.N., Ziauddin, M., Xiao, Z., Lecerf, B., Bulte, H. and Fuller, M. 2009a. Method for Single-Stage Treatment of Siliceous Subterranean Formations. US Application Patent No. 2009/0192057.
- Frenier, W.W., Fu, D., Davies, S.N., Ziauddin, M., Xiao, Z., Lecerf, B. and Bulte, H. 2012. Method for Single-Stage Treatment of Siliceous Subterranean Formations. US Patent No. 8,312,929.
- Frenier, W.W., Growcock, F.B., and Lopp, V.R. 1988. -Alkenylphenones — A New Class of Acid Corrosion Inhibitors. *Corrosion* **44** (9): 590–598. <http://dx.doi.org/10.5006/1.3584970>.
- Frenier, W.W., Growcock, F.B., Lopp, V.R., and Dixon, R.E. 1991. Process and Composition for Inhibiting Iron and Steel Corrosion. US Patent No. 5,013,483.
- Frenier, W.W., Wilson, D., Crump, D. et al. 2000. Use of Highly Acid-Soluble Chelating Agents in Well Stimulation Services. Presented at the SPE Annual Technical Conference and Exhibition, Dallas, 1–4 October. SPE-63242-MS. <http://dx.doi.org/10.2118/63242-MS>.
- Frenier, W.W., Ziauddin, M. and Venkatesan, R. 2010. *Organic Deposits in Oil and Gas Production*. Richardson, Texas: Society of Petroleum Engineers.
- Frenier, W.W., Ziauddin, M., Davies, S. and Chang, F.F. 2009b. Composition Comprising a Fully Dissolved Non-HF Fluoride Source and Method for Treating a Subterranean Formation. US Patent No. 7,589,050.

- Friberg, S. 2007. Micellization. In *Asphaltenes, Heavy Oil, and Petroleomics*. ed. O.C. Mullins, E.Y. Sheu, A. Hammami, and A. G. Marshall. New York: Springer.
- Frick, T.P., Kurmayr, M., and Economides, M.J. 1994. Modeling of Fractal Patterns in Matrix Acidizing and Their Impact on Well Performance. *SPE Prod & Oper* **9** (1): 61–68. SPE-23789-MS. <http://dx.doi.org/10.2118/23789-PA>.
- Friedmann, F. and Jensen, J.A. 1986. Some Parameters Influencing the Formation and Propagation of Foams in Porous Media. Presented at the SPE California Regional Meeting, Oakland, California, USA, 2–4 April. SPE-15087-MS. <http://dx.doi.org/10.2118/15087-MS>.
- Frost, K., Daussin, R., and Van Domelen, M. 2008. New, Highly Effective Asphaltene Removal System With Favorable HSE Characteristics. Presented at the SPE International Symposium and Exhibition on Formation Damage Control, Lafayette, Louisiana, USA, 13–15 February. SPE-112420-MS. <http://dx.doi.org/10.2118/112420-MS>.
- FTS. 2011. *Eco-Green Stimulation Services*. Cisco, TX: Frac Tech Services. <http://www.ftsi.com/operations/fluids/Pages/default.aspx>.
- Fu, B. 2007. Development of Non-Interfering Corrosion Inhibitors for Sour Gas Pipelines with Co-Injection of Kinetic Hydrate Inhibitors. Paper NACE 07666 presented at NACE International Corrosion 2007, Nashville, Tennessee, 11–15 March.
- Fu, B., Neff, S., Mathur, A. et al. 2001. Novel Low Dosage Hydrate Inhibitors for Deepwater Operations. Presented at the SPE Annual Technical Conference and Exhibition, New Orleans, Louisiana, 30 September–3 October 2001. SPE-71472-MS. <http://dx.doi.org/10.2118/71472-MS>.
- Fu, D. 2010. Self-Diverting Pre-Flush Acid for Sandstone. US Patent No. 7,666,821.
- Fu, P., Johnson, S.M. and Carrigan, C.R. 2011. Simulating Complex Fracture Systems in Geothermal Reservoirs Using an Explicitly Coupled Hydro-Geomechanical Model. Paper ARMA 11-244 presented at the 45th US Rock Mechanics/Geomechanics Symposium of the American Rock Mechanics Association, San Francisco, California, 26–29 June.
- Fuller, M.J., Fu, D., Garcia-Lopez De Victoria, M., Kef, S. and Panga, M.K.R. 2009. Self Diverting Matrix Acid US Patent No. 7,575,054.
- Fulton, D.D., Terracina, J. and Milson, S.L. 2010. Method for Diversion of Hydraulic Fracture Treatments. US Application Patent No. 20100212906.
- Furui, K., Burton, R.C., Burkhead, D.W. et al. 2010. A Comprehensive Model of High-Rate Matrix Acid Stimulation for Long Horizontal Wells in Carbonate Reservoirs. Presented at the SPE Annual Technical Conference and Exhibition, Florence, Italy, 19–22 September. SPE-134265-MS. <http://dx.doi.org/10.2118/134265-MS>.
- Gagner, M.G. and Wolfe, B. 2010. An ESP Lift Reliability Process: Making the Most of Limited Manpower and Field Experience to Promote Field Optimization – Case Study. Presented at the SPE Annual Technical Conference and Exhibition, Florence, Italy, 19–22 September. SPE-134233-MS. <http://dx.doi.org/10.2118/134233-MS>.
- Gaillard, N., Giovannetti, B., and Favero, C. 2010. Improved Oil Recovery using Thermally and Chemically Protected Compositions Based on co- and ter-polymers Containing Acrylamide. Presented at the SPE Improved Oil Recovery Symposium, Tulsa, 24–28 April. SPE-129756-MS. <http://dx.doi.org/10.2118/129756-MS>.
- Gall, B. 1985. Degredation of Fracturing Fluid Polymers, Report OE1B. Bartlesville, Oklahoma: US Department of Energy and Gas Research Institute.
- Gallus, J.P. and Pye, D.S. 1969. Deformable Diverting Agent for Improved Well Stimulation. *J Pet Technol* **21** (4): 497–504. SPE-2161-PA. <http://dx.doi.org/10.2118/2161-PA>.
- Gardner, D.C. and Eikerts, J.V. 1982. The Effects of Shear and Proppant on the Viscosity of Cross-Linked Fracturing Fluids. Presented at the SPE Annual Technical Conference and Exhibition, New Orleans, 26–29 September. SPE-11066-MS. <http://dx.doi.org/10.2118/11066-MS>.
- Gauglitz, P.A., Friedmann, F., Kam, S.I. et al. 2002. Foam generation in homogeneous porous media. *Chem. Eng. Sci.* **57** (19): 4037–4052. [http://dx.doi.org/http://dx.doi.org/10.1016/S0009-2509\(02\)00340-8](http://dx.doi.org/http://dx.doi.org/10.1016/S0009-2509(02)00340-8).

- Gdanski, R. 1995. Fractional Pore Volume Acidizing Flow Experiments. Presented at the SPE European Formation Damage Conference, The Hague, Netherlands, 15–16 May 1995. SPE-30100-MS. <http://dx.doi.org/10.2118/30100-MS>.
- Gdanski, R. 1998. Kinetics of Tertiary Reactions of Hydrofluoric Acid on Aluminosilicates. *SPE Prod & Oper* **13** (2): 75–80. SPE-31076-PA. <http://dx.doi.org/10.2118/31076-PA>.
- Gdanski, R. 1999. A Fundamentally New Model of Acid Wormholing in Carbonates. Presented at the SPE European Formation Damage Conference, The Hague, 31 May–1 June 1999. SPE-54719-MS. <http://dx.doi.org/10.2118/54719-MS>.
- Gdanski, R. 2001. Modeling Acid Returns Profiles After HF Acidizing Treatments. Presented at the SPE International Symposium on Oilfield Chemistry, Houston, 13–16 February. SPE-65035-MS. <http://dx.doi.org/10.2118/65035-MS>.
- Gdanski, R.D. 1985. AlCl_3 Retards HF Acid for More Effective Stimulation. *Oil and Gas J.* **83** (42): 111–115.
- Gdanski, R.D. 1993. Experience and Research Show Best Designs for Foam-Diverted Acidizing. *Oil and Gas J.* **91** (36): 85–86.
- GE. 2012. *GE Water in Unconventional Gas*. Treviso, PA: GE Power and Water Water and Process Technologies.
- Geertsma, J. and Klerk, F.d. 1969. A Rapid Method of Predicting Width and Extent of Hydraulically Induced Fractures. *J Pet Technol* **21** (12): 1571–1581. SPE-2458-PA. <http://dx.doi.org/10.2118/2458-PA>.
- Goel, N. and Shah, S. 2001. A Rheological Criterion for Fracturing Fluids to Transport Proppant during a Stimulation Treatment. Presented at the SPE Annual Technical Conference and Exhibition, New Orleans, 30 September–3 October. SPE-71663-MS. <http://dx.doi.org/10.2118/71663-MS>.
- Geraci, J.R. and Aubin, D.J.S. 1988. Synthesis of Effects of Oil on Marine Mammals, OCS Study MMS 88-0049. Washington, DC: Department of Interior Minerals Management Service.
- Gharfeh, S.G., Singh, P., Kraiwattanawong, K. et al. 2007. A General Study of Asphaltene Flocculation Prediction at Field Conditions. *SPE Prod & Oper* **22** (3): 277–284. SPE-112782-PA. <http://dx.doi.org/10.2118/112782-PA>.
- Ghiselin, D. 2009 *Arkoma Basin: The Playbook*. Houston: Hart Energy Publishing www.UGcenter.com
- Gidley, J.L., Holditch, S.A., Nierode, D.E. et al. 1989. *Recent Advances in Hydraulic Fracturing*, No. 12. Richardson, Texas: Monograph Series, SPE.
- Gijtenbeek, K.A.W.v., Neyfeld, A.P., and Prudnikova, A. 2006. One-Molar Salt Solutions Used for Clay Control in Water-Based Frac Fluids in Western Siberia. Presented at the SPE Russian Oil and Gas Technical Conference and Exhibition, Moscow, Russia, 3–6 October 2006. SPE-101203-MS. <http://dx.doi.org/10.2118/101203-MS>.
- Gillard, M.R., Medvedev, O.O., Hosein, P.R. et al. 2010. A New Approach to Generating Fracture Conductivity. Presented at the SPE Annual Technical Conference and Exhibition, Florence, Italy, 19–22 September. SPE-135034-MS. <http://dx.doi.org/10.2118/135034-MS>.
- Glasbergen, G., Kalia, N., and Talbot, M. 2009. The Optimum Injection Rate for Wormhole Propagation: Myth or Reality? Presented at the 8th European Formation Damage Conference, Scheveningen, The Netherlands, 27–29 May. SPE-121464-MS. <http://dx.doi.org/10.2118/121464-MS>.
- Glynn, P.D., Parkhurst, D.L., and Plummer, L.N. 1992. *Principles and Applications of Modeling Chemical Reactions in Ground Water. Igwmc Short Course*. Golden, Colorado: Colorado School of Mines.
- Gogarty, W.B. and Tosch, W.C. 1968. Miscible-Type Waterflooding: Oil Recovery with Micellar Solutions. *J Pet Technol* **20** (12): 1407–1414. SPE-1847-1-PA. <http://dx.doi.org/10.2118/1847-1-PA>.
- Goldszal, A. and Bourrel, M. 2000. Demulsification of Crude Oil Emulsions: Correlation to Microemulsion Phase Behavior. *Ind. Eng. Chem. Res.* **39** (8): 2746–2751. <http://dx.doi.org/10.1021/ie990922e>.

- Gomaa, A.M. and Nasr-El-Din, H.A. 2010. New Insights Into the Viscosity of Polymer-Based In-Situ-Gelled Acids. *SPE Prod & Oper* **25** (3): pp. 367-375. SPE-121728-PA. <http://dx.doi.org/10.2118/121728-PA>.
- Gomaa, A.M., Mahmoud, M.A., and Nasr-El-Din, H.A. 2011. Effect of Shear Rate on the Propagation of Polymer-Based In-Situ-Gelled Acids Inside Carbonate Cores. *SPE Prod & Oper* **26** (1): 41–54. SPE-142927-PA. <http://dx.doi.org/10.2118/142927-PA>.
- Gonzalez, D.L., Vargas, F.M., Hirasaki, G.J. et al. 2007. Modeling Study of CO₂-Induced Asphaltene Precipitation. *Energy Fuels* **22** (2): 757–762. <http://dx.doi.org/10.1021/ef700369u>.
- Gougler Jr., P.D., Hendrick, J.E., and Coulter, A.W. 1985. Field Investigation Identifies Source and Magnitude of Iron Problems. Presented at the SPE Production Operations Symposium, Oklahoma City, Oklahoma, 10–12 March. SPE-13812-MS. <http://dx.doi.org/10.2118/13812-MS>.
- Graham, A., Vieille, E., Boak, L. and Neville, A. 2004. Effect of Temperature and Flow on the the Surface Nucleation and Growth of Barium Sulphate in the Presence of PPCA. *Flow Assurance and Scale Control JIP*, 2001–2004 Progress Report 5, Section 6, Heriot Watt University.
- Graham, G.M. and McMahon, C.P. 2002. The Effect of Scale Inhibitor Performance Against Bulk (Homogeneous) and Surface (Heterogeneous) Scale Nucleation and Growth by the Addition of Film Forming Corrosion Inhibitors. Presented at the NACE International CORROSION, Denver, Colorado, 7–11 April. NACE-02315.
- Graham, G.M., Boak, L.S., and Sorbie, K.S. 2003. The Influence of Formation Calcium and Magnesium on the Effectiveness of Generically Different Barium Sulphate Oilfield Scale Inhibitors. *SPE Prod & Oper* **18** (1): 28–44. SPE-81825-PA. <http://dx.doi.org/10.2118/81825-PA>.
- Graham, G.M., Frigo, D.M., McCracken, I.R. et al. 2001. The Influence of Corrosion Inhibitor / Scale Inhibitor Interference on the Selection of Chemical Treatments Under Harsh (HP/HT/HS) Reservoir Conditions. Presented at the International Symposium on Oilfield Scale, Aberdeen, United Kingdom, 30–31 January. SPE-68330-MS. <http://dx.doi.org/10.2118/68330-MS>.
- Grattan, K.T.V. and Meggitt, B.T., eds. 2000. *Optical Fiber Sensor Technology: Advanced Applications—Bragg Gratings and Distributed Sensors*. London: Springer.
- Grattoni, C.A., Chiotis, E.D., and Dawe, R.A. 1995. Determination of relative wettability of porous sandstones by imbibition studies. *J. Chem. Technol. Biotechnol.* **64** (1): 17–24. <http://dx.doi.org/10.1002/jctb.280640104>.
- Graue, D.J. and Johnson Jr., C.E. 1974. Field Trial of Caustic Flooding Process. *J Pet Technol* **26** (12): 1353–1358. SPE-4740-PA. <http://dx.doi.org/10.2118/4740-PA>.
- Grebe, J. 1935. Treatment of Wells. US Patent No. 1,989,479.
- Grebe, J.J. and Stoesser, M. 1935. Increasing Crude Production 20,000,000 Bbl From Established Fields. *World Petroleum J.* (August): 473–482.
- Green, D.W. and Willhite, G.P. 1998. *Enhanced Oil Recovery*, 6. Richardson, Texas: Textbook Series, SPE.
- Greenwald, H.L., Brown, G.L. and Fineman, M.N. 1956. Development of Method for Measurement of Relative Solubility of Nonionic Surfactants. *Analytical Chemistry* **28**(11): 1693–1697.
- Gregory, D.P. and Riddiford, A.C. 1956. Transport to the Surface of a Rotating Disc. *J. Chem. Soc. Paper 731*: 3756–3764. DOI: 10.1039/JR9560003756
- GRI. 1990. *Coal Seam Stimulation Manual*. Chicago, Illinois: Gas Research Institute.
- Grieser, B., Hobbs, J., Hunter, J., and Ables, J. 2003. A Concise Guide to Water Frac Design. *World Oil* **224** (111): 1–10.
- Griffin, W.C. 1954. Calculation of HLB Values of Non-Ionic Surfactants. *J. of the Society of Cosmetic Chemists* **5**: 235–249.
- Griffith, A.A. 1921. The phenomena of rupture and flow in solids. *Philosophical Transactions of the Royal Society of London. A* **221**: 163–198.
- Groat, C.G. and Grimshaw, T.W. 2012. *Fact-Based Regulation for Environmental Protection in Shale Gas Development*. Austin, Texas: The Energy Institute, University of Texas, Austin.

- Gröllmann, U. and Schnabel, W. 1982. Free radical-induced oxidative degradation of polyacrylamide in aqueous solution. *Polym. Degrad. Stab.* **4** (3): 203–212. [http://dx.doi.org/10.1016/0141-3910\(82\)90027-1](http://dx.doi.org/10.1016/0141-3910(82)90027-1).
- Growcock, F. 2005. *Composition and Properties of Drill Fluids*, fifth edition. Burlington, Massachusetts: Butterworth-Heinemann.
- Growcock, F.B. and Lopp, V.R. 1988. The inhibition of steel corrosion in hydrochloric acid with 3-phenyl-2-propyn-1-ol. *Corros. Sci.* **28** (4): 397–410. [http://dx.doi.org/10.1016/0010-938X\(88\)90059-5](http://dx.doi.org/10.1016/0010-938X(88)90059-5).
- Growcock, F.B., Frenier, W.W. and Lopp, V.R. 1985. Corrosion Inhibition of Steel in HCl by 1-Octyn-3-ol. I Kinetics. Presented at the 6th European Symposium Corrosion Inhibitors, Ferrara Italy, 16–20 September.
- Growcock, F.B., Frenier, W.W., and Andreozzi, P.A. 1989. Inhibition of Steel Corrosion in HCl by Derivatives of Cinnamaldehyde: Part II. Structure–Activity Correlations. *Corrosion* **45** (12): 1007–1015. <http://dx.doi.org/10.5006/1.3585008>.
- Guichard III, J.A., Allison, D., Gdanski, R.D. et al. 1996. An Overview of HF Acid as Applied to the Wilcox Sand in Reddell Field, Southwest Louisiana. Presented at the SPE Formation Damage Control Symposium, Lafayette, Louisiana, 14–15 February. SPE-31139-MS. <http://dx.doi.org/10.2118/31139-MS>.
- Guillot, D. and Dunand, A. 1985. Rheological Characterization of Fracturing Fluids by Using Laser Anemometry. *SPE J.* **25** (1): 39–45. SPE-12030-PA. <http://dx.doi.org/10.2118/12030-PA>.
- Gulbis, J. and Hodge, R.M. 2001. Fracturing Fluid Chemistry and Proppants. In *Formation Stimulation*, third edition, ed. M.J. Economides and K.G. Nolte. Chichester: John Wiley and Sons.
- Gulbis, J., King, M.T., Hawkins, G.W. et al. 1992. Encapsulated Breaker for Aqueous Polymeric Fluids. *SPE Prod Eng* **7** (1): 9–14. SPE-19433-PA. <http://dx.doi.org/10.2118/19433-PA>.
- Gupta, D.V.S. 1998. What Is Green? Paper NACE 98206 presented at NACE International CORROSION 98, San Diego, California, March 22–27.
- Gupta, D.V.S. and Hlidek, B.T. 2010. Frac-Fluid Recycling and Water Conservation: A Case History. *SPE Production and Operations* **25** (1): 65–69. SPE-119478-PA. <http://dx.doi.org/10.2118/119478-PA>.
- Gupta, D.V.S. and Prasek, B.B. 1995. Method for Fracturing Subterranean Formations Using Controlled Release Breakers and Compositions. US Patent No. 5,437,331.
- Gupta, D.V.S., Brown, J.M., and Szymczak, S. 2010. A 5-Year Survey of Applications and Results of Placing Solid Chemical Inhibitors in the Formation via Hydraulic Fracturing. Presented at the SPE Annual Technical Conference and Exhibition, Florence, Italy, 19–22 September. SPE-134414-MS. <http://dx.doi.org/10.2118/134414-MS>.
- Gupta, D.V.S., Hlidek, B.T., Hill, E.S.W. et al. 2007. Fracturing Fluid for Low-Permeability Gas Reservoirs: Emulsion of Carbon Dioxide With Aqueous Methanol Base Fluid: Chemistry and Applications. Presented at the SPE Hydraulic Fracturing Technology Conference, College Station, Texas, U.S.A., 29–31 January. SPE-106304-MS. <http://dx.doi.org/10.2118/106304-MS>.
- Gupta, D.V.S., Szymczak, S., and Brown, M. 2009. Solid Production Chemicals Added with the Frac for Scale, Paraffin and Asphaltene Inhibition. Presented at the SPE Hydraulic Fracturing Technology Conference, The Woodlands, Texas, 19–21 January. SPE-119393-MS. <http://dx.doi.org/10.2118/119393-MS>.
- GWPC. 2011. *Fracfocus Chemical Disclosure Registry*. GroundWater Protection Council and Interstate Oil and Gas Compact commission. Oklahoma City, Oklahoma: FracFocus. <http://fracfocus.org/>.
- Hagen, G. 1839. Über Die Bewegung Des Wassers in Engen Zylinderschen. *Ann. Phys. Chem.* **46**: 423–442.
- Hall, B.E. and Dill, W.R. 1988. Iron Control Additives for Limestone and Sandstone Acidizing of Sweet and Sour Wells. Presented at the SPE Formation Damage Control Symposium, Bakersfield, California, 8–9 February. SPE-17157-MS. <http://dx.doi.org/10.2118/17157-MS>.

- Halliburton. 2005a. Choosing Fracturing Sand to Optimize Permeability Achieved Vs. Costs Brochure. Houston: Halliburton Services.
- Halliburton. 2005b. Surgifracsm Brochure H03297. Houston: Halliburton Services.
- Halliburton. 2006. Cementing Truck Brochure Hal 18296. Houston: Halliburton.
- Halliburton. 2011a. *Cleanwavesm Water Treatment Service*. Houston: Halliburton Services. http://www.halliburton.com/public/pe/contents/Presentations/CleanWave_Service.pdf.
- Halliburton. 2011b. Biovert[®] NWB Biodegradable Diverting Agent, Brochure H08003 06/11. Houston: Halliburton.
- Halliburton. 2012. *RapidfracTM System*. Houston: Halliburton Services <http://www.halliburton.com/ps/default.aspx?pageid=5313&prodid=PRN::LK0BSD15>.
- Hamadi, A.S. and Mahmood, L.H. 2010. Demulsifiers for Simulated Basrah Crude Oil. *Eng. & Tech. J.* **28** (1): 54–64.
- Hammami, A. and Ratulowski, J. 2007. Precipitation and Deposition of Asphaltenes in Production Systems: A Flow Assurance Overview. In *Asphaltenes, Heavy Oils, and Petroleomics*, eds. O. Mullins, E. Sheu, A. Hammami, and A. Marshall, 23, 617–660. New York: Springer. http://dx.doi.org/10.1007/0-387-68903-6_23.
- Hansen, C.M. 1967. The Three Dimensional Solubility Parameter - Key to Paint Component Affinities: I Solvents, Plasticizers, Polymeres, and Resins. *J. Paint Tech.* **39** (505): 104–117.
- Hansen, C.M. 2000. *Hansen Solubility Parameters: A User's Handbook*. Boca Raton, Florida: CRC Press LLC.
- Hansen, E.W.M. 2005. *Separation Offshore Survey - Design/Redesign of Gravity Separators - Expro*. The Oil and Gas Review 2 1–4 London: Touch Group http://www.touchoilandgas.com/publications.cfm?publication_id=67&level=2.
- Harris Jr, W. 1999. Non-Aqueous Slurries of Water Soluble Polymers US Patent No. 5,969,012.
- Harris, F.N. 1961. Applications of Acetic Acid to Well Completion, Stimulation and Reconditioning. *J Pet Technol* **13** (7): 637–639. SPE-63-PA. <http://dx.doi.org/10.2118/63-PA>.
- Harris, P.C. and Batenburg, D.v. 1999. A Comparison of Freshwater- and Seawater-Based Borate-Crosslinked Fracturing Fluids. Presented at the SPE International Symposium on Oilfield Chemistry, Houston, 16–19 February. SPE-50777-MS. <http://dx.doi.org/10.2118/50777-MS>.
- Harris, P.C. and Sabhapondit, A. 2009. Chemistry Applied to Fracture Stimulation of Petroleum Wells. Presented at the SPE Middle East Oil and Gas Show and Conference, Bahrain, Bahrain, 15–18 March. SPE-120029-MS. <http://dx.doi.org/10.2118/120029-MS>.
- Harris, P.C. and Walters, H. 2000. Real-Time Control of Low-Polymer Fracturing Fluids. Presented at the SPE Annual Technical Conference and Exhibition, Dallas, Texas, 1–4 October. SPE-63238-MS. <http://dx.doi.org/10.2118/63238-MS>.
- Harris, P.C., Walters, H.G., and Bryant, J. 2009. Prediction of Proppant Transport From Rheological Data. *SPE Prod & Oper* **24** (4): 550–555. SPE-115298-PA. <http://dx.doi.org/10.2118/115298-PA>.
- Harrison, N.W. 1972. Diverting Agents-History and Application. *J Pet Technol* **24** (5): 593–598. SPE-3653-PA. <http://dx.doi.org/10.2118/3653-PA>.
- Hartman, R.L., Lecerf, B., Frenier, W. et al. 2003. Acid Sensitive Aluminosilicates: Dissolution Kinetics and Fluid Selection for Matrix Stimulation Treatments. Presented at the SPE European Formation Damage Conference, The Hague, 13–14 May. SPE-82267-MS. <http://dx.doi.org/10.2118/82267-MS>.
- Hartman, R.L., Lecerf, B., Frenier, W.W. et al. 2006. Acid-Sensitive Aluminosilicates: Dissolution Kinetics and Fluid Selection for Matrix-Stimulation Treatments. *SPE Prod & Oper* **21** (2): 194–204. SPE-82267-PA. <http://dx.doi.org/10.2118/82267-PA>.
- Hassler, G.L. 1944. Method and Apparatus for Permeability Measurements. US Patent No. 2,345,935.
- Hausler, R.H. 1983. *Developed the Only Qualified Corrosion Inhibitor for Nuclear Steam Generator Cleaning, NP-3030*. Palo Alto, California: Electric Power Research Institute.

- Havlik, W., Thayer, K., and Oberndorfer, M. 2007. Production of Wet Natural Gas Containing Corrosive Components: Four Case Histories. *SPE Prod & Oper* **22** (3): 319-325. SPE-100219-PA. <http://dx.doi.org/10.2118/100219-PA>.
- Hawkins, M.F.J. 1956. A Note on the Skin Effect. *J Pet Technol* **8** (12): 65–66. SPE-732-G. <http://dx.doi.org/10.2118/732-G>.
- Haynes, H.H. and Lenderman, G.L. 1986. Cost-Effective Paraffin Inhibitor Squeezes Can Improve Production Economics. Presented at the SPE Rocky Mountain Regional Meeting, Billings, Montana, 19–21 May. SPE-15178-MS. <http://dx.doi.org/10.2118/15178-MS>.
- HealthCanada. 2011. *Environmental and Workplace Health*. Ottawa, California: Health Canada. <http://www.hc-sc.gc.ca/ewh-semt/legislation/index-eng.php>.
- Heidersbach, R. 2011. *Metallurgy and Corrosion Control in Oil and Gas Production*. Hoboken, New Jersey: John Wiley and Sons, Inc.
- Hekim, Y., Fogler, H.S., and McCune, C.C. 1982. The Radial Movement of Permeability Fronts and Multiple Reaction Zones in Porous Media (includes associated papers 11284 and 11590). *Society of Petroleum Engineers Journal* **22** (1): 99–107. SPE-9495-PA. <http://dx.doi.org/10.2118/9495-PA>.
- Hendrickson, A.R. 1972. Stimulation of Carbonate Reservoirs. In *Oil and Gas Production from Carbonate Rocks*. ed. G.V. Chilingar, R.W. Manson, and H.H. Ricke, 309-339. New York: Elsevier.
- Henriksen, N., Christensen, T., Fareid, E., and Kjolberg, S.A. 1984. Degassing of Water Using Inert Gas. German Patent No. GB2127711.
- Henry, H., Meyer, R., Hicks, K., and Horsup, D.I. 2005. The Design and Synthesis of Improved Corrosion Inhibitors. Paper NACE 05282 presented at Corrosion/2005, NACE International, Houston, Texas, 3–7 April.
- Henthorne, L. and Wodehouse, J. 2012. The Science of Membrane Technology to Further Enhance Oil Recovery. Presented at the SPE Improved Oil Recovery Symposium, Tulsa, Oklahoma, USA, 14–18 April. SPE-154281-MS. <http://dx.doi.org/10.2118/154281-MS>.
- Herschel, W. and Bulkley, R. 1926. Konsistenzmessungen von Gummi-Benzollösungen. *Kolloid-Zeitschrift* **39** (4): 291–300. <http://dx.doi.org/10.1007/bf01432034>.
- Hess, G. 2010. Drilling Process Draws Scrutiny. *Chemical & Engineering News Archive* **88** (22): 42-45. <http://dx.doi.org/10.1021/cen-v088n022.p042>.
- Hexion. 2008. *Considerations for Fracturing with Resin Coated Proppants*. Houston, Texas: Hexon Oilfield Technologies. <http://www.hexionfracline.com/fall2008/resinconsiderations.php>.
- HFF. 2010. *Hydraulic Fracturing Facts*. Oklahoma City, Oklahoma: Chesapeake Energy, <http://www.hydraulicfracturing.com/Pages/information.aspx>.
- Hidu, H. 1965. Effects of Synthetic Surfactants on the Larvae of Clams (*M. Mercenaria*) and Oysters (*C. Virginica*). *J. of the Water Pollution Control Federation* **37** (2): 262–270.
- Hildebrand, J.H. and Scott, R.L. 1950. Solutions of Nonelectrolytes. *Annu. Rev. Phys. Chem.* **1** (1): 75–92. <http://dx.doi.org/10.1146/annurev.pc.01.100150.000451>.
- Hill, A.D. and Schechter, R.S. 2001. Fundamentals of Acid Stimulation. In *Reservoir Stimulation*, third edition. ed. M.J. Economides and K.G. Nolte, 16-1-27. New York: John Wiley and Sons.
- Hill, A.D., Lindsay, D.M., Silberberg, I.H. et al. 1981. Theoretical and Experimental Studies of Sandstone Acidizing. *Society of Petroleum Engineers Journal* **21** (1): 30–42. SPE-6607-PA. <http://dx.doi.org/10.2118/6607-PA>.
- Hill, A.D., Pournik, M., Zou, C. et al. 2007. Small-Scale Fracture Conductivity Created by Modern Acid-Fracture Fluids. Presented at the SPE Hydraulic Fracturing Technology Conference, College Station, Texas, USA, 29–31 January. SPE-106272-MS. <http://dx.doi.org/10.2118/106272-MS>.
- Hill, D.G. 1982. Clay Stabilization - Criteria for Best Performance. Presented at the SPE Formation Damage Control Symposium, Lafayette, Louisiana, 24–25 March. SPE-10656-MS. <http://dx.doi.org/10.2118/10656-MS>.
- Hill, D.G. 2005. Gelled Acid. US Application Patent No. 2005/0065041.
- Hill, D.G., Dismuke, K., Shepherd, W. et al. 2003. Development Practices and Achievements for Reducing the Risk of Oilfield Chemicals. Presented at the SPE/EPA/DOE Exploration and

- Production Environmental Conference, San Antonio, Texas, 10–12 March. SPE-80593-MS. <http://dx.doi.org/10.2118/80593-MS>.
- Hill, D.G., Liétard, O.M., Piot, B.M., and King, George E. 2001. Formation Damage: Origin, Diagnosis and Treatment Strategy. In *Reservoir Stimulation*. ed. M.J. Economides and K.G. Nolte, 14.1-14.39. New York: John Wiley and Sons.
- Himes, R.E. and Vinson, E.F. 1989. Fluid Additive and Method for Treatment of Subterranean Formations. US Patent No. 4,842,073.
- Hinkel, J., Brown, E., Boney, C. and Sutton, G. 2005. Fracturing Fluid and Method of Use. Patent No. 6,929,069.
- Hinkel, J.J. and England, K.W. 2001. Fluids and Techniques for Maximizing Fracture Clean-Up. US Patent No. 6,192,985.
- Hirasaki, G., Miller, C.A., and Puerto, M. 2011. Recent Advances in Surfactant EOR. *SPE J.* **16** (4): pp. 889-907. SPE-115386-PA. <http://dx.doi.org/10.2118/115386-PA>.
- Hirasaki, G.J., Miller, C.A. and Pope, G.A. 2006. Surfactant Based Enhanced Oil Recovery and Foam Mobility Control, Report, final, DE-FC26-03NT15406. Bartlesville, Oklahoma: National Energy Technology Laboratory, Department of Energy.
- Hirasaki, G.J., Miller, C.A., Pope, G.A. and Jackson, R.E. 2004. Surfactant Based Enhanced Oil Recovery and Foam Mobility Control, Report, Interim, DE-FC26-03NT15406. Washington, DC: Department of Energy.
- Hlideo, B.T. and Rieb, B.A. 2011. Fracture Stimulation Treatment Best Practices in the Bakken Oil Shale. Presented at the SPE Hydraulic Fracturing Technology Conference, The Woodlands, Texas, USA, 24–26 January 2011. SPE-140252-MS. <http://dx.doi.org/10.2118/140252-MS>.
- HMMG. 2010. Liquitote[®] Brochure. Houston, Texas: Hoover Material Handling Group, Inc.
- Hodge, R.M. 1989. Delayed Crosslinker Composition Containing Organic Titanium Complexes and Hydroxycarboxylic Acids. US Patent No. 4,861,500.
- Hoefler, A.M., Sullivan, P.F., Salamat, G., Boney, C.L., Lee, J.C., Chen, Y., Willberg, D.M., Bulova, M., Fredd, C.N., et al. 2008. Well Treatment with Dissolvable Polymer. US Patent No. 7,398,826.
- Hoefner, M.L. and Fogler, H.S. 1988. Pore Evolution and Channel Formation During Flow and Reaction in Porous Media. *AIChE J.* **34** (1): 45–54. <http://dx.doi.org/10.1002/aic.690340107>.
- Hoefner, M.L. and Fogler, H.S. 1989. Fluid-Velocity and Reaction-Rate Effects During Carbonate Acidizing: Application of Network Model. *SPE Prod Eng* **4** (1): 56–62. SPE-15573-PA. <http://dx.doi.org/10.2118/15573-PA>.
- Hoffman, B.T. 2012. Comparison of Various Gases for Enhanced Recovery from Shale Oil Reservoirs. Presented at the SPE Improved Oil Recovery Symposium, Tulsa, 14–18 April. SPE-154329-MS. <http://dx.doi.org/10.2118/154329-MS>.
- Holditch, S.A., Ely, J.W., and Carter, R.H. 1989. Development of a Coal Seam Fracture Design Manual. Paper SPE 8976 presented at the 1989 Coalbed Methane Symposium in Tuscaloosa, Alabama, 17–20 April. <http://dx.doi.org/10.2118/8976-MS>.
- Holditch, S.A., Perry, K., and Lee, J. 2007. *Unconventional Gas Reservoirs—Tight Gas, Coal Seams, and Shales, Working Document of the Npc Global Oil and Gas Study*. Washington, D.C.: National Petroleum Council.
- Hollenbeak, K.H. and Brown-Jr, P.S. 1985. Clay Stabilizing Agent Preparation and Use. US Patent No. 4,693,639.
- Holm, L.W. and Josendal, V.A. 1974. Mechanisms of Oil Displacement By Carbon Dioxide. *J Pet Technol* **26** (12): 1427–1438. SPE-4736-PA. <http://dx.doi.org/10.2118/4736-PA>.
- Holstein, E.D., ed. 2007. *Petroleum Engineering Handbook, Volume V: Reservoir Engineering and Petrophysics*. Richardson, TX: SPE.
- Hongkun, Y., Jincai, C., Xianke, Y., Yuping, F., and Yunzhang, Z. 1998. Clay Swelling Control to Improve Steam Stimulation Results, 1998.138. Liaohe, China: Liaohe Petroleum Exploration Bureau, CNPC.
- Horner, D.R. 1951. Pressure Build-up in Wells. Presented at the Third World Petroleum Conference, The Hague, The Netherlands, 28 May–6 June. Sec II, 503-523.

- Hou, Q., Zhu, Y., Luo, Y. et al. 2012. Studies on Foam Flooding EOR Technique for Daqing Reservoirs After Polymer Flooding. Presented at the SPE Improved Oil Recovery Symposium, Tulsa, 14–18 April. SPE-151955-MS. <http://dx.doi.org/10.2118/151955-MS>.
- Howard, G.C. and Fast, C.R. 1970. *Hydraulic Fracturing*, No. 2. Richardson, Texas: Monograph Series, SPE.
- Howard, P., Mukhopadhyay, S., Moniaga, N. et al. 2010. Comparison of Flowback Aids: Understanding Their Capillary Pressure and Wetting Properties. *SPE Prod & Oper* **25** (3): pp. 376–387. SPE-122307-PA. <http://dx.doi.org/10.2118/122307-PA>.
- Huang, T. and Crews, J.B. 2007. Fluid-Loss Control Improves Performance of Viscoelastic-Surfactant Fluids. Presented at the International Symposium on Oilfield Chemistry, Houston, 28 February–2 March. SPE-106227-MS. <http://dx.doi.org/10.2118/106227-MS>.
- Huang, T., Crews, J.B., and Treadway-Jr, J.H. 2009. Fluid Loss Control Agents for Viscoelastic Surfactant Fluids. US Patent No. 7,550,413.
- Huang, T., Crews, J.B., Willingham, J.R., Pace, J.R., and Belcher, C.K. 2010. Nano-Sized Particle-Coated Proppants for Formation Fines Fixation in Proppant Packs. US Patent No. 7,721,803.
- Huang, T., Hill, A.D., and Schechter, R.S. 1997. Reaction Rate and Fluid Loss: The Keys to Wormhole Initiation and Propagation in Carbonate Acidizing. Presented at the International Symposium on Oilfield Chemistry, Houston, 18–21 February. SPE-37312-MS. <http://dx.doi.org/10.2118/37312-MS>.
- Huang, T., Ostensen, L., and Hill, A.D. 2000. Carbonate Matrix Acidizing with Acetic Acid. Presented at the SPE International Symposium on Formation Damage Control, Lafayette, Louisiana, USA, 23–24 February. SPE-58715-MS. <http://dx.doi.org/10.2118/58715-MS>.
- Hubert, C., Voordouw, G., Nemati, M. and Jenneman, G.E. 2004. Is Souring and Corrosion by Sulfate-Reducing Bacteria in Oil Fields Reduced More Efficiently by Nitrate or by Nitrite?. Paper NACE 04762 presented at NACE International CORROSION 2004, New Orleans, 28 March–1 April.
- Huh, C. 1979. Interfacial tensions and solubilizing ability of a microemulsion phase that coexists with oil and brine. *J. Colloid Interface Sci.* **71** (2): 408–426. [http://dx.doi.org/10.1016/0021-9797\(79\)90249-2](http://dx.doi.org/10.1016/0021-9797(79)90249-2).
- Huizinga, S. and Liek, W.E. 1994. Corrosion Behavior of 13% Chromium Steel in Acid Stimulation. *Corrosion* **50** (7): 555–566. <http://dx.doi.org/10.5006/1.3294357>.
- Hung, K.M., Hill, A.D., and Sepehrnoori, K. 1989. A Mechanistic Model of Wormhole Growth in Carbonate Matrix Acidizing and Acid Fracturing. *J Pet Technol* **41** (1): 59–66. SPE-16886-PA. <http://dx.doi.org/10.2118/16886-PA>.
- Hunter, J. and Walker, R.N.J. 1991. Clean Frac Fluids Improve Load Recovery, Tight-Gas Production. *World Oil* **212** (10): 76–78.
- Hurst, R.E. and Smith, C.F. 1968. Method of Well Treatment Employing Volatile Fluid Compositions. US Patent No. 3,368,627.
- Husen, A., Ali, A., Frenier, W.W. et al. 2002. Chelating Agent-Based Fluids for Optimal Stimulation of High-Temperature Wells. Presented at the SPE Annual Technical Conference and Exhibition, San Antonio, Texas, 29 September–2 October. SPE-77366-MS. <http://dx.doi.org/10.2118/77366-MS>.
- Hutchins, R.D., and Dovan, H.T. 1995. Composition for Selectively Reducing Subterranean Formation Permeability US Patent No. 5,418,217.
- Hutchins, R.D., and Saunders, D.L. 1993. Tracer Chemicals for Monitoring Subterranean Fluids. US Patent No. 5,246,860.
- Hutchins, R.D., Daniel, S., Wirajati, A. Y. et al. 2011. Polymer Chemistry Improves Productivity in Tight Gas Hydraulic Fracturing. Presented at the SPE International Symposium on Oilfield Chemistry, The Woodlands, Texas, USA, 11–13 April. SPE-141597-MS. <http://dx.doi.org/10.2118/141597-MS>.
- Hutchins, R.D., Dessinges, M.N., and Mukhopadhyay, S. 2009. Treatment Fluid with Non-Symmetrical Peroxide Breaker and Method. US Application Patent No. 2009/0088347.

- Hutchins, R.D., Ladva, H.K., Williamson, D., and Daniel, S. 2010. Methods of Limiting Leak Off and Damage in Hydraulic Fractures. US Patent No. 7,779,915.
- IDA. 2006. 19th Desalination Plant Inventory. Topsfield, Massachusetts: Global Water Intelligence and International Desalination Association.
- Iler, R.K. 1979. *The Chemistry of Silica: Solubility, Polymerization, Colloid and Surface Properties and Biochemistry of Silica*. New York: John Wiley & Sons.
- Isidore, C. 2006. New Worry for Drivers: BP Shuts Oilfield. Damaged Pipeline in Alaska Affects 8% of U.S. Oil Production; Crude Surges; Record Gas Prices Seen. http://money.cnn.com/2006/08/07/news/international/oil_alaska/index.htm.
- Islam, M.R. and Farouq Ali, S.M. 1993. Use of silica gel for improving waterflooding performance of bottom-water reservoirs. *J. Pet. Sci. Eng.* **8** (4): 303–313. [http://dx.doi.org/http://dx.doi.org/10.1016/0920-4105\(93\)90007-2](http://dx.doi.org/http://dx.doi.org/10.1016/0920-4105(93)90007-2).
- ISO International Standards. 2012. Geneva, Switzerland: International Standards Organization.
- ISO 13503-2, *Measurement of Properties of Proppants Used in Hydraulic Fracturing and Gravel-Packing Operations*. 2006. Geneva, Switzerland: International Organization of Standards.
- ISO 3104:1994, *Petroleum Products—Transparent and Opaque Liquids—Determination of Kinematic Viscosity and Calculation of Dynamic Viscosity*. 1994. Geneva: International Standards Organization.
- Jack, T.R., Grigoryan, A., Lambo, A. et al. 2009. Troubleshooting Nitrate Field Injections for Control of Reservoir Souring. Presented at the SPE International Symposium on Oilfield Chemistry, The Woodlands, Texas, 20–22 April 2009. SPE-121573-MS. <http://dx.doi.org/10.2118/121573-MS>.
- Jacob, S.M. and Bergman, R.F. 2001. Water Based Oil Dispersant. US Patent No. 6,261,463.
- Jacobs, I.C. and Thorne, M.A. 1986. Asphaltene Precipitation During Acid Stimulation Treatments. Presented at the SPE Formation Damage Control Symposium, Lafayette, Louisiana, 26–27 February. SPE-14823-MS. <http://dx.doi.org/10.2118/14823-MS>.
- Jaffe, A.M. 2010. Shale Gas Will Rock the World. *Wall Street Journal*, 10 May, <http://online.wsj.com/article/SB10001424052702303491304575187880596301668.html>.
- Jaramillo, O.J., Romero, R., Ortega, A. et al. 2010. Matrix Acid Systems for Formations With High Clay Content. Presented at the SPE International Symposium and Exhibition on Formation Damage Control, Lafayette, Louisiana, USA, 10–12 February. SPE-126719-MS. <http://dx.doi.org/10.2118/126719-MS>.
- Jarrell, P., Fox, C., Stein, M. et al. 2002. *Practical Aspects of CO₂ Flooding*, No. 22. Richardson, Texas: Monograph Series, SPE.
- Jasinski, R., Frenier, W. and Grannan, S. 1988. Inhibiting HCl Corrosion of High Chrome Tubular Steels. Paper NACE 88188 presented at NACE International Corrosion '88, St. Louis, Missouri, 14–18 March.
- Jasinski, R.J. and Frenier, W.W. 1992. Process and Composition for Protecting Chrome Steel. US Patent No. 5,120,471.
- Jauregui, J.A.L., Malik, A.R., Garcia, W.N. et al. 2010. Field Trials of a Novel Fiber-Laden Self-Diverting Acid System for Carbonates in Saudi Arabia. Presented at the SPE Deep Gas Conference and Exhibition, Manama, Bahrain, 24–26 January. SPE-132003-MS. <http://dx.doi.org/10.2118/132003-MS>.
- Jauregui, J.A.L., Malik, A.R., Garcia, W.N. et al. 2011. Successful Application of Novel Fiber Laden Self-Diverting Acid System during Fracturing Operations of Naturally Fractured Carbonates in Saudi Arabia. Presented at the SPE Middle East Oil and Gas Show and Conference, Manama, Bahrain, 25–28 September. SPE-142512-MS. <http://dx.doi.org/10.2118/142512-MS>.
- Jayakumar, S. and Lane, R.H. 2012. Delayed Crosslink Polymer Flowing Gel System for Water Shutoff in Conventional and Unconventional Oil and Gas Reservoirs. Presented at the SPE International Symposium and Exhibition on Formation Damage Control, Lafayette, Louisiana, USA, 15–17 February. SPE-151699-MS. <http://dx.doi.org/10.2118/151699-MS>.
- Jayaraman, A. and Saxena, R.C. 1996. Corrosion Inhibitors in Hydrocarbon Systems. Paper NACE 96221 presented at NACE International CORROSION/ 96, Denver, 24–29 March.

- Jenkins, A. 2010. The Application of Corrosion Inhibitors to Prevent Localized Corrosion in a Sour Oilfield. Paper NACE 10330 presented at NACE International CORROSION 2010, San Antonio, Texas, 14–18 March.
- Jenkins, A. 2011a. Performance of High-Temperature, Biodegradable Corrosion Inhibitors. Paper NACE 11272 presented at NACE International CORROSION 2011, Houston, Texas, 13–17 March.
- Jenkins, A. 2011b. Organic Corrosion Inhibitor Package for Organic Acids. US Application Patent No. 2011/0028360.
- Jennings-Jr, A.R. 1993. Method of Matrix Acidizing. US Patent No. 5,207,778.
- Jermelov, A. 2010. How to Defend against Future Oil Spills. *Nature* **466** (7303): 182–183. <http://dx.doi.org/10.1038/466182a>.
- Jimenez-Bueno, O., Ramirez, G.R., Quevedo, M. et al. 2012. Pushing the Limits: HT Carbonate Acidizing. Presented at the SPE International Symposium and Exhibition on Formation Damage Control, Lafayette, Louisiana, USA, 15–17 February. SPE-151740-MS. <http://dx.doi.org/10.2118/151740-MS>.
- Jofa, Z.A. 1965. Adsorption of Inhibitors of the Acid Corrosion of Iron & the Mechanism of Their Action. Presented at the 2nd European Symposium on Corrosion Inhibitors, Ferrara, Italy, 13–17 September.
- Jones, A.H. and Cutler, R.A. 1985. Hollow Proppants and a Process for Their Manufacture. US Patent No. 4,547,468.
- Jones, C.K. 2000. Method of Reducing the Concentration of Metal Soaps of Partially Esterified Phosphates from Hydrocarbon Flowback Fluids. US Patent No. 6,133,205.
- Jones, J.R. and Britt, L.K. 2009. *Design and Appraisal of Hydraulic Fractures*. Richardson, Texas: SPE.
- Jones, P.W. and Williams, D.R. 2001. Chemical Speciation Used to Assess [S,S']-Ethylenediaminedisuccinic Acid (EDDS) as a Readily-Biodegradable Replacement for EDTA in Radiochemical Decontamination Formulations. *Applied Radiation and Isotopes* **54** (4): 587–593.
- Jordan, M., Sorhaug, E., Marlow, D., and Graham, G. 2010. Red; Vs. Green Scale Inhibitors for Extending Squeeze Life—a Case Study from North Sea, Norwegian Sector. Paper NACE 10137 presented at NACE International CORROSION 2010 San Antonio, Texas, March 14–18.
- Jordan, M.M. 2012. Simultaneous Well Stimulation and Scale Squeeze Treatments in Sandstone and Carbonate Reservoirs. Presented at the SPE International Production and Operations Conference & Exhibition, Doha, Qatar, 14–16 May. SPE-156804-MS. <http://dx.doi.org/10.2118/156804-MS>.
- Jordan, M.M. and Feasey, N.D. 2008. Meeting the Flow Assurance Challenges of Deepwater Developments: From Capex Development to Field Start Up. Presented at the SPE North Africa Technical Conference & Exhibition, Marrakech, Morocco, 12–14 March. SPE-112472-MS. <http://dx.doi.org/10.2118/112472-MS>.
- Joseph, D.D. 1997. Understanding Foams & Foaming, Report NSF-GOALI grant in collaboration with INTEVEP S.A. Minneapolis, Minnesota: University of Minnesota.
- Jubran, B.A., Zurigat, Y.H., and Goosen, M.F.A. 2005. Drag Reducing Agents in Multiphase Flow Pipelines: Recent Trends and Future Needs. *Petroleum Science and Technology* **23** (11-12): 1403–1424. <http://dx.doi.org/10.1081/lft-200038223>.
- Judzis, A., Felder, R., Curry, D., and Seiller, B. 2011. The Five R&D Grand Challenges Plus One. *J. Pet Tech* **63**(5): 34–35.
- Kabir, M.M.R., Dashti, Q.M., Singh, J.R. et al. 2011. Extending Well Productive Life by Acid Refracturing in a High Pressure/High Temperature Tight Gas/Condensate Carbonate Reservoir in the Jurassic Formation of North Kuwait. Presented at the SPE Middle East Unconventional Gas Conference and Exhibition, Muscat, Oman, 31 January–2 February. SPE-142444-MS. <http://dx.doi.org/10.2118/142444-MS>.
- Kakadjian, S., Rauseo, O., Marquez, R. et al. 2001. Crosslinked Emulsion To Be Used as Fracturing Fluids. Presented at the SPE International Symposium on Oilfield Chemistry, Houston, 13–16 February. SPE-65038-MS. <http://dx.doi.org/10.2118/65038-MS>.
- Kakadjian, S.R., Zamora, F., Garza, T., De Santis, L.M., and Salager, J.-L. 2009. Composition and Methods for Gas Well Treatments. US Application Patent No. 20090200033.

- Kalantari-Dahaghi, A., Moghadasi, J., Gholami, V. et al. 2006. Formation Damage Due to Asphaltene Precipitation Resulting From CO₂ Gas Injection in Iranian Carbonate Reservoirs. Presented at the SPE Europec/EAGE Annual Conference and Exhibition, Vienna, Austria, 12–15 June. SPE-99631-MS. <http://dx.doi.org/10.2118/99631-MS>.
- Kalfayan, L. 2008. *Production Enhancement with Acid Stimulation*, second edition. Tulsa: PennWell.
- Kalfayan, L.J. 2007. Fracture Acidizing: History, Present State, and Future. Presented at the SPE Hydraulic Fracturing Technology Conference, College Station, Texas USA, 29–31 January. SPE-106371-MS. <http://dx.doi.org/10.2118/106371-MS>.
- Kalra, A., Venkatraman, A., Raney, K.H. et al. 2012. Prediction and Experimental Measurements of Water-in-Oil Emulsion Viscosities During Alkaline/Surfactant Injections. *Oil and Gas Facilities* **1** (3): 34–43. SPE-143992-PA. <http://dx.doi.org/10.2118/143992-PA>.
- Kam, S.I. and Rossen, W.R. 2003. A Model for Foam Generation in Homogeneous Porous Media. *SPE J.* **8** (4): 417–425. SPE-87334-PA. <http://dx.doi.org/10.2118/87334-PA>.
- Kam, S.I., Frenier, W.W., Davies, S.N. et al. 2007. Experimental study of high-temperature foam for acid diversion. *J. Pet. Sci. Eng.* **58** (1-2): 138–160. <http://dx.doi.org/10.1016/j.petrol.2006.12.005>.
- Kamel, A.H.A. and Shah, S.N. 2008. Investigation of the Complex Flow Behaviour of Surfactant-Based Fluids in Straight Tubing. Presented at the Canadian International Petroleum Conference, Calgary, Alberta, 17–19 June. PETSOC-2008-185. <http://dx.doi.org/10.2118/2008-185>.
- Kamel, A.H.A. and Shah, S.N. 2010. Friction Pressure Losses of Surfactant-Based Fluids Flowing in Coiled Tubing. Presented at the SPE Production and Operations Conference and Exhibition, Tunis, Tunisia, 8–10 June. SPE-135826-MS. <http://dx.doi.org/10.2118/135826-MS>.
- Kan, A.T., Fu, G., Al-Saiari, H. et al. 2009. Enhanced Scale-Inhibitor Treatments With the Addition of Zinc. *SPE J.* **14** (4): 617–626. SPE-114060-PA. <http://dx.doi.org/doi:10.2118/114060-PA>.
- Karazincir, O., Thach, S., Wei, W. et al. 2011. Scale Formation Prevention During ASP Flooding. Presented at the SPE International Symposium on Oilfield Chemistry, The Woodlands, Texas, USA, 11–13 April. SPE-141410-MS. <http://dx.doi.org/10.2118/141410-MS>.
- Kargbo, D.M., Wilhelm, R.G., and Campbell, D.J. 2010. Natural Gas Plays in the Marcellus Shale: Challenges and Potential Opportunities. *Environ. Sci. Technol.* **44** (15): 5679–5684. <http://dx.doi.org/10.1021/es903811p>.
- Kaufman, P.B., Penny, G.S., and Paktinat, J. 2008. Critical Evaluation of Additives Used in Shale Slickwater Fracs. Presented at the SPE Shale Gas Production Conference, Fort Worth, Texas, USA, 16–18 November. SPE-119900-MS. <http://dx.doi.org/10.2118/119900-MS>.
- Kayhan, M. 1982. Proposed Classification and Definitions of Heavy Crude Oils and Tar Sands. Presented at the 2nd UNITAR Conference on Heavy Crude and Tar Sands, Caracas, Venezuela, 7–17 February.
- Keck, R.G., Nehmer, W., and Strumolo, G.S. 1992. A New Method for Predicting Friction Pressures and Rheology of Proppant-Laden Fracturing Fluids. *SPE Prod Eng* **7** (1): 21–28. SPE-19771-PA. <http://dx.doi.org/10.2118/19771-PA>.
- Kefi, S., Lee, J., Nelson, E., Hernandez, A.N., Olsen, T., Parlar, M., Powers, B., Roy, A., Wilson, A., et al. 2004. Expanding Applications for Viscoelastic Surfactants. *Oilfield Review* **16** (4): 10–23.
- Keijzer, P.P.M., H.M., M., Rosmalen Janssen-van, R. et al. 1986. Application of Steam Foam in the Tia Juana Field, Venezuela: Laboratory Tests and Field Results. Presented at the SPE Enhanced Oil Recovery Symposium, Tulsa, 20–23 April. SPE-14905-MS. <http://dx.doi.org/10.2118/14905-MS>.
- Kell, S. 2009. Modern Shale Gas Development in the United States: A Primer. Report DE-FG26-04NT15455, US Department of Energy Office of Fossil Energy, Oklahoma City, Oklahoma, Ground Water Protection Council.
- Kelland, M.A. 2009. *Production Chemicals for the Oil and Gas Industry*. Boca Raton, Florida: CRC Press.

- Kelland, M.A., Svartaas, T.M., and Dybvik, L. 1995. A New Generation of Gas Hydrate Inhibitors. Presented at the SPE Annual Technical Conference and Exhibition, Dallas, 22–25 October. SPE-30695-MS. <http://dx.doi.org/10.2118/30695-MS>.
- Khilar, K. and Fogler, H. 1998. *Migrations of Fines and Porous Media*. Dordrecht/London/Boston: Kulwer Academic Publishers.
- Khristianovich, S.A. and Zheltov, Y.P. 1955. Formation of vertical fractures by means of highly viscous liquid. *Proc.*, Fourth World Petroleum Congress, Rome, Italy, 6–15 June, 2, 579–586.
- Kiel, O.M. 1974. Fracturing Method Using Acid External Emulsions. US Patent No. 3,799,266.
- Kim, B.-Y., Moon, J.H., Sung, T.-H. et al. 2002. Demulsification of water-in-crude oil emulsions by a continuous electrostatic dehydrator. *Sep. Sci. Technol.* **37** (6): 1307–1320. <http://dx.doi.org/10.1081/ss-120002613>.
- Kim, Y.H. and Wasan, D.T. 1996. Effect of Demulsifier Partitioning on the Destabilization of Water-in-Oil Emulsions. *Ind. Eng. Chem. Res.* **35** (4): 1141–1149. <http://dx.doi.org/10.1021/ie950372u>.
- King, G.E. 2010. Thirty Years of Gas Shale Fracturing: What Have We Learned? Presented at the SPE Annual Technical Conference and Exhibition, Florence, Italy, 19–22 September. SPE-133456-MS. <http://dx.doi.org/10.2118/133456-MS>.
- Kirkby, L.L. and Rockefeller, H.A. 1985. Proppant Settling Velocities in Nonflowing Slurries. Presented at the SPE/DOE Low Permeability Gas Reservoirs Symposium, Denver, 19–22 March. SPE-13906-MS. <http://dx.doi.org/10.2118/13906-MS>.
- Kirkpatrick, W.H., Seale, V.L., and Berkley, R.E. 1965. Emulsifier Compositions and Uses Thereof. US Patent No. 3,169,113.
- Kleverlaan, M., Noort, R.H.v., and Jones, I. 2005. Deployment of Swelling Elastomer Packers in Shell E&P. Presented at the SPE/IADC Drilling Conference, Amsterdam, Netherlands, 23–25 February. SPE-92346-MS. <http://dx.doi.org/10.2118/92346-MS>.
- Kline, W.E. 1980. *The Catalyzed Dissolution of Silicate Materials in Hydrofluoric Acid*. PhD dissertation, University of Michigan, Ann Arbor, Michigan.
- Kline, W.E. and Fogler, H.S. 1981. Dissolution kinetics: Catalysis by strong acids. *J. Colloid Interface Sci.* **82** (1): 93–102. [http://dx.doi.org/10.1016/0021-9797\(81\)90127-2](http://dx.doi.org/10.1016/0021-9797(81)90127-2).
- Kohler, N. and Zaitoun, A. 1992. Method and Composition for Selectively Reducing Permeability to Water in Hydrocarbon Reservoirs Which Are Hot and Saline. US Patent No. 5,082,577.
- Kohler, N., Bazin, B., Zaitoun, A. and Johnson, T. 2004. Green Inhibitors for Squeeze Treatments: A Promising Alternative. Paper NACE 04537 presented at NACE International Corrosion/2004, New Orleans, Louisiana, 28 March–1 April.
- Kohler, N., Courbin, C., Estievenart, C., and Ropital, F. 2002. Polyaspartates: Biodegradable Alternates to Polyacrylates or Noteworthy Multifunctional Inhibitors? Paper NACE 02411 presented at the NACE International CORROSION 2002, Denver, 7–11 April.
- Kokal, S. and Wingrove, M. 2000. Emulsion Separation Index: From Laboratory to Field Case Studies. Presented at the SPE Annual Technical Conference and Exhibition, Dallas, 1–4 October. SPE-63165-MS. <http://dx.doi.org/10.2118/63165-MS>.
- Kokal, S.L. 2006. Crude Oil Emulsions. In *Petroleum Engineering Handbook, Vol. 1—General Engineering*, ed. J.R. Fanchi. Richardson, Texas: Society of Petroleum Engineers.
- Kozora, C.J. 2010. Water Management: Treatment of Frac Water at Wellhead. Paper IWC-10-63 presented at the 71st International Water Conference, San Antonio, Texas, 24–28 October.
- Krawczyk, M.A., Wasan, D.T., and Shetty, C. 1991. Chemical demulsification of petroleum emulsions using oil-soluble demulsifiers. *Ind. Eng. Chem. Res.* **30** (2): 367–375. <http://dx.doi.org/10.1021/ie00050a014>.
- Krumrine, P.H. and Falcone Jr., J.S. 1983. Surfactant, Polymer, and Alkali Interactions in Chemical Flooding Processes. Presented at the SPE Oilfield and Geothermal Chemistry Symposium, Denver, Colorado, 1–3 June 1983. SPE-11778-MS. <http://dx.doi.org/10.2118/11778-MS>.
- Kubala, G. and Mackay, B.G. 2010. Use of Carbon Dioxide Based Fracturing Fluids. US Patent No. 7,726,404.

- Kulawardana, E.U., Koh, H., Kim, D.H. et al. 2012. Rheology and Transport of Improved EOR Polymers under Harsh Reservoir Conditions. Presented at the SPE Improved Oil Recovery Symposium, Tulsa, 14–18 April. SPE-154294-MS. <http://dx.doi.org/10.2118/154294-MS>.
- Kulkarni, M.C. 2008. *Characterization of Light Weight Composit Proppants*. MS thesis, Texas A&M University, College Station, Texas.
- Kume, N., Melsen, R.V., Erhahon, L. et al. 1999. New HF Acid System Improves Sandstone Matrix Acidizing Success Ratio By 400% Over Conventional Mud Acid System in Niger Delta Basin. Presented at the SPE Annual Technical Conference and Exhibition, Houston, 3–6 October. SPE-56527-MS. <http://dx.doi.org/10.2118/56527-MS>.
- Kuron, D. 1995. Corrosion inhibitors—A working party report of the European Federation of Corrosion (EFC), Publication Nr. 11. Hrsg. The Institute of Materials, 163 Seiten, Book Nr. 559, London 1994. *Mater. Corros.* **46** (5): 336–336. <http://dx.doi.org/10.1002/maco.19950460514>.
- Kwak., T.Y., Benmekki, E.H., and Mansoori, C.A. 1985. *Van Der Waals Mixing Rules for Cubic Equations of State (Applications for Supercritical Fluid Extraction Modeling and Phase Equilibrium Calculations)*. Report, Department of Chemical Engineering, University of Illinois, Chicago.
- Labrid, J.C. 1975. Thermodynamic and Kinetic Aspects of Argillaceous Sandstone Acidizing. *Society of Petroleum Engineers Journal* **15** (2): 117–128. SPE-5156-PA. <http://dx.doi.org/10.2118/5156-PA>.
- LaFollette, R.F. and Holcomb, W.D. 2011. Practical Data Mining: Lessons-Learned From the Barnett Shale of North Texas. Presented at the SPE Hydraulic Fracturing Technology Conference, The Woodlands, Texas, USA, 24–26 January. SPE-140524-MS. <http://dx.doi.org/10.2118/140524-MS>.
- Lager, A., Webb, K.J., and Black, C.J.J. 2007. Impact of Brine Chemistry on Oil Recovery. Presented at the 14th European Symposium on Improved Oil Recovery, Cairo, 22–24 April. A24.
- Lager, A., Webb, K.J., Collins, I.R. et al. 2008. LoSal™ Enhanced Oil Recovery: Evidence of Enhanced Oil Recovery at the Reservoir Scale. Presented at the SPE/DOE Symposium on Improved Oil Recovery, Tulsa, 20–23 April. SPE-113976-MS. <http://dx.doi.org/10.2118/113976-MS>.
- Laing, N., Graham, G.M., and Dyer, S.J. 2003. Barium Sulphate Inhibition in Subsea Systems - The Impact of Cold Seabed Temperatures on the Performance of Generically Different Scale Inhibitor Species. Presented at the International Symposium on Oilfield Chemistry, Houston, 5–7 February. SPE-80229-MS. <http://dx.doi.org/10.2118/80229-MS>.
- Lakatos, I.J., Bodi, T., Lakatos-Szabo, J. et al. 2010. Mitigation of Formation Damage Caused by Water-Based Drilling Fluid in Unconventional Gas Reservoirs. Presented at the SPE International Symposium and Exhibiton on Formation Damage Control, Lafayette, Louisiana, USA, 10–12 February. SPE-127999-MS. <http://dx.doi.org/10.2118/127999-MS>.
- Lake, L. 2010. *Enhanced Oil Recovery*. Richardson, Texas: Society of Petroleum Engineers.
- Lake, L.W. 2007. *Fundamentals of Enhanced Oil Recovery*. Richardson, Texas: Society of Petroleum Engineers.
- Lake, L.W. and Walsh, M.P. 2008. *Enhanced Oil Recovery (EOR) Field Data Literature Search*. Report, Department of Petroleum and Geosystems Engineering University of Texas at Austin, Austin, Texas.
- Lake, L.W., Schmidt, R.L., and Venuto, P.B. 1992. A Niche for Enhanced Oil Recovery in the 1990s. *Oilfield Review* **4** (1): 55–60.
- Lambert, M.E. 1981. *A Statistical Study of Reservoir Heterogeneity*. MS thesis, The University of Texas at Austin, Austin, Texas.
- Langelier, W.G. 1988. The Analytical Control of Anti-Corrosion Water Treatment. *JAWWA* **28** (10): 1500–1521.
- Langmuir, D. 1997. *Aqueous Environmental Geochemistry*. New Jersey: Prentice Hall.
- Langston, M.V., Hoadley, S.F., and Young, D.N. 1988. Definitive CO₂ Flooding Response in the SACROC Unit. Presented at the SPE Enhanced Oil Recovery Symposium, Tulsa, 16–21 April. SPE-17321-MS. <http://dx.doi.org/10.2118/17321-MS>.

- Larsen, J., Rasmussen, K., Pedersen, H., Sørensen, K., Lundgaard, T., and Skovhus, T.L. 2010. Consortia of Mic Bacteria and Archaea Causing Pitting Corrosion in Top Side Oil Production Facilities. Paper NACE 10252 presented at NACE International CORROSION 2010, San Antonio, Texas, 14–18 March.
- Larsen, J., Sorenson, K., Hojris, K., and Skovhus, T.L. 2009. Significance of Troublesome Sulfate-Reducing Prokaryotes (Srp) in Oilfield Systems. Paper NACE 09389 presented at NACE International CORROSION 2009, Houston, 2–4 February.
- Lau, J.C.S. 2005. Husky Energy Successfully Implements Alkaline-Surfactant-Polymer (ASP) Flood Technology. Calgary: Husky Energy.
- Le, H. and Dawson, J. 1995. Controlled Degradation of Polymer Based Aqueous Gels. US Patent No. 5,447,199.
- Le, H., Kesavan, S., Dawson, J., Mack, D.J., and Nelson, S.G. 2001. Composition and Methods for Hydraulic Fracturing. US Patent No. 6,169,058.
- Lei, C. and Clark, P.E. 2004. Crosslinking of Guar and Guar Derivatives. Presented at the SPE Annual Technical Conference and Exhibition, Houston, 26–29 September. SPE-90840-MS. <http://dx.doi.org/10.2118/90840-MS>.
- Leinweber, D., Scherl, F.-X., Wasmund, E., and Rausch, H. 2010. Alkoxylated, Cross-Linked Polyglycerols and Use Thereof as Biodegradable Demulsifier. US Patent No. 7,671,098.
- Lemon, P.E., Zeinijahromi, A., Bedrikovetsky, P.G. et al. 2011. Effects of Injected Water Chemistry on Waterflood Sweep Efficiency via Induced Fines Migration. Presented at the SPE International Symposium on Oilfield Chemistry, The Woodlands, Texas, USA, 11–13 April 2011. SPE-140141-MS. <http://dx.doi.org/10.2118/140141-MS>.
- Leontaritis, K.J. 1998. Asphaltene Near-wellbore Formation Damage Modeling. Presented at the SPE Formation Damage Control Conference, Lafayette, Louisiana, 18–19 February. SPE-39446-MS. <http://dx.doi.org/10.2118/39446-MS>.
- LePage, J.N., Wolf, C.D., Bemelaar, J. et al. 2009. An Environmentally Friendly Stimulation Fluid for High-Temperature Applications. Presented at the SPE International Symposium on Oilfield Chemistry, The Woodlands, Texas, 20–22 April. SPE-121709-MS. <http://dx.doi.org/10.2118/121709-MS>.
- Lessard, R.R., Becker, K.W., Canevari, G.P., George-Ares, A., and Fiocco, R.J. 2001. Chemical Dispersants for Oil Spills. US Patent No. 6,194,473.
- Levich, V.G. 1962. *Physicochemical Hydrodynamics*. Englewood Cliffs, New Jersey: Prentice-Hall.
- Levitt, D.B. and Pope, G.A. 2008. Selection and Screening of Polymers for Enhanced-Oil Recovery. Presented at the SPE/DOE Symposium on Improved Oil Recovery, Tulsa, 19–23 April. SPE 113845. <http://dx.doi.org/10.2118/113845-MS>.
- Levitt, D.B., Jackson, A.C., Heinson, C. et al. 2009. The Identification and Evaluation of High-Performance EOR Surfactants. *SPE Res Eval & Eng* **12** (2): 243–253. SPE-100089-PA. <http://dx.doi.org/10.2118/100089-PA>.
- Lewis, A. 2001. Oil Spill Dispersants. Report, SINTEF, Trondheim, Norway.
- Li, L., Abad, C., and Lin, L. 2008a. Internal Breakers for Viscoelastic Surfactant Fluids. US Application Patent No. 2008/0269081.
- Li, L., Eliseeva, K.E., Eliseev, V. et al. 2009. Well Treatment Fluids Prepared With Oilfield Produced Water. Presented at the SPE Annual Technical Conference and Exhibition, New Orleans, 4–7 October. SPE-124212-MS. <http://dx.doi.org/10.2118/124212-MS>.
- Li, L., Nasr-El-Din, H.A., and Cawiezel, K.E. 2010. Rheological Properties of a New Class of Viscoelastic Surfactant. *SPE Prod & Oper* **25** (3): pp. 355–366. SPE-121716-PA. <http://dx.doi.org/10.2118/121716-PA>.
- Li, L., Nasr-El-Din, H.A., Chang, F. et al. 2008b. Reaction of Simple Organic Acids and Chelating Agents With Calcite. Presented at the International Petroleum Technology Conference, Kuala Lumpur, 3–5 December. IPTC-12886-MS. <http://dx.doi.org/10.2523/12886-MS>.
- Li, Y., Wang, F., Wu, J. et al. 2008c. Current Status and Prospects of ASP Flooding in Daqing Oil Fields. Presented at the SPE/DOE Symposium on Improved Oil Recovery, Tulsa, Oklahoma, 20–23 April. SPE-114343-MS. <http://dx.doi.org/10.2118/114343-MS>.

- Li, Z., Zhou, G., and Zhou, Z. 2006. The Feasibility Studies of Polymer Foam Flooding in Gudao Oil Field. Presented at the SPE Asia Pacific Oil & Gas Conference and Exhibition, Adelaide, Australia, 11–13 September. SPE-101189-MS. <http://dx.doi.org/10.2118/101189-MS>.
- Liang, J.-T., Sun, H., and Seright, R.S. 1995. Why Do Gels Reduce Water Permeability More Than Oil Permeability? *SPE Res Eng* **10** (4): 282–286. SPE-27829-PA. <http://dx.doi.org/10.2118/27829-PA>.
- Lim, F.H., Munoz, E., and Joshi, N.B. 2008. Design and Initial Results of EOR and Flow Assurance Lab Tests for K2 Field Development in the Deepwater Gulf of Mexico. Presented at the Offshore Technology Conference, Houston, 5–8 May. OTC-19624-MS. <http://dx.doi.org/10.4043/19624-MS>.
- Lin, L., Abad, C., Baser, B., and Li, L. 2008. Oxidative Internal Breaker System with Breaking Activators for Viscoelastic Surfactant Fluids. US Application Patent No. 20080070806.
- Lin, L., Danican, S.C., and Mueller, F.A. 2009. A Novel Foaming Agent for Hydraulic Fracturing: Laboratory Investigation and Field Usage. Presented at the SPE Eastern Regional Meeting, Charleston, West Virginia, USA, 23–25 September. SPE-125745-MS. <http://dx.doi.org/10.2118/125745-MS>.
- Lindley, J.R. 2001a. Chemical Recovery. National Energy Technology Laboratory, Department of Energy, Bartlesville, Oklahoma, <http://www.netl.doe.gov/technologies/oil-gas/publications/EORdrawings/Color/colhf.pdf>.
- Litt, M. and Serad, G. 1964. Chemical reactions on a rotating disk. *Chem. Eng. Sci.* **19** (11): 867–884. [http://dx.doi.org/http://dx.doi.org/10.1016/0009-2509\(64\)85065-X](http://dx.doi.org/http://dx.doi.org/10.1016/0009-2509(64)85065-X).
- Litt, N.D., Jerat, A.C., Gupta, D.V.S., and Pierce, R. 2006. Fracturing Fluids Containing Borate Esters as Crosslinking Agents and Method of Using Same. US Patent No. 7,007,757.
- Liu, S., Feng Li, R., Miller, C.A. et al. 2010. Alkaline/Surfactant/Polymer Processes: Wide Range of Conditions for Good Recovery. *SPE J.* **15** (2): 282–293. SPE-113936-PA. <http://dx.doi.org/10.2118/113936-PA>.
- Lockwood, L., and Kordziel, W. 2010. Acid Systems Give Old Wells New Life. *The American Oil and Gas Reporter* (December).
- Lohne, A., Han, L., Zwaag, C.v.d. et al. 2010. Formation-Damage and Well-Productivity Simulation. *SPE J.* **15** (3): 751–769. SPE-122241-PA. <http://dx.doi.org/10.2118/122241-PA>.
- Lord, P.D., Terracina, J., and Slabaugh, B. 2005. High Temperature Seawater-Based Cross-Linked Fracturing Fluids and Methods. US Patent No. 6,911,419.
- Lorenz, P.B. and Tham, M.K. 1981. Calcium Effects in the DOE Surfactant-Polymer Pilot Test. Presented at the SPE/DOE Enhanced Oil Recovery Symposium, Tulsa, 5–8 April. SPE-9814-MS. <http://dx.doi.org/10.2118/9814-MS>.
- Lumcon. 2008. Dispersant Bibliography. Cocodrie, Louisiana: Louisiana Universities Marine Consortium. <http://www.lumcon.edu/library/dispersants/>.
- Lund, K. and Fogler, H.S. 1976. Acidization—V: The prediction of the movement of acid and permeability fronts in sandstone. *Chem. Eng. Sci.* **31** (5): 381–392. [http://dx.doi.org/http://dx.doi.org/10.1016/0009-2509\(76\)80008-5](http://dx.doi.org/http://dx.doi.org/10.1016/0009-2509(76)80008-5).
- Lund, K., Fogler, H.S., and McCune, C.C. 1973. Acidization—I. The dissolution of dolomite in hydrochloric acid. *Chem. Eng. Sci.* **28** (3): 691–IN1. [http://dx.doi.org/http://dx.doi.org/10.1016/0009-2509\(77\)80003-1](http://dx.doi.org/http://dx.doi.org/10.1016/0009-2509(77)80003-1).
- Lund, K., Fogler, H.S., McCune, C.C. et al. 1975. Acidization—II. The dissolution of calcite in hydrochloric acid. *Chem. Eng. Sci.* **30** (8): 825–835. [http://dx.doi.org/http://dx.doi.org/10.1016/0009-2509\(75\)80047-9](http://dx.doi.org/http://dx.doi.org/10.1016/0009-2509(75)80047-9).
- Lungwitz, B., Fredd, C., Brady, M. et al. 2007. Diversion and Cleanup Studies of Viscoelastic Surfactant-Based Self-Diverting Acid. *SPE Prod & Oper* **22** (1): 121–127. SPE-86504-PA. <http://dx.doi.org/10.2118/86504-PA>.
- Luo, M., Liu, J., Wen, Q., Lliu, H., and Jia, Z. 2011. Fracturing Cleanup Effectiveness Improved by Environment-Friendly Mes Middle Phase Microemulsion. *ACTA Petrolei Sinica (Petroleum Processing Section)* **27** (3): 454–460.

- Lutnaes, B.F., Brandal, Ø., Sjoblom, J. et al. 2006. Archaeal C80 isoprenoid tetraacids responsible for naphthenate deposition in crude oil processing. *Org. Biomol. Chem.* **4** (4): 616–620. <http://dx.doi.org/10.1039/b516907k>.
- Ma, S.M., Zhang, X., Morrow, N.R. et al. 1999. Characterization of Wettability From Spontaneous Imbibition Measurements. *J Can Pet Technol* **38** (13). PETSOC-99-13-49. <http://dx.doi.org/10.2118/99-13-49>.
- Macdonald, B.A. and Engwall, S.J. 1983. High-Volume Electrical Submersible Pumping in the Sulphate-Sacling Environment of the Piper Field. Presented at the Offshore Europe, Aberdeen, United Kingdom, 6–9 September. SPE-11882-MS. <http://dx.doi.org/10.2118/11882-MS>.
- Mach, J., Proano, E.A., and Brown, K.E. 1982. Application of Production Systems Analysis to Determine Completion Sensitivity on Gas Well Production. *J. Energy Resour. Technol.* **104** (2): 162–169. <http://dx.doi.org/10.1115/1.3230394>.
- Mack, M.G., and Warpinski, N.R. 2001. Mechanics of Hydraulic Fracturing. In *Reservoir Stimulation*, third edition, ed. M.J. Economides and K.G. Nolte, 6.1-6.48. New York: John Wiley and Sons.
- Madyanova, M., Hezmela, R., Carvalho, C.R.G.D. et al. 2012. Effective Matrix Stimulation of High-Temperature Carbonate Formations in South Sumatra Through the Combination of Emulsified and Viscoelastic Self-Diverting Acids. Presented at the SPE International Symposium and Exhibition on Formation Damage Control, Lafayette, Louisiana, USA, 15–17 February. SPE-151070-MS. <http://dx.doi.org/10.2118/151070-MS>.
- Maerker, J.M. and Gale, W.W. 1992. Surfactant Flood Process Design for Loudon. *SPE Res Eng* **7** (1): 36–44. SPE-20218-PA. <http://dx.doi.org/10.2118/20218-PA>.
- Mahmoud, M.A., Nasr-El-Din, H.A., Wolf, C.D. et al. 2010. Optimum Injection Rate of a New Chelate That Can Be Used To Stimulate Carbonate Reservoirs. Presented at the SPE Annual Technical Conference and Exhibition, Florence, Italy, 19–22 September. SPE-133497-MS. <http://dx.doi.org/10.2118/133497-MS>.
- Mahmoud, M.A., Nasr-El-Din, H.A., Wolf, C.D. et al. 2011a. Evaluation of a New Environmentally Friendly Chelating Agent for High-Temperature Applications. *SPE J.* **16** (3): 559-574. SPE-127923-PA. <http://dx.doi.org/10.2118/127923-PA>.
- Mahmoud, M.A., Nasr-El-Din, H.A., Wolf, C.D. et al. 2011b. Sandstone Acidizing Using A New Class of Chelating Agents. Presented at the SPE International Symposium on Oilfield Chemistry, The Woodlands, Texas, USA, 11–13 April. SPE-139815-MS. <http://dx.doi.org/10.2118/139815-MS>.
- Makogon, T., and Sloan, E.D., Jr. 2002. Mechanism of Kinetic Hydrate Inhibitors. Presented at the 4th International Conference on Gas Hydrates, Yokohama, Japan, May 19–23.
- Malate, R.C.M., Austria, J.J.C., Sarmiento, Z.F., DiLullo, G., Sookprasong, P.A., and Francis, E.S. 1998. Matrix Stimulation Treatment of Geothermal Wells Using Sandstone Acid. Paper SGP-TR-IS8 presented at the 23rd Workshop on Geothermal Reservoir Engineering, Stanford University, Stanford, California, 26–28 January.
- Malhotra, S. and Sharma, M.M. 2011. A General Correlation for Proppant Settling in VES Fluids. Presented at the SPE Hydraulic Fracturing Technology Conference, The Woodlands, Texas, USA, 24–26 January. SPE-139581-MS. <http://dx.doi.org/10.2118/139581-MS>.
- Malik, M.A. and Hill, A.D. 1989. A New Technique for Laboratory Measurement of Acid Fracture Conductivity. Presented at the SPE Annual Technical Conference and Exhibition, San Antonio, Texas, 8–11 October. SPE-19733-MS. <http://dx.doi.org/10.2118/19733-MS>.
- Malik, Q.M. and Islam, M.R. 2000. CO₂ Injection in the Weyburn Field of Canada: Optimization of Enhanced Oil Recovery and Greenhouse Gas Storage With Horizontal Wells. Presented at the SPE/DOE Improved Oil Recovery Symposium, Tulsa, 3–5 April. SPE-59327-MS. <http://dx.doi.org/10.2118/59327-MS>.
- Malone, M.R., Nelson, S.G., and Greenlees, W.M. 2004. Fracture Stimulation of the Morrow Formation with Crosslinked Methanol: A Case History. Presented at the SPE International Symposium and Exhibition on Formation Damage Control, Lafayette, Louisiana, 18–20 February. SPE-86482-MS. <http://dx.doi.org/10.2118/86482-MS>.

- Malpani, R.V. 2006. *Selection of Fracturing Fluid for Stimulating Tight Gas Reservoirs*. MS thesis, Texas A&M University, College Station, Texas.
- Malvern 2003. Zeta Potential Theory. In *Zetasizer Nano Series*, sixteenth edition. Worcestershire, United Kingdom: Malvern Instruments Ltd.
- Mangold, D.C. and Tsang, C.-F. 1991. A summary of subsurface hydrological and hydrochemical models. *Rev. Geophys.* **29** (1): 51–79. <http://dx.doi.org/10.1029/90rg01715>.
- Manning, F.S., and Thompson, R.E. 1995. *Oilfield Processing of Petroleum: Crude Oil*. Tulsa: PennWell Publishing Co.
- Mannistu, K.D., Yarranton, H.W., and Masliyah, J.H. 1997. Solubility Modeling of Asphaltenes in Organic Solvents. *Energy Fuels* **11** (3): 615–622. <http://dx.doi.org/10.1021/ef9601879>.
- Manrique, E.J., Muci, V.E., and Gurfinkel, M.E. 2007. EOR Field Experiences in Carbonate Reservoirs in the United States. *SPE Res Eval & Eng* **10** (6): 667–686. SPE-100063-PA. <http://dx.doi.org/10.2118/100063-PA>.
- Mansfield, R.C., Morrison, J.G., and Schmidle, C.J. 1959. Corrosion Inhibiting Compositions. US Patent No. 2,874,119.
- Martell, A.E. and Smith, R.S. 1978. *Critical Stability Constants*. New York: Plenum Press.
- Martin, R.L., McMahon, J.A., and B., O.A. 1995. Biodegradable Corrosion Inhibitors of Low Toxicity. US Patent No. 5,393,464.
- Marty, L., Green, D.W., and Willhite, G.P. 1991. The Effect of Flow Rate on the In-Situ Gelation of a Chrome/Redox/Polyacrylamide System. *SPE Res Eng* **6** (2): 219–224. SPE-18504-PA. <http://dx.doi.org/10.2118/18504-PA>.
- Masel, R.I. 1996. *Principles of Adsorption and Reaction on Solid Surfaces*. New York: John Wiley and Sons, Inc.
- Masliyah, J. and Bhattacharjee, S. 2006. *Electrokinetic and Colloid Transport Phenomena*. New York: John Wiley & Sons.
- Masoudi, R. and Tohidi, B. 2005. Experimental Investigation on the Effect of Commercial Oilfield Scale Inhibitors on the Performance of Low Dosage Hydrate Inhibitors (LDHI). Presented at the 5th International Conference on Gas Hydrates, Trondheim, Norway, June 13–16.
- Matsuhisa, S. and Bird, R.B. 1965. Analytical and numerical solutions for laminar flow of the non-Newtonian ellis fluid. *AIChE J.* **11** (4): 588–595. <http://dx.doi.org/10.1002/aic.690110407>.
- Matthews, W.R. and Kelly, J. 1967. How to predict formation pressure and fracture gradient from electric and sonic logs. *Oil Gas J.* **62**: 92–106.
- McCarthy, K., Rojas, K., Niemann, M., Palmowski, D., Peters, K., and Stankiewicz, A. 2011. Basic Petroleum Geochemistry for Source Rock Evaluation. *Oilfield Review* **23** (2): 32–44.
- McDaniel, G.A., Abbott, J., Mueller, F.A. et al. 2010. Changing the Shape of Fracturing: New Proppant Improves Fracture Conductivity. Presented at the SPE Annual Technical Conference and Exhibition, Florence, Italy, 19–22 September. SPE-135360-MS. <http://dx.doi.org/10.2118/135360-MS>.
- McDuff, D., Shuchart, C.E., Jackson, S. et al. 2010. Understanding Wormholes in Carbonates: Unprecedented Experimental Scale and 3-D Visualization. Presented at the SPE Annual Technical Conference and Exhibition, Florence, Italy, 19–22 September. SPE-134379-MS. <http://dx.doi.org/10.2118/134379-MS>.
- McFarland, S., Pit, H., Unsal, R. et al. 2008. Development of Corrosion Inhibitor and Kinetic Hydrate Inhibitor for the Pearl GTL Project. Presented at the International Petroleum Technology Conference, Kuala Lumpur, Malaysia, 3–5 December. IPTC-12405-MS. <http://dx.doi.org/10.2523/12405-MS>.
- McGowen, J.M. and Vitthal, S. 1997. Evaluation of Particulate and Hydrocarbon Fracturing Fluid-Loss Additives Under Dynamic Conditions. Presented at the SPE Production Operations Symposium, Oklahoma City, Oklahoma, USA, 9–11 March. SPE-37488-MS. <http://dx.doi.org/10.2118/37488-MS>.
- McGowen, J.M., Vitthal, S., Parker, M.A. et al. 1993. Fluid Selection for Fracturing High-Permeability Formations. Presented at the SPE Annual Technical Conference and Exhibition, Houston, 4–6 October. SPE-26559-MS. <http://dx.doi.org/10.2118/26559-MS>.

- McGuire, D., and Jakhete, S. 2010. Enhanced Water Treatment for Reclamation of Waste Fluids and Increased Efficiency Treatment of Potable Waters. US Patent No. 7,699,994.
- McIlroy, J.G. 2009. The Use of a Plume Modelling Study to Reduce the Risk of H₂S Release in an Exploration Well to As Low As Reasonably Practicable (ALARP). Presented at the International Petroleum Technology Conference, Doha, Qatar, 7–9 December. IPTC-13636-MS. <http://dx.doi.org/10.2523/13636-MS>.
- McLendon, W.J., Koronaos, P., McNulty, S. et al. 2012. Assessment of CO₂-Soluble Surfactants for Mobility Reduction using Mobility Measurements and CT Imaging. Presented at the SPE Improved Oil Recovery Symposium, Tulsa, 14–18 April. SPE-154205-MS. <http://dx.doi.org/10.2118/154205-MS>.
- McLeod, H.O. 2007. Matrix Acidizing. In *Petroleum Engineering Handbook Volume IV. Production Operations Engineering*, ed. J.D.Clegg. Richardson, Texas: SPE.
- McLeod, H.O. and Norman, W.D. 2001. Sandstone Acidizing. In *Reservoir Stimulation*, third edition, ed. M.J. Economides and K. G. Nolte. New York: John Wiley & Sons.
- Medvedev, A., Kraemer, C., Pena, A. et al. 2013. On the Mechanisms of Channel Fracturing. Presented at the 2013 SPE Hydraulic Fracturing Technology Conference, The Woodlands, Texas, USA, 4–6 February. SPE-163836-MS. <http://dx.doi.org/10.2118/163836-MS>.
- Melo, R.C.B.D., Curtis, J.A., Gomez, J.R. et al. 2012. Phosphonic/Hydrofluoric Acid: A Promising New Weapon in the Tortuosity Remediation Arsenal for Fracturing Treatments. Presented at the SPE Hydraulic Fracturing Technology Conference, The Woodlands, Texas, USA, 6–8 February. SPE-152624-MS. <http://dx.doi.org/10.2118/152624-MS>.
- Menjivar, J. 1986. Use of Gelation Theory to Characterize Metal Cross-Linked Polymer Gels. In *In Water-Soluble Polymers*, ed. J.E. Glass, 209–226. Washington, DC: American Chemical Society.
- Merdhah, A.B.B. and Yassin, A.M. 2008. Formation Damage Due to Scale Formation in Porous Media Resulting from Water Injection. *Emirates J. for Engineering Research* **13** (3): 69–79.
- Merdhah, A.B.B. and Yassin, A.A.M. 2009. Scale Formation Due to Water Injection in Malaysian Sandstone Cores. *American J. of Applied Sciences* **6** (8): 1531–1538.
- Messina. 2004. *Stimulation Chemicals—Fluid Loss Additives*. Dallas: Messina Oilfield Chemicals. <http://www.messina-oilchem.com/>.
- Metcalf, A.S., Boles, J.L., and Parker, C.P. 2006. Increasing Reaction Efficiency of Acetic Acid. US Patent No. 7,086,469.
- Metcalf, A.S., Orna, S., and Kretzschmer, G. 2007. Case Histories of Successful Acid Stimulation of Carbonate Completed With Horizontal Openhole Wellbores. Presented at the Canadian International Petroleum Conference, Calgary, 12–14 June. PETSOC-2007-085. <http://dx.doi.org/10.2118/2007-085>.
- Metcalf, S., Lopez, H., Hoff, C. et al. 2000. Gas Production From Low Permeability Carbonates Enhanced Through Usage of New Acid Polymer System. Presented at the SPE/CERI Gas Technology Symposium, Calgary, 3–5 April. SPE-59756-MS. <http://dx.doi.org/10.2118/59756-MS>.
- Meyer & Associates Inc. 2008. *Meyer Fracturing Simulators—User's Guide for MFRAC Software Used to Do Hydraulic Fracturing Simulations*. Natrona Heights, Pennsylvania: Baker Hughes Inc.
- Meyer, B.R. and Bazan, L.W. 2011. A Discrete Fracture Network Model for Hydraulically Induced Fractures: Theory, Parametric and Case Studies. Presented at the SPE Hydraulic Fracturing Technology Conference, The Woodlands, Texas, USA, 24–26 January. SPE-140514-MS. <http://dx.doi.org/10.2118/140514-MS>.
- Meyer, B.R. 1986. Generalized Drag Coefficient Applicable for All Flow Regimes. *Oil & Gas Journal* **86** (18): 71–77.
- Meyer, J.P. 2007. Summary of Carbon Dioxide Enhanced Oil Recovery (CO₂EOR) Injection Well Technology. Report, American Petroleum Institute, Washington D.C.
- Meyer. 2010. MFRAC computer program. Natrona Heights, Pennsylvania: Myers & Associates, Inc.

- Miles, A.F., Bourne, H.M., Smith, R.G. et al. 2003. Development of a Novel Water in Oil Microemulsion Based Scale Inhibitor Delivery System. Presented at the SPE International Symposium on Oilfield Scale, Aberdeen, 29–30 January. SPE-80390-MS. <http://dx.doi.org/10.2118/80390-MS>.
- Miller, J.F., Sheely, C.O., Wimberley, J.W., and Howard, R.A. 1993. Use of Nonradioactive Complex Metal Anion as Tracer in Subterranean Reservoirs. US Patent No. 5,246,861.
- Ming, G., and El-Rabaa, W. 2001. Method for Optimizing Acid Injection Rate in Carbonate Acidizing Process. US Patent No. 6,196,318.
- Mohamed, S.K., Nasr-El-Din, H.A., and Al-Furaidan, Y.A. 1999. Acid Stimulation of Power Water Injectors and Saltwater Disposal Wells in a Carbonate Reservoir in Saudi Arabia: Laboratory Testing and Field Results. Presented at the SPE Annual Technical Conference and Exhibition, Houston, 3–6 October. SPE-56533-MS. <http://dx.doi.org/10.2118/56533-MS>.
- Mohammadi, H. and Jerauld, G. 2012. Mechanistic Modeling of the Benefit of Combining Polymer with Low Salinity Water for Enhanced Oil Recovery. Presented at the SPE Improved Oil Recovery Symposium, Tulsa, 14–18 April. SPE-153161-MS. <http://dx.doi.org/10.2118/153161-MS>.
- Mohammadi, H., Delshad, M., and Pope, G.A. 2009. Mechanistic Modeling of Alkaline/Surfactant/Polymer Floods. *SPE Res Eval & Eng* **12** (4): 518–527. SPE-110212-PA. <http://dx.doi.org/10.2118/110212-PA>.
- Mohanty, K. 2009. Improvement of Fracturing for Gas Shales. Topical Progress Report, University of Texas, Dept. Petroleum and Geosystem Engineering, Austin, TX.
- Mohanty, K.K. 2003. Dilute Surfactant Methods for Carbonate Formations. Report DE-FC26-02NT 15322, Department of Energy, Washington, D.C.
- Mohnot, S.M., Bae, J.H., and Foley, W.L. 1987. A Study of Mineral/Alkali Reactions. *SPE Res Eng* **2** (4): 653–663. SPE-13032-PA. <http://dx.doi.org/10.2118/13032-PA>.
- Mokhtari, M. and Ozbayoglu, M.E. 2010. Laboratory Investigation on Gelation Behavior of Xanthan Crosslinked With Borate Intended to Combat Lost Circulation. Presented at the SPE Production and Operations Conference and Exhibition, Tunis, Tunisia, 8–10 June. SPE-136094-MS. <http://dx.doi.org/10.2118/136094-MS>.
- Molchanov, V.S., Philippova, O.E., Khokhlov, A.R., Kovalev, Y.A., and Kuklin, A.I. 2006. Self-Assembled Networks Highly Responsive to Hydrocarbons. *Langmuir* **23** (1): 105–111.
- Moloney, J., Mok, W., and Gamble, C. 2008. Corrosion and Hydrate Control in Wet Sour Gas Transmission Systems. Presented at the SPE Asia Pacific Oil and Gas Conference and Exhibition, Perth, Australia, 20–22 October. SPE-115074-MS. <http://dx.doi.org/10.2118/115074-MS>.
- Monroe, R.F., Kucera, C.H., Oakes, B.D., and Johnston, N.G. 1963. Composition for Inhibiting Corrosion. US Patent No. 3 077 454.
- Montgomerie, H., Chen, P., Hagen, T., Wat, R., and Selle, O.M. 2010. Well Treatment. US Application Patent No. 2010/0273682.
- Moore, J., and Liu, J.-F. 2009. Corrosion Inhibitors in the Presence of Elemental Sulfur. Paper NACE 09363 presented at NACE International CORROSION 2009, Atlanta, Georgia, 22–26 March.
- Moore, J., Vers, L.V., and Conrad, P. 2009. SS: Flow Assurance: Understanding Kinetic Hydrate Inhibitor and Corrosion Inhibitor Interactions. Presented at the Offshore Technology Conference, Houston, 4–7 May. OTC-19869-MS. <http://dx.doi.org/10.4043/19869-MS>.
- Moradi-Araghi, A., Johnston, E.L., Zornes, D.R. et al. 1997. Laboratory Evaluation of Surfactants for CO₂-Foam Applications at the South Cowden Unit. Presented at the International Symposium on Oilfield Chemistry, Houston, 18–21 February. SPE-37218-MS. <http://dx.doi.org/10.2118/37218-MS>.
- Morales, R.H., Brady, B.H., and Ingraffea, A.R. 1993. Three-Dimensional Analysis and Visualization of the Wellbore and the Fracturing Process in Inclined Wells. Presented at the Low Permeability Reservoirs Symposium, Denver, 26–28 April. SPE-25889-MS. <http://dx.doi.org/10.2118/25889-MS>.

- Morales, R.H., Profinet, J., Piedras, J. et al. 2003. Optimization of Frac/Pack Completions Based on Field Experience. Presented at the SPE Annual Technical Conference and Exhibition, Denver, 5–8 October. SPE-84263-MS. <http://dx.doi.org/10.2118/84263-MS>.
- Morel, D.C., Vert, M., Jouenne, S. et al. 2010. First Polymer Injection in Deep Offshore Field Angola: Recent Advances on Dalia/Camelia Field Case. Presented at the SPE Annual Technical Conference and Exhibition, Florence, Italy, 19–22 September. SPE 135735. <http://dx.doi.org/10.2118/135735-MS>.
- Moreno, B., Haydell, G.A., and Landry, L. 2009. Critical Data Needs for Design of FracPack Completions in Today's Oilfield Environment. Presented at Offshore Europe, Aberdeen, 8–11 September. SPE-124389-MS. <http://dx.doi.org/10.2118/124389-MS>.
- Morgenthaler, L.N., Lawson, J.B., Faircloth, R.J. et al. 1993. Scale Prediction and Control in the Denver Unit CO₂ Flood. Presented at the SPE Annual Technical Conference and Exhibition, Houston, 3–6 October. SPE-26603-MS. <http://dx.doi.org/10.2118/26603-MS>.
- Morgenthaler, L.N., Rhodes, P.R., and Wheaton, L.L. 1997. Testing the Corrosivity of Spent HCl/HF Acid to 22 Cr and 13 Cr Stainless Steels. Presented at the International Symposium on Oilfield Chemistry, Houston, 18–21 February. SPE-37278-MS. <http://dx.doi.org/10.2118/37278-MS>.
- Morrow, N. and Buckley, J. 2011. Improved Oil Recovery by Low-Salinity Waterflooding. *J Pet Technol* **63** (5): 106–112. SPE-129421-MS. <http://dx.doi.org/10.2118/129421-MS>.
- Morvan, M., Degre, G., Beaumont, J. et al. 2012. Optimization of Viscosifying Surfactant Technology for Chemical EOR. Presented at the SPE Improved Oil Recovery Symposium, Tulsa, 14–18 April. SPE-154053-MS. <http://dx.doi.org/10.2118/154053-MS>.
- Morvan, M., Lannisbois Drean, H., and Bende-Jacq, D. 2010. Enhanced Crude Oil Recovery. US Application Patent No. 2010/0069272.
- Morvan, M., Moreau, P., Degre, G. et al. 2009. New Viscoelastic Fluid for Chemical EOR. Presented at the SPE International Symposium on Oilfield Chemistry, The Woodlands, Texas, 20–22 April. SPE-121675-MS. <http://dx.doi.org/10.2118/121675-MS>.
- Motekaitis, R.J., Martell, A.E., Hayes, D., and Frenier, W.W. 1980. The Iron(III)-Catalyzed Oxidation of EDTA in Aqueous Solution. *Can. J. Chem.* **58** (19): 1999–2005. <http://dx.doi.org/10.1139/v80-318>.
- Mou, J., Zhu, D., and Hill, A.D. 2010. Acid-Etched Channels in Heterogeneous Carbonates—a Newly Discovered Mechanism for Creating Acid-Fracture Conductivity. *SPE J.* **15** (2): pp. 404–416. SPE-119619-PA. <http://dx.doi.org/10.2118/119619-PA>.
- MSNBC. 2010a. New Microbe Discovered Eating Gulf Oil Spill, <http://www.msnbc.msn.com/id/38834330/>.
- MSNBC. 2010b. BP Testing 'Static Kill' after Valves Fixed, http://www.msnbc.msn.com/id/38518874/ns/disaster_in_the_gulf/.
- Muhr, A.H. and Blanshard, J.M.V. 1982. Diffusion in gels. *Polymer* **23** (7): 1012–1026. [http://dx.doi.org/http://dx.doi.org/10.1016/0032-3861\(82\)90402-5](http://dx.doi.org/http://dx.doi.org/10.1016/0032-3861(82)90402-5).
- Mukherjee, H. and Cudney, G. 1993. Extension of Acid Fracture Penetration by Drastic Fluid-Loss Control. *J Pet Technol* **45** (2): 102–105. SPE-25395-PA. <http://dx.doi.org/10.2118/25395-PA>.
- Mulder, M. 1996. *Basic Principles of Membrane Technology*, second edition. Dordrecht, The Netherlands: Kluwer Academic Publishers.
- Mulkins-Phillips, G.J., and Stewart, J.E. 1974. Effect of Four Dispersants on Biodegradation and Growth of Bacteria on Crude Oil. *Applied Microbiology* **28** (4): 547–552.
- Mullins, O.C. and Sheu, E.Y. 2005. Molecular Structure and Aggregation of Asphaltenes and Petroleomics. Presented at the SPE Annual Technical Conference and Exhibition, Dallas, 9–12 October. SPE-95801-MS. <http://dx.doi.org/10.2118/95801-MS>.
- Mullins, O.C., Sheu, E.Y., Hammami, A., and Marshall, A. 2007. *Asphaltenes, Heavy Oils, and Petroleomics*. London: Springer.
- Multiscalelab. 2011. Multiscale Barcelona. Spain: Multiscalelab.
- Munday, K. 2003. Reducing Water Flow. US Patent No. 6,516,885.

- Mungan, N. 1981. Carbon Dioxide Flooding—fundamentals. *J Can Pet Technol* **20**(1). PETSOC-81-01-03. <http://dx.doi.org/10.2118/81-01-03>.
- NACE ANSI/NACE SP0502, *Pipeline External Corrosion Direct Assessment Methodology*. 2010. Houston: NACE International.
- NACE RP0497, *Field Corrosion Evaluation Using Metallic Test Specimens*. 2004. Houston: NACE International.
- NACE *Standards and Reports*. 2012. Houston, TX: NACE International.
- NACE TM0169-2000, *Laboratory Corrosion Testing of Metals*. 2000. Houston: NACE International.
- Nagel, N.B., Gil, I., Sanchez-nagel, M. et al. 2011. Simulating Hydraulic Fracturing in Real Fractured Rocks - Overcoming the Limits of Pseudo3D Models. Presented at the SPE Hydraulic Fracturing Technology Conference, The Woodlands, Texas, USA, 24–26 January. SPE-140480-MS. <http://dx.doi.org/10.2118/140480-MS>.
- Naraghi, A.R., and Obeyesekere, N.U. 2002. Corrosion Inhibitors with Low Environmental Toxicity. US Patent No. 6,475,431.
- Nasr-El-Din, H.A. and Samuel, M. 2007. Lessons Learned From Using Viscoelastic Surfactants in Well Stimulation. *SPE Prod & Oper* **22** (1): 112–120. SPE-90383-PA. <http://dx.doi.org/10.2118/90383-PA>.
- Nasr-El-Din, H.A., A.A. Zahrani, A.A., Garzon, F.O. et al. 2009a. Acid Fracturing of Gas Wells by Use of an Acid Precursor in the Form of Solid Beads: Lessons Learned From First Field Application. *SPE Prod & Oper* **24** (2): 320–335. SPE-110895-PA. <http://dx.doi.org/10.2118/110895-PA>.
- Nasr-El-Din, H.A., Al-Anazi, H.A., and Mohamed, S.K. 1999. Stimulation of Water Disposal Wells Using Acid-In-Diesel Emulsion: Case Histories. Presented at the SPE International Symposium on Oilfield Chemistry, Houston, 16–19 February. SPE-50739-MS. <http://dx.doi.org/10.2118/50739-MS>.
- Nasr-El-Din, H.A., Al-Anazi, H.A., and Mohamed, S.K. 2000a. Stimulation of Water-Disposal Wells Using Acid-in-Diesel Emulsions: Case Histories. *SPE Prod & Oper* **15** (3): 176–182. SPE-65069-PA. <http://dx.doi.org/10.2118/65069-PA>.
- Nasr-El-Din, H.A., Al-Dirweesh, S., and Samuel, M. 2008. Development and Field Application of a New, Highly Stable Emulsified Acid. Presented at the SPE Annual Technical Conference and Exhibition, Denver, 21–24 September. SPE-115926-MS. <http://dx.doi.org/10.2118/115926-MS>.
- Nasr-El-Din, H.A., Al-Humaidan, A.Y., Fadhel, B.A. et al. 2000b. Investigation of Sulfide Scavengers in Well Acidizing Fluids. Presented at the SPE International Symposium on Formation Damage Control, Lafayette, Louisiana, 23–24 February. SPE-58712-MS. <http://dx.doi.org/10.2118/58712-MS>.
- Nasr-El-Din, H.A., Al-Nakhli, A.R., Al-Driweesh, S.M. et al. 2009b. Application of Cationic Surfactant-Based Fluids for Acid Diversion. *SPE Prod & Oper* **24** (1): 124–134. SPE-107687-PA. <http://dx.doi.org/10.2118/107687-PA>.
- Nasr-El-Din, H.A., Fadhel, B.A., Al-Humaidan, A.Y. et al. 2000c. An Experimental Study of Removing Iron Sulfide Scale from Well Tubulars. Presented at the International Symposium on Oilfield Scale, Aberdeen, 26–27 January. SPE-60205-MS. <http://dx.doi.org/10.2118/60205-MS>.
- Nasr-El-Din, H.A., Hill, A.D., Chang, F.F. et al. 2007a. Chemical Diversion Techniques Used for Carbonate Matrix Acidizing: An Overview and Case Histories. Presented at the International Symposium on Oilfield Chemistry, Houston, 28 February–2 March. SPE-106444-MS. <http://dx.doi.org/10.2118/106444-MS>.
- Nasr-El-Din, H.A., Kelkar, S.K., and Samuel, M. 2007b. Development and Field Application of a New Hydrogen Sulfide Scavenger for Acidizing Sour-Water Injectors. Presented at the International Symposium on Oilfield Chemistry, Houston, 28 February–2 March. SPE-106442-MS. <http://dx.doi.org/10.2118/106442-MS>.
- Nasr-El-Din, H.A., Li, L., Crews, J.B. et al. 2011. Impact of Organic Acids/Chelating Agents on the Rheological Properties of an Amidoamine-Oxide Surfactant. *SPE Prod & Oper* **26** (1): 30–40. SPE-128091-PA. <http://dx.doi.org/10.2118/128091-PA>.

- Navarrete, R.C., Holms, B.A., McConnell, S.B. et al. 1998a. Emulsified Acid Enhances Well Production in High-Temperature Carbonate Formations. Presented at the European Petroleum Conference, The Hague, 20–22 October. SPE-50612-MS. <http://dx.doi.org/10.2118/50612-MS>.
- Navarrete, R.C., Holms, B.A., McConnell, S.B. et al. 2000. Laboratory, Theoretical, and Field Studies of Emulsified Acid Treatments in High-Temperature Carbonate Formations. *SPE Prod & Oper* **15** (2): 96–106. SPE-63012-PA. <http://dx.doi.org/10.2118/63012-PA>.
- Navarrete, R.C., Miller, M.J., and Gordon, J.E. 1998b. Laboratory and Theoretical Studies for Acid Fracture Stimulation Optimization. Presented at the SPE Permian Basin Oil and Gas Recovery Conference, Midland, Texas, 23–26 March. SPE-39776-MS. <http://dx.doi.org/10.2118/39776-MS>.
- Nedwed, T., Coolbaugh, T., and Demarco, G. 2012. The Value of Dispersants for Offshore Oil Spill Response. Presented at the Offshore Technology Conference, Houston, 30 April–3 May. OTC-23359-MS. <http://dx.doi.org/10.4043/23359-MS>.
- Needham, R.B., Threlkeld, C.B., and Gall, J.W. 1974. Control of Water Mobility using Polymers and Multivalent Cations. Presented at the SPE Improved Oil Recovery Symposium, Tulsa, 22–24 April. SPE-4747-MS. <http://dx.doi.org/10.2118/4747-MS>.
- Nelson, E., Cawiezel, K., and Constien, V.G. 1995. Delayed Borate Crosslinked Fracuring Fluid Having Increased Temperature Range. US Patent No. 5,445,223.
- Nelson, E.B., and Guillot, D., ed. 2005. *Well Cementing*, second edition. Sugar Land, Texas: Schlumberger Technology Corporation.
- Nelson, P.H. 2009. Pore-Throat Sizes in Sandstones, Tight Sandstones, and Shales. *AAPG Bulletin* **93** (3): 329–340. <http://dx.doi.org/10.1306/10240808059>.
- NETL. 2001. Exploration and Production Technologies. Bartlesville, Oklahoma: National Energy Technology Laboratory, Department of Energy, <http://www.netl.doe.gov/technologies/oil-gas/ep-technologies/ExplorationTechnologies/EORdraw.html>.
- NETL. 2008. DOE's Enhanced Oil Recovery Program. Washington, DC: Department of Energy, <http://www.fossil.energy.gov/programs/oilgas/EOR/index.html>.
- NETL. 2010. Carbon Dioxide Enhanced Oil Recovery, Brochure. Morgantown, West Virginia: National Energy Technology Laboratory, U.S. DOE.
- NETL. 2011. Carbon Dioxide Enhanced Oil Recovery and CCS. US Department of Energy, Washington, D.C., http://www.uscsc.org/Files/Admin/Educational_Papers/Enhanced%20Oil%20Recovery%20and%20CCS-Jan%202011.pdf.
- Neumann, L.F., Sousa, J.L.A.O., Brandao, E.M. et al. 2012. Acid Fracturing: New Insights on Acid Etching Patterns from Experimental Investigation. Presented at the SPE Hydraulic Fracturing Technology Conference, The Woodlands, Texas, USA, 6–8 February. SPE-152179-MS. <http://dx.doi.org/10.2118/152179-MS>.
- Newman, S.H., Ziccardi, M.H., Berknerj, A.B., Holcomb, A.Y., Clumpner, C. and Mazet, J.A.K. 2003. A Historical Account of Oiled Wildlife Care in California. *Marine Ornithology* **31** (1): 59–64.
- NGS. 2010. Gulf Oil Spill a “Dead Zone in the Making”? National Geographic Society, Washington D.C., http://www.tiehh.ttu.edu/documents/Nat'l_Geo_Oil_Spill-552010.pdf.
- Nickel, E.H. 1995. Definition of a Mineral. *Mineralogical Magazine* **59** (397): 767–768.
- Nierode, D.E. and Kruk, K.F. 1973. An Evaluation of Acid Fluid Loss Additives, Retarded Acids, and Acidized Fracture Conductivity. Presented at the Fall Meeting of the Society of Petroleum Engineers of AIME, Las Vegas, Nevada, USA, 30 September–3 October. SPE-4549-MS. <http://dx.doi.org/10.2118/4549-MS>.
- Nierode, D.E. and Williams, B.B. 1971. Characteristics of Acid Reaction in Limestone Formations. *SPE J.* **11** (4): 406–418. SPE-3101-PA. <http://dx.doi.org/10.2118/3101-PA>.
- Nieto, C.M., Pournik, M., and Hill, A.D. 2008. The Texture of Acidized Fracture Surfaces: Implications for Acid Fracture Conductivity. *SPE Prod & Oper* **23** (3): 343–352. SPE-102167-PA. <http://dx.doi.org/10.2118/102167-PA>.
- Nieuwerf, J. 2009. *Asp Flooding*. Jan Nieuwerf at SGS Horizon, <http://www.youtube.com/watch?v=aLe55iEBSpo>.

- Niiler, E. 2012. Geologists Say Ohio Quakes Directly Tied to Fracking Process Uses Deep Wells in Rock to Dispose of Liquid Wastes During Natural Gas Drilling, http://www.msnbc.msn.com/id/45903873/ns/technology_and_science-science/t/geologists-say-ohio-quakes-directly-tied-fracking/.
- Nimerick, K., and Hinkel, J.J. 1993. Method of Enhancing Methane Production from Coal Seams by Dewatering. US Patent No. 5,229,017.
- Nimerick, K.H., McConnell, S.B., and Samuelson, M.L. 1992. Compatibility of Resin-Coated Proppants With Crosslinked Fracturing Fluids. *SPE Prod Eng* 7 (1): 29–33. SPE-20639-PA. <http://dx.doi.org/10.2118/20639-PA>.
- NIMS. 2008. National Incident Management System. Washington, DC. <http://www.fema.gov/national-incident-management-system>.
- NIST. 2012. *Online Scientific Databases*. Washington, D.C.: National Institute of Standards and Testing, <http://www.nist.gov/srd/online.cfm>.
- NNI. 2011. *National Nanotechnology Initiative*. Washington, D.C.: US Government, <http://www.nano.gov/about-nni>.
- NOAA. 2005. *Emergency Response Dispersants Tour*. Washington D.C.: National Oceanic and Atmospheric Administration, www.response.restoration.noaa.gov/dispersantstour.
- Nordgren, R.P. 1972. Propagation of a Vertical Hydraulic Fracture. *SPE J.* 12 (4): 306–314. SPE-3009-PA. <http://dx.doi.org/10.2118/3009-PA>.
- Norman, W.D., Jasinski, R.J., and Nelson, E.B. 1995. Hydraulic Fracturing Process and Compositions. US Patent No. 5,551,516.
- Norris, M., Perez, D., Bourne, H.M. et al. 2001. Maintaining Fracture Performance Through Active Scale Control. Presented at the International Symposium on Oilfield Scale, Aberdeen, United Kingdom, 30–31 January 2001. SPE-68300-MS. <http://dx.doi.org/10.2118/68300-MS>.
- NRS. 2009. *National Response System*. Washington, D.C., US Environmental Protection Agency, <http://www.epa.gov/ceppo/web/content/nrs/>.
- NSI. 2011. Stimplan V 4.0, Computer Program. Tulsa: NSI, Inc.
- Nutting, P.G. 1925. Chemical Problems in the Water Driving of Petroleum from Oil Sands. *Ind. Eng. Chem.* 17 (10): 1035–1036. <http://dx.doi.org/10.1021/ie50190a014>.
- Nyborg, R. and Gulbrandsen, E., 2007. Specialised Corrosion Inhibitor Test Protocols Developed in Iife Joint Industry Project. Report, Institute for Energy Technology, Kjeller, Norway.
- Oakes, B.D. 1972. Report of the Power Station Chemistry Subcommittee. Washington, DC: The Edison Electric Institute.
- Obeyesekere, N.U., Naraghi, A.R., Chen, L., Zhou, S. and Abayarathn, D. 2004. Environmentally Friendly Corrosion Inhibitors for Sweet and Sour Gas Corrosion. Paper NACE 04733 presented at NACE International CORROSION 2004, New Orleans, 28 March–1 April.
- O'Donoghue, M. 1990. *Rocks and Minerals, American Nature Guides*. New York.: Gallery Books.
- OERB. 2000. Bureau of Land Management Lease Operations Environmental Guidance Document. Oklahoma City, Oklahoma: Oklahoma Energy Resources Board.
- Ogbe, D.O., and Zhu, T. 2002. Solvent-Based Enhanced Oil Recovery Processes to Develop West Sak Alaska North Slope Heavy Oil Resources. Report, National Energy Technology Lab, US Department of Energy, Bartlesville, Oklahoma.
- Oliveira, T.J.L.D., Melo, A.R.D., Oliveira, J.A.A. et al. 2012. Numerical Simulation of the Acidizing Process and PVBT Extraction Methodology Including Porosity/Permeability and Mineralogy Heterogeneity. Presented at the SPE International Symposium and Exhibition on Formation Damage Control, Lafayette, Louisiana, USA, 15–17 February. SPE-151823-MS. <http://dx.doi.org/10.2118/151823-MS>.
- Osterloh, W.T. and Jante Jr., M.J. 1992. Effects of Gas and Liquid Velocity on Steady-State Foam Flow at High Temperature. Presented at the SPE/DOE Enhanced Oil Recovery Symposium, Tulsa, 22–24 April. SPE-24179-MS. <http://dx.doi.org/10.2118/24179-MS>.
- Otott-Jr, G.E. 2007. History of Advanced Recovery Technologies in the Wilmington Field. In *AAPG Pacific Section, 2007 - Old Oil Fields and New Life: A Visit to the Giants of the Los Angeles Basin, 1996*. Presented at the AAPG Annual Meeting, Long Beach, California, 2 April.

- Oussoltsev, D., Butula, K.K., Klyubin, A. et al. 2008. Fiber-Based Fracture Fluid Technology a First for Oil Reservoirs in Western Siberia. Presented at the SPE International Symposium and Exhibition on Formation Damage Control, Lafayette, Louisiana, USA, 13–15 February. SPE-112438-MS. <http://dx.doi.org/10.2118/112438-MS>.
- Outotec. 2008. *Processing for Proppants*. Physical Separation Technology External Newsletter, July, 1 1-11, Jacksonville, Florida: Outotec, <http://www.outotec.com/37368.epibrw>.
- Oyemade, S.N., Al Harthy, S.A., Jaspers, H.F., Van Wunnik, J., de Kruijf, A., Stoll, M. 2010. Alkaline - Surfactant - Polymer Flood (ASP): Single Well Chemical Tracer Tests - Design, Implementation and Performance. Presented at the SPE EOR Conference at Oil & Gas West Asia, Muscat, Oman, 11–13 April. SPE-130042-MS. <http://dx.doi.org/10.2118/130042-MS>.
- Özbayoglu, E.M., Miska, S.Z., Reed, T. et al. 2003. Cuttings Transport with Foam in Horizontal & Highly-Inclined Wellbores. Presented at the SPE/IADC Drilling Conference, Amsterdam, 19–21 February. SPE-79856-MS. <http://dx.doi.org/10.2118/79856-MS>.
- Paccaloni, G. 1995. A New, Effective Matrix Stimulation Diversion Technique. *SPE Prod & Fac* **10** (3): 151–156. SPE-24781-PA. <http://dx.doi.org/10.2118/24781-PA>.
- Paccaloni, G. and Tambini, M. 1993. Advances in Matrix Stimulation Technology. *J Pet Technol* **45** (3): 256–263. SPE-20623-PA. <http://dx.doi.org/10.2118/20623-PA>.
- PackersPlus. 2011a. Rapidmatrix Multi-Stage Stimulation System. Brochure, Houston: Packers Plus Energy Services Inc.
- PackersPlus. 2011b. Stackfrac Hd High Density Multi-Stage Fracturing System. Brochure, Houston: Packers Plus Energy Services Inc.
- Page, C.A., Bonner, J.S., Sumner, P.L. et al. 2000. Solubility of petroleum hydrocarbons in oil/water systems. *Mar. Chem.* **70** (1–3): 79–87. [http://dx.doi.org/http://dx.doi.org/10.1016/S0304-4203\(00\)00016-5](http://dx.doi.org/http://dx.doi.org/10.1016/S0304-4203(00)00016-5).
- Palisch, T.T., Duenckel, R., Chapman, M.A. et al. 2010a. How To Use and Misuse Proppant Crush Tests: Exposing the Top 10 Myths. *SPE Prod & Oper* **25** (3): 345-354. SPE-119242-PA. <http://dx.doi.org/10.2118/119242-PA>.
- Palisch, T.T., Vincent, M., and Handren, P.J. 2010b. Slickwater Fracturing: Food for Thought. *SPE Prod & Oper* **25** (3): pp. 327-344. SPE-115766-PA. <http://dx.doi.org/10.2118/115766-PA>.
- Palmer, J.W., Hedges, W., and Dawson, J.L., ed. 2004. *Use of Corrosion Inhibitors in Oil and Gas Production: (EFC 39)*. Leeds, UK: Maney Publishing.
- Panda, M.N. and Lake, L.W. 1995. A Physical Model of Cementation and Its Effects on Single-Phase Permeability. *AAPG Bulletin* **79** (3): 431–443.
- Pandey, V. 2004. Wellbore Treatment Fluid Selection Guide. US Patent No. 6,826,482.
- Pandey, V.J. 2001. Friction Pressure Correlation for Guar-Based Hydraulic Fracturing Fluids. Presented at the SPE Rocky Mountain Petroleum Technology Conference, Keystone, Colorado, 21–23 May. SPE-71074-MS. <http://dx.doi.org/10.2118/71074-MS>.
- Panga, M.K.R., Balakotaiah, V., and Ziauddin, M. 2002. Modeling, Simulation and Comparison of Models for Wormhole Formation during Matrix Stimulation of Carbonates. Presented at the SPE Annual Technical Conference and Exhibition, San Antonio, Texas, 29 September–2 October. SPE-77369-MS. <http://dx.doi.org/10.2118/77369-MS>.
- Panga, M.K.R., Ziauddin, M., and Balakotaiah, V. 2005. Two-scale continuum model for simulation of wormholes in carbonate acidization. *AIChE J.* **51** (12): 3231–3248. <http://dx.doi.org/10.1002/aic.10574>.
- Park, N.G., Morello, L., and Abriam, G. 2009. Understanding Inhibition of Sour Systems with Water Soluble Corrosion Inhibitors. Paper NACE 09362 presented at NACE International CORROSION 2009, Atlanta, Georgia, 22–26 March.
- Parkinson, M., Munk, T.K., Brookley, J.G. et al. 2010. Stimulation of Multilayered High-Carbonate-Content Sandstone Formations in West Africa Using Chelant-Based Fluids and Mechanical Diversion. Presented at the SPE International Symposium and Exhibition on Formation Damage Control, Lafayette, Louisiana, USA, 10–12 February. SPE-128043-MS. <http://dx.doi.org/10.2118/128043-MS>.

- Parlar, M., Parris, M.D., Jasinski, R.J. et al. 1995. An Experimental Study of Foam Flow Through Berea Sandstone With Applications to Foam Diversion in Matrix Acidizing. Presented at the SPE Western Regional Meeting, Bakersfield, California, USA, 8–10 March. SPE-29678-MS. <http://dx.doi.org/10.2118/29678-MS>.
- Patterson, D.E., Kendrick, M., Williams, W.H. et al. 2012. Squimulation: Simultaneous Well Stimulation and Scale Squeeze Treatments in Deep Water, West Africa. Presented at the SPE International Symposium and Exhibition on Formation Damage Control, Lafayette, Louisiana, USA, 15–17 February. SPE-151863-MS. <http://dx.doi.org/10.2118/151863-MS>.
- Paul, B.K. and Moulik, S.P. 2001. Uses and Applications of Microemulsions. *Current Science* **80** (8): 990–1001.
- Pauls, R.W., Ford, W.G.F., and Hollenbeak, K.H. 1994. Low Viscosity Acid-in-Oil Emulsions and Methods. US Patent No. 5,355,958.
- Pauls, R.W., Ford, W.G.F., and Hollenbeak, K.H. 1995. Low Viscosity Acid-in-Oil Emulsions and Methods. US Patent No. 5,427,699.
- PDHengineer. 2004. *Waterflood History and Design Fundamentals, Course O-2004*. Houston: PDHengineer, www.PDHengineer.com.
- Pena, A., Salamat, G., and Lin, L. 2009. Energized Fluids and Methods of Use Thereof. US Patent No. 7,494,957.
- Penny, G.S. 1987. An Evaluation of the Effects of Environmental Conditions and Fracturing Fluids Upon the Long-Term Conductivity of Proppants. Presented at the SPE Annual Technical Conference and Exhibition, Dallas, 27–30 September. SPE-16900-MS. <http://dx.doi.org/10.2118/16900-MS>.
- Perkins, T.K. and Kern, L.R. 1961. Widths of Hydraulic Fractures. *J Pet Technol* **13** (9): 937–949. SPE-89-PA. <http://dx.doi.org/10.2118/89-PA>.
- Perry, S.C. and Williams, M.E. 2009. Composition for Denaturing and Breaking Down Friction-Reducing Polymer and for Destroying Other Oil Well Contaminants. US Patent No. 7,615,518.
- Petrov, A.D. and Ivanov, I.Z. 1932. Formation of Naphthenic Acids I. *J. Am. Chem. Soc.* **54** (1): 239–242. <http://dx.doi.org/10.1021/ja01340a035>.
- Peytavy, J.-L., Glenat, P., and Bourg, P. 2007. Kinetic Hydrate Inhibitors—Sensitivity Towards Pressure and Corrosion Inhibitors. Presented at the International Petroleum Technology Conference, Dubai, UAE, 4–6 December. IPTC-11233-MS. <http://dx.doi.org/10.2523/11233-MS>.
- Pezron, E., Leibler, L., Ricard, A. et al. 1989. Complex formation in polymer-ion solution. 1. Polymer concentration effects. *Macromolecules* **22** (3): 1169–1174. <http://dx.doi.org/10.1021/ma00193a030>.
- Pezron, E., Ricard, A., Lafuma, F. et al. 1988. Reversible gel formation induced by ion complexation. 1. Borax-galactomannan interactions. *Macromolecules* **21** (4): 1121–1125. <http://dx.doi.org/10.1021/ma00182a045>.
- PHYWE. 2004. Surface Tension by the Ring Method (Du Nouy Method). Report, PHYWE System GMBH Göttingen, Germany.
- Poiseuille, J.L. 1840. Recherches Expérimentelles Sur Le Mouvement Des Liquids Dans Les Tubes De Très Petits Diamètres. *Compte Rendus* **11**: 961.
- Pope, G.A. 2007a. Chemical Flooding Overview, Technical Advisory Board Meeting, Enhanced Oil Recovery Institute, University of Wyoming, Laramie, Wyoming, 18 July.
- Pope, G.A. 2007b. Overview of Chemical EOR. Enhanced Oil Recovery Quarterly meeting, Casper EOR workshop, Casper, Wyoming, 26 October.
- Pope, G.A. 2009. Program *UTCHEM*, Austin, Texas, University of Texas.
- Pope, G.A., Weerasooriya, U.P., Nguyen, P.D., and Britton, L.N. 2011. Di-Functional Surfactants for Enhanced Oil Recovery. US Application Patent No. 20110048721.
- Portier, S., André, L., and Vuataz, F.-D. 2007. Review on Chemical Stimulation Techniques in Oil Industry and Applications to Geothermal Systems. Report, Deep Heat Mining Association, Neuchâtel, Switzerland.
- POSC. 2006. Life Cycle. Petrochemical Open Standards Consortium, Houston.

- Potter, J.M. and Dibble, W.E. Jr. 1985. Chemical Aspects of Iron Colloid Plugging in Quartz Sands and Implications for Formation Damage. *J Pet Technol* **37** (9): 1682–1688. SPE-11801-PA. <http://dx.doi.org/10.2118/11801-PA>.
- Pournik, M., Gomaa, A.M., and Nasr-El-Din, H.A. 2010. Influence of Acid-Fracture Fluid Properties on Acid-Etched Surfaces and Resulting Fracture Conductivity. Presented at the SPE International Symposium and Exhibiton on Formation Damage Control, Lafayette, Louisiana, USA, 10–12 February. SPE-128070-MS. <http://dx.doi.org/10.2118/128070-MS>.
- Pournik, M., Nasr-El-Din, H.A., and Mahmoud, M.A. 2011. A Novel Application of Closed-Fracture Acidizing. *SPE Prod & Oper* **26** (1): pp. 18-29. SPE-124874-PA. <http://dx.doi.org/10.2118/124874-PA>.
- Prasad, S.K. 2008. *Modern Concepts in Nanotechnology*. New Delhi, India: Discovery Publishing House.
- Prats, M. 1961. Effect of Vertical Fractures on Reservoir Behavior—Incompressible Fluid Case. *SPE J.* **1** (2). SPE-1575-G. <http://dx.doi.org/10.2118/1575-G>.
- Pu, H., Yin, D., Chen, Y. et al. 2008. Feasibility Study and Pilot Test of Polymer Flooding in Third Class Reservoir of Daqing Oilfield. Presented at the SPE North Africa Technical Conference & Exhibition, Marrakech, Morocco, 12–14 March. SPE-111720-MS. <http://dx.doi.org/10.2118/111720-MS>.
- Purinton, J., R.J. and Manning, T.S. 1996. The New Role of HSE in Chemical Product Development. Presented at the SPE Health, Safety and Environment in Oil and Gas Exploration and Production Conference, New Orleans, 9–12 June. SPE-35822-MS. <http://dx.doi.org/10.2118/35822-MS>.
- Pursell, D.A. 1987. *Laboratory Investigation of Inertial Flow in High Strength Fracture Proppants*. MS thesis, Texas A&M University, College Station, Texas.
- Pursley, J.T., Holcomb, D.L., and Penny, G.S. 2008. Composition and Process for Well Cleaning. Patent No. 7,380,606.
- Putzig, D.E. 2009. Zirconium-Based Cross-Linking Composition for Use with High pH Polymer Solutions. US Application Patent No. 2009/0227479.
- Putzig, D.E. and St.Clair, J.D. 2007. A New Delay Additive for Hydraulic Fracturing Fluids. Presented at the SPE Hydraulic Fracturing Technology Conference, College Station, Texas USA, 29–31 January. SPE-105066-MS. <http://dx.doi.org/10.2118/105066-MS>.
- Qiu, X.W., Chang, F.F., and Tustin, G. 2009. Acidizing Treatment Compositions and Methods. US Application Patent No. 2009/0209439.
- Qu, Q. and Wang, X. 2010. Method of Acid Fracturing a Sandstone Formation. US Patent No. 7,704,927.
- Quinn, M.A., Lake, L.W., and Schechter, R.S. 1997. Designing Effective Sandstone Acidizing Treatments Through Geochemical Modeling. Presented at the SPE European Formation Damage Conference, The Hague, Netherlands, 2–3 June. SPE-38173-MS. <http://dx.doi.org/10.2118/38173-MS>.
- Rabie, A., Mahmoud, M.A., and Nasr-El-Din, H.A. 2011. Reaction of GLDA with Calcite: Reaction Kinetics and Transport Study. Presented at the SPE International Symposium on Oilfield Chemistry, The Woodlands, Texas, USA, 11–13 April. SPE-139816-MS. <http://dx.doi.org/10.2118/139816-MS>.
- Rae, P. and di Lullo, G. 1996. Fracturing Fluids and Breaker Systems - A Review of the State-of-the-Art. Presented at the SPE Eastern Regional Meeting, Columbus, Ohio, 23–25 October. SPE-37359-MS. <http://dx.doi.org/10.2118/37359-MS>.
- Rae, P.J. and Lullo, G. 2007. Single Step Matrix Acidising With HF—Eliminating Preflushes Simplifies the Process, Improves the Results. Presented at the European Formation Damage Conference, Scheveningen, The Netherlands, 30 May–1 June. SPE-107296-MS. <http://dx.doi.org/10.2118/107296-MS>.
- Rahim, Z., Bartko, K.A., and Al-Qahtani, M.A. 2002. Hydraulic Fracturing Case Histories in the Carbonate and Sandstone Reservoirs of Khuff and Pre-Khuff Formations, Ghawar Field, Saudi

- Arabia. Presented at the SPE Annual Technical Conference and Exhibition, San Antonio, Texas, USA, 29 September–2 October. SPE-77677-MS. <http://dx.doi.org/10.2118/77677-MS>.
- Ramachandran, S., and Jovancievcic, V. 1998. Molecular Modeling of the Inhibition of Mild Steel CO₂ Corrosion by Imidazolines. Paper NACE 98017 presented at NACE International CORROSION 98, San Diego, California, 22–27 March.
- Ramachandran, S., Campbell, S., and Ward, M.B. 2000. The Interactions and Properties of Corrosion Inhibitors with Byproduct Layers. Paper NACE 00025 presented at NACE International CORROSION 2000, Orlando, Florida, 26–31 March.
- Ramachandran, S., Ward, M.B., and Bartrip, K.A. 2002. Molecular Modeling of Corrosion of Iron in H₂S Environments. Paper NACE 02240 presented at NACE International CORROSION 2002, Denver, 7–11 April.
- Raman, A. and Labine, P., ed. 1993. *Reviews of Corrosion Inhibitor Science and Technology*. Houston: NACE International.
- Ramsey, J.E. and Cenegy, L.M. 1985. A Laboratory Evaluation of Barium Sulfate Scale Inhibitors at Low pH for Use in Carbon Dioxide EOR Floods. Presented at the SPE Annual Technical Conference and Exhibition, Las Vegas, Nevada, 22–26 September. SPE-14407-MS. <http://dx.doi.org/10.2118/14407-MS>.
- Rassenfoss, S. 2011a. From Flowback to Fracturing: Water Recycling Grows in the Marcellus Shale. *J. Pet Tech* **63** (7): 48–51.
- Rehm, D. 2011. *Growing Concerns over Fracking*. Radio Broadcast WAMU. Wasington, DC <http://thedianerehmshow.org/shows/2011-08-29/growing-concerns-over-fracking>.
- Reichenbach-Klinke, R., Langlotz, B., Wenzke, B. et al. 2011. Hydrophobic Associative Copolymer with Favorable Properties for the Application in Polymer Flooding. Presented at the SPE International Symposium on Oilfield Chemistry, The Woodlands, Texas, USA, 11–13 April. SPE 141107. <http://dx.doi.org/10.2118/141107-MS>.
- Reichenbach-Klinke, R., Pfeuffer, T., Schmidt, K., Ostrowski, T., Leyrer, R.J., Fogel, Y., Friedrich, S., Gaerberlein, P., Orleans, A., et al. 2010. Hydrophobically Associating Copolymers. US Application Patent No. 2010/0331510.
- Reidenbach, V.G., Harris, P.C., Lee, Y.N. et al. 1986. Rheological study of foam fracturing fluids using nitrogen and carbon dioxide. *SPE Prod Eng* **1** (1): 31–41. SPE-12026-PA. <http://dx.doi.org/10.2118/12026-PA>.
- Reyes, R.P., Yeager, V.J., Glasbergen, G. et al. 2011. DTS Sensing: An Introduction To Permian Basin With A West-Texas Operator. Presented at the SPE Annual Technical Conference and Exhibition, Denver, 30 October–2 November. SPE-145055-MS. <http://dx.doi.org/10.2118/145055-MS>.
- RezaeiDoust, A., Puntervold, T., Strand, S. et al. 2009. Smart Water as Wettability Modifier in Carbonate and Sandstone: A Discussion of Similarities/Differences in the Chemical Mechanisms. *Energy Fuels* **23** (9): 4479–4485. <http://dx.doi.org/10.1021/ef900185q>.
- Rhine, T., Loayza, M.P., Kirkham, B. et al. 2011. Channel Fracturing in Horizontal Wellbores: the New Edge of Stimulation Techniques in the Eagle Ford Formation. Presented at the SPE Annual Technical Conference and Exhibition, Denver, 30 October–2 November. SPE-145403-MS. <http://dx.doi.org/10.2118/145403-MS>.
- Riazi, M.R. 2005. *Characterization and Properties of Petroleum Fractions*. West Conshohocken, PA: ASTM International.
- Ribeiro, L.H. and Sharma, M.M. 2012. Multiphase Fluid-Loss Properties and Return Permeability of Energized Fracturing Fluids. *SPE Prod & Oper* **27** (3): 265–277. SPE-139622-PA. <http://dx.doi.org/10.2118/139622-PA>.
- Rickards, A.R., Brannon, H.D., Rae, P.J., DiLullo, G.A., and Stephenson, C.J. 2000. Formation Treatment Method Using Deformable Particles. US Patent No. 6,059,034.
- Rickards, A.R., Brannon, H.D., Wood, W.D. et al. 2003. High Strength, Ultra-Lightweight Proppant Lends New Dimensions to Hydraulic Fracturing Applications. Presented at the SPE Annual

- Technical Conference and Exhibition, Denver, 5–8 October. SPE-84308-MS. <http://dx.doi.org/10.2118/84308-MS>.
- Riggs, O.L.J. 1973. Theoretical Aspects of Corrosion Inhibitors and Inhibition. In *Corrosion Inhibitors*, ed. C.C. Nathan, 7-27. Houston: NACE International.
- Rimassa, S.M., Samuel, M., and Mason, S. 2009. Temperature-Extended Enzyme Systems. US Application Patent No. 2009/0137429.
- Ritter, S. 2011. Shedding Nanoparticles. *Chemical and Engineering News* **89** (43): 5.
- Robert, J.A. and Crowe, C.W. 2001. Carbonate Acidizing Design. In *Reservoir Stimulation*, ed. M.J. Economides and K. G. Nolte. New York: John Wiley & Sons.
- Robert, J.A. and Rossen, W.R. 2001. Fluid Placement and Pumping Strategy. In *Formation Stimulation*, third edition, ed. M.J. Economides and K. G. Nolte. New York: John Wiley and Sons.
- Robinson, G., Ross-Murphy, S.B., and Morris, E.R. 1982. Viscosity-molecular weight relationships, intrinsic chain flexibility, and dynamic solution properties of guar galactomannan. *Carbohydr. Res.* **107** (1): 17–32. [http://dx.doi.org/10.1016/S0008-6215\(00\)80772-7](http://dx.doi.org/10.1016/S0008-6215(00)80772-7).
- Robinson, J.S. 1979. *Corrosion Inhibitors: Recent Developments*. Park Ridge, New Jersey: Noyes Data Corp.
- Rodoplu, S., Zhu, D., Hill, A.D. et al. 2003. Development and Validation of a Sandstone Acidizing Model With a New Permeability Response Model. Presented at the SPE Annual Technical Conference and Exhibition, Denver, 5–8 October. SPE-84132-MS. <http://dx.doi.org/10.2118/84132-MS>.
- Rodriguez, J., Stopi, S., Krause, G., and Friedrich, B. 2007. Feasibility Assessment of Electrocoagulation Towards a New Sustainable Wastewater Treatment. *Environmental Science and Pollution Research* **14** (7): 477–482. <http://dx.doi.org/10.1065/espr2007.05.424>.
- Rong, J.G. 2002. *Experimental Evaluation of Foam in Environmental Remediation*. PhD dissertation, The University of Texas at Austin, Austin, TX.
- Ross, G.J. 1969. Acid Dissolution of Chlorites: Release of Magnesium, Iron and Aluminum and Mode of Acid Attack. *Clays and Clay Minerals* **17** (6): 347–354. <http://dx.doi.org/10.1346/CCMN.1969.0170604>.
- Rossen, W.R. 2005. Mechanistic Studies of Improved Foam EOR Processes. Report, FC26-01BC15318, Final Report – 1, US Department of Energy, Washington, DC.
- Rossen, W.R. and Gauglitz, P.A. 1990. Percolation Theory of Creation and Mobilization of Foam in Porous Media. *AIChE J.* **36** (8): 1176–1188. <http://dx.doi.org/10.1002/aic.690360807>.
- Rousseau, D., Renard, S., Prempain, B. et al. 2012. CO₂ Mobility Control With Dissolved Polymers: A Core-Scale Investigation Of Polymer-Rock and Polymer-Oil Interactions. Presented at the SPE Improved Oil Recovery Symposium, Tulsa, 14–18 April. SPE-154055-MS. <http://dx.doi.org/10.2118/154055-MS>.
- Rousseau, G., Zhou, H., and Hurtevent, C. 2001. Calcium Carbonate and Naphthenate Mixed Scale in Deep-Offshore Fields. Presented at the International Symposium on Oilfield Scale, Aberdeen, 30–31 January. SPE-68307-MS. <http://dx.doi.org/10.2118/68307-MS>.
- Royce, B., Kaplan, E., Garrell, M., and Geffen, T.M. 1984. Enhanced Oil Recovery Water Requirements. *Environmental Geochemistry and Health* **6** (2): 44–53.
- Rozenfeld, I.L. 1981. *Corrosion Inhibitors*. New York: McGraw-Hill.
- Rozo, R.E., Paez, J., Rojas, A.M. et al. 2007. Combining Acid- and Hydraulic-Fracturing Technologies Is the Key to Successfully Stimulating the Orito Formation. Presented at the SPE Hydraulic Fracturing Technology Conference, College Station, Texas USA, 29–31 January. SPE-104610-MS. <http://dx.doi.org/10.2118/104610-MS>.
- RRC. 2011. Eagle Ford Information. Brochure, Railroad Commission of Texas, Austin.
- Ruseska, I., Robbins, J., Costerton, J.W., and Lashen, E.S. 1982. Biocide Testing against Corrosion-Causing Oil-Field Bacteria Helps Control Plugging. *Oil and Gas J.* **80** (3) 253-260.
- Saad, N. 1989. Field Studies with 3D Chemical Flooding Simulator. PhD dissertation, University of Texas, Austin, Texas.
- Saito, M., Yamamoto, T., and Soya, S. 2000. Cleaning Agent Composition. US Patent No. 6,013,612.

- Salager, J.L. 2005. *FIRP Booklet # E705-A, Principles of the Spinning Drop Tensiometer*. Mérida, Venezuela: Laboratorio FIRP, Escuela De Ingenieria Quimica, Universidad De Los Andes.
- Salager, J.L. 1977. *Physico-Chemical Properties of Surfactant-Water-Oil Mixtures: Phase Behavior, Microemulsion Formation and Interfacial Tension*. PhD dissertation, University of Texas, Austin, Texas.
- Salathiel, W.M., W.Muecke, T., Cooke, C.E., and Li., N.N. 1980. Well Treatments with Emulsions Dispersions. US Patent No. 4,233,165.
- Salinas-Nolasco, M.F., Méndez-Vivar, J., Lara, V.c.H. et al. 2004. Passivation of the calcite surface with malonate ion. *J. Colloid Interface Sci.* **274** (1): 16–24. <http://dx.doi.org/http://dx.doi.org/10.1016/j.jcis.2003.10.027>.
- Samuel, M., Card, R., Nelson, E.B. et al. 1997. Polymer-Free Fluid for Hydraulic Fracturing. Presented at the SPE Annual Technical Conference and Exhibition, San Antonio, Texas, USA, 5–8 October. SPE 38622. <http://dx.doi.org/10.2118/38622-MS>.
- Samuel, M.M., Mohsen, A.H.A., Ejan, A.B. et al. 2009. Novel Enzyme Stabilizers for Applications at Extreme High Temperatures. Presented at the SPE Annual Technical Conference and Exhibition, New Orleans, 4–7 October. SPE-125024-MS. <http://dx.doi.org/10.2118/125024-MS>.
- Samuelson, M.L. 1991. Development of a Low Toxicity Solvent for Paraffin, Asphaltene and Pipe Dope Solvents. Report DL 10639, Schlumberger Technology Corporation, Sugar Land, Texas.
- Saneifar, M., Nasralla, R.A., Nasr-El-Din, H.A. et al. 2011. Surface Tension of Spent Acids at High Temperature and Pressure. Presented at the SPE/DGS Saudi Arabia Section Technical Symposium and Exhibition, Al-Khobar, Saudi Arabia, 15–18 May. SPE-149109-MS. <http://dx.doi.org/10.2118/149109-MS>.
- San-Miguel, L., Dickson, K.R., Stephens, W.T. et al. 2010. High Strength Proppants. US Application Patent No. 20100113251.
- Sasol. 2012. Alfoterra® Surfactants, Matching Surfactant to Reservoir with HLB Concept. Report, Sasol North America, Houston.
- Saukaitis, A.J. and Gardner, G.S. 1956. Derivatives of Rosin Amines. US Patent No. 2,758,970.
- Sayed, M.A.I. and Nasr-El-Din, H.A. 2012. Reaction Rate of Emulsified Acids and Dolomite. Presented at the SPE International Symposium and Exhibition on Formation Damage Control, Lafayette, Louisiana, USA, 15–17 February. SPE-151815-MS. <http://dx.doi.org/10.2118/151815-MS>.
- Sayed, M.A.I., Assem, A.I., and Nasr-El-Din, H.A. 2012. Effect of Presence of Crude Oil on the Performance of Emulsified Acids. Presented at the North Africa Technical Conference and Exhibition, Cairo, Egypt, 20–22 February. SPE-152844-MS. <http://dx.doi.org/10.2118/152844-MS>.
- Schechter, R.S. 1992. *Oil Well Stimulation*. New Jersey: Prentice Hall Inc.
- Schechter, R.S. and Gidley, J.L. 1969. The change in pore size distribution from surface reactions in porous media. *AIChE J.* **15** (3): 339–350. <http://dx.doi.org/10.1002/aic.690150309>.
- Scherubel, G.A. and Crowe, C.W. 1978. Foamed Acid, A New Concept in Fracture Acidizing. Presented at the SPE Annual Technical Conference and Exhibition, Houston, 1–3 October. SPE-7568-MS. <http://dx.doi.org/10.2118/7568-MS>.
- Schlumberger. 2004a. Equipment-Mixing and Blending, Brochure. Sugar Land, Texas: Schlumberger Technology Corporation.
- Schlumberger. 2004b. Sandstone Acidizing, Mechanisms and Fluids. Sugar Land, Texas: Schlumberger Technology Corporation.
- Schlumberger. 2008. Characterization of Fractured Reservoirs. Sugar Land, Texas: Schlumberger Technology Corporation.
- Schlumberger. 2009a. FRACADE V 6, Brochure. Sugar Land, Texas: Schlumberger Technology Corporation.
- Schlumberger. 2009b. 4D Reservoir Geomechanics, Brochure. Sugar Land Texas: Schlumberger Technology Corporation.
- Schlumberger. 2010a. Coilflute through-Tubing Inflatable Packer, Brochure. Sugar Land, Texas: Schlumberger Technology Company.

- Schlumberger. 2010b. 5 Spot, Brochure. Sugar Land, Texas: Schlumberger Technology Corporation.
- Schlumberger. 2010c. Schlumberger Openfrac, Brochure. Sugar Land, Texas: Schlumberger Technology Corporation.
- Schlumberger. 2010d. EFP Crude Oil Treatment, Brochure. Sugar Land, Texas: Schlumberger Technology Corporation.
- Schlumberger. 2012a. Multi-Isotope Log, <http://www.glossary.oilfield.slb.com/Display.cfm?Term=multiple-isotope%20log>.
- Schlumberger. 2012b. *Wireline Logs*. Sugarland, Texas: Schlumberger Technology Corporation. http://www.slb.com/services/characterization/wireline_open_hole/nmr.aspx.
- Schmitt, G. and Bedbur, K. 1985. Investigations on structural and electronic effects in acid inhibitors by AC impedance. *Mater. Corros.* **36** (6): 273–278. <http://dx.doi.org/10.1002/maco.19850360603>.
- Schmitt, G. and Labus, B.N. 1994. Effect of Surfactants on Inhibitor Performance in CO₂ Corrosion of Steel under Highly Turbulent Flow Conditions. Paper NACE 94037 presented at NACE International Corrosion/94, Baltimore, Maryland, 27 February–4 March.
- Schmitt, G. and Olbertz, B. 1980. Acid Inhibitors. II. Influence of Quarternary Ammonium Salts on the Hydrogen Absorption of Mild Steel in H₂S-Free and H₂S-Saturated Hydrochloric Acid. Presented at the 5th European Symposium Corrosion Inhibitors, Ferrara, Italy, 15–19 September.
- Schofield, M. and Stott, J. 2012. Assessing Magnitude and Consequences of Reservoir Souring. *J. Pet Tech* **64** (5): 76–79.
- Schols, R.S. and Visser, W. 1974. Proppant Bank Buildup in a Vertical Fracture Without Fluid Loss. Presented at the SPE European Spring Meeting, Amsterdam, 29–30 May. SPE-4834-MS. <http://dx.doi.org/10.2118/4834-MS>.
- Scholz, M. and Tapp, J. 2005. Development of a Revised Capillary Suction Time (CST) Test. *Water Conditioning and Purification* **48** (1): 46–52.
- Schubert, J.S. 2010. Precipitation Reactions in Hydrofrac Wastewater Treatments. Paper IWC 10-64 presented at the 71st International Water Conference, San Antonio, Texas, 24–28 October.
- Schultz, R.K. and Myers, R.R. 1969. The Chemorheology of Poly(vinyl alcohol)-Borate Gels. *Macromolecules* **2** (3): 281–285. <http://dx.doi.org/10.1021/ma60009a014>.
- Sciencelab. 2012. Material Safety Data Sheet. Houston: Guar Gum Science lab.com.
- Seagraves, S. 2007. Microbiological Influences in Mid-Continent Oil and Gas Production. Presented at the NACE International Central Area Conference, Tulsa, 25–28 September.
- Seale, R.A. 2007. An Efficient Horizontal Openhole Multi-Stage Fracturing and Completion System. Presented at the International Oil Conference and Exhibition in Mexico, Veracruz, Mexico, 27–30 June. SPE-108712-MS. <http://dx.doi.org/10.2118/108712-MS>.
- Sears, F.W. and Zemanski, M.W. 1955. *University Physics*, second edition. Boston, Massachusetts: Addison Wesley.
- Sedeh, I.F., Sjöberg, S., and Öhman, L.-O. 1993. Equilibrium and structural studies of silicon(IV) and aluminum(III) in aqueous solution. 31. Aqueous complexation between silicic acid and the catecholamines dopamine and L-DOPA. *J. Inorg. Biochem.* **50** (2): 119–132. [http://dx.doi.org/10.1016/0162-0134\(93\)80019-6](http://dx.doi.org/10.1016/0162-0134(93)80019-6).
- Selle, O.M., Wat, R.M.S., Vikane, O. et al. 2003. A Way Beyond Scale Inhibitors - Extending Scale Inhibitor Squeeze Life Through Bridging. Presented at the International Symposium on Oilfield Scale, Aberdeen, 29–30 January. SPE-80377-MS. <http://dx.doi.org/10.2118/80377-MS>.
- Seright, R.S. 1997. Minutes and Key Points of SPE Applied Technology Workshop on Water Conformance Dunkeld, Scotland, 19–22 May. Prepared by Bob Eden, SPE, Richardson, Texas.
- Seright, R.S. and Liang, J. 1994. A Survey of Field Applications of Gel Treatments for Water Shutoff. Presented at the SPE Latin American and Caribbean Petroleum Engineering Conference, Buenos Aires, 27–29 April. SPE-26991-MS. <http://dx.doi.org/10.2118/26991-MS>.
- Seright, R.S., Campbell, A.R., Mozley, P.S. et al. 2010. Stability of Partially Hydrolyzed Polyacrylamides at Elevated Temperatures in the Absence of Divalent Cations. *SPE J.* **15** (2): 341–348. SPE-121460-PA. <http://dx.doi.org/10.2118/121460-PA>.

- Seright, R.S., Fan, T., Wavrik, K. et al. 2011. Rheology of a New Sulfonic Associative Polymer in Porous Media. *SPE Res Eval & Eng* **14** (6): pp. 726-734. SPE-141355-PA. <http://dx.doi.org/10.2118/141355-PA>.
- Settari, A. 1993. Modeling of Acid-Fracturing Treatments. *SPE Prod & Fac* **8** (1): 30–38. SPE-21870-PA. <http://dx.doi.org/10.2118/21870-PA>.
- Settari, A., Sullivan, R.B., and Hansen, C. 2001. A New Two-Dimensional Model for Acid-Fracturing Design. *SPE Prod & Oper* **16** (4): 200–209. SPE-73002-PA. <http://dx.doi.org/10.2118/73002-PA>.
- Shah, S.N. and Lee, Y.N. 1986. Friction Pressures of Proppant-Laden Hydraulic Fracturing Fluids. *SPE Prod Eng* **1** (6): 437–445. SPE-13836-PA. <http://dx.doi.org/10.2118/13836-PA>.
- Shah, S.N. and Vyas, A. 2010. Temperature and Salinity Effects on Drag-Reduction Characteristics of Polymers in Coiled Tubing. Presented at the SPE/ICoTA Coiled Tubing and Well Intervention Conference and Exhibition, The Woodlands, Texas, USA, 23–24 March. SPE-130685-MS. <http://dx.doi.org/10.2118/130685-MS>.
- Sharma, G.D. 1995. Study of Hydrocarbon Miscible Solvent Slug Injection Process for Improved Recovery of Heavy Oil from Schrader Bluff Pool, Milne Point Unit, Alaska Annual Report for the Period January 1, 1994 to December 31, 1994. DOE/BC/14864- 1 4 Distribution Category UC-122. Washington, D.C.: US Department of Energy.
- Sharma, M.M. 2007. Formation Damage. In *Production Operations Engineering, Vol. IV.*, ed. J. D. Clegg, IV. Richardson, Texas: SPE.
- Sharma, M.M., Gadde, P.B., Sullivan, R. et al. 2004. Slick Water and Hybrid Fracs in the Bossier: Some Lessons Learnt. Presented at the SPE Annual Technical Conference and Exhibition, Houston, 26–29 September. SPE-89876-MS. <http://dx.doi.org/10.2118/89876-MS>.
- Sharma, S.C., Shrestha, L.K., Tsuchiya, K., Sakai, K., Sakai, H., and Abe, M. 2009. Viscoelastic Wormlike Micelles of Long Polyoxyethylene Chain Phytosterol with Lipophilic Nonionic Surfactant in Aqueous Solution. *The J. of Physical Chemistry B* **113** (10): 3043–3050. <http://dx.doi.org/10.1021/jp8102244>.
- Shashkina, J.A., Philippova, O.E., Zaroslov, Y.D., Khokhlov, A.R., Pryakhina, T.A., and Blagodatskikh, I.V. 2005. Rheology of Viscoelastic Solutions of Cationic Surfactant. Effect of Added Associating Polymer. *Langmuir* **21**(4): 1524–1530.
- Shaughnessy, C.M. and Kline, W.E. 1983. EDTA Removes Formation Damage at Prudhoe Bay. *J Pet Technol* **35** (10): 1783–1791. SPE-11188-PA. <http://dx.doi.org/10.2118/11188-PA>.
- Shen, D., Shcolnik, D., Perkins, R. et al. 2012. Evaluation of Scale Inhibitors in Marcellus High-Iron Waters. *Oil and Gas Facilities* **1** (5): pp. 34-42. SPE-141145-PA. <http://dx.doi.org/10.2118/141145-PA>.
- Sheng, J. 2011. *Modern Chemical Enhanced Oil Recovery: Theory and Practice*. Burlington, Massachusetts: Gulf Professional Publishing Elsevier.
- Shepherd, A.G., Mcgregor, S., Trompert, R.A. et al. 2012. Integrated Production Chemistry Management of the Schoonebeek Heavy Oil Redevelopment in the Netherlands: From Project to Start-up and Steady State Production. Presented at the SPE Heavy Oil Conference Canada, Calgary, 12–14 June. SPE-150635-MS. <http://dx.doi.org/10.2118/150635-MS>.
- Shepherd, A.G., Thomson, G., Westacott, R. et al. 2005. A Mechanistic Study of Naphthenate Scale Formation. Presented at the SPE International Symposium on Oilfield Chemistry, The Woodlands, Texas, USA, 2–4 February. SPE-93407-MS. <http://dx.doi.org/10.2118/93407-MS>.
- Sherik, A.M., Zaidi, S.R., Tuzan, E.V., and Perez, J.P. 2008. Black Powder in Gas Transmission Systems. Paper NACE 08415 presented at NACE International CORROSION 2008, New Orleans, 16–20 March.
- Shiau, B.J.B., Hsu, T.-P., Lohateeraparp, P. et al. 2012. Improved Oil Recovery by Chemical Flood from A High Salinity Reservoir. Presented at the SPE Improved Oil Recovery Symposium, Tulsa, 14–18 April. SPE-154260-MS. <http://dx.doi.org/10.2118/154260-MS>.
- Shimokata, N. and Yamada, Y. 2010. Troubles, Problems and Improvements of ESP. Presented at the Abu Dhabi International Petroleum Exhibition and Conference, Abu Dhabi, UAE, 1–4 November. SPE-137337-MS. <http://dx.doi.org/10.2118/137337-MS>.

- Shoaib, S. and Hoffman, B.T. 2009. CO₂ Flooding the Elm Coulee Field. Presented at the SPE Rocky Mountain Petroleum Technology Conference, Denver, 14–16 April. SPE-123176-MS. <http://dx.doi.org/10.2118/123176-MS>.
- Shukla, S., Zhu, D., and Hill, A.D. 2006. The Effect of Phase Saturation Conditions on Wormhole Propagation in Carbonate Acidizing. *SPE J.* **11** (3): 273–281. SPE-82273-PA. <http://dx.doi.org/10.2118/82273-PA>.
- Shuler, P. 1991. Method for Prolonging the Useful Life of Scale Inhibitors Injected within a Formation. US Patent No. 5,038,861.
- Shuler, P. 1993. Method for Prolonging the Useful Life of Polymeric or Blended Scale Inhibitor. US Patent No. 5,181,567.
- Siddiqui, S., Nasr-El-Din, H.A., and Khamees, A.A. 2006. Wormhole initiation and propagation of emulsified acid in carbonate cores using computerized tomography. *J. Pet. Sci. Eng.* **54** (3-4): 93–111. <http://dx.doi.org/10.1016/j.petrol.2006.08.005>.
- Siddiqui, S., Talabani, S., Yang, J. et al. 2003. An experimental investigation of the diversion characteristics of foam in Berea sandstone cores of contrasting permeabilities. *J. Pet. Sci. Eng.* **37** (1–2): 51–67. [http://dx.doi.org/http://dx.doi.org/10.1016/S0920-4105\(02\)00310-8](http://dx.doi.org/http://dx.doi.org/10.1016/S0920-4105(02)00310-8).
- Silverman, D.C. 1990. Rotating Cylinder Electrode -an Approach for Predicting Velocity Sensitive Corrosion. Paper NACE 90013 presented at NACE International Corrosion/90, Las Vegas, Nevada, 23–27 April.
- Simanzhenkov, V. and Idem, R. 2003. *Crude Oil Chemistry*. New York: Marcel Dekker, Inc.
- Simon, D.E. and Anderson, M.S. 1990. Stability of Clay Minerals in Acid. Presented at the SPE Formation Damage Control Symposium, Lafayette, Louisiana, 22–23 February. SPE-19422-MS. <http://dx.doi.org/10.2118/19422-MS>.
- Sims, P. 2010. The Next Generation Separator; Changing the Rules. *Oilfield Review* **22** (3): 50–54.
- Singer, M., Brown, B., Camacho, A., and Nesic, S. 2007. Combined Effect of CO₂, H₂S and Acetic Acid on Bottom of the Line Corrosion. Paper NACE 07661 presented at NACE International CORROSION 2007, Nashville, Tennessee, 11–15 March.
- Singh, S.P. and Kiel, O.G. 1982. Waterflood Design (Pattern, Rate, and Timing). Presented at the International Petroleum Exhibition and Technical Symposium, Beijing, 17–24 March. SPE-10024-MS. <http://dx.doi.org/10.2118/10024-MS>.
- Singh, W.P. and Bockris, J.O. 1996. Toxicity Issues of Organic Corrosion Inhibitor: Application of Qsar Model. Paper NACE 96225 presented at NACE International CORROSION 96, Denver, 24–29 March.
- Singh, W.P., Bockris, J.O., Lin, G.H., and Kang, Y. 1998. Designing Green Corrosion Inhibitors Using Chemical Computational Methods. Paper NACE 98208 presented at NACE International CORROSION 98, San Diego, California, 22–27 March.
- Sinkankas, J. 1966. *Mineralogy, First Course*. Princeton, New Jersey: D. Van Nostrand Company.
- Sinton, S.W. 1987. Complexation chemistry of sodium borate with poly(vinyl alcohol) and small diols: a boron-11 NMR study. *Macromolecules* **20** (10): 2430–2441. <http://dx.doi.org/10.1021/ma00176a018>.
- Sitdikov, S.S., Serdyuk, A., Nikitin, A. et al. 2009. Fiber-Laden Fluid: Applied Solution for Addressing Multiple Challenges of Hydraulic Fracturing in Western Siberia. Presented at the SPE Hydraulic Fracturing Technology Conference, The Woodlands, Texas, 19–21 January. SPE-119825-MS. <http://dx.doi.org/10.2118/119825-MS>.
- Sitz, C., Frenier, W.W., and Vallejo, C.M. 2012. Acid Corrosion Inhibitors with Improved Environmental Profiles. Presented at the SPE International Conference and Exhibition on Oilfield Corrosion, Aberdeen, 28–29 May. SPE-155966-MS. <http://dx.doi.org/10.2118/155966-MS>.
- Sjöblom, J., Aske, N., Harald Aulfem, I. et al. 2003. Our current understanding of water-in-crude oil emulsions.: Recent characterization techniques and high pressure performance. *Adv. Colloid Interface Sci.* **100–102** (0): 399–473. [http://dx.doi.org/http://dx.doi.org/10.1016/S0001-8686\(02\)00066-0](http://dx.doi.org/http://dx.doi.org/10.1016/S0001-8686(02)00066-0).

- Sjöblom, J., Hemmingsen, P., and Kallevik, H. 2007. The Role of Asphaltenes in Stabilizing Water-in-Crude Oil Emulsions. In *Asphaltenes, Heavy Oils, and Petroleomics*, O. Mullins, E. Sheu, A. Hammami, and A. Marshall, 21, 549-587. New York: Springer, http://dx.doi.org/10.1007/0-387-68903-6_21.
- Skauge, T., Spildo, K., and Skauge, A. 2010. Nano-sized Particles For EOR. Presented at the SPE Improved Oil Recovery Symposium, Tulsa, 24–28 April. SPE-129933-MS. <http://dx.doi.org/10.2118/129933-MS>.
- Smith, C., Oswald, D., and Daffin, M.D. 2006. Clay Control Additive for Wellbore Fluids. US Application Patent No. 2006/0289164 A1.
- Smith, C., Oswald, D., and Daffin, M.D. 2010. Clay Control Additive for Wellbore Fluids. US Patent No. 7,740,071.
- Smith, C., Oswald, D., Skibinski, D., and Sylvestre, N. 2011a. Single Fluid Acidizing Treatment. US Patent No. 7,915,205.
- Smith, C.F., Crowe, C.W., and Nolan, T.J.I. 1969. Secondary Deposition of Iron Compounds Following Acidizing Treatment. *J Pet Technol* **21** (9): 1121–1129. SPE-2358-PA. <http://dx.doi.org/10.2118/2358-PA>.
- Smith, C.F., Ross, W.M., and Hendrickson, A.R. 1965. Hydrofluoric Acid Stimulation Developments For Field Application. Presented at the Fall Meeting of the Society of Petroleum Engineers of AIME, Denver, 3–6 October. SPE-1284-MS. <http://dx.doi.org/10.2118/1284-MS>.
- Smith, M.B. and Shlyapobersky, J.W. 2001. Basics of Hydraulic Fracturing. In *Reservoir Stimulation*, third edition, ed. M. J. Economides and K. G. Nolte, 5-1 - 5-27. New York: John Wiley & Sons Ltd.
- Smith, R.J., Loscutova, J.R., Coker, C., Barron, A.R., and Skala, R.D. 2011b. Composition and Method for Making a Proppant. Patent No. 8,012,533.
- Smith, R.J., Loscutova, J.R., Whitsitt, E.A., Coker, C.E., Barron, A.R., Wiesner, M., Costantino, S.A., and Bordia, R.K. 2008. Composition and Method for Making a Proppant. US Patent No. 7,459,209.
- Smith, S.N. and Pacheco, J.L. 2002. Predicting Corrosion in Slightly Sour Environments. Paper NACE 02241 presented at NACE International CORROSION 2002, Denver, 7–11 April.
- SNF. 2010. Chemical Pump (Dr Injection Pump). Brochure, SNF SAS - ZAC de Milieux, Andrézieux, France.
- Soeder, D.J. 1988. Porosity and Permeability of Eastern Devonian Gas Shale. *SPE Form Eval* **3** (1): 116–124. SPE-15213-PA. <http://dx.doi.org/10.2118/15213-PA>.
- Solairaj, S., Britton, C., Kim, D.H. et al. 2012. Measurement and Analysis of Surfactant Retention. Presented at the SPE Improved Oil Recovery Symposium, Tulsa, 14–18 April. SPE-154247-MS. <http://dx.doi.org/10.2118/154247-MS>.
- Solomons, T.W.G. 1992a. Carbohydrates. In *Organic Chemistry*, fifth edition, ed. T. W. G. Solomons, 997-1039. New York: John Wiley & Sons.
- Solomons, T.W.G. 1992b. Esters. In *Organic Chemistry*, fifth edition, ed. T. W. G. Solomons, 778-786. New York: John Wiley and Sons.
- Somasundaran, P. and Hanna, H.S. 1979. Adsorption of Sulfonates on Reservoir Rocks. *Society of Petroleum Engineers Journal* **19** (4): 221–232. SPE-7059-PA. <http://dx.doi.org/10.2118/7059-PA>.
- Sorbie, K.S. and Laing, N. 2004. How Scale Inhibitors Work: Mechanisms of Selected Barium Sulphate Scale Inhibitors Across a Wide Temperature Range. Presented at the SPE International Symposium on Oilfield Scale, Aberdeen, 26–27 May. SPE-87470-MS. <http://dx.doi.org/10.2118/87470-MS>.
- Soulgani, B.S., Jamialahmadi, M., Rashtchian, D. et al. 2009. A New Thermodynamic Scale Equation for Modelling of Asphaltene Precipitation Form Live Oil. Presented at the Canadian International Petroleum Conference, Calgary, 16–18 June. PETSOC-2009-147. <http://dx.doi.org/10.2118/2009-147>.
- Southard, M.Z., Green, D.W., and Willhite, G.P. 1984. Kinetics of the Chromium(VI)/Thiourea Reaction in the Presence of Polyacrylamide. Presented at the SPE Enhanced Oil Recovery Symposium, Tulsa, 15–18 April. SPE-12715-MS. <http://dx.doi.org/10.2118/12715-MS>.
- SPE. 2010. FAQs on Deepwater Drilling, Gulf of Mexico Spill. SPE Notes, <http://www.spe.org/notes/2010/07/faqs-on-deepwater-drilling-gulf-spill/>.

- SPE. 2011. Grand Challenges Facing E&P Industry, <http://www.spe.org/industry/globalchallenges.php.7/10/11>.
- Srivastava, M., Zhang, J., Nguyen, Q.P. et al. 2009. A Systematic Study of Alkaline-Surfactant-Gas Injection as an EOR Technique. Presented at the SPE Annual Technical Conference and Exhibition, New Orleans, 4–7 October. SPE-124752-MS. <http://dx.doi.org/10.2118/124752-MS>.
- Stalkup, F.I. Jr. 1992. *Miscible Displacement*. Richardson, Texas: SPE.
- Stanitzek, T., Wolf, C.D., Gerdes, S. et al. 2012. Field Treatment to Stimulate a Deep, Sour, Tight Gas Well using a New, Low Corrosive and Environmentally Friendly Fluid. Presented at the 2012 SPE Kuwait International Petroleum Conference and Exhibition, Kuwait City, Kuwait, 10–12 December. SPE-163332-MS. <http://dx.doi.org/10.2118/163332-MS>.
- Statoil. 2009. Chemical Flooding, <http://www.statoil.com/en/TechnologyInnovation/OptimizingReservoirRecovery/RecoveryMethods/WaterAssistedMethodsImprovedOilRecoveryIOR/Pages/ChemicalFlooding.aspx>.
- Steinbrenner, U., Bittner, C., Oetter, G., and Guzman, M. 2009. Use of Surfactant Mixtures for Tertiary Mineral Oil Extraction. US Application Patent No. 2009/0270281.
- Stiff Jr., H.A. and Davis, L.E. 1952. A Method for Predicting the Tendency of Oil Field Waters To Deposit Calcium Carbonate. *J Pet Technol* **4** (9): 213–216. SPE-952213-G. <http://dx.doi.org/10.2118/952213-G>.
- Still, J.W., Dismuke, K.D., and Frenier, W.W. 2007. Generating Acid Downhole in Acid Fracturing. US Patent No. 7,166,560.
- Still, J.W., McConnell, S.B., and Miller, M.J. 2003. An Improved Encapsulated Breaker To Decrease Hydrostatic Release and Increase Thermal Stability. Presented at the International Symposium on Oilfield Chemistry, Houston, 5–7 February. SPE-80220-MS. <http://dx.doi.org/10.2118/80220-MS>.
- Stoll, W.M., al Shureqi, H., Finol, J. et al. 2010. Alkaline-Surfactant-Polymer Flood: From the Laboratory to the Field. Presented at the SPE EOR Conference at Oil & Gas West Asia, Muscat, Oman, 11–13 April. SPE 129164. <http://dx.doi.org/10.2118/129164-MS>.
- Strand, S., Austad, T., Puntervold, T. et al. 2008. “Smart Water” for Oil Recovery from Fractured Limestone: A Preliminary Study. *Energy Fuels* **22** (5): 3126–3133. <http://dx.doi.org/10.1021/ef800062n>.
- Street-Jr., E.H. 1979. Process for Sequestering Iron While Acidizing a Reservoir. US Patent No. 4,167,214.
- Sulejmanov, A.B., Geokchaev, T.B., and Dashdiev, R.A. 1993. Removal of Petroleum Spillages from Water Surface. US Patent No. 1803418-A.
- Sullivan, A.P. and Kilpatrick, P.K. 2002. The Effects of Inorganic Solid Particles on Water and Crude Oil Emulsion Stability. *Ind. Eng. Chem. Res.* **41** (14): 3389–3404. <http://dx.doi.org/10.1021/ie010927n>.
- Sun, H., Wood, B., Stevens, R.F. et al. 2011. A Nondamaging Friction Reducer for Slickwater Frac Applications. Presented at the SPE Hydraulic Fracturing Technology Conference, The Woodlands, Texas, USA, 24–26 January. SPE-139480-MS. <http://dx.doi.org/10.2118/139480-MS>.
- Sun, S.Q. 1995. Dolomite Reservoirs: Porosity Evolution and Reservoir Characteristics. *AAPG Bulletin* **79** (2): 186–204.
- Sun, W. 2006. *Kinetics of Iron Carbonate and Iron Sulfide Scale Formation in CO₂/H₂S Corrosion*. PhD dissertation, Russ College Of Engineering And Technology, Ohio University, Athens, Ohio.
- Sun, W., Chokshi, K., and Nestic, S. 2005. Iron Carbonate Scale Growth and the Effect of Inhibition in CO₂ Corrosion of Mild Steel. Presented at the Corrosion 2005, Houston, 3–7 April. NACE-05285.
- Sunde, E., Lillebo, B.-L.P., Bodtke, G., and Thorstenson, T. 2004. H₂S Inhibition by Nitrate Injection on the Gullfaks Field. Paper NACE 04760 presented at NACE International CORROSION/2004, New Orleans, 28 March–1 April.
- Surkalo, H. 2012. Chemical Floods since 1985. Brochure, Golden, Colorado, Surtek.
- Swanson, T.A., Petrie, M., and Sifferman, T.R. 2005. The Successful Use of Both Kinetic Hydrate and Paraffin Inhibitors Together in a Deepwater Pipeline with a High Water Cut in the Gulf of Mexico.

- Presented at the SPE International Symposium on Oilfield Chemistry, The Woodlands, Texas, 2–4 February 2005. SPE-93158-MS. <http://dx.doi.org/10.2118/93158-MS>.
- Sweatman, R.E., Parker, M.E., and Crookshank, S.L. 2009. Industry Experience With CO₂-Enhanced Oil Recovery Technology. Presented at the SPE International Conference on CO₂ Capture, Storage, and Utilization, San Diego, California, USA, 2–4 November. SPE 126446. <http://dx.doi.org/10.2118/126446-MS>.
- Syahputra, A.E., Tsau, J.-S., and Grigg, R.B. 2000. Laboratory Evaluation of Using Lignosulfonate and Surfactant Mixture in CO₂ Flooding. Presented at the SPE/DOE Improved Oil Recovery Symposium, Tulsa, 3–5 April. SPE-59368-MS. <http://dx.doi.org/10.2118/59368-MS>.
- Syrinek, A.R. and Huddleston, A. 1988. Hydrocarbon Gellant. US Patent No. 4,781,845.
- Szymczak, S., Shen, D., Higgins, R. et al. 2012. Minimizing Environmental and Economic Risks with a Proppant-Sized Solid Scale Inhibitor Additive in the Bakken Formation. Presented at the SPE Annual Technical Conference and Exhibition, San Antonio, Texas, USA, 8–10 October. SPE-159701-MS. <http://dx.doi.org/10.2118/159701-MS>.
- Taber, J.J., Martin, F.D., and Seright, R.S. 1997. EOR Screening Criteria Revisited - Part 1: Introduction to Screening Criteria and Enhanced Recovery Field Projects. *SPE Res Eng* **12** (3): 189–198. SPE-35385-PA. <http://dx.doi.org/10.2118/35385-PA>.
- Tadmor, R. 2004. Line Energy and the Relation between Advancing, Receding, and Young Contact Angles. *Langmuir* **20** (18): 7659–7664. <http://dx.doi.org/10.1021/la049410h>.
- Taha, R., Hill, A.D., and Sepohnoori, K. 1989. Sandstone Acidizing Design With a Generalized Model. *SPE Prod Eng* **4** (1): 49–55. SPE-16885-PA. <http://dx.doi.org/10.2118/16885-PA>.
- Tandy, S., Bossart, K., Mueller, R. et al. 2003. Extraction of Heavy Metals from Soils Using Biodegradable Chelating Agents. *Environ. Sci. Technol.* **38** (3): 937–944. <http://dx.doi.org/10.1021/es0348750>.
- Tang, G.Q. and Morrow, N.R. 1997. Salinity, Temperature, Oil Composition, and Oil Recovery by Waterflooding. *SPE Res Eng* **12** (4): 269–276. SPE-36680-PA. <http://dx.doi.org/10.2118/36680-PA>.
- Tang, G.-Q. and Morrow, N.R. 1999. Oil Recovery by Waterflooding and Imbibition – Invading Brine Cation Valency and Salinity. Presented at the 1999 International Symposium of the Society of Core Analysts, Golden, Colorado, USA, 1–4 August. SCA-9911.
- Tardy, P.M.J. and Chang, F.F. 2011. Determining Matrix Treatment Performance From Downhole Pressure And Temperature Distribution: A Model. Presented at the 2011 International Petroleum Technology Conference, Bangkok, Thailand, 15–17 November. IPTC-15118-MS. <http://dx.doi.org/10.2523/15118-MS>.
- Taylor, G.N. and Matherly, R. 2011. The Laboratory Evaluation and Optimization of Hydrogen Sulphide Scavengers Using Sulphur Specific Flame Photometric Gas Chromatography. Presented at the SPE International Symposium on Oilfield Chemistry, The Woodlands, Texas, USA, 11–13 April. SPE-140401-MS. <http://dx.doi.org/10.2118/140401-MS>.
- Taylor, K.C., Nasr-El-Din, H.A., and Al-Alawi, M.J. 1998. A Systematic Study of Iron Control Chemicals Used During Well Stimulation. Presented at the SPE Formation Damage Control Conference, Lafayette, Louisiana, 18–19 February. SPE-39419-MS. <http://dx.doi.org/10.2118/39419-MS>.
- Taylor, R., Khallad, A., Cheng, A. et al. 2002. Optimized Gas-Well Stimulating using CO₂-Miscible, Viscosified Hydrocarbon Fracturing Fluids. Presented at the SPE Gas Technology Symposium, Calgary, 30 April–2 May. SPE-75666-MS. <http://dx.doi.org/10.2118/75666-MS>.
- Taylor, R.S., Stemler, P., Cheng, A. et al. 2004. Refinery Plugging by Residual Oil Gellant Chemicals in Crude: Understanding and Preventing the Problem Through New Oil Gellant Chemistry. Presented at the Canadian International Petroleum Conference, Calgary, 8–1 June. PETSOC-2004-049. <http://dx.doi.org/10.2118/2004-049>.
- Teas, J.P. 1968. Graphic Analysis of Resin Solubilities. *J. of Paint Technology* **40** (516): 19–25.
- Thiercelin, M.C. and Roegiers, J.-C. 2001. Formation Characterization: Rock Mechanics. In *Reservoir Stimulation*, third edition, ed. M.J. Economides and K.G. Nolte. New York: John Wiley & Sons.

- Thomas, A., Gaillard, N. and Favero, C. 2012. Some Key Features to Consider When Studying Acrylamide-Based Polymers for Chemical Enhanced Oil Recovery. *Oil & Gas Science and Technology – Rev. IFP Energies nouvelles* **67** (6): 887–902. <http://dx.doi.org/10.2516/ogst2012065>.
- Thomas, F.B. and Bennion, D.B. 1999. Development and Evaluation of Paraffin Technology: Current Status. *J Pet Technol* **51** (2): 60–61. SPE-8344-MS. <http://dx.doi.org/10.2118/50561-MS>.
- Thomas, R.L. 1979. Method for Acidizing a Subterranean Formation. US Patent No. 4,151,879.
- Thomas, R.L. and Crowe, C.W. 1981. Matrix Treatment Employs New Acid System for Stimulation and Control of Fines Migration in Sandstone Formations. *J Pet Technol* **33** (8): 1491–1500. SPE-7566-PA. <http://dx.doi.org/10.2118/7566-PA>.
- Thomas, R.L. and Morgenthaler, L.N. 2001. Introduction to Matrix Stimulation. In *Reservoir Stimulation*, third edition, ed. M.J. Economides and K.G. Nolte. New York: John Wiley & Sons.
- Thomas, R.L. and Nasr-El-Din, H.A. 2003. Field Validation of a Carbonate Matrix Acidizing Model: A Case Study of Seawater Injection Wells in Saudi Arabia. Presented at the SPE European Formation Damage Conference, The Hague, 13–14 May. SPE-82271-MS. <http://dx.doi.org/10.2118/82271-MS>.
- Thomas, S. 2008. Enhanced Oil Recovery- an Overview. *Oil and Gas Science and Technology- Rev. IFP* **63** (1): 9–19.
- Thomas, S. and Ali, S.M.F. 2001. Micellar Flooding and ASP-Chemical Methods for Enhanced Oil Recovery. *J Can Pet Technol* **40** (2). PETSOC-01-02-04. <http://dx.doi.org/10.2118/01-02-04>.
- Thomas, S., Ali, S.M.F., and Daharu, R. 1986. Tertiary Recovery Of Two Alberta Oils By Micellar Flooding. Presented at the Annual Technical Meeting, Calgary, 8–11 June. PETSOC-86-37-54. <http://dx.doi.org/10.2118/86-37-54>.
- Thompson, K.E. and Gdanski, R.D. 1993. Laboratory Study Provides Guidelines for Diverting Acid With Foam. *SPE Prod & Fac* **8** (4): 285–290. SPE-23436-PA. <http://dx.doi.org/10.2118/23436-PA>.
- Thorstenon, T., Sunde, E., Bodtker, G., Lillebo, B.-L., Torsvik, T., and Beeder, J. 2002. Biocide Replacement by Nitrate in Sea Water Injection Systems. Paper NACE 02033 presented at NACE International CORROSION 2002, Denver, 7–11 April.
- Tibbles, R.J., Mehmet, P., Chang, F.F., Fu, D., Davison, J.M., Morris, E.W.A., Wierenga, A.M., and Vinod, P.S. 2003. Fluids and Techniques for Hydrocarbon Well Completion. US Patent No. 6,638,896.
- Tielong, C., Zhengyu, S., Fan, Y. et al. 1998. A Pilot Test of Polymer Flooding in an Elevated-Temperature Reservoir. *SPE Res Eval & Eng* **1** (1): 24–29. SPE-36708-PA. <http://dx.doi.org/10.2118/36708-PA>.
- Tiler, F.M. 1981. Revision of Sedimentation Theory. *AIChE J.* **27**(5): 823–828. <http://dx.doi.org/10.1002/aic.690270517>.
- Tinto, J. and Solomon, R. 2010. Water Recovery Via Thermal Evaporative Processes for High Saline Frac Water Flowback. Paper IWC-10-66 presented at the 71st International Water Conference, San Antonio, Texas, 24–28 October.
- Tiyaboonchai, W., Woiszwilllo, J., and Middaugh, C.R. 2003. Formulation and characterization of DNA–polyethylenimine–dextran sulfate nanoparticles. *Eur. J. Pharm. Sci.* **19** (4): 191–202. [http://dx.doi.org/http://dx.doi.org/10.1016/S0928-0987\(03\)00102-7](http://dx.doi.org/http://dx.doi.org/10.1016/S0928-0987(03)00102-7).
- Tjon-Joe-Pin, R. 1993. Enzyme Breaker for Glactomannan Based Fracturing Fluids. US Patent No. 5,201,370.
- Tjon-Joe-Pin, R., Thompson, J.E., and Ault, M.G. 2001. Stable Breaker-Complexer-Polymer Complex and Method of Use in Completion and Stimulation. US Patent No. 6,186,235.
- Todd, B.L., Slabaugh, B.F., Munoz, T. Jr., and Parker, M. 2005. Fluid Loss Control Additives for Use in Fracturing Subterranean Formations. World Application Patent No. WO/2005/071223.
- Trabelsi, S. and Kakadjian, S. 2013. Comparative Study Between Guar and Carboxymethylcellulose Used as Gelling Systems in Hydraulic Fracturing Application. Presented at the 2013 SPE Production and Operations Symposium, Oklahoma City, Oklahoma, USA, 23–26 March. SPE-164486-MS. <http://dx.doi.org/10.2118/164486-MS>.

- Trehan, R., Jones, N.D., and Haney, J.A. 2012. Acidizing Optimization: Monterey Shale, California. Presented at the SPE Western Regional Meeting, Bakersfield, California, USA, 21–23 March. SPE-154257-MS. <http://dx.doi.org/10.2118/154257-MS>.
- Tsau, J.-S. and Heller, J.P. 1992. Evaluation of Surfactants for CO₂-Foam Mobility Control. Presented at the Permian Basin Oil and Gas Recovery Conference, Midland, Texas, 18–20 March. SPE-24013-MS. <http://dx.doi.org/10.2118/24013-MS>.
- Tsui, K., Wong, J.E., and Park, N. 2010. Effect of Corrosion Inhibitor Active Components on Corrosion Inhibition in a Sweet Environment. Paper NACE 10326 presented at NACE International Corrosion 2010, San Antonio, Texas, 14–18 March.
- Tuedor, F.E., Xiao, Z., Frenier, W.W. et al. 2006. A Breakthrough Fluid Technology in Stimulation of Sandstone Reservoirs. Presented at the International Symposium and Exhibition on Formation Damage Control, Lafayette, Louisiana USA, 15–17 February. SPE-98314-MS. <http://dx.doi.org/10.2118/98314-MS>.
- Turner, M.S. and Smith, P.C. 2005. Controls On Soap Scale Formation, Including Naphthenate Soaps - Drivers And Mitigation. Presented at the SPE International Symposium on Oilfield Scale, Aberdeen, 11–12 May. SPE-94339-MS. <http://dx.doi.org/10.2118/94339-MS>.
- Uchendu, C.V., Nwoke, L.A., Akinlade, O. et al. 2006. A New Approach to Matrix Sandstone Acidizing Using a Single Step HF System: A Niger Delta Case Study. Presented at the SPE Annual Technical Conference and Exhibition, San Antonio, Texas, USA, 24–27 September. SPE-103041-MS. <http://dx.doi.org/10.2118/103041-MS>.
- Uhlig, H.H. 1971. *Corrosion and Corrosion Control*. New York: John Wiley and Sons.
- Urbina, I. 2011. Danger to the Environment and Health from “Fracking” Is Greater Than Previously Understood. *N.Y. Times*, 27 February 2011.
- Uribe, O. 2006. *After-Closure Analysis of Mini-Frac Tests in Naturally Fractured Reservoirs*. MS thesis, University of Oklahoma, Norman, Oklahoma.
- Urum, K., Pekdemir, T. and Copur, M. 2005. Screening of Biosurfactants for Crude Oil Contaminated Soil Washing. *J. of Environmental Engineering and Science* 4 (6): 487–496. <http://dx.doi.org/10.1139/s04-073>.
- USDOE. 2000. University of Oklahoma Fracturing Fluid Characterization Facility, DE - FC 21 - 92MC29077. Washington, DC: Department of Energy.
- USDOE. 2004. Hydraulic Fracturing White Paper. Washington DC: US Department of Energy.
- USDOE. 2007. US DOE Produced Water Fact Sheet. US Department of the Environment, Washington DC, <http://www.netl.doe.gov/technologies/pwmis/techdesc/discharge/index.html> (accessed 19 July 2010).
- USEPA. 2010a. Radioactive Waste Disposal: An Environmental Perspective, EPA 402-K-94-00.1. Washington DC: U.S. Environmental Protection Agency.
- USEPA. 2010b. Hydrafacts. Washington DC: US Environmental Protection Agency, http://www.epa.gov/safewater/uic/wells_hydrofrac.html.
- USEPA. 2011a. Priority Pollutants from Clean Water Act, Appendix A to 40 CFR Part 423. Washington DC: US Environmental Protection Agency.
- USEPA. 2011b. Class II Wells - Oil and Gas Related Injection Wells (Class II). Washington DC: US Environmental Protection Agency, <http://water.epa.gov/type/groundwater/uic/class2/>.
- van der Heijde, P.K.M. and Elnawawy, O.A. 1993. Compilation of Ground-Water Models, EPA/600/R-93/118. US Environmental Protection Agency, US Office of Research and Development.
- Van Domelen, M.S., Talib, N.N., and Glasbergen, G. 2011. Return to Basics and Proper Planning Opens the Possibility to Acid Stimulate a Difficult Chalk Formation. Presented at the SPE European Formation Damage Conference, Noordwijk, The Netherlands, 7–10 June. SPE-144159-MS. <http://dx.doi.org/10.2118/144159-MS>.
- van Everdingen, A.F. and Hurst, W. 1949. The Application of the Laplace Transformation to Flow Problems in Reservoirs. *J Pet Technol* 1 (12): 305–324. <http://dx.doi.org/10.2118/949305-G>.

- van Poolen, H.K. and Hoover, D.B. 1970. Waste Disposal and Earthquakes at the Rocky Mountain Arsenal, Derby, Colorado. *J Pet Technol* **22** (8): 983–993. SPE-2558-PA. <http://dx.doi.org/10.2118/2558-PA>.
- Veedu, F.K., Delshad, M., and Pope, G.A. 2010. Scaleup Methodology for Chemical Flooding. Presented at the SPE Annual Technical Conference and Exhibition, Florence, Italy, 19–22 September. SPE-135543-MS. <http://dx.doi.org/10.2118/135543-MS>.
- Vehlow, J., Bergfeldt, B., Visser, R. et al. 2007. European Union waste management strategy and the importance of biogenic waste. *J. Mater. Cycles Waste Manage.* **9** (2): 130–139. <http://dx.doi.org/10.1007/s10163-007-0178-9>.
- Veil, J.A. 2009. Produced Water Management Options –One Size Does Not Fit Allproduced—All One All. Society of Petroleum Engineers, <http://www.spe.org/dl/docs/2009/Veil.pdf>.
- Veley, C.D. 1969. How Hydrolyzable Metal Ions React with Clays to Control Formation Water Sensitivity. *J Pet Technol* **21** (9): 1111–1118. SPE-2188-PA. <http://dx.doi.org/10.2118/2188-PA>.
- Venugopal, K.N. and Abhilash, M. 2010. Study of Hydration Kinetics and Rheological Behaviour of Guar Gum. *International J. of Pharma Sciences and Research* **1** (1): 28–39.
- Verga, F. 2009. *Drive Mechanisms and Displacement Processes*. Milan, Italy: ENI Encyclopedia of Hydrocarbons ENI, http://www.treccani.it/export/sites/default/Portale/sito/altre_aree/Tecnologia_e_Scienze_applicate/enciclopedia/inglese/inglese_vol_1/pag509-526ing3.pdf.
- Vindstad, J.E., Grande, K.V., and Mediaas, H. 2007. Efficient Management of Calcium Naphthenate Deposition Deposition at Oil Fields. TEKNA–Separation Technology 2007, Stavanger, Norway, 26–27 September.
- Voderbruggen, M.A. and Williams, D.A. 2000. Acid Corrosion Inhibitors. US Patent No. 6,117,364.
- Vogel, J.V. 1968. Inflow Performance Relationships for Solution-Gas Drive Wells. *J Pet Technol* **20** (1): 83–92. SPE-1476-PA. <http://dx.doi.org/10.2118/1476-PA>.
- Volz, H.A. 1977. Subterranean Formations Are Fractured by Means of an Acid Foam Which Can Contain Propping Materials. Patent No. 4,044,833.
- Vreeburg, R.-J., Roodhart, L.P., Davies, D.R. et al. 1994. Proppant Backproduction During Hydraulic Fracturing - A New Failure Mechanism for Resin-Coated Proppants. *J Pet Technol* **46** (10): 884–889. SPE-27382-PA. <http://dx.doi.org/10.2118/27382-PA>.
- Wagner, H.L. 1985. The Mark-Houwink-Sakurada Equation for the Viscosity of Atactic Polystyrene. *J. Phys. Chem. Ref. Data*, **14** (4): 1101–1106. <http://dx.doi.org/10.1063/1.555740>.
- Walker, M.L., Shuchart, C.E., Yaritz, J.G. et al. 1995. Effects of Oxygen on Fracturing Fluids. Presented at the SPE International Symposium on Oilfield Chemistry, San Antonio, Texas, 14–17 February. SPE-28978-MS. <http://dx.doi.org/10.2118/28978-MS>.
- Walters, H.G., Slabaugh, B.F., and Bryant, J. 2008. Polymer Mixture for Crosslinked Fluids. US Patent No. 7,445,044.
- Walters, H.G., Stegent, N.A., and Harris, P.C. 2009. New Frac Fluid Provides Excellent Proppant Transport and High Conductivity. Presented at the SPE Hydraulic Fracturing Technology Conference, The Woodlands, Texas, 19–21 January. SPE-119380-MS. <http://dx.doi.org/10.2118/119380-MS>.
- Wamser, C.A. 1948. Hydrolysis of Fluoboric Acid in Aqueous Solution. *J. Am. Chem. Soc.* **70** (3): 1209–1215. <http://dx.doi.org/10.1021/ja01183a101>.
- Wang, D., Seright, R.S., and Zhang, J. 2012a. Wettability Survey in Bakken Shale Using Surfactant Formulation Imbibition. Presented at the SPE Improved Oil Recovery Symposium, Tulsa, 14–18 April. SPE-153853-MS. <http://dx.doi.org/10.2118/153853-MS>.
- Wang, D., Wang, X., Liu, G. et al. 2012b. A New Way of Staged Fracturing Using Ball Sealers. *SPE Prod & Oper* **27** (3): pp. 278–283. SPE-140529-PA. <http://dx.doi.org/10.2118/140529-PA>.
- Wang, W., Kan, A., and Tomson, M. 2013. A Novel and Comprehensive Study of Polymeric and Traditional Phosphonate Inhibitors for High-Temperature Scale Control. *SPE J.* **18** (3): pp. 575–582. SPE-155108-PA. <http://dx.doi.org/10.2118/155108-PA>.
- Wang, X., Zou, H., Chen, Y. et al. 2004. Development of a Novel Alcoholic Acid System for Removal Damage Resulting from Hydraulic Fracturing in the Tight Gas Reservoir. Presented at the SPE

- International Symposium and Exhibition on Formation Damage Control, Lafayette, Louisiana, 18–20 February. SPE-86552-MS. <http://dx.doi.org/10.2118/86552-MS>.
- Wang, Y., Hill, A.D., and Schechter, R.S. 1993. The Optimum Injection Rate for Matrix Acidizing of Carbonate Formations. Presented at the SPE Annual Technical Conference and Exhibition, Houston, 3–6 October. SPE-26578-MS. <http://dx.doi.org/10.2118/26578-MS>.
- Warpinski, N.R. and Teufel, L.W. 1987. Influence of Geologic Discontinuities on Hydraulic Fracture Propagation (includes associated papers 17011 and 17074). *J Pet Technol* **39** (2): 209–220. SPE-13224-PA. <http://dx.doi.org/10.2118/13224-PA>.
- Washburn, E.W. 1921. The Dynamics of Capillary Flow. *Physical Review* **17** (3): 273–283. <http://dx.doi.org/10.1103/PhysRev.17.273>.
- Waters, G. 2011. Shale Completion and Production Technologies, Brochure. Sugar Land, Texas: Schlumberger Technology Company.
- Watkins, E.K., Wendorff, C.L., and Ainley, B.R. 1983. A New Crosslinked Foamed Fracturing Fluid. Presented at the SPE Annual Technical Conference and Exhibition, San Francisco, 5–8 October. SPE-12027-MS. <http://dx.doi.org/10.2118/12027-MS>.
- Wattebled, L. and Laschewsky, A. 2007. Effects of Organic Salt Additives on the Behavior of Dimeric (“Gemini”) Surfactants in Aqueous Solution. *Langmuir* **23** (20): 10044–10052. <http://dx.doi.org/10.1021/la701542k>.
- Waxman, H.A., Markey, E.J., and DeGette, D. 2011. Chemicals Used in Hydraulic Fracturing. Report, Washington DC, US Congress.
- WDNR. 2012. Silica Sand Mining in Wisconsin January 2012. Report, Madison, Wisconsin, Wisconsin Department of Natural Resources.
- Weaver, J., Gdanski, R., and Karcher, A. 2003. Guar Gum Degradation: A Kinetic Study. Presented at the International Symposium on Oilfield Chemistry, Houston, 5–7 February. SPE-80226-MS. <http://dx.doi.org/10.2118/80226-MS>.
- Webber, S.J. 1994. *An Expert System for Hydraulic Fracturing*. PhD Dissertation, University of Oklahoma, Norman, Oklahoma.
- Weerasooriya, U.P. and Pope, G.A. 2011a. Styrylphenol Alkoxylate Sulfate as a New Surfactant Composition for Enhanced Oil Recovery Applications. US Application Patent No. 2011/0190174.
- Weerasooriya, U.P. and Pope, G.A. 2011b. Process of Using Hard Brine at High Alkalinity for Enhanced Oil Recovery (EOR) Applications. US Application Patent No. 2011/0059873A1.
- Weerasooriya, U.P., Pope, G.A., and Nguyen, Q.P. 2011. Method of Manufacture and Use of Large Hydrophobe Ether Sulfate Surfactants in Enhanced Oil Recovery (EOR) Applications. US Application Patent No. 2011/0071057.
- Wehunt, C.D., Van Arsdale, H., Warner, J.L. et al. 1993. Laboratory Acidization of an Eolian Sandstone at 380F. Presented at the SPE International Symposium on Oilfield Chemistry, New Orleans, 2–5 March. SPE-25211-MS. <http://dx.doi.org/10.2118/25211-MS>.
- Weiss, J. 2008. Emulsion Processing-Homogenization Emulsion Workshop, University of Massachusetts, Amherst, Massachusetts, 13–14 November.
- Weitz, D., Wyss, H. and Larsen, R. 2007. Oscillatory Rheology. *G.I.T. Laboratory J.* **3-4**: 68–70.
- Wellcare. 2003. Closing an Abandoned Well. Report. Washington, DC: Water Systems Council.
- Welton, T.D. and Domelen, M.S.V. 2008. High-Viscosity-Yield Acid Systems for High-Temperature Stimulation. *SPE Prod & Oper* **23** (2): 177–183. SPE-98237-PA. <http://dx.doi.org/10.2118/98237-PA>.
- Welton, T.D., Lewis, S.J., and Funkhouser, G.P. 2007. Viscoelastic Surfactant Fluids and Associated Diverting Methods. US Patent No. 7,303,019.
- Welton, T.D., Todd, B.L., and Eoff, L.S. 2009. Methods of Diverting Chelating Agents in Subterranean Treatments. US Application Patent No. 2009/0291863.
- Wendorff, C.L. and Ainley, B.R. 1981. Massive Hydraulic Fracturing Of High-Temperature Wells With Stable Frac Foams. Presented at the SPE Annual Technical Conference and Exhibition, San Antonio, Texas, 4–7 October. SPE-10257-MS. <http://dx.doi.org/10.2118/10257-MS>.

- Weng, X., Kresse, O., Cohen, C.-E. et al. 2011. Modeling of Hydraulic-Fracture-Network Propagation in a Naturally Fractured Formation. *SPE Prod & Oper* **26** (4): 368-380. SPE-140253-PA. <http://dx.doi.org/10.2118/140253-PA>.
- Westenhaus, B. 2012. Get Ready for Super Fracking! New Energy and Fuel, January 16, 2012, <http://newenergyandfuel.com/2012/01/16/get-ready-for-super-fracking/>.
- Whitaker, S. 1986. Flow in porous media I: A theoretical derivation of Darcy's law. *Transport Porous Media* **1** (1): 3–25. <http://dx.doi.org/10.1007/bf01036523>.
- Whitehead, D. 1968. *The Dow Story: The History of the Dow Chemical Company*. New York: McGraw-Hill.
- Wickstrom, L., Perry, C., Riley, R., and Erenpreiss, M. 2012. The Utica-Point Pleasant Shale Play of Ohio, Ohio Department of Natural Resources Division of Geological Survey, Columbus, Ohio.
- Wikipedia. 2009a. Viscometer (19 July 2009 revision), <http://en.wikipedia.org/wiki/Viscometer> (accessed 28 July 2009).
- Wikipedia. 2009b. West Texas Intermediate (5 May 2009 revision). http://en.wikipedia.org/wiki/West_Texas_Intermediate (accessed 28 July 2009).
- Wikipedia. 2010a. Deepwater Horizon Oil Spill (25 July 2010 revision). http://en.wikipedia.org/wiki/Deepwater_Horizon_oil_spill (accessed 25 July 2010).
- Wikipedia. 2010b. Shale (22 June 2010 revision). <http://en.wikipedia.org/wiki/Shale> (accessed 25 July 2010).
- Wikipedia. 2010c. Phenol Formaldehyde Resin (22 June 2010 revision). http://en.wikipedia.org/wiki/Phenol_formaldehyde_resin (accessed 24 June 2010).
- Wikipedia. 2010d. Spinning Drop Method (3 April 2010 revision). http://en.wikipedia.org/wiki/Spinning_Drop_Method (accessed 15 April 2010).
- Wikipedia. 2010e. Surface Tensions (28 July 2010 revision). http://en.wikipedia.org/wiki/Surface_tension (accessed 31 July 2010).
- Wikipedia. 2010f. Coalbed Methane (11 July 2010 revision). http://en.wikipedia.org/wiki/Coalbed_methane (accessed 12 July 2010).
- Wikipedia. 2010g. Du Nouy Ring (25 March 2010 revision). http://en.wikipedia.org/wiki/Du_No%C3%BCy_ring_method (accessed 23 August 2010).
- Wikipedia. 2011a. (25 July 2011 revision). Bayer Process. http://en.wikipedia.org/wiki/Bayer_process (accessed 7 November 2011).
- Wikipedia. 2011b. Supercritical Carbon Dioxide (27 March 2011 revision). http://en.wikipedia.org/wiki/Supercritical_carbon_dioxide (accessed 22 April 2011).
- Wikipedia. 2011c. Eagle Ford Formation (16 October 2010 revision). http://en.wikipedia.org/wiki/Eagle_Ford_Formation (accessed 4 March 2011).
- Wiles, C. and Watts, P. 2010. The Scale-up of Organic Synthesis Using Micro Reactors. *Chemistry Today (chimica oggi)* **28** (3): 3–5.
- Wiles, C. and Watts, P. 2011. *Micro Reaction Technology in Organic Synthesis*. Boca Raton, Florida: CRC Press, Taylor and Francis Group.
- Willberg, D.M., Miller, M.J., Thiercelin, M.J., and Kosarev, I.V. 2009. Method for Hydraulic Fracturing of Subterranean Formation. US Application Patent No. 2009/0044945.
- Willberg, D.M., Nelson, E., and Frenier, W. 2006. Proppants Useful for Prevention of Scale Deposition. US Application Patent No. 20060272816.
- Willcox, M. 2000. Soap. In *Poucher's Perfumes, Cosmetics and Soaps*, tenth edition, ed. H. Butler, 453. Dordrecht: Kluwer Academic Publishers.
- Willhite, G.P. 1986. *Waterflooding*. Richardson, Texas: Society of Petroleum Engineers.
- Williams, B.B. and Nierode, D.E. 1972. Design of Acid Fracturing Treatments. *J Pet Technol* **24** (7): 849–859. SPE-3720-PA. <http://dx.doi.org/10.2118/3720-PA>.
- Williams, D., Holifield, P.K., Looney, J.R., and McDougall, L.A. 1992. Method of Inhibiting Corrosion in Acidizing Wells. US Patent No. 5,089,153.
- Williams, D., Holifield, P.K., Looney, J.R., and McDougall, L.A. 1993a. Inhibited Acid System for Acidizing Wells. US Patent No. 5,209,859.

- Williams, D., Holifield, P.K., Looney, J.R., and McDougall, L.A. 1993b. Method of Inhibiting Corrosion in Acidizing Wells. US Patent No. 5,200,096.
- Williamson, C.D. and Allenson, S.J. 1989. A New Nondamaging Particulate Fluid-Loss Additive. Presented at the SPE International Symposium on Oilfield Chemistry, Houston, 8–10 February. SPE-18474-MS. <http://dx.doi.org/10.2118/18474-MS>.
- Willmon, J.G. and Edwards, M.A. 2006. From Precommissioning to Startup: Getting Chemical Injection Right. *SPE Prod & Oper* **21** (4): 483–491. SPE-96144-PA. <http://dx.doi.org/10.2118/96144-PA>.
- Wilson, D.A. and Crump, D.K. 1999. Succinic Acid Derivative Biodegradable Chelants and Uses and Compositions Thereof. US Patent No. 5,859,273.
- Winsor, P.A. 1954. *Solvent Properties of Amphiphilic Compounds*. London: Buttersorth's Scientific Publications.
- Wolery, T.J. 1992. EQ3/6, a Software Package for Geochemical Modeling of Aqueous Systems: Package Overview and Installation Guide, Version 7.0. Livermore, California: Lawrence Livermore National Laboratory.
- Wong, J.E. and Park, N. 2008. Effect of Corrosion Inhibitor Active Components on the Growth of Iron Carbonate Scale under CO₂ Conditions. Paper NACE 08345 presented at NACE International CORROSION 2008, New Orleans, 16–20 March.
- Wong, J.E. and Park, N. 2009. Further Investigation on the Effect of Corrosion Inhibitor Actives on the Formation of Iron Carbonate on Carbon Steel. Paper NACE 09569 presented at NACE International CORROSION 2009, Atlanta, Georgia, 22–26 March.
- Wood, W.R. 2008. Fluid Loss Control in Viscoelastic Surfactant Fracturing Fluids Using Water Soluble Polymers. US Application Patent No. 2008/0161209.
- Wu, Q., Ma, Y., Sun, Y. et al. 2013. The Flow Behavior of Friction Reducer in Microchannels During Slickwater Fracturing. Presented at the 2013 SPE Production and Operations Symposium, Oklahoma City, Oklahoma, USA, 23–26 March. SPE-164476-MS. <http://dx.doi.org/10.2118/164476-MS>.
- Wu, Y., Wang, K.-S., Hu, Z. et al. 2009. A New Method for Fast Screening of Long Term Thermal Stability of Water-Soluble Polymers For Reservoir Conformance Control. Presented at the SPE Annual Technical Conference and Exhibition, New Orleans, 4–7 October. SPE-124257-MS. <http://dx.doi.org/10.2118/124257-MS>.
- Wyld, J.J. and O'Neil, B.J. 2011. Environmentally-acceptable Replacement of 2-Butoxyethanol: A High Performance Alternative for Fracturing Applications. Presented at the SPE International Symposium on Oilfield Chemistry, The Woodlands, Texas, USA, 11–13 April. SPE-141099-MS. <http://dx.doi.org/10.2118/141099-MS>.
- Wyld, J.J. and Slayer, J. 2009. Development, Testing and Field Application of a Heavy Oil Pipeline Cleaning Chemical: A Cradle to Grave Case History. Presented at the SPE Western Regional Meeting, San Jose, California, 24–26 March. SPE-119688-MS. <http://dx.doi.org/10.2118/119688-MS>.
- Wyld, J.J., Coscio, S.E., and Barbu, V. 2010. A Case History of Heavy-Oil Separation in Northern Alberta: A Singular Challenge of Demulsifier Optimization and Application. *SPE Prod & Oper* **25** (1): 19–24. SPE-117177-PA. <http://dx.doi.org/10.2118/117177-PA>.
- Xie, T., Li, C., Pournik, M. et al. 2005. An Experimental and Modeling Investigation of Acid-Created Channels in Sandstone. Presented at the SPE European Formation Damage Conference, Sheveningen, The Netherlands, 25–27 May. SPE-94566-MS. <http://dx.doi.org/10.2118/94566-MS>.
- Xu, B., Hill, A.D., Zhu, D. et al. 2011. Experimental Evaluation of Guar Fracture Fluid Filter Cake Behavior. Presented at the SPE Hydraulic Fracturing Technology Conference, The Woodlands, Texas, USA, 24–26 January. SPE-140686-MS. <http://dx.doi.org/10.2118/140686-MS>.
- Xu, L. and Fu, Q. 2012. Proper Selection of Surfactant Additive Ensures Better Well Stimulation in Unconventional Oil and Gas Formations. Presented at the SPE Middle East Unconventional Gas Conference and Exhibition, Abu Dhabi, UAE, 23–25 January. SPE-153265-MS. <http://dx.doi.org/10.2118/153265-MS>.

- Xu, W., Thiercelin, M.J., Ganguly, U. et al. 2010. Wiremesh: A Novel Shale Fracturing Simulator. Presented at the International Oil and Gas Conference and Exhibition in China, Beijing, 8–10 June. SPE-132218-MS. <http://dx.doi.org/10.2118/132218-MS>.
- Yaghoobi, H. 1994. Laboratory Investigation of Parameters Affecting CO₂-Foam Mobility in Sandstone at Reservoir Conditions. Presented at the SPE Eastern Regional Meeting, Charleston, West Virginia, 8–10 November. SPE-29168-MS. <http://dx.doi.org/10.2118/29168-MS>.
- Yang, C. 1995. The Alkaline-Surfactant-Polymer Combination Flooding and Application to Oilfield EOR. Presented at the Eighth EAPG Improved Oil Recovery Symposium Vienna, Austria, 15–17 May.
- Yang, F., Nasr-El-Din, H.A., and Al-Harbi, B.M. 2012. Acidizing Sandstone Reservoirs Using HF and Formic Acids. Presented at the SPE International Symposium and Exhibition on Formation Damage Control, Lafayette, Louisiana, USA, 15–17 February. SPE-150899-MS. <http://dx.doi.org/10.2118/150899-MS>.
- Yang, J. 2002. Viscoelastic wormlike micelles and their applications. *Curr. Opin. Colloid Interface Sci.* **7** (5–6): 276–281. [http://dx.doi.org/10.1016/S1359-0294\(02\)00071-7](http://dx.doi.org/10.1016/S1359-0294(02)00071-7).
- Yang, J. and Jovancevic, V. 2009a. Corrosion Inhibitors for Oilfield Applications. US Application Patent No. 20090181867.
- Yang, J. and Jovancevic, V. 2009b. Microemulsions Containing Oil Field Chemicals Useful for Oil and Gas Field Applications. US Patent No. 7,615,516.
- Yang, J. and Jovancevic, V. 2010. Microemulsion Containing Oil Field Chemicals Useful for Oil and Gas Field Applications. US Patent No. 7,851,414.
- Yi, T., Fadili, A., Ibrahim, M.N. et al. 2009. Modeling the Effect of Asphaltene on the Development of the Marrat Field. Presented at the 8th European Formation Damage Conference, Scheveningen, The Netherlands, 27–29 May. SPE-120988-MS. <http://dx.doi.org/10.2118/120988-MS>.
- Yin, G., Grigg, R.B., and Svec, Y. 2009. Oil Recovery and Surfactant Adsorption during CO₂-Foam Flooding. Presented at the Offshore Technology Conference, Houston, 4–7 May. OTC-19787-MS. <http://dx.doi.org/10.4043/19787-MS>.
- Youngman, R., Okell, P.R., and Akbar, S. 2002. Proppant Composition for Gas and Oil Well Fracturing. US Patent No. 6,372,678.
- Yousef, A.A., Al-Saleh, S., and Al-Jawfi, M.S. 2012. Improved/Enhanced Oil Recovery from Carbonate Reservoirs by Tuning Injection Water Salinity and Ionic Content. Presented at the SPE Improved Oil Recovery Symposium, Tulsa, USA, 14–18 April. SPE-154076-MS. <http://dx.doi.org/10.2118/154076-MS>.
- Youssef, N., Elshahed, M.S. and McInerney, M.J. 2009. Microbial Processes in Oil Fields: Culprits, Problems, and Opportunities. In *Advances in Applied Microbiology*, ed. Laskin, A. Sariaslani, S. Gadd, G. Vol. 66, 141-251. Burlington: Academic Press. [http://dx.doi.org/10.1016/S0065-2164\(08\)00806-X](http://dx.doi.org/10.1016/S0065-2164(08)00806-X).
- Zaitoun, A. 2009. Improved Oil and Gas Recovery by Polymer Technology: Epr, Water Shutoff and Sand Control. SPE Distinguished Lecturer Program, Society of Petroleum Engineers, Richardson, Texas.
- Zaitoun, A. and Kohler, N. 1989. Process for the Selective Reduction of Water Inflows in Oil or Gas Producing Wells. US Patent No. 4,842,071.
- Zaitoun, A., Kohler, N., Bossie-Codreanu, D. et al. 1999. Water Shutoff by Relative Permeability Modifiers: Lessons from Several Field Applications. Presented at the SPE Annual Technical Conference and Exhibition, Houston, 3–6 October. SPE-56740-MS. <http://dx.doi.org/10.2118/56740-MS>.
- Zaitoun, A., Makakou, P., Blin, N. et al. 2012. Shear Stability of EOR Polymers. *SPE J.* **17** (2): pp. 335-339. SPE-141113-PA. <http://dx.doi.org/10.2118/141113-PA>.
- Zaitoun, A., Rahbari, R., and Kohler, N. 1991. Thin Polyacrylamide Gels for Water Control in High-Permeability Production Wells. Presented at the SPE Annual Technical Conference and Exhibition, Dallas, 6–9 October. SPE-22785-MS. <http://dx.doi.org/10.2118/22785-MS>.

- Zaitoun, A., Tabary, R., Rousseau, D. et al. 2007. Using Microgels To Shut Off Water in a Gas Storage Well. Presented at the International Symposium on Oilfield Chemistry, Houston, 28 February–2 March. SPE-106042-MS. <http://dx.doi.org/10.2118/106042-MS>.
- Zaltoun, A. and Berton, N. 1992. Stabilization of Montmorillonite Clay in Porous Media by High-Molecular-Weight Polymers. *SPE Prod Eng* 7 (2): 160–166. SPE-19416-PA. <http://dx.doi.org/10.2118/19416-PA>.
- Zaltoun, A., Kohler, N., and Guerrinl, Y. 1991. Improved Polyacrylamide Treatments for Water Control in Producing Wells. *J Pet Technol* 43 (7): 862–867. SPE-18501-PA. <http://dx.doi.org/10.2118/18501-PA>.
- Zemaitis, Jr., J.F., Clark, D. M., Rafal, M., Scrivner, N.C. 1986. *Handbook of Aqueous Electrolyte Thermodynamics: Theory and Application*. New York: DIPR, American Institute of Chemical Engineers.
- Zenone, V.E., Allen, H.L., and Edenbor, H.M. 2002. Bioremediation as a Removal Response Action at OPA Sites. Presented at the International Oil Spill Conference's Freshwater Spills Symposium Cleveland, Ohio, 19–21 March.
- Zerhoub, M., Touboul, E., Ben-Naceur, K. et al. 1994. Matrix Acidizing: A Novel Approach to Foam Diversion. *SPE Prod & Oper* 9 (2): 121–126. SPE-22854-PA. <http://dx.doi.org/10.2118/22854-PA>.
- Zhang, H. and Bai, B. 2010. Preformed Particle Gel Transport Through Open Fractures and its Effect on Water Flow. Presented at the SPE Improved Oil Recovery Symposium, Tulsa, 24–28 April. SPE-129908-MS. <http://dx.doi.org/10.2118/129908-MS>.
- Zhang, N.S., Somerville, J.M., and Todd, A.C. 1993. An Experimental Investigation of the Formation Damage Caused by Produced Oily Water Injection. Presented at the Offshore Europe, Aberdeen, 7–10 September. SPE-26702-MS. <http://dx.doi.org/10.2118/26702-MS>.
- Zhang, Y., Gao, K. and Schmitt, G. 2011. Inhibiting Steel Corrosion in Aqueous Supercritical CO₂ Conditions. *Materials Performance* 50 (9): 54–59.
- Zhou, D., Yan, M., and Calvin, W.M. 2012. Optimization of a Mature CO₂ Flood - from Continuous Injection to WAG. Presented at the SPE Improved Oil Recovery Symposium, Tulsa, 14–18 April. SPE-154181-MS. <http://dx.doi.org/10.2118/154181-MS>.
- Zhou, Z. and Law, D.H.S. 1998. Swelling Clays in Hydrocarbon Reservoirs: The Bad, the Less Bad, and the Useful, Report, Research Council, Edmonton, Alberta.
- Zhou, Z.J., Gunter, W.O., and Jonasson, R.G. 1995. Controlling Formation Damage Using Clay Stabilizers: A Review. Presented at the Annual Technical Meeting, Calgary, 7–9 June. PETSOC-95-71. <http://dx.doi.org/10.2118/95-71>.
- Ziauddin, M. 2011. Some Fundamentals of CO₂ EOR. Sugar Land, Texas: Schlumberger Technology Company.
- Ziauddin, M., Frenier, W.W., and Lecerf, B. 2002a. Evaluation of Kaolinite Clay Dissolution by Various Mud Acid Systems (Regular, Organic and Retarded). Presented at the 5th International Conference and Exhibition on Chemistry and Industry, Manana, Bahrain, 14–16 October.
- Ziauddin, M., Kotlar, H.K., Vikane, O. et al. 2002b. The Use of a Virtual Chemistry Laboratory for the Design of Matrix Stimulation Treatments in the Heidrun Field. Presented at the European Petroleum Conference, Aberdeen, 29–31 October. SPE-78314-MS. <http://dx.doi.org/10.2118/78314-MS>.
- Ziauddin, M.E. and Bize, E. 2007. The Effect of Pore-Scale Heterogeneities on Carbonate Stimulation Treatments. Presented at the SPE Middle East Oil and Gas Show and Conference, Kingdom of Bahrain, 11–14 March. SPE-104627-MS. <http://dx.doi.org/10.2118/104627-MS>.
- Ziauddin, Murtaza. 2012. Personal Communication. Sugarland, Texas: Schlumberger Technology Company.
- Zou, C. 2006. *Development and Testing of an Advanced Acid Fracture Conductivity Apparatus*. MS thesis, Texas A&M University, College Station, Texas.

AUTHOR INDEX

A

- Abad, C., 273, 322
Abass, H.H., 339
Abayarathn, D., 118
Abbott, J., 344, 345
Abdallah, W., 40, 88, 97, 105, 191, 374, 381, 392
Abdel-Aal, H.K., 75
Abdou, M., 79, 80
Abdulahad, G., 130
Abe, M., 308
Abhilash, M., 295
Ables, J., 292
Abou-Sayed, I., 256
Abriam, G., 70
Acharya, A.R., 280
Achour, M., 143, 478
Acock, A.M., 227, 228
Acosta, E.J., 429
Adachi, J., 355, 357
Adams, T.A., 330
Adkins, S., 434
Aggour, M., 75
Ahmad, A.J., 178, 179, 181, 199
Ahmad, T., 225
Ahmadi, M., 98
Ahmed, J., 66
Ainley, B.R., 324, 475
Akbar, A., 69
Akbar, S., 209, 210, 339
Akbarzadeh, K., 103, 104
Akinlade, O., 178
Akrad, O.M., 263, 268, 351
Al Harthy, S.A., 459
al Shureqi, H., 391, 395, 439
Al-Abduwani, F.A.H., 94
Al-Alawi, M.J., 195
Al-Anazi, H.A., 244, 255
Al-Anzi, E., 223
Al-Asmi, K., 99
Al-Awadi, M., 132, 143
Al-Dahlan, M.N., 175, 177
Al-Dirweesh, S.M., 244
Al-Driweesh, S.M., 224–226, 478
Alexander, T., 38
Al-Farisi, O., 133
Al-Felasi, A., 133
Al-Furaidan, Y.A., 219
Al-Ghamdi, A.H., 225
Al-Hamaidan, A.Y., 197
Al-Harbi, B.G., 175, 177
Al-Harbi, B.M., 177
Al-Harthy, S., 123, 125, 156–158, 180, 181, 183
Al-Humaidan, A.Y., 72, 197, 198
Al-Humaidi, A.S., 211
Ali, A., 157
Ali, S.A., 98, 165, 174, 176, 181, 182, 184, 191, 193, 194, 199, 201–203, 230, 259
Ali, S.M.F., 432, 440
Al-Jawfi, M.S., 400, 401
Al-Jubran, H.H., 249, 364
Alkafeef, S.F., 460
Al-Khonaini, T., 211
Alleman, D., 228
Allen, H.L., 491, 504
Allen, T.E., 497
Allenson, S.J., 315
Allison, D., 177
Al-Marzouqi, M., 133
Al-Mayouf, A.M., 159
Al-Mjeni, R., 377, 384, 387, 388
Almond, S.W., 297
Al-Muhaish, A.S., 192, 194
Al-Mutairi, S.H., 138, 139, 145, 146, 243, 478
Al-Mutawa, M., 223
Al-Naimi, K.M., 249, 364
Al-Najim, A., 211
Al-Nakhli, A.R., 224–226
Al-Obied, M.A., 138, 139, 146
Al-Qahtani, M.A., 366
Al-Saiari, H., 78, 84
Al-Saleh, S., 400, 401
Alshehri, A., 383
Alvarado, V., 461
Al-Yami, A., 211
Al-Yami, I., 138, 139, 146
Ammer, J.R., 421, 423, 425
Amott, E., 392, 393
Anderson, G.A., 456, 461
Anderson, M.S., 169
Anderson, W.G., 379, 381–383
André, L., 125
Andreozzi, P.A., 188
Appel, C., 380
Appicciutoli, D., 245
Arachchilage, G.P., 434
Arceneaux, C., 467
Arf, T.G., 430–431
Armstrong, K., 283, 289, 290, 342
Arnab, W.D.V., 211
Arora, S.M., 377, 384, 387, 388, 456
Arthur, J.D., 144, 260, 263, 264, 349, 354, 484
Asen, S.M., 402

- Asheim, T.I., 77, 78
 Aske, N., 102–107
 Assem, A.I., 138, 146
 Aubin, D.J.S., 498–500
 Augustinovic, A., 408, 409, 505
 Ault, M.G., 318
 Austad, T., 399–402
 Austria, J.J.C., 178, 181
 Aveyard, R., 116
 Awan, A.R., 389
 Ayello, F., 67
 Ayoub, J.A., 314
 Azem, W., 476, 483
- B**
- Babcock, R.E., 279
 Bae, J.H., 394, 438, 439
 Bai, B., 446
 Baihly, J., 38
 Bakeev, K.N., 85
 Baker, H.R., 312
 Baker, R.W., 204
 Bakke, J.M., 73
 Balakotaiah, V., 140, 141
 Bale, G.E., 209
 Ball, C.L., 197
 Balzer, D., 115
 Bang, V.S.S., 98
 Baranet, S.E., 241
 Barati, R., 320, 321, 452
 Barbu, V., 119
 Barnes, J.R., 429
 Barrett, N.D., 245
 Barron, A.R., 335, 336
 Barthelmy, D., 34
 Bartko, K.A., 366
 Barton, A.F.M., 25
 Bartosek, M., 83
 Bas, F.v.d., 314
 Baser, B., 210, 322
 Batenburg, D.v., 292, 302
 Batrakov, V.V., 186
 Baumgarten, D., 249, 250, 364
 Baycroft, P.D., 261, 474
 Bazan, L.W., 355, 359
 Bazin, B., 97–99, 118, 130, 219
 Beal, C., 3
 Beale, J.A.F., 187
 Beaman, D.J., 225
 Beaumont, J., 455
 Becker, J.R., 61, 63, 99
 Becker, K.W., 497, 500, 501
 Beckwith, R., 293, 299, 350, 472, 490–492
 Bedbur, K., 196
 Bedrikovetsky, P.G., 455
 Beeder, J., 409
 Behrmann, L.A., 285
 Belcher, C.K., 329, 330
 Bell, T., 83
 Bemelaar, J., 151, 160, 195
 Benayan, M., 99
 Bende-Jacq, D., 455
 Benham, A.L., 419
 Benmekki, E.H., 13
 Ben-Naceur, K., 218
 Bennion, B., 87, 92
 Bennion, D.B., 87
 Bergfeldt, B., 481
 Bergman, R.F., 497, 501
 Berkhof, R., 115
 Berkland, C., 321, 452
 Berkley, R.E., 244
 Berkner, A.B., 505
 Bernard, G.C., 421
 Berry, S.L., 196
 Bersworth, F.C., 149, 196
 Berton, N., 200, 202
 Bhakta, A.S., 429
 Bhardwaja, A., 114
 Bhattacharjee, S., 202
 Bhuyan, D., 443
 Binks, B.P., 116
 Bird, R.B., 33
 Birketveit, O., 408, 409, 505
 Birou, P., 225
 Bittner, C., 432
 Bivins, C.H., 280, 281, 287, 288, 342, 343
 Bize, E., 135, 136
 Bjørnstad, T., 457
 Black, C.J.J., 401
 Blagodatskikh, I.V., 309
 Blanshard, J.M.V., 241
 Blauch, M.E., 478, 486
 Blevins, S., 67
 Blin, N., 412
 Blumer, D., 143, 478
 Boak, L., 62
 Boak, L.S., 424
 Bobrosky, D., 249, 250, 364
 Bockris, J.O., 66
 Bodi, T., 90, 97
 Bodtker, G., 409
 Boek, E.S., 93
 Bohm, B.K., 144, 260, 263, 264, 349, 354, 484
 Boles, J.L., 149, 196
 Bolster, R.N., 312
 Bomgardner, M.M., 483, 486, 488
 Boney, C.L., 11, 12, 123, 210, 214, 280, 281, 287, 288, 342, 343, 351, 362, 363
 Bonis, M.R., 67
 Bonner, J.S., 18
 Boonstra, T.O., 160
 Bordia, R.K., 335
 Børeng, R., 79
 Boschee, P., 476, 478, 483, 484, 486, 488, 490
 Bossart, K., 159
 Bossie-Codreanu, D., 445–448
 Boswood, D.W., 193
 Bourg, P., 85
 Bourne, H.M., 20, 79, 330
 Bourrel, M., 114
 Boyd, P.A., 316
 Boyer, C., 38, 263–265
 Brady, B., 231
 Brady, B.H., 356
 Brady, M., 156–158, 181, 183, 192, 193, 225, 228, 246, 247

- Brandao, E.M., 239
 Brandes, B.E., 501
 Brannon, H.D., 283, 285, 318, 320, 341
 Bredal, F., 143, 478
 Breukel, B., 240
 Brezinski, M.M., 190, 195
 Britt, L.K., 124, 245, 250, 346, 351, 352
 Britton, C., 435
 Britton, L.N., 428, 434
 Brookley, J.G., 157, 182
 Brooks, F.A., 4
 Brown, B., 64
 Brown, E., 285, 351, 465
 Brown, G.L., 110
 Brown, J.E., 252, 253
 Brown, J.M., 79, 330
 Brown, K.E., 4
 Brown, L.D., 56
 Brown, M., 79
 Brown-Jr, P.S., 202, 204
 Brunauer, S., 171
 Bryant, J., 298, 299, 311
 Bryant, S.L., 98, 173
 Bryndza, H.E., 505
 Buckley, J.S., 40, 88, 97, 103, 105, 191, 374, 381, 392, 398, 399
 Buckley, S.E., 375, 376
 Buhaug, J., 73
 Buijse, M.J., 141, 240, 253
 Bulkley, R., 314
 Buller, D.C., 98, 263
 Bulova, M., 214
 Bulova, M.N., 343, 362
 Bulte, H., 152, 166, 179
 Bunge, A.L., 437
 Burke, J., 25–27
 Burke, P., 398
 Burman, J.W., 324
 Burnett, D.B., 411, 482, 484
 Buske, G.R., 197
 Bustos, O.A., 123, 125, 180, 181, 220, 245, 256, 265, 308, 369
 Butler, J.N., 25
 Butula, K.K., 343
 Byars, H.G., 61, 63, 67
- C**
- Caili, D., 451
 Calvin, W.M., 420
 Camacho, A., 64
 Campbell, A.R., 411, 412
 Campbell, D.J., 475, 478, 485
 Campbell, S., 68, 70
 Candler, J., 476, 483
 Canevari, G.P., 497, 500, 501
 Cantu, L.A., 316
 Card, R., 221
 Card, R.J., 283, 287, 289–291, 306, 339, 342
 Carman, P.S., 305, 319
 Carnegie, A., 40, 79, 80, 88, 97, 105, 191, 374, 381, 392
 Carpenter, J.F., 328
 Carrigan, C.R., 359
 Carrillo, A.L., 203
 Carruthers, N., 66
 Carstens, A., 160
 Carter, R.H., 348
 Carvalho, C.R.G.D., 226
 Casero, A., 253
 Cassidy, J.M., 193, 194
 Casto, W., 337
 Castro Dantas, T.N., 308
 Caveny, W.J., 342
 Cawiezal, K.E., 223, 225, 286, 287, 319
 Cayias, J.L., 429
 Cenegy, L.M., 332, 424, 478
 Chambers, David J., 22, 324
 Chambers, R., 83
 Chan, K., 228, 246
 Chang, F.F., 31, 126, 146–149, 151–157, 160, 178–180, 211, 213, 220–223, 224, 226–228, 238, 240, 242, 245, 306
 Chang, H.L., 377
 Chang, S.-H., 421
 Chapman, M.A., 333, 334, 336, 338, 353
 Chappell, G.D., 424
 Charbonnel, P., 219
 Charkhutian, K.B., 159, 160
 Chase, B., 221, 306
 Chatriwala, S., 223
 Chauveteau, G., 448
 Chekhonin, E., 371
 Chen, F., 450
 Chen, L., 118
 Chen, P., 75, 77, 78
 Chen, T., 75
 Chen, Y., 193, 214, 308, 343, 362, 369, 403
 Cheng, A., 474
 Cheng, J., 406
 Cheng, L., 217
 Cheng, X., 144
 Cheng, Y., 300, 320
 Cherian, J., 376
 Cherukupalli, P.K., 377, 384, 387, 388, 456
 Chesnut, G.R., 424
 Chik, J., 300
 Chiotis, E.D., 43, 44
 Chmilowski, W., 221, 306
 Choi, N.H., 256
 Chokshi, K., 68
 Christensen, T., 328
 Chuang, J., 85
 Cinco-Ley, H., 267
 Cipolla, C.L., 269–271, 279, 350, 357, 358
 Civan, F., 9, 89, 455
 Clampitt, R.L., 405
 Clark, B., 263–265
 Clark, P.E., 295–297, 303–304
 Clark, W.J., 132, 143, 165, 259
 Clarke, J., 181, 182
 Clayton, J.R. Jr., 492, 494–497, 499, 500
 Clegg, J.D., 4
 Clements, K., 408, 409, 505
 Clewlow, P.J., 66
 Clouse, D., 475
 Clum, E., 210
 Clumpher, C., 505

- Coffey, M.D., 91
 Cogley, D.R., 25
 Cohen, C.-E., 213, 226, 355, 357, 359
 Coker, C.E., 335
 Colaco, A., 226
 Collins, I.R., 19, 20, 75, 101, 400, 401
 Conrad, P., 85, 86
 Constien, V.G., 33, 275–283, 286, 287, 294–296, 305
 Cooke, C.E., 221
 Coolbaugh, T., 502
 Copur, M., 499
 Cordova, M., 321, 452
 Correria, S., 83
 Coscio, S.E., 119
 Costantino, S.A., 335
 Costerton, J.W., 273
 Cotton, F.A., 4, 200
 Coughlin, B.J., 260, 263, 264, 349, 354
 Couillet, I., 308
 Coulter, A.W., 195, 245
 Courbin, C., 75
 Coviello, T., 298
 Cowan, J.C., 59
 Crabtree, M., 58, 59, 61, 62
 Craig, F.F. Jr., 382
 Crameik, T.D., 420
 Cramer, D.D., 262, 263, 349, 351, 366
 Crank, J., 251
 Crawford, C.C., 436
 Crawford, D.L., 312
 Crawford, M.E., 436
 Crawshaw, J.P., 93
 Creek, J.L., 79, 103, 373
 Crews, J.B., 224, 225, 261, 273, 316, 321, 322, 329, 330, 474
 Cribbs, M., 79, 373
 Crolet, J.L., 67
 Crookshank, S.L., 416, 423
 Crowe, C.W., 146, 175, 180, 194, 195, 213, 218, 229, 230, 241, 245, 246
 Crump, D.K., 128–130, 160, 195, 196
 Cudney, G., 218
 Curry, D., 505
 Curtis, J.A., 181
 Cussler, E.L., 204
 Cutler, R.A., 335
- D**
- da Motta, E.P., 173
 Dabbousi, B.O., 192, 194
 Daccord, G., 122, 140, 141
 Daffin, M.D., 200, 204
 Daharu, R., 432
 Dake, L.P., 4
 Daling, P.S., 496, 498, 502
 Dalmazzone, C., 115
 Dalrymple, E.D., 228
 Damaskin, B.B., 186
 Daneshy, A.A., 367
 Danican, S.C., 324, 325
 Daniel, S., 316
 Daniels, J., 357
 Dantas Neto, A.A., 308
 Darcy, H., 4, 45
 Darley, H.C.H., 4
 Darling, D., 467
 Dashdiev, R.A., 501
 Dashti, Q.M., 256
 Daussin, R., 26, 27
 Davidson, B.M., 357
 Davies, D.R., 311, 341
 Davies, J.T., 113, 429
 Davies, M., 61, 390
 Davies, S.N., 152, 166, 179, 180, 193, 214–217, 325, 422, 454
 Davis, L.E., 60
 Davison, J.M., 221, 306
 Dawe, R.A., 43, 44
 Dawson, J.C., 302, 315, 317
 Dawson, J.L., 64
 de Boer, P., 240
 De Cordt, F.L.M., 159, 160
 de Kruijff, A., 459
 de Kruijff, A.S., 311
 de Rozieres, J., 31, 238, 242
 De Santis, L.M., 313
 Dean Rhue, R., 380
 DeGette, D., 472
 Degre, G., 455
 DeKerlegand, K., 467
 Del Villano, L., 471
 Delshad, M., 217, 426, 428, 434, 436, 442–444, 456, 461
 Demarco, G., 502
 Deng, J., 251
 Denney, D., 213, 502
 Desai, B., 190
 Dessinges, M.N., 317
 Deutch, J., 467, 479
 DeVine, C.S., 474
 Dewprashad, B., 339
 d'Huteau, E., 361
 Di Lullo Arias, G.F., 178, 179, 181, 199
 di Lullo, G., 297, 299
 Dibble, W.E. Jr., 500, 501
 Dickson, K.R., 341
 Dietz, D.N., 455
 Dill, W.R., 194, 195
 Dillon, E.T., 73
 DiLullo, G.A., 178, 181, 341
 Ding, Y., 144
 Dirkwager, H., 429
 Dismuke, K., 471, 476
 Dismuke, K.D., 190, 204, 241, 248, 317
 Dixon, R.E., 187
 Dobos, K., 113
 Domelen, M.S.V., 240, 430, 432, 439
 Donaldson, E.C., 394
 Dong, C., 79, 373
 Dong, Z., 262
 Dovan, H.T., 451
 Dowden, W.E., 419
 Drzewinski, M.A., 85
 Duenckel, R., 333, 334, 336, 338, 353
 Duffin, G.F., 188
 Dunand, A., 32

Dunlop, A.K., 64
 Dybvik, L., 471
 Dyer, S.J., 424
 Dzubin, B., 350

E

Earl, R.B., 312
 Earle, S.A., 498, 502
 Eaton, B.A., 48
 Economides, M.J., 7, 11, 12, 123–125, 130, 141, 355, 356
 Edenbor, H.M., 491, 504
 Edwards, M.A., 471
 Efird, K.D., 67
 Efroymsen, R.A., 502, 503
 Ehlig-Economides, C., 7
 Eikerts, J.V., 277
 Ejan, A.B., 319–321
 Elbel, J., 231, 245, 250
 Elbel, J.L., 328, 346, 352
 Eliseev, V., 484
 Eliseeva, K.E., 484
 El-Monier, E.A., 98, 200–203, 329
 Elnawawy, O.A., 25
 El-Rabaa, W., 133, 154
 Elshahed, M.S., 409
 Ely, J.W., 312, 314, 345, 346, 348
 Emmett, P.H., 171
 Emmons, D.H., 424
 England, K.W., 326
 Engwall, S.J., 61
 Enick, R.M., 421, 423, 425
 Eoff, L.S., 228
 Erbstoesser, S.R., 208, 209
 Erenpreiss, M., 264
 Erhahon, L., 178
 Ermel, E., 181, 182
 Estievenart, C., 75
 Ettinger, R.A., 21, 214
 Ewing, J., 486
 Eykamp, W., 204
 Eylander, J.G.R., 39

F

Fadhel, B.A., 72, 197, 198
 Fadili, A., 93
 Fahim, M.A., 75
 Faircloth, R.J., 423
 Falcone, J.S. Jr., 435
 Falls, A.H., 214
 Fan, T., 405
 Fan, Y., 87, 113, 405, 410
 Fan, Z., 189
 Fareid, E., 328
 Farlow, J.S., 492, 494–497, 499, 500
 Farouq Ali, S.M., 450
 Fast, C.R., 282
 Faust, M., 116, 117
 Favero, C., 305, 404, 410, 411, 413
 Feasey, N., 19, 101
 Feasey, N.D., 204, 470
 Felder, R., 505
 Feng Li, R., 442
 Feng, X., 112

Feraud, J.-P., 287, 291, 339, 342
 Fetkovich, M.J., 7
 Fineman, M.N., 110
 Fink, J.K., 4, 65, 92, 99, 111, 112, 116, 184, 199, 200,
 202–204, 314, 315, 329, 332, 404, 430, 449, 450,
 457, 490, 496–498, 500, 501, 504
 Finol, J., 391, 395, 439
 Fiocco, R.J., 497, 500, 501
 Fischer, E.R., 66
 Fisher, M.K., 357
 Fisher, R.S., 477
 Fjelde, I., 402
 Fletcher, P.D.I., 116
 Fogel, Y., 405
 Fogler, H.S., 39, 98, 127–130, 133, 141, 143, 144,
 146–148, 151–154, 156, 172–174, 455
 Foley, W.L., 394, 438, 439
 Fontana, M.G., 63
 Ford, W.G.F., 129, 196, 245
 Førdedal, H., 104
 Foster, J.P. Jr., 505
 Fox, C., 417
 Francini, P.-A., 228, 246
 Francis, E.S., 178, 181
 Frasch, H., 126
 Fredd, C.N., 129, 133, 140, 141, 146–148, 151–157,
 160, 214, 225, 228, 246, 247, 280, 281, 287, 288,
 342, 343, 362, 363
 Frenier, W.W., 2, 3, 9, 10, 13, 25, 31, 38, 55–61, 64, 65,
 67, 72, 75–79, 82–86, 93, 95, 103, 106, 117, 128–
 130, 143–145, 149–160, 164–167, 172, 174–176,
 179–181, 183, 185–190, 192, 193, 195–198, 200,
 203, 204, 207, 214–217, 220–223, 230, 240, 241,
 248, 306, 317, 325, 330–332, 389, 394, 411, 417,
 422–424, 429, 437, 441, 442, 446, 454, 463, 469,
 477, 478, 499
 Friberg, S., 103
 Frick, T.P., 130, 141
 Friedmann, F., 215
 Friedrich, B., 487
 Friedrich, S., 405
 Frigo, D.M., 39, 85
 Frost, K., 26, 27
 Fu, B., 85, 228
 Fu, D., 152, 166, 179, 221, 227, 228, 252, 253, 306
 Fu, G., 78, 84
 Fu, P., 359
 Fu, Q., 327
 Fuller, M.J., 179, 227, 228
 Fulton, D.D., 213
 Funkhouser, G.P., 228, 306

G

Gaeberlein, P., 405
 Gagner, M.G., 84
 Gaillard, N., 305, 404, 410, 411, 413
 Gale, W.W., 385
 Gall, B., 318
 Gall, J.W., 398
 Gallus, J.P., 315
 Galvan, J., 476, 483
 Gamble, C., 85
 Ganguly, U., 359

- Gao, K., 63
 Garcia, M., 79
 Garcia, W.N., 213, 226, 247
 Garcia-Lopez De Victoria, M., 227, 228
 Gardner, D.C., 277
 Gardner, G.S., 187
 Garrell, M., 410
 Garvin, T.R., 297
 Garza, T., 313
 Garzon, F.O., 241
 Gauglitz, P.A., 214, 215
 Gdanski, R.D., 141, 169, 170, 172, 174, 177, 214, 317
 Geertsma, J., 275, 355
 Geffen, T.M., 410
 Geoghagan, A., 227, 228
 Geokchaev, T.B., 501
 George, E., 165, 229
 George-Ares, A., 500
 Geraci, J.R., 498–500
 Gerdes, S., 162
 Ghaeli, H., 297
 Gharfeh, S.G., 103
 Ghiselin, D., 265
 Gholami, V., 83
 Gidley, J.L., 143, 273, 274, 312, 345
 Gijtenbeek, K.A.W.v., 200
 Gil, I., 355, 359
 Gillard, M.R., 360–363, 366
 Giovannetti, B., 411
 Glasbergen, G., 130, 143, 211, 212
 Glenat, P., 85
 Glynn, P.D., 25
 Goel, N., 311
 Gogarty, W.B., 432
 Goldszal, A., 114
 Gomaa, A.M., 220, 247, 248
 Gomez, J.R., 181
 Gonzalez, D.L., 83
 Goosen, M.F.A., 116
 Gordon, J.E., 236, 243
 Gougler, P.D. Jr., 195
 Graham, A., 62
 Graham, G.M., 83, 85, 118, 424
 Grande, K.V., 102
 Grannan, S., 143, 144, 189
 Grant, W.D., 178
 Grassi, M., 298
 Grattan, K.T.V., 211
 Grattoni, C.A., 43, 44
 Graue, D.J., 437
 Gray, G.R., 4
 Grebe, J.J., 126
 Green, D.W., 371, 404, 450
 Greenlees, W.M., 313
 Greenwald, H.L., 110
 Gregory, D.P., 127
 Grieser, B., 292
 Griffin, W.C., 113
 Grigg, R.B., 421, 422
 Grigoryan, A., 409
 Grimshaw, T.W., 473
 Groat, C.G., 473
 Gröllmann, U., 411
 Growcock, F.B., 4, 90, 186–188
 Guggenheim, D.E., 498, 502
 Guichard, J.A. III, 177
 Guillot, D., 4, 32, 472
 Gulbis, J., 272, 276, 283, 286, 287, 289–291, 297–301, 304, 312, 316, 318, 319, 324, 328, 333, 334, 336, 338, 339
 Gulbrandsen, E., 67
 Gunter, W.O., 201
 Gupta, D.V.S., 79, 305, 312, 313, 320, 330, 467, 485
 Gurfinkel, M.E., 387, 436, 461
 Guzman, M., 432
- H**
 Haddad, Z.A., 351
 Hagen, G., 8
 Hagen, T., 77, 78
 Hall, B.E., 194, 324
 Halterman, M.P., 129, 196
 Halvaci, M., 297
 Hamadi, A.S., 115
 Hammami, A., 94, 103, 104
 Han, L., 90
 Han, W., 442, 456
 Handren, P.J., 292, 305
 Haney, J.A., 178
 Hanna, H.S., 430
 Hansen, C.M., 25, 26, 250
 Hansen, E.W.M., 108
 Harald Aulfem, I., 102–107
 Harris, F.N., 126
 Harris, P.C., 260, 292, 298, 302, 303, 311, 324
 Harris, W. Jr., 285
 Harrison, N.W., 126
 Hartlanda, S., 114
 Hartman, R.L., 38, 164, 167, 172, 180, 331
 Hartog, F.A., 39
 Harvey, C.P., 421
 Haselgrave, J.A., 66
 Hassell, H.L., 64
 Hassler, G.L., 129
 Hausler, R.H., 186
 Havlik, W., 118
 Hawkins, G.W., 33, 275–277, 279–283, 290, 291, 294–296, 305, 318
 Hawkins, M.F.J., 6
 Haydell, G.A., 269
 Hayes, D., 411
 Haynes, H.H., 84
 Heath, S.M., 79, 330
 Hedges, W., 64
 Heidersbach, R., 63, 69
 Heiken, K.R., 256, 265
 Heinson, C., 427, 428, 430, 433, 434
 Hekim, Y., 173
 Heller, J.P., 421
 Hemmingsen, P., 103, 104
 Hendrick, J.E., 195
 Hendrickson, A.R., 126, 133
 Henriksen, N., 328
 Henry, H., 68
 Henry, W., 37
 Henthorne, L., 398, 413

- Hernandez, A.N., 222, 227, 306, 307, 321, 322, 348
Herschel, W., 314
Hess, G., 11, 472
Heus, M., 160
Hewartson, J.A., 19, 75
Hezar, L., 99
Hezmela, R., 226
Hicks, K., 68
Higgins, R., 79, 330
Hildebrand, J.H., 25
Hill, A.D., 7, 39, 130, 133, 137, 141–148, 151, 153, 163, 165, 173, 174, 178, 236, 239, 243, 246, 250, 251, 313, 314
Hill, D.G., 72, 165, 190, 194, 197, 200, 204, 219, 225, 229, 241, 246, 411, 471, 475, 476
Hill, E.S.W., 312
Himes, R.E., 200, 204
Hinkel, J.J., 20, 98, 184, 191, 193, 194, 199, 201–203, 326, 351
Hirasaki, G.J., 83, 214, 426, 432, 435, 436, 444
Hlidek, B.T., 312, 349, 367, 368, 485
Hoadley, S.F., 420, 421
Hobbs, J., 292
Hodge, R.M., 272, 276, 286, 287, 289, 297–301, 304, 312, 316, 319, 324, 328, 333, 334, 336, 338, 339
Hoefler, A.M., 214, 343, 362
Hoefner, M.L., 133, 141, 143, 153
Hoff, C., 242
Hoffman, B.T., 416
Hojris, K., 408
Holcomb, A.Y., 505
Holcomb, D.L., 326
Holcomb, W.D., 367
Holditch, S.A., 261, 262, 273, 274, 312, 345, 348, 351, 467, 479
Hollifield, P.K., 189
Hollenbeak, K.H., 202, 204, 245
Hollier, R., 330
Holm, L.W., 419, 421
Holms, B.A., 145, 220, 236, 244
Holstein, E.D., 38
Hongkun, Y., 204
Hoover, D.B., 488
Horner, D.R., 89
Horstmann, D., 456
Horsup, D.I., 68
Hosein, P.R., 360–363, 366
Hou, Q., 454
Howard, G.C., 282
Howard, P.R., 42, 43, 287, 290, 291, 325–327, 339, 342, 351
Howard, R.A., 458
Hsu, T.-P., 411, 426, 428, 456, 459
Hu, X., 69
Hu, Z., 440
Huang, T., 141, 148, 151, 273, 316, 321, 322, 329, 330
Hubert, C., 409
Huddleston, A., 312
Hughes, T., 308
Huh, C., 427, 429, 430
Huizinga, S., 143, 478
Hung, K.M., 141, 153
Hunter, J., 292, 297
Hurst, R.E., 475
Hurtevent, C., 102
Husen, A., 157
Hutchins, R.D., 314, 316, 317, 451, 458
Hutchinson, B.H., 245
- I**
Ibrahim, M.N., 93
Idem, R., 3
Iler, R.K., 165
Ingraffea, A.R., 356
Isidore, C., 63
Islam, M.R., 420, 450
Ivanov, I.Z., 102
- J**
Jack, T.R., 409
Jackson, A.C., 427, 428, 430, 433, 434
Jackson, R.E., 432, 435, 436
Jackson, S., 122, 130
Jacob, S.M., 497, 501
Jacobs, I.C., 98
Jaffe, A.M., 11, 490
Jakhete, S., 328
Jamialahmadi, M., 81
Jante, M.J. Jr., 215
Jaramillo, O.J., 176
Jarrell, P., 417
Jasinski, R.J., 143, 144, 189, 215, 216, 221, 306
Jaspers, H.F., 459
Jauregui, J.A.L., 213, 226, 247
Jayakumar, S., 452
Jayaraman, A., 65
Jenkins, A., 66, 71, 190, 469
Jenneman, G.E., 409
Jennings-Jr, A.R., 218
Jensen, J.A., 215
Jerat, A.C., 313
Jerauld, G., 413
Jermelov, A., 490
Jia, Z., 327
Jimenez-Bueno, O., 157, 158
Jincai, C., 204
Jochen, V., 263–265
Jofa, Z.A., 186
Johnson, C.E. Jr., 437
Johnson, S.J., 320, 321, 452
Johnson, S.M., 359
Johnson, T., 118
Johnston, B.B., 249, 364
Johnston, E.L., 421
Johnston, N.G., 187
Jonasson, R.G., 201
Jones, A.H., 335
Jones, C.K., 484
Jones, I., 211
Jones, J.R., 124
Jones, N.D., 178
Jones, P.W., 147
Jordan, M.M., 19, 78, 101, 118, 204, 470
Josendal, V.A., 419
Joseph, D.D., 22
Joshi, N.B., 390

Jouenne, S., 406
 Jovancevic, V., 67, 75, 76
 Jubran, B.A., 116
 Judzis, A., 505

K

Kabir, M.M.R., 256
 Kakadjian, S.R., 299, 302, 313, 317, 325
 Kalantari-Dahaghi, A., 83
 Kalfayan, L.J., 125, 184, 197, 208, 211, 229, 236, 253,
 332, 478
 Kalia, N., 130
 Kallevik, H., 103, 104
 Kalra, A., 99, 101, 445
 Kam, S.I., 21, 22, 193, 214–217, 325, 422, 454
 Kamel, A.H.A., 279, 307, 308
 Kan, A., 79
 Kan, A.T., 78, 84
 Kang, Y., 66
 Kaplan, E., 410
 Karazincir, O., 441
 Karcher, A., 317
 Kargbo, D.M., 475, 478, 485
 Kaufman, P.B., 264, 323, 328, 331, 349, 485
 Kayhan, M., 3
 Keck, R., 228
 Keck, R.G., 279
 Kefi, S., 222, 227, 228, 306, 307, 321, 322, 348
 Kehle, R.O., 279
 Keijzer, P.P.M., 454
 Kelkar, S.K., 198, 212
 Kell, S., 266, 348–350, 472, 477, 478, 481, 482
 Kelland, M.A., 4, 65–67, 72, 75, 77, 99, 106, 108,
 110–112, 116–117, 151, 184, 203, 241, 246, 323,
 327, 328, 404, 446–450, 453, 467, 471, 472
 Kelly, J., 48
 Kendrick, M., 78
 Kennedy, W.C., 31
 Kern, L.R., 355
 Kesavan, S., 315
 Khaldi, M.H., 175, 177
 Khallad, A., 474
 Khamees, A.A., 129, 130, 135, 145
 Kharrat, A., 103, 104
 Khilar, K., 98, 455
 Khokhlov, A.R., 309, 310
 Khristianovich, S.A., 355
 Kiel, O.G., 377, 378, 396, 397
 Kiel, O.M., 244, 245
 Kilpatrick, P.K., 106
 Kim, B.-Y., 107, 108
 Kim, D.H., 412, 434, 435
 Kim, Y.H., 115
 King, C.L.B., 456, 461
 King, G.E., 264, 349, 351, 363
 King, M.T., 283, 290, 291, 318
 Kirkby, L.L., 297
 Kirkham, B., 362
 Kirkpatrick, W.H., 244
 Kiser, C.E., 193, 194
 Kjolberg, S.A., 328
 Klaus, E.E., 430–431
 Kleppe, J., 389
 Klerk, F.d., 275, 355

Kleverlaan, M., 211
 Kline, W.E., 126, 152, 167, 172
 Klyubin, A., 343
 Knox, J.A., 195
 Koh, H., 412, 434
 Kohler, N., 75, 118, 445–448, 451
 Kokal, S.L., 17, 18, 99–101, 103–105, 107–111
 Kommedal, R., 471
 Komunjer, L., 115
 Kordziel, W., 457
 Koronaios, P., 422
 Kosarev, I.V., 361
 Kotlar, H.K., 167, 174
 Kovalev, Y.A., 310
 Kovscek, A.R., 383
 Kozora, C.J., 484
 Kraemer, C., 361, 362
 Kraiwattanawong, K., 103
 Krause, G., 487
 Krawczyk, M.A., 115
 Kreh, K.A., 193
 Kresse, O., 355, 357, 359
 Kretzschmer, G., 254
 Kruk, K.F., 234, 236, 241, 245
 Krumrine, P.H., 435
 Krupp, F., 467, 479
 Kubala, G., 267, 312, 475
 Kucera, C.H., 187
 Kuklin, A.I., 310
 Kulawardana, E.U., 412, 434
 Kulkarni, M.C., 335, 341
 Kume, N., 178
 Kunzman, W.J., 419
 Kurmayr, M., 130, 141
 Kuron, D., 65, 185
 Kwak, T.Y., 13
 Kwekkeboom, H., 115

L

LaBelle, G., 430–431
 Labine, P., 65
 Labrid, J.C., 173, 174, 183
 Labus, B.N., 65
 Ladva, H.K., 93, 316
 LaFollette, R.F., 367
 Lafuma, F., 303
 Lager, A., 400, 401
 Laing, N., 424
 Lakatos, I.J., 90, 97
 Lakatos-Szabo, J., 90, 97
 Lake, L.W., 174, 371, 374, 376–382, 384, 385,
 387–389, 395, 402–404, 407, 410, 411, 415–417,
 420, 425, 429–431, 433, 434, 436, 443
 Lambert, M.E., 174
 Lambo, A., 409
 Lamy, F., 97–99
 Landry, L., 269
 Lane, J.L., 193, 194
 Lane, R.H., 452
 Langelier, W.G., 59
 Langlotz, B., 405
 Langmuir, D., 23–25
 Langston, M.V., 420, 421
 Lannisbois Drean, H., 455

- Lara, V.c.H., 380
 Larsen, J., 408
 Larsen, R., 296
 Laschewsky, A., 308, 309
 Lashen., E.S., 273
 Lau, J.C.S., 440
 Law, D.H.S., 199, 200
 Lawson, J.B., 214, 423
 Layne, M., 144, 349, 484
 Le Calvez, J., 357
 Le, H., 315, 317
 Leach, P.B., 312
 Lecerf, B., 38, 152, 164, 166, 167, 172, 174–176, 179, 180, 230, 331
 Lee, B.O., 249, 364
 Lee, J.C., 214, 222, 227, 261, 306, 307, 321, 322, 343, 348, 351, 362, 369
 Lee, Y.N., 278, 324
 Lei, C., 295, 296, 303–304
 Leibler, L., 303
 Leinweber, D., 116
 Lemon, P.E., 455
 Lenderman, G.L., 84
 Lenormand, R., 122, 140, 141
 Leontaritis, K.J., 92
 LePage, J.N., 151, 160, 195
 Lesko, T.M., 213, 226
 Lessard, R.R., 497, 500, 501
 Leverett, M.C., 375, 376
 Levich, V.G., 126
 Levitt, D.B., 390, 411, 427, 428, 430, 433, 434
 Lewis, A., 496, 498, 502, 503
 Lewis, S.J., 228, 306
 Leyrer, R.J., 405
 Li, C., 165
 Li, F., 226
 Li, L., 146–148, 224, 225, 273, 322, 484
 Li, N.N., 221
 Li, Y., 144, 440
 Li, Z., 454
 Liang, J., 445
 Liang, J.-T., 321, 447, 448, 452
 Libutti, B.L., 159, 160
 Liek, W.E., 143, 478
 Liétard, O., 141
 Liétard, O.M., 165, 229
 Lliu, H., 327
 Lillebo, B.-L.P., 409
 Lim, F.H., 390
 Lin, G.H., 66
 Lin, L., 273, 322, 324, 325
 Lindley, J.R., 371, 373
 Lindsay, D.M., 173
 Lindvig, T., 148, 213, 240
 Litt, M., 127
 Litt, N.D., 313
 Liu, F., 189
 Liu, G., 208, 360
 Liu, J., 327
 Liu, J.-F., 70
 Liu, S., 442
 Llave, F.M., 87
 Loayza, M.P., 362
 Lockwood, L., 457
 Lohateeraparp, P., 411, 426, 428, 456, 459
 Lohne, A., 90
 Lolon, E.P., 350
 Looney, J.R., 189
 Lopez, H., 242
 Lopp, V.R., 186, 187
 Lord, P.D., 299, 302
 Lorenz, P.B., 394, 411
 Loscutova, J.R., 335
 Loveless, C.F., 501
 Lullo, G., 181
 Lund, K., 39, 127, 128, 130, 143, 144, 147, 174
 Lundgaard, T., 408
 Lungwitz, B., 225, 246, 247
 Luo, M., 327
 Luo, Y., 454
- M**
 Ma, L.Q., 380
 Ma, S.M., 392
 Ma, Y., 271, 305
 Macdonald, B.A., 61
 Mach, J., 4
 Mack, D.J., 315
 Mack, M.G., 231, 233, 235, 236, 355, 356
 Mackay, B.G., 267, 312, 475
 Maddin, C.M., 195
 Madyanova, M., 226
 Maerker, J.M., 385
 Mahmood, L.H., 115
 Mahmoud, M.A., 160–162, 183, 220, 248
 Maier, R., 253
 Maier, R.W., 245
 Maitland, G., 308
 Makakou, P., 412
 Makogon, T., 85
 Malate, R.C.M., 178, 181
 Malhotra, S., 310
 Malik, A.R., 213, 226, 247
 Malik, M.A., 236
 Malik, Q.M., 420
 Malone, M.R., 313
 Malpani, R.V., 291, 350–352
 Mangold, D.C., 25
 Manning, T.S., 468, 471
 Mannistu, K.D., 26
 Manrique, E.J., 387, 436, 461
 Mansfield, R.C., 187
 Mansoori, C.A., 13
 Marchand, J.-P., 226
 Marcinew, R., 221, 306
 Markey, E.J., 472
 Marlow, D., 118
 Marquez, R., 313
 Marshall, A., 103
 Martell, A.E., 147, 411
 Martin, F.D., 384–386, 446, 450
 Martin, R.C., 241
 Martin, R.L., 66
 Marty, L., 450
 Masel, R.I., 14
 Masliyah, J.H., 26, 112, 202
 Masmonteil, J., 218
 Masoudi, R., 86

- Matherly, R., 73, 74
 Mathews, S.G., 79, 80
 Mathur, A., 85
 Matsuhisa, S., 33
 Matthews, W.R., 48
 Mayerhofer, M., 269–271, 279, 357, 358
 Mazet, J.A.K., 505
 Mcafee, C.A., 332, 478
 McBride, E.F., 316
 McCarthy, K., 2, 38, 262–264
 McCartney, J.H., 505
 McConnell, S.B., 145, 220, 236, 244, 317, 339, 363
 McCool, C.S., 450
 McCool, S., 320, 321, 452
 McCoy, J.C., 211
 McCracken, I.R., 85
 McCune, C.C., 39, 127, 128, 130, 143, 144, 147, 173
 McDaniel, G.A., 344, 345
 McDougall, L.A., 189
 McDuff, D., 122, 130
 McElfresh, P.M., 261, 474
 McFarland, S., 85
 McGowan, G.R., 241
 McGowen, J.M., 314, 315, 347
 Mcgregor, S., 117, 119, 120
 McGuire, D., 328
 McIlroy, J.G., 467
 McInerney, M.J., 409
 McKay, S., 79, 330
 Mclendon, W.J., 422
 McLeod, H.O., 88, 89, 175, 229, 230
 McMahan, C.P., 83
 McMahan, J.A., 66
 McNulty, S., 422
 McVay, D., 262
 Meadows, D.L., 339
 Mediaas, H., 102
 Medvedev, A., 361, 362
 Medvedev, O.O., 360–363, 366
 Meggitt, B.T., 211
 Mehmet, P., 221, 306
 Melo, A.R.D., 142
 Melo, R.C.B.D., 181
 Melsen, R.V., 178
 Méndez-Vivar, J., 380
 Menjivar, J., 286
 Merdhah, A.B.B., 95, 96
 Metcalf, A.S., 149, 254
 Metcalf, S., 242
 Meyer, B.R., 280, 355, 359
 Meyer, J.P., 423, 425
 Meyer, R., 68
 Michaelis, A.M., 241
 Middaugh, C.R., 320
 Miles, A.F., 20
 Miller, C.A., 426, 432, 435, 436, 442, 444
 Miller, J.F., 458
 Miller, M.J., 126, 140, 221, 223, 224, 226, 236, 243, 306, 317, 361
 Milson, S.L., 213
 Ming, G., 133, 154
 Miska, S.Z., 324
 Miskimins, J.L., 263, 268, 351
 Moghadasi, J., 83
 Mohamed, S.K., 219, 244, 255
 Mohammadi, H., 413, 428, 434, 442–444
 Mohanty, K., 335, 349, 353, 432
 Mohnot, S.M., 394, 438, 439
 Mohsen, A.H.A., 319–321
 Mok, W., 85
 Mokhtari, M., 298
 Molchanov, V.S., 310
 Moloney, J., 85
 Moniaga, N., 42, 43, 290, 325–327, 351
 Monroe, R.F., 187, 312
 Montgomerie, H., 75, 77, 78
 Moon, J.H., 107, 108
 Moore, J., 85, 86
 Moore, T., 478, 486
 Moore, W.R., 132, 143, 165, 259
 Moradi-Araghi, A., 421
 Morales, R.H., 261, 356, 368
 Moreau, P., 455
 Morel, D.C., 406
 Morello, L., 70
 Moreno, B., 269
 Morgenthaler, L.N., 125, 423, 478
 Morris, E.R., 294, 295
 Morris, E.W.A., 221, 306
 Morrison, J.G., 187
 Morrow, N.R., 392, 398, 399
 Morvan, M., 455
 Motekaitis, R.J., 411
 Mou, J., 250, 251
 Moulik, S.P., 20, 430
 Mozley, P.S., 411, 412
 Muci, V.E., 387, 436, 461
 Muecke, T., 221
 Mueller, F.A., 324, 325, 344, 345
 Mueller, R., 159
 Muhr, A.H., 241
 Mukherjee, H., 218
 Mukhopadhyay, S., 42, 43, 290, 317, 325–327, 351
 Mulkins-Phillips, G.J., 498
 Mullins, O.C., 81, 103
 Munday, K., 453
 Mungan, N., 417–419
 Munk, T.K., 157, 182
 Munoz, E., 390
 Munoz, T. Jr., 315
 Murillo, C.A., 4, 200
 Myers, R.R., 302, 478, 486
- N**
- Nagel, N.B., 355, 359
 Nalepa, C.J., 328
 Naraghi, A.R., 118
 Nasralla, R.A., 194
 Nasr-El-Din, H.A., 72, 98, 129, 130, 135, 138, 140, 145–148, 160–162, 177, 183, 192, 194, 195, 197, 198, 200–203, 211–213, 219, 220, 223–226, 240, 241, 243, 244, 247, 248, 254, 255, 329, 478
 Navarrete, R.C., 145, 220, 236, 243, 244, 283, 289, 290, 342
 Nedwed, T., 502
 Needham, R.B., 398
 Neff, S., 85

Nehmer, W., 279
 Nelson, E.B., 4, 221, 222, 227, 286, 287, 306, 307, 321, 322, 330, 348, 472
 Nelson, P.H., 44
 Nelson, S.G., 313, 315
 Nemati, M., 409
 Nesic, S., 64, 68
 Neumann, L.F., 239
 Neville, A., 62, 69
 Newman, S.H., 505
 Neyfeld, A.P., 200
 Nguyen, P.D., 342, 428, 434
 Nguyen, Q.P., 427, 428, 434, 440, 441
 Nickel, E.H., 34
 Nicolette, J.P., 502, 503
 Niemann, M., 2, 38, 262–264
 Nierode, D.E., 126, 153, 234, 236, 241, 245, 250, 273, 274, 312, 345
 Nieto, C.M., 239
 Nieuwerf, J., 440, 441
 Niiler, E., 488
 Nikitin, A., 343
 Nimerick, K.H., 326, 339
 Nodland, E., 104
 Noïk, C., 115
 Nolan, T.J.I., 195
 Nolte, K.G., 124, 125, 355, 356
 Noort, R.H.v., 211
 Nordgren, R.P., 355
 Norman, W.D., 175, 221, 229, 230, 306
 Norris, M., 79
 Nosova, K.E., 343
 Nutting, P.G., 382
 Nwoke, L.A., 178
 Nyborg, R., 67

O

Oakes, B.D., 185, 187
 Oberndorfer, M., 118
 Obeyesekere, N.U., 118
 O'Donoghue, M., 35
 Oetter, G., 432
 Ogbe, D.O., 415
 Öhman, L.-O., 165
 Okell, P.R., 209, 210, 339
 Olbertz, B., 188
 Oliveira, J.A.A., 142
 Oliveira, T.J.L.D., 142
 Olsen, D.K., 421, 423, 425
 Olsen, T., 222, 227, 306, 307, 321, 322, 348
 Omari, A., 448
 Omekeh, A.V., 402
 Onaisi, A., 219
 O'Neil, B.J., 192
 Orleans, A., 405
 Orona, S., 254
 Ortega, A., 176
 Oryszczak, R., 203
 Osborne, M.W., 316
 Ostensen, L., 148, 151
 Osterloh, W.T., 215
 Ostrowski, T., 405
 Oswald, D., 82, 193, 200, 204
 Otott-Jr, G.E., 377

Oussoltsev, D., 343
 Oyemade, S.N., 459
 Özbayoglu, E.M., 298, 324

P

Paccaloni, G., 208, 254
 Pace, J.R., 329, 330
 Pacheco, J.L., 64
 Paez, J., 348
 Page, C.A., 18
 Paktinat, J., 264, 323, 328, 331, 349, 485
 Palisch, T.T., 292, 305, 333, 334, 336, 338, 353
 Palleschi, A., 298
 Palmer, J.W., 64
 Palmowski, D., 2, 38, 262–264
 Panda, M.N., 174
 Pandey, V., 353
 Panga, M.K.R., 140, 141, 227, 228
 Park, N.G., 70
 Park, N.G., 68, 69
 Parker, C.P., 149
 Parker, J.E. III, 66
 Parker, M.A., 315, 347
 Parker, M.E., 416, 423
 Parkhurst, D.L., 25
 Parkinson, M., 157, 182
 Parlar, M., 215, 216, 222, 227, 306, 307, 321, 322, 348
 Parris, M.D., 215, 216
 Parshin, A., 371
 Patterson, D.E., 78
 Paul, B.K., 20, 430
 Pauls, R.W., 245
 Payne, J.R., 492, 494–497, 499, 500
 Pedersen, H., 408
 Peirce, A., 355, 357
 Pekdemir, T., 499
 Pena, A., 324, 325, 361, 362
 Penny, G.S., 264, 316, 323, 326, 328, 331, 349, 485
 Perez, D., 79
 Perez, J.P., 83
 Perkins, R., 330, 331, 479
 Perkins, T.K., 355
 Perry, C., 264
 Perry, K., 261, 351
 Perry, S.C., 484
 Peters, K., 2, 38, 262–264
 Petrie, M., 84
 Petrii, O.A., 186
 Petrov, A.D., 102
 Peysson, Y., 97–99
 Peytavy, J.-L., 85
 Pezron, E., 303
 Pfeuffer, T., 405
 Philippova, O.E., 309, 310
 Piedras, J., 261, 368
 Pierce, R., 313
 Piot, B.M., 165, 229
 Pissarenko, D., 371
 Pit, H., 85
 Plassey, J.A., 420
 Plavnik, B., 173
 Plummer, L.N., 25
 Poiseuille, J.L., 8

- Pope, G.A., 98, 390, 391, 394, 395, 403, 407, 410, 411, 413, 426–428, 432, 434–436, 442–444, 456
- Pope, T.L., 369
- Portier, S., 125
- Potter, J.M., 500, 501
- Pournik, M., 165, 239, 246–248
- Powers, B., 222, 227, 306, 307, 321, 322, 348
- Prasad, M., 263, 268, 351
- Prasad, S.K., 21
- Prasek, B.B., 320
- Prats, M., 267
- Prempain, B., 423
- Proano, E.A., 4
- Profinet, J., 261, 368
- Prokop, C.L., 279
- Prud'homme, R.K., 33, 275–277, 279–283, 294–296, 300, 301, 305, 320
- Prudnikova, A., 200
- Pryakhina, T.A., 309
- Pu, H., 403
- Puerto, M., 432, 444
- Pulsinelli, R.J., 283
- Punternold, T., 398–402
- Purinton, J., 468, 471
- Pursell, D.A., 236–238
- Pursley, J.T., 326
- Putzig, D.E., 300, 302
- Pye, D.S., 315
- Pyle, R., 83
- Q**
- Qiu, X.W., 149
- Qu, Q., 126, 220–223, 224, 226, 228, 252, 306
- Quevedo, M., 157, 158
- Quinn, M.A., 174
- R**
- Rabie, A., 160–162
- Radke, C.J., 21, 214, 437
- Rae, P.J., 181, 297, 299, 341
- Rahbari, R., 448
- Rahim, Z., 366
- Rakshpal, R., 467
- Ramachandran, S., 67, 68, 70
- Raman, A., 65
- Ramirez, G.R., 157, 158
- Ramsey, J.E., 424
- Raney, K.H., 99, 101, 445
- Rashtchian, D., 81
- Rasmussen, K., 408
- Rassenfoss, S., 481, 507
- Ratulowski, J., 94
- Rausch, H., 116
- Rauseo, O., 313
- Reddy, B.R., 228
- Reed, T., 324
- Rehm, D., 323
- Reichenbach-Klinke, R., 405
- Reid, T.B., 405
- Reidenbach, V.G., 324
- Renard, S., 423
- Reyes, R.P., 211, 212
- RezaeiDoust, A., 398, 401, 402
- Rhine, T., 362
- Rhodes, P.R., 64, 478
- Riazi, M.R., 30
- Ribeiro, L.H., 283, 325
- Ricard, A., 303
- Richter, S., 67
- Rickards, A.R., 341
- Riddiford, A.C., 127
- Rieb, B.A., 349, 367, 368
- Riggs, O.L.J., 185
- Riha, J., 73
- Riley, R., 264
- Ritter, S., 21
- Robbins, J., 273
- Robbins, W., 67
- Robert, J.A., 146, 207, 208, 210, 212, 213, 229, 230, 241
- Robinson, G., 294, 295
- Robinson, J.S., 186
- Rockefeller, H.A., 297
- Rodoplu, S., 173
- Rodriguez, J., 487
- Rodriguez, V.O., 369
- Roegiers, J.-C., 46, 48
- Rojas, A.M., 348
- Rojas, K., 2, 38, 262–264
- Romero, R., 176
- Rong, J.G., 215
- Roodhart, L.P., 311, 341
- Ropital, F., 75
- Rosine, R., 211
- Rosmalen Janssen-van, R., 454
- Ross, G.J., 169
- Ross, W.M., 126
- Rossen, W.R., 21, 22, 207, 208, 210, 212–215, 422, 453, 454
- Ross-Murphy, S.B., 294, 295
- Rousseau, D., 423, 449
- Rousseau, G., 102
- Roy, A., 222, 227, 306, 307, 321, 322, 348
- Royce, B., 410
- Rozenfeld, I.L., 186
- Roza, R.E., 348
- Ruseska, I., 273
- S**
- Saad, N., 442
- Sabhaponnit, A., 260
- Sagatov, E., 383
- Saito, M., 159
- Sakai, H., 308
- Sakai, K., 308
- Salager, J.-L., 313, 426, 428–430, 434
- Salamat, G., 214, 324, 325, 343, 362
- Salathiel, W.M., 145, 221, 245
- Salinas-Nolasco, M.F., 380
- Samaniego-V., F., 267
- Samuel, M.M., 123, 125, 180, 181, 198, 212, 220, 221, 244, 245, 254, 306, 319–321
- Samuelson, M.L., 27, 339
- Sanchez-nagel, M., 355, 359
- Saneifar, M., 194
- San-Miguel, L., 341
- Santanna, V.C., 308
- Sarmiento, Z.F., 178, 181

- Saukaitis, A.J., 187
 Saunders, D.L., 458
 Saxena, R.C., 65
 Sayed, M.A.I., 138, 146, 243
 Schechter, R.S., 39, 130, 133, 135, 140–144, 146, 147, 163, 165, 173, 174, 178, 429
 Scherl, F.-X., 116
 Scherubel, G.A., 246
 Schmidle, C.J., 187
 Schmidt, K., 405
 Schmidt, R.L., 387, 388, 395
 Schmidt, T., 79
 Schmitt, G., 63, 65, 188, 196
 Schnabel, W., 411
 Schofield, M., 407–409
 Schols, R.S., 279–280
 Scholz, M., 200
 Schubert, J.S., 477
 Schultz, R.K., 302
 Scott, P.J.B., 61, 390
 Scott, R.L., 25
 Seagraves, S., 408
 Seale, R.A., 365
 Seale, V.L., 244
 Sedeh, I.F., 165
 Seibrits, E., 355, 357
 Seiller, B., 505
 Selle, O.M., 77, 78
 Sepehrnoori, K., 141, 153, 173, 426, 436
 Serad, G., 127
 Serdyuk, A., 343
 Seright, R.S., 384–386, 393, 394, 405, 411, 412, 445–448, 450
 Seth, K., 330
 Settari, A., 235, 250
 Settineri, W.J., 186
 Shah, S.N., 278, 279, 307, 308, 311, 323
 Sharma, G.D., 415
 Sharma, M.M., 9, 87–92, 96–98, 283, 310, 325
 Sharma, S.C., 308
 Shashkina, J.A., 309
 Shaughnessy, C.M., 126, 152
 Shaw, S.D., 498, 502
 Shcolnik, D., 330, 331, 479
 Sheely, C.O., 458
 Shekarchian, M., 474
 Shen, D., 79, 330, 331, 479
 Shen, Y.-F., 203
 Sheng, J., 371, 380
 Shepherd, A.G., 102, 117, 119, 120
 Shepherd, W., 190, 204, 471, 476
 Sherik, A.M., 83
 Shetty, C., 115
 Sheu, E.Y., 103
 Shiau, B.J.B., 411, 426, 428, 456, 459
 Shimokata, N., 84
 Shirzadi, A., 94
 Shlyapobersky, J.W., 49, 231–233, 268, 287–289, 310
 Shoaib, S., 416
 Shourbagi, S.M., 249, 364
 Shrestha, L.K., 308
 Shuchart, C.E., 122, 130, 256, 328
 Shukla, S., 137
 Shuler, P., 77, 78
 Siddiqui, S., 129, 130, 135, 145, 218
 Sievert, C.J., 369
 Sifferman, T.R., 84
 Silberberg, I.H., 173
 Silverman, D.C., 129
 Simanzhenkov, V., 3
 Simon, D.E., 169
 Simon, S.b., 113
 Simoni, M.D., 83
 Sims, P., 108
 Sinclair, A.R., 209, 210
 Singer, M., 64
 Singh, J.R., 256
 Singh, P., 103
 Singh, S.P., 377, 378, 396, 397
 Singh, W.P., 66
 Sinkankas, J., 35
 Sinton, S.W., 302, 303
 Sitdikov, S.S., 343
 Sitz, C., 189
 Sjöberg, S., 165
 Sjöblom, J., 102–107, 113
 Skala, R.D., 335
 Skauge, A., 452
 Skauge, T., 452
 Skibinski, D., 82, 193
 Skovhus, T.L., 408
 Slabaugh, B.F., 298, 299, 302, 311, 315
 Slayer, J., 82
 Sloan, E.D. Jr., 85
 Smit, J.R., 429
 Smith, C.F., 82, 126, 193, 195, 200, 204, 475
 Smith, J.L., 67
 Smith, K.L., 196
 Smith, M.B., 49, 231–233, 268, 287–289, 310, 351
 Smith, P.C., 107
 Smith, R.G., 20
 Smith, R.J., 335
 Smith, R.S., 147
 Smith, S.N., 64
 Soeder, D.J., 264
 Solairaj, S., 434, 435
 Solomon, R., 483, 485
 Solomons, T.W.G., 4, 293
 Somasundaran, P., 430
 Somerville, J.M., 94
 Song, K., 406
 Sookprasong, P.A., 178, 181
 Sorbie, K.S., 424
 Sørensen, K., 408
 Sorhaug, E., 118
 Sousa, J.L.A.O., 239
 Soya, S., 159
 Spildo, K., 452
 Srivastava, M., 440, 441
 Stalkup, F.I. Jr., 414
 Stanitzek, T., 162
 Stankiewicz, A., 2, 38, 262–264
 St. Clair, J.D., 300, 302
 Stegent, N.A., 298, 303, 311
 Stein, M., 417
 Steinbrenner, U., 432
 Stemler, P., 474
 Stephens, W.T., 341

- Stephenson, C.J., 341
 Stevens, R.F., 323
 Stewart, J.E., 498
 Stewart, M.E., 256, 265
 Stiff, H.A. Jr., 60
 Still, J.W., 241, 248, 252, 253, 317
 Stoesser, M., 126
 Stoll, M., 459
 Stoll, W.M., 391, 395, 439
 Stopi, S., 487
 Stott, J., 407–409
 Strand, S., 398–400
 Street-Jr., E.H., 195
 Strippoli, P., 245
 Strumolo, G.S., 279
 Sulejmanov, A.B., 501
 Sullivan, A.P., 106
 Sullivan, P.F., 214, 308, 343, 362
 Sullivan, R.B., 31, 238, 242, 250
 Sumner, P.L., 18
 Sun, H., 323, 447, 448
 Sun, S.Q., 143
 Sun, W., 64, 68
 Sun, Y., 271, 305
 Sunde, E., 409
 Sung, T.-H., 107, 108
 Surkalo, H., 402
 Suter, G.W. II, 502, 503
 Sutton, G., 351
 Svartaas, T.M., 471
 Svec, Y., 422
 Swanson, S.R., 335
 Swanson, T.A., 84
 Sweatman, R.E., 416, 423
 Syahputra, A.E., 422
 Sylvestre, N., 82, 193
 Syrinek, A.R., 312
 Szymczak, S., 79, 330
- T**
- Tabary, R., 448, 449
 Taber, J.J., 384–386, 446, 450
 Tadmor, R., 42
 Taha, R., 173
 Talabani, S., 218
 Talbot, M., 130
 Talib, N.N., 143
 Tambini, M., 208
 Tandy, S., 159
 Tang, G.-Q., 398
 Tapp, J., 200
 Tardy, P.M.J., 211, 213, 226
 Taylor, G.N., 73, 74
 Taylor, K.C., 195
 Taylor, R.S., 474
 Teas, J.P., 25, 27
 Teigland, R., 389
 Teller, E., 171
 Terracina, J., 213, 299, 302
 Teufel, L.W., 357
 Thach, S., 441
 Tham, M.K., 411
 Thayer, K., 118
 Thiercelin, M.C., 46, 48
 Thiercelin, M.J., 359, 361
 Thomas, A., 305, 404, 410, 413
 Thomas, F.B., 87
 Thomas, R.D., 394
 Thomas, R.L., 125, 140, 175, 178, 180, 199, 328
 Thomas, S., 3, 371, 372, 374, 375, 379, 384, 389, 397, 414, 415, 426, 432, 440
 Thompson, J.E., 318
 Thompson, K.E., 214
 Thompson, R.E., 110
 Thomson, G., 102
 Thorne, M.A., 98
 Thorstenson, T., 409
 Thrasher, R.W., 285, 465
 Threlkeld, C.B., 398
 Tibbles, R.J., 221, 306
 Tielong, C., 405, 410
 Tiler, F.M., 287
 Tinto, J., 483, 485
 Tiyaboonchai, W., 320
 Tjon-Joe-Pin, R., 318, 320
 Todd, A.C., 94
 Todd, B.L., 228, 315
 Tohidi, B., 86
 Tomson, M., 79
 Torsvik, T., 409
 Tosch, W.C., 432
 Touboul, E., 140, 141, 218
 Trabelsi, S., 299, 302, 317, 325
 Treadway-Jr, J.H., 316
 Trehan, R., 178
 Trittipi, B.L., 245
 Trompert, R.A., 117, 119, 120
 Tsang, C.-F., 25
 Tsau, J.-S., 421, 422
 Tsuchiya, K., 308
 Tsui, K., 69
 Tuedor, F.E., 180
 Turner, M.S., 107
 Tustin, G., 149
 Tuzan, E.V., 83
- U**
- Uchendu, C.V., 178
 Uhlig, H.H., 63
 Unsal, R., 85
 Urbina, I., 477, 478
 Uribe, O., 314
 Urum, K., 499
- V**
- Vallejo, C.M., 189
 Van Arsdale, H., 169
 van den Brock, W.M.G.T., 94
 van der Heijde, P.K.M., 25
 Van Domelen, M.S., 26, 27, 143
 van Poollen, H.K., 488
 Van Wunnik, J., 459
 Vargas, F.M., 83
 Vavra, C.J., 411, 482, 484
 Veedu, F.K., 456
 Vehlow, J., 481
 Veil, J.A., 479, 507
 Veley, C.D., 201–203

- Venkatesan, R., 2, 3, 9, 10, 13, 25, 55–58, 64, 67, 72,
 82–85, 93, 103, 106, 117, 165, 192, 389, 417, 423,
 429, 437, 499
 Venkatraman, A., 99, 101, 445
 Venugopal, K.N., 295
 Venuto, P.B., 387, 388, 395
 Verga, F., 377–379, 414
 Vers, L.V., 85, 86
 Vert, M., 406
 Vervoort, I., 20, 75
 Vieille, E., 62
 Vikane, O., 77–79, 167, 174
 Vincent, M., 292, 305
 Vindstad, J.E., 102
 Vinod, P.S., 221, 306
 Vinson, E.F., 200, 204
 Visser, R., 481
 Visser, W., 279–280
 Vitthal, S., 314, 315, 347
 Voderbruggen, M.A., 188
 Vogel, J.V., 7
 Volz, H.A., 246
 Voordouw, G., 409
 Vreeburg, R.-J., 341
 Vuataz, F.-D., 125
 Vyas, A., 323
- W**
- Wade, W.H., 429
 Wagner, H.L., 295
 Walker, M.L., 129, 195, 196, 328
 Walker, R.N.J., 297
 Walsh, M.P., 389, 402, 403, 416, 420, 436
 Walters, H., 311
 Walters, H.G., 298, 299, 303, 311
 Wamser, C.A., 175
 Wang, D., 208, 360, 393, 394
 Wang, F., 440
 Wang, J., 103, 105
 Wang, K.-S., 440
 Wang, W., 79
 Wang, X., 193, 208, 252, 360
 Wang, Y., 141, 143, 144, 189
 Ward, M.B., 68, 70
 Warner, J.L., 169
 Warpinski, N.R., 233, 235, 236, 269–271, 279, 355–358
 Wasan, D.T., 115
 Washburn, E.W., 44
 Wasmund, E., 116
 Wat, R., 77, 78
 Wat, R.M.S., 77, 78
 Waters, G., 350, 357, 487
 Watkins, E.K., 324
 Wattebled, L., 308, 309
 Watts, P., 46
 Wavrik, K., 405
 Waxman, H.A., 472
 Weathers, T., 116, 117
 Weaver, J.D., 317, 342
 Webb, K.J., 400, 401
 Webber, S.J., 259, 273
 Weerasooriya, U.P., 411, 427, 428, 434, 435
 Wehunt, C.D., 169
 Wei, J., 406
 Wei, W., 441
 Weintritt, D.J., 59
 Weiss, J., 19
 Weitz, D., 296
 Welton, T.D., 228, 240, 306, 430, 432, 439
 Wen, Q., 327
 Wendorff, C.L., 324
 Weng, X., 355, 357, 359
 Wenzke, B., 405
 Westacott, R., 102
 Westenhaus, B., 366
 Wheaton, L.L., 478
 Whitaker, S., 45
 Whitehead, D., 507
 Whitsitt, E.A., 335
 Wickstrom, L., 264
 Wierenga, A.M., 221, 306
 Wiesner, M., 335
 Wiles, C., 46
 Wilhelm, R.G., 475, 478, 485
 Wilkinson, G., 4, 200
 Willberg, D.M., 214, 330, 343, 361, 362
 Willcox, M., 437
 Willhite, G.P., 371, 379–381, 395, 404, 450
 Williams, B.B., 126, 153, 250
 Williams, D.A., 188, 189
 Williams, D.R., 147
 Williams, M.E., 484
 Williams, W.H., 78
 Williamson, C.D., 315
 Williamson, D., 316
 Willingham, J.R., 329, 330
 Willmon, J.G., 471
 Wilson, A., 222, 227, 306, 307, 321, 322, 348
 Wilson, D.A., 128–130, 160, 195, 196
 Wilson, S., 249, 364
 Wimberley, J.W., 458
 Wingrove, M., 110
 Winsor, P.A., 20, 429, 430
 Wirajati, A.Y., 316
 Wodehouse, J., 398, 413
 Woiszwilllo, J., 320
 Wolery, T.J., 25
 Wolf, C.D., 151, 160–162, 183, 195
 Wolfe, B., 84
 Wong, J.E., 68, 69
 Wood, B., 323
 Wood, W.D., 341, 474
 Wood, W.R., 316
 Wright, C.A., 357
 Wu, J., 440
 Wu, Q., 271, 305
 Wu, Y., 390
 Wylde, J.J., 82, 119, 192
 Wyss, H., 296
- X**
- Xianke, Y., 204
 Xiao, Z., 152, 166, 179, 180
 Xie, T., 165
 Xu, B., 313, 314
 Xu, L., 327
 Xu, W., 359
 Xu, Z., 112

Y

Yamada, Y., 84
Yamamoto, T., 159
Yan, M., 420
Yang, C., 385
Yang, F., 177
Yang, J., 15, 75, 76, 218
Yaritz, J.G., 328
Yarranton, H.W., 26
Yassin, A.M., 95, 96
Yeager, V.J., 211, 212
Yi, T., 93
Yin, C., 189
Yin, D., 403
Yin, G., 422
You, Q., 451
Young, D.N., 420, 421
Youngman, R., 339
Yousef, A.A., 400, 401
Youssef, N., 409
Yuan, J.S., 429
Yuhong, X., 451
Yunzhang, Z., 204
Yuping, F., 204

Z

Zahedi, A., 211
Zahrani, A.A., 241
Zaid, A.M., 460
Zaidi, S.R., 83
Zaitoun, A., 118, 200, 202, 402, 403, 412, 445–448, 449, 451
Zamora, F., 313

Zaroslov, Y.D., 309
Zeinijahromi, A., 455
Zemaitis, J.F. Jr., 23
Zenone, V.E., 491, 504
Zerhoub, M., 218
Zhang, H., 189, 446
Zhang, J., 189, 393, 394, 440, 441
Zhang, N.S., 94
Zhang, X., 392
Zhang, Y., 63
Zheltoy, Y.P., 355
Zhengyu, S., 405, 410
Zhou, D., 420
Zhou, G., 454
Zhou, H., 102
Zhou, S., 118
Zhou, Z., 454
Zhou, Z.J., 199–201
Zhu, D., 137, 173, 250, 251, 313, 314
Zhu, T., 415
Zhu, Y., 454
Ziauddin, M.E., 2, 3, 9, 10, 13, 25, 55–61, 64, 65, 67, 72, 75–79, 82–86, 93, 95, 103, 106, 117, 129, 135, 136, 140, 141, 145, 152, 159, 165–167, 174–176, 179, 180, 185, 187, 189, 192, 198, 200, 204, 207, 240, 330, 332, 389, 394, 411, 417, 423, 424, 429, 437, 441, 442, 446, 477, 478, 499
Ziccardi, M.H., 505
Zornes, D.R., 421
Zou, C., 236–238, 243, 244, 246
Zou, H., 193
Zurigat, Y.H., 116
Zwaag, C.v.d., 90

SUBJECT INDEX

A

- acidic breakers, 316–317
- acidizing
 - carbonates, matrix and fracture, 123
 - fracture, 121
 - models
 - kinetic-controlled reactions, geochemical models, 174
 - two-acid, three-mineral models, 173
 - two-mineral models, 173
 - oilfield emulsions, 106
 - reactive chemicals, formation stimulation, 125–126
 - sandstone fracture, 252–253
 - stimulation method, 125–126
- additives, reactive fluid
 - agent types, 184
 - CCCs, 199–204
 - CIs [see corrosion inhibitors (CIs)]
 - composition, 184
 - definition, 184
 - HSE activities and considerations, 205–206
 - iron control agents, 194–196
 - oilfield properties, 205
 - physical and chemical attributes, 204–205
 - selection properties, 205
 - sulfide control chemicals, 196–198
 - surface active agent
 - alcohols, 193
 - antisludging agents, 193–194
 - damage types and solvents, 191
 - mutual solvents, 192–193
 - single-stage acid microemulsion fluid, 193
 - surfactants types, 191
- alkaline flooding
 - acid number, 436
 - kaolinite, 438
 - MP and ASP methods, 439
 - natural surfactants, 437
 - static dissolution tests, 438
- alkaline-surfactant polymer (ASP)
 - chemicals and economic constraints, 440
 - component, 439
 - Daqing field, 440
 - emulsification, 440, 441
 - features, 442
 - improved oil recovery (IOR), 372–373, 385
 - macro push, 440, 441
 - polymer push, 440, 441
 - soap/surfactant gradient, 442
 - test parameters, 443–444
 - UTCHEM-ASP model, 443

aluminosilicates

- carbonate formations, 35
 - category, 38
 - characteristics, 168
 - clays, 35, 91, 170
 - HCl treatments, 98
 - mineral ratio elemental analysis, 168
 - tertiary reactions, 172
 - zeolites, 170
- Amott–Harvey index number calculation, 393–394
- analcime, 169–171

B

- ¹¹B nuclear magnetic resonance (NMR) methods, 303

C

- capillary suction time (CST) test, 200
- carbohydrates
 - biopolymers
 - linear-gel fluid system, 298–299
 - scleroglucan, 298
 - xanthan polymer, 297–298
 - cellulose derivatives, 299
 - dicarbohydrates, 293
 - glucose equilibrium, 292–293
 - guar-based fluids
 - DOR methods, 303
 - effects of polymer (HPG), 303–304
 - galactomannan-borax systems, reversible gels, 303
 - NMR methods, 303
 - poly(vinyl alcohol) (PVA), 302–303
 - guar-based polymers
 - carboxymethyl HPG (CMHPG), 297
 - concentration curve changes, 295–296
 - DOR, 296
 - galactose and mannose monomers, 294
 - HPG concentrations, 296–297
 - hydration, 295
 - intrinsic viscosity, 294–295
 - molecular weight (MW), 294–295
 - shear thinning, 296
 - structure, 294
 - HPG, use, 292
 - metallic compounds, crosslinking
 - borate, 300–302
 - HPG fluids, viscosity, 299, 300
 - metal, 301
 - polymer fracturing fluids, 299–300
 - seawater-delayed crosslinking system, 302

- titanium complex, 301
- polymer chemistry, 304
- viscosity modifiers, 304
- carbonates
 - acidizing, 123
 - carboxylic compounds, 399
 - formations, matrix stimulation
 - dissolution pattern, 133
 - dolomites, 132–133
 - limestone (calcite), 132
 - numerical acidizing models, 140–142
 - reaction of acids, 134–138
 - rocks, 133
 - wormholes, 133–134, 138–140
 - ionic composition, 400
 - low-salinity waterflooding (LSWF), 399–400
 - matrix reactive fluid treatments
 - coreflood tests, 129–130
 - radial flow experiments, 130
 - RD methods, 126–129
 - propped fracturing chemistry and applications, 259
 - reactive chemicals, formations
 - matrix and fracture acidizing, 123
 - stimulation treatments, 125, 255–258
 - wormhole formation, 124
 - reservoirs
 - calcite dissolution capacity, various dissolvers, 150–151
 - carboxylic acid, 150
 - conical wormhole, limestone, 155
 - core breakthrough/pump rate relationships, 154
 - coreflood data, 156
 - diammonium EDTA (DAE), 152
 - emulsified/gelled acids, 145–146
 - HCl, 142–145
 - organic acids, acetic and formic acid (FA), 146–149
 - phosphonate acid, 150
 - pore volume to breakthrough (PVBT) values, 155
 - rotating disk tests, reaction rates, 152
 - technologies, 159–162
 - temperature dependency, 153
 - traditional, 151–158
 - seawater wettability mechanism, 399–400
- cationic inorganic polymers (CIP), 201
- CCCs. *See* clay control chemicals (CCCs)
- CDG. *See* colloidal dispersion gels (CDG)
- CFTs. *See* coreflood tests (CFTs)
- chemical/engineering practices, production enhancement
 - problems analysis
 - external reservoir boundary, 6
 - Fanning friction factor, 8
 - Hawkin's formula, 6
 - inflow and outflow performance curves, 7
 - inflow performance relationship (IPR) curve, 4–5
 - oil and gas production system, 5
 - permeability, 6
 - potential energy pressure drop, 7
 - pressure and radial distance, 6
 - two-phase fluid flow, 8
 - Vogel relationship, 7
 - processes
 - drilling additional wells, 10
 - EOR processes, 10
 - inflow and outflow performance, 8
 - matrix treatments and hydraulic fracturing (HF), 9
 - near-wellbore (NWB) damage, 9
 - pressure maintenance, 10
 - relative formation areas, 10
 - scale/corrosion inhibitor treatments, 11
- chemicals and produced fluids
 - emergency plans/operations, spill control, 463
 - flowback fluids
 - handling, reuse, and disposal, 476–479
 - planned waste disposal options, 479–488
 - health and safety, 463
 - HSE management
 - chemical selection, 467–472
 - improved environmental control, 474–476
 - tight gas production and fracturing processes, 472–474
 - inhalation of toxic gases, 464
 - Material Safety Data Sheets (MSDSs), 464, 469
 - oilfield chemistry
 - benzene-containing diesel fuel, 505–506
 - fresh brines, 507
 - petroleum product supply chain, 506
 - SPE Research and Development Grand Challenges, 505
 - well fluids, 506–507
 - personal safety equipment (PSE), 464–465
 - previous incidents/accidents
 - energized fluid, precautions, 465
 - environmental considerations, 465
 - flammable fluids, precautions, 465
 - PSE, 464
 - RP Table of Contents, 466–467
 - safety meeting, 464
 - well control, 464–465
 - production enhancement operations, 463–467
 - reactive hazards, 464
 - safely dispose/reuse, 463
 - spills, water bodies and land
 - contaminated soil and wildlife, 503–505
 - control and planning, 489–492
 - remediation chemicals, 492–503
 - toxicity, 463
- chemical tracers, EOR
 - description, 456–457
 - passive tracers, 457–458
 - reactive tracers
 - chemical partitioning, 458–459
 - oil and water phases, 459–460
- chlorite, 169–170
- CIs. *See* corrosion inhibitors (CIs)
- clay control chemicals (CCCs)
 - capillary suction time (CST) test, 200
 - cards macrostructure, 199
 - cation exchange, 201
 - cationic inorganic polymers (CIP), 201
 - coating, as control mechanism, 202
 - compounds, 201–204
 - ion exchange control mechanisms, 200–202
 - potassium salts, 200

- stabilization, 200
 - surface affinity modification, 202
 - testing, 200
 - tetramethylammonium chloride (TMAC), 201, 203
 - colloidal dispersion gels (CDG), 452–453
 - CO₂ miscible floods
 - API, 425
 - corrosion and inhibitor, scale, 423–424
 - displacement tests, 419
 - economic challenges, 424
 - EOR mechanism, 418
 - foamed CO₂/brine
 - flooding parameters, 422
 - mobility reduction, 421
 - nonylphenol ethoxylates, 422
 - SAG, 422
 - surfactant adsorption equilibrium, 423
 - injection project, 420
 - miscible zone formation, 416–417
 - oil cut, 420
 - oil density, 417
 - phase diagram, 417–418
 - technical challenges, 424
 - thickeners, 423
 - WAG, 421
 - conventional reservoirs, oil and gas, 261
 - coreflood tests (CFTs)
 - acid injection, 134
 - CDG process and, 453
 - ICPOES methods, 130
 - pore volume to breakthrough (PVBT), 129
 - rock/fluid interactions, 394–395
 - sandstone formation rocks, 131
 - short core and long core tests, 130
 - silicate formations, test methods, 131
 - surfactant evaluation methods, 426, 428
 - corrosion inhibitors (CIs)
 - chemistry
 - “greener” petroleum production inhibitors, 67
 - inhibitor structures, 65
 - marine toxicity, 66–67
 - water-soluble inhibitors, 67
 - HCl solvents
 - corrosion rates, 188
 - eleosteric imidazolineamine, 189–190
 - imidazolines, 189
 - nitrogen quats, 189
 - oxygen containing inhibitors, 188
 - phenyl ketone inhibitors, 187
 - polymer film, formation, 186
 - Priority Pollutant List, 189
 - quaternary ammonium salts, 188
 - organic acids and chelating agents, 190–191
 - production, mechanisms of action
 - crude/brine mixtures, corrosivity, 67
 - evaluation, tests types, 67
 - film forming inhibitor mechanism, 66–67
 - hydrocarbon/brines, corrosivity, 67
 - imidazolines derivatives, 67
 - IST/steel wettability and adsorption tests, 67
 - structures, 65, 67
 - Young’s modulus, corrosion product scale, 68
 - reactive fluid inhibitor mechanisms, 185–186
 - and scale inhibitors
 - chemical structure, 76
 - delivery, improvements, 76
 - hydraulic fracturing treatments, 79
 - imidazoline dimer-type compounds, 76
 - “Live Formation Water” *in-situ* analyses, 79–80
 - microemulsions, 75–76
 - squeeze treatments (*see* “squeeze enhancement” methods, SIs)
 - sour brine
 - CO₂ inhibitors, 70
 - H₂S corrosion, 70
 - pitting corrosion rates, 71
 - production stage CIs, 71
 - “sweet (CO₂)” fluid
 - bis amine (quat) inhibitors, 68
 - imidazoline inhibitor and Fe²⁺, 69
 - imidazolium CIs, 68
 - iron carbonate and inhibitor types, 69–70
 - rotating cylinder electrode methods, 68–69
 - critical micelle concentration (CMC)
 - anionic/nonionic polymers, 202
 - corrosion inhibition performance, 69
 - crosslinked, 302
 - definition, 14
 - EOR fluids, properties, 390
 - IST and CMS, surfactants, 495
 - measurements, 16, 103
 - crude oil emulsion tests, 391
- D**
- diesel-substitute-based (DiSub) system, 474–475
 - diffusivity, 31, 140
 - dispersions
 - emulsions
 - cosurfactant, 19–20
 - external phase, 17
 - internal phase, 17
 - microemulsions (MEs), 19–20
 - oil field treatment fluids, 17
 - oil in water (O/W) and water in oil (W/O), 17–18
 - paraffin mineral oils, 18
 - physicochemical processes, 19
 - rate of breaking, 19
 - solubility values, 18
 - Winsor microemulsion phase diagram, 20–21
 - foams
 - bulk foams, 21
 - component, 21
 - energized fluids, 22
 - half-life, 22
 - liquid drains, 21
 - quality, 22
 - settling, 22
 - homogenized milk, 17
 - nanoparticles, in oil and gas production, 21
 - semistable, 17
 - slurries, 22
 - drag reducing agents (DRAs), 116–117
 - dynamic oscillatory rheometry (DOR)
 - definition, 33–34

fluid transport, 311
 gels formation, 303
 guar-type polymers, 296

E

electrical submersible pumps (ESP), 61, 84, 94
 emulsions

chocolate mousse emulsion, 99–100
 demulsification, chemical methods
 anti-emulsifiers, 111
 API bottle test, 110
 crude oil/water emulsions, 111
 demulsifier categories, 115
 ESI test, 110
 HLB concept, 113–114
 microemulsion phase, 114
 oil-soluble DMs, 115
 polyacrylamide polymer, 115
 polysiloxane molecules, 115
 RSN, 110–111
 small molecules DMs, 112
 water-in-crude oil emulsions, 116
 W/O and O/W emulsions, materials, 112

oil droplets in water (O/W), 99

oilfield emulsions

acidizing and fracturing procedures, 106
 aggregation, 101
 “ARN Acids,” 102
 asphaltene precipitation, 103–104
 brine composition, 107
 chemical factors, 106
 CMC measurements, 103
 coalescence, 101
 CO₂/light hydrocarbons, 106
 fatty acids, 102
 mechanical and chemical methods, 107
 naphthenic acid category of chemicals, 102
 organic soaps and solids, control, 107
 sedimentation, 101
 shear forces and emulsifying agents, 101
 solids in stabilizing emulsions, 105
 stabilizing agents (or emulsifiers), 101, 104–105
 wettability of particles, 105–106
 W/O emulsion, 103

production phase mechanisms

microemulsions, 101
 oilfield emulsions, 100
 rheological properties, 101
 W/O emulsions, 100

resolving emulsions, mechanical methods

centrifugation, 108
 demulsification process, 108
 EFP separator, 108, 109
 electrostatic methods, 108
 gravity settler, 108
 sedimentation (settling), 107
 separation process, 108
 thermal (heat) breaking methods, 107
 three-phase separator, 108, 109
 water droplets in oil (W/O), 99

emulsion separation index (ESI) test, 110

enhanced-oil-recovery (EOR) processes

carbon dioxide flooding, 461
 case histories and practices, 460–462

CO₂ injection, 462
 miscible displacement processes, 414
 optimum design, 461
 polymer flooding, 398
 produced water, injection, 94
 screening analysis, 460
 surfactant adsorption, 215
 synthetic surfactant, 429–430
 targets, 371–372
 waterflooding, 379
 wetting characteristics, 10

enzyme breakers

α-amylase enzyme, structure, 319
 encapsulated enzyme breaker, 320
 galactomannanase, 320
 guar galactomannan, degradation, 320
 nanotechnology materials, 321
 pH and temperature, 319–320
 polyethyleneimine (PEI)-dextran sulfate,
 320–321
 reaction-diffusion model, 320
 stability enzymes, 321
 subterranean formation, 320

EOR processes. *See* enhanced-oil-recovery (EOR) processes

ESI. *See* emulsion separation index (ESI) test

ESP. *See* electrical submersible pumps (ESP)

F

flow assurance (FA), 11, 56–57

flowback fluids

acid flowback, 478–479
 dissolved salts, 478
 flowback activities, 476–479
 NORM, 477
 planned waste disposal options (*see* waste disposal options)
 production engineers, concerns, 477
 shale formations, 477
 TDS, 478
 use/reuse, 477–478

flow enhancers

biphasic viscosity reducer chemicals, 117
 dehydration/demulsification methods, 117
 drag reducing agents (DRAs), 116–117
 fracturing fluids, 116

fluid loss (FL) agents

carbohydrate fluids
 deformable/degradable polymers, 315–316
 filtration process, 314
 formation type and permeability, 314
 gel damage/filtration process, 313–314
 inorganic solids (silica flour), 314
 leakoff volume, 313–314
 resin hydrocarbon, 314–315
 yield stress, 314
 dynamic fluid loss cell, 282
 filter cake, 282–283
 reservoir fluids, 280–281
 static fluid loss cell, 282
 VES fluids, 316

fluids

chemistries
 dispersions, 17–22

- hydrated chloride anionon, 13
- monomer and salt solutions, 12–13
- polymer fluids (see fluids)
- solutions of monomers and salts, 12
- surfactant fluids (see surfactants)
- macroscopic displacement
 - fingering, 377, 378
 - heterogeneity and vertical sweep, 378–379
 - immiscible displacement, 376
 - injection/producer patterns, 377, 378
 - reservoir rock, 375
 - sweep efficiency, 377–378
 - volume sweep efficiency, 377, 379
 - volumetric factors, 376, 377
 - water fraction and saturation, 376, 377
- microscopic displacement
 - capillary pressure, 381–382
 - gravity parameters, 383
 - IOR/EOR activities, 380
 - IST, 381
 - oil and water, pore spaces, 380
 - surfactants and solvents, 383–384
 - water-wet reservoir, 382
 - wettability, 381
- polymer
 - additives, 17
 - ethylenediamine, 16
 - polymer additives, 16
 - random coil, 16–17
 - scale/deposit inhibitors, 17
 - thickening agents, 17
- properties, 390–391
- surface wetting, 374
- transport properties
 - diffusivity, 31
 - thermal conductivity, 29, 31–32
 - viscosity, 29–31
- fluids injection, into earth
 - mobility control, 49
 - reservoir geomechanics
 - fracture mechanics, 47–48
 - fracture pressure, 48–49
 - geologic layers, depiction, 46
 - stress-strain curve, 47
 - tangent modulus, 47
 - tensile modulus, 47
 - surface chemistry, wetting and nonwetting surfaces
 - contact angle values, 41
 - Du Nouy ring manual method, 42–43
 - forces, at surfaces, 40
 - IST values, 41
 - sessile drop method, 42
 - Washburn equation, 44
 - water/oil/mineral surface, 40
 - Wilhemly plate method, 42–43
 - tubing and porous media, 44–46
- foam
 - liquid ratio and resistance factor, 454
 - matrix fluids
 - bulk-foam stability, 216–217
 - data-acquisition system, 217
 - foamed acid, 216
 - foaming tests, 216
 - generation, 214–215
 - HT tests, surfactants description, 216
 - laboratory sand pack apparatus, 217
 - mobilization, 214
 - parameters, 215
 - strong and weak, 214
 - mobilization and division, 453
 - operating parameters, 454
 - and polymers, 454
- formation damage, production impairment processes
 - analyses
 - asphaltenes and hydrates, 88
 - flow reduction effect, 88–89
 - NWB areas, pressure drop, 87
 - organic solids damage, 87
 - paraffin deposition, 87
 - types of damage, 88
 - drilling- and completion-induced damage
 - dimethylbenzylauryl ammonium chloride, 90
 - Horner plot, 89–90
 - oil-based drilling mud, 90–91
 - water-based drilling fluids, 90
 - finest migration
 - clay micro and macrostructure, 91
 - clay swelling, 92
 - sandstone, 91
 - water shock test, 91, 92
 - in-situ emulsification, 96
 - organic solids and inorganic scales
 - asphaltenes, 92–93
 - flash scaling, 93, 94
 - produced water, injection, 94–95
 - seawater injection
 - permeability loss, 96
 - on sandstone cores, effects, 95
 - scale damage, well system, 96
 - stimulation treatments
 - asphaltene precipitation, 98–99
 - clay stabilizers, 99
 - fracturing treatments, 99
 - HCl treatments, 98
 - water block and wettability alterations
 - return permeability values, 97–98
 - surface energy and wetting technologies, 96–97
 - water-wet and oil-wet formation, 97
- frac additives
 - biocides, 328
 - flowback aids
 - flowback additives, 326
 - microemulsion (ME), 326–327
 - oil-wetting additive, 326, 327
 - water-wetting additives, 326–327
 - fluid and formation stabilizers
 - buffers, 329
 - clay control chemicals, 329–330
 - fracturing-fluid additives, 330–331
 - SIs, 330
 - foams and foaming agents
 - base fluids and gas, 325
 - dynamic FL cells, 325
 - foam stability, 324–325
 - nonionic, ionic, and amphoteric surfactants, 324
 - FR/DR agents, 323

- oxygen scavengers/reducing agents, 328
 - fracture fluid chemicals
 - additives, types, 273, 274
 - cost effective, 275–276
 - formation fluids and materials, 274
 - fracture width, 274
 - low FL, 274
 - low-friction properties, 275
 - preparation, in field, 275
 - proppants, types, 273
 - propped frac base fluids, 272–273
 - removal, fracture, 275
 - viscosity throughout treatment, 275
 - fracture stimulation, reactive fluids
 - acid frac mechanics, 235
 - carbonates
 - acid frac models, 250–252
 - acid fracturing process, 233–234
 - benefits, 236
 - conductivity, 233
 - fluid capacity, 235
 - viscosity, 234
 - conductivity and reactivity
 - acid etching procedure, 238
 - acid frac conductivity flow system, 237
 - chalk, 239
 - diffusion, 238–239
 - dolomite, 239
 - limestone, 239
 - measurement procedure, 238
 - modified API cell, 236–237
 - platens, 237–238
 - profilometer, 239
 - RD procedure, 239
 - frac support in proppant and acid fracs, 233
 - hydraulic fracturing, 231
 - mechanical placement
 - multistage fracturing systems, 249–250
 - openhole packer system, 249
 - polymer-based leakoff control acid, 249–250
 - reactivity and leakoff management
 - carbonate acid fracturing, 248
 - conductivity vs. closure stress, 248
 - foamed acid, 246
 - gelled acids, 241–242, 246
 - methods to reduce, 245–246
 - oil outer phase emulsions (W/O), 242–245
 - organic acids and chelating agents, 240–241
 - particulate diverters, 246
 - pumping schedule for multifract treatment, 249
 - VES materials, 246–247
 - sandstone fracture acidizing, 252–253
 - stresses, 231
 - fracturing-fluid selection
 - for coal seams
 - choice of fracturing fluid, 348
 - DOE CBM fracturing fluid selection guide, 347–348
 - laboratory retained permeability, 348
 - factors considerations, 345
 - guides, 345–346
 - for high carbon shales
 - amine oxides, 351
 - crosslinked gels, 350
 - effects of frac fluids, 351
 - guar-based fluid, 350–351
 - SW formulation, 349–350
 - oil or gas wells, 346
 - for TG, 351–352
 - FR/DR agents. *See* friction reducers (FRs)/drag reducer (DR) agents
 - friction reducers (FRs)/drag reducer (DR) agents, 323
- ## H
- harmonized mandatory control scheme (HMCS), 469, 470
 - HCl, carbonate reservoirs
 - adsorption data, 144
 - chalk formations, stimulation, 143
 - corrosion and inhibition, 143
 - densities and reactivates, 144
 - dolomitic reservoirs, 144
 - limestone and dolomite reactions, 144
 - oilfield steels, corrosion inhibition, 145
 - precipitate formation, 142–143
 - PVBT vs. injection rate plots, 143–144
 - reactivity and viscosity, 145
 - rotating disk electrode (RDE) methods, 143–144
 - sandstone acidization, 142–143
 - viscoelastic surfactants (VESs), 145
 - wormholes, 143
 - health, safety, and environmental (HSE) management
 - additives, reactive fluid, 205–206
 - chemical selection
 - environmental screening, 469
 - exposure hazards, 469
 - Global “Restricted Use” Considerations, 468
 - HMCS, 469, 470
 - HSE issues, 470
 - injection issues, functions, 471
 - physical/chemical properties, 468, 470–471
 - improved environmental control
 - CO₂ use, 475
 - DiSub system, 474–475
 - drum and tank recycling, 475
 - fluorocarbons, use, 475
 - LPG, 475
 - recyclable tote, 475–476
 - tight gas production and fracturing processes
 - FracFocus, 474
 - hazards, 473
 - hydraulic fracturing products, 472
 - methane emissions, 472
 - Phosphorus Project Group, 474
 - refinery distillation tower plugging, 474
 - state-drafted regulation, 474
 - toxic chemicals, 472–473
 - well construction, 472
 - HEC. *See* hydroxyethyl cellulose (HEC)
 - high-strength proppant (HSP), 333, 339, 341
 - HMCS. *See* harmonized mandatory control scheme (HMCS)
 - HPG. *See* hydroxypropyl guar (HPG)
 - HSP. *See* high-strength proppant (HSP)

- hydrolyzed polyacrylamides (HPAAs), 272
 - hydrophilic and lipophilic balance (HLB) values, 499, 500
 - hydroxyethyl cellulose (HEC), 272, 299, 306–307
 - hydroxypropyl guar (HPG)
 - flowback and cleanup
 - ammonium peroxydisulfate, 289–291
 - conditions, 289
 - curable-RCPs, 290–291
 - fluids and additives
 - aqueous and nonaqueous, 291
 - borate-crosslinked HPG fluid, 291
 - foamed fluids, 291
 - preparation and mixing
 - guar polymer, 285
 - HPG monomer, 284
 - hydrocarbon fluids, 285
 - proppant blenders, 285
 - propagation
 - conditions, 287
 - filter cake leakoff effects, 289
 - FL, zones, 287, 288
 - infiltration of particles, 289, 290
 - proppant settling, 287
 - Stokes' law and Kynch sedimentation, 287, 288
 - pumping through tubing
 - borate crosslinking mechanism, 286
 - pH, borate ion concentration, 286, 287
 - working conditions, 285
- I**
- illite, 170–173
 - improved oil recovery (IOR)
 - ASP, 372–373
 - capillary number, 374, 375
 - CFTs, 394–395
 - chemical tracers (see chemical tracers, EOR)
 - crude oil emulsion tests, 391
 - and EOR, 371–372, 460–462
 - fluids (see fluids)
 - formation particles, oil and water wetting, 374
 - hydraulic fracturing, 373
 - immiscible displacement processes
 - AMPS, 410
 - ATBS and VP groups, 412–413
 - degradation/failure modes, 413
 - iron, 411
 - LSWF, 398–402
 - polymer floods, 402–407
 - polymer retention, 411
 - shear degradation, 412
 - SRB, 407–408
 - waterflooding (see waterflooding)
 - water quality, 409–410
 - miscible displacement processes
 - alkaline flooding, 436–439
 - ASP (see alkaline-surfactant polymer (ASP))
 - CO₂ miscible floods, 414, 416–425
 - gas drives, 414–415
 - single miscible contact slug, 415
 - solvents, 414
 - surfactant floods, 425–436
 - surfactant method technologies, 444–445
 - VAPEX, 415–416
 - VGDs, 415
 - water and ethanol, 414
 - mobility control
 - coil tubing, 446
 - excessive water production, 445
 - foam, 453–455
 - particles and VES, 456
 - RPM [see relative permeability polymers (RPM)]
 - treatment, 445
 - waterflood/EOR operation, 446
 - water shutoff operations, 446
 - mobility ratio, displaceable oil, 375
 - physical/chemical procedures, 371–372
 - processes, 1
 - production methods, 374
 - reservoir fluid properties, 389–390
 - rock matrix minerals, 394
 - treatment
 - ASP, 385
 - carbonate reservoirs, 387
 - EOR technology, 389
 - initial oil recovery values, 384
 - methods, 371, 372, 384
 - TDSs, 386
 - WAG, 388
 - USBM test, 394
 - viscosity measurements, 390
 - wettability and imbibition tests (see wettability and imbibition tests)
- inductively coupled plasma optical emission spectrophotometry (ICPOES), 129
 - inflow performance relationship (IPR) curve, 4–5
 - inorganic deposits formation
 - barium sulfate crystals, 61, 62
 - corrosion inhibitors (CIs), 61
 - debris, 59
 - electrical submersible pumps (ESP), 61
 - formation mechanisms, 61, 62
 - homogeneous/heterogeneous nucleation, 61, 62
 - iron-based scale forms, 61
 - mixed deposit chemistries
 - asphaltenes and scale, 83, 84
 - CaCO₃ scale deposition, 84
 - CO₂ injection, 83–84
 - naturally occurring minerals, 82, 83
 - in pipeline, 83
 - mixed inhibitor treatments, complex deposits
 - CI/KHI interactions, 85–86
 - interference experiments, chemicals, 86
 - kinetic hydrate inhibitor (KHI), 84–85
 - low dose hydrate inhibitors (LDHIs), 85
 - LUVICAP, 86
 - squeeze treatment method, step-by-step procedure, 84
 - naphthenates, 82
 - oil and gas production, 63
 - salt formers, 61
 - saturation index (SI), 60
 - saturation ratio (SR), 59–60
 - inorganic scaling and corrosion control technology
 - carbon steel, 63
 - chemicals, 61

- corrosion pit and scale, 63
 - FeS and FeCO₃, precipitation regimes, 64
 - H₂S and FeS precipitation, 71–72, 75
 - production CIs [see corrosion inhibitors (CIs)]
 - scales, 58–60
 - scaling and emulsion studies, 57
 - siderite, 63
 - sour brine CIs [see corrosion inhibitors (CIs)]
 - sulfide scavengers
 - formaldehyde, 73, 74
 - glyoxal, 73, 74
 - hexamethylene tetraamine, 73
 - reactions of aldehydes, 72
 - reactions of triazines, 72, 73
 - tris (2-hydroxyethyl)hexahydro-s-triazine (THHT), 73, 74
 - “sweet (CO₂)” fluid CIs [see corrosion inhibitors (CIs)]
 - interfacial surface tension (IST), 381, 426
 - intermediate strength proppant (ISP)
 - highly spherical ISP, 339–441
 - ultralightweight (ULW) proppants, 341
 - IST. See interfacial surface tension (IST)
- K**
- kaolinite
 - dissolution
 - Al concentration, 438
 - with DAE and ABF, 180
 - Si concentration, 438
 - porosity reduction, 124
 - sandstone formations, 167–171
 - SEM photo, 36
 - Kauri-Butanol number (KB), 27
 - kinetic hydrate inhibitor (KHI), 84–85
- L**
- lightweight proppants (LWPs)
 - ceramic spheres, 335, 336
 - proppants, 273, 333
 - shale formations, 349, 353
 - synthesis method, 335–336
 - liquefied petroleum gas (LPG), 475
 - low dose hydrate inhibitors (LDHIs), 85–87
 - low-salinity waterflooding (LSWF)
 - carbonates, 399–400
 - carboxylic compounds, 399
 - ionic composition, 400
 - sandstone, 400–402
 - seawater dilution, 400, 401
 - “smart water”, 398
 - wettability mechanism, seawater, 399–400
 - LSWF. See low-salinity waterflooding (LSWF)
 - LWPs. See lightweight proppants (LWPs)
- M**
- mass transfer limited (MTL) rate, 130
 - matrix fluids, placement
 - acid treatment plan, 229
 - carbonate fluid selection, 230
 - chemical diversion methods
 - biodegradable particle diverting agent, 213
 - foam diversion, 214–218
 - multicore system, 220
 - PAA gel crosslink mechanism, 219
 - self-generated gel diversion and emulsified acids, 218–221
 - solid diverting agents, 212–214
 - VESs [see viscoelastic surfactants (VESs)]
 - correct fluid placement, 207
 - liquid products, 230
 - mechanical placement methods
 - ball sealers, 208–210
 - maximum pressure differential and injection rates (MAPDIR) technique, 208
 - placement devices, packers and CT, 210–212
 - oilfield chemicals, wellsite delivery, 230
 - planning and fluid selection, 228–230
 - sandstone formations, 230
 - solid products, 231
 - three-layer formation, 207
- matrix reactive fluid treatments
 - carbonates
 - coreflood tests, 129–130
 - radial flow experiments, 130
 - RD methods, 126–129
 - silicate formations, test methods
 - coreflood tests, 131
 - slurry batch reactor, 130–132
- microreaction technologies (MRT), 46
- minerals chemistry
 - amorphous structure, 34
 - barium sulfate, 35
 - carbonate formations, 35
 - clays, 35–36
 - crystalline, 34
 - database, 34
 - hydrodynamic shear, surface, 37
 - kaolinite, SEM photo, 36
 - montmorillonite structure, 36
 - phyllosilicates structures, 35
 - reaction, 38–39
 - shales, 38
 - tectosilicate structure, 38
 - unit cell, 35
 - zeta potential, 37
- monomer and salt solutions, 12–13
- N**
- National Incident Management System (NIMS), 490
 - National Oil and Hazardous Substances Pollution Contingency Plan (NCP), 490
 - National Oil Spill Response and Renewable Energy Test Facility (NOSRRETF), 491
 - National Response System (NRS), 504
 - naturally occurring radioactive materials (NORM), 477, 478
 - near wellbore (NWB) matrix
 - chemical/engineering practices, production enhancement, 9
 - formation damage, 87
 - production impairment processes, 55–56
 - net environmental benefit analysis (NEBA) method, 502–503

- NIMS. See National Incident Management System (NIMS)
- nonwater-based fluids
 alcohols, 312–313
 CO₂, 312
 emulsions, 313
 foamed fluids, 313
 gelled oil, 312
- NORM. See naturally occurring radioactive materials (NORM)
- NOSRRETF. See National Oil Spill Response and Renewable Energy Test Facility (NOSRRETF)
- NRS. See National Response System (NRS)
- O**
- oilfield chemistry information, electronic sources, 53–54
- organic acids, acetic and formic acid (FA)
 calcareous materials, 149
 calcite formations, stimulation, 147
 calcium acetate, 146
 carboxylic acid, 149
 chelating agents, 148
 O/G fields, 146
 proton attack, 148
 reactive chemicals, characteristics, 147
 wormhole formation, 148
- organic-based fluids, solubility and solubility parameters
 asphaltenes precipitation, 25
 ASTM method, 27
 crude oil fluids, behavior, 25
 functional group, 27
 Hansen plot, 26
 Hansen solubility parameters, 26
 interactions, 26
 Kauri-Butanol number (KB), 27
 Teas classes, 27
- organic deposits formation
 asphaltenes (unsaturated and cyclic hydrocarbons), 58, 80, 81
 control technology, 81–82
 corrosion process, 58
 crude oil, chemical types, 80–81
 fouling solids, 58–59
 hetero atoms, 80
 water production, 80–81
 waxes (saturated hydrocarbons), 58, 81
- oxidizing agent breakers
 advantages, 317
 breaker-crosslinker-polymer complex, 318
 cumene hydroperoxide, 317
 gellable fracturing fluid, formation, 319
 guar, 317–318
 organic peroxides, 317
 viscosity and molecular weight (MW) reduction, 318
- P**
- polyethyleneimine (PEI)-nanoparticle, 452
- polymer floods
 AM and AMPS monomers, 404
 areal sweep efficiency, 402–403
 Dalia field, 406–407
 EOR projects, 402
- HPAA, 403–404
 injection, 405
 macro analyses, 406
 mechanisms, 402
 resistance factor, 404
 tetra-polymer, 405
- production chemistry economics
 flow assurance (FA) activities, 11
 indicators
 corporate goals and risk, 12
 net present value (NPV), 11
 payout time, 11
 rate of return, 12
 return on investment (ROI), 12
 stimulation/intervention method, 12
 matrix chemical fluids, 11
 retrievable liquid hydrocarbons, 11
- production impairment processes
 case histories
 corrosion mitigation chemicals, 118
 demulsification, 119
 multichemical application, 119–120
 scale inhibitor improvements, 118–119
 emulsions, formation and control (see emulsions)
 flow assurance (FA), 56, 57
 flow enhancers, 116–117
 formation damage
 analyses, 87–89
 drilling- and completion-induced damage, 89–91
 production processes, 91–99
 inorganic scaling and emulsion studies, 57
 mixed deposit environment, 56, 57
 near wellbore (NWB) matrix, 55–56
 organic and inorganic deposits
 corrosion process, 58
 formation and control, 80–82
 inorganic scale, 58, 61–75
 production corrosion and scale inhibitors, 75–80
 scale blocking formation pores, 59
 wax blocking tubing, 58–59
 production chemicals, 55
 Reynolds number, 55
 scale and organic solids formation in well, 56
- proppants
 benefits, 344
 characteristics, 333–335
 conductivity and closure stress, 334
 crush-test procedures, 333–334
 cylindrical and spherical, 344
 deformable particles, 341–342
 fiber-laden low-viscosity fluid technology, 343–344
 fibers stabilized sand-pack treatment, 342–343
 fracture conductivity, 344–345
 high-strength, 341
 ISP, 339–341
 LWPs, 335–336
 nondeformable core, 342
 RCP
 curable proppants, 338
 pack strength, 341
 partially cured or curable-resin coating, 338–339

602 Subject Index

- phenol-formaldehyde resins, 339, 340
 - precured resin coatings, 338
 - red mud, 341
 - sand
 - API RP 56*, 337
 - choice of proppant, 337–338
 - frac sand, 336, 337
 - silica sands, 336
 - selection, 352–353
 - transport
 - chemistry, 310–311
 - DOR methods, 311
 - effect of viscosity, 280
 - fluid chemistry, 311
 - Newtonian fluids, 310–311
 - properties, 279
 - slot-flow model, 280–281
 - Stokes law, 281
 - viscosity, proppant settling rate, 280–281
 - types, 333
 - propped fracturing chemistry and applications
 - acid fracturing, 259–260
 - additional frac additives (see frac additives)
 - carbonates and silicate formations, 259
 - case histories and best practices
 - frac pack, 368–369
 - horizontal completions, 367–368
 - tight gas (TG) and shale gas, 366–367
 - VES fluids, 369
 - chemicals (see fracture fluid chemicals)
 - conventional reservoirs, oil and gas, 261
 - drilling and mechanical frac placement, 364
 - FL agents [see fluid loss (FL) agents]
 - fluid efficiency and leakoff, 268
 - fluid/proppant chemistry, HPG [see hydroxypropyl guar (HPG)]
 - fluid selection (see fracturing-fluid selection)
 - formation minerals, reactions, 331–332
 - fracture models
 - design elements, 353–354
 - 3D fracture models, 356
 - 2D models, 355
 - geometry simulation, 354
 - KGD model, 355–356
 - PKN model, 355
 - planar-3D models, 356
 - pseudo-3D models, 356–357
 - fracture treatment, tasks, 260–261
 - fracturing fluids
 - base fluid rheology, 276–278
 - FL, 280–283
 - fracture conductivity, 283–284
 - proppant transport, 279–280
 - slurry rheology and friction pressure, 277–279
 - hydraulic fracturing (HF), 259
 - interactive selection systems, 353
 - long, deviated wells, frac placement
 - ball-activated frac ports (FPs), 365–366
 - directional drilling, 364
 - multiple-stage fracturing process, 364, 365
 - stress field, 364
 - mechanical parameters
 - complex fractures, 269–271
 - fluid efficiency and leakoff, 268
 - fracture conductivity, 267–268
 - fracture geometry, 268–269
 - nonplanar fractures, 269
 - planar fractures, 269
 - reservoir contact area, 270–271
 - transverse and longitudinal fractures, 269
 - nonwater-based fluids (see nonwater-based fluids)
 - placement methods
 - channeled frac pack, 361, 363
 - fibers, 362, 363
 - frac conductivity, 360–361
 - low-permeability formations, 363
 - permeability vs. channel formation, 362
 - pumping schedule, 361
 - sealing-ball staged fracturing, 360
 - proppants (see proppants)
 - unconventional reservoirs (see unconventional reservoirs)
 - viscosity
 - breakers, carbohydrate frac fluids, 316–322
 - causing agents, 260
 - water-based fluids (see water-based fluids)
 - well fluids, reactions, 332
- ## R
- radial flow experiments, matrix reactive fluid treatments, 130
 - RCP. See resin-coated proppant (RCP)
 - reaction of acids, carbonate rocks
 - Austin chalk, 136–137
 - fluid saturations, 137–138
 - injection rate, effect, 135
 - rock type, effect, 135–137
 - RRT, 135–136
 - tomogram, core, 135
 - Winterset limestone, 136–137
 - wormhole velocity vs. interstitial velocity, 137–138
 - reactive chemicals, formation stimulation
 - acidizing, 125–126
 - additives (see additives, reactive fluid)
 - carbonates
 - matrix and fracture acidizing, 123
 - matrix stimulation (see carbonates)
 - stimulation treatments, 125, 255–258
 - wormhole formation, 124
 - corrosion inhibitors (CIs), 123
 - diversion/fluid loss, 253–255
 - fracture acidizing, 121
 - fracture stimulation (see fracture stimulation, reactive fluids)
 - hydraulic fracturing treatments, 124
 - matrix fluids, placement (see matrix fluids, placement)
 - matrix reactive fluid treatments (see matrix reactive fluid treatments)
 - matrix stimulation, 121, 124
 - productivity index (PI), 123
 - pumping rate and well pressure, 121–122
 - sandstone
 - and carbonate treatment methods, radial view, 122

- matrix stimulation, 124, 125 (*see also* sandstone)
 - steel well tubing, 125
 - tubing cleanout treatments, 125
 - wormhole structures, top and side views, 123
 - relative permeability polymers (RPM)
 - chemicals, 449
 - HPAA, 448
 - materials, 448
 - nonionic polyacrylamides, 448
 - particles and VES, 455–456
 - polymers and microgels, 448–449
 - principle, 447–448
 - scleroglucan, 448
 - tests and field evaluation, 456
 - water shutoff chemicals
 - aldehyde compound, 451–452
 - CDG, 452–453
 - chromium (III), 450
 - description, 449
 - gel treatments, 450
 - PEI, 452
 - polymer treatment process, 451
 - sodium silicate solutions, 450
 - relative solubility number (RSN), 110–111
 - remediation chemicals, water bodies
 - biodegradation, 496
 - BPMTDH spill, 502
 - dispersants
 - characteristics, 496–497
 - compounds, 499
 - HLB values, 499, 500
 - hydrocarbon solvents, 499
 - nonionic surfactants, 499
 - oil-soluble surfactant, 501
 - oxyethylated fatty alcohols, 501–502
 - petroleum-based dispersants, 498
 - seawater oil dispersants, 500, 501
 - water-soluble surfactant, 501
 - effectiveness tests, 497–498
 - hydrocarbon spills, 492
 - IST and CMS for surfactants, 495
 - lab-level tests, 497
 - Laurel sulfate, 494
 - NCP product schedule, 497
 - NEBA method, 502–503
 - safety/ecotox test methods, 498
 - simplified dispersant mechanism, 494–495
 - US EPA, 497
 - wave basin tests, 497
 - reservoir life cycle, chemical applications
 - global oil field chemical market, 4
 - petroleum liquids, API gravity, 3
 - refiners, 3
 - sub phases
 - primary, 2
 - secondary, 2–3
 - tertiary, 3
 - total organic carbon analysis, 2
 - viscosity, 3–4
 - water-based and oil-based fluids, 2
 - well, chemistry in production phases, 2
 - resin-coated proppant (RCP), 338–340
 - rheology
 - apparent viscosity, 33
 - definition, 32
 - dynamic oscillatory rheometry (DOR), 33–34
 - hydroxypropyl guar (HPG), 32–33
 - Newtonian fluids, 32
 - rheometers, 34
 - rheopectic, 33
 - shear thickening and thinning, 32, 33
 - thixotropy, 33
 - rock reservoir types (RRT), 135–136
 - rotating disk (RD) methods
 - angular velocity, 128
 - description, 127
 - diffusion coefficient, 127
 - fluid motion, 127
 - HP reactor and RDE, 128
 - ICPOES, 129
 - infinite disk spinning, 127
 - laminar conditions, 127
 - measured reaction rate, 128
 - RPM. *See* relative permeability polymers (RPM)
- S**
- sandstone
 - acid formulations
 - antiprecipitation and retarded formulations, 176–179
 - MA, 174–175
 - retarded acid containing fluoboric acid, 175–176
 - acidizing models
 - kinetic-controlled reactions, geochemical models, 174
 - two-acid, three-mineral models, 173
 - two-mineral models, 173
 - acid stages number, systems for reducing
 - Berea sandstone, 183
 - bottomhole temperatures (BHTs), 182
 - carbonate salts (calcite/dolomite) organic acids, 181
 - chelating agent formulations, 179
 - coreflood tests, 180
 - damage field cores, 181
 - GLDA-based fluids, 183
 - HEDTA fluids, 182
 - HF-containing fluids, 180
 - kaolinite dissolution, 180
 - low bottomhole pressure, 183
 - mechanical diversion, 183
 - retarding agents, 179–180
 - single-stage sandstone acid, 181
 - single-stage sandstone fluid (SSF), 179–180
 - slurry reactor tests, 181
 - Berea sandstone core, micrograph, 163
 - constituents, 163
 - coreflood tests (CFTs), 131
 - formation damage, 91, 95
 - fracture stimulation, reactive fluids, 252–253
 - HCl, carbonate reservoirs, 142–143
 - LSWF, 400–402
 - minerals dissolution, mechanisms, 164–166

- organic material, 401
 - permeability response, 174
 - polar oil components, 402
 - reactions and reaction rates
 - aluminosilicates, 172
 - analcime, 169
 - batch reactor experimental data, 171
 - chlorite, 169–170
 - clay-type minerals, dissolution, 167
 - components, 166
 - illite, 170
 - kaolinite, 167–169, 172
 - mineral compositions, 167
 - porosity-permeability relationship, 173
 - secondary acidizing precipitates, 167
 - zeolites, 170–171
 - silicate compositions, 164
 - stimulation treatments, 125
 - surfactant evaluation methods, 426
 - SWTT, 401
 - scale inhibitors (SIs)
 - additional frac additives, 329–331
 - fracture treatments, 327
 - thermal stability determination, 79
 - seawater wettability mechanism, 399–400
 - single well tracer test (SWTT), 401, 456, 459
 - slickwater (SW) fracturing fluids
 - AMPS polymer viscosity, 306
 - HPAA gels, 305
 - polyacrylamide (PAA), 305
 - and synthetic polymers, 305
 - slurry batch reactor, 130–132
 - solids and liquids, mechanical properties
 - Poisson effect, 28
 - shear modulus, 29
 - shear strain, 28
 - strain, 27–29
 - stress, 27–29
 - spills, control and remediation
 - contaminated soil and wildlife
 - bioremediation, 504
 - hydrocarbon impacted soils, restoration, 504
 - salt-impacted soils, restoration, 503–504
 - wildlife and birds, cleaning of, 505
 - control and planning
 - Abandoned Oil and Gas Wells, 491
 - Bureau of Land Management by OERB (2000), 492
 - containment/removal, 492
 - contamination of groundwater, 491
 - EMSA (2010) system, 490
 - NCP, 490
 - NIMS, 490
 - NOSRRETF, 491
 - NRS, 504
 - oilfield fluids, 490
 - oil release, 490
 - spill plans, 492
 - remediation chemicals (see remediation chemicals, water bodies)
 - “squeeze enhancement” methods, SIs
 - charged polymers, 77–78
 - polyquaternary amines, 78
 - precipitation squeeze, 76–77
 - scale delay tests and chemical analyses, 79
 - SIs with acids, 78–79
 - structures of bridging agents, 77
 - Zn²⁺-scale inhibitor salts, 78
 - surface chemistry, wetting and nonwetting surfaces
 - contact angle values, 41
 - Du Nouy ring manual method, 42–43
 - forces, at surfaces, 40
 - IST values, 41
 - sessile drop method, 42
 - Washburn equation, 44
 - water/oil/mineral surface, 40
 - Wilhemly plate method, 42–43
 - surface reaction rate (SRR)
 - carbonates, 126
 - coefficients, 147
 - constant, 128
 - dissolution rate, 39
 - surfactant-alternating gas (SAG), 422
 - surfactants
 - adsorption, 444
 - evaluation methods
 - HLB, 429
 - laboratory models, 426
 - oil solubilization ratio, 427
 - phase-behavior tests, 426
 - sandstone formations, 426
 - solubilization phase behavior, 427–428
 - floods
 - alkalinity, 432
 - aqueous and oil phase, 432
 - EOR anionic, 430–431
 - evaluation methods, 426–429
 - hydrophobe surfactants, 434–435
 - IST, 426
 - micellar/polymer flood sequence, 425
 - optimal microemulsion formulation, 433–434
 - PO sulfonate, 430, 431
 - SP and ASP formulations, 435
 - SS processes, 429–430
 - test, 433
 - fluids
 - CMC, 14, 16
 - Langmuir adsorption, 14–15
 - Langmuir equation, 14
 - micelle in water, 15
 - micelles/vesicles, 14
 - molecules associations, 15
 - rough inhomogeneous surfaces, 14
 - surfactant dipole, 13
 - types, 14
 - viscoelastic surfactants, 15
 - wormlike micelle aggregation, 15–16
 - SW fracturing fluids. *See* slickwater (SW) fracturing fluids
 - SWTT. *See* single well tracer test (SWTT)
- T**
- TDSs. *See* total dissolved solids (TDSs)
 - tetramethylammonium chloride (TMAC), 201, 203
 - thermodynamic equilibrium processes

- activity coefficients, 25
- chemical system, 23
- pressure dependence, equilibrium constant, 24
- reactants and products at equilibrium, 23
- standard enthalpy change, 24
- tight gas (TG)
 - fluids for, 351–352
 - fracturing, 260, 349
 - sands, 262, 310
 - shale gas reservoirs, 349, 366–367
 - unconventional reservoirs, 265–266
- total dissolved solids (TDSs), 386, 478, 484–485
- true vertical depth (TVD), 254
- tubing cleanout treatments, 125

U

- ultralightweight (ULW) proppants, 341
- unconventional reservoirs
 - complex fracture network, 357–358
 - innovative drilling, pumping, and placement strategies, 360
 - nonplanar, complex-fracture pattern, 359, 360
 - oil and gas
 - coalbed methane (CBM), 266–267
 - Eagle Ford shale group, 264
 - fissility, 263
 - geographic distribution, 262
 - low-permeability reservoirs, 261
 - Marcellus shale, 264
 - massive hydraulic frac, 264, 267
 - natural gas production, 262–263
 - organic shale, 263
 - resource plays, 262
 - rock matrix, 262
 - shale bed with multiple fractures, 264, 266
 - shale gas, 264–266
 - silicate formation, 263
 - slates, 263
 - TG, 265–266
 - proppant distribution scenarios, 358–359
 - wire-mesh model, 359
- US Bureau of Mines (USBM) test, 392, 394

V

- vaporizing gas drive (VGD), 414–415
- VES. *See* viscoelastic surfactants (VESs)
- viscoelastic surfactants (VESs)
 - acid diverter process, 227
 - acid diverting agents, 226
 - amidoamine oxide, surfactant, 224
 - amine oxide structures, 225
 - amphoteric betaine surfactants, 222
 - diversion methods, 223, 227–228
 - fluids compositions, 226
 - fracturing fluids
 - cosurfactants, 308
 - effects of temperature, 307
 - and HEC shear viscosity profiles, 306–307
 - HPAA network, 309–310
 - and hydrotropes, 308–309
 - viscosified fluids, 310
 - in-situ gelled acid diversion system, 221
 - multicore flow study, 224

- reversible gel, 222
- rod-like micelles, 221
- SGAD gels, 223
- surfactant-based acid systems, 224
- surfactants, 223
- types, 224
- viscosity profile, 223
- viscosity
 - AMPS polymer, 306
 - biphasic viscosity reducer chemicals, 117
 - breakers, carbohydrate frac fluids
 - acidic, 316–317
 - enzyme, 319–321
 - oxidizing agent, 317–319
 - VES fluids, 321–322
 - carbonates, 234
 - causing agents, 260
 - fluids, transport properties, 29–31
 - guar-based polymers, 294–295
 - HPG fluids, 299, 300
 - improved oil recovery (IOR), 390
 - modifiers, 304
 - proppants transport, 280–281
 - reactivity and, 145
 - reservoir life cycle, chemical applications, 3–4
 - rheology, 33
 - throughout treatment, 275
 - viscoelastic surfactants (VESs), 223

W

- waste disposal options
 - chemical and mechanical processes
 - acid mine drainage (AMD) water, 485
 - CleanWaveT, 486
 - Devon Energy Corporation (Devon) reports, 486
 - electrocoagulation/flotation, 487
 - evaporation/crystallization, 486
 - fixed-site treatment operations, 486
 - frac return water, 485
 - frac water lagoon and treatment plant, 486
 - guar-based fracturing fluids, 484
 - hydrocarbon flowback fluid, 484
 - hydrolyzed polyacrylamide polymer, 484
 - lowest TDS, 484–485
 - polysaccharide-based fracturing fluids, 484
 - scale forming constituents, 485
 - shale formations, 485
 - shallow-gas fracturing, 485
 - thermal evaporation, 485
 - water management options, 487
 - disposal in injection wells/surface streams
 - Class II injection, 488–489
 - earthquake activities, 488
 - surface water discharge treatment operations, 488, 490
 - EU directives, 481
 - gas/liquid separation and collection system, 479–480
 - general treatment and recycle methods
 - frac flowback pit, 483
 - frac water treatment for recycle, 483–484
 - oil/water separator, 483

- separation of phases, 483
 - methods for reducing water entry, 479
 - recycle/reuse, 480–481
 - shale gas production, 481–482
 - treatment/disposal, 481
 - water minimization, 480
 - well treatment water cycle, 487–488
 - water-alternating gas (WAG)
 - carbon dioxide flooding, 388, 420–421, 461
 - EOR technologies, 389
 - mobility control, 425
 - water-based fluids
 - carbohydrates (*see* carbohydrates)
 - chemistry of proppant transport, 310–311
 - fracturing-fluid business, nomenclature, 292
 - SW [*see* slickwater (SW) fracturing fluids]
 - VES [*see* viscoelastic surfactants (VESs)]
 - water frac (WF), 292
 - waterflooding
 - Buckley-Leverett method, 396
 - factors, 395
 - polymer flooding, 398
 - pressure maintenance, 397
 - salinity control, 398
 - water cycle, EOR, 395, 396
 - wellsite, treating equipment
 - chemist and chemical engineers, 49
 - heat/cooling, 52–53
 - material requirements, 51
 - matrix acid and cement placement, pumper, 50
 - mixing, 50
 - placement and control, 51–52
 - portable high pressure frac pump, 51
 - pumping, 50–51
 - rig down and flowback fluids disposal, 53
 - transportation and storage, 50
 - treatment evaluation, 53
 - wettability and imbibition tests
 - Amott–Harvey index number calculation, 393, 394
 - capillary pressure, water, 392
 - coreflood tests, 393
 - imbibition test, 392
 - rock surfaces, 391
 - USBM, 392
 - wormhole formation
 - clean and hydrocarbon soaked cores, 139
 - dissolution rate, 138
 - limestone-dolomite mixtures, 142
 - organic acids, acetic and formic acid (FA), 148
 - processes, 139
 - reactive chemicals, 123–124
 - theories and model characteristics, 140–141
- Z**
- zeolites
 - “acid-sensitive”, 38
 - aluminosilicates, 170–171
 - sandstone formations, 38
 - sensitive clays, 164
 - tectosilicates, 165